University of Fribourg
Department of Medicine
Domain of Physiology
Switzerland

A WINDOW INTO THE PLASTICITY OF THE SENSORIMOTOR SYSTEM IN ADULT PRIMATES USING EEG: INSIGHTS FROM LESION, REPEATED STIMULATION AND TOUCHSCREEN USE

THESIS

Presented to the Faculty of Science of the University of Fribourg (Switzerland)

in consideration for the award of the academic grade of *Doctor rerum naturalium*

by

Anne-Dominique Gindrat

from

Porrentruy, Switzerland

Thesis No 1923

Imprimerie Saint-Paul

2015

University of Fribourg
Department of Medicine
Domain of Physiology
Switzerland

A WINDOW INTO THE PLASTICITY OF THE SENSORIMOTOR SYSTEM IN ADULT PRIMATES USING EEG: INSIGHTS FROM LESION, REPEATED STIMULATION AND TOUCHSCREEN USE

THESIS

Presented to the Faculty of Science of the University of Fribourg (Switzerland)

in consideration for the award of the academic grade of *Doctor rerum naturalium*

by

Anne-Dominique Gindrat

from

Porrentruy, Switzerland

Thesis No 1923

Imprimerie Saint-Paul

2015

Accepted by the Faculty of Science of the University of Fribourg (Switzerland) upon the recommendation of Professor Eric M. Rouiller, Professor Jean-Marie Annoni, Professor Hansjörg Scherberger and Professor Jean-Pierre Bresciani

Fribourg, 18th Septembre 2015

Thesis supervisor:

Prof. Eric M. Rouiller

Dean:

Prof. Fritz Müller

A vous qui avez toujours cru en moi

« Je n'écris, pour ma part, ni un roman ni des Mémoires. J'essaie de comprendre le peu que j'ai fait et comment tout cela s'est emmanché. Je n'écris pas pour passer le temps ni pour donner des leçons. Je n'écris pas pour faire le malin ni pour ouvrir, comme ils disent, des voies nouvelles à la littérature. Pouah ! Je n'écris pas pour faire joli ni pour défendre quoi que ce soit. J'écris pour y voir un peu plus clair et pour ne pas mourir de honte sous les sables de l'oubli. »

Jean d'Ormesson, *Qu'ai-je donc fait*, 2008

Remerciements - Acknowledgements

« Nullum enim officium referenda gratia magis necessarium est. »

[« Car la reconnaissance est le premier de tous les devoirs. »]

Cicéron, *De officiis*, *Liber primus*

Réaliser une thèse de doctorat en sciences naturelles est une expérience unique et enrichissante sous plusieurs aspects. En effet, cela a constitué ma première vraie expérience professionnelle, avec tous les avantages … et les inconvénients qui en résultent. D'un point de vue humain et plus personnel, ma thèse a représenté une tranche de vie non négligeable de plus de 5 ans! Cette période a été rythmée par le plaisir et l'enthousiasme que j'ai eus à réaliser les expériences pratiques, à collecter des données, amenant parfois à des résultats prometteurs, parfois à des périodes de doute et de découragement, le tout entremêlé de préparations de posters et de présentations, de participations à des congrès et bien évidemment la rédaction de ma thèse. Maintenant que je suis enfin arrivée au bout de mes peines, le sentiment le plus excitant est celui d'avoir peut-être contribué quelque peu à la recherche scientifique. Néanmoins, cela n'aurait jamais été possible sans l'aide des personnes ci-dessous.

Je voudrais pour commencer exprimer ma gratitude au Professeur Eric Rouiller qui m'a accueillie dans son laboratoire depuis que je suis étudiante en Bachelor. Grâce à lui, j'ai découvert l'univers fascinant des Neurosciences et de la recherche scientifique. Sa rigueur scientifique, son caractère très humain et son soutien permanent tout au long de mes études m'ont permis de réaliser ma thèse dans les meilleures conditions. Il a toujours cru en moi et m'a toujours témoigné sa pleine confiance alors que souvent je doutais moi-même de mes réelles capacités ! Il a également toujours tâché de partager son optimisme et de m'encourager lorsque je me trouvais dans des moments de découragement. J'ai passé dans son laboratoire mes plus belles années d'étude ! Je regrette d'ailleurs sincèrement de partir…

Un grand merci au Professeur Hansjörg Scherberger et au Professeur Jean-Marie Annoni d'avoir accepté d'être les co-examinateurs du jury de ma thèse. Merci pour leur lecture attentive de mon manuscrit pendant l'été.

I would like to deeply thank Dr Arko Ghosh. I have learnt a lot by working with him! It may have been quite stressful but always fruitful!

Je tiens également à remercier vivement le Dr Charles Quairiaux, le Dr Juliane Britz et le Professeur Christoph Michel qui m'ont initiée à l'enregistrement et à l'analyse des potentiels évoqués somatosensoriels. J'associe également à mes remerciements Denis Brunet et le Dr Laurent Spinelli. Merci pour tout le temps qu'ils m'ont consacré !

Je voudrais aussi remercier particulièrement le Professeur Roland S. Johansson et le Professeur Jean-Marie Annoni pour les clarifications apportées à mes questions.

Un merci tout particulier au Dr Mélanie Kaeser. J'ai commencé par être sa « bachelorette » à mon arrivée au laboratoire. A ce moment-là, je l'appelais encore timidement « Madame » ! Puis au fil du temps s'est nouée entre nous une sincère amitié. Tout comme M. Rouiller, elle a toujours cru en moi et en mes aptitudes, alors que j'en doutais souvent fortement moi-même. Merci également de m'avoir fourni la figure 14A du Chapitre 5. Toi aussi, tu vas me manquer…

Je voudrais remercier chaleureusement Myriam Balerna et Magali Chytiris, les deux étudiantes de Bachelor avec lesquelles nous avons mené à bien nos études « smartphone ». J'ai eu un réel plaisir à travailler avec elles car elles ont toutes deux toujours fait preuve d'une grande motivation et d'une efficacité redoutable !

Mes sincères remerciements vont bien sûr également au Dr Florian Lanz pour sa précieuse aide pendant les enregistrements EEG, son ingéniosité, et sa bonne humeur !

Merci à Michela Fregosi et Julie Savidan pour leur aide concernant l'utilisation du microscope et de Neurolucida.

Merci également aux autres étudiants du laboratoire pour les bons moments que nous avons passés ensemble, que ce soit autour d'un café, lors de soupers « labo » ou pendant les différents congrès : Pauline Chatagny, Camille Roux, Simon Borgognon, Jérôme Cottet, Simon Badoud, Katia Fortis, Dr Marie-Laure Beaud, Dr Adjia Hamadjida…

Je suis également très reconnaissante envers les animaliers, Laurent Bossy et Jacques Maillard, qui font un travail inestimable. Merci pour leur grande disponibilité, leur efficacité et leur gentillesse !

Merci au Dr Loïc Chareyron et au Professeur Pierre Lavenex pour nous avoir fourni leur protocole histologique de coloration de la myéline.

Merci à Christine Roulin et Christiane Marti pour leur excellent travail histologique.

Merci à Françoise Tinguely et Michela Fregosi qui m'ont aidée à entraîner mes singes.

Je souhaite aussi remercier vivement Laurent Monney pour sa contribution informatique plus que nécessaire ! Il a su redonner vie à mon ordinateur à plusieurs reprises !

Merci aussi à Karine Sciboz, André Gaillard, Bernard Aebischer, Andrea Francovich et David Michel pour leur gentillesse et les nombreux services rendus.

Je remercie toute l'équipe du laboratoire pour son accueil, son aide et sa bonne humeur. Les repas de St-Martin à Chevenez resteront pour moi de merveilleux souvenirs. Je ne regrette qu'une seule chose : ne pas avoir fait les voyages en train avec vous !

Merci aux bibliothécaires de la DOKPE Halim Zinaoui et François Rappaz pour m'avoir fourni les articles dont j'avais besoin.

Pour finir, si j'en suis arrivée là à ce jour, je le dois en premier lieu à mes parents qui m'ont permis de faire mes études dans les meilleures conditions et qui m'ont toujours accordé leur soutien. J'y associe bien évidemment également ma sœur et mon frère qui m'ont soutenue et qui m'ont permis de me changer les idées pendant les quelques petits « entre-deux » que nous avons passés ensemble !

Table of contents

Abbreviations **1**
Abstract **4**
Résumé **7**
Preamble **10**

GENERAL INTRODUCTION **14**
General context **15**
Electroencephalography **16**
The pioneers of electroencephalography 18
The brain as a volume-conductor 21
Electrical neuroimaging 27
Evoked potentials 28
Somatosensory evoked potentials 30
Somatosensory system **33**
Some definitions about somesthesic perceptions 33
Peripheral receptors involved in tactile sensation 35
Somatosensory pathways 43
Dorsal column-medial lemniscal system *45*
Anterolateral system *50*
Somatosensory cortical areas 52
Motor control of voluntary movements **61**
Motor cortical areas 61
Primary motor cortex *61*
Association motor cortices *64*
Motor pathways 68
Corticospinal tract *69*
Other descending pathways *76*
Voluntary hand motor control 81
Functional sensorimotor system in primates **84**
Emergence of the concept of *sensorimotor cortex* in primates 84
M1 and S1 have dense reciprocal anatomical connections 87
The somatosensory cortical areas contribute to movements 89
Somatosensory processing takes place in M1 93
A disruption of somatosensory input induces motor deficits 94
A disruption of motor output induces modifications in somatosensory processing 96

Neuroplasticity **98**
Definition of neuroplasticity 99
Use-dependent plasticity in the adult 100
Use-dependent plasticity in animals *101*
Use-dependent plasticity in human *104*
Special forms of use-dependent plasticity in human *109*
Lesion-dependent plasticity in the adult 111
Lesion-induced plasticity in adult monkeys *111*
Example of plasticity following a motor cortex lesion in monkeys *112*
How does neuroplasticity operate ? 114
Biology of the long-tailed macaque **116**
General aims of the thesis **117**
References **118**

GENERAL MATERIALS AND METHODS **178**
Subjects **179**
Behavioural tasks **180**
General training 180
Modified Brinkman board task 182
Brinkman box task 184
EEG recording of somatosensory evoked potentials **184**
Electroencephalographic recordings (EEG) 184
Peripheral electrical stimulation 185
Peripheral tactile stimulation 185
EEG data analysis 185
Lesion **185**
Injection of BDA neuronal tracer **188**
End of the experimental protocol **189**
Histology **190**
Nissl staining 190
SMI staining 191
BDA histochemistry 192
Cytochrome oxidase staining 192
Myelin staining 193
References **194**

CHAPTER 1

Whole-scalp EEG mapping of somatosensory evoked potentials in macaque monkeys 200

Supplementary Figures 223

CHAPTER 2

Cortical and subcortical alterations of somatosensory processing from the distal forelimb after a dominant M1 lesion in non-human primate: a case report 231

Abstract 232

Introduction 233

Materials and Methods 237

Monkey 237
Cortical lesion 238
Behavioural task 238
EEG and electrical stimulation 238
Injection of BDA neuronal tracer 241
End of the experimental protocol 241
Histology 241
Neuroanatomical reconstruction 242

Results 243

Description and characterisation of the lesion 243
Impact of the lesion on fine manual dexterity 247
Subcortical potentials of SSEPs 248
Cortical potential of SSEPs 250
Relationship between subcortical volleys and cortical output 252
Reconstruction of BDA labelling 256

Discussion 257

Extent of the lesion 257
Effect of the cortical lesion on subcortical processing of peripheral inputs 259
Origin of subcortical potential 262
Effect of the cortical lesion on cortical potential 263
Effect of the cortical lesion on the relationship between subcortical volleys and cortical output 265
Post-lesion cortical reorganisation 267
Electrical stimulation 270
Relevance of single-trial analysis 271
Impact of the lesion on hand motor control 272
Further remarks 273

Conclusion **274**
Acknowledgements **274**
References **275**
Supplementary Figures **292**

CHAPTER 3

Impact of a dominant M1 lesion on cortical tactile processing from the fingertips in adult macaque monkey: a case report **303**

Abstract **304**
Introduction **305**
Materials and Methods **312**
Monkey 312
Behavioural task 312
EEG and tactile stimulation 314
EEG data analysis 315
Results **315**
EEG and tactile stimulation 315
Impact of the lesion on fine manual dexterity 319
Discussion **325**
Justifications for EEG investigations on a non-human primate model 325
Extent of the lesion 326
Impact of the dominant M1 lesion on hand sensorimotor control 328
Post-lesion cortical reorganisation highlighted by tactile stimulation to the fingertips 331
Arguments against volume-conduction artifacts 337
Electrical versus tactile stimulation 339
Originality of our lesion study 341
Prospects 343
Conclusion **344**
Acknowledgements **345**
References **345**

CHAPTER 4

Adaptation of the cortical somatosensory evoked potentials following a repeated tactile stimulation of the fingertips in macaque monkeys **369**

Abstract **370**
Introduction **371**

Materials and Methods **377**
Monkeys 377
EEG and tactile stimulation 377
EEG and electrical stimulation 378
Anaesthesia 379
Data analysis 379
Results **380**
Adaptation resulting from tactile stimulation of the fingertips 380
Adaptation resulting from electrical stimulation of the median nerve at the wrist 388
Discussion **389**
About the use of *adaptation* rather than *fatigue* or *habituation* 389
Mechanoreceptors involved in tactile SSEPs from the fingertips 391
Inter-individual variability in tactile SSEPs from the fingertips 391
Intra-individual variability in tactile SSEPs and in adaptation patterns across the fingers 393
Differences between adaptation after tactile versus electrical stimulation 394
Latency adaptation in the literature 396
Hypotheses about the origin of adaptation 397
Side-effect of anaesthesia ? *398*
Peripheral effect ? *401*
Changes in the pattern of contribution of neuronal populations to the cortical component ? *401*
Spike-timing dependent plasticity ? *403*
Originality of the present study 404
Relevance of the present study 405
Prospects 406
Conclusion **407**
Acknowledgements **408**
References **409**
Supplementary Figures **426**

CHAPTER 5

Sensorimotor functional recovery of manual dexterity in non-human primates following a motor cortex lesion assessed with the Brinkman box task **429**

Abstract **430**
Introduction **431**
The outstanding primate hand 431
Assessment of the fine manual dexterity in non-human primates 433

Present study ... 440
Materials and Methods ... 441
Macaque monkeys ... 441
Brinkman box task ... 442
Data analysis ... 445
Lesion ... 450
Treatments ... 451
Histology ... 452
Results ... 452
Extent of the lesions ... 452
Post-lesion deficits ... 453
Impact of the lesion on contralesional manual dexterity without vision ... 454
Impact of the lesion on contralesional manual dexterity with vision ... 457
Impact of visual feedback on contralesional functional recovery from the lesion ... 459
Somatosensory-related errors in contralesional manual dexterity without vision 461
Relationship between the contra- and the ipsilesional hand functional recovery ... 465
Strategy of prehension ... 467
Impact of a prefrontal (dlPFC) cortical biopsy on manual dexterity ... 470
Discussion ... 473
Relevance of our analysis method to assess manual dexterity in non-human primates ... 474
Relevance of a blind task ... 476
Somatosensory-related errors ... 477
Correlation between lesion extent and manual dexterity ... 479
Remarks on the effects of the treatments ... 481
Comparison between contra- and ipsilesional manual dexterity ... 482
Effect of a prefrontal cortical biopsy on ipsilesional manual dexterity ... 483
Post-lesion deficits ... 485
Further remarks ... 486
Conclusion ... 486
References ... 487
Supplementary Data ... 503
Impact of the lesion on ipsilesional manual dexterity ... 547

CHAPTER 6

Use-Dependent Cortical Processing from Fingertips in Touchscreen Phone Users ... 549
Supplementary Figures ... 558
Appendix: Survey ... 560

CHAPTER 7

Imprint of historical touchscreen minutes in cortical tactile processing.. 567

Abstract....568

Introduction....568

Materials and Methods....569

Volunteers and touchscreen behavioral log.... 569

Touchscreen-finger interaction survey.... 569

Somatosensory evoked potentials and multiple regression analysis.... 570

Results....570

Discussion....575

Acknowledgements....576

References....576

CHAPTER 8

May one conceive research in Neuroscience without animal models ?..... 579

Introduction....580

Our brain, this fascinating organ....580

Ethical dilemma....583

Application fields of research based on animal models....584

Animal models involved in biomedical research....587

The situation in Switzerland....587

The non-human primate as model of choice in Neuroscience....591

Contributions of non-human primates to biomedical progress in Neuroscience....598

Neuroprosthetics.... 599

The successful story of anti-Nogo-A: examples of CNS lesions.... 601

Parkinson's disease.... 609

Concluding remarks....613

References....615

Supplementary Figures....640

GENERAL DISCUSSION.... 643

Summary of the main results....644

Potential limitations of our studies and perspectives....647

Plasticity as the driving force of brain activity....651

EEG as an imaging tool **651**
Importance to comprehend the sensorimotor system as a whole **654**
Uniqueness of the thumb **655**
Conclusion **656**
References **656**

APPENDIXES **661**
Appendix 1 ..... **662**
Appendix 2 ..... **674**
Appendix 3 ..... **687**
Appendix 4 ..... **709**

Curriculum vitae **746**

Abbreviations

ABC: avidin-biotin complex

AEP: auditory evoked potentials

ATP: adenosine triphosphate

BAEP: brainstem auditory evoked potential

BDA: biotinylated dextran amine

C.O.: cytochrome oxidase

CD: current density

CM: corticomotoneuronal

CMA: cingulate motor area

CNS: central nervous system

CST: corticospinal tract

DAB: diaminobenzidine

DBS: deep-brain stimulation

dlPFC: dorsolateral prefrontal cortex

DTI: diffusion tensor imaging

ECG: electrocardiogram

EEG: electroencephalogram

EMG: electromyogram

EP: evoked potential

EPSP: excitatory postsynaptic potential

ERP: event-related potential

fMRI: functional magnetic resonance imaging

GA: grand average

GABA: γ-aminobutyric acid

GEV: global explained variance

GFP: global field power

i.m.: intramuscular

i.v.: intravenous

ICMS: intracortical microstimulation

IPSP: inhibitory postsynaptic potential

LFP: local field potential

LH: left hand

LORETA: low-resolution electromagnetic tomography

LSI: laser speckle imaging

LTD: long-term depression

LTP: long-term potentiation

M1: primary motor cortex

M1c: caudal part of the primary motor cortex

M1r: rostral part of the primary motor cortex

MEG: magnetoencephalography

MEP: motor evoked potentials

Mk: monkey

MPTP: 1-methyl-4-phenyl-1,2,3,6-tetrahydropyridine

MRI: magnetic resonance imaging

PBS: phosphate-buffered saline solution

PET: positron emission tomography

PM: premotor cortex

PMd: dorsal part of the premotor cortex

PMv: ventral part of the premotor cortex

PMvr: rostral part of PMv

PNS: peripheral nervous system

Pulo: anterior pulvinar

PV: parietal ventral area

RER: rough endoplasmic reticulum

S1: primary somatosensory cortex

RH: right hand

RNA: ribonucleic acid

s.c.: subcutaneous

S2: secondary somatosensory cortex

SC: spatial correlation

SD: standard deviation

SE: standard error

SMA: supplementary motor area

SPECT: single-photon emission computerised tomography

SSEP: somatosensory evoked potential

VEP: visual evoked potential

VL: thalamic ventrolateral nucleus

VP: thalamic ventroposterior complex

VPL: thalamic ventroposterolateral nucleus

Abstract

Somatosensory and motor cortical areas of the primate brain are functionally linked into a global sensorimotor system that integrates somatosensory information from the periphery into movement production. Plastic modifications take place continuously in this large-scale network and are of prime importance throughout life, for instance during daily sensory experience, for skill learning and for functional recovery after a brain lesion.

In order to provide a fresh insight into the dynamics of sensorimotor cortical activity in non-human primates in the general context of a motor cortex lesion, we developed a methodological approach allowing to record the whole-scalp electroencephalogram (EEG) from 32 electrodes in anaesthetised macaque monkeys. Somatosensory evoked potentials (SSEPs) in response to the electrical stimulation of the median nerve at the wrist were mapped non-invasively from the whole scalp with submillisecond temporal resolution. We aimed at using EEG measurement of SSEPs to study the reorganisation of the somatosensory processing following a focal cortical lesion of the primary motor cortex (M1), requiring a craniotomy. Consequently, we fully validated our EEG method by demonstrating that a craniotomy performed in the context of a cortical lesion did not induce major distortions in the EEG signal measured at the scalp. From then on, we were able to confidently use this EEG technique to investigate the effects of a cortical lesion on brain activity and the mechanisms involved in subsequent cortical reorganisation.

Lesion-induced plasticity was investigated in one monkey subjected to a unilateral permanent lesion of the hand representation in M1, resulting in strong deficits of contralesional fine manual dexterity. Regular pre- and post-lesion EEG measurements of median nerve SSEPs showed that the M1 lesion induced extensive plastic modifications in somatosensory processing that were not restricted to the somatosensory cortical level but, surprisingly, affected the subcortical level as well. To elaborate, experiments revealed a reduction of the amplitude of subcortical potential after the lesion. Moreover, the lesion resulted in a constant gain added in the somatosensory processing at the cortical level while the sensitivity itself of somatosensory cortex to fluctuating inputs from the subcortical level was maintained.

We complemented our investigations on the same monkey by recording EEG measurement of SSEPs elicited by a more naturalistic, tactile stimulation to the fingertips (thumb, index and middle fingers) in order to overcome some major drawbacks inherent in artificial, electrical stimulations. As a result, we observed that the M1 lesion induced drastic alterations in tactile sensory processing from the fingertips, especially from the thumb tip although the lesion affected the entire hand representation in M1. Interestingly, detailed behavioural observations revealed that these cortical modifications were associated with differential alterations and recovery of the use of the different fingers in a precision grip task (opposition of the thumb and index finger) performed with or without visual control. Behavioural analyses extended to other monkeys involved in the same task confirmed the presence of somatosensory-related behavioural deficits after a motor cortex lesion. This pilot study illustrates that sustained changes in motor output and sensorimotor connectivity after a motor cortex lesion were sufficient to induce deep plastic reorganisation of the somatosensory processing over the post-lesion recovery period in an adult macaque monkey.

In a separate study, we took advantage of the high temporal resolution of EEG to investigate in greater detail the effects of the aforementioned repeated tactile stimulation to the fingertips on somatosensory processing, in three intact adult monkeys. By using a 1-Hz stimulation repetition rate, which is actually low as compared to many other studies using repeated stimulations, we demonstrated that cortical adaptation is not limited to the well-known reduction in amplitude of cortical activity over time, but surprisingly the latency of EEG signal was linearly increasing over time in response to a repeated tactile stimulation to each of the fingertips. These rapid plastic modifications of the somatosensory cortical activity may correspond to a unique and specific “cortical signature” of fingertip tactile stimulation and may enable the brain to prioritise novel stimuli by delaying the sensory processing of repeated and thus meaningless inputs. Moreover, these results suggest that latency adaptation is a significant process that should be carefully considered in case of repeated tactile stimulations, even at a low stimulus repetition rate.

Finally, we provided significant insights into use-dependent plasticity by moving to EEG investigations on human. While a wealth of studies on use-dependent plasticity has focused on highly skilled expert people so far, we investigated the plasticity of the sensorimotor cortex in daily, unconstrained conditions by measuring EEG on adult

touchscreen smartphone users and nonusers (used only old-technology mobile phones) in response to tactile stimulations to the fingertips (thumb, index and middle fingers). In addition, we took advantage of the intrinsic technology of touchscreen smartphones which store built-in battery logs to document participants' activity on these devices. In this way, we were able to relate past sensory activity on the phone with cortical somatosensory processing from the fingertips. Briefly, we found that the repetitive finger interactions on a smooth touchscreen led to deep reshaping of tactile sensory processing from the fingers in smartphone users. Remarkably, we demonstrated that use-dependent plasticity can operate very rapidly by daily updating the somatosensory cortical representation of the thumb in particular. In a subsequent study, we investigated in greater detail the brain cortical imprinting of sensory behavioural activity on the touchscreen. In short, we observed that different temporal features of touchscreen experiences and related hand actions are strongly imprinted at distinct stages of tactile sensory processing in the contemporary brain.

Taken all these results together, we were able to confirm by using EEG that brain activity in adult primates cannot be dissociated from the concept of neuroplasticity, whether during daily sensory experiences or after a brain lesion. Furthermore, we confirmed that M1 is definitely not a purely motor structure but, on the contrary, is important for somatosensory processing as well in primates.

Résumé

Chez les primates, les aires corticales somatosensorielles et motrices sont liées fonctionnellement sous la forme d'un système sensorimoteur plus global, intégrant les informations somatosensorielles de la périphérie pour produire les mouvements. Ce réseau à grande échelle est constamment sujet à des modifications plastiques cruciales, que ce soit dans nos expériences sensorielles quotidiennes, pour acquérir de nouvelles habiletés ou lors de la récupération fonctionnelle suite à une lésion cérébrale, entre autres.

Afin d'approfondir nos connaissances sur la dynamique de l'activité corticale sensorimotrice chez le primate non-humain dans le contexte général d'une lésion du cortex moteur primaire (M1), nous avons développé une approche méthodologique permettant d'enregistrer l'électroencéphalogramme (EEG) chez le macaque anesthésié, au moyen de 32 électrodes distribuées régulièrement sur toute la surface du cuir chevelu. Ce faisant, nous avons pu cartographier de manière non-invasive sur le cuir chevelu les potentiels évoqués somatosensoriels (SSEPs) en réponse à une stimulation électrique du nerf médian au poignet, avec une résolution temporelle inférieure à la milliseconde. Notre but final était d'utiliser ensuite cette méthode pour étudier la réorganisation du traitement de l'information somatosensorielle suite à une lésion focale de M1, cette dernière procédure impliquant la réalisation d'une craniotomie. Nous avons alors validé complètement notre technique d'enregistrement EEG en montrant qu'une craniotomie n'induisait pas de distorsions majeures dans le signal EEG mesuré au niveau du cuir chevelu. Dès lors, nous étions en mesure d'appliquer l'enregistrement EEG de SSEPs pour étudier les effets d'une lésion corticale cérébrale sur l'activité du cerveau et ainsi mieux appréhender les mécanismes de la réorganisation corticale inhérente à la lésion.

Nous avons étudié la plasticité cérébrale induite par une lésion chez un singe ayant subi une lésion unilatérale permanente de la représentation corticale de la main dans M1, perturbant profondément sa dextérité manuelle fine contralésionnelle. Par des acquisitions EEG de SSEPs du nerf médian réalisées régulièrement avant et après la lésion, nous avons observé que la lésion de M1 a induit d'importantes modifications plastiques du traitement de l'information somatosensorielle. A notre plus grande surprise, ces modifications n'étaient pas limitées au cortex somatosensoriel mais elles s'étendaient également au niveau sous-cortical sous la forme d'une diminution de l'amplitude du potentiel sous-cortical

après la lésion. L'activité corticale post-lésionnelle était, elle, caractérisée par une augmentation du potentiel somatosensoriel sous la forme d'un gain constant ajouté, alors que la sensibilité du cortex somatosensoriel aux afférences sous-corticales variables était elle-même conservée après la lésion.

Les stimulations périphériques électriques comme celles appliquées ici au nerf médian comportent de nombreux inconvénients, notamment parce qu'elles sont très artificielles. Pour contourner ce problème, nous avons alors mis au point, chez ce même animal, l'enregistrement EEG de SSEPs obtenus par une stimulation tactile de l'extrémité des doigts (pouce, index et majeur), correspondant à une activation plus naturelle des voies somatosensorielles afférentes. Nous avons alors observé que la lésion de M1 a modifié de manière profonde le traitement cortical de l'information sensorielle tactile provenant des doigts, en particulier du pouce, alors que la lésion corticale s'étendait sur la représentation complète de la main dans M1. De plus, en parallèle à ces modifications corticales, la lésion a altéré de manière distincte l'usage puis la récupération fonctionnelle des différents doigts dans une tâche comportementale basée sur l'utilisation de la pince de précision (opposition du pouce et de l'index), réalisée avec ou sans contrôle visuel. Des analyses comportementales réalisées sur d'autres singes impliqués dans cette même tâche ont confirmé qu'une lésion corticale motrice induisait des déficits comportementaux en lien avec le traitement somatosensoriel. Cette étude pilote démontre que les changements majeurs opérés au niveau du cortex moteur et de la connectivité sensorimotrice ont été suffisants pour provoquer une profonde réorganisation plastique du traitement de l'information somatosensorielle au cours de la période de récupération qui a suivi la lésion, chez un macaque adulte.

Dans une autre étude, nous avons profité de l'excellente résolution temporelle offerte par l'EEG pour étudier dans plus de détails l'impact de la stimulation tactile répétée décrite ci-dessus, sur le traitement de l'information somatosensorielle provenant de l'extrémité des doigts. Pour ce faire, nous avons délivré des simulations tactiles répétées aux doigts de trois singes adultes intacts avec un taux de répétition de 1 Hz (faible valeur en comparaison de beaucoup d'autres études utilisant un paradigme de stimulation répétée). Nous avons alors observé que l'adaptation corticale ne se limite pas à la réduction de l'amplitude corticale au cours du temps, comme généralement décrite. En effet nous avons mis en évidence que la latence du signal EEG augmentait de manière linéaire durant la période de stimulation tactile répétée de chaque doigt. Ces modifications plastiques rapides de

l'activité du cortex somatosensoriel pourraient correspondre à une « signature corticale » unique et spécifique de la stimulation tactile de l'extrémité des doigts et pourraient permettre au cerveau de traiter en priorité de nouveaux stimuli en retardant le traitement sensoriel de l'information répétée et ainsi moins pertinente. De plus, nos résultats suggèrent que l'adaptation de la latence est un processus significatif qu'il faut considérer avec attention dans les protocoles impliquant une stimulation tactile répétée, et ce même lorsque le taux de répétition du stimulus est faible.

Pour finir, nous avons étudié dans de plus amples détails la plasticité liée à l'usage en concentrant nos investigations EEG sur l'homme. Alors que le concept de plasticité liée à l'usage est le plus souvent associé à la pratique soutenue et spécialisée d'une activité par des sujets experts, nous nous sommes intéressés à la plasticité du cortex sensorimoteur associée aux conditions non contraintes de la vie quotidienne. Pour ce faire, nous avons mesuré l'activité EEG en réponse à la stimulation tactile du pouce, de l'index et du majeur chez des utilisateurs adultes de smartphones à écran tactile et des non-utilisateurs (sujets restés fidèles à des téléphones d'ancienne génération, sans écran tactile). De plus, nous avons utilisé l'historique de la décharge de la batterie des smartphones pour en suivre l'utilisation faite par leur propriétaire. Ainsi, nous avons pu établir un lien entre l'activité sensorielle précédemment opérée sur le téléphone et le traitement cortical somatosensoriel associé aux doigts. Nous avons alors mis en évidence que les interactions répétées des doigts sur un écran tactile lisse ont provoqué un remodelage important du traitement cortical tactile chez les utilisateurs de smartphone. Nous avons en particulier observé que la plasticité liée à l'usage est un phénomène qui opère très rapidement en permettant d'actualiser quotidiennement la représentation corticale somatosensorielle du pouce, en particulier. Dans une dernière étude, nous nous sommes intéressés à l'empreinte corticale laissée dans le cerveau par le comportement sensoriel sur les écrans tactiles. Il ressort que différentes caractéristiques temporelles de l'expérience tactile et de l'usage de la main sur le smartphone sont fortement représentées à différentes étapes du traitement sensoriel tactile dans le cerveau des utilisateurs d'écran tactile.

Les investigations EEG présentées ici confirment que l'activité corticale du cerveau du primate adulte est intimement liée à la notion de plasticité, que ce soit dans les expériences sensorielles quotidiennes ou après une lésion cérébrale. Nous avons aussi confirmé que M1 n'est pas une structure purement motrice mais au contraire qu'elle est également impliquée dans le traitement somatosensoriel chez les primates.

Preamble

The present manuscript summarises the work I have carried out during my PhD thesis in the laboratory of Professor Eric Rouiller at the University of Fribourg, from March 2010 to September 2015. I assembled texts from peer-reviewed published articles for which I wrote most of the text (**Chapter 1** and French review in **Chapter 6**) and/or contributed substantially to the study design and data collection (**Chapters 1** and **6**), a submitted paper (**Chapter 7**), and other chapters that are still not so completely achieved but that may result, in a more condensed form, in future publications as well (**Chapters 2 to 5**), explaining why some repetitions may occur as the text progresses. Finally, four other peer-reviewed published articles reporting studies which I took part in as well are compiled in the **Appendixes**.

Each chapter of the main text is connected either to one or to both of the central themes of my thesis, namely the electroencephalography (EEG) and the plasticity of the sensorimotor system in primates. I have gathered the methodological parts that were common to several chapters together in the **Chapter General Materials and Methods**, unless an entire chapter was specifically devoted to a particular methodological aspect.

The **General Introduction** and the **Chapter General Materials and Methods** are presented first. Then the results are divided into 7 chapters, followed by the transcription of a public conference I hold, followed by a **General Discussion**, and finally the **Appendixes**.

The **Chapter 1** describes the methodology of scalp EEG recordings in macaque monkeys following an electrical peripheral stimulation. This constitutes a general introduction to the methodology used throughout the **Chapters 2** to **4** dealing EEG recordings in macaque monkeys specifically. We also put a special emphasis on evaluating the impact of a craniotomy on brain potentials recorded at the scalp. This work was published in *Brain Structure and Function* in 2014. This study was already initiated as I was a Master student in the laboratory of Prof. E. Rouiller.

The **Chapter 2** is focused on evaluating the impacts of a motor cortical lesion on brain activities elicited by an electrical peripheral stimulation, by using EEG in one macaque monkey.

At the time I started my PhD project, we intended to measure the brain activity evoked by an electrical stimulation delivered to peripheral nerves in macaque monkeys to investigate the effects of a cortical lesion on brain activity and to follow the subsequent brain reorganisation. Nevertheless, even though the convenience of this technique, the electrical stimulation of large peripheral mixed nerves presents several drawbacks. Consequently, we improved our study design by adding EEG recording of brain activity elicited by a more naturalistic stimulation. These results are presented in **Chapter 3**, exploring still in the same animal the impacts of the cortical lesion on brain activity elicited now by delivering a peripheral tactile stimulation to the fingertips, with the advantage to activate specific classes of mechanoreceptors and therefore to selectively engage some afferent fibres.

The **Chapter 4** shows how a repeated peripheral stimulation (either tactile or electrical) can lead to adaptation in cortical activity assessed by scalp EEG, both in the time domain, which was really surprising, and in the amplitude domain, which was more expected.

The **Chapter 5** is again a more methodological section describing a behavioural task implemented to evaluate the integrity of the sensorimotor system in macaque monkeys. This chapter does not directly relate to EEG recording but it deals with interesting behavioural observations that may complement electrophysiological information in order to go deeper in our understanding of mechanisms underlying the brain reorganisation following a focal and permanent cortical lesion in macaque monkeys.

The **Chapter 6** presents the results of an EEG study conducted in human in collaboration with Dr Arko Ghosh (University of Zürich and ETH Zürich). We were here interested to investigate the plasticity of the sensorimotor cortex in relation to the use of touchscreen smartphones. These results were published originally in *Current Biology* in 2015. A short French review about the same topic was published in *Médecine/sciences* as well in 2015 and is also included here.

The **Chapter 7** is the direct continuation of the study presented in **Chapter 6**. Here we investigated in greater detail how the touchscreen behavioural statistics are imprinted through the different stages of sensory processing in the cerebral cortex. This paper has been submitted for publication in the *Annals of Neurology*.

Finally, the **Chapter 8** is the written and refined version of a public conference I hold about the use of non-human primates in scientific research, and more specifically in Neuroscience. I found important to integrate some ethical aspects about animal research in the present manuscript because the achievement of my PhD project would never have been possible without the invaluable contribution of some macaque monkeys.

15th June 2015 Anne-Dominique Gindrat

GENERAL INTRODUCTION

General context

This PhD thesis comes within the scope of research already initiated from many years in the laboratory of Prof. Eric Rouiller to document the mechanisms of functional recovery of manual dexterity (both time course and extent) following a lesion affecting the corticospinal system. To this end, an adult macaque monkey model of cervical spinal cord lesion (Beaud et al., 2008; Beaud et al., 2012; Freund et al., 2006; Freund et al., 2007; Freund et al., 2009; Hoogewoud et al., 2013; Schmidlin et al., 2004; Schmidlin et al., 2005; Wannier et al., 2005; Wannier-Morino et al., 2008), and an adult macaque monkey model of motor cortex lesion (Bashir et al., 2012; Hamadjida et al., 2012; Hoogewoud et al., 2013; Kaeser et al., 2010; Kaeser et al., 2011; Liu and Rouiller, 1999; Peuser et al., 2011; Rouiller and Olivier, 2004; Wyss et al., 2013) were developed, the ultimate goal being to transpose findings obtained in the non-human primate model to human patients suffering a spinal cord injury or a stroke, for instance. In particular, the major ongoing area of research is now about unravelling the mechanisms of cortical reorganisation within the brain, underlying functional recovery of hand sensorimotor control after a permanent focal lesion of the hand representation in the primary motor cortex (M1). To investigate this topic, several approaches have been developed:

The first experimental front deals with testing different therapeutic approaches: the therapeutic strategy *anti-Nogo-A*, already proven to be efficient on the rodent model (Schwab, 2004) and aiming at improving the functional recovery of manual dexterity following a lesion in the central nervous system (CNS), was tested and validated on spinal cord injured monkeys as well (Freund et al., 2006; Freund et al., 2007; Freund et al., 2009) and ongoing investigations are performed to test its safety and effectiveness on macaque monkeys subjected to a motor cortex lesion (Hamadjida et al., 2012; Wyss et al., 2013) (see **Chapter 8** for greater detail). In parallel, another therapy based on grafting autologous adult neural progenitor cells has been developed (Brunet et al., 2005; Kaeser, 2010; Kaeser et al., 2011) and experiments are still in progress to test its safety and effectiveness on a parkinsonian macaque monkey model, among others.

A second experimental approach, presented in **Chapters 1-4** of this PhD thesis, was to develop non-invasive measurements of brain activity in macaque monkeys by using electroencephalogram (EEG), in order to investigate the post-lesion cortical reorganisation within the brain repeatedly and over the long-term.

In addition, several behavioural tasks challenging fine manual dexterity, in particular the precision grip, were developed to precisely characterise functional deficits after the CNS lesion (Chatagny et al., 2013; Kaeser et al., 2014; Schmidlin et al., 2011).

In parallel with experiments on non-human primates, another ongoing area of research has been developed in collaboration with Dr Arko Ghosh (University of Zürich and ETH Zürich). Essentially, we are interested in studying how use-dependent plasticity of the brain is implemented in human daily life. To this end, EEG experiments were and are conducted on smartphone users and nonusers(see **Chapters 6** and **7**).

Electroencephalography

The human's fascination for the brain and its mysteries, on the one hand, and the increasing prevalence of neurological disorders (see for instance the Swiss Health Statistics 2014[1] or the Health statistics from WHO[2]) and their associated devastating aftereffects, on the other hand, have motivated the development of innovative technologies and their subsequent improvements to investigate the functioning of the brain and monitor its activity (**Figure 1**). These techniques are not only relevant for medicine to detect neurological disorders, but also to study the normal functions of the brain. The brain monitoring methods currently used in human and in animal models have each their own advantages and limitations (see e.g. Boas and Dunn, 2010; Buzsáki, 2006; Logothetis, 2008; Small and Heeger, 2013; Taulu et al., 2014).

[1] http://www.bfs.admin.ch/bfs/portal/fr/index/news/publikationen.html?publicationID=%205766
[2] http://www.who.int/healthinfo/global_burden_disease/estimates/en/index2.html

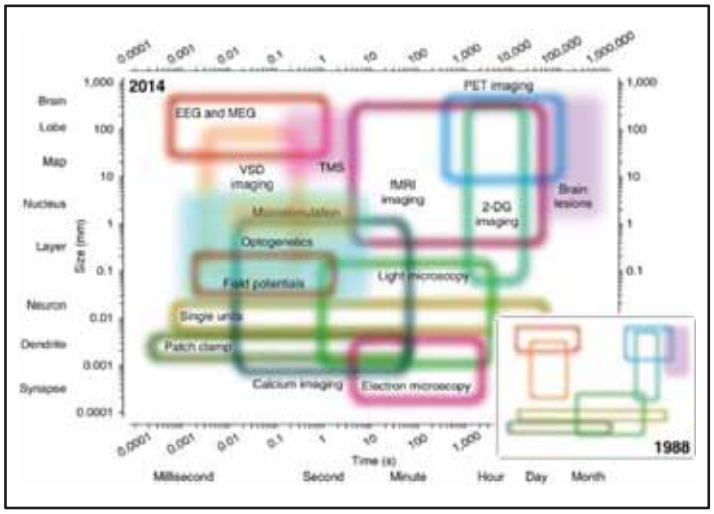

Figure 1: Biological data in Neuroscience span over a wide range of temporal (x-axis) and spatial (y-axis) scales and are optimally collected by brain imaging techniques with specific temporal and spatial resolutions. Note the very submilisecond resolution of EEG, counterbalanced by a low spatial resolution. There has been a tremendous development in brain imaging technologies in the last decades. For comparison, the state in 1988 is depicted on the lower right corner. Open rectangles show measurement techniques and filled rectangles represent perturbation techniques. VSD, voltage-sensitive dye; TMS, transcranial magnetic stimulation; 2-DG, 2-deoxyglucose (from Sejnowski et al., 2014).

The electroencephalography is a technique for recording the neural electrical activity of the brain by using electrodes. In particular, recording the *spontaneous* electrical activity of the brain is defined as an electroencephalogram or EEG (Berger, 1929). Populations of neurons in the superficial layers of the cortex generate electrical impulses fluctuating rhythmically according to different patterns (Lopes da Silva, 2011a). When derived non-invasively at the scalp, the field potential at each electrode (voltage difference with the reference electrode, in the order of μV) is the spatiotemporally smoothed version of the local field potential (LFP) generated by the electrical activity from neuronal populations in deeper cortical layers and then integrated over an area of about 10 cm^2 (Buzsáki, 2006; Buzsáki et al., 2012). The EEG activity is not directly linked to the spiking patterns of the individual neurons generating it because of the smearing effects of the successive tissue layers between the current generator and the recording electrode at the scalp (Nunez, 1998; Nunez, 2000) (see below the section *The brain as a volume-conductor*). Nevertheless, the use of high-density EEG caps associated with source-localisation techniques allow to remedy partially these volume-conduction effects and greatly improve the spatial resolution of EEG (see below the section *Electrical neuroimaging*) (Brandeis et al., 2009; Buzsáki et al., 2012; Michel et al., 2004b; Michel and He, 2011). These concepts will be developed in the following paragraphs.

EEG has several great advantages over the other brain imaging techniques. The first one is to provide a direct, real-time monitoring of neuronal activity at the scalp, not a correlate of it, by non-invasively directly detecting the electrical activity of the neurons within the brain. For comparison, the functional magnetic resonance imaging (fMRI), the positron emission tomography (PET) or the single-photon emission computerised tomography (SPECT) all detect the haemodynamic response and hence metabolic changes resulting from the brain activity and not changes in brain activity itself (Bear et al., 2007; Kayser and Logothetis, 2013; Purves et al., 2008; Small and Heeger, 2013). A second invaluable advantage of this technique is its high temporal resolution (in the order of the millisecond) able to resolve the fast changes of neuronal activity and therefore to document the dynamic processes taking place within the brain, contrary to fMRI, PET of SPECT (Jurcak et al., 2007; Michel and Murray, 2012; Nunez, 1993). Third, when recorded at the scalp, EEG is a completely non-invasive, safe and painless procedure, allowing to investigate the same brain in a repeated manner. Fourth, EEG is much less expensive than magnetoencephalography (MEG) (Taulu et al., 2014), fMRI, PET or SPECT. Fifth, as compared to invasive procedures currently used in neurophysiology, such as intracortical microstimulation (ICMS) or Laser Speckle Imaging (LSI) (see **Appendix 1**), EEG recorded at the scalp with a high density of electrodes is powerful to monitor the cortical activity of the whole brain, meaning that investigations are not restricted over a small brain region. Last but not least, EEG has proven to be a powerful diagnostic tool, for instance to localise an epileptic focus (Brodbeck et al., 2009; Brodbeck et al., 2010; Brodbeck et al., 2011; Michel et al., 2004a; Michel and Murray, 2012; Sperli et al., 2006).

The evoked potential (EP) recording is another powerful, non-invasive method to investigate the whole brain activity. This tool, corresponding to time-locked voltage fluctuations derived from the ongoing EEG signal in response to a specific peripheral sensory (Lopes da Silva, 2011b), will be discussed in greater detail below.

The pioneers of electroencephalography[3]

The first measurements of both spontaneous and evoked brain electrical activity were very likely accomplished by Richard Caton (1842-1926) (**Figure 2A**), a physician from

[3] For an extensive and illustrated historical review from the birth of EEG until 1960, see Grass (Grass, 1984).

Liverpool, from the brains of rabbits and monkeys, by using a galvanometer and two electrodes at the scalp (Caton, 1875; Caton, 1887; for historical reviews, see Brazier, 1963; Cohen of Birkenhead, 1959; Haas, 2003; Niedermeyer and Schomer, 2011; and Ormerod, 2006). More specifically, Caton noticed that the spontaneous electrical activity of the rabbit's and monkey's brains was changing in response to visual stimulation (Caton, 1875; Caton, 1887). Strictly speaking, this was not EEG yet because the recorded activity was projected on the wall and not written as "*graphein*" means. Nevertheless, these first observations constitute a milestone in the birth of electroencephalography.

From 1924, Hans Berger (1873-1941) (**Figure 2B**), a German neuropsychiatrist, developed an electroencephalograph, an instrument with which he measured and recorded the first spontaneous human EEG activity, first from patients with large skull defects, then from healthy people (**Figure 2C, D**) (Berger, 1929; for historical reviews, see Haas, 2003; Millett, 2001; and Niedermeyer and Schomer, 2011). From then on, the term *electro-* (registration of brain electrical activities) *encephalo-* (emitting the signals from the head) *gram* (drawing or writing) was proposed to describe the electrical neural activity of the brain. Interestingly, he reported that photic stimulation generated small potentials in the occipital region ("the driving response") and that potentials could be evoked by auditory stimulation during sleep (K-complexes) (Berger, 1930). At the time, the development of EEG to record brain activity represented a breakthrough by providing a new neurological and psychiatric diagnostic tool and the contribution of these EEG pioneers is still of prime importance nowadays because EEG is still one of the most widely used tools to investigate the brain electrical activity.

Figure 2 (next page): The fathers of electroencephalography. (A) Richard Caton (from Brazier, 1963). (B) Hans Berger (from Millett, 2001). (C) EEG recorded on Klaus Berger, 16 years old, Hans Berger's son. First line: scalp EEG, bipolar recording with fronto-occipital subcutaneous needle electrodes, second line: ECG, third line: time scale (10 cycles/s sine wave) (from Berger, 1929). (D) Berger's subject with pad EEG electrodes on the scalp (from Grass, 1984) (E) George D. Dawson. (F) Averaged evoked response (below) by the overtrace method from the 55 individual traces superimposed (above) after electrical stimulation of the left ulnar nerve at the wrist, bipolar electrode montage (left side). As a control, the averaging of 55 traces of the calibration pulse (5 μv) is shown on the right. Time scale: 20 ms. (E and F from Merton and Morton, 1984).

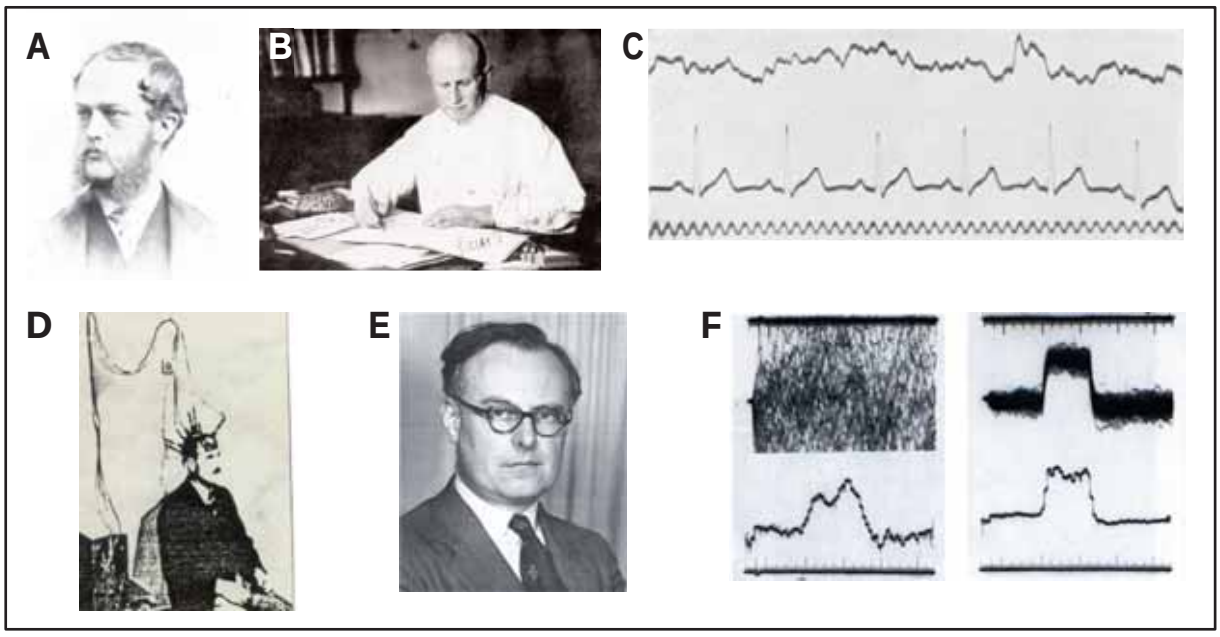

The related fields of EEG developed in parallel with the EEG as well. In particular, EP recording was used to map several cortical areas in response to sensory stimulation in animals. For instance, Frederic Bremer (1892-1982) located precisely the auditory cortex of cats using two cotton electrodes and clicks as auditory stimuli (Bremer and Dow, 1939). Then, Edgar Douglas Adrian (1889-1977) confirmed Berger's observations (Adrian and Matthews, 1934) and mapped the "somatic receiving area", i.e. the somatosensory cortex, in several mammals by recording brain activity with electrodes placed on the surface of the cortex or with intracortical electrodes, in response to mechanical stimulations of the skin and pressure receptors (Adrian, 1941). By using peripheral stimulations and recordings at the scalp, Marshall et al. (1941; 1937) were able to map the somatosensory cortex in cats and monkeys.

Subsequently, George D. Dawson (1912-1983) (**Figure 2E**) applied the technique of EP recording to human patients suffering from myoclonus (Dawson, 1947b; Dawson, 1950) and to healthy human subjects (Dawson, 1947a; Dawson, 1950). Later on, Dawson contributed to one of the most important advances in EP recording: by measuring brain activity after electrical stimulation of the ulnar nerve, he realised the urgent need to solve the signal-to-noise issue inherent to EP recording. To this end, he established the first summation and averaging method, namely the responses evoked by each repetitive stimulus were displayed on an oscilloscope and superimposed on a photographic film. In

this way, the time-locked brain activity resulted in an overexposure in one portion of the film whereas random activity only lightly exposed all of the film (**Figure 2F**). This photographic *overtrace method* allowed thus suppressing spontaneous nonrelated potentials while extracting the low-amplitude "significant phases of the response" evoked by the stimulation (Dawson, 1951; Dawson, 1954; for reviews, see Desmedt, 1987; Erwin et al., 1987; and Niedermeyer and Schomer, 2011). Due to this major impact on the field, George D. Dawson is usually considered as the father of EP studies. From then on, the EP technique developed, improved and became an independent field of electrophysiology. In particular, the averaging method was afterward further improved to lead to the current digital computerised averaging methods that permit the averaging of multiple responses, and the old galvanometers were progressively replaced by highly sensitive amplifiers (for reviews, see Desmedt, 1987; and Niedermeyer and Schomer, 2011). Since then, the measurement of EPs has become widely employed in human clinics, for instance to non-invasively assess the processing integrity in sensory systems (Nuwer et al., 1992; Nuwer, 1998; Nuwer et al., 2012), and EP recording is now an increasingly popular neuroscientific tool as well (see e.g. Andrew et al., 2014; Zeller et al., 2014).

The brain as a volume-conductor

The volume-conduction or electrical spread is defined as the passage of an electrical current through a conducting substance (Fisch, 2011). ln electroencephalography more specifically, the brain can be considered as a volume-conductor, meaning that each ionic current produced locally through the membrane of an active neuron generates then an electrical field in the surrounding medium (Buzsáki et al., 2012; Nunez and Srinivasan, 2006). Current dipoles are generated in individual neurons, resulting in ohmic return currents flowing through the surrounding area. The EEG electrodes at the scalp surface capture then the differences in potential of the return currents (for a more biophysics-oriented review, see Buzsáki et al., 2012; Westbrook, 2013; Wolters and Munck, 2007).

To elaborate, it is now accepted that the high-frequency electrical activity in single cells, such as action potentials, is largely filtered out by the brain tissues and therefore does not contribute to the EEG signal at the scalp. Conversely, the EEG activity mainly results from slower-frequency voltage fluctuations across cell membranes, such as the summated effects of many excitatory postsynaptic potentials (EPSPs) and inhibitory postsynap-

tic potentials (IPSPs) upon pyramidal cells (Gloor, 1985; Pascual-Marqui et al., 2009; Speckmann et al., 2011; Westbrook, 2013). Indeed, the EEG signal derived at the scalp reflects predominantly the synchronous activity of populations of cortical neurons close to the scalp electrodes, i.e. the pyramidal cells, meaning that deep brain structures do not largely contribute to the scalp EEG (Buzsáki, 2006). The pyramidal cells constitute the main projection neurons in the cerebral cortex; they are oriented perpendicularly to the cortical surface and many synapses are formed with their dendrites.

The activation of an excitatory synapse (EPSP) on the apical dendrite of a pyramidal neuron, in layers II and III, by a contralateral cortical afferent axon (**Figure 3A** and **C**) causes an inward flow of cations into the dendrite at the synaptic site where the EPSP is generated, resulting in the formation of a current sink. This current flows then down the dendrite and crosses the membrane to go back in the extracellular space, forming a loop. This creates at this site a current source. If an extracellular electrode is placed at the current sink, near the site of EPSP generation, current flowing away from the electrode into the intracellular space will be detected and recorded as a negative deflection. On the contrary, if an extracellular electrode is inserted close to the current source, near the cell body, a positive deflection will be recorded, as a result of current flowing out of the cell towards the electrode.

The activity of pyramidal neurons is mainly influenced and synchronised by subcortical inputs, particularly from the thalamus and from the high brainstem reticular formation (Westbrook, 2013). In the case of excitatory (EPSP) thalamocortical afferent axons, giving rise to synapses on the proximal dendrites in layers IV and V (**Figure 3B**), current flows are reversed as compared to the case of contralateral cortical afferent axons, where the synapses are established with the distal dendrite: an extracellular electrode inserted superficially will record a positive deflection as current flows out of the cell towards the electrode. Conversely, an electrode inserted deeply will show a negative deflection as current flows away from the electrode into the intracellular space. IPSP in deeper layers results in a negative scalp potential in the same manner as EPSP in superficial layers, because the EEG surface electrode is close to the current sink. On the other hand, IPSP in superficial layers appears as a positive scalp potential like EPSP in deeper layers because the EEG surface electrode is near the current source. As a consequence, it

is not possible to distinguish between such cortical synaptic potentials unambiguously using only EEG signals.

At the larger population level, when neurons are synchronously activated, the longitudinal (parallel to the elongated apical dendrites) components of the current flows add each other, while their transverse components cancel each other, resulting in a laminar current along the main axis of the pyramidal neurons (Lopes da Silva, 2011a; Lopes da Silva, 2013).

To sum up, the location of the synaptic activity in the cortex determines the polarity of the EEG scalp signals (**Figure 3B** and **C**) (Gloor, 1985). The cortical electrical activity captured by scalp electrodes consists of slow, simultaneous, summated EPSP and IPSP generated by large populations of pyramidal cells (Gloor, 1985). Note that the amplitude of the EEG signal recorded at the scalp depends on both the strength of individual current dipole and the temporal synchronisation of their activity (Gloor, 1985; Musall et al., 2014; Nunez and Srinivasan, 2006).

Figure 3 (next page) : (A) Current flow generated by an EPSP from a contralateral cortical afferent axon on the distal dendrite of a pyramidal neuron in the cerebral cortex. The electrical activity is recorded from 4 electrodes: superficial intracellular (1) and extracellular (2) electrodes located near the EPSP generation site, and deeper extracellular (3) and intracellular (4) electrodes located near the cell body. Current flows from the extra- to the intracellular space at the EPSP generation site (current sink), flows down the dendrite and goes out of the cell, so as to form a current loop (current source). The potentials recorded from each electrode are represented: both intracellular electrodes record potentials with the same polarity whereas potentials of both extracellular electrodes display opposite polarities. Ra, Rm and Re refer to the cytoplasmic, membranar and extracellular resistances, respectively. (B) and (C) The location of the synaptic activity in the cortex determines the polarity of the EEG scalp signals. (B) When excitatory thalamocortical afferent axons do synapse with proximal dendrites in layers IV and V, a positive deflection is recorded at the surface of the scalp because the EEG surface electrode is located near the current source. (C) When excitatory contralateral cortical afferent axons do synapse with distal dendrites in layers II and III, a negative deflection is observed at the scalp as the EEG electrodes are near the current sink (from Holmes and Khazipov, 2007, p. 30-31; Westbrook, 2013, p. 1122-1123).

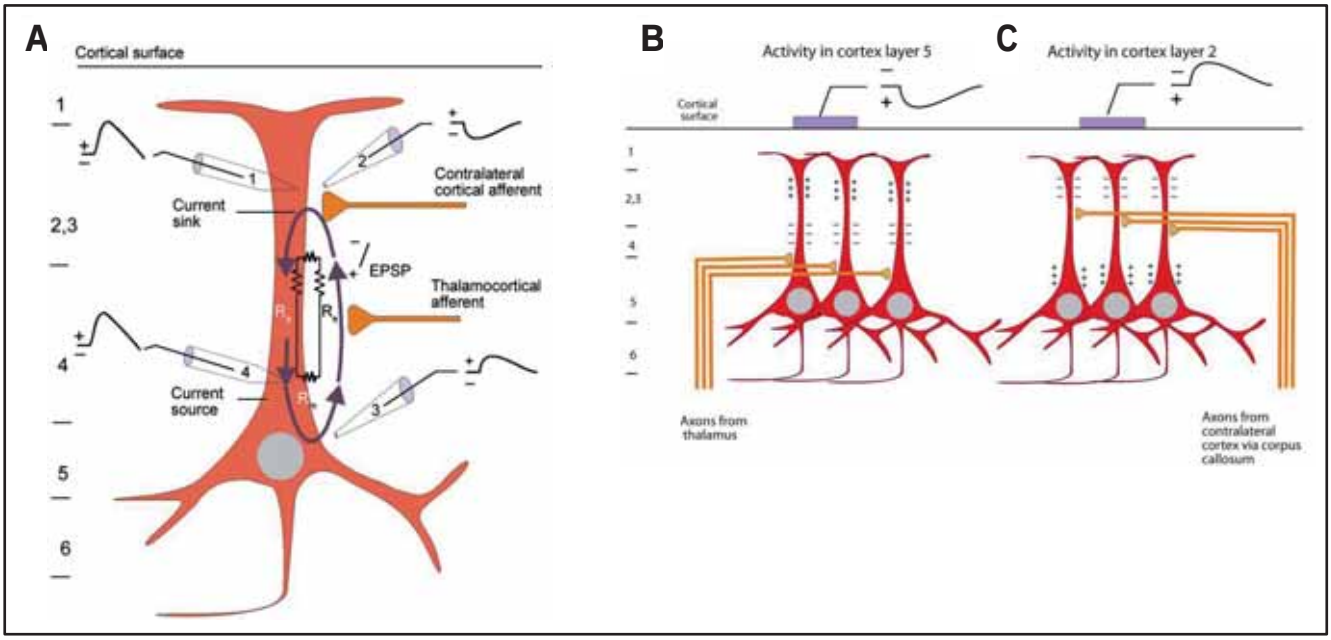

As a matter of fact, because the electrical activity originates from neurons in the underlying brain tissue, the EEG signal captured at the scalp strongly depends on the orientation and distance between the neuronal generator and the recording electrodes. More specifically, the convolutional organisation of the brain induces different configurations of electrical fields recorded at the scalp (Gloor, 1985). Within the neocortex, pyramidal neurons are organised into columns perpendicular to the cortical surface (Amaral and Strick, 2013; Mountcastle, 1997; Powell and Mountcastle, 1959b; Szentáigothai, 1983), i.e. with the apical dendrites parallel to each other and at the same time perpendicular to the cortical surface. These assemblies of neurons of sufficient size constitute spatially-organised functional entities that can be synchronously activated such that the resulting electrical field may be captured at some distance, such as from the scalp (Lopes da Silva, 2011a; Lopes da Silva, 2013). The populations of vertically oriented pyramidal cells constitute then sheets of electrical dipoles that are parallel to the cortical surface: these dipole sheet layers have uniform and opposite voltage polarities and only one polarity (one side of the dipole layer) is captured at the scalp surface (Fisch, 2011; Gloor, 1985). This corresponds to radial dipoles (at 90°) to the scalp. Conversely, the populations of pyramidal cells in the walls of the sulci are horizontally oriented with regard to the scalp surface (i.e. parallel to the scalp) with their dipole layers now perpendicular to the scalp surface, corresponding to a tangential dipole to the scalp surface (both ends of the dipole are captured by scalp electrodes). Such configuration of tangential dipoles contrib-

utes only few to the EEG signal at the scalp because they do not strongly project negativity or positivity to the scalp surface. Furthermore, dipole layers located in the walls of sulci facing each other tend to mutually cancel at the scalp surface (**Figure 4**). In sum, the EEG field is differentially sensitive to both tangential and radial components of dipolar sources.

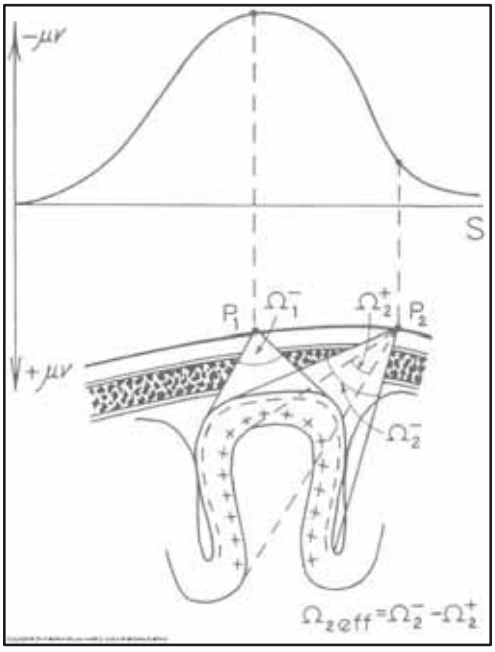

Figure 4 : Example of volume-conduction for a cortical source generating synchronous activity located in the crown of a gyrus and its two sides. The curve S represents the distribution of the voltage magnitude reaching the scalp surface. The amount of current captured by a scalp electrode (P_1 or P_2 here) from the cortical source corresponds to the area between the lines originating at the cortex and converging on the corresponding electrode. P_1, located at the top of the gyrus convexity, captures only the negative side of the dipole layer in the crown of the gyrus and its sides (Ω_1^-). For P_2, located laterally to the gyrus convexity, the source projects both negativity from the outer surface of the cortex (Ω_2^-) and positivity (Ω_2^+) from the inner vertical part of cortex (corresponds to the area between the dashed lines converging to P_2). Currents from the inner cortex and the outer cortex cancelled each other (the positivity -area within the dashed lines- subtracted from the negativity - area within the solid lines converging on P_2), resulting in a reduced voltage of the signal captured by P_2 ($\Omega_{2\ eff}$) as compared to P_1 (see curve S). The potential profile (S) is therefore bell-shaped. Actually, the scheme should be considered in 3D space with the lines originating from the cortex to electrodes representing the sides of approximately conical spaces. The amount of current measured at P_1 and P_2 should be therefore a volume Ω and not an area (from Fisch, 2011; Gloor, 1985).

The volume-conductive properties of the brain, i.e. the passive resistive process by which the amplitude of an extracellular potential decreases according to the increasing distance from the active neuronal membrane (Holsheimer and Feenstra, 1977), mean that the activity of neurons can still be detected quite far from their membrane and therefore that the activity of given neurons can be picked up by several electrodes. The EEG technique takes advantage of this property of the brain by measuring at the scalp

the electrical open field (i.e. detected at some distance from the neuronal sources (Lopes da Silva, 2013)) from neuronal populations located quite far from the recording electrodes, corresponding therefore to the summed activity of neuronal populations. Nevertheless, the potentials generated within the brain are further blurred and distorted by going through several filtering and attenuating biological layers (cortical layers, blood vessels, meninges, cerebrospinal fluid, skull, muscles, skin) (Flemming et al., 2005; Lopes da Silva, 2011a; Lopes da Silva, 2013; van den Broek et al., 1998; Westbrook, 2013), each of them with specific properties of electrical propagation, electrical resistance and complex geometry, before being picked up by scalp electrodes. As a result, the amplitude of EEG signals at the scalp (in μV) is much smaller than the voltage changes occurring in a single neuron (in mV). In EEG signals with frequency below 1000 Hz, one can reasonably neglect the capacitive component of tissue impedance, the inductive effect and the electromagnetic propagation effect without inducing errors (Wolters and Munck, 2007). It results that the transmission of brain activity through the different biological tissues depends only on their conductivity and can be described with the quasi-static Maxwell equations (de Munck and, 1991; Plonsey and Heppner, 1967; Sarvas, 1987). In sum, volume-conduction causes blurring and attenuation of the effect of the neural generators at the scalp surface, decreasing the EEG spatial resolution.

For a long time, EEG has been commonly used as a diagnostic tool and nowadays a further step has been achieved with the use of electrical source imaging based on inverse solution methods. In both cases, it is mandatory to know if a given change in EEG signal comes from a modification in brain activity itself or alternatively if that change merely reflects volume-conduction effects, such as the anisotropy of the skull, the one of the white matter, a change in skull conductivity following a craniotomy, a brain lesion, or the presence of fluid-filled compartments (van den Broek et al., 1998). This serious issue has often been underestimated and resulted in massive errors in source localisation because the head models used did not include the relevant features, for instance (Aydin et al., 2014; Benar and Gotman, 2002; Chauveau et al., 2004; Vanrumste et al., 2000).

Actually there is still some uncertainty concerning the influence of volume-conduction effects on scalp EEG. This means that there is still no perfect model of the head (forward problem) able to integrate realistically all the volume-conduction properties of the brain

but progresses are ongoing (Hallez et al., 2007; Huiskamp et al., 1999; Michel et al., 2004b; Wolters et al., 2004).

Electrical neuroimaging

A major problem in the interpretation of EEG signal is the impossibility to localise the generators uniquely on the basis of the potentials that are measured at the scalp. One possibility to overcome this situation is to use a high density of electrodes at the scalp to measure the EEG activity simultaneously at many locations (Brandeis et al., 2009; Buzsáki et al., 2012; Michel et al., 2004b; Michel and He, 2011). With several recording electrodes at the scalp, a map of the voltage changes in the brain can be then constructed. Finally, by using EEG inverse solution based on some assumptions, the underlying generators can be reconstructed by determining the relationship between the signals measured from the different locations (Michel et al., 2004b; Ryynanen et al., 2004; Ryynanen et al., 2006).

Understanding the relation between the generators in the brain and the activity measured at the scalp may be considered from two distinct points of view: either using a forward approach or an inverse approach. The *EEG forward problem* consists in computing the electrical field at the scalp generated by electrical sources within the brain by modeling the volume-conduction properties of the head (using realistic head models and applying actual values of skull-to-brain resistivity ratios) (Hallez et al., 2007; Pascual-Marqui et al., 2009).

Conversely, the *EEG inverse problem* aims at reconstructing the electrical sources within the brain from the EEG signals measured over the scalp (Grave de Peralta et al., 2009; Lopes da Silva, 2011a; Michel and Brandeis, 2009; Pascual-Marqui, 1999; Pascual-Marqui et al., 2009; Spinelli et al., 2000) by using the model of field distribution of a current dipole in the given volume-conductor provided by the forward problem. To put it another way, it corresponds to the process of imaging the brain activity that generates the voltage distribution observed at the scalp. Nevertheless, as reviewed by Michel (2004b), there is an "*ambiguity of the underlying static electromagnetic inverse problem* (Helmholtz, 1853)", meaning that the EEG signals measured over the scalp do not indicate unambiguously the location of the generators because the inverse problem has an

unlimited number of solutions in case no constraints are used. The consequence is that a given distribution of potentials over the scalp can be actually generated by different source configurations within the brain (this problematics has been discussed by Fender, 1987). On the other hand, different topographies at the scalp obligatorily result from different sources within the brain. In sum, the maximal brain activity measured at a given electrode does not necessarily mean that the corresponding generator is located immediately under the electrode. Electrical source imaging, or electrical neuroimaging, applies inverse source estimation methods to EEG recorded with multiple electrodes arrayed across the whole scalp (Grave de Peralta Menendez et al., 2004; Michel et al., 2001; Michel et al., 2004b; Michel and He, 2011; Michel and Murray, 2012). As explained, several a priori assumptions about the intracerebral sources are required to solve this ambiguous problem in addition to modeling the head and especially determining the conductive properties of the different structures involved in the conduction of the EEG activity from the generator to the scalp electrodes (Michel et al., 2004b). Such electrical neuroimaging analyses are currently successfully used in clinics, for instance to localise the brain structures responsible for epileptic seizures (Brodbeck et al., 2009; Brodbeck et al., 2010; Brodbeck et al., 2011; Michel et al., 2004a; Michel and Murray, 2012; Sperli et al., 2006).

Evoked potentials

The evoked potentials (EPs) are the brief changes in EEG signals *evoked* by external peripheral stimulations (Lopes da Silva, 2011b). Essentially, in response to a peripheral or external stimulus, the resulting afferent sensory volley travels from the sensory receptor at the stimulation site to the cortex by being processed at each neuronal population level –the neural generators– along the involved afferent pathway and then further transmitted to the next relay (Aminoff and Eisen, 1998; Cruccu et al., 2008; Desmedt, 1987; Freye, 2005; Mauguière, 2011). As explained above, the synchronous activity at the level of neuronal populations results in current dipoles that can be measured with electrodes along the stimulated pathway, and especially at the scalp.

The brain activity generated in response to each individual stimulation is of very small amplitude (usually in the order of 1-30 μV) and is mixed up with the large-amplitude spontaneous activity of the brain (Freye, 2005; Mauguière and Fischer, 1990). To cir-

cumvent this inherent limitation, the stimulation is repeated many times so as to obtain a large number of EEG signals or *trials*, each of them being time-locked to one repetition of the stimulus. Then, in order to increase the signal-to-noise ratio and thus to reveal the brain activity specifically elicited by the stimulation, an averaging of the individual trials is performed, based on the method originally developed by Dawson (Dawson, 1951; Dawson, 1954). Simply put, responses are added up each other in such a way that those generated synchronously with the stimulation are amplified (Desmedt, 1987; Mauguière and Fischer, 1990). Conversely, randomly generated spontaneous signals are not time-locked to the stimulus and cancel out each other due to their variable polarity. An EP corresponds therefore to the brain activity that is precisely time-locked to the stimulation. The resulting EP is a waveform containing several successive peaks or components and troughs or valleys, each of these components being characterised by specific amplitude (represents the extent of neural activity), latency (represents the timing of activation) and scalp distribution (represents the pattern of the voltage gradient of a component at the scalp at any time point) that reflect the activity of a given neural generator along the afferent pathway (Sanei and Chambers, 2007).

Depending on the modality of the peripheral or external stimulation, one can distinguish between somatosensory evoked potentials (SSEPs) (see below), auditory evoked potentials (AEPs) including brainstem auditory evoked potentials (BAEPs) if the very early components are considered (Celesia, 2011), visual evoked potentials (VEPs) (Celesia and Peachey, 2011), pain- and laser-evoked potentials (LEPs) (Treede, 2005), and motor evoked potentials (MEPs) (Legatt et al., 2011), among others.

In human clinics, the different modalities of EPs are relevant to assess the integrity of sensory processes in real time. Simply put, the presence of lesions in a specific relay along the stimulated pathway can be inferred from the absence or alteration of the corresponding component, sometimes associated with delays of subsequent waves as well (Starr, 1978; Tandon, 1998). Even though this tool tends to be supplanted nowadays by functional imaging, EPs have proven to be highly relevant to diagnose some neurological disorders, such as nerve conduction impairments (Lascano et al., 2009; for reviews, see Michel and Murray, 2012; Morizot-Koutlidis et al., 2015; Sand et al., 2013), to predict outcome and disabilities such as in comatose patients (Carter and Butt, 2001; Carter and Butt, 2005; for a review, see Sand et al., 2013; Tzovara et al., 2013) or in patients with

multiple sclerosis (Schlaeger et al., 2014), to perform intraoperative monitoring (Korn et al., 2015; for reviews, see Freye, 2005; Nitzschke et al., 2012; and Nuwer et al., 2012; Nwachuku et al., 2015; Stecker, 2012; Tamkus et al., 2015), or to obtain a presurgical mapping of the cortex (Lascano et al., 2014), among others.

Somatosensory evoked potentials

The SSEPs are EEG signals, usually recorded from the scalp, that result from the sequential activation of neural structures along the somatosensory pathway from the peripheral receptors to the somatosensory cortex, in response to the repeated application of a peripheral somatosensory stimulation, either electrical (**Figure 5**) or mechanical (**Figure 6**) (Allison et al., 1991a; Aminoff and Eisen, 1998; Arezzo et al., 1979; Arezzo et al., 1981; Berger and Blum, 2007; Legatt, 2014; Mauguière et al., 1999; Mauguière, 2011). Electrical stimulations at bearable stimulation intensity are usually delivered on the skin over the trajectory of a peripheral nerve by using a bipolar transcutaneous stimulator, resulting in a small twitch in the muscles innervated by the stimulated nerve when the latter contains some motor fibres as well (i.e. mixed nerve, such as the median nerve) (Cruccu et al., 2008; Freye, 2005; Mauguière et al., 1999). SSEPs can be virtually elicited from any peripheral nerve, even though the median nerve and posterior tibial nerve are most commonly used in clinics (Mauguière et al., 1999). Mechanical stimulations can be delivered among others by using either solenoid tappers (see **Chapters 3** and **4** for greater detail), or pneumatic stimulators (Lascano et al., 2014; Wienbruch et al., 2006), or air-puff stimulators (**Figure 6**) (Hashimoto et al., 1989; Hashimoto et al., 2000), or moving coil vibrators (Pratt et al., 1979a; Pratt et al., 1979b; Pratt et al., 1980).

A peripheral stimulation at bearable stimulation intensity, as routinely used in clinics, activates the rapidly conducting, large myelinated fibres mediating touch and proprioception, but muscle afferents may be activated as well after posterior tibial nerve stimulation (Mauguière et al., 1999). Conversely, both electrical and mechanical stimulations virtually do not activate the small myelinated or unmyelinated afferent fibres mediating thermoreception and nociception, meaning that SSEPs are primarily mediated by the dorsal column-medial lemniscal tract, as confirmed by experiments on monkeys (Allison et al., 1991a; Cruccu et al., 2008; Cusick et al., 1979; Freye, 2005; Legatt and Benbadis, 2014; Sances et al., 1978; Toleikis, 2005).

However, nociceptive and thermoreceptive afferent fibres can be selectively stimulated by delivering brief heat pulses by means of a CO_2 laser beam applied to the skin surface, for instance (Kunde and Treede, 1993; Mauguière et al., 1999; Treede, 2005; Valeriani et al., 2000). These specific EPs are commonly called laser-evoked potentials or LEPs. More information about the activated fibres in response to electrical and mechanical stimulations is provided in the *Discussion* of **Chapter 3**.

SSEP recordings are influenced by several factors, such as the consciousness level, the administration of drugs, the repetition rate of the stimulation, the stimulation amplitude, the body temperature, the age, gender and size of the subject, among others (for reviews, see Banoub et al., 2003; Mauguière et al., 1999; and Mauguière, 2011).

Cornerstone work in the field of SSEP recordings in monkeys was established by Truett Allison and collaborators from the 1980s. By measuring scalp EEG, epidural EEG, cortical-surface EEG and intracerebral activity on awake or anaesthetised macaque monkeys, either control animals or animals after removal of a specific brain region, they were able to locate the generators of median nerve SSEPs. Essentially, they found that the precentral potentials P10-N20 (**Figure 5**, left side), inverting through the central sulcus into the postcentral potentials N10-P20, were most probably generated by a tangential dipole in the posterior wall of the central sulcus, corresponding primarily to the area 3b. In addition, the potentials P12-N25, recorded near the CS, were proposed to originate from a radial generator in areas 1 and 2. Conversely, they excluded the presence of any generator in areas 3a and 4 (Allison et al., 1991b; McCarthy et al., 1991). Nevertheless, the role of M1 in the generation of N20-P20 and P22 (human components) SSEPs is under debate, some studies on human and monkeys reporting generators located in the area 4 (for a review, see Mauguière, 2011).

Importantly, Allison and collaborators also demonstrated that comparable median nerve SSEPs were obtained on macaque monkeys and human, fully justifying then translational studies using median nerve SSEP recordings on macaque monkeys as animal models, before transposing the results to human. To elaborate, they showed that early median nerve SSEPs (i.e. generated from the peripheral nerve to the primary somatosensory cortex (S1), and corresponding to human potentials with a latency shorter than 40 ms) measured in macaque monkeys were similar to the human SSEPs in terms of waveform, relative latency and topography. More specifically, the cortical SSEPs P10-N20, N10-20

and P12-N25 in macaque monkeys corresponded to human SSEPs P20-N30, N20-P30 and P25-N35, respectively (Allison et al., 1991a; Allison and Hume, 1981; McCarthy et al., 1991) (**Figure 5**). Nevertheless, as expected, the absolute latencies recorded in monkeys were about 10 ms shorter than the human's ones because of the shorter somatosensory pathways in monkeys than in human (Allison et al., 1991a; McCarthy et al., 1991). Based on these results, the authors therefore concluded that the same neuronal activity and voltage topography were present in both species (Allison et al., 1991a; Allison and Hume, 1981; McCarthy et al., 1991).

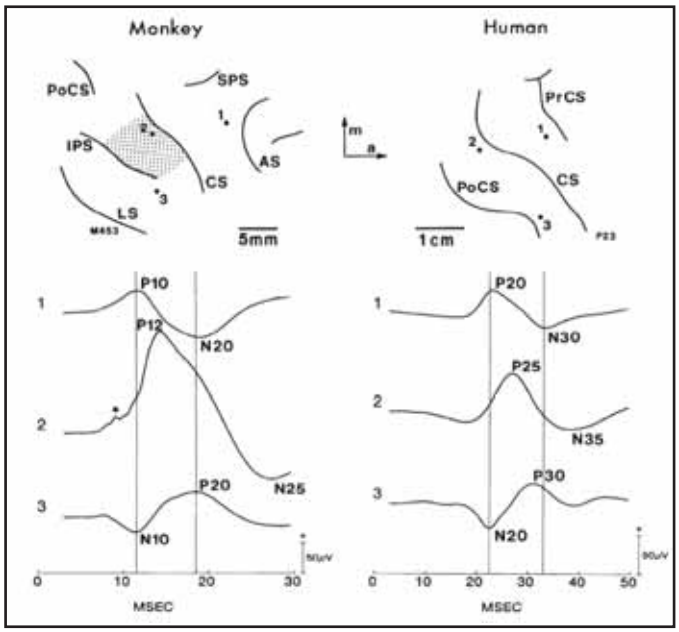

Figure 5: Comparison of SSEPs obtained after electrical stimulation of the left median nerve, in macaque monkey and in human, under similar stimulation and recording conditions. Cortical surface recordings were performed at three sites (precentral, pericentral and postcentral, respectively) on the right sensorimotor cortex in monkeys and human, both under anaesthesia. The gray zone on monkey's cortex represents the primary somatosensory cortex (S1) hand area. AS: arcuate sulcus, CS: central sulcus, IPS: intraparietal sulcus, LS: lateral sulcus, PrCS: precentral sulcus, PoCS: postcentral sulcus, SPS: superior precentral sulcus. The stimulus was delivered at 0 ms (from McCarthy et al., 1991).

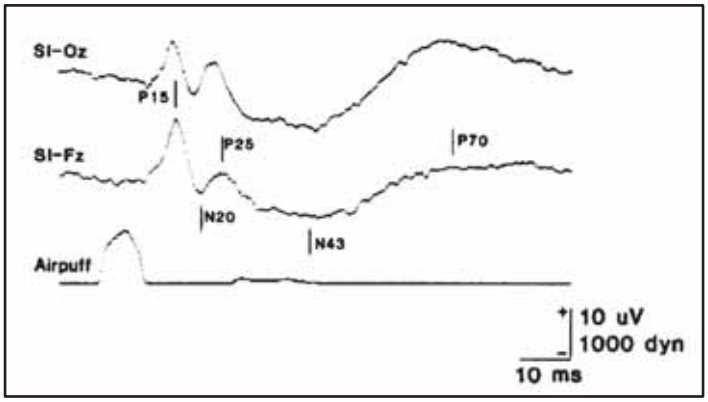

Figure 6: Cortical tactile SSEPs recorded in an awake macaque monkey from an epidural electrode over the contalateral area 1 in response to air-puff stimulation of the volar forearm. P15 was shown to originate from areas 3b and 1 and P25 from areas 3b, 1 and other posterior parietal cortical areas (from Gardner et al., 1984).

Somatosensory system[4]

In primates, the fine voluntary motor control from the hand depends on the integrity of the major afferent and efferent pathways of the cervical cord, namely the dorsal column-medial lemniscal system and the spinothalamic pathway for the afferent pathways and predominantly the corticospinal tract for the motor pathway. For instance, by manipulating a small object with the fingers, the brain is continuously flooded with many different tactile afferent inputs linked with the time course, the amplitude, the direction and the spatial distribution of the contact forces, the shapes and structure of the object being contacted as well as the frictions generated between the object and the fingers (Johansson and Flanagan, 2008; Johansson, 1991; Johansson et al., 1992; Johansson, 1998; Johansson, 2002; Johansson and Cole, 1992; Johansson and Flanagan, 2009a; Johansson and Flanagan, 2009b; Johansson and Flanagan, 2009c; Johansson and Westling, 1990; Johansson and Westling, 1991; Johansson, 1996; Macefield et al., 1996; Macefield and Johansson, 1996).

The somatosensory system is involved in processing sensory information from the skin or from organs and structures within the body. It provides information for instance about the location of a touch stimulus on a given body part or about the texture of an object being manipulated with the fingers. In addition to mediating such discriminative touch, the somatosensory system plays a role in vibration sense and proprioception. As a whole, the somatosensory system provides our ability to recognise objects, to discriminate textures, it gives sensorimotor feedback and plays a key role in social interactions as well (Abraira and Ginty, 2013; Keysers et al., 2010; McGlone et al., 2014).

In the next sections, we will present the somatosensory system, beginning from the skin and ending in the cerebral cortex.

Some definitions about somesthesic perceptions

The somatosensory system mediates several types of conscious somesthesic perceptions (Patestas and Gartner, 2013; Strominger et al., 2012).

[4] For a comprehensive description of mechanoreceptors, somatosensory pathways and somatosensory areas, see Darian-Smith (1984), Nieuwenhuys et al. (2007, chapter 16) and Gardner (Gardner and Johnson, 2013a; Gardner, 2010).

Depending on the mechanical stimuli applied on the body surface, two types of tactile sensations may be evoked, namely: (1) the nondiscriminative or crude touch, usually elicited by applying light strokes on the skin with hair or cotton. This sensation does not provide detailed information about the stimulus, and is considered as a poorly localised perception. (2) The discriminative or fine touch, namely the ability to localise and perceive the fine details of an object by palpation, such as its shape, size, and texture, even with closed eyes. This is also called stereognosis (perception of the three-dimensionality of an object). To put it another way, the discriminative touch corresponds to the ability to distinguish two stimuli separated in space, tested by using the so-called "two-point discrimination test" (Weber et al., 1996). This perception of spatial resolution strongly depends on the receptor density, as it will be discussed below.

In addition, tactile perception is linked to pressure sense from the body, and perception of vibration. This latter is usually tested by applying the stem of a vibrating tuning fork on a joint or other body parts.

Conscious proprioception is elicited by the mechanical displacement of muscles, ligaments, and joints and has several facets as well: (1) the static proprioception or static position sense, namely the awareness of position of body parts, especially joints; (2) the dynamic proprioception or kinesthetic sense, namely the awareness of body and limb movement, direction and balance (Patestas and Gartner, 2013; Strominger et al., 2012).

A *passive* tactile perception (*being touched*) is obtained by stimulating the inactive fingers or hand with an external stimulus (moving or static) while *active* tactile perception (*touching*) (Gibson, 1962), also known as haptic perception, haptics or tactile scanning, is defined as the sense through which we perceive our environment by actively exploring it with our body, especially the active exploration and manipulation of surfaces and objects by palpation with the hands (Ballesteros and Heller, 2008; Hollins, 2002). During environment exploration, exteroceptive inputs are generated by extracting relevant sensory information about texture and shape for further processing, in addition to proprioceptive inputs (Lederman et al., 1986; Lederman and Klatzky, 1987; Lederman and Klatzky, 1996). Movements of the hand are here exploratory and not performatory and induce changes in the stimulus itself, enhancing some features and decreasing some others. Passive touch relies only on the excitation of receptors in the skin and underlying tissues. Conversely, active touch includes additionally the excitation of joint and tendon

receptors, as well as continuous inputs from vestibular organs. Simply put, active touch involves the integration of inputs from the whole skeleto-muscular system (Ballesteros and Heller, 2008).

Peripheral receptors involved in tactile sensation

Discriminative touch is elicited by several kinds of mechanoreceptors (here receptors activated by the physical deformation or stretch of the skin) located in surface layers of the skin and subcutaneous tissue in body parts that actively contact objects, i.e. the glabrous skin of the hand and fingertips, the sole of the foot, the lips, the tongue and the oral mucosa (Johansson and Flanagan, 2009a). In human[5], the glabrous surface of the hand constitutes one of the most sensitive body parts (behind the lips and the tongue, see Sathian and Zangaladze, 1996; and Van Boven and Johnson, 1994), with about 20'000 mechanoreceptors, among them 2'000 on each fingertip (see for instance Pacinian corpuscles in **Figure 7E**) (Johansson and Flanagan, 2009b; Johansson and Vallbo, 1979b). The elastic properties of the skin make it actually a perfect sensory organ because objects then leave their print on it, allowing us to discriminate their size, shape and texture (Gardner, 2010).

The tactile mechanoreceptors are specialised exteroceptors (specialised receptors to detect sensory information from the external environment) associated with myelin-free, encapsulated nerve endings (Andres and von Düring, 1973; Cauna and Mannan, 1958; Chambers et al., 1972; Darian-Smith, 1984; Iggo and Andres, 1982; Iggo and Muir, 1969) (**Figure 7**) arising from large diameter, fast-conducting (Aβ), myelinated afferent neurons (Burgess and Perl, 1973) (**Table 1**). The transduction of mechanical stimulus into electrical activity takes place directly in these myelin-free nerve endings.

[5] The differences in tactile innervation of the fingertips between macaque monkeys and human (Paré et al., 2002) will be presented in **Chapter 4**.

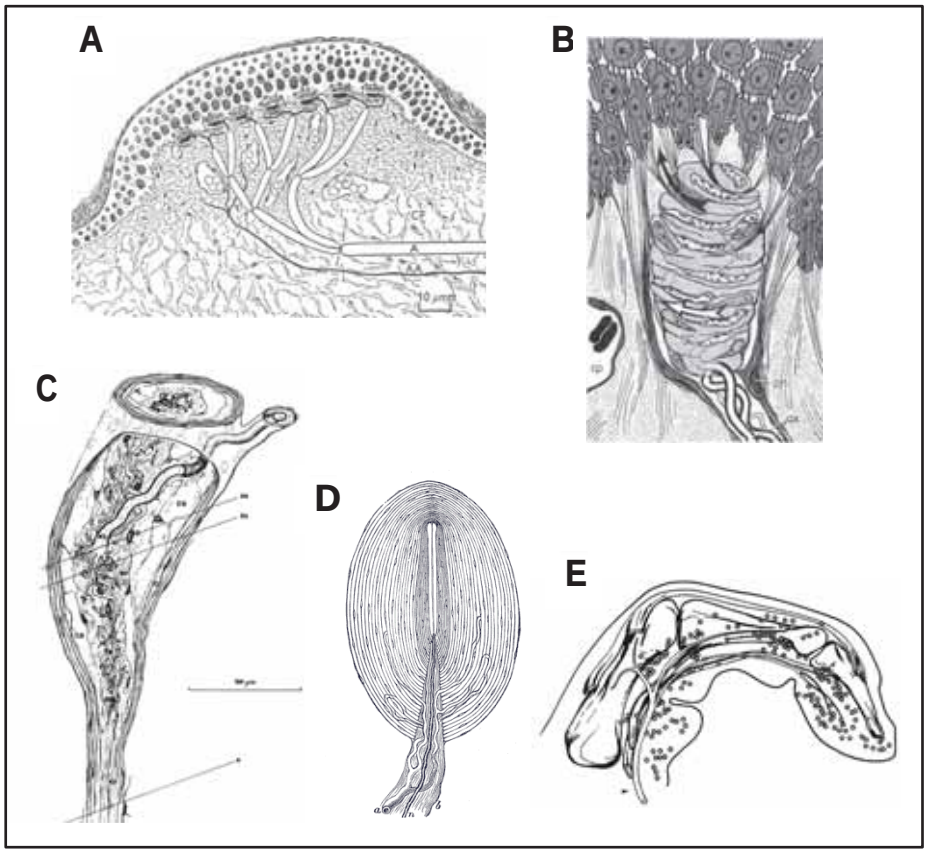

Figure 7: Encapsulated tactile mechanoreceptors. (A) Merkel cell-neurite complexes are branched receptors. Each terminal consists of a disk-shaped Merkel cell in close apposition with an expanded disk-shaped nerve terminal (from Iggo and Muir, 1969). (B) Meissner corpuscles are made of a connective tissue capsule containing stacks of flattened Schwann cells envelopping the nerve terminal (from Andres and von Düring, 1973). (C) Ruffini endings are branched nerve fibres intertwining around a core of collagen fibres, inside an elongated, lamellated, cylindrical capsule (from Chambers et al., 1972). (D) Pacinian corpuscles are large layered onion-like capsules (connective tissue) surrounding the nerve terminal. A fluid-filled space separates the compact inner core of membrane lamellae (made of modified fibroblasts) from the outer lamella of the capsule (from Gray, 1893). (E) Londitudinal section through the index finger (radial half) showing the distribution of Pacinian corpuscles (open circles) in a 7-month foetus (from Cauna and Mannan, 1959).

Fiber type	Diameter, micrometers	Myelinated or nonmyelinated	Conduction velocity, m/sec	Structures innervated
Aα (Ia, Ib)	Largest diameter (13–22 μm)	Myelinated	Fastest conduction 70–120 m/sec	Alpha motoneurons; neuromuscular spindles (primary fibers for muscle length and rate of change of length) and neurotendinous spindles (muscle tension)
Aβ (II)	Large diameter (8–13 μm)	Myelinated	Fast conduction 69.1 ± 7.4 m/sec (range 25–75)	Neuromuscular spindles (secondary fibers), tactile disks (contact, pressure, form, texture = light touch), tactile corpuscles (contact, velocity, movement = discriminative touch), lamellar corpuscles (pressure, high frequency vibration, stretch), Ruffini corpuscles (contact and skin stretch = light touch) and nociceptors
Aγ	Medium diameter (4–8 μm)	Myelinated	Medium conduction 15–40 m/sec	Gamma motoneurons
Aδ (III)	Small diameter (1–4 μm)	Myelinated	Slow conduction 10. 6 ± 2.1 m/sec (range 5–30)	Free nerve endings (sharpness, pinprick or first pain) and free nerve endings (coolness, 15–45°C)
B	Very small diameter (1–3 μm)	Lightly myelinated	Very slow conduction 3–14 m/sec	Preganglionic autonomic efferents and visceral afferents
C (IV)	Smallest diameter (0.4–1.2 μm)	Nonmyelinated	Slowest conduction 1.2 ± 0.2 m/sec (range 0.5–2.0)	Postganglionic autonomic, free nerve endings (slow, burning second pain, heat pain, cold pain), free nerve endings (warmth, 20–40°C), blood vessels, sweat glands, and arrector pili muscles

Modified from Hagbarth, 1979; Light and Perl, 1993; Tran et al., 2001; Djouhri and Lawson, 2004; Mann, 2004; Mountcastle, 2005.

Table 1: Classification of peripheral nerve fibres according to their diameter, myelination, conduction velocity and localisation. Fibres located in peripheral nerves are divided into unmyelinated (C) and myelinated fibres (A), the latter being further divided into 4 classes (α-δ) based on their properties of conduction and diameter. Fibres innervating the musculoskeletal system are classified into 4 groups (I-IV) (from Augustine, 2008, p. 84).

The mechanoreceptors and their associated afferent fibres were studied in detail in human by using a technique called microneurography (for a review, see Vallbo, 1989; Vallbo and Hagbarth, 1968). Essentially, a fine needle electrode was carefully inserted through the skin into individual afferent fibres of peripheral nerves along the arm, in conscious subjects, so as to measure and record the activity elicited in response to mechanical stimulation delivered on the skin surface, here the hand. In this way, receptive fields were determined, i.e. the skin area from which a primary afferent fibre is activated when an appropriate stimulus is applied on. When a stimulus was applied within the receptive field, already a weak stimulus elicited a strong response in the activated fibre. Conversely, if the stimulus was delivered on the boundaries of or outside the receptive field, a much stronger stimulation was required to activate the corresponding nerve fibre (Johansson, 1978). Moreover, receptive fields were shown to not be uniform in the sense that there are some spots with especially low activation threshold, corresponding to the location of individual nerve endings resulting from the branching pattern of the

fibre extremity (Johansson, 1978). Moreover, an individual fibre is preferentially activated by one submodality, such as light pressure, low-frequency vibration or high-frequency vibration.

Four types of tactile afferents in the glabrous skin of the hand were described (Johansson and Vallbo, 1983), each of them allowing a sophisticated processing of touch stimulation to take place already in the skin (**Figure 8A**). To elaborate, there are two types of somatosensory mechanoreceptor afferents based on contrasting properties of adaptation of firing rate in response to a stimulus: slowly adapting (SA) mechanoreceptor afferents (Merkel cell-neurite complexes innervated by SA-I afferents, and Ruffini endings innervated by SA-II afferents) show a sustained firing rate as long as the skin is stimulated and exhibit only very mild decline in activity in response to prolonged skin indenting stimulus. Therefore, SA fibres inform about how strongly the fingers are grasping an object or how heavy are the feet pressing on the ground, for instance. Conversely, activity in fast adapting (FA) mechanoreceptor afferents (Meissner corpuscles innervated by FA-I or RA afferents, and Pacinian corpuscles innervated by FA-II or PC afferents) is rapidly changing and restricted to modifications in stimulation, i.e. the stimulus onset and offset, in the form of brief bursts of action potentials. Consequently, FA afferents primarily inform about the dynamic properties of mechanical stimuli. The adaptation properties are, in part, determined by the dynamic filtering properties of the encapsulated structures of the mechanoreceptors. Regarding the Pacinian corpuscles, for instance, Loewenstein compared the activity of an intact isolated receptor from the cat with the one of a decapsulated isolated nerve ending (**Figure 9**). Essentially, a brief pulse of compression applied to the Pacinian corpuscle in an intact receptor elicited a brief receptor potential only at the onset and offset of the stimulus (**Figure 9A**). This was explained by the fact that the compression of the fibre ending was largely attenuated by the redistribution of the mechanical pressure throughout the fluid-filled capsule and its lamellae, surrounding the nerve terminal (Loewenstein and Skalak, 1966). Conversely, when the mechanical compression was applied to the decapsulated nerve ending, a prolonged receptor potential was generated, lasting for the entire stimulus and thus matching now a slowly-adapting receptors, even though the amplitude slowly decreased during the pulse (**Figure 9B**). But interestingly, even after removal of the Pacinian capsule, the fibre still produced only a brief burst of action potentials in the axon in response to the mechanical pulse (not shown here, but see Loewenstein and Mendelson,

1965; Loewenstein, 1971), meaning that the axon itself had similar adaptation properties as those of the intact Pacinian corpuscle associated with the nerve ending.

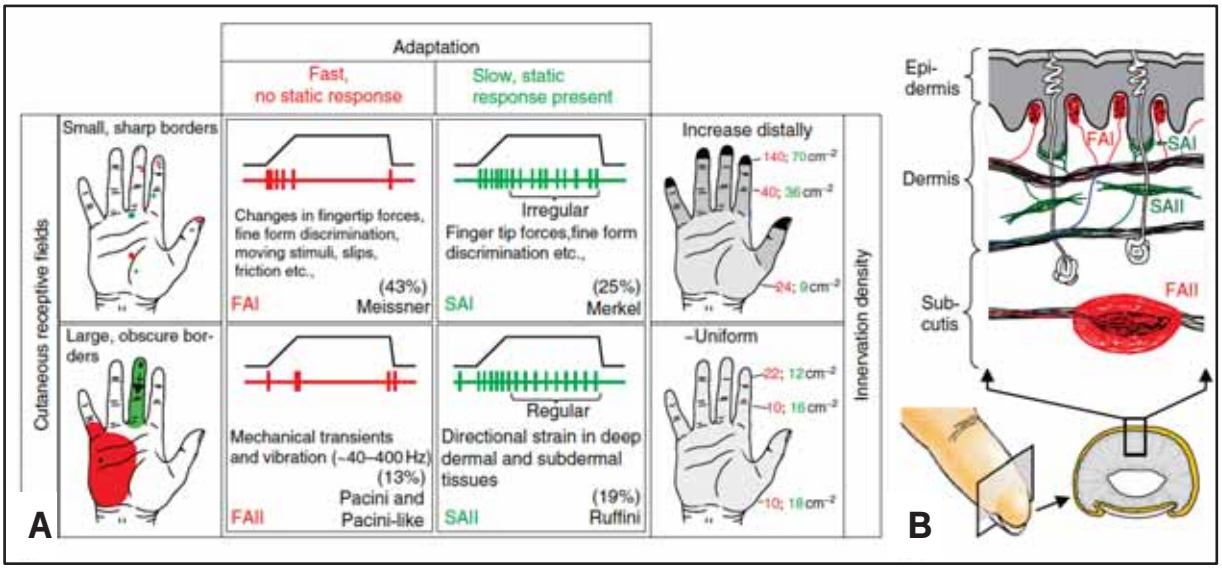

Figure 8: (A) Classification of the mechanoreceptors located in the glabrous skin of the human hand. The middle panels represent the impulse discharges of the 4 types of mechanoreceptors (lower traces) in response to a skin indentation (perpendicular ramp, upper traces). The fast adapting (FA, in red) receptor cells show a rapid adaptation in response to a continuous deformation of the skin, meaning that they discharge only when the application of the stimulus changes. The slowly adapting (SA, in green) receptor cells show a continuous discharge during the entire presentation of the stimulus. The relative occurrence frequency and the probable associated end structures for each mechanoreceptor type are given. The left panels show the receptive fields of the different mechanoreceptors. Note that Meissner's corpuscles are the most common mechanoreceptors in glabrous hand skin. Upper left: 15 different receptive fields of FA-I and SA-I receptor cells. These receptive fields are small and precisely delimited on the skin (around 10 mm^2). Lower left: 2 receptive fields of FA-II and SA-II receptor cells. They are larger and less precisely delimited than those of FA-I and SA-I receptor cells. The right panels illustrate the density of the mechanoreceptors on the skin. For FA-I and SA-I receptor cells, the innervation density increases from the palm to the very fingertips (upper right panel, FA-I density per cm^2 in red and SA-I density per cm^2 in green). For FA-II and SA-II receptor cells, the innervation density is more constant over the glabrous skin and lower than the one of FA-I and SA-I receptor cells (lower right panel, FA-II density per cm^2 in red and SA-II density per cm^2 in green). Note that the type II receptors are present in all fibrous tissues in the body. (B) Cross section through a human fingertip showing the location of the nerve endings and their associated mechanoreceptors. Merkel cell-

neurite complexes (innervated by SA-I afferents) are located at the border between the epidermis and dermis, aligned with the dermal papillae. Meissner corpuscles (innervated by FA-I afferents) are located between the dermal papillae just, just below the epidermis. Ruffini endings (innervated by SA-II afferents) are located in the dermis, and Pacinian corpuscles (innervated by FA-II afferents) are located deeply, in the subcutis. Note that free nerve endings, involved in temperature, itch and pain sensation are not represented here (from Johansson and Flanagan, 2009b).

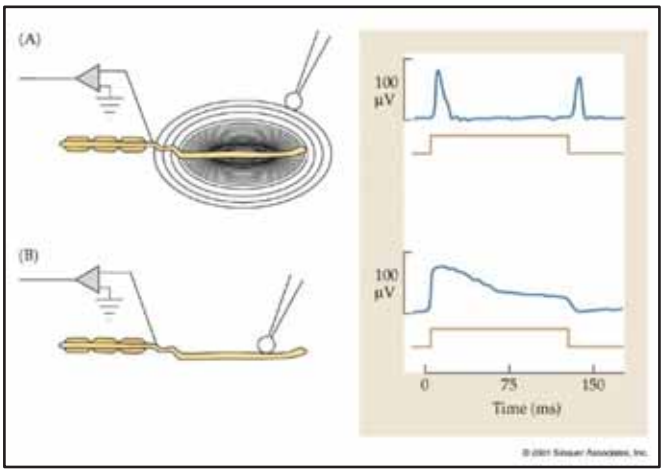

Figure 9: Adaptation in the cat Pacinian corpuscle, demonstrated in Loewenstein's experiments. (A) When a mechanical compression (yellow trace on the right) is applied to an intact Pacinian corpuscle (left), a transient deformation travels through the capsule layers to the nerve ending only at the onset and offset of the stimulus and the receptor potential rapidly adapts (blue trace on the right). (B) After removal of the capsule, the same stimulus induces a prolonged receptor potential lasting for the entire application of the stimulus, even though its amplitude decreases. This decapsulation experiment shows that adaptation in Pacinian receptor primarily results from the capsule, but also from axon properties (from Nicholls et al., 2001, p.340).

These 4 types of mechanoreceptors also differ in their location in the skin and in receptive field properties (Johansson and Vallbo, 1983; Johnson, 2001). On the one hand, SA-I afferents and FA-I afferents are both located in the superficial layers of the skin (**Figure 8B**). Their receptive fields are small and circumscribed, allowing the most precise localisation and finest discrimination of touch, such as for Braille reading (Phillips et al., 1990). More precisely, SA-I afferents are located in the stratum basale of the epidermis

and are for instance involved in the high-quality perception of coarse structures (Nicholls et al., 2012), shapes, edges and roughness of surface (Hsiao et al., 1993). FA-I afferents are located in the dermal papillae of the glabrous hand (also in dermal papillae of the glabrous skin of the lips, forearm, and foot sole, as well as in the connective tissue papillae of the tongue) and are important for the perception of moving stimuli and low-frequency vibration (up to 50 Hz) (Coleman et al., 2001; LaMotte and Mountcastle, 1975; Lundström and Johansson, 1986). On the other hand, SA-II afferents and FA-II afferents are located in deeper skin layers and have therefore large and diffuse receptive fields. FA-II afferents are located in the subcutis (and in gut mesenteries, pancreas, peritoneum, muscles, ligaments, joint capsules, external genitalia, and interosseous membranes). They are mainly activated by transient mechanical stimuli that deform the skin depth and high-frequency vibratory stimuli, including tickling. Conversely, SA-II afferents are located in the dermis and in subcutis, especially at the base of the fingernails and in the hand palm (and in ligaments and joins), with their long axis usually parallel to the stretch lines in skin (Paré et al., 2002). They are activated by stimuli that induce a strain or compression in the dermis and subcutis (Bolanowski et al., 1988) and respond to the direction of motion, stretch, and vibration. They are not activated by an electrical stimulation.

Equally important, there is a differential innervation pattern of the glabrous hand skin, with the fingertips showing the largest innervation density (Bensmaia et al., 2005; Darian-Smith and Kenins, 1980; Johansson and Vallbo, 1976; Johansson and Vallbo, 1979b; Johansson and Vallbo, 1983; Leung et al., 2005; Talbot et al., 1968; Vallbo and Johansson, 1984). See the legend of **Figure 8A** for greater detail.

Skin vibration below 40 Hz is usually reported as flutter, while touch stimulations with a repetition rate between 80 and 300 Hz are described as hum or buzz (LaMotte and Mountcastle, 1975). Interestingly, it was demonstrated that the psychophysical properties of the stimuli (frequency-dependence of the tactile perception) are directly linked with the tuning of FA afferents, similarly in human and monkeys (LaMotte and Mountcastle, 1975). To elaborate, FA-I afferents preferentially discharge in response to 30-40-Hz stimulation (Konietzny and Hensel, 1977) while FA-II afferents preferentially discharge in response to 250-Hz vibration (LaMotte and Mountcastle, 1975; Talbot et al., 1968) and FA-II afferents have a lower response threshold than FA-I afferents. However,

note that, contrary to what was traditionally reported, FA-I afferents have a much broader tuning range by being able to respond to vibratory stimuli > 1000 Hz (Prof. Roland Johansson, personal communication, April 24, 2015).

In natural unconstrained conditions, stimuli usually activate several kinds of receptors simultaneously such that the different aspects of the stimulus are coded by the different receptors. The mechanoreceptors are important in passive touch to give sensory information about the size, shape, and texture of objects. Moreover, they play an important role during skilled movements, such as object manipulation. Simply put, by handling an object, tactile afferent signals provide information about object texture among others, allowing to identify this object and to produce the appropriate motor plan to prevent the object slipping through the hands. SA and FA afferents contribute differently due to their characteristics: for instance, the vibration sensitivity of FA afferents is important since the slipping of an object being gripped with the fingers transmits skin vibrations (Brisben et al., 1999). Moreover, SA-II receptors, located in the depth of the skin, are activated by stretch stimulus in a particular direction during object grasping and thus inform about stimulus direction. The critical importance of tactile feedbacks in the control of the fine manual dexterity has been investigated in depth in human by Johansson and collaborators by using microneurography as an object was first contacted by the fingers, grasped between the thumb and index finger, then lifted, held for a while above a table, lowered, and returned back to the rest position (Johansson and Flanagan, 2008; Johansson, 1991; Johansson et al., 1992; Johansson, 1998; Johansson, 2002; Johansson and Cole, 1992; Johansson and Flanagan, 2009a; Johansson and Flanagan, 2009b; Johansson and Flanagan, 2009c; Johansson and Westling, 1990; Johansson and Westling, 1991; Johansson, 1996; Macefield et al., 1996; Macefield and Johansson, 1996). Essentially, all types of mechanoreceptors are specifically involved in a particular phase during object grasp. For instance, the FA-I, FA-II, and SA-I afferents signal finger-object contact when an object is first touched. Then, the SA-I afferents inform about the amount of grip force applied with each finger while the FA-I afferents measure the speed of the grasp being applied. The FA-II afferents detect the small vibrations transmitted by the object being lifted. Due to their rapid adaptation properties, the FA-I and FA-II afferents stop responding after grasp has been established. Conversely, the SA-II afferents detect flexion or extension of the fingers during grasp or release of the object and thereby inform about the hand posture during movements. In sum, the signals about object shape,

size, and texture originating from the four types of afferences are used to adjust the level of forces that are applied during an object grasping. In case these afferent inputs are completely prevented, for instance by a local anaesthesia of the fingertips (inactivates probably some proprioceptive inputs as well), then fine object grasping is strongly impaired (Johansson et al., 1992; Johansson and Westling, 1984; Monzée et al., 2003)[6].

In sum, the combination of the different properties observed among the four cutaneous afferent systems makes each of them being functionally specialised to process some specific features of tactile stimuli (Johnson, 2001) during both passive and active touch, and thus constitute an anatomical and functional substrates for the richness of touch perception (Zimmerman et al., 2014).

In addition to the four aforementioned mechanoreceptors, discriminative touch is also mediated by free nerve endings and peritrichial endings, associated with hair follicles.

Proprioception is mediated by proprioceptors, such as the muscle spindles, Golgi tendon organs, joint capsule receptors and stretch-sensitive free endings. These afferents are fast-conducting, myelinated fibres located in deeper skin layers, joint capsules, ligaments, tendons, muscles, and periosteum and are activated by the physical deformation of the structures which they are located in (**Table 1**). For instance, muscle spindles and Golgi tendon organs continuously measure the level of muscle contraction and tension within the tendons, respectively, so as to provide information about the state of the muscles, the configuration of the joints, the position of the body or a limb in space (Gardner and Johnson, 2013a). But they are beyond the scope of the present thesis and therefore will not be described in greater detail.

Somatosensory pathways[7]

The dorsal column-medial lemniscal system and the anterolateral system are the two most important structures conveying somatosensory information from the periphery to the brain, leading to somatosensory sensations (**Figure 10**). In addition, the postsynaptic dorsal column pathway, the spinocervical tract, the spinocerebellar tract, the spino-

[6] See also https://www.youtube.com/watch?v=0LfJ3M3Kn80&feature=player_embedded

[7] This section is primarily based on textbooks (Bear et al., 2007; Cruccu et al., 2008; Kandel et al., 2013; Nicholls et al., 2001; Purves et al., 2008; Shimoji and Willis, 2008) in addition to more specific references mentioned in the text.

tectal tract, the spinoreticular tract, and the spinomesencephalic tract contribute as well, but to a lesser extent, to somatosensory processing. Moreover, there are several other ascending pathways such as the spinohypothalamic tract, the spinoparabrachial tract, and several tracts projecting directly to the amygdala and other telencephalic limbic structures that are involved in different limbic system-related functions (Shimoji and Willis, 2008).

These different systems process information linked with different types of bodily sensations, namely the discriminative touch (perception of size, shape, texture, movement of an object on the skin, as well as vibration and pressure), nondiscriminative touch (crude or poorly localised tactile perception), the proprioception (perception of static position and movements of the own limbs and body mediated by the measurement of muscles stretch, tendon tension and joint position), the nociception (sensation of pain or itching due to a physically damaging or threatening stimulus), the temperature sense or thermoreception (distinction between warmth and cold) and the viscероception (perception of the physiological state of internal organs, part of the autonomous nervous system).

The present thesis is primarily concerned with discriminative touch processing. However, even though there are segregated pathways for tactile stimulus processing and thermal/painful stimulus processing, both systems are linked and interact with each other. Indeed, in the skin, the mechanoreceptors are largely intermixed with thermoreceptors and nociceptors. Moreover, a painful stimulus inevitably activates tactile receptors as well, located in close vicinity with the painful stimulus given that the activation threshold of the large-diameter fibres mediating touch is lower than the one of Aδ and C fibres. Reciprocally, in case the intensity of a given tactile stimulus is strong enough, nociceptive-sensitive afferent fibres may be activated as well. Such interactions between both systems are exemplified by the gating effect of touch stimulus on pain (Melzack and Wall, 1967). Moreover, in a very recent study on musicians experiencing chronic pain, a clear link was demonstrated between the increase in pain sensitivity and a decrease in tactile acuity (Zamorano et al., 2015).

Therefore, we will focus in further detail first on the dorsal column-medial lemniscal system, mediating touch among others, and then on the spinothalamic tract, mediating pain among others (but we will not discuss somatosensory pathway from the head and face). Both ascending tracts share similar organisation patterns. First, both pathways

involve 3 successive neurons, the cell body of the first one being located in a dorsal root ganglion. In other words, the activation of cortical neurons is separated from the peripheral stimulus by 3 synapses only. Second, an orderly representation of the body is preserved along each level in the pathways. Third, both pathways send a crossed projection to the cortex, resulting in the representation of the left half of the body onto the right somatosensory cortex and vice-versa. Fourth, both pathways mediate a conscious perception of sensory information from external stimuli to the ventral posterior lateral nucleus of the thalamus. Conversely, sensations that do not reach consciousness are mediated by the spinoreticular tract, spinomesencephalic tract, spinotectal tract, spinohypothalamic tract, anterior, posterior, and rostral spinocerebellar tracts, and cuneocerebellar tract, ending in the reticular formation, mesencephalon, hypothalamus and cerebellum, respectively. In particular, non-conscious proprioceptive inputs are transmitted directly to the cerebellum (Patestas and Gartner, 2013).

Dorsal column-medial lemniscal system

The dorsal column-medial lemniscal system (**Figure 10**) relays primarily discriminative touch, pressure sensation, vibratory sense and proprioception. This system is highly sensitive. Namely, based on microneurographic investigations, Johansson and Vallbo (1979a) demonstrated that a skin indentation of as small as 10 µm, most probably producing a single action potential in a single FA-I afferent, was sufficient to induce a touch sensation that the subject was able to perceive and report! The transmission of peripheral inputs to the cortex along the different relays of the pathway is remarkably sensitive as well because only 3 synapses are involved and each of them transmits information with high security and temporal fidelity (Huang et al., 2010; Rowe, 2001; Zachariah et al., 2001). It results virtually in a one-for-one transmission from the periphery to the cortex (Nicholls et al., 2001).

Tactile and proprioceptive stimuli at the periphery are transduced into action potentials by the large-diameter (Aα and Aβ) afferent sensory fibres (see **Table 1**) associated with the aforementioned peripheral nerve endings (see the description of mechanoreceptors and proprioceptors above) located in the skin, joint capsules and muscles. These cells constitute the first-order sensory neurons and their cell bodies are located in the ipsilateral dorsal root ganglia. Each ganglion is associated with a segmental spinal nerve. The

afferent fibres are grouped into peripheral nerves entering the spinal cord through the dorsal roots and terminating in Rexed laminae II-V in the dorsal horn. In particular, afferent tactile and proprioceptive inputs from the skin and deeper tissues of the hand enter the cervical spinal cord via dorsal roots C5-C8 (Darian-Smith, 2007). Once in the spinal cord, the central process of each afferent fibre divides and one axon collateral synapses on neurons in the spinal gray matter already at that level. The other, ascending branch of the first-order sensory neuron projects ipsilaterally through the dorsal column (in the fasciculus cuneatus and fasciculus gracilis) to the caudal part of the medulla oblongata and ends in the dorsal column nuclei, either the nucleus gracilis or the nucleus cuneatus, depending on the origin of the first-order neuron (Rustioni et al., 1979): first-order neurons entering the spinal cord via a dorsal root caudal to T6 ascend the spinal cord through to the fasciculus gracilis and establish a synapse on second-order neurons located in the nucleus gracilis (Qi and Kaas, 2006). Conversely, first-order neurons originating from a dorsal root rostrally to T6 travel in the fasciculus cuneatus and to the nucleus cuneatus to synapse second-order neurons. Second-order neurons originate from the dorsal column nuclei, project their axon across the midline in the medulla (sensory decussation), ascend then contralaterally in the medial lemniscus (fibre bundle) to reach the thalamus and finally synapse in the contralateral thalamic ventroposterolateral nucleus (VPL, mainly the caudal VPL, but also the oral VPL, the anterior pulvinar (Pulo) and the suprageniculate nucleus of the thalamus) on third order neurons (Darian-Smith, 2007; Darian-Smith and Darian-Smith, 1993). The thalamocortical projections from the VPL nucleus ascend through the posterior limb of the internal capsule to finally project to S1 and other secondary areas of the somatosensory cortex (Darian-Smith et al., 1996c). The thalamocortical projections from the Pulo terminate in S1 as well, but also in the posterior parietal cortexand even in the caudal motor cortex (Darian-Smith, 2007).

In brief, the left hemisphere receives sensory information from the right side of the body and conversely. Along the entire afferent pathway, ascending axons are organised and terminate in their target in a somatotopic manner (see below the section *Somatosensory cortical areas* for greater detail about somatotopy) (Qi and Kaas, 2006).

The face is sensitively innervated by the trigeminal somatosensory system (beyond the scope of this work).

Note the presence of the postsynaptic dorsal column pathway as well: second-order neurons originating from the dorsal horn receive afferent synaptic input from dorsal root ganglion collateral fibres, travel in the dorsal columns and project to the dorsal column nuclei. They synapse another neuron projecting to the VPL thalamic nucleus (Jones, 1983) that in turn projects to the somatosensory cortex. This tract conveys mechanosensory information from the posterior third of the head and the rest of the body.

Proprioception from the lower extremity is mediated by afferent fibres ascending in the fasciculus gracilis and synapse on second-order neurons in Clarke's column (in cats and probably in human as well (Lloyd and McIntyre, 1950)). These latter neurons project then to the medulla oblongata along with the dorsal spinocerebellar tract (Grant et al., 1973). On the contrary, proprioceptive fibres from the upper limb travel through the fasciculus cuneatus to the nucleus cuneatus and the lateral cuneate nucleus (Whitsel et al., 1969a). These two nuclei send then axons to the contralateral VLP thalamic nucleus that in turn projects to somatosensory cortical neurons. Note that the lateral cuneate nucleus sends axons to the cerebellum as well through the cuneocerebellar tract.

The dorsal column usually does not process pain or thermal stimuli even though some unmyelinated axons originating from the dorsal root ganglion cells, containing peptides such as substance P and calcitonin gene-related peptide, and projecting to the dorsal column nuclei, have been shown in rats (Patterson et al., 1989; Patterson et al., 1990). In the same way, there are some postsynaptic dorsal column neurons and some neurons in the nucleus gracilis responding to noxious stimulation (Al-Chaer et al., 1998; Ferrington et al., 1988).

Figure 10 (next page): Organisation of the two major afferent somatosensory pathways from the limbs and trunk to the cerebral cortex in human. The discriminative tactile sensation and the proprioception are mediated by the dorsal column-medial lemniscal system (in dark orange) towards the cortex, whereas the temperature, pain and crude tactile perceptions are conveyed towards the cortex by the spinothalamic tract (in dark brown). In the dorsal column medial-lemniscal system in particular, the first sensory fibres mediating tactile sense from the lower limb ascend the dorsal columns by being located medially. By ascending progressively the spinal cord, the newly entering fibres, e.g. from the upper limb, are added progressively more lateraly within the dorsal column, resulting in inputs from the leg being located more medially than those from the arm, for instance. This somatotopic organisation is conserved along the entire pathway. Afferent fibres entering the spinal cord below level T6 convey inputs from the lower limb and lower half of the trunk and afferent fibres entering the spinal cord at level T6 and above convey inputs from the upper half of the trunk and upper limb. The upper right figure represents the location of S1 (in orange) on a lateral view of the brain, in the postcentral gyrus in the anterior parietal lobe. The planes of the successive transverse sections through the spinal cord and medulla and the coronal section of the brain through the postcentral gyrus used to represent the pathways are indicated by the black lines (Gardner and Johnson, 2013a, p. 493).

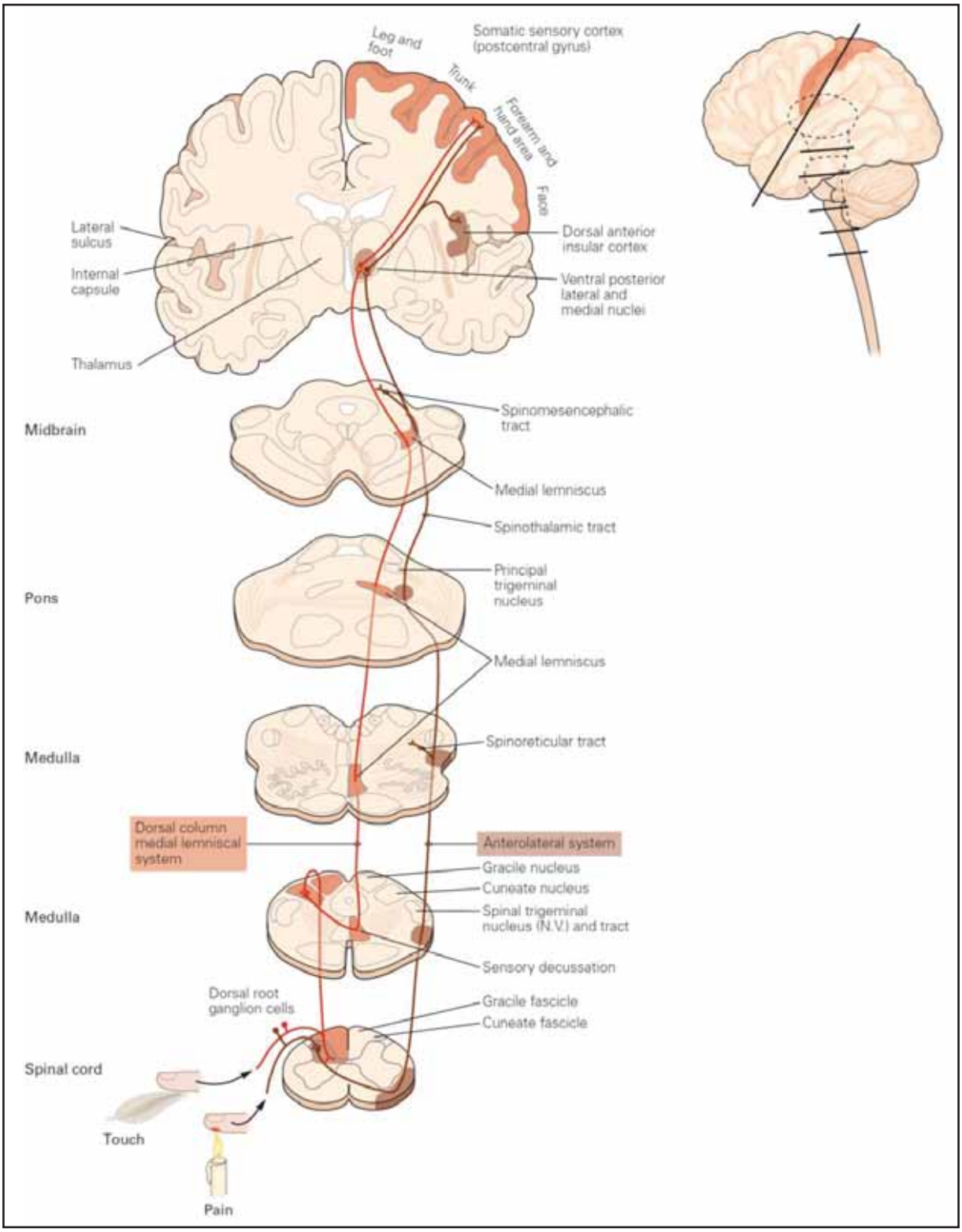
Somatic sensory cortex (postcentral gyrus)
Leg and foot
Trunk
Forearm and hand area
Face
Lateral sulcus
Internal capsule
Thalamus
Dorsal anterior insular cortex
Ventral posterior lateral and medial nuclei
Midbrain
Spinomesencephalic tract
Medial lemniscus
Spinothalamic tract
Pons
Principal trigeminal nucleus
Medial lemniscus
Medulla
Spinoreticular tract
Dorsal column medial lemniscal system
Anterolateral system
Gracile nucleus
Cuneate nucleus
Medulla
Spinal trigeminal nucleus (N.V.) and tract
Sensory decussation
Dorsal root ganglion cells
Gracile fascicle
Cuneate fascicle
Spinal cord
Touch
Pain

Anterolateral system

The spinothalamic tract, a component of the anterolateral system (**Figure 10**), relays thermoreception, nociception, itch sensation, viscerоception, as well as nondiscriminative (crude) touch, pressure sensation, and some proprioceptive sensation from the periphery to the brain[8]. These sensations are mediated by small-diameter (group III and IV, and Aδ and C, see **Table 1**) myelinated and unmyelinated afferent fibres with free nerve endings located in the skin and other tissues (bones, joint capsules, tendons, muscles, and many visceral organs). Contrary to the encapsulated mechanoreceptors described above, the free nerve endings do not contain any specialised structure but can be classified into different classes according to the modality they convey at best, such as mechanical deformation (mechanoreceptors), heating or cooling (thermoreceptors), or painful stimuli (nociceptors) (Burgess and Perl, 1973; Hensel, 1973; Willis, 2007; Willis and Coggeshall, 2004). Nociceptive and thermoreceptive afferent fibres are of two types: small-diameter (1-5 μm) myelinated Aδ fibres, conducting at about 6-25 m/s, and unmyelinated (0.1-1 μm in diameter) C fibres, conducting at 0.5-2 m/s (**Table 1**).

Following a thermal or painful stimulation, action potentials are generated in the axons of the first-order sensory neurons whose terminals are the aforementioned free nerve endings. In the same way as the dorsal column-medial lemniscal pathway, the cell bodies of these first-order neurons are located in ipsilateral dorsal root ganglia. These small fibres reach, in part, the ipsilateral dorsal horn (marginal zone and substantia gelatinosa, Rexed laminae I and II) and, in part, the intermediate region and ventral horn of the spinal cord (Willis, 2007), and synapse on second-order neurons. These second-order neurons cross immediately the midline of the spinal cord to the contralateral side in the ventral white commissure (Nathan et al., 2001), and then ascend in the anterolateral quadrant of the spinal cord white matter (forming the lateral and the ventral spinothalamic tracts) (Apkarian and Hodge, 1989a; Zhang et al., 2000a; Zhang et al., 2000b) to reach the third-order neurons located in different thalamic nuclei, such as the ventral posterior lateral (VPL), ventral posterior inferior (VPI), posterior (Po), and central lat-

[8] This is here the classical textbook view of thermoreception, nociception, itch sensation and other crude sensations from the body. Nevertheless, there is emerging evidence that the emotions and motivations linked to temperature, pain, itch processings, viscerоception and non-discriminative affective touch, among others, are mediated by another pathway (interoceptive pathway), distinct from tactile mechanoreception and proprioception at all levels, and projecting to the insular cortex, the anterior cingulate cortex and prefrontal cortex, among others (for further detail, see Couto et al., 2014; Craig, 2009; Craig, 2013; Craig, 2014; Craig and Zhang, 2006; McGlone et al., 2014 (see in particular their Figure 5); Morrison et al., 2010; Wiech et al., 2001).

eral (CL) nuclei (Apkarian and Hodge, 1989b; Boivie, 1979; Mehler, 1962). The VPL nucleus sends then axons to S1 and to other secondary somatosensory areas (sensory discriminative aspects, i.e. the intensity and location of pain) while some other thalamic nuclei convey nociceptive information to the anterior cingulate gyrus and to the insula (emotional and motivational processing of nociceptive input) (Craig, 2009; Craig, 2013; Craig, 2014; Craig and Zhang, 2006; Dum et al., 2009; Willis, 2003). The spinothalamic tract is responsible for noxious, thermal and visceral sensations from the posterior third of the head and the rest of the body. The face is innervated for these sensations by the spinal trigeminal tract (beyond the scope of this thesis).

Besides the spinothalamic tract, the anterolateral system also includes the spinoreticular, the spinomesencephalic, the spinotectal, and the spinohypothalamic tracts, all these pathways also mediating predominantly nociception, thermoreception, viscerоception, nondiscriminative touch, itch sensation, pressure, and some proprioceptive sensation from the periphery, but to other regions in the nervous system (see Patestas and Gartner, 2013 for greater detail).

Most importantly, note that there are feedback projections from high motor levels (cortex, brainstem nuclei) to all the levels of the somatosensory pathways in the form of inhibitory projections controlling sensory ascending pathways (Darian-Smith, 2007; Towe, 1973; Zimmermann, 1989). For instance, motor areas send premovement inputs to S1 so as to modulate its excitability (Jiang et al., 1991; Nelson, 1987; Nelson et al., 1991; Salimi et al., 1999; Williams and Chapman, 2002; Williams et al., 1998). Corticospinal tract fibres from M1 send collaterals to the cuneate nucleus, and these projections are of prime importance during the execution of fine skilled movements involving tactile sensory feedback from the hand (Darian-Smith, 2007). In addition, each level of the somatosensory pathway projects down to preceding levels, such that somatosensory areas project back to the same thalamic, brainstem and spinal cord relays from which they received afferent inputs (Nicholls et al., 2012). This top-down control modulates ascending somatosensory transmission by making a selective filtering of signal transmission and increases the specification of signal processing in the different relays of the somatosensory pathways (Johansson and Flanagan, 2009a). These feedback effects have high temporal and spatial specificity, such that tactile perception from the hand decreases when

the arm is reaching an object and is increased during object manipulation (tactile gating) (Chapman, 1994; Chapman and Beauchamp, 2006; Jiang et al., 1991).

Somatosensory cortical areas

In primates, the primary somatosensory cortex, shorten to S1, is located in the post-central gyrus, in the anterior parietal cortex (**Figure 11**) (Kaas, 2004a; Kaas, 2004b; Kaas and Collins, 2001; Krubitzer and Disbrow, 2005). S1 contains a large density of granules (stellates) in layer IV, typical for the sensory areas, corresponding to the synaptic projections of the thalamocortical fibres (Jones, 1975; Jones and Powell, 1973).

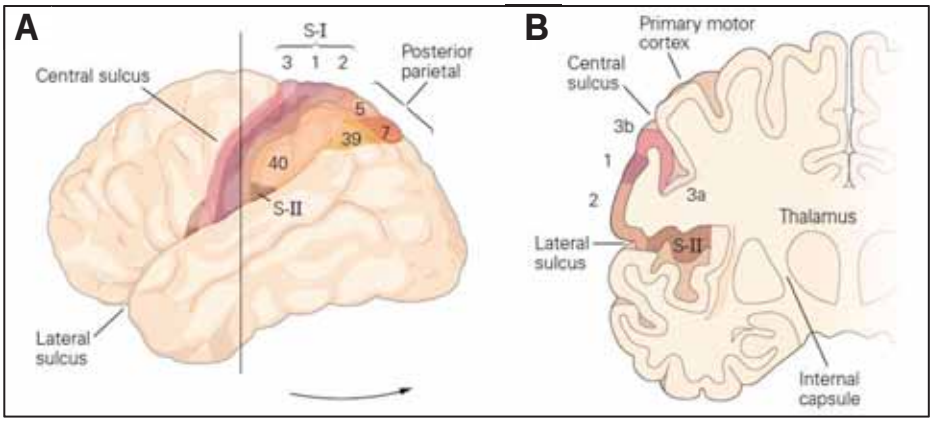

Figure 11: Somatosensory cortex in human. (A) Location of the somatosensory areas on a lateral view of the brain. The somatosensory cortex is composed of three areas, namely S1 (S-I, Brodmann's areas 3a, 3b, 1, and 2), S2 (S-II) and the posterior parietal cortex (Brodmann's areas 5 and 7). S1 is located posterior to the primary motor cortex (Brodmann's area 4) and anterior to the posterior parietal cortex. (B) Coronal section through the postcentral gyrus (section plane shown in A) showing the cytoarchitectonic subdivisions of S1 and the location of S2 (from Gardner and Johnson, 2013b, p. 512; and Gardner, 2010).

Early studies on rats, rabbits, cats and monkeys (**Figure 12A-C**) by Woolsey and collaborators (Marshall et al., 1941; Marshall et al., 1937; Woolsey et al., 1942; Woolsey, 1958; Woolsey, 1964) and on human patients undergoing a surgical ablation of epileptic foci by Penfield and collaborators (Penfield and Boldrey, 1937; Penfield and Jasper, 1954; Penfield and Rasmussen, 1950; Woolsey et al., 1979; Woolsey and Erickson, 1949), using electrical stimulation of the cortical surface or SSEP recordings, revealed that the soma-

tosensory cortex is somatotopically organised, meaning that neighbouring body parts are represented as neighbouring points on the cortical surface (**Figure 12D, E**). In primates, the genitals, the foot and the leg are represented most medially on the interhemispheric aspect of S1, followed by the trunk, then the hand more laterally, then the face and finally the tongue most laterally. Moreover, the representation of the body is not a one-to-one map but some body parts, such as the hand, fingers, foot, lips and tongue, are largely over-represented with respect to cortical territory. The cortical magnification[9] (Sur et al., 1980) of these body parts in S1 results from a particularly dense tactile innervation of the palm of the hands, the soles of the feet, the tongue and lips, some body surfaces that are usually in tight contact with objects, surface and textures. For instance, as already mentioned, each fingertip in human contains about 2'000 tactile afferent fibres (Johansson and Flanagan, 2009b). Moreover, the oral cavity and the tongue are regularly in tight contact with food and are involved in speech production as well, both situations generating strong tactile inputs. Conversely, the trunk and the leg do not have such a strong endowment of tactile receptors. The resulting disproportionate human body with huge hands, feet, lips and tongue relative to their normal proportions was called sensory homunculus ("little man") by Penfield (Penfield and Boldrey, 1937; Penfield and Rasmussen, 1950) and the corresponding distorted monkey body was called sensory simiusculus ("little monkey") by Woolsey (Woolsey et al., 1952; Woolsey, 1958). Later on, non-invasive imaging techniques provided finer detail about the somatotopic organisation of the somatosensory cortex (Blankenburg et al., 2003; Buchner et al., 1995; Hlustik et al., 2001; Inoue et al., 2013; Jamali and Ross, 2012; Martuzzi et al., 2014; Nelson and Chen, 2008; Overduin and Servos, 2004; van Westen et al., 2004; Zeharia et al., 2015). In fact, the somatosensory representation of the body in S1 follows probably the same overlapping mosaic principles as described for the primary motor cortex (see below).

[9] The star-nosed moles remarkably illustrate the principle of cortical magnification with 52% of the somatosensory representation devoted to their pink fleshy appendages ringing the snout (Catania, 1999; Catania and Kaas, 1997; Sachdev and Catania, 2002). These highly innervated structures are moved as tactile probes to find food and explore the environment.

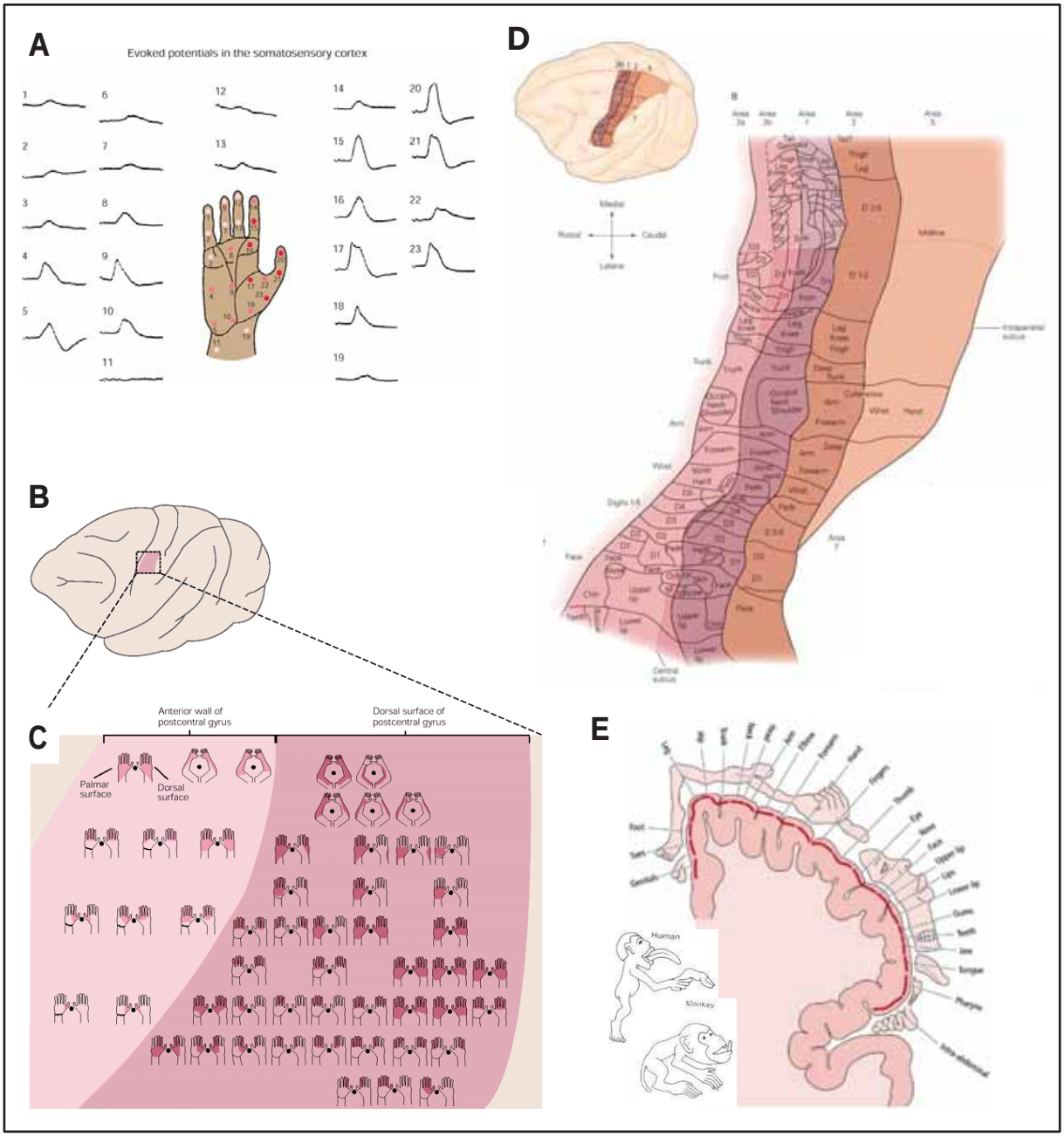

Figure 12: Somatotopy in S1. (A-C) The organisation of S1 was established by recording SSEPs in monkeys, among others by Marshall et al. (1941). Here, SSEPs (A) were measured on the pial surface of S1, in the left postcentral gyrus (B) of rhesus monkeys, after a repeated light touch stimulation at different points on the right hand palm (A) (from Kandel, 2013, p. 374). (C) Magnification of the recorded region showing the precise location of the recording electrodes (black dots). At each site, the coloured hand region corresponded to the stimulated area that evoked a SSEP at that location. The light pink area on the left represents approximately areas 3a and 3b, whereas the dark pink area on the right corresponds more or less to area 1 ((B) and (C) from Kandel, 2013, p. 375). (D) Topographic organisation of S1 in macaque monkeys, based on

microelectrode recordings in S1 by Nelson and by Pons. The location of S1 in the anterior partietal cortex is shown on a dorsolateral view of the brain, on the small left inset. The detailed representation of the different body surfaces in the areas 3a, 3b, 1, 2 and 5 is depicted. Note that the cortical surface along the central sulcus was unfolded. The depth of the sulcus is represented by the long dotted line. The mesial aspect of the hemisphere was flattened as well (short horizontal dotted line). The areas 3a and 2 receive mainly proprioceptive inputs from deep tissues, while the areas 3b and 1 are primarily activated by cutaneous inputs. The representations in areas 3b and 1 are parallel and largely mirror images along the mediolateral axis. A clearly distinct representation of each finger is visible in the areas 3b and 1 whereas receptive fields in the area 2 are more complex and represent the convergent inputs from several fingers. A careful examination of the map indicates that the entire finger representation covers a larger extent of cortical surface than e.g. the back representation (about 100 times more cortical columns per unit of body surface responding to touch stimulus on the fingers than on the trunk, in owl monkeys (Sur et al., 1980)). The area 5 in macaque monkeys is homologous to the areas 5 and 7 in human. D1-D5: fingers 1-5 of the hand (lateral)/foot (medial) (from Kandel, 2013, p. 517). (E) Section along the postcentral gyrus (S1) in human, illustrating the somatotopic representation of the entire body on the surface of S1 and the sensory homunculus and simiusculus (insets on the bottom left). Body parts which are particularly involved in tactile discrimination, essentially because of their dense somatosensory innervation, i.e. the face, the hand, the fingers and the foot, have a disproportionately extended representation on the somatosensory cortex (from Kandel and Jessell, 1991, p. 373; and Patestas and Gartner, 2013, p. 152).

Furthermore, the somatotopic architecture of S1 is reflected at the level of cortical columns as well: cells located in the same vertical cortical column in S1 share similar properties in terms of receptor class, i.e. preference of stimulus modality and adaptation of the mechanoreceptors, and receptive field location (Amaral and Strick, 2013; Jones and Powell, 1973; Mountcastle, 1997; Powell and Mountcastle, 1959b; Szentáigothai, 1983).

Finally, as already mentioned, the somatotopic organisation is not restricted to the cortical level but sensory inputs from the different body parts are conveyed towards the cortex according to a somatotopic organisation as well, as demonstrated for instance in both cuneate and gracile nuclei (Culberson and Brushart, 1989; Florence et al., 1989; Strata et al., 2003) and in the thalamic VPL nucleus (Jones et al., 2002).

S1 is architectonically subdivided into Brodmann's area 1, 2 and 3, the latter being further divided into areas 3a and 3b (**Figure 11**) (Brodmann, 1909; Geyer et al., 1999; Jones, 1975; Powell and Mountcastle, 1959a; von Economo, 1927). This organisation also reflects functional differences within each area, each of them being involved in specific processing. Moreover, the general classical somatotopic organisation described above is actually distinctly represented in a more or less elaborated form in each area of S1 (Kaas et al., 1979): area 1 (Kaas et al., 1981; Merzenich et al., 1978; Merzenich et al., 1981; Merzenich et al., 1987; Nelson et al., 1980), area 2 (Pons et al., 1985), area 3a (Geyer et al., 1999; Huffman and Krubitzer, 2001; Jones and Porter, 1980; Kaas and Collins, 2001; Krubitzer et al., 2004) and area 3b (Cusick et al., 1989; Jain et al., 1998; Jain et al., 2001; Kaas et al., 1981; Manger et al., 1997; Merzenich et al., 1978; Merzenich et al., 1981; Merzenich et al., 1987; Nelson et al., 1980; Pons et al., 1987; Qi and Kaas, 2004). Taken together, it means that S1 is characterised by parallel processing in different areas, and contains several modality-specific body representations. These distinct somatosensory areas are described in further detail below (for a review, see Krubitzer and Disbrow, 2005).

The area 3a is buried in the fundus of the central sulcus, in direct continuity with the area 4 (Geyer et al., 1999; Huffman and Krubitzer, 2001; Jones and Porter, 1980; Kaas and Collins, 2001; Krubitzer et al., 2004). This subdivision of S1 receives primarily inputs from muscle spindle receptors and other deep receptors (Tanji and Wise, 1981; Tanji, 1976; Wise and Tanji, 1981; Yumiya et al., 1974) via thalamocortical afferent fibres originating from the thalamic ventroposterior (VP) complex (Kaas, 2004a; Kaas, 2004b), and is involved in the coding of muscle stretch, movement velocity and limb position to adapt the posture (Tanji, 1976; Wise and Tanji, 1981). Nevertheless, some neurons in the hand representation of area 3a also process cutaneous stimuli (Tanji and Wise, 1981; Wise and Tanji, 1981) and noxious stimuli (Whitsel et al., 2009). The area 3a is densely interconnected with other ipsilateral areas such as areas 3b, 4 (Huerta and Pons, 1990; Kaas, 2004b), 6 (SMA), 2, 5, S2, PV, the cingulate cortex and the insular cortex (Huffman and Krubitzer, 2001; Krubitzer and Disbrow, 2005).

Proceeding then posteriorly, the area 3b is mostly activated by inputs from cutaneous receptors (Pons et al., 1987; Tanji and Wise, 1981), conveyed through thalamocortical afferent fibres originating from the thalamic VP complex (Kaas, 2004a; Krubitzer and

Kaas, 1990). In addition, the area 3b is activated by nociceptive inputs as well (Keysers et al., 2010). The receptive fields are relatively simple, small and cutaneous (Pons et al., 1987). This area is characterised by a high expression of myelin and cytochrome oxidase (C.O.) (Kaas and Collins, 2001). Remarkably, it was demonstrated that the fine-scale somatotopic representation within area 3b was correlated with regional patterns of myelin and C.O. expression (Jain et al., 1998; Jain et al., 2001; Qi and Kaas, 2004). The area 3b is interconnected predominantly with areas 3a, 1 and 2, S2, PV and M1 (Krubitzer and Disbrow, 2005).

The area 1 is located immediately posterior to the area 3b (Kaas and Collins, 2001). This area is primarily activated by inputs from 3b (Kaas, 2004a; Keysers et al., 2010) and its activity is modulated by cutaneous thalamic inputs from the thalamic VP complex (Kaas, 2004a). The somatotopic organisation in area 1 is approximately the mirror reversal of the one described in area 3b along their common border. Receptive fields usually have a center-surround organisation with separate 'on' and 'off' zones, and are larger than in area 3b (Sur et al., 1985). The area 1 has broad connections with areas 3b, 2, S2/PV, 5, AIP/7b, and more sparsely with area 3a, M1, and the frontal cortex (Krubitzer and Disbrow, 2005).

The area 2 lies in the most caudal part of S1. It receives tactile and proprioceptive information from areas 3a, 3b and 1 (Keysers et al., 2010) and muscle spindle receptor information from the thalamic VP complex (Kaas, 2004a; Kaas, 2004b; Keysers et al., 2010), and sends dense projections to the posterior parietal cortex (Kaas, 2004b). The area 2 is activated not as consistently and homogeneously as more rostral somatosensory areas (Pons et al., 1985), but instead more complex stimuli are required than in 3b. As a result, some area 2 neurons were shown for instance to preferentially respond to curvature (Yau et al., 2013), others were activated by the perception and discrimination of objects with a particular form by using haptic palpation (Iwamura and Tanaka, 1978; Keysers et al., 2010), and some neurons were also responding to stimuli on both the ipsilateral and the contralateral hands during bimanual exploration (Keysers et al., 2010). In addition the somatotopic organisation in area 2 is more complex than the one described in more rostral areas (Pons et al., 1985). The area 2 is interconnected with all the other areas of S1, with M1, with some areas in the intraparietal sulcus and in the inferior pari-

etal lobule, and with the contralateral area 2 (Keysers et al., 2010; Krubitzer and Disbrow, 2005).

In sum, the characteristics of the receptive fields evolve hierarchically along the rostro-caudal axis of S1. More specifically, from area 3b to area 1 and later on to area 2, the receptive fields become more complex and more extended, and feature-specific responses such as center-surround organisation (Friedman et al., 2008; Sripati et al., 2006; Sur, 1980), direction selectivity of the stimulus, or submodality integration become more obvious (Iwamura et al., 1993; Iwamura, 1998; Iwamura, 2007; Nicholls et al., 2001). Tract-tracing studies confirmed that there is a strong and sequential outflow of connections from area 3 to areas 1 and 2, then from area 1 to area 2 (and then from area 2 to area 5 and rostral area 7) (Vogt and Pandya, 1978). A summary of the afferent input modalities to the areas of S1 and characteristics of their receptive fields are provided in **Figure 13**.

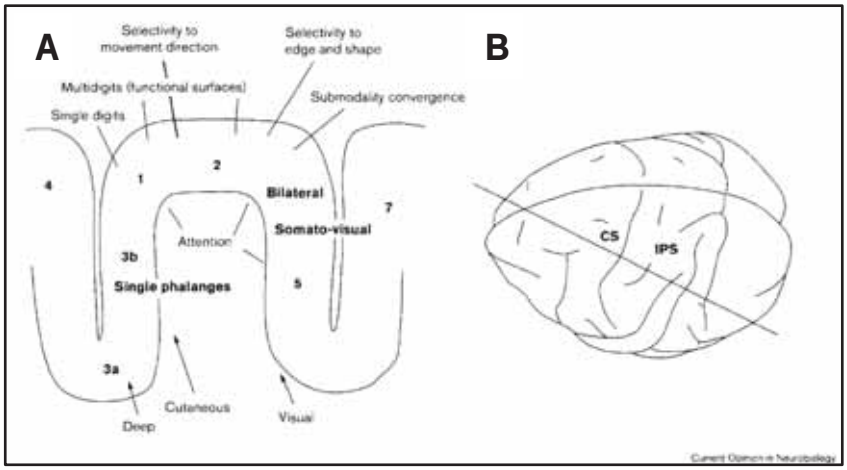

Figure 13: Hierarchical processing along the rostro-caudal axis of the postcentral gyrus in monkey. (A) Sagittal histological section across the postcentral gyrus, showing the architectonic divisions of S1, the input modality (under) and the properties of the receptive fields of S1 areas. (B) Lateral view of a monkey's brain with the section plane shown in (A). CS: central sulcus, IPS: intraparietal sulcus (from Iwamura, 1998).

From S1, the somatosensory information is sent through reciprocal projections to the secondary somatosensory cortex (S2) (Jiang et al., 1997), containing another somatotopic somatosensory representation (Burton and Robinson, 1981; Cusick et al., 1989; Friedman et al., 1980; Friedman, 1981; Whitsel et al., 1969b). This area is located in the

upper bank of the lateral sulcus and on the parietal operculum (**Figure 11**) (Cusick et al., 1989; Kaas and Collins, 2001; Keysers et al., 2010). S2 receives strong afferent inputs from the thalamus as well (Kaas, 2004b; Keysers et al., 2010). S2 was shown to be involved in a hierarchical information processing from S1 to S2, for instance regarding texture discrimination. Essentially, monkeys had to evaluate the presence or absence of texture changes on a surface by using the fingertips: while S1 neurons linearly encoded texture changes, a more complex feature extraction was performed in S2 (Jiang et al., 1997). Other studies confirmed that S2 is involved in a sophisticated extraction of somatosensory features (Fitzgerald et al., 2006), for instance by demonstrating the presence of larger receptive fields in S2 than in area 3b (Cusick et al., 1989) and bilateral receptive fields (Whitsel et al., 1969b). This is accompanied by a large number of interconnections with other sensory and associative areas (Keysers et al., 2010), allowing a high level of information integration to build up a representation of tactile objects (Haggard, 2006). For further detail about the role of S2, see Keysers et al. (2010).

In addition, Kaas and collaborators identified an additional area, namely a parietal ventral area (PV), as a subdivision of S2. PV is located caudal to S2, along the upper bank of the lateral sulcus, and shares the same connectivity as S2 (Kaas, 2004b; Keysers et al., 2010). Moreover, the respective somatotopic representations of S2 and PV are the mirror reversal of each other along their common border.

The posterior parietal cortex is located in the parietal lobe caudal to area 2 but without including the cortex of the lateral sulcus nor the supplementary sensory area of the medial wall (Kaas, 2004c). This brain region is particularly well developed in macaque monkeys (Kaas, 2004b) and is composed of at least 8-10 separate sensorimotor and visuomotor areas, among others the Brodmann's areas 5 and 7, the ventral (VIP), lateral (LIP), medial (MIP), and anterior (AIP) sensorimotor areas (Kaas, 2004c). It is considered as the somatosensory association cortex. The rostral areas receive principally somatosensory inputs, mainly from area 2 and from areas of the lateral parietal cortex, and they project to M1 and to premotor areas. The caudal areas receive auditory and particularly visual information, and send projections to premotor areas. By integrating somatosensory inputs with inputs from other sensory modalities, the posterior parietal cortex is largely involved in the perception of the body in relation to the surrounding environment, such as in guided motor behaviours (see e.g. Baumann et al., 2009; Borra

et al., 2008; Brochier and Umiltà, 2007; Buneo and Andersen, 2006; Davare et al., 2011; Gardner et al., 2007; Janssen and Scherberger, 2015; Kaas, 2004a; Kaas, 2004b; Lehmann and Scherberger, 2013; Mountcastle et al., 1975; Murata et al., 2000; Schaffelhofer et al., 2015; Townsend et al., 2011). A summary of somatosensory afferences and efferences of S1 is presented in **Figure 14**.

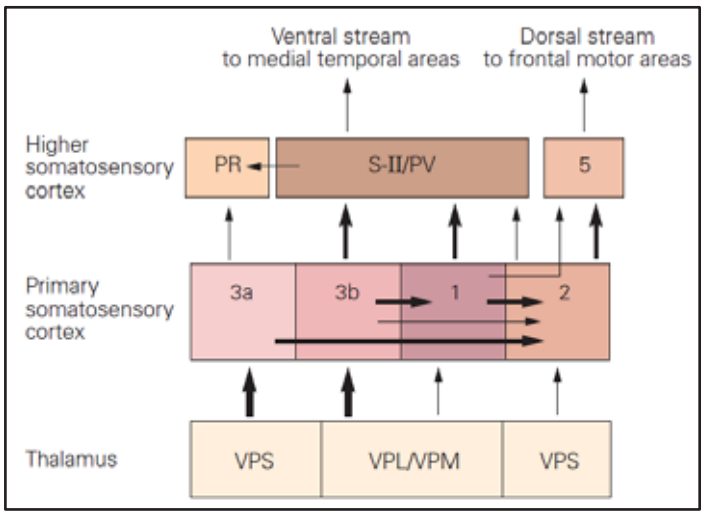

Figure 14: Summary of the afferences and efferences of the somatosensory cortical areas. The thalamus sends direct thalamocortical afferent fibres from the ventroposterior (VP) complex primarily to the areas 3b and 3a but also to the areas 1 and 2. The area 3b receives massive projections from the core of the thalamic ventroposterior complex, while the other 3 areas receive less dense inputs from the shell areas surrounding the core of the thalamic ventroposterior complex. In S1, neurons of areas 3a and 3b project to areas 1 and 2. Information from all the four S1 areas is then transmitted for further processing to neurons in the posterior parietal cortex (area 5), in S2/PV and in M1 (not shown here). From then on, information is further processed in higher-order associative cortical areas: the ventral pathway originates from S2 and is involved in tactile object recognition (specific shape and texture, context, behavioural relevance). The dorsal pathway begins in the parietal lobe and is involved in the sensorimotor guidance of movements. Tactile inputs can be conveyed to frontal areas directly from S1. In addition, other tactile inputs are conveyed to several areas of the posterior parietal cortex (areas 5, 7, 39, 40) where a multimodal integration takes place. The information is then sent to premotor areas in the frontal lobe to be integrated into complex movement sequences. In sum, tactile and proprioceptive inputs (in addition to visual ones) play an important feedback role that can modify behaviour during object manipulation. PR: parietal rostroventral cortex; PV: parietal ventral cortex: VPL, thalamic

ventroposterolateral nucleus; VPI, thalamic ventroposteroinferior nucleus; VPS, thalamic ventroposterosuperior nucleus (from Gardner and Johnson, 2013b, p. 512; Gardner, 2010; and Patestas and Gartner, 2013, p. 151).

Motor control of voluntary movements[10]

Contrary to reflexes, voluntary movements depend on the activity of supraspinal centers, among them motor cortical areas that exert control on the effector muscles via descending pathways running down the spinal cord. Here we will review the organisation of the motor system involved in the generation of voluntary movements, such as the fine manual dexterity that characterises primates. We will describe first the motor cortex, and then the main descending pathways in the spinal cord.

Motor cortical areas

In primates, the frontal cortex contains several motor areas (Amaral and Strick, 2013; Dum and Strick, 2002; Luppino and Rizzolatti, 2000; Matelli et al., 2004; Rizzolatti and Luppino, 2001; Rouiller, 1996; Rouiller and Olivier, 2004; Strick et al., 1998; Wiesendanger, 1981): the primary motor cortex (M1) and several association or secondary motor areas, all of them sharing at least one of the following characteristics: the area contains corticospinal neurons, it directly projects to M1, electrical stimulation to it does elicit movements and tonic contractions mostly on the contralateral half of the body, but also to a lesser extent on the ipsilateral side (Wiesendanger, 1981), it possesses a connection with a thalamic nucleus, its neuronal activity is clearly related to the execution of a conditional motor task (Rouiller and Olivier, 2004).

Primary motor cortex

The primary motor cortex (M1) is architectonically defined as Brodmann's area 4 (Brodmann, 1909; von Economo, 1927) (**Figure 15A**), characterised by the absence of a granular layer IV and the presence of very large pyramidal cells in layer V (Stepniewska

[10] For a comprehensive description of the motor areas and motor pathways, consult Lemon (2008b) and Nieuwenhuys et al. (2007, chapter 21).

et al., 1993). Physiologically, M1 is defined as the region of electrically excitable cortex where the lowest-intensity stimulus is able to evoke a contralateral isolated movement of skeletal muscles (Nudo et al., 2001; Sessle and Wiesendanger, 1982; Strick and Preston, 1978a). Similarly to the somatosensory cortex, studies on animals (Fritsch and Hitzig, 1870; Leyton and Sherrington, 1917; Woolsey et al., 1952; Woolsey, 1958; Woolsey, 1964) and on human patients (Foerster, 1936; Penfield and Boldrey, 1937; Penfield and Jasper, 1954; Penfield and Rasmussen, 1950; Woolsey et al., 1979) demonstrated using electrical stimulation of the cortical surface that there is a somatotopic organisation of the body in the motor cortex. To elaborate, muscles of the contralateral body are represented on the cortex, for instance with muscles of the head and face being represented in the most lateral part of the precentral gyrus, those of the leg and tail in the paracentral lobule on the medial surface of the cerebral hemisphere, and those of the hand in between, in the lateral surface of the precentral gyrus (**Figure 15B**). Furthermore, as for the somatotopy in S1, this body representation is not a one-to-one map but there is a cortical magnification of some body parts with respect to cortical territory: the body parts able to produce the finest movements and therefore with a large number of M1 neurons involved in controlling these movements, i.e. distal parts of the extremities, especially of the hand, as well as the lips and tongue, have a larger cortical representation in M1 than the body parts used in gross movements such as locomotion. Thus, the resulting motor homunculus (Penfield and Boldrey, 1937; Penfield and Rasmussen, 1950) and motor simiusculus (Woolsey et al., 1952; Woolsey, 1958) have highly disproportionate hands, lips and tongue relative to their normal proportions (Schieber and Baker, 2013) (an illustrated comparison of the motor somatotopic organisation in human and in macaque monkey in provided in **Chapter 8**, **Figure 6**).

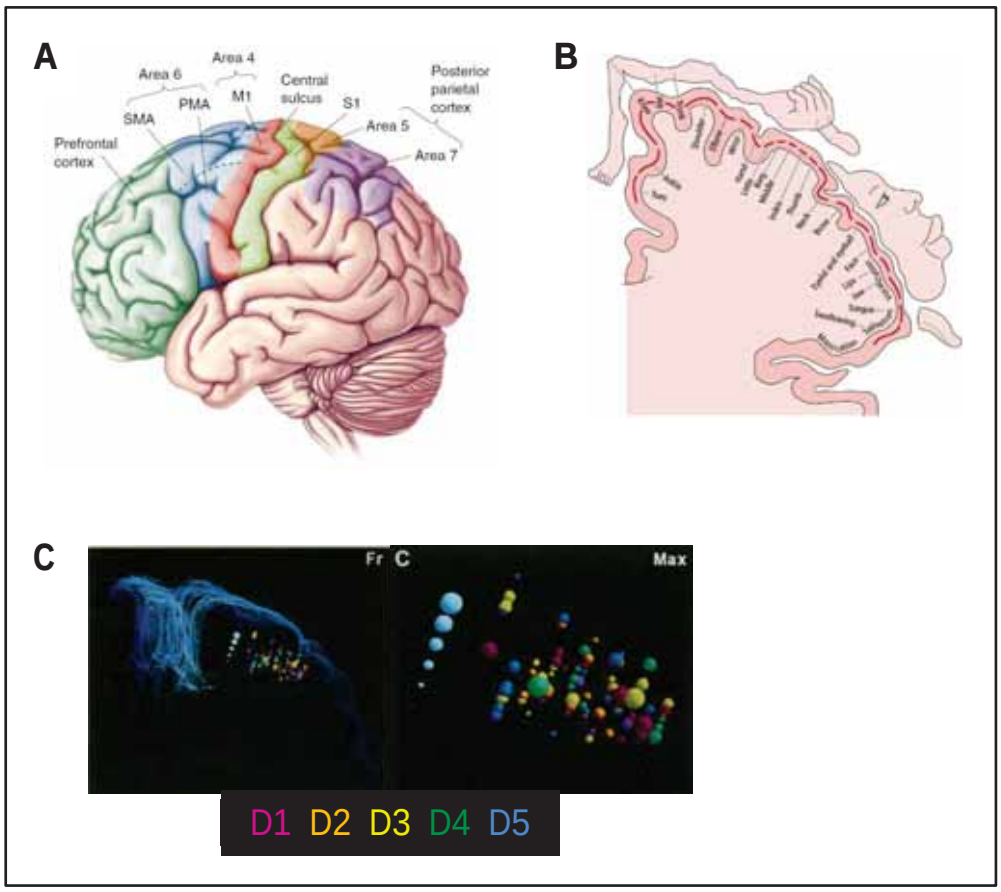

Figure 15 : Organisation of M1. (A) Neocortical areas involved in voluntary motor control, on a lateral view of the left hemisphere surface in human. M1 is located in the precentral gyrus. A more detailed representation of the motor areas is provided in Figure 16 (from Bear et al., 2007, p. 460). (B) Somatotopic representation of the body on the surface of M1 in human, and the resulting motor homunculus, superimposed on a coronal section along the precentral gyrus. The body muscles are organised in an orderly manner but there is a disproportionally large representation of the finger muscles and the oral cavity muscles, resulting from the fine motor control needed for object manipulation with the fingers and for speech production (from Patestas and Gartner, 2013). (C) Distributed and overlapping mosaic organisation of M1 neurons involved in finger movements throughout the hand representation, in monkeys. Each coloured sphere represents a single neuron recorded in left M1 (frontal pole reconstruction on the left side, and magnification on the right side) during individuated finger flexion or extension. The larger the sphere diameter, the larger the spiking frequency of the neuron under consideration (from Schieber and Hibbard, 1993).

Later on, this concept of somatotopy in M1 was refined, especially for the hand representation. Studies on monkeys (Kwan et al., 1978; Lemon, 1988; Rathelot and Strick, 2006; Schieber and Hibbard, 1993; Schieber and Poliakov, 1998) and then on human

(Schieber, 1999) demonstrated that finger movements were actually represented in a distributed and overlapping mosaic fashion in M1 (**Figure 15C**) rather than only in the strict strip-like pattern originally proposed by Penfield and contemporaries (Foerster, 1936; Penfield and Boldrey, 1937; Penfield and Jasper, 1954; Penfield and Rasmussen, 1950; Woolsey et al., 1979). To put it another way, even though there is a tendency for the more radial fingers to be represented more laterally and the more ulnar fingers to be represented more medially (Hwang et al., 2014; Schieber, 1999), each finger movement is still represented at many locations in the whole hand representation (Kwan et al., 1978; Schieber, 2001; Schieber, 1999; Schieber and Poliakov, 1998). Consequently, the neuronal populations controlling a given finger movement topographically overlap with those involved in the motor control of other finger movements in order to create synergies between movements of different muscles and fingers (Hepp-Reymond et al., 1996). More recently, the general somatotopic organisation of the motor cortex as well as the distributed motor control of the fingers was confirmed by using fMRI, among others (Beisteiner et al., 2001; Dechent and Frahm, 2003; Hlustik et al., 2001; Indovina and Sanes, 2001; Kleinschmidt et al., 1997; Lotze et al., 2000; Rao et al., 1995; Zeharia et al., 2015).

By using the technique of spike-triggered averaging on rhesus monkeys, Park and collaborators (2001; 2004) extended to the whole upper limb the concept of synergy between muscle representations. Namely, they highlighted a "horseshoe-like" representation of the upper limb in M1 with three different zones identified across several monkeys: a mediolaterally-oriented central zone along the caudal border of M1 containing distal muscle synergies, surrounded by a first zone representing synergies between distal and proximal muscles, itself surrounded by a zone representing proximal muscle synergies only. This means that the wrist representation in M1, for instance, is in part intermingled with the finger representation and the shoulder representation as well.

Association motor cortices

In addition to M1 itself, 6 spatially separate premotor areas (**Figure 16**) have been identified in the frontal lobe of monkeys by using retrograde labelling in parallel with physiological ICMS mapping. Each of them projects massively and directly to M1 (Dum and Strick, 1991; Dum and Strick, 2002; Felix and Wiesendanger, 1970; Picard and Strick,

1996; Strick et al., 1998; Wiesendanger, 1981): the ventral premotor area (PMv) and the dorsal premotor area (PMd), both located just rostrally to M1 on the lateral surface of the hemisphere in Brodmann's area 6; the supplementary motor area (SMA, Brodmann's area 6) and three cingulate motor areas (CMA) -the rostral, the dorsal and the ventral cingulate motor areas (CMAr, CMAd and CMAv, in Brodmann's areas 23 and 24)- all four located on the medial wall of the hemisphere. SMA can be further divided into a rostral part (pre-SMA) and a caudal part (SMA-proper), PMd into a rostral and a caudal part (PMdr and PMdc) and PMv into a rostral and a caudal part (PMvr and PMvc) (Gentilucci et al., 1988; Luppino et al., 1991; Matelli et al., 1991; Matelli et al., 1985; Rizzolatti et al., 1988; Rizzolatti et al., 1998; Rouiller and Olivier, 2004). Note that the nomenclature of motor areas varies across authors (**Figure 16B**).

A

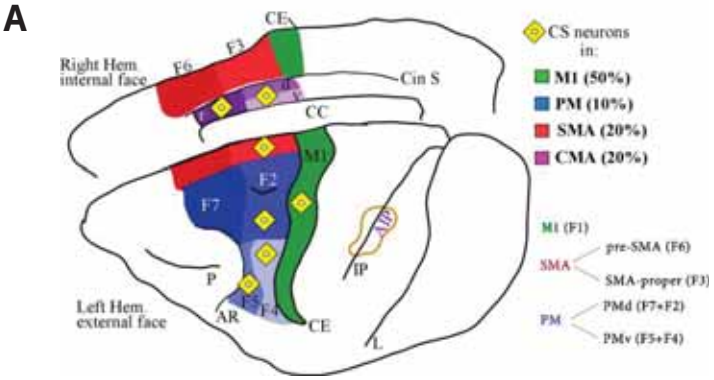

B

Matelli *et al.* nomenclature	Brodmann's nomenclature	Most widely used terminology in the functional literature
F1	Area 4	Primary motor cortex
F2	Dorsal sector of area 6, caudal part	Dorsal premotor cortex, caudal part (PMdc)
F3	Mesial sector of area 6, caudal part	Supplementary motor area proper (SMA proper)
F4	Ventral sector of area 6, caudal part	Ventral premotor cortex, caudal part (PMvc)
F5	Ventral sector of area 6, rostral part	Ventral premotor cortex, rostral part (PMvr)
F6	Mesial sector of area 6, rostral part	Presupplementary motor area (Pre-SMA)
F7	Dorsal sector of area 6, rostral part	Dorsal premotor cortex, rostral part (PMdr)

Figure 16 : Motor areas in the macaque monkey. (A) Localisation of the frontal and cingulate motor areas on the lateral and mesial surfaces of the hemispheres. Each colour field represents a distinct cytoarchitectonic area. Yellow diamonds: origin of corticospinal (CS) neurons projecting to cervical motoneurons in the spinal cord. The % of distribution of CS neurons is indicated (even though some parietal CS neurons were omitted here). AIP: anterior intraparietal area (tightly interconnected with F5 and plays a key role in grasping. For a review, see Janssen and Scherberger, 2015); AR: arcuate sulcus; CC: corpus callosum; Cin S: cingulate sulcus; CMA: cingulate motor areas

(further divided into rostral or 'r', ventral or 'v' and dorsal or 'd' subareas); CE: central sulcus; IP: intraparietal sulcus; P: principal sulcus (modified from Rouiller, 2012; and Rouiller and Olivier, 2004). (B) Different nomenclatures have been used to describe the motor areas in primates, among them Matelli et al. nomenclature (Matelli et al., 1991; Matelli et al., 1985), Brodmann's nomenclature of the agranular frontal areas (Brodmann, 1909), and a commonly used functional nomenclature (from Matelli et al., 2004).

Again by using retrograde labelling, it was shown that the premotor areas have massive direct projections to the spinal cord, forming corticospinal tracts with a precise topographical organisation, i.e. distinct projections for the upper and lower limb motoneurons were observed in the cervical and lombar segments of the spinal cord, respectively (see e.g. Biber et al., 1978; Coulter and Jones, 1977; Dum and Strick, 1991; He et al., 1993; He et al., 1995; Jones and Wise, 1977). At the cortical level, a more or less elaborated somatotopic organisation was observed in each of the premotor areas (but not as clear as in M1) by using ICMS (Mitz and Wise, 1987; Preuss et al., 1996) or neural tract-tracing. To elaborate, in all areas but PMv, distinct projections to upper and lower cervical segments were further identified, meaning that those areas contain separate proximal and distal upper limb representations. Conversely, PMv was shown to project only to the upper cervical motoneurons (Dum and Strick, 1991; He et al., 1993; He et al., 1995). The total number of corticospinal neurons identified in these 6 areas was equal to or sometimes even larger than the number of corticospinal neurons located in M1. The termination of the corticospinal fibres from SMA, CMAr, CMAd and CMAv in the spinal cord was studied by injecting anterograde tracers in each area individually as well as retrograde tracers in the cervical spinal cord (Dum and Strick, 1996a; Martino and Strick, 1987; Rouiller et al., 1996): it was shown that the corticospinal axons project mainly to different portions of the intermediate zone of the cervical spinal cord and less densely to the ventral horn of the lower cervical spinal cord where motoneurons controlling distal upper limb muscles are located (i.e. like M1). Another study combining anterograde tracer injection in SMA and retrograde labelling from distal hand muscles confirmed that there were direct connections from the hand area of SMA to motoneurons in the cervical spinal cord (Rouiller et al., 1996). In sum, these motor areas establish direct connections with cervical motoneurons, like M1, especially the ones innervating distal muscles of the upper limb.

The function of these areas was assessed by using ICMS (Luppino et al., 1991; Mitz and Wise, 1987; Takada et al., 2001): in SMA and CMAs, proximal and distal movements of both upper and lower limbs were evoked, although the threshold was higher and the probability to observe a movement was lower than with a similar stimulation in M1. As mentioned above, corticospinal fibres from PMv project only to upper segments of the cervical spinal cord (normally involved in the control of proximal upper limb) (He et al., 1993; Martino and Strick, 1987). But the same region of PMv sends very dense projections to the finger representations in M1 as well (Dum and Strick, 2002; Tokuno and Tanji, 1993). The function of this conflicting organisation of PMv was clarified by using ICMS in the posterior bank of the arcuate sulcus, the region of origin of the PMv corticospinal fibres projecting to upper cervical motoneurons in the spinal cord. ICMS resulted in movements of the distal upper limb, in particular thumb and fingers movements whereas movements of the proximal upper limb, i.e. the elbow, were much more rarely observed (Dum and Strick, 1991; He et al., 1993; Martino and Strick, 1987). Interestingly, the stimulation thresholds were as low as the ones usually used to elicit movements by ICMS in M1. It was therefore concluded that this region of PMv, in particular PMvr, is important for the motor control of the distal upper limb (Cerri et al., 2003; Dum and Strick, 2005; Gentilucci et al., 1988; He et al., 1993; Kurata and Tanji, 1986; Rizzolatti et al., 1988; Shimazu et al., 2004). These neural tract-tracing studies and ICMS studies indicate that premotor areas can influence the motor control either through M1 (Cerri et al., 2003; Maier et al., 2013; Schmidlin et al., 2008; Shimazu et al., 2004) or more directly as well through corticomotoneuronal projections (see below for more detail about corticomotoneuronal pathway) (Rouiller et al., 1996). Dum (2002) suggested that each premotor area works actually as a functionally distinct efferent system in parallel with M1 and is able to produce and control specific aspects of motor behaviour.

The premotor cortex (PM) and SMA are intimately involved in planning and programming sequences of movements, in particular complex motor sequences of the distal musculature, by integrating all the information they receive from the posterior parietal cortex. SMA activity is essential for the organisation of movements, particularly in case of a sequential performance of multiple movements as well as bilateral movements (Brinkman, 1984; Brinkman and Porter, 1979; Brinkman, 1981; Kazennikov et al., 1999; Kermadi et al., 1997; Kermadi et al., 1998; Kermadi et al., 2000; Larsson et al., 1996; Luders, 1996; Picard and Strick, 1996; Roland et al., 1980; Seitz and Roland, 1992; Shima

and Tanji, 1998a; Tanji, 1994; Wiesendanger, 1986). In addition, SMA is important for initiating self-paced sequences of movements (Kermadi et al., 1997; Larsson et al., 1996; Roland et al., 1980).

PM is involved in programming motor sequence as well (Kurata and Tanji, 1986; Rijntjes et al., 1999; Weinrich et al., 1984; Weinrich and Wise, 1982) but primarily based on external cues. For instance, it was demonstrated that the activity of PM is tightly linked to visuospatial signals and sensory guidance of movement (Picard and Strick, 1996; Weinrich et al., 1984; Weinrich and Wise, 1982). Moreover, PMv (F5) contains mirror neurons (di Pellegrino et al., 1992; Rizzolatti and Fogassi, 2014). Regarding PMvr in greater detail, this area is involved in goal-related (Rizzolatti et al., 1988) and visually-guided movements of the hand during fine manipulation of objects (Chouinard and Paus, 2006; Umilta et al., 2007), in coding for object shape (Murata et al., 1997), grasping movements (Bonini et al., 2010; Spinks et al., 2008; Umilta et al., 2007), grip type and object orientation (Fluet et al., 2010; Schaffelhofer et al., 2015; Townsend et al., 2011), reach and gaze representation (Lehmann and Scherberger, 2013), 3-D objects (Janssen and Scherberger, 2015), and in exerting a facilitatory effect on M1 output to upper limb motoneurons (Cerri et al., 2003; Maier et al., 2013; Schmidlin et al., 2008; Shimazu et al., 2004). This last observation suggests that PMvr may be involved in the control of grasp movements essentially through corticocortical projections to M1, and less through its corticospinal tract projections to motoneurons innervating hand muscles because these latter are few in number. In addition, it was recently demonstrated that PMv could also exert an inhibitory effect on M1 (Kraskov et al., 2011).

CMA, which is a part of the limbic system, plays a motor role as well, in particular in voluntary movements involving emotions and motivation (Craig, 2009; Craig, 2014). More specifically, the neuronal activity in CMA is modulated during selection of voluntary movements based on the expectation of a reward (Shima and Tanji, 1998b).

Motor pathways

In primates, the main descending pathways (for a definition of a descending pathway, see Lemon, 2008b) that project directly or indirectly on spinal cord motoneurons originate from the cerebral cortex and from the brainstem and terminate either within the dorsolateral or the ventromedial part of the intermediate zone of the spinal gray matter

(Kuypers, 1981; Kuypers, 1987; Kuypers and Brinkman, 1970). There are two major dorsolateral pathways, namely the ***lateral corticospinal tract***, originating from the cerebral cortex, and the ***rubrospinal tract***, coming from the red nucleus in the brainstem. They supply a monosynaptic and polysynaptic innervation largely on lateral motoneurons that can recruit small groups of distal muscles in order to exert a fine motor control. Regarding the ventromedial pathways, one can distinguish the ***ventral corticospinal tract***, coming from the cerebral cortex, the ***lateral*** and ***medial vestibulospinal tracts***, originating from the vestibular nuclei, the ***pontine*** and ***medullary reticulospinal tracts***, originating from the pontine and medullary reticular formations, respectively, and the ***tectospinal tract***, originating from the superior colliculus. These ventromedial pathways mainly supply innervation of medial and ventral motoneurons that control large groups of axial and proximal muscles, in order to regulate the body position and posture (Nicholls et al., 2001).

Corticospinal tract

The corticospinal tract (CST), also known as pyramidal tract, is the major descending motor pathway involved in voluntary motor control through skeletal muscles and its lateral component, in particular, plays a critical role in fine skilled movements of the hands and fingers (**Figure 17**) (for reviews, see Lemon, 2008b; and Schieber, 2007). To put it briefly, the CST projects from the cerebral cortex to the motoneurons located in the brainstem and in the spinal cord. This pathway can be either direct or indirect (via interneurons). The upper motoneurons are located in upper portion of the system, from the cerebral cortex to the anterior horn cells in the spinal cord. The lower motor neurons are located in the lower portion of the system, corresponding to the anterior horn cells and their associated axon.

It was conventionally established that the human CST tract originated exclusively from M1 although Penfield described in an early study that some movements were also elicited by postcentral electrical cortical stimulations in human patients (Penfield and Boldrey, 1937). But as described above, it is now well known that the upper motoneurons of the CST are located in several cortical areas of the frontal lobe (M1, SMA, PMd, PMv, CMAs) (**Figure 16A**) and parietal lobe (S1, posterior parietal cortex, parietal operculum (S2)) (Biber et al., 1978; Cheema et al., 1983; Coulter and Jones, 1977; Darian-

Smith et al., 1996b; Dum and Strick, 1991; Galea and Darian-Smith, 1994; He et al., 1993; He et al., 1995; Jones and Wise, 1977; Kumar et al., 2009; Lemon, 2008b; Lemon and Griffiths, 2005; Liu and Chambers, 1964; Maier et al., 2002; Nieuwenhuys et al., 2007; Nudo and Masterton, 1990; Ralston and Ralston, 1985; Rouiller et al., 1996; Schieber, 2007; Seo and Jang, 2013; Sessle and Wiesendanger, 1982; Toyoshima and Sakai, 1982; Wiesendanger, 1981). There are anatomical differences between the different CSTs: for instance, corticospinal fibres from M1 project mainly to the contralateral intermediate zone of the spinal cord and especially on lateral nuclei supplying the muscles for the upper limb (Armand et al., 1997), whereas corticospinal fibres from S1 project primarily to the contralateral dorsal horn (see below the section *Functional sensorimotor system* for greater detail). Moreover, there are considerably more axon terminals in the lamina IX (motor nuclei) from M1 than from SMA or the CMAs (Dum and Strick, 1996b; Schieber, 2007) and direct projection (corticomotoneuronal fibres, see below) from M1 are much denser and stronger than those from SMA (Boudrias et al., 2006; Maier et al., 2002; Rouiller et al., 1996). As a matter of fact, the multiple origins of the CSTs suggest that these pathways are involved in several functions, in addition to the execution of movements through the CST from M1 (Lemon, 2008b; Lemon and Griffiths, 2005). For instance, it has been shown that CST fibres from PMv do not reach the lower cervical cord (subserving hand muscles) in macaque monkeys but they rather terminate at more rostral cervical levels (He et al., 1993). Therefore it is expected that they do not directly exert a descending motor control through corticomotoneuronal neurons. In fact, it is now proposed that the CST from PMv may be involved in unwanted movement suppression during action observation since CST neurons with mirror properties were discovered in PMv (Kraskov et al., 2014; Kraskov et al., 2009; Rizzolatti and Fogassi, 2014; Vigneswaran et al., 2013). Regarding the CST originating from SMA, the existence of a direct CM projection strongly suggests that this pathway can contribute directly to the control of hand movements (Rouiller et al., 1996). More specifically, a very recent study demonstrated that this pathway is recruited when manual force control requires a high degree of precision (Chen et al., 2013). The putative function of CST originating from S1 will be developed below (see the section below *Functional sensorimotor system* for greater detail). In sum, corticospinal projections from non-primary cortical motor areas usually provide less direct access to motoneurons than the projection from M1 does (Schieber, 2007).

The upper motoneurons at the origin of the CST (**Figure 17A**) are mainly the pyramidal cells of cortical layer V (Biber et al., 1978; Jones and Wise, 1977; Nudo and Masterton, 1990; Schieber, 2007) made up of the Betz cells (**Figure 17B, C**), characterised by a large soma, and non-Betz pyramidal neurons. Very recently, it was demonstrated that the CST may contain much more very thin axonal fibres than reported until now, i.e. <1 µm in diameter as compared to large fibres up to 13 µm in diameter (Porter and Lemon, 1993), even though their origin and activity pattern are still not well understood (Firmin et al., 2014). The upper motoneurons give rise to axon bundles that descend via the posterior limb of internal capsule to the cerebral peduncle, on the ventral surface of the midbrain. The axon bundles branch among the transverse pontine fibres and the nuclei of the basal pontine gray matter by entering the pons via the base of the pons, and coalesce again by entering the pyramids, on the ventral surface of medulla. In the caudal part of the medulla, most pyramidal fibres (90%, but note that there are variations across studies) cross the midline (decussation of pyramids) and descend in the dorsolateral columns of the spinal cord on the opposite side to form the ***lateral CST***. But some fibres (8%) enter the spinal cord without crossing the midline (Darian-Smith, 2007; Galea and Darian-Smith, 1994) and travel then downward in the ipsilateral dorsolateral CST to form the ipsilateral ***lateral CST***. These projections are of prime importance in case of a lesion of the CST, by constituting a substrate for some functional recovery. Some other CST fibres descend bilaterally in the ventral funiculus to form the bilateral ***anterior CST*** (or ***ventral CST***) (2%) (Darian-Smith, 2007). These ventral CST fibres arise primarily from dorsal and medial regions of the motor cortex that subserve axial and proximal limb muscles, the same divisions of the motor cortex that give rise to projections to the reticular formation as well. Some anterior CST fibres send collateral branches through the midline via the ventral white commissure in the spinal cord to terminate in the contralateral ventral funiculus. The upper motoneurons of CST establish then synapses at the spinal cord level, mostly in the intermediate zone (contralateral fibres terminals in Rexed laminae I to IX, but most densely in lamina V-VII, vs ipsilateral fibres terminals in Rexed laminae V to X) (**Figure 17D**) (Cheema et al., 1984; Coulter and Jones, 1977; Lemon and Griffiths, 2005; Liu and Chambers, 1964; Morecraft et al., 2013; Ralston and Ralston, 1985; Schieber, 2007; Wiesendanger, 1969; Wiesendanger, 1981): lateral CST fibres synapse most predominantly on interneurons and α-motoneurons in the ipsilateral lateral gray matter of the spinal cord, present in the cer-

vical and lumbar enlargements (Biber et al., 1978). These α-motoneurons control distal limb muscles and are usually involved in phasic activities, for instance the fine manipulation of small objects. On the contrary, anterior CST fibres synapse mostly on interneurons in the anterior gray matter. The anterior α-motoneurons control more proximal and axial muscles and are mainly involved in sustained activities, for instance muscle control for stance and posture adjustments. Indeed, α-motoneurons show an orderly somatotopic organisation in the gray matter of the spinal cord (**Figure 17D, E**) (Bossy and Ferratier, 1968). Essentially, those α-motoneurons innervating extensor muscles are located more ventral than those α-motoneurons controlling flexor muscles. In addition, α-motoneurons innervating trunk muscles and proximal limb muscles, such as the shoulder musculature, are located on the medial and ventral parts of the ventral horn, respectively. Proceeding more laterally, ventral α-motoneurons innervate the arm and then the forearm musculature, respectively the thigh and then the leg musculature, and they are mostly controlled by interneurons travelling over many spinal cord segments. Finally, the lateral α-motoneurons in the cervical and lumbar enlargements control distal limb muscles, and are coordinated by short spinal interneurons, such as the system of C3–C4 propriospinal neurons.

Very recently, the existence of commissural premotor interneurons synapsing on cervical motoneurons (i.e. innervating intrinsic hand muscles) and receiving inputs from the periphery as well as from descending pathways was demonstrated in macaque monkeys (Soteropoulos et al., 2013). The authors suggested that these interneurons may represent a substrate of bilateral coordination during fine fractionated voluntary movements of the hands.

Figure 17 (next page): (A) Organisation of the corticospinal tract in human. The upper motoneuron fibres send collaterals to brainstem nuclei (cranial nerve nuclei, reticular formation, red nucleus, basilar pontine nuclei) (Lemon, 2008b) but they are not represented here. Note the direct projection of some corticospinal neurons on motoneurons in the lateral horn of the spinal cord (modified from Patestas and Gartner, 2013). (B) Histological photomicrograph of a SMI-32-stained frontal section in M1 cortex. Strongly stained neurons are Betz cells, in cortical layer V. Bar: 1 mm. (C) Magnification of the delineated rectangle in (B), showing 3 stained Betz cells. Bar: 100 µm. (D) Transverse section of the spinal cord showing projections of lateral and ventral corticospinal neurons on distinct pools of spinal α-motoneurons, based on the somatotopic organisation of α-motoneurons supplying the trunk, upper and lower extremities (from Patestas and Gartner, 2013). (E) Transverse section of the spinal cord showing the detail of the orderly somatotopic organisation of α-motoneurons in the ventral and lateral horns: muscles of the shoulder and arm, respectively thigh and leg, are represented most medially, while distal muscles are represented most laterally. Extensor muscles are controlled by α-motoneurons located in the most ventral part of the spinal gray matter while flexor muscles are controlled by more central α-motoneurons (from Patestas and Gartner, 2013).

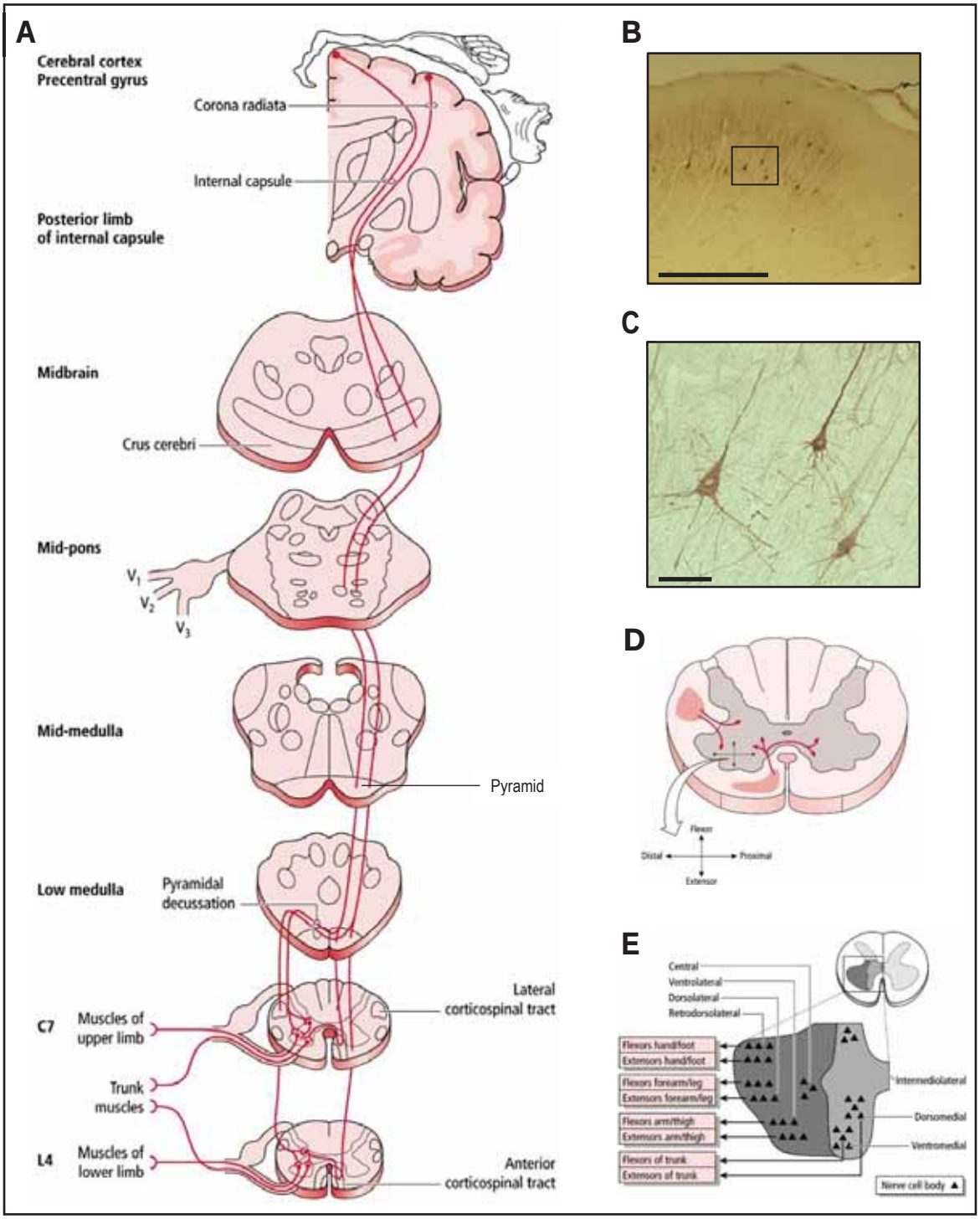

Of prime importance, many primates, among them macaque monkeys and human, developed a specialisation of the lateral CST during the evolution (see **Figure 7** in **Chapter 8**), the so-called ***corticomotoneuronal tract*** (CM tract): essentially, many upper motoneurons of the lateral CST establish direct monosynaptic excitatory projections on α-motoneurons innervating the distal limb muscles, especially hand muscles (Alstermark et al., 2004; Bennett and Lemon, 1996; Bernhard and Bohm, 1954; Cheney and Fetz,

1985; Courtine et al., 2007; Fetz et al., 1976; Fetz and Cheney, 1980; Lawrence et al., 1985; Lemon et al., 1991; Lemon, 1993; Lemon, 1997; for a review about Leyton's study, see Lemon, 2008a; Lemon, 2008b; Lemon and Griffiths, 2005; Leyton and Sherrington, 1917; Porter and Lemon, 1993; Rouiller et al., 1996; Wiesendanger, 1969), but also hindlimb distal muscles (see e.g. Asanuma et al., 1979a; Porter and Lemon, 1993) and tail muscles (Lemon, 2008b). In macaque monkeys, most of CST fibres terminate in the intermediate zone of the spinal gray matter but, in addition, in the cervical enlargement (and lombar enlargement as well), many CST fibres project more ventrally into the lamina IX of the spinal gray matter as well, where they establish then a direct synaptic connection with α-motoneurons (Dum and Strick, 1996b; Kuypers, 1982; Liu and Chambers, 1964; for greater detail, see Morecraft et al., 2013; Schieber, 2007). This direct motor cortical control on distal muscles allows the recruitment of small groups of muscles in a highly selective manner and thereby represents the anatomical support of the exquisite manual dexterity and independent finger movements that characterise some primates (Bennett and Lemon, 1996; Bernhard and Bohm, 1954; Bortoff and Strick, 1993; Buys et al., 1986; Darian-Smith et al., 1996a; Lawrence and Hopkins, 1976; Lemon et al., 1991; Lemon, 2008b; Lemon and Griffiths, 2005; Porter and Lemon, 1993). This is illustrated by their unique ability to perform the precision grip, i.e. the opposition of the thumb and another finger, usually the index finger (Napier, 1956; Napier, 1960; Napier, 1961; Napier, 1962). In addition, it was recently demonstrated that CM tract is also involved in tool use in macaque monkeys (Quallo et al., 2012). As a matter of fact, the CM pathway is a unique feature to primates and is especially well developed in the most skillful species (Courtine et al., 2007). But note that even in these species, the CM pathway coexists with the indirect CST, involving segmental interneurons and propriospinal neurons (Lemon, 2008b). CM fibres control mainly distal, intrinsic hand muscles (Buys et al., 1986; Lemon et al., 1986; Maier et al., 2002; Nakajima et al., 2000) and, to a lesser extent, upper limb proximal muscles (de Noordhout et al., 1999; Lemon, 2008b; Lemon and Griffiths, 2005). In addition, CM fibres from M1 are more numerous and activate α-motoneurons for upper limb muscles in a stronger way than CM fibres from SMA (Maier et al., 2002).

As a consequence, the interruption of the lateral CST in human or in non-human primates (either by section of the spinal cord or cortical lesion, usually in M1) results immediately in a dramatic loss of the ability to perform independent finger movements and consequently in a strong impairment to perform fine skilled movements with the

hand (**Figure 18**) (Freund et al., 2007; Hepp-Reymond, 1988; Hoogewoud et al., 2013; Kaeser et al., 2010; Kaeser et al., 2011; Kazennikov et al., 1998; Kermadi et al., 1997; Kuypers, 1974; Kuypers, 1981; Kuypers, 1987; Lawrence and Kuypers, 1968a; Lemon et al., 2012; Liu and Rouiller, 1999; Rouiller et al., 1998; Rouiller and Olivier, 2004; Wyss et al., 2013).

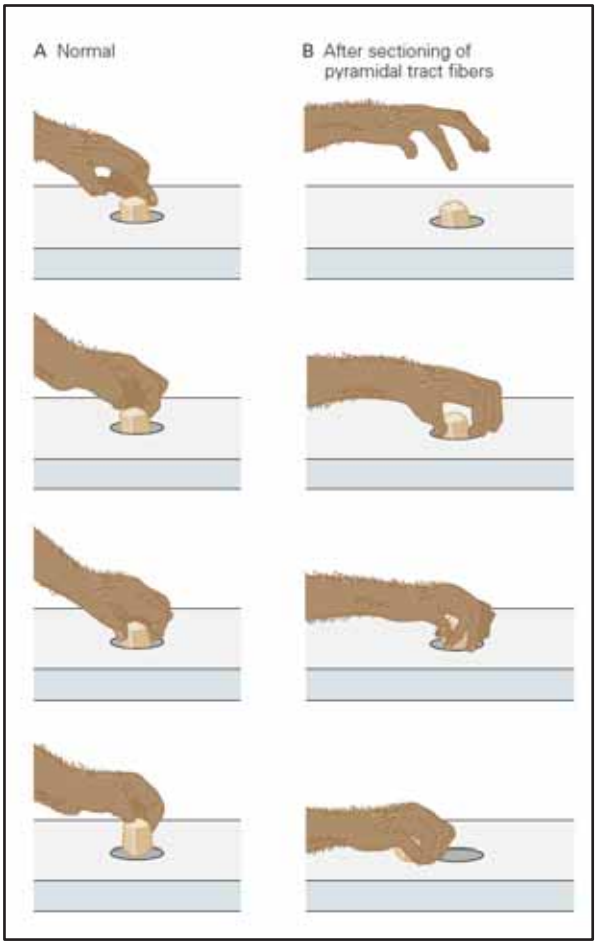

Figure 18 : Successive schematic frames reproduced from the seminal work of Lawrence and Kuypers (Lawrence and Kuypers, 1968a), demonstrating that the corticospinal tract subserves fine and individuated finger movements, such as the precision grip. (A) Intact monkey grasping a small food morsel from a well on a Klüver board by using the precision grip. (B) Following a bilateral section (here 5 months after the lesion) of the pyramidal tract (inducing thereby the loss of the direct control by the corticomotoneuronal fibres), the animal is not able any more to produce individuated finger movements, but can only remove food from the well by grabbing it with the whole hand (power grasp) (from Kalaska and Rizzolatti, 2013, p. 847).

Other descending pathways

Even though the CST is undoubtedly the major descending pathway in intact primates, there is now a growing body of evidence that some of the other descending pathways, originating from the brainstem, establish monosynaptic projections to motoneurons innervating distal muscles as well: the rubrospinal tract, the reticulospinal tract and the vestibulospinal tract (Cheney et al., 1991; Lemon, 2008b; Lemon and Griffiths, 2005). These tracts may play an important role in voluntary hand motor control, in parallel with the CST. Note that these pathways are under the control of motor cortex as well.

Regarding dorsolateral descending pathways, the ***rubrospinal tract*** (**Figure 19A**) is particularly well developed in cats (Fujito et al., 1991; Fujito and Aoki, 1995; Pettersson et al., 1997) but probably not as prominent in primates, especially in human (Kennedy, 1990; Nathan and Smith, 1982) because of the increasing significance of the CST and especially the CM pathway during the evolution of primates. The rubrospinal tract emerges from the magnocellular part of the red nucleus, a somatotopically organised structure located in the ventral midbrain (Murray and Haines, 1975) that receives excitatory inputs from the motor cortex and the cerebellum (Humphrey et al., 1984). Then, rubrospinal fibres cross the midline in the ventral midbrain (ventral tegmental decussation) and project down along the spinal cord to synapse on contralateral interneurons in the dorsolateral region of the intermediate zone of the spinal horn and, in some cases, directly on lateral α-motoneurons innervating distal muscles (Cheney, 1980; Isa et al., 2013; Kuypers, 1981; Kuypers, 1987; Lemon, 2008b; Shapovalov et al., 1971). This pathway primarily controls proximal and axial muscles and is usually involved in gross automated movements, such as the maintenance of body orientation and posture (Deliagina et al., 2014). Moreover, it has been demonstrated in lesion studies that this pathway can compensate to some extent for the loss of descending CST input. For instance, in one of their famous experiments, Lawrence and Kuypers (1968a) lesioned bilaterally the CST of rhesus monkeys. After an initial strong impairment of hand motor control, the animals progressively recovered some manual dexterity although individuated finger movements remained largely affected. Then, in case these monkeys were subjected to a second lesion targeted now towards the rubrospinal tract, manual dexterity was again completely abolished but never recovered subsequently (Lawrence and Kuypers, 1968b). In another study where monkeys were subjected to a cervical spinal cord injury, Belhaj-Saïf and Cheney (2000) observed some post-lesion reorganisation in the magnocellular red nucleus that may have contributed to the spontaneous functional recovery of the forelimb that had been observed in these animals. These results associated with others (Cheney et al., 1991; Kennedy, 1990) strongly suggest that the rubrospinal tract can in part duplicate some functions of the CST if the latter is lesioned and consequently that the rubrospinal tract may play an important role in voluntary hand motor control, in parallel with the CST.

Regarding now ventromedial descending pathways, the ***pontine*** (or ***medial***) ***reticulospinal tract*** (**Figure 19A**) originates from the reticular formation in the pons and de-

scends ipsilaterally to project on segmental interneurons. These latter establish then bilateral excitatory projections on medial extensor motoneurons and thereby enhance antigravity reflexes. The ***medullary*** (or ***lateral***) ***reticulospinal tract*** (**Figure 19A**) originates from the reticular formation in the medulla and travels bilaterally down the spinal cord to inhibit motoneurons innervating the proximal limbs, thus inhibiting antigravity reflexes (Nicholls et al., 2001). In sum, both pathways are mainly involved in the control of proximal and axial muscles, and are usually the substrate for gross movements such as locomotion (Matsuyama et al., 2004), reaching and postural correction (Lemon, 2008b). However, the reticulospinal tract modulates its activity during the execution of fine movements of the hand (Soteropoulos et al., 2012) and some fibres from the reticular formation can also establish direct excitatory projections on motoneurons innervating distal hand muscles (Baker, 2011; Riddle et al., 2009) that may influence hand movements (for a review, see Baker et al., 2015).

Regarding the vestibulospinal tract, the ***lateral vestibulospinal tract*** (**Figure 19B**) originates from the lateral vestibular nucleus that receives itself information from the ipsilateral utricles of the labyrinth and from the cerebellum. The lateral vestibulospinal tract descends in the ipsilateral spinal cord to the anterior spinal gray matter innervating the axial and proximal limb muscles and establishes a monosynaptic excitatory projection on motoneurons innervating extensor muscles and a disynaptic inhibitory projection on motoneurons innervating flexor muscles. This tract is mainly involved in postural maintenance and in the regulation of extensor tone (Nicholls et al., 2001; Purves et al., 2008). The ***medial vestibulospinal tract*** (**Figure 19B**) emerges from the medial vestibular nucleus, itself getting inputs from the semicircular canals of the vestibular system and from stretch receptors located in the neck musculature. The medial vestibulospinal tract projects ipsilaterally through the medial longitudinal fasciculus to the medial part of the ventral gray matter in the cervical-midthoracic spinal segments to adjust the posture of the neck (Sugiuchi et al., 2004) and upper limbs during angular acceleration (Nicholls et al., 2001). In addition, some vestibulospinal fibres also make synaptic connections with motoneurons supplying distal limb muscles (Cheney et al., 1991).

The ***tectospinal tract*** (**Figure 19C**) originates from the superior colliculus. These axons travel around the periaqueductal gray, decussate (dorsal tegmental decussation), join the medial longitudinal fasciculus in the medulla, and project down along the anterior

funiculus of the spinal cord to upper cervical segments of the spinal cord. This tract is involved in directing head and eye movements in response to visual and auditory stimuli (Nicholls et al., 2001).

Finally, the role of cortical excitation to upper limb motoneurons by the system of C3–C4 propriospinal neurons in the macaque monkey is still under debate, some studies demonstrating its involvement (Isa et al., 2007; Isa et al., 2013; Kinoshita et al., 2012; Sasaki et al., 2004) but another infirming its presence (Olivier et al., 2001) (for a review, see Baker et al., 2015).

Figure 19 (next page): (A) Rubrospinal tract and reticulospinal tracts. (B) Vestibulospinal tracts. MLF: medial longitudinal fasciculus. (C) Tectospinal tract. Note that all these pathways also receive descending cortical inputs but they are not represented here (from Patestas and Gartner, 2013).

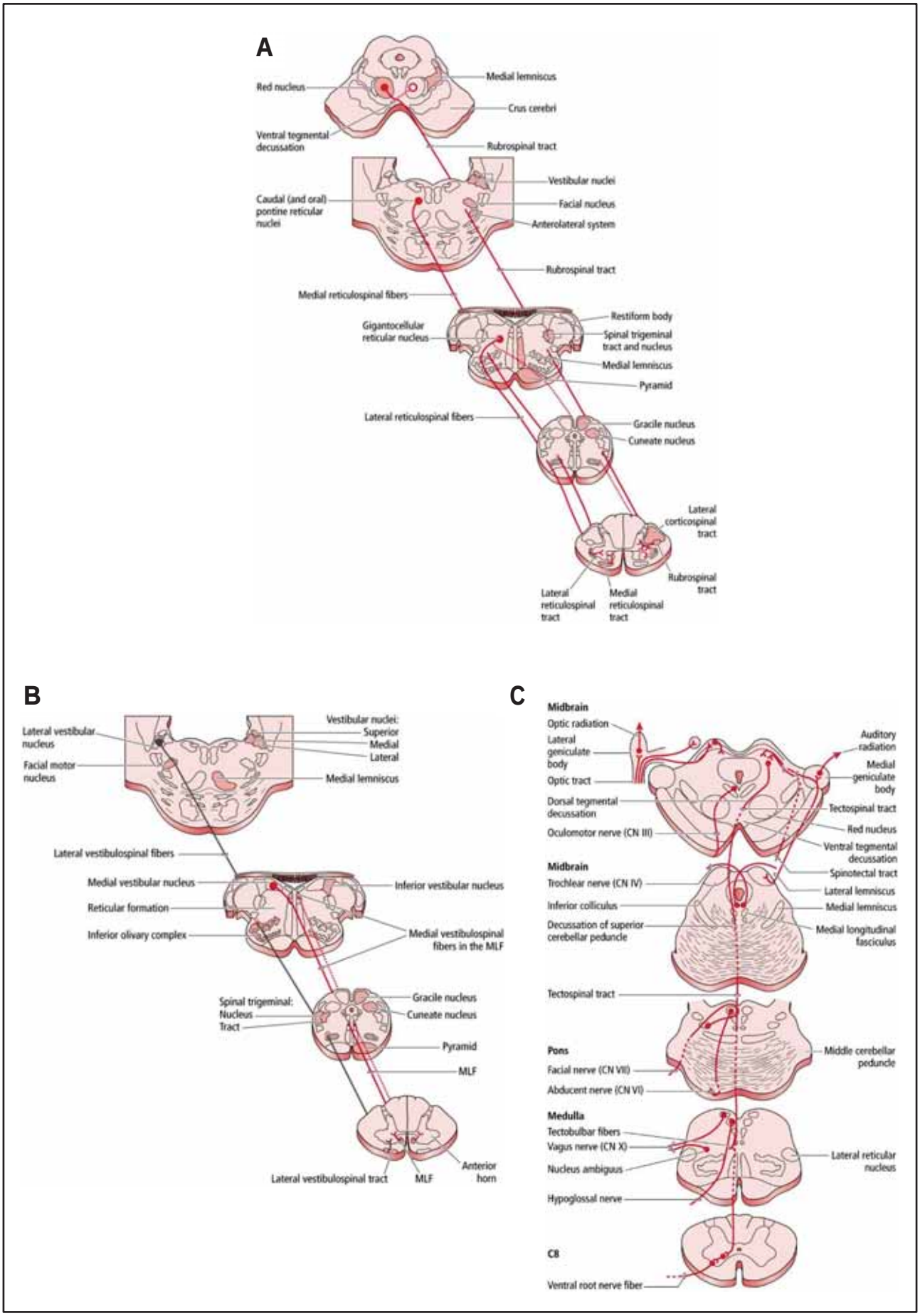
A
Red nucleus
Medial lemniscus
Crus cerebri
Ventral tegmental decussation
Rubrospinal tract
Vestibular nuclei
Caudal (and oral) pontine reticular nuclei
Facial nucleus
Anterolateral system
Rubrospinal tract
Medial reticulospinal fibers
Restiform body
Gigantocellular reticular nucleus
Spinal trigeminal tract and nucleus
Medial lemniscus
Pyramid
Lateral reticulospinal fibers
Gracile nucleus
Cuneate nucleus
Lateral corticospinal tract
Rubrospinal tract
Lateral reticulospinal tract
Medial reticulospinal tract
B
Lateral vestibular nucleus
Vestibular nuclei:
Superior
Medial
Lateral
Facial motor nucleus
Medial lemniscus
Lateral vestibulospinal fibers
Medial vestibular nucleus
Inferior vestibular nucleus
Reticular formation
Inferior olivary complex
Medial vestibulospinal fibers in the MLF
Spinal trigeminal:
Nucleus
Tract
Gracile nucleus
Cuneate nucleus
Pyramid
MLF
Lateral vestibulospinal tract
MLF
Anterior horn
C
Midbrain
Optic radiation
Lateral geniculate body
Optic tract
Auditory radiation
Medial geniculate body
Dorsal tegmental decussation
Tectospinal tract
Oculomotor nerve (CN III)
Red nucleus
Ventral tegmental decussation
Midbrain
Trochlear nerve (CN IV)
Spinotectal tract
Lateral lemniscus
Inferior colliculus
Medial lemniscus
Decussation of superior cerebellar peduncle
Medial longitudinal fasciculus
Tectospinal tract
Pons
Middle cerebellar peduncle
Facial nerve (CN VII)
Abducent nerve (CN VI)
Medulla
Tectobulbar fibers
Vagus nerve (CN X)
Lateral reticular nucleus
Nucleus ambiguus
Hypoglossal nerve
C8
Ventral root nerve fiber

Riddle and Baker (2010) showed that the reticulospinal tract, medial vestibulospinal tract and tectospinal tract largely parallel the CST that projects on spinal interneurons in the cervical spinal cord of rhesus monkeys, i.e. involved in the indirect control of hand muscles. The authors suggested that these indirect pathways as well may be involved in functional recovery after a lesion of the CST. This was confirmed later in monkeys subjected to a CST lesion: mono- and disynaptic EPSPs elicited from the medial longitudinal fasciculus (contains reticulospinal, medial vestibulospinal, and some tectospinal fibres) were significantly larger after recovery in motor neurons innervating forearm flexor and intrinsic hand muscles. Conversely no new connections from the intact ipsilateral CST were observed. They concluded that the reticulospinal tract, in particular, was most probably involved in some functional recovery after the lesion (Zaaimi et al., 2012).

In sum, in case of a lesion affecting the CST in primates, other motor pathways, especially the rubrospinal pathway and the reticulospinal pathway, may influence, at least in part, upper limb motor control and thereby may be involved in the functional recovery by assuming some motor control previously predominantly achieved by the CST.

Voluntary hand motor control

The role of the brain is to generate our behaviour, among them voluntary movements. M1, the association motor areas and the somatosensory areas all are involved in motor control but each with a different role (as well as basal ganglia and the cerebellum). During the execution of simple voluntary movements, the brain activity is restricted to M1 and S1 (Roland et al., 1980). But in case of more demanding tasks, the generation of complex movements requires the involvement of other brain areas (Georgopoulos, 1991; Larsson et al., 1996; Roland et al., 1980; Seitz and Roland, 1992), among them the aforementioned association motor areas. These areas have dense reciprocal connections with several other brain areas in the parietal lobe and in the prefrontal lobe which represent the highest levels in motor control hierarchy because they are involved in the decision of action choice and in the anticipation of the likely outcome. In particular, grasping an object with the hand constitutes a highly complex sensorimotor process (Janssen and Scherberger, 2015). Visual inputs, for instance, are of prime importance: the brain needs information about the precise spatial location of the object in relation to the hand as well as information about the intrinsic properties of the object (Davare et al., 2011).

Then premotor areas integrate sensory information and motor programs into an appropriate motor command to produce the hand movement.

For reminder, M1 is supplied with somatosensory information directly from the somatosensory cortex as well as from premotor areas. These latter receive strong inputs from the association sensory areas such as the posterior parietal region, where multimodal integration takes place (see **Figure 14**), for instance regarding the spatial perception of the position of the body and limbs (proprioception). To elaborate, to perform a movement, the motor system needs a spatial coordinate system that is provided in part from motor areas themselves (Kakei et al., 1999) but also from association areas in the parietal lobe that integrate many sensory modalities (Brozzoli et al., 2011; Fogassi and Luppino, 2005; Matelli and Luppino, 2001; Mountcastle et al., 1975; Mountcastle, 1995; Rizzolatti et al., 1997).

Visual information about the object to be grasped is conveyed from the visual cortex to association areas along two processing paths. Briefly, the more ventral pathway projects on the inferotemporal cortex and is involved in object recognition by providing information about the visual properties of the objects to be grasped (i.e. size, colour, form, …) and these inputs are used to direct reaching and grasping behaviour. This information may be probably then conveyed towards posterior parietal cortex, in the anterior intraparietal area (AIP) (Davare et al., 2011; Janssen and Scherberger, 2015). The more dorsal pathway terminates in the posterior parietal cortex, in particular in AIP, and is involved in the control of specific movements and in visuomotor transformation by providing information to act on objects and to locate them in space (Rizzolatti and Strick, 2013). Thereby AIP is a key structure for processing grasp-related object properties because inputs from both dorsal and ventral visual pathways may converge there (Davare et al., 2011; Janssen and Scherberger, 2015). From then on, the resulting multisensory integrated information is sent to premotor areas, in particular to PMv, through reciprocal connections (Davare et al., 2011; Janssen and Scherberger, 2015; Tanné-Gariépy et al., 2002). As mentioned above, premotor areas are linked with planning and programming complex motor sequences such as hand movements. They integrate the representations from the external environment with intentions and motor plans, and work with the cerebellum in order to identify from the available motor repertoire the precise sequence of muscle contractions that is needed to achieve the planned motor ac-

tion. In sum, the AIP–PMv (F5) network is essential in the motor planning and control (with M1) of visually guided grasp because it is tightly interconnected with other parietal, premotor and prefrontal areas as well as subcortical structures and thereby receives all intentional inputs, perceptual inputs and spatial object information (Davare et al., 2011; Davare et al., 2008; Davare et al., 2009; Janssen and Scherberger, 2015).

Then, the motor program is transmitted from premotor areas to the M1 hand representation, through strong reciprocal connections, for the motor execution itself (Davare et al., 2011; Davare et al., 2009; Kraskov et al., 2011; Umilta et al., 2007). In case of fine hand movement, the projection from PMv on M1 is the predominant frontal input to M1 (Dum and Strick, 2005). M1 commands the precise contractions of all muscles needed for the given action (Cheney and Fetz, 1985; Fetz et al., 1976; Fetz and Cheney, 1980) by projecting descending fibres through the brainstem and the spinal cord. To this end, M1 is involved in coding many aspects of movements: M1 neurons clearly show movement-related activity, for instance by discharging preferentially during flexion or extension of the wrist (Evarts, 1968), by coding for the amplitude of muscle forces (Wannier et al., 1991), by coding the posture of the hand (Kakei et al., 1999), by coding in detail the trajectory of movements (Hocherman and Wise, 1990), by broadly coding the movement direction (at the population level) and the final position of the hand (Amirikian and Georgopoulos, 2000; Caminiti et al., 1990; Georgopoulos et al., 1982; Georgopoulos, 1994; Georgopoulos et al., 2007; Georgopoulos, 2014; Merchant et al., 2008; Schwartz et al., 1988; Scott and Kalaska, 1995). Moreover, some neurons clearly show a change in tuning from spatial location to muscle activity, by first encoding the location of a target, and later encoding the resulting movement towards the target (Shen and Alexander, 1997). In addition, some M1 neurons specifically code a chosen category of tactile stimulus, meaning that decision making takes place in M1 as well (Salinas and Romo, 1998). M1 sends this elaborated motor command to interneurons and motoneurons in the brainstem and spinal cord that produce the intended movement and the postural adjustments that accompany it.

Functional sensorimotor system in primates

The sensorimotor cortex is well documented in rodents (Diamond et al., 2008; Feldmeyer et al., 2013; Ferezou et al., 2007; Petersen, 2009) and in marsupial mammals (Frost et al., 2000; for a review, see Kaas, 2004b; Lende, 1963) but the use of the expression "sensorimotor cortex" or even "sensorimotor system" in primates may appear strange because the common practice is to split the somatosensory system on the one side and the motor system on the other side, as usually seen with individual large sections dedicated to each of them in most Neuroscience reference textbooks (see e.g. Kandel et al., 2013; Purves et al., 2008; Squire et al., 2012). Moreover, the macroscopic separation by the central sulcus may be interpreted as a strong boundary between motor and somatosensory areas.

Nevertheless, there is strong evidence that somatosensory and motor systems are divisions of a larger, more complex functional and global sensorimotor system and thus that they participate together to the motor control, as summarised by Wiesendanger (1981):

"In a general way, the dichotomy in "motor" and "sensory" is perhaps not very meaningful, since processing of sensory information usually leads to motor behavior. In this sense the term sensorimotor is certainly justified. "

Simply put, the somatosensory cortical areas are not purely sensory areas and the motor areas are not exclusively motor areas but somatosensory and motor cortical areas of the primate brain are functionally linked into a global sensorimotor system that integrates somatosensory information from the periphery into movement production, a process called sensorimotor integration. In the following sections, we will present a brief historical review followed by more recent evidence in favour of the existence of a sensorimotor system in primates.

Emergence of the concept of *sensorimotor cortex* in primates

The concept of sensorimotor cortex in primates is not new. Historically, the first experiments investigating the pericentral region led to the well accepted idea of a broad, overlapping sensorimotor cortex. For instance, by electrically stimulating some parts of the brain in monkeys, Ferrier already noticed in 1876 that it was possible to elicit some

movements from the postcentral cortex, in addition to the precentral cortex (Ferrier, 1876). Then, in 1878, Luciani and Tamburini were the firsts to introduce the concept of a combined sensorimotor cortex, based on their investigation on the localisation of brain functions and on epilepsy (Luciani and Tamburini, 1878). At the same time, other neurosurgeons investigating brain functions, such as Mills (**Figure 20A**), also observed that movements of the body were elicited by electrically stimulating the precentral gyrus and the postcentral gyrus, either on epileptic patients or on animals (for a historical review, see Uematsu et al., 1992).

The original idea of a discrete precentral motor cortex completely separated from a postcentral sensory cortex was originally proposed by Charles Sherrington, a surgeon who actually attempted to delimit the motor and sensory cortices, by performing electrical stimulation of the precentral cortex and histological analyses (**Figure 20B**) (Grünbaum and Sherrington, 1901; Leyton and Sherrington, 1917). His colleague Harvey Cushing, one of the first modern neurosurgeons, confirmed Sherrington's ideas by locating the somatosensory cortex only in the postcentral gyrus, and was the first to use the term "narrow motor strip" to describe the motor cortex (**Figure 20C**) (for a historical review, see Uematsu et al., 1992). Even though there were some oppositions from other scientists, the conception of a purely precentral motor cortex and a separate postcentral somatosensory cortex proposed by Sherrington became accepted as the rule by most neuroscientists at that time.

Figure 20 (next page): (A) Map of the human brain drawn by the neurosurgeon Mills, in 1888. The face, finger, wrist, elbow, shoulder, hip, knee, foot, and toe motor representations extended over both pre- and postcentral gyri (from Uematsu et al., 1992). (B) Map of the chimpanzee's brain drawn by Sherrington, in 1901. The location of the motor cortex, strictly restricted to the precentral gyrus, is depicted by steeples and the different representations are indicated in red. Many stimulated sites evoking a motor response were located in the depth of the sulci as well. This map became a standard for teaching. Note that Sherrington already noticed that many representations were actually overlapping but this pattern was impossible to be represented on such a drawing (from Grünbaum and Sherrington, 1901). (C) Map of the human motor and sensory cortices drawn by the neurosurgeon Cushing, in 1906. The motor representations (in red) are restricted to the precentral gyrus and the somatosensory representations to the postcentral gyrus (in blue). We are indebted to Cushing for the use of the red colour to represent the motor cortex

and the blue colour to represent the somatosensory cortex, a colour code that is still commonly used in some modern textbooks (from Uematsu et al., 1992).

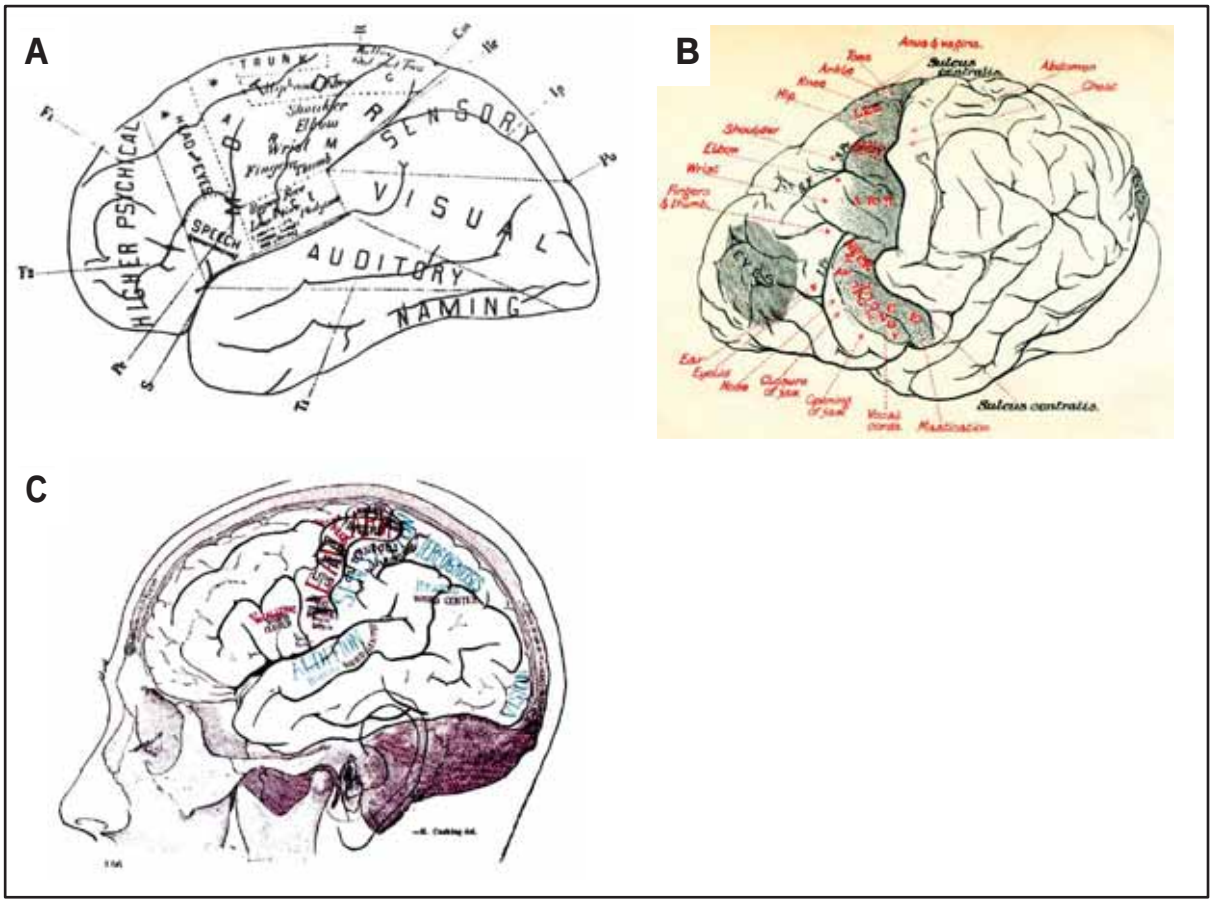

From the 1920s, more extensive electrical brain stimulation studies (e.g. Foerster, 1936; Vogt and Vogt, 1926) and histological studies (e.g. Vogt and Vogt, 1926) were performed on human patients and the original idea of a much more complex and broader motor representation became popular again. Based on his results from electrical brain stimulations on epileptic patients, Penfield wrote: "*Often we have found it impossible to confine functional representation within strict cytoarchitectural boundaries*." (Penfield and Boldrey, 1937). Then, Woolsey performed similar detailed brain mapping on macaque monkeys, among others, and he observed that somatosensory and motor functions of the cortex were not segregated into separate cortical areas (Woolsey et al., 1953; Woolsey et al., 1952; Woolsey, 1958; Woolsey, 1964). For instance, even after the complete ablation of the precentral gyrus and SMA, electrical stimulation of the postcentral gyrus elicited well-organised motor responses (Woolsey et al., 1953). Moreover, by using electrical stimulation of the medullary pyramid in macaque monkeys, Woolsey also

noticed that antidromic brain activation was not restricted to the precentral gyrus and SMA, but the whole parietal lobe was activated as well (Woolsey and Chang, 1947).

Regarding somatosensory activity in M1, Penfield and Boldrey (1937) observed during surgeries on human epileptic patients that it was actually possible to elicit tactile sensation by electrically stimulating the cortical surface over M1 such that one sixth of the sensations felt in fingers were evoked by stimulating the precentral gyrus. Similarly, Woolsey (1958) reported that evoked responses were recorded in the precentral gyrus of monkeys, in addition to the well-established potentials in the postcentral gyrus, following stimulation of a spinal dorsal root ganglion in monkey.

Based on his observations, Woolsey (1964) proposed the denomination of somatic sensory-motor area I (Sm I) for the postcentral gyrus, somatic sensory-motor area II (Sm II) for the secondary sensory area (S2), somatic motor-sensory area I (Ms I) for the precentral motor area, and somatic motor-sensory area II (Ms II) for SMA.

M1 and S1 have dense reciprocal anatomical connections

In primates, motor areas and somatosensory areas from the same hemisphere are densely anatomically interconnected, in particular M1 and S1 (Kaas, 2004a; Kaas, 2004b).

Evidence of extensive reciprocal fibres connections between M1 and S1 was obtained in macaque monkeys (Cole and Glees, 1954; for a review, see Jones, 1999; Jones and Powell, 1969; Jones and Powell, 1970; Vogt and Pandya, 1978) by studying the pattern of Wallerian axonal degeneration from a given brain region by damaging that region (for instance by using the Swank-Davenport Marchi method for staining degenerated myelinated fibres, or the Nauta technique using reduced silver impregnation for the staining of myelinated or unmyelinated degenerated axons (Bancroft and Gamble, 2008)). Then deeper insights were obtained among others by means of anterograde and retrograde labelling in several monkey species: in sum, reciprocal connections were observed between the different cytoarchitectonic areas 1, 2, 3a, 3b, 5 and 7 with the area 4 (see e.g. Burton and Fabri, 1995; Darian-Smith et al., 1993; Huerta and Pons, 1990; Huffman and Krubitzer, 2001; Jones et al., 1978; Jones and Porter, 1980; Jones, 1986; Künzle, 1978; Leichnetz, 1986; Liao et al., 2013; Stepniewska et al., 1993; Tokuno and Tanji, 1993).

Remarkably, it was demonstrated that fibres interconnecting S1 and M1 were organised in a somatotopic manner, meaning that representations of the same body part are usually interconnected (Burton and Fabri, 1995; Huerta and Pons, 1990; Jones et al., 1978; Jones and Porter, 1980; Jones and Powell, 1968; Jones, 1986; Stepniewska et al., 1993; Tokuno and Tanji, 1993). Consequently, CST neurons in M1 hand representation get a complete somatosensory representation of the hand (Lemon, 2010), during both passive and active movements (Lemon, 1981). Nevertheless, there were some exceptions as well. For instance, in addition to the somatotopic and homotopic organisation of fibres between the area 4 and the areas 3, 1, 2 and 5 in macaque monkeys, Künzle (1978) observed that there were some heterotopic projections from M1 to S1 as well, for instance from the M1 leg representation to the S1 finger representation or from the M1 face representation to the S1 toe representation.

It is well known that the motor cortex of primates can be divided into a rostral part (M1r) and a caudal part (M1c), both containing a motor representation of the hand (see e.g. Geyer et al., 1996; Rathelot and Strick, 2009; Strick and Preston, 1982a; Strick and Preston, 1982b; Strick and Preston, 1978a). Differences were reported concerning their connectivity with somatosensory areas. In non-human primates such as owl monkeys, M1c has been shown to be connected mainly with the somatosensory areas 3a, 1, S2, PV area and to a lesser extent to areas 2 and 3b. On the other hand, M1r has connections mostly with the areas 2 and S2 and to a lesser extent with areas 1, 3a, 5 and 7b (Stepniewska et al., 1993). Strick and Preston (1978b) also demonstrated that in squirrel monkeys, cutaneous inputs primarily project to M1c while deep inputs mainly project to M1r.

Some authors examined the M1-S1 connections at the laminar level in greater detail. For instance, Sloper (1973) combined electron microscopy and a modified Nauta technique in rhesus monkeys and demonstrated that afferent S1 neurons (comprised between the postcentral gyrus and the anterior bank of the intraparietal sulcus) connected M1 neurons in all the cortical layer of this area, but however predominantly in the upper half of M1 cortex. Moreover, he observed that 82% of asymmetric axo-dendritic synapses from S1 axons terminated on dendritic spines belonging most probably to pyramidal cells, i.e. on M1 efferent neurons, and only 18% on dendritic shafts of large stellate cells. Later, Ghosh and Porter (1988) stimulated the cortical surface of S1 in macaque monkeys and

labelled the neurons responding orthodromically to such stimuli by using intracellular ionophoresis of horseradish peroxidase. The resulting strongest labelling was observed in pyramidal layers III and V of M1. In addition, they reported that M1 pyramidal neurons were excited at short latency by stimulation of the somatosensory cortex (1.1-6.5 ms), confirming that S1 sends strong monosynaptic inputs onto M1 efferent neurons. Then, Huerta and Pons (1990) used retrograde labelling from restricted portions of M1 in order to study in particular muscle inputs from the area 3a. They showed that afferent projections from the area 3a primarily originated from layer III, with fewer cells labelled in layers V and IV of area 3a as well. In sum, the aforementioned studies confirmed that M1 and S1 are densely interconnected and a large proportion of projection neurons in M1 receives direct inputs from S1. Moreover, somatosensory inputs are conveyed to M1 directly through the thalamus as well (Jones, 1987; Lemon, 1981, see the *Introduction* of **Chapter 3** for greater detail).

The somatosensory cortical areas contribute to movements

Woolsey's and Penfield's observations were carried out by using massive electrical stimulations at the surface of the cortex. Their results were later confirmed thanks to the development of ICMS, allowing a cortical mapping with finer resolution: in owl monkeys, stimulation in areas 3a and 3b, for instance, elicited some movements, even though the stimulation threshold was higher than in M1 (Lemon and Van der Burg, 1979; Preuss et al., 1996). Note however that higher stimulation thresholds were required to produce movements from the postcentral gyrus with ICMS in macaque monkeys (Sessle and Wiesendanger, 1982). Moreover, electrical stimulation of the postcentral gyrus following ablation of the precentral cortex remained effective to elicit movements, probably ruling out that the postcentral motor effects were only the result of electrical spread of the stimulus to the precentral cortex or resulted from cortico-cortical transmission (Woolsey et al., 1953).

According to Rizzolatti (1998), the electrical excitability of a brain area (providing correct stimulation parameters) is correlated with the presence of CST neurons in this latter. Indeed, as already described above, the lamina V in somatosensory cortical areas (S1, S2, posterior parietal cortex) does contain CST neurons (Biber et al., 1978; Cheema et al., 1983; Cole and Glees, 1954; Coulter and Jones, 1977; Darian-Smith et al., 1996b;

Galea and Darian-Smith, 1994; Jones and Wise, 1977; Kumar et al., 2009; Lemon, 1997; Lemon, 2008b; Lemon and Griffiths, 2005; Nieuwenhuys et al., 2007; Nudo and Masterton, 1990; Ralston and Ralston, 1985; Schieber, 2007; Seo and Jang, 2013; Sessle and Wiesendanger, 1982; Toyoshima and Sakai, 1982; Wiesendanger, 1981). These CST fibres from the parietal lobe descend in the capsula interna more posteriorly than CST from M1 (Schieber, 2007). Investigations on macaque monkeys revealed some differences between the CST from S1 and the CST from M1: first, the mean surface of the corticospinal cell soma was observed to be smaller in the areas 3a, 3b, 1 and 2 than in the area 4. Nevertheless, none corticospinal S1 cell was smaller than the smallest corticospinal cells in the area 4 (Jones and Wise, 1977). Second, clusters of corticospinal cells usually contained fewer cells in the 4 areas of S1 than in the area 4 (Jones and Wise, 1977). Third, the corticospinal projection from S1 terminated mainly in the dorsal horn of the contralateral spinal cord (from Rexed lamina I to VII, but primarily in Rexed laminae III-VI) as compared to the intermediate zone for CST from M1 (from Rexed lamina I to IX, but most densely in laminae V-VII) (**Figure 21**) (Cheema et al., 1984; Coulter and Jones, 1977; Lemon and Griffiths, 2005; Liu and Chambers, 1964; Morecraft et al., 2013; Ralston and Ralston, 1985; Schieber, 2007; Wiesendanger, 1969; Wiesendanger, 1981). Ralston and Ralston (1985) also reported few ipsilateral CST fibres from S1. Galea and Darian-Smith (1994) estimated in macaque monkeys the contribution of each cortical origin to the CST to be (% of total CST population): 2.2% from the area 3a, 9% from the areas 3b/1, 13% from the areas 2/5 and 3.4% from the area S2/insula (as compared to 35% from M1, 6% from PMd, 2.6% from PMv, 15% from SMA, and 10% from CMA among others).

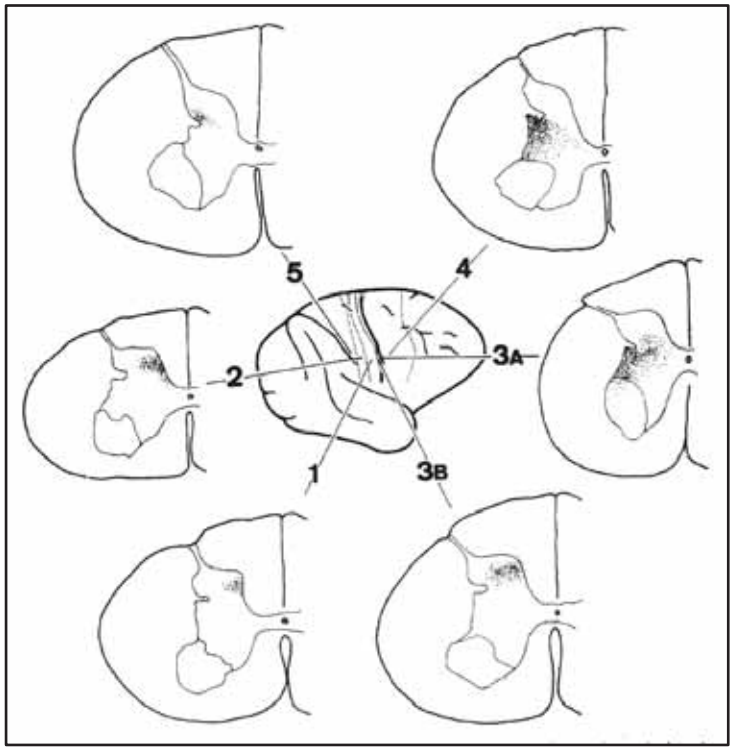

Figure 21: Differential distribution of corticospinal projection from M1 and S1 in the cynomolgus monkey's spinal cord assessed by means of terminal labelling (stipple) following injections of the anterograde tracer horseradish peroxidase individually in the areas 1, 2, 3a, 3b, 4 and 5. Each spinal reconstruction was obtained from 5 sections (1-mm interval) in the cervical enlargement (from Coulter and Jones, 1977).

Recently, by using diffusion tensor imaging (DTI), Seo and Jang (2013) were able to reconstruct the different cortical origins of the human CST in M1, S1, SMA and PM. Interestingly, the authors showed that M1 and S1 send CST projections with similar DTI properties, namely the fractional anisotropy (measure of the directional dependence of water molecule diffusion within nervous system tissues, depends e.g. on the axonal integrity, myelination, axon diameter and density (Zatorre et al., 2012)) and mean diffusivity (i.e. the magnitude of free diffusion of water molecules). Moreover, by reconstructing the volume of the different CSTs, they reported that the CST from S1 was the second largest source of CST fibres after M1, i.e. before SMA and before PM, contrary to what was reported until now (see e.g. Galea and Darian-Smith, 1994). The authors linked this finding with the reorganisation in S1 often observed following a stroke in M1.

There were few mentions about the existence of direct CM cells from S1. For instance, by using the very elegant method of retrograde transneuronal transport of rabies virus from single muscles in macaque monkeys, allowing to specifically label CM cells (provided that the timing of the experiment is precisely and closely controlled), Rathelot and Strick (2006; 2009) observed that some CM cells were labelled in the areas 3a as well. Previous observations of CM fibres from S1 based on tract-tracing experiments were also reported (see e.g. Cheema et al., 1984 below).

An important issue concerns the functional role of the CST from S1. Essentially, is the CST from S1 directly involved in motor control or does it modulate ascending somatosensory transmission?

The exact function of the CST terminating in the dorsal horn of the spinal gray matter, originating largely from S1 and actually present in all mammals (Lemon and Griffiths, 2005), is still not fully understood. Based on the pattern of projection in the dorsal gray matter, it seems that this pathway is mostly involved in sensory processing and is probably important for the descending control and gating of ascending somatosensory inputs, especially proprioceptive inputs generated by movements, and may act by modulating the flow of movement-associated afferent inputs both to spinal cord reflexes and interneuron systems and to afferent spinothalamic and spinocerebellar pathways (Lemon, 2008b; Lemon and Griffiths, 2005; Porter and Lemon, 1993; Schieber, 2007; Sessle and Wiesendanger, 1982). Rathelot and Strick (2006) proposed that the CST fibres from S1, in particular the CM fibres from the area 3a, may establish monosynaptic connections with γ-motoneurons, involved in the control of the sensitivity of muscle spindle afferents. In this way, the CM cells from the area 3a may provide an efferent control over the afferent proprioceptive inputs (Rathelot and Strick, 2006). Indeed, it has been reported since a long time that electrical stimulation of S1 strongly modulated the transmission of somatosensory inputs at several levels of the ascending pathway such as in the spinal cord (Towe, 1973; Wiesendanger, 1969). Moreover, direct CM projections from S1 were shown to terminate into laminae I and II of the spinal cord in macaque monkeys, suggesting that these CM fibres may directly modulate the transmission of nociceptive inputs in the most superficial laminae of the spinal gray matter (Cheema et al., 1984). As a consequence, a lesion of the CST does not only induce motor deficits, but also results in sensory impairments, such as tactile placing and deficits to perform a rapid matching of tactile inputs to motor outputs (Lemon and Griffiths, 2005).

To sum up, S1 has CST fibres that may operate the descending control of afferent information during movement.

Somatosensory processing takes place in M1[11]

There is a wealth of literature about somatosensory processing recorded in M1. In addition to the early observations already mentioned above, many other studies reported that M1 neurons can be activated in response to somatosensory stimulation (Adrian and Moruzzi, 1939; Barbay et al., 2005; Lemon et al., 1976; Lemon, 1981; Lemon and Porter, 1976; Malis et al., 1953; Moore et al., 2000; Strick and Preston, 1982b; Tanji and Wise, 1981; Wannier et al., 1991; Wise and Tanji, 1981). More specifically, neurons of forelimb and hindlimb representations in M1c were shown to respond predominantly to cutaneous stimulation while neurons of forelimb and hindlimb representations in M1r responded predominantly to proprioceptive stimulation (muscle stimulation and joint manipulation) (Boudreau and Smith, 2001; Lemon and Porter, 1976; Picard and Smith, 1992a; Picard and Smith, 1992b; Strick and Preston, 1982b; Tanji and Wise, 1981).

Extensive work in the field was performed by Asanuma and co-workers (Asanuma, 1973; Asanuma, 1975; Asanuma and Rosén, 1972; Asanuma et al., 1979b; Rosén and Asanuma, 1972; Tanji and Wise, 1981), among others. A review of their work is proposed in the introduction of the **Chapter 3.** Very briefly, they observed that the activity of a given columnar array of M1 neurons, producing the contraction of a target muscle, was tightly associated with somatosensory feedback directly generated by the contraction of that target muscle, constituting a closed-loop circuit (homonymous coupling between sensory inputs to M1 and motor output). Regarding the functional role of sensory inputs to M1, they may be involved in the sequencing of voluntary movements by facilitating and/or setting up the excitability level of corticofugal M1 neurons by positive feedback, both before and during voluntary movements (Lemon, 1981; Liepert et al., 2003; Murray and Keller, 2011) and may be particularly important for the learning of motor skills (Lemon, 1981; Pavlides et al., 1993). Tactile exploration (Darian-Smith, 2007) and real-time adjustments during object manipulation (Gardner et al., 2007; Monzée et al., 2003; Wannier et al., 1991) with the fingers and the hand in particular were shown to strongly depend on a continuous afferent positive feedback of peripheral inputs to M1 (Lemon, 1981).

To sum up, M1 is not a purely motor area but is involved in somatosensory processing as well.

[11] This topic will be presented in greater detail in the introduction of the **Chapter 3**.

A disruption of somatosensory input induces motor deficits

"The body of an animal must have tactile sensation, if the animal is to survive."

(Aristotle, 350 B.C.)

As developed previously, dexterous hand movements require obviously the integrity of the motor cortex and CST. In addition, the fine motor control is strongly associated with different sensory inputs from the periphery, among them somatosensory inputs (Lemon, 1999; Lemon and Porter, 1976; Twitchell, 1954), so that the brain remains constantly informed about the outcome of each executed movement as well as supplied with proprioceptive inputs. These latter are transmitted from muscle and joint receptors to S1 and then directly or indirectly to motor areas, or directly from the thalamus to M1 (Asanuma and Arissian, 1984; Jones, 1987; Lemon and Van der Burg, 1979) that integrates this sensory information to generate appropriate movements (Jones, 1996). In case these inputs are abolished, such as in deafferented patients[12], the consequences regarding the execution of movements are disastrous because these patients are usually simply unable to maintain static postures and to correctly reproduce even simple movements (Cole and Paillard, 1995; Sainburg et al., 1993; Sainburg et al., 1995; Sanes and Shadmehr, 1995; Volpe et al., 1979). Despite almost no deficit in motor power and the conserved ability to perform voluntary movements, they cannot carry out many simple tasks of daily life because they have no more automatic reflex correction, they cannot judge the weight of objects and they cannot execute without visual feedback correct movements requiring complex muscle synergies (Cole and Sedgwick, 1992; Ghez et al., 1995; Gordon et al., 1995; Rothwell et al., 1982; Sanes et al., 1984).

Tactile inputs are even more fundamental and vital. This is demonstrated by the lack of any identified congenital absence of touch in newborns (Tan and Katsanis, 2009) while genetic mutations leading to complete deafness (Smith et al., 1999), blindness (Graw, 2003), deafblindness at birth (Ask Larsen and Damen, 2014) or even to congenital insensitivity to pain at birth (see e.g. Cox et al., 2006; Goldberg et al., 2007) are known and viable. As predicted by Aristotle, this suggests that any mutation inducing an absence of touch sensation during development is simply lethal before or around birth (Poole et al., 2011).

[12] See for instance http://www.dailymotion.com/video/x12647t_the-man-who-lost-his-body-bbc-documentary_tech

From a motor point of view, tactile inputs from the fingers are essential to control movements, as extensively investigated by Johansson and collaborators (see previous sections): for instance, by locally anaesthetising the fingers, a procedure that completely removed tactile inputs (and probably some proprioceptive inputs as well), as already mentioned above (Johansson et al., 1992; Johansson and Westling, 1984; Monzée et al., 2003), the subjects were unable to correctly execute very simple grasping tasks and object slipping was thus frequent, illustrating that tactile inputs are required in order to adapt the force used to grasp an object with the fingers. In sum, somatosensory inputs from the periphery are integrated with the motor commands originating from the motor cortex to control the body movements.

The first observations on deafferented subjects were actually carried out on monkeys:

Mott and Sherrington (1894) already reported long time ago that in macaque monkeys, the sections of sensory spinal roots from either the upper limb or the lower limb, at their entry in the spinal cord, induced strong and permanent motor deficits, such that the movements of the hand or foot were nearly completely abolished and the animals were not able any more to perform grasping movement, whereas movement of more proximal joints were less affected. They demonstrated thereby the essential contribution of muscular and cutaneous inputs to voluntary motor control of the limbs in monkeys. Later, other studies on monkeys confirmed the strong inability to use a deafferented limb (see e.g. Twitchell, 1954).

Another experiment on macaque monkeys, subjected now to a small lesion (either unilateral or bilateral) of the hand representation in S1 (areas 1, 2 and 3), resulted in a strong loss of motor power and dexterity in addition to tactile and proprioceptive deficits, followed by a massive, and sometimes complete, recovery of all deficits (Cole and Glees, 1954). Interestingly, the authors were already aware that "*[…] the sensory and motor cortices form a single unit, although when viewed macroscopically the depth of the central sulcus suggests at first a separation, as lines so often indicate boundaries*."

Similarly, a small lesion of the area 3b in squirrel and owl monkeys did not only result in impaired tactile sensations from the contralesional hand, but the contralesional manual dexterity was severely affected as well, such that the monkeys were unable to produce independent and precisely coordinated finger movements. Here again, the animals then

progressively recovered their sensorimotor skills (Xerri et al., 1998). Based on these observations, the authors proposed that S1 provides an important sensory feedback to motor areas during object manipulation and palpation and this sensory afferent input contributes to regulate 1) the forces involved during grasping and 2) the generation of fine finger movements, such as the precision grip.

Additional insight into the motor deficits resulting from an alteration in somatosensory inputs was obtained in macaque monkeys by reversibly inactivating some restricted portions of the finger representation in S1 with microinfusion of muscimol. The disruption of fine manual dexterity, assessed by means of specific behavioural tasks, was then characterised by a loss of finger coordination, an abnormal placement of the fingers on the objects, and an impaired control of prehensile and lifting forces (Brochier et al., 1999; Hikosaka et al., 1985).

Further detail about the impact of the loss of somatosensory inputs on the M1 organisation was obtained by ICMS mapping of M1: in addition to deficits in the execution of fine fractionated finger movements, an injury of the hand representation in the dorsal column of macaque monkeys induced fine modifications in the representation of the finger movements in M1 (less extension-flexion sites, more adduction-abduction sites, higher ICMS thresholds) (Kambi et al., 2011; Qi et al., 2010).

A disruption of motor output induces modifications in somatosensory processing

Following an ischemic lesion of the hand representation in M1c (receiving predominantly cutaneous inputs) in squirrel monkeys, Nudo and collaborators observed that the somatosensory processing from the contralesional hand was affected in parallel with the motor control itself (Friel et al., 2005; Nudo et al., 2000). More specifically, a positive correlation was described between the increase in sensory errors reminiscent of human sensory agnosia and the deterioration of manual dexterity in the Klüver board task. The authors interpreted this finding as either a deficit in processing of cutaneous information or a failure to integrate cutaneous information with motor commands. Conversely, when the lesion targeted the hand representation in M1r (receiving predominantly proprioceptive inputs), the monkeys did many reaching errors, such that the animals

failed to direct the hand correctly towards the wells of the Klüver board. The authors proposed that this may reflect either a dysfunction in proprioceptive processing or the loss of integration of proprioceptive information with motor commands (Friel et al., 2005). These differential results are fully in accordance with the contrasting somatosensory processing in M1c as compared to M1r described above.

Sasaki and Gemba (1984) performed an elegant study in conscious macaque monkeys by using the method of transient lesioning of a brain region with a cooling chamber. In parallel, they recorded cortical field potentials in the hand representation of M1 and S1 while the monkeys were doing a behavioural task consisting in visually-guided hand movements. After a cooling lesion of the hand representation in M1 specifically, and while the animals were performing the behavioural task, the authors observed that, within a few minutes, the associated premovement cortical activity in M1 was strongly reduced compared to the baseline and this electrophysiological modulation was accompanied with a slowness and weakness of the contralesional hand movements and an increase in the reaction time during the behavioural task. Remarkably, by simultaneously recording the S1 hand representation, they observed an increase in the premovement cortical activity in S1. Most interestingly, the latency of the movement from the premovement potential was similar or even larger for the potential recorded in S1 than the one in M1 under normal condition (i.e. without lesion), indicating that S1 could be activated earlier in relation to movement onset than when the premovement potential originated from M1. Conversely, cooling of S1 had usually only a weak effect on movements. Then, in case the cooling lesion affected the hand representation both in M1 and in S1, the contralateral hand movements of the animal were severely impaired. These results indicate that when the lesion affected M1 only, S1 could partially (because of the behavioural deficit) take up the motor function previously assumed by M1, corresponding to the increase in premovement cortical activity measured in S1. To put it another way, the role of S1 in motor control was significant when M1 was transiently lesioned. Note that no changes in activity were observed in premotor areas (Sasaki and Gemba, 1984). Even though the premotor activity in M1 can be compensated by the one in S1, still it does not allow for a complete functional recovery. Therefore, in accordance with the evidence that the CST from S1 usually does not directly contribute to movement, it may be proposed that M1 networks usually subserve motor activities, probably with a modest contribution from S1. When M1 is lesioned, S1 is recruited to compensate for the loss of mo-

tor function, explaining the enhanced activity in S1 during M1 cooling, but S1 cannot completely assume the motor functions of M1. This study is in line with some observations that, in monkeys, CST neurons from S1 share similar properties of activities to CST neurons from M1, such that in addition to their sensory function, CST neurons from S1 could be directly involved in motor control (Evarts, 1974; Fromm and Evarts, 1982).

To sum up, the integrity of the somatosensory processing depends on the integrity of the descending motor pathways, meaning that sensorimotor interactions allow M1 and S1 to adapt their activity to changes at the periphery.

By way of conclusion of this section, both motor and somatosensory systems, and in particular M1 and S1, work together as a functional and global sensorimotor system and sensorimotor cortex that are involved in processing peripheral inputs and in executing movement, rather than two completely separated entities.

Neuroplasticity[13]

"Once the development was ended, the founts of growth and regeneration of the axons and dendrites dried up irrevocably. In the adult centers, the nerve paths are something fixed, ended, and immutable. Everything may die, nothing may be regenerated."

(Ramon y Cajal, 1913)

Nowadays, this citation appears unrealistic in view of our fresh knowledge about the plasticity of the brain. Cajal's words were however the dominant view among neurobiologists until the middle of the 20th century. Before Altman's studies (Altman, 1962; Altman and Das, 1965), it had been proposed that the nervous system was a machine with static properties, containing its maximal amount of neurons at birth, and that new neurons were not added to the adult mammalian brain, except in the hippocampus to some extent, once the critical period of the brain had been reached (for a review, see Braun and Jessberger, 2014; Colucci-D'Amato et al., 2006; Jäncke, 2009).

[13] For a comprehensive historical review about the "birth" of the concept of neuroplasticity, see Doidge (2007).

This central dogma in Neuroscience implied also that a given function was strictly located in a specific brain region (proposed by F.J. Gall, 1758-1828) and that any changes in the brain or functional recovery were merely some exceptions to this cornerstone principle. Ramon y Cajal (1913) was nevertheless conscious that this central dogma of neurobiology might one day change as he continued his paragraph with: "*It is for the science of the future to change, if possible, this harsh decree.*". Actually, he had previously written:

"*[…] the work of a pianist […] is inaccessible for the untrained human, as the acquisition of new abilities requires many years of mental and physical practice. In order to fully understand this complicated phenomenon it is necessary to admit, in addition to the strengthening of pre-established organic pathways, the establishment of new ones, through ramification and progressive growth of dendritic arborizations and nervous terminals. […] Such a development takes place in response to exercise, while it stops and may be reversed in brain spheres that are not cultivated.*" (Ramon y Cajal, 1904, translated and cited in Pascual-Leone, 2001).

In truth, we already have reached the *future* of Cajal's predictions! At the present time, we know that the basic architecture of the brain is not completely hard-wired and there is strong evidence that its organisation can actually change throughout the lifespan (Kempermann, 2006), as perfectly summarised by Michael Merzenich: "*The brain was constructed to change.*" (Holloway, 2003).

Definition of neuroplasticity

The term *neuroplasticity* was first introduced by Konorski in 1948 (Konorski, 1948). The neuroplasticity or brain plasticity (from the Greek verb *plássein* meaning to mold) refers to the intrinsic ability of the brain (and the nervous system) to continuously reshape its own structural and functional organisation in response to environmental demand, either modifications in the external environment or within the body, in order to adapt to these environmental changes (Nudo, 2006b; Pascual-Leone et al., 2005). More precisely, the brain plasticity corresponds to the ability of neuronal networks and neural systems to modify their topography and their local organisation in response to new information.

Brain plasticity is the strongest during childhood. Nevertheless the adult brain conserves the ability to continuously reshape itself over the entire lifespan (Boyke et al.,

2008; Pascual-Leone et al., 2005; Sanes and Donoghue, 2000), although usually in a more selective manner than during childhood (Bengtsson et al., 2005) and by using different mechanisms. Plastic modifications of the cortical representations are the normal ongoing state of the brain over time and take place under many circumstances (Ward and Frackowiak, 2004), e.g. during the development of the nervous system (for a review, see Stiles and Jernigan, 2010; Zilles, 1992), during sensory information reinforcement through experience, such as training (Adkins et al., 2006; Cannonieri et al., 2007; Chang, 2014; Dayan and Cohen, 2011; Lamprecht and LeDoux, 2004; Nudo et al., 1996; Pascual-Leone et al., 1995a; Pascual-Leone et al., 2005), in learning and memory processes (Draganski et al., 2006; Mahncke et al., 2006; Merzenich and Sameshima, 1993; Takeuchi et al., 2010), in cognitive processes (e.g. during reading acquisition, in Dehaene et al., 2015; or for spatial orientation, see the famous example of the London taxi drivers in Maguire et al., 2000), in functional recovery after a dysfunction or a damage, such as a sensorimotor deprivation, a peripheral injury, or a brain injury (see below), and in our daily activities as well, depending on the amount of use of the corresponding body part (see below).

Brain plasticity results from the combination of different events taking place at several levels, from the gene expression or molecular level (see e.g. Garraghty et al., 1991; Hendry and Jones, 1986; Jones, 1993; Kleim et al., 2006; Zatorre et al., 2012) to the behaviour (see e.g. Di Paola et al., 2013), through the cellular (see e.g. Kolb et al., 2008; Zatorre et al., 2012), anatomical (see e.g. Draganski et al., 2004; Kolb and Whishaw, 1998) and functional (see e.g. Calvo-Merino et al., 2005; Kelly and Garavan, 2005; Lotze et al., 2003) levels.

In sum, there are many different forms of brain plasticity. Here, we will focus in greater detail on two of them, namely the use-dependent plasticity and the lesion-induced plasticity in the primate sensorimotor system more particularly.

Use-dependent plasticity in the adult

Use is a decisive factor underlying the plasticity of cortical processing and cortical representations. Thus, *use-dependent neuroplasticity* or *use-dependent brain plasticity* corresponds to the outstanding property of the brain to selectively adjust the amount of neu-

ronal activity associated with a given body part in response to behavioural changes in the use of this body part (Dayan and Cohen, 2011; Nudo, 2006b; Pascual-Leone et al., 2005).

In the next two sections, we will present some examples of use-dependent plasticity, first in monkeys, then in human, with a special emphasis on plasticity in the sensorimotor system.

Use-dependent plasticity in animals

The first key principles of use-dependent plasticity were demonstrated in animals, in particular in adult monkeys, by Jon Kaas, Michael Merzenich and their collaborators, by modifying monkeys' sensory inputs to cortex and studying the impact on cortical sensory representation by mapping the receptive fields. For instance, some monkeys were trained to perform a sustained and specific use of the hand (Byl et al., 1996; Byl et al., 1997; Jenkins et al., 1990; Kaas, 1991; Recanzone et al., 1992b; Wang et al., 1995), and the associated receptive fields were mapped at the cortical level before and after the "intervention": in one study, adult owl monkeys were trained to regularly apply their index, middle and fourth fingertips to a rotating disc, for about 10 days. After this sustained tactile "practice", the representations of those fingertips, specifically, were substantially enlarged in 3b and invaded 3a as well (**Figure 22**) (Jenkins et al., 1990), meaning that the overuse induced a clear change in the cortical representation of the trained skin.

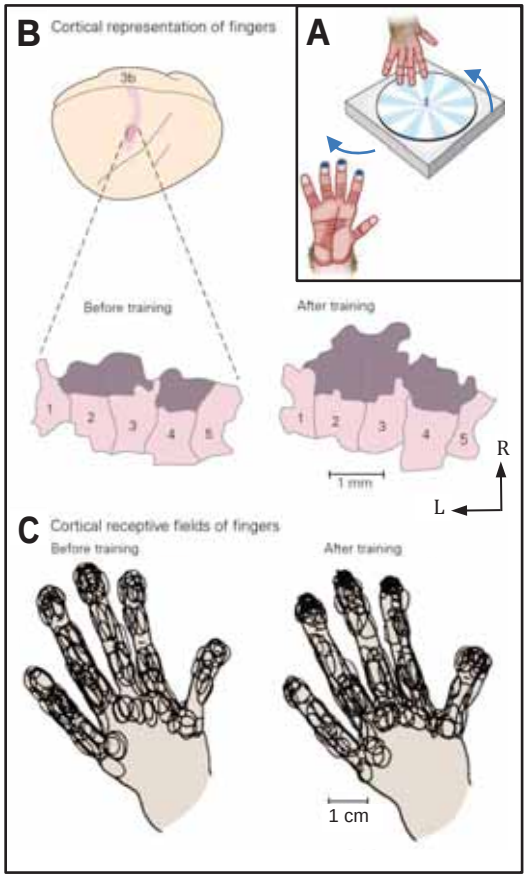

Figure 22: Jenkins' experiment on use-dependent plasticity in an adult owl monkey. (A) The animal was conditioned to freely apply the index, middle and fourth fingertips on a rotating disk for about 10 days (corresponding to about 1.5 cumulated hours of tactile stimulation a day), to create a controlled and sustained tactile experience (modified from Vinogradov et al., 2012, itself modified from Jenkins et al., 1990). (B) Somatosensory representation of the monkey's fingers in contralateral area 3b, before training (left) and 3.5 months after training (right). R: rostral, L: lateral. Note the considerable functional expansion of the cortical representation of the stimulated fingertips specifically, after training (purple). These cortical representations were obtained by determining the receptive fields on the glabrous fingerskin (C) before and after training. More and smaller receptive fields were identified on those fingertips that experienced sustained tactile stimulation, after the training (B and C modified from Kandel, 2013, itself modified from Jenkins et al., 1990).

In another series of studies, adult owl monkeys were trained to discriminate differences in the frequency of a vibrating stimulus applied to one fingertip (Recanzone et al., 1991). Here again, this training by overuse induced a clear cortical expansion of the representation of the stimulated finger in S1, more specifically in the area 3b, by a factor of 1.5 to 3 (depending on the animals) as compared to the untrained hand (Recanzone et al., 1992b). Remarkably, this spatial modification of the sensory cortical representation after training was accompanied by an improved tactile discrimination (Recanzone et al., 1992a), as well as a larger, earlier and temporally sharper neuronal activity in area 3b. The authors found that the behavioural improvement was linked with a decrease in the variance of the neuronal representation of the vibrating stimulus (Recanzone et al., 1992c). To put it another way, there was an improvement in the temporal precision of neuronal responses to the vibrating stimulus. Interestingly, based on these observations, the authors proposed that both spatial and temporal functional organisations of S1

should always reflect the recent behaviourally relevant history of stimulation as well as the current perceptual abilities of the subject.

Another intriguing finding was obtained by intensively training adult owl monkeys to a tactile discrimination task where several fingers were stimulated simultaneously, for 4-5 weeks. Essentially, after the training, the cortical maps of S1 were reorganised in such a way that there was now a large continuous cortical zone in which all neurons had the same large receptive field covering the simultaneously stimulated fingers. To put it another way, the cortical representations of the stimulated fingers were integrated into neurons showing a single large multi-finger receptive field covering the different trained fingers, and the normally segregated representations of adjacent fingers completely disappeared for these stimulated fingers. This learning-induced cortical representational remodeling was shown to be cortical in origin and did not result from remodeling already taking place at subcortical levels because no similar integrated receptive fields were observed in the thalamic VPL nucleus (Wang et al., 1995).

In some cases, the training by overuse was intentionally forced to create monkey models for focal hand dystonia (Blake et al., 2002; Byl et al., 1996; Byl et al., 1997). Here, adult owl monkeys were trained to perform a repetitive finger squeezing daily for several weeks. The repetition of highly stereotyped hand movements induced disorders in motor control and a degradation of the cortical sensory representation of the hand in area 3b. To elaborate, the hand overuse resulted in the dedifferentiation of the sensory cortical representation of the hand skin in the form of strongly enlarged receptive fields, the development of many new receptive fields extending each over the whole glabrous surface of a given finger or even extending over several fingers, the emergence of intermingled representations of glabrous finger skin with hairy finger skin, and the loss of the normal local shifted-overlap topography of the receptive fields (Blake et al., 2002; Byl et al., 1996; Byl et al., 1997). Moreover, stimulations on the face skin revealed the emergence of face-responding sites within the representation initially devoted to the hand in S1 (Blake et al., 2002). In sum, the extreme and repetitive overtraining of the hand led to the development of maladaptive plasticity, characterised by a degradation of the S1 hand representation that was normally involved in the fine sensorimotor control of the hand. These aberrant sensory representations induced thereby an abnormal motor con-

trol that itself strengthened sensory abnormalities, leading to focal hand dystonia (Blake et al., 2002).

Taken all together, these studies on owl monkeys demonstrate that the specificity of the cortical neuronal response, and therefore the resulting cortical maps, is a dynamic process with plastic changes in the cerebral cortex that strongly depend on the inputs delivered on the skin.

The plastic properties of M1 cortical representations were investigated as well. Normal adult squirrel monkeys were trained to perform a behavioural task consisting in the skilled retrieving of small pieces of food with the fingers. After a period of training, the ICMS mapping of M1 revealed an enlarged finger representation at the expense of the wrist and forearm representations, as compared to the pre-training representations. Conversely, monkeys engaged in a task involving mainly the use of the forearm presented an enlarged forelimb representation in M1 after training, at the expense of more distal representations (Nudo et al., 1996). This study demonstrated that plastic modifications were highly specific to the muscles involved in a given task.

Use-dependent plasticity in human

Further studies on use-dependent brain plasticity were also performed in parallel on human subjects, in particular on people presenting a long-lasting and exceptional use of a particular body part, such as the fingers and the hand, leading to the development of extraordinary skills or expertise (for a review, see Chang, 2014). Musicians, for instance, present such outstanding skills (Gaser and Schlaug, 2003; for reviews, see Jäncke, 2009; Munte et al., 2002; Pascual-Leone, 2001; and Wan and Schlaug, 2010). In a very elegant study, Elbert et al. (1995) demonstrated that in adult string players, the S1 representation of the left little finger –particularly engaged on the instrument– was larger in comparison with the same finger of their right hand or in comparison with the corresponding finger of control subjects (**Figure 23**).

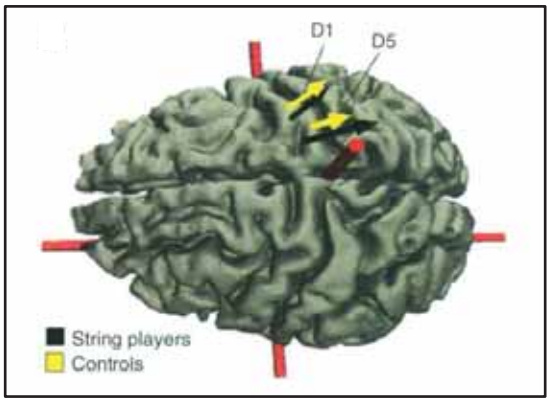

Figure 23: Elbert's experiment on use-dependent plasticity in adult string players. Light pneumatic stimulation was separately delivered to the left thumb tip (D1) and fifth fingertip (D5) and brain activity was measured by magnetoencephalography (MEG) to estimate the size of the cortical representation of the fingers. As compared to non-musicians, string players had an enlarged S1 cortical representation of the left fifth fingertip –the finger that strongly interacts with the strings– represented by a stronger equivalent current dipole (D5 black arrow vs yellow arrow). Conversely, the cortical enlargement was only very small for the left thumb representation, a finger that is used to stabilise the violin. In addition, there was a topographic shift towards the midsagittal plane for both fingers in musicians, indicating an enlarged representation of their left fingers as compared to non-musicians (from Elbert et al., 1995).

Professional pianists constitute another group of music experts. Here, a larger finger representation was bilaterally observed in motor cortex as compared to non-musicians (Amunts et al., 1997; Schlaug, 2001; Watson, 2006). But interestingly, the hand representation was especially more extended on the right hemisphere (i.e. controlling the subdominant left hand) than on the left hemisphere (i.e. controlling the dominant right hand) (Amunts et al., 1997). In addition, professional pianists were shown to have a significantly higher tactile acuity than non-musicians (Ragert et al., 2004).

In addition, a DTI study demonstrated that the CST was more structured (indicating a higher integrity of the fibre system) in professional pianists than in control non-musicians. Interestingly, a positive correlation was highlighted between the total amount of practice and organisation of the CTS (Bengtsson et al., 2005).

Still in musicians, differential neuroplastic changes were even observed depending on the instrument played, such that pianists (more pronounced use of the right hand than the left hand) had a hand representation more clearly defined (in terms of Omega sign) in left motor cortical area. Conversely, string players (implying a more predominant use of the left hand as compared to the right hand) had a hand representation more clearly defined in the right motor cortical area (Bangert and Schlaug, 2006).

Interestingly, the acquisition of new motor skills in control subjects, such as the piano practice, is linked to rapid plastic changes as well. A study focused on non-musician volunteers who learned to play a specific five-finger exercise on the piano, with one hand, for 2 hours a day (Pascual-Leone et al., 1995a). By using TMS just after the daily practice to map motor cortical outputs, it was observed that the motor cortical output maps to the muscles involved in the task became progressively enlarged over 5 days of piano practice, as the volunteers became more skillful in the task. These changes in motor output were specific to the hand involved in the piano training. Some other volunteers did not learn the specific piano sequence but were free to play the piano at will during the same 2 hours a day of musical practice. Interestingly, the motor output maps to the free playing hand increased as well in these subjects during the 5 days of practice, but to a lesser extent as compared to the trained volunteers. Then, some volunteers were followed up during four additional weeks of training and motor output maps were obtained each Monday (after 2 days off) and each Friday (after 5 days of piano training). Interestingly, the maps measured on Fridays progressively decreased over the course of the four weeks of practice, even though the practice continued. In addition, the maps obtained on Mondays, i.e. after 2 days without piano training, showed a slight decrease as compared to the map obtained 3 days before, and then, the motor output maps increased again throughout the week of practice. Conversely, a control group did not have the 4 additional weeks of piano practice. As a result, their maps returned to baseline already after a week rest and did not evolve any more thereafter (Pascual-Leone, 2001; Pascual-Leone et al., 2005). This study demonstrated that plastic changes were very rapid and reversible. Based on these results, the authors proposed that such use-dependent plasticity occurs in two steps: the first step involving flexible and rapid modulations of already existing pathways (such as unmasking previously existing connections), leading then to deeper changes in the organisation of intracortical and subcortical networks over the longer term, as the subject develops the skills (Pascual-Leone, 2001; Pascual-Leone et al., 2005).

Experienced Braille readers represent another excellent human model for studying the changes in the brain induced by intensive, specialised, sensorimotor skills (for a review, see Elbert and Rockstroh, 2004). For instance, the cortical sensorimotor representation of their right (reading) index finger was shown to be significantly larger (at the expense of the representation of other fingers) than the one of their left index finger or than the

one of the right index finger of non-Braille readers (Hamilton and Pascual-Leone, 1998; Pascual-Leone and Torres, 1993), and this cortical reorganisation was accompanied by an increased tactile spatial acuity of the reading fingertip, interpreted as the potential behavioural correlate of plastic changes observed at the cortical level (Van Boven et al., 2000). Remarkably, changes in motor cortical output, assessed by using TMS, were even observed within a day when Braille reading was intensively practiced (about 6h/day) after a day off practice: for instance, after a working day spent reading Braille, the motor cortical output maps to a muscle of the reading finger were significantly enlarged as compared to the maps of the contralateral finger muscle and to the maps of an ipsilateral hand muscle not involved in Braille reading. Conversely, after a day without Braille reading activity, the maps for the reading finger muscle remained small, suggesting that a very rapid update of the motor cortical output took place within the brain to adjust the brain activity to the demand of the task being performed (Pascual-Leone et al., 1995b).

Use-dependent plasticity was investigated in athletes as well because they usually develop high sensorimotor skills through disciplined and long-lasting periods of practice (Nielsen and Cohen, 2008). A study based on TMS focused on the CM projection to the hand in elite racquet players. Essentially, elite racquet players were shown to have larger motor evoked potentials (MEPs) as compared to social players and control volunteers. Moreover, a shift in the motor cortical representation of the playing hand was systematically observed in all elite players and some of them even had lower cortical motor thresholds of MEPs. Conversely, the social players did not differ from the non-players in the MEPs. These findings indicate that a functional reorganisation of the motor system, and in particular the CM pathway, took place in the athletes specifically, that is most probably the anatomical support of the acquisition and retention of the highly developed sensorimotor skills observed in these athletes (Pearce et al., 2000).

The sensorimotor control is especially well developed in athletes using actively both hands. A very new study investigated this particular topic in professional handball players. To elaborate, by using fMRI and DTI, some structural brain changes were observed in these athletes as compared to control non-player subjects, in the form of an enlargement of the right sensorimotor cortex, of the SMA and CMA bilaterally, and of the left intraparietal sulcus. Moreover, the DTI properties of the right CST were shown to significantly differ from those in control non-players. Equally interesting, the authors were

able to demonstrate that the age at beginning of the athletic practice was inversely correlated with the volume of both right and left sensorimotor cortices, supporting the fact that the intensive training induced neuroplastic adaptations in the sensorimotor system of these athletes (Hänggi et al., 2015).

In these examples of skill learning and expertise, the brain increases its computational capacities associated with the body part being used and these use-dependent adaptations in the nervous system may be useful (Dayan and Cohen, 2011). More specifically, the structural brain plasticity is usually characterised by an increase in the volume and gray matter density of those brain areas that are involved in the sustained practice of the task (Chang, 2014). Moreover, these use-dependent structural changes are rapid (Pascual-Leone, 2001; Pascual-Leone et al., 2005) and reversible, meaning that they can rapidly disappear in case of interruption of the practice (Chang, 2014; Draganski et al., 2004; Pascual-Leone, 2001; Pascual-Leone et al., 2005; Pascual-Leone et al., 1995b). One special feature of neuroplasticity observed mainly in expert musicians is the direct link between the amount of brain reorganisation and the age at beginning of the musical training (Amunts et al., 1997; Elbert et al., 1995; Wan and Schlaug, 2010). This suggests that there may be sensitive periods beyond which music-induced plastic changes and learning effects may become less pronounced (Chang, 2014). But note that such a correlation was very recently observed in elite handball players as well (Hänggi et al., 2015).

The use-dependent plasticity of the body representations in the nervous system, and in the sensorimotor cortex more specifically, is not limited to extraordinary skills. For instance, in a very recent study about the effect of age and expertise on tactile processing from the fingertips in human, it was observed that a period of as short as 30 minutes of repeated tactile stimulation to the fingertips was sufficient to induce significant plastic modifications in the brain activity visible on EEG signals (P300), in addition to an improvement in tactile discrimination performance (Reuter et al., 2014).

In addition, we demonstrated that the brain was able to conform its activity according to practice performed in our everyday, unconstrained life as well (see Gindrat et al., 2015 in **Chapter 6**; and see **Chapter 7** as well): in short, we observed that sensory processing from the fingertips in touchscreen smartphone users was reshaped by their repetitive interactions on the smooth surface of their smartphone. More specifically, the thumb representation was daily adjusted in a use-dependent manner.

Special forms of use-dependent plasticity in human

The examples provided so far described plastic changes usually associated with an increase in brain activity or in cortical volume. The opposite process, resulting from periods of disuse or non-use of a given body part, affects cortical representations and perception as well, and this kind of plastic changes is sometimes called *deprivation-related neuroplasticity* (Hänggi et al., 2015; Makin et al., 2013). For instance, a decrease in cortical thickness of the contralateral sensorimotor cortex was observed in patients after a short-term (16 days) upper limb immobilisation in a plaster cast because of an upper limb injury (Langer et al., 2012). Another study demonstrated that, in addition to the reduction of activation of the finger representations in S1, a limb immobilisation for 4-10 weeks led to an impairment of tactile acuity. Remarkably, the authors observed that the more severe the tactile deficits, the larger the decrease in cortical somatosensory representation (Lissek et al., 2009). Equally interesting, the brain activity related to the non-immobilised hand was shown to increase during the immobilisation period (Langer et al., 2012; Weibull et al., 2011), and the tactile perception was significantly better than the one of control subjects (Lissek et al., 2009), meaning that the immobilisation of one limb led to a skill transfer to the intact limb. Finally, while perceptual and cortical changes associated with the immobilised hand completely recovered after cast removal, the improved tactile perceptive abilities of the intact hand were conserved (Lissek et al., 2009).

As already mentioned by reviewing studies on monkey models of focal hand dystonia (Blake et al., 2002; Byl et al., 1996; Byl et al., 1997), use-dependent brain plasticity can be detrimental as well and can lead to maladaptive brain plasticity (Pascual-Leone et al., 2005), meaning that a cortical representation becomes functionally innervated by surrounding cortical representations, leading to misperceptions. Syndactyly is an interesting example of maladaptive changes: a study demonstrated that the artificial finger webbing for 5 hours only was sufficient to deeply reorganise the finger representation in S1 in human (Stavrinou et al., 2007). Conversely, recovery of a nearly normal somatotopic finger representation was observed in S1 in an adult patient after surgery to correct syndactyly (Mogilner et al., 1993).

Another famous example is provided by patients who experience phantom sensations and phantom limb pain, for instance after an amputation (Birbaumer et al., 1997;

Dettmers et al., 2001; Elbert and Rockstroh, 2004; Flor et al., 1995; for a review, see Flor et al., 2006; Kaas et al., 1997; Ramachandran et al., 1995; Ramachandran and Hirstein, 1998; Ramachandran and Rogers-Ramachandran, 2000). The sensory deprivation resulting from an amputation can induce maladaptive cortical changes in S1, in the form of a functional invasion of the deafferented cortex by surrounding representations. This disorganisation of S1 and the inability to receive afferent inputs from the amputated limb often lead to phantom limb pain. Interestingly, a high correlation was observed between the intensity of phantom limb pain sensation and the extent of cortical reorganisation in S1 (Flor et al., 1995). Moreover phantom sensations such as referred sensations on the phantom limb can appear as well when adjacent sites are stimulated, such that tactile sensations on the phantom hand can be evoked by touching the face, for instance (Ramachandran and Hirstein, 1998; Ramachandran and Rogers-Ramachandran, 2000). Another study (Makin et al., 2013) revealed that the concept of maladaptive plasticity resulting from sensory deprivation may not work in amputees, and the authors proposed instead a reverse mechanism, i.e. that adaptive patterns of limb use (both intact and residual limb) after amputation do drive cortical plasticity (instead of sensory deprivation leading to maladaptive changes). This study suggests therefore a tight link between deprivation-related neuroplasticity and use-dependent neuroplasticity.

Maladaptation was also reported in patients after limb replantation, in the form of an increased activity in S1, and the amount of pain in this reimplanted body part was inversely proportional to the amount of cortical reorganisation in S1 (Blume et al., 2014). In addition, maladaptation induced by the overuse of a given body part has been demonstrated in Braille readers in the form of an alteration of touch perception (Sterr et al., 1999), and in professional pianists or hand writers with painful focal hand dystonia (Aranguiz et al., 2011; Elbert et al., 1998; Lim et al., 2004; Murase et al., 2000; Neychev et al., 2011; Quartarone and Hallett, 2013; Quartarone and Pisani, 2011; Zamorano et al., 2015). In these dystonic subjects, the hand representation in S1 was found to be altered, with a reduction of inhibitory cortical activity (Abbruzzese et al., 2001; Murase et al., 2000; Neychev et al., 2011; Pascual-Leone, 2001; Pascual-Leone et al., 2005; Pujol et al., 2000; Quartarone and Hallett, 2013; Tamburin et al., 2002; Tamura et al., 2009; Tamura et al., 2008).

Before closing this section about use-dependent neuroplasticity, note that brain plasticity can be cross-modal as well, as demonstrated for instance by the pioneering development of prosthetic devices to substitute vision in blind subjects via tactile inputs (Bach-y-Rita et al., 1969; Bach-y-Rita, 1983; Bach-y-Rita, 1967) and later by the observation of a shift in modality (from vision to somatosensory processing from the reading finger) in the visual cortex of Braille readers (Cohen et al., 1997; Pascual-Leone et al., 2005; Sadato et al., 1998; Sadato et al., 1996).

To sum up so far, the brain conserves throughout life the ability to operate plastic changes in the cortical representations of the body based on environmental demand, i.e. fine adjustements in the topographic representation of the body in the cortex, as illustrated here in particular with the sensorimotor representation. As a general principle, selected body parts are represented over an expanded cortical region when their use is amplified, for instance in response to a specific training or to shifts in sensory demands. In some cases, the expanded cortical representations, i.e. the larger number of cortical cells involved in the processing of the relevant stimuli, may be associated with an improvement of sensory perception. But in some cases, an unwanted cortical reorganisation takes place and leads to misperceptions.

Lesion-dependent plasticity in the adult

Brain plasticity operates after a lesion affecting the nervous system as well. More specifically, changes in the body such as a peripheral lesion (loss of a limb, nerve degeneration, …) or a CNS lesion (spinal cord injury, brain cortical lesion) induce plastic modifications in the cortex as well.

Lesion-induced plasticity in adult monkeys

The fundamental principles of lesion-induced plasticity in the adult nervous system were demonstrated in monkeys in the 1980s, first by Michael Merzenich and collaborators (Kaas et al., 1983; Merzenich et al., 1983a; Merzenich et al., 1983b), then by others.

These pioneering studies (followed then by others) focused on the cortical modifications taking place in S1 after an alteration in somatosensory inputs, either by performing peripheral nerve injuries (Jones et al., 2002; Kaas et al., 1983; Kaas, 1991; Kaas et al., 1997; Merzenich et al., 1983a; Merzenich et al., 1983b; Wall et al., 1986; Wall et al., 1983), or by performing amputations (Florence et al., 1998; Florence et al., 2000; Florence and Kaas, 1995; Kaas, 1991; Kaas et al., 1997; Manger et al., 1996; Merzenich et al., 1984), or by inducing finger syndactyly (Allard et al., 1991; Clark et al., 1988) or by lesioning the spinal cord (Kambi et al., 2014) or S1 (Xerri et al., 1998). For instance, immediately after a finger amputation, say the middle finger, the S1 cortical representation associated with this finger became completely unresponsive. But later on, the region was found to be progressively invaded by the representation of the intact, adjacent fingers, i.e. the index and fourth fingers, now with smaller receptive fields on the skin. To put it another way, a dynamic functional remapping took place in the form of a contraction of the sensory-deprived representation followed by a cortical enlargement of the somatosensory representation of adjacent fingers into the deprived cortical area (Merzenich et al., 1984).

Example of plasticity following a motor cortex lesion in monkeys

The mechanisms of brain plasticity operating after a motor cortex lesion in the adult monkey have been already extensively studied as well, for instance by E. Rouiller, R. Nudo, and their co-workers, among others.

In case of a very restricted unilateral lesion of M1 in monkeys, the cortical reorganisation remains restricted to this region and the regions immediately adjacent. Essentially, the non-damaged zones immediately around the lesion can reorganise themselves to assume now the functions that were previously fulfilled by the damaged tissue as it was intact (Nudo, 2006b; Nudo and Milliken, 1996; Rouiller et al., 1998; Rouiller and Olivier, 2004).

But in case of more extended M1 lesions, it has been demonstrated that other intact, more remote brain regions do contribute, at least in part, to the post-lesion recovery (for reviews, see Dancause and Nudo, 2011; Nudo, 2006a; and Rouiller and Olivier, 2004), such as the premotor areas: for instance, a unilateral permanent lesion of the hand representation dominantly in M1 was performed on adult macaque monkeys (Liu and

Rouiller, 1999; Rouiller and Olivier, 2004). This intervention resulted in the complete abolition of the contralesional dexterous hand use such that the monkeys were not able any more to perform fine fractionated finger movements for 1 to 2 months after the cortical lesion. Then, a progressive spontaneous functional recovery developed, lasting for 3 to 4 months, before reaching a stable but still incomplete level of manual dexterity (about 30% of the pre-lesion value). An ICMS mapping showed that it was now impossible to evoke any visible movement of the recovered hand by electrically stimulating the lesioned M1 cortex and the surrounding sites where more proximal representations were visible before the lesion, indicating that the adjacent M1 representations did not reorganise to contribute to the post-lesion motor recovery, contrary to what was observed after a more restricted cortical lesion. Later on, the transient inactivation of PM specifically (PMv+PMd) of the lesioned hemisphere using the GABA agonist muscimol resulted in the complete loss of the recovered manual dexterity, strongly suggesting that the incomplete functional recovery observed after the relatively extended permanent lesion was, at least partly, mediated by ipsilesional PM. Other neurophysiological studies confirmed that PM, in particular PMv, was reorganised after a similar M1 lesion (Frost et al., 2003; Murata et al., 2015). A very recent study gave more insight into the potential time course of the reorganisation by showing that PMv is involved in the early post-lesion recovery period, whereas the late post-lesion recovery period implies perilesional reorganisation of M1 itself (Murata et al., 2015). Others observed the potential involvement of SMA in the functional recovery after a permanent lesion of the M1 hand representation in monkeys (Eisner-Janowicz et al., 2008; McNeal et al., 2010).

An anatomical study confirmed the contribution of non-primary motor cortical areas in recovery after an M1 lesion (Dancause et al., 2005). Briefly, squirrel monkeys were subjected to a unilateral lesion of the hand representation in M1. After injection of the tracer biotinylated dextran amine (BDA) into the ipsilesional PMv, the authors were able to reconstruct the afferent and efferent projections of this area. Remarkably, they observed a prominent new corticocortical projection between PMv and the areas 1 and 2 in S1, most probably mediated by PMv fibres that reoriented their trajectory by approaching the lesion, travelling now towards S1 instead of M1. This study did not only confirm the role of PM, but also suggested the potential implication of S1 in the functional recovery after an M1 lesion. To put it another way, the sensorimotor cortex may have developed a repair strategy by reconnecting motor areas with somatosensory areas (Nudo, 2006b).

Taken all together, these lesion studies all converge to demonstrate that, after a lesion of the M1 hand representation, plastic modification took place at the cortical level and involved cortical areas quite remote from the lesion site, in particular premotor areas.

After a lesion, the cortical reorganisation and the associated functional recovery can be promoted by using some treatments, such as anti-Nogo-A antibody. This topic is presented in greater detail in **Chapter 8**. In addition, the use of autologous adult neural progenitor cells was shown to be effective in enhancing functional recovery after an M1 lesion as compared to control animals (Kaeser et al., 2011).

After a very extended cortical lesion, such as after a stroke in human patients, plastic modifications were shown to involve not only the peri-infarct cortex, but also more remote areas, such as the contralesional hemisphere (Nudo, 2006b). But note that this situation is less probable in animal models because lesions are usually relatively well restricted, at least in comparison with lesions observed in human subjects following a stroke.

In sum, cortical representations in adult primates are not immutable and can reshape according to the sensorimotor changes resulting from a peripheral nervous system (PNS) lesion or a CNS lesion.

How does neuroplasticity operate ?

The specific mechanisms underlying neuroplastic changes are still far from full knowledge. In particular, the cellular and molecular processes remain elusive, as well as the precise time scale of these neural changes.

It has been proposed that brain plasticity operates at several microscopic and mesoscopic levels and is visible in the form of modifications in cortical representations (see above), morphological changes of synapses, morphological and contact changes in dendrites and dendritic spines (Chen and Nedivi, 2013; Churchill et al., 2004; Harms et al., 2008; Holtmaat et al., 2006; Knott et al., 2006; Trachtenberg et al., 2002), modification in the trajectory of axons (Dancause et al., 2005), modulation in the neurotransmitters concentration, such as a reduction of GABA (Chen and Nedivi, 2013; Frias and Wierenga, 2013; Garraghty et al., 1991; Griffen and Maffei, 2014; Jones, 1993; Kullmann

et al., 2012), short-term strengthening, respectively weakening of existing synapses via the induction of long-term potentiation (LTP), respectively long-term depression (LTD) (Martin and Morris, 2001), changes in glial number and morphology, angiogenesis, and neurogenesis (Gould et al., 1999), to a limited extent (Nudo, 2006b). For further detail, see e.g. Zatorre (2012).

Regarding use-dependent plasticity, in particular, the purpose and significance of such plastic modifications in the adult brain are not completely understood, especially if one considers maladaptive changes such as dystonia or phantom-limb pain.

Use-dependent modifications in the cortical representations can appear very rapidly (remember e.g. that 5 hours of artificial finger webbing were enough to elicit visible modifications in the cortical representation (Stavrinou et al., 2007)). This means that they most probably do not depend on neurogenesis or on the formation of new projections between distinct brain areas. Several other mechanisms are possible immediately after the event (experience, lesion, …) (Kaas, 2000): 1) Changes in the balance of excitation and inhibition can be achieved very quickly. Already existing connections that where kept silenced until now through strong inhibition can become rapidly unmasked due to disinhibition, probably mediated by a the removal of local GABAergic inhibition (Dancause and Nudo, 2011). 2) The synaptic efficacy in existing neural circuits can be modulated by LTP (leading to an increase of synaptic efficacy) or LTD (leading to a decrease of synaptic efficacy. 3) The neuronal membrane excitability can change.

Then, in a second phase, lasting at least several weeks, changes operate over the longer time (Dancause and Nudo, 2011). Structural changes appear, such as the formation of new dendritic spines and changes in dendritic arborisation, followed by sprouting of new axonal terminals, and the formation of new synapses between neurons. In case of a lesion, the remainder of the deprived cortex undergoes some gradual modifications and becomes responsive to other inputs (Dancause and Nudo, 2011). Note that these mechanisms are not mutually exclusive because plastic changes are expected to occur over several time scales.

Biology of the long-tailed macaque

Long-tailed macaques, also known as crab-eating macaques or cynomolgus monkeys (*Macaca fascicularis*, Raffles, 1821) belong to the Primate order, the Cercopithecidae family and the Cercopithecinae subfamily (Groves, 2005). Males usually measure between 40 cm and 65 cm, and weigh between 5 kg and 10 kg whereas females range between 40 cm and 50 cm and weigh between 2.5 kg and 7 kg. Another characteristic of the sexual dimorphism is the much more prominent canine teeth in males than in females (Cawthon Lang, 2006). According to their name, the tail is longer than the rest of the body. The back, leg, and arm fur of long-tailed macaques ranges usually from light brown or grayish to brown. A small hair crest is usually present in the midline on head (Groves, 2005).

The long-tailed macaques originate from islands of Southeast Asia and mainland Asia and usually live in coastal, mangrove, swamp, and riverine forests from 0 up to 2000 m above sea level and favour habitats near water such as riverbanks, lakeshores, or seacoast. They primarily eat fruits but also some small invertebrates, insects, eggs, frogs, crabs, shrimps and octopus (Cawthon Lang, 2006). These animals usually store food in their cheek pouches during foraging in order to eat later quietly, especially for dominated animals.

Long-tailed macaques are social animals and live in highly hierarchical groups. In the wild, macaque monkeys live in large multi-male, multi-female groups made of about 40 animals, usually with a ratio of one male for every 2.4 females. On the one hand, female offspring keeps the maternal hierarchical rank and remains closely associated with its group and hierarchical status throughout its life. On the other hand, male offspring leaves its birth group at sexual maturity to attempt to incorporate into a new group, meaning that its hierarchical status evolves throughout its life depending on its age, temperament and group size (Tardif et al., 2012). Long-tailed macaques reach sexual maturity at the age of 3 (females) or 4 (males) years old and may become as old as 30 years old. The period of pregnancy in females is 165 days (Groves, 2005; Tardif et al., 2012).

General aims of the thesis

As discussed above, the motor control cannot be fully understood without considering its somatosensory component. However, until now, most studies in the laboratory have focused on the post-lesion reorganisation taking place in the motor system itself, after an M1 lesion (Hamadjida et al., 2012; Liu and Rouiller, 1999; Rouiller et al., 1998; Rouiller and Olivier, 2004; Wyss et al., 2013). Conversely, relatively little attention has been given to the reorganisation of the somatosensory system after an M1 lesion.

Based on this situation, the first aim was to develop a methodological approach allowing to investigate the reorganisation of the somatosensory system in macaque monkeys after an M1 lesion. To this end, during my Master thesis, already carried out in the laboratory of Prof. Eric Rouiller, I have already contributed towards the early developments of a method of whole-scalp EEG mapping of SSEPs in anaesthetised macaque monkeys. We decided to focus on the EEG technique because this non-invasive tool provides an instant reflection of the ongoing neurophysiological processes taking place within the cerebral cortex. At that time, EEG recordings were obtained from intact monkeys only. Thus, in order to use this recently introduced EEG technique for post-lesion investigations of the cortical reorganisation, a second aim was to verify that a craniotomy itself – required to perform an M1 lesion– did not induce any artifact in the EEG signals recorded at the scalp.

From the moment that we fully validated the EEG recording of SSEPs after a craniotomy, the third aim of the present thesis was to apply the EEG measurement of SSEPs to document the mechanisms of reorganisation taking place in the somatosensory system following a permanent lesion of the hand representation in M1. Essentially, was the somatosensory processing affected by the M1 lesion? If yes, were the plastic modifications restricted to the cortical level? Could one gain more knowledge about the mechanisms of cortical reorganisation by using different stimulation paradigms to elicit SSEPs?

In addition, measuring SSEPs means that a large number of stimuli are presented in a repeated manner, what is known to induce adaptation in some cases. Consequently, the fourth aim was to determine to what extent the simulation paradigm used was affected by adaptation.

The sensorimotor system is the anatomical substrate of motor behaviour. A behavioural task allowing to assess more specifically the effects of an M1 lesion on the somatosensory system itself has been previously developed but there was no conclusive method to analyse the collected data until now. Thus, based on these already existing data, the fifth aim was to develop an effective analysis method able to document somatosensory impairments resulting from the M1 lesion, in case they were some.

Besides these projects involving macaque monkeys, we started a collaboration with Dr Arko Ghosh (University of Zürich and ETH Zürich), aiming at investigating how past sensory experiences of the daily, unconstrained life shape the sensory cortical processing in the adult brain, i.e. how use-dependent plasticity is implemented in daily life. By focusing on smartphone users and nonusers, we were interested in particular in investigating the impact of smartphone daily use on tactile sensory processing in the brain. In addition, we intended to better understand how the different temporal features of our tactile behaviour on a smartphone touchscreen are imprinted in brain cortical activity.

More specific aims will be declared in each result chapter.

References

Abbruzzese, G., Marchese, R., Buccolieri, A., Gasparetto, B., Trompetto, C., 2001. Abnormalities of sensorimotor integration in focal dystonia: a transcranial magnetic stimulation study. Brain 124, 537-545.

Abraira, V.E., Ginty, D.D., 2013. The Sensory Neurons of Touch. Neuron 79, 618-639.

Adkins, D.L., Boychuk, J., Remple, M.S., Kleim, J.A., 2006. Motor training induces experience-specific patterns of plasticity across motor cortex and spinal cord. J Appl.Physiol 101, 1776-1782.

Adrian, E.D., 1941. Afferent discharges to the cerebral cortex from peripheral sense organs. J Physiol 100, 159-191.

Adrian, E.D., Matthews, B.H., 1934. The interpretation of potential waves in the cortex. J Physiol 81, 440-471.

Adrian, E.D., Moruzzi, G., 1939. Impulses in the pyramidal tract. J.Physiol 97, 153-199.

Al-Chaer, E.D., Feng, Y., Willis, W.D.Jr., 1998. A Role for the Dorsal Column in Nociceptive Visceral Input Into the Thalamus of Primates. Journal of Neurophysiology 79, 3143-3150.

Allard, T., Clark, S.A., Jenkins, W.M., Merzenich, M.M., 1991. Reorganization of somatosensory area 3b representations in adult owl monkeys after digital syndactyly. J Neurophysiol. 66, 1048-1058.

Allison, T., Hume, A.L., 1981. A comparative analysis of short-latency somatosensory evoked potentials in man, monkey, cat, and rat. Exp.Neurol. 72, 592-611.

Allison, T., McCarthy, G., Wood, C.C., Jones, S.J., 1991a. Potentials evoked in human and monkey cerebral cortex by stimulation of the median nerve. A review of scalp and intracranial recordings. Brain 114 (Pt 6), 2465-2503.

Allison, T., Wood, C.C., McCarthy, G., Spencer, D.D., 1991b. Cortical somatosensory evoked potentials. II. Effects of excision of somatosensory or motor cortex in humans and monkeys. J Neurophysiol 66, 64-82.

Alstermark, B., Ogawa, J., Isa, T., 2004. Lack of Monosynaptic Corticomotoneuronal EPSPs in Rats: Disynaptic EPSPs Mediated Via Reticulospinal Neurons and Polysynaptic EPSPs Via Segmental Interneurons. Journal of Neurophysiology 91, 1832-1839.

Altman, J., 1962. Are New Neurons Formed in the Brains of Adult Mammals? Science 135, 1127-1128.

Altman, J., Das, G.D., 1965. Post-Natal Origin of Microneurones in the Rat Brain. Nature 207, 953-956.

Amaral, D.G., Strick, P.L., 2013. The Organization of the Central Nervous System. In: Kandel, E.R., Schwartz, J.H., Jessell, T.M., Siegelbaum, S.A., Hudspeth, A.J. (Eds.), Principles of Neural Science, Fifth Edition. McGraw-Hill Education, pp. 337-355.

Aminoff, M.J., Eisen, A.A., 1998. AAEM minimonograph 19: somatosensory evoked potentials. Muscle Nerve 21, 277-290.

Amirikian, B., Georgopoulos, A.P., 2000. Directional tuning profiles of motor cortical cells. Neuroscience Research 36, 73-79.

Amunts, K., Schlaug, G., Jäncke, L., Steinmetz, H., Schleicher, A., Dabringhaus, A., Zilles, K., 1997. Motor cortex and hand motor skills: structural compliance in the human brain. Human Brain Mapping 5, 206-215.

Andres, K.H., von Düring, M., 1973. Morphology of cutaneous receptors., Somatosensory system. Springer, pp. 3-28.

Andrew, D., Haavik, H., Dancey, E., Yielder, P., Murphy, B., 2014. Somatosensory evoked potentials show plastic changes following a novel motor training task with the thumb. Clin.Neurophysiol.

Apkarian, A.V., Hodge, C.J., 1989a. A dorsolateral spinothalamic tract in macaque monkey. Pain 37, 323-333.

Apkarian, A.V., Hodge, C.J., 1989b. Primate spinothalamic pathways: III. Thalamic terminations of the dorsolateral and ventral spinothalamic pathways. The Journal of Comparative Neurology 288, 493-511.

Aranguiz, R., Chana-Cuevas, P., Alburquerque, D., Leon, M., 2011. Focal dystonia in musicians. Neurologia 26, 45-52.

Arezzo, J.C., Legatt, A.D., Vaughan, H.G.Jr., 1979. Topography and intracranial sources of somatosensory evoked potentials in the monkey. I. Early components. Electroencephalogr.Clin.Neurophysiol 46, 155-172.

Arezzo, J.C., Vaughan, H.G.Jr., Legatt, A.D., 1981. Topography and intracranial sources of somatosensory evoked potentials in the monkey. II. Cortical components. Electroencephalogr.Clin.Neurophysiol 51, 1-18.

Aristotle, 350 B.C. de Anima, [Ensouled Body] Book III. Centre for the Development of Artist's Books and Limited Editions.

Armand, J., Olivier, E., Edgley, S.A., Lemon, R.N., 1997. Postnatal development of corticospinal projections from motor cortex to the cervical enlargement in the macaque monkey. J Neurosci. 17, 251-266.

Asanuma, H., 1973. Cerebral cortical control of movement. Physiologist 16, 143-166.

Asanuma, H., 1975. Recent developments in the study of the columnar arrangement of neurons within the motor cortex. Physiol Rev 55, 143-156.

Asanuma, H., Arissian, K., 1984. Experiments on functional role of peripheral input to motor cortex during voluntary movements in the monkey. J.Neurophysiol. 52, 212-227.

Asanuma, H., Rosén, I., 1972. Functional role of afferent inputs to the monkey motor cortex. Brain Res 40, 3-5.

Asanuma, H., Zarzecki, P., Jankowska, E., Hongo, T., Marcus, S., 1979a. Projection of individual pyramidal tract neurons to lumbar motor nuclei of the monkey. Exp Brain Res 34, 73-89.

Asanuma, H., Larsen, K.D., Yumiya, H., 1979b. Direct sensory pathways to the motor cortex in the monkey: a basis of cortical reflexes. In: Asanuma, H., Wilson, V.J. (Eds.), Integration in the nervous system. Igaku-shoin Tokyo, pp. 223-238.

Ask Larsen, F., Damen, S., 2014. Definitions of deafblindness and congenital deafblindness. Research in Developmental Disabilities 35, 2568-2576.

Augustine, J.R., 2008. Human neuroanatomy. Academic Press.

Aydin, U., Vorwerk, J., Kupper, P., Heers, M., Kugel, H., Galka, A., Hamid, L., Wellmer, J., Kellinghaus, C., Rampp, S., Wolters, C.H., 2014. Combining EEG and MEG for the Reconstruction of Epileptic Activity Using a Calibrated Realistic Volume Conductor Model. PLoS One 9, e93154.

Bach-y-Rita, P., 1983. Tactile Vision Substitution: Past and Future. International Journal of Neuroscience 19, 29-36.

Bach-y-Rita, P., Collins, C.C., Saunders, F.A., White, B., Scadden, L., 1969. Vision substitution by tactile image projection. Nature 221, 963-964.

Bach-y-Rita, P., 1967. Sensory plasticity. Acta Neurologica Scandinavica 43, 417-426.

Baker, S.N., 2011. The primate reticulospinal tract, hand function and functional recovery. J Physiol 589, 5603-5612.

Baker, S.N., Zaaimi, B., Fisher, K.M., Edgley, S.A., Soteropoulos, D.S., 2015. Pathways mediating functional recovery. In: Dancause, N., Nadeau, S., Rossignol, S. (Eds.), Progress in Brain Research, Sensorimotor Rehabilitation At the Crossroads of Basic and Clinical Sciences, Volume 218. Elsevier, pp. 389-412.

Ballesteros, S., Heller, M.A., 2008. Haptic object identification., Human Haptic Perception: Basics and Applications. Springer, pp. 207-222.

Bancroft, J.D., Gamble, M., 2008. Theory and Practice of Histological Techniques. Churchill Livingstone.

Bangert, M., Schlaug, G., 2006. Specialization of the specialized in features of external human brain morphology. European Journal of Neuroscience 24, 1832-1834.

Banoub, M., Tetzlaff, J.E., Schubert, A., 2003. Pharmacologic and physiologic influences affecting sensory evoked potentials: implications for perioperative monitoring. Anesthesiology 99, 716-737.

Barbay, S., Zoubina, E.V., Nudo, R.J., 2005. Neural Plasticity in Adult Motor Cortex. In: Ebner, F.F. (Ed.), Neural Plasticity in Adult Somatic Sensory-Motor Systems. CRC Press, Nashville, TN, pp. 155-188.

Bashir, S., Kaeser, M., Wyss, A., Hamadjida, A., Liu, Y., Bloch, J., Brunet, J.F., Belhaj-Saïf, A., Rouiller, E.M., 2012. Short-term effects of unilateral lesion of the primary motor cortex (M1) on ipsilesional hand dexterity in adult macaque monkeys. Brain Struct.Funct. 217, 63-79.

Baumann, M.A., Fluet, M.C., Scherberger, H., 2009. Context-Specific Grasp Movement Representation in the Macaque Anterior Intraparietal Area. The Journal of Neuroscience 29, 6436-6448.

Bear, M.F., Connors, B.W., Paradiso, M.A., 2007. Neuroscience: Exploring the Brain, 3rd ed. Lippincott Williams & Wilkins.

Beaud, M.L., Rouiller, E.M., Bloch, J., Mir, A., Schwab, M.E., Wannier, T., Schmidlin, E., 2012. Invasion of lesion territory by regenerating fibers after spinal cord injury in adult macaque monkeys. Neuroscience 227, 271-282.

Beaud, M.L., Schmidlin, E., Wannier, T., Freund, P., Bloch, J., Mir, A., Schwab, M.E., Rouiller, E.M., 2008. Anti-Nogo-A antibody treatment does not prevent cell body shrinkage in the motor cortex in adult monkeys subjected to unilateral cervical cord lesion. BMC.Neurosci. 9, 5.

Beisteiner, R., Windischberger, C., Lanzenberger, R., Edward, V., Cunnington, R., Erdler, M., Gartus, A., Streibl, B., Moser, E., Deecke, L., 2001. Finger somatotopy in human motor cortex. Neuroimage 13, 1016-1026.

Belhaj-Saif, A., Cheney, P.D., 2000. Plasticity in the distribution of the red nucleus output to forearm muscles after unilateral lesions of the pyramidal tract. J Neurophysiol 83, 3147-3153.

Benar, C.G., Gotman, J., 2002. Modeling of post-surgical brain and skull defects in the EEG inverse problem with the boundary element method. Clin.Neurophysiol 113, 48-56.

Bengtsson, S.L., Nagy, Z., Skare, S., Forsman, L., Forssberg, H., Ullen, F., 2005. Extensive piano practicing has regionally specific effects on white matter development. Nat Neurosci 8, 1148-1150.

Bennett, K.M., Lemon, R.N., 1996. Corticomotoneuronal contribution to the fractionation of muscle activity during precision grip in the monkey. J.Neurophysiol. 75, 1826-1842.

Bensmaia, S.J., Leung, Y.Y., Hsiao, S.S., Johnson, K.O., 2005. Vibratory adaptation of cutaneous mechanoreceptive afferents. J Neurophysiol. 94, 3023-3036.

Berger, H., 1929. Ueber das Elektrenkephalogramm des Menschen, 1st report. Archiv für Psychiatrie 87, 527-570.

Berger, H., 1930. Ueber das Elektrenkephalogram des Menschen, II. Mitteilung. J.Psychol.Neurol.(Lpz) 40, 160-179.

Berger, J.R., Blum, A.S., 2007. Somatosensory evoked potentials. In: Blum, A.S., Rutkove, S.B. (Eds.), The Clinical Neurophysiology Primer. Humana Press Totowa, New Jersey, pp. 485-495.

Bernhard, C.G., Bohm, E., 1954. Cortical representation and functional significance of the corticomotoneuronal system. AMA.Arch.Neurol.Psychiatry 72, 473-502.

Biber, M.P., Kneisley, L.W., LaVail, J.H., 1978. Cortical neurons projecting to the cervical and lumbar enlargements of the spinal cord in young and adult rhesus monkeys. Experimental Neurology 59, 492-508.

Birbaumer, N., Lutzenberger, W., Montoya, P., Larbig, W., Unertl, K., Töpfner, S., Grodd, W., Taub, E., Flor, H., 1997. Effects of Regional Anesthesia on Phantom Limb Pain Are Mirrored in Changes in Cortical Reorganization. The Journal of Neuroscience 17, 5503-5508.

Blake, D.T., Byl, N.N., Cheung, S., Bedenbaugh, P., Nagarajan, S., Lamb, M., Merzenich, M., 2002. Sensory representation abnormalities that parallel focal hand dystonia in a primate model. Somatosensory & Motor Research 19, 347-357.

Blankenburg, F., Ruben, J., Meyer, R., Schwiemann, J., Villringer, A., 2003. Evidence for a Rostral-to-Caudal Somatotopic Organization in Human Primary Somatosensory Cortex with Mirror-reversal in Areas 3b and 1. Cerebral Cortex 13, 987-993.

Blume, K.R., Dietrich, C., Huonker, R., Gotz, T., Sens, E., Friedel, R., Hofmann, G.O., Miltner, W.H., Weiss, T., 2014. Cortical reorganization after macroreplantation at the upper extremity: a magnetoencephalographic study. Brain 137, 757-769.

Boas, D.A., Dunn, A.K., 2010. Laser speckle contrast imaging in biomedical optics. Journal of Biomedical Optics 15, 011109.

Boivie, J., 1979. An anatomical reinvestigation of the termination of the spinothalamic tract in the monkey. The Journal of Comparative Neurology 186, 343-369.

Bolanowski, S.J.Jr., Gescheider, G.A., Verrillo, R.T., Checkosky, C.M., 1988. Four channels mediate the mechanical aspects of touch. The Journal of the Acoustical Society of America 84, 1680-1694.

Bonini, L., Rozzi, S., Serventi, F.U., Simone, L., Ferrari, P.F., Fogassi, L., 2010. Ventral premotor and inferior parietal cortices make distinct contribution to action organization and intention understanding. Cereb.Cortex 20, 1372-1385.

Borra, E., Belmalih, A., Calzavara, R., Gerbella, M., Murata, A., Rozzi, S., Luppino, G., 2008. Cortical Connections of the Macaque Anterior Intraparietal (AIP) Area. Cerebral Cortex 18, 1094-1111.

Bortoff, G.A., Strick, P.L., 1993. Corticospinal terminations in two new-world primates: further evidence that corticomotoneuronal connections provide part of the neural substrate for manual dexterity. J Neurosci 13, 5105-5118.

Bossy, J.G., Ferratier, R., 1968. Studies of the spinal cord of Galago senegalensis, compared to that in man. The Journal of Comparative Neurology 132, 485-498.

Boudreau, M.J., Smith, A.M., 2001. Activity in rostral motor cortex in response to predictable force-pulse perturbations in a precision grip task. J Neurophysiol. 86, 1079-1085.

Boudrias, M.H., Belhaj-Saïf, A., Park, M.C., Cheney, P.D., 2006. Contrasting properties of motor output from the supplementary motor area and primary motor cortex in rhesus macaques. Cereb.Cortex 16, 632-638.

Boyke, J., Driemeyer, J., Gaser, C., Büchel, C., May, A., 2008. Training-induced brain structure changes in the elderly. The Journal of Neuroscience 28, 7031-7035.

Brandeis, D., Michel, C.M., Amzica F., 2009. From neuronal activity to scalp potential fields. In: Michel, C.M., Koenig, T., Brandeis, D., Gianotti, L.R.R., Wackermann, J. (Eds.), Electrical neuroimaging. Cambridge University Press, pp. 1-24.

Braun, S.M., Jessberger, S., 2014. Adult neurogenesis: mechanisms and functional significance. Development 141, 1983-1986.

Brazier, M.A.B., 1963. The history of the electrical activity of the brain as a method for localizing sensory function. Medical History 7, 199-211.

Bremer, F., Dow, R.S., 1939. The cerebral acoustic area of the cat - A combined oscillographic and cytoarchitectonic study. Journal of Neurophysiology 2, 308-318.

Brinkman, C., 1984. Supplementary motor area of the monkey's cerebral cortex: short- and long-term deficits after unilateral ablation and the effects of subsequent callosal section. J Neurosci. 4, 918-929.

Brinkman, C., Porter, R., 1979. Supplementary motor area in the monkey: activity of neurons during performance of a learned motor task. Journal of Neurophysiology 42, 681-709.

Brinkman, C., 1981. Lesions in supplementary motor area interfere with a monkey's performance of a bimanual coordination task. Neuroscience Letters 27, 267-270.

Brisben, A.J., Hsiao, S.S., Johnson, K.O., 1999. Detection of Vibration Transmitted Through an Object Grasped in the Hand. Journal of Neurophysiology 81, 1548-1558.

Brochier, T., Boudreau, M.J., Paré, M., Smith, A.M., 1999. The effects of muscimol inactivation of small regions of motor and somatosensory cortex on independent finger movements and force control in the precision grip. Exp Brain Res 128, 31-40.

Brochier, T., Umiltà, M.A., 2007. Cortical control of grasp in non-human primates. Current Opinion in Neurobiology 17, 637-643.

Brodbeck, V., Lascano, A.M., Spinelli, L., Seeck, M., Michel, C.M., 2009. Accuracy of EEG source imaging of epileptic spikes in patients with large brain lesions. Clin.Neurophysiol 120, 679-685.

Brodbeck, V., Spinelli, L., Lascano, A.M., Pollo, C., Schaller, K., Vargas, M.I., Wissmeyer, M., Michel, C.M., Seeck, M., 2010. Electrical source imaging for presurgical focus localization in epilepsy patients with normal MRI. Epilepsia 51, 583-591.

Brodbeck, V., Spinelli, L., Lascano, A.M., Wissmeier, M., Vargas, M.I., Vulliemoz, S., Pollo, C., Schaller, K., Michel, C.M., Seeck, M., 2011. Electroencephalographic source imaging: a prospective study of 152 operated epileptic patients. Brain 134, 2887-2897.

Brodmann, K., 1909. Vergleichende Lokalisationslehre der Grosshirnrinde: in ihren Prinzipien dargestellt auf Grund des Zellenbaues. Verlag von Johann Ambrosius Barth, Leipzig.

Brozzoli, C., Makin, T.R., Cardinali, L., Holmes, L.P., Farnè, A., 2011. Peripersonal Space: A Multisensory Interface for Body–Object Interactions. In: Murray, M.M., Wallace, M.T. (Eds.), The neural bases of multisensory processes. CRC Press.

Brunet, J.F., Rouiller, E.M., Wannier, T., Villemure, J.G., Bloch, J., 2005. Primate adult brain cell autotransplantation, a new tool for brain repair? Exp.Neurol. 196, 195-198.

Buchner, H., Adams, L., Muller, A., Ludwig, I., Knepper, A., Thron, A., Niemann, K., Scherg, M., 1995. Somatotopy of human hand somatosensory cortex revealed by dipole source analysis of early somatosensory evoked potentials and 3D-NMR tomography. Electroencephalogr.Clin.Neurophysiol 96, 121-134.

Buneo, C.A., Andersen, R.A., 2006. The posterior parietal cortex: Sensorimotor interface for the planning and online control of visually guided movements. Neuropsychologia 44, 2594-2606.

Burgess, P.R., Perl, E.R., 1973. Cutaneous Mechanoreceptors and Nociceptors. In: Iggo, A. (Ed.), Somatosensory System, 2nd ed. Springer Berlin Heidelberg, pp. 29-78.

Burton, H., Fabri, M., 1995. Ipsilateral intracortical connections of physiologically defined cutaneous representations in areas 3b and 1 of macaque monkeys: projections in the vicinity of the central sulcus. J Comp Neurol. 355, 508-538.

Burton, H., Robinson, C.J., 1981. Organization of the S II Parietal Cortex. In: Woolsey, C. (Ed.), Cortical Sensory Organization, 1st ed. Humana Press, pp. 67-119.

Buys, E.J., Lemon, R.N., Mantel, G.W., Muir, R.B., 1986. Selective facilitation of different hand muscles by single corticospinal neurones in the conscious monkey. J Physiol 381, 529-549.

Buzsáki, G., 2006. Rhythms of the Brain. Oxford University Press.

Buzsáki, G., Anastassiou, C.A., Koch, C., 2012. The origin of extracellular fields and currents - EEG, ECoG, LFP and spikes. Nat Rev Neurosci 13, 407-420.

Byl, N.N., Merzenich, M.M., Cheung, S., Bedenbaugh, P., Nagarajan, S.S., Jenkins, W.M., 1997. A primate model for studying focal dystonia and repetitive strain injury: effects on the primary somatosensory cortex. Phys.Ther. 77, 269-284.

Byl, N.N., Merzenich, M.M., Jenkins, W.M., 1996. A primate genesis model of focal dystonia and repetitive strain injury: I. Learning-induced dedifferentiation of the representation of the hand in the primary somatosensory cortex in adult monkeys. Neurology 47, 508-520.

Calvo-Merino, B., Glaser, D.E., Grèzes, J., Passingham, R.E., Haggard, P., 2005. Action Observation and Acquired Motor Skills: An fMRI Study with Expert Dancers. Cerebral Cortex 15, 1243-1249.

Caminiti, R., Johnson, P.B., Urbano, A., 1990. Making arm movements within different parts of space: dynamic aspects in the primate motor cortex. The Journal of Neuroscience 10, 2039-2058.

Cannonieri, G.C., Bonilha, L., Fernandes, P.T., Cendes, F., Li, L.M., 2007. Practice and perfect: length of training and structural brain changes in experienced typists. Neuroreport 18, 1063-1066.

Carter, B.G., Butt, W., 2001. Review of the use of somatosensory evoked potentials in the prediction of outcome after severe brain injury. Crit Care Med. 29, 178-186.

Carter, B.G., Butt, W., 2005. Are somatosensory evoked potentials the best predictor of outcome after severe brain injury? A systematic review. Intensive Care Med. 31, 765-775.

Catania, K.C., 1999. A nose that looks like a hand and acts like an eye: the unusual mechanosensory system of the star-nosed mole. Journal of Comparative Physiology A 185, 367-372.

Catania, K.C., Kaas, J.H., 1997. Somatosensory fovea in the star-nosed mole: Behavioral use of the star in relation to innervation patterns and cortical representation. The Journal of Comparative Neurology 387, 215-233.

Caton, R., 1875. The electric currents of the brain. The British Medical Journal, 278.

Caton, R., 1887. Researches on electrical phenomena of cerebral gray matter. Transactions International Medical Congress, Washington, D.C.Sec.9 III, 246-249.

Cauna, N., Mannan, G., 1958. The structure of human digital Pacinian corpuscles (corpuscula lamellosa) and its functional significance. Journal of Anatomy 92, 1-20.

Cauna, N., Mannan, G., 1959. Development and postnatal changes of digital Pacinian corpuscles (corpuscula lamellosa) in the human hand. Journal of Anatomy 93, 271-286.

Cawthon Lang, K.A., 2006. Primate Factsheets: Long-tailed macaque (*Macaca fascicularis*) Taxonomy, Morphology, & Ecology.

Celesia, G.G., 2011. Brainstem Auditory Evoked Potentials (BAEPs) and Other Auditory Evoked Potentials. In: Schomer, D.L., Lopes da Silva, F.H. (Eds.), Niedermeyer's Electroencephalography: Basic Principles, Clinical Applications, and Related Fields, 6th ed. Lippincott Williams & Wilkins, pp. 975-1002.

Celesia, G.G., Peachey, N.S., 2011. Visual Evoked Potentials and Electroretinograms. In: Schomer, D.L., Lopes da Silva, F.H. (Eds.), Niedermeyer's Electroencephalography: Basic Principles, Clinical Applications, and Related Fields, 6th ed. Lippincott Williams & Wilkins, pp. 949-973.

Cerri, G., Shimazu, H., Maier, M.A., Lemon, R.N., 2003. Facilitation From Ventral Premotor Cortex of Primary Motor Cortex Outputs to Macaque Hand Muscles. Journal of Neurophysiology 90, 832-842.

Chambers, M.R., Andres, K.H., Duering, M., Iggo, A., 1972. The structure and function of the slowly adapting type II mechanoreceptor in hairy skin. Quarterly Journal of Experimental Physiology and Cognate Medical Sciences 57, 417-445.

Chang, Y., 2014. Reorganization and plastic changes of the human brain associated with skill learning and expertise. Front Hum.Neurosci. 8, 35.

Chapman, C.E., 1994. Active versus passive touch: factors influencing the transmission of somatosensory signals to primary somatosensory cortex. Canadian journal of physiology and pharmacology 72, 558-570.

Chapman, C.E., Beauchamp, E., 2006. Differential Controls Over Tactile Detection in Humans by Motor Commands and Peripheral Reafference. Journal of Neurophysiology 96, 1664-1675.

Chatagny, P., Badoud, S., Kaeser, M., Gindrat, A.D., Savidan, J., Fregosi, M., Moret, V., Roulin, C., Schmidlin, E., Rouiller, E.M., 2013. Distinction between hand dominance and hand preference in primates: a behavioral investigation of manual dexterity in nonhuman primates (macaques) and human subjects. Brain and Behavior 3, 575-595.

Chauveau, N., Franceries, X., Doyon, B., Rigaud, B., Morucci, J.P., Celsis, P., 2004. Effects of skull thickness, anisotropy, and inhomogeneity on forward EEG/ERP computations using a spherical three-dimensional resistor mesh model. Hum.Brain Mapp. 21, 86-97.

Cheema, S.S., Rustioni, A., Whitsel, B.L., 1983. Corticospinal projections from pericentral and supplementary cortices in macaques as revealed by anterograde transport of horseradish peroxidase. Neurosci.Letters.suppl. 14, 62.

Cheema, S.S., Rustioni, A., Whitsel, B.L., 1984. Light and electron microscopic evidence for a direct corticospinal projection to superficial laminae of the dorsal horn in cats and monkeys. The Journal of Comparative Neurology 225, 276-290.

Chen, J.L., Nedivi, E., 2013. Highly specific structural plasticity of inhibitory circuits in the adult neocortex. Neuroscientist. 19, 384-393.

Chen, S., Entakli, J., Bonnard, M., Berton, E., De Graaf, J.B., 2013. Functional Corticospinal Projections from Human Supplementary Motor Area Revealed by Corticomuscular Coherence during Precise Grip Force Control. PLoS One 8, e60291.

Cheney, P.D., 1980. Response of rubromotoneuronal cells identified by spike-triggered averaging of EMG activity in awake monkeys. Neuroscience Letters 17, 137-141.

Cheney, P.D., Fetz, E.E., 1985. Comparable patterns of muscle facilitation evoked by individual corticomotoneuronal (CM) cells and by single intracortical microstimuli in primates: evidence for functional groups of CM cells. J Neurophysiol 53, 786-804.

Cheney, P.D., Fetz, E.E., Mewes, K., 1991. Neural mechanisms underlying corticospinal and rubrospinal control of limb movements. In: Holstege, G. (Ed.), Progress in Brain Research, Role of The Forebrain in Sensation and Behavior, Volume 87. Elsevier, pp. 213-252.

Chouinard, P.A., Paus, T., 2006. The primary motor and premotor areas of the human cerebral cortex. neuroscientist 12, 143-152.

Churchill, J., Tharp, J., Wellman, C., Sengelaub, D., Garraghty, P., 2004. Morphological correlates of injury-induced reorganization in primate somatosensory cortex. BMC Neuroscience 5, 43.

Clark, S.A., Allard, T., Jenkins, W.M., Merzenich, M.M., 1988. Receptive fields in the body-surface map in adult cortex defined by temporally correlated inputs. Nature 332, 444-445.

Cohen of Birkenhead, 1959. Richard Caton (1842-1926) Pioneer Electrophysiologist. Proc.R.Soc.Med. 52, 645-651.

Cohen, L.G., Celnik, P., Pascual-Leone, A., Corwell, B., Faiz, L., Dambrosia, J., Honda, M., Sadato, N., Gerloff, C., Dolores, M., Hallett, M., 1997. Functional relevance of cross-modal plasticity in blind humans. Nature 389, 180-183.

Cole, J., Glees, P., 1954. Effects of small lesions in sensory cortex in trained monkeys. J Neurophysiol. 17, 1-13.

Cole, J.D., Sedgwick, E.M., 1992. The perceptions of force and of movement in a man without large myelinated sensory afferents below the neck. J.Physiol 449, 503-515.

Cole, J., Paillard, J., 1995. Living without touch and peripheral information about body position and movement: Studies with deafferented subjects. The body and the self, 245-266.

Coleman, G.T., Bahramali, H., Zhang, H.Q., Rowe, M.J., 2001. Characterization of Tactile Afferent Fibers in the Hand of the Marmoset Monkey. Journal of Neurophysiology 85, 1793-1804.

Colucci-D'Amato, L., Bonavita, V., di Porzio, U., 2006. The end of the central dogma of neurobiology: stem cells and neurogenesis in adult CNS. Neurol.Sci. 27, 266-270.

Coulter, J.D., Jones, E.G., 1977. Differential distribution of corticospinal projections from individual cytoarchitectonic fields in the monkey. Brain Research 129, 335-340.

Courtine, G., Bunge, M.B., Fawcett, J.W., Grossman, R.G., Kaas, J.H., Lemon, R.N., Maier, I., Martin, J., Nudo, R.J., Ramon-Cueto, A., Rouiller, E.M., Schnell, L., Wannier, T., Schwab, M.E., Edgerton, V.R., 2007. Can experiments in nonhuman primates expedite the translation of treatments for spinal cord injury in humans? Nat.Med. 13, 561-566.

Couto, B., Salles, A., Sedeño, L., Peradejordi, M., Barttfeld, P., Canales-Johnson, A., Dos Santos, Y.V., Huepe, D., Bekinschtein, T., Sigman, M., Favaloro, R., Manes, F., Ibanez, A., 2014. The man who feels two hearts: the different pathways of interoception. Social Cognitive and Affective Neuroscience 9, 1253-1260.

Cox, J.J., Reimann, F., Nicholas, A.K., Thornton, G., Roberts, E., Springell, K., Karbani, G., Jafri, H., Mannan, J., Raashid, Y., Al-Gazali, L., Hamamy, H., Valente, E.M., Gorman, S., Williams, R., McHale, D.P., Wood, J.N., Gribble, F.M., Woods, C.G., 2006. An SCN9A channelopathy causes congenital inability to experience pain. Nature 444, 894-898.

Craig, A.D., 2009. How do you feel - now? The anterior insula and human awareness. Nat Rev Neurosci 10, 59-70.

Craig, A.D., 2013. Cooling, pain, and other feelings from the body in relation to the autonomic nervous system. In: Ruud, M.B.a.D. (Ed.), Handbook of Clinical Neurology Autonomic Nervous System, Volume 117. Elsevier, pp. 103-109.

Craig, A.D., 2014. How do you feel ? an interoceptive moment with your neurobiological self.

Craig, A.D., Zhang, E.T., 2006. Retrograde analyses of spinothalamic projections in the macaque monkey: Input to posterolateral thalamus. The Journal of Comparative Neurology 499, 953-964.

Cruccu, G., Aminoff, M.J., Curio, G., Guerit, J.M., Kakigi, R., Mauguière, F., Rossini, P.M., Treede, R.D., Garcia-Larrea, L., 2008. Recommendations for the clinical use of somatosensory-evoked potentials. Clin.Neurophysiol 119, 1705-1719.

Culberson, J.L., Brushart, T.M., 1989. Somatotopy of digital nerve projections to the cuneate nucleus in the monkey. Somatosensory & Motor Research 6, 319-330.

Cusick, C.G., Wall, J.T., Felleman, D.J., Kaas, J.H., 1989. Somatotopic organization of the lateral sulcus of owl monkeys: Area 3b, s-II, and a ventral somatosensory area. The Journal of Comparative Neurology 282, 169-190.

Cusick, J.F., Myklebust, J.B., Larson, S.J., Sances, A., 1979. Spinal cord evaluation by cortical evoked responses. Archives of Neurology 36, 140-143.

Dancause, N., Barbay, S., Frost, S.B., Plautz, E.J., Chen, D., Zoubina, E.V., Stowe, A.M., Nudo, R.J., 2005. Extensive cortical rewiring after brain injury. J.Neurosci. 25, 10167-10179.

Dancause, N., Nudo, R.J., 2011. Shaping plasticity to enhance recovery after injury. Progress in brain research 192, 273-295.

Darian-Smith, C., 2007. Monkey Models of Recovery of Voluntary Hand Movement After Spinal Cord and Dorsal Root Injury. ILAR Journal 48, 396-410.

Darian-Smith, C., Darian-Smith, I., 1993. Thalamic projections to areas 3a, 3b, and 4 in the sensorimotor cortex of the mature and infant macaque monkey. The Journal of Comparative Neurology 335, 173-199.

Darian-Smith, C., Darian-Smith, I., Burman, K., Ratcliffe, N., 1993. Ipsilateral cortical projections to areas 3a, 3b, and 4 in the macaque monkey. The Journal of Comparative Neurology 335, 200-213.

Darian-Smith, I., Kenins, P., 1980. Innervation density of mechanoreceptive fibres supplying glabrous skin of the monkey's index finger. J Physiol 309, 147-155.

Darian-Smith, I., 1984. The Sense of Touch: Performance and Peripheral Neural Processes. In: Brookhart, J.M., Mountcastle, V.B. (Eds.), Handbook of Physiology, The Nervous System, Sensory Processes. John Wiley & Sons, Inc., pp. 739-788.

Darian-Smith, I., Galea, M.P., Darian-Smith, C., Sugitani, M., Tan, A., Burman, K., 1996a. Corticospinal Connections in the Primate., The Anatomy of Manual Dexterity, Advances in Anatomy Embryology and Cell Biology, Volume 133. Springer Berlin Heidelberg, pp. 17-63.

Darian-Smith, I., Galea, M.P., Darian-Smith, C., 1996b. Manual dexterity: how does the cerebral cortex contribute? Clinical and Experimental Pharmacology and Physiology 23, 948-956.

Darian-Smith, I., Galea, M.P., Darian-Smith, C., Sugitani, M., Tan, A., Burman, K., 1996c. The Primate Sensorimotor Thalamus., The Anatomy of Manual Dexterity, Advances in Anatomy Embryology and Cell Biology, Volume 133. Springer Berlin Heidelberg, pp. 64-105.

Davare, M., Kraskov, A., Rothwell, J.C., Lemon, R.N., 2011. Interactions between areas of the cortical grasping network. Curr.Opin.Neurobiol. 21, 565-570.

Davare, M., Lemon, R., Olivier, E., 2008. Selective modulation of interactions between ventral premotor cortex and primary motor cortex during precision grasping in humans. The Journal of physiology 586, 2735-2742.

Davare, M., Montague, K., Olivier, E., Rothwell, J.C., Lemon, R.N., 2009. Ventral premotor to primary motor cortical interactions during object-driven grasp in humans. Cortex 45, 1050-1057.

Dawson, G.D., 1947a. Cerebral Responses to Electrical Stimulation of Peripheral Nerve in Man. Journal of Neurology Neurosurgery and Psychiatry 10, 134-140.

Dawson, G.D., 1947b. Investigations on a patient subject to myoclonic seizures after sensory stimulation. J Neurol.Neurosurg.Psychiatry 10, 141-162.

Dawson, G.D., 1950. Cerebral responses to nerve stimulation in man. Br.Med.Bull. 6, 326-329.

Dawson, G.D., 1951. A summation technique for detecting small signals in a large irregular background. The Journal of physiology (London) 115, 2P.

Dawson, G.D., 1954. A summation technique for the detection of small evoked potentials. Electroencephalography and Clinical Neurophysiology 6, 65-84.

Dayan, E., Cohen, L.G., 2011. Neuroplasticity subserving motor skill learning. Neuron 72, 443-454.

de Munck and, J.C., 1991. Symmetry considerations in the quasi-static approximation of volume conductor theory. Physics in Medicine and Biology 36, 521.

de Noordhout, A.M., Rapisarda, G., Bogacz, D., Gerard, P., De Pasqua, V., Pennisi, G., Delwaide, P.J., 1999. Corticomotoneuronal synaptic connections in normal man: an electrophysiological study. Brain 122 (Pt 7), 1327-1340.

Dechent, P., Frahm, J., 2003. Functional somatotopy of finger representations in human primary motor cortex. Hum.Brain Mapp. 18, 272-283.

Dehaene, S., Cohen, L., Morais, J., Kolinsky, R., 2015. Illiterate to literate: behavioural and cerebral changes induced by reading acquisition. Nat Rev Neurosci 16, 234-244.

Deliagina, T.G., Beloozerova, I.N., Orlovsky, G.N., Zelenin, P.V., 2014. Contribution of supraspinal systems to generation of automatic postural responses. Frontiers in Integrative Neuroscience 8.

Desmedt, J.E., 1987. Physiologie et physiopathologie des sensations somatiques étudiées chez l'Homme par la méthode des potentiels évoqués, [Physiology and physiopathology of somatic sensations studied in man by the method of evoked potentials]. J Physiol (Paris) 82, 64-136.

Dettmers, C., Adler, T., Rzanny, R., van Schayck, R., Gaser, C., Weiss, T., Miltner, W.H., Brückner, L., Weiller, C., 2001. Increased excitability in the primary motor cortex and supplementary motor area in patients with phantom limb pain after upper limb amputation. Neuroscience Letters 307, 109-112.

Di Paola, M., Caltagirone, C., Petrosini, L., 2013. Prolonged rock climbing activity induces structural changes in cerebellum and parietal lobe. Human Brain Mapping 34, 2707-2714.

di Pellegrino, G., Fadiga, L., Fogassi, L., Gallese, V., Rizzolatti, G., 1992. Understanding motor events: a neurophysiological study. Exp Brain Res 91, 176-180.

Diamond, M.E., von Heimendahl, M., Knutsen, P.M., Kleinfeld, D., Ahissar, E., 2008. 'Where' and 'what' in the whisker sensorimotor system. Nat.Rev.Neurosci. 9, 601-612.

Doidge, N., 2007. The brain that changes itself: Stories of personal triumph from the frontiers of brain science. Penguin.

Draganski, B., Gaser, C., Busch, V., Schuierer, G., Bogdahn, U., May, A., 2004. Neuroplasticity: Changes in grey matter induced by training. Nature 427, 311-312.

Draganski, B., Gaser, C., Kempermann, G., Kuhn, H.G., Winkler, J., Büchel, C., May, A., 2006. Temporal and Spatial Dynamics of Brain Structure Changes during Extensive Learning. The Journal of Neuroscience 26, 6314-6317.

Dum, R.P., Strick, P.L., 1991. The origin of corticospinal projections from the premotor areas in the frontal lobe. J Neurosci. 11, 667-689.

Dum, R.P., Strick, P.L., 1996a. Spinal cord terminations of the medial wall motor areas in macaque monkeys. J Neurosci. 16, 6513-6525.

Dum, R.P., Strick, P.L., 2002. Motor areas in the frontal lobe of the primate. Physiol Behav. 77, 677-682.

Dum, R.P., Strick, P.L., 2005. Frontal lobe inputs to the digit representations of the motor areas on the lateral surface of the hemisphere. J Neurosci. 25, 1375-1386.

Dum, R.P., Levinthal, D.J., Strick, P.L., 2009. The Spinothalamic System Targets Motor and Sensory Areas in the Cerebral Cortex of Monkeys. The Journal of Neuroscience 29, 14223-14235.

Dum, R.P., Strick, P.L., 1996b. Spinal Cord Terminations of the Medial Wall Motor Areas in Macaque Monkeys. The Journal of Neuroscience 16, 6513-6525.

Eisner-Janowicz, I., Barbay, S., Hoover, E., Stowe, A.M., Frost, S.B., Plautz, E.J., Nudo, R.J., 2008. Early and late changes in the distal forelimb representation of the supplementary motor area after injury to frontal motor areas in the squirrel monkey. J Neurophysiol 100, 1498-1512.

Elbert, T., Candia, V., Altenmuller, E., Rau, H., Sterr, A., Rockstroh, B., Pantev, C., Taub, E., 1998. Alteration of digital representations in somatosensory cortex in focal hand dystonia. Neuroreport 9, 3571-3575.

Elbert, T., Pantev, C., Wienbruch, C., Rockstroh, B., Taub, E., 1995. Increased cortical representation of the fingers of the left hand in string players. Science 270, 305-307.

Elbert, T., Rockstroh, B., 2004. Reorganization of human cerebral cortex: the range of changes following use and injury. neuroscientist 10, 129-141.

Erwin, C.W., Rozear, M.P., Radtke, R.A., Erwin, A.C., 1987. Somatosensory evoked potentials. In: Niedermeyer, E., Lopes da Silva, F.H. (Eds.), Electroencephalography: Basic Principles, Clinical Applications and Related Fields, 2nd ed. Urban & Schwarzenberg, pp. 817-833.

Evarts, E.V., 1968. Relation of pyramidal tract activity to force exerted during voluntary movement. Journal of Neurophysiology 31, 14-27.

Evarts, E.V., 1974. Precentral and postcentral cortical activity in association with visually triggered movement. J Neurophysiol. 37, 373-381.

Feldmeyer, D., Brecht, M., Helmchen, F., Petersen, C.C., Poulet, J.F., Staiger, J.F., Luhmann, H.J., Schwarz, C., 2013. Barrel cortex function. Prog.Neurobiol. 103, 3-27.

Felix, D., Wiesendanger, M., 1970. Cortically induced inhibition in the dorsal column nuclei of monkeys. Pflugers Arch. 320, 285-288.

Fender, D.H., 1987. Source localization of brain electrical activity. In: Gevins, A.S., Remond, A. (Eds.), Handbook of electroencephalography and clinical neurophysiology, vol. 1. Methods of analysis of brain electrical and magnetic signals. Elsevier, Amsterdam, pp. 355-399.

Ferezou, I., Haiss, F., Gentet, L.J., Aronoff, R., Weber, B., Petersen, C.C., 2007. Spatiotemporal dynamics of cortical sensorimotor integration in behaving mice. Neuron 56, 907-923.

Ferrier, D., 1876. The functions of the brain. GP Putnam's Sons.

Ferrington, D.G., Downie, J.W., Willis, W.D.Jr., 1988. Primate nucleus gracilis neurons: responses to innocuous and noxious stimuli. Journal of Neurophysiology 59, 886-907.

Fetz, E.E., Cheney, P.D., 1980. Postspike facilitation of forelimb muscle activity by primate corticomotoneuronal cells. Journal of Neurophysiology 44, 751-772.

Fetz, E.E., Cheney, P.D., German, D.C., 1976. Corticomotoneuronal connections of precentral cells detected by post-spike averages of EMG activity in behaving monkeys. Brain Research 114, 505-510.

Firmin, L., Field, P., Maier, M.A., Kraskov, A., Kirkwood, P.A., Nakajima, K., Lemon, R.N., Glickstein, M., 2014. Axon diameters and conduction velocities in the macaque pyramidal tract. Journal of Neurophysiology 112, 1229-1240.

Fisch, B.J., 2011. Polarity and field determination. In: Niedermeyer, E., Schomer, D.L., da Silva, F.H.L. (Eds.), Niedermeyer's Electroencephalography: Basic Principles, Clinical Applications, and Related Fields. Wolters Kluwer Health/Lippincott Williams & Wilkins, pp. 143-151.

Fitzgerald, P.J., Lane, J.W., Thakur, P.H., Hsiao, S.S., 2006. Receptive Field (RF) Properties of the Macaque Second Somatosensory Cortex: RF Size, Shape, and Somatotopic Organization. The Journal of Neuroscience 26, 6485-6495.

Flemming, L., Wang, Y., Caprihan, A., Eiselt, M., Haueisen, J., Okada, Y., 2005. Evaluation of the distortion of EEG signals caused by a hole in the skull mimicking the fontanel in the skull of human neonates. Clin.Neurophysiol 116, 1141-1152.

Flor, H., Elbert, T., Knecht, S., Wienbruch, C., Pantev, C., Birbaumers, N., Larbig, W., Taub, E., 1995. Phantom-limb pain as a perceptual correlate of cortical reorganization following arm amputation. Nature 375, 482-484.

Flor, H., Nikolajsen, L., Staehelin, J.T., 2006. Phantom limb pain: a case of maladaptive CNS plasticity? Nat.Rev.Neurosci. 7, 873-881.

Florence, S.L., Hackett, T.A., Strata, F., 2000. Thalamic and Cortical Contributions to Neural Plasticity After Limb Amputation. Journal of Neurophysiology 83, 3154-3159.

Florence, S.L., Kaas, J.H., 1995. Large-scale reorganization at multiple levels of the somatosensory pathway follows therapeutic amputation of the hand in monkeys. J.Neurosci. 15, 8083-8095.

Florence, S.L., Taub, H.B., Kaas, J.H., 1998. Large-scale sprouting of cortical connections after peripheral injury in adult macaque monkeys. Science 282, 1117-1121.

Florence, S.L., Wall, J.T., Kaas, J.H., 1989. Somatotopic organization of inputs from the hand to the spinal gray and cuneate nucleus of monkeys with observations on the cuneate nucleus of humans. The Journal of Comparative Neurology 286, 48-70.

Fluet, M.C., Baumann, M.A., Scherberger, H., 2010. Context-Specific Grasp Movement Representation in Macaque Ventral Premotor Cortex. The Journal of Neuroscience 30, 15175-15184.

Foerster, O., 1936. The motor cortex in man in the light of Hughlings Jackson's doctrines. Brain 59, 135-159.

Fogassi, L., Luppino, G., 2005. Motor functions of the parietal lobe. Current Opinion in Neurobiology 15, 626-631.

Freund, P., Schmidlin, E., Wannier, T., Bloch, J., Mir, A., Schwab, M.E., Rouiller, E.M., 2006. Nogo-A-specific antibody treatment enhances sprouting and functional recovery after cervical lesion in adult primates. Nat.Med. 12, 790-792.

Freund, P., Schmidlin, E., Wannier, T., Bloch, J., Mir, A., Schwab, M.E., Rouiller, E.M., 2009. Anti-Nogo-A antibody treatment promotes recovery of manual dexterity after unilateral cervical lesion in adult primates--re-examination and extension of behavioral data. Eur.J Neurosci. 29, 983-996.

Freund, P., Wannier, T., Schmidlin, E., Bloch, J., Mir, A., Schwab, M.E., Rouiller, E.M., 2007. Anti-Nogo-A antibody treatment enhances sprouting of corticospinal axons rostral to a unilateral cervical spinal cord lesion in adult macaque monkey. J Comp Neurol. 502, 644-659.

Freye, E., 2005. Cerebral monitoring in the operating room and the intensive care unit - an introductory for the clinician and a guide for the novice wanting to open a window to the brain. Part II: Sensory-evoked potentials (SSEP, AEP, VEP). J Clin.Monit.Comput. 19, 77-168.

Frias, C.P., Wierenga, C.J., 2013. Activity-dependent adaptations in inhibitory axons. Front Cell Neurosci 7, 219.

Friedman, D.P., Jones, E.G., Burton, H., 1980. Representation pattern in the second somatic sensory area of the monkey cerebral cortex. Journal of Comparative Neurology 192, 21-41.

Friedman, D.P., 1981. Body Topography in the Second Somatic Sensory Area: Monkey SII Somatotopy. In: Woolsey, C. (Ed.), Cortical Sensory Organization, 1st ed. Humana Press, pp. 121-165.

Friedman, R.M., Chen, L.M., Roe, A.W., 2008. Responses of areas 3b and 1 in anesthetized squirrel monkeys to single- and dual-site stimulation of the digits. J Neurophysiol. 100, 3185-3196.

Friel, K.M., Barbay, S., Frost, S.B., Plautz, E.J., Hutchinson, D.M., Stowe, A.M., Dancause, N., Zoubina, E.V., Quaney, B.M., Nudo, R.J., 2005. Dissociation of sensorimotor deficits after rostral versus caudal lesions in the primary motor cortex hand representation. J Neurophysiol. 94, 1312-1324.

Fritsch, G., Hitzig, E., 1870. Electric excitability of the cerebrum [Über die elektrische Erregbarkeit des Grosshirns]. Arch Anat Physiol Wissen 37, 300-332.

Fromm, C., Evarts, E.V., 1982. Pyramidal tract neurons in somatosensory cortex: central and peripheral inputs during voluntary movement. Brain Research 238, 186-191.

Frost, S.B., Barbay, S., Friel, K.M., Plautz, E.J., Nudo, R.J., 2003. Reorganization of remote cortical regions after ischemic brain injury: a potential substrate for stroke recovery. J Neurophysiol 89, 3205-3214.

Frost, S.B., Milliken, G.W., Plautz, E.J., Masterton, R.B., Nudo, R.J., 2000. Somatosensory and motor representations in cerebral cortex of a primitive mammal (*Monodelphis domestica*): A window into the early evolution of sensorimotor cortex. The Journal of Comparative Neurology 421, 29-51.

Fujito, Y., Aoki, M., 1995. Monosynaptic rubrospinal projections to distal forelimb motoneurons in the cat. Exp Brain Res 105, 181-190.

Fujito, Y., Imai, T., Aoki, M., 1991. Monosynaptic excitation of motoneurons innervating forelimb muscles following stimulation of the red nucleus in cats. Neuroscience Letters 127, 137-140.

Galea, M.P., Darian-Smith, I., 1994. Multiple Corticospinal Neuron Populations in the Macaque Monkey Are Specified by Their Unique Cortical Origins, Spinal Terminations, and Connections. Cerebral Cortex 4, 166-194.

Gardner, E.P., Hamalainen, H.A., Warren, S., Davis, J., Young, W., 1984. Somatosensory evoked potentials (SEPs) and cortical single unit responses elicited by mechanical tactile stimuli in awake monkeys. Electroencephalogr.Clin.Neurophysiol 58, 537-552.

Gardner, E.P., Johnson, K.O., 2013a. The Somatosensory System: Receptors and Central Pathways. In: Kandel, E.R., Schwartz, J.H., Jessell, T.M., Siegelbaum, S.A., Hudspeth, A.J. (Eds.), Principles of Neural Science, Fifth Edition. McGraw-Hill Education, pp. 475-497.

Gardner, E.P., Johnson, K.O., 2013b. Touch. In: Kandel, E.R., Schwartz, J.H., Jessell, T.M., Siegelbaum, S.A., Hudspeth, A.J. (Eds.), Principles of Neural Science, Fifth Edition. McGraw-Hill Education, pp. 498-529.

Gardner, E.P., Ro, J.Y., Babu, K.S., Ghosh, S., 2007. Neurophysiology of prehension. II. Response diversity in primary somatosensory (S-I) and motor (M-I) cortices. J.Neurophysiol. 97, 1656-1670.

Gardner, E.P., 2010. Touch., Encylclopedia of Life Sciences. John Wiley & Sons, Ltd, pp. 1-12.

Garraghty, P.E., Lachica, E.A., Kaas, J.H., 1991. Injury-Induced Reorganization of Somatosensory Cortex Is Accompanied by Reductions in GABA Staining. Somatosensory & Motor Research 8, 347-354.

Gaser, C., Schlaug, G., 2003. Brain structures differ between musicians and non-musicians. J Neurosci. 23, 9240-9245.

Gentilucci, M., Fogassi, L., Luppino, G., Matelli, M., Camarda, R., Rizzolatti, G., 1988. Functional organization of inferior area 6 in the macaque monkey. Exp Brain Res 71, 475-490.

Georgopoulos, A.P., 1991. Higher Order Motor Control. Annual Review of Neuroscience 14, 361-377.

Georgopoulos, A.P., Kalaska, J.F., Caminiti, R., Massey, J.T., 1982. On the relations between the direction of two-dimensional arm movements and cell discharge in primate motor cortex. The Journal of Neuroscience 2, 1527-1537.

Georgopoulos, A.P., 1994. New concepts in generation of movement. Neuron 13, 257-268.

Georgopoulos, A.P., 2014. Cell directional spread determines accuracy, precision, and length of the neuronal population vector. Exp Brain Res 232, 2391-2405.

Georgopoulos, A.P., Merchant, H., Naselaris, T., Amirikian, B., 2007. Mapping of the preferred direction in the motor cortex. Proceedings of the National Academy of Sciences 104, 11068-11072.

Geyer, S., Ledberg, A., Schleicher, A., Kinomura, S., Schormann, T., Burgel, U., Klingberg, T., Larsson, J., Zilles, K., Roland, P.E., 1996. Two different areas within the primary motor cortex of man. Nature 382, 805-807.

Geyer, S., Schleicher, A., Zilles, K., 1999. Areas 3a, 3b, and 1 of Human Primary Somatosensory Cortex: 1. Microstructural Organization and Interindividual Variability. Neuroimage 10, 63-83.

Ghez, C., Gordon, J., Ghilardi, M.F., 1995. Impairments of reaching movements in patients without proprioception. II. Effects of visual information on accuracy. J Neurophysiol. 73, 361-372.

Ghosh, S., Porter, R., 1988. Corticocortical synaptic influences on morphologically identified pyramidal neurones in the motor cortex of the monkey. J.Physiol 400, 617-629.

Gibson, J.J., 1962. Observations on active touch. Psychological review 69, 477.

Gindrat, A.D., Chytiris, M., Balerna, M., Rouiller, E.M., Ghosh, A., 2015. Use-Dependent Cortical Processing from Fingertips in Touchscreen Phone Users. Current Biology 25, 109-116.

Gloor, P., 1985. Neuronal Generators and the Problem of Localization in Electroencephalography: Application of Volume Conductor Theory to Electroencephalography. Journal of Clinical Neurophysiology 2.

Goldberg, Y.P., MacFarlane, J., MacDonald, M.L., Thompson, J., Dube, M.P., Mattice, M., Fraser, R., Young, C., Hossain, S., Pape, T., Payne, B., Radomski, C., Donaldson, G.,

Ives, E., Cox, J., Younghusband, H.B., Green, R., Duff, A., Boltshauser, E., Grinspan, G.A., Dimon, J.H., Sibley, B.G., Andria, G., Toscano, E., Kerdraon, J., Bowsher, D., Pimstone, S.N., Samuels, M.E., Sherrington, R., Hayden, M.R., 2007. Loss-of-function mutations in the Nav1.7 gene underlie congenital indifference to pain in multiple human populations. Clinical Genetics 71, 311-319.

Gordon, J., Ghilardi, M.F., Ghez, C., 1995. Impairments of reaching movements in patients without proprioception. I. Spatial errors. J Neurophysiol. 73, 347-360.

Gould, E., Reeves, A.J., Graziano, M.S.A., Gross, C.G., 1999. Neurogenesis in the Neocortex of Adult Primates. Science 286, 548-552.

Grant, G., Boivie, J., Silfvenius, H., 1973. Course and termination of fibres from the nucleus Z of the medulla oblongata. An experimental light microscopical study in the cat. Brain Research 55, 55-70.

Grass, A.M., 1984. The Electroencephalographic Heritage Until 1960. American Journal of EEG Technology 24, 133-173.

Grave de Peralta Menendez, R., Murray, M.M., Michel, C.M., Martuzzi, R., Gonzalez Andino, S.L., 2004. Electrical neuroimaging based on biophysical constraints. Neuroimage. 21, 527-539.

Grave de Peralta, R., Hauk, O., Gonzalez, S.L., 2009. The neuroelectromagnetic inverse problem and the zero dipole localization error. Comput.Intell.Neurosci., 659247.

Graw, J., 2003. The genetic and molecular basis of congenital eye defects. Nat Rev Genet 4, 876-888.

Gray, H., 1893. Anatomy, descriptive and surgical. Lea Brothers & Company.

Griffen, T.C., Maffei, A., 2014. GABAergic synapses: their plasticity and role in sensory cortex. Front Cell Neurosci 8, 91.

Groves, C., 2005. The Taxonomy of Primates in the Laboratory Context. In: Sonia, W.C. (Ed.), The Laboratory Primate, Handbook of Experimental Animals. Academic Press, London, pp. 3-15.

Grünbaum, A.S.F., Sherrington, C.S., 1901. Observations on the Physiology of the Cerebral Cortex of Some of the Higher Apes. (Preliminary Communication.). Proceedings of the Royal Society of London 69, 206-209.

Haas, L.F., 2003. Hans Berger (1873-1941), Richard Caton (1842-1926), and electroencephalography. J Neurol.Neurosurg.Psychiatry 74, 9.

Haggard, P., 2006. Sensory Neuroscience: From Skin to Object in the Somatosensory Cortex. Current Biology 16, R884-R886.

Hallez, H., Vanrumste, B., Grech, R., Muscat, J., De Clercq, W., Vergult, A., D'Asseler, Y., Camilleri, K.P., Fabri, S.G., Van Huffel, S., Lemahieu, I., 2007. Review on solving the forward problem in EEG source analysis. J Neuroeng.Rehabil. 4, 46.

Hamadjida, A., Wyss, A.F., Mir, A., Schwab, M.E., Belhaj-Saïf, A., Rouiller, E.M., 2012. Influence of anti-Nogo-A antibody treatment on the reorganization of callosal connectivity of the premotor cortical areas following unilateral lesion of primary motor cortex (M1) in adult macaque monkeys. Exp.Brain Res. 223, 321-340.

Hamilton, R.H., Pascual-Leone, A., 1998. Cortical plasticity associated with Braille learning. Trends Cogn Sci. 2, 168-174.

Hänggi, J., Langer, N., Lutz, K., Birrer, K., Mérillat, S., Jäncke, L., 2015. Structural Brain Correlates Associated with Professional Handball Playing. PLoS One 10, e0124222.

Harms, K.J., Rioult-Pedotti, M.S., Carter, D.R., Dunaevsky, A., 2008. Transient spine expansion and learning-induced plasticity in layer 1 primary motor cortex. J Neurosci. 28, 5686-5690.

Hashimoto, I., Yoshikawa, K., Kimura, T., 2000. Somatosensory evoked potentials to a threshold air-puff can predict stimulus detection in human subjects. Neurosci.Lett. 282, 181-184.

Hashimoto, I., Yoshikawa, K., Sasaki, M., Gatayama, T., Nomura, M., 1989. Sensory nerve action potentials elicited by mechanical air-puff stimulation of the index finger in man. Electroencephalography and Clinical Neurophysiology 72, 321-333.

He, S.Q., Dum, R.P., Strick, P.L., 1993. Topographic organization of corticospinal projections from the frontal lobe: motor areas on the lateral surface of the hemisphere. J Neurosci. 13, 952-980.

He, S.Q., Dum, R.P., Strick, P.L., 1995. Topographic organization of corticospinal projections from the frontal lobe: motor areas on the medial surface of the hemisphere. J Neurosci. 15, 3284-3306.

Helmholtz, H., 1853. Ueber einige Gesetze der Vertheilung elektrischer Ströme in körperlichen Leitern mit Anwendung auf die thierisch-elektrischen Versuche. Annalen der Physik 165, 211-233.

Hendry, S.H.C., Jones, E.G., 1986. Reduction in number of immunostained GABAergic neurones in deprived-eye dominance columns of monkey area 17. Nature 320, 750-753.

Hensel, H., 1973. Cutaneous thermoreceptors., Somatosensory system. Springer, pp. 79-110.

Hepp-Reymond, M.-C., 1988. Functional organization of motor cortex and its participation in voluntary movements. In: Seklis, H.D., Erwin, J. (Eds.), Comparative Primate Biology, Vol 4: Neurosciences. Alan R. Liss, New York, pp. 501-624.

Hepp-Reymond, M.C., Huesler, E.J., Maier, M.A., 1996. Precision Grip in Humans: Temporal and Spatial Synergies. In: Flanagan, A.M.W. (Ed.), Hand and Brain. Academic Press, San Diego, pp. 37-68.

Hikosaka, O., Tanaka, M., Sakamoto, M., Iwamura, Y., 1985. Deficits in manipulative behaviors induced by local injections of muscimol in the first somatosensory cortex of the conscious monkey. Brain Research 325, 375-380.

Hlustik, P., Solodkin, A., Gullapalli, R.P., Noll, D.C., Small, S.L., 2001. Somatotopy in Human Primary Motor and Somatosensory Hand Representations Revisited. Cerebral Cortex 11, 312-321.

Hocherman, S., Wise, S.P., 1990. Trajectory-selective neuronal activity in the motor cortex of rhesus monkeys (*Macaca mulatta*). Behavioral Neuroscience 104, 495-499.

Hollins, M., 2002. Touch and Haptics. In: Pashler, H., Yantis, S. (Eds.), Stevens' Handbook of Experimental Psychology, Sensation and Perception, 3 ed. John Wiley & Sons, New York, pp. 585-618.

Holloway, M., 2003. The mutable brain. Scientific American 289, 78-85.

Holmes, G.L., Khazipov, R., 2007. Basic Neurophysiology and the Cortical Basis of EEG. In: Blum, A.S., Rutkove, S.B. (Eds.), The Clinical Neurophysiology Primer. Humana Press, pp. 19-33.

Holsheimer, J., Feenstra, B.W., 1977. Volume conduction and EEG measurements within the brain: a quantitative approach to the influence of electrical spread on the linear relationship of activity measured at different locations. Electroencephalogr.Clin.Neurophysiol. 43, 52-58.

Holtmaat, A., Wilbrecht, L., Knott, G.W., Welker, E., Svoboda, K., 2006. Experience-dependent and cell-type-specific spine growth in the neocortex. Nature 441, 979-983.

Hoogewoud, F., Hamadjida, A., Wyss, A.F., Mir, A., Schwab, M.E., Belhaj-Saïf, A., Rouiller, E.M., 2013. Comparison of functional recovery of manual dexterity after unilateral spinal cord lesion or motor cortex lesion in adult macaque monkeys. Front Neurol. 4, 101.

Hsiao, S.S., Johnson, K.O., Twombly, I.A., 1993. Roughness coding in the somatosensory system. Acta Psychologica 84, 53-67.

Huang, C.H., Bao, J., Sakaba, T., 2010. Multivesicular Release Differentiates the Reliability of Synaptic Transmission between the Visual Cortex and the Somatosensory Cortex. The Journal of Neuroscience 30, 11994-12004.

Huerta, M.F., Pons, T.P., 1990. Primary motor cortex receives input from area 3a in macaques. Brain Res. 537, 367-371.

Huffman, K.J., Krubitzer, L., 2001. Area 3a: topographic organization and cortical connections in marmoset monkeys. Cereb.Cortex 11, 849-867.

Huiskamp, G., Vroeijenstijn, M., van Dijk, R., Wieneke, G., van Huffelen, A.C., 1999. The need for correct realistic geometry in the inverse EEG problem. IEEE Trans.Biomed.Eng 46, 1281-1287.

Humphrey, D.R., Gold, R., Reed, D.J., 1984. Sizes, laminar and topographic origins of cortical projections to the major divisions of the red nucleus in the monkey. The Journal of Comparative Neurology 225, 75-94.

Hwang, K.J., Park, K.C., Chang, D.I., Yoon, S.S., 2014. Isolated Weakness of Radial-side Fingers Due to a Small Cortical Infarction. Journal of the Korean Society of Magnetic Resonance in Medicine 18, 362-365.

Iggo, A., Andres, K.H., 1982. Morphology of Cutaneous Receptors. Annual Review of Neuroscience 5, 1-31.

Iggo, A., Muir, A.R., 1969. The structure and function of a slowly adapting touch corpuscle in hairy skin. The Journal of physiology 200, 763-796.

Indovina, I., Sanes, J.N., 2001. On somatotopic representation centers for finger movements in human primary motor cortex and supplementary motor area. Neuroimage 13, 1027-1034.

Inoue, K., Nakanishi, K., Hadoush, H., Kurumadani, H., Hashizume, A., Sunagawa, T., Ochi, M., 2013. Somatosensory mechanical response and digit somatotopy within cortical areas of the postcentral gyrus in humans: an MEG study. Hum.Brain Mapp. 34, 1559-1567.

Isa, T., Ohki, Y., Alstermark, B., Pettersson, L.G., Sasaki, S., 2007. Direct and indirect cortico-motoneuronal pathways and control of hand/arm movements. Physiology.(Bethesda.) 22, 145-152.

Isa, T., Kinoshita, M., Nishimura, Y., 2013. Role of direct vs indirect pathways from the motor cortex to spinal motoneurons in the control of hand dexterity. Frontiers in Neurology 4.

Iwamura, Y., 1998. Hierarchical somatosensory processing. Current Opinion in Neurobiology 8, 522-528.

Iwamura, Y., 2007. Somatosensory Processing in the Postcentral, Intraparietal and Parietal Opercular Cortical Regions. In: Wu, J., Ito, K., Tobimatsu, S., Nishida, T., Fukuyama, H. (Eds.), Complex Medical Engineering. Springer Japan, pp. 423-437.

Iwamura, Y., Tanaka, M., 1978. Postcentral neurons in hand region of area 2: their possible role in the form discrimination of tactile objects. Brain Research 150, 662-666.

Iwamura, Y., Tanaka, M., Sakamoto, M., Hikosaka, O., 1993. Rostrocaudal gradients in the neuronal receptive field complexity in the finger region of the alert monkey's postcentral gyrus. Exp Brain Res 92, 360-368.

Jain, N., Catania, K.C., Kaas, J.H., 1998. A histologically visible representation of the fingers and palm in primate area 3b and its immutability following long-term deafferentations. Cereb.Cortex 8, 227-236.

Jain, N., Qi, H.X., Catania, K.C., Kaas, J.H., 2001. Anatomic correlates of the face and oral cavity representations in the somatosensory cortical area 3b of monkeys. The Journal of Comparative Neurology 429, 455-468.

Jamali, S., Ross, B., 2012. Precise mapping of the somatotopic hand area using neuromagnetic steady-state responses. Brain Res 1455, 28-39.

Jäncke, L., 2009. The plastic human brain. Restorative Neurology and Neuroscience 27, 521-538.

Janssen, P., Scherberger, H., 2015. Visual Guidance in Control of Grasping. Annual Review of Neuroscience.

Jenkins, W.M., Merzenich, M.M., Ochs, M.T., Allard, T., Guic-Robles, E., 1990. Functional reorganization of primary somatosensory cortex in adult owl monkeys after behaviorally controlled tactile stimulation. J Neurophysiol. 63, 82-104.

Jiang, W., Chapman, C.E., Lamarre, Y., 1991. Modulation of the cutaneous responsiveness of neurones in the primary somatosensory cortex during conditioned arm movements in the monkey. Exp Brain Res 84, 342-354.

Jiang, W., Tremblay, F., Chapman, C.E., 1997. Neuronal Encoding of Texture Changes in the Primary and the Secondary Somatosensory Cortical Areas of Monkeys During Passive Texture Discrimination. Journal of Neurophysiology 77, 1656-1662.

Johansson, R., Flanagan, J., 2008. Tactile Sensory Control of Object Manipulation in Humans., Volume 6: Somatosensation, 6th ed. Elsevier, pp. 67-86.

Johansson, R., Vallbo, A.B., 1976. Skin mechanoreceptors in the human hand: an inference of some population properties. In: Zotterman, Y. (Ed.), Sensory Functions of the Skin in Primates, Wenner–Gren Center International Symposium Series. Pergamon, pp. 171-184.

Johansson, R.S., 1978. Tactile sensibility in the human hand: receptive field characteristics of mechanoreceptive units in the glabrous skin area. The Journal of physiology 281, 101-125.

Johansson, R.S., 1991. How is grasping modified by somatosensory input. Motor control: concepts and issues, 331-355.

Johansson, R.S., 1998. Sensory input and control of grip. In: Bock, G.R., Goode, J.A. (Eds.), Novartis Foundation Symposium 218 - Sensory Guidance of Movement. Wiley, Chichester, pp. 45-63.

Johansson, R.S., 2002. Dynamic Use of Tactile Afferent Signals in Control of Dexterous Manipulation. In: Gandevia, S.C., Proske, U., Stuart, D. (Eds.), Sensorimotor Control of Movement and Posture, 508 ed. Springer US, pp. 397-410.

Johansson, R.S., Cole, K.J., 1992. Sensory-motor coordination during grasping and manipulative actions. Curr.Opin.Neurobiol. 2, 815-823.

Johansson, R.S., Flanagan, J.R., 2009a. Coding and use of tactile signals from the fingertips in object manipulation tasks. Nat Rev Neurosci 10, 345-359.

Johansson, R.S., Flanagan, J.R., 2009b. Sensorimotor Control of Manipulation. In: Squire, L.R. (Ed.), Encyclopedia of Neuroscience. Academic Press, Oxford, pp. 583-594.

Johansson, R.S., Flanagan, J.R., 2009c. Sensory control of object manipulation. In: Nowak, D.A., Hermsdörfer, J. (Eds.), Sensorimotor control of grasping: physiology and pathophysiology. Cambridge University Press, Cambridge, pp. 141-160.

Johansson, R.S., Hger, C., Backstrom, L., 1992. Somatosensory control of precision grip during unpredictable pulling loads. III. Impairments during digital anesthesia. Exp.Brain Res 89, 204-213.

Johansson, R.S., Vallbo, A.B., 1979a. Detection of tactile stimuli. Thresholds of afferent units related to psychophysical thresholds in the human hand. The Journal of physiology 297, 405-422.

Johansson, R.S., Vallbo, A.B., 1979b. Tactile sensibility in the human hand: relative and absolute densities of four types of mechanoreceptive units in glabrous skin. The Journal of physiology 286, 283-300.

Johansson, R.S., Westling, G., 1984. Roles of glabrous skin receptors and sensorimotor memory in automatic control of precision grip when lifting rougher or more slippery objects. Exp Brain Res 56, 550-564.

Johansson, R.S., Westling, G., 1990. Tactile afferent signals in the control of precision grip., Attention and Performance, vol. XIII. Lawrence Erlbaum Associates, Inc, pp. 677-713.

Johansson, R.S., Westling, G., 1991. Afferent signals during manipulative tasks in humans. In: Franzén, O., Westman, J. (Eds.), Somatosensory Mechanisms. Macmillan Academic Press, London, p. 25.

Johansson, R.S., 1996. Sensory control of dexterous manipulation in humans., Hand and brain: The neurophysiology and psychology of hand movements, 1st ed. Academic, San Diego, pp. 381-414.

Johansson, R.S., Vallbo, A.B., 1983. Tactile sensory coding in the glabrous skin of the human hand. Trends in Neurosciences 6, 27-32.

Johnson, K.O., 2001. The roles and functions of cutaneous mechanoreceptors. Curr.Opin.Neurobiol. 11, 455-461.

Jones, E.G., 1975. Lamination and differential distribution of thalamic afferents within the sensory–motor cortex of the squirrel monkey. Journal of Comparative Neurology 160, 167-203.

Jones, E.G., 1983. Distribution patterns of individual medial lemniscal axons in the ventrobasal complex of the monkey thalamus. The Journal of Comparative Neurology 215, 1-16.

Jones, E.G., 1987. Ascending Inputs to, and Internal Organization of, Cortical Motor Areas., Ciba Foundation Symposium 132 - Motor Areas of the Cerebral Cortex. John Wiley & Sons, Ltd., pp. 21-39.

Jones, E.G., 1993. GABAergic Neurons and Their Role in Cortical Plasticity in Primates. Cerebral Cortex 3, 361-372.

Jones, E.G., 1999. Making brain connections: neuroanatomy and the work of TPS Powell, 1923-1996. Annu.Rev.Neurosci. 22, 49-103.

Jones, E.G., Coulter, J.D., Hendry, S.H.C., 1978. Intracortical connectivity of architectonic fields in the somatic sensory, motor and parietal cortex of monkeys. The Journal of Comparative Neurology 181, 291-347.

Jones, E.G., Porter, R., 1980. What is area 3a? Brain Res. 203, 1-43.

Jones, E.G., Powell, T.P., 1969. Connexions of the somatic sensory cortex of the rhesus monkey. I. Ipsilateral cortical connexions. Brain 92, 477-502.

Jones, E.G., Powell, T.P.S., 1968. The ipsilateral cortical connexions of the somatic sensory areas in the cat. Brain Research 9, 71-94.

Jones, E.G., Powell, T.P.S., 1970. An anatomical study of converging sensory pathways within the cerebral cortex of the monkey. Brain 93, 793-820.

Jones, E.G., Powell, T.P.S., 1973. Anatomical Organization of the Somatosensory Cortex. In: Iggo, A. (Ed.), Somatosensory System, 2 ed. Springer Berlin Heidelberg, pp. 579-620.

Jones, E.G., Wise, S.P., 1977. Size, laminar and columnar distribution of efferent cells in the sensory-motor cortex of monkeys. The Journal of Comparative Neurology 175, 391-437.

Jones, E.G., Woods, T.M., Manger, P.R., 2002. Adaptive responses of monkey somatosensory cortex to peripheral and central deafferentation. Neuroscience 111, 775-797.

Jones, E.G., 1986. Connectivity of the Primate Sensory-Motor Cortex. In: Jones, E.G., Peters, A. (Eds.), Sensory-Motor Areas and Aspects of Cortical Connectivity, 5th ed. Springer US, pp. 113-183.

Jones, L., 1996. Proprioception and Its Contribution to Manual Dexterity. In: Flanagan, A.M.W. (Ed.), Hand and Brain. Academic Press, San Diego, pp. 349-362.

Jurcak, V., Tsuzuki, D., Dan, I., 2007. 10/20, 10/10, and 10/5 systems revisited: their validity as relative head-surface-based positioning systems. Neuroimage. 34, 1600-1611.

Kaas, J.H., 1991. Plasticity of sensory and motor maps in adult mammals. Annu.Rev.Neurosci. 14, 137-167.

Kaas, J.H., 2004a. Evolution of somatosensory and motor cortex in primates. Anat.Rec.A Discov.Mol.Cell Evol.Biol. 281, 1148-1156.

Kaas, J.H., 2004b. Evolution of the Large, Complex Sensorimotor Systems of Anthropoid Primates. In: Pellis, S., Marino, L. (Eds.), Special Issue: Evolution of the Vertebrate Brain and Behavior, International Journal of Comparative Psychology 17, pp. 34-52.

Kaas, J.H., 2004c. Somatosensory system. In: Paxinox, G., Mai, J.K. (Eds.), The human nervous system, 2nd ed. Elsevier Academic Press, New York, pp. 1059-1092.

Kaas, J.H., Collins, C.E., 2001. The organization of sensory cortex. Curr.Opin.Neurobiol. 11, 498-504.

Kaas, J.H., Florence, S.L., Jain, N., 1997. Reorganization of sensory systems of primates after injury. neuroscientist 3, 123-130.

Kaas, J.H., Merzenich, M.M., Killackey, H.P., 1983. The reorganization of somatosensory cortex following peripheral nerve damage in adult and developing mammals. Annu.Rev.Neurosci. 6, 325-356.

Kaas, J.H., Nelson, R.J., Sur, M., Lin, C.S., Merzenich, M.M., 1979. Multiple representations of the body within the primary somatosensory cortex of primates. Science 204, 521-523.

Kaas, J.H., 2000. The Reorganization of Sensory and Motor Maps after Injury in Adult Mammals. In: Gazzaniga, M.S. (Ed.). MIT Press, pp. 223-236.

Kaas, J.H., Sur, M., Nelson, R.J., Merzenich, M.M., 1981. The Postcentral Somatosensory Cortex. In: Woolsey, C. (Ed.), Cortical Sensory Organization, 1st ed. Humana Press, pp. 29-45.

Kaeser, M., 2010. Transplantation of autologous adult brain progenitor cells in a non-human primate model of motor cortex lesion. Doctoral thesis. University of Fribourg, Imprimerie Saint-Paul.

Kaeser, M., Brunet, J.F., Wyss, A., Belhaj-Saïf, A., Liu, Y., Hamadjida, A., Rouiller, E.M., Bloch, J., 2011. Autologous adult cortical cell transplantation enhances functional recovery following unilateral lesion of motor cortex in primates: a pilot study. Neurosurgery 68, 1405-1416.

Kaeser, M., Chatagny, P., Gindrat, A.D., Savidan, J., Badoud, S., Fregosi, M., Moret, V., Roulin, C., Schmidlin, E., Rouiller, E.M., 2014. Variability of manual dexterity performance in non-human primates (*Macaca fascicularis*). International Journal of Comparative Psychology 27, 295-325.

Kaeser, M., Wyss, A.F., Bashir, S., Hamadjida, A., Liu, Y., Bloch, J., Brunet, J.F., Belhaj-Saïf, A., Rouiller, E.M., 2010. Effects of unilateral motor cortex lesion on ipsilesional hand's reach and grasp performance in monkeys: relationship with recovery in the contralesional hand. J Neurophysiol 103, 1630-1645.

Kakei, S., Hoffman, D.S., Strick, P.L., 1999. Muscle and movement representations in the primary motor cortex. Science 285, 2136-2139.

Kalaska, J.F., Rizzolatti, G., 2013. Voluntary Movement: The Primary Motor Cortex. In: Kandel, E.R., Schwartz, J., Jessell, T. (Eds.), Principles of neural science. McGraw-Hill Education, pp. 835-864.

Kambi, N., Tandon, S., Mohammed, H., Lazar, L., Jain, N., 2011. Reorganization of the primary motor cortex of adult macaque monkeys after sensory loss resulting from partial spinal cord injuries. J.Neurosci. 31, 3696-3707.

Kambi, N., Halder, P., Rajan, R., Arora, V., Chand, P., Arora, M., Jain, N., 2014. Large-scale reorganization of the somatosensory cortex following spinal cord injuries is due to brainstem plasticity. Nat Commun 5.

Kandel, E.R., Jessell, T.M., 1991. Touch. In: Kandel, E.R., Schwartz, J.H., Jessell, T.M. (Eds.), Principles of Neural Science, 3rd ed. Elsevier, pp. 367-384.

Kandel, E.R., Schwartz, J.H., Jessell, T.M., Siegelbaum, S.A., Hudspeth, A.J., 2013. Principles of Neural Science, Fifth Edition. McGraw-Hill Education.

Kandel, E.R., 2013. From Nerve Cells to Cognition: The Internal Representations of Space and Action. In: Kandel, E.R., Schwartz, J., Jessell, T. (Eds.), Principles of Neural Science, Fifth Edition. McGraw-Hill Education, pp. 370-391.

Kayser, C., Logothetis, N.K., 2013. The Electrophysiological Background of the fMRI Signal. In: Ulmer, S., Jansen, O. (Eds.), fMRI. Springer Berlin Heidelberg, pp. 25-36.

Kazennikov, O., Hyland, B., Corboz, M., Babalian, A., Rouiller, E.M., Wiesendanger, M., 1999. Neural activity of supplementary and primary motor areas in monkeys and its relation to bimanual and unimanual movement sequences. Neuroscience 89, 661-674.

Kazennikov, O., Hyland, B., Wicki, U., Perrig, S., Rouiller, E.M., Wiesendanger, M., 1998. Effects of lesions in the mesial frontal cortex on bimanual co-ordination in monkeys. Neuroscience 85, 703-716.

Kelly, A.M.C., Garavan, H., 2005. Human Functional Neuroimaging of Brain Changes Associated with Practice. Cerebral Cortex 15, 1089-1102.

Kempermann, G., 2006. Adult Neurogenesis. In: Baltes, P.B., Reuter-Lorenz, P.A., Rösler, F. (Eds.), Lifespan development and the brain. Cambridge University Press, pp. 82-108.

Kennedy, P.R., 1990. Corticospinal, rubrospinal and rubro-olivary projections: a unifying hypothesis. Trends in Neurosciences 13, 474-479.

Kermadi, I., Liu, Y., Rouiller, E.M., 2000. Do bimanual motor actions involve the dorsal premotor (PMd), cingulate (CMA) and posterior parietal (PPC) cortices? Comparison with primary and supplementary motor cortical areas. Somatosens.Mot.Res. 17, 255-271.

Kermadi, I., Liu, Y., Tempini, A., Calciati, E., Rouiller, E.M., 1998. Neuronal activity in the primate supplementary motor area and the primary motor cortex in relation to spatio-temporal bimanual coordination. Somatosens.Mot.Res. 15, 287-308.

Kermadi, I., Liu, Y., Tempini, A., Rouiller, E.M., 1997. Effects of reversible inactivation of the supplementary motor area (SMA) on unimanual grasp and bimanual pull and grasp performance in monkeys. Somatosens.Mot.Res. 14, 268-280.

Keysers, C., Kaas, J.H., Gazzola, V., 2010. Somatosensation in social perception. Nat Rev Neurosci 11, 417-428.

Kinoshita, M., Matsui, R., Kato, S., Hasegawa, T., Kasahara, H., Isa, K., Watakabe, A., Yamamori, T., Nishimura, Y., Alstermark, B., Watanabe, D., Kobayashi, K., Isa, T., 2012. Genetic dissection of the circuit for hand dexterity in primates. Nature 487, 235-238.

Kleim, J.A., Chan, S., Pringle, E., Schallert, K., Procaccio, V., Jimenez, R., Cramer, S.C., 2006. BDNF val66met polymorphism is associated with modified experience-dependent plasticity in human motor cortex. Nat Neurosci 9, 735-737.

Kleinschmidt, A., Nitschke, M.F., Frahm, J., 1997. Somatotopy in the Human Motor Cortex Hand Area. A High-Resolution Functional MRI Study. European Journal of Neuroscience 9, 2178-2186.

Knott, G.W., Holtmaat, A., Wilbrecht, L., Welker, E., Svoboda, K., 2006. Spine growth precedes synapse formation in the adult neocortex in vivo. Nat Neurosci 9, 1117-1124.

Kolb, B., Cioe, J., Comeau, W., 2008. Contrasting effects of motor and visual spatial learning tasks on dendritic arborization and spine density in rats. Neurobiology of learning and memory 90, 295-300.

Kolb, B., Whishaw, I.Q., 1998. Brain plasticity and behavior. Annual Review of Psychology 49, 43-64.

Konietzny, F., Hensel, H., 1977. Response of rapidly and slowly adapting mechanoreceptors and vibratory sensitivity in human hairy skin. Pflugers Arch. 368, 39-44.

Konorski, J., 1948. Conditioned reflexes and neuron organization. Cambridge University Press.

Korn, A., Halevi, D., Lidar, Z., Biron, T., Ekstein, P., Constantini, S., 2015. Intraoperative neurophysiological monitoring during resection of intradural extramedullary spinal cord tumors: experience with 100 cases. Acta neurochir 157, 819-830.

Kraskov, A., Philipp, R., Waldert, S., Vigneswaran, G., Quallo, M.M., Lemon, R.N., 2014. Corticospinal mirror neurons. Philosophical Transactions of the Royal Society of London B: Biological Sciences 369.

Kraskov, A., Dancause, N., Quallo, M.M., Shepherd, S., Lemon, R.N., 2009. Corticospinal Neurons in Macaque Ventral Premotor Cortex with Mirror Properties: A Potential Mechanism for Action Suppression? Neuron 64, 922-930.

Kraskov, A., Prabhu, G., Quallo, M.M., Lemon, R.N., Brochier, T., 2011. Ventral Premotor–Motor Cortex Interactions in the Macaque Monkey during Grasp: Response of Single Neurons to Intracortical Microstimulation. The Journal of Neuroscience 31, 8812-8821.

Krubitzer, L., Disbrow, E.A., 2005. The Evolution of Parietal Areas Involved in Hand Use in Primates. In: Kaas, J.H., Gardner, E.P. (Eds.), The senses: a comprehensive reference, Volume 6: Somatosensation. Elsevier, pp. 183-214.

Krubitzer, L., Huffman, K.J., Disbrow, E., Recanzone, G., 2004. Organization of area 3a in macaque monkeys: contributions to the cortical phenotype. J Comp Neurol. 471, 97-111.

Krubitzer, L.A., Kaas, J.H., 1990. The organization and connections of somatosensory cortex in marmosets. J Neurosci. 10, 952-974.

Kullmann, D.M., Moreau, A.W., Bakiri, Y., Nicholson, E., 2012. Plasticity of inhibition. Neuron 75, 951-962.

Kumar, A., Juhasz, C., Asano, E., Sundaram, S.K., Makki, M.I., Chugani, D.C., Chugani, H.T., 2009. Diffusion tensor imaging study of the cortical origin and course of the corticospinal tract in healthy children. AJNR Am.J Neuroradiol. 30, 1963-1970.

Kunde, V., Treede, R.D., 1993. Topography of middle-latency somatosensory evoked potentials following painful laser stimuli and non-painful electrical stimuli. Electroencephalogr.Clin.Neurophysiol 88, 280-289.

Künzle, H., 1978. Cortico-cortical efferents of primary motor and somatosensory regions of the cerebral cortex in *Macaca fascicularis*. Neuroscience 3, 25-39.

Kurata, K., Tanji, J., 1986. Premotor cortex neurons in macaques: activity before distal and proximal forelimb movements. The Journal of Neuroscience 6, 403-411.

Kuypers, H.G., 1974. Recovery of Motor Function in Rhesus Monkeys. Neurosci.Res.Program Bull. 12, 240-244.

Kuypers, H.G.J.M., 1981. Anatomy of the Descending Pathways., Handbook of Physiology: The nervous system, vol. 2: Motor Control. John Wiley & Sons, Inc., pp. 597-666.

Kuypers, H.G.J.M., 1982. A New Look at the Organization of the Motor System. Progress in brain research 57, 381-403.

Kuypers, H.G.J.M., 1987. Some aspects of the organization of the output of the motor cortex. In: Bock, G., O'Connor, M., Marsh, J. (Eds.), Motor Areas of the Cerebral Cortex, 713 ed. John Wiley & Sons, pp. 63-82.

Kuypers, H.G.J.M., Brinkman, J., 1970. Precentral projections to different parts of the spinal intermediate zone in the rhesus monkey. Brain Research 24, 29-48.

Kwan, H.C., MacKay, W.A., Murphy, J.T., Wong, Y.C., 1978. Spatial organization of precentral cortex in awake primates. II. Motor outputs. J Neurophysiol. 41, 1120-1131.

LaMotte, R.H., Mountcastle, V.B., 1975. Capacities of humans and monkeys to discriminate vibratory stimuli of different frequency and amplitude: a correlation between neural events and psychological measurements. Journal of Neurophysiology 38, 539-559.

Lamprecht, R., LeDoux, J., 2004. Structural plasticity and memory. Nat Rev Neurosci 5, 45-54.

Langer, N., Hanggi, J., Muller, N.A., Simmen, H.P., Jancke, L., 2012. Effects of limb immobilization on brain plasticity. Neurology 78, 182-188.

Larsson, J., Gulyás, B., Roland, P.E., 1996. Cortical representation of self-paced finger movement. Neuroreport 7.

Lascano, A.M., Brodbeck, V., Lalive, P.H., Chofflon, M., Seeck, M., Michel, C.M., 2009. Increasing the diagnostic value of evoked potentials in multiple sclerosis by quantitative topographic analysis of multichannel recordings. J Clin.Neurophysiol 26, 316-325.

Lascano, A.M., Grouiller, F., Genetti, M., Spinelli, L., Seeck, M., Schaller, K., Michel, C.M., 2014. Surgically relevant localization of the central sulcus with high-density somatosensory-evoked potentials compared with functional magnetic resonance imaging. Neurosurgery 74, 517-526.

Lawrence, D.G., Hopkins, D.A., 1976. The development of motor control in the rhesus monkey: evidence concerning the role of corticomotoneuronal connections. Brain 99, 235-254.

Lawrence, D.G., Kuypers, H.G., 1968a. The functional organization of the motor system in the monkey. I. The effects of bilateral pyramidal lesions. Brain 91, 1-14.

Lawrence, D.G., Kuypers, H.G., 1968b. The functional organization of the motor system in the monkey. II. The effects of lesions of the descending brain-stem pathways. Brain 91, 15-36.

Lawrence, D.G., Porter, R., Redman, S.J., 1985. Corticomotoneuronal synapses in the monkey: Light microscopic localization upon motoneurons of intrinsic muscles of the hand. The Journal of Comparative Neurology 232, 499-510.

Lederman, S.J., Klatzky, R.L., 1987. Hand movements: A window into haptic object recognition. Cognitive Psychology 19, 342-368.

Lederman, S.J., Klatzky, R.L., 1996. Action for Perception: Manual Exploratory Movements for Haptically Processing Objects and Their Features. In: Flanagan, A.M.W. (Ed.), Hand and Brain. Academic Press, San Diego, pp. 431-446.

Lederman, S.J., Thorne, G., Jones, B., 1986. Perception of texture by vision and touch: Multidimensionality and intersensory integration. Journal of Experimental Psychology: Human Perception and Performance 12, 169-180.

Legatt, A.D., Pascual-Leone, A., Rotenberg, A., 2011. Technical Aspects of Transcranial Magnetic and Electrical Stimulation of the Brain. In: Schomer, D.L., Lopes da Silva, F.H. (Eds.), Niedermeyer's Electroencephalography: Basic Principles, Clinical Applications, and Related Fields, 6th ed. Lippincott Williams & Wilkins, pp. 1129-1138.

Legatt, A., 2014. General Principles of Somatosensory Evoked Potentials. Medscape.

Legatt, A., Benbadis, S.R., 2014. General Principles of Somatosensory Evoked Potentials. Medscape.

Lehmann, S.J., Scherberger, H., 2013. Reach and Gaze Representations in Macaque Parietal and Premotor Grasp Areas. The Journal of Neuroscience 33, 7038-7049.

Leichnetz, G.R., 1986. Afferent and efferent connections of the dorsolateral precentral gyrus (area 4, hand/arm region) in the macaque monkey, with comparisons to area 8. J.Comp Neurol. 254, 460-492.

Lemon, R.N., 1981. Functional properties of monkey motor cortex neurones receiving afferent input from the hand and fingers. J.Physiol 311, 497-519.

Lemon, R.N., 1993. The G. L. Brown Prize Lecture. Cortical control of the primate hand. Exp.Physiol 78, 263-301.

Lemon, R.N., 1997. Mechanisms of cortical control of hand function. neuroscientist 3, 389-398.

Lemon, R.N., 1999. Neural control of dexterity: what has been achieved? Exp.Brain Res. 128, 6-12.

Lemon, R.N., 2008a. An enduring map of the motor cortex. Experimental Physiology 93, 798-802.

Lemon, R.N., 2008b. Descending pathways in motor control. Annu.Rev.Neurosci. 31, 195-218.

Lemon, R.N., Bennett, K.M., Werner, W., 1991. The Cortico-Motor Substrate for Skilled Movements of the Primate Hand. In: Requin, J., Stelmach, G.E. (Eds.), Tutorials in Motor Neuroscience, 62 ed. Springer Netherlands, pp. 477-495.

Lemon, R.N., Griffiths, J., 2005. Comparing the function of the corticospinal system in different species: organizational differences for motor specialization? Muscle Nerve 32, 261-279.

Lemon, R.N., Hanby, J.A., Porter, R., 1976. Relationship between the activity of precentral neurones during active and passive movements in conscious monkeys. Proc.R.Soc.Lond B Biol.Sci. 194, 341-373.

Lemon, R.N., Landau, W., Tutssel, D., Lawrence, D.G., 2012. Lawrence and Kuypers (1968a, b) revisited: copies of the original filmed material from their classic papers in Brain. Brain.

Lemon, R.N., Mantel, G.W., Muir, R.B., 1986. Corticospinal facilitation of hand muscles during voluntary movement in the conscious monkey. J Physiol 381, 497-527.

Lemon, R.N., Porter, R., 1976. Afferent input to movement-related precentral neurones in conscious monkeys. Proc.R.Soc.Lond B Biol.Sci. 194, 313-339.

Lemon, R.N., Van der Burg, J., 1979. Short-latency peripheral inputs to thalamic neurones projecting to the motor cortex in the monkey. Exp.Brain Res. 36, 445-462.

Lemon, R., 1988. The output map of the primate motor cortex. Trends in Neurosciences 11, 501-506.

Lemon, R.N., 2010. What drives corticospinal output? F1000 biology reports 2.

Lende, R.A., 1963. Cerebral Cortex: A Sensorimotor Amalgam in the Marsupialia. Science 141, 730-732.

Leung, Y.Y., Bensmaia, S.J., Hsiao, S.S., Johnson, K.O., 2005. Time-course of vibratory adaptation and recovery in cutaneous mechanoreceptive afferents. J Neurophysiol. 94, 3037-3045.

Leyton, A.S.F., Sherrington, C.S., 1917. Obervartions on the excitable cortex of the chimpanzee, orang-utan and gorilla. Quarterly Journal of Experimental Physiology 11, 135-222.

Liao, C.C., Gharbawie, O.A., Qi, H., Kaas, J.H., 2013. Cortical connections to single digit representations in area 3b of somatosensory cortex in squirrel monkeys and prosimian galagos. J Comp Neurol 521, 3768-3790.

Liepert, J., Gorsler, A., van Eimeren, T., Münchau, A., Weiller, C., 2003. Motor excitability in a patient with a somatosensory cortex lesion. Clinical Neurophysiology 114, 1003-1008.

Lim, V.K., Bradshaw, J.L., Nicholls, M.E., Altenmuller, E., 2004. Abnormal sensorimotor processing in pianists with focal dystonia. Adv.Neurol 94, 267-273.

Lissek, S., Wilimzig, C., Stude, P., Pleger, B., Kalisch, T., Maier, C., Peters, S.A., Nicolas, V., Tegenthoff, M., Dinse, H.R., 2009. Immobilization Impairs Tactile Perception and Shrinks Somatosensory Cortical Maps. Current Biology 19, 837-842.

Liu, C.N., Chambers, W.W., 1964. An experimental study of the cortico-spinal system in the monkey (*Macaca mulatta*). The spinal pathways and preterminal distribution of degenerating fibers following discrete lesions of the pre- and postcentral gyri and bulbar pyramid. The Journal of Comparative Neurology 123, 257-283.

Liu, Y., Rouiller, E.M., 1999. Mechanisms of recovery of dexterity following unilateral lesion of the sensorimotor cortex in adult monkeys. Exp.Brain Res. 128, 149-159.

Lloyd, D.P.C., McIntyre, A.K., 1950. Dorsal column conduction of group i muscle afferent impulses and their relay through Clarke's column. Journal of Neurophysiology 13, 39-54.

Loewenstein, W.R., Mendelson, M., 1965. Components of receptor adaptation in a Pacinian corpuscle. The Journal of physiology 177, 377-397.

Loewenstein, W.R., Skalak, R., 1966. Mechanical transmission in a Pacinian corpuscle. An analysis and a theory. The Journal of physiology 182, 346-378.

Loewenstein, W.R., 1971. Mechano-electric Transduction in the Pacinian Corpuscle. Initiation of Sensory Impulses in Mechanoreceptors. In: Loewenstein, W.R. (Ed.), Principles of Receptor Physiology, 1st ed. Springer Berlin Heidelberg, pp. 269-290.

Logothetis, N.K., 2008. What we can do and what we cannot do with fMRI. Nature 453, 869-878.

Lopes da Silva, F.H., 2011a. Biophysical Aspects of EEG and Magnetoencephalogram Generation. In: Schomer, D.L., Lopes da Silva, F.H. (Eds.), Niedermeyer's Electroencephalography: Basic Principles, Clinical Applications, and Related Fields, 6th ed. Lippincott Williams & Wilkins, pp. 91-110.

Lopes da Silva, F.H., 2011b. Event-Related Potentials: General Aspects of Methodology and Quantification. In: Schomer, D.L., Lopes da Silva, F.H. (Eds.), Niedermeyer's Electroencephalography: Basic Principles, Clinical Applications, and Related Fields, 6th ed. Lippincott Williams & Wilkins, pp. 923-933.

Lopes da Silva, F.H., 2013. EEG and MEG: relevance to neuroscience. Neuron 80, 1112-1128.

Lotze, M., Erb, M., Flor, H., Huelsmann, E., Godde, B., Grodd, W., 2000. fMRI Evaluation of Somatotopic Representation in Human Primary Motor Cortex. Neuroimage 11, 473-481.

Lotze, M., Scheler, G., Tan, H.-R., Braun, C., Birbaumer, N., 2003. The musician's brain: functional imaging of amateurs and professionals during performance and imagery. Neuroimage 20, 1817-1829.

Luciani, L., Tamburini, A., 1878. Ricerche sperimentali sui centri psico-motori corticali. Bologna.

Luders, H.O., 1996. The supplementary sensorimotor area. An overview. Adv.Neurol. 70, 1-16.

Lundström, R.J.I., Johansson, R.S., 1986. Acute impairment of the sensitivity of skin mechanoreceptive units caused by vibration exposure of the hand. Ergonomics 29, 687-698.

Luppino, G., Matelli, M., Camarda, R.M., Gallese, V., Rizzolatti, G., 1991. Multiple representations of body movements in mesial area 6 and the adjacent cingulate cortex: An intracortical microstimulation study in the macaque monkey. The Journal of Comparative Neurology 311, 463-482.

Luppino, G., Rizzolatti, G., 2000. The Organization of the Frontal Motor Cortex. News Physiol Sci. 15, 219-224.

Macefield, V.G., Häger-Ross, C., Johansson, R.S., 1996. Control of grip force during restraint of an object held between finger and thumb: responses of cutaneous afferents from the digits. Exp Brain Res 108, 155-171.

Macefield, V.G., Johansson, R.S., 1996. Control of grip force during restraint of an object held between finger and thumb: responses of muscle and joint afferents from the digits. Experimental brain research 108, 172-184.

Maguire, E.A., Gadian, D.G., Johnsrude, I.S., Good, C.D., Ashburner, J., Frackowiak, R.S., Frith, C.D., 2000. Navigation-related structural change in the hippocampi of taxi drivers. Proc.Natl.Acad.Sci.USA 97, 4398-4403.

Mahncke, H.W., Connor, B.B., Appelman, J., Ahsanuddin, O.N., Hardy, J.L., Wood, R.A., Joyce, N.M., Boniske, T., Atkins, S.M., Merzenich, M.M., 2006. Memory enhancement in healthy older adults using a brain plasticity-based training program: A randomized, controlled study. Proceedings of the National Academy of Sciences 103, 12523-12528.

Maier, M.A., Armand, J., Kirkwood, P.A., Yang, H.W., Davis, J.N., Lemon, R.N., 2002. Differences in the corticospinal projection from primary motor cortex and supplementary motor area to macaque upper limb motoneurons: an anatomical and electrophysiological study. Cereb.Cortex 12, 281-296.

Maier, M.A., Kirkwood, P.A., Brochier, T., Lemon, R.N., 2013. Responses of single corticospinal neurons to intracortical stimulation of primary motor and premotor cortex in the anesthetized macaque monkey. Journal of Neurophysiology 109, 2982-2998.

Makin, T.R., Cramer, A.O., Scholz, J., Hahamy, A., Henderson Slater, D., Tracey, I., Johansen-Berg, H., 2013. Deprivation-related and use-dependent plasticity go hand in hand. eLife 2.

Malis, L.I., Pribram, K.H., Kruger, L., 1953. Action potentials in motor cortex evoked by peripheral nerve stimulation. J Neurophysiol. 16, 161-167.

Manger, P.R., Woods, T.M., Jones, E.G., 1996. Plasticity of the Somatosensory Cortical Map in Macaque Monkeys after Chronic Partial Amputation of a Digit. Proceedings: Biological Sciences 263, 933-939.

Manger, P.R., Woods, T.M., Muñoz, A., Jones, E.G., 1997. Hand/Face Border as a Limiting Boundary in the Body Representation in Monkey Somatosensory Cortex. The Journal of Neuroscience 17, 6338-6351.

Marshall, W.H., Woolsey, C.N., Bard, P., 1941. Observations on cortical somatic sensory mechanisms of cat and monkey. Journal of Neurophysiology 4, 1-24.

Marshall, W.H., Woolsey, C.N., Bard, P., 1937. Cortical representation of tactile sensibility as indicated by cortical potentials. Science 85, 388-390.

Martin, S.J., Morris, R.G., 2001. Cortical plasticity: It's all the range! Curr.Biol. 11, R57-R59.

Martino, A.M., Strick, L., 1987. Corticospinal projections originate from the arcuate premotor area. Brain Research 404, 307-312.

Martuzzi, R., van der Zwaag, W., Farthouat, J., Gruetter, R., Blanke, O., 2014. Human finger somatotopy in areas 3b, 1, and 2: a 7T fMRI study using a natural stimulus. Hum.Brain Mapp. 35, 213-226.

Matelli, M., Luppino, G., Rizzolatti, G., 1991. Architecture of superior and mesial area 6 and the adjacent cingulate cortex in the macaque monkey. The Journal of Comparative Neurology 311, 445-462.

Matelli, M., Luppino, G., 2001. Parietofrontal Circuits for Action and Space Perception in the Macaque Monkey. Neuroimage 14, S27-S32.

Matelli, M., Luppino, G., Geyer, S., Zilles, K., 2004. Motor Cortex. In: Mai, J., Paxinox, G. (Eds.), The Human Nervous System (Second Edition). Academic Press, San Diego, pp. 973-996.

Matelli, M., Luppino, G., Rizzolatti, G., 1985. Patterns of cytochrome oxidase activity in the frontal agranular cortex of the macaque monkey. Behavioural Brain Research 18, 125-136.

Matsuyama, K., Mori, F., Nakajima, K., Drew, T., Aoki, M., Mori, S., 2004. Locomotor role of the corticoreticular–reticulospinal–spinal interneuronal system. In: Shigemi Mori, D.G.S. (Ed.), Progress in Brain Research, Brain Mechanisms for the Integration of Posture and Movement, Volume 143. Elsevier, pp. 239-249.

Mauguière, F., 2011. Somatosensory-evoked potentials: Normal Responses, Abnormal Waveforms, and Clinical Applications in Neurologic Diseases. In: Schomer, D.L., Lopes da Silva, F.H. (Eds.), Niedermeyer's Electroencephalography: Basic Principles, Clinical Applications, and Related Fields, 6th ed. Lippincott Williams & Wilkins, pp. 1003-1056.

Mauguière, F., Allison, T., Babiloni, C., Buchner, H., Eisen, A.A., Goodin, D.S., Jones, S.J., Kakigi, R., Matsuoka, S., Nuwer, M., 1999. Somatosensory evoked potentials. The International Federation of Clinical Neurophysiology. Electroencephalography and clinical neurophysiology.Supplement 52, 79.

Mauguière, F., Fischer, C., 1990. Les potentiels évoqués en neurologie, Editions Techniques ed.

McCarthy, G., Wood, C.C., Allison, T., 1991. Cortical somatosensory evoked potentials. I. Recordings in the monkey *Macaca fascicularis*. J Neurophysiol 66, 53-63.

McGlone, F., Wessberg, J., Olausson, H., 2014. Discriminative and Affective Touch: Sensing and Feeling. Neuron 82, 737-755.

McNeal, D.W., Darling, W.G., Ge, J., Stilwell-Morecraft, K.S., Solon, K.M., Hynes, S.M., Pizzimenti, M.A., Rotella, D.L., Tyler, V., Morecraft, R.J., 2010. Selective long-term reorganization of the corticospinal projection from the supplementary motor cortex following recovery from lateral motor cortex injury. Journal of Comparative Neurology 518, 586-621.

Mehler, W.R., 1962. The anatomy of the so-called "pain tract" in man: an analysis of the course and distribution of the ascending fibers of the fasciculus anterolateralis. In: Thomas, C.C. (Ed.), Basic research in paraplegia. Thomas Springfield, pp. 26-55.

Melzack, R., Wall, P.D., 1967. Pain mechanisms: a new theory. Survey of Anesthesiology 11, 89-90.

Merchant, H., Naselaris, T., Georgopoulos, A.P., 2008. Dynamic Sculpting of Directional Tuning in the Primate Motor Cortex during Three-Dimensional Reaching. The Journal of Neuroscience 28, 9164-9172.

Merton, P.A., Morton, H.B., 1984. George Dawson (1912–1983) and the invention of averaging techniques in physiology. Trends in Neurosciences 7, 371-374.

Merzenich, M.M., Kaas, J.H., Wall, J., Nelson, R.J., Sur, M., Felleman, D., 1983a. Topographic reorganization of somatosensory cortical areas 3b and 1 in adult monkeys following restricted deafferentation. Neuroscience 8, 33-55.

Merzenich, M.M., Kaas, J.H., Wall, J.T., Sur, M., Nelson, R.J., Felleman, D.J., 1983b. Progression of change following median nerve section in the cortical representation of the hand in areas 3b and 1 in adult owl and squirrel monkeys. Neuroscience 10, 639-665.

Merzenich, M.M., Nelson, R.J., Stryker, M.P., Cynader, M.S., Schoppmann, A., Zook, J.M., 1984. Somatosensory cortical map changes following digit amputation in adult monkeys. J Comp Neurol 224, 591-605.

Merzenich, M.M., Kaas, J.H., Sur, M., Lin, C.–S., 1978. Double representation of the body surface within cytoarchitectonic area 3b and 1 in "S1"in the owl monkey (*Aotus trivirgatus*). Journal of Comparative Neurology 181, 41-73.

Merzenich, M.M., Nelson, R.J., Kaas, J.H., Stryker, M.P., Jenkins, W.M., Zook, J.M., Cynader, M.S., Schoppmann, A., 1987. Variability in hand surface representations in areas 3b and 1 in adult owl and squirrel monkeys. Journal of Comparative Neurology 258, 281-296.

Merzenich, M.M., Sameshima, K., 1993. Cortical plasticity and memory. Current Opinion in Neurobiology 3, 187-196.

Merzenich, M.M., Sur, M., Nelson, R.J., Kaas, J.H., 1981. Organization of the S I Cortex - Multiple Cutaneous Representations in Areas 3b and 1 of the Owl Monkey. In: Woolsey, C. (Ed.), Cortical Sensory Organization, 1st ed. Humana Press, pp. 47-66.

Michel, C.M., Brandeis, D., 2009. Data acquisition and pre-processing standards for electrical neuroimaging. In: Michel, C.M., Koenig, T., Brandeis, D., Gianotti, L.R.R., Wackermann, J. (Eds.), Electrical neuroimaging. Cambridge University Press, pp. 79-92.

Michel, C.M., He, B., 2011. EEG Mapping and Source Imaging. In: Schomer, D.L., Lopes da Silva, F.H. (Eds.), Niedermeyer's Electroencephalography: Basic Principles, Clinical Applications, and Related Fields, 6th ed. Lippincott Williams & Wilkins, pp. 1179-1202.

Michel, C.M., Lantz, G., Spinelli, L., De Peralta, R.G., Landis, T., Seeck, M., 2004a. 128-channel EEG source imaging in epilepsy: clinical yield and localization precision. J Clin.Neurophysiol 21, 71-83.

Michel, C.M., Murray, M.M., 2012. Towards the utilization of EEG as a brain imaging tool. Neuroimage 61, 371-385.

Michel, C.M., Murray, M.M., Lantz, G., Gonzalez, S., Spinelli, L., Grave de Peralta, R., 2004b. EEG source imaging. Clin.Neurophysiol 115, 2195-2222.

Michel, C.M., Thut, G., Morand, S., Khateb, A., Pegna, A.J., Grave de Peralta, R., Gonzalez, S., Seeck, M., Landis, T., 2001. Electric source imaging of human brain functions. Brain Res.Brain Res.Rev. 36, 108-118.

Millett, D., 2001. Hans Berger: from psychic energy to the EEG. Perspect.Biol.Med. 44, 522-542.

Mitz, A.R., Wise, S.P., 1987. The somatotopic organization of the supplementary motor area: intracortical microstimulation mapping. The Journal of Neuroscience 7, 1010-1021.

Mogilner, A., Grossman, J.A., Ribary, U., Joliot, M., Volkmann, J., Rapaport, D., Beasley, R.W., Llinas, R.R., 1993. Somatosensory cortical plasticity in adult humans revealed by magnetoencephalography. Proc.Natl.Acad.Sci.USA 90, 3593-3597.

Monzée, J., Lamarre, Y., Smith, A.M., 2003. The Effects of Digital Anesthesia on Force Control Using a Precision Grip. Journal of Neurophysiology 89, 672-683.

Moore, C.I., Stern, C.E., Corkin, S., Fischl, B., Gray, A.C., Rosen, B.R., Dale, A.M., 2000. Segregation of somatosensory activation in the human rolandic cortex using fMRI. J Neurophysiol. 84, 558-569.

Morecraft, R.J., Ge, J., Stilwell-Morecraft, K.S., McNeal, D.W., Pizzimenti, M.A., Darling, W.G., 2013. Terminal distribution of the corticospinal projection from the hand/arm region of the primary motor cortex to the cervical enlargement in rhesus monkey. Journal of Comparative Neurology 521, 4205-4235.

Morizot-Koutlidis, R., André-Obadia, N., Antoine, J.C., Attarian, S., Ayache, S.S., Azabou, E., Benaderette, S., Camdessanché, J.P., Cassereau, J., Convers, P., d'Anglejean, J., Delval, A., Durand, M.C., Etard, O., Fayet, G., Fournier, E., Franques, J., Gavaret, M., Guehl, D., Guerit, J.M., Krim, E., Kubis, N., Lacour, A., Lozeron, P., Mauguière, F., Merle, P.E., Mesrati, F., Mutschler, V., Nicolas, G., Nordine, T., Pautot, V., Péréon, Y., Petiot, P., Pouget, J., Praline, J., Salhi, H., Trébuchon, A., Tyvaert, L., Vial, C., Zola, J.M., Zyss, J., Lefaucheur, J.P., 2015. Somatosensory evoked potentials in the assessment of peripheral neuropathies: Commented results of a survey among French-speaking practitioners and recommendations for practice. Neurophysiologie Clinique/Clinical Neurophysiology.

Morrison, I., Löken, L.S., Olausson, H., 2010. The skin as a social organ. Exp Brain Res 204, 305-314.

Mott, F.W., Sherrington, C.S., 1894. Experiments upon the influence of sensory nerves upon movement and nutrition of the limbs. Preliminary communication. Proceedings of the Royal Society of London 57, 481-488.

Mountcastle, V.B., 1997. The columnar organization of the neocortex. Brain 120 (Pt 4), 701-722.

Mountcastle, V.B., Lynch, J.C., Georgopoulos, A., Sakata, H., Acuna, C., 1975. Posterior parietal association cortex of the monkey: command functions for operations within extrapersonal space. Journal of Neurophysiology 38, 871-908.

Mountcastle, V.B., 1995. The parietal system and some higher brain functions. Cerebral Cortex.

Munte, T.F., Altenmuller, E., Jancke, L., 2002. The musician's brain as a model of neuroplasticity. Nat.Rev.Neurosci. 3, 473-478.

Murase, N., Kaji, R., Shimazu, H., Katayama-Hirota, M., Ikeda, A., Kohara, N., Kimura, J., Shibasaki, H., Rothwell, J.C., 2000. Abnormal premovement gating of somatosensory input in writer's cramp. Brain 123, 1813-1829.

Murata, A., Fadiga, L., Fogassi, L., Gallese, V., Raos, V., Rizzolatti, G., 1997. Object Representation in the Ventral Premotor Cortex (Area F5) of the Monkey. Journal of Neurophysiology 78, 2226-2230.

Murata, A., Gallese, V., Luppino, G., Kaseda, M., Sakata, H., 2000. Selectivity for the Shape, Size, and Orientation of Objects for Grasping in Neurons of Monkey Parietal Area AIP. Journal of Neurophysiology 83, 2580-2601.

Murata, Y., Higo, N., Hayashi, T., Nishimura, Y., Sugiyama, Y., Oishi, T., Tsukada, H., Isa, T., Onoe, H., 2015. Temporal Plasticity Involved in Recovery from Manual Dexterity Deficit after Motor Cortex Lesion in Macaque Monkeys. The Journal of Neuroscience 35, 84-95.

Murray, H.M., Haines, D.E., 1975. The Rubrospinal Tract in a Prosimian Primate *Galago senegalensis*. Brain, Behavior and Evolution 12, 311-333.

Murray, P.D., Keller, A., 2011. Somatosensory response properties of excitatory and inhibitory neurons in rat motor cortex. J Neurophysiol 106, 1355-1362.

Musall, S., von Pföstl, V., Rauch, A., Logothetis, N.K., Whittingstall, K., 2014. Effects of Neural Synchrony on Surface EEG. Cerebral Cortex 24, 1045-1053.

Nakajima, K., Maier, M.A., Kirkwood, P.A., Lemon, R.N., 2000. Striking differences in transmission of corticospinal excitation to upper limb motoneurons in two primate species. J Neurophysiol. 84, 698-709.

Napier, J.R., 1956. The prehensile movements of the human hand. J Bone Joint Surg.Br 38-B, 902-913.

Napier, J.R., 1960. Studies of the hands of living primates. Proc.Zool.Soc.London 134, 647-657.

Napier, J.R., 1961. Prehensility an opposability in the hands of primates. Symposia of the Zoological Society,London 5, 115-132.

Napier, J., 1962. The evolution of the hand. Scientific American 207, 56-62.

Nathan, P.W., Smith, M.C., 1982. The rubrospinal and central tegmental tracts in man. Brain 105, 223-269.

Nathan, P.W., Smith, M., Deacon, P., 2001. The crossing of the spinothalamic tract. Brain 124, 793-803.

Nelson, A.J., Chen, R., 2008. Digit Somatotopy within Cortical Areas of the Postcentral Gyrus in Humans. Cerebral Cortex 18, 2341-2351.

Nelson, R.J., 1987. Activity of monkey primary somatosensory cortical neurons changes prior to active movement. Brain Research 406, 402-407.

Nelson, R.J., Smith, B.N., Douglas, V.D., 1991. Relationships between sensory responsiveness and premovement activity of quickly adapting neurons in areas 3b and 1 of monkey primary somatosensory cortex. Exp Brain Res 84, 75-90.

Nelson, R.J., Sur, M., Felleman, D.J., Kaas, J.H., 1980. Representations of the body surface in postcentral parietal cortex of *Macaca fascicularis*. J.Comp Neurol. 192, 611-643.

Neychev, V.K., Gross, R.E., Lehericy, S., Hess, E.J., Jinnah, H.A., 2011. The functional neuroanatomy of dystonia. Neurobiol.Dis. 42, 185-201.

Nicholls, J.G., Robert Martin, A., Fuchs, P.A., Brown, D.A., Diamond, M.E., Weisblat, D.A., 2012. From Neuron to Brain, 5th ed. Sinauer Associates, Inc, Sunderland, Massachusetts, USA.

Nicholls, J.G., Robert Martin, A., Wallace, B.G., Fuchs, P.A., 2001. From Neuron to Brain, 4th ed. Sinauer Associates, Inc.

Niedermeyer, E., Schomer, D.L., 2011. Historical Aspects of EEG. In: Schomer, D.L., Lopes da Silva, F.H. (Eds.), Niedermeyer's Electroencephalography: Basic Principles, Clinical Applications, and Related Fields, 6th ed. Lippincott Williams & Wilkins, pp. 1-16.

Nielsen, J.B., Cohen, L.G., 2008. The Olympic brain. Does corticospinal plasticity play a role in acquisition of skills required for high-performance sports? J Physiol 586, 65-70.

Nieuwenhuys, R., Voogd, J., Voogd, J., van Huijzen, C., 2007. The Human Central Nervous System: A Synopsis and Atlas. Springer.

Nitzschke, R., Hansen-Algenstaedt, N., Regelsberger, J., Goetz, A.E., Goepfert, M.S., 2012. Intraoperatives elektrophysiolo-gisches Monitoring mit evozierten Potenzialen, [Intraoperative electrophysiological monitoring with evoked potentials]. Anaesthesist 61, 320-335.

Nudo, R.J., 2006a. Mechanisms for recovery of motor function following cortical damage. Curr.Opin.Neurobiol. 16, 638-644.

Nudo, R.J., 2006b. Plasticity. NeuroRx. 3, 420-427.

Nudo, R.J., Friel, K.M., Delia, S.W., 2000. Role of sensory deficits in motor impairments after injury to primary motor cortex. Neuropharmacology 39, 733-742.

Nudo, R.J., Masterton, R.B., 1990. Descending pathways to the spinal cord, III: Sites of origin of the corticospinal tract. The Journal of Comparative Neurology 296, 559-583.

Nudo, R.J., Milliken, G.W., 1996. Reorganization of movement representations in primary motor cortex following focal ischemic infarcts in adult squirrel monkeys. J Neurophysiol 75, 2144-2149.

Nudo, R.J., Milliken, G.W., Jenkins, W.M., Merzenich, M.M., 1996. Use-dependent alterations of movement representations in primary motor cortex of adult squirrel monkeys. J Neurosci 16, 785-807.

Nudo, R.J., Plautz, E.J., Frost, S.B., 2001. Role of adaptive plasticity in recovery of function after damage to motor cortex. Muscle & Nerve 24, 1000-1019.

Nunez, P.L., 1993. High-resolution EEG: applications in medicine and cognitive science. Proc.SPIE 1887, Physiological Imaging, Spectroscopy, and Early-Detection Diagnostic Methods, 22 (August 27, 1993), 22-39.

Nunez, P.L., 1998. Neocortical dynamics of macroscopic-scale EEG measurements. IEEE Eng Med.Biol.Mag. 17, 110-117.

Nunez, P.L., 2000. Toward a quantitative description of large-scale neocortical dynamic function and EEG. Behav.Brain Sci. 23, 371-398.

Nunez, P.L., Srinivasan, R., 2006. Electric fields and currents in biological tissue., Electric Fields of the Brain: The Neurophysics of EEG, 2nd ed. Oxford University Press, USA.

Nuwer, M.R., 1998. Fundamentals of evoked potentials and common clinical applications today. Electroencephalogr.Clin.Neurophysiol 106, 142-148.

Nuwer, M.R., Banoczi, W.R., Cloughesy, T.F., Hoch, D.B., Peacock, W., Levesque, M.F., Black, K.L., Martin, N.A., Becker, D.P., 1992. Topographic mapping of somatosensory evoked potentials helps identify motor cortex more quickly in the operating room. Brain Topogr. 5, 53-58.

Nuwer, M.R., Emerson, R.G., Galloway, G., Legatt, A.D., Lopez, J., Minahan, R., Yamada, T., Goodin, D.S., Armon, C., Chaudhry, V., Gronseth, G.S., Harden, C.L., 2012. Evidence-based guideline update: intraoperative spinal monitoring with somatosensory and transcranial electrical motor evoked potentials: report of the Therapeutics and Technology Assessment Subcommittee of the American Academy of Neurology and the American Clinical Neurophysiology Society. Neurology 78, 585-589.

Nwachuku, E.L., Balzer, J.R., Yabes, J.G., Habeych, M.E., Crammond, D.J., Thirumala, P.D., 2015. Diagnostic value of somatosensory evoked potential changes during carotid endarterectomy: A systematic review and meta-analysis. JAMA Neurology 72, 73-80.

Olivier, E., Baker, S.N., Nakajima, K., Brochier, T., Lemon, R.N., 2001. Investigation into non-monosynaptic corticospinal excitation of macaque upper limb single motor units. J Neurophysiol 86, 1573-1586.

Ormerod, W., 2006. Richard Caton (1842-1926): pioneer electrophysiologist and cardiologist. J Med.Biogr. 14, 30-35.

Overduin, S.A., Servos, P., 2004. Distributed digit somatotopy in primary somatosensory cortex. Neuroimage. 23, 462-472.

Paré, M., Smith, A.M., Rice, F.L., 2002. Distribution and terminal arborizations of cutaneous mechanoreceptors in the glabrous finger pads of the monkey. The Journal of Comparative Neurology 445, 347-359.

Park, M.C., Belhaj-Saïf, A., Gordon, M., Cheney, P.D., 2001. Consistent features in the forelimb representation of primary motor cortex in rhesus macaques. J Neurosci. 21, 2784-2792.

Park, M.C., Belhaj-Saïf, A., Cheney, P.D., 2004. Properties of Primary Motor Cortex Output to Forelimb Muscles in Rhesus Macaques. Journal of Neurophysiology 92, 2968-2984.

Pascual-Leone, A., 2001. The brain that plays music and is changed by it. Ann.N.Y.Acad.Sci. 930, 315-329.

Pascual-Leone, A., Amedi, A., Fregni, F., Merabet, L.B., 2005. The plastic human brain cortex. Annu.Rev.Neurosci. 28, 377-401.

Pascual-Leone, A., Nguyet, D., Cohen, L.G., Brasil-Neto, J.P., Cammarota, A., Hallett, M., 1995a. Modulation of muscle responses evoked by transcranial magnetic stimulation during the acquisition of new fine motor skills. J Neurophysiol. 74, 1037-1045.

Pascual-Leone, A., Torres, F., 1993. Plasticity of the sensorimotor cortex representation of the reading finger in Braille readers. Brain 116 (Pt 1), 39-52.

Pascual-Leone, A., Wassermann, E.M., Sadato, N., Hallett, M., 1995b. The role of reading activity on the modulation of motor cortical outputs to the reading hand in Braille readers. Annals of Neurology 38, 910-915.

Pascual-Marqui, R.D., 1999. Review of methods for solving the EEG inverse problem. International Journal of Bioelectromagnetism 1, 75-86.

Pascual-Marqui, R.D., Sekihara, K., Brandeis, D., Michel, C.M., 2009. Imaging the electric neuronal generators of EEG/MEG. In: Michel, C.M., Koenig, T., Brandeis, D., Gianotti, L.R.R., Wackermann, J. (Eds.), Electrical neuroimaging. Cambridge University Press, pp. 49-78.

Patestas, M., Gartner, L.P., 2013. A textbook of neuroanatomy. John Wiley & Sons.

Patterson, J.T., Coggeshall, R.E., Lee, W.T., Chung, K., 1990. Long ascending unmyelinated primary afferent axons in the rat dorsal column: Immunohistochemical localizations. Neuroscience Letters 108, 6-10.

Patterson, J.T., Head, P.A., McNeill, D.L., Chung, K., Coggeshall, R.E., 1989. Ascending unmyelinated primary afferent fibers in the dorsal funiculus. The Journal of Comparative Neurology 290, 384-390.

Pavlides, C., Miyashita, E., Asanuma, H., 1993. Projection from the sensory to the motor cortex is important in learning motor skills in the monkey. J Neurophysiol. 70, 733-741.

Pearce, A.J., Thickbroom, G.W., Byrnes, M.L., Mastaglia, F.L., 2000. Functional reorganisation of the corticomotor projection to the hand in skilled racquet players. Exp.Brain Res. 130, 238-243.

Penfield, W., Boldrey, E., 1937. Somatic motor and sensory representation in the cerebral cortex of man as studied by electrical stimulation. Brain 60, 389-443.

Penfield, W., Jasper, H.H., 1954. Epilepsy and the Functional Anatomy of the Human Brain. Little, Brown.

Penfield, W., Rasmussen, T., 1950. The cerebral cortex of man; a clinical study of localization of function.

Petersen, C.C., 2009. Genetic manipulation, whole-cell recordings and functional imaging of the sensorimotor cortex of behaving mice. Acta Physiol (Oxf) 195, 91-99.

Pettersson, L.G., Lundberg, A., Alstermark, B., Isa, T., Tantisira, B., 1997. Effect of spinal cord lesions on forelimb target-reaching and on visually guided switching of target-reaching in the cat. Neuroscience Research 29, 241-256.

Peuser, J., Belhaj-Saïf, A., Hamadjida, A., Schmidlin, E., Gindrat, A.D., Volker, A.C., Zakharov, P., Hoogewoud, H.M., Rouiller, E.M., Scheffold, F., 2011. Follow-up of cortical activity and structure after lesion with laser speckle imaging and magnetic resonance imaging in nonhuman primates. J Biomed.Opt. 16, 096011-1-096011-11.

Phillips, J.R., Johansson, R.S., Johnson, K.O., 1990. Representation of braille characters in human nerve fibres. Exp Brain Res 81, 589-592.

Picard, N., Smith, A.M., 1992a. Primary motor cortical activity related to the weight and texture of grasped objects in the monkey. J Neurophysiol. 68, 1867-1881.

Picard, N., Smith, A.M., 1992b. Primary motor cortical responses to perturbations of prehension in the monkey. J Neurophysiol. 68, 1882-1894.

Picard, N., Strick, P.L., 1996. Motor Areas of the Medial Wall: A Review of Their Location and Functional Activation. Cerebral Cortex 6, 342-353.

Plonsey, R., Heppner, D.B., 1967. Considerations of quasi-stationarity in electrophysiological systems. Bulletin of Mathematical Biophysics 29, 657-664.

Pons, T.P., Garraghty, P.E., Cusick, C.G., Kaas, J.H., 1985. The somatotopic organization of area 2 in macaque monkeys. The Journal of Comparative Neurology 241, 445-466.

Pons, T.P., Wall, J.T., Garraghty, P.E., Cusick, C.G., Kaas, J.H., 1987. Consistent Features of the Representation of the Hand in Area 3b of Macaque Monkeys. Somatosensory & Motor Research 4, 309-331.

Poole, K., Lechner, S.G., Lewin, G.R., 2011. The molecular and genetic basis of touch. The Handbook of Touch, Hertenstein MJ, Weiss SJ (eds) pp, 59-84.

Porter, R., Lemon, R., 1993. Corticospinal Function and Voluntary Movement. Clarendon Press, Oxford.

Powell, T.P., Mountcastle, V.B., 1959a. The cytoarchitecture of the postcentral gyrus of the monkey *Macaca mulatta*. Bulletin of the Johns Hopkins Hospital 105, 108.

Powell, T.P.S., Mountcastle, V.B., 1959b. Some aspects of the functional organization of the cortex of the postcentral gyrus of the monkey: a correlation of findings obtained in a single unit analysis with cytoarchitecture. Bull Johns Hopkins Hosp 105, 133-162.

Pratt, H., Amlie, R.N., Starr, A., 1979a. Short latency mechanically evoked somatosensory potentials in humans. Electroencephalography and Clinical Neurophysiology 47, 524-531.

Pratt, H., Politoske, D., Starr, A., 1980. Mechanically and electrically evoked somatosensory potentials in humans: effects of stimulus presentation rate. Electroencephalogr.Clin.Neurophysiol 49, 240-249.

Pratt, H., Starr, A., Amlie, R.N., Politoske, D., 1979b. Mechanically and electrically evoked somatosensory potentials in normal humans. Neurology 29, 1236.

Preuss, T.M., Stepniewska, I., Kaas, J.H., 1996. Movement representation in the dorsal and ventral premotor areas of owl monkeys: a microstimulation study. Journal of Comparative Neurology 371, 649-676.

Pujol, J., Roset-Llobet, J., Rosinés-Cubells, D., Deus, J., Narberhaus, B., Valls-Solé, J., Capdevila, A., Pascual-Leone, A., 2000. Brain Cortical Activation during Guitar-Induced Hand Dystonia Studied by Functional MRI. Neuroimage 12, 257-267.

Purves, D., Augustine, G.A., Fitzpatrick, D., Hall, W., LaMantia, A.-S., McNamara, J.O., Williams, S.M., 2008. Neuroscience, 4th ed. Sinauer Associates, Incorporated.

Qi, H.X., Jain, N., Collins, C.E., Lyon, D.C., Kaas, J.H., 2010. Functional organization of motor cortex of adult macaque monkeys is altered by sensory loss in infancy. Proc.Natl.Acad.Sci.USA 107, 3192-3197.

Qi, H.X., Kaas, J.H., 2004. Myelin stains reveal an anatomical framework for the representation of the digits in somatosensory area 3b of macaque monkeys. J.Comp Neurol. 477, 172-187.

Qi, H.X., Kaas, J.H., 2006. Organization of primary afferent projections to the gracile nucleus of the dorsal column system of primates. The Journal of Comparative Neurology 499, 183-217.

Quallo, M.M., Kraskov, A., Lemon, R.N., 2012. The activity of primary motor cortex corticospinal neurons during tool use by macaque monkeys. J.Neurosci. 32, 17351-17364.

Quartarone, A., Hallett, M., 2013. Emerging concepts in the physiological basis of dystonia. Mov Disord. 28, 958-967.

Quartarone, A., Pisani, A., 2011. Abnormal plasticity in dystonia: Disruption of synaptic homeostasis. Neurobiol.Dis. 42, 162-170.

Ragert, P., Schmidt, A., Altenmuller, E., Dinse, H.R., 2004. Superior tactile performance and learning in professional pianists: evidence for meta-plasticity in musicians. Eur.J Neurosci. 19, 473-478.

Ralston, D.D., Ralston, H.J.I., 1985. The terminations of corticospinal tract axons in the macaque monkey. J Comp Neurol. 242, 325-337.

Ramachandran, V.S., Hirstein, W., 1998. The perception of phantom limbs. The D. O. Hebb lecture. Brain 121, 1603-1630.

Ramachandran, V.S., Rogers-Ramachandran, D., 2000. Phantom limbs and neural plasticity. Archives of Neurology 57, 317-320.

Ramachandran, V.S., Rogers-Ramachandran, D., Cobb, S., 1995. Touching the phantom limb. Nature 377, 489-490.

Ramon y Cajal, S., 1904. Textura del Sistema Nervioso del Hombre y de los Vertebrados. Madrid.

Ramon y Cajal, S., 1913. Degeneration and Regeneration of the Nervous System. Oxford Univ Press, London.

Rao, S.M., Binder, J.R., Hammeke, T.A., Bandettini, P.A., Bobholz, J.A., Frost, J.A., Myklebust, B.M., Jacobson, R.D., Hyde, J.S., 1995. Somatotopic mapping of the human primary motor cortex with functional magnetic resonance imaging. Neurology 45, 919-924.

Rathelot, J.A., Strick, P.L., 2006. Muscle representation in the macaque motor cortex: an anatomical perspective. Proc.Natl.Acad.Sci.USA 103, 8257-8262.

Rathelot, J.A., Strick, P.L., 2009. Subdivisions of primary motor cortex based on cortico-motoneuronal cells. Proceedings of the National Academy of Sciences 106, 918-923.

Recanzone, G.H., Jenkins, W.M., Hradek, G.T., Merzenich, M.M., 1992a. Progressive improvement in discriminative abilities in adult owl monkeys performing a tactile frequency discrimination task. Journal of Neurophysiology 67, 1015-1030.

Recanzone, G.H., Merzenich, M.M., Jenkins, W.M., Grajski, K.A., Dinse, H.R., 1992b. Topographic reorganization of the hand representation in cortical area 3b owl monkeys trained in a frequency-discrimination task. J.Neurophysiol. 67, 1031-1056.

Recanzone, G.H., Merzenich, M.M., Schreiner, C.E., 1992c. Changes in the distributed temporal response properties of SI cortical neurons reflect improvements in performance on a temporally based tactile discrimination task. Journal of Neurophysiology 67, 1071-1091.

Recanzone, G.H., Jenkins, W.M., Hradek, G.T., Merzenich, M.M., 1991. A behavioral frequency discrimination paradigm for use in adult primates. Behavior Research Methods, Instruments, & Computers 23, 357-369.

Reuter, E.M., Voelcker-Rehage, C., Vieluf, S., Godde, B., 2014. Effects of age and expertise on tactile learning in humans. European Journal of Neuroscience 40, 2589-2599.

Riddle, C.N., Baker, S.N., 2010. Convergence of pyramidal and medial brain stem descending pathways onto macaque cervical spinal interneurons. J Neurophysiol 103, 2821-2832.

Riddle, C.N., Edgley, S.A., Baker, S.N., 2009. Direct and indirect connections with upper limb motoneurons from the primate reticulospinal tract. J Neurosci. 29, 4993-4999.

Rijntjes, M., Dettmers, C., Büchel, C., Kiebel, S., Frackowiak, R.S.J., Weiller, C., 1999. A Blueprint for Movement: Functional and Anatomical Representations in the Human Motor System. The Journal of Neuroscience 19, 8043-8048.

Rizzolatti, G., Camarda, R., Fogassi, L., Gentilucci, M., Luppino, G., Matelli, M., 1988. Functional organization of inferior area 6 in the macaque monkey. II. Area F5 and the control of distal movements. Exp Brain Res 71, 491-507.

Rizzolatti, G., Luppino, G., Matelli, M., 1998. The organization of the cortical motor system: new concepts. Electroencephalogr.Clin.Neurophysiol 106, 283-296.

Rizzolatti, G., Fogassi, L., 2014. The mirror mechanism: recent findings and perspectives. Philosophical Transactions of the Royal Society of London B: Biological Sciences 369.

Rizzolatti, G., Fogassi, L., Gallese, V., 1997. Parietal cortex: from sight to action. Current Opinion in Neurobiology 7, 562-567.

Rizzolatti, G., Luppino, G., 2001. The Cortical Motor System. Neuron 31, 889-901.

Rizzolatti, G., Strick, P.L., 2013. Cognitive Functions of the Premotor Systems. In: Kandel, E.R., Schwartz, J.H., Jessell, T.M., Siegelbaum, S.A., Hudspeth, A.J. (Eds.). McGraw-Hill, pp. 412-425.

Roland, P.E., Larsen, B., Lassen, N.A., Skinhoj, E., 1980. Supplementary motor area and other cortical areas in organization of voluntary movements in man. Journal of Neurophysiology 43, 118-136.

Rosén, I., Asanuma, H., 1972. Peripheral afferent inputs to the forelimb area of the monkey motor cortex: input-output relations. Exp.Brain Res. 14, 257-273.

Rothwell, J.C., Traub, M.M., Day, B.L., Obeso, J.A., Thomas, P.K., Marsden, C.D., 1982. Manual motor performance in a deafferented man. Brain 105 (Pt 3), 515-542.

Rouiller, E.M., 1996. Multiple Hand Representations in the Motor Cortical Areas. In: Flanagan, A.M.W. (Ed.), Hand and Brain. Academic Press, San Diego, pp. 99-124.

Rouiller, E.M., 2012. What can we learn from animal models? In: Gollhofer, A., Taube, W., Bo Nielsen, J. (Eds.), Routledge Handbook of Motor Control and Motor Learning. Routledge.

Rouiller, E.M., Moret, V., Tanne, J., Boussaoud, D., 1996. Evidence for direct connections between the hand region of the supplementary motor area and cervical motoneurons in the macaque monkey. Eur.J Neurosci. 8, 1055-1059.

Rouiller, E.M., Olivier, E., 2004. Functional recovery after lesions of the primary motor cortex. Prog.Brain Res. 143, 467-475.

Rouiller, E.M., Yu, X.H., Moret, V., Tempini, A., Wiesendanger, M., Liang, F., 1998. Dexterity in adult monkeys following early lesion of the motor cortical hand area: the role of cortex adjacent to the lesion. Eur.J.Neurosci. 10, 729-740.

Rowe, M.J., 2001. Transmission security across central synapses for tactile and kinaesthetic signals., Somatosensory processing: from single neuron to brain imaging. Harwood Academic publishers, Sydney, pp. 77-100.

Rustioni, A., Hayes, N.L., O'Neill, S., 1979. Dorsal column nuclei and ascending spinal afferents in macaques. Brain 102, 95-125.

Ryynanen, O.R., Hyttinen, J.A., Laarne, P.H., Malmivuo, J.A., 2004. Effect of electrode density and measurement noise on the spatial resolution of cortical potential distribution. IEEE Trans.Biomed.Eng 51, 1547-1554.

Ryynanen, O.R., Hyttinen, J.A., Malmivuo, J.A., 2006. Effect of measurement noise and electrode density on the spatial resolution of cortical potential distribution with different resistivity values for the skull. IEEE Trans.Biomed.Eng 53, 1851-1858.

Sachdev, R.N.S., Catania, K.C., 2002. Receptive Fields and Response Properties of Neurons in the Star-Nosed Mole's Somatosensory Fovea. Journal of Neurophysiology 87, 2602-2611.

Sadato, N., Pascual-Leone, A., Grafman, J., Deiber, M.P., Ibanez, V., Hallett, M., 1998. Neural networks for Braille reading by the blind. Brain 121, 1213-1229.

Sadato, N., Pascual-Leone, A., Grafman, J., Ibanez, V., Deiber, M.P., Dold, G., Hallett, M., 1996. Activation of the primary visual cortex by Braille reading in blind subjects. Nature 380, 526-528.

Sainburg, R.L., Ghilardi, M.F., Poizner, H., Ghez, C., 1995. Control of limb dynamics in normal subjects and patients without proprioception. Journal of Neurophysiology 73, 820-835.

Sainburg, R.L., Poizner, H., Ghez, C., 1993. Loss of proprioception produces deficits in interjoint coordination. Journal of Neurophysiology 70, 2136-2147.

Salimi, I., Brochier, T., Smith, A.M., 1999. Neuronal activity in somatosensory cortex of monkeys using a precision grip. I. Receptive fields and discharge patterns. J Neurophysiol. 81, 825-834.

Salinas, E., Romo, R., 1998. Conversion of Sensory Signals into Motor Commands in Primary Motor Cortex. The Journal of Neuroscience 18, 499-511.

Sances, A.Jr., Larson, S.J., Cusick, J.F., Myklebust, J., Ewing, C.L., Jodat, R., Ackmann, J.J., Walsh, P., 1978. Early somatosensory evoked potentials. Electroencephalogr.Clin.Neurophysiol 45, 505-514.

Sand, T., Kvaloy, M.B., Wader, T., Hovdal, H., 2013. Evoked potential tests in clinical diagnosis. Tidsskr.Nor Laegeforen. 133, 960-965.

Sanei, S., Chambers, J.A., 2007. Event-Related Potentials., EEG signal processing. John Wiley & Sons, Ltd, pp. 127-159.

Sanes, J.N., Donoghue, J.P., 2000. Plasticity and primary motor cortex. Annu.Rev.Neurosci. 23, 393-415.

Sanes, J.N., Mauritz, K.H., Evarts, E.V., Dalakas, M.C., Chu, A., 1984. Motor deficits in patients with large-fiber sensory neuropathy. Proc.Natl.Acad.Sci.USA 81, 979-982.

Sanes, J.N., Shadmehr, R., 1995. Sense of muscular effort and somesthetic afferent information in humans. Canadian journal of physiology and pharmacology 73, 223-233.

Sarvas, J., 1987. Basic mathematical and electromagnetic concepts of the biomagnetic inverse problem. Physics in Medicine and Biology 32, 11.

Sasaki, K., Gemba, H., 1984. Compensatory motor function of the somatosensory cortex for the motor cortex temporarily impaired by cooling in the monkey. Exp.Brain Res 55, 60-68.

Sasaki, S., Isa, T., Pettersson, L.G., Alstermark, B., Naito, K., Yoshimura, K., Seki, K., Ohki, Y., 2004. Dexterous finger movements in primate without monosynaptic corticomotoneuronal excitation. J Neurophysiol 92, 3142-3147.

Sathian, K., Zangaladze, A., 1996. Tactile spatial acuity at the human fingertip and lip Bilateral symmetry and interdigit variability. Neurology 46, 1464.

Schaffelhofer, S., Agudelo-Toro, A., Scherberger, H., 2015. Decoding a Wide Range of Hand Configurations from Macaque Motor, Premotor, and Parietal Cortices. The Journal of Neuroscience 35, 1068-1081.

Schieber, M.H., 2001. Constraints on somatotopic organization in the primary motor cortex. J Neurophysiol 86, 2125-2143.

Schieber, M.H., Hibbard, L.S., 1993. How somatotopic is the motor cortex hand area? Science 261, 489-492.

Schieber, M.H., 1999. Somatotopic gradients in the distributed organization of the human primary motor cortex hand area: evidence from small infarcts. Exp Brain Res 128, 139-148.

Schieber, M.H., 2007. Comparative anatomy and physiology of the corticospinal system. In: Andrew, A.E.a.P. (Ed.), Handbook of Clinical Neurology, Motor neuron disorders and related diseases, Volume 82. Elsevier, pp. 15-37.

Schieber, M.H., Baker, J.F., 2013. Control of Movement. In: Spitzer, L.R.S. (Ed.), Fundamental Neuroscience (Fourth Edition). Academic Press, San Diego, pp. 631-651.

Schieber, M.H., Poliakov, A.V., 1998. Partial Inactivation of the Primary Motor Cortex Hand Area: Effects on Individuated Finger Movements. The Journal of Neuroscience 18, 9038-9054.

Schlaeger, R., D'Souza, M., Schindler, C., Grize, L., Kappos, L., Fuhr, P., 2014. Prediction of MS disability by multimodal evoked potentials: Investigation during relapse or in the relapse-free interval? Clinical Neurophysiology 125, 1889-1892.

Schlaug, G., 2001. The brain of musicians. A model for functional and structural adaptation. Ann.N.Y.Acad.Sci. 930, 281-299.

Schmidlin, E., Kaeser, M., Gindrat, A.D., Savidan, J., Chatagny, P., Badoud, S., Hamadjida, A., Beaud, M.L., Wannier, T., Belhaj-Saïf, A., Rouiller, E.M., 2011. Behavioral assessment of manual dexterity in non-human primates. J.Vis.Exp., e3258.

Schmidlin, E., Wannier, T., Bloch, J., Belhaj-Saïf, A., Wyss, A.F., Rouiller, E.M., 2005. Reduction of the hand representation in the ipsilateral primary motor cortex following unilateral section of the corticospinal tract at cervical level in monkeys. BMC.Neurosci. 6, 56.

Schmidlin, E., Wannier, T., Bloch, J., Rouiller, E.M., 2004. Progressive plastic changes in the hand representation of the primary motor cortex parallel incomplete recovery from a unilateral section of the corticospinal tract at cervical level in monkeys. Brain Res. 1017, 172-183.

Schmidlin, E., Brochier, T., Maier, M.A., Kirkwood, P.A., Lemon, R.N., 2008. Pronounced Reduction of Digit Motor Responses Evoked from Macaque Ventral Premotor Cortex after Reversible Inactivation of the Primary Motor Cortex Hand Area. The Journal of Neuroscience 28, 5772-5783.

Schwab, M.E., 2004. Nogo and axon regeneration. Curr.Opin.Neurobiol. 14, 118-124.

Schwartz, A.B., Kettner, R.E., Georgopoulos, A.P., 1988. Primate motor cortex and free arm movements to visual targets in three- dimensional space. I. Relations between single cell discharge and direction of movement. The Journal of Neuroscience 8, 2913-2927.

Scott, S.H., Kalaska, J.F., 1995. Changes in motor cortex activity during reaching movements with similar hand paths but different arm postures. Journal of Neurophysiology 73, 2563-2567.

Seitz, R.J., Roland, P.E., 1992. Learning of Sequential Finger Movements in Man: A Combined Kinematic and Positron Emission Tomography (PET) Study. European Journal of Neuroscience 4, 154-165.

Sejnowski, T.J., Churchland, P.S., Movshon, J.A., 2014. Putting big data to good use in neuroscience. Nat Neurosci 17, 1440-1441.

Seo, J.P., Jang, S.H., 2013. Different characteristics of the corticospinal tract according to the cerebral origin: DTI study. AJNR Am.J Neuroradiol. 34, 1359-1363.

Sessle, B.J., Wiesendanger, M., 1982. Structural and functional definition of the motor cortex in the monkey (*Macaca fascicularis*). J Physiol 323, 245-265.

Shapovalov, A.I., Karamjan, O.A., Kurchavyi, G.G., Repina, Z.A., 1971. Synaptic actions evoked from the red nucleus on the spinal alpha-motoneurons in the rhesus monkey. Brain Research 32, 325-348.

Shen, L., Alexander, G.E., 1997. Neural Correlates of a Spatial Sensory-To-Motor Transformation in Primary Motor Cortex. Journal of Neurophysiology 77, 1171-1194.

Shima, K., Tanji, J., 1998a. Both Supplementary and Presupplementary Motor Areas Are Crucial for the Temporal Organization of Multiple Movements. Journal of Neurophysiology 80, 3247-3260.

Shima, K., Tanji, J., 1998b. Role for Cingulate Motor Area Cells in Voluntary Movement Selection Based on Reward. Science 282, 1335-1338.

Shimazu, H., Maier, M.A., Cerri, G., Kirkwood, P.A., Lemon, R.N., 2004. Macaque ventral premotor cortex exerts powerful facilitation of motor cortex outputs to upper limb motoneurons. J Neurosci. 24, 1200-1211.

Shimoji, K., Willis, W.D.Jr., 2008. Evoked Spinal Cord Potentials: An illustrated Guide to Physiology, Pharmocology, and Recording Techniques. Springer.

Sloper, J.J., 1973. An electron microscope study of the termination of afferent connections to the primate motor cortex. J.Neurocytol. 2, 361-368.

Small, S.A., Heeger, D.J., 2013. Functional Imaging of Cognition. In: Kandel, E.R., Schwartz, J., Jessell, T. (Eds.), Principles of Neural Science, Fifth Edition. McGraw-Hill Education, pp. 426-442.

Smith, R.J.H., Shearer, A.E., Hildebrand, M.S., Van Camp, G., 1999. Deafness and hereditary hearing loss overview. In: Pagon, R.A., Adam, M.P., Ardiger, H.H. (Eds.), GeneReviews® [Internet], [Updated 2014 Jan 9]. University of Washington, Seattle.

Soteropoulos, D.S., Edgley, S.A., Baker, S.N., 2013. Spinal Commissural Connections to Motoneurons Controlling the Primate Hand and Wrist. The Journal of Neuroscience 33, 9614-9625.

Soteropoulos, D.S., Williams, E.R., Baker, S.N., 2012. Cells in the monkey ponto-medullary reticular formation modulate their activity with slow finger movements. The Journal of physiology 590, 4011-4027.

Speckmann, E.J., Elger, C.E., Gorji, A., 2011. Neurophysiologic basis of EEG and DC potentials. In: Niedermeyer, E., Schomer, D.L., da Silva, F.H.L. (Eds.), Niedermeyer's Electroencephalography: Basic Principles, Clinical Applications, and Related Fields. Wolters Kluwer Health/Lippincott Williams & Wilkins, pp. 17-31.

Sperli, F., Spinelli, L., Seeck, M., Kurian, M., Michel, C.M., Lantz, G., 2006. EEG source imaging in pediatric epilepsy surgery: a new perspective in presurgical workup. Epilepsia 47, 981-990.

Spinelli, L., Andino, S.G., Lantz, G., Seeck, M., Michel, C.M., 2000. Electromagnetic inverse solutions in anatomically constrained spherical head models. Brain Topogr. 13, 115-125.

Spinks, R.L., Kraskov, A., Brochier, T., Umilta, M.A., Lemon, R.N., 2008. Selectivity for grasp in local field potential and single neuron activity recorded simultaneously from M1 and F5 in the awake macaque monkey. J.Neurosci. 28, 10961-10971.

Squire, L., Berg, D., Bloom, F.E., du Lac, S., Ghosh, A., Spitzer, N.C., 2012. Fundamental Neuroscience. Elsevier Science.

Sripati, A.P., Yoshioka, T., Denchev, P., Hsiao, S.S., Johnson, K.O., 2006. Spatiotemporal Receptive Fields of Peripheral Afferents and Cortical Area 3b and 1 Neurons in the Primate Somatosensory System. The Journal of Neuroscience 26, 2101-2114.

Starr, A., 1978. Sensory evoked potentials in clinical disorders of the nervous system. Annu.Rev.Neurosci. 1, 103-127.

Stavrinou, M.L., Della, P.S., Pizzella, V., Torquati, K., Cianflone, F., Franciotti, R., Bezerianos, A., Romani, G.L., Rossini, P.M., 2007. Temporal dynamics of plastic changes in human primary somatosensory cortex after finger webbing. Cereb.Cortex 17, 2134-2142.

Stecker, M.M., 2012. A review of intraoperative monitoring for spinal surgery. Surg.Neurol.Int. 3, S174-S187.

Stepniewska, I., Preuss, T.M., Kaas, J.H., 1993. Architectonics, somatotopic organization, and ipsilateral cortical connections of the primary motor area (M1) of owl monkeys. Journal of Comparative Neurology 330, 238-271.

Sterr, A., Muller, M., Elbert, T., Rockstroh, B., Taub, E., 1999. Development of cortical reorganization in the somatosensory cortex of adult Braille students. Electroencephalogr.Clin.Neurophysiol.Suppl 49, 292-298.

Stiles, J., Jernigan, T.L., 2010. The Basics of Brain Development. Neuropsychology Review 20, 327-348.

Strata, F., Coq, J.O., Kaas, J.H., 2003. The chemo- and somatotopic architecture of the Galago cuneate and gracile nuclei. Neuroscience 116, 831-850.

Strick, P.L., Preston, J.B., 1982a. Two representations of the hand in area 4 of a primate. I. Motor output organization. J.Neurophysiol. 48, 139-149.

Strick, P.L., Preston, J.B., 1982b. Two representations of the hand in area 4 of a primate. II. Somatosensory input organization. J.Neurophysiol. 48, 150-159.

Strick, P.L., Dum, R.P., Picard, N., 1998. Motor Areas on the Medial Wall of the Hemisphere. In: Bock, G.R., Goode, J.A. (Eds.), Novartis Foundation Symposium 218 - Sensory Guidance of Movement. John Wiley & Sons, Ltd., pp. 64-80.

Strick, P.L., Preston, J.B., 1978a. Multiple representation in the primate motor cortex. Brain Research 154, 366-370.

Strick, P.L., Preston, J.B., 1978b. Sorting of somatosensory afferent information in primate motor cortex. Brain Research 156, 364-368.

Strominger, N.L., Demarest, R.J., Laemle, L.B., 2012. Discriminative General Senses, Crude Touch, and Proprioception., The Human Nervous System, 7th ed. Humana Press, New York, pp. 175-189.

Sugiuchi, Y., Kakei, S., Izawa, Y., Shinoda, Y., 2004. Functional synergies among neck muscles revealed by branching patterns of single long descending motor-tract axons. In: Shigemi Mori, D.G.S. (Ed.), Progress in Brain Research, Brain Mechanisms for the Integration of Posture and Movement, Volume 143. Elsevier, pp. 411-421.

Sur, M., 1980. Receptive fields of neurons in areas 3b and 1 of somatosensory cortex in monkeys. Brain Res 198, 465-471.

Sur, M., Garraghty, P.E., Bruce, C.J., 1985. Somatosensory cortex in macaque monkeys: laminar differences in receptive field size in areas 3b and 1. Brain Res 342, 391-395.

Sur, M., Merzenich, M.M., Kaas, J.H., 1980. Magnification, receptive-field area, and "hypercolumn" size in areas 3b and 1 of somatosensory cortex in owl monkeys. Journal of Neurophysiology 44, 295-311.

Szentáigothai, J., 1983. The modular architectonic principle of neural centers. Reviews of Physiology, Biochemistry and Pharmacology 98, 11-61.

Takada, M., Tokuno, H., Hamada, I., Inase, M., Ito, Y., Imanishi, M., Hasegawa, N., Akazawa, T., Hatanaka, N., Nambu, A., 2001. Organization of inputs from cingulate motor areas to basal ganglia in macaque monkey. European Journal of Neuroscience 14, 1633-1650.

Takeuchi, H., Sekiguchi, A., Taki, Y., Yokoyama, S., Yomogida, Y., Komuro, N., Yamanouchi, T., Suzuki, S., Kawashima, R., 2010. Training of Working Memory Impacts Structural Connectivity. The Journal of Neuroscience 30, 3297-3303.

Talbot, W.H., Darian-Smith, I., Kornhuber, H.H., Mountcastle, V.B., 1968. The sense of flutter-vibration: comparison of the human capacity with response patterns of mechanoreceptive afferents from the monkey hand. J Neurophysiol. 31, 301-334.

Tamburin, S., Manganotti, P., Marzi, C.A., Fiaschi, A., Zanette, G., 2002. Abnormal somatotopic arrangement of sensorimotor interactions in dystonic patients. Brain 125, 2719-2730.

Tamkus, A.A., Scott, A.F., Khan, F.R., 2015. Neurophysiological Monitoring During Spinal Cord Stimulator Placement Surgery. Neuromodulation: Technology at the Neural Interface.

Tamura, Y., Ueki, Y., Lin, P., Vorbach, S., Mima, T., Kakigi, R., Hallett, M., 2009. Disordered plasticity in the primary somatosensory cortex in focal hand dystonia. Brain 132, 749-755.

Tamura, Y., Matsuhashi, M., Lin, P., Ou, B., Vorbach, S., Kakigi, R., Hallett, M., 2008. Impaired intracortical inhibition in the primary somatosensory cortex in focal hand dystonia. Movement Disorders 23, 558-565.

Tan, P.L., Katsanis, N., 2009. Thermosensory and mechanosensory perception in human genetic disease. Human Molecular Genetics 18, R146-R155.

Tandon, O.P., 1998. Average evoked potentials--clinical applications of short latency responses. Indian J Physiol Pharmacol. 42, 172-188.

Tanji, J., Wise, S.P., 1981. Submodality distribution in sensorimotor cortex of the unanesthetized monkey. J.Neurophysiol. 45, 467-481.

Tanji, J., 1976. Selective activation of neurons in cortical area 3a associated with accurate maintenance of limb positions. Brain Research 115, 328-333.

Tanji, J., 1994. The supplementary motor area in the cerebral cortex. Neuroscience Research 19, 251-268.

Tanné-Gariépy, J., Rouiller, E.M., Boussaoud, D., 2002. Parietal inputs to dorsal versus ventral premotor areas in the macaque monkey: evidence for largely segregated visuomotor pathways. Exp Brain Res 145, 91-103.

Tardif, S., Carville, A., Elmore, D., Williams, L.E., Rice, K., 2012. Chapter 8 - Reproduction and Breeding of Nonhuman Primates. In: Morris, C.R.A. (Ed.), Nonhuman Primates in Biomedical Research (Second Edition). Academic Press, Boston, pp. 197-249.

Taulu, S., Simola, J., Nenonen, J., Parkkonen, L., 2014. Novel Noise Reduction Methods. In: Supek, S., Aine, C.J. (Eds.), Magnetoencephalography. Springer, Berlin Heidelberg, pp. 35-71.

Tokuno, H., Tanji, J., 1993. Input organization of distal and proximal forelimb areas in the monkey primary motor cortex: a retrograde double labeling study. J Comp Neurol. 333, 199-209.

Toleikis, J.R., 2005. Intraoperative monitoring using somatosensory evoked potentials. A position statement by the American Society of Neurophysiological Monitoring. J Clin.Monit.Comput. 19, 241-258.

Towe, A.L., 1973. Somatosensory cortex: descending influences on ascending systems., Somatosensory System. Springer, pp. 701-718.

Townsend, B.R., Subasi, E., Scherberger, H., 2011. Grasp Movement Decoding from Premotor and Parietal Cortex. The Journal of Neuroscience 31, 14386-14398.

Toyoshima, K., Sakai, H., 1982. Exact cortical extent of the origin of the corticospinal tract (CST) and the quantitative contribution to the CST in different cytoarchitectonic areas. A study with horseradish peroxidase in the monkey. J Hirnforsch. 23, 257-269.

Trachtenberg, J.T., Chen, B.E., Knott, G.W., Feng, G., Sanes, J.R., Welker, E., Svoboda, K., 2002. Long-term in vivo imaging of experience-dependent synaptic plasticity in adult cortex. Nature 420, 788-794.

Treede, R.D., 2005. Funktionsprüfung der nozizeptiven Bahnen durch SEP nach schmerzhaften Laser-Hitzereizen., Evozierte Potenziale. Springer Berlin Heidelberg, pp. 599-621.

Twitchell, T.E., 1954. Sensory factors in purposive movement. J.Neurophysiol. 17, 239-252.

Tzovara, A., Rossetti, A.O., Spierer, L., Grivel, J., Murray, M.M., Oddo, M., De Lucia, M., 2013. Progression of auditory discrimination based on neural decoding predicts awakening from coma. Brain 136, 81-89.

Uematsu, S., Lesser, R.P., Gordon, B., 1992. Localization of sensorimotor cortex: the influence of Sherrington and Cushing on the modern concept. Neurosurgery 30, 904-912.

Umilta, M.A., Brochier, T., Spinks, R.L., Lemon, R.N., 2007. Simultaneous Recording of Macaque Premotor and Primary Motor Cortex Neuronal Populations Reveals Different Functional Contributions to Visuomotor Grasp. Journal of Neurophysiology 98, 488-501.

Valeriani, M., Le Pera, D., Niddam, D., Arendt-Nielsen, L., Chen, A.C., 2000. Dipolar source modeling of somatosensory evoked potentials to painful and nonpainful median nerve stimulation. Muscle Nerve 23, 1194-1203.

Vallbo, A.B., 1989. Single Fibre Microneurography and Sensation. In: Kennard, C., Swash, M. (Eds.), Hierarchies in Neurology. Springer London, pp. 93-109.

Vallbo, A.B., Hagbarth, K.E., 1968. Activity from skin mechanoreceptors recorded percutaneously in awake human subjects. Experimental Neurology 21, 270-289.

Vallbo, A.B., Johansson, R.S., 1984. Properties of cutaneous mechanoreceptors in the human hand related to touch sensation. Hum Neurobiol 3, 3-14.

Van Boven, R.W., Hamilton, R.H., Kauffman, T., Keenan, J.P., Pascual-Leone, A., 2000. Tactile spatial resolution in blind Braille readers. Neurology 54, 2230-2236.

Van Boven, R.W., Johnson, K.O., 1994. The limit of tactile spatial resolution in humans: Grating orientation discrimination at the lip, tongue, and finger. Neurology 44, 2361.

van den Broek, S.P., Reinders, F., Donderwinkel, M., Peters, M.J., 1998. Volume conduction effects in EEG and MEG. Electroencephalogr.Clin.Neurophysiol. 106, 522-534.

van Westen, D., Fransson, P., Olsrud, J., Rosen, B., Lundborg, G., Larsson, E.M., 2004. Fingersomatotopy in area 3b: an fMRI-study. BMC Neuroscience 5, 28.

Vanrumste, B., Van Hoey, G., Van de Walle, R., D'Have, M., Lemahieu, I., Boon, P., 2000. Dipole location errors in electroencephalogram source analysis due to volume conductor model errors. Med.Biol.Eng Comput 38, 528-534.

Vigneswaran, G., Philipp, R., Lemon, R.N., Kraskov, A., 2013. M1 Corticospinal Mirror Neurons and Their Role in Movement Suppression during Action Observation. Current Biology 23, 236-243.

Vinogradov, S., Fisher, M., de Villers-Sidani, E., 2012. Cognitive training for impaired neural systems in neuropsychiatric illness. Neuropsychopharmacology 37, 43-76.

Vogt, B.A., Pandya, D.N., 1978. Cortico-cortical connections of somatic sensory cortex (areas 3, 1 and 2) in the rhesus monkey. The Journal of Comparative Neurology 177, 179-191.

Vogt, C., Vogt, O., 1926. Die vergleichend-architektonische und die vergleichend-reizphysiologische Felderung der Grosshirnrinde unter besonderer Berücksichtigung der menschlichen. Naturwissenschaften 14, 1190-1194.

Volpe, B.T., LeDoux, J.E., Gazzaniga, M.S., 1979. Spatially oriented movements in the absence of proprioception. Neurology 29, 1309.

von Economo, C., 1927. Zellaufbau der Grosshirnrinde des Menschen. Zehn Vorlesungen mit 61 Abbildungen. Verlag Julius Springer, Berlin.

Wall, J.T., Kaas, J.H., Sur, M., Nelson, R.J., Felleman, D.J., Merzenich, M.M., 1986. Functional reorganization in somatosensory cortical areas 3b and 1 of adult monkeys after median nerve repair: possible relationships to sensory recovery in humans. J Neurosci. 6, 218-233.

Wall, J.T., Felleman, D.J., Kaas, J.H., 1983. Recovery of normal topography in the somatosensory cortex of monkeys after nerve crush and regeneration. Science 221, 771-773.

Wan, C.Y., Schlaug, G., 2010. Music Making as a Tool for Promoting Brain Plasticity across the Life Span. the neuroscientist 16, 566-577.

Wang, X., Merzenich, M.M., Sameshima, K., Jenkins, W.M., 1995. Remodelling of hand representation in adult cortex determined by timing of tactile stimulation. Nature 378, 71-75.

Wannier, T., Schmidlin, E., Bloch, J., Rouiller, E.M., 2005. A unilateral section of the corticospinal tract at cervical level in primate does not lead to measurable cell loss in motor cortex. Journal of Neurotrauma 22, 703-717.

Wannier, T.M., Maier, M.A., Hepp-Reymond, M.C., 1991. Contrasting properties of monkey somatosensory and motor cortex neurons activated during the control of force in precision grip. J Neurophysiol. 65, 572-589.

Wannier-Morino, P., Schmidlin, E., Freund, P., Belhaj-Saïf, A., Bloch, J., Mir, A., Schwab, M.E., Rouiller, E.M., Wannier, T., 2008. Fate of rubrospinal neurons after unilateral section of the cervical spinal cord in adult macaque monkeys: effects of an antibody treatment neutralizing Nogo-A. Brain Res. 1217, 96-109.

Ward, N.S., Frackowiak, R.S.J., 2004. Towards a New Mapping of Brain Cortex Function. Cerebrovascular Diseases 17 (suppl 3), 35-38.

Watson, A.H., 2006. What can studying musicians tell us about motor control of the hand? J Anat. 208, 527-542.

Weber, E.H., Ross, H.E., Murray, D.J., 1996. EH Weber: on the tactile senses, 2nd ed. Erlbaum (UK) Taylor & Francis Hove.

Weibull, A., Flondell, M., Rosen, B., Bjorkman, A., 2011. Cerebral and clinical effects of short-term hand immobilisation. Eur.J Neurosci 33, 699-704.

Weinrich, M., Wise, S.P., 1982. The premotor cortex of the monkey. The Journal of Neuroscience 2, 1329-1345.

Weinrich, M., Wise, S.P., Mauritz, K.H., 1984. A neurophysiological study of the premotor cortex in the rhesus monkey. Brain 107, 385-414.

Westbrook, G.L., 2013. Seizures and Epilepsy. In: Kandel, E.R., Schwartz, J., Jessell, T. (Eds.), Principles of Neural Science, Fifth Edition. McGraw-Hill Education, pp. 1116-1139.

Whitsel, B.L., Petrucelli, L.M., Sapiro, G., 1969a. Modality representation in the lumbar and cervical fasciculus gracilis of squirrel monkeys. Brain Research 15, 67-78.

Whitsel, B.L., Petrucelli, L.M., Werner, G., 1969b. Symmetry and connectivity in the map of the body surface in somatosensory area II of primates. Journal of Neurophysiology 32, 170-183.

Whitsel, B.L., Favorov, O.V., Li, Y., Quibrera, M., Tommerdahl, M., 2009. Area 3a Neuron Response to Skin Nociceptor Afferent Drive. Cerebral Cortex (New York, NY) 19, 349-366.

Wiech, K., Preissl, H., Birbaumer, N., 2001. Neuronale Netzwerke und Schmerzverarbeitung, Ergebnisse bildgebender Verfahren, [Neural networks and pain processing. New insights from imaging techniques]. Der Anaesthesist 50, 2-12.

Wienbruch, C., Candia, V., Svensson, J., Kleiser, R., Kollias, S.S., 2006. A portable and low-cost fMRI compatible pneumatic system for the investigation of the somatosensensory system in clinical and research environments. Neurosci.Lett. 398, 183-188.

Wiesendanger, M., 1969. The pyramidal tract recent investigations on its morphology and function. Springer, pp. 72-136.

Wiesendanger, M., 1981. Organization of Secondary Motor Areas of Cerebral Cortex., Comprehensive Physiology. John Wiley & Sons, Inc., pp. 1121-1147.

Wiesendanger, M., 1986. Recent developments in studies of the supplementary motor area of primates., Reviews of Physiology, Biochemistry and Pharmacology, Volume 103. Springer Berlin Heidelberg, pp. 1-59.

Williams, S.R., Chapman, C.E., 2002. Time course and magnitude of movement-related gating of tactile detection in humans. III. Effect of motor tasks. J Neurophysiol. 88, 1968-1979.

Williams, S.R., Shenasa, J., Chapman, C.E., 1998. Time Course and Magnitude of Movement-Related Gating of Tactile Detection in Humans. I. Importance of Stimulus Location. Journal of Neurophysiology 79, 947-963.

Willis, W.D.Jr., 2003. Thalamo-cortical system of nociception in animals. In: Chen, J., Chen, A.C.N., Han, J.S., Willis, W.D.Jr. (Eds.), Experimental pathological pain: from molecules to brain functions. Science Press, Beijing, pp. 165-196.

Willis, W.D.Jr., 2007. The somatosensory system, with emphasis on structures important for pain. Brain Research Reviews 55, 297-313.

Willis, W.D.Jr., Coggeshall, R.E., 2004. Sensory receptors and peripheral nerves., Sensory Mechanisms of the Spinal Cord. Springer, pp. 19-90.

Wise, S.P., Tanji, J., 1981. Neuronal responses in sensorimotor cortex to ramp displacements and maintained positions imposed on hindlimb of the unanesthetized monkey. Journal of Neurophysiology 45, 482-500.

Wolters, C., Munck, J.C.d., 2007. Volume conduction. Scholarpedia 2, 1738.

Wolters, C.H., Anwander, A., Maess, B., Macleod, R.S., Friederici, A.D., 2004. The influence of volume conduction effects on the EEG/MEG reconstruction of the sources of the Early Left Anterior Negativity. Conf.Proc.IEEE Eng Med Biol.Soc. 5, 3569-3572.

Woolsey, C.N., Travis, A.M., Barnard, J.W., Ostenso, R.S., 1953. Motor representation in the postcentral gyrus after chronic ablation of precentral and supplementary motor areas. In: Erickson, C.C., Handler, P., Pfeiffer, C.C., Essex, H.E., Orten, J.M., Sugg, J.Y.,

Lee, M.O. (Eds.), Federation Proceedings, volume 12. Federation of Amercian Societies for experimental Biology, Washington, D.C., p. 160.

Woolsey, C.N., 1958. Organization of somatic sensory and motor areas of the cerebral cortex. In: Harlow, H.F., Woolsey, C.N. (Eds.), Biological and biochemical bases of behavior. The University of Wisconsin Press, pp. 63-81.

Woolsey, C.N., 1964. Cortical localization as defined by evoked potential and electrical stimulation studies. Cerebral localization and organization, 17-26.

Woolsey, C.N., Chang, H.t., 1947. Activation of the cerebral cortex by antidromic volleys in the pyramidal tract. Research publications-Association for Research in Nervous and Mental Disease 27, 146-161.

Woolsey, C.N., Erickson, T.C., 1949. Study of the postcentral gyrus of man by the evoked potential technique. Transactions of the American Neurological Association 51, 50-52.

Woolsey, C.N., Erickson, T.C., Gilson, W.E., 1979. Localization in somatic sensory and motor areas of human cerebral cortex as determined by direct recording of evoked potentials and electrical stimulation. J Neurosurg. 51, 476-506.

Woolsey, C.N., Marshall, W.H., Bard, P., 1942. Representation of cutaneous tactile sensibility in the cerebral cortex of the monkey as indicated by evoked potentials. Bull Johns Hopkins Hosp 70, 399-441.

Woolsey, C.N., Settlage, P.H., Meyer, D.R., Sencer, W., Pinto Hamuy, T., Travis, A.M., 1952. Patterns of localization in precentral and "supplementary" motor areas and their relation to the concept of a premotor area. Res.Publ.Assoc.Res.Nerv.Ment.Dis. 30, 238-264.

Wyss, A.F., Hamadjida, A., Savidan, J., Liu, Y., Bashir, S., Mir, A., Schwab, M.E., Rouiller, E.M., Belhaj-Saïf, A., 2013. Long-term motor cortical map changes following unilateral lesion of the hand representation in the motor cortex in macaque monkeys showing functional recovery of hand functions. Restor.Neurol Neurosci. 31, 733-760.

Xerri, C., Merzenich, M.M., Peterson, B.E., Jenkins, W., 1998. Plasticity of primary somatosensory cortex paralleling sensorimotor skill recovery from stroke in adult monkeys. J Neurophysiol. 79, 2119-2148.

Yau, J.M., Connor, C.E., Hsiao, S.S., 2013. Representation of tactile curvature in macaque somatosensory area 2. Journal of Neurophysiology 109, 2999-3012.

Yumiya, H., Kubota, K., Asanuma, H., 1974. Activities of neurons in area 3a of the cerebral cortex during voluntary movements in the monkey. Brain Res 78, 169-177.

Zaaimi, B., Edgley, S.A., Soteropoulos, D.S., Baker, S.N., 2012. Changes in descending motor pathway connectivity after corticospinal tract lesion in macaque monkey. Brain 135, 2277-2289.

Zachariah, M.K., Coleman, G.T., Mahns, D.A., Zhang, H.Q., Rowe, M.J., 2001. Transmission Security for Single, Hair Follicle–Related Tactile Afferent Fibers and Their Target Cuneate Neurons in Cat. Journal of Neurophysiology 86, 900-911.

Zamorano, A.M., Riquelme, I., Kleber, B., Altenmüller, E., Hatem, S., Montoya, P., 2015. Pain sensitivity and tactile spatial acuity are altered in healthy musicians as in chronic pain patients. Frontiers in Human Neuroscience 8.

Zatorre, R.J., Fields, R.D., Johansen-Berg, H., 2012. Plasticity in gray and white: neuroimaging changes in brain structure during learning. Nat Neurosci 15, 528-536.

Zeharia, N., Hertz, U., Flash, T., Amedi, A., 2015. New Whole-Body Sensory-Motor Gradients Revealed Using Phase-Locked Analysis and Verified Using Multivoxel Pattern Analysis and Functional Connectivity. The Journal of Neuroscience 35, 2845-2859.

Zeller, D., Litvak, V., Friston, K.J., Classen, J., 2014. Sensory Processing and the Rubber Hand Illusion — An Evoked Potentials Study. Journal of Cognitive Neuroscience 27, 573-582.

Zhang, X., Honda, C.N., Giesler, G.J., 2000a. Position of Spinothalamic Tract Axons in Upper Cervical Spinal Cord of Monkeys. Journal of Neurophysiology 84, 1180-1185.

Zhang, X., Wenk, H.N., Honda, C.N., Giesler, G.J., 2000b. Locations of Spinothalamic Tract Axons in Cervical and Thoracic Spinal Cord White Matter in Monkeys. Journal of Neurophysiology 83, 2869-2880.

Zilles, K., 1992. Neuronal plasticity as an adaptive property of the central nervous system. Annals of Anatomy - Anatomischer Anzeiger 174, 383-391.

Zimmerman, A., Bai, L., Ginty, D.D., 2014. The gentle touch receptors of mammalian skin. Science 346, 950-954.

Zimmermann, M., 1989. The Somatovisceral Sensory System. In: Schmidt, R.F., Thews, G. (Eds.), Human Physiology. Springer Berlin Heidelberg, pp. 196-222.

GENERAL MATERIALS AND METHODS

In this chapter, we will expose the general methodology of the experiments involving non-human primate subjects. Results of these experiments are presented in **Chapters 1** to **5**. More specific methodology to each chapter is presented in the corresponding chapter.

Subjects

Experiments were planned to be conducted on three adult macaque monkeys (*Macaca fascicularis*) (1 male: Mk-EN, and 2 females: Mk-AT, Mk-DI) (**Figure 1**). Unfortunately, much before the completion of all the experiments, Mk-AT prematurely died of a peritonitis. In addition, Mk-EN had to be euthanised because of a chronic incurable scalp infection. Therefore the data presented in **Chapters 2** and **3** were obtained from Mk-DI only. Additional animals were involved in the other projects and are mentioned accordingly in the appropriate chapters.

Figure 1 : The three monkeys I was in charge of during my PhD thesis. Note the presence of Mk-EN in a primate chair, here with both frontal doors removed, giving free access for both upper limbs.

Mk-AT (female, age: 5-8 years old during the experiments, weight: 3.2-3.8 kg) and Mk-DI (female, age: 5.5-10 years old during the experiments, weight: 3.1-3.8 kg) were housed in the animal facility in a group with three other congeners, in a 45-m^3 room (12 hours light/12 hours dark cycle). Moreover, they had a regular access to an outside facility (21 m^3) with a high degree of enrichment (trees, branches, ladders, large pipes to hide, dif-

ferent toys, foraging devices, etc.) for a part of the day or night. Before September 2010, Mk-EN (male, age: 4-9 years old during the experiments, weight: 3.1-8.3 kg) was housed in the animal facility with another congener in a 15-m^3 room (12 hours light/12 hours dark cycle), with regular access to an outside facility. In September 2010, the Swiss legislation about animal welfare was updated with new guidelines. From this time point, Mk-EN and its roommate moved in a 45-m^3 room (12 hours light/12 hours dark cycle), with regular access to a similar outside facility (13 m^3) as for both females. The monkeys were daily weighted and on no account food- or water-deprived (see e.g. Kaeser, 2010; Schmidlin et al., 2011). All procedures and animal care were conducted in accordance with the Guide for the Care and Use of Laboratory Animals (Committee for the Update of the Guide for the Care and Use of Laboratory Animals and National Research Council, 2011) and were designed to minimise the animals' pain and suffering. Moreover, all procedures were approved by local (Canton of Fribourg) and federal (Swiss) veterinary authorities. The experiments involving these monkeys were covered by the official authorisation numbers FR 17/09, FR 18/10 and FR 23765.

Behavioural tasks

General training

A comprehensive description of the daily routine and different tasks performed by the monkeys is provided in Schmidlin et al. (2011) and available in **Appendix 2**[14]. The first step had been to train the monkeys to cooperate from the moment they arrived in our animal facility. To this aim, animals were first trained to go freely from their home room into a smaller transitional cage and then from this cage into a primate chair (**Figure 1**) through a tunnel (**Figure 2**). The primate chair was made of Plexiglas® and contained a sliding opening on the top for the head and two independent sliding doors at the front, one for each upper limb. The size of the chair and the one of the upper opening were adapted to each animal. The next step was to get them to extract the head out of the primate chair on a voluntary basis. This long training phase was adapted to the character of each monkey and was absolutely essential to form a relationship based on mutual

[14] For short videos sequences illustrating the behavioural tasks, see also http://www.unifr.ch/neuro/rouiller/research/motorcontcadre.php

trust. This ensured that the monkeys remained calm and not stressed in my presence, in order to subsequently get valid behavioural data from them.

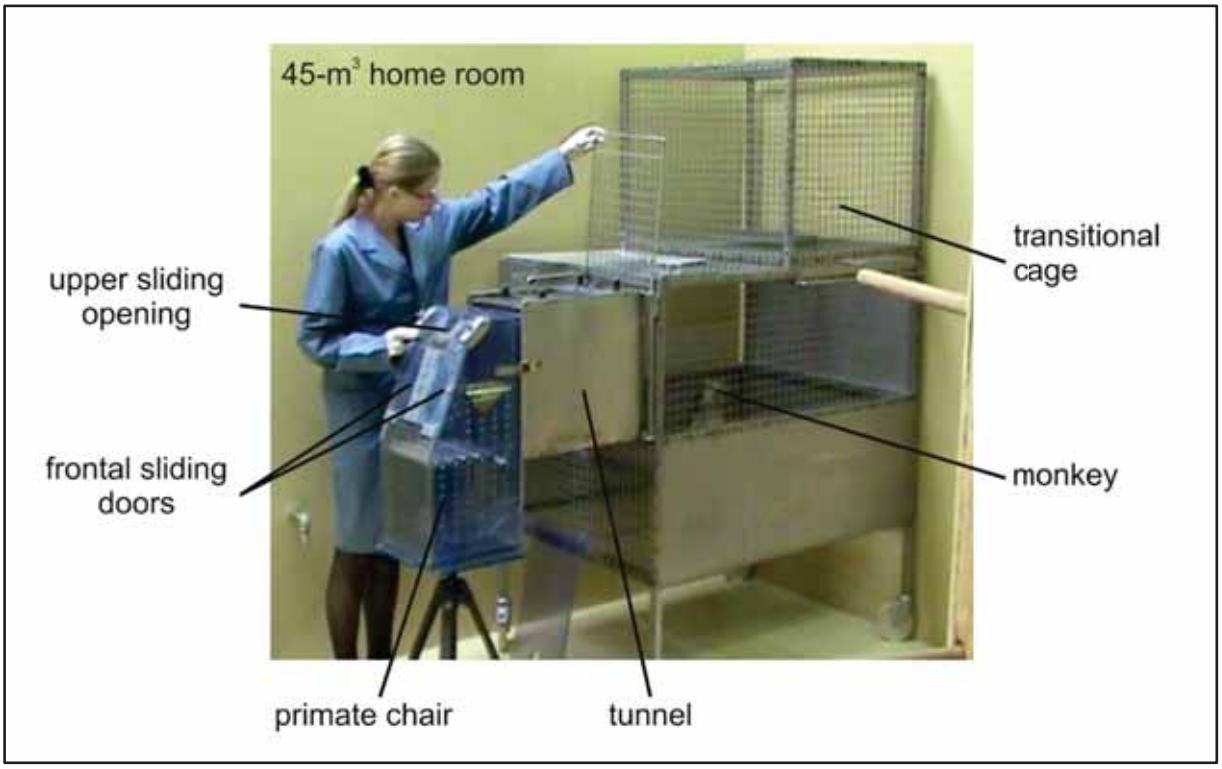

Figure 2 : Transfer of a monkey of its own free will from the transitional cage into the primate chair through a tunnel (from Schmidlin et al., 2011).

Once this first step had been achieved, the animals were trained to perform several behavioural tasks to assess their fine manual dexterity. For all these tests, the animals were sitting in the aforementioned primate chair. The daily behavioural training, usually lasting for about one hour, included the modified Brinkman board task, the Brinkman box task, the rotating Brinkman board task and the reach and grasp drawer task. However the latter two tasks will not be considered here (for greater detail, see Schmidlin et al., 2011 in **Appendix 2**). After completion of the daily training, the animals were fed (mix of fruits, vegetables, cereal croquettes and dried fruits) and then brought back to their home room and were then free to interact with their congeners until the next training session, usually the day after. Food access was limited to a 1-to-2-hour period after the end of the training session and the remaining non-eaten food was removed after that period. Note however that the monkeys had a continuous free access to water. Importantly, for each animal the different behavioural tasks were carried out at a very sim-

ilar schedule from one day to the next in order to establish a routine, a prerequisite for the monkeys to be motivated to work.

Modified Brinkman board task

The fine manual dexterity of monkeys was assessed by using the modified Brinkman board task (**Figure 3**). This test has been specifically designed to challenge the precision grip ability (Napier, 1956) in macaque monkeys (Brinkman and Kuypers, 1973) and its original version was improved into a modified version currently used in our laboratory (Chatagny et al., 2013; Liu and Rouiller, 1999; Rouiller et al., 1998; Schmidlin et al., 2005; Schmidlin et al., 2011) (see also the *Introduction* of **Chapter 5**). The modified Brinkman board set-up (**Figure 3A**) consisted of a rectangular board (40° angle above the horizontal) in green Perspex® (22 cm long, 12 cm wide) containing 25 vertically- and 25 horizontally-oriented rounded rectangular wells (15 mm x 7.5 mm, 6 mm deep), each filled with a 45-mg banana pellet (about 4 mm diameter, Bio-Serv, US and Canada, www.bio-serv.com) (**Figure 3B**). The task for the monkeys consisted of unimanually retrieving the pellet from each well. A fine finger motor control was required to perform the test, usually achieved by first introducing one finger (mostly the index finger or the thumb) into the well to establish a contact with the pellet, followed by the contact of a second finger (mostly the thumb or the index finger) to grasp the pellet with a precision grip while keeping the 3 other fingers flexed (**Figure 3C**). Collecting pellets from the horizontal wells required additionally ulnar or radial deviations and was therefore much more challenging than collecting pellets from the vertical wells, usually performed with the wrist in a neutral position (see e.g. Chatagny et al., 2013; Hoogewoud et al., 2013).

In practice, the monkey sat in its primate chair (**Figure 1**). The two independent sliding doors allowed the animals to work with either hand individually (Schmidlin et al., 2011). The monkey was placed in front of the modified Brinkman board with the door of the tested hand centred in front of the set-up (the distance between the door and the set-up was about 3 cm and the height at the basis of the board fitted the height at the basis of the door of the primate chair). Tests were conducted with each hand individually, and alternating between the first tested hand from one session to the next. Usually, this test was conducted from twice to five times a week, with a musical background to mask disturbing noise from outside. Each test session was videotaped (25 frames/s) using 3

standard digital cameras (Sony Handycam DCR-SX33, 25 frames/s, one above the board and one on either side) (**Figure 3A**). This task was straightforward to learn for the monkeys because they were simply reaching for food. Importantly, the animals performed the task in a free-will basis, meaning that there was neither constraint of score level nor speed to achieve. Short video sequences illustrating this task are available at http://www.unifr.ch/neuro/rouiller/research/MBB.php. Video sequences of the modified Brinkman board task performed with the right (contralesional, in Mk-DI) hand were analysed frame by frame (25 frames/s) with the software Virtualdub-MPEG2 1.6.19. The *score in 30 s* was established, i.e. the number of pellets correctly retrieved during the first 30 s of the task, independently for the vertical and horizontal wells as well as for all wells. Then, we defined a pre-lesion plateau of performance and a post-lesion plateau of performance based on all wells and compared both of them with a Mann-Whitney rank-sum test (SigmaPlot 12.5). The *contact time* was obtained for the first five vertical pellets and the first five horizontal pellets collected in the sessions of the pre-lesion plateau and post-lesion plateau. This measure was defined as the time interval between the first contact established by a finger with a pellet in a precision grip and the time point at which the fingers left the well with the pellet. A Mann-Whitney rank-sum test was used to compare pre- and post-lesion values distinctly for each well orientation (SigmaPlot 12.5).

Some additional information about this task is available in **Appendix 2**.

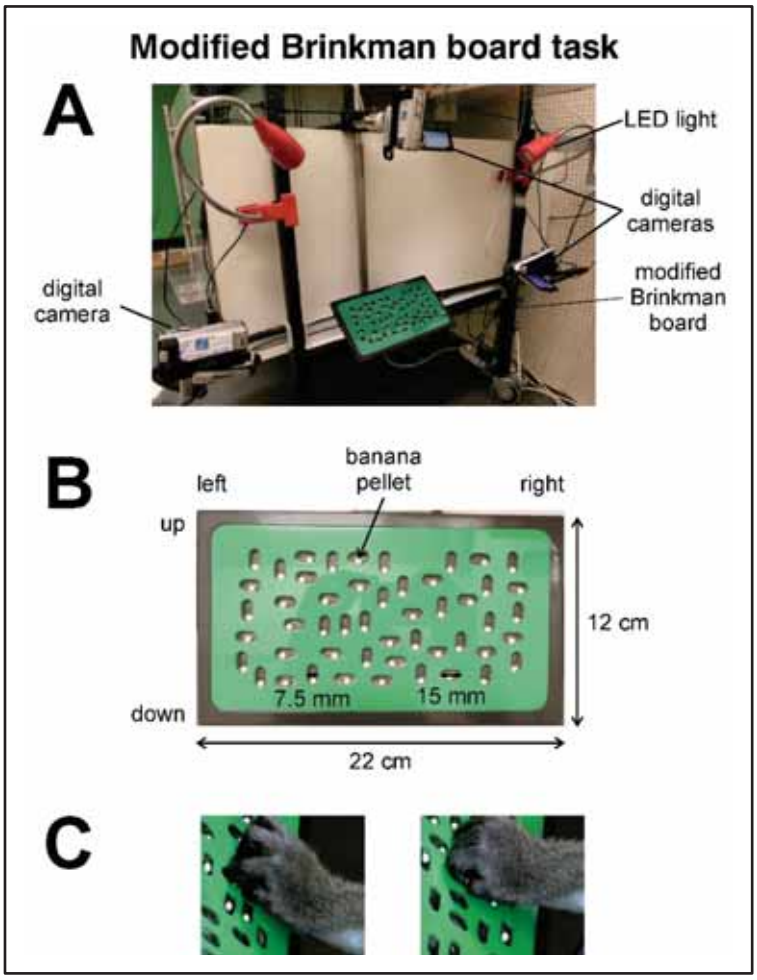

Figure 3 : Modified Brinkman board set-up. (A) General view of the set-up. Data were simultaneously acquired from one digital camera above the board and 2 lateral digital cameras. Lightening was provided by 2 LED lights. (B) Detail of the board and its sizes. (C) Detail of the initiation (left) and completion (right) of a pellet picking from a vertical well by using a precision grip. The index finger was first inserted in the well to establish a contact with the pellet and the thumb was then brought to pinch the pellet between the thumb tip and index fingertip.

Brinkman box task

In addition to the modified Brinkman board task, we assessed the integrity of the monkey's sensorimotor system by using the Brinkman box task, relying on motor exploration by palpation. Both tasks were usually performed in the same behavioural session, beginning with the modified Brinkman board task and then the Brinkman box task. A comprehensive description of the latter task and its analysis method are presented in **Chapter 5**.

EEG recording of somatosensory evoked potentials

Electroencephalographic recordings (EEG)

A comprehensive description of the protocol dealing with EEG recordings in anaesthetised macaque monkeys is presented in **Chapter 1**.

Peripheral electrical stimulation

The protocol of peripheral electrical stimulation is described in **Chapters 1**, **2** and **4**.

Peripheral tactile stimulation

The protocol of peripheral tactile stimulation is described in **Chapters 3** and **4**.

EEG data analysis

The specific protocol for EEG data analysis is presented in each corresponding chapter (**Chapters 1-4**).

Lesion

When Mk-DI reached a behavioural plateau in aforementioned manual dexterity tests, a unilateral permanent cortical lesion was performed in the hand representation of left M1 by infusion of ibotenic acid in order to impair the dominant, right hand (defined according to the criteria established in Chatagny et al., 2013, see **Appendix 3**). The procedure of unilateral permanent cortical lesion by microinfusion of ibotenic acid at multiple sites within the hand representation of M1 in *awake* monkeys (having a chronic recording chamber implanted on the skull) was already reported previously (see e.g. Hamadjida et al., 2012; Kaeser et al., 2010; Kaeser et al., 2011; Liu and Rouiller, 1999; Peuser et al., 2011; Rouiller et al., 1993; Wyss et al., 2013). In these animals, the hand representation had been first mapped by using intracortical microstimulation (ICMS). In the present thesis, the lesion was performed on an *anaesthetised* monkey and without previous ICMS mapping because Mk-DI had no chronic recording chamber, in order to keep an intact skull to measure scalp EEG. Nevertheless, the very standard anatomy of the precentral gyrus allowed an easy identification of the "hand knob", corresponding to the hand representation in M1 (Hopkins et al., 2014; Yousry et al., 1997). Ibotenic acid microinfusion creates a permanent and focal excitotoxic lesion (Boegman et al., 1992; Inglis and Semba, 1997; Jarrard, 1989; Watkins and Evans, 1981; Zinkand et al., 1992).

Mk-DI was first sedated with an intramuscular (i.m.) injection of ketamine hydrochloride (Ketasol 100®, 100 mg/ml, Graeub AG, 10 mg/kg), midazolam hydrochloride (Dormicum®, 5 mg/ml, Roche Pharma SA, 0.1 mg/kg) and methadone (Methadone®, 10 mg/ml, Streuli Pharma AG, 0.2 mg/kg). The premedication also included atropine (Atropinum sulf®, 0.5 mg/ml, Sintetica SA, 0.05 mg/kg, i.m.) to reduce bronchial secretions, the analgesic carprofen (Rimadyl®, 50 mg/ml, Pfizer Animal Health, 4 mg/kg, subcutaneous (s.c.)), the antibiotics Amoxicillin/clavulanic acid (Synulox® Suspension, 140 mg/ml Amoxicillin and 35 mg/ml clavulanic acid, Pfizer Animal Health, 30 mg/kg, s.c.) and dexamethasone (Dexadreson®, 2 mg/ml, Intervet, 0.3 mg/kg, i.m.) to prevent brain oedema. The surgery itself was performed under sterile conditions. The animal was placed in ventral decubitus position on a heating blanket regulated according to the animal's rectal temperature. In addition, single-use gloves filled with warm water were placed along the monkey's sides and the animal was isolated with bubble wrap. Eye drops (Lacryvisc® SE, Alcon) were administrated to prevent exsiccation of the cornea. The intra-operative monitoring was the same as described for SSEP acquisition (see **Chapters 1** and **2**) and included in addition body temperature monitoring.

The animal was intubated and put under sevoflurane anaesthesia (Sevorane®, Abbott, 2.5%-4%, in 50% O_2 and 50% air). An intravenous (i.v.) catheter was placed in the saphenous vein to induce propofol anaesthesia (mixture of propofol 1% MCT (Fresenius Kabi AG) and Ringer lactate (1:2), 1.8 ml/kg/h) and Ringer lactate infusion (8 ml/kg/h). The monkey's head was then fixed in a stereotaxic frame (Narishige, Japan) using ear bars coated with lubricating gel (Lidohex®, Dr. G. Bichsel AG). The skin was incised along the anteroposterior axis of the head, in the midline. This zone had been locally anaesthetised with several s.c. injections of lidocaine 1% (Rapidocain® 1%, 10 mg/ml, Sintetica SA, 2 ml in total). The muscles were incised and reclined. A craniotomy (**Figure 4A**) was performed by drilling a rectangular bone flap (22 mm mediolaterally x 30 mm anteroposteriorally) over the left hemisphere (i.e. contralateral to right median nerve), whose centre was localised 15 mm rostral and 15 mm lateral from the reference point of the stereotaxic frame (half distance between both ear bars) and with an angle of 30° with respect to the mid-sagittal plane (Shimazu et al., 2004), giving access to the hand area in the left sensorimotor cortex. Then, the dura was carefully incised, giving directly access to the sensorimotor cortex (**Figure 4B**). Twenty-one microinfusions of ibotenic acid (1 mg ibotenic acid in 50 µl phosphate buffered saline, Sigma 95%) were performed in the

hand representation of M1 (1.8-2.1 µl at each site, total volume of 39.7 µl) with a 10-µl Hamilton microsyringe guided with a 3 axes micromanipulator fixed on the stereotaxic frame (**Figure 4C** and **D**). In order to target the hand representation folded into the depth of the central sulcus, microinfusions were performed at 3 different depths (2-3 mm distant from each other) along the same microsyringe penetration in sites along the rostral bank of the central sulcus. Injections were performed at sites located from 2 to 9 mm below the cortical (pial) surface, depending on their location. To compensate for the neuroprotective effect of sevoflurane and propofol anaesthesia (Adembri et al., 2007; Engelhard et al., 2003; Jain, 2011a; Jain, 2011b; Velly et al., 2003; Werner, 2009; Wu et al., 2011), a twice as concentrated solution of ibotenic acid was used as in previous monkeys in the laboratory (Hamadjida et al., 2012; Kaeser et al., 2010; Kaeser et al., 2011; Liu and Rouiller, 1999; Peuser et al., 2011; Rouiller et al., 1993; Wyss et al., 2013) and electrical stimulation was delivered continuously to the right median nerve (1.98 mA, 0.5-Hz repetition rate, 400-µs duration) to increase the excitability of the neurons. A constant small twitch of the thumb was observed during the whole procedure. After completion of the ibotenic acid microinfusions, the dura was sutured. The bone flap was then repositioned and sealed with a calcium phosphate cement converting to hydroxy-apatite (HydroSet Injectable HA Bone Substitute, Stryker®; Chow and Takagi, 2001; Dickson et al., 2002; Larsson, 2006; Van Lieshout et al., 2011) as previously reported (see Gindrat et al., 2014 in **Chapter 1**) (**Figure 4E**). The muscles and the skin were then sutured. During painful phases (e.g. bone drilling), fentanyl was delivered (Fentanyl Curamed®, 0.1 mg/ 2 ml, Actavis Switzerland AG, 0.1 µg/kg/min diluted 1:1 in saline, i.v.). Following surgery, the monkey was treated for 8 days with carprofen (Rimadyl®, 50 mg/ml, Pfizer Animal Health, 4 mg/kg/day, s.c.) and antibiotics Amoxicillin/clavulanic acid (Synulox® Suspension, 140 mg/ml Amoxicillin and 35 mg/ml clavulanic acid, Pfizer Animal Health, 30 mg/kg/day, s.c.).

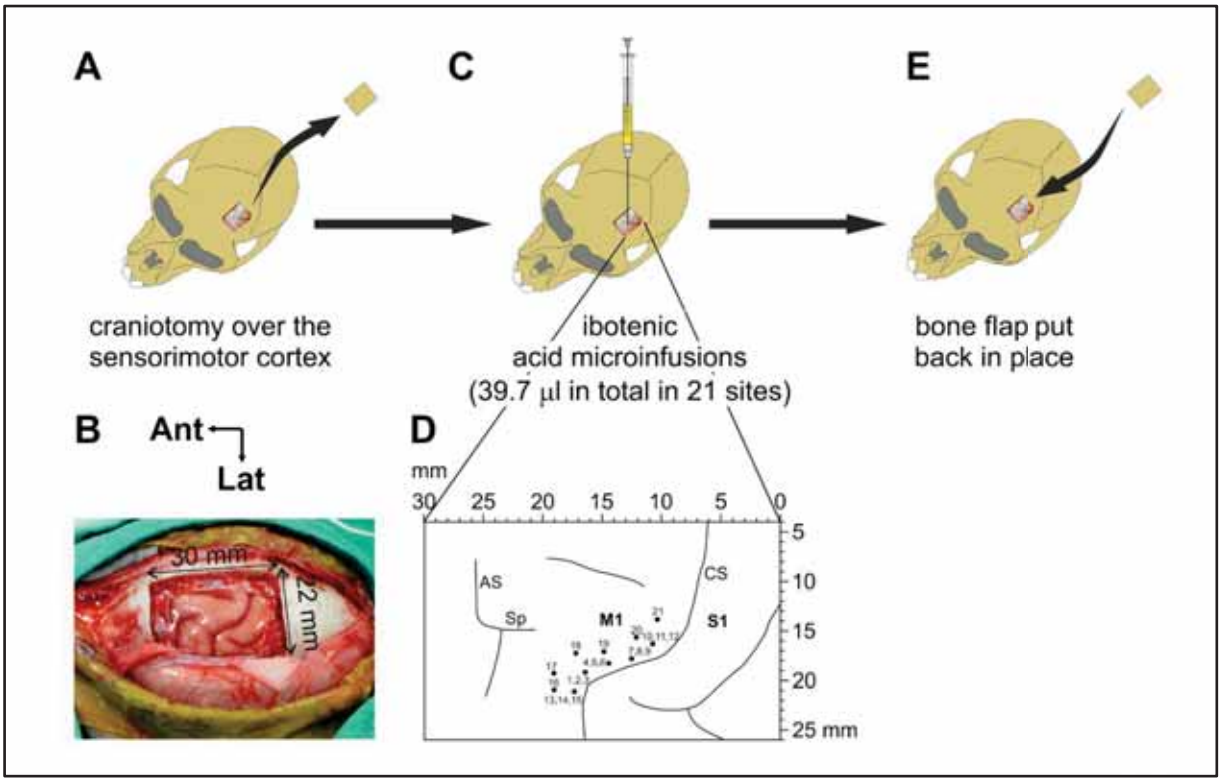

Figure 4: Overview of the M1 lesion procedure. (A) A craniotomy was performed over the left sensorimotor cortex by removing a 22-mm x 30-mm bone flap. (B) Exposed cortical surface after incision of the dura. Note the well defined "hand knob" in the precentral gyrus, corresponding to the hand representation in M1. (C) A unilateral permanent lesion targeting the hand representation in M1 was performed by microinfusion of ibotenic acid at 21 locations (D) in the precentral "hand knob". For the 5 sites along the rostral bank of the central sulcus, microinfusions were performed at 3 different depths along the same microsyringe penetration. Stereotaxic coordinates in the anteroposterior and mediolateral axes from the reference (midpoint between ear bars at the vertex with an angle of 30° with respect to the mid-sagittal plane) are given. (E) After ibotenic acid microinfusion, the dura was closed, the bone flap was put back in place and sealed by using bone cement. Finally, the muscles and skin were sutured. Ant: anterior, AS: arcuate sulcus, CS: central sulcus, Lat: lateral, Sp: spur of arcuate sulcus.

Injection of BDA neuronal tracer

Once the acquisition of the electrophysiological and behavioural data was achieved for Mk-DI, the experiment was completed with the injection of the bidirectional neuronal tracer biotinylated dextran amine (BDA; 5% BDA in saline solution; 10,000 MW (high

molecular weight) conjugated to lysine; Molecular Probes, Eugene, OR) into the distal forelimb representation in S1 in left hemisphere (i.e. ipsilateral to the lesion) (see **Chapter 2**, **Supplementary Figure 3**) by using a 10-µl Hamilton syringe. Injections were targeted at 2 cortical locations and at 2 depths each (injected volume = 4 x 1 µl), 2 and 5 mm below the dura mater to attempt to label all six layers of the gray matter. Due to the previous surgery having aimed at lesioning M1, the dura matter was strongly adhering to the brain and was consequently not reopened. Therefore, injections were performed directly through the dura matter, decreasing partially the accuracy of the injections. This surgery was performed under the same conditions as already described for the M1 lesion.

End of the experimental protocol

After a survival period of 22 days following BDA injection, Mk-DI was first anaesthetised with an i.m. injection of ketamine hydrochloride (Ketasol 100®, 100 mg/ml, Graeub AG, 1 ml), followed by an i.v. lethal dose of sodium pentobarbital (60 mg/kg body weight) and an injection of heparin (Heparin-Natrium, 5000 IE/ml, B. Braun Medical AG, 1 ml) in the left ventricle. A transcardiac perfusion with 0.9% saline (400-500 ml) was performed, followed by a perfusion with fixative (4 ℓ of 4% phosphate-buffered paraformaldehyde in 0.1 M phosphate buffer, pH 7.6) and 3 subsequent solutions of the same fixative in increasing concentrations of sucrose (10%, 20% and 30%; 2 ℓ each). After decapitation, the brain was removed, dissected and then stored for 1 week in a 30% sucrose solution (in phosphate buffer) for cryoprotection. Eight series of frozen sections were then performed in the frontal plane at a 50-µm thickness (400 µm between two successive sections of the same series) by using a freezing cryotome (HM560, MICROM, Volketswil, Switzerland). Until further use, the obtained brain slices were stored at -20°C in a cryoprotective phosphate buffer solution (50 mM, pH 7.4) containing 25% glycerol (G7893, Sigma Aldrich, St. Louis, MO, USA) and 30% ethylene glycol (33068, Ridel-de-Haën, Seelze, Germany).

Histology

Three brain series were then prepared for Nissl staining, SMI-32 staining and BDA histochemistry, respectively, as follows below (for greater detail, see e.g. Beaud et al., 2008; Liu et al., 2002; Wannier et al., 2005). In a later step, a selected rostrocaudal portion of the brain comprising M1 and S1 was processed using 2 series of sections, to reveal cytochrome oxidase (C.O.) and myelin, respectively, using previously published protocols.

Nissl staining

The Nissl bodies, Nissl granules, tigroid bodies or Nissl substance refer to the basophilic (due to ribosomal RNA) aggregations of rough endoplasmic reticulum (RER or ergastoplasm) (Bancroft and Gamble, 2008; Kiernan, 2010). These structures were named after Franz Nissl. This German neuropsychiatrist (1860-1919) developed the so-called Nissl staining method that revealed the Nissl bodies as darkly stained granules in the neuronal perikaria in brain sections stained with cationic dyes such as methylene blue or cresyl violet. Based on the perikarion localisation of the RER, the Nissl technique preferentially stains the soma and to some extent the axonal hillock of neurons (Bancroft and Gamble, 2008; Garman, 2011). The Nissl staining method allows to identify the different layers constituting the gray matter in the nervous system as the amount, distribution and size of the Nissl bodies vary according to the cell types. Moreover, in case of degenerating neurons, for example after a lesion, ribosomes separate from RER, resulting in very badly labelled neurons with the Nissl technique given that it is based on RER staining (Garman, 2011).

In Mk-DI, every eighth section (50 µm, i.e. at 400-µm interval), corresponding to a first section series, was histologically prepared to stain the Nissl substance with cresyl violet. Brain tissue was first treated to remove fat residuals by incubating for 1 hour in 1:1 chloroform-alcohol 100%, then in alcohol 100% twice for 3 min each time, and finally 3 min in alcohol 95%. At the end, sections were dried at 37°C. Then, sections were incubated subsequently in alcohol 70% for 2 min, in alcohol 50% for 1 min and in distilled H_2O for 30 s. Staining was performed by incubating sections at 40°C in 0.5% cresyl violet (diluted in distilled H_2O, natrium acetate and acetic acid) for 2 to 7 min. Sections were then rinsed twice to three times for 1 min 30 s in distilled H_2O, and incubated subse-

quently in alcohol 70% for 3 min, in alcohol 80%-acetic acid for 6 min, in alcohol 95% for 1 min, twice in alcohol 100% for 1 min each time, in butanol for 5 to 45 min, and finally twice in xylol for 5 min each time. At the end, sections were mounted on slides by using Eukit.

SMI staining

The SMI-32 monoclonal antibody recognises a non-phosphorylated epitope of neurofilaments H (Sternberger and Sternberger, 1983). The SMI-32 immunoreactivity highlights the cell bodies, the dendrites and some thick axons of some pyramidal neurons in the neocortex (Campbell and Morrison, 1989).

For Mk-DI, every eighth section was histologically prepared for SMI-32 staining. Free-floating sections were first rinsed several times in phosphate-buffered saline solution (PBS, 0.1 M, pH 7.2) and then incubated for 10 min in 1.5% H_2O_2 (750 µl 30% H_2O_2 in 50 ml PBS) to remove the endogenous peroxidase activity. Sections were rinsed twice in PBS for 10 min each time and then incubated overnight at room temperature in SMI-32P mouse monoclonal antibody (anti-Neurofilament H Non-Phosphorylated, BioLegend, by LubioScience GmbH, Luzern, Switzerland) diluted 1:3000 in 2% normal horse serum and PBS-T (0.1 M, pH 7.2, Triton 0.2%). The following day, the tissue was washed three times in PBS for 10 min each time, then incubated for 30 min at room temperature in 0.5% biotinylated anti-mouse secondary antibody (BA-2000, Vector Laboratories, Inc., Burlingame, CA), 2% horse serum and PBS, and rinsed again three times in PBS for 10 min each time. The avidin-biotin complex (ABC) reaction was subsequently performed by using the ABC immunoperoxidase method (VECTASTAIN ABC Kit, peroxidase standard PK 4000, Vector Laboratories, Inc.): sections were incubated at room temperature in 1% ABC solution (400 µl A and 400 µl B in 40 ml PBS-T) and then firstly rinsed twice in PBS for 10 min each time and secondly once in Tris-HCl buffer (pH 7.7). Finally, the visualising reaction with diaminobenzidine (DAB, 3,3-diaminobenzidine tetrahydrochloride) as a chromogen was performed with 0.05% DAB diluted with 0.05% Tris-HCl buffer (pH 7.7) and H_2O_2 (0.03%). Brain sections were finally washed twice in Tris-HCl buffer (pH 7.7), then twice in PBS, and immediately mounted on gelatin-coated slides, dehydrated and coverslipped.

BDA histochemistry

Within the injection site, the neuronal tracer biotinylated dextran amine (BDA) is taken up by the neuronal cell bodies and is then transported anterogradely to label the axon fibres, the collaterals and the synaptic boutons (terminal fields and *boutons en passant*) (Brandt and Apkarian, 1992; Morecraft et al., 2014). Moreover, low molecular weight BDA can also be retrogradely taken up at the injection site, resulting in retrogradely labelled fibres and cell bodies. Nevertheless, for high molecular weight BDA, such as in our study (i.e. 10,000 MW), anterograde labelling is much more effective than retrograde labelling (Negyessy et al., 2013; Rockland and Knutson, 2000).

A third series of sections was histologically prepared to study the anterograde and retrograde distributions of BDA after injection in S1. Processing was performed using a VECTASTAIN ABC Kit (peroxidase standard PK 4000, Vector Laboratories, Inc.). After sectioning, the free-floating sections were collected into PBS (pH 7.4, 0.1 M). The tissue was then washed three times in PBS-T (phosphate buffer 0.01M pH 7.4, NaCl 0.9%, Triton 0.3%) for 10 min each. Then the ABC reaction was performed: sections were overnighted at room temperature in a solution of 10 ml PBS-T, 2 drops of A and 2 drops of B. The following day, the tissue was rinsed three times in PBS (without Triton) and then a DAB reaction was performed to reveal BDA: sections were incubated in a DAB solution (20 ml PBS 0.1 M pH 7.4, 10 mg DAB, 660 µl H_2O_2 0.3%) for around 20 min or until the background came up. The tissue was then rinsed three times in PBS (0.1 M pH 7.4). Finally, the sections were mounted on subbed slides and dried overnight, before being coverslipped the day after.

Cytochrome oxidase staining

The cytochrome oxidases (C.O.) are energy-deriving mitochondrial enzymes responsible for electron transport and oxidative phosphorylation, ultimately producing ATP (adenosine triphosphate) (Voet and Voet, 2004). ATP is linked to vital processes, meaning that the brain is highly dependent of these reactions due to its high metabolic needs (Herculano-Houzel, 2011). Briefly, the C.O. is sensitive to changes in neuronal activity. Accordingly, histochemical analyses of brain tissue revealed variable levels of C.O. activity from one region of the brain to another (Carroll and Wong-Riley, 1984; Matelli et al.,

1985; Wong-Riley, 1979; Wong-Riley and Carroll, 1984), demonstrating that this enzyme could be used as a functional and anatomical marker.

A selected rostrocaudal portion of a fourth series of MK-DI's brain sections, comprising M1 and S1, was incubated for C.O. activity by using the method described by Wong-Riley (Carroll and Wong-Riley, 1984; Wong-Riley, 1979). To this end, sections were rinsed in 0.1 M phosphate buffer for 5 minutes, then in 10% sucrose-phosphate buffer for 5 min and finally in 20% sucrose-phosphate buffer for 5 min. Next, sections were incubated for 4 hours at room temperature in a solution of 0.1 M phosphate buffer containing 4% sucrose, 50 mg of DAB and 0.04% cytochrome c from horse heart (Sigma n° C2506) per 100 ml of buffer. Catalase (about 10 mg/100ml, Sigma n° C40 (500mg)) was used to eliminate the presence of any endogenous H_20_2 but no detectable difference was noted with sections processed without catalase. The staining reaction was stopped by washing sections three times for 5 min each time in 0.1 M phosphate buffer. Sections were finally mounted, dehydrated in a series of graded alcohols, defatted in xylenes before being coverslipped.

Myelin staining

The myelin sheath is formed by compacted superimposed layers of neuroglial membranes (oligodendrocytes in the CNS and Schwann cells in the PNS) surrounding axons and constituting axonal insulator to improve the conduction of action potentials by saltatory conduction (Greenstein and Greenstein, 2000; Huxley and Stämpfli, 1949; Rushton, 1951; Tasaki, 1939). A myelin staining is therefore a marker for the white matter in the nervous system. The different techniques of myelin staining are based on the myelin composition rich in phospholipids and basic proteins essential for proper neuronal function (Bancroft and Gamble, 2008; Savaskan et al., 2009). Interestingly, in case of neuronal degeneration or axonal damage, the myelin sheath degenerates as well, meaning that myelin staining can be used as an anatomical marker of lesion (Kiernan, 2010).

A portion of a fifth series of MK-DI's brain sections, comprising M1 and S1, was histologically prepared to stain myelin (protocol generously provided by Dr Loïc Chareyron and Prof. Pierre Lavenex, improved from Quinn and Graybiel, 1994) in order to assess if the

cortical lesion affected white matter as well. To this end, free-floating sections were first rinsed three times for 10 min each in a solution of PBS (0.02 M) with 0.6% NaCl (pH 7.2-7.4; 100 ml PO_4 0.1 M + 400 ml H_2O + 3 g NaCl) and then incubated with rotation for 1 hour in a gold chloride solution (0.2% $HAuCl_4 \cdot 3H_2O$, 0.012% H_2O_2 in 0.6% NaCl-PBS solution) at room temperature. The development was stopped by rinsing the sections with normal saline (NaCl 0.9%) for 10 min and brain tissue was then fixed with 5% sodium thiosulphate for 5 min. Sections were then rinsed three times for 10 min each in PBS, mounted in PO_4 (0.02 M) and dried for 3-4 hours in a 37°C oven. Then, sections were hydrated in a descending series of ethanol solutions (from 100% to 50% in 5 successive baths, for 2 min each), followed by several dips in distilled water. Counterstaining was then performed with 0.25% thionin (Fisher Scientific, Waltham, MA; catalog n° T-409) for 4 s followed again by several dips in distilled water. Sections were then dehydrated in an ascending series of ethanol solutions (from 50% to 100% in 5 successive baths, for 4 min each), with the adjunction of 7 drops of acetic acid (1 min) in 95% ethanol between the 2nd and 3rd ethanol baths to differentiate the sections. Sections on glass slides were imbibed with xylene and coverslipped by using mountant DPX (BDH Laboratories Supplies, Poole, UK).

References

Adembri, C., Venturi, L., Pellegrini-Giampietro, D.E., 2007. Neuroprotective effects of propofol in acute cerebral injury. CNS.Drug Rev 13, 333-351.

Bancroft, J.D., Gamble, M., 2008. Theory and Practice of Histological Techniques. Churchill Livingstone.

Beaud, M.L., Schmidlin, E., Wannier, T., Freund, P., Bloch, J., Mir, A., Schwab, M.E., Rouiller, E.M., 2008. Anti-Nogo-A antibody treatment does not prevent cell body shrinkage in the motor cortex in adult monkeys subjected to unilateral cervical cord lesion. BMC.Neurosci. 9, 5.

Boegman, R.J., Cockhill, J., Jhamandas, K., Beninger, R.J., 1992. Excitotoxic lesions of rat basal forebrain: Differential effects on choline acetyltransferase in the cortex and amygdala. Neuroscience 51, 129-135.

Brandt, H.M., Apkarian, A.V., 1992. Biotin-dextran: a sensitive anterograde tracer for neuroanatomic studies in rat and monkey. J.Neurosci.Methods 45, 35-40.

Brinkman, J., Kuypers, H.G., 1973. Cerebral control of contralateral and ipsilateral arm, hand and finger movements in the split-brain rhesus monkey. Brain 96, 653-674.

Campbell, M.J., Morrison, J.H., 1989. Monoclonal antibody to neurofilament protein (SMI-32) labels a subpopulation of pyramidal neurons in the human and monkey neocortex. J.Comp Neurol. 282, 191-205.

Carroll, E.W., Wong-Riley, M.T.T., 1984. Quantitative light and electron microscopic analysis of cytochrome oxidase-rich zones in the striate cortex of the squirrel monkey. The Journal of Comparative Neurology 222, 1-17.

Chatagny, P., Badoud, S., Kaeser, M., Gindrat, A.D., Savidan, J., Fregosi, M., Moret, V., Roulin, C., Schmidlin, E., Rouiller, E.M., 2013. Distinction between hand dominance and hand preference in primates: a behavioral investigation of manual dexterity in nonhuman primates (macaques) and human subjects. Brain and Behavior 3, 575-595.

Chow, L.C., Takagi, S., 2001. A natural bone cement - A laboratory novelty led to the development of revolutionary new biomaterials. Journal of Research of the National Institute of Standards and Technology 106, 1029-1033.

Committee for the Update of the Guide for the Care and Use of Laboratory Animals, National Research Council, 2011. Guide for the Care and Use of Laboratory Animals, Eighth ed. The National Academies Press.

Dickson, K.F., Friedman, J., Buchholz, J.G., Flandry, F.D., 2002. The use of BoneSource hydroxyapatite cement for traumatic metaphyseal bone void filling. J.Trauma 53, 1103-1108.

Engelhard, K., Werner, C., Hoffman, W.E., Matthes, B., Blobner, M., Kochs, E., 2003. The Effect of Sevoflurane and Propofol on Cerebral Neurotransmitter Concentrations During Cerebral Ischemia in Rats. Anesthesia & Analgesia 97.

Garman, R.H., 2011. Histology of the central nervous system. Toxicol.Pathol. 39, 22-35.

Gindrat, A.D., Quairiaux, C., Britz, J., Brunet, D., Lanz, F., Michel, C.M., Rouiller, E.M., 2014. Whole-scalp EEG mapping of somatosensory evoked potentials in macaque monkeys. Brain Struct.Funct., 1-22.

Greenstein, B., Greenstein, A., 2000. Color Atlas of Neuroscience: Neuroanatomy and Neurophysiology. Thieme.

Hamadjida, A., Wyss, A.F., Mir, A., Schwab, M.E., Belhaj-Saïf, A., Rouiller, E.M., 2012. Influence of anti-Nogo-A antibody treatment on the reorganization of callosal connectivity of the premotor cortical areas following unilateral lesion of primary motor cortex (M1) in adult macaque monkeys. Exp.Brain Res. 223, 321-340.

Herculano-Houzel, S., 2011. Scaling of brain metabolism with a fixed energy budget per neuron: implications for neuronal activity, plasticity and evolution. PLoS One 6, e17514.

Hoogewoud, F., Hamadjida, A., Wyss, A.F., Mir, A., Schwab, M.E., Belhaj-Saïf, A., Rouiller, E.M., 2013. Comparison of functional recovery of manual dexterity after unilateral spinal cord lesion or motor cortex lesion in adult macaque monkeys. Front Neurol. 4, 101.

Hopkins, W.D., Meguerditchian, A., Coulon, O., Bogart, S., Mangin, J.F., Sherwood, C.C., Grabowski, M.W., Bennett, A.J., Pierre, P.J., Fears, S., Woods, R., Hof, P.R., Vauclair, J., 2014. Evolution of the central sulcus morphology in primates. Brain Behav.Evol. 84, 19-30.

Huxley, A.F., Stämpfli, R., 1949. Evidence for saltatory conduction in peripheral myelinated nerve fibres. J Physiol 108, 315-339.

Inglis, W.L., Semba, K., 1997. Discriminable excitotoxic effects of ibotenic acid, AMPA, NMDA and quinolinic acid in the rat laterodorsal tegmental nucleus. Brain Res 755, 17-27.

Jain, K.K., 2011a. Neuroprotection During Anesthesia and Surgery., The Handbook of Neuroprotection. Humana Press, pp. 509-528.

Jain, K.K., 2011b. Neuroprotective Agents., The Handbook of Neuroprotection. Humana Press, pp. 25-139.

Jarrard, L.E., 1989. On the use of ibotenic acid to lesion selectively different components of the hippocampal formation. Journal of Neuroscience Methods 29, 251-259.

Kaeser, M., 2010. Transplantation of autologous adult brain progenitor cells in a non-human primate model of motor cortex lesion. Doctoral thesis. University of Fribourg, Imprimerie Saint-Paul.

Kaeser, M., Brunet, J.F., Wyss, A., Belhaj-Saïf, A., Liu, Y., Hamadjida, A., Rouiller, E.M., Bloch, J., 2011. Autologous adult cortical cell transplantation enhances functional recovery following unilateral lesion of motor cortex in primates: a pilot study. Neurosurgery 68, 1405-1416.

Kaeser, M., Wyss, A.F., Bashir, S., Hamadjida, A., Liu, Y., Bloch, J., Brunet, J.F., Belhaj-Saïf, A., Rouiller, E.M., 2010. Effects of unilateral motor cortex lesion on ipsilesional hand's reach and grasp performance in monkeys: relationship with recovery in the contralesional hand. J Neurophysiol 103, 1630-1645.

Kiernan, J.A., 2010. Staining Sections of the Central Nervous System. In: Kumar, G.L., Kiernan, J.A. (Eds.), Special Stains and H & E, Second Edition. Dako, pp. 67-74.

Larsson, S., 2006. Injectable Phosphate Cements – A Review., Uppsala, Sweden, pp. 1-12.

Liu, J., Morel, A., Wannier, T., Rouiller, E.M., 2002. Origins of callosal projections to the supplementary motor area (SMA): a direct comparison between pre-SMA and SMA-proper in macaque monkeys. J Comp Neurol. 443, 71-85.

Liu, Y., Rouiller, E.M., 1999. Mechanisms of recovery of dexterity following unilateral lesion of the sensorimotor cortex in adult monkeys. Exp.Brain Res. 128, 149-159.

Matelli, M., Luppino, G., Rizzolatti, G., 1985. Patterns of cytochrome oxidase activity in the frontal agranular cortex of the macaque monkey. Behavioural Brain Research 18, 125-136.

Morecraft, R.J., Ugolini, G., Lanciego, J.L., Wouterlood, F.G., Pandya, D.N., 2014. Classic and Contemporary Neural Tract-Tracing Techniques. In: Johansen-Berg, H., Behrens, T.E.J. (Eds.), Diffusion MRI (Second Edition). Academic Press, San Diego, pp. 359-399.

Napier, J.R., 1956. The prehensile movements of the human hand. J Bone Joint Surg.Br 38-B, 902-913.

Negyessy, L., Palfi, E., Ashaber, M., Palmer, C., Jakli, B., Friedman, R.M., Chen, L.M., Roe, A.W., 2013. Intrinsic horizontal connections process global tactile features in the primary somatosensory cortex: neuroanatomical evidence. J.Comp Neurol. 521, 2798-2817.

Peuser, J., Belhaj-Saïf, A., Hamadjida, A., Schmidlin, E., Gindrat, A.D., Volker, A.C., Zakharov, P., Hoogewoud, H.M., Rouiller, E.M., Scheffold, F., 2011. Follow-up of cortical activity and structure after lesion with laser speckle imaging and magnetic resonance imaging in nonhuman primates. J Biomed.Opt. 16, 096011-1-096011-11.

Quinn, B., Graybiel, A.M., 1994. Myeloarchitectonics of the Primate Caudate-Putamen. In: Percheron, G., McKenzie, J.S., Féger, J. (Eds.), The Basal Ganglia IV, New Ideas and Data on Structure and Function. Springer US, pp. 35-41.

Rockland, K.S., Knutson, T., 2000. Feedback connections from area MT of the squirrel monkey to areas V1 and V2. J.Comp Neurol. 425, 345-368.

Rouiller, E.M., Moret, V., Liang, F., 1993. Comparison of the connectional properties of the two forelimb areas of the rat sensorimotor cortex: support for the presence of a premotor or supplementary motor cortical area. Somatosens.Mot.Res. 10, 269-289.

Rouiller, E.M., Yu, X.H., Moret, V., Tempini, A., Wiesendanger, M., Liang, F., 1998. Dexterity in adult monkeys following early lesion of the motor cortical hand area: the role of cortex adjacent to the lesion. Eur.J.Neurosci. 10, 729-740.

Rushton, W.A.H., 1951. A theory of the effects of fibre size in medullated nerve. The Journal of physiology 115, 101-122.

Savaskan, N.E., Weinmann, O., Heimrich, B., Eyupoglu, I.Y., 2009. High resolution neurochemical gold staining method for myelin in peripheral and central nervous system at the light- and electron-microscopic level. Cell Tissue Res 337, 213-221.

Schmidlin, E., Kaeser, M., Gindrat, A.D., Savidan, J., Chatagny, P., Badoud, S., Hamadjida, A., Beaud, M.L., Wannier, T., Belhaj-Saïf, A., Rouiller, E.M., 2011. Behavioral assessment of manual dexterity in non-human primates. J.Vis.Exp., e3258.

Schmidlin, E., Wannier, T., Bloch, J., Belhaj-Saïf, A., Wyss, A.F., Rouiller, E.M., 2005. Reduction of the hand representation in the ipsilateral primary motor cortex

following unilateral section of the corticospinal tract at cervical level in monkeys. BMC.Neurosci. 6, 56.

Shimazu, H., Maier, M.A., Cerri, G., Kirkwood, P.A., Lemon, R.N., 2004. Macaque ventral premotor cortex exerts powerful facilitation of motor cortex outputs to upper limb motoneurons. J Neurosci. 24, 1200-1211.

Sternberger, L.A., Sternberger, N.H., 1983. Monoclonal antibodies distinguish phosphorylated and nonphosphorylated forms of neurofilaments in situ. Proc.Natl.Acad.Sci.USA 80, 6126-6130.

Tasaki, I., 1939. The electro-saltatory transmission of the nerve impulse and the effect of narcosis upon the nerve fiber. American Journal of Physiology 127, 211-227.

Van Lieshout, E.M., Van Kralingen, G.H., El-Massoudi, Y., Weinans, H., Patka, P., 2011. Microstructure and biomechanical characteristics of bone substitutes for trauma and orthopaedic surgery. BMC.Musculoskelet.Disord. 12, 34.

Velly, L.J., Guillet, B.A., Masmejean, F.M., Nieoullon, A.L., Bruder, N.J., Gouin, F.M., Pisano, P.M., 2003. Neuroprotective effects of propofol in a model of ischemic cortical cell cultures: role of glutamate and its transporters. Anesthesiology 99, 368-375.

Voet, D., Voet, J.G., 2004. Biochemistry, 3rd ed. John Wiley and Sons, New York.

Wannier, T., Schmidlin, E., Bloch, J., Rouiller, E.M., 2005. A unilateral section of the corticospinal tract at cervical level in primate does not lead to measurable cell loss in motor cortex. Journal of Neurotrauma 22, 703-717.

Watkins, J.C., Evans, R.H., 1981. Excitatory amino acid transmitters. Annu.Rev.Pharmacol.Toxicol. 21, 165-204.

Werner, C., 2009. Anesthetic drugs and sustained neuroprotection in acute cerebral ischemia: can we alter clinical outcomes? Can J Anaesth 56, 883-888.

Wong-Riley, M., 1979. Changes in the visual system of monocularly sutured or enucleated cats demonstrable with cytochrome oxidase histochemistry. Brain Research 171, 11-28.

Wong-Riley, M.T.T., Carroll, E.W., 1984. Quantitative light and electron microscopic analysis of cytochrome oxidase-rich zones in V II prestriate cortex of the squirrel monkey. The Journal of Comparative Neurology 222, 18-37.

Wu, G.J., Chen, W.F., Hung, H.C., Jean, Y.H., Sung, C.S., Chakraborty, C., Lee, H.P., Chen, N.F., Wen, Z.H., 2011. Effects of propofol on proliferation and anti-apoptosis of neuroblastoma SH-SY5Y cell line: new insights into neuroprotection. Brain Research 1384, 42-50.

Wyss, A.F., Hamadjida, A., Savidan, J., Liu, Y., Bashir, S., Mir, A., Schwab, M.E., Rouiller, E.M., Belhaj-Saïf, A., 2013. Long-term motor cortical map changes following unilateral

lesion of the hand representation in the motor cortex in macaque monkeys showing functional recovery of hand functions. Restor.Neurol Neurosci. 31, 733-760.

Yousry, T.A., Schmid, U.D., Alkadhi, H., Schmidt, D., Peraud, A., Buettner, A., Winkler, P., 1997. Localization of the motor hand area to a knob on the precentral gyrus. A new landmark. Brain 120 (Pt 1), 141-157.

Zinkand, W.C., Moore, W.C., Thompson, C., Salama, A., Patel, J., 1992. Ibotenic acid mediates neurotoxicity and phosphoinositide hydrolysis by independent receptor mechanisms. Molecular and Chemical Neuropathology 16, 1-10.

CHAPTER 1

Whole-scalp EEG mapping of somatosensory evoked potentials in macaque monkeys

Gindrat AD*, Quairiaux C*, Britz J, Brunet D, Lanz F, Michel CM, Rouiller EM (2014). Brain Structure and Function 1-22. DOI: 10.1007/s00429-014-0776-y

* Equal first authorship

Brain Struct Funct
DOI 10.1007/s00429-014-0776-y

ORIGINAL ARTICLE

Whole-scalp EEG mapping of somatosensory evoked potentials in macaque monkeys

Anne-Dominique Gindrat · Charles Quairiaux · Juliane Britz · Denis Brunet · Florian Lanz · Christoph M. Michel · Eric M. Rouiller

Received: 17 December 2013 / Accepted: 7 April 2014

Abstract High-density scalp EEG recordings are widely used to study whole-brain neuronal networks in humans non-invasively. Here, we validate EEG mapping of somatosensory evoked potentials (SSEPs) in macaque monkeys (*Macaca fascicularis*) for the long-term investigation of large-scale neuronal networks and their reorganisation after lesions requiring a craniotomy. SSEPs were acquired from 33 scalp electrodes in five adult anaesthetized animals after electrical median or tibial nerve stimulation. SSEP scalp potential maps were identified by cluster analysis and identified in individual recordings. A distributed, linear inverse solution was used to estimate the intracortical sources of the scalp potentials. SSEPs were characterised by a sequence of components with unique scalp topographies. Source analysis confirmed that median nerve SSEP component maps were in accordance with the somatotopic organisation of the sensorimotor cortex. Most importantly, SSEP recordings were stable both intra- and inter-individually. We aim to apply this method to the study of recovery and reorganisation of large-scale neuronal networks following a focal cortical lesion requiring a craniotomy. As a prerequisite, the present study demonstrated that a 300-mm^2 unilateral craniotomy over the sensorimotor cortex necessary to induce a cortical lesion, followed by bone flap repositioning, suture and gap plugging with calcium phosphate cement, did not induce major distortions of the SSEPs. In conclusion, SSEPs can be successfully and reproducibly recorded from

A.-D. Gindrat and C. Quairiaux equal first authorship.
C. M. Michel and E. M. Rouiller equal senior authorship.

Electronic supplementary material The online version of this article (doi:10.1007/s00429-014-0776-y) contains supplementary material, which is available to authorized users.

A.-D. Gindrat (✉) · F. Lanz · E. M. Rouiller
Domain of Physiology, Department of Medicine, Faculty of Sciences and Fribourg Center for Cognition, University of Fribourg, Chemin du Musée 5, 1700 Fribourg, Switzerland
e-mail: anne-dominique.gindrat@unifr.ch

F. Lanz
e-mail: florian.lanz@unifr.ch

E. M. Rouiller
e-mail: eric.rouiller@unifr.ch

C. Quairiaux
Department of Fundamental Neurosciences, Faculty of Medicine, University of Geneva, Rue Michel-Servet 1, 1206 Geneva, Switzerland
e-mail: Charles.Quairiaux@unige.ch

C. Quairiaux · J. Britz · D. Brunet · C. M. Michel
Functional Brain Mapping Laboratory, Departments of Clinical and Fundamental Neurosciences, University Medical School, Rue Michel-Servet 1, 1206 Geneva, Switzerland
e-mail: Juliane.Britz@unige.ch

D. Brunet
e-mail: Denis.Brunet@unige.ch

C. M. Michel
e-mail: Christoph.Michel@unige.ch

J. Britz · D. Brunet · C. M. Michel
EEG Brain Mapping Core, Center for Biomedical Imaging (CIBM), University Hospital and University of Geneva, 1211 Geneva, Switzerland

Published online: 04 May 2014

high-density EEG caps in macaque monkeys before and after a craniotomy, opening new possibilities for the long-term follow-up of the cortical reorganisation of large-scale networks in macaque monkeys after a cortical lesion.

Keywords Craniotomy · Electrical neuroimaging · High-density EEG · LORETA inverse solution · Non-human primate · Sensorimotor cortex

Abbreviations

CD	Current density
EEG	Electroencephalography
EPs	Evoked potentials
GA	Grand average
GEV	Global explained variance
GFP	Global field power
ICMS	Intracortical microstimulation
im	Intramuscular
iv	Intravenous
LORETA	Low-resolution electromagnetic tomography
LSI	Laser speckle imaging
M1	Primary motor cortex
MRI	Magnetic resonance imaging
S1	Primary somatosensory cortex
SC	Spatial correlation
sc	Subcutaneous
SD	Standard deviation
SE	Standard error
SSEPs	Somatosensory evoked potentials

Introduction

Cortical plasticity promotes some functional recovery by allowing reorganisation of neuronal connections after a brain insult (e.g. Bütefisch 2004; Nudo 2006, 2007; Pascual-Leone et al. 2005). Different approaches such as intracortical microstimulation (ICMS) (Eisner-Janowicz et al. 2008; Liu and Rouiller 1999; Nudo and Milliken 1996; Rouiller et al. 1998; Rouiller and Olivier 2004; Wyss et al. 2013), laser speckle imaging (LSI) (Peuser et al. 2011) or magnetic resonance imaging (MRI) (Peuser et al. 2011) have been used to study cortical reorganisation accompanying functional recovery of manual dexterity after a motor cortex lesion in non-human primates. However, these techniques have major limitations: MRI has a great cost and a limited temporal resolution preventing time-sensitive assessment of the brain activity whereas ICMS and LSI are invasive methods limiting repetitive and long-term follow-up of functional reorganisation and their limited spatial coverage does not allow to investigate large-scale, whole-brain network recovery. In contrast, electroencephalographic (EEG) recordings of evoked potentials (EPs) are non-invasive, easy to use and to repeat, and offer high temporal resolution. The poor spatial resolution of conventional EEG techniques can be compensated using high-density scalp recordings and mapping analysis tools that render EEG a true brain mapping technique, i.e. providing spatiotemporal information on normal and pathologic brain functions (Jurcak et al. 2007; Michel and Murray 2012; Nunez 1993), as reported in humans (e.g. Hardmeier et al. 2013; Lascano et al. 2009, 2010; Lopez et al. 2011; Toepel et al. 2012; van de Wassenberg et al. 2008a, b, 2009) and in rodents (Megevand et al. 2008; Quairiaux et al. 2010). However, these tools have not yet been systematically used in monkeys. EEG recordings in monkeys were classically restricted to invasive electrocorticography or epidural recordings over a limited brain area (Allison et al. 1991a, b; Allison and Hume 1981; Arezzo et al. 1979, 1981; Chao et al. 2010; McCarthy et al. 1991) or were performed with surface electrodes along the stimulated afferent pathway (Hernandez-Godinez et al. 2011 (4 electrodes in *Macaca mulatta*)), on the skull (Reinhart et al. 2012 (14 electrodes in *Macaca radiata*); Tamura et al. 2013 (2 electrodes in *Macaca fuscata*)) or at the scalp with poor spatial resolution (Ferrari et al. 2012 (6 electrodes in newborn *M. mulatta*); Shimazu et al. 2000 (5 electrodes in *M. fuscata*); Ueno et al. 2008 (5 electrodes in *Pan troglodytes*)). To the best of our knowledge, only two studies involving whole-brain EEG recordings in monkeys have been reported, focusing on electrical source imaging of brainstem auditory evoked potentials (Fontanarosa et al. 2004, 32 electrodes in *M. mulatta*) and auditory event-related potentials (Gil-da-Costa et al. 2013, 22 electrodes in *M. mulatta*).

Motor areas and somatosensory areas are densely interconnected in primates and participate together to the motor control, forming the functional sensorimotor system (e.g. Huffman and Krubitzer 2001; Kaas 2004; Krakauer and Ghez 2000; Krubitzer and Disbrow 2005; Krubitzer and Kaas 1990; Shinoura et al. 2005; Stepniewska et al. 1993). The primary somatosensory cortex (S1) sends corticocortical inputs to the primary motor cortex (M1) (Ghosh and Porter 1988; Huerta and Pons 1990; Sloper 1973) and somatosensory corticospinal projections (Lemon 2008; Seo and Jang 2013), contributing to the control of voluntary movements (Murray and Keller 2011). After a lesion in caudal M1 in monkeys, the somatosensory system is affected in parallel with the motor control itself (Friel et al. 2005; Nudo et al. 2000) and in the same line, following a stroke, an increase of activity in S1 is associated with a better motor recovery in humans (Laible et al. 2012). It is therefore expected that, after a lesion in M1, S1 functions will also be affected in parallel with the motor control itself. Our long-term goal is to show that after a permanent lesion of the motor cortex, a rearrangement of

connections, including also areas remote from the lesion, can be monitored at repetitive time points during the functional recovery using high-density EEG recordings of somatosensory evoked potentials (SSEPs).

To validate our approach of whole-scalp EEG mapping of SSEPs in macaque monkeys, a prerequisite is to demonstrate the intraindividual stability and interindividual reproducibility of SSEP signals. The present study intends therefore to demonstrate that SSEPs can be successfully and reproducibly recorded with good temporal and spatial resolution from a high-density EEG cap covering the entire skull in anaesthetized macaque monkeys. To this aim, we developed customised EEG caps with 33 channels for macaque monkeys. Median and tibial nerve SSEP recordings were regularly performed in five macaque monkeys to obtain stable baseline data. We assessed the intraindividual stability and interindividual reproducibility of the SSEPs with classical component analyses as well as topographical analysis tools as used in human studies. Furthermore, we evaluated for the first time the ability of SSEP source imaging to provide spatial information on brain somatosensory processing in macaque monkeys.

The experimental brain lesion of the motor cortex used in our non-human primate model requires a craniotomy (see e.g. Hamadjida et al. 2012; Kaeser et al. 2010, 2011; Liu and Rouiller 1999; Wyss et al. 2013). It is well-known from the literature that an opening in the skull may produce a strong distortion in the pattern of electrical fields recorded at the scalp due to a leakage of current through this hole and the surrounding skull (Brigo et al. 2011; Cobb et al. 1979; Cobb and Sears 1960; van Doorn and Cherian 2008). Therefore, the second goal of this study was to assess whether a craniotomy followed by bone flap replacement, suture and use of calcium phosphate cement to fill the gaps around the flap, would distort the SSEPs recorded from the scalp after surgery as compared to before surgery. This evaluation also has important implications for human EEG studies investigating recordings before and after surgery, e.g. in epileptic patients that are not seizure free after a surgery intended to remove the epileptic foci (see e.g. Jung et al. 2013; Moosa et al. 2013; Roulet-Perez et al. 2010; Sheybani et al. 2012; Simasathien et al. 2013).

Materials and methods

Macaque monkeys

Experiments were conducted on five adult macaque monkeys (*M. fascicularis*): three males (Mk-BB, Mk-DG, Mk-EN) and two females (Mk-AT, Mk-DI). Their age/weight ranges were 6 years/5.5 kg (Mk-BB), 9 years/8.5 kg (Mk-DG), 7–8 years/7.7–8.3 kg (Mk-EN), 7 years/3.3 kg (Mk-AT) and 8 years/3.4 kg (Mk-DI) at the time of the experiments. They were housed in the animal facility with one to three other congeners in a 45-m^3 room (12 h light/dark cycle). The weight of the animals was checked daily. The animals were on no account food- or water-deprived (see e.g. Kaeser et al. 2010; Schmidlin et al. 2011). All procedures and animal care were conducted in accordance with the Guide for the Care and Use of Laboratory Animals (Committee for the Update of the Guide for the Care and Use of Laboratory Animals, National Research Council 2011) and were approved by local (Canton of Fribourg) and federal (Swiss) veterinary authorities. The present experiments were covered by the official authorisation numbers FR 22668, FR 18/10, FR 17/09, FR 156/08 and FR 22010. Experimental procedures were designed to minimise the animals' pain and suffering.

SSEP acquisitions

Anaesthesia and procedure

SSEP acquisitions were performed under sevoflurane anaesthesia (Sevorane®, Abbott) delivered with a mask by a cassette vaporiser inserted in an anaesthesia machine (ADU AS/3, Datex-Engström Division, Instrumentarium Corp., Helsinki, Finland). In case of low tolerance for the mask and also to decrease the level of stress in highly restless monkeys, a pre-anaesthesia with *S*-ketamine hydrochloride (Keta-S®, 60 mg/ml, Graeub AG, 5 mg/kg, im (intramuscular)) could be administrated as a first step. Data presented in this study were, however, obtained without this pre-anaesthesia. To induce a rapid gas anaesthesia, a bolus was first given at a concentration of 6.5 % of sevoflurane (1–2 l/min air; 1–2 l/min O_2) for about 4–5 min, while the monkey sat in a Plexiglas® primate chair (Schmidlin et al. 2011). Then, the concentration of sevoflurane was reduced and maintained at 2.5 % (0.3–1 l/min air; 0.3–1 l/min O_2 for Mk-AT, Mk-BB and Mk-EN) or 3.5 % (0.7–1 l/min air; 0.7–1 l/min O_2 for Mk-DG and Mk-DI) for the continuation of the experiment, suppressing the lid reflex. At that time, the monkey was placed in a metal tilted chair with the forearms on armrests and the hind legs laying horizontally on a platform in the prolongation of the chair. Monkey's back and nape of the neck were maintained in an adequate position with a customised thermoplastic shell (Turbocast without perforation, Art.-nr 636025, FREY Orthopädie-Bedarf AG, Othmarsingen, Switzerland). The monkey's head was shaved and washed vigorously with alcohol to eliminate fat secretion on the scalp. The EEG cap was then placed and maintained in the correct position using a chest strap. Body temperature was maintained by covering the animal with bubble wrap and single-use gloves filled with warm water. During the experiment, the level of anaesthesia

was regularly evaluated by checking the lid reflex. Moreover, the electrocardiogram, the cardiac pulse frequency, the respiratory frequency, the expired CO_2 and blood saturation rate in oxygen were continuously monitored with the anaesthesia machine.

Usually, a 30- to 50-min period was necessary between the induction of the anaesthesia and the first recordings to set up the EEG cap (see below) and to ensure equilibration of the anaesthetic concentration.

At the end of the recordings, the sevoflurane delivery was stopped and a mixture of O_2 and air was delivered via the mask to the monkey. All SSEP recordings were performed in a Faraday cage room. The entire experimental session typically lasted about 2–3 h.

Peripheral nerve stimulation

An electrical pulse stimulation was delivered to the median nerve at the wrist or to the tibial nerve at the ankle, successively on both sides through a surface stimulator (barrette with 2 electrodes, 1 cm apart) attached around the corresponding limb with a Velcro® strip. A silver-impregnated conductive Velcro® ground electrode (model F-E10SG1, Grass Instruments Division, Astro-Med, Inc., West Warwick, RI, USA) was placed around the stimulated limb, proximally to the stimulation site. The regions where the stimulator and the ground electrode were applied were shaved and cleaned with alcohol and the electrodes of the stimulator were moistened with saline solution. Stimuli consisted of monophasic square wave electrical pulses of 400-μs duration delivered via an isolation unit (Stimulus isolator A365R, World Precision Instruments, Sarasota, USA) every 2 s (0.5 Hz) for periods of 3 min (corresponding to a total of about 90 stimuli delivered at each of the 4 stimulation sites). Stimulation intensities corresponded to the visual threshold of the motor response of the muscles innervated by the stimulated nerve (between 0.55 and 4.75 mA at the wrist and between 0.32 and 2.6 mA at the ankle, depending on the animal's corpulence), i.e. eliciting a small twitch of the thumb after median nerve stimulation and a plantar flexion of the toes after tibial nerve stimulation. The visual motor threshold was used as an indicator of the stimulation intensity because it is a simple and position-independent criterion to visualise the effectiveness of the electrical stimulation. Moreover, this technique is widely used in clinics, e.g. to reliably localise a nerve or a plexus during peripheral nerve blockade (Tsui 2007) or to evaluate curarisation level in anaesthetised patients (Baurain et al. 1998) or animals (Martin-Flores et al. 2008). To reduce the likelihood of anodal block, the cathode of the stimulator was placed proximally and the anode more distally on the stimulated limb (Cruccu et al. 2008).

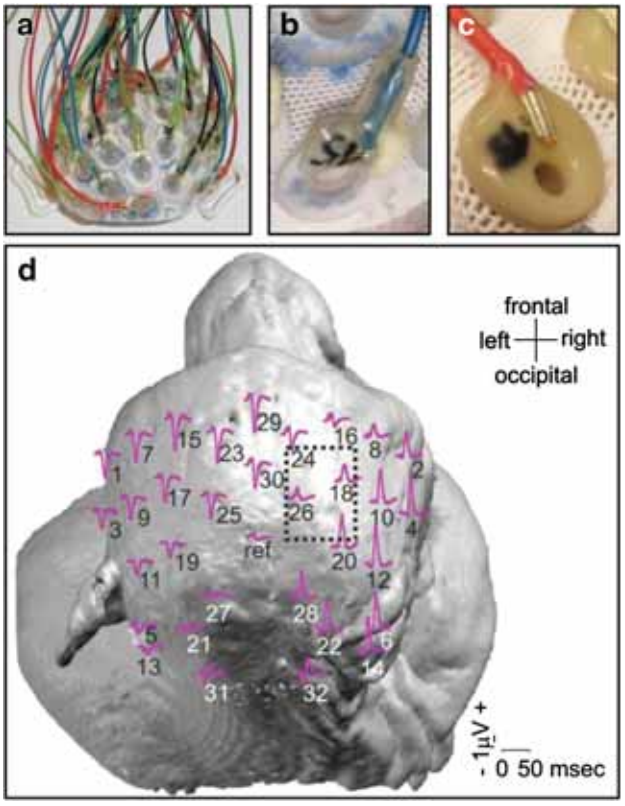

Fig. 1 SSEP acquisitions and craniotomy. **a** View of Mk-EN's EEG cap from the top (frontal: down, occipital: up, right side: *left*, left side: *right*). **b** Detail of an electrode of Mk-EN's cap. The electrode is mounted on a 14-mm circular support which is inserted in the cap. **c** Detail of an electrode of Mk-AT, Mk-BB and MK-DI's cap. The electrode is fixed on the cap via a 9.5-mm circular glue support. **d** Location of the 33 electrodes and their waveform after left median nerve SSEPs (GA of 9 recordings), projected on Mk-EN's MRI head surface viewed from above (frontal: *up*, occipital: *down*, right side: *right*, left side: *left*). Interval: 0.0 to 50.0 ms post-stimulus. The perimeter of the bone flap of the craniotomy is indicated by *dotted lines*. *ref* reference electrode

Scalp SSEP recording

Recordings were performed at the scalp with a customised EEG cap made of synthetic elastic tissue (EASYCAP GmbH, Herrsching, Germany) with slits for the ears and 32 sintered Ag/AgCl electrodes (EASYCAP, Catalogue-Nr. B12-HS-200) (Fig. 1a) in reference to a vertex electrode. The EEG was grounded at an electrode just left to the reference one. Electrodes were 2 mm in diameter and embedded on a circular support 14 mm in diameter for Mk-DG and Mk-EN's cap (Fig. 1b) and 9.5 mm in diameter for Mk-AT, Mk-BB and Mk-DI's caps (Fig. 1c). Electrodes were inserted in the cap in a symmetrical and regular manner between both hemispheres, based on the International 10–10 System (American Clinical Neurophysiology Society 2006) to cover the whole scalp (Fig. 1d). The montage included 2 midline sites and 15 sites over each

hemisphere. The inter-electrode distance was between 1.5 and 2 cm for Mk-DG and Mk-EN's cap and between 1 and 2 cm for the other caps.

The EEG was recorded using a BrainAmp DC amplifier (Brain Products GmbH, Gilching, Germany) with a band-pass filter between 0.1 Hz and 1 kHz and sampled at 5 kHz, with a resolution of 0.1 μV and 16 bit A/D conversion. Signals were displayed online and stored on hard drive using a conventional human EEG software (BrainVision professional Recorder 1.20, Brain Products GmbH, Gilching, Germany). Impedance minimisation was obtained with a high-chloride, abrasive electrolyte gel (Abralyt HiCl, EASY CAP). The impedances were kept below 5 kΩ.

SSEP analysis

SSEP data averaging

Data analysis was performed using the Cartool software developed by Denis Brunet (Geneva University Hospital and Medical School, Geneva, Switzerland; https://sites.google.com/site/fbmlab/cartool, Brunet et al. 2011).

Prior to averaging, the EEG was filtered offline between 8 and 300 Hz, and the DC component (0 Hz) was removed. When the signals were contaminated with 50-Hz noise, an additional 50-Hz notch filter was used. Signals were re-referenced offline against the average reference and the reference electrode became therefore a 33rd electrode. Before averaging, responses to each stimulus were visually selected offline to ensure that they were not contaminated by noise in addition to a threshold criterion of 100 μV. All SSEPs were finally obtained by averaging about 80 sweeps. Data were baseline corrected, based on the −80 to −30 ms pre-stimulus period. For Mk-EN, several SSEP grand averages (GAs) were calculated based on different recordings made at days to weeks intervals before and after a 15 × 20-mm^2 craniotomy performed over the right parietal bone (see below "Surgery and craniotomy").

Classical component analysis

The effect of a craniotomy on EEG signals recorded at the scalp was first assessed by statistically comparing at each time frame the amplitude of left median nerve SSEP signal recorded at each electrode between 4 pre-craniotomy sessions and 4 post-craniotomy sessions. A two two-tailed unpaired *t* test with Bonferroni correction for the number of electrodes was performed in Cartool with a *p* value threshold at 0.01.

Moreover, to assess the effects of the craniotomy on SSEP signals and at the same time the stability of recordings, we also performed classical component analysis on the global field power (GFP) waveform and at two selected electrodes: electrode 32 (e32), located in right occipital region presumably over the right half of the brainstem, and electrode 12 (e12) presumably located over the sensorimotor cortex of the right hemisphere (see Fig. 1d for precise location of the electrodes). The arrival of the afferent volleys at the brainstem (brainstem component) and the main cortical component were characterised both on the GFP waveform, on e32 for the former and on e12 for the latter. Both components measured at peak were analysed in terms of absolute amplitude and latency from the stimulation onset on the 4 pre-craniotomy sessions and on the 4 post-craniotomy sessions. Pre- and post-craniotomy values were compared using unpaired *t* tests with SigmaPlot 12.0 (*p* value threshold at 0.01).

Identification of SSEP maps by cluster analysis

The spatiotemporal dynamics of the SSEPs can be represented by maps of the scalp potentials, i.e. a succession of non-overlapping periods of stable scalp voltage topographies of variable duration and intensities and separated by sharp transitions. Such SSEP component maps are thought to represent the different processing steps in the brain activity evoked by a stimulus (Brandeis and Lehmann 1986; Lehmann et al. 2009; Michel et al. 2009; Pascual-Marqui et al. 1995). These maps represent the voltage distribution on the scalp produced by all concurrently active intracranial generators during this processing step (Koenig et al. 2013; Michel and Murray 2012): different scalp topographies necessarily result from different generators (Helmholtz 1853; Michel et al. 2004; Pascual-Marqui et al. 1995; Vaughan 1982).

Topographical analyses of SSEPs have many advantages over the classical component analysis of SSEPs, namely SSEP maps are reference–independent and are not limited by a priori time periods and components of interest in a subset of electrodes (Geselowitz 1998; Michel et al. 2004; Murray et al. 2008).

To determine the most important stable maps optimally summarising the data, we applied a K-means clustering algorithm (Murray et al. 2009; Pascual-Marqui et al. 1995) to the GAs from 6- to 50-ms post-stimulus for median nerve SSEPs and from 10.8- to 60-ms post-stimulus for tibial nerve SSEPs. Clusters shorter than 0.4 ms (2 time frames) were excluded and associated with the preceding or the following one, depending on which they correlated better with. Clusters with a correlation coefficient >92 % were merged together. The optimal number of clusters was determined using either the Krzanowski–Lai criterion (Krzanowski and Lai 1988) or the cross-validation criterion (Brunet et al. 2011).

Potential values were averaged during each cluster at each electrode and interpolated with Delaunay

triangulation for graphical representations of mean SSEP maps. For further details about the whole segmentation process, see Brunet et al. (2011) and Cartool Reference Guide (Brunet 1996).

Statistical analyses on SSEP component maps

To determine in how far the templates (or maps) identified by the cluster analysis are represented in the data of each individual recording session, we computed a strength-independent spatial correlation (SC) between the templates identified in the GA cluster analysis and the EPs of each individual recording session (fitting) (Megevand et al. 2008). The SC measures the topographical similarity between two maps:

$$\mathrm{SC} = \frac{\sum_{i=1}^{n} (u_i \cdot v_i)}{\sqrt{\sum_{i=1}^{n} u_i^2} \cdot \sqrt{\sum_{i=1}^{n} v_i^2}},$$

where n is the number of electrodes and u_i and v_i are the voltages against the average reference at electrode i for the two maps (Lehmann and Skrandies 1980). No SC between the template and the individual data results in SC = 0, whereas a perfect SC between them yields SC = 1. This fitting process assigns at each time frame and for each individual recording the component map obtained by cluster analysis having the highest SC. Segments shorter than or equal to 0.4 ms were rejected. No smoothing was applied to the data. Eight different topographical parameters were then computed for each component map in each individual recording: latency at first onset, duration, global explained variance (GEV), latency at best SC, mean SC, maximum of GFP, latency at maximum of GFP and mean GFP. The GEV is the sum of the explained variances weighted by the GFP at each time. For further details about these parameters, see Brunet et al. (2011), Koenig and Gianotti (2009) and Cartool Reference Guide (Brunet 1996).

The intraindividual stability of SSEPs was tested across 9 recording sessions. Unpaired t tests or Mann–Whitney U rank sum tests when normality tests failed were performed with SigmaPlot 12.0 to compare the latency at first onset and the latency at best SC from each individual recording session between pairs of successive component maps obtained after median nerve stimulation and tibial nerve stimulation (the p value threshold at 0.01 was adapted using Bonferroni correction for the number of electrodes). The total GEV for each recording session was also computed by adding the GEVs obtained from each template map, and these values were then averaged across the 9 recording sessions.

Moreover, two-tailed unpaired t tests with Bonferroni correction for the number of electrodes were performed with Cartool with a p value threshold at 0.01 to compare the 8 topographical parameters of the fitting before and after the craniotomy.

SSEP source estimation method

MRI acquisition, electrode position reconstruction and lead field model

Because any voltage topography recorded at the scalp can be generated in principle by an infinite number of different source combinations within the brain, no unambiguous statement about which brain areas contribute to what extent to the EPs can be made on the basis of scalp EEG data alone. To estimate the electrical source activity, we used a low-resolution electromagnetic tomography (LORETA) distributed, linear inverse solution based on the estimation of current density (CD) distribution in the whole brain (Pascual-Marqui et al. 1994, 2009) combined with a lead field model (or forward solution model) based on the individual CT scan and MRI of Mk-EN.

For the MRI acquisition, the monkey Mk-EN was first sedated with an im injection of ketamine hydrochloride (Ketasol 100®, 100 mg/ml, Graeub AG, 10 mg/kg) and midazolam hydrochloride (Dormicum®, 5 mg/ml, Roche Pharma SA, 0.1 mg/kg), allowing to transport the animal from the animal facility of the University to the HFR Hôpital cantonal of Fribourg. The transport by car was approved by local (Canton of Fribourg) veterinary authorities. The MRI investigations were conducted according to guidelines established by the Hospital's authorities.

Once in the MRI anteroom at the Hospital, the EEG cap was positioned on the animal's head and a small spot of EEG paste (high-chloride electrolyte gel Lectron III-10, EASY CAP) was put at each electrode location. This EEG paste was used because it is easily visible in T1-weighted MR images. The EEG cap was then carefully removed, leaving the electrode positions labelled with EEG paste. An intravenous (iv) catheter was placed in the saphenous vein to induce propofol anaesthesia (mixture of propofol 1 % MCT (Fresenius Kabi AG) and Ringer lactate (1:1), and 1.25 ml ketamine hydrochloride (Ketasol 100®, 100 mg/ml, Graeub AG), 1.2–3.6 ml/kg/h). The monkey was placed in lateral decubitus position and insulated with bubble wrap. The monkey's head was carefully positioned on the side inside the head coil. During the MRI acquisition, the animal's cardiac pulse frequency and blood saturation rate in oxygen were continuously monitored and the animal was provided with a continuous O_2 flow. The electrode positions were determined with the EEG paste positions in the MRI space: an Ax FSPGR 3D full head MRI (TE = 3.6 ms, TR = 8,000 ms, ET = 1, flip angle =

10°, acquisition matrix = 240 × 240, 1 excitation) of Mk-EN was acquired on a Discovery MR750 3.0T scanner (GE Medical Systems) with a 32-channel head coil. A total of 312 slices were recorded with a 1.2-mm slice thickness, a 0.6-mm gap between slices and an in-plane resolution of 0.625 × 0.625 mm^2.

The lead field model was computed with the Cartool software from the CT scan and MRI acquisitions and from the electrode positions. An analytical head model using a manifold of locally adapted spheres to calculate the lead field for each of the 33 electrodes was used (Brunet et al. 2011). The radiuses for the scalp, skull and brain were kept constant (scalp at 100 %, outer skull boundary at 78 % and brain/inner skull boundary at 68 %). Skull stripping was performed with Cartool to obtain the isolated brain. The whole brain, i.e. white and grey matter combined, was used to define a solution space of 3,000 discrete points, because the MRI quality did not provide enough separation between white and grey matter. The relative conductivity of the skull was set to 0.05.

Inverse solution

The obtained lead field matrix of Mk-EN was used to compute a LORETA inverse matrix with the Cartool software. A range of 13 Tikhonov regularisations was pre-computed to allow the right amount of regularisation to be selected according to the noise level found in the data.

Left and right median nerve SSEPs from 9 recording sessions in Mk-EN (before the craniotomy) were considered for this analysis. We estimated the CDs (mA/mm^3) for each source and at each time point. The 100-ms prestimulus CD period was used as a baseline. Then, we compared the baseline CDs with the post-stimulus CDs across all the epochs of the different recording sessions using paired *t* tests performed with Matlab (*p* value threshold at 0.05) to assess when stimulus-evoked CDs exceeded the baseline activity (Plomp et al. 2010). The paired samples were the average baseline CD and the evoked CD within each epoch at each time point between 0 and 200 ms after stimulus onset, and for each source point. The *t* values were averaged across each component map and colour-scaled.

Surgery and craniotomy

The animals of the present study are included in a protocol of cortical lesion of the hand area of M1 (see e.g. Hamadjida et al. 2012; Kaeser et al. 2010, 2011; Wyss et al. 2013). To this aim, animals were trained to perform several manual dexterity tasks (for more details, see Schmidlin et al. 2011) in parallel with SSEPs recordings. The next step in the protocol is to perform a lesion by microinfusion of ibotenic acid at multiple sites within the hand area of M1 (see e.g. Hamadjida et al. 2012; Kaeser et al. 2010, 2011; Liu and Rouiller 1999), requiring consequently a craniotomy to expose the sensorimotor cortex. To evaluate the effect of the craniotomy itself on the SSEPs, a "sham lesion" consisting in the craniotomy alone was first performed in Mk-EN, with the bone flap put back in place.

To perform the craniotomy, the monkey Mk-EN was first sedated with an im injection of ketamine hydrochloride (Ketasol 100®, 100 mg/ml, Graeub AG, 10 mg/kg), midazolam hydrochloride (Dormicum®, 5 mg/ml, Roche Pharma SA, 0.1 mg/kg) and methadone (Methadone®, 10 mg/ml, Streuli Pharma AG, 0.2 mg/kg). The premedication also included atropine (Atropinum sulf®, 0.5 mg/ml, Sintetica SA, 0.05 mg/kg, im) to reduce bronchial secretions, the analgesics carprofen (Rimadyl®, 50 mg/ml, Pfizer Animal Health, 4 mg/kg, subcutaneous (sc)), the antibiotics ampicillin 10 % (Betamox LA®, 150 mg/ml, Arovet SA, 30 mg/kg, sc) and dexamethasone (Dexamethasone®, 5 mg/ml, Helvepharm AG, 0.15 mg/kg diluted 1:1 in saline, im) to prevent brain oedema. The surgery itself was performed under sterile conditions. The animal was placed in ventral decubitus position on a heating blanket regulated according to the animal's rectal temperature, and isolated with bubble wrap. Eye drops (Neosporin®, GlaxoSmithKline Inc.) were administrated to prevent exsiccation of the cornea. The intra-operative monitoring was the same as described above for SSEP acquisition (see "Anaesthesia and procedure") and included in addition body temperature monitoring.

The animal was intubated and put under sevoflurane anaesthesia (Sevorane®, Abbott, 2.5 %, in 50 % O_2 and 50 % air). An iv catheter was placed in the saphenous vein to induce propofol anaesthesia (mixture of propofol 1 % MCT (Fresenius Kabi AG) and Ringer lactate (1:2), 1.8 ml/kg/h) and Ringer lactate infusion (8 ml/kg/h). The monkey's head was then fixed in a stereotaxic frame (Narishige, Japan) using ear bars coated with lubricating gel (Lidohex®, Dr. G. Bichsel AG). The skin was incised along the anteroposterior axis of the head, in the midline. This zone had been locally anaesthetized with several sc injections of lidocaine 1 % (Rapidocain® 1 %, 10 mg/ml, Sintetica SA, 2 ml in total). The muscles were incised and reclined. A craniotomy was performed by drilling a rectangular bone flap (15 mm mediolaterally × 20 mm anteroposteriorally) over the right hemisphere (i.e. contralateral to left median nerve), whose centre was localised 15 mm rostral and 15 mm lateral from the reference point of the stereotaxic frame (half-distance between both ear bars) and with an angle of 30° with respect to the midsagittal plane (Shimazu et al. 2004), giving access to the hand area in the right

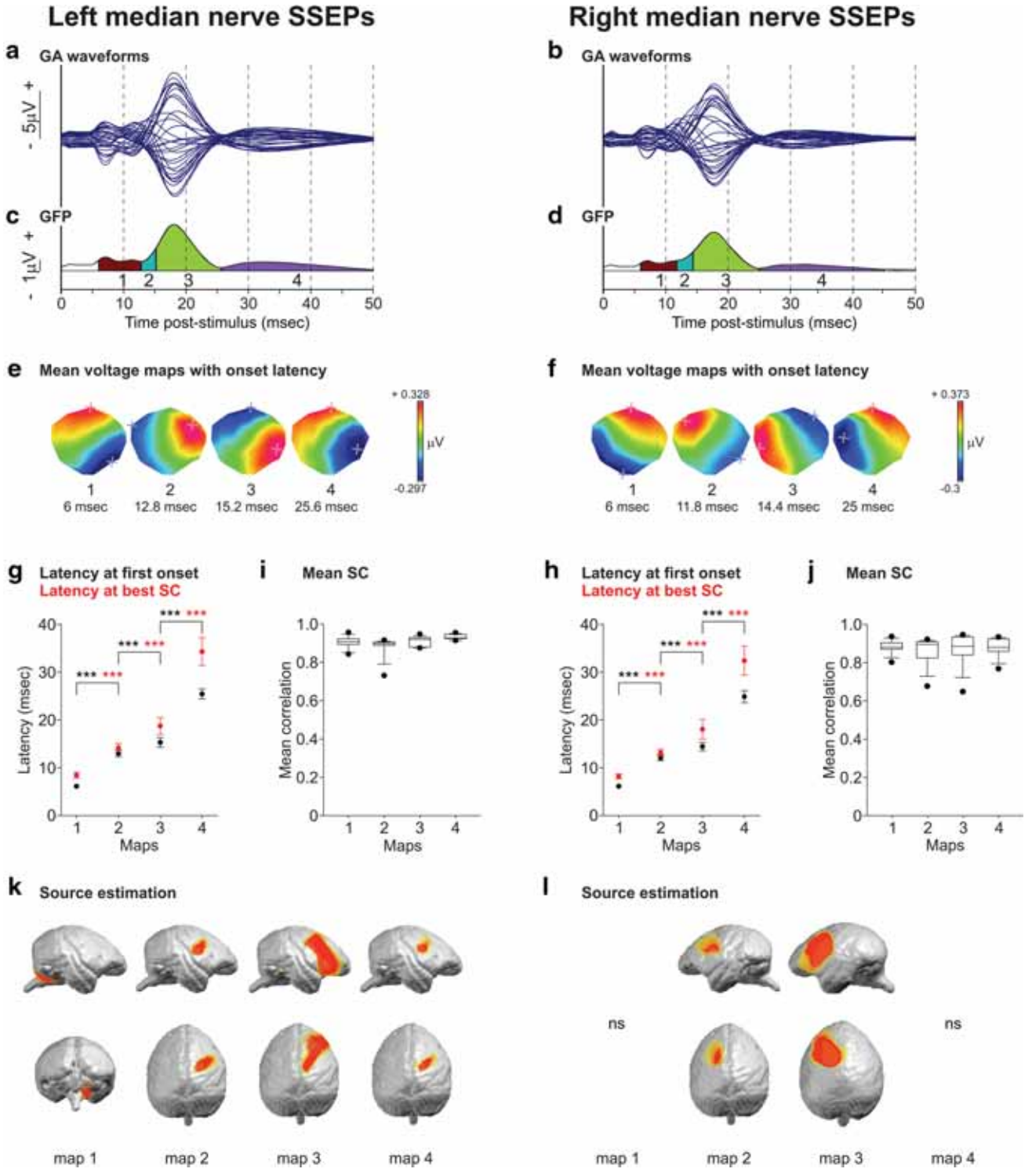

motor cortex (Fig. 1d). The dura mater was left in place. The bone flap was then repositioned and sutured with 2 stitches, one on the midline anterior part and one on the midline posterior part of the bone flap. To this aim, two small holes were beforehand drilled through the bone flap and two through the skull. A calcium phosphate cement converting to hydroxyapatite (HydroSet Injectable HA Bone Substitute, Stryker®; Chow and Takagi 2001; Dickson et al. 2002; Larsson 2006; Van Lieshout et al. 2011) was then applied all around the bone flap and over the stitches to seal the gaps. HydroSet is a synthetic material formed by a sterile white powder (dicalcium phosphate dihydrate, tetracalcium phosphate and trisodium citrate) which has to be mixed with liquid (sodium phosphate,

◀**Fig. 2** Median nerve SSEPs in Mk-EN. **a**, **b** Overlapped SSEP waveforms at all electrodes after left and right median nerve stimulations (GA of 9 recordings in each case), computed against the average reference, during the first 50 ms following the stimulation. Positive voltages are plotted upward. **c**, **d** Global field power (*GFP*) waveform during the first 50 ms following the stimulation, and temporal extent of the SSEP component maps obtained by cluster analysis. **e**, **f** Colour-scaled mean voltage maps obtained for each cluster shown in **c**, **d**. The *colour* scaling was adapted for each map (positive voltage: *red*, negative voltage: *blue*). *Red* "+" indicates the electrode with the most positive voltage value and *blue* "+" the electrode with the most negative voltage value. The latency at *onset* is indicated for each map. Maps are oriented so that the frontal part points up, the occipital part points down, the left part points left and the right part points right. **g**, **h** Latency at first onset and latency at best spatial correlation (*SC*) for the 4 maps obtained after left and right median nerve stimulations in each of the 9 recording sessions used to compute the GAs shown in **a**, **b**. The mean latency ± SD is shown. 9 unpaired *t* tests and 3 Mann–Whitney *U* rank sum tests when normality tests failed were performed (the *p* value threshold at 0.01 was adapted using Bonferroni correction for the number of electrodes; *** $p \leq 0.01$) to compare the latencies of pairs of successive maps. **i**, **j** *Box plots* of the mean SC of each map measured for each of the 9 individual recordings used to compute the GAs shown in **a**, **b**. The *bottom* of the *boxes* indicates the 25th percentile, the line within the *boxes* marks the median, and the *top* of the *boxes* indicates the 75th percentile. Whiskers below and above the boxes display the 10th and 90th percentiles, respectively. *Outliers* are represented by *black dots*. **k**, **l** The estimated source localisations obtained with LORETA inverse solution are plotted for each map after left and right median nerve stimulations. *Coloured* areas indicate regions of significant deflection from baseline projected onto Mk-EN's brain (*t* values are averaged across each component map and colour-scaled, only significant *t* values at $p < 0.05$ are shown, paired *t* tests, *ns* statistically non-significant)

polyvinylpyrrolidone and water) to form a malleable paste. It was mixed and applied with a thin spatula. The muscles and the skin were then sutured. During painful phases (e.g. bone drilling), fentanyl was delivered (Fentanyl Curamed®, 0.1 mg/2 ml, Actavis Switzerland AG, 0.1 µg/kg/min diluted 1:1 in saline, iv). Following surgery, the monkey was treated for 9 days with carprofen (Rimadyl®, 50 mg/ml, Pfizer Animal Health, 4 mg/kg/day, sc) and ampicillin 10 % (Betamox LA®, 150 mg/ml, Arovet SA, 30 mg/kg every second day, sc).

Results

Median nerve SSEPs

Electrical stimulation of the left median nerve at the wrist elicited a complex response derived at the scalp (Fig. 2a, b). In Mk-EN, the earliest component was recorded with largest amplitude (mean −2.770 µV, standard deviation (SD) 0.196; mean across 4 pre-craniotomy recording sessions, used for further comparison with 4 post-craniotomy recording sessions, see below "Effect of craniotomy on left median nerve SSEPs") at 6.9 ms (mean, SD 0.258) (Fig. 3b, c pre) at a contralateral occipital electrode (e32). These spatiotemporal characteristics presumably correspond to the arrival of the afferent volleys in the brainstem (see also results of the inverse solution); this component was consequently called brainstem component. The next major component was recorded with the largest amplitude (mean 6.603 µV, SD 2.428) at 17.9 ms (mean, SD 1.039) (Fig. 3e, f pre) at a contralateral electrode located on the sensorimotor cortex (e12). This component was called here main cortical component.

To characterise the spatiotemporal dynamics of the scalp SSEPs, signals after left and right median nerve stimulations were each averaged from 9 recording sessions regularly distributed at different days over an 11-week period and the GAs were then segmented (GAs of 9 recording sessions performed with Mk-EN, 2 independent clusterings, Fig. 2). The Krzanowski–Lai criterion yielded 4 template maps as the best solution of the K-means cluster analysis (Fig. 2c, d) which explained 97.33 % of the GEV of the sequence of brain activity evoked after left median nerve stimulation and 96.18 % of the GEV of the sequence of brain activity evoked after right median nerve stimulation.

Following left median nerve stimulation, the first SSEP component map lasted from 6 to 12.8 ms after the stimulation (map 1, Fig. 2e) and was characterised by a positive amplitude above the ipsilateral frontal part of the scalp and a strong focal negative amplitude above the contralateral most occipital part of the scalp. The next component map was very short (map 2, from 12.8 to 15.2 ms), with a positive amplitude above the contralateral fronto-parietal cortex and a negative amplitude above the ipsilateral parieto-temporal part of the scalp. Then, the positivity spread towards contralateral parietal electrodes and the negativity became more frontal (map 3, from 15.2 to 25.6 ms). The last component map (map 4, from 25.6 to 50 ms) was characterised by a voltage inversion as compared to map 3. As expected, voltage topographies of SSEPs obtained after left and right median nerve stimulations were essentially mirror images in relation to the anteroposterior axis (Fig. 2e, f). Moreover, the latencies for each component map were highly conserved between both stimulated sides.

A crucial issue is how stable the SSEP signals are in a given monkey across recording sessions from different days since the EEG cap might not be positioned precisely in the same way between recording sessions. The high stability of left median nerve SSEPs was first confirmed by the small SD in amplitude and latency of the brainstem and main cortical components measured on the GFP and, respectively, on e32 and e12, as illustrated in Fig. 3. To address the stability of the component maps across recording sessions, the sequence of 4 templates identified from the GAs was fitted back to the 9 individual recordings (a summary of the raw voltage maps can be found in

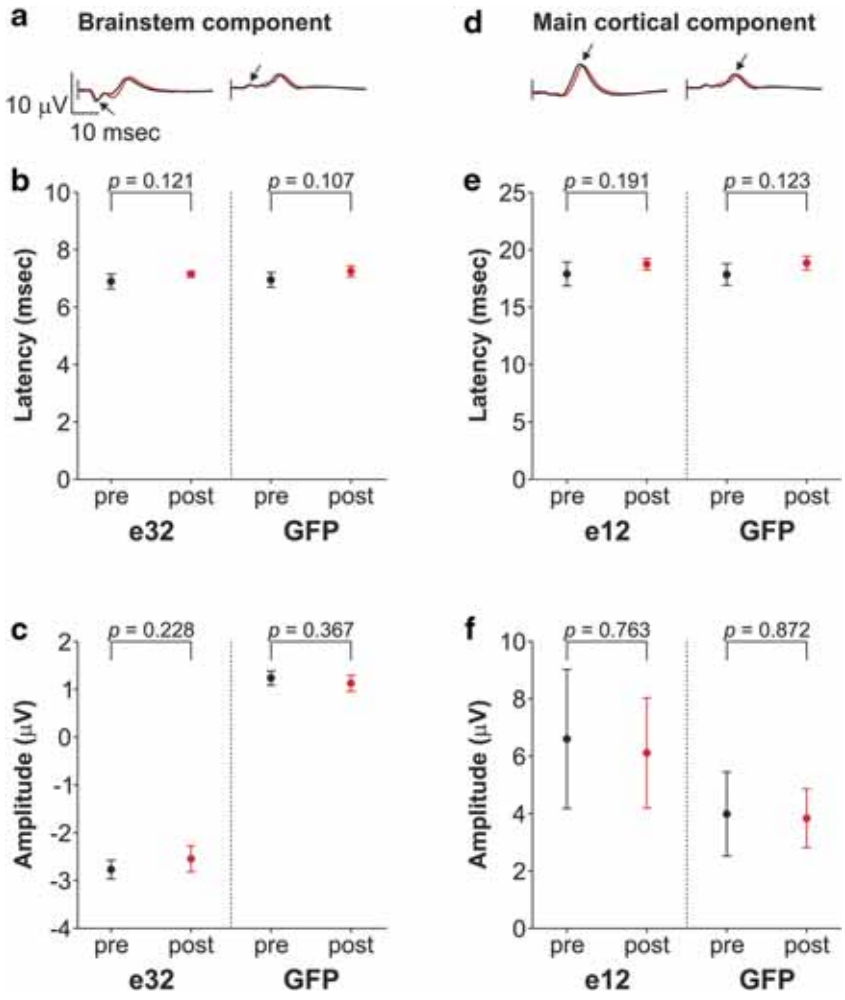

Fig. 3 Latencies and amplitudes of left median nerve SSEP components in Mk-EN. **a** Waveform at electrode 32 (e32) (*left*) and GFP waveform (*right*) before (*black*) and after (*red*) craniotomy. The *small black arrow* shows the brainstem component on each waveform. **b** Latency from stimulation onset of the brainstem component measured on e32 and on the GFP waveform before (pre, *black*) and after (post, *red*) craniotomy. **c** Amplitude of the brainstem component measured on e32 and on the GFP waveform. **d** Waveform at electrode 12 (e12) (*left*) and GFP waveform (*right*) before (*black*) and after (*red*) craniotomy. The *small black arrow* shows the main cortical component on each waveform. **e** Latency from stimulation onset of the main cortical component measured on e12 and on the GFP waveform. **f** Amplitude of the main cortical component measured on e12 and on the GFP waveform. The mean ± SD values from 4 pre-craniotomy SSEP (pre) and from 4 post-craniotomy SSEP (post) recordings are plotted for each condition. *p* values obtained with unpaired *t* tests at $p < 0.01$ are indicated. See Fig. 1d for the location of e32 and e12

Online Resource Supplementary Figures 1 and 2). The GEVs of each of the 4 templates of a recording session were added and then averaged across the 9 recording sessions, resulting in remarkably strong mean GEV of 94.64 % (SD 2.26) for left median nerve SSEPs and 93.90 % (SD 0.93) for right median nerve SSEPs. Moreover, the mean latency at first onset and the mean latency at best SC for each component map across the 9 recording sessions were very similar between both right and left median nerve SSEPs and exhibited a very small SD (Fig. 2g, h; Table 1); and the mean SC for each map from the 9 recording sessions was very high for both stimulated sides (Fig. 2i, j; Table 1). Equally important, we observed that the differences in mean latencies at first onset and the differences in mean latencies at best SC between pairs of successive component maps were all highly statistically significant, both after left and right median nerve stimulations (all *p* values $\leq 10^{-3}$ for each comparison of two successive map latencies, 9 unpaired *t* tests and 3 Mann–Whitney *U* rank sum tests because normality test failed, Fig. 2g, h; Table 1), indicating that the sequence of component maps was similar across recording sessions. All these observations demonstrate that median nerve SSEPs in macaque monkeys are characterised by a succession of 4 stable component maps highly reproducible across recordings sessions (Fig. 2e, f).

Table 1 Fitting parameters of median and tibial nerve SSEPs

	Latency at first onset (ms)		Latency at best SC (ms)		Mean SC		
	Mean	SD	Mean	SD	Mean	SD	Median
Left median nerve SSEPs							
Map 1	6.00	0.00	8.46	0.62	0.90	0.03	0.91
Map 2	13.00	0.68	14.18	0.91	0.88	0.06	0.90
Map 3	15.31	1.02	18.76	1.78	0.91	0.03	0.92
Map 4	25.44	1.04	34.30	2.89	0.93	0.01	0.93
Right median nerve SSEPs							
Map 1	6.00	0.00	8.20	0.52	0.88	0.04	0.88
Map 2	12.09	0.62	13.16	0.71	0.85	0.08	0.90
Map 3	14.44	0.86	18.07	2.05	0.86	0.09	0.89
Map 4	25.05	0.87	32.40	3.04	0.88	0.05	0.88
Left tibial nerve SSEPs							
Map 1	10.91	0.33	12.71	0.96	0.86	0.05	0.85
Map 2	16.53	1.09	22.00	3.21	0.87	0.04	0.88
Map 1	29.31	1.08	40.82	3.92	0.79	0.09	0.83
Right tibial nerve SSEPs							
Map 1	10.94	0.38	12.94	1.08	0.78	0.14	0.82
Map 2	15.76	0.64	21.60	3.32	0.89	0.04	0.89
Map 3	28.97	1.87	40.13	8.25	0.83	0.05	0.84

Latency at first onset, latency at best spatial correlation (SC) and mean SC resulting from the fitting of the templates (maps) obtained by cluster analysis back to the 9 individual recording sessions of left and right median nerve SSEPs (Fig. 2) and left and right tibial nerve SSEPs (Fig. 4). Values correspond to the mean, SD and median (for mean SC only) across the 9 recording sessions. For reminder, no correlation between the templates and the individual data leads to SC = 0, whereas a whole correlation between them results in SC = 1

The spatiotemporal propagation of activity described by this sequence of component maps seems to correspond well to the expected propagation of sensory evoked processing following median nerve stimulation. During map 1, the strong negative voltage deflections above the contralateral posterior part of the map may correspond to the early processing of the afferent sensory volleys in the dorsal column nuclei in the brainstem. During the 3 following maps, the locations of the strongest voltage values in the contralateral parietal and frontal cortices, first positive during maps 2 and 3, then negative during map 4, may correspond to activation of sensory and motor hand representations. However, no unambiguous statement about the contributing brain areas can be made on the basis of surface topographies alone. Consequently, we used the LORETA distributed, linear inverse solution adapted to Mk-EN's brain to localise the generators of the observed scalp EEG activities. Figure 2k, l shows the surface representations of the significant intracerebral source estimates during the 4 SSEP maps in response to left and right median nerve stimulations. For left median nerve SSEPs, it confirmed that during map 1, the contralateral dorsal region of the brainstem was active. From maps 2 to 4, activity invaded successively an anterior medial region of the contralateral parietal cortex, then the posterior medial region of the frontal cortex and finally back to the parietal cortex (Fig. 2k). After right median nerve stimulation, similar results were obtained for maps 2 and 3 (Fig. 2l). However, no significant source estimates could be calculated using our algorithm at $p < 0.05$ for maps 1 and 4. This difficulty to localise evoked activity source estimates may be due to morphological differences between the two hemispheres or to the skull altering the positioning of the electrodes above the left and right hemispheres and reducing the signal-to-noise ratio asymmetrically.

Tibial nerve SSEPs

Although we were interested mainly in the arm representation of the sensorimotor cortex, we also recorded left and right tibial nerve SSEPs (Fig. 4a, b). SSEP signals were averaged from 9 recording sessions regularly distributed over an 11-week period and the GAs were then segmented (GAs of 9 recording sessions performed with Mk-EN, 2 independent clusterings, Fig. 4). The spatiotemporal dynamics of evoked brain activity was summarised by 3 different component maps (Fig. 4e, f) by the K-means cluster analysis (Fig. 4c, d), explaining 97.29 % of the GEV of left tibial nerve SSEPs and 98.04 % of the GEV of right tibial nerve SSEPs. This sequence of 3 templates was then fitted back to the 9 individual recordings. The GEVs of the 3 templates of a recording session were added and then averaged across the 9 recording sessions, yielding a mean GEV of 89.55 % (SD 4.00) for left tibial nerve SSEPs and 90.66 % (SD 3.34) for right tibial nerve SSEPs. Once again, the SD in mean latencies at first onset and in mean latencies at best SC from the 9 recording sessions was small (Fig. 4g, h; Table 1), these latencies were similar between both stimulated sides (Table 1) and the mean SC for each map across the recordings was very high for both left tibial nerve SSEPs and right tibial nerve SSEPs (Fig. 2i, j, Table 1). These findings demonstrate here again that the succession of brain activity components was stable and reproducible across recordings and consequently that the intraindividual variability of tibial nerve SSEP maps was minimal over time.

The differences in mean latencies at first onset and the differences in latencies at best SC between pairs of successive component maps were all highly statistically significant, both after left and right tibial nerve stimulations (all p values $\leq 10^{-3}$ for each comparison of two successive map latencies, 4 unpaired t tests and 4 Mann–Whitney U rank sum tests because normality test failed, Fig. 4g, h; Table 1). Thus, tibial nerve SSEPs in macaque monkeys

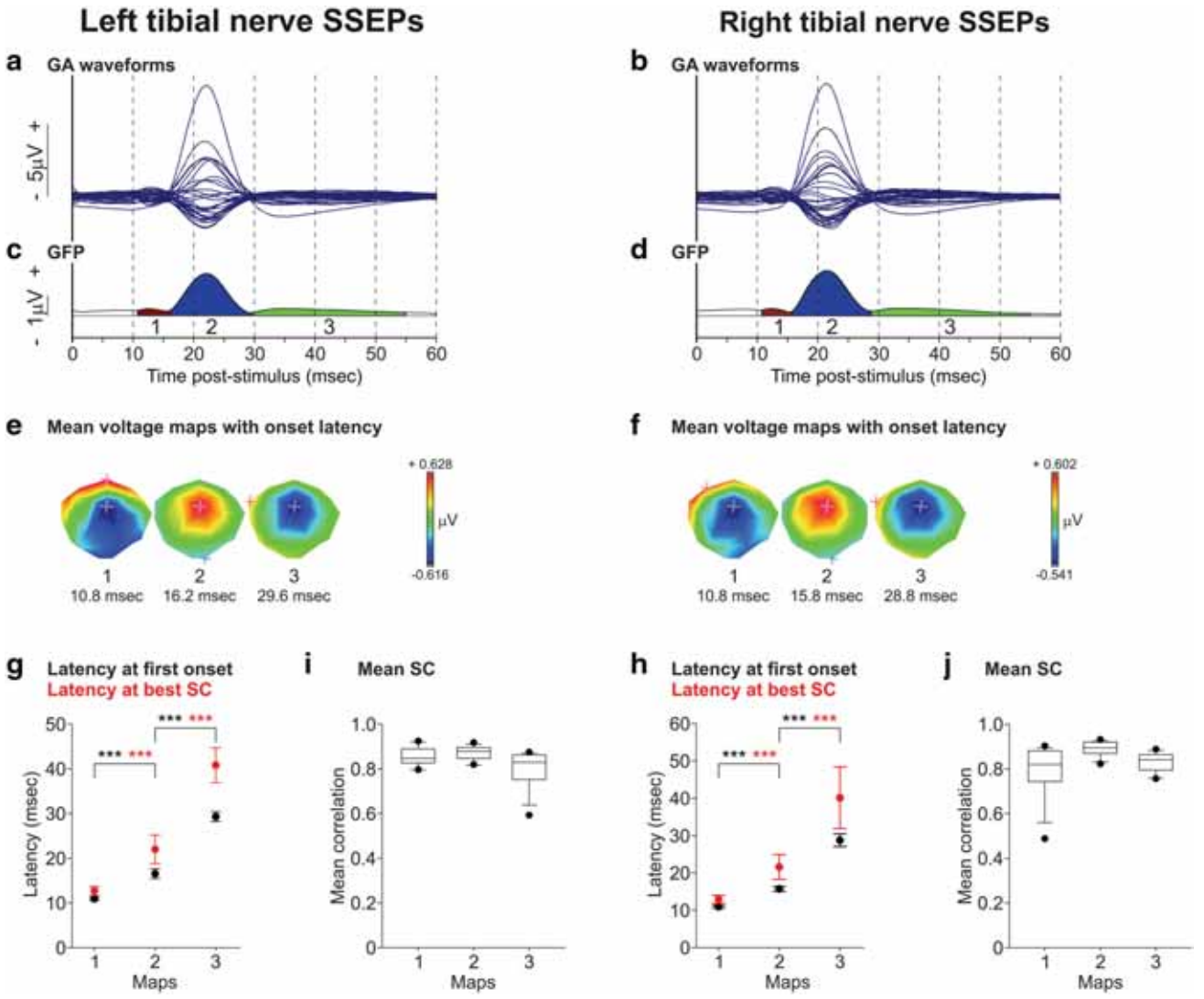

Fig. 4 Tibial nerve SSEPs in Mk-EN. **a**, **b** Overlapped SSEP waveforms at all electrodes after left and right tibial nerve stimulations (GA of 9 recordings in each case), during the first 60 ms following the stimulation. **c**, **d** GFP waveform during the first 60 ms following the stimulation, and temporal extent of the SSEP component maps obtained by cluster analysis. **e**, **f** Colour-scaled mean voltage maps obtained for each cluster shown in **c**, **d**. **g**, **h** Latency at first onset and latency at best SC for the 3 maps obtained after left and right tibial nerve stimulations in each of the 9 recording sessions used to compute the GAs shown in **a**, **b**. The mean latency ± SD is shown. 4 unpaired *t* tests and 4 Mann–Whitney *U* rank sum tests when normality tests failed were performed (the *p* value threshold at 0.01 was adapted using Bonferroni correction for the number of electrodes; *** $p \leq 0.01$) to compare the latencies of pairs of successive maps. **i**, **j** *Box plots* of the mean SC of each map measured for each of the 9 individual recordings used to compute the GAs shown in **a**, **b**. Same conventions as in Fig. 2

are remarkably stable across recording sessions (which is also visible in the raw voltage maps in Online Resource Supplementary Figures 3 and 4) and can be characterised by a succession of 3 stable component maps (Fig. 4e, f).

Following left and right tibial nerve stimulations, the SSEPs exhibited first a negative amplitude in the central part of the scalp (fronto-parietal region) and a positive amplitude at the most frontal electrodes (map 1) (Fig. 4e, f). A strong central positive amplitude appeared above midline in the fronto-parietal scalp region during map 2, situated above the expected sensorimotor somatotopic representation of the contralateral leg along the medial longitudinal fissure and reversed during map 3. The similarity of voltage topographies of the SSEPs obtained after left and right tibial nerve stimulations is presumably due to the fact that the leg representation in the sensorimotor cortex is located on either side of the medial longitudinal fissure.

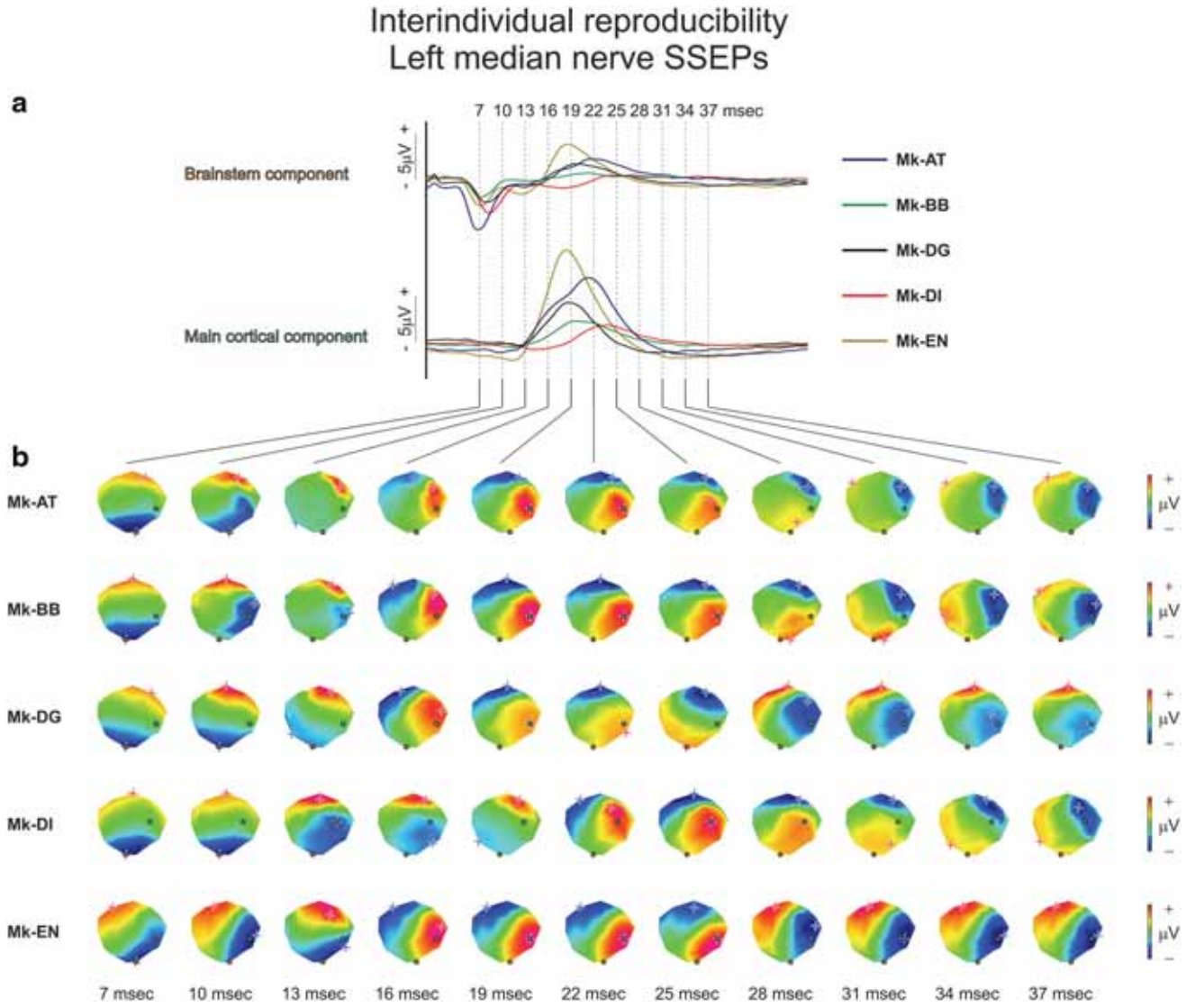

Fig. 5 Interindividual reproducibility of left median nerve SSEPs. **a** Brainstem component and main cortical component SSEP waveforms after left median nerve stimulation in five monkeys: Mk-AT (*blue*), Mk-BB (*green*), Mk-DG (*black*), Mk-DI (*red*), and Mk-EN (*yellow*), during the first 50 ms following the stimulation. These data were obtained from 1 recording session in each animal. **b** Colour-scaled voltage maps obtained from 7 to 37 ms post-stimulus, at 3-ms interval. The colour scaling in microvolts is indicated for each animal and was adapted for each map. All the maps were obtained using the same cap model (Mk-EN). The locations of the electrodes where both components were recorded with the largest amplitude are represented on the maps with *orange circles* (brainstem component) and *light green circles* (main cortical component). Note that these locations can vary between animals. Same conventions as in Fig. 2

Interindividual reproducibility of SSEPs

The results presented in Figs. 2 and 4, acquired in a single animal (Mk-EN), showed high stability across recording sessions. Median nerve and tibial nerve SSEP recordings were also performed in four other monkeys (Mk-AT, Mk-BB, Mk-DG, Mk-DI). A qualitative analysis based on left median nerve SSEPs obtained from 1 recording session in the five animals showed that there were some differences in the relative amplitude and some shifts in latencies of the different SSEP components among the animals (Fig. 5a), i.e. the voltage maps at a given time point may differ slightly across animals. For example, maps from 13 ms in Mk-DI were delayed by 3–6 ms relative to the ones in the other monkeys. More importantly, however, voltage topographies at the scalp were conserved both in terms of spatial configuration and temporal sequence across the five individuals (Fig. 5b). This reproducibility of surface topographies across animals was also true for right median nerve SSEPs and left and right tibial nerve SSEPs (Online Resource Supplementary Figures 5–7).

Effect of craniotomy on left median nerve SSEPs

A 300-mm^2 craniotomy was performed over the hand representation in the right sensorimotor cortex followed by bone flap repositioning in Mk-EN. Subsequently, post-craniotomy SSEPs were acquired and compared to pre-craniotomy data, to investigate whether the craniotomy had an impact on the scalp SSEPs. Four post-craniotomy SSEPs in response to left median nerve stimulation (therefore contralateral to the craniotomy) were recorded at regular time points over a 7-week period and compared to 4 pre-craniotomy SSEPs recorded over an 11-week period. No statistically significant differences appeared in the amplitude of the signal before and after the craniotomy when the statistical analysis was performed on each electrode at each time frame (two-tailed unpaired t test at $p < 0.01$, Bonferroni corrected for the number of electrodes). Moreover, post-craniotomy waveforms did not show any artefact.

The effect of craniotomy on left median nerve SSEPs was then classically assessed by comparing the absolute amplitude and the latency from the stimulation onset of the brainstem and main cortical components on two electrodes of interest (e12 and e32) and on the GFP (Fig. 3). No statistically significant differences in amplitude and in latency were observed between pre- and post-craniotomy data (all p values >0.1 for each comparison of pre- and post-craniotomy data, 8 unpaired t tests).

The effect of craniotomy was also tested using topographical analyses of surface SSEPs (Fig. 6). To this aim, the GA of the 4 pre-craniotomy sessions and the GA of the 4 post-craniotomy sessions used in Fig. 3 were subjected to a common K-means clustering. This segmentation process found the same sequence of 4 SSEP component maps before (Fig. 6c, e) and after (Fig. 6d, f) the surgery with quite similar latencies at first onset, suggesting that craniotomy by itself did not induce major changes in the spatial configuration and the temporal sequence of the component maps. To confirm this result, the 4 maps were fitted back to each of the 4 pre-craniotomy and 4 post-craniotomy recordings (Fig. 6g). Two-tailed unpaired t tests were performed to compare 8 topographical parameters (latency at first onset, duration, GEV, latency at best SC, mean SC, maximum of GFP, latency at maximum of GFP and mean GFP) for each component map before and after the craniotomy (Fig. 6h). Despite a seeming increase in cluster 2 duration, no statistically significant differences appeared between both conditions for any map parameter (all p values >0.15 for each comparison of pre- and post-craniotomy parameters), except a statistically higher post-craniotomy map 2 GEV (mean 0.101, standard error (SE) 0.005) than pre-craniotomy (mean 0.020, SE 0.007; p value 0.0045). This confirmed the absence of any strong adverse effect of craniotomy on our surface EEG and again the intraindividual stability of SSEP recordings over time.

Discussion

The present study showed that scalp SSEPs can be successfully and reproducibly recorded from a high-density EEG cap in anaesthetized macaque monkeys. Using detailed analyses of waveform components, voltage topographies and source localisation methods, we described the spatiotemporal propagation of SSEPs across the brain and demonstrated the stability of EEG recordings over time and across animals. We also demonstrated that a craniotomy followed by bone flap replacement with calcium phosphate cement suture did not affect the SSEPs in macaque monkeys, confirming that topographical analyses of SSEP are a valid and promising method to assess the reorganisation of the somatosensory network after lesions requiring a craniotomy. This study hence opens up new possibilities for the non-invasive long-term follow-up of cortical reorganisation in macaque monkeys after a cortical lesion or any injury affecting other parts of the central nervous system.

Intraindividual stability and interindividual reproducibility of the SSEPs

SSEPs recorded over several daily sessions in the same monkey were highly stable in terms of shapes of the waveform components as well as in terms of scalp topographies. This finding is not trivial because it is impossible to position the EEG cap exactly at the same location from one recording session to the next and the impedance of the electrodes also vary between recording sessions. The intraindividual stability of the SSEPs was demonstrated with the fitting process: it is a highly demanding procedure because it tries to allocate the clustering template fitting with the highest SC to the voltage topography of each time frame independently, and in each individual recording independently. Therefore, obtaining a coherent succession of voltage topographies in each recording and conserved across the recordings demonstrates and also proves the high quality and the stability of the SSEP data. Highly reproducible EP recordings from one session to the next were already demonstrated in mice in response to whisker stimulation (Megevand et al. 2008). Between monkeys, the same components were present, although we observed some differences in latencies and amplitudes. These differences in latency and amplitude might be due to intrinsic physiological differences between animals. Latency differences may also be due to anatomical variations, such as the size of the limbs, inducing differences in the length of

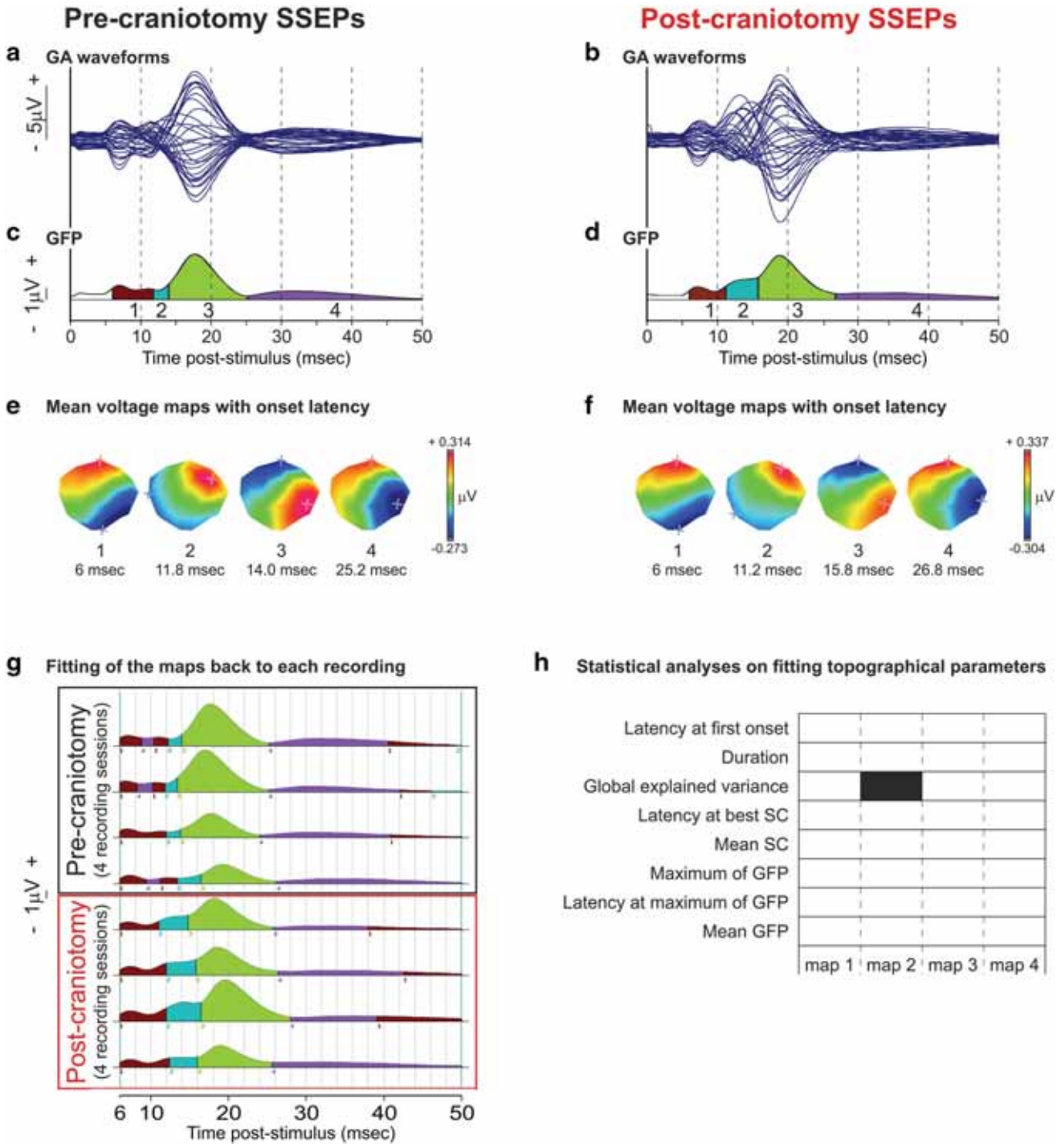

Fig. 6 Effect of the craniotomy on the spatiotemporal pattern of left median nerve SSEPs in Mk-EN. **a**, **b** Overlapped SSEP waveforms at all electrodes after left median nerve stimulation obtained before and after craniotomy (GA of 4 recordings in each case). **c**, **d** GFP and temporal extent of the SSEP component maps obtained by cluster analysis. **e**, **f** Colour-scaled mean voltage maps obtained for each cluster shown in **c**, **d**. Same conventions as in Fig. 2. **g**, **h** Fitting process of the 4 distinct clusters obtained by cluster analysis in **c**, **d** back to each of the 8 recordings. **g** GFP waveforms and temporal extent of the 4 different SSEP component maps for each of the 4 pre-craniotomy (*black*) and 4 post-craniotomy (*red*) individual recordings used to compute the GAs shown in **a** and **b**, from 6 to 50 ms following the stimulation. **h** Two-tailed unpaired *t* tests at $p < 0.01$ performed on the fitting results, between the pre- and post-craniotomy recording sessions: *black bars* indicate for each parameter the maps during which *p* values are statistically significant

the nerve tracts from the peripheral receptors to the brain (Chu 1986). Moreover, some variability may result from differences in the EEG caps and electrode types used for the different animals or differences in the signal-to-noise ratios. Nevertheless, voltage topographies were well conserved among the five monkeys. Taken together, the intraindividual stability and the interindividual reproducibility of SSEPs prove the high quality of our data and support the potential of our method of whole-scalp EEG mapping of SSEPs in non-human primates, e.g. in the context of a regular evaluation of the cortical reorganisation following a cortical lesion.

Spatiotemporal propagation of SSEPs

Here, we described EPs recorded in macaque monkeys as a succession of stable brain states called functional microstates (Lehmann et al. 1987, 2009; Michel et al. 2009). Their presence was demonstrated in many human multichannel EP studies (for reviews, see Brandeis and Lehmann 1986; Michel et al. 1999, 2001; Murray et al. 2008) as well as in rodents in response to whisker stimulation (Megevand et al. 2008, 2009; Quairiaux et al. 2010, 2011). SSEP voltage maps obtained here in monkeys are quite similar to the ones obtained in human with high-resolution EEG mapping of SSEPs (Lascano et al. 2009; van de Wassenberg et al. 2008a) using the same kind of stimulation. The differences in latency observed between both species are due to the longer human sensory pathways as compared to the ones in macaque monkeys. As reported here, scalp topographies of right and left median nerve SSEPs in human are mirror images in relation to the anteroposterior axis (Lascano et al. 2009), which could be of importance to study the effects of unilateral brain lesions (Quairiaux et al. 2010).

Source imaging

Based on anatomical knowledge, one could localise the main deep generators of the median nerve SSEPs recorded at occipital electrodes to the brainstem and at contralateral parietal and frontal electrodes to the underneath cortical areas, as already demonstrated in human (Finke et al. 2013; He et al. 2002) and in accordance with a response of the dorsal column nuclei following an electrical stimulation of the median nerve at the wrist in macaque monkeys (Moller et al. 1989) and close to the expected location of the somatosensory representation of the hand in macaque monkeys (Nelson et al. 1980). Moreover, as expected, the scalp SSEP response after tibial nerve stimulation was medial to the one after median nerve stimulation. Nevertheless due to the volume conduction problem and to the distance to the generators, the validity and the spatial resolution of such observations are limited. Classically, the localisation of generators of brain activity was investigated in monkeys using invasive recordings on the surface of or within the cortex (for a review, see e.g. Allison et al. 1991a). Here, we used a distributed source localisation method on the scalp EEG of macaque monkeys. Distributed source localisation methods have been successfully used in many previous human experimental studies (for reviews, see e.g. He et al. 2011; Michel et al. 2001, 2004; Michel and He 2011) and clinical studies in the context of the localisation of epileptic foci (see e.g. Plummer et al. 2010). Our results could be of interest for future lesion-induced plasticity experiments. To the best of our knowledge, LORETA source analyses based on high-density EEG have been used only in two other studies with monkeys (Fontanarosa et al. 2004; Gil-da-Costa et al. 2013). The present study confirms the feasibility of recording scalp EEGs from a high-density electrode array in non-human primates and of localising the cortical generators of EPs with LORETA. Moreover, our study on SSEPs is original from several points of view: first of all, we developed for the first time scalp EEG recordings of SSEPs in adult *M. fascicularis* with a large number of scalp electrodes. Such whole-scalp recordings allow to record large-scale neuronal networks and their reorganisation following a disruption. We can assume that we recorded EEG with a higher density of scalp electrodes as compared to 22 electrodes (Gil-da-Costa et al. 2013) and 32 electrodes (Fontanarosa et al. 2004) in adult *M. mulatta*, that have a larger head than *M. fascicularis* (Hamada et al. 2006), although the size and weight of the animals involved in both studies were not mentioned. Then, we demonstrated that SSEP signals were topographically stable over time in the same animal and across several animals, which is required to prove the validity of our method of EEG mapping of SSEPs in macaque monkeys. To this aim, we introduced for the first time a cluster analysis of monkey SSEPs with detailed statistical analyses of the voltage topographies which are reference-independent instead of waveforms at selected electrodes (Geselowitz 1998; Michel et al. 2004; Murray et al. 2008). Equally important, we developed and applied a LORETA inverse solution to SSEP signals in macaque monkeys. Last but not least, we demonstrated that a replaced, sutured and cemented bone flap following a craniotomy had a negligible effect on the recorded EEG signals in macaque monkeys.

Effect of craniotomy on scalp SSEPs

EEGs in patients with a skull defect or a skull lesion are characterised by a "breach rhythm" that is not suppressed in all cases after skull reconstruction (Brigo et al. 2011;

Cobb et al. 1979; Cobb and Sears 1960; van Doorn and Cherian 2008). The breach rhythm signals are a mu-like activity and exhibit a higher overall power as compared to normal scalp spontaneous EEGs and EPs (Lee et al. 2010a; Pfurtscheller et al. 1982; Tatum et al. 2011; Voytek et al. 2010). These signals reflect probably the reduction of the filtering and of high resistive properties normally exerted by the intact skull, resulting in a higher current flow from the brain to the scalp (Brigo et al. 2011; Chauveau et al. 2004). The amplitude of these signals depends among others on the distance between the recording electrode and the hole, on the hole size and conductivity, and on the orientation and location of the source in relation to the skull defect (Benar and Gotman 2002; Chauveau et al. 2004; Flemming et al. 2005; Heasman et al. 2002; Li et al. 2007; Oostenveld and Oostendorp 2002). Thus, the signal distortion is variable for the different components of EPs, depending on the location of the involved source in relation to the skull defect (Flemming et al. 2005). It is important to take this EEG alteration into account to achieve an accurate EEG source localisation (Benar and Gotman 2002; Chauveau et al. 2004; Chen et al. 2010; Heasman et al. 2002; Oostenveld and Oostendorp 2002). In addition to these breach rhythms, a recent publication (Suzuki et al. 2012) reports that a craniotomy may induce artifactual glial activation (Xu et al. 2007) due to mechanical stimulation (Davalos et al. 2005), and cortical inflammation due to inflammatory blood cell leakage from damaged vessels.

The effect of the craniotomy on SSEP signals was assessed by two complementary approaches: the classical analysis gives information about differences in the signal amplitude and latency between two situations, whereas the topographical analysis illustrates changes in the electrical field distribution (Astle et al. 2009). Classical analyses showed no statistically significant effect of craniotomy. No differences were observed in the topographical parameters studied here except the GEV of map 2 that was higher in post-craniotomy recordings. As reminder, the GEV is the percentage of the data variance explained by a given voltage topography and therefore should indicate the importance of a given map (Brunet 1996, Cartool Reference Guide; Koban et al. 2012). It means that the significance of map 2 was higher after than before the craniotomy but the topography, the latency at first onset, the duration, the SC and the GFP of this map were not affected by the surgery, i.e. the syntax (temporal sequence and duration) of the SSEP component maps did not significantly change after craniotomy.

The observation that craniotomy followed by bone flap repositioning had a negligible effect on the SSEP signals in macaque monkeys shows the beneficial effect of using calcium phosphate cement to plug the entire perimeter of the bone flap. Such hydroxyapatite bone substitutes present several advantages: they can be resorbed and then replaced by natural bone under physiological conditions (osteoconductive properties) because they support bone proliferation; they are biocompatible; they have a long working time (time from start of mixing, allowing to manipulate the cement) and a short setting time; they can be set in a wet field environment; they do not release any heat during setting (isothermic properties) and finally they can be applied by simple injection (Adams et al. 2011; Clarkin et al. 2009a, b; Hannink et al. 2008). Our results contrast with the "breach rhythm" reported by Cobb et al. (1979) in some patients after skull reconstruction following craniotomy. Nevertheless, we should keep in mind that immediately after a surgery breach rhythms can be absent and develop progressively instead (Pfurtscheller et al. 1982). In a recent study using median nerve and tibial nerve SSEPs to evaluate the extent of surgical decompression in children affected by Chiari type 1 malformation (Chen et al. 2012), the bone flap was not replaced at the end of the surgery (craniectomy) in some patients whereas it was (craniotomy) in the others. Nevertheless, there was no difference in the pattern of decrease of SSEP latency during the surgery between both groups of subjects, meaning that the replacement of the bone did not influence SSEPs and therefore that the EP latency decrease observed during the surgery was the result of the decompression on its own (by craniectomy and durotomy). This finding goes in the same direction as the results obtained here in macaque monkeys. The demonstration of negligible effect of the craniotomy on SSEPs is important in the context of a future unilateral lesion of M1 requiring a craniotomy, to distinguish the possible modulations generated by the craniotomy from the consequences of the lesion itself on SSEP responses.

Future perspectives

Based on previous studies (Bazley et al. 2011; Hu et al. 2011), SSEPs are expected to help to investigate the post-lesional cortical reorganisation of neuronal networks, especially to highlight which areas of the monkey's brain may take over the functions of M1 affected by the lesion. From a clinical point of view, we also hope that post-lesional modifications in SSEP signals will help us to predict the level of recovery after the lesion (Carter and Butt 2005; Feys et al. 2000; Lee et al. 2010b, c; Su et al. 2010; Tzvetanov et al. 2005; Tzvetanov and Rousseff 2005; Zhang et al. 2011).

To sum up, the present study demonstrated the feasibility of high-density scalp SSEP recordings during the pre- and post-lesional follow-up of cortical activity in macaque monkeys. Not only is EEG relatively inexpensive and non-invasive as compared to other imaging techniques, allowing repeated acquisitions in the same animal, but it also

allows to study cortical reorganisation at the whole-brain level and with high temporal resolution, i.e. in the ms time scales, a temporal resolution consistent with the speed of information processing (Michel and Murray 2012; Nunez 1993). Therefore, SSEPs might give additional information to ICMS or LSI approaches from a temporal and large-scale networks point of view and will help to unravel the different mechanisms involved in cortical reorganisation following a brain lesion. Future perspectives will include EEG recordings of SSEPs following a unilateral permanent lesion of the hand representation in M1 in macaque monkeys, and subsequently the application of this EEG method in awake monkeys.

Acknowledgments We thank Josef Corpataux, Laurent Bossy, Jacques Maillard (animal care taking), André Gaillard (mechanics), Bernard Aebischer, Jean-Pierre Rossier (electronics), Laurent Monney (informatics) and Gijs Plomp (inverse solution estimation). The Cartool software (https://sites.google.com/site/fbmlab/cartool) has been programmed by Denis Brunet, from the Functional Brain Mapping Laboratory, Geneva, Switzerland, and is supported by the Center for Biomedical Imaging (CIBM) of Geneva and Lausanne. This work was supported by the Swiss National Science Foundation grants 310000-110005, 31003A-132465, 310030B-149643, FZFS-0_144990 (EMR) and 310030-132952 (CMM), the National Centre of Competence in Research (NCCR) "Neural plasticity and repair" and the SPCCR (Swiss Primate Competence Center for Research: www.unifr.ch/neuro/rouiller/SPCCR).

Conflict of interest The authors declare no conflict of interest.

References

Adams DL, Economides JR, Jocson CM, Parker JM, Horton JC (2011) A watertight acrylic-free titanium recording chamber for electrophysiology in behaving monkeys. J Neurophysiol 106:1581–1590. doi:10.1152/jn.00405.2011

Allison T, Hume AL (1981) A comparative analysis of short-latency somatosensory evoked potentials in man, monkey, cat, and rat. Exp Neurol 72:592–611. doi:10.1016/0014-4886(81)90008-X

Allison T, McCarthy G, Wood CC, Jones SJ (1991a) Potentials evoked in human and monkey cerebral cortex by stimulation of the median nerve. A review of scalp and intracranial recordings. Brain 114(6):2465–2503. doi:10.1093/brain/114.6.2465

Allison T, Wood CC, McCarthy G, Spencer DD (1991b) Cortical somatosensory evoked potentials. II. Effects of excision of somatosensory or motor cortex in humans and monkeys. J Neurophysiol 66:64–82

American Clinical Neurophysiology Society (2006) Guideline 5: guidelines for standard electrode position nomenclature. J Clin Neurophysiol 23:107–110. doi:10.1097/00004691-200604000-00006

Arezzo JC, Legatt AD, Vaughan HGJr (1979) Topography and intracranial sources of somatosensory evoked potentials in the monkey. I. Early components. Electroencephalogr Clin Neurophysiol 46:155–172. doi:10.1016/0013-4694(79)90065-8

Arezzo JC, Vaughan HGJr, Legatt AD (1981) Topography and intracranial sources of somatosensory evoked potentials in the monkey. II. Cortical components. Electroencephalogr Clin Neurophysiol 51:1–18. doi:10.1016/0013-4694(81)91505-4

Astle DE, Nobre AC, Scerif G (2009) Applying an attentional set to perceived and remembered features. PLoS ONE 4:e7613. doi:10.1371/journal.pone.0007613

Baurain MJ, Hennart DA, Godschalx A, Huybrechts I, Nasrallah G, d'Hollander AA, Cantraine F (1998) Visual evaluation of residual curarization in anesthetized patients using one hundred-hertz, five-second tetanic stimulation at the adductor pollicis muscle. Anesth Analg 87:185–189. doi:10.1213/00000539-199807000-00038

Bazley FA, All AH, Thakor NV, Maybhate A (2011) Plasticity associated changes in cortical somatosensory evoked potentials following spinal cord injury in rats. Conf Proc IEEE Eng Med Biol Soc 2011:2005–2008. doi:10.1109/IEMBS.2011.6090564

Benar CG, Gotman J (2002) Modeling of post-surgical brain and skull defects in the EEG inverse problem with the boundary element method. Clin Neurophysiol 113:48–56. doi:10.1016/S1388-2457(01)00714-3

Brandeis D, Lehmann D (1986) Event-related potentials of the brain and cognitive processes: approaches and applications. Neuropsychologia 24:151–168. doi:10.1016/0028-3932(86)90049-7

Brigo F, Cicero R, Fiaschi A, Bongiovanni LG (2011) The breach rhythm. Clin Neurophysiol 122:2116–2120. doi:10.1016/j.clinph.2011.07.024

Brunet D (1996) Cartool Reference Guide. https://sites.googlecom/site/fbmlab/cartool/

Brunet D, Murray MM, Michel CM (2011) Spatiotemporal analysis of multichannel EEG: CARTOOL. Comput Intell Neurosci 2011(813870):15. doi:10.1155/2011/813870

Bütefisch CM (2004) Plasticity in the human cerebral cortex: lessons from the normal brain and from stroke. Neuroscientist 10:163–173. doi:10.1177/1073858403262152

Carter BG, Butt W (2005) Are somatosensory evoked potentials the best predictor of outcome after severe brain injury? A systematic review. Intensive Care Med 31:765–775. doi:10.1007/s00134-005-2633-1

Chao ZC, Nagasaka Y, Fujii N (2010) Long-term asynchronous decoding of arm motion using electrocorticographic signals in monkeys. Front Neuroeng 3:3. doi:10.3389/fneng.2010.00003

Chauveau N, Franceries X, Doyon B, Rigaud B, Morucci JP, Celsis P (2004) Effects of skull thickness, anisotropy, and inhomogeneity on forward EEG/ERP computations using a spherical three-dimensional resistor mesh model. Hum Brain Mapp 21:86–97. doi:10.1002/hbm.10152

Chen FM, Hallez H, Staelens S (2010) Influence of skull conductivity perturbations on EEG dipole source analysis. Med Phys 37:4475–4484. doi:10.1118/1.3466831

Chen JA, Coutin-Churchman PE, Nuwer MR, Lazareff JA (2012) Suboccipital craniotomy for Chiari I results in evoked potential conduction changes. Surg Neurol Int 3:165. doi:10.4103/2152-7806.105277

Chow LC, Takagi S (2001) A natural bone cement: a laboratory novelty led to the development of revolutionary new biomaterials. J Res Nat Inst Stand Technol 106:1029–1033. doi:10.6028/jres.106.053

Chu NS (1986) Somatosensory evoked potentials: correlations with height. Electroencephalogr Clin Neurophysiol 65:169–176. doi:10.1016/0168-5597(86)90051-1

Clarkin OM, Boyd D, Madigan S, Towler MR (2009a) Comparison of an experimental bone cement with a commercial control, Hydroset. J Mater Sci Mater Med 20:1563–1570. doi:10.1007/s10856-009-3701-9

Clarkin OM, Boyd D, Towler MR (2009b) Comparison of failure mechanisms for cements used in skeletal luting applications.

J Mater Sci Mater Med 20:1585–1594. doi:10.1007/s10856-009-3724-2

Cobb WA, Sears TA (1960) A study of the transmission of potentials after hemispherectomy. Electroencephalogr Clin Neurophysiol 12:371–383. doi:10.1016/0013-4694(60)90012-2

Cobb WA, Guiloff RJ, Cast J (1979) Breach rhythm: the EEG related to skull defects. Electroencephalogr Clin Neurophysiol 47:251–271. doi:10.1016/0013-4694(79)90278-5

Committee for the Update of the Guide for the Care and Use of Laboratory Animals, National Research Council (2011) Guide for the Care and Use of Laboratory Animals: Eighth Edition. The National Academies Press (ISBN 978-0-309-15400-0)

Cruccu G, Aminoff MJ, Curio G, Guerit JM, Kakigi R, Mauguiere F, Rossini PM, Treede RD, Garcia-Larrea L (2008) Recommendations for the clinical use of somatosensory-evoked potentials. Clin Neurophysiol 119:1705–1719. doi:10.1016/j.clinph.2008.03.016

Davalos D, Grutzendler J, Yang G, Kim JV, Zuo Y, Jung S, Littman DR, Dustin ML, Gan WB (2005) ATP mediates rapid microglial response to local brain injury in vivo. Nat Neurosci 8:752–758. doi:10.1038/nn1472

Dickson KF, Friedman J, Buchholz JG, Flandry FD (2002) The use of BoneSource hydroxyapatite cement for traumatic metaphyseal bone void filling. J Trauma 53:1103–1108. doi:10.1097/01.TA.0000033760.65011.52

Eisner-Janowicz I, Barbay S, Hoover E, Stowe AM, Frost SB, Plautz EJ, Nudo RJ (2008) Early and late changes in the distal forelimb representation of the supplementary motor area after injury to frontal motor areas in the squirrel monkey. J Neurophysiol 100:1498–1512. doi:10.1152/jn.90447.2008

Ferrari PF, Vanderwert RE, Paukner A, Bower S, Suomi SJ, Fox NA (2012) Distinct EEG amplitude suppression to facial gestures as evidence for a mirror mechanism in newborn monkeys. J Cogn Neurosci 24:1165–1172. doi:10.1162/jocn_a_00198

Feys H, Van Hees J, Bruyninckx F, Mercelis R, De WW (2000) Value of somatosensory and motor evoked potentials in predicting arm recovery after a stroke. J Neurol Neurosurg Psychiatry 68:323–331. doi:10.1136/jnnp.68.3.323

Finke S, Gulrajani RM, Gotman J, Savard P (2013) Conventional and reciprocal approaches to the inverse dipole localization problem for N(20)-P (20) somatosensory evoked potentials. Brain Topogr 26:24–34. doi:10.1007/s10548-012-0238-x

Flemming L, Wang Y, Caprihan A, Eiselt M, Haueisen J, Okada Y (2005) Evaluation of the distortion of EEG signals caused by a hole in the skull mimicking the fontanel in the skull of human neonates. Clin Neurophysiol 116:1141–1152. doi:10.1016/j.clinph.2005.01.007

Fontanarosa JB, Lasky RE, Lee HC, van Drongelen W (2004) Localization of brainstem auditory evoked potentials in primates: a comparison of localization techniques applied to deep brain sources. Brain Topogr 17:99–108. doi:10.1007/s10548-004-1007-2

Friel KM, Barbay S, Frost SB, Plautz EJ, Hutchinson DM, Stowe AM, Dancause N, Zoubina EV, Quaney BM, Nudo RJ (2005) Dissociation of sensorimotor deficits after rostral versus caudal lesions in the primary motor cortex hand representation. J Neurophysiol 94:1312–1324. doi:10.1152/jn.01251.2004

Geselowitz DB (1998) The zero of potential. IEEE Eng Med Biol Mag 17:128–132. doi:10.1109/51.646230

Ghosh S, Porter R (1988) Corticocortical synaptic influences on morphologically identified pyramidal neurones in the motor cortex of the monkey. J Physiol 400:617–629

Gil-da-Costa R, Stoner GR, Fung R, Albright TD (2013) Nonhuman primate model of schizophrenia using a noninvasive EEG method. Proc Natl Acad Sci USA 110:15425–15430. doi:10.1073/pnas.1312264110

Hamada Y, Urasopon N, Hadi I, Malaivijitnond S (2006) Body size and proportions and pelage color of free-ranging Macaca mulatta from a zone of hybridization in northeastern Thailand. Int J Primatol 27:497–513. doi:10.1007/s10764-006-9033-4

Hamadjida A, Wyss AF, Mir A, Schwab ME, Belhaj-Saif A, Rouiller EM (2012) Influence of anti-Nogo-A antibody treatment on the reorganization of callosal connectivity of the premotor cortical areas following unilateral lesion of primary motor cortex (M1) in adult macaque monkeys. Exp Brain Res 223:321–340. doi:10.1007/s00221-012-3262-x

Hannink G, Wolke JG, Schreurs BW, Buma P (2008) In vivo behaviour of a novel injectable calcium phosphate cement compared with two other commercially available calcium phosphate cements. J Biomed Mater Res B Appl Biomater 85:478–488. doi:10.1002/jbm.b.30969

Hardmeier M, Hatz F, Naegelin Y, Hight D, Schindler C, Kappos L, Seeck M, Michel CM, Fuhr P (2013) Improved characterization of visual evoked potentials in multiple sclerosis by topographic analysis. Brain Topogr 27:318–327. doi:10.1007/s10548-013-0318-6

He B, Zhang X, Lian J, Sasaki H, Wu D, Towle VL (2002) Boundary element method-based cortical potential imaging of somatosensory evoked potentials using subjects' magnetic resonance images. Neuroimage 16:564–576. doi:10.1006/nimg.2002.1127

He B, Yang L, Wilke C, Yuan H (2011) Electrophysiological imaging of brain activity and connectivity-challenges and opportunities. IEEE Trans Biomed Eng 58:1918–1931. doi:10.1109/TBME.2011.2139210

Heasman BC, Valentin A, Alarcon G, Garcia Seoane JJ, Binnie CD, Guy CN (2002) A hole in the skull distorts substantially the distribution of extracranial electrical fields in an in vitro model. J Clin Neurophysiol 19:163–171. doi:10.1097/00004691-200203000-00008

Helmholtz H (1853) Ueber einige Gesetze der Vertheilung elektrischer Ströme in körperlichen Leitern mit Anwendung auf die thierisch-elektrischen Versuche. Ann Phys 165:211–233. doi:10.1002/andp.18531650702

Hernandez-Godinez B, Ibanez-Contreras A, Durand-Rivera A, Reyes-Pantoja SA, Ramirez-Hernandez R, Rodriguez-Guzman P, Tena-Betancourt E (2011) Somatosensory evoked potentials of median and tibial nerves in rhesus monkeys (*Macaca mulatta*) under captivity: influence of ontogenic status in neonatal, infant, young, adult, and senile stages. J Med Primatol 40:79–87. doi:10.1111/j.1600-0684.2010.00458.x

Hu Y, Wen CY, Li TH, Cheung MM, Wu EX, Luk KD (2011) Somatosensory-evoked potentials as an indicator for the extent of ultrastructural damage of the spinal cord after chronic compressive injuries in a rat model. Clin Neurophysiol 122:1440–1447. doi:10.1016/j.clinph.2010.12.051

Huerta MF, Pons TP (1990) Primary motor cortex receives input from area 3a in macaques. Brain Res 537:367–371. doi:10.1016/0006-8993(90)90388-R

Huffman KJ, Krubitzer L (2001) Area 3a: topographic organization and cortical connections in marmoset monkeys. Cereb Cortex 11:849–867. doi:10.1093/cercor/11.9.849

Jung R, Aull-Watschinger S, Moser D, Czech T, Baumgartner C, Bonelli-Nauer S, Pataraia E (2013) Is reoperation an option for patients with temporal lobe epilepsy after failure of surgery? Seizure 22:502–506. doi:10.1016/j.seizure.2012.11.011

Jurcak V, Tsuzuki D, Dan I (2007) 10/20, 10/10, and 10/5 systems revisited: their validity as relative head-surface-based positioning systems. Neuroimage 34:1600–1611. doi:10.1016/j.neuroimage.2006.09.024

Kaas JH (2004) Evolution of the large, complex sensorimotor systems of anthropoid primates. In: Pellis S, Marino L (eds) Special issue: evolution of the vertebrate brain and behaviour. International Journal of Comparative Psychology 17, pp 34–52

Kaeser M, Wyss AF, Bashir S, Hamadjida A, Liu Y, Bloch J, Brunet JF, Belhaj-Saif A, Rouiller EM (2010) Effects of unilateral motor cortex lesion on ipsilesional hand's reach and grasp performance in monkeys: relationship with recovery in the contralesional hand. J Neurophysiol 103:1630–1645. doi:10.1152/jn.00459.2009

Kaeser M, Brunet JF, Wyss A, Belhaj-Saif A, Liu Y, Hamadjida A, Rouiller EM, Bloch J (2011) Autologous adult cortical cell transplantation enhances functional recovery following unilateral lesion of motor cortex in primates: a pilot study. Neurosurgery 68:1405–1416. doi:10.1227/NEU.0b013e31820c02c0

Koban L, Pourtois G, Bediou B, Vuilleumier P (2012) Effects of social context and predictive relevance on action outcome monitoring. Cogn Affect Behav Neurosci 12:460–478. doi:10.3758/s13415-012-0091-0

Koenig T, Gianotti LRR (2009) Scalp field maps and their characterization. In: Michel CM, Koenig T, Brandeis D, Gianotti LRR, Wackermann J (eds) Electrical neuroimaging. Cambridge University Press, Cambridge, pp 25–48 (ISBN 978-0-521-87979-8)

Koenig T, Stein M, Grieder M, Kottlow M (2013) A tutorial on data-driven methods for statistically assessing ERP topographies. Brain Topogr 27:72–83. doi:10.1007/s10548-013-0310-1

Krakauer J, Ghez C (2000) Voluntary movement. In: Kandel ER, Schwartz M, Jessell TM (eds) Principles of neural science, 4th edn. McGraw-Hill Medical, New York, pp 756–781 (ISBN 0-8385-7701-6)

Krubitzer L, Disbrow EA (2005) The evolution of parietal areas involved in hand use in primates. In: Kaas JH, Gardner EP (eds) The senses: a comprehensive reference, vol 6, somatosensation. Elsevier, New York, pp 183–214. doi:10.1016/B978-012370880-9.00352-2

Krubitzer LA, Kaas JH (1990) The organization and connections of somatosensory cortex in marmosets. J Neurosci 10:952–974

Krzanowski WJ, Lai YT (1988) A criterion for determining the number of groups in a data set using sum-of-squares clustering. Biometrics 44:23–34. doi:10.2307/2531893

Laible M, Grieshammer S, Seidel G, Rijntjes M, Weiller C, Hamzei F (2012) Association of activity changes in the primary sensory cortex with successful motor rehabilitation of the hand following stroke. Neurorehabil Neural Repair 26:881–888. doi:10.1177/1545968312437939

Larsson S (2006) Injectable phosphate cements: a review. Uppsala, Sweden 2006:1–12

Lascano AM, Brodbeck V, Lalive PH, Chofflon M, Seeck M, Michel CM (2009) Increasing the diagnostic value of evoked potentials in multiple sclerosis by quantitative topographic analysis of multichannel recordings. J Clin Neurophysiol 26:316–325. doi:10.1097/WNP.0b013e3181baac00

Lascano AM, Hummel T, Lacroix JS, Landis BN, Michel CM (2010) Spatio-temporal dynamics of olfactory processing in the human brain: an event-related source imaging study. Neuroscience 167:700–708. doi:10.1016/j.neuroscience.2010.02.013

Lee JW, Tanaka N, Shiraishi H, Milligan TA, Dworetzky BA, Khoshbin S, Stufflebeam SM, Bromfield EB (2010a) Evaluation of postoperative sharp waveforms through EEG and magnetoencephalography. J Clin Neurophysiol 27:7–11. doi:10.1097/WNP.0b013e3181c9b283

Lee SY, Lim JY, Kang EK, Han MK, Bae HJ, Paik NJ (2010b) Prediction of good functional recovery after stroke based on combined motor and somatosensory evoked potential findings. J Rehabil Med 42:16–20. doi:10.2340/16501977-0475

Lee YC, Phan TG, Jolley DJ, Castley HC, Ingram DA, Reutens DC (2010c) Accuracy of clinical signs, SEP, and EEG in predicting outcome of hypoxic coma: a meta-analysis. Neurology 74:572–580. doi:10.1212/WNL.0b013e3181cff761

Lehmann D, Skrandies W (1980) Reference-free identification of components of checkerboard-evoked multichannel potential fields. Electroencephalogr Clin Neurophysiol 48:609–621. doi:10.1016/0013-4694(80)90419-8

Lehmann D, Ozaki H, Pal I (1987) EEG alpha map series: brain micro-states by space-oriented adaptive segmentation. Electroencephalogr Clin Neurophysiol 67:271–288. doi:10.1016/0013-4694(87)90025-3

Lehmann D, Pascual-Marqui RD, Michel CM (2009) EEG microstates. Scholarpedia 4:7632. doi:10.4249/scholarpedia.7632

Lemon RN (2008) Descending pathways in motor control. Annu Rev Neurosci 31:195–218. doi:10.1146/annurev.neuro.31.060407.125547

Li J, Wang K, Zhu S, He B (2007) Effects of holes on EEG forward solutions using a realistic geometry head model. J Neural Eng 4:197–204. doi:10.1088/1741-2560/4/3/004

Liu Y, Rouiller EM (1999) Mechanisms of recovery of dexterity following unilateral lesion of the sensorimotor cortex in adult monkeys. Exp Brain Res 128:149–159. doi:10.1007/s002210050830

Lopez C, Mercier MR, Halje P, Blanke O (2011) Spatiotemporal dynamics of visual vertical judgments: early and late brain mechanisms as revealed by high-density electrical neuroimaging. Neuroscience 181:134–149. doi:10.1016/j.neuroscience.2011.02.009

Martin-Flores M, Campoy L, Ludders JW, Erb HN, Gleed RD (2008) Comparison between acceleromyography and visual assessment of train-of-four for monitoring neuromuscular blockade in horses undergoing surgery. Vet Anaesth Analg 35:220–227. doi:10.1111/j.1467-2995.2007.00380.x

McCarthy G, Wood CC, Allison T (1991) Cortical somatosensory evoked potentials. I. Recordings in the monkey *Macaca fascicularis*. J Neurophysiol 66:53–63

Megevand P, Quairiaux C, Lascano AM, Kiss JZ, Michel CM (2008) A mouse model for studying large-scale neuronal networks using EEG mapping techniques. Neuroimage 42:591–602. doi:10.1016/j.neuroimage.2008.05.016

Megevand P, Troncoso E, Quairiaux C, Muller D, Michel CM, Kiss JZ (2009) Long-term plasticity in mouse sensorimotor circuits after rhythmic whisker stimulation. J Neurosci 29:5326–5335. doi:10.1523/JNEUROSCI.5965-08.2009

Michel CM, He B (2011) EEG mapping and source imaging. In: Schomer DL, Da Silva Lopes FH (eds) Niedermeyer's electroencephalography: basic principles, clinical applications, and related fields, 6th edn. Lippincott Williams & Wilkins, New York, pp 1179–1202 (ISBN 978-0-7817-8942-4)

Michel CM, Murray MM (2012) Towards the utilization of EEG as a brain imaging tool. Neuroimage 61:371–385. doi:10.1016/j.neuroimage.2011.12.039

Michel CM, Seeck M, Landis T (1999) Spatiotemporal dynamics of human cognition. News Physiol Sci 14:206–214

Michel CM, Thut G, Morand S, Khateb A, Pegna AJ, Grave de Peralta R, Gonzalez S, Seeck M, Landis T (2001) Electric source imaging of human brain functions. Brain Res Brain Res Rev 36:108–118. doi:10.1016/S0165-0173(01)00086-8

Michel CM, Murray MM, Lantz G, Gonzalez S, Spinelli L, Grave de Peralta R (2004) EEG source imaging. Clin Neurophysiol 115:2195–2222. doi:10.1016/j.clinph.2004.06.001

Michel CM, Koenig T, Brandeis D (2009) Electrical neuroimaging in the time domain. In: Michel CM, Koenig T, Brandeis D, Gianotti LRR, Wackermann J (eds) Electrical neuroimaging. Cambridge University Press, Cambridge, pp 111–144 ISBN 978-0-521-87979-8

Moller AR, Sekiya T, Sen CN (1989) Responses from dorsal column nuclei (DCN) in the monkey to stimulation of upper and lower

limbs and spinal cord. Electroencephalogr Clin Neurophysiol 73:353–361. doi:10.1016/0013-4694(89)90113-2
Moosa AN, Gupta A, Jehi L, Marashly A, Cosmo G, Lachhwani D, Wyllie E, Kotagal P, Bingaman W (2013) Longitudinal seizure outcome and prognostic predictors after hemispherectomy in 170 children. Neurology 80:253–260. doi:10.1212/WNL.0b013e31827dead9
Murray PD, Keller A (2011) Somatosensory response properties of excitatory and inhibitory neurons in rat motor cortex. J Neurophysiol 106:1355–1362. doi:10.1152/jn.01089.2010
Murray MM, Brunet D, Michel CM (2008) Topographic ERP analyses: a step-by-step tutorial review. Brain Topogr 20:249–264. doi:10.1007/s10548-008-0054-5
Murray MM, De LM, Brunet D, Michel CM (2009) Principles of topographic analyses for electrical neuroimaging. In: Handy TC (ed) Brain signal analysis: advances in neuroelectric and neuromagnetic methods. MIT Press, Cambridge, pp 21–52 (ISBN:978-0-262-01308-6)
Nelson RJ, Sur M, Felleman DJ, Kaas JH (1980) Representations of the body surface in postcentral parietal cortex of Macaca fascicularis. J Comp Neurol 192:611–643. doi:10.1002/cne.901920402
Nudo RJ (2006) Plasticity. NeuroRx 3:420–427. doi:10.1016/j.nurx.2006.07.006
Nudo RJ (2007) Post infarct cortical plasticity and behavioral recovery. Stroke 38:840–845. doi:10.1161/01.STR.0000247943.12887.d2
Nudo RJ, Milliken GW (1996) Reorganization of movement representations in primary motor cortex following focal ischemic infarcts in adult squirrel monkeys. J Neurophysiol 75:2144–2149
Nudo RJ, Friel KM, Delia SW (2000) Role of sensory deficits in motor impairments after injury to primary motor cortex. Neuropharmacology 39:733–742. doi:10.1016/S0028-3908(99)00254-3
Nunez PL (1993) High-resolution EEG: applications in medicine and cognitive science. In: Proceedings of SPIE 1887, physiological imaging, spectroscopy, and early-detection diagnostic Methods, 22 (Aug 27, 1993), pp 22–39. doi:10.1117/12.151186
Oostenveld R, Oostendorp TF (2002) Validating the boundary element method for forward and inverse EEG computations in the presence of a hole in the skull. Hum Brain Mapp 17:179–192. doi:10.1002/hbm.10061
Pascual-Leone A, Amedi A, Fregni F, Merabet LB (2005) The plastic human brain cortex. Annu Rev Neurosci 28:377–401. doi:10.1146/annurev.neuro.27.070203.144216
Pascual-Marqui RD, Michel CM, Lehmann D (1994) Low resolution electromagnetic tomography: a new method for localizing electrical activity in the brain. Int J Psychophysiol 18:49–65. doi:10.1016/0167-8760(84)90014-X
Pascual-Marqui RD, Michel CM, Lehmann D (1995) Segmentation of brain electrical activity into microstates: model estimation and validation. IEEE Trans Biomed Eng 42:658–665. doi:10.1109/10.391164
Pascual-Marqui RD, Sekihara K, Brandeis D, Michel CM (2009) Imaging the electric neuronal generators of EEG/MEG. In: Michel CM, Koenig T, Brandeis D, Gianotti LRR, Wackermann J (eds) Electrical neuroimaging. Cambridge University Press, Cambridge, pp 49–78 (ISBN 978-0-521-87979-8)
Peuser J, Belhaj-Saif A, Hamadjida A, Schmidlin E, Gindrat AD, Volker AC, Zakharov P, Hoogewoud HM, Rouiller EM, Scheffold F (2011) Follow-up of cortical activity and structure after lesion with laser speckle imaging and magnetic resonance imaging in nonhuman primates. J Biomed Opt 16:096011. doi:10.1117/1.3625287
Pfurtscheller G, Auer L, Oberbauer R (1982) The influence of skull defects and reperfusion after extra-intracranial arterial bypass surgery on the sensorimotor EEG rhythm. J Neurol Neurosurg Psychiatry 45:1106–1112. doi:10.1136/jnnp.45.12.1106
Plomp G, Michel CM, Herzog MH (2010) Electrical source dynamics in three functional localizer paradigms. Neuroimage 53:257–267. doi:10.1016/j.neuroimage.2010.06.037
Plummer C, Wagner M, Fuchs M, Vogrin S, Litewka L, Farish S, Bailey C, Harvey AS, Cook MJ (2010) Clinical utility of distributed source modelling of interictal scalp EEG in focal epilepsy. Clin Neurophysiol 121:1726–1739. doi:10.1016/j.clinph.2010.04.002
Quairiaux C, Sizonenko SV, Megevand P, Michel CM, Kiss JZ (2010) Functional deficit and recovery of developing sensorimotor networks following neonatal hypoxic-ischemic injury in the rat. Cereb Cortex 20:2080–2091. doi:10.1093/cercor/bhp281
Quairiaux C, Megevand P, Kiss JZ, Michel CM (2011) Functional development of large-scale sensorimotor cortical networks in the brain. J Neurosci 31:9574–9584. doi:10.1523/JNEUROSCI.5995-10.2011
Reinhart RM, Heitz RP, Purcell BA, Weigand PK, Schall JD, Woodman GF (2012) Homologous mechanisms of visuospatial working memory maintenance in macaque and human: properties and sources. J Neurosci 32:7711–7722. doi:10.1523/JNEUROSCI.0215-12.2012
Rouiller EM, Olivier E (2004) Functional recovery after lesions of the primary motor cortex. Prog Brain Res 143:467–475. doi:10.1016/S0079-6123(03)43044-6
Rouiller EM, Yu XH, Moret V, Tempini A, Wiesendanger M, Liang F (1998) Dexterity in adult monkeys following early lesion of the motor cortical hand area: the role of cortex adjacent to the lesion. Eur J Neurosci 10:729–740. doi:10.1046/j.1460-9568.1998.00075.x
Roulet-Perez E, Davidoff V, Mayor-Dubois C, Maeder-Ingvar M, Seeck M, Ruffieux C, Villemure JG, Deonna T (2010) Impact of severe epilepsy on development: recovery potential after successful early epilepsy surgery. Epilepsia 51:1266–1276. doi:10.1111/j.1528-1167.2009.02487.x
Schmidlin E, Kaeser M, Gindrat AD, Savidan J, Chatagny P, Badoud S, Hamadjida A, Beaud ML, Wannier T, Belhaj-Saif A, Rouiller EM (2011) Behavioral assessment of manual dexterity in non-human primates. J Vis Exp 57:e3258. doi:10.3791/3258
Seo JP, Jang SH (2013) Different characteristics of the corticospinal tract according to the cerebral origin: DTI study. AJNR Am J Neuroradiol 34:1359–1363. doi:10.3174/ajnr.A3389
Sheybani L, Korff C, Maier O, Vargas MI, Schaller K, Seeck M (2012) Postoperative EEG in hemimegalencephaly. Eur Neurol 68:358–360. doi:10.1159/000342239
Shimazu H, Kaji R, Tsujimoto T, Kohara N, Ikeda A, Kimura J, Shibasaki H (2000) High-frequency SEP components generated in the somatosensory cortex of the monkey. Neuro Report 11:2821–2826. doi:10.1097/00001756-200008210-00042
Shimazu H, Maier MA, Cerri G, Kirkwood PA, Lemon RN (2004) Macaque ventral premotor cortex exerts powerful facilitation of motor cortex outputs to upper limb motoneurons. J Neurosci 24:1200–1211. doi:10.1523/JNEUROSCI.4731-03.2004
Shinoura N, Suzuki Y, Yamada R, Kodama T, Takahashi M, Yagi K (2005) Fibers connecting the primary motor and sensory areas play a role in grasp stability of the hand. Neuroimage 25:936–941. doi:10.1016/j.neuroimage.2004.12.060
Simasathien T, Vadera S, Najm I, Gupta A, Bingaman W, Jehi L (2013) Improved outcomes with earlier surgery for intractable frontal lobe epilepsy. Ann Neurol 73:646–654. doi:10.1002/ana.23862
Sloper JJ (1973) An electron microscope study of the termination of afferent connections to the primate motor cortex. J Neurocytol 2:361–368. doi:10.1007/BF01103794
Stepniewska I, Preuss TM, Kaas JH (1993) Architectonics, somatotopic organization, and ipsilateral cortical connections of the

primary motor area (M1) of owl monkeys. J Comp Neurol 330:238–271. doi:10.1002/cne.903300207

Su YY, Xiao SY, Haupt WF, Zhang Y, Zhao H, Pang Y, Wang L, Ding JP, Zhao JW (2010) Parameters and grading of evoked potentials: prediction of unfavorable outcome in patients with severe stroke. J Clin Neurophysiol 27:25–29. doi:10.1097/WNP.0b013e3181cb4282

Suzuki T, Sakata H, Kato C, Connor JA, Morita M (2012) Astrocyte activation and wound healing in intact-skull mouse after focal brain injury. Eur J Neurosci 36:3653–3664. doi:10.1111/j.1460-9568.2012.08280.x

Tamura R, Nishida H, Eifuku S, Fushiki H, Watanabe Y, Uchiyama K (2013) Sleep-stage correlates of hippocampal electroencephalogram in primates. PLoS ONE 8:e82994. doi:10.1371/journal.pone.0082994

Tatum WO, Dworetzky BA, Schomer DL (2011) Artifact and recording concepts in EEG. J Clin Neurophysiol 28:252–263. doi:10.1097/WNP.0b013e31821c3c93

Toepel U, Knebel JF, Hudry J, le CJ, Murray MM (2012) Gender and weight shape brain dynamics during food viewing. PLoS ONE 7:e36778. doi:10.1371/journal.pone.0036778

Tsui BCH (2007) Electrical nerve stimulation. In: Tsui BCH, Chan V, Finucane BT, Grau T, Walji AH (eds) Atlas of ultrasound- and nerve stimulation-guided regional anesthesia. Springer, Berlin, pp 9–18 (ISBN 978-0-387-68158-0)

Tzvetanov P, Rousseff RT (2005) Predictive value of median-SSEP in early phase of stroke: a comparison in supratentorial infarction and hemorrhage. Clin Neurol Neurosurg 107:475–481. doi:10.1016/j.clineuro.2004.12.008

Tzvetanov P, Rousseff RT, Atanassova P (2005) Prognostic value of median and tibial somatosensory evoked potentials in acute stroke. Neurosci Lett 380:99–104. doi:10.1016/j.neulet.2005.01.023

Ueno A, Hirata S, Fuwa K, Sugama K, Kusunoki K, Matsuda G, Fukushima H, Hiraki K, Tomonaga M, Hasegawa T (2008) Auditory ERPs to stimulus deviance in an awake chimpanzee (Pan troglodytes): towards hominid cognitive neurosciences. PLoS ONE 3:e1442. doi:10.1371/journal.pone.0001442

van de Wassenberg WJ, Kruizinga WJ, van der Hoeven JH, Leenders KL, Maurits NM (2008a) Multichannel recording of tibial-nerve somatosensory evoked potentials. Neurophysiol Clin 38:277–288. doi:10.1016/j.neucli.2008.07.002

van de Wassenberg WJ, van der Hoeven J, Leenders K, Maurits N (2008b) Multichannel recording of median nerve somatosensory evoked potentials. Neurophysiol Clin 38:9–21. doi:10.1016/j.neucli.2007.08.002

van de Wassenberg WJ, van der Hoeven JH, Leenders KL, Maurits NM (2009) 128-channel somatosensory evoked potentials in the differential diagnosis of parkinsonian disorders. Parkinsonism Relat Disord 15:564–571. doi:10.1016/j.parkreldis.2009.02.002

van Doorn J, Cherian PJ (2008) Neurological picture. Breach rhythm related to a solitary skull lesion caused by multiple myeloma. J Neurol Neurosurg Psychiatry 79:819. doi:10.1136/jnnp.2007.129528

Van Lieshout EM, Van Kralingen GH, El-Massoudi Y, Weinans H, Patka P (2011) Microstructure and biomechanical characteristics of bone substitutes for trauma and orthopaedic surgery. BMC Musculoskelet Disord 12:34. doi:10.1186/1471-2474-12-34

Vaughan HGJr (1982) The neural origins of human event-related potentials. Ann N Y Acad Sci 388:125–138. doi:10.1111/j.1749-6632.1982.tb50788.x

Voytek B, Secundo L, Bidet-Caulet A, Scabini D, Stiver SI, Gean AD, Manley GT, Knight RT (2010) Hemicraniectomy: a new model for human electrophysiology with high spatio-temporal resolution. J Cogn Neurosci 22:2491–2502. doi:10.1162/jocn.2009.21384

Wyss AF, Hamadjida A, Savidan J, Liu Y, Bashir S, Mir A, Schwab ME, Rouiller EM, Belhaj-Saif A (2013) Long-term motor cortical map changes following unilateral lesion of the hand representation in the motor cortex in macaque monkeys showing functional recovery of hand functions. Restor Neurol Neurosci 31:733–760. doi:10.3233/RNN-130344

Xu HT, Pan F, Yang G, Gan WB (2007) Choice of cranial window type for in vivo imaging affects dendritic spine turnover in the cortex. Nat Neurosci 10:549–551. doi:10.1038/nn1883

Zhang Y, Su YY, Ye H, Xiao SY, Chen WB, Zhao JW (2011) Predicting comatose patients with acute stroke outcome using middle-latency somatosensory evoked potentials. Clin Neurophysiol 122:1645–1649. doi:10.1016/j.clinph.2010.11.016

Supplementary Figures

Whole-scalp EEG mapping of somatosensory evoked potentials in macaque monkeys

Gindrat Anne-Dominique[1,*], Quairiaux Charles[2,3,*], Britz Juliane[3,4], Brunet Denis[3,4], Lanz Florian[1], Michel Christoph M.[3,4,&] and Rouiller Eric M.[1,&]

[1] Domain of Physiology, Department of Medicine, Faculty of Sciences and Fribourg Center for Cognition, University of Fribourg, Chemin du Musée 5, CH-1700 Fribourg, Switzerland.

[2] Faculty of Medicine, Department of Fundamental Neurosciences, University of Geneva, rue Michel-Servet 1, CH-1206 Geneva, Switzerland

[3] Functional Brain Mapping Laboratory, Departments of Clinical and Fundamental Neurosciences, University Medical School, rue Michel-Servet 1, CH-1206 Geneva, Switzerland

[4] EEG Brain Mapping Core, Center for Biomedical Imaging (CIBM), University Hospital and University of Geneva, CH-1211 Geneva, Switzerland

* Equal first authorship

& Equal senior authorship

Correspondence:

Prof. Eric M. Rouiller (same address as above): eric.rouiller@unifr.ch, phone: + 41 26 300 86 09

or

Prof. C. Michel (same address as above): Christoph.Michel@unige.ch, phone: +41 22 379 54 57

Supplementary Fig. 1 Intraindividual stability of left median nerve SSEPs in Mk-EN. Colour-scaled voltage maps of each of the 9 individual SSEP recording sessions from different days used to compute the GA shown in Figure 2A, obtained from 7 to 40 ms post-stimulus at 3-ms interval. Same conventions as in Figure 2.

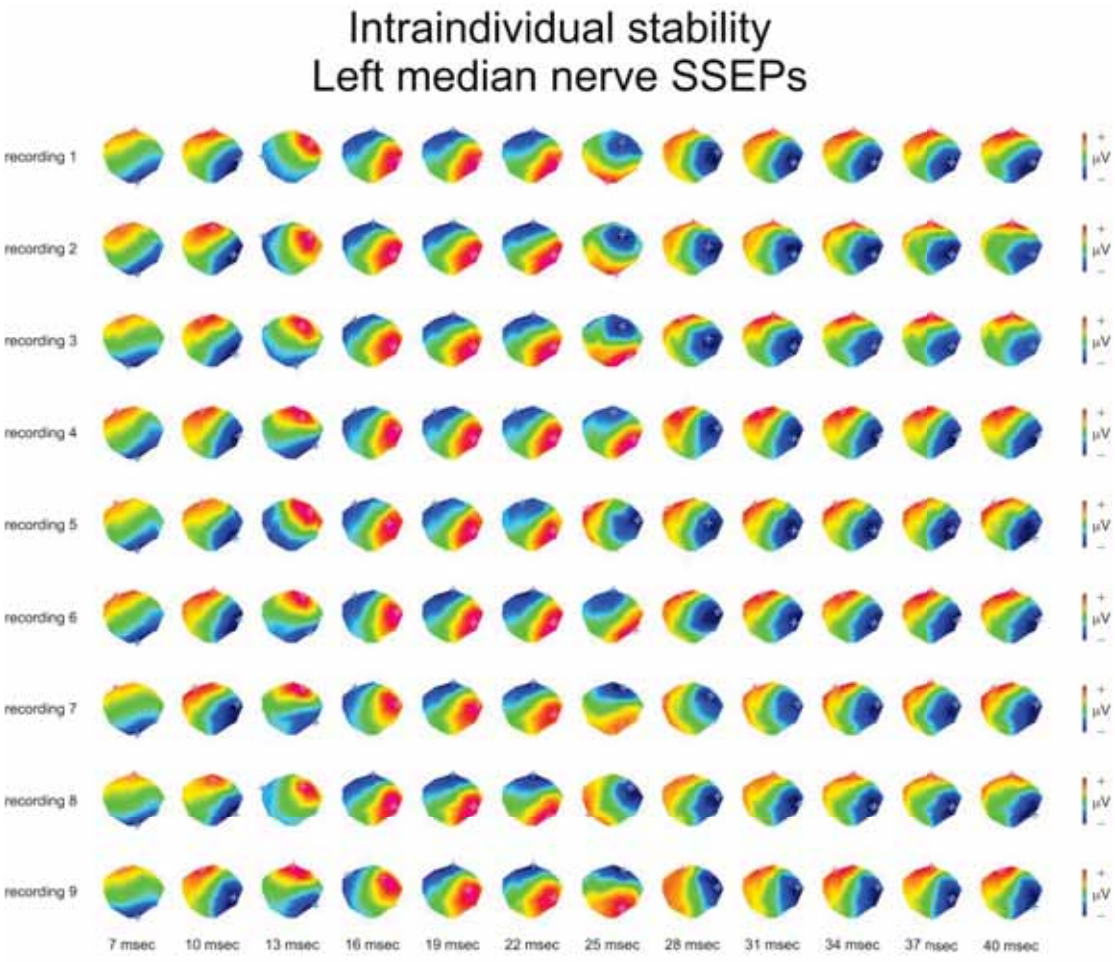

Suppl Fig 1

Supplementary Fig. 2 Intraindividual stability of right median nerve SSEPs in Mk-EN. Colour-scaled voltage maps of each of the 9 individual SSEP recording sessions from different days used to compute the GA shown in Figure 2B, obtained from 7 to 40 ms post-stimulus at 3-ms interval. Same conventions as in Figure 2.

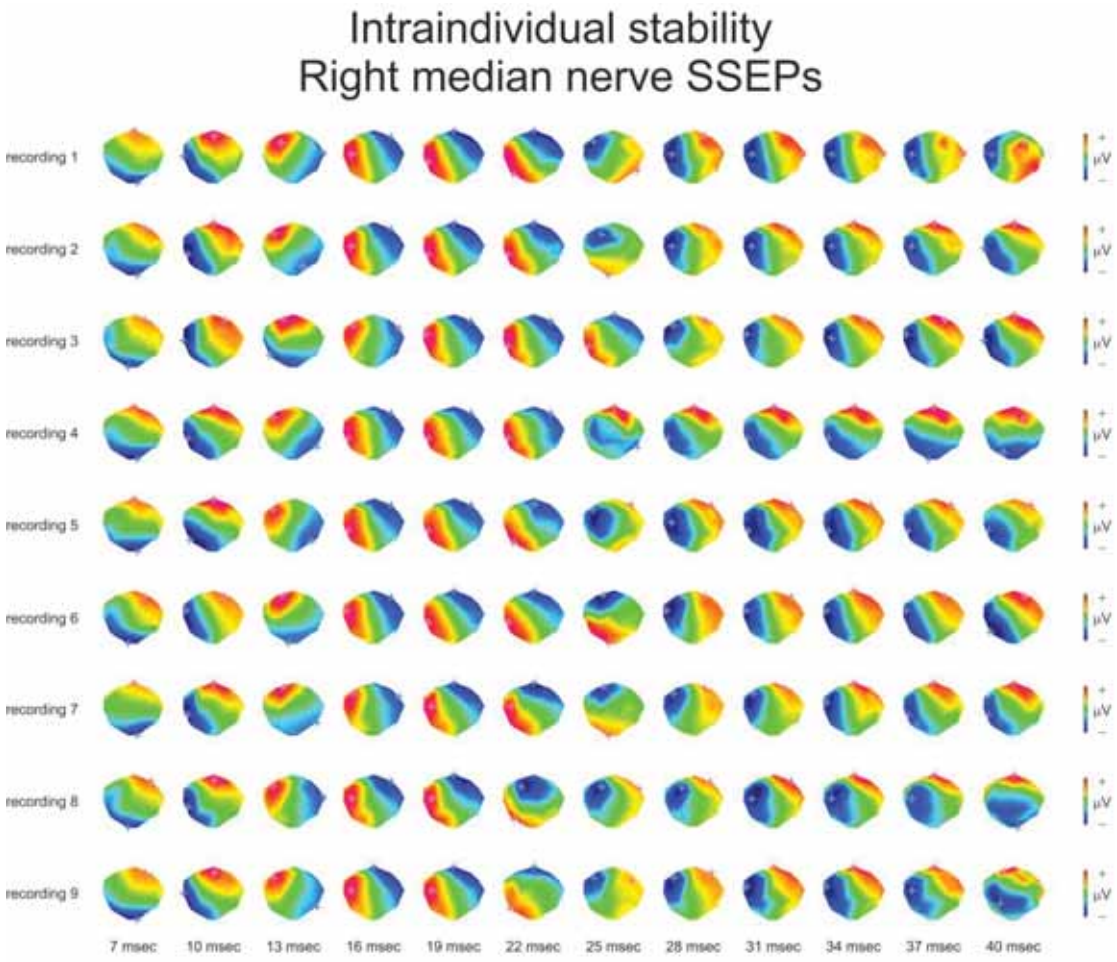

Suppl Fig 2

Supplementary Fig. 3 Intraindividual stability of left tibial nerve SSEPs in Mk-EN. Colour-scaled voltage maps of each of the 9 individual SSEP recording sessions from different days used to compute the GA shown in Figure 4A, obtained from 12 to 45 ms post-stimulus at 3-ms interval. Same conventions as in Figure 2.

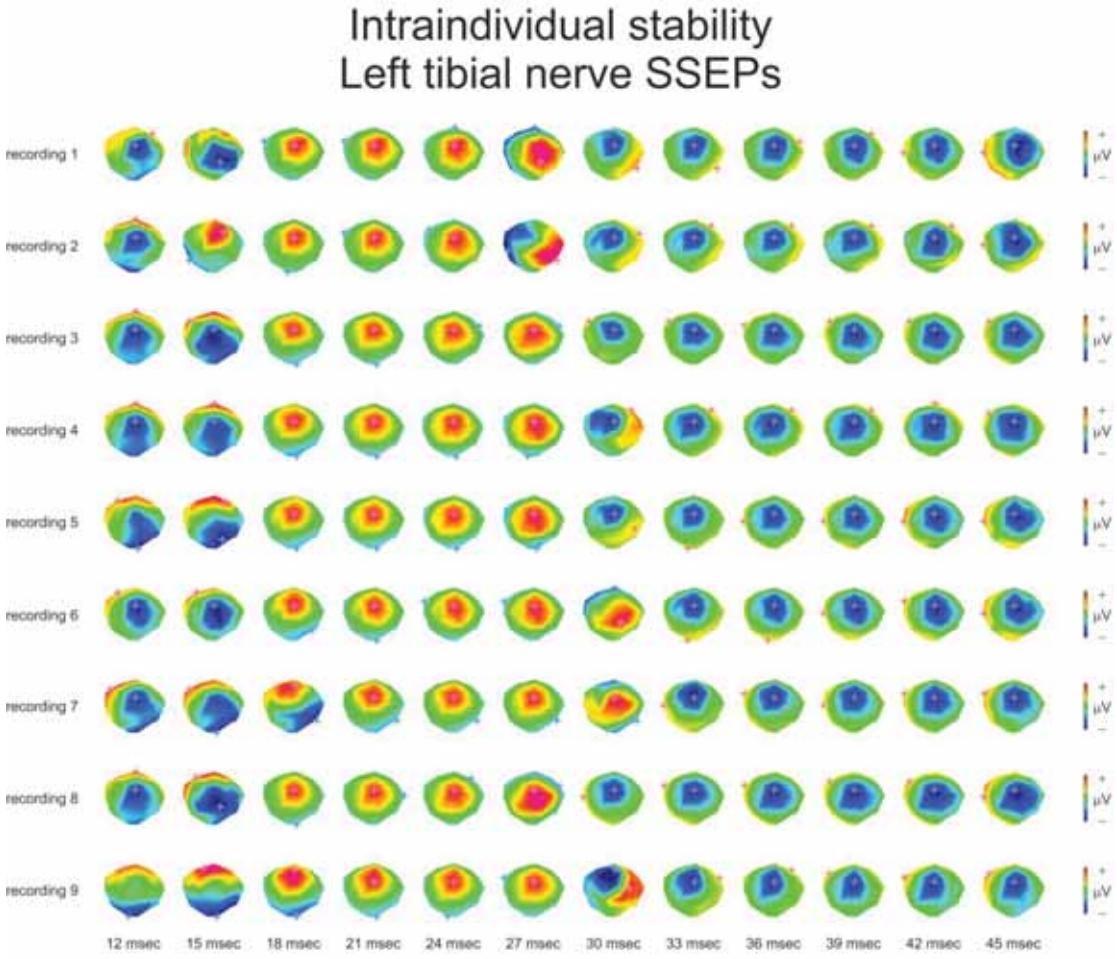

Supplementary Fig. 4 Intraindividual stability of right tibial nerve SSEPs in Mk-EN. Colour-scaled voltage maps of each of the 9 individual SSEP recording sessions from different days used to compute the GA shown in Figure 4B, obtained from 12 to 45 ms post-stimulus at 3-ms interval. Same conventions as in Figure 2.

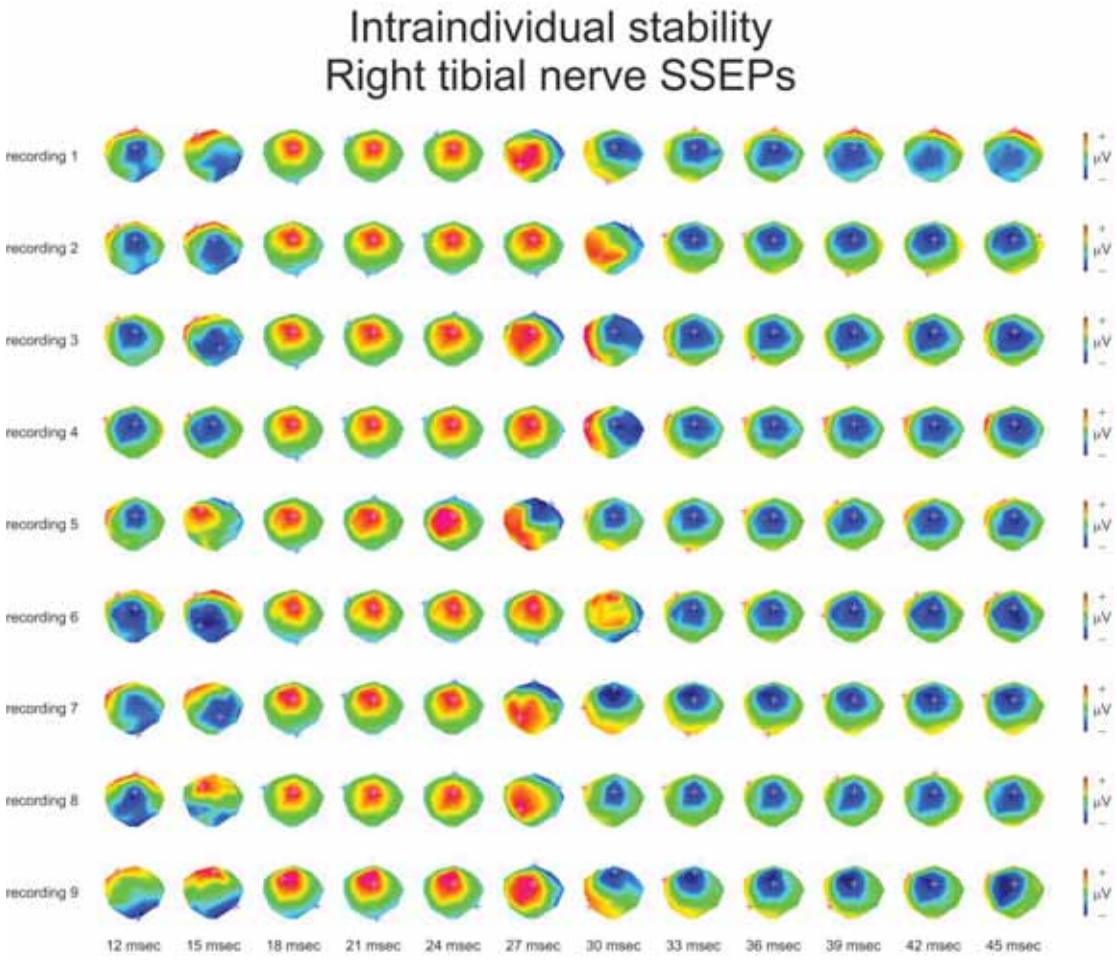

Suppl Fig 4

Supplementary Fig. 5 Interindividual reproducibility of right median nerve SSEPs. (A) Brainstem component and main cortical component SSEP waveforms after right median nerve stimulation in 5 monkeys: Mk-AT, Mk-BB, Mk,-DG, Mk-DI, and Mk-EN, during the first 50 ms following the stimulation. These data were obtained from 1 recording session in each animal. **(B)** Colour-scaled voltage maps obtained from 7 to 37 ms post-stimulus, at 3-ms interval. Same conventions as in Figures 2 and 5.

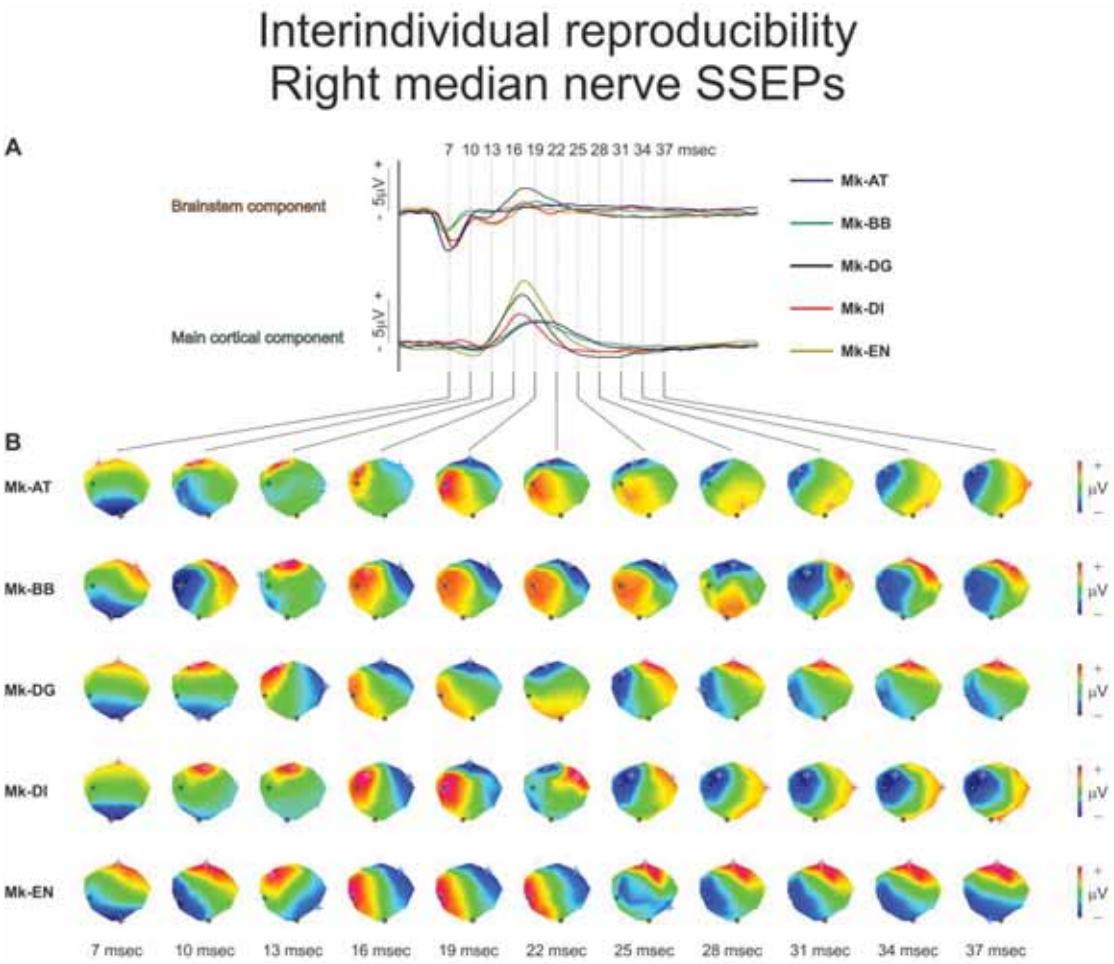

Suppl Fig 5

Supplementary Fig. 6 Interindividual reproducibility of left tibial nerve SSEPs. (A) Brainstem component and main cortical component SSEP waveforms after left tibial nerve stimulation in 5 monkeys: Mk-AT, Mk-BB, Mk,-DG, Mk-DI, and Mk-EN, during the first 60 ms following the stimulation. These data were obtained from 1 recording session in each animal. **(B)** Colour-scaled voltage maps obtained from 12 to 42 ms post-stimulus, at 3-ms interval. Same conventions as in Figures 2 and 5.

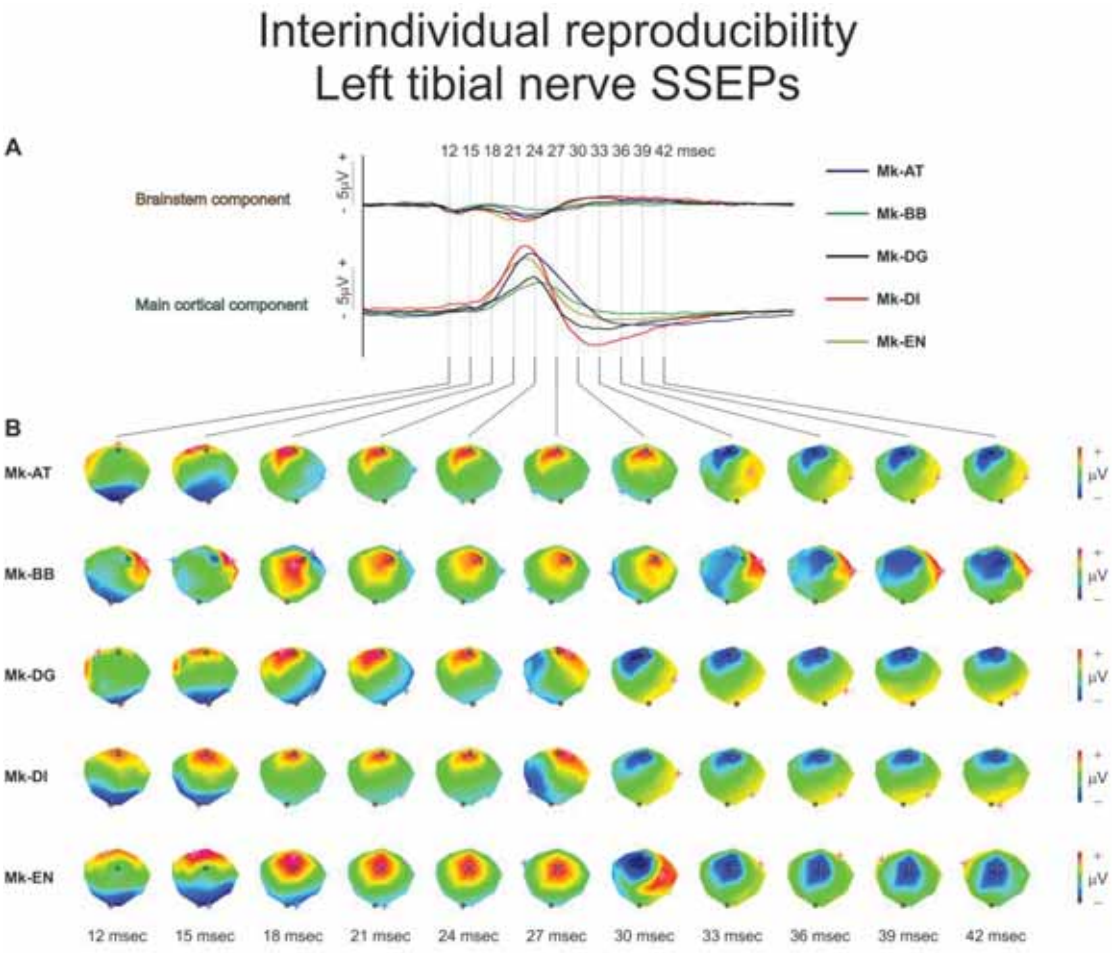

Suppl Fig 6

Supplementary Fig. 7 Interindividual reproducibility of right tibial nerve SSEPs. (A) Brainstem component and main cortical component SSEP waveforms after right tibial nerve stimulation in 5 monkeys: Mk-AT, Mk-BB, Mk,-DG, Mk-DI, and Mk-EN, during the first 60 ms following the stimulation. These data were obtained from 1 recording session in each animal. **(B)** Colour-scaled voltage maps obtained from 12 to 42 ms post-stimulus, at 3-ms interval. Same conventions as in Figures 2 and 5.

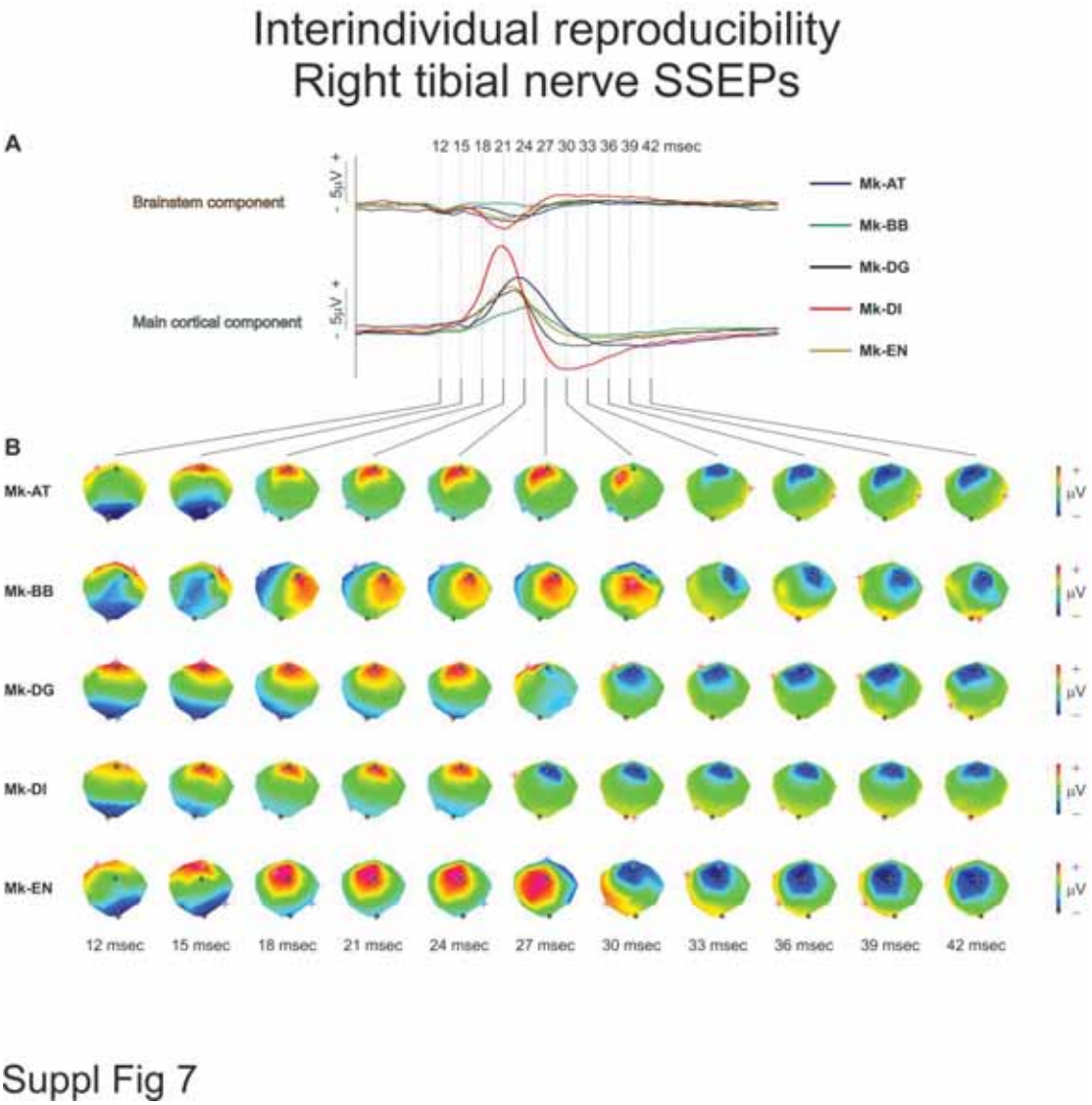

Suppl Fig 7

CHAPTER 2

Cortical and subcortical alterations of somatosensory processing from the distal forelimb after a dominant M1 lesion in non-human primate: a case report

Anne-Dominique Gindrat, Arko Ghosh and Eric M Rouiller

Abstract

A cortical lesion affecting mostly the hand representation in primary motor cortex (M1) was performed in an adult macaque monkey, resulting in a severe deficit of fine manual dexterity of the contralesional hand. By using electroencephalography (EEG) at the scalp, we measured the brain activity in response to electrical stimulation to the median nerve at the wrist before and after the lesion to investigate in greater detail the post-lesion plastic mechanisms involved in brain reorganisation underlying spontaneous functional recovery. Importantly and as expected for somatosensory evoked potentials (SSEPs) after an M1 lesion, we did not observe any post-lesion alteration of the voltage topography at the scalp, confirming that the lesion itself did not induce volume-conducted effects. But surprisingly, the lesion resulted in a reduction of the amplitude of subcortical potential after stimulation of contralesional as well as ipsilesional median nerves, whereas the amplitude of the cortical potential in the lesioned hemisphere increased after the lesion when the contralesional median nerve was stimulated. By focusing then our analysis on single trials, we showed that there was a significant linear relationship between the amplitude of afferent volleys at the subcortical level and the amplitude of outputs at the cortical level before the lesion. Surprisingly, after the cortical lesion, the somatosensory cortex continued to maintain this sensitivity to fluctuating inputs from the subcortical level. The lesion resulted rather in a constant gain added in the somatosensory processing. Moreover, a slight change in precision of the cortical processing was observed through the post-lesion period. This suggests that the cortical sensitivity could be fully achieved very locally by structures spared by the lesion whereas the dominant M1 lesion probably affected some structures of the sensorimotor cortex normally involved in a global control of the somatosensory output. In sum, the present data indicate that plastic modifications of the neural circuits occurred both at subcortical and cortical levels after a cortical lesion but the clear functional implications of such changes for behavioural recovery still need further investigations. In the discussion, we propose some hypotheses about the origin of the brain reorganisation and functional recovery.

Introduction

Afferent sensory signals from the periphery to the cerebral cortex through the dorsal column-medial lemniscal pathway and through the spinothalamic tract play a critical role by continuously informing the brain about the current state of somatosensory interactions between the environment and the body and thus contribute to regulate the functional state of the brain (Kandel et al., 2013; Purves et al., 2008). Moreover, somatosensory information from the periphery is crucial for motor control such as manual dexterity (Smith, 2009). Understanding how the surrounding sensory events are further reflected in neural activity in the CNS and then transformed through successive populations of neurons is crucial, for instance how they influence motor commands. Peripheral inputs are already processed at several subcortical levels before reaching the cerebral cortex. For instance, potentials intrinsically generated within the lumbosacral spinal cord were recorded from the surface and directly within the spinal cord of monkeys following cutaneous stimulation delivered at the limb (Beall et al., 1977). Evidence of potentials generated by afferences to the dorsal column nuclei was obtained as well in monkeys by electrical stimulation to the median nerve at the wrist among others (Moller et al., 1986; Moller et al., 1989). Equally important, these volleys generated in the afferent pathways before reaching the cortex were shown to coincide with the potentials recorded simultaneously at the scalp (Moller et al., 1986). By simultaneously recording potentials at the surface of the scalp, spinal cord and peripheral nerve, from epidural electrodes over the brain and by using intracranial electrodes in the medial lemniscus, the ventral thalamus and the internal capsula in macaque monkeys, Arezzo et al. (1979) demonstrated that several early potentials in response to electrical stimulation of the median nerve were generated in the medial lemniscus, the thalamus and the pons, respectively. Lesion-based evidence of early potentials generated in the brainstem and the thalamus after electrical stimulation of the median nerve was also obtained from human subjects affected by very specific damages in these structures (Barba et al., 2005; Mauguière et al., 1983; Mauguière and Ibanez, 1985; Sonoo et al., 1992).

In spite of the abundance of evidence of volleys generated already at subcortical level after a peripheral stimulation, we still do not fully understand the subcortical influences on the cortical activity, i.e. the response function of the different structures involved in the processing of peripheral stimulation. More specifically, how is the processing of af-

ferent volleys at the brainstem level then reflected in the cortical processing? To investigate this particular process in greater detail, it is necessary to measure both potentials captured at the brainstem level and potentials generated at the cortical level after a peripheral stimulation and then evaluate whether there is a relationship between them. To put it another way, how is the cortex responding to a given amount of brainstem afferent volleys? Is there a linear signal transfer from subcortical to cortical structures? Based on previous reports, one can reasonably expect that there is actually a clear link between subcortical and cortical processing. The properties of the different synaptic relays of somatosensory afferent pathways have been investigated long time ago by measuring the outputs at several levels of inputs in the spinal cord, the brainstem or the somatosensory cortex of cats (Krnjevic and Morris, 1976; Lloyd and McIntyre, 1950; Mark and Steiner, 1958; McIntyre and Mark, 1960; Mountcastle et al., 1957; Walsh and Whitehorn, 1981). However, the results were not always consistent. For instance, input-output curves best fitted by a power function with 0.5 exponent were obtained in the nucleus cuneatus of decerebrate cats after stimulation of afferences to this nucleus, suggesting a high sensitivity and responsiveness of this pathway to a wide range of inputs used (Krnjevic and Morris, 1976). Walsh (Walsh and Whitehorn, 1981) used a simple saturation model to describe the input-output function for the same nucleus, still in anaesthetised cats. Others hypothesised linear conductions through the relays along the somatosensory afferent pathways (Mountcastle, 1965). More recently, a study on auditory evoked potentials (AEPs) reported that an increase in brainstem synchrony (i.e. a faster encoding based on a more precise timing in generating and transmitting auditory information to further relays) was strongly correlated with a more robust auditory cortical processing in normal children, in the form of a more consistently precise timing in processing repetitive auditory stimuli in a noisy background (Wible et al., 2005). In musicians exposed to different series of vowels, the spectral magnitude of F1 brainstem response (encoding the voice timbre) was shown to be predictive of the amplitude of cortical P2 component and this coordinated plasticity was proposed to be the substrate of the higher categorical speech perception in musicians as compared to non-musicians (Bidelman et al., 2014). But, to the best of our knowledge, such a relationship has never been investigated in a straightforward way in SSEPs in primates so far by comparing for instance the amplitude of both brainstem volleys and cortical potentials at the single trial level.

In monkeys, a focal lesion of the hand representation in M1 results in an immediate strong impairment of the fine manual dexterity of the contralesional hand, followed by a progressive but incomplete spontaneous recovery (Darling et al., 2014; Frost et al., 2003; Glees and Cole, 1950; Hoogewoud et al., 2013; Liu and Rouiller, 1999; Murata et al., 2008; Murata et al., 2015; Nudo and Milliken, 1996; Pizzimenti et al., 2007; Plautz et al., 2003; Rouiller et al., 1998; Wyss et al., 2013). The neuronal substrate of the cortical reorganisation underlying the functional recovery has been already investigated (Dancause et al., 2005; Dancause et al., 2006b; Dancause, 2006; Frost et al., 2003; Liu and Rouiller, 1999; McNeal et al., 2010; Nudo and Milliken, 1996; Plautz et al., 2003; Rouiller and Olivier, 2004; Wyss et al., 2013), suggesting a role played by intact ipsilesional non-primary motor cortical areas, such as PM or SMA. However, many questions still remain, in particular about the role of the somatosensory system in the cortical reorganisation. SSEPs are a powerful tool to evaluate the plastic changes occurring in the CNS. Allison et al. (1991b) previously demonstrated that SSEPs recorded in macaque monkeys with latencies from 10 to 25 ms are generated in S1 but not in M1, meaning consequently that any modification in somatosensory processing and any involvement of S1 in the brain reorganisation after an M1 lesion should be highlighted with this method. Given the bidirectional tight connections between M1 and S1 in primates (Burton and Fabri, 1995; Jones et al., 1978; Jones and Porter, 1980; Jones, 1986; Kaas, 2004b; Liao et al., 2013; Stepniewska et al., 1993; Tokuno and Tanji, 1993), and the modulatory effect of motor areas on the somatosensory pathway (Jiang et al., 1991; Nelson, 1987; Nelson et al., 1991; Salimi et al., 1999; Williams and Chapman, 2002), lesion performed in the motor cortex can affect the somatosensory processing as well. Indeed somatosensory impairments were observed in squirrel monkeys after a lesion of M1 hand representation (Friel et al., 2005; Nudo et al., 2000) and an increase of activity in S1 forelimb area was shown in macaque monkeys during the reversible inactivation of the M1 forelimb area (Sasaki and Gemba, 1984). Although it is known that M1 is involved in somatosensory processing in primates (Jones, 1986), the neuronal processes of this sensorimotor integration remain poorly understood. Actually, the motor and somatosensory systems of primates should be considered more globally as a functional sensorimotor system instead of two distinct entities (Jones, 1986; Kaas, 2004a; Kaas, 2004b; Kaas, 2008; Tanji and Wise, 1981; Uematsu et al., 1992; Wise and Tanji, 1981; Woolsey, 1964).

The aim of this study was to assess the impact of a permanent lesion, targeting primarily the M1 hand representation, on somatosensory information processing from the distal forelimb in macaque monkeys. Our working hypothesis was that the somatosensory processing from the distal forelimb was affected by the cortical injury. To test this hypothesis, we examined here the relationship between processing of peripheral electrical stimuli at the subcortical level and at the cortical level in an adult macaque monkey by using scalp EEG recording of SSEPs. We were particularly interested to investigate: (1) whether there was a correlation between inputs provided by subcortical volleys and output measured at the cortical level, (2) in case such a relationship existed, whether and how a dominant M1 lesion would affect it. More specifically, are the effects of a lesion at high hierarchical brain level visible on lower level structures as well? Is the plasticity of the somatosensory pathway restricted to the cortical level? Such questions have been largely under-investigated so far in case of motor cortex lesion. We performed our study on a non-human primate because this model is very close to human in terms of anatomy and physiology of the nervous system, especially the motor system (see e.g. Courtine et al., 2007). Moreover, it offers also the unique opportunity to collect "pre-intervention" data, then to perform a lesion in controlled conditions, followed by a regular and dense follow-up over the long-term during the post-intervention phase, both in terms of behavioural tests and electrophysiological measurements, which is in principle not possible to achieve in studies with human patients (see the *Discussion* in **Chapter 3** for more detailed justifications for EEG investigations in a non-human primate model).

In brief, we first demonstrated that there was a significant relationship between the amount of information processing at brainstem level and the amount of information processing at cortical level. Second, we found that a dominant M1, permanent lesion induced post-lesion alterations in somatosensory processing that were by no means confined to the sole S1. Rather, we observed a subcortical modulation of afferent volley after peripheral electrical stimulation to the contralateral as well as ipsilateral median nerve at the wrist after the lesion. In addition, the cortical amplitude over the sensorimotor cortex was increased. Finally, the relationship observed between subcortical volleys and cortical processing was partly affected after the lesion. Based on the present results, we propose some hypotheses about the mechanisms involved in the post-lesion reorganisation of the sensorimotor cortex.

Materials and Methods

Monkey

Experiments were conducted on one adult female macaque monkey (*Macaca fascicularis*) (Mk-DI, age: 8-10 years old during the experiments, weight: 3.3-3.8 kg). The animal was housed in the animal facility in a group of 4-5 congeners, in a 45-m^3 room (12 hours light/12 hours dark cycle), with a regular access to an outside facility (21.12 m^3) for a part of the day or night. The monkey was daily weighted and on no account food- or water-deprived (see e.g. Kaeser, 2010; Schmidlin et al., 2011). All procedures and animal care were conducted in accordance with the Guide for the Care and Use of Laboratory Animals (Committee for the Update of the Guide for the Care and Use of Laboratory Animals and National Research Council, 2011) and were approved by local (Canton of Fribourg) and federal (Swiss) veterinary authorities. The present experiments were covered by the official veterinary authorisations FR 17/09, FR 18/10 and FR 23765. Experimental procedures were designed to minimise the animal's pain and suffering.

EEG mapping of SSEPs was routinely recorded on Mk-DI under anaesthesia, as described previously (see Gindrat et al., 2014 in **Chapter 1**). Essentially, SSEP acquisitions were performed under sevoflurane anaesthesia (Sevorane®, Abbott). To induce a rapid gas anaesthesia, a bolus was first given at a concentration of 6.5% of sevoflurane (1-2 ℓ/min air; 1-2 ℓ/min O_2) for about 4-5 minutes while the monkey sat in a Plexiglas® primate chair (Schmidlin et al., 2011). Then, the concentration of sevoflurane was reduced and maintained between 4.0% and 5.5% (0.75-1 ℓ/min air; 0.75-1 ℓ/min O_2) for the continuation of the experiment, adjusted on the basis of the cardiac pulse frequency and the respiratory frequency. Body temperature was maintained by covering the animal with bubble wrap and single-use gloves filled with warm water. During the experiment, the level of anaesthesia was regularly evaluated by checking the lid reflex. Moreover, the electrocardiogram (ECG), the cardiac pulse frequency, the respiratory frequency, the expired CO_2 and blood saturation rate in oxygen were continuously monitored with the anaesthesia machine. The EEG recordings under general anaesthesia ensured highly controlled recording conditions (e.g. decreased muscular and movement artifacts) so as to increase the sensitivity to detect small changes in brain potentials between different conditions.

Cortical lesion

A unilateral permanent cortical lesion was performed in the hand representation of left M1 in anaesthetised Mk-DI in order to impair the right, dominant hand. Ibotenic acid microinfusion was performed in the "hand knob" in M1 (Hopkins et al., 2014; Yousry et al., 1997) (see **Chapter General Materials and Methods** for additional information).

Behavioural task

The monkey's manual dexterity was assessed by using the modified Brinkman board task, consisting in unimanually retrieving food pellets from horizontal and vertical wells by using the precision grip (Napier, 1956). Here we present only the data from the right, contralesional hand. Collecting pellets from the horizontal wells required ulnar or radial deviations and was therefore much more challenging than collecting pellets from the vertical wells, usually performed with the wrist in a neutral position (see e.g. Chatagny et al., 2013; Hoogewoud et al., 2013) (see **Chapter General Materials and Methods** and **Appendix 2** for further detail).

The *score in 30 s* was established, i.e. the number of pellets correctly retrieved during the first 30 s of the task, independently for the vertical and horizontal wells as well as for all wells. Then, we defined a pre-lesion plateau of performance and a post-lesion plateau of performance based on all wells and compared both of them with a Mann-Whitney rank-sum test (SigmaPlot 12.5). The *contact time* was obtained for the first five vertical pellets and the first five horizontal pellets collected in the sessions of the pre-lesion plateau and post-lesion plateau. This measure was defined as the time interval between the first contact established by a finger with a pellet in a precision grip and the time point at which the fingers left the well with the pellet. A Mann-Whitney rank-sum test was used to compare pre- and post-lesion values distinctly for each well orientation (SigmaPlot 12.5).

EEG and electrical stimulation

We investigated the brain activity by using high-density EEG in order to survey large populations of neurons in a non-invasive way. The procedure of brain activity measure-

ment following peripheral electrical stimulation by using high-density EEG recording on anaesthetised macaque monkeys was already described in detail previously (see Gindrat et al., 2014 in **Chapter 1**). Essentially, electrical stimulation to the median nerve at the wrist (right and left) was delivered with a surface stimulator (intensity slightly above the motor threshold, 0.5-Hz repetition rate, 400-μs duration). The stimulation intensity was based on visual motor threshold of thumb twitch given that it is a straightforward and position-independent criterion to assess the effectiveness of electrical stimulation, in addition to be commonly used in clinics (Baurain et al., 1998; Tsui, 2007). EEG signals were obtained from an elastic cap (EasyCap) containing 32 electrodes regularly distributed over the whole scalp. The position of the electrodes at the scalp was obtained from MRI scanning of spots of EEG paste (high-chloride electrolyte gel Lectron III, EASY CAP) at the electrode locations. The EEG signals were recorded with a 5-kHz sampling rate against a vertex reference, amplified with an AC/DC amplifier (BrainAmp, Brain Products) and digitized using a 16 bit A/D converter. Further offline analysis was performed using the Cartool software (Brunet et al., 2011): the data were re-referenced offline to the average signal from all the scalp electrodes (average reference), band-pass filtered between 8 Hz and 300 Hz, baseline corrected with a pre-stimulation period of 50 ms and artifacts were removed (threshold at 100 μV and visual inspection of all the epochs). SSEPs were obtained by averaging 80 accepted epochs per recording. Raw accepted epochs were saved as well for further analysis at the single-trial level.

The single-trial analysis was achieved by processing the raw accepted epochs in the following way: filters between 8 Hz and 300 Hz, 50-Hz notch when needed, baseline correction: 10 ms, average reference. This led to the *processed accepted epochs*.

The latency of both subcortical peak (at about 7 ms, most probably from the brainstem) and main cortical peak (at about 18 ms) was obtained from every average SSEP from the electrode with the largest signal amplitude. The amplitude of these components at those latencies was then measured on the *processed accepted epochs* at the corresponding electrodes using the *Export tracks* tool in Cartool. As a control, the amplitude of EEG signals was also extracted both at 5 ms and at 27 ms on the 2 selected electrodes. Median peak amplitudes across the single trials were then obtained for each recording, both before and after the M1 lesion. Linear regressions were computed between the brainstem peak amplitude and the cortical peak amplitude among all pre-lesion sessions on the one

hand and among all post-lesion sessions on the other hand by using MATLAB® (MATLAB R2013b). We chose to focus our analysis only on the electrodes measuring the largest brainstem potential and the largest cortical potential, respectively, because previous a inverse solution on median nerve SSEPs in our macaque monkeys confirmed that the initial brainstem component was generated at the brainstem level and the main cortical component was generated at the sensorimotor cortex level (see Gindrat et al., 2014 in **Chapter 1**). Therefore, we are confident that the activity at these 2 electrodes reflects the brainstem input and the cortical output, respectively.

The amplitude of potentials recorded on specific electrodes was compared before and after the lesion by using a two-tailed unpaired t-test with Bonferroni correction for multiple comparisons (Cartool). We evaluated the effect of an M1 lesion on the relationship between subcortical (brainstem) input and cortical output in the brain by using a linear regression between the amplitude of the cortical component as the response variable and the amplitude of the brainstem component as the predictor variable in the average of all single trials per recording, both before and after the lesion. The y-axis intercept of the regression line was interpreted as a correlate of a constant gain added or removed to the cortical processing, the slope was a measure of the sensitivity or responsiveness of the cortex to changes in subcortical input, and the residuals, assessed by the coefficient of correlation R, corresponded to the precision of the prediction of cortical output from subcortical input, or noise in the data. A One-Way Analysis of Covariance for Independent Samples (ANCOVA) (*aoctool* function implemented in MATLAB) was used to statistically compare the slope and y-axis intercept of both pre- and post-lesion regression lines. The significance of the difference between the coefficients of correlation R of two groups was assessed by using a Fisher r-to-z transformation.

Data were obtained from 18 pre-lesion sessions and 13 post-lesion sessions for right median nerve SSEPs and from 12 pre-lesion and 9 post-lesion sessions for left median nerve stimulation. The reduced amount of left median nerve SSEP data as compared to right median nerve ones comes from our experiment design: right median nerve SSEPs were obtained at the beginning of the recording session whereas left median nerve SSEPs were recorded at the end (tibial nerve SSEPs were performed in between but these data are not presented here.). At the end of some sessions, the anaesthesia was not as stable as at the beginning and we had to interrupt the EEG acquisition before per-

forming left median nerve stimulation or the data were contamined by artifacts (muscular activity, higher electrode impedance, …), reducing the quality of the signals.

Injection of BDA neuronal tracer

Once the acquisition of the electrophysiological and behavioural data was achieved, the neuronal tracer biotinylated dextran amine (BDA) was injected in the distal forelimb representation in S1 in left hemisphere (i.e. ipsilateral to the lesion) (see **Supplementary Figure 3** at the end of this chapter, and **Chapter General Materials and Methods** for more information).

End of the experimental protocol

After a survival period of 22 days following tracer injection, the animal was euthanised (see **Chapter General Materials and Methods** for further detail). The brain was removed and eight series of frozen sections were then performed in the frontal plane at a 50-μm thickness (400 μm between two successive sections of the same series).

Histology

A series of brain frontal sections was histologically prepared to stain the Nissl substance with cresyl violet. A second series of MK-DI's brain sections was histologically prepared for SMI-32 staining and a third one for BDA histochemistry to study the anterograde and retrograde distributions of BDA after injection in S1, using previously published protocols (for greater detail, see e.g. Beaud et al., 2008; Liu et al., 2002; Wannier et al., 2005). In a later step, a selected rostro-caudal portion of the brain comprising M1 and S1 was processed using two series of sections, to reveal cytochrome oxidase (C.O.) activity by using the method described by Wong-Riley (Carroll and Wong-Riley, 1984; Wong-Riley, 1979), and myelin, respectively (see **Chapter General Materials and Methods** for further detail).

Neuroanatomical reconstruction

Data were analysed by using Neurolucida 9.12 32-bit (MBF Bioscience, Williston, VT, USA) both for charting the sections and then reconstructing serial sections. The software was working with a computer-interfaced Olympus BX40 microscope (Olympus Schweiz AG), a computer-controlled motorised stage (Märzhäuser Wetzlar GmbH & Co. KG, type EK 32 75 x 50) and a digital camera (Olympus U-PMTVC). Frontal brain sections were examined under bright-field illumination. Photomicrographs taken with the digital camera were further edited in CorelDRAW (the colour, brightness and contrast were not modified).

The lesion location was reconstructed on the basis of frontal Nissl-stained sections. To this aim, we first determined the extent of the lesion by selecting all the Nissl-stained sections where the lesion was present. Then the contour of the brain sections and some anatomical landmarks such as the ventricles and the white matter/gray matter border were mapped at 1.25x-4x (objective magnification), and the contour of the lesion in gray matter was drawn at 4x-10x for each selected brain section. The outer and inner boundaries of the lesion were the actual neuronal layers at the boundary of the lesion in the gray matter. The area of the lesioned site was reconstructed on each section by using the same location on the intact hemisphere as model given that a brain lesion induces brain atrophy (Seghier et al., 2014) at the lesion site itself in addition to either some tissue missing or conversely some cavitation. Each reconstructed brain section was then carefully realigned with the previous ones by using anatomical landmarks (such as the cut edges of the section and the ventricles). The cortical lesioned area was reconstructed by using the serial section reconstruction function implemented in Neurolucida Explorer (MBF Bioscience, Williston, VT, USA) and its volume was estimated by using the Cavalieri estimator (see e.g. Pizzimenti et al., 2007) based on Cavalieri's principle (Cavalieri, 1653) and running on the same software. The extent and location of the lesion were projected onto a lateral view of the cortical surface of the lesioned hemisphere for display.

The BDA injection site was reconstructed by drawing a contour at 4x-10x on the corresponding BDA-stained sections (at 400-µm interval) around the injection core (dense dark zone, center of the injections) and part of the surrounding transition zone (less dense zone, halo), in addition to the contour of the brain sections and some anatomical landmarks such as the ventricles at 4x. The dense core and the halo were determined in

the same way as previously defined by Dancause et al. (2005; 2006a, see their Figure 1A and B), namely the dense core is the part of the injection site where cell bodies, axonal fibres and synaptic boutons cannot be individually distinguished from the others and the halo is the transition zone where one begins to distinguish each of these structures separately from the others. Therefore, the injection site, as defined here, comprised the injection core and part of the surrounding halo as the border between these two zones was not always clearly identifiable. The sections were realigned with the previous ones and the volume of the injection site was then determined with Neurolucida Explorer in the same way as explained above for the cortical lesion reconstruction. The location of the tracer injection sites in terms of gray matter versus white matter and cytoarchitecture was determined by examining the corresponding Nissl-stained sections and the corresponding site in the contralateral intact hemisphere.

Results

Description and characterisation of the lesion

A unilateral permanent lesion of the hand representation predominantly in M1, in the left hemisphere, was performed by microinfusion of 39.7 µl ibotenic acid in total distributed in 21 sites in the "hand knob" (Hopkins et al., 2014; Yousry et al., 1997) of the precentral gyrus (see **Figure 4** in **Chapter General Materials and Methods**). The cortical volume of the lesion on the basis of reconstructions from Nissl-stained sections (**Supplementary Figure 1**) was estimated at 68.46 mm^3, in the range of the largest lesions previously performed in our laboratory (Hamadjida et al., 2012; Kaeser et al., 2010; Wyss et al., 2013). The lesioned sites were characterised by a clear diminution or even a complete absence of magnocellular cell bodies, replaced then by gliotic tissue. The transition from non-lesioned to lesioned tissue was usually clear, in the form of a loss of the precise cortical laminar cytoarchitecture and a change in the shape of cell nuclei from being large, darkly stained and with a nearly oval shape in intact tissue to being small, lighter and with an irregular shape in lesioned tissue (Nissl staining). In some sections, the damaged tissue was even absent, forming cavities. Nevertheless, there was neither sign of oedema nor calcification. A careful examination of each individual section showed that the lesion extended from section 27 to section 48, confirming that the corti-

cal lesion targeted M1 but possibly extended also somewhat into the ventrocaudal part of PM (PMvc, sections 27-28; corresponding to the transition zone between PM and M1), in the white matter, and into about 15-20% of the hand representation of area 3a in direct continuity with area 4 in the fundus of the central sulcus. More specifically, about 50% of the medial part of the median third of the hand representation of area 3a was lesioned (sections 36-41 included), but the full rostral and caudal thirds of the hand representation of area 3a remained intact (**Figure 1A** and **Supplementary Figure 1**). All subcortical gray matter structures such as basal ganglia and thalamic nuclei were intact as well. Our estimation of the lesion affecting a small portion of median area 3a was based on criteria previously reported by others (Geyer et al., 1999; Krubitzer et al., 2004; White et al., 1997): by using the intact hemisphere as a reference, this region showed no strict architectonic borders but appeared much more as a transition zone from densely distributed large pyramidal cells in area 4 towards sparse and less evenly distributed large pyramidal cells in area 3a, in parallel with the progressive emergence of the internal granular layer IV in area 3a that was largely absent in area 4. This was visible on Nissl-stained sections, on SMI-32-stained sections, on C.O.-stained sections, and on myelin-stained sections (**Figure 1B-G**). The detailed representation of the lesion reconstruction on consecutive Nissl-stained sections is available in **Supplementary Figure 1**.

Figure 1 (next page): Extent of the lesion. (A) On the basis of Nissl-stained sections, the lesion (hatched area) extended from section 27 to section 48 (red boundaries). The lesion was dominantly located in the hand representation of M1, but most likely extended also in the ventrocaudal part of the premotor cortex (PM) and in a small portion of the medial part of the median third of the hand representation of area 3a (see text for greater detail). The landmark of some sections is given, as well as the rostro-caudal coordinates (in mm) relative to interaural axis (based on Paxinos' atlas (Paxinos et al., 1999)). Ant: anterior, Med: medial. (B) *Camera lucida* **reconstruction of the frontal Nissl-stained section 39, with the lesion (red) putatively extending into the area 3a. The border between gray matter and white matter is represented in light blue. (C)** *Camera lucida* **reconstruction of the frontal Nissl-stained section 45, with the lesion (red) restricted to area 4. (D-G) Nissl staining (D), cytochrome oxidase staining (E), SMI-32 staining (F), and myelin staining (G) of the lesion, for both sections 39 and 45, first at 1.25x magnification (left panels for each section, see rectangle delimited in B and C), then at 4x magnification (right panels for each section, see rectangle delimited in 1.25x sections). In the intact cortex, CST neurons are visible in the layer V (see SMI-32 staining at 4x magnification). Our estimation of the anterior border of the lesioned cortex is shown with a dotted line on Nissl-stained sections, cytochrome oxidase-stained sections and myelin-stained sections.**

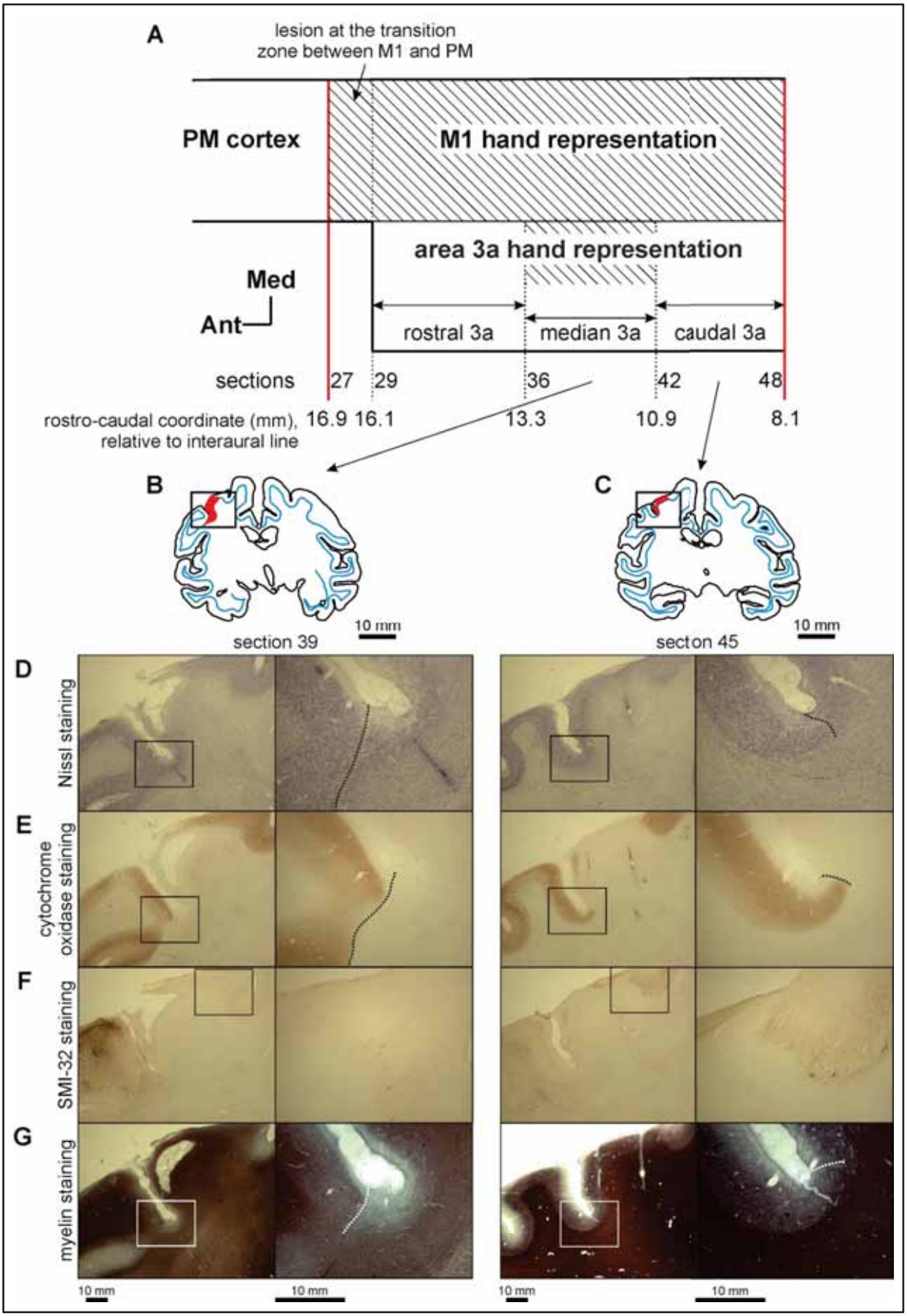
A
lesion at the transition zone between M1 and PM
PM cortex
M1 hand representation
area 3a hand representation
Med
Ant
rostral 3a
median 3a
caudal 3a
sections
27
29
36
42
48
rostro-caudal coordinate (mm), relative to interaural line
16.9
16.1
13.3
10.9
8.1
B
C
10 mm
section 39
secton 45
D
Nissl staining
E
cytochrome oxidase staining
F
SMI-32 staining
G
myelin staining

Impact of the lesion on fine manual dexterity

We tested the monkey's ability to achieve precision grip by using the modified Brinkman board task repeatedly performed before and after the lesion and we quantified its performance with the *score in 30 s* (**Figure 2A**). We defined plateaux of stable performance based on previously established criteria (Chatagny et al., 2013; Kaeser et al., 2014) and also on the ability of the monkey to collect again pellets from the horizontal wells (see below). A stable pre-lesion plateau of performance was defined between from day 141 to day 4 before the lesion based on the *score in 30 s* obtained from all wells (median total plateau: 29; median vertical plateau: 14; median horizontal plateau: 15). The lesion induced then several marked behavioural deficits for the contralesional hand: in the first post-lesion days, the animal showed only very little voluntary use of the hand, either for collecting the small pellets in this behavioural task, or for natural behaviours in the animal facility and kept its hand hanging out. The monkey kept its hand in a flexed resting posture of the wrist and was actually completely unable to perform the task, as reflected by a *score in 30 s* at 0. Then we observed a progressive and regular improvement in the performance from day 16 to day 69. During this period, the animal collected only pellets from the vertical wells and was completely unable to collect those from the horizontal wells. This strongly reflected an impairment to perform either ulnar or radial deviation with the wrist. From day 72, the animal began to collect horizontal pellets as well but to a lesser extent than vertical ones and its performance did not increase any more. Therefore, we considered the post-lesion plateau of the *score in 30 s* from day 72 to day 187 (median total plateau: 10; median vertical plateau: 10; median horizontal plateau: 1). The post-lesion score at plateau in all wells was statistically lower than the pre-lesion score ($p < 0.001$, Mann-Whitney rank-sum test) and the percentage of spontaneous recovery based on this score was then estimated at 34.48%. The post-lesion score in vertical wells (recovery: 71.43%, $p < 0.001$, Mann-Whitney rank-sum test) and the one in horizontal wells (recovery: 6.67%, $p < 0.001$, Mann-Whitney rank-sum test) were statistically lower than the pre-lesion scores as well. Moreover, as expected, the *contact time* in both vertical (pre- vs post-lesion median: 0.25 s vs 0.56 s) and horizontal wells (pre- vs post-lesion median: 0.36 s vs 0.68 s) was significantly increased after the lesion ($p \leq 0.001$ for both tests, Mann-Whitney rank-sum tests). Moreover, the *contact time* was significantly shorter in vertical wells than in horizontal ones both before ($p \leq 0.001$,

Mann-Whitney rank-sum test) and after the lesion (p ≤0.008, Mann-Whitney rank-sum test) (**Figure 2B**).

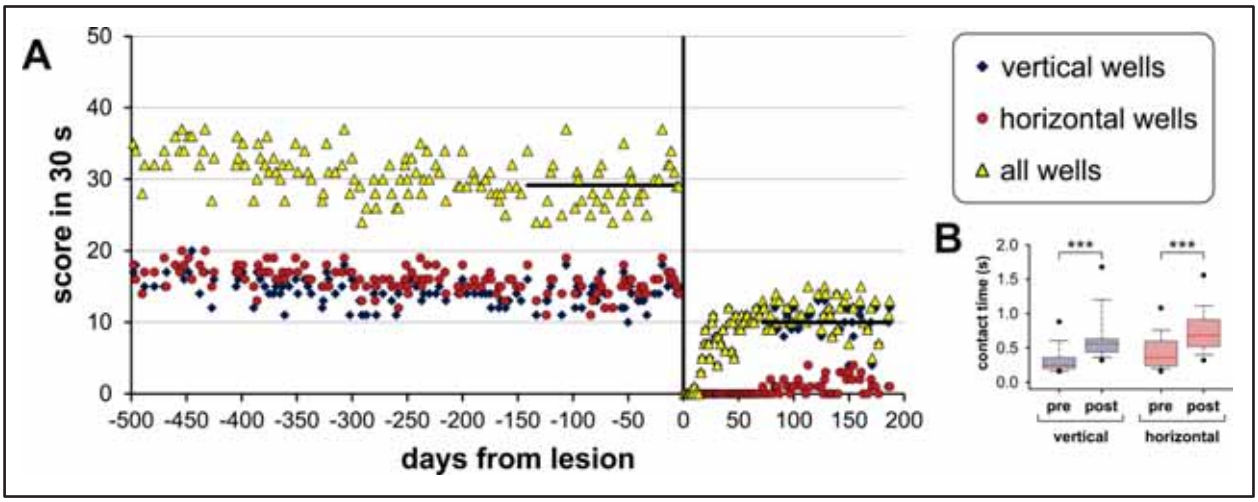

Figure 2: Behavioural task. (A) Score in 30 s in the modified Brinkman board task with the right hand (contralesional hand), separately for the vertical wells (blue diamonds), the horizontal wells (red circles) and the sum of them (yellow triangles). The lesion was performed at day 0. The pre- and post-lesion plateaux of score based on all the wells are indicated by black horizontal lines. (B) Contact time in the modified Brinkman board task with the right hand (contralesional hand), separately for the vertical wells (blue box plots) and the horizontal wells (red box plots), both before and after the lesion. Box plot description: box, 25th and 75th percentiles, whiskers, 10th and 90th percentiles, black dots: 5th and 95th percentiles, red line: median. ***: p <0.001, Mann-Whitney rank-sum test.

Subcortical potentials of SSEPs

We investigated whether the somatosensory brain activity evoked by an electrical stimulation applied to the median nerve (independently on both sides) at the wrist was affected by the cortical lesion. To this end, we used 32 surface electrodes distributed over the whole scalp to detect brain potentials evoked by electrical stimulation (monophasic square wave electrical pulses of 400-µs duration) to the median nerve at the right (contralesional) and left (ipsilesional) wrists. SSEPs were then obtained by averaging 80 trials.

It appeared that the dominant M1 lesion induced changes in the early potential measured with maximal negativity from the two most caudal electrodes, located on either side of the midline just below the external occipital protuberance, both after stimulation to the right and left median nerves, respectively. For right median nerve stimulation, the amplitude of the post-lesion SSEP was significantly smaller than the amplitude of the pre-lesion SSEP from 6 ms to 8.4 ms on the left-side electrode and from 5.6 ms to 8.2 ms on the right-side electrode ($p < 0.05$, two-tailed unpaired t-tests with Bonferroni correction for multiple comparisons) (**Figure 3A** and **B**). For left median nerve SSEPs, the post-lesion amplitude was significantly reduced from 5.8 ms to 8.0 ms on the left-side electrode and from 5.6 ms to 8.2 ms on the right-side electrode ($p < 0.05$, two-tailed unpaired t-tests with Bonferroni correction for multiple comparisons) (**Figure 3C** and **D**). Conversely, no statistical difference between pre- and post-lesion potentials was observed for either of the two electrodes in the pre-stimulation baseline period, strongly suggesting a true post-stimulation difference between both groups instead of an artifact. The period around the stimulation onset was not considered in this analysis because it was contaminated with some stimulation artifacts. Based on previous studies on the latency and amplitude of these potentials (Gindrat et al., 2014; Hashimoto, 1984), we propose that these signals originated from the brainstem (see the section *Discussion* for further detail). Therefore, from now on we refer to this potential as *brainstem peak*, captured from the 2 *subcortical electrodes*.

Figure 3 (next page): Brainstem potential of SSEPs following electrical stimulation to the median nerve. (A) The brainstem potential was captured with maximal negativity from the two most caudal scalp electrodes, located on either side of the midline just below the external occipital protuberance. Grand averages of the SSEPs ± SEM (lighter shade) from the left subcortical electrode (red dot) in response to electrical stimulation to the right median nerve at the wrist before (dark blue) and after (light blue) the lesion. The lighter gray areas comprise the latencies at which statistical analyses between both conditions were performed. The darker area depicts significant differences between both groups, $p < 0.05$, $|T| > 1$ and minimum of 10 successive significant time frames (=2 ms) (two-tailed unpaired t-tests with Bonferroni correction for multiple comparisons). The zigzag arrow above the traces points at the stimulation onset (i.e. 0 ms). (B)

Same as (A) but for the right subcortical electrode, before (red) and after (orange) the lesion. (C) and (D) Same as (A) and (B), respectively, but for left median nerve stimulation.

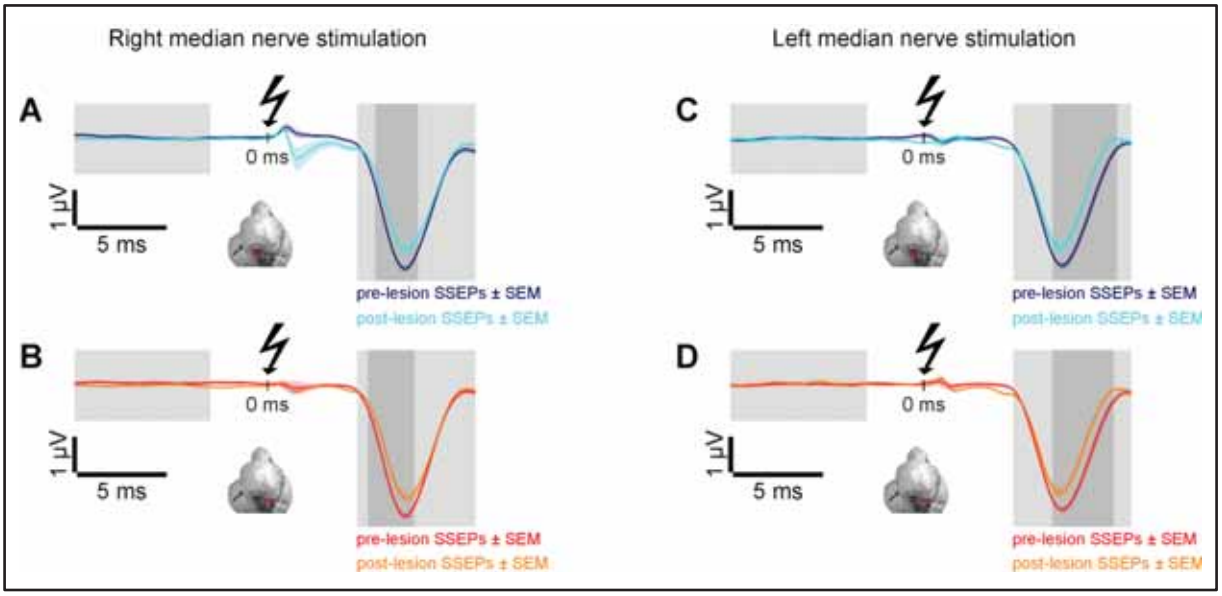

In sum, the cortical lesion induced already subcortical alterations. Moreover, this effect of the lesion was obtained after stimulation of both contralesional and ipsilesional median nerves.

Cortical potential of SSEPs

Based on a previous study in our laboratory, we defined the *cortical peak* as the potential measured at the scalp at about 18 ms (Gindrat et al., 2014). The lesion did not induce noticeable changes in voltage topography at the scalp in right SSEPs (**Figure 4A**), except an increase in voltage amplitude of the cortical peak, as exemplified here at 18 ms post-stimulation whereas there was no topography difference in the baseline before the initiation of the cortical peak (e.g. at 10 ms). This increase in amplitude of the cortical peak was further confirmed throughout the signal: the post-lesion potential was significantly larger than the pre-lesion potential between 11 ms and 21.4 ms after the stimulation on the electrode capturing the largest potential before and after the lesion ($p < 0.05$, two-tailed unpaired t-test with Bonferroni correction for multiple comparisons) (**Figure 4B**).

As a control, there was neither difference in topography nor in the amplitude of the cortical component of left median nerve SSEPs measured on the electrode capturing the largest potential before and after the lesion (ns, two-tailed unpaired t-test with Bonferroni correction for multiple comparisons) (**Figure 4C** and **D**).

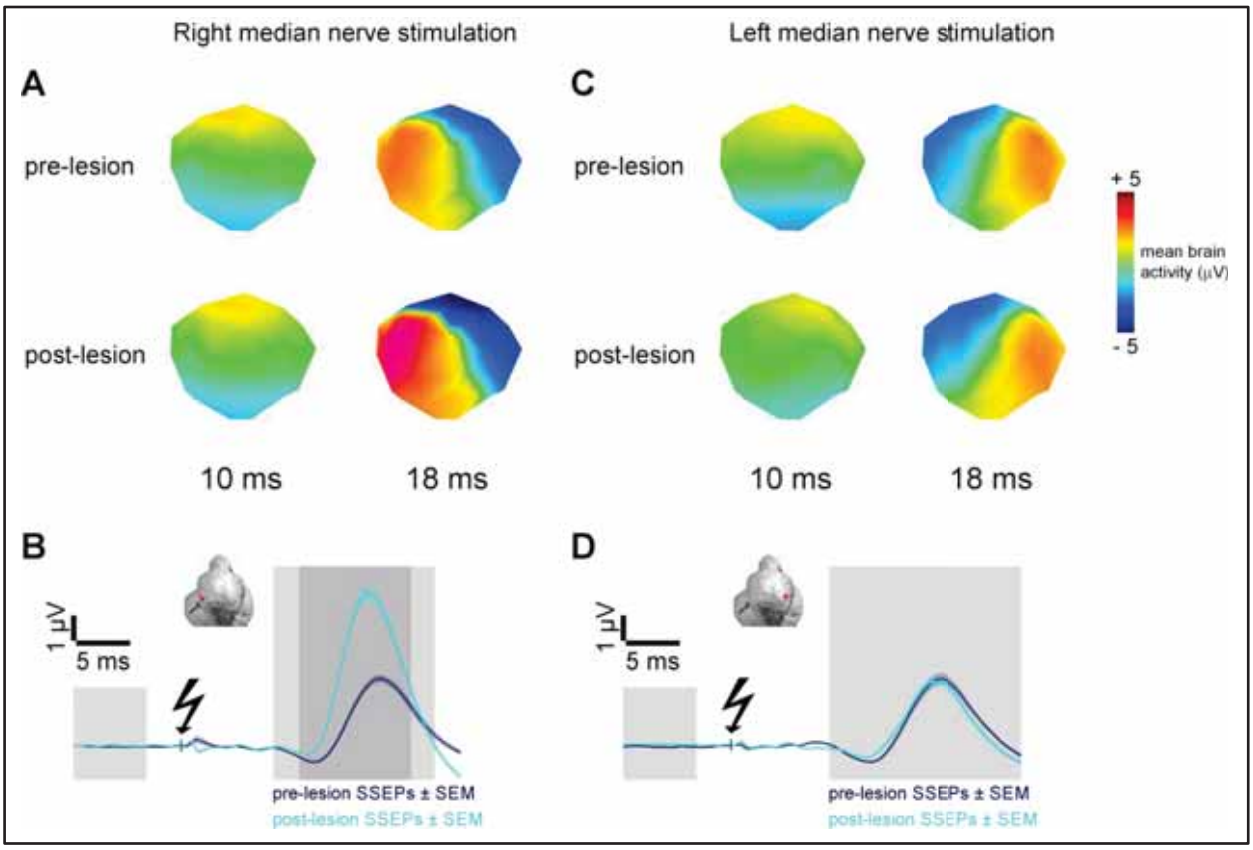

Figure 4: Cortical potential of SSEPs following electrical stimulation to the median nerve. (A) Voltage topographies as the scalp before and after the lesion, before the initiation of the cortical peak (10 ms) and at the cortical peak (18 ms). The orientation of the maps is frontal-up and right side-right. (B) The cortical potential was captured with maximal positivity from the contralateral scalp electrode indicated in red. Grand averages of the SSEPs ± SEM (lighter shade) in response to electrical stimulation to the right median nerve at the wrist before (dark blue) and after (light blue) the lesion. Same conventions as in Figure 3. (C) and (D) Same as (A) and (B), respectively, but for left median nerve stimulation.

Relationship between subcortical volleys and cortical output

Based on the assumption that early alterations do influence later potentials and consequently that we cannot explain the putative cortical modifications without understanding the earlier ones at subcortical level, we focused on the relationship between afferent volleys from the brainstem and output at the cortical level in right and then left median nerve SSEPs. To this aim, we measured the amplitude of the brainstem component in each single trial at the electrode with maximal negativity and the amplitude of the cortical component in each single trial at the electrode with maximal positivity in pre-lesion sessions and in post-lesion sessions. Then, we performed linear regressions between the median brainstem peaks and the median cortical peaks obtained from each recording available in each recording session, independently for the pre-lesion sessions and the post-lesion sessions. Interestingly, for right median nerve SSEPs, we observed a significant, negative linear relationship between both components among the pre-lesion sessions ($R = -0.55$, $p = 0.0003$) (**Figure 5A**), meaning that a substantial portion of the variability observed among the amplitude of the cortical peak was explained by differences in the amplitude of the brainstem peak. In essence, the more negative the amplitude of the brainstem peak, the larger the positive amplitude of the cortical component. We performed the same regression analysis among post-lesion data and, surprisingly, we still observed a significant linear relationship among them as well ($R = -0.63$, $p = 0.0004$). The next step was to compare both regression lines to assess how the lesion of the finger representation in M1 affected the relationship between subcortical volleys from the brainstem and output at cortical level. To this end, we performed a One-Way Analysis of Covariance for Independent Samples (ANCOVA) to compare the slope and the y-axis intercept of both regression lines and the coefficients of correlation R were compared with a Fisher r-to-z transformation. For the ANCOVA implemented in MATLAB, different models to fit were available (single mean ignoring groups, separate mean to each group, single line ignoring groups, parallel line to each group, separate line to each group (with no constraints)). In our situation, the regression line slope is a measure of the average amount by which the cortical peak increases or decreases as a function of a given change of the brainstem peak, i.e. a measure of the sensitivity of the cortex to brainstem changes. The y-axis intercept is a measure of a constant input or gain to the cortical processing. Finally, the R indicates the level of noise or variability in the data. By fitting the separate line model, we did not observe any significant change in slope ($F = 0.31$, p

=0.5806) but the y-axis intercept of the regression line was significantly higher after the lesion than before the lesion (T =2.89, p =0.0054). No changes in R (z =0.46, ns) was observed between both groups. In sum, the dominant M1 lesion resulted in a constant gain added to S1 output, without affecting the sensitivity of the cortex to process somatosensory inputs, nor the noise/variability level of the somatosensory processing.

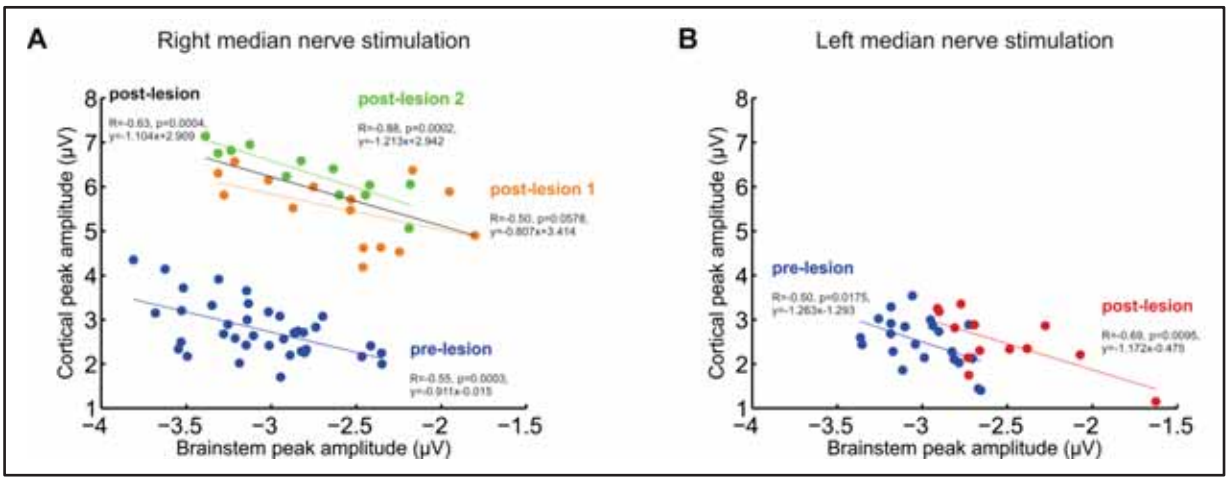

Figure 5: Relationship between subcortical volleys and cortical processing. (A) To investigate how the lesion affected the relationship between subcortical input and output at the cortical level, we measured the amplitude of the brainstem peak in each single trial at the electrode with maximal negativity and the amplitude of the cortical peak in each single trial at the electrode with maximal positivity in pre-lesion sessions and in post-lesion sessions. Then, we performed linear regressions between the median brainstem peaks and the median cortical peaks obtained from each session, both before (dark blue) and after the lesion (orange and green). We further splitted the post-lesion data into 2 groups (closer to the lesion in orange and further from lesion in green). The regression line, the coefficient of correlation (R), the p-value of the linear regression (p) and the regression line equation (y) are indicated for each group. (B) Same as (A) but for left median nerve (ipsilesional) SSEPs. Here post-lesion data were pooled into a single group. Note that the same scales are used on both graphs.

To go further into the evolution of post-lesion brain activity, we separated the post-lesion data into 2 sets: the first one (*post-lesion 1*) containing the data from the 7 sessions performed 9 to 56 days after the lesion and the second one (*post-lesion 2*) contain-

ing the data from the next 6 sessions, from day 63 to day 134 after the lesion. No change appeared between *post-lesion 1* and *post-lesion 2* groups either in terms of slope (ANCOVA, F =0.66, p =0.4238) or y-axis intercept (ANCOVA, T =0.35, p =0.7323). The Fisher r-to-z transformation resulted in a very close to significance difference between both R (z =1.83, one-tailed p =0.0336 and two-tailed p =0.0673). We report here the p-value for both one-tailed and two-tailed z tests because we do not see any indication to favour one test over the other. In any case, it reveals that the difference between the R of both post-lesion groups is modest and very close to the significance level, either just above or just below, depending on the test. This suggests that there is a small reduction in the noise level of the cortical processing throughout the post-lesion phase.

Similar statistical comparisons between the pre-lesion group and the *post-lesion 1* group confirmed the absence of change in slope and the difference in y-axis intercept (slope: F =0.07, p =0.7993, ANCOVA; y-axis intercept: T =2.99, p =0.0043, ANCOVA; R: z =-0.22, ns, Fisher-r-to-z transformation) whereas interestingly there was a significant difference in R (Fisher-r-to-z transformation, z =1.96, one-tailed p =0.025 and two-tailed p =0.05) between the pre-lesion group and the *post-lesion 2* group in the form of a reduction of noise in the *post-lesion 2* group without any changes in slope (ANCOVA, F =0.58, p =0.4517) but again in y-axis intercept (ANCOVA, T =2.57, p =0.0134).

One may argue that the post-lesion shift in the regression line is due to a general increase in the baseline EEG activity at the cortical level, and not to a specific modification in the relationship between subcortical input and cortical output of right median nerve SSEPs. To address this question, we applied the same analysis to SSEPs obtained in response to electrical stimulation to the left median nerve, i.e. originating from the non-lesioned hemisphere. There was neither significant modification after the lesion in the slope (ANCOVA, F =0.02, p =0.8838) nor in the y-axis intercept (ANCOVA, T =0.47, p =0.6439) nor in the R (z =0.75, ns, Fisher-r-to-z transformation) of the regression lines (**Figure 5B**). The absence of alteration in the y-axis intercept confirms that the lesion did not induce a global increase in the cortical activity but only a specific effect in the lesioned hemisphere.

One may also argue that the relationship between brainstem peak and cortical peak observed across several recording sessions both before and after the lesion is only a noise correlation resulting from data contamination by a recurrent electrical artifact across

the sessions, such as mains frequency. Artifacts are any transient or periodic electrical activities that can be recorded by the EEG electrodes (in our situation) but that are not originating from cerebral components (Talsma and Woldorff, 2005). Transient artifacts include electromyographic (EMG) activity, movements, ECG artifacts and equipment problems. Periodic noise comprises interferences from power lines (50 Hz), light sources and equipment. We paid much attention to avoid electrical noise (1) by impedance minimisation of the electrodes below 5 kΩ and regular check during the experiments to avoid "electrode popping", (2) by performing the recordings in a Faraday room to reduce non-physiological artifacts such as the interference from electrical devices, and (3) by performing the recordings in an anaesthetised animal to avoid muscular and blinking artifacts. However, these precautions do not guarantee a completely artifact-free situation and noise-free data because ECG artifacts or salt bridge artifacts may still appear. Therefore, as a control, we measured the amplitude of the brain activity at 5 ms and at 27 ms for right median nerve SSEPs, both on the subcortical electrode and on the cortical electrode, in the same way as the brainstem peak and the cortical peak. Both activities at 5 ms and at 27 ms were outside any peaks and were therefore considered as a more random signal as compared to the brainstem peak and the cortical peak. In case of completely artifact-free data, there should be no strongly significant correlation between the amplitude of the 5-ms signal recorded at the subcortical electrode and at the cortical electrode, and the same principle applies for the measurement of the 27-ms amplitude as well. These expectations were verified: there was no strongly significant correlation between the 5-ms amplitude recorded at the subcortical electrode and at the cortical electrode, either across the pre-lesion sessions ($R = 0.32$, $p = 0.052$) or across the post-lesion sessions ($R = -0.23$, $p = 0.248$). In the same way, there was no significant correlation between the 27-ms amplitude recorded at the subcortical electrode and the corresponding measure at the cortical electrode across the sessions either before ($R = -0.30$, $p = 0.070$) or after the lesion ($R = 0.20$, $p = 0.327$) (**Supplementary Figure 2**).

At the single-trial level, a significant regression between two amplitudes measured outside of a peak is not sufficient to infer noise contamination of the data because the background activity of the brain is not completely random (Spencer, 2005), as previously claimed (Graben et al., 2000). However, in case of significant relationship between 2 amplitudes measured at each trial, a recurrent artifact in the data should result in a highly reproductive slope of the regression line, meaning a suspicious reproducible

trend, from one session to next. That has however never been observed by considering the regression among single trials in each recording, either for the brainstem peak vs cortical peak, or the amplitude at 5 ms vs the amplitude at 27 ms on the subcortical electrode, or the amplitude at 5 ms vs the amplitude at 27 ms on the cortical electrode, or the amplitude at 5 ms on the subcortical electrode vs the amplitude at 27 ms on the cortical electrode, or the amplitude at 5 ms on the cortical electrode vs the amplitude at 27 ms on the subcortical electrode. Taken together, these results strongly suggest that we described a true lesion effect in **Figure 5** and not an artifact.

Reconstruction of BDA labelling

Tract-tracing analyses of brain sections after post-lesion injection of the tracer BDA in S1 should provide more insight into the post-lesion input and output projections of this area. Here, BDA was infused in 4 sites and injection site reconstruction was localised into the areas 3b and 1 of S1, both in gray matter and white matter, from section 35 to section 43 (see **Supplementary Figure 4**). The section showing the largest injection site area (section 41) contained 2 distinct patches of labelling (areas of 4.01 mm^2 and 1.18 mm^2, respectively), both regions containing a dense plexus of labelled neuronal fibres, cell bodies and synaptic boutons and a surrounding halo (**Supplementary Figure 3A**). The volume of the injection site comprising the injection core and some part of the halo was estimated at 4.78 mm^3 with the Cavalieri estimator. We were able to distinguish different labelled structures such as fibres, synaptic boutons and cell bodies (**Supplementary Figure 3B-D**).

Given that similar BDA injections in S1 have never been performed either in control monkeys or in other lesioned monkeys until now, we were not able to directly compare our neuroanatomical data and provide quantitative analyses and therefore we were not able to investigate whether the motor cortex lesion affected the projections from and to S1. Nevertheless, we suggested here an interesting complementary approach to the behavioural and electrophysiological readouts presented in this study. We hope that similar analyses will be pursued in the future and that this material will be useful. The reconstruction of BDA-labelled sections is presented for information in **Supplementary Figure 4**.

Discussion

Understanding the mechanisms of brain plasticity following a cerebral damage is of critical importance for the clinics but this field still contains many gray areas. Here, by using scalp EEG recording of SSEPs in an adult macaque monkey, we found that a dominant M1 lesion induced alterations in somatosensory processing. Our first surprise was that the post-lesion modulations were by no means restricted only to S1 but on the contrary, we also observed a post-lesion reduction in the amplitude of subcortical volleys. In addition, even though there was no change in voltage topography at the scalp after the lesion, the somatosensory cortical potential from the lesioned hemisphere was increased. Our second surprise was that the significant linear relationship between the amount of subcortical volleys and the amount of cortical output observed before the lesion after stimulation to the contralesional median nerve was partly maintained after the lesion in the form of a conserved cortical sensitivity to fluctuating volleys from the brainstem. Conversely, the lesion resulted in a constant gain added in the somatosensory processing irrespective of the amount of subcortical volley, as well as in a slight reduction of noise level of the cortical processing through the post-lesion period.

Extent of the lesion

The characteristics of the lesioned tissue reported here correspond to the cellular distortion previously described in other studies involving cortical lesions by using microinfusion of ibotenic acid in monkeys (Liu and Rouiller, 1999; Murata et al., 2008; Murata et al., 2015; Newsome et al., 1985a; Newsome et al., 1985b). The lesion was performed to damage the M1 finger representation only but actually it extended unintentionally to some extent in PMvc or more likely to the transition zone between M1 and PM (see below the section *Post-lesion cortical reorganisation* for further detail), in the white matter and maybe in area 3a as well. This is probably due to some spread and to the large volume and high concentration (twice as usually used in our laboratory) of ibotenic acid injected to circumvent the neuroprotective effect of the anaesthesia during the lesion surgery. Moreover, the large variations in area 3a position among different monkeys within the same species make very challenging to predict and then to spare its exact location at the moment of the lesion (Krubitzer et al., 2004). Previous studies already re-

ported the difficulty to perform very focal lesions restricted to the hand representation in M1 and described some damage in the neighbouring areas as well, such as S1 or PM (Kaeser et al., 2010; Lashley, 1924; Liu and Rouiller, 1999; Murata et al., 2008; Ogden and Franz, 1917). In particular, the lesion described in Murata et al. (2008), involving the fundus of the central sulcus, seems to be very close to the one performed in our study. This situation probably mimics to some extent the complex brain injuries observed in human as well, usually not restricted to a single architectonic area (see e.g. Kim and Lee, 1994). Although we acknowledge that the lesion may have damaged a small portion of the area 3a as well, more specifically the rostral part located in direct continuity with the area 4 in the fundus of the central sulcus, we are confident that the post-lesion alterations in SSEPs and manual dexterity changes described here cannot be only attributed to a damage of area 3a for the following reasons: (1) No generator of median nerve SSEPs has been found in area 3a in macaque monkeys using either epidural and intracranial recordings (Allison et al., 1991a; Allison et al., 1991b; McCarthy et al., 1991) or dipole localization method (Hayashi et al., 1994; Hayashi et al., 1995) (for a recent review about median nerve SSEP generators, see Mauguière, 2011). More specifically, the cortical potential recorded in our study at about 18 ms corresponds probably to the component P20 reported previously in anaesthetised macaque monkeys and whose generator was shown to be in area 3b (McCarthy et al., 1991). (2) Manual dexterity was previously compared in squirrel monkeys after a lesion of the rostral vs caudal portion of M1 (Friel et al., 2005). A caudal M1 lesion may be reasonably compared with the lesion performed in our study. The striking difference between both groups of monkeys was demonstrated using a behavioural task involving the precision grip performed under visual control (Klüver board): animals with a caudal M1 lesion often had to visually inspect the empty palm of their working hand after a pellet retrieval to realise that they really collected the pellet or not even though the whole task was under visual control, which the authors compared to somatosensory agnosia observed in humans. Although such a behaviour was observed in some monkeys in our laboratory (unpublished data, see **Chapter 5**), it was not the case in Mk-DI.

In spite of the absence of ICMS mapping of the lesioned area to directly assess its extent, there are several lines of evidence that the lesion most likely targeted the entire hand representation. First, in the 3 days following the lesion, the monkey presented a paresis of the ipsilateral (to the impaired hand) face, a severe paralysis of the ipsilateral

hindlimb in addition to a complete paralysis of the contralesional hand, wrist, elbow and shoulder to some extent. Normal movements of the face, shoulder, elbow and hindlimb were progressively recovered in the following days but the daily video follow-up of the animal performing the different behavioural tasks confirmed that finger and wrist movements remained partially altered throughout the post-lesion period. The transitory motor impairment of the face and hindlimb, in addition to the permanent deficit of the fingers and wrist throughout the post-lesion recovery phase strongly suggest that the lesion actually targeted the whole hand representation because the general somatotopic representation of the fingers is located between the representation of the face (more laterally) and the representation of the wrist and then the one of the leg (more medially). Second, *post mortem* histological analyses confirmed the large extent of the lesion, covering most likely the whole hand representation in the antero-posterior axis given that small portions of PMvc and maybe of the area 3a were damaged as well. Moreover, our neuroanatomical results were in accordance with other reports of lesions affecting the whole hand in *M. fascicularis* (see e.g. Qi et al., 2000; Sessle and Wiesendanger, 1982; Woolsey et al., 1952; and Wyss et al., 2013).

Effect of the cortical lesion on subcortical processing of peripheral inputs

Our first surprise was that a lesion performed at the cortical level induced massive alterations at the subcortical level as well, more specifically a reduction of the brainstem potential generated after stimulation of the median nerve of either side. We are confident that the modification observed here in subcortical sensory processing is not due to alteration in volume-conduction that may result from the lesion because the generator of this potential is very distant from the lesion.

A quite old study in cats mentioned that a drug-induced epileptic seizure originating at several sensory cortical areas drove then epileptic activity in sensory relay thalamic nuclei as well and both activities were synchronous and similar in shape, suggesting that subcortical activity was subordinate to cortical activity (Starzl et al., 1953). Moreover, subcortical modifications of several receptor systems after a ischemic lesion of prefrontal, motor, and somatosensory cortices were reported in rats (Dawson et al., 1994). These alterations were explained as an attempt of the damaged structures to compensate for the decrease of innervation following the cortical lesion. Another study in rats

showed some alterations of BAEPs after partial ablation of the auditory cortex (Lamas et al., 2013). But to the best of our knowledge, no mention of subcortical reorganisation after a cortical lesion is available in the EP literature either in non-human primates or in human (Green and McLeod, 1979; Kileny et al., 1987; Kraus et al., 1982; Ozdamar et al., 1982). On the contrary, a lesion in the afferent pathways usually induced abnormalities in signal from the latency corresponding to the structure itself targeted by the lesion (Green and McLeod, 1979; Sonoo et al., 1991; Stohr et al., 1983).

Other studies in rodents (Ghosh et al., 2009; Ghosh et al., 2010; Ghosh et al., 2012) and in primates (Bowes et al., 2013; Kaas et al., 1997; Kaas, 2000; Kaas et al., 2008; Nishimura and Isa, 2009; Nishimura and Isa, 2012; Schneider, 1990) already demonstrated that a spinal cord injury, a pyramidotomy or a dorsal column section all induced reorganisation at the cortical level. For instance, a partial dorsal column section in primates sparing afferences from fourth and fifth fingers induced a cortical reorganisation of the somatosensory cortex in the form of an expansion of the representation of both these spared fingers into territories previously devoted to the other fingers (Kaas et al., 1997). In case of a complete cervical dorsal column section, the former cortical representation of the fingers in S1 was then even invaded by cutaneous afferences from the face (Kaas et al., 1997). This confirms the general idea that an alteration at low-hierarchical level in a system induced further alteration at higher-hierarchical level ("magnification concept", Wall et al., 2002) in that system during reorganisation processes after a lesion. Essentially, according to this theory, the small subcortical changes induced by a lesion are substantially amplified in the cortex (Kaas et al., 1997).

But the reverse situation is not intuitive and was a real surprise for us from two points of view. First, our results suggest that a modification in motor output is able to induce itself a modification in sensory afferent processing as well, more specifically in the brainstem relay involved in somatosensory processing. Second, this suggests that a modification performed at a high-hierarchical level (the cortex in this case) results in further visible effects downwards in the hierarchical organisation of the nervous system, essentially implying that subcortical structures are under constant control of the cortex (see **General Introduction** for more information).

How can we interpret the reduction of brainstem volleys after the lesion? Does this reflect a use-dependent modulation? The sudden post-lesion decrease of use of the con-

tralesional upper limb may have induced a decreased sensory feedback from this particular body part to the brainstem, in the form of a smaller afferent volley at the brainstem level. The flow of sensory information from the periphery to the cortex via subcortical relay stations corresponds actually to the integration of ascending afferent pathways, intrinsic circuits and descending pathways from the neocortex as well (Nunez and Buno, 2001). Does the subcortical alteration correspond to a spinal, a subcortical or a cortical modulation on the brainstem by an increase of inhibition by lesion-induced plasticity in these structures? For instance, some topographically restricted corticocunate projections have been already demonstrated in monkeys (Cheema et al., 1985). These questions remain open. But still this does not explain the similar decrease in brainstem volley observed after stimulation of the ipsilesional median nerve as well.

The similarly significant post-lesion decrease of the brainstem volley observed after stimulation of the ipsilesional median nerve suggests that the lesion induced massive reorganisation in subcortical sensory processing, i.e. that the unilateral lesion affected indiscriminately and bilaterally subcortical structures, instead of inducing a more focal and lateralised alteration. This may reflect either a strong cortical modulation on brainstem structures through bilateral projections after the lesion, or that alteration in processing from the contralesional median nerve are sufficient to induce alteration in processing from the ipsilesional median nerve, maybe through extensive bilateral connections at the brainstem level. Interestingly, even though the subcortical volleys after ipsilesional median nerve stimulation were decreased, the cortical signal and the brainstem input-cortical output relationship were not altered by the lesion, meaning that the post-lesion modulation in processing from the ipsilesional median nerve was restricted to subcortical structures only.

In sum, based on the data presented here, we can only speculate about the origin of the brainstem alterations after the lesion and not favour one hypothesis over the others.

We cannot exclude that the cortical lesion may have induced some other subcortical alterations, for instance in the thalamus or in the thalamocortical projections. Nevertheless, our study design did not allow us to investigate these possibilities.

Origin of subcortical potential

An important issue concerns the precise origin of the generation of the subcortical potential of median nerve SSEPs. Previous source localisation of median nerve SSEPs in our macaque monkeys confirmed the brainstem origin of this signal (Gindrat et al., 2014). Nevertheless, this first result did not allow to distinguish between intrinsic tissue activity at the brainstem level and axonal volleys in pathways along the brainstem. The ultimate proof of the origin of this signal would be provided of course by several intracellular recordings in the brainstem during electrical stimulation of the median nerve. A previous study of SSEP recordings in *M. mulatta*, by using surface electrodes, array of epidural electrodes over S1 and intracortical electrodes, reported that the early potentials P5.3 and P6.2 were generated by "*bursts of highly synchronised action potentials travelling along the medial lemniscus*" and that the potential P7.2 was "*generated within the thalamocortical radiations*" (Arezzo et al., 1979). Based on our previous study using electrical source imaging (Gindrat et al., 2014), we may reasonably assume that the P6.4 potential corresponds to the brainstem potential recorded in the present study and therefore that the brainstem potential in our study is generated by an afferent volley at the brainstem level. The slightly longer latency we reported here (about 7 ms) is probably due to the different body sizes of the animals involved in each study (*M. fascicularis* in the present study versus *M. mulatta* in Arezzo's paper) (Hamada et al., 2006). The difference in polarity of the potentials (negative brainstem peak here versus positive P6.2 ms in Arezzo's paper) is probably due to the difference in electrode montage design (average reference here versus left wrist reference in Arezzo's paper) (Dien, 1998; Murray et al., 2008; Yao et al., 2007).

Another study supports this hypothesis: an interpretation of the origin of human short-latency brainstem potentials recorded using intracranial and scalp electrodes was proposed on the basis of spatial gradients of latency and amplitude changes in the recorded potentials (Hashimoto, 1984). On the one hand, the authors classified components such as P11 as *volume-conducted far-field activity* because neither shift in latency nor changes in amplitude of the potential were observed along the successive electrodes in the intracranial array, meaning that this activity was not affected by the relative distance of the recording electrodes. On the other hand, for other components such as P13, a latency shift was present along the electrode array from the pons to the diencephalon, then a

very similar potential waveform was measured from 2 close electrodes in the midbrain at the medial lemniscus level, followed by a volume-conducted far-field activity recorded close to the lateral ventricle and at the scalp surface. This activity was proposed to correspond to a synchronised volley of action potentials within the medial lemniscus from the brainstem to the thalamus. In our study we picked up this brainstem signal from all the electrodes at the scalp with some changes in latency and amplitude but this component was with maximal amplitude and very similar waveform in the two most caudal electrodes, located on either side of the midline just below the external occipital protuberance. By applying the same reasoning as in Hashimoto's paper (1984) but by being well aware that this potential was derived only from scalp electrodes in our study, we can conclude again that the brainstem activity may represent a synchronised axonal volley travelling in fibre tracts at the level of these recording electrodes.

Effect of the cortical lesion on cortical potential

The cortical lesion induced modifications at the cortical level itself, in the form of an increased amplitude of the cortical potential measured over the ipsilesional sensorimotor cortex even though the voltage topography was not affected. Given the very close distance between the S1 generator of this potential (Allison et al., 1991a; Allison et al., 1991b; Hayashi et al., 1994; Hayashi et al., 1995; McCarthy et al., 1991) and the cortical lesion, we are aware that this alteration in the amplitude of cortical signal may result from modification in volume-conduction properties induced by the lesion itself, in addition to a real modification of the brain activity. The biophysical properties of volume-conduction of EEG signal from the generators through brain tissues to the scalp electrodes remain largely elusive and have been only investigated by using models so far (van den Broek et al., 1998). We still do not know exactly how the signal is conducted through the living tissues of the head and modified before reaching the recording electrodes at the scalp. Therefore, we cannot predict then how a cortical lesion will modify the volume-conduction properties of the brain. Nevertheless, we do not think that the sole lesion-induced distortions in volume-conduction could explain the post-lesion EEG signature observed at the scalp for the following reasons: (1) The cortical potential recorded in our study at about 18 ms corresponds probably to the component P20 reported previously in anaesthetised macaque monkeys. The generator of this potential was

shown to be located in area 3b (McCarthy et al., 1991), i.e. in the posterior bank of the central sulcus. This generator is therefore tangentially oriented to the scalp surface. Previous models of the effect of a brain lesion on volume-conduction demonstrated that volume-conduction artifacts from tangential generators close to the lesion were smaller than from radial generators (van den Broek et al., 1998). (2) Modification in volume-conduction induces most certainly strong distortions in voltage topography at the scalp (van den Broek et al., 1998). But here, we did not observe any topographical changes at the scalp after the lesion. (3) The dipole location relative to the lesion and to the inner skull surface is crucial for the presence or absence of volume-conduction artifacts (van den Broek et al., 1998). Essentially, the closer the lesion is to the dipole, the larger volume-conduction artifacts are, especially if the lesion is located in between the dipole and the head surface. We do not expect such a configuration of the lesion-generator localisation here. (4) We already demonstrated that the craniotomy itself required in our lesional protocol did not induce artifact in brain activity recorded at the scalp (see Gindrat et al., 2014 in **Chapter 1**). (5) The significant linear relationship between brainstem input and cortical output observed before the lesion cannot objectively be attributed to any volume-conduction artifact because the monkey's head and brain had not been subjected to any intervention during this pre-lesion period. The evidence of a preserved cortical sensitivity to changes in brainstem input after the lesion indicates that the cortical potential was not fully altered and we can then reasonably assume that the post-lesion relationship is real as well and is not merely the result of volume-conduction effect.

Of course further evidence against volume-conduction artifact would have been to confirm the post-lesion increased cortical amplitude of contralesional SSEPs by using another imaging technique such as magnetoencephalography (MEG) that is known to be less affected by volume-conduction issues than EEG (Mondt, 1989; van den Broek et al., 1998; Winter et al., 2007).

In brief, all these observations suggest that the modulation of brain activity observed after the lesion are not only due to volume-conduction effects resulting from the lesion but correspond to true alterations in brain activity after the lesion.

Effect of the cortical lesion on the relationship between subcortical volleys and cortical output

We demonstrated here that the spontaneous cortical reorganisation after the permanent cortical lesion was characterised by a modification of the relationship between subcortical volleys and cortical output after contralesional electrical stimulation. But in spite of the large extent of the cortical lesion, this relationship was not fully altered. On the contrary, the lesion induced very specific modulations of this relationship: we interpreted the post-lesion increase of the y-axis intercept value as a constant gain added to the somatosensory cortical processing, i.e. an increase of somatosensory output. The slight post-lesion decrease in R indicated a small reduction in the noise level of the cortical processing. The absence of any modification in the slope of the regression lines suggested a conserved sensitivity of S1 to subcortical volleys. This post-lesion EEG signature is interesting from several points of view.

First, surprisingly, the sensitivity of the somatosensory cortex to fluctuating subcortical volleys was maintained after the lesion in spite of a decreased processing at the brainstem level. This suggests that the S1 sensitivity could still be fully achieved even with impaired afferent information. Moreover, it indicates that this specific process does not require the involvement of the large sensorimotor cortical networks and subcortical networks that may have been damaged by the lesion performed here. Rather we propose that the sensitivity of S1 was performed very locally by S1 itself. Another possibility would be that the lesion had destroyed the neuronal network responsible for this particular process as well but then that the post-lesion plastic reorganisation at the cortical level resulted in the complete recovery of the sensitivity of the somatosensory cortex. Nevertheless, given that we demonstrated that the same cortical sensitivity as observed before the lesion was still present in the first post-lesion data in spite of the large extent of the lesion, we do not think that this is a putative hypothesis.

Second, intriguingly, the cortical lesion resulted in a constant gain added in the somatosensory cortical process and maybe a slight post-lesion evolution in the control of noise in somatosensory processing. This suggests that the control of the somatosensory output and the one of noise normally depended on a more global and larger cortical network probably affected by the lesion, in addition to S1 itself.

Third, this observation suggests that the post-lesion increase of somatosensory output was not accompanied with any clear benefit for S1 in terms of processing improvement, given the conserved sensitivity of S1.

The demonstration of a similar relationship between subcortical input and somatosensory cortical output in both left and right median nerve SSEPs before the lesion is important. First, it confirms that this relationship was not an artifact in our data. Second, it suggests that this process of cortical sensitivity is not linked to hand dominance but is rather a general feature of somatosensory processing, at least from the median nerve. Furthermore, the completely conserved relationship between subcortical input and somatosensory cortical output in left, ipsilesional median nerve SSEPs confirmed that the lesion did not induce a global change in brain activity that may be attributed to an artifact but rather that the gain added at the cortical level was restricted to S1 in the lesioned hemisphere.

We demonstrated here that the relationship between subcortical afferent volleys and cortical output after electrical stimulation to the median nerve in macaque monkey was linear. This result is not in agreement with previous observations of non-linear conductions through relays in the somatosensory afferent pathways (Krnjevic and Morris, 1976; Walsh and Whitehorn, 1981). Nevertheless, a direct comparison with them is not appropriate because both these earlier studies were performed in cats, under very unnatural conditions (decerebrate animals or paralysed and artificially respired animals) and did not involve the same structures, nor exactly the same kind of measurement nor the same analysis.

In sum, we propose that the lesion-induced alterations in somatosensory pathway already observed at the subcortical level are further transmitted at the cortical level by ascending projections from the periphery to the cortex. The preserved linear relationship observed between brainstem input and cortical output after the lesion does not support the “magnification concept” (Wall et al., 2002) of subcortical inputs at the cortex level during post-lesion reorganisation processes where small subcortical changes induced by a lesion are substantially amplified in the cortex (Kaas et al., 1997). The present data rather suggest that extensive alterations are already present at the brainstem level, in accordance with the “multiple substrate view” (Wall et al., 2002). But the observation that, after the lesion, a reduced activity at the brainstem level was related to an

increased activity at the cortical level ruled out the hypothesis of a simple, passive and complete reflection of brainstem alterations at the cortical level, but rather suggested the additional involvement of "supra-brainstem" mechanisms, for instance in the form of other cortical areas sending inputs to S1 and/or intrinsic reorganisation in S1, both resulting in a constant gain added to cortical output.

Post-lesion cortical reorganisation

Then, how can we interpret the increased output from S1? Does that correspond to an internal reorganisation in S1 or do some inputs come from other areas? Moreover, is/are the increased somatosensory output and/or the improved control of noise level contributing to the functional recovery? This will be discussed here.

There was some spontaneous functional recovery of the contralesional hand dexterity after the lesion although the hand area in left M1 had been permanently destroyed, meaning that there were compensatory mechanisms underlying the partial functional recovery of the contralesional finger use. The increased output from S1 and the slightly improved control of noise in S1 processing may be one neuronal substrate of functional recovery among others because the involvement of S1 in post-lesion cortical reorganisation after a similar injury in squirrel monkeys was already demonstrated (Dancause et al., 2005) as well as the role of S1 in functional recovery after a stroke in human (Jang et al., 2002; Jang et al., 2004; Laible et al., 2012; Pineiro et al., 2001; Schaechter et al., 2012). Remarkably, an increase in sensorimotor cortex responsiveness to tactile stimulation of impaired fingers correlated strongly with the level of functional motor recovery during subacute post-stroke period (less than one year after stroke, corresponding to the same time period as the post-lesion phase investigated in our study) in human patients (Schaechter et al., 2012). S1 is a contributor of the CST (Biber et al., 1978; Cheema et al., 1983; Cole and Glees, 1954; Coulter and Jones, 1977; Darian-Smith et al., 1996; Galea and Darian-Smith, 1994; Jones and Wise, 1977; Kumar et al., 2009; Lemon, 1997; Lemon, 2008; Lemon and Griffiths, 2005; Nieuwenhuys et al., 2007; Nudo and Masterton, 1990; Ralston and Ralston, 1985; Schieber, 2007; Seo and Jang, 2013; Sessle and Wiesendanger, 1982; Toyoshima and Sakai, 1982; Wiesendanger, 1981). One may therefore speculate that the partial functional recovery and changes in strategy observed after the lesion are at least partially mediated through an increased contribution

of S1 to the CST output. Alternatively, this increase in S1 output may come from aberrant projections to S1 and therefore represent a maladaptive activation of S1, interfering with functional recovery. Based on our results, we cannot invalidate this hypothesis.

What is the origin of this constant input to the somatosensory cortex? If the linear relationship between the brainstem input and the cortical output is always true, irrespective of the brainstem input, we expect that a constant input is added to the somatosensory output, even without any subcortical input. This suggests that this gain added at the cortical level is independent from the subcortical activity. Putative explanations are exposed here:

(1) The post-lesion increase of background activity at the somatosensory cortex level may correspond to a post-lesion activity-related reorganisation in S1 itself in the form of an increase of self-generated, intrinsic activity in S1. We expect that the M1 lesion resulted not only in sustained changes in motor output, but it should have also damaged the strong sensorimotor connectivity between M1 and S1. It has been proposed that the amount of inhibitory inputs to sensory cortices is strongly linked to long-term activity levels (Kaas et al., 1997): deprived areas are less inhibited, for instance by a reduction of GABA activity (Chen and Nedivi, 2013; Garraghty et al., 1991; Griffen and Maffei, 2014; Hendry and Jones, 1986; Jones, 1993; Kullmann et al., 2012; Redecker et al., 2000) or ACh activity (Avendano et al., 1995) among others. Conversely highly stimulated areas get much more inhibition. This means that S1 was then largely deprived of intracortical inhibitory connections from M1, leading to an increase in intrinsic S1 activity. Similar phenomena of increase of activity in sensory cortex have been already suggested to explain some phantom perceptions such as tinnitus (Chen et al., 2014; Lockwood et al., 1999; Norena and Eggermont, 2003) or phantom limb pain (Bolognini et al., 2013; Dettmers et al., 2001).

This leads then to ask the question about the functional significance of this motor inhibition in normal situations. During motor exploration by active touch from the fingers for instance, the somatosensory system is exposed to many different stimuli but has to concentrate on the most important ones only, in order to send the most relevant sensory feedback to M1. This gating of sensory input to M1 may be achieved at the cortical level (Seki and Fetz, 2012) by temporarily upregulating intracortical inhibition from M1 to S1.

(2) A second hypothesis involves an acute plastic reorganisation of the connections from and to S1, such as a constant input to the somatosensory cortex coming from another remote area of the brain involved in post-lesion reorganisation. Based on previous studies, a strong candidate is PM that was shown to be involved in functional recovery (Liu and Rouiller, 1999; Murata et al., 2015) and reorganised as well after a large M1 lesion of the hand representation of M1 in non-human primates (Frost et al., 2003; Murata et al., 2015). More specifically, the ventrorostral part of PM (PMvr or F5 (Matelli et al., 1985)), in the postarcuate cortex, may be involved because there is a large body of evidence that the PMv hand representation is actually located in PMvr (Cerri et al., 2003; Dum and Strick, 2005; Gentilucci et al., 1988; Gerbella et al., 2011; He et al., 1993; Kurata and Tanji, 1986; Lehmann and Scherberger, 2013; Rizzolatti et al., 1988; Shimazu et al., 2004). For instance, we propose that some cortical inputs from PMvr targeting originally M1 may have been redirected to S1 after the lesion, as already observed (Dancause et al., 2005), or some pre-lesion existing but inactive inputs from PMvr to S1 may have been desilenced after the lesion. Importantly, although some portions of PMvc were lesioned, PMvr remained intact, supporting the hypothesis of a post-lesion contribution of PMv.

(3) Maybe some other remote, non-primary motor areas in the lesioned hemisphere could contribute in the same way by projecting on S1, such as the SMA (Eisner-Janowicz et al., 2008; McNeal et al., 2010) or the CMA because existing projections from SMA (DeVito and Smith, 1959; Huffman and Krubitzer, 2001; Jones et al., 1978; Jürgens, 1984) and CMA to S1 were already observed in control monkeys as from PM to S1 (Dancause et al., 2005).

All these potential phenomena may result in a completely new cortical output from S1 and may actually coexist as well. However, this does not fully explain our data because we did not observe any massive post-lesion evolution in S1 processing and output, if not a slight improvement in the control of noise level, whereas the monkey showed a progressive functional recovery of fine manual dexterity. This implies that some additional contributions are expected to underlie the partial functional recovery, for instance originating from other non-primary motor cortical areas in the frontal cortex. SMA, PMv or CMA all contain a hand representation and CST neurons as well and may therefore either increase the strength of their projections in the CST or the strength of projections to some spared portions of M1 (Borra et al., 2010; Boudrias et al., 2010; Darian-Smith et al.,

1999; Dum and Strick, 1991; Dum and Strick, 2002; Dum and Strick, 1996; He et al., 1993; He et al., 1995; Kantak et al., 2012; Liu and Rouiller, 1999; McNeal et al., 2010; Rouiller et al., 1996). What about the involvement of contralesional areas (Nudo, 2006)? The recruitment of the intact hemisphere such as the intact sensorimotor cortex (Cramer et al., 1997; Liepert et al., 2000; Schaechter et al., 2008; Schaechter et al., 2012) has already been observed, especially in case of largely extended lesions (Nudo, 2013). Here the lesion was extended in the sense that it covered the whole hand representation of M1. Nevertheless, back in the clinical context, this corresponds to a very focal lesion, meaning that the implication of the intact hemisphere is unlikely. One may expect contribution from the intact hemisphere in case of an extended lesion affecting not only M1 but other non-primary motor areas as well, such as PM or SMA, as observed in stroke patients.

We should not forget that plastic changes mediating functional reorganisation are actually dynamic over time. A very recent study on *M. mulatta* revealed that after an M1 hand lesion, the early post-recovery period involved the activation of ipsilesional PMv whereas the functional recovery during the later post-recovery period was mediated primarily by the peri-lesional intact portion of M1 (Murata et al., 2015). This suggests that during the early post-lesion stage, the brain resorted to available pre-existing neural substrates by simply reducing inhibitory control on them, whereas during the late post-lesion stage original structures were again involved by plastic changes of the neural circuits (Nishimura and Isa, 2009).

In sum, based on the present data, we cannot favour one scenario over the others.

Electrical stimulation

We used here electrical peripheral stimulation at the wrist because it activates synchronously a large amount of afferent fibres not restricted to tactile afferences (Allison et al., 1991a; Aminoff and Eisen, 1998; Desmedt, 1987; Legatt, 2014; Mauguière, 2011; Regan, 1989; Walsh et al., 2005; York, 1985). Testing this nonspecific activation by using electrical stimulation may be relevant in case of a neurological impairment affecting differentially the different types of fibres. Moreover electrical peripheral stimulation generates a robust response at the scalp (Dawson, 1956; York, 1985). This was a prerequisite

for data analysis at single-trial level. Moreover, this type of stimulation is user-friendly and has some advantages over other types of stimulation, such as the brevity and strict temporal control of stimulus onset and cutoff (Mauguière, 2011). Consequently, it is commonly used in clinical investigations (American Clinical Neurophysiology Society, 2006; Cruccu et al., 2008), increasing then the relevance of our results.

We delivered electrical stimulation to the median nerve instead of the ulnar nerve because the ratio of skin afferents to muscle afferents from the hand is higher in median nerve than in ulnar nerve (Dawson, 1956). Actually, cerebral potentials evoked by electrical stimulation to a nerve are primarily produced by the large-diameter and low-threshold sensory afferent fibres form the skin, as compared to the sensory afferences from the hand muscles (Dawson, 1956).

Relevance of single-trial analysis

We considered median nerve SSEPs at the single-trial level and performed regressions between the subcortical peak and the cortical peak over each recording in a single subject. The standard method of event-related potential (ERP) analysis and interpretation assumes (1) that ERPs are essentially stable over time across many trials (stationary hypothesis) and (2) that ERPs are superimposed on an uncorrelated stochastic background EEG activity (Graben et al., 2000). Therefore brain responses related to a given similar stimulus are usually averaged across trials and across subjects to enhance signal-to-noise ratio. Nevertheless this approach fails to consider that ERPs are influenced by some important factors over time, such as learning, plasticity, adaptation, and background EEG activity, resulting consequently in variability across trials, in addition to inter-individual variability (McLaughlin and Kelly, 1993; Spencer, 2005). The physiological information contained in each trial is partially lost when data are averaged in a given subject (Pernet et al., 2011) and averaging brain activity across subjects can result in false interpretations by summarising the brain activity into patterns that are not present at the single-subject level (Gaspar et al., 2011). What is even more important, the high temporal resolution of EEG constitutes a unique opportunity to access the real temporal dynamics of the brain processing incoming stimuli. These elements have led to consider the variance of brain activity within subjects already at the level of the single trials. Single-trial analysis allows to address the fundamental question of relationship between

sensory inputs to the brain and cortical output activity over time and to get more knowledge about the different mechanisms underlying brain plasticity. Moreover, this method enables statistical analysis already at the single-subject level, which is crucial when the subject cannot be easily included in a larger group, for instance in animal research with only few animals involved in a protocol, or in clinics with patients presenting very specific deficits. From the point of view of basic neurophysiology, by going deeper than the averaged brain activity, a more detailed description of the data allows to get additional insight into the mechanisms of ERP generation: the activity at each single trial is the correlate of post-synaptic potentials of neuronal populations in the cortex.

Impact of the lesion on hand motor control

The cortical lesion induced severe motor deficits in manual dexterity with an initial complete loss of finger movements followed by a spontaneous gradual functional recovery. Although some relatively independent fingers movements were restored, allowing to perform some precision grip, the ability to perform fine fractionated fingers movements was permanently reduced, as indicated by the *score in 30 s* and the *contact time*. Moreover, the larger impairment to collect horizontal pellets as compared to vertical ones reflects a permanent deficit to perform wrist deviations associated to precision grip. This is in accordance with previous reports of motor cortex lesions of the hand representation in non-human primates performed in our laboratory (Hoogewoud et al., 2013; Kaeser et al., 2011; Liu and Rouiller, 1999; Rouiller et al., 1998; Wyss et al., 2013), and in other groups (Darling et al., 2014; Frost et al., 2003; Glees and Cole, 1950; Nudo and Milliken, 1996; Pizzimenti et al., 2007; Plautz et al., 2003). The lesion performed in our study has most probably extensively damaged the populations of CM cells in M1 normally involved in the control of the distal muscles of the contralateral arm (Buys et al., 1986; Lemon, 1993; Lemon, 1997; Lemon, 2008; Lemon and Porter, 1976).

The clear functional implications of the post-lesion EEG alterations observed here for behavioural recovery are unknown and would still need further investigations. Nevertheless, the increase of cortical activity may be reminiscent of the increase in premovement cortical activity measured in S1 after cooling of the M1 hand representation in macaque monkeys, previously described by Sasaki and Gemba (1984). It is tempting to speculate that S1 may be recruited to compensate for the loss of motor function, explain-

ing the enhanced activity in S1 after M1 lesion. This is in line with some observations that, in monkeys, CST neurons from S1 share similar properties of activities to CST neurons from M1, such that in addition to their sensory function, CST neurons from S1 could be directly involved in motor control (Evarts, 1974; Fromm and Evarts, 1982). Our data suggest a slight decrease in the amount of noise in cortical processing from *post-lesion 1* group (post-lesion days 9 to 56) to *post-lesion 2* group (post-lesion days 63 to 134). Such decrease in the noise of cortical processing through the post-lesion recovery period may correspond to functional recovery in the form of the transition from reacquisition to stabilisation of the performance of the contralesional hand observed from post-lesion day 72. This observation does not necessarily mean that the slightly reduced noise in processing induced the partial functional recovery of manual dexterity of the contralesional hand, nor the opposite, but this suggests that the two phenomena may be linked. Many questions remain open at that level.

Further remarks

This study is a case report. Evidently, we will need to confirm the EEG signature of a lesion of the M1 hand representation in more animals. Moreover, we could refine our study by analysing other SSEP components and by increasing the number of trials in order to get a finer and more robust analysis. It would be also interesting to use other stimulations paradigms, by changing for instance the stimulus length, stimulus amplitude (Lesser et al., 1979; Rappaport et al., 1992a; Rappaport et al., 1992b) or repetition rate (Araki et al., 1999; Fujii et al., 1994; Pratt et al., 1980; Robinson and Micklesen, 2010; Valeriani et al., 1998), and to investigate in particular if the relationship observed between brainstem volleys and cortical output does depend on these stimulation parameters.

The power of our study resides in the acquisition of whole-scalp EEG signals very frequently over time, both before and after the lesion, associated with a simple but even so fruitful data analysis to obtain a detailed follow-up of the cortical reorganisation. Although subcortical evoked signals usually have a lower signal-to-noise ratio as compared to cortical evoked potentials, we were able to extract both potentials already at the single-trial level and demonstrate that there is actually a significant linear relationship between them.

We demonstrated that the lesion-induced changes in motor output and sensorimotor connectivity were sufficient to reorganise the somatosensory system at several levels, meaning that a lesion in the motor system induces extensive plasticity in the somatosensory system as well that may be involved in functional recovery (Schaechter et al., 2012). Therefore these results may be relevant for the clinics, where neurorehabilitation strategies for stroke patients for instance should target more intensively the somatosensory system as well, in parallel with the recovery of motor functions themselves, as already initiated in some studies (Byl et al., 2003; Laible et al., 2012; Sawaki et al., 2006).

Conclusion

By way of conclusion, we presented here an additional window into the mechanisms of sensorimotor reorganisation underlying functional recovery after a cortical lesion in non-human primates. More specifically, the present data showed that the somatosensory processing was deeply reorganised in the form of plastic modifications both at subcortical and cortical levels after a dominant motor cortex lesion. This indicates that the sustained changes in motor output and sensorimotor connectivity induced by the lesion were sufficient to reorganise extensively the somatosensory system as well. We provided here additional information about the post-lesion compensatory mechanisms of subcortical structures interacting with the cortex, shedding light on another facet of lesion-induced plasticity. This further confirms that the motor cortex is not a purely motor structure (Asanuma, 1981; Asanuma and Rosén, 1972; Jones, 1986; Rosen and Asanuma, 1972). Equally important, this supports that the sensorimotor cortical representations are plastic in adult macaque monkeys. However the clear functional implications of the changes described here for behavioural recovery still need further investigations.

Acknowledgements

We thank Laurent Bossy, Jacques Maillard (animal care taking), Christiane Marti, Christine Roulin (histology), André Gaillard (mechanics), Bernard Aebischer, Andrea Francovich (electronics), Laurent Monney (informatics) and Véronique Gindrat (help in behavioural data analysis). We also thank Dr Charles Quairiaux for his helpful comments.

The Cartool software (http://www.fbmlab.com/cartool-software/) has been programmed by Denis Brunet, from the Functional Brain Mapping Laboratory, Geneva, Switzerland, and is supported by the Center for Biomedical Imaging (CIBM) of Geneva and Lausanne. This work was supported by the Swiss National Science Foundation grants 31-61857.00, 310000-110005, 31003A-132465 (EMR), the National Centre of Competence in Research (NCCR) on "Neural plasticity and repair", Novartis Foundation, The Christopher Reeves Foundation (Springfield, NJ, USA) and the SPCCR (Swiss Primate Competence Center for Research: http://www.unifr.ch/spccr/).

References

Allison, T., McCarthy, G., Wood, C.C., Jones, S.J., 1991a. Potentials evoked in human and monkey cerebral cortex by stimulation of the median nerve. A review of scalp and intracranial recordings. Brain 114 (Pt 6), 2465-2503.

Allison, T., Wood, C.C., McCarthy, G., Spencer, D.D., 1991b. Cortical somatosensory evoked potentials. II. Effects of excision of somatosensory or motor cortex in humans and monkeys. J Neurophysiol 66, 64-82.

American Clinical Neurophysiology Society, 2006. Guideline 9D: guidelines on short-latency somatosensory evoked potentials. American journal of electroneurodiagnostic technology 46, 287.

Aminoff, M.J., Eisen, A.A., 1998. AAEM minimonograph 19: somatosensory evoked potentials. Muscle Nerve 21, 277-290.

Araki, A., Takada, A., Yasuhara, A., Kobayashi, Y., 1999. The effects of stimulus rates on the amplitude of median nerve somatosensory evoked potentials: the developmental change. Brain Dev. 21, 118-121.

Arezzo, J.C., Legatt, A.D., Vaughan, H.G.Jr., 1979. Topography and intracranial sources of somatosensory evoked potentials in the monkey. I. Early components. Electroencephalogr.Clin.Neurophysiol 46, 155-172.

Asanuma, H., 1981. Functional role of sensory inputs to the motor cortex. Prog.Neurobiol. 16, 241-262.

Asanuma, H., Rosén, I., 1972. Functional role of afferent inputs to the monkey motor cortex. Brain Res 40, 3-5.

Avendano, C., Umbriaco, D., Dykes, R.W., Descarries, L., 1995. Decrease and long-term recovery of choline acetyltransferase immunoreactivity in adult cat somatosensory

cortex after peripheral nerve transections. The Journal of Comparative Neurology 354, 321-332.

Barba, C., Valeriani, M., Colicchio, G., Mauguière, F., 2005. Short and middle-latency Median Nerve (MN) SEPs recorded by depth electrodes in human pre-SMA and SMA-proper. Clin.Neurophysiol 116, 2664-2674.

Baurain, M.J., Hennart, D.A., Godschalx, A., Huybrechts, I., Nasrallah, G., d'Hollander, A.A., Cantraine, F., 1998. Visual evaluation of residual curarization in anesthetized patients using one hundred-hertz, five-second tetanic stimulation at the adductor pollicis muscle. Anesth.Analg. 87, 185-189.

Beall, J.E., Applebaum, A.E., Foreman, R.D., Willis, W.D.Jr., 1977. Spinal cord potentials evoked by cutaneous afferents in the monkey. J Neurophysiol 40, 199-211.

Beaud, M.L., Schmidlin, E., Wannier, T., Freund, P., Bloch, J., Mir, A., Schwab, M.E., Rouiller, E.M., 2008. Anti-Nogo-A antibody treatment does not prevent cell body shrinkage in the motor cortex in adult monkeys subjected to unilateral cervical cord lesion. BMC.Neurosci. 9, 5.

Biber, M.P., Kneisley, L.W., LaVail, J.H., 1978. Cortical neurons projecting to the cervical and lumbar enlargements of the spinal cord in young and adult rhesus monkeys. Experimental Neurology 59, 492-508.

Bidelman, G.M., Weiss, M.W., Moreno, S., Alain, C., 2014. Coordinated plasticity in brainstem and auditory cortex contributes to enhanced categorical speech perception in musicians. European Journal of Neuroscience 40, 2662-2673.

Bolognini, N., Olgiati, E., Maravita, A., Ferraro, F., Fregni, F., 2013. Motor and parietal cortex stimulation for phantom limb pain and sensations. Pain 154, 1274-1280.

Borra, E., Belmalih, A., Gerbella, M., Rozzi, S., Luppino, G., 2010. Projections of the hand field of the macaque ventral premotor area F5 to the brainstem and spinal cord. J Comp Neurol. 518, 2570-2591.

Boudrias, M.H., Lee, S.P., Svojanovsky, S., Cheney, P.D., 2010. Forelimb muscle representations and output properties of motor areas in the mesial wall of rhesus macaques. Cereb.Cortex 20, 704-719.

Bowes, C., Burish, M., Cerkevich, C., Kaas, J., 2013. Patterns of cortical reorganization in the adult marmoset after a cervical spinal cord injury. Journal of Comparative Neurology 521, 3451-3463.

Brunet, D., Murray, M.M., Michel, C.M., 2011. Spatiotemporal analysis of multichannel EEG: CARTOOL. Comput.Intell.Neurosci. 2011 (ID 813870), 15 pages.

Burton, H., Fabri, M., 1995. Ipsilateral intracortical connections of physiologically defined cutaneous representations in areas 3b and 1 of macaque monkeys: projections in the vicinity of the central sulcus. J Comp Neurol. 355, 508-538.

Buys, E.J., Lemon, R.N., Mantel, G.W., Muir, R.B., 1986. Selective facilitation of different hand muscles by single corticospinal neurones in the conscious monkey. J Physiol 381, 529-549.

Byl, N., Roderick, J., Mohamed, O., Hanny, M., Kotler, J., Smith, A., Tang, M., Abrams, G., 2003. Effectiveness of sensory and motor rehabilitation of the upper limb following the principles of neuroplasticity: patients stable poststroke. Neurorehabil Neural Repair 17, 176-191.

Carroll, E.W., Wong-Riley, M.T.T., 1984. Quantitative light and electron microscopic analysis of cytochrome oxidase-rich zones in the striate cortex of the squirrel monkey. The Journal of Comparative Neurology 222, 1-17.

Cavalieri, B., 1653. Geometria indivisibilibus continuorum nova quadam ratione promota. typis C. Ferronii, Bologna.

Cerri, G., Shimazu, H., Maier, M.A., Lemon, R.N., 2003. Facilitation From Ventral Premotor Cortex of Primary Motor Cortex Outputs to Macaque Hand Muscles. Journal of Neurophysiology 90, 832-842.

Chatagny, P., Badoud, S., Kaeser, M., Gindrat, A.D., Savidan, J., Fregosi, M., Moret, V., Roulin, C., Schmidlin, E., Rouiller, E.M., 2013. Distinction between hand dominance and hand preference in primates: a behavioral investigation of manual dexterity in nonhuman primates (macaques) and human subjects. Brain and Behavior 3, 575-595.

Cheema, S., Rustioni, A., Whitsel, B.L., 1985. Sensorimotor cortical projections to the primate cuneate nucleus. The Journal of Comparative Neurology 240, 196-211.

Cheema, S.S., Rustioni, A., Whitsel, B.L., 1983. Corticospinal projections from pericentral and supplementary cortices in macaques as revealed by anterograde transport of horseradish peroxidase. Neurosci.Letters.suppl. 14, 62.

Chen, J.L., Nedivi, E., 2013. Highly specific structural plasticity of inhibitory circuits in the adult neocortex. Neuroscientist. 19, 384-393.

Chen, Y.C., Zhang, J., Li, X.W., Xia, W., Feng, X., Gao, B., Ju, S.H., Wang, J., Salvi, R., Teng, G.J., 2014. Aberrant spontaneous brain activity in chronic tinnitus patients revealed by resting-state functional MRI. NeuroImage: Clinical 6, 222-228.

Cole, J., Glees, P., 1954. Effects of small lesions in sensory cortex in trained monkeys. J Neurophysiol. 17, 1-13.

Committee for the Update of the Guide for the Care and Use of Laboratory Animals, National Research Council, 2011. Guide for the Care and Use of Laboratory Animals, Eighth ed. The National Academies Press.

Coulter, J.D., Jones, E.G., 1977. Differential distribution of corticospinal projections from individual cytoarchitectonic fields in the monkey. Brain Research 129, 335-340.

Courtine, G., Bunge, M.B., Fawcett, J.W., Grossman, R.G., Kaas, J.H., Lemon, R.N., Maier, I., Martin, J., Nudo, R.J., Ramon-Cueto, A., Rouiller, E.M., Schnell, L., Wannier, T., Schwab, M.E., Edgerton, V.R., 2007. Can experiments in nonhuman primates expedite the translation of treatments for spinal cord injury in humans? Nat.Med. 13, 561-566.

Cramer, S.C., Nelles, G., Benson, R.R., Kaplan, J.D., Parker, R.A., Kwong, K.K., Kennedy, D.N., Finklestein, S.P., Rosen, B.R., 1997. A Functional MRI Study of Subjects Recovered From Hemiparetic Stroke. Stroke 28, 2518-2527.

Cruccu, G., Aminoff, M.J., Curio, G., Guerit, J.M., Kakigi, R., Mauguière, F., Rossini, P.M., Treede, R.D., Garcia-Larrea, L., 2008. Recommendations for the clinical use of somatosensory-evoked potentials. Clin.Neurophysiol 119, 1705-1719.

Dancause, N., 2006. Vicarious function of remote cortex following stroke: recent evidence from human and animal studies. Neuroscientist. 12, 489-499.

Dancause, N., Barbay, S., Frost, S.B., Plautz, E.J., Chen, D., Zoubina, E.V., Stowe, A.M., Nudo, R.J., 2005. Extensive cortical rewiring after brain injury. J.Neurosci. 25, 10167-10179.

Dancause, N., Barbay, S., Frost, S.B., Plautz, E.J., Popescu, M., Dixon, P.M., Stowe, A.M., Friel, K.M., Nudo, R.J., 2006a. Topographically divergent and convergent connectivity between premotor and primary motor cortex. Cereb.Cortex 16, 1057-1068.

Dancause, N., Barbay, S., Frost, S.B., Zoubina, E.V., Plautz, E.J., Mahnken, J.D., Nudo, R.J., 2006b. Effects of small ischemic lesions in the primary motor cortex on neurophysiological organization in ventral premotor cortex. J Neurophysiol 96, 3506-3511.

Darian-Smith, I., Burman, K., Darian-Smith, C., 1999. Parallel pathways mediating manual dexterity in the macaque. Exp Brain Res 128, 101-108.

Darian-Smith, I., Galea, M.P., Darian-Smith, C., 1996. Manual dexterity: how does the cerebral cortex contribute? Clinical and Experimental Pharmacology and Physiology 23, 948-956.

Darling, W.G., Morecraft, R.J., Rotella, D.L., Pizzimenti, M.A., Ge, J., Stilwell-Morecraft, K.S., Zhang, H., Soliman, H., Seecharan, D., Edwards, I., McNeal, D., Nudo, R.J., Cheney, P., 2014. Recovery of precision grasping after motor cortex lesion does not require forced use of the impaired hand in macaca mulatta. Exp Brain Res.

Dawson, G.D., 1956. The relative excitability and conduction velocity of sensory and motor nerve fibres in man. J.Physiol 131, 436-451.

Dawson, V.L., Hsu, C.Y., Liu, T.H., Dawson, T.M., Wamsley, J.K., 1994. Receptor Alterations in Subcortical Structures after Bilateral Middle Cerebral Artery Infarction of the Cerebral Cortex. Experimental Neurology 128, 88-96.

Desmedt, J.E., 1987. Physiologie et physiopathologie des sensations somatiques étudiées chez l'Homme par la méthode des potentiels évoqués, [Physiology and

physiopathology of somatic sensations studied in man by the method of evoked potentials]. J Physiol (Paris) 82, 64-136.

Dettmers, C., Adler, T., Rzanny, R., van Schayck, R., Gaser, C., Weiss, T., Miltner, W.H., Brückner, L., Weiller, C., 2001. Increased excitability in the primary motor cortex and supplementary motor area in patients with phantom limb pain after upper limb amputation. Neuroscience Letters 307, 109-112.

DeVito, J.L., Smith, O.A., 1959. Projections from the mesial frontal cortex (supplementary motor area) to the cerebral hemispheres and brain stem of the *Macaca mulatta*. The Journal of Comparative Neurology 111, 261-277.

Dien, J., 1998. Issues in the application of the average reference: Review, critiques, and recommendations. Behavior Research Methods Instruments & Computers 30, 34-43.

Dum, R.P., Strick, P.L., 1991. The origin of corticospinal projections from the premotor areas in the frontal lobe. J Neurosci. 11, 667-689.

Dum, R.P., Strick, P.L., 2002. Motor areas in the frontal lobe of the primate. Physiol Behav. 77, 677-682.

Dum, R.P., Strick, P.L., 2005. Frontal lobe inputs to the digit representations of the motor areas on the lateral surface of the hemisphere. J Neurosci. 25, 1375-1386.

Dum, R.P., Strick, P.L., 1996. Spinal Cord Terminations of the Medial Wall Motor Areas in Macaque Monkeys. The Journal of Neuroscience 16, 6513-6525.

Eisner-Janowicz, I., Barbay, S., Hoover, E., Stowe, A.M., Frost, S.B., Plautz, E.J., Nudo, R.J., 2008. Early and late changes in the distal forelimb representation of the supplementary motor area after injury to frontal motor areas in the squirrel monkey. J Neurophysiol 100, 1498-1512.

Evarts, E.V., 1974. Precentral and postcentral cortical activity in association with visually triggered movement. J Neurophysiol. 37, 373-381.

Friel, K.M., Barbay, S., Frost, S.B., Plautz, E.J., Hutchinson, D.M., Stowe, A.M., Dancause, N., Zoubina, E.V., Quaney, B.M., Nudo, R.J., 2005. Dissociation of sensorimotor deficits after rostral versus caudal lesions in the primary motor cortex hand representation. J Neurophysiol. 94, 1312-1324.

Fromm, C., Evarts, E.V., 1982. Pyramidal tract neurons in somatosensory cortex: central and peripheral inputs during voluntary movement. Brain Research 238, 186-191.

Frost, S.B., Barbay, S., Friel, K.M., Plautz, E.J., Nudo, R.J., 2003. Reorganization of remote cortical regions after ischemic brain injury: a potential substrate for stroke recovery. J Neurophysiol 89, 3205-3214.

Fujii, M., Yamada, T., Aihara, M., Kokubun, Y., Noguchi, Y., Matsubara, M., Yeh, M.H., 1994. The effects of stimulus rates upon median, ulnar and radial nerve somatosensory evoked potentials. Electroencephalogr.Clin Neurophysiol. 92, 518-526.

Galea, M.P., Darian-Smith, I., 1994. Multiple Corticospinal Neuron Populations in the Macaque Monkey Are Specified by Their Unique Cortical Origins, Spinal Terminations, and Connections. Cerebral Cortex 4, 166-194.

Garraghty, P.E., Lachica, E.A., Kaas, J.H., 1991. Injury-Induced Reorganization of Somatosensory Cortex Is Accompanied by Reductions in GABA Staining. Somatosensory & Motor Research 8, 347-354.

Gaspar, C.M., Rousselet, G.A., Pernet, C.R., 2011. Reliability of ERP and single-trial analyses. Neuroimage. 58, 620-629.

Gentilucci, M., Fogassi, L., Luppino, G., Matelli, M., Camarda, R., Rizzolatti, G., 1988. Functional organization of inferior area 6 in the macaque monkey. Exp Brain Res 71, 475-490.

Gerbella, M., Belmalih, A., Borra, E., Rozzi, S., Luppino, G., 2011. Cortical connections of the anterior (F5a) subdivision of the macaque ventral premotor area F5. Brain Struct.Funct. 216, 43-65.

Geyer, S., Schleicher, A., Zilles, K., 1999. Areas 3a, 3b, and 1 of Human Primary Somatosensory Cortex: 1. Microstructural Organization and Interindividual Variability. Neuroimage 10, 63-83.

Ghosh, A., Haiss, F., Sydekum, E., Schneider, R., Gullo, M., Wyss, M.T., Mueggler, T., Baltes, C., Rudin, M., Weber, B., Schwab, M.E., 2010. Rewiring of hindlimb corticospinal neurons after spinal cord injury. Nat.Neurosci. 13, 97-104.

Ghosh, A., Peduzzi, S., Snyder, M., Schneider, R., Starkey, M., Schwab, M.E., 2012. Heterogeneous spine loss in layer 5 cortical neurons after spinal cord injury. Cereb.Cortex 22, 1309-1317.

Ghosh, A., Sydekum, E., Haiss, F., Peduzzi, S., Zörner, B., Schneider, R., Baltes, C., Rudin, M., Weber, B., Schwab, M.E., 2009. Functional and anatomical reorganization of the sensory-motor cortex after incomplete spinal cord injury in adult rats. J Neurosci. 29, 12210-12219.

Gindrat, A.D., Quairiaux, C., Britz, J., Brunet, D., Lanz, F., Michel, C.M., Rouiller, E.M., 2014. Whole-scalp EEG mapping of somatosensory evoked potentials in macaque monkeys. Brain Struct.Funct., 1-22.

Glees, P., Cole, J., 1950. Recovery of skilled motor functions after small repeated lesions of motor cortex in macaque. Journal of Neurophysiology 13, 137-148.

Graben, P., Saddy, J.D., Schlesewsky, M., Kurths, J., 2000. Symbolic dynamics of event-related brain potentials. Phys.Rev.E.Stat.Phys.Plasmas.Fluids Relat Interdiscip.Topics. 62, 5518-5541.

Green, J.B., McLeod, S., 1979. Short latency somatosensory evoked potentials in patients with neurological lesions. Arch.Neurol 36, 846-851.

Griffen, T.C., Maffei, A., 2014. GABAergic synapses: their plasticity and role in sensory cortex. Front Cell Neurosci 8, 91.

Hamada, Y., Urasopon, N., Hadi, I., Malaivijitnond, S., 2006. Body size and proportions and pelage color of free-ranging *Macaca mulatta* from a zone of hybridization in northeastern Thailand. International Journal of Primatology 27, 497-513.

Hamadjida, A., Wyss, A.F., Mir, A., Schwab, M.E., Belhaj-Saïf, A., Rouiller, E.M., 2012. Influence of anti-Nogo-A antibody treatment on the reorganization of callosal connectivity of the premotor cortical areas following unilateral lesion of primary motor cortex (M1) in adult macaque monkeys. Exp.Brain Res. 223, 321-340.

Hashimoto, I., 1984. Somatosensory evoked potentials from the human brain-stem: origins of short latency potentials. Electroencephalogr.Clin.Neurophysiol 57, 221-227.

Hayashi, N., Nishijo, H., Endo, S., Fukuda, M., Homma, S., Ono, T., 1994. Dipole tracing of monkey somatosensory evoked potentials. Brain Research Bulletin 33, 231-235.

Hayashi, N., Nishijo, H., Ono, T., Endo, S., Tabuchi, E., 1995. Generators of somatosensory evoked potentials investigated by dipole tracing in the monkey. Neuroscience 68, 323-338.

He, S.Q., Dum, R.P., Strick, P.L., 1993. Topographic organization of corticospinal projections from the frontal lobe: motor areas on the lateral surface of the hemisphere. J Neurosci. 13, 952-980.

He, S.Q., Dum, R.P., Strick, P.L., 1995. Topographic organization of corticospinal projections from the frontal lobe: motor areas on the medial surface of the hemisphere. J Neurosci. 15, 3284-3306.

Hendry, S.H.C., Jones, E.G., 1986. Reduction in number of immunostained GABAergic neurones in deprived-eye dominance columns of monkey area 17. Nature 320, 750-753.

Hoogewoud, F., Hamadjida, A., Wyss, A.F., Mir, A., Schwab, M.E., Belhaj-Saïf, A., Rouiller, E.M., 2013. Comparison of functional recovery of manual dexterity after unilateral spinal cord lesion or motor cortex lesion in adult macaque monkeys. Front Neurol. 4, 101.

Hopkins, W.D., Meguerditchian, A., Coulon, O., Bogart, S., Mangin, J.F., Sherwood, C.C., Grabowski, M.W., Bennett, A.J., Pierre, P.J., Fears, S., Woods, R., Hof, P.R., Vauclair, J., 2014. Evolution of the central sulcus morphology in primates. Brain Behav.Evol. 84, 19-30.

Huffman, K.J., Krubitzer, L., 2001. Area 3a: topographic organization and cortical connections in marmoset monkeys. Cereb.Cortex 11, 849-867.

Jang, S.H., Cho, S.H., Kim, Y.H., Kwon, Y.H., Byun, W.M., Lee, S.J., Park, S.M., Chang, C.H., 2004. Cortical activation changes associated with motor recovery in patients with precentral knob infarct. Neuroreport 15.

Jang, S.H., Han, B.S., Chang, Y., Byun, W.M., Lee, J., Ahn, S.H., 2002. Functional MRI Evidence for Motor Cortex Reorganization Adjacent to a Lesion in a Primary Motor Cortex. American Journal of Physical Medicine & Rehabilitation 81.

Jiang, W., Chapman, C.E., Lamarre, Y., 1991. Modulation of the cutaneous responsiveness of neurones in the primary somatosensory cortex during conditioned arm movements in the monkey. Exp Brain Res 84, 342-354.

Jones, E.G., 1993. GABAergic Neurons and Their Role in Cortical Plasticity in Primates. Cerebral Cortex 3, 361-372.

Jones, E.G., Coulter, J.D., Hendry, S.H.C., 1978. Intracortical connectivity of architectonic fields in the somatic sensory, motor and parietal cortex of monkeys. The Journal of Comparative Neurology 181, 291-347.

Jones, E.G., Porter, R., 1980. What is area 3a? Brain Res. 203, 1-43.

Jones, E.G., Wise, S.P., 1977. Size, laminar and columnar distribution of efferent cells in the sensory-motor cortex of monkeys. The Journal of Comparative Neurology 175, 391-437.

Jones, E.G., 1986. Connectivity of the Primate Sensory-Motor Cortex. In: Jones, E.G., Peters, A. (Eds.), Sensory-Motor Areas and Aspects of Cortical Connectivity, 5th ed. Springer US, pp. 113-183.

Jürgens, U., 1984. The efferent and afferent connections of the supplementary motor area. Brain Research 300, 63-81.

Kaas, J.H., 2000. The reorganization of somatosensory and motor cortex after peripheral nerve or spinal cord injury in primates. Prog.Brain Res. 128, 173-179.

Kaas, J.H., 2004a. Evolution of somatosensory and motor cortex in primates. Anat.Rec.A Discov.Mol.Cell Evol.Biol. 281, 1148-1156.

Kaas, J.H., 2004b. Evolution of the Large, Complex Sensorimotor Systems of Anthropoid Primates. In: Pellis, S., Marino, L. (Eds.), Special Issue: Evolution of the Vertebrate Brain and Behavior, International Journal of Comparative Psychology 17, pp. 34-52.

Kaas, J.H., 2008. The evolution of the complex sensory and motor systems of the human brain. Brain Res.Bull. 75, 384-390.

Kaas, J.H., Florence, S.L., Jain, N., 1997. Reorganization of sensory systems of primates after injury. neuroscientist 3, 123-130.

Kaas, J.H., Qi, H.X., Burish, M.J., Gharbawie, O.A., Onifer, S.M., Massey, J.M., 2008. Cortical and subcortical plasticity in the brains of humans, primates, and rats after damage to sensory afferents in the dorsal columns of the spinal cord. Exp.Neurol. 209, 407-416.

Kaeser, M., 2010. Transplantation of autologous adult brain progenitor cells in a non-human primate model of motor cortex lesion. Doctoral thesis. University of Fribourg, Imprimerie Saint-Paul.

Kaeser, M., Brunet, J.F., Wyss, A., Belhaj-Saïf, A., Liu, Y., Hamadjida, A., Rouiller, E.M., Bloch, J., 2011. Autologous adult cortical cell transplantation enhances functional recovery following unilateral lesion of motor cortex in primates: a pilot study. Neurosurgery 68, 1405-1416.

Kaeser, M., Chatagny, P., Gindrat, A.D., Savidan, J., Badoud, S., Fregosi, M., Moret, V., Roulin, C., Schmidlin, E., Rouiller, E.M., 2014. Variability of manual dexterity performance in non-human primates (*Macaca fascicularis*). International Journal of Comparative Psychology 27, 295-325.

Kaeser, M., Wyss, A.F., Bashir, S., Hamadjida, A., Liu, Y., Bloch, J., Brunet, J.F., Belhaj-Saïf, A., Rouiller, E.M., 2010. Effects of unilateral motor cortex lesion on ipsilesional hand's reach and grasp performance in monkeys: relationship with recovery in the contralesional hand. J Neurophysiol 103, 1630-1645.

Kandel, E.R., Schwartz, J.H., Jessell, T.M., Siegelbaum, S.A., Hudspeth, A.J., 2013. Principles of Neural Science, Fifth Edition. McGraw-Hill Education.

Kantak, S.S., Stinear, J.W., Buch, E.R., Cohen, L.G., 2012. Rewiring the brain: potential role of the premotor cortex in motor control, learning, and recovery of function following brain injury. Neurorehabil Neural Repair 26, 282-292.

Kileny, P., Paccioretti, D., Wilson, A.F., 1987. Effects of cortical lesions on middle-latency auditory evoked responses (MLR). Electroencephalography and Clinical Neurophysiology 66, 108-120.

Kim, J.S., Lee, M.C., 1994. Writing tremor after discrete cortical infarction. Stroke 25, 2280-2282.

Kraus, N., Ozdamar, O., Hier, D., Stein, L., 1982. Auditory middle latency responses (MLRs) in patients with cortical lesions. Electroencephalogr.Clin.Neurophysiol. 54, 275-287.

Krnjevic, K., Morris, M.E., 1976. Input-output relation of transmission through cuneate nucleus. J Physiol 257, 791-815.

Krubitzer, L., Huffman, K.J., Disbrow, E., Recanzone, G., 2004. Organization of area 3a in macaque monkeys: contributions to the cortical phenotype. J Comp Neurol. 471, 97-111.

Kullmann, D.M., Moreau, A.W., Bakiri, Y., Nicholson, E., 2012. Plasticity of inhibition. Neuron 75, 951-962.

Kumar, A., Juhasz, C., Asano, E., Sundaram, S.K., Makki, M.I., Chugani, D.C., Chugani, H.T., 2009. Diffusion tensor imaging study of the cortical origin and course of the corticospinal tract in healthy children. AJNR Am.J Neuroradiol. 30, 1963-1970.

Kurata, K., Tanji, J., 1986. Premotor cortex neurons in macaques: activity before distal and proximal forelimb movements. The Journal of Neuroscience 6, 403-411.

Laible, M., Grieshammer, S., Seidel, G., Rijntjes, M., Weiller, C., Hamzei, F., 2012. Association of Activity Changes in the Primary Sensory Cortex With Successful Motor Rehabilitation of the Hand Following Stroke. Neurorehabil Neural Repair 26, 881-888.

Lamas, V., Alvarado, J.C., Carro, J., Merchan, M.A., 2013. Long-term evolution of brainstem electrical evoked responses to sound after restricted ablation of the auditory cortex. PLoS One 8, e73585.

Lashley, K.S., 1924. Studies of cerebral function in learning: V. The retention of motor habits after destruction of the so-called motor areas in primates. Archives of Neurology & Psychiatry 12, 249-276.

Legatt, A., 2014. General Principles of Somatosensory Evoked Potentials. Medscape.

Lehmann, S.J., Scherberger, H., 2013. Reach and Gaze Representations in Macaque Parietal and Premotor Grasp Areas. The Journal of Neuroscience 33, 7038-7049.

Lemon, R.N., 1993. The G. L. Brown Prize Lecture. Cortical control of the primate hand. Exp.Physiol 78, 263-301.

Lemon, R.N., 1997. Mechanisms of cortical control of hand function. neuroscientist 3, 389-398.

Lemon, R.N., 2008. Descending pathways in motor control. Annu.Rev.Neurosci. 31, 195-218.

Lemon, R.N., Griffiths, J., 2005. Comparing the function of the corticospinal system in different species: organizational differences for motor specialization? Muscle Nerve 32, 261-279.

Lemon, R.N., Porter, R., 1976. Afferent input to movement-related precentral neurones in conscious monkeys. Proc.R.Soc.Lond B Biol.Sci. 194, 313-339.

Lesser, R.P., Koehle, R., Lueders, H., 1979. Effect of stimulus intensity on short latency somatosensory evoked potentials. Electroencephalogr.Clin.Neurophysiol 47, 377-382.

Liao, C.C., Gharbawie, O.A., Qi, H., Kaas, J.H., 2013. Cortical connections to single digit representations in area 3b of somatosensory cortex in squirrel monkeys and prosimian galagos. J Comp Neurol 521, 3768-3790.

Liepert, J., Hamzei, F., Weiller, C., 2000. Motor cortex disinhibition of the unaffected hemisphere after acute stroke. Muscle & Nerve 23, 1761-1763.

Liu, J., Morel, A., Wannier, T., Rouiller, E.M., 2002. Origins of callosal projections to the supplementary motor area (SMA): a direct comparison between pre-SMA and SMA-proper in macaque monkeys. J Comp Neurol. 443, 71-85.

Liu, Y., Rouiller, E.M., 1999. Mechanisms of recovery of dexterity following unilateral lesion of the sensorimotor cortex in adult monkeys. Exp.Brain Res. 128, 149-159.

Lloyd, D.P.C., McIntyre, A.K., 1950. Dorsal column conduction of group I muscle afferent impulses and their relay through Clarke's column. Journal of Neurophysiology 13, 39-54.

Lockwood, A.H., Salvi, R.J., Burkard, R.F., Galantowicz, P.J., Coad, M.L., Wack, D.S., 1999. Neuroanatomy of tinnitus. Scand.Audiol.Suppl 51, 47-52.

Mark, R.F., Steiner, J., 1958. Cortical projection of impulses in myelinated cutaneous afferent nerve fibres of the cat. The Journal of physiology 142, 544-562.

Matelli, M., Luppino, G., Rizzolatti, G., 1985. Patterns of cytochrome oxidase activity in the frontal agranular cortex of the macaque monkey. Behavioural Brain Research 18, 125-136.

Mauguière, F., 2011. Somatosensory-evoked potentials: Normal Responses, Abnormal Waveforms, and Clinical Applications in Neurologic Diseases. In: Schomer, D.L., Lopes da Silva, F.H. (Eds.), Niedermeyer's Electroencephalography: Basic Principles, Clinical Applications, and Related Fields, 6th ed. Lippincott Williams & Wilkins, pp. 1003-1056.

Mauguière, F., Desmedt, J.E., Courjon, J., 1983. Neural generators of N18 and P14 far-field somatosensory evoked potentials studied in patients with lesion of thalamus or thalamo-cortical radiations. Electroencephalography and Clinical Neurophysiology 56, 283-292.

Mauguière, F., Ibanez, V., 1985. The dissociation of early SEP components in lesions of the cervico-medullary junction: a cue for routine interpretation of abnormal cervical responses to median nerve stimulation. Electroencephalogr.Clin.Neurophysiol 62, 406-420.

McCarthy, G., Wood, C.C., Allison, T., 1991. Cortical somatosensory evoked potentials. I. Recordings in the monkey *Macaca fascicularis*. J Neurophysiol 66, 53-63.

McIntyre, A.K., Mark, R.F., 1960. Synaptic linkage between afferent fibres of the cat's hind limb and ascending fibres in the dorsolateral funiculus. J Physiol 153, 306-330.

McLaughlin, D.F., Kelly, E.F., 1993. Evoked potentials as indices of adaptation in the somatosensory system in humans: a review and prospectus. Brain Res.Brain Res.Rev. 18, 151-206.

McNeal, D.W., Darling, W.G., Ge, J., Stilwell-Morecraft, K.S., Solon, K.M., Hynes, S.M., Pizzimenti, M.A., Rotella, D.L., Tyler, V., Morecraft, R.J., 2010. Selective long-term reorganization of the corticospinal projection from the supplementary motor cortex

following recovery from lateral motor cortex injury. Journal of Comparative Neurology 518, 586-621.

Moller, A.R., Jannetta, P.J., Burgess, J.E., 1986. Neural generators of the somatosensory evoked potentials: recording from the cuneate nucleus in man and monkeys. Electroencephalogr.Clin.Neurophysiol 65, 241-248.

Moller, A.R., Sekiya, T., Sen, C.N., 1989. Responses from dorsal column nuclei (DCN) in the monkey to stimulation of upper and lower limbs and spinal cord. Electroencephalogr.Clin.Neurophysiol. 73, 353-361.

Mondt, J.P., 1989. On the effects on source localisation of volume currents in neuroelectric and neuromagnetic signals. Physics in Medicine and Biology 34, 1073.

Mountcastle, V.B., 1965. The Neural Replication of Sensory Events in the Somatic Afferent System. In: Eccles, J.C. (Ed.), Brain and Conscious Experience. Springer Berlin Heidelberg, pp. 85-115.

Mountcastle, V.B., Davies, P.W., Berman, A.L., 1957. Response properties of neurons of cat's somatic sensory cortex to peripheral stimuli. J.Neurophysiol. 20, 374-407.

Murata, Y., Higo, N., Oishi, T., Yamashita, A., Matsuda, K., Hayashi, M., Yamane, S., 2008. Effects of motor training on the recovery of manual dexterity after primary motor cortex lesion in macaque monkeys. J Neurophysiol 99, 773-786.

Murata, Y., Higo, N., Hayashi, T., Nishimura, Y., Sugiyama, Y., Oishi, T., Tsukada, H., Isa, T., Onoe, H., 2015. Temporal Plasticity Involved in Recovery from Manual Dexterity Deficit after Motor Cortex Lesion in Macaque Monkeys. The Journal of Neuroscience 35, 84-95.

Murray, M.M., Brunet, D., Michel, C.M., 2008. Topographic ERP analyses: a step-by-step tutorial review. Brain Topogr. 20, 249-264.

Napier, J.R., 1956. The prehensile movements of the human hand. J Bone Joint Surg.Br 38-B, 902-913.

Nelson, R.J., 1987. Activity of monkey primary somatosensory cortical neurons changes prior to active movement. Brain Research 406, 402-407.

Nelson, R.J., Smith, B.N., Douglas, V.D., 1991. Relationships between sensory responsiveness and premovement activity of quickly adapting neurons in areas 3b and 1 of monkey primary somatosensory cortex. Exp Brain Res 84, 75-90.

Newsome, W.T., Wurtz, R.H., Dursteler, M.R., Mikami, A., 1985a. Deficits in visual motion processing following ibotenic acid lesions of the middle temporal visual area of the macaque monkey. The Journal of Neuroscience 5, 825-840.

Newsome, W.T., Wurtz, R.H., Dursteler, M.R., Mikami, A., 1985b. Punctate chemical lesions of striate cortex in the macaque monkey: effect on visually guided saccades. Exp Brain Res 58, 392-399.

Nieuwenhuys, R., Voogd, J., Voogd, J., van Huijzen, C., 2007. The Human Central Nervous System: A Synopsis and Atlas. Springer.

Nishimura, Y., Isa, T., 2009. Compensatory changes at the cerebral cortical level after spinal cord injury. neuroscientist 15, 436-444.

Nishimura, Y., Isa, T., 2012. Cortical and subcortical compensatory mechanisms after spinal cord injury in monkeys. Experimental Neurology 235, 152-161.

Norena, A.J., Eggermont, J.J., 2003. Changes in spontaneous neural activity immediately after an acoustic trauma: implications for neural correlates of tinnitus. Hearing Research 183, 137-153.

Nudo, R.J., 2006. Plasticity. NeuroRx. 3, 420-427.

Nudo, R.J., 2013. Recovery after brain injury: mechanisms and principles. Front Hum.Neurosci. 7, 887.

Nudo, R.J., Friel, K.M., Delia, S.W., 2000. Role of sensory deficits in motor impairments after injury to primary motor cortex. Neuropharmacology 39, 733-742.

Nudo, R.J., Masterton, R.B., 1990. Descending pathways to the spinal cord, III: Sites of origin of the corticospinal tract. The Journal of Comparative Neurology 296, 559-583.

Nudo, R.J., Milliken, G.W., 1996. Reorganization of movement representations in primary motor cortex following focal ischemic infarcts in adult squirrel monkeys. J Neurophysiol 75, 2144-2149.

Nunez, A., Buno, W., 2001. Properties and plasticity of synaptic inputs to rat dorsal column neurones recorded in vitro. J Physiol 535, 483-495.

Ogden, R., Franz, S.I., 1917. On cerebral motor control: The recovery from experimentally produced hemiplegia. Psychobiology 1, 33.

Ozdamar, O., Kraus, N., Curry, F., 1982. Auditory brain stem and middle latency responses in a patient with cortical deafness. Electroencephalogr.Clin.Neurophysiol. 53, 224-230.

Paxinos, G., Huang, X.F., Toga, A.W., 1999. The rhesus monkey brain in stereotaxic coordinates.

Pernet, C.R., Sajda, P., Rousselet, G.A., 2011. Single-trial analyses: why bother? Front Psychol. 2, 322.

Pineiro, R., Pendlebury, S., Johansen-Berg, H., Matthews, P.M., 2001. Functional MRI detects posterior shifts in primary sensorimotor cortex activation after stroke: evidence of local adaptive reorganization? Stroke 32, 1134-1139.

Pizzimenti, M.A., Darling, W.G., Rotella, D.L., McNeal, D.W., Herrick, J.L., Ge, J., Stilwell-Morecraft, K.S., Morecraft, R.J., 2007. Measurement of reaching kinematics and prehensile dexterity in nonhuman primates. J Neurophysiol. 98, 1015-1029.

Plautz, E.J., Barbay, S., Frost, S.B., Friel, K.M., Dancause, N., Zoubina, E.V., Stowe, A.M., Quaney, B.M., Nudo, R.J., 2003. Post-infarct cortical plasticity and behavioral recovery using concurrent cortical stimulation and rehabilitative training: a feasibility study in primates. Neurol.Res. 25, 801-810.

Pratt, H., Politoske, D., Starr, A., 1980. Mechanically and electrically evoked somatosensory potentials in humans: effects of stimulus presentation rate. Electroencephalogr.Clin.Neurophysiol 49, 240-249.

Purves, D., Augustine, G.A., Fitzpatrick, D., Hall, W., LaMantia, A.-S., McNamara, J.O., Williams, S.M., 2008. Neuroscience, 4th ed. Sinauer Associates, Incorporated.

Qi, H.X., Stepniewska, I., Kaas, J.H., 2000. Reorganization of primary motor cortex in adult macaque monkeys with long-standing amputations. J Neurophysiol. 84, 2133-2147.

Ralston, D.D., Ralston, H.J.I., 1985. The terminations of corticospinal tract axons in the macaque monkey. J Comp Neurol. 242, 325-337.

Rappaport, M., Leonard, J., Ruiz, P.S., 1992a. Effects of anesthesia and stimulus intensity on posterior tibial nerve somatosensory evoked potentials. Clin.Electroencephalogr. 23, 24-30.

Rappaport, M., Ruiz, P.S., Leonard, J., 1992b. Effects of stimulus intensity on posterior tibial nerve somatosensory evoked potentials. Clin.Electroencephalogr. 23, 89-94.

Redecker, C., Luhmann, H.J., Hagemann, G., Fritschy, J.M., Witte, O.W., 2000. Differential Downregulation of GABAA Receptor Subunits in Widespread Brain Regions in the Freeze-Lesion Model of Focal Cortical Malformations. The Journal of Neuroscience 20, 5045-5053.

Regan, D., 1989. Human brain electrophysiology: evoked potentials and evoked magnetic fields in science and medicine. Elsevier.

Rizzolatti, G., Camarda, R., Fogassi, L., Gentilucci, M., Luppino, G., Matelli, M., 1988. Functional organization of inferior area 6 in the macaque monkey. II. Area F5 and the control of distal movements. Exp Brain Res 71, 491-507.

Robinson, L.R., Micklesen, P.J., 2010. Does stimulus rate matter when performing somatosensory evoked potentials for coma patients? Neurocrit.Care 12, 69-73.

Rosen, I., Asanuma, H., 1972. Peripheral afferent inputs to the forelimb area of the monkey motor cortex: input-output relations. Exp Brain Res 14, 257-273.

Rouiller, E.M., Moret, V., Tanne, J., Boussaoud, D., 1996. Evidence for direct connections between the hand region of the supplementary motor area and cervical motoneurons in the macaque monkey. Eur.J Neurosci. 8, 1055-1059.

Rouiller, E.M., Olivier, E., 2004. Functional recovery after lesions of the primary motor cortex. Prog.Brain Res. 143, 467-475.

Rouiller, E.M., Yu, X.H., Moret, V., Tempini, A., Wiesendanger, M., Liang, F., 1998. Dexterity in adult monkeys following early lesion of the motor cortical hand area: the role of cortex adjacent to the lesion. Eur.J.Neurosci. 10, 729-740.

Salimi, I., Brochier, T., Smith, A.M., 1999. Neuronal activity in somatosensory cortex of monkeys using a precision grip. I. Receptive fields and discharge patterns. J.Neurophysiol. 81, 825-834.

Sasaki, K., Gemba, H., 1984. Compensatory motor function of the somatosensory cortex for the motor cortex temporarily impaired by cooling in the monkey. Exp.Brain Res 55, 60-68.

Sawaki, L., Wu, C.W., Kaelin-Lang, A., Cohen, L.G., 2006. Effects of somatosensory stimulation on use-dependent plasticity in chronic stroke. Stroke 37, 246-247.

Schaechter, J.D., Perdue, K.L., Wang, R., 2008. Structural damage to the corticospinal tract correlates with bilateral sensorimotor cortex reorganization in stroke patients. Neuroimage. 39, 1370-1382.

Schaechter, J.D., van Oers, C.A., Groisser, B.N., Salles, S.S., Vangel, M.G., Moore, C.I., Dijkhuizen, R.M., 2012. Increase in sensorimotor cortex response to somatosensory stimulation over subacute poststroke period correlates with motor recovery in hemiparetic patients. Neurorehabil Neural Repair 26, 325-334.

Schieber, M.H., 2007. Comparative anatomy and physiology of the corticospinal system. In: Andrew, A.E.a.P. (Ed.), Handbook of Clinical Neurology, Motor neuron disorders and related diseases, Volume 82. Elsevier, pp. 15-37.

Schmidlin, E., Kaeser, M., Gindrat, A.D., Savidan, J., Chatagny, P., Badoud, S., Hamadjida, A., Beaud, M.L., Wannier, T., Belhaj-Saïf, A., Rouiller, E.M., 2011. Behavioral assessment of manual dexterity in non-human primates. J.Vis.Exp., e3258.

Schneider, R.J., 1990. Loss of information concerning hair displacement and other somatic stimuli in the first somatic sensory cortex of unanesthetized *Macaca mulatta* monkeys following dorsal funiculus transections. Exp Brain Res 83, 105-114.

Seghier, M.L., Ramsden, S., Lim, L., Leff, A.P., Price, C.J., 2014. Gradual lesion expansion and brain shrinkage years after stroke. Stroke 45, 877-879.

Seki, K., Fetz, E.E., 2012. Gating of Sensory Input at Spinal and Cortical Levels during Preparation and Execution of Voluntary Movement. The Journal of Neuroscience 32, 890-902.

Seo, J.P., Jang, S.H., 2013. Different characteristics of the corticospinal tract according to the cerebral origin: DTI study. AJNR Am.J Neuroradiol. 34, 1359-1363.

Sessle, B.J., Wiesendanger, M., 1982. Structural and functional definition of the motor cortex in the monkey (*Macaca fascicularis*). J Physiol 323, 245-265.

Shimazu, H., Maier, M.A., Cerri, G., Kirkwood, P.A., Lemon, R.N., 2004. Macaque ventral premotor cortex exerts powerful facilitation of motor cortex outputs to upper limb motoneurons. J Neurosci. 24, 1200-1211.

Smith, A.M., 2009. The neurohaptic control of the hand. In: Nowak, D.A., Hermsdörfer, J. (Eds.), Sensorimotor Control of Grasping: Physiology and Pathophysiology. Cambridge University Press, pp. 178-192.

Sonoo, M., Shimpo, T., Takeda, K., Genba, K., Nakano, I., Mannen, T., 1991. SEPs in two patients with localized lesions of the postcentral gyrus. Electroencephalogr.Clin.Neurophysiol 80, 536-546.

Sonoo, M., Genba, K., Zai, W., Iwata, M., Mannen, T., Kanazawa, I., 1992. Origin of the widespread N18 in median nerve SEP. Electroencephalography and Clinical Neurophysiology/Evoked Potentials Section 84, 418-425.

Spencer, K.M., 2005. Averaging, detection, and classification of single-trial ERPs. In: Handy, T.C. (Ed.), Event-related Potentials: A Methods Handbook. MIT Press, Cambridge, pp. 209-227.

Starzl, T.E., Niemer, W.T., Dell, M., Forgrave, P.R., 1953. Cortical and subcortical electrical activity in experimental seizures induced by metrazol. Journal of neuropathology and experimental neurology 12, 262-276.

Stepniewska, I., Preuss, T.M., Kaas, J.H., 1993. Architectonics, somatotopic organization, and ipsilateral cortical connections of the primary motor area (M1) of owl monkeys. Journal of Comparative Neurology 330, 238-271.

Stohr, M., Dichgans, J., Voigt, K., Buettner, U.W., 1983. The significance of somatosensory evoked potentials for localization of unilateral lesions within the cerebral hemispheres. J Neurol.Sci. 61, 49-63.

Talsma, D., Woldorff, M.G., 2005. Methods for the Estimation and Removal of Artifacts and Overlap in ERP Waveforms. In: Handy, T.C. (Ed.), Event-related Potentials: A Methods Handbook. MIT Press, pp. 115-148.

Tanji, J., Wise, S.P., 1981. Submodality distribution in sensorimotor cortex of the unanesthetized monkey. J.Neurophysiol. 45, 467-481.

Tokuno, H., Tanji, J., 1993. Input organization of distal and proximal forelimb areas in the monkey primary motor cortex: a retrograde double labeling study. J Comp Neurol. 333, 199-209.

Toyoshima, K., Sakai, H., 1982. Exact cortical extent of the origin of the corticospinal tract (CST) and the quantitative contribution to the CST in different cytoarchitectonic areas. A study with horseradish peroxidase in the monkey. J Hirnforsch. 23, 257-269.

Tsui, B.C.H., 2007. Electrical Nerve Stimulation. In: Tsui, B.C.H., Chan, V., Finucane, B.T., Grau, T., Walji, A.H. (Eds.), Atlas of Ultrasound- and Nerve Stimulation-Guided Regional Anesthesia. Springer, pp. 9-18.

Uematsu, S., Lesser, R.P., Gordon, B., 1992. Localization of sensorimotor cortex: the influence of Sherrington and Cushing on the modern concept. Neurosurgery 30, 904-912.

Valeriani, M., Restuccia, D., Di Lazzaro, V., Le Pera, D., Barba, C., Tonali, P., Mauguière, F., 1998. Dipolar sources of the early scalp somatosensory evoked potentials to upper limb stimulation. Effect of increasing stimulus rates. Exp.Brain Res. 120, 306-315.

van den Broek, S.P., Reinders, F., Donderwinkel, M., Peters, M.J., 1998. Volume conduction effects in EEG and MEG. Electroencephalogr.Clin.Neurophysiol. 106, 522-534.

Wall, J.T., Xu, J., Wang, X., 2002. Human brain plasticity: an emerging view of the multiple substrates and mechanisms that cause cortical changes and related sensory dysfunctions after injuries of sensory inputs from the body. Brain Research Reviews 39, 181-215.

Walsh, J.P., Whitehorn, D., 1981. An input-output analysis of the dorsal column nuclei. Experimental Neurology 73, 186-198.

Walsh, P., Kane, N., Butler, S., 2005. The clinical role of evoked potentials. J Neurol.Neurosurg.Psychiatry 76 Suppl 2, ii16-ii22.

Wannier, T., Schmidlin, E., Bloch, J., Rouiller, E.M., 2005. A unilateral section of the corticospinal tract at cervical level in primate does not lead to measurable cell loss in motor cortex. Journal of Neurotrauma 22, 703-717.

White, L.E., Andrews, T.J., Hulette, C., Richards, A., Groelle, M., Paydarfar, J., Purves, D., 1997. Structure of the human sensorimotor system. I: Morphology and cytoarchitecture of the central sulcus. Cereb.Cortex 7, 18-30.

Wible, B., Nicol, T., Kraus, N., 2005. Correlation between brainstem and cortical auditory processes in normal and language-impaired children. Brain 128, 417-423.

Wiesendanger, M., 1981. Organization of Secondary Motor Areas of Cerebral Cortex., Comprehensive Physiology. John Wiley & Sons, Inc., pp. 1121-1147.

Williams, S.R., Chapman, C.E., 2002. Time course and magnitude of movement-related gating of tactile detection in humans. III. Effect of motor tasks. J Neurophysiol. 88, 1968-1979.

Winter, W.R., Nunez, P.L., Ding, J., Srinivasan, R., 2007. Comparison of the effect of volume conduction on EEG coherence with the effect of field spread on MEG coherence. Statistics in Medicine 26, 3946-3957.

Wise, S.P., Tanji, J., 1981. Neuronal responses in sensorimotor cortex to ramp displacements and maintained positions imposed on hindlimb of the unanesthetized monkey. Journal of Neurophysiology 45, 482-500.

Wong-Riley, M., 1979. Changes in the visual system of monocularly sutured or enucleated cats demonstrable with cytochrome oxidase histochemistry. Brain Research 171, 11-28.

Woolsey, C.N., 1964. Cortical localization as defined by evoked potential and electrical stimulation studies. Cerebral localization and organization, 17-26.

Woolsey, C.N., Settlage, P.H., Meyer, D.R., Sencer, W., Pinto Hamuy, T., Travis, A.M., 1952. Patterns of localization in precentral and "supplementary" motor areas and their relation to the concept of a premotor area. Res.Publ.Assoc.Res.Nerv.Ment.Dis. 30, 238-264.

Wyss, A.F., Hamadjida, A., Savidan, J., Liu, Y., Bashir, S., Mir, A., Schwab, M.E., Rouiller, E.M., Belhaj-Saïf, A., 2013. Long-term motor cortical map changes following unilateral lesion of the hand representation in the motor cortex in macaque monkeys showing functional recovery of hand functions. Restor.Neurol Neurosci. 31, 733-760.

Yao, D., Wang, L., Arendt-Nielsen, L., Chen, A.C., 2007. The effect of reference choices on the spatio-temporal analysis of brain evoked potentials: the use of infinite reference. Comput Biol.Med. 37, 1529-1538.

York, D.H., 1985. Somatosensory evoked potentials in man: differentiation of spinal pathways responsible for conduction from the forelimb vs hindlimb. Prog.Neurobiol. 25, 1-25.

Yousry, T.A., Schmid, U.D., Alkadhi, H., Schmidt, D., Peraud, A., Buettner, A., Winkler, P., 1997. Localization of the motor hand area to a knob on the precentral gyrus. A new landmark. Brain 120 (Pt 1), 141-157.

Supplementary Figures

Supplementary Figure 1 (next page): Histological reconstruction of the cortical lesion in Mk-DI. Complete series of individual Nissl-stained sections in the frontal plane where the lesion was visible. The cortical lesion in gray matter (red area) extended from Nissl-stained section 27 to section 48. The border between gray matter and white matter is shown in blue. The extent of the cortical lesion (insert in the lower right corner), based on Nissl-stained sections, was orthogonally projected onto the surface of the left hemisphere. When the lesion extended in the depth of the central sulcus, the lower extremity of the red bars was represented crossing the central sulcus in direction of the postcentral gyrus. The landmark of some sections is given.

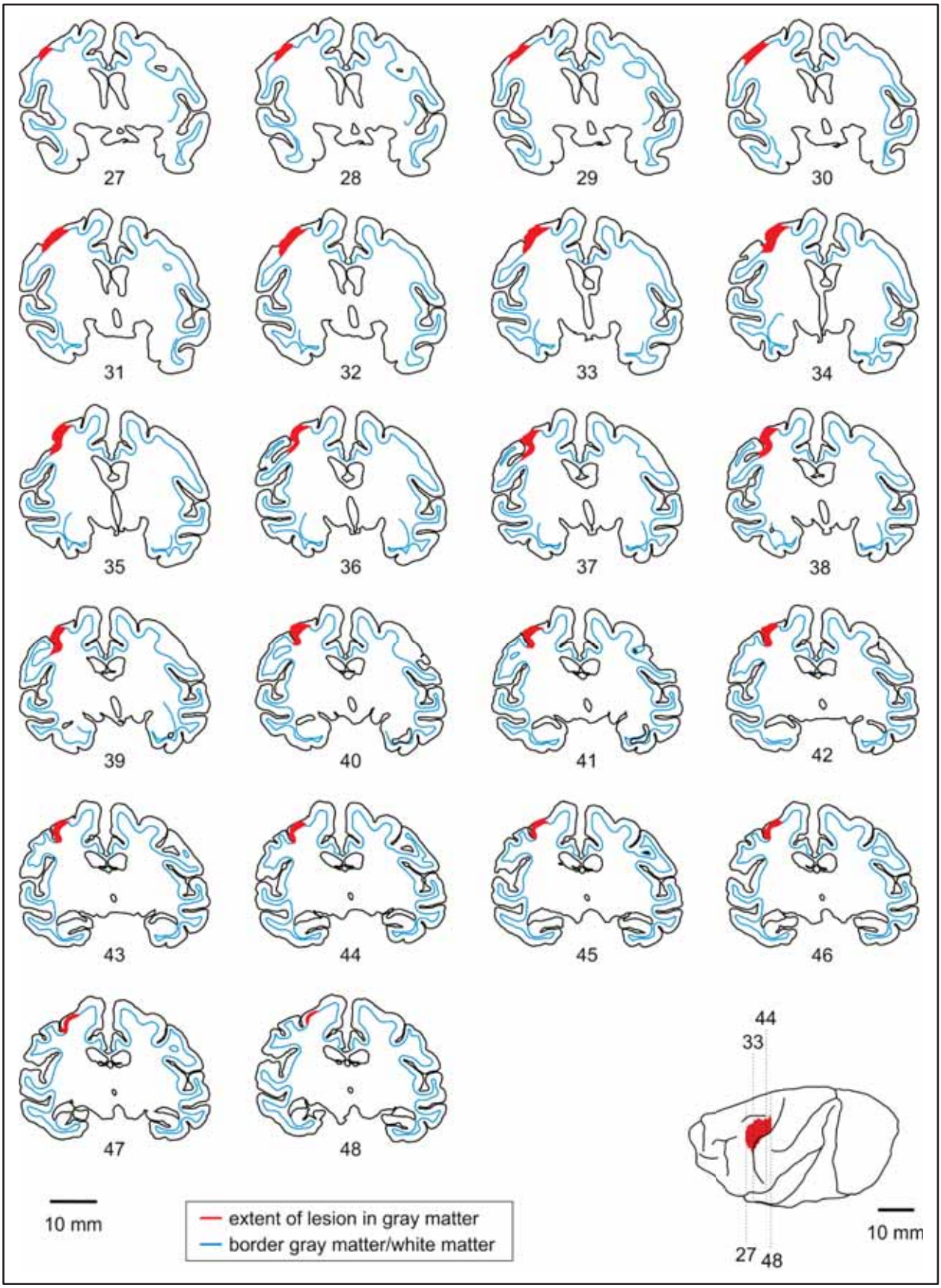
27
28
29
30
31
32
33
34
35
36
37
38
39
40
41
42
43
44
45
46
47
48
10 mm
extent of lesion in gray matter
border gray matter/white matter
44
33
27 48
10 mm

Supplementary Figure 2: 5-ms signal and 27-ms signal captured at the subcortical and cortical electrodes. (A) Relationship between the amplitude of the 5-ms signal from the subcortical electrode and from the cortical electrode before the lesion. (B) Same as (A) but after the lesion. (C) and (D) Same as (A) and (B) but for the amplitude of the 27-ms signal.

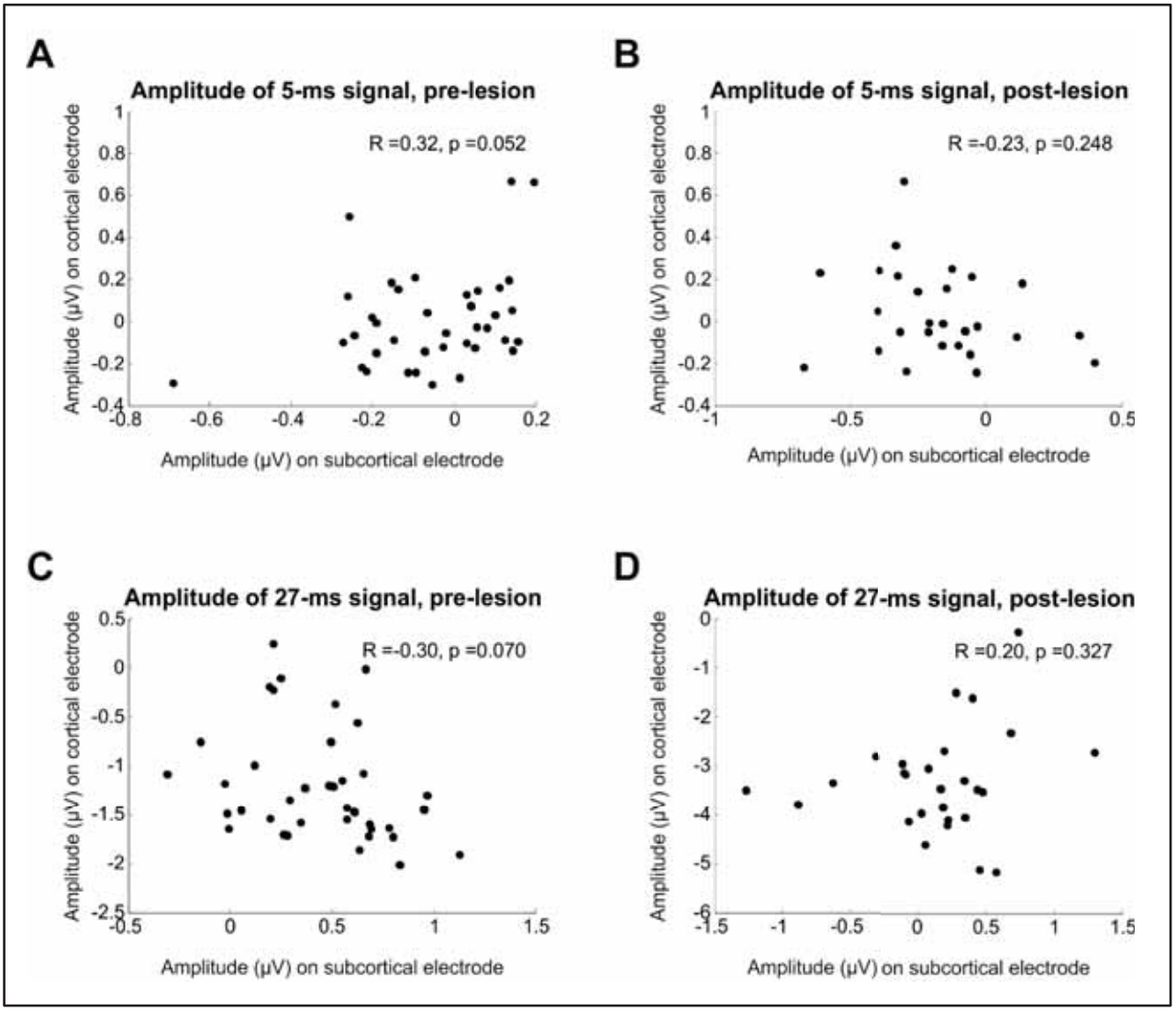

Supplementary Figure 3: BDA labelling. (A) Injection core on section 41, and magnification (on the right). (B) Labelled fibres in PM, M1 and S1. (C) Retrogradely labelled cell bodies in M1 and S1. (D) Labelled synaptic boutons in S1.

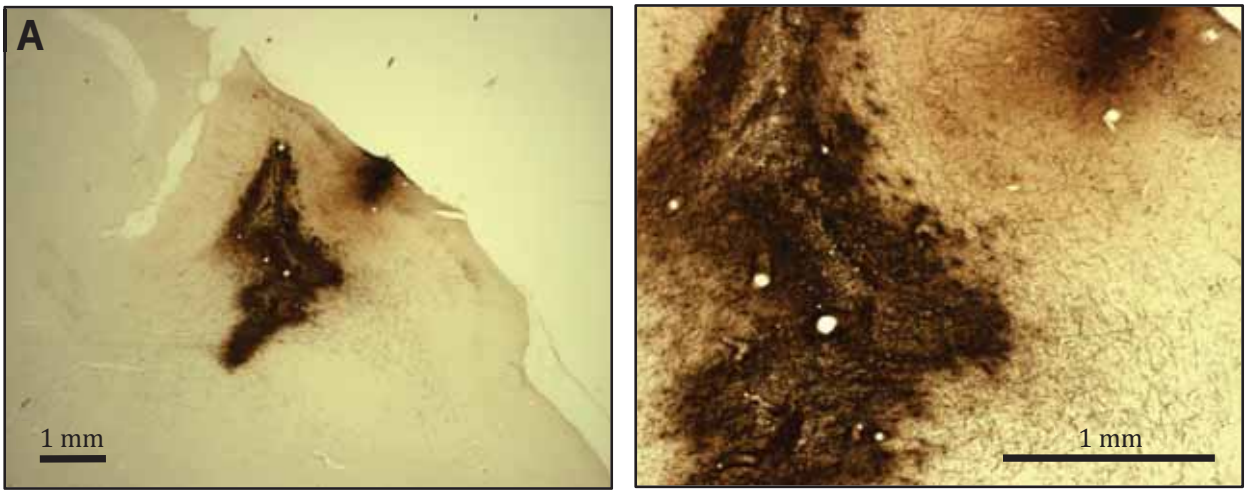

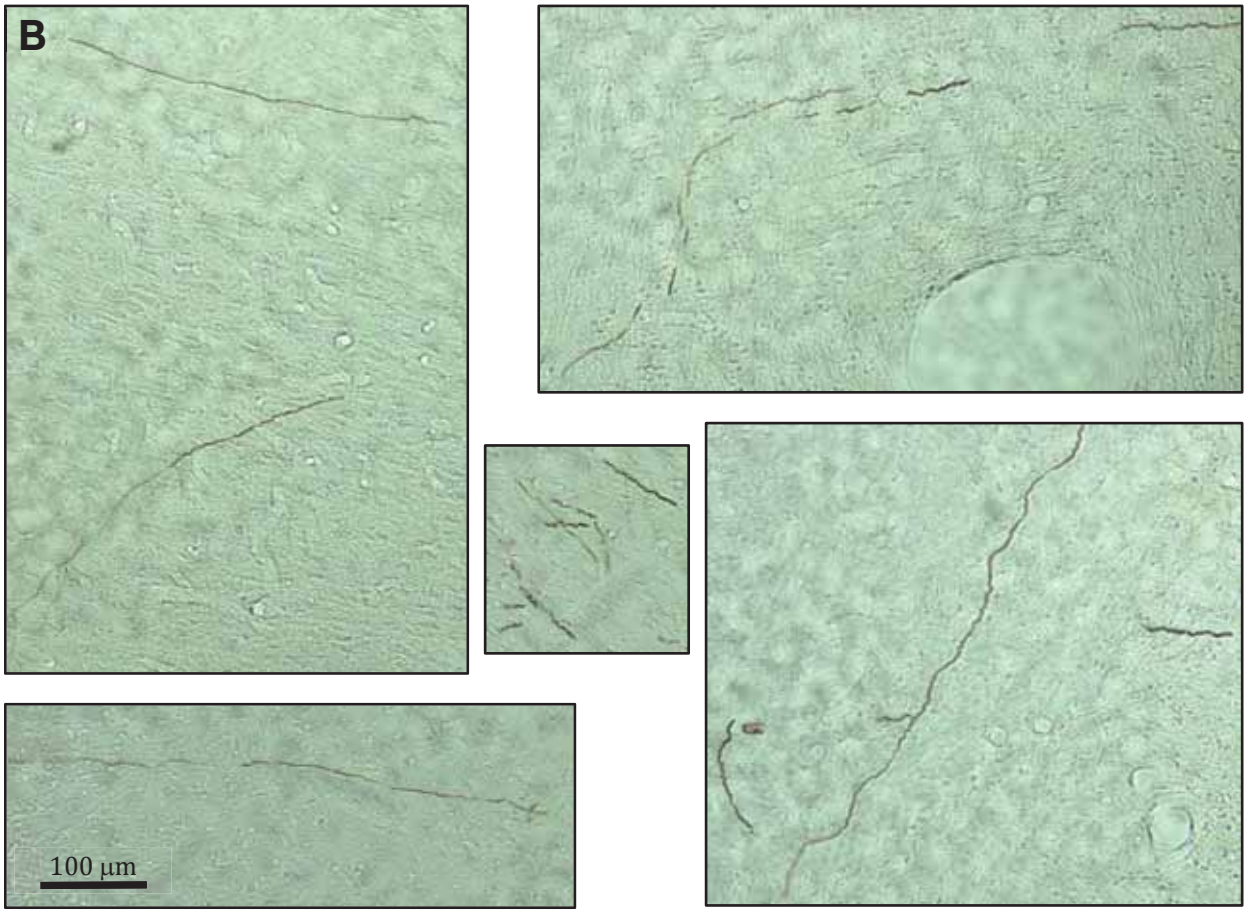

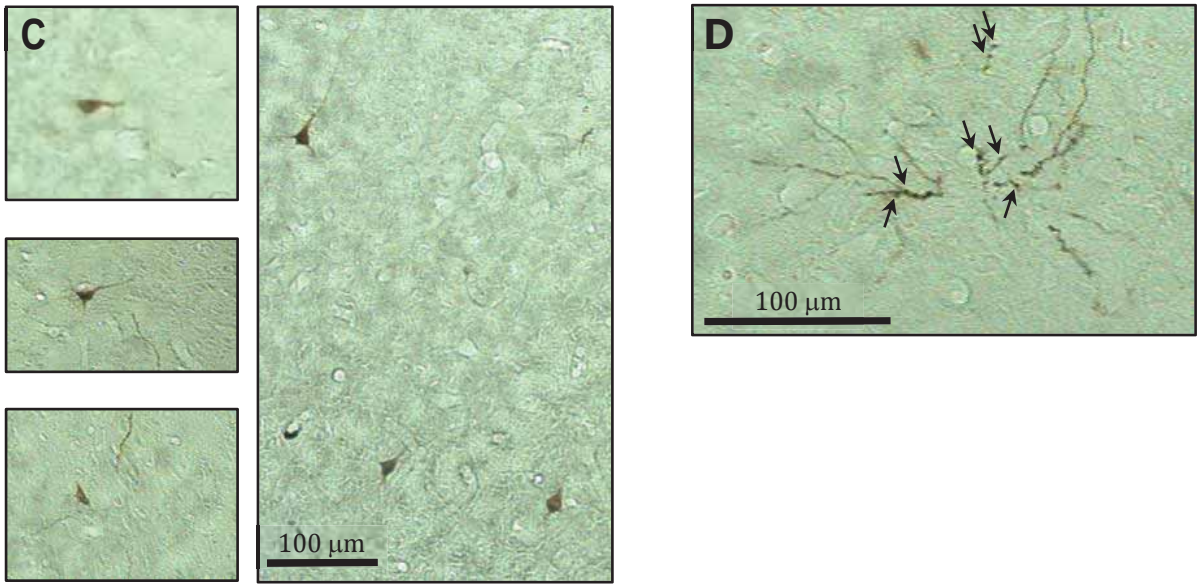

Supplementary Figure 4 (next 6 pages): Reconstruction of BDA labelling. Series of individual BDA-stained sections (11-44) with visible ipsilateral BDA labelling after BDA injection into left S1. Sections before 27 showed labelling primarily in PM while posterior sections from 27 showed labelling in M1 and in the different areas of S1. For sections 35-44, some labelled structures in S1 were not drawn here due to the highly dense labelling, especially around the injection site. Note that BDA-labelled structures were present caudal to section 44 as well but were not investigated here. Labelling in the right hemisphere was not reconstructed. Given the absence of information about the distribution of labelled structures following an injection in S1 in intact animals, we cannot provide here any quantitative data but the following sections are shown for information.

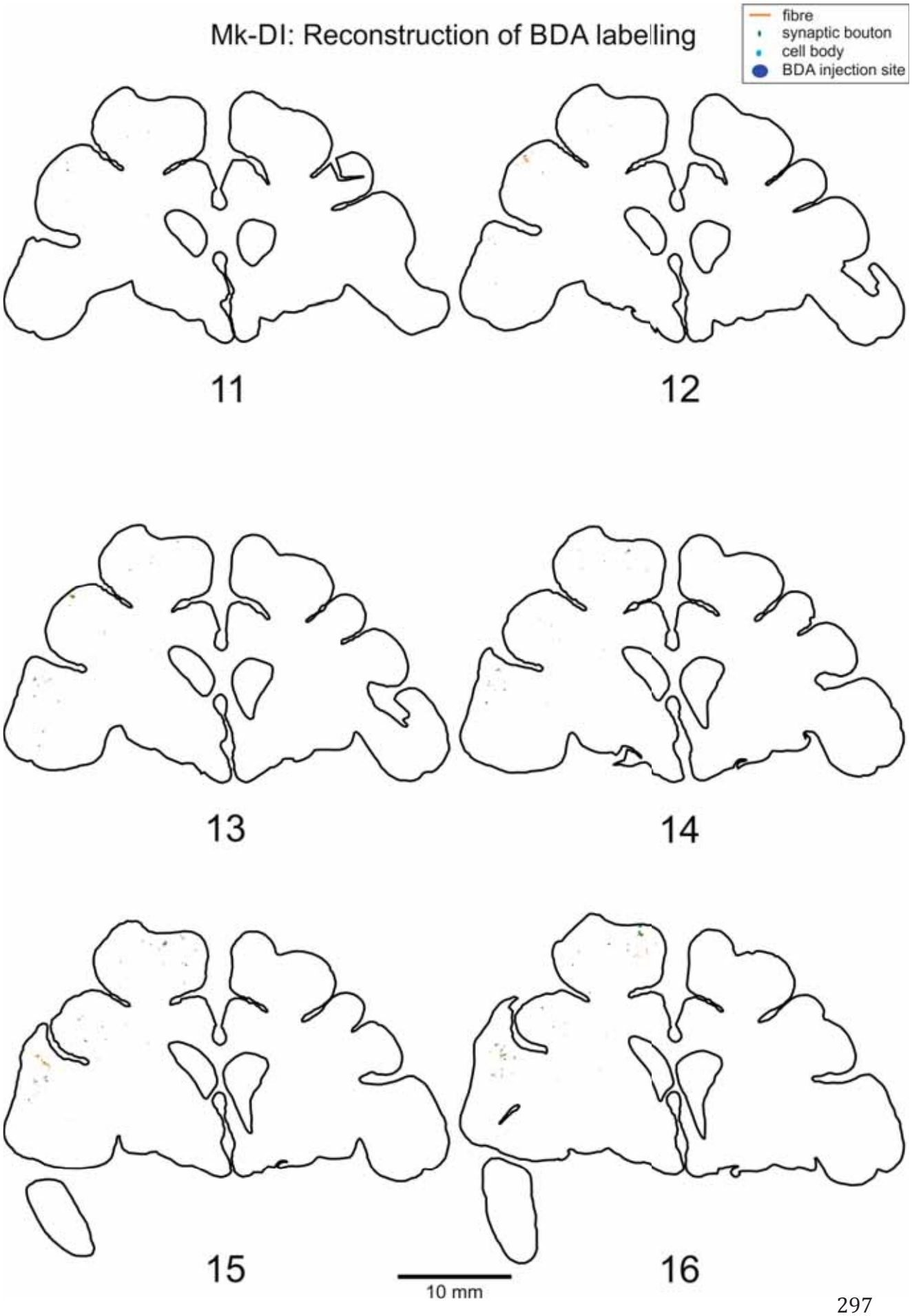
Mk-DI: Reconstruction of BDA labelling
fibre
synaptic bouton
cell body
BDA injection site
11
12
13
14
15
16
10 mm

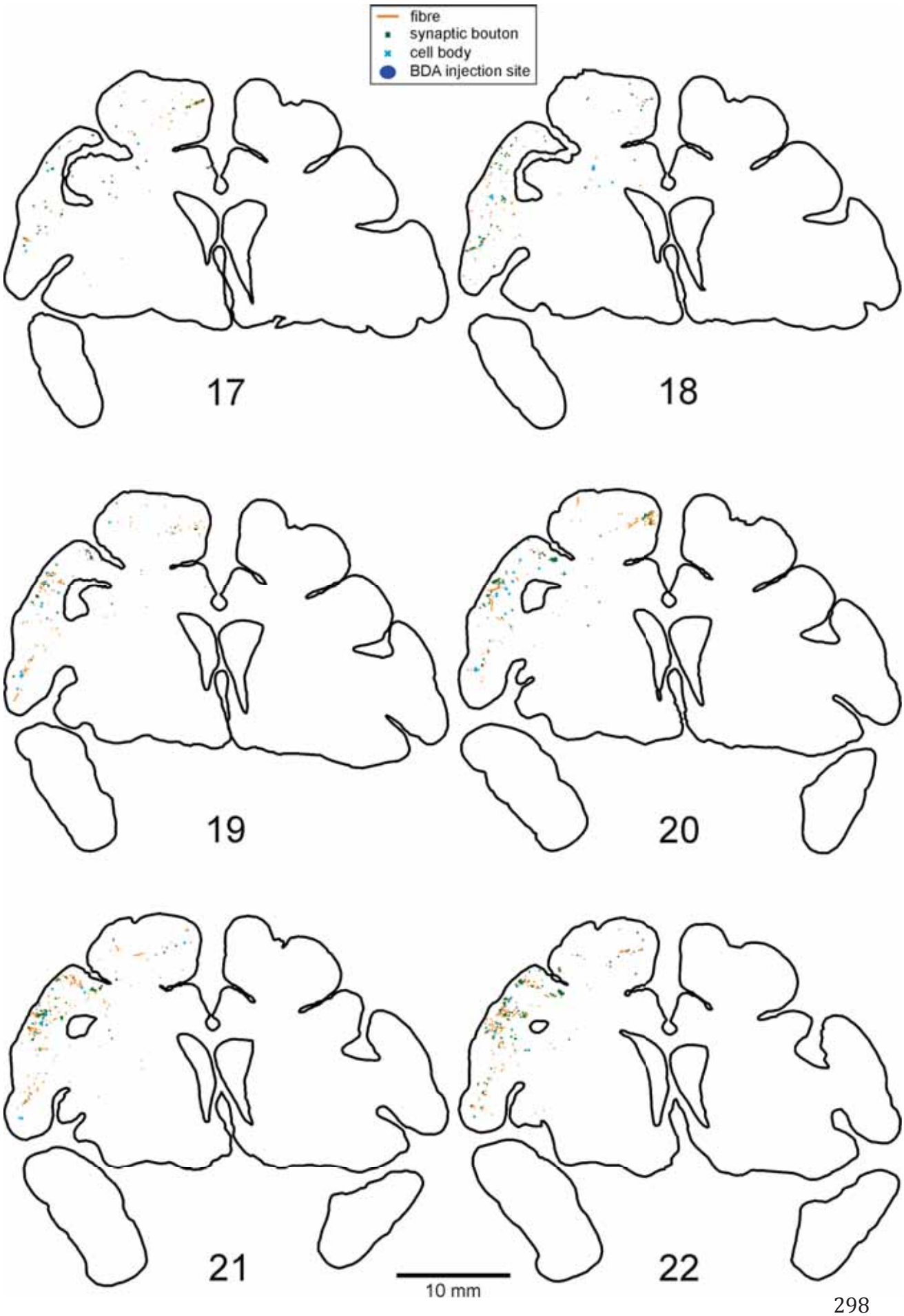
fibre
synaptic bouton
cell body
BDA injection site
17
18
19
20
21
22
10 mm

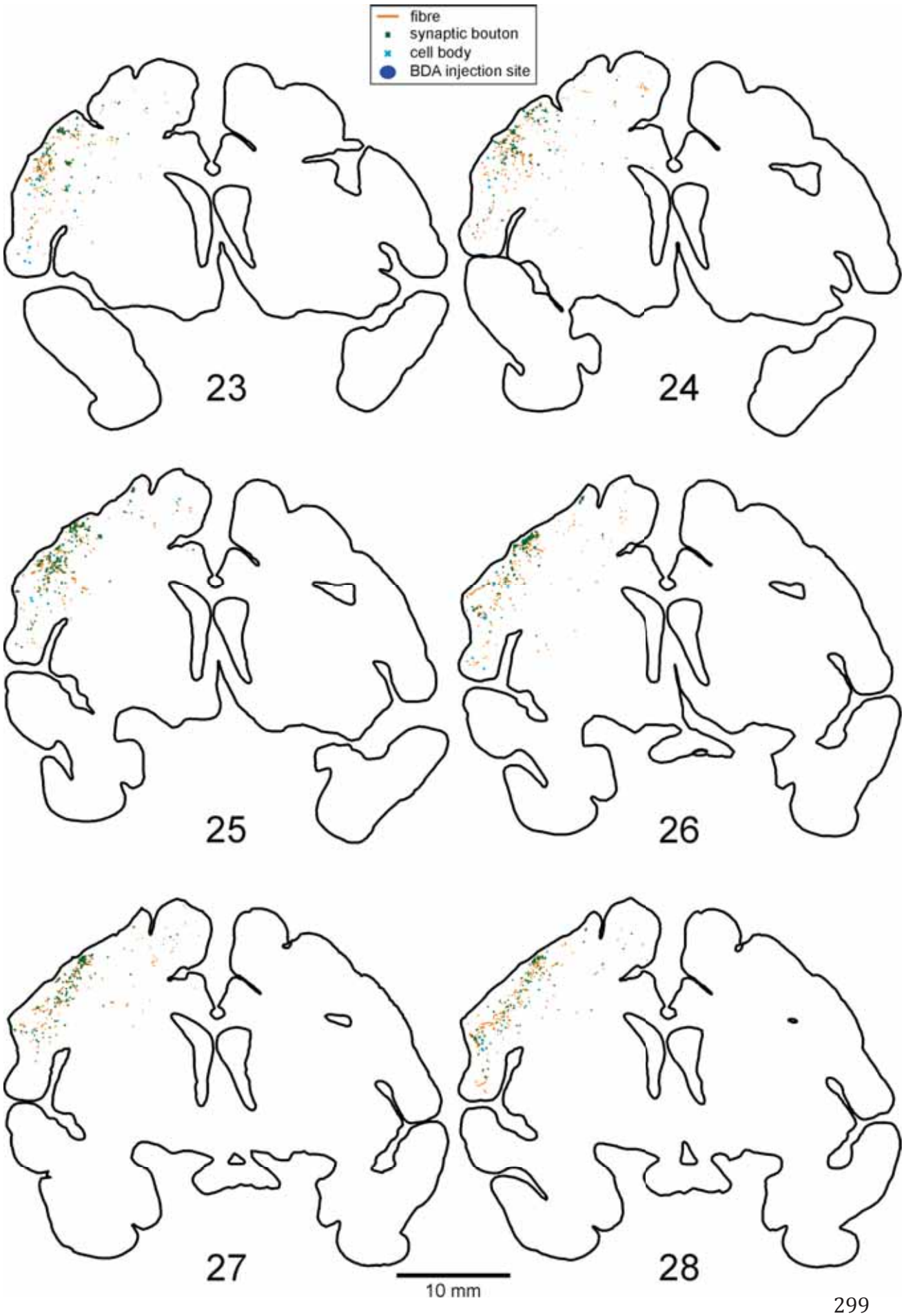
fibre
synaptic bouton
cell body
BDA injection site
23
24
25
26
27
28
10 mm

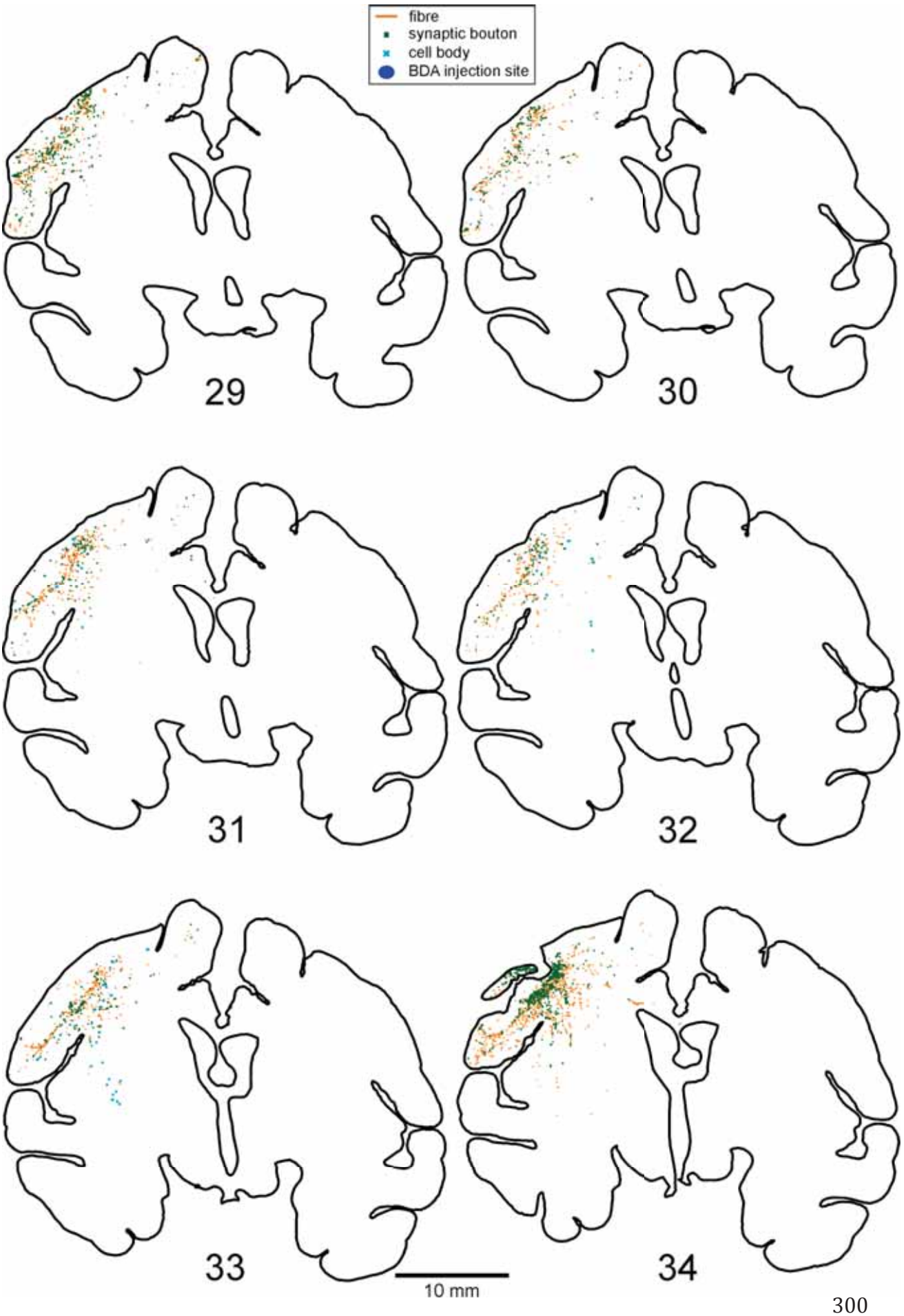
fibre
synaptic bouton
cell body
BDA injection site
29
30
31
32
33
34
10 mm

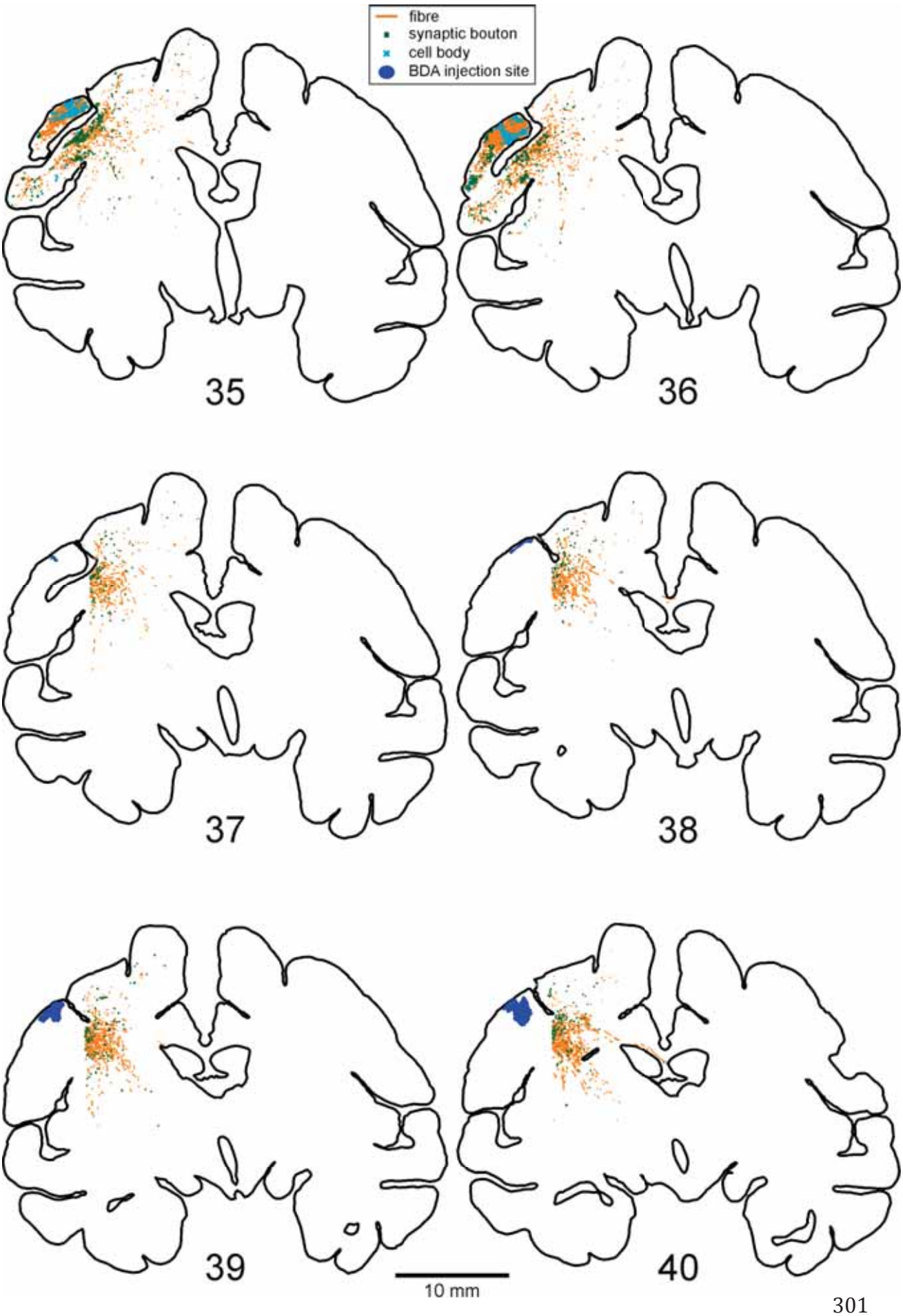
fibre
synaptic bouton
cell body
BDA injection site
35
36
37
38
39
40
10 mm

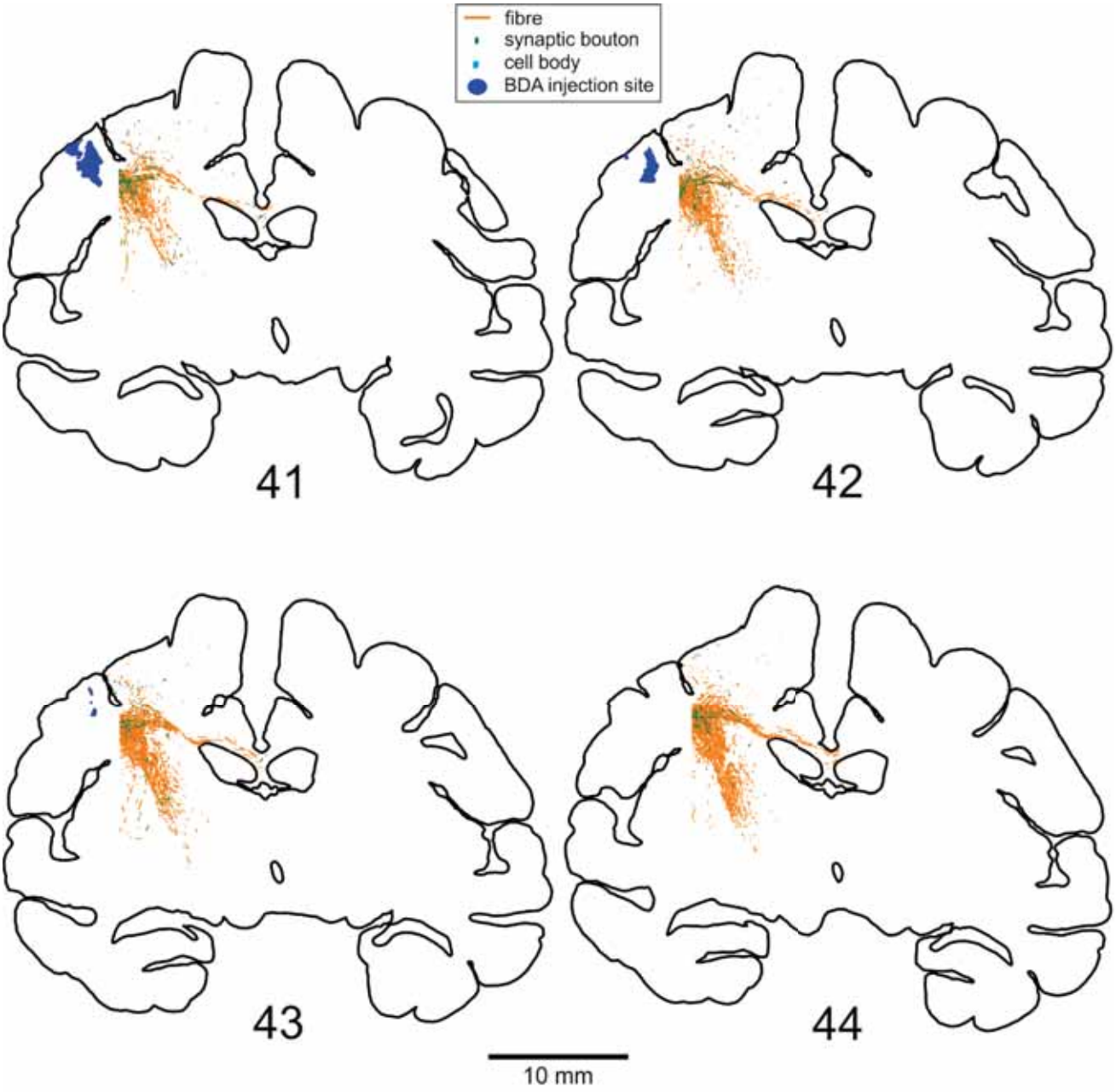
fibre
synaptic bouton
cell body
BDA injection site
41
42
43
44
10 mm

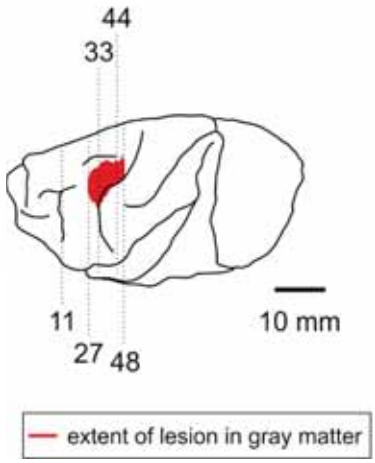
44
33
11
27
48
10 mm
extent of lesion in gray matter

CHAPTER 3

Impact of a dominant M1 lesion on cortical tactile processing from the fingertips in adult macaque monkey: a case report

Anne-Dominique Gindrat, Eric M Rouiller and Arko Ghosh

Abstract

Sensory information from the hand is crucial for motor control and the disruption of these inputs due to a nervous system injury or disease results in numb and clumsy hands. The fingertips, in particular, are well endowed with tactile receptors but how these inputs are computationally linked to motor control is not entirely clear. Here, our goal was to profit from the high temporal resolution and non-invasiveness of scalp EEG to study the changes in tactile information processing from the fingertips following a highly focal cortical lesion in a non-human primate, in order to complement our understanding of post-lesion mechanisms involved in brain plastic reorganisation.

To this end, in parallel with the previous study (**Chapter 2**) involving scalp EEG measurements of the processing of electrical stimulation to the median nerve, we recorded the cortical activity associated with the fingertips in the same anaesthetised macaque monkey as well, both before and at several time points (5-week interval) after the dominant M1 lesion. Tactile stimulations were applied by using computer-controlled solenoid tappers placed over the contralesional thumb, index and middle fingertips.

The pre-lesion recordings from the electrodes over the contralateral somatosensory cortex revealed a large positive peak at 33-37 ms post-stimulus. After the lesion, we observed major changes in brain activity following tactile stimulation to the contralesional fingertips: interestingly, although the lesion targeted the whole hand representation in M1, the alterations were the most prominent for the thumb and were further enhanced over post-lesion time. Similar effects were observed for the index finger but to a lesser extent. In parallel, the animal displayed impairment in contralesional thumb use in favour of the index finger when manual dexterity was assessed in a task without visual feedback. The alterations in sensory processing may partially explain the behavioural deficits observed after the lesion.

We hypothesise that the dominant M1 lesion may have damaged the pre-existing strong sensorimotor interactions which are normally biased towards the thumb sensorimotor control. Equally importantly, several observations suggest that the post-lesion changes in scalp signals are unlikely to result from lesion-induced distortions in volume-conduction.

In sum, the present data show that the dominant M1 lesion interfered with the processing of fingertip inputs in the cerebral cortex and suggest that normal tactile sensory processing is modulated by motor cortical activity.

Introduction

This chapter should be considered as the direct and complementary succession of **Chapter 2**. In the latter, we presented the impact of a motor cortex lesion on somatosensory processing of electrical stimulation to the median nerve in Mk-DI. Here we will explore the impact of the same lesion on tactile processing from the fingertips in the same animal. Before concluding, we will discuss the present results in relation with those of **Chapter 2**.

Sensory and motor capabilities of the primate hand evolved to eventually reach the ultimate refinement in prehensility that characterises primates (Old World monkeys and Humans) (Napier, 1962) and confers them a very special evolutionary advantage in the sense that they can directly interact with the physical environment and partly control it (Napier, 1993). Indeed, the primate hand is able to fully achieve dual complementary functions, namely to finely manipulate objects as well as to be used as a sensory organ to get somatosensory feedback, especially during discriminative touch and haptic perception (Chapman et al., 1996; Napier, 1993). Such sophisticated sensorimotor control of the hand is first assumed by M1 and S1 and relies on a uniqueness of S1 among the different primary sensory areas in being directly and intimately connected with M1 through strong bidirectional projections (Hendry and Hsiao, 2013).

The crucial role of this sensorimotor integration has been already demonstrated by lesioning one of these 2 areas. For instance, a muscimol-mediated reversible inactivation of S1 hand representation (Hikosaka et al., 1985) or electrocoagulation-mediated permanent inactivation of S1 hand representation (Xerri et al., 1998), both in monkeys, resulted in strong but temporary deficits in fine manual dexterity. Conversely, somatosensory impairments were observed in squirrel monkeys after lesion of M1 hand representation (Friel et al., 2005; Nudo et al., 2000) and an increase of activity in S1 forelimb area was described in macaque monkeys during reversible inactivation of the M1 forelimb area (Sasaki and Gemba, 1984). These descriptions of impairments highlight the im-

portance of the strong connectivity between M1 and S1 in primates (Cole and Glees, 1954; Jones et al., 1978; Jones and Powell, 1970; Jones, 1986; Kaas, 2004; Stepniewska et al., 1993).

In addition to these corticocortical connections between M1 and S1, short-latency peripheral somatosensory inputs were shown to reach M1 directly from the thalamus (Asanuma et al., 1979a). More specifically, thalamic inputs from the distal upper limb originate primarily from the oral subdivision of VPL (VPLo) (Asanuma et al., 1979c; Horne and Tracey, 1979; Lemon and Van der Burg, 1979; Strick, 1976) while thalamic inputs from the proximal upper limb project mostly from the ventrolateral nucleus (VL, both oral and caudal parts) (Darian-Smith and Darian-Smith, 1993; Holsapple et al., 1991; Leichnetz, 1986; Matelli et al., 1989; Rouiller et al., 1999; Shindo et al., 1995; Strick, 1976; Strick, 1975). These thalamic inputs are mediated mainly through the dorsal column-medial lemniscal system (Asanuma et al., 1980; Brinkman et al., 1978) in monkeys while they reached S1 through both the dorsal column-medial lemniscal system and spinothalamic tract (Asanuma et al., 1979b; Asanuma et al., 1980; Brinkman et al., 1978; Darian-Smith et al., 1996a; Darian-Smith et al., 1996b).

The existence of afferent feedback to higher levels of the nervous system involved in motor control is known since a very long time (Francois-Franck, 1887). Peripheral afferent inputs to the motor system were reported in the form of pyramidal tract neurons responding to peripheral nerve stimulations (Adrian and Moruzzi, 1939), cutaneous stimulation or passive limb movements (see e.g. Wannier et al., 1991). Then pioneering extensive work in the field of relation between motor function and peripheral input was performed in particular by Asanuma and co-workers (for a review, see Asanuma, 1981), first in cats (Asanuma, 1959; Asanuma et al., 1968; Asanuma, 1973; Asanuma, 1975; Asanuma et al., 1979b; Asanuma and Rosén, 1972; Asanuma and Sakata, 1967; Asanuma et al., 1979c; Stoney et al., 1968; Thompson et al., 1970) then in awake monkeys (Asanuma, 1973; Asanuma, 1975; Asanuma and Rosén, 1972; Asanuma et al., 1979c; Rosén and Asanuma, 1972). Some other groups later confirmed their results again in cats (Murphy et al., 1975) and in monkeys (Brinkman et al., 1985; Colebatch et al., 1990; Murphy et al., 1978; Wiesendanger, 1973; Wong et al., 1978). In practical, by using microelectrode penetrations in M1, Asanuma and co-workers combined at a given cortical site both receptive field determination with natural stimuli and passive movement and

then ICMS. In this way they were able to map and then to reconstruct the cortical volume in charge of a given muscle or movement, with the aim to correlate it with the afferent inputs projecting to this cortical region. They discovered a columnar organisation within the motor cortex where neurons of the same column were shown to control movements of the same body part. In particular they demonstrated that M1 neurons controlling finger movements received polymodal afferent inputs from peripheral receptors activated by light touch, skin pressure or passive finger movements. For instance, tactile afferences elicited by stimulating the glabrous volar surface of the hand projected on neurons of the hand cortical area controlling finger flexions. In the same way, most of the cells activated by passive joint movements (receptors in muscles and joints) projected on neurons involved in the motor control of that joint that sent peripheral input to the given cortical region. More generally, they highlighted an input-output organisation where each M1 cortical region received afferent inputs associated with the movement produced by the activity of that zone, because peripheral receptors (skin, joint and muscle receptors) were located in the same region potentially stimulated by the contraction of the target muscle. The motor cortex received in particular dense peripheral sensory inputs from the distal forelimb areas. Asanuma and co-workers described in greater detail the columnar organisation within M1 and observed that cells responding to peripheral inputs were mostly located in layers II to IV whereas cell controlling movements of the corresponding body parts originated mostly in layer V. They suggested a loop organisation between peripheral inputs and motor cortex but excluded a direct initiation of movements by peripheral inputs because these inputs projected on cells of superficial layers with a high activation threshold to generate movements. Conversely, cells in layer V were rarely activated directly by peripheral inputs. Asanuma et al. concluded therefore that these inputs were actually relayed from superficial layers to a restricted group of neurons located in deeper layers of the same cortical column by interneurons.

Remarkably, a mostly somatotopic organisation of afferent sensory inputs to M1 was demonstrated by using EPs (Woolsey et al., 1942; Woolsey, 1958; Woolsey, 1964) and intracortical microelectrode recordings (Brooks et al., 1961; Buser and Imbert, 1961; Lemon and Porter, 1976; Murphy et al., 1978; Rosén and Asanuma, 1972; Wong et al., 1978) in cats and in monkeys, in a similar way as inputs to S1. Some exceptions to this topographical organisation of afferent inputs were nevertheless reported (Lemon et al., 1976; Lemon and Porter, 1976). Moreover, a segregation between cutaneous and deep

afferent inputs emerged in M1: neurons receiving substantial cutaneous input were concentrated in the caudal M1 hand representation while those driven by non-cutaneous, deep input were located in the rostral M1 hand representation in monkeys (Strick and Preston, 1982; Strick and Preston, 1978; Tanji and Wise, 1981). Consequently, Strick and Preston (1978) suggested that the caudal motor representation may control movements using tactile input for their execution and guidance, such as in tactile exploration, while the rostral motor representation may control movements using kinesthetic input for their execution and guidance, such as in load compensation.

The functional role of sensory inputs to motor control are still under debate although their importance was already demonstrated long time ago, for instance by Claude Bernard (1858) in frogs and in dogs. Namely he wrote: « *Les racines postérieures, nerfs du sentiment, semblent […] avoir une certaine influence sur les propriétés motrices des racines antérieures. Chez les grenouilles, cette influence ne paraît pas sensible, et nous avons vu qu'en privant un membre postérieur de tous ses nerfs de sensibilité, il se meut encore assez bien en harmonie avec celui du côté opposé dans les mouvements de natation ou de saut qu'exécute l'animal. Cependant, quand on coupe la racine postérieure des deux membres postérieurs à la fois, il y a moins d'ensemble dans les mouvements auxquels tous deux prennent part. Chez les chiens, cette influence est beaucoup plus manifeste. Cette influence du sentiment sur le mouvement est un fait important qui, je crois, n'a pas été remarqué par les expérimentateurs.* » (Bernard, 1858). Similar observations of motor impairment of the limbs, especially for distal hand and foot muscles, followed or not by partial functional recovery, were then reported in macaque monkeys after dorsal root sections (Darian-Smith and Ciferri, 2005; Darian-Smith, 2007; Mott and Sherrington, 1894). In human severe motor deficits were observed after local finger anaesthesia (Johansson et al., 1992; Johansson and Westling, 1984; Monzée et al., 2003) or after severe deafferentation (Rothwell et al., 1982; Sanes et al., 1984). Moreover, cortical reorganisation emerged in M1 after reduced somatosensory inputs, either by unilateral section of the dorsal columns in macaque monkeys (Kambi et al., 2011; Qi et al., 2010) or by limb amputation (Qi et al., 2000).

Some hypotheses about the functional role of these sensory inputs to M1 were proposed. For instance Brooks suggested these inputs to have integrative functions (Brooks et al., 1961). Asanuma and co-workers (Asanuma and Arissian, 1984) investigated the ques-

tion in detail in awake macaque monkeys by interrupting each of the 2 major sources of peripheral input to M1, namely 1) the dorsal column, sending direct projection from the periphery to M1 through the thalamus, 2) S1, sending association fibres to M1. The removal of a large portion of S1 (from the neck representation to hindlimb representation) resulted only in very slight and transient (about 1 week) finger motor deficits. In the same way, very few and short-lasting (about 2 weeks) motor deficits (loss of orientation and coordination) were observed after section of the dorsal column, and afferent peripheral inputs to M1 recovered in parallel. But, when S1 was removed in animals that just recovered from the transient motor deficits of dorsal column sections, or the opposite situation -meaning that both lesions were now combined in the same animal- then very strong and permanent motor deficits emerged, characterised by a profound impairment of fine manual dexterity associated with a loss of orientation within extrapersonal space. Similarly, after dorsal column section, a subsequent lesion of the association fibres between S1 and M1 was performed on some monkeys, resulting in strong permanent impairment to perform individuated fine finger movements and to orient the hand in space, in addition to a loss of the pre-lesion receptive fields in M1. Taken together, these results suggest that sensory inputs from the periphery to M1 can be mediated either through the dorsal column and then direct thalamocortical fibres to M1 or indirectly from S1 to M1 through association fibres. Both play a key role in the execution of voluntary movements (Wiesendanger, 1973) and deficits produced by the loss of one source of inputs can be compensated by the function of the other source of inputs (Brinkman et al., 1978).

Asanuma and co-workers integrated all their findings in a model called cortico-peripheral loop (Asanuma, 1973; Asanuma, 1981). Essentially, the pyramidal system is involved among others in the control of fine movements of the hand and fingers (Lemon, 1997; Lemon, 2008). The activity in CST fibres from a given columnar efferent zone in M1 produces the contraction of a target muscle. In parallel, the same M1 region receives afferent peripheral inputs directly from receptors associated with the contraction of the target muscle, constituting a closed-loop circuit. In addition, afferent inputs from these receptors project to S1 as well. In sum, there are direct and indirect loop circuits between M1 and the periphery.

In conclusion, Asanuma, Murphy (Murphy et al., 1978) and their co-workers suggested that the homonymous coupling between sensory inputs to M1 and motor outputs was involved in the sequencing of voluntary movements with sensory inputs facilitating and/or setting up the excitability level of corticofugal neurons in M1 by positive feedback, both before and during voluntary movements. Tactile exploration (Darian-Smith, 2007) and real-time adjustments during object manipulation (Gardner et al., 2007; Monzée et al., 2003; Wannier et al., 1991) with the fingers and the hand, in particular, were shown to strongly depend on a continuous afferent positive feedback of peripheral inputs to M1 (Lemon, 1981).

SSEPs in human and in non-human primates have been traditionally investigated primarily by using a punctate electrical stimulation delivered percutaneously to a peripheral nerve because of the convenience of this technique (see e.g. Allison et al., 1989a; Allison et al., 1989b; Allison et al., 1991a; Allison et al., 1991b; Allison et al., 1996; Aminoff and Eisen, 1998; Arezzo et al., 1979; Arezzo et al., 1981; Desmedt and Cheron, 1980a; Desmedt and Cheron, 1980b; Desmedt and Cheron, 1981; Desmedt and Nguyen, 1984; McCarthy et al., 1991; Nuwer et al., 1994; Perot et al., 1983; Stohr et al., 1983; Valeriani et al., 2000; van de Wassenberg et al., 2008). We used this classical stimulation paradigm in **Chapter 1** and **Chapter 2** as well. Such responses to electrical shocks led to important discoveries about the neural basis (i.e. generators) of these potentials (Allison et al., 1989a; see e.g. Allison et al., 1989b; Allison et al., 1991b; Desmedt and Cheron, 1982; Mauguière et al., 1983; Valeriani et al., 2000; Vaughan, 1982). Nevertheless, electrical stimulation represents a very artificial stimulation because it is targeted directly on the nerve trunk and in this way completely bypasses the terminal nerve fibres (Brown, 1984; Starr et al., 1982), and fibre activation is nonspecific (Pratt et al., 1979a). Moreover, the use of electrical stimulation resulted in discrepancies between electrophysiological and psychophysical thresholds (Rosner and Goff, 1967; Uttal and Cook, 1964).

Conversely, natural stimulation such as taps or vibrations delivered to the skin, the fingernails or the pads, has been used more sporadically so far (see e.g. Breitwieser et al., 2011; Breitwieser et al., 2012; Budd and Timora, 2013; Colon et al., 2012; Hari, 1980; Hashimoto et al., 2000; Hashimoto et al., 1990; Johnson et al., 1975; Pokorny et al., 2013; Pratt et al., 1979b; Pratt et al., 1980; Soininen and Jarvilehto, 1983; Starr et al., 1982) but

presents actually several advantages over electrical stimulation: natural stimulation activates the afferents through their receptors and thus involves the most distal segments of the peripheral nerves as well (Caruso et al., 1994; Pratt et al., 1979a; Pratt et al., 1979b; Starr et al., 1982). Moreover, here the perceptual estimations were shown to be linearly related to the amplitude of mechanical stimulation (Franzén and Offenloch, 1969; Johnson et al., 1975). In addition, natural stimulation has already been shown to be physiologically appropriate to clarify mechanisms of both normal somatosensory processing (Adrian, 1941; Caruso et al., 1994; Gardner et al., 1984; Gindrat et al., 2015; Hari, 1980; Marshall et al., 1941; McLaughlin and Makeig, 1995; McLaughlin and Kelly, 1993; Nakanishi et al., 1973; Pratt et al., 1979a; Reuter et al., 2014; Soininen and Jarvilehto, 1983; Woolsey et al., 1942; Woolsey and Erickson, 1950; Zeller et al., 2014) and clinical disorders of somatosensory processing (Lascano et al., 2014; Maitre et al., 2012; Pokorny et al., 2013; Vanhatalo et al., 2009).

Although it is known from the aforementioned evidence that peripheral afferent inputs in primates are not restricted to S1 but project to M1 as well, meaning that M1 is indisputably involved in somatosensory processing, the neuronal mechanisms of this sensorimotor integration and its involvement in the execution of motor commands remain poorly understood. Therefore, in parallel with our first investigations with median nerve stimulation (**Chapter 2**), we were interested here to study in the same monkey the impacts of the motor cortex lesion on somatosensory processing of a more naturalistic and more physiological stimulation, namely a purely passive tactile stimulation to the hand fingertips. Based on the observations presented in **Chapter 2**, our working hypothesis was that tactile processing of information originating from the distal forelimb in non-human primates was affected by a motor cortex injury. Our second hypothesis was that recording the brain activity evoked by different types of stimulation applied to the somatosensory pathway would provide further and complementary insights into the mechanisms involved in post-lesion plastic reorganisation of the brain. To test these hypotheses, we measured brain activity (EEG) at the scalp in response to a tactile stimulation to the fingertips of the hand in Mk-DI, before and after a permanent cortical lesion of the hand representation in M1.

Materials and Methods

Monkey

This experiment was performed on Mk-DI in parallel with the study presented in **Chapter 2**. Therefore, all the general procedures introduced in **Chapter 2** apply here as well (anaesthesia, cortical lesion, EEG acquisition, end of procedure, histology, neuroanatomical reconstruction) except the behavioural task, the peripheral stimulation and the EEG data analysis. These specific aspects will be developed below.

Behavioural task

We assessed the integrity of the sensorimotor control of the monkey's hand from a behavioural point of view by using the Brinkman box task. The full description of this task is provided in **Chapter 5**. Briefly, this grasping task is based on the use of the precision grip (Napier, 1956) and was specifically designed to be performed either without or with visual feedback. In particular without visual feedback, the Brinkman box task was expected to challenge the motor exploration by palpation and the precision grip ability by relying mostly on tactile sense and proprioceptive inputs. Such fine fractionated movements of the fingers during active tactile exploration without visual feedback involve the activation of M1 neurons through glabrous afferent inputs (Lemon, 1981).

In this study, we were particularly interested in the use of the fingers. To this end, we quantified for each pellet being collected using a precision grip which was the first finger in contact with this given pellet, and we divided then the total score of each finger by the number of pellets retrieved to express the use of each finger as a percentage of the total finger use (*% of first finger use*). We also measured the percentage of effective contacts established with each finger in the first 30 s of the task *(% of effective contacts*), defined as the number of pellets successfully retrieved in the first 30 s divided by the number of contacts established with pellets in the first 30 s, for each individual finger. The ability to conform a precision grip was evaluated by measuring firstly the *precision grip shaping time* for the first 5 collected pellets, defined as the time interval between the well detection by a finger and the first contact between a finger and the pellet in this given well in order to make a precision grip. Secondly, we measured the *contact time* for the first 10 pellets as the time interval between the first contact established by a finger with a pellet

in a precision grip and the time point at fingers going out of the well with the pellet. The *time interval* between 2 pellets, defined as the time difference between the time point of pellet retrieval from a well and the time point of first contact established by a finger with the next pellet to be collected, was used to quantify the duration of motor exploration by palpation. To this end, the *time interval* in the task with vision, corresponding to the sole travelling time from the box to the mouth and vice-versa, was removed from the *time interval* in the task without vision (travelling time + motor exploration by palpation) to estimate the duration of pure motor exploration. In the same way, the *precision grip shaping time* obtained with vision (time to conform a precision grip) was removed from the *precision grip shaping time* obtained without vision (time to conform a precision grip + time of motor exploration) to derive another measurement of motor exploration. The motor performance at the wrist level was assessed by quantifying the *% of wrist orientation* in the form of radial deviation, neutral position and ulnar deviation at the moment when fingers went out of a well with a pellet. Both ulnar and radial deviations are especially needed to retrieve pellets from horizontal wells (see e.g. Chatagny et al., 2013; Hoogewoud et al., 2013) whereas collecting pellets from the vertical wells can usually be performed less challengingly with the wrist in a neutral position.

For the parameters under investigation here, we defined a pre-lesion plateau of performance and a post-lesion plateau of performance (same dates for each parameter, based on visual appreciation, with the goal to find the time period being the most stable across the different parameters under consideration and in accordance with the plateaux defined in the modified Brinkman board task, see **Chapter 2**) and compared both of them with either a Mann-Whitney test, or a z-test for comparing proportions, as the case may be. Statistical analyses were performed with SigmaPlot 12.5. We chose to perform Mann-Whitney tests even in some cases when a t-test was possible, in order to be fully consistent across the data. Moreover, in case of a small sample size, such as the data sample considered in each plateau, Mann-Whitney tests are known to perform better than t-tests (Fay and Proschan, 2010; Ludbrook and Dudley, 1998).

Further detail about the analysis of the behavioural data of the Brinkman box task is given in **Chapter 5**.

EEG and tactile stimulation

The cortical activity at the scalp was measured after a peripheral tactile stimulation by using high-density EEG recordings on Mk-DI under sevoflurane anaesthesia, as already described in detail previously (see Gindrat et al., 2014 in **Chapter 1**, and **Chapter 2**). EEG recordings under general anaesthesia ensured that the animal was exposed to purely passive touch stimulations (see below) in addition to highly controlled conditions (e.g. decreased muscular and movement artifacts, and reduced cardiovascular and autonomic responses that are usually associated with unanticipated stimulus exposure in conscious subjects) so as to increase the sensitivity to detect small changes in brain signals between different conditions.

The passive tactile stimulation was randomly and individually delivered to the volar pad of the tips of the thumb, index finger and middle finger of the right hand (i.e. contralesional) using solenoid tappers (Heijo Research Electronics) (**Figure 1**) that were precisely computer-controlled (IBM ThinkPad T43) in time via a stimulation box using a customised MATLAB® script (MATLAB R2011b). The tappers were designed to apply single pulses of 2-ms-long suprathreshold touch stimulus (square wave pulse) with an interstimulus interval of 1000 ± 250 ms, resulting in a <0.4-mm indentation on the pulp. A 0.4-mm skin indentation was measured in human (see **Chapters 6** and **7** for a use of the same tappers in human). Nevertheless, because of the thicker skin at the fingertips in monkeys than in human, we can expect that the indentation generated here was somewhat less prominent than in human. Brain activity was measured at the scalp in the same way as described in **Chapters 1** and **2**. Regular breaks in acquisition were made during the experiments to visually check the state of the monkey, in addition to the continuous monitoring of vital parameters.

The cortical activity associated with the fingertips was recorded both before (3 sessions) and after (4 sessions at 5-week interval) the dominant M1 lesion.

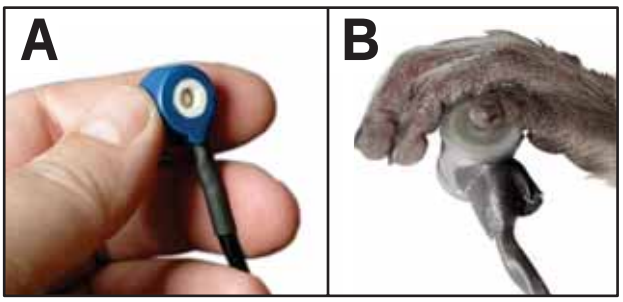

Figure 1 : Solenoid tapper used for tactile stimulations. (A) A small magnet is inserted at the centre of the cylinder. Under activation, the magnet moves then forward and backward, inducing a small depression of the skin surface and generating a sensation of touch (Image from manufacturer Heijo Electronics). (B) Tapper positioned on the monkey's right thumb. Some additional tape was added to secure the position of the tapper on fingertips during the experiments.

EEG data analysis

The EEG signal was re-referenced offline to the average reference using EEGLAB (an open source MATLAB toolbox (Delorme and Makeig, 2004)), then band-pass filtered between 5 and 100 Hz, and baseline corrected by using the pre-stimulus period from -100 ms to -10 ms. Artifact-contaminated amplitudes were rejected by using both a ±20-µV threshold and the kurtosis and joint probability distribution of the recordings (the threshold was set at 3 SD). SSEPs for each fingertip stimulation were then obtained by averaging a total of about 500 epochs (from -100 ms to +100 ms) per recording. All of the analyses were conducted with customised scripts on MATLAB and EEGLAB.

Results

EEG and tactile stimulation

In parallel with the electrical stimulation protocol (**Chapter 2**), we investigated in Mk-DI the impact of the dominant M1 lesion on somatosensory processing of passive tactile stimulation to the contralesional, right fingertips (thumb, index and middle fingers) as well. Such stimulation is more natural and more physiological because the afferents are now activated through their receptors and thus the most distal segments are involved.

Before the lesion, the passive tactile stimulation to all three fingertips resulted in a dipole field around the contralateral (to stimulation) sensorimotor cortex (**Figure 2**), with signal onset at about 22 ms and prominent positive peak at 33 ms (on grand average

waveforms) for the thumb and the index finger stimulation and with signal onset at about 25 ms and large positive peak at 37 ms (on grand average waveforms) for the middle finger stimulation (**Figure 3**). At the peak for all three fingertips, positive SSEPs were recorded from electrodes in the contralateral and central fronto-parietal electrodes, and negative SSEPs were obtained from bilateral temporo-occipital electrodes (**Figure 2**).

The lesion induced major changes in voltage topography at the scalp, especially after tactile stimulation applied to the thumb tip: by considering maps at the same latency, the strong pre-lesion central fronto-parietal positivity was now shifted on contralateral parieto-temporal electrodes, as exemplified at 33 ms after the stimulation (**Figure 2**). Post-lesion alterations in voltage topography were less prominent for index fingertip SSEPs, characterised by a shift of the pre-lesion central fronto-parietal positivity towards central and contralateral parieto-temporal electrodes. Conversely, no clear alteration of voltage topography was observed in middle fingertip SSEPs, except a post-lesion increase in amplitude of the positivity, as exemplified at 43 ms and 50 ms after the stimulation (**Figure 2**). Note however that a similar increase in amplitude of the positivity emerged after the lesion for the thumb tip and index fingertip SSEPs as well at 41 ms.

These post-lesion changes in voltage topography were visible throughout the signal as well (**Figure 3**): for thumb tip stimulation, the first component (a in **Figure 3**) largely decreased in amplitude (a' in **Figure 3**) after the lesion whereas the second component (b in **Figure 3**) largely increased in amplitude (b' in **Figure 3**) after the lesion. Moreover, the latency of both components was smaller after than before the lesion. Essentially, both early and late tactile sensory inputs were treated differently at the cortical level after the M1 lesion. The same post-lesion changes were observed for index fingertip stimulation as well, but less pronounced than for thumb tip stimulation, whereas any post-lesion effect on middle fingertip SSEPs was difficult to identify. Based on the signal latency and topography, we are confident that these potentials were of cortical origin. Namely, cortical components generated in areas 3b and 1 were observed already at 15 ms after a mechanical tactile stimulation by air-puff to the hand or forearm in awake macaque monkeys (Gardner et al., 1984).

The impacts of the dominant M1 lesion on voltage topographies and waveforms were obvious already with the naked eye, explaining our choice for a qualitative rather than

quantitative analysis with sophisticated statistics. In addition, we decided to pool all post-lesion data together into a grand average to represent the voltage topography at the scalp because we did not observe any strong evolution in topography throughout the post-lesion sessions. The same applies to pre-lesion data.

By considering the post-lesion potentials in greater detail, we observed that brain signals did evolve over time during the 4 post-lesion sessions in the form of the amplitude of the second component usually further increasing over time after the lesion (b' in **Figure 3**, from dark red to light orange) for thumb and index finger SSEPs. Simply put, this means that the alterations in cortical sensory processing induced by the lesion were further enhanced over time. While the post-lesion topographies never recovered towards the pre-lesion configuration (the waveforms conserved the same altered shape throughout the post-lesion period), there was a trend towards an increase in amplitude of cortical sensory signal during post-lesion recovery phase.

In sum, the dominant M1 lesion affected drastically tactile sensory processing primarily from the thumb and to a lesser extent from the index finger, in terms of voltage topography, amplitude and latency of SSEPs. Additionally, the post-lesion alterations in SSEP amplitude were further enhanced over time.

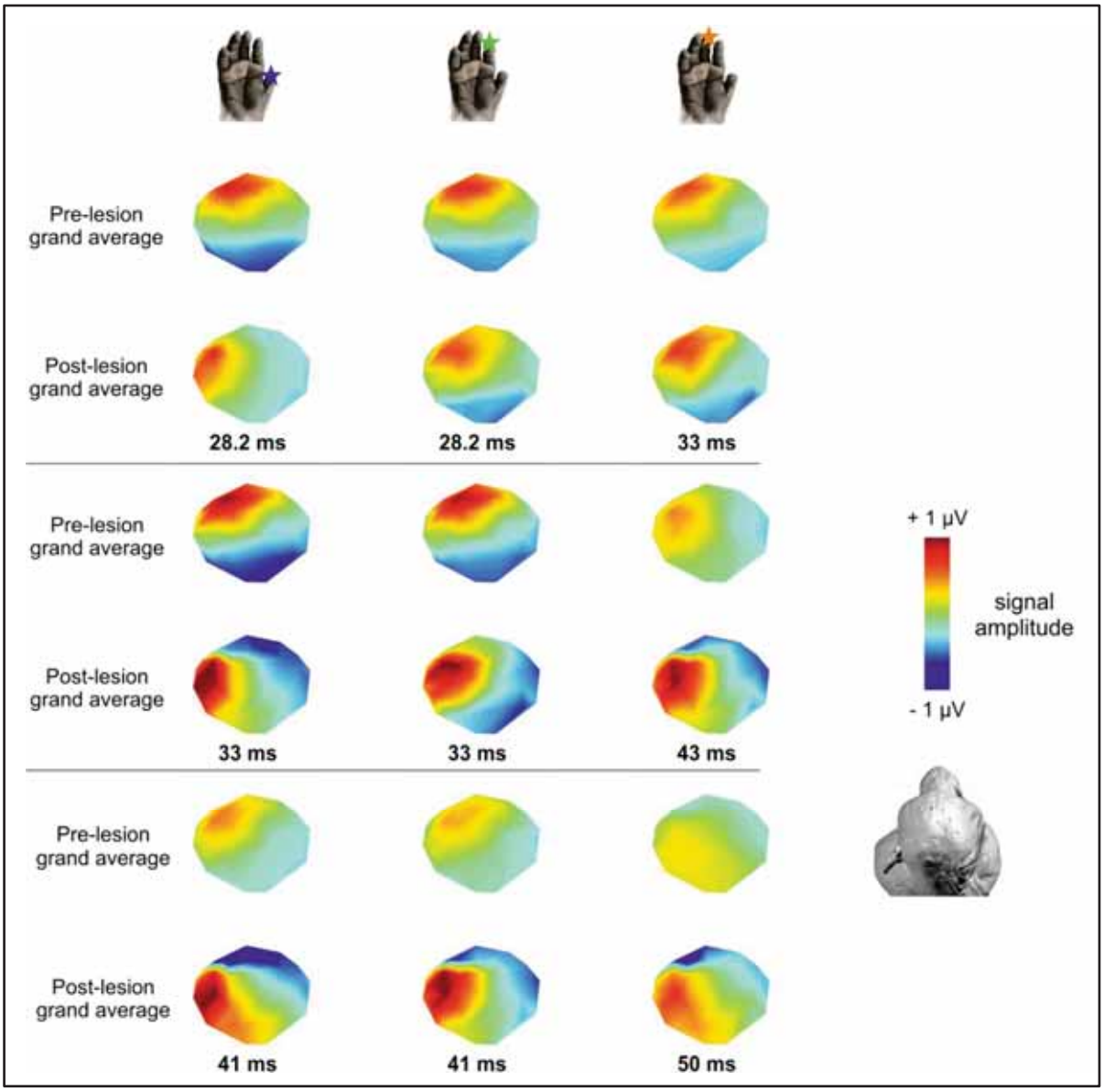

Figure 2 : Lesion-induced modifications in voltage topography of tactile SSEPs at the scalp. Colour-scaled voltage maps of pre-lesion and post-lesion SSEP grand averages, at three time points, for the three stimulated fingertips. The orientation of the maps is given on the right: frontal-up, left side-left. Thumb tip and index fingertip SSEPs had similar latency, shorter than middle fingertip SSEPs. Therefore, in order to present maps at corresponding parts of the signal for the three stimulation sites, maps for middle fingertip SSEPs are shown at a later latency than maps for the other two fingertip SSEPs.

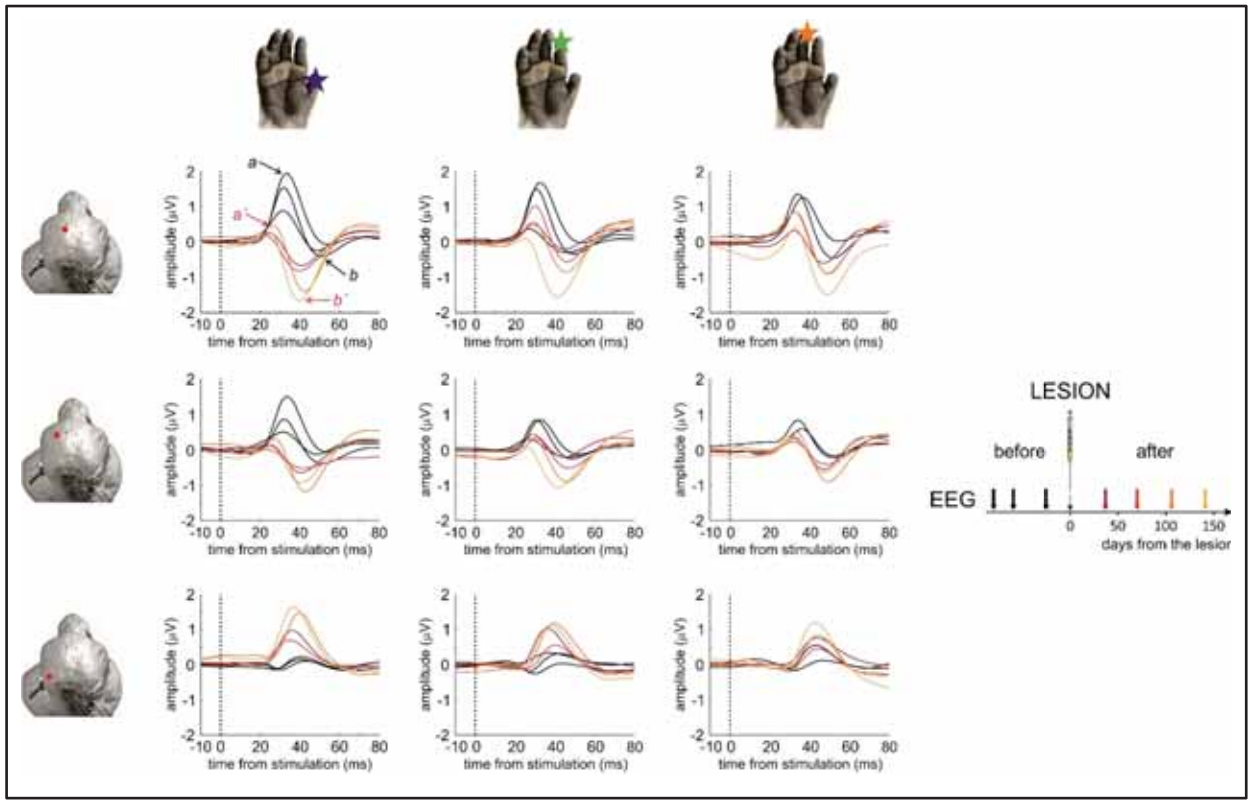

Figure 3 : Lesion-induced modifications in amplitude and latency of tactile SSEP signal. Individual pre-lesion and post-lesion SSEPs at three scalp electrodes of interest (red dot on the head representations on the left) over the ipsilesional hemisphere in response to right thumb tip, index fingertip and middle fingertip stimulation, respectively. The colour code of the signal is given on the right: pre-lesion sessions in black, post-lesion sessions in a gradient from dark red (earliest post-lesion session) to light orange (latest post-lesion session). Average reference.

Impact of the lesion on fine manual dexterity

In order to provide a more complete description of the lesion-induced alterations in sensorimotor processing, Mk-DI was tested for haptic touch as well, in addition to passive tactile stimulation processing.

Along with alteration in cortical processing of tactile inputs to the fingertips, the lesion induced several behavioural deficits of fine manual dexterity highlighted with the Brinkman box task: the most striking effect was a complete opposite **pattern of use of the thumb and index finger** after the lesion, in the sense that the thumb was much more affected by the lesion than the index finger. To elaborate, this was visible immediately after the lesion on the *% of first finger use* both in the task performed with visual

feedback and in the task performed without visual feedback (**Figure 4A** and **B**, **Table 1**). Before the lesion, first contacts with pellets were usually established as often with the thumb as with the index finger, in both conditions of the task. After the lesion, there was a huge decrease in the use of the thumb in favour of a proportional increase in index finger use. But even more surprisingly, this pattern of finger use evolved then differentially over post-lesion time according to the task: the use of both fingers recovered partially towards pre-lesion level in the Brinkman box task with vision (**Figure 4A**, **Table 1**) whereas the thumb use further deteriorated when the task was performed without vision, in favour of the index finger use (**Figure 4B**, **Table 1**). This behavioural readout reflects the active tactile component of the precision grip in the sense that it was required to first actively establish a tactile contact (Gibson, 1962) with a pellet in order to localise it before collecting it strictly speaking (Smith, 2009). Once a pellet contact was established, the lesion affected the ability to retrieve the pellet as well, as measured by the *% of effective contacts in 30 s* in both conditions of the task (**Figure 4C** and **D**, **Table 1**). This parameter corresponds now to the true ability to perform a precision grip, i.e. it reflects the fine manipulation ability of the hand, once a contact with a pellet has been established. Here again, the percentage of effective contacts was much more affected by the lesion for the thumb than for the index finger, in both conditions of the task. The post-lesion use of the index finger nearly reached the pre-lesion level in both conditions of the task. But whereas the animal then partially recovered the use of the thumb when visual feedback was provided, it was not able any more to perform effective contacts with the thumb in the blind condition of the task, at least in the first 30 s of the task (**Figure 4D**). In sum, we observed a non-uniform behavioural adaptation of the finger use over post-lesion time, the thumb use being more impaired than the index finger use.

The decreased ability to perform **fine finger movements** was confirmed by a significant increase in the *contact time* with horizontal and vertical pellets both in the Brinkman box task with vision (2.2-fold increase for vertical pellets and 1.8-fold increase for horizontal pellets after the lesion) and without vision (2.7-fold increase for vertical pellets and 3.4-fold increase for horizontal pellets after the lesion) (**Figure 4E** and **F**, **Table 1**). This was accompanied with a significant increase in the *precision grip shaping time* in both conditions of the task (**Figure 4G** and **H**, **Table 1**). Simply put, the animal needed significantly more time after the lesion to conform a precision grip once a first finger had already contacted a pellet. Here this lesion-induced increase appeared to be slightly

more pronounced in the task with vision (2.5-fold increase after the lesion) than without vision (2.1-fold increase after the lesion).

Then, the duration of **motor exploration by palpation** between the contact of 2 successive pellets, derived from the median *time interval* without vision – median *time interval* with vision, was severely increased after the lesion (pre-lesion: 0.62 s vs post-lesion: 2.64 s) (**Figure 4I** and **J**, **Table 1**). Another measurement of the motor exploration was provided by the median *precision grip shaping time* without vision - median *precision grip shaping time* with vision (**Figure 4G** and **H**, **Table 1**), and resulted in a higher post-lesion value as well (pre-lesion: 0.16 s vs post-lesion: 0.30 s).

In addition, **general movements** of the contralesional hand were slower after the lesion, as reflected by the significant increase in the *time interval* between 2 successive pellets in both conditions of the task (**Figure 4I** and **J**, **Table 1**). Note that this lesion effect was stronger in the task without (3.5-fold increase after the lesion) than with vision (2.8-fold increase after the lesion).

Moreover, the animal presented a strong impairment to perform **wrist deviations** (**Figure 4K** and **L**, **Table 1**). More specifically, we observed a post-lesion permanent deficit in performing ulnar deviation in favour of an increase in neutral position of the wrist in both conditions of the task, though much more prominent in the absence of vision. Note that the use of radial deviation was already absent in the pre-lesion period. The post-lesion consequence was therefore a stronger impairment to retrieve pellets from the more challenging horizontal wells compared to the vertical wells, reflected by the strong decrease in the number of horizontal pellets collected after the lesion (note the very few orange triangles in post-lesion period in **Figure 4E** and **F**). This large difference in the number of vertical vs horizontal pellets collected after the lesion may probably explain that we did not observe any statistical difference between horizontal *contact time* and vertical *contact time* in both tasks after the lesion although there was a visible trend towards larger *contact time* with horizontal pellets at least in the blind task (**Figure 4F**). For reminder, we observed a significantly longer *contact time* for horizontal pellets compared to vertical ones both before and after the lesion in the modified Brinkman board task (see **Chapter 2**).

To sum up, the dominant M1 lesion induced a large range of deficits in fine manual dexterity, characterised among others by a striking alteration in finger use when the behavioural task was performed without visual feedback. Taken as a whole, the post-lesion impairment was more prominent in the blind task than in the task with visual feedback.

Figure 4 (next page): Impact of the lesion on the fine manual dexterity of the contralesional hand assessed with the Brinkman box task performed with vision (left column) and without vision (right column). Time course of the % of first finger use in the task with vision (A) and without vision (B), the % of effective contacts with pellets in the first 30 s of the task with vision (C) and without vision (D), the contact time with pellets in the task with vision (E) and without vision (F), the precision grip shaping time in the task with vision (G) and without vision (H), the time interval between 2 pellets in the task with vision (I) and without vision (J), the % of 3 wrist orientations in the task with vision (K) and without vision (L). The colour codes are given on the right. The cortical lesion was performed at day 0 (x-axis). Pre- and post-lesion plateaux (see Table 1) are shown in a lighter colour than the corresponding data. When data were partly or completely missing, mostly after the lesion, a red star was indicated at the highest value for the corresponding time point.

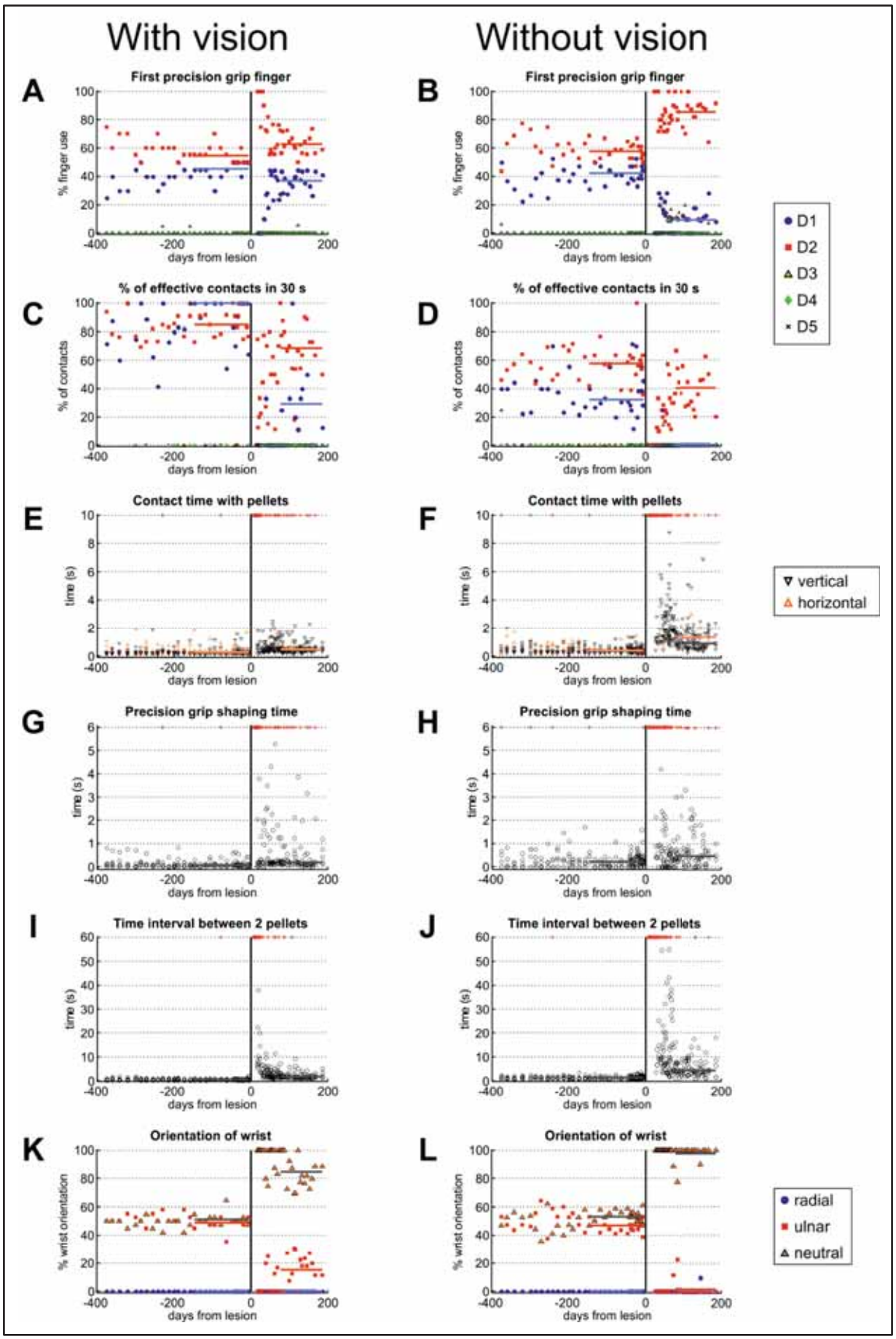
With vision
Without vision
A
First precision grip finger
% finger use
days from lesion
B
First precision grip finger
C
% of effective contacts in 30 s
% of contacts
D
% of effective contacts in 30 s
D1
D2
D3
D4
D5
E
Contact time with pellets
time (s)
F
Contact time with pellets
vertical
horizontal
G
Precision grip shaping time
H
Precision grip shaping time
I
Time interval between 2 pellets
J
Time interval between 2 pellets
K
Orientation of wrist
% wrist orientation
L
Orientation of wrist
radial
ulnar
neutral

Table 1 : Brinkman box task. Detail of values at the pre- and post-lesion plateaux for several readouts of the monkey's fine manual dexterity, in the task with vision (upper part) and without vision (lower part). Plateau values were expressed either as a median or a proportion of the given parameter among all observations. Pre- and post-lesion plateaux were compared for each parameter using either a Mann-Whitney test or a z-test for comparing proportions (SigmaPlot 12.5). We chose to perform Mann-Whitney tests even in some cases when a t-test was possible, in order to be fully consistent across the data. Pre-lesion plateaux were defined between day -147 and day -6 (lesion: day 0) and post-lesion plateaux were defined between day 76 and day 186.

With vision	pre-lesion	post-lesion	p-value, test
first finger use, thumb, proportion	0.453	0.368	p =0.04, z-test
first finger use, index finger, proportion	0.547	0.629	p =0.049, z-test
% of effective contacts, thumb, median	100	29.17	p ≤0.001, Mann-Whitney test
% of effective contacts, index finger, median	84.62	68.33	p =0.002, Mann-Whitney test
contact time, vertical wells, median	0.20 s	0.44 s	p ≤0.001, Mann-Whitney test
contact time, horizontal wells, median	0.28 s	0.50 s	p ≤0.001, Mann-Whitney test
precision grip shaping time, median	0.08 s	0.20 s	p ≤0.001, Mann-Whitney test
time interval, median	0.64 s	1.8 s	p ≤0.001, Mann-Whitney test
wrist orientation, neutral position, proportion	0.5137	0.8495	p ≤0.001, z-test
wrist orientation, radial deviation, proportion	0	0	
wrist orientation, ulnar deviation, proportion	0.4863	0.1505	p ≤0.001, z-test
Without vision			
first finger use, thumb, proportion	0.4221	0.0977	p ≤0.001, z-test
first finger use, index finger, proportion	0.5779	0.8563	p ≤0.001, z-test
% of effective contacts, thumb, median	32.29	0	p ≤0.001, Mann-Whitney test
% of effective contacts, index finger, median	57.74	40.4	p ≤0.001, Mann-Whitney test
contact time, vertical wells, median	0.36 s	0.96 s	p ≤0.001, Mann-Whitney test
contact time, horizontal wells, median	0.40 s	1.36 s	p ≤0.001, Mann-Whitney test
precision grip shaping time, median	0.24 s	0.50 s	p ≤0.001, Mann-Whitney test
time interval, median	1.26 s	4.44 s	p ≤0.001, Mann-Whitney test
wrist orientation, neutral position, proportion	0.5328	0.9773	p ≤0.001, z-test
wrist orientation, radial deviation, proportion	0	0.0076	p =0.611, z-test
wrist orientation, ulnar deviation, proportion	0.4672	0.0152	p ≤0.001, z-test

Discussion

Here, by using again scalp EEG recording of SSEPs in the same macaque monkey, we complemented results from the previous chapter (**Chapter 2**) by demonstrating that a dominant M1 lesion induced drastic alterations in tactile sensory processing from the fingertips, in addition to alteration in somatosensory processing from the median nerve. With this stimulation paradigm as well, several surprising results emerged: first, although the lesion was not restricted to the thumb representation in M1, the tactile sensory processing from the thumb was mostly affected, followed by processing from the index finger while no obvious post-lesion modification was observed in tactile processing from the middle finger. Second, equally interesting, a trend towards a continuous evolution of the cortical signal throughout the post-lesion recovery phase emerged. Finally, the post-lesion evolution of fine manual dexterity, assessed with the Brinkman box task, was striking as well, characterised among others by a differential alteration in finger use according to the conditions of the task. Taken together, our results confirm that M1 is important for tactile somatosensory processing from the fingers in primates.

Justifications for EEG investigations on a non-human primate model

By reading so far, one may wonder why a non-human primate model was actually required for this EEG study. Several reasons motivated the choice to perform our research on a macaque monkey model. First, as exposed briefly in the previous chapter (**Chapter 2**), non-human primates and Old World monkeys in particular are very close to human in terms of anatomy and physiology of the motor system, and of particular interest here regarding hand motor control (see e.g. Courtine et al., 2007 and Figure 7 in Chapter 8). Findings obtained on monkeys can then be transposed to human more easily than findings obtained on rodents, for instance.

Second, investigating on a non-human primate model offers the unique opportunity to collect already "pre-intervention" data, then to carry out experimental interventions in controlled conditions (here a cortical lesion), and then to obtain a regular and dense follow-up over the long-term during the post-intervention phase, both in terms of behavioural readouts and electrophysiological measurements (EEG in our case, particularly visible in **Chapter 2**), which is not possible to achieve in studies with human patients.

Here we intended in particular to investigate in detail the impact of a motor cortex lesion on somatosensory processing.

Third, non-human primate models constitute the exclusive occasion to perform lesions restricted to a very precise brain region, for instance here a lesion dominantly limited to M1, to investigate the deficits specifically associated with that brain region. Such very focal lesions restricted to a small brain area are very rare in human.

Fourth, equally important, detailed histological analyses of the brain tissue are mandatory at the end of the experiment in order to precisely document the lesion and thus to better interpret our results.

Fifth, by specifically considering the protocol of tactile stimulation to the fingertips, we were interested to deliver a purely passive tactile stimulation. Due to the low signal-to-noise ratio of such tactile SSEPs, this stimulation paradigm requires a high number of trials to be averaged (Krarup and Trojaborg, 1994; Starr et al., 1982; York, 1985) and recordings should be insulated from movements and muscular artifacts as much as possible in order to obtain a reliable signal at the scalp. These requirements could be suited with ease by performing EEG recordings on a monkey under anaesthesia.

Extent of the lesion

The much stronger post-lesion impairment observed both in tactile processing from the fingertip and in behaviour for the thumb as compared to the other fingers may have resulted from an incomplete lesion of the hand representation in M1 in the form of a permanent lesion affecting the fingers with a decreasing gradient from the most radial (i.e. the thumb) to the most ulnar (i.e. the middle finger here) finger. The absence of ICMS mapping of the lesioned area does not allow to directly rule out such a possibility. Nevertheless, there are several lines of evidence against such a hypothesis.

First, previous studies on monkeys (Kwan et al., 1978; Lemon, 1988; Rathelot and Strick, 2006; Schieber and Hibbard, 1993; Schieber and Poliakov, 1998) and then on human (Beisteiner et al., 2001; Indovina and Sanes, 2001; Schieber, 1999) demonstrated that finger movements were represented in a distributed and overlapping mosaic fashion in M1 rather than only in the simplified strip-like pattern originally proposed by Penfield

and contemporaries (Foerster, 1936; Penfield and Boldrey, 1937; Penfield and Jasper, 1954; Penfield and Rasmussen, 1950; Woolsey et al., 1979). This misleading interpretation was sometimes observed in studies using ICMS mapping as well and was due to the fact that only the muscular response appearing at the lowest stimulation intensity (threshold) was reported for a given stimulation site, occulting the other movements that would probably have been elicited at higher stimulation intensities at the same or at different depths in the cortex (Andersen et al., 1975; Foerster, 1936; Sessle and Wiesendanger, 1982). Actually, both organisation patterns are superimposed, meaning that there is a tendency for the more radial fingers to be represented more laterally and the more ulnar fingers to be represented more medially in M1 (Hwang et al., 2014; Schieber, 1999) but each finger movement is still represented at many locations in the whole hand representation (Kwan et al., 1978; Schieber, 2001; Schieber, 1999; Schieber and Poliakov, 1998). Consequently, the neuronal populations controlling a given finger movement topographically overlap with those involved in the motor control of other finger movements in order to create synergies between movements of different muscles and fingers, meaning that it is very difficult to precisely isolate the brain territory controlling a single finger. This makes a selective lesion of the thumb representation highly improbable. Nevertheless, due to the general gradient from thumb represented laterally to middle finger more medially in M1, one may still oppose that the lesion affected mostly the lateral part of the finger representation.

The arguments based on behavioural observations and histological analyses developed in the discussion of **Chapter 2** in favour of a lesion extending over the entire hand representation imply therefore that the lesion did not target the thumb representation selectively. For reminder, there were some transient motor impairments of the contralesional face and hindlimb immediately after the lesion, together with permanent partial motor deficits of the contralesional fingers and wrist throughout the post-lesion recovery phase, suggesting a large mediolateral extent of the lesion. Nevertheless, we are aware that the wrist representation is in part intermingled with the finger representation as well rather than being completely separated from it (Nudo and Milliken, 1996; Park et al., 2001; Park et al., 2004; Schieber, 1999).

To sum up, we are confident that the differential impairments of the finger use and tactile SSEPs observed here did not result from a lesion that would have damaged the

thumb representation much more than the representation of the other fingers but rather that the lesion damaged the entire finger representation in M1.

Impact of the dominant M1 lesion on hand sensorimotor control

The functional consequence of the lesion-induced sensory changes for motor behaviour is not clear. But, interestingly, the post-lesion changes in brain signals were associated in particular with behavioural adaptation of the finger use over time highlighted with the Brinkman box task. This test designed to assess the integrity of the hand sensorimotor control after an M1 lesion revealed that both motor and tactile components of the precision grip were affected in Mk-DI after the lesion. A more comprehensive discussion about the pertinence of this behavioural task will be presented in **Chapter 5**.

After the lesion, we observed a nearly complete recovery of both thumb and index finger motor behaviours by focusing on the first finger used to establish contact with a pellet in a precision grip in the Brinkman box task *with* visual feedback. On the other hand, when the task was performed *without* visual feedback, relying therefore mainly on tactile and proprioceptive inputs from the fingertips, an inverse pattern emerged: the use of the thumb decreased over time and never recovered, in favour of the use of the index finger which showed a proportionally more pronounced use after the lesion as compared to before. Such a non-uniform impairment of the finger use observed in the task without visual feedback is in accordance with our suggested model of sensorimotor impairment biased towards the thumb (see below the section *Post-lesion cortical reorganisation highlighted by tactile stimulation to the fingertips*). Equally interestingly, the distinct post-lesion evolution of the finger use according to the behavioural task condition suggests that the post-lesion alteration in tactile sensory processing and the further deterioration of cortical tactile processing over post-lesion time highlighted with SSEP recording was specifically related to behavioural deficits in the corresponding unisensory context (no vision + touch) but not in a multisensory condition (vision + touch). However, we are aware that tactile stimulation to the fingertips corresponds to passive touch whereas the motor exploration by palpation involved in our behavioural task corresponds to active touch. Our data support the idea that the post-lesion tactile cortical signals were not a substitute for the normal tactile signals given that the animal was unable to regain its pre-lesion sensorimotor behaviour in the blind behavioural task.

One may argue that picking very small objects with the thumb first, in the absence of visual feedback, is not an instinctive behaviour, explaining its absence after the lesion. Here, interestingly, the monkey relied often on its thumb to establish a precision grip before the lesion, even in the absence of visual feedback. This demonstrates that the animal performed the task very efficiently and proficiently before the lesion. As a consequence, one cannot impute the post-lesion deficits with the thumb to a not fully acquired behaviour but rather to a true sensorimotor deficit.

The neural control of fine fractionated finger movements, such as the precision grip in primates, depends to a large extent on the motor cortex and the CST (Lemon et al., 1991; Lemon, 1993; Lemon, 1997; Lemon, 2008). More specifically, many electrophysiological studies on primates demonstrated that performing the precision grip involves the activity of monosynaptic CM cells (Bennett and Lemon, 1996; Bortoff and Strick, 1993; Buys et al., 1986; Cheney and Fetz, 1985; Fetz and Cheney, 1980; Lawrence and Hopkins, 1976). In case of a lesion of the hand representation in M1 (Darling et al., 2014; Frost et al., 2003; Glees and Cole, 1950; Hoogewoud et al., 2013; Liu and Rouiller, 1999; Nudo and Milliken, 1996; Passingham et al., 1983; Pizzimenti et al., 2007; Rouiller et al., 1998b; Rouiller and Olivier, 2004; Wyss et al., 2013) or of the CST at cervical level (Freund et al., 2006; Freund et al., 2009; Galea and Darian-Smith, 1997; Hoogewoud et al., 2013; Lawrence and Kuypers, 1968; Nishimura et al., 2007; Schmidlin et al., 2004; Zaaimi et al., 2012), severe impairments of hand dexterity have been described in non-human primate models. In the same way, alteration in fine fractionated finger movements (Beebe and Lang, 2008; Han et al., 2006; Hwang et al., 2014; Kim, 2001; Kim et al., 2002; Kobayashi et al., 2004; Lang and Schieber, 2003; Lang and Schieber, 2004; Lang et al., 2009; Lee et al., 1998; Schieber, 1999; Schieber et al., 2009; Terao et al., 1993; Thielbar et al., 2014; Uribe Roca et al., 2002) with a reduction of muscle selectivity (Lang and Schieber, 2003; Lang and Schieber, 2004) were reported in human after an injury affecting the motor cortex or the CST.

While some studies mentioned that all fingers were similarly affected in motor behaviour after the lesion (Beebe and Lang, 2008; Darling et al., 2014; Schieber, 1999), other groups reported differential motor deficits across the fingers. For instance Murata et al. (2008) described a sequential recovery of the use of the fingers during the first weeks after a lesion of the M1 hand representation in three macaque monkeys, charac-

terised by the reappearance of index finger movements first, and subsequently thumb movements, suggesting a stronger impairment for the thumb than for the index finger. Similar stronger impairments for the thumb in particular were reported after section of the CST in spinal cord in macaque monkeys (Galea and Darian-Smith, 1997; Schmidlin et al., 2004).

Similarly, a report mentioned a human stroke patient with an impairment restricted to thumb sensorimotor control (Terao et al., 1993). Some other studies reported cases of human patients with motor impairment predominantly of the contralateral radial-sided fingers (from thumb to middle finger) (Hwang et al., 2014; Kim, 2001; Lang and Schieber, 2003; Lee et al., 1998; Schieber, 1999; Uribe Roca et al., 2002), and sometimes even in a decreasing degree of severity from the thumb (Hwang et al., 2014; Lee et al., 1998; Schieber, 1999; Uribe Roca et al., 2002), following small discrete strokes located either only in the posterior bank of the precentral gyrus or affecting the anterior bank of the postcentral gyrus as well (Uribe Roca et al., 2002). Conversely, some stroke patients presented motor impairment predominantly of radial-sided fingers other than the thumb (Hwang et al., 2014; Kim et al., 2002; Kobayashi et al., 2004) or selectively on the ulnar-sided fingers (from middle to little fingers) (Han et al., 2006; Kim, 2001; Schieber, 1999) after small cortical infarctions in the precentral gyrus. Some authors also reported that patients had sensory deficits in addition to motor impairments (Kim, 2001; Terao et al., 1993; Uribe Roca et al., 2002). But as Schieber (1999) mentioned, most of the stroke patients with an M1 lesion affecting differentially the fingers presented a larger deficit in thumb motor control compared to the other fingers, confirming that due to the larger thumb representation throughout M1 compared to the one of the other fingers, a lesion of the hand representation would affect the thumb more than the other fingers.

The finger independency in macaque monkeys is nearby but still lower than the human one (for detailed hypotheses about the origin of these differences, see Häger-Ross and Schieber, 2000; Schieber, 1991), meaning that we should not have expected such a large post-lesion discrepancy in thumb versus index finger use in our monkey compared with studies on human stroke patients. A previous study on human subjects with a pure motor hemiparesis resulting either from motor cortex or CST lesion, showed a differential effect of the lesion on the motor behaviour of the five fingers, in the form of an increas-

ing loss of independent finger movements from the thumb (not impaired) to the little finger (largely impaired), but without any mention of somatosensory deficit (Lang and Schieber, 2003). This distinct pattern of post-lesion finger impairment was explained first by the rehabilitative training therapies in humans usually designed to reinforce the independent use of the thumb and index finger as compared to the other fingers, and second by the naturally stronger independent motor control of the thumb as compared to the other fingers. At a first glance, our behavioural results may appear conflicting with this study. Nevertheless, a direct comparison is not suitable here because we cannot consider the behavioural tasks performed by our monkeys as an intensive rehabilitative training towards improving individual finger movements, as targeted in human rehabilitation. Indeed, although our monkeys are usually performing several manual dexterity tasks involving the precision grip 3-5 days a week, both before and after the lesion, these tasks are performed on a free-will basis, meaning that there is neither constraint of time nor predefine level to reach for the animals. The tasks are only based on the motivation to get additional food rewards, complementing the sufficient daily food already provided. Moreover, the variable nature of the lesions inducing the pure motor paresis observed in the human study makes a direct comparison with our results in monkey difficult because actually only one subject in Lang and Schieber's study (2003) had a lesion affecting selectively the precentral gyrus.

Post-lesion cortical reorganisation highlighted by tactile stimulation to the fingertips

Although the dominant M1 lesion most probably extended over the entire hand representation in M1 (see above the section *Extent of the lesion*), tactile sensory processing from the fingertips was not evenly impaired after the lesion. We observed rather a decreasing degree of severity of alterations in tactile processing from the thumb tip to the middle fingertip. To explain this finding, we base our argument on the cortico-peripheral loop model proposed earlier by Asanuma (Asanuma, 1973; Asanuma, 1981) and we hypothesise that the lesion may have damaged the pre-existing strong sensorimotor interactions which are normally biased towards the thumb sensorimotor control. In the control situation, we expect that the thumb has the strongest sensorimotor connectivity, followed by the index finger, itself followed by the middle finger (i.e. weakest sensorimotor

connectivity among the three fingers) given that macaque monkeys have a fully opposable thumb (Darian-Smith, 1984; Napier, 1961; Napier, 1962; Napier, 1993) (**Figure 5A**). To put it another way, the motor cortex of the hand may be primarily devoted to the thumb motor control that may be itself tightly linked to a very strong tactile sensory processing from the thumb. M1 is hypothesised to get sensory feedback directly through the thalamus or indirectly from S1 (see the section *Introduction* for greater detail).

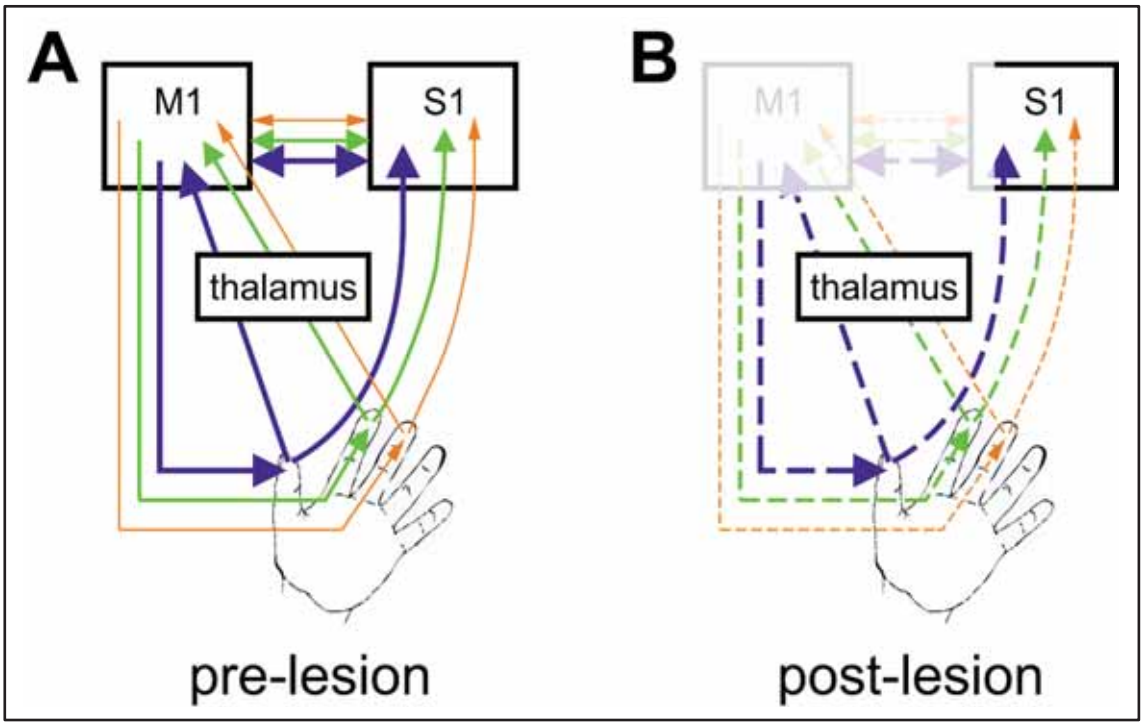

Figure 5 : Model based on a pre-existing differential sensorimotor connectivity of the fingers. (A) Control pre-lesion situation. (B) Post-lesion situation. The dominant M1 lesion (lighter area) damaged the hand representation in M1, most probably a small portion of the area 3a and the connections between M1 and S1 (see Chapter 2 for greater detail). The thickness of the arrows indicates the strength of the projections for the 3 fingers. Nevertheless, we cannot provide hard connectional data on the relative strength of sensory projections to M1 either from S1 or from the thalamus. See text for greater detail (inspired from Asanuma, 1981).

The assumption of the motor control in M1 hand representation primarily focused towards the thumb, followed by the index finger one and finally the middle finger one, is derived from previous mappings of M1 in macaque monkeys by cortical surface stimulation (Woolsey et al., 1952) or ICMS (Liu and Rouiller, 1999), confirming the large representation of the thumb as compared to the other fingers. ICMS investigations also re-

vealed the usually lower intensity threshold needed to elicit thumb movements compared to other finger movements (Sessle and Wiesendanger, 1982) and the production of isolated thumb movements but not isolated index finger nor isolated middle finger movements (Kwan et al., 1978). In addition, the activity in M1 neurons was shown to be much more correlated with thumb movements than with movements of the other fingers (Kirsch et al., 2014). Finally, the decreasing individuation index of the macaque fingers from thumb to middle finger through index finger on the one hand (Schieber, 1991), and post-spike facilitations primarily on thumb muscles when CM cells were observed to facilitate only a single intrinsic hand muscle (Buys et al., 1986; Lemon et al., 1991) on the other hand, also suggest a highly selective control of the thumb in particular. Of course this difference in the relative amount of the M1 representation of each finger is not incompatible with the distributed and overlapping mosaic finger representation described in M1 (see above the section *Extent of the lesion*).

Regarding the finger representation in S1, more receptive fields involving the thumb alone were recorded in S1 in macaque monkeys as compared to receptive fields of other individual fingers (Iwamura et al., 1980). The different areas of S1 were then investigated in greater detail and it was demonstrated that receptive fields for the thumb and the index finger in area 2 of macaque monkeys were smaller and rarely involved more than one finger, contrary to the other three fingers and a greater cortical magnification (i.e. the extent of cortical representation divided by that of the skin surface represented) was observed for the thumb and the index finger compared to the other three fingers (Pons et al., 1985). Similarly, a decreasing gradient of cortical magnification of the glabrous part of the fingers was observed in area 3b from the thumb (the largest) to the little finger (the smallest) and the cortical magnification of the thumb was shown to be also much larger than the one of the index and middle fingers in area 1 in squirrel monkeys and owl monkeys (Merzenich et al., 1987). In addition, electrophysiological mapping of areas 3a and 3b in macaque monkeys revealed larger thumb and index finger representations than the ones of the other fingers (Krubitzer et al., 2004). Finally, a larger thumb representation in somatosensory cortex as compared to the other fingers was reported in an optical imaging study on intrinsic signal in *M. fascicularis* after mild tactile stimulation to the fingertips (Shoham and Grinvald, 2001).

A lamellar somatotopy of the body representation in the thalamic nuclei VPLo (mostly afferent inputs from distal upper limb) and VL (mostly afferent inputs from proximal upper limb), the relays of peripheral inputs to M1, was described by Vitek et al. (1994) but the detail of the finger representation was not shown. Nevertheless, an organisation of VPLo similar to the arm representation in M1 was suggested by Strick (1976) and Matelli et al. (1989).

A mostly somatotopic organisation of afferent sensory inputs to M1 was demonstrated (Murphy et al., 1978; Rosén and Asanuma, 1972; Wong et al., 1978; Woolsey et al., 1942; Woolsey, 1958; Woolsey, 1964) in monkeys. In particular, Wannier et al. (1991) were able to record receptive fields in M1 in macaque monkeys after either cutaneous stimulation or passive finger movements and reported that the thumb had the largest number of M1 receptive fields, followed then by the index finger, itself followed by the middle finger. Moreover, M1 receptive fields devoted exclusively to a single finger were obtained both after cutaneous stimulation and joint manipulation of the thumb only whereas the other fingers were represented in pair in the other receptive fields (Wong et al., 1978).

Taken all these results together, we can then reasonably assume that the thumb normally has the strongest pre-existing sensorimotor connectivity (**Figure 5A**). Consequently, a dominant M1 lesion of the hand representation should have the largest impact on the sensorimotor processing from the thumb as compared to the one of the other fingers (**Figure 5B**). By recording SSEPs at the scalp, we were able to assess the integrity of somatosensory processing from the periphery to S1 through the dorsal column–medial lemniscal system (Allison et al., 1991a; Cruccu et al., 2008; Freye, 2005; Legatt, 2014; York, 1985) and we observed that the tactile processing from the fingertips was affected by the dominant M1 lesion. Conversely, we are not in a position to obtain here information about the direct sensory processing from the periphery to M1 through the thalamus. We assumed arbitrarily in our model that this processing was altered as well after the lesion (**Figure 5B**), on the basis of the subcortical alteration highlighted by using electrical stimulation in **Chapter 2**, but this is only a speculation. In sum, the aforementioned studies and our model emphasize that M1 is important for tactile somatosensory processing from the fingers in primates, in addition to motor control.

Interestingly we observed that the post-lesion alteration in tactile signals from the thumb tip and index fingertip was further enhanced over time, in the form of an increasing amplitude of the 2nd component studied throughout the post-lesion recovery period. In parallel a differential functional recovery appeared over time depending on the task. Hypotheses about cortical mechanisms underlying this recovery process have been already proposed in **Chapter 2**. We can now refine our explanations with the idea that the neural components involved in recovery, probably non-primary motor areas such as SMA or PMvr, do not allow for a better compensation of the thumb sensorimotor function compared to the other fingers. This may suggest that the relative differences in the extent of representation of the different fingers are probably not as prominent in non-primary motor areas as in M1. This makes sense if we consider both SMA-proper and PMvr areas and their role in further detail.

Regarding SMA, a somatotopic organisation was highlighted (Indovina and Sanes, 2001; Mitz and Wise, 1987; Woolsey et al., 1952) but the representation of the different body parts obtained by ICMS in SMA-proper (F3, Matelli et al., 1985) appeared less detailed and more intermingled than in M1 (Chen et al., 1991; Luppino et al., 1991; Macpherson et al., 1982; Maier et al., 2002; Mitz and Wise, 1987; Tanji, 1994) and higher stimulation thresholds were often required to elicit movements (Chen et al., 1991; Luppino et al., 1991; Macpherson et al., 1982; Maier et al., 2002; Rouiller et al., 1994; Rouiller et al., 1996; Woolsey et al., 1952). More specifically, the hand representation in F3 was clearly not as enlarged as in M1 and global finger movements rather than fluent and smooth individual finger movements were obtained by ICMS (Kalaska and Rizzolatti, 2013; Luppino et al., 1991; Rouiller et al., 1994; Rouiller et al., 1996; Rouiller et al., 1998a). Actually, SMA (both F3 and F6) was shown to be more often involved in controlling bilateral movements and quite demanding tasks than M1 and plays a crucial role in the organisation of movements, particularly in sequential performance of multiple movements (Brinkman and Porter, 1979; Kermadi et al., 1998; Tanji, 1994).

Contrary to SMA, PMvr (F5, Matelli et al., 1985) does contain a detailed hand representation (Cerri et al., 2003; Dum and Strick, 2005; Gentilucci et al., 1988; Gerbella et al., 2011; He et al., 1993; Kurata and Tanji, 1986; Lehmann and Scherberger, 2013; Rizzolatti et al., 1988; Shimazu et al., 2004). But similarly to SMA, the hand representation was smaller in PMvr than in M1 (Dancause et al., 2006), higher stimulation thresh-

olds were often required to elicit movements in PMvr during ICMS (Cerri et al., 2003; Gentilucci et al., 1988; Schmidlin et al., 2008; Umilta et al., 2007), ICMS responses were less robust than in M1 (Cerri et al., 2003; Gentilucci et al., 1988) and often elicited movements of several articulations including the mouth as well (Gentilucci et al., 1988). The role of F5 as well was shown to be more complex than the one of M1: F5 was demonstrated to be involved in goal-related (Rizzolatti et al., 1988) and visually-guided movements of the hand during fine manipulation of objects (Chouinard and Paus, 2006; Umilta et al., 2007), to code for object shapes (Murata et al., 1997), grasping movements (Bonini et al., 2010; Spinks et al., 2008; Umilta et al., 2007) and object orientation (Fluet et al., 2010; Schaffelhofer et al., 2015; Townsend et al., 2011), reach and gaze representation (Lehmann and Scherberger, 2013) and to exert a facilitatory effect on M1 output to upper limb motoneurons (Cerri et al., 2003; Schmidlin et al., 2008; Shimazu et al., 2004).

In sum, both SMA and PMvr contain a somatotopic representation of the body and of the hand in particular but neither as clear nor as robust as the one observed in M1, suggesting that both areas may probably not be able to exert a much stronger motor control on the thumb than on the other fingers, or at least may not be able to compensate for the larger thumb impairment as compared to the other fingers.

By comparing post-lesion signals to pre-lesion signals, one may claim that the post-lesion changes in amplitude we suggested here are questionable given the large variability already present in the pre-lesion data. We propose two arguments against that: first, the variability in the amplitude of the pre-lesion waveforms was not consistent with time, meaning that we did not observe any regular evolution (increase or decrease) in the amplitude of the signals during the pre-lesion recording sessions, but the amplitude changes were random across the sessions (**Figure 6**). Second, even though there was obviously some pre-lesion variability, the general shape of the pre-lesion waveforms was conserved and was in no way at all similar to any of the post-lesion waveforms, therefore strongly suggesting a true alteration in post-lesion potentials.

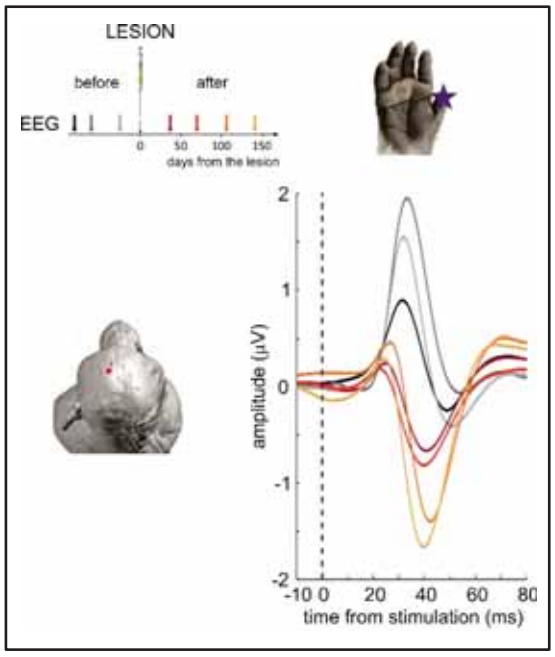

Figure 6 : Variability in the signal. Same individual pre-lesion and post-lesion potentials as shown in Figure 3 (first graph at the top-left) in response to right thumb tip stimulation. The pre-lesion potentials are displayed here in a gradient from dark gray (first pre-lesion session) to light gray (last pre-lesion session) and the post-lesion sessions in a gradient from dark red (earliest post-lesion session) to light orange (late post-lesion session). Same conventions as in Figure 3.

Moreover, another confounding factor may arise by interpreting post-lesion waveforms. At a first glance, one may pretend that the lesion induced a complete shift in polarity of the signals, especially if one compares the largest pre-lesion positive component with the largest post-lesion negative component. A more careful examination of the waveforms indicated instead that there was a non-uniform change in amplitude for both early and late components but still with the same polarity, in the form of a large reduction in the amplitude of the first component and a large increase in the amplitude of the second component, associated with a decrease in latency for both components after the lesion.

Arguments against volume-conduction artifacts

As already mentioned in **Chapter 2**, we acknowledge an important caveat in our study, namely the very close distance between the S1 generator of tactile potentials (Gardner et al., 1984) and the cortical lesion affecting most probably a small portion of area 3a as well. This means that the alteration in cortical signal measured at the scalp may result from modification in volume-conduction properties secondary induced by the lesion itself (van den Broek et al., 1998) in addition to a truly altered functioning of the brain.

There are nevertheless some observations allowing to reduce the likelihood that the post-lesion brain alteration is only due to lesion-induced distortions in volume-conduction within the brain.

First, both latencies and amplitudes of tactile SSEPs were substantially altered after the lesion. Volume-conduction artifacts secondary affect the conduction of brain signal that has been already generated, on its way from its generator to the scalp. Therefore, we can expect that volume-conduction alteration would have resulted in massive changes in amplitudes at the scalp due to inhomogeneous tissue for instance (van den Broek et al., 1998), but we cannot figure out how secondary alteration in volume-conduction induced by the lesion could result in an obvious shift in latency of brain activity at the scalp as we observed here.

Second, the dominant M1 lesion affected mainly the thumb tip-related brain activity, and to a lesser extent the index fingertip-related brain activity, but the middle fingertip signals remained largely unaffected. Given that these three signals were most probably generated by very close dipoles within the brain, volume-conduction effects would have affected them in a very similar manner but we did not observe such a scenario.

Third, the prominent stimulus specificity of the effects induced by the lesion further favours that we recorded real alterations in brain processing after the lesion. Namely, while we reported post-lesion modifications in voltage distribution at the scalp in tactile SSEPs, voltage topographies of median nerve SSEPs remained largely unaffected after the lesion (**Chapter 2**), suggesting that the cortex was dealing both kinds of peripheral stimulation very differently. We suppose that the large population of neurons involved in generating median nerve SSEPs produced a dipole whose activity was strong enough to mask volume-conduction effects resulting from the small damage in area 3a if there were some. Conversely tactile SSEPs were generated by a much less widespread subset of neurons (McLaughlin and Kelly, 1993; Pratt et al., 1979b; Starr et al., 1982) within the ones involved in the production of median nerve SSEPs, most probably in areas 3b, 1 and S2 (Gardner et al., 1984). It is therefore much less likely that the generator of tactile SSEPs has been damaged by the lesion, suggesting that is it not very likely that we observed here only purely conduction artifact rather than truly altered brain activity after the dominant M1 lesion.

Fourth, as already mentioned in **Chapter 2**, the dipole location and orientation relative to the lesion, and relative to the inner skull surface are crucial for the presence or absence of volume-conduction artifacts (van den Broek et al., 1998). Essentially, the closer the lesion is to the dipole, the larger volume-conduction artifacts are, especially if the

lesion is located in between the dipoles and the head surface. Here again, we do not expect that the lesion was in between the dipole and the head surface.

Taken together, these arguments suggest here again that the modulations in tactile processing observed after the lesion were not only due to volume-conduction effects resulting from the lesion but reflected true alterations in brain activity.

Electrical versus tactile stimulation

The stimulus specificity of the effects induced by the dominant M1 lesion on somatosensory processing probably results in part from the dual properties of electrical and tactile stimulations. Some of them are exposed here.

The activation of the median nerve by means of an electrical shock delivered to the overlying skin represents a very artificial stimulation because it is targeted directly on the nerve trunk and bypasses the terminal nerve fibres (Brown, 1984; Mauguière, 2011; Starr et al., 1982). Following the stimulation, the nerve impulses are generated nearly simultaneously (Larsson and Prevec, 1970), resulting in SSEPs that are time-locked to the stimulation onset, but the afferences are activated nonspecifically on the basis of their electrical threshold and their relative position to the cathode rather than by their functional type (Brown, 1984; Mauguière, 2011; Starr et al., 1982). The median nerve is a mixed nerve, containing both sensory and motor fibres. Nevertheless, the response volley to electrical stimulation is primarily conducted along the large myelinated and low-threshold sensory fibres because the sensory conduction velocity is about 8% faster than the motor conduction velocity (Dawson, 1956; Krarup and Trojaborg, 1994). Actually, an electrical stimulation of the median nerve at the wrist can antidromically activate many conducting motor fibres as well. But these activations do not propagate further along the ascending pathways of the spinal cord after synapses in the anterior horn, leading to a subsequent decrease in SSEP amplitude at the spinal level (Pratt et al., 1979b). An electrical stimulation delivered at normally bearable intensity recruits the large-diameter, fast-conducting myelinated sensory afferent fibres of group I (or Aα) mostly, and on occasion group II (or Aβ) as well at thumb twitch threshold, at least in human. These sensory fibres innervate cutaneous receptors, muscle spindles (primary and secondary endings), Golgi tendon organs and receptors in the joint capsules (Allison

et al., 1991a; Aminoff and Eisen, 1998; Desmedt, 1987; Legatt, 2014; Mauguière, 2011; Regan, 1989; Walsh et al., 2005; York, 1985). The visible motor response is due to the concomitant depolarisation of motor axons at the site of electrical stimulation (Allison et al., 1991a). In sum, an electrical stimulation prevents a natural activation of the somatosensory system by engaging afferent and efferent fibres in abnormal patterns (McLaughlin and Kelly, 1993).

Tactile stimulation is delivered by using a mechanical or air-puff device to tap the skin, the fingernails or the pads or to stretch muscles and provide cutaneous input. As opposed to an electrical stimulation to the skin overlying directly the nerve trunk, a tactile stimulation activates the afferents through their receptors and thus involves the most distal segments of the sensory nerve fibres as well, corresponding to a more physiological and more naturalistic stimulus for the somatosensory system (Caruso et al., 1994; McLaughlin and Kelly, 1993; Nakanishi et al., 1973; Pratt et al., 1979a; Pratt et al., 1979b; Starr et al., 1982). A tactile stimulation produces a very focal and selective activation of some mechanoreceptors (compared to a larger number of nerve fibres with electrical stimuli) (Caruso et al., 1994; Larsson and Prevec, 1970) and therefore elicits smaller peripheral (Hashimoto et al., 1989; Krarup and Trojaborg, 1994; McLaughlin and Kelly, 1993) and central (Pratt et al., 1979b; Starr et al., 1982) responses than an electrical stimulation does, and consequently requires a larger number of trials to be averaged to obtain a SSEP (York, 1985). While electrical stimulation results in synchronous nerve action potentials in a larger number of fibres, mechanical taps induces a repetitive firing in some uniform populations of mechanoreceptive fast-conducting afferent fibres (Larsson and Prevec, 1970; Pratt et al., 1979b). It is known from the literature that the waveforms of SSEPs elicited by mechanical and electrical stimulations are generally similar but the initial negative component present in electrical SSEPs is usually absent in tactile SSEPs (Larsson and Prevec, 1970; Manzano and Kohn, 2000). Our data with the initial brainstem component observed in electrical SSEPs but not in tactile SSEPs confirmed this last observation. Moreover, the latency of mechanical SSEPs is longer than with electrical stimulation (Brown, 1984; Larsson and Prevec, 1970; Nakanishi et al., 1973; Onofrj et al., 1990; York, 1985). This latency difference is due to the time interval between the stimulation onset and the actual excitation of the receptors, the additional conduction along thin distal fibre portions in case of tactile stimulation and a difference in conduction velocities of the fibre types recruited by an electrical stimulation com-

pared to a mechanical stimulation (Krarup and Trojaborg, 1994; Nakanishi et al., 1973; Pratt et al., 1979b; York, 1985). Moreover, voltage topographies at the scalp may differ between electrical and tactile SSEPs because a median nerve stimulation simultaneously engages afferent fibres from several fingers and different modalities, resulting in a spread of activation at the cortical level (McLaughlin and Kelly, 1993).

An additional hypothesis about the differences between electrical and mechanical SSEPs was proposed by Larsson and Prevec (1970): following peripheral stimulation to the first-order neuron, synchronous volleys induce repetitive discharges in the second-order neurons, and then in the third-order neurons, i.e. in the thalamocortical tract fibres. But there are then differences in the thalamocortical repetitive activity following either electrical or mechanical stimulation. An electrical stimulation generates bursts of thalamocortical activity with a comparatively higher degree of synchronicity between different thalamocortical fibres compared to a mechanical stimulation, meaning a high reproducibility of the signal. Conversely, a mechanical stimulation induces thalamocortical bursts which are well defined for each single neuronal fibre, but less synchronised and less reproducible in relation to each other. This may help to explain the absence of the initial negative peak in tactile SSEPs specifically and the longer latency of tactile SSEPs compared to electrical SSEPs.

Originality of our lesion study

Our EEG experiments on Mk-DI in the context of an M1 lesion are original for several points of view: first, in addition to the processing of electrical stimulus presented in **Chapter 2,** in order to document in detail plastic reorganisation of the sensorimotor system after dominant M1 lesion, we assessed here both active (behavioural task) and passive touch (EEG measurement of brain activity at the scalp) processing. We combined tests of both tactile perceptions because it is obvious that both processes largely differ (Gibson, 1962) and testing one cannot be a substitute of testing the other (Gibson, 1962; Heller, 1984; Heller et al., 1990). Moreover, SSEPs in response to tactile stimulation of the upper limb have only been rarely performed in non-human primates until now (see e.g. Gardner et al., 1984; Marshall et al., 1937; Woolsey et al., 1942). Conversely, SSEPs were rather usually obtained by electrical stimulation of a peripheral nerve (see e.g. McCarthy et al., 1991). To the best of our knowledge, there is no existing report about

whole-scalp EEG mapping of tactile SSEPs in non-human primates but previous tactile SSEP measurements were restricted to invasive electrocorticography or epidural recordings over a limited brain area (Gardner et al., 1984; Marshall et al., 1937; Woolsey et al., 1942) or whole-head MEG (Wilson et al., 2009).

Second, both here and even more prominent in the previous chapter (**Chapter 2**), we used a high density of EEG recordings over time both before and after the lesion to provide a detailed follow-up of the time course of cortical reorganisation. Conversely, most studies using EEG on non-human primates (Allison et al., 1991a; Allison et al., 1991b) or on patients with brain or spinal cord lesion for instance usually reported data acquisition at a single time point after the nervous system insult (Ferri et al., 2001; see e.g. Finnigan et al., 2004; Giblin, 1964; Green et al., 1999a; Green et al., 1999b; Han et al., 2013; Jabbari et al., 1987; Lee et al., 2010; Riquelme et al., 2014; Slimp et al., 1986; Sonoo et al., 1991; Stohr et al., 1983; Tsuji et al., 1988; Tzvetanov et al., 2005; Tzvetanov and Rousseff, 2005; Watanabe et al., 1989; Wong et al., 1982; Zeman and Yiannikas, 1989).

Third, by considering again the results exposed in the previous chapter as well, we combined two different types of peripheral stimulations for the somatosensory modality, namely either direct stimulation of sensory nerve trunk with an electrical stimulator or stimulation of the corresponding mechanoreceptors with tactile stimulators. In this way, we were able to obtain complementary information about the effects of a dominant M1 lesion on somatosensory processing at different levels of the somatosensory pathway.

Finally, we presented in this chapter a detailed description of sensorimotor impairment of the fingers by using the Brinkman box task. We showed in particular that the lesion induced differential deficits between the thumb and the index finger. Whereas differential weakness in the fingers are known and well described in human stroke patients, only few studies mentioned such a similar phenomenon in non-human primates (Galea and Darian-Smith, 1997; Murata et al., 2008; Schmidlin et al., 2004). Actually, *manual dexterity*, *agility* or *skill* have been usually described globally without distinction of impairment between the fingers after a lesion affecting the motor system in most studies so far (Freund et al., 2006; Freund et al., 2009; Frost et al., 2003; Hoogewoud et al., 2013; Lawrence and Kuypers, 1968; Liu and Rouiller, 1999; Nishimura et al., 2007; Nudo and

Milliken, 1996; Passingham et al., 1983; Pizzimenti et al., 2007; Rouiller et al., 1998b; Rouiller and Olivier, 2004; Wyss et al., 2013; Zaaimi et al., 2012).

Prospects

The case report presented here in combination with **Chapter 2** confirmed that SSEP recording is a relevant technique for assessing the integrity of the somatosensory pathway to the cortical sensory areas. We demonstrated in one monkey the potential of our EEG technique and we hope that similar experiments will be carried out on additional animals to confirm our preliminary findings. In particular we propose to refine future investigations by testing additional stimulation paradigms, for instance by changing the stimulus length, stimulus amplitude or repetition rate (Huttunen and Hömberg, 1991; Popescu et al., 2010; Pratt et al., 1980) to verify the consistency of the results. It would be also relevant to include some tests of tactile perception to better document touch processing. Then with these additional data it would be possible to investigate at the population level whether there is a link between abnormality in brain potential after the lesion and the extent of the cortical lesion, sensory deficits or functional recovery of manual dexterity, as it was already demonstrated in human (Jabbari et al., 1987; Watanabe et al., 1989).

Another improvement would be to apply tactile stimulation to the non-affected limb as well given that it is known that the intact hemisphere may be involved in functional recovery, especially in case of an extended brain lesion in human (Liepert et al., 2000; Netz et al., 1997; Serrien et al., 2004; Shimizu et al., 2002). In addition, Watanabe showed that the amplitude ratio of ipsilesional SSEP component to contralesional SSEP component after median nerve stimulation was significantly correlated with sensory disturbance in a large population of stroke patients (Watanabe et al., 1989). Finally, we will demonstrate in **Chapter 5** that fine manual dexterity of the non-affected limb is slightly modified as well after a focal cortical lesion of the hand representation in M1 in our macaque monkeys, confirming that it is of definite relevance to extend investigation to the intact hemisphere as well.

We demonstrated that the lesion-induced changes in motor output and sensorimotor connectivity were sufficient to reorganise the somatosensory system, meaning that a le-

sion in the motor system induces extensive plasticity in the somatosensory system as well that may be involved in functional recovery (Schaechter et al., 2012). Therefore these results may be relevant for the clinics, where neurorehabilitation strategies for stroke patients for instance should target more intensively the somatosensory system as well in parallel with the recovery of motor functions themselves (Byl et al., 2003; Laible et al., 2012; Sawaki et al., 2006).

Conclusion

In sum, the present data show that the dominant M1 lesion interfered with tactile input processing from the fingertips in the cerebral cortex, suggesting that normal tactile sensory processing is modulated by motor cortical activity. The alterations in sensory processing documented here may partially explain the motor deficits observed after the lesion.

By way of conclusion of this chapter and the previous one, we presented complementary insights into the mechanisms of sensorimotor reorganisation underlying functional recovery after a cortical lesion in non-human primates. We used the technique of scalp EEG to address the impact of a dominant M1 lesion on somatosensory processing from the distal forelimb in one adult macaque monkey and we observed distinct effects of the lesion on the somatosensory processing from the hand by applying either direct electrical stimulation to a sensory nerve or tactile stimulation to the corresponding mechanoreceptors.

Our results may be relevant for clinical neurophysiologists by combining different methods to quantify the sensorimotor function in patients (Pratt et al., 1979a; Pratt et al., 1979b). Both peripheral stimulation paradigms used in our study were shown to have particular advantages and revealed different facets of plastic reorganisation in the sensorimotor system. Electrical stimulation is user-friendly and results in relatively large-amplitude components. Nevertheless, it may be painful and there is no specificity in the type of fibres activated. Conversely, mechanical stimulation to the fingertips is absolutely not painful, it involves the entire afferent pathways, it elicits information processing in a specific group of receptors and their nerve pathways, but signal is smaller. In sum, both methods could be combined in patients with problems of sensorimotor

processing that characterise neurologic disorders, in order to unravel the localisation and the mechanisms of the neurological impairment.

These data confirm that the somatosensory cortical representations are plastic in adult macaque monkeys in the sense that sustained changes in motor output and sensorimotor connectivity induced by a lesion were sufficient to deeply reorganise the somatosensory processing, in addition to the control of fine manual dexterity. In other words, by using EEG, we were able to demonstrate here lesion-induced plasticity in the somatosensory pathway.

Last but not least, our results further demonstrate that the motor cortex is definitely not a purely motor structure (Asanuma, 1981; Asanuma and Rosén, 1972; Jones, 1986; Rosén and Asanuma, 1972). On the contrary, M1 is also important for somatosensory processing from the forelimb in primates.

Acknowledgements

We thank Laurent Bossy, Jacques Maillard (animal care taking), Christiane Marti, Christine Roulin (histology), André Gaillard (mechanics), Bernard Aebischer, Andrea Francovich (electronics) and Laurent Monney (informatics). This work was supported by the Swiss National Science Foundation grants 31-61857.00, 310000-110005, 31003A-132465 (EMR), the National Centre of Competence in Research (NCCR) on "Neural plasticity and repair", Novartis Foundation, The Christopher Reeves Foundation (Springfield, NJ, USA), the SPCCR (Swiss Primate Competence Center for Research: http://www.unifr.ch/spccr/) and Society in Science - the BrancoWeiss Fellowship (AG).

References

Adrian, E.D., 1941. Afferent discharges to the cerebral cortex from peripheral sense organs. J Physiol 100, 159-191.

Adrian, E.D., Moruzzi, G., 1939. Impulses in the pyramidal tract. J.Physiol 97, 153-199.

Allison, T., McCarthy, G., Wood, C.C., Darcey, T.M., Spencer, D.D., Williamson, P.D., 1989a. Human cortical potentials evoked by stimulation of the median nerve. I. Cytoarchitectonic areas generating short-latency activity. J Neurophysiol 62, 694-710.

Allison, T., McCarthy, G., Wood, C.C., Jones, S.J., 1991a. Potentials evoked in human and monkey cerebral cortex by stimulation of the median nerve. A review of scalp and intracranial recordings. Brain 114 (Pt 6), 2465-2503.

Allison, T., McCarthy, G., Wood, C.C., Williamson, P.D., Spencer, D.D., 1989b. Human cortical potentials evoked by stimulation of the median nerve. II. Cytoarchitectonic areas generating long-latency activity. J Neurophysiol 62, 711-722.

Allison, T., Wood, C.C., McCarthy, G., Spencer, D.D., 1991b. Cortical somatosensory evoked potentials. II. Effects of excision of somatosensory or motor cortex in humans and monkeys. J Neurophysiol 66, 64-82.

Allison, T., McCarthy, G., Luby, M., Puce, A., Spencer, D.D., 1996. Localization of functional regions of human mesial cortex by somatosensory evoked potential recording and by cortical stimulation. Electroencephalography and Clinical Neurophysiology/Evoked Potentials Section 100, 126-140.

Aminoff, M.J., Eisen, A.A., 1998. AAEM minimonograph 19: somatosensory evoked potentials. Muscle Nerve 21, 277-290.

Andersen, P., Hagan, P.J., Phillips, C.G., Powell, T.P., 1975. Mapping by microstimulation of overlapping projections from area 4 to motor units of the baboon's hand. Proc.R.Soc.Lond B Biol.Sci. 188, 31-36.

Arezzo, J.C., Legatt, A.D., Vaughan, H.G.Jr., 1979. Topography and intracranial sources of somatosensory evoked potentials in the monkey. I. Early components. Electroencephalogr.Clin.Neurophysiol 46, 155-172.

Arezzo, J.C., Vaughan, H.G.Jr., Legatt, A.D., 1981. Topography and intracranial sources of somatosensory evoked potentials in the monkey. II. Cortical components. Electroencephalogr.Clin.Neurophysiol 51, 1-18.

Asanuma, H., 1959. Microelectrode studies on the evoked activity of a single pyramidal tract cell in the somato-sensory area in cats. Jpn.J Physiol 9, 94-105.

Asanuma, H., 1973. Cerebral cortical control of movement. Physiologist 16, 143-166.

Asanuma, H., 1975. Recent developments in the study of the columnar arrangement of neurons within the motor cortex. Physiol Rev 55, 143-156.

Asanuma, H., 1981. Functional role of sensory inputs to the motor cortex. Prog.Neurobiol. 16, 241-262.

Asanuma, H., Arissian, K., 1984. Experiments on functional role of peripheral input to motor cortex during voluntary movements in the monkey. J.Neurophysiol. 52, 212-227.

Asanuma, H., Larsen, K., Yumiya, H., 1980. Peripheral input pathways to the monkey motor cortex. Exp Brain Res 38, 349-355.

Asanuma, H., Larsen, K.D., Yumiya, H., 1979a. Receptive fields of thalamic neurons projecting to the motor cortex in the cat. Brain Research 172, 217-228.

Asanuma, H., Larsen, K.D., Zarzecki, P., 1979b. Peripheral input pathways projecting to the motor cortex in the cat. Brain Research 172, 197-208.

Asanuma, H., Rosén, I., 1972. Functional role of afferent inputs to the monkey motor cortex. Brain Res 40, 3-5.

Asanuma, H., Sakata, H., 1967. Functional Organization of a Cortical Efferent System Examined with Focal Depth Stimulation in Cats. Journal of Neurophysiology 30, 35-54.

Asanuma, H., Stoney, S.D.Jr., Abzug, C., 1968. Relationship between afferent input and motor outflow in cat motorsensory cortex. J.Neurophysiol. 31, 670-681.

Asanuma, H., Larsen, K.D., Yumiya, H., 1979c. Direct sensory pathways to the motor cortex in the monkey: a basis of cortical reflexes. In: Asanuma, H., Wilson, V.J. (Eds.), Integration in the nervous system. Igaku-shoin Tokyo, pp. 223-238.

Beebe, J.A., Lang, C.E., 2008. Absence of a proximal to distal gradient of motor deficits in the upper extremity early after stroke. Clinical Neurophysiology 119, 2074-2085.

Beisteiner, R., Windischberger, C., Lanzenberger, R., Edward, V., Cunnington, R., Erdler, M., Gartus, A., Streibl, B., Moser, E., Deecke, L., 2001. Finger somatotopy in human motor cortex. Neuroimage 13, 1016-1026.

Bennett, K.M., Lemon, R.N., 1996. Corticomotoneuronal contribution to the fractionation of muscle activity during precision grip in the monkey. J.Neurophysiol. 75, 1826-1842.

Bernard, C., 1858. Leçons sur la physiologie et la pathologie du système nerveux: cours de Médecine du Collège de France, 2nd ed. J.-B. Baillière et fils.

Bonini, L., Rozzi, S., Serventi, F.U., Simone, L., Ferrari, P.F., Fogassi, L., 2010. Ventral premotor and inferior parietal cortices make distinct contribution to action organization and intention understanding. Cereb.Cortex 20, 1372-1385.

Bortoff, G.A., Strick, P.L., 1993. Corticospinal terminations in two new-world primates: further evidence that corticomotoneuronal connections provide part of the neural substrate for manual dexterity. J Neurosci 13, 5105-5118.

Breitwieser, C., Kaiser, V., Neuper, C., Muller-Putz, G.R., 2012. Stability and distribution of steady-state somatosensory evoked potentials elicited by vibro-tactile stimulation. Med.Biol.Eng Comput 50, 347-357.

Breitwieser, C., Pokorny, C., Neuper, C., Muller-Putz, G.R., 2011. Somatosensory evoked potentials elicited by stimulating two fingers from one hand - Usable for BCI? Conf.Proc.IEEE Eng Med.Biol.Soc. 2011, 6373-6376.

Brinkman, C., Porter, R., 1979. Supplementary motor area in the monkey: activity of neurons during performance of a learned motor task. Journal of Neurophysiology 42, 681-709.

Brinkman, J., Bush, B.M., Porter, R., 1978. Deficient influence of peripheral stimuli on precentral neurones in monkeys with dorsal column lesions. The Journal of physiology 276, 27-48.

Brinkman, J., Colebatch, J.G., Porter, R., York, D.H., 1985. Responses of precentral cells during cooling of post-central cortex in conscious monkeys. J Physiol 368, 611-625.

Brooks, V.B., Rudomin, P., Slayman, C.L., 1961. Peripheral receptive fields of neurons in the cat's cerebral cortex. Journal of Neurophysiology 24, 302-325.

Brown, W.F., 1984. Evoked potentials. In: Brown, W.F. (Ed.), The Physiological and Technical Basis of Electromyography. Butterworth-Heinemann, pp. 169-221.

Budd, T.W., Timora, J.R., 2013. Steady state responses to temporally congruent and incongruent auditory and vibrotactile amplitude modulated stimulation. Int J Psychophysiol. 89, 419-432.

Buser, P., Imbert, M., 1961. Sensory projections to the motor cortex in cats: a microelectrode study., Sensory communication. MIT Press, pp. 607-626.

Buys, E.J., Lemon, R.N., Mantel, G.W., Muir, R.B., 1986. Selective facilitation of different hand muscles by single corticospinal neurones in the conscious monkey. J Physiol 381, 529-549.

Byl, N., Roderick, J., Mohamed, O., Hanny, M., Kotler, J., Smith, A., Tang, M., Abrams, G., 2003. Effectiveness of sensory and motor rehabilitation of the upper limb following the principles of neuroplasticity: patients stable poststroke. Neurorehabil Neural Repair 17, 176-191.

Caruso, G., Nolano, M., Lullo, F., Crisci, C., Nilsson, J.B., Massini, R., 1994. Median nerve sensory responses evoked by tactile stimulation of the finger proximal and distal phalanx in normal subjects. Muscle & Nerve 17, 269-275.

Cerri, G., Shimazu, H., Maier, M.A., Lemon, R.N., 2003. Facilitation From Ventral Premotor Cortex of Primary Motor Cortex Outputs to Macaque Hand Muscles. Journal of Neurophysiology 90, 832-842.

Chapman, C.E., Tremblay, F., Ageranioti-Bélanger, S.A., 1996. Role of Primary Somatosensory Cortex in Active and Passive Touch. In: Flanagan, A.M.W. (Ed.), Hand and Brain. Academic Press, San Diego, pp. 329-347.

Chen, D.F., Hyland, B., Maier, V., Palmeri, A., Wiesendanger, M., 1991. Comparison of Neural Activity in the Supplementary Motor Area and in the Primary Motor Cortex in Monkeys. Somatosensory & Motor Research 8, 27-44.

Cheney, P.D., Fetz, E.E., 1985. Comparable patterns of muscle facilitation evoked by individual corticomotoneuronal (CM) cells and by single intracortical microstimuli in primates: evidence for functional groups of CM cells. J Neurophysiol 53, 786-804.

Chouinard, P.A., Paus, T., 2006. The primary motor and premotor areas of the human cerebral cortex. neuroscientist 12, 143-152.

Cole, J., Glees, P., 1954. Effects of small lesions in sensory cortex in trained monkeys. J Neurophysiol. 17, 1-13.

Colebatch, J.G., Sayer, R.J., Porter, R., White, O.B., 1990. Responses of monkey precentral neurones to passive movements and phasic muscle stretch: relevance to man. Electroencephalography and Clinical Neurophysiology 75, 44-55.

Colon, E., Legrain, V., Mouraux, A., 2012. Steady-state evoked potentials to study the processing of tactile and nociceptive somatosensory input in the human brain. Neurophysiol.Clin. 42, 315-323.

Courtine, G., Bunge, M.B., Fawcett, J.W., Grossman, R.G., Kaas, J.H., Lemon, R.N., Maier, I., Martin, J., Nudo, R.J., Ramon-Cueto, A., Rouiller, E.M., Schnell, L., Wannier, T., Schwab, M.E., Edgerton, V.R., 2007. Can experiments in nonhuman primates expedite the translation of treatments for spinal cord injury in humans? Nat.Med. 13, 561-566.

Cruccu, G., Aminoff, M.J., Curio, G., Guerit, J.M., Kakigi, R., Mauguière, F., Rossini, P.M., Treede, R.D., Garcia-Larrea, L., 2008. Recommendations for the clinical use of somatosensory-evoked potentials. Clin.Neurophysiol 119, 1705-1719.

Dancause, N., Barbay, S., Frost, S.B., Plautz, E.J., Popescu, M., Dixon, P.M., Stowe, A.M., Friel, K.M., Nudo, R.J., 2006. Topographically divergent and convergent connectivity between premotor and primary motor cortex. Cereb.Cortex 16, 1057-1068.

Darian-Smith, C., Ciferri, M.M., 2005. Loss and recovery of voluntary hand movements in the macaque following a cervical dorsal rhizotomy. J.Comp Neurol. 491, 27-45.

Darian-Smith, C., 2007. Monkey Models of Recovery of Voluntary Hand Movement After Spinal Cord and Dorsal Root Injury. ILAR Journal 48, 396-410.

Darian-Smith, C., Darian-Smith, I., 1993. Thalamic projections to areas 3a, 3b, and 4 in the sensorimotor cortex of the mature and infant macaque monkey. The Journal of Comparative Neurology 335, 173-199.

Darian-Smith, I., 1984. The Sense of Touch: Performance and Peripheral Neural Processes. In: Brookhart, J.M., Mountcastle, V.B. (Eds.), Handbook of Physiology, The Nervous System, Sensory Processes. John Wiley & Sons, Inc., pp. 739-788.

Darian-Smith, I., Galea, M.P., Darian-Smith, C., Sugitani, M., Tan, A., Burman, K., 1996a. Introduction., The Anatomy of Manual Dexterity, Advances in Anatomy Embryology and Cell Biology, Volume 133. Springer Berlin Heidelberg, pp. 1-16.

Darian-Smith, I., Galea, M.P., Darian-Smith, C., Sugitani, M., Tan, A., Burman, K., 1996b. The Primate Sensorimotor Thalamus., The Anatomy of Manual Dexterity, Advances in Anatomy Embryology and Cell Biology, Volume 133. Springer Berlin Heidelberg, pp. 64-105.

Darling, W.G., Morecraft, R.J., Rotella, D.L., Pizzimenti, M.A., Ge, J., Stilwell-Morecraft, K.S., Zhang, H., Soliman, H., Seecharan, D., Edwards, I., McNeal, D., Nudo, R.J., Cheney, P., 2014. Recovery of precision grasping after motor cortex lesion does not require forced use of the impaired hand in *Macaca mulatta*. Exp Brain Res.

Dawson, G.D., 1956. The relative excitability and conduction velocity of sensory and motor nerve fibres in man. J.Physiol 131, 436-451.

Delorme, A., Makeig, S., 2004. EEGLAB: an open source toolbox for analysis of single-trial EEG dynamics including independent component analysis. J Neurosci Methods 134, 9-21.

Desmedt, J.E., 1987. [Physiology and physiopathology of somatic sensations studied in man by the method of evoked potentials]. J Physiol (Paris) 82, 64-136.

Desmedt, J.E., Cheron, G., 1980a. Central somatosensory conduction in man: neural generators and interpeak latencies of the far-field components recorded from neck and right or left scalp and earlobes. Electroencephalogr.Clin.Neurophysiol 50, 382-403.

Desmedt, J.E., Cheron, G., 1980b. Somatosensory evoked potentials to finger stimulation in healthy octogenarians and in young adults: wave forms, scalp topography and transit times of parietal and frontal components. Electroencephalogr.Clin.Neurophysiol 50, 404-425.

Desmedt, J.E., Cheron, G., 1981. Non-cephalic reference recording of early somatosensory potentials to finger stimulation in adult or aging normal man: differentiation of widespread N18 and contralateral N20 from the prerolandic P22 and N30 components. Electroencephalogr.Clin.Neurophysiol 52, 553-570.

Desmedt, J.E., Cheron, G., 1982. Somatosensory evoked potentials in man: subcortical and cortical components and their neural basis. Ann.N.Y.Acad.Sci. 388, 388-411.

Desmedt, J.E., Nguyen, T.H., 1984. Bit-mapped colour imaging of the potential fields of propagated and segmental subcortical components of somatosensory evoked potentials in man. Electroencephalogr.Clin.Neurophysiol 58, 481-497.

Dum, R.P., Strick, P.L., 2005. Frontal lobe inputs to the digit representations of the motor areas on the lateral surface of the hemisphere. J Neurosci. 25, 1375-1386.

Fay, M.P., Proschan, M.A., 2010. Wilcoxon-Mann-Whitney or t-test? On assumptions for hypothesis tests and multiple interpretations of decision rules. Statistics surveys 4, 1.

Ferri, R., Elia, M., Musumeci, S.A., Cosentino, F.I., Roccasalva, G., Spada, R.S., Toscano, G., 2001. Somatosensory evoked potentials in patients affected by unilateral cerebrovascular lesions with onset during the perinatal period or adulthood. J Child Neurol. 16, 541-547.

Fetz, E.E., Cheney, P.D., 1980. Postspike facilitation of forelimb muscle activity by primate corticomotoneuronal cells. Journal of Neurophysiology 44, 751-772.

Finnigan, S.P., Rose, S.E., Walsh, M., Griffin, M., Janke, A.L., McMahon, K.L., Gillies, R., Strudwick, M.W., Pettigrew, C.M., Semple, J., Brown, J., Brown, P., Chalk, J.B., 2004. Correlation of quantitative EEG in acute ischemic stroke with 30-day NIHSS score: comparison with diffusion and perfusion MRI. Stroke 35, 899-903.

Fluet, M.C., Baumann, M.A., Scherberger, H., 2010. Context-Specific Grasp Movement Representation in Macaque Ventral Premotor Cortex. The Journal of Neuroscience 30, 15175-15184.

Foerster, O., 1936. The motor cortex in man in the light of Hughlings Jackson's doctrines. Brain 59, 135-159.

Francois-Franck, C.E., 1887. Leçons sur les fonctions motrices du cerveau. Paris, Doin.

Franzén, O., Offenloch, K., 1969. Evoked response correlates of psychophysical magnitude estimates for tactile stimulation in man. Exp Brain Res 8, 1-18.

Freund, P., Schmidlin, E., Wannier, T., Bloch, J., Mir, A., Schwab, M.E., Rouiller, E.M., 2006. Nogo-A-specific antibody treatment enhances sprouting and functional recovery after cervical lesion in adult primates. Nat.Med. 12, 790-792.

Freund, P., Schmidlin, E., Wannier, T., Bloch, J., Mir, A., Schwab, M.E., Rouiller, E.M., 2009. Anti-Nogo-A antibody treatment promotes recovery of manual dexterity after unilateral cervical lesion in adult primates--re-examination and extension of behavioral data. Eur.J Neurosci. 29, 983-996.

Freye, E., 2005. Cerebral monitoring in the operating room and the intensive care unit - an introductory for the clinician and a guide for the novice wanting to open a window to the brain. Part II: Sensory-evoked potentials (SSEP, AEP, VEP). J Clin.Monit.Comput. 19, 77-168.

Friel, K.M., Barbay, S., Frost, S.B., Plautz, E.J., Hutchinson, D.M., Stowe, A.M., Dancause, N., Zoubina, E.V., Quaney, B.M., Nudo, R.J., 2005. Dissociation of sensorimotor deficits after rostral versus caudal lesions in the primary motor cortex hand representation. J Neurophysiol. 94, 1312-1324.

Frost, S.B., Barbay, S., Friel, K.M., Plautz, E.J., Nudo, R.J., 2003. Reorganization of remote cortical regions after ischemic brain injury: a potential substrate for stroke recovery. J Neurophysiol 89, 3205-3214.

Galea, M.P., Darian-Smith, I., 1997. Manual dexterity and corticospinal connectivity following unilateral section of the cervical spinal cord in the macaque monkey. J Comp Neurol. 381, 307-319.

Gardner, E.P., Hamalainen, H.A., Warren, S., Davis, J., Young, W., 1984. Somatosensory evoked potentials (SEPs) and cortical single unit responses elicited by mechanical tactile stimuli in awake monkeys. Electroencephalogr.Clin.Neurophysiol 58, 537-552.

Gardner, E.P., Ro, J.Y., Babu, K.S., Ghosh, S., 2007. Neurophysiology of prehension. II. Response diversity in primary somatosensory (S-I) and motor (M-I) cortices. J.Neurophysiol. 97, 1656-1670.

Gentilucci, M., Fogassi, L., Luppino, G., Matelli, M., Camarda, R., Rizzolatti, G., 1988. Functional organization of inferior area 6 in the macaque monkey. Exp Brain Res 71, 475-490.

Gerbella, M., Belmalih, A., Borra, E., Rozzi, S., Luppino, G., 2011. Cortical connections of the anterior (F5a) subdivision of the macaque ventral premotor area F5. Brain Struct.Funct. 216, 43-65.

Giblin, D.R., 1964. Somatosensory evoked potentials in healthy subjects and in patients with lesions of the nervous system. Ann.N.Y.Acad.Sci. 112, 93-142.

Gibson, J.J., 1962. Observations on active touch. Psychological review 69, 477.

Gindrat, A.D., Quairiaux, C., Britz, J., Brunet, D., Lanz, F., Michel, C.M., Rouiller, E.M., 2014. Whole-scalp EEG mapping of somatosensory evoked potentials in macaque monkeys. Brain Struct.Funct., 1-22.

Gindrat, A.D., Chytiris, M., Balerna, M., Rouiller, E.M., Ghosh, A., 2015. Use-Dependent Cortical Processing from Fingertips in Touchscreen Phone Users. Current Biology 25, 109-116.

Glees, P., Cole, J., 1950. Recovery of skilled motor functions after small repeated lesions of motor cortex in macaque. Journal of Neurophysiology 13, 137-148.

Green, J.B., Bialy, Y., Sora, E., Ricamato, A., 1999a. High-resolution EEG in poststroke hemiparesis can identify ipsilateral generators during motor tasks. Stroke 30, 2659-2665.

Green, J.B., Sora, E., Bialy, Y., Ricamato, A., Thatcher, R.W., 1999b. Cortical motor reorganization after paraplegia: an EEG study. Neurology 53, 736-743.

Häger-Ross, C., Schieber, M.H., 2000. Quantifying the Independence of Human Finger Movements: Comparisons of Digits, Hands, and Movement Frequencies. The Journal of Neuroscience 20, 8542-8550.

Han, E.Y., Jung, H.Y., Kim, M.O., 2013. Absent median somatosensory evoked potential is a predictor of type I complex regional pain syndrome after stroke. Disabil.Rehabil.

Han, Y.S., Ha, S.W., Cho, J.S., Park, S.E., Kim, J.M., Han, J.H., Cho, E.K., Kim, D.E., 2006. Isolated Weakness of Middle, Ring, and Little Fingers due to a Small Cortical Infarction in the Medial Precentral Gyrus. Journal of Clinical Neurology (Seoul, Korea) 2, 146-148.

Hari, R., 1980. Evoked potentials elicited by long vibrotactile stimuli in the human EEG. Pflügers Arch. 384, 167-170.

Hashimoto, I., Yoshikawa, K., Kimura, T., 2000. Somatosensory evoked potentials to a threshold air-puff can predict stimulus detection in human subjects. Neurosci.Lett. 282, 181-184.

Hashimoto, I., Yoshikawa, K., Sasaki, M., Gatayama, T., Nomura, M., 1989. Sensory nerve action potentials elicited by mechanical air-puff stimulation of the index finger in man. Electroencephalography and Clinical Neurophysiology 72, 321-333.

Hashimoto, I., Yoshikawa, K., Sasaki, M., 1990. Latencies of peripheral nerve and cerebral evoked responses to air-puff and electrical stimuli. Muscle & Nerve 13, 1099-1104.

He, S.Q., Dum, R.P., Strick, P.L., 1993. Topographic organization of corticospinal projections from the frontal lobe: motor areas on the lateral surface of the hemisphere. J Neurosci. 13, 952-980.

Heller, M.A., 1984. Active and Passive Touch: The Influence of Exploration Time on form Recognition. Journal of General Psychology 110, 243.

Heller, M.A., Rogers, G.J., Perry, C.L., 1990. Tactile pattern recognition with the optacon: Superior performance with active touch and the left hand. Neuropsychologia 28, 1003-1006.

Hendry, S.H., Hsiao, S.S., 2013. Fundamentals of Sensory Systems. In: Spitzer, L.R.S. (Ed.), Fundamental Neuroscience (Fourth Edition). Academic Press, San Diego, pp. 499-511.

Hikosaka, O., Tanaka, M., Sakamoto, M., Iwamura, Y., 1985. Deficits in manipulative behaviors induced by local injections of muscimol in the first somatosensory cortex of the conscious monkey. Brain Research 325, 375-380.

Holsapple, J.W., Preston, J.B., Strick, P.L., 1991. The origin of thalamic inputs to the "hand" representation in the primary motor cortex. J Neurosci. 11, 2644-2654.

Hoogewoud, F., Hamadjida, A., Wyss, A.F., Mir, A., Schwab, M.E., Belhaj-Saïf, A., Rouiller, E.M., 2013. Comparison of functional recovery of manual dexterity after unilateral spinal cord lesion or motor cortex lesion in adult macaque monkeys. Front Neurol. 4, 101.

Horne, M.K., Tracey, D.J., 1979. The afferents and projections of the ventroposterolateral thalamus in the monkey. Exp.Brain Res 36, 129-141.

Huttunen, J., Hömberg, V., 1991. Influence of stimulus repetition rate on cortical somatosensory potentials evoked by median nerve stimulation: Implications for generation mechanisms. Journal of the Neurological Sciences 105, 37-43.

Hwang, K.J., Park, K.C., Chang, D.I., Yoon, S.S., 2014. Isolated Weakness of Radial-side Fingers Due to a Small Cortical Infarction. Journal of the Korean Society of Magnetic Resonance in Medicine 18, 362-365.

Indovina, I., Sanes, J.N., 2001. On somatotopic representation centers for finger movements in human primary motor cortex and supplementary motor area. Neuroimage 13, 1027-1034.

Iwamura, Y., Tanaka, M., Hikosaka, O., 1980. Overlapping representation of fingers in the somatosensory cortex (area 2) of the conscious monkey. Brain Research 197, 516-520.

Jabbari, B., Vance, S.C., Harper, M.G., Salazar, A.M., Smutok, M.A., Amin, D., 1987. Clinical and radiological correlates of somatosensory evoked potentials in the late phase of head injury: a study of 500 Vietnam veterans. Electroencephalogr.Clin.Neurophysiol 67, 289-297.

Johansson, R.S., Hger, C., Backstrom, L., 1992. Somatosensory control of precision grip during unpredictable pulling loads. III. Impairments during digital anesthesia. Exp.Brain Res 89, 204-213.

Johansson, R.S., Westling, G., 1984. Roles of glabrous skin receptors and sensorimotor memory in automatic control of precision grip when lifting rougher or more slippery objects. Exp Brain Res 56, 550-564.

Johnson, D., Jürgens, R., Kongehl, G., Kornhuber, H.H., 1975. Somatosensory evoked potentials and magnitude of perception. Exp Brain Res 22, 331-334.

Jones, E.G., Coulter, J.D., Hendry, S.H.C., 1978. Intracortical connectivity of architectonic fields in the somatic sensory, motor and parietal cortex of monkeys. The Journal of Comparative Neurology 181, 291-347.

Jones, E.G., Powell, T.P.S., 1970. An anatomical study of converging sensory pathways within the cerebral cortex of the monkey. Brain 93, 793-820.

Jones, E.G., 1986. Connectivity of the Primate Sensory-Motor Cortex. In: Jones, E.G., Peters, A. (Eds.), Sensory-Motor Areas and Aspects of Cortical Connectivity, 5th ed. Springer US, pp. 113-183.

Kaas, J.H., 2004. Evolution of the Large, Complex Sensorimotor Systems of Anthropoid Primates. In: Pellis, S., Marino, L. (Eds.), Special Issue: Evolution of the Vertebrate Brain and Behavior, International Journal of Comparative Psychology 17, pp. 34-52.

Kalaska, J.F., Rizzolatti, G., 2013. Voluntary Movement: The Primary Motor Cortex. In: Kandel, E.R., Schwartz, J., Jessell, T. (Eds.), Principles of neural science. McGraw-Hill Education, pp. 835-864.

Kambi, N., Tandon, S., Mohammed, H., Lazar, L., Jain, N., 2011. Reorganization of the primary motor cortex of adult macaque monkeys after sensory loss resulting from partial spinal cord injuries. J.Neurosci. 31, 3696-3707.

Kermadi, I., Liu, Y., Tempini, A., Calciati, E., Rouiller, E.M., 1998. Neuronal activity in the primate supplementary motor area and the primary motor cortex in relation to spatio-temporal bimanual coordination. Somatosens.Mot.Res. 15, 287-308.

Kim, J.S., 2001. Predominant involvement of a particular group of fingers due to small, cortical infarction. Neurology 56, 1677-1682.

Kim, J.S., Chung, J.P., Ha, S.W., 2002. Isolated weakness of index finger due to small cortical infarction. Neurology 58, 985.

Kirsch, E., Rivlis, G., Schieber, M.H., 2014. Primary Motor Cortex Neurons during Individuated Finger and Wrist Movements: Correlation of Spike Firing Rates with the Motion of Individual Digits versus Their Principal Components. Front Neurol. 5, 70.

Kobayashi, M., Sonoo, M., Shimizu, T., 2004. Pure motor stroke with major involvement of the index finger. Journal of Neurology, Neurosurgery & Psychiatry 75, 507-508.

Krarup, C., Trojaborg, W., 1994. Compound sensory action potentials evoked by tactile and by electrical stimulation in normal median and sural nerves. Muscle Nerve 17, 733-740.

Krubitzer, L., Huffman, K.J., Disbrow, E., Recanzone, G., 2004. Organization of area 3a in macaque monkeys: contributions to the cortical phenotype. J Comp Neurol. 471, 97-111.

Kurata, K., Tanji, J., 1986. Premotor cortex neurons in macaques: activity before distal and proximal forelimb movements. The Journal of Neuroscience 6, 403-411.

Kwan, H.C., MacKay, W.A., Murphy, J.T., Wong, Y.C., 1978. Spatial organization of precentral cortex in awake primates. II. Motor outputs. J Neurophysiol. 41, 1120-1131.

Laible, M., Grieshammer, S., Seidel, G., Rijntjes, M., Weiller, C., Hamzei, F., 2012. Association of Activity Changes in the Primary Sensory Cortex With Successful Motor Rehabilitation of the Hand Following Stroke. Neurorehabil Neural Repair 26, 881-888.

Lang, C.E., Schieber, M.H., 2003. Differential impairment of individuated finger movements in humans after damage to the motor cortex or the corticospinal tract. J.Neurophysiol. 90, 1160-1170.

Lang, C.E., Schieber, M.H., 2004. Reduced muscle selectivity during individuated finger movements in humans after damage to the motor cortex or corticospinal tract. J Neurophysiol. 91, 1722-1733.

Lang, C.E., DeJong, S.L., Beebe, J.A., 2009. Recovery of Thumb and Finger Extension and Its Relation to Grasp Performance After Stroke. Journal of Neurophysiology 102, 451-459.

Larsson, L.E., Prevec, T.S., 1970. Somato-sensory response to mechanical stimulation as recorded in the human EEG. Electroencephalography and Clinical Neurophysiology 28, 162-172.

Lascano, A.M., Grouiller, F., Genetti, M., Spinelli, L., Seeck, M., Schaller, K., Michel, C.M., 2014. Surgically relevant localization of the central sulcus with high-density somatosensory-evoked potentials compared with functional magnetic resonance imaging. Neurosurgery 74, 517-526.

Lawrence, D.G., Hopkins, D.A., 1976. The development of motor control in the rhesus monkey: evidence concerning the role of corticomotoneuronal connections. Brain 99, 235-254.

Lawrence, D.G., Kuypers, H.G., 1968. The functional organization of the motor system in the monkey. I. The effects of bilateral pyramidal lesions. Brain 91, 1-14.

Lee, P.H., Han, S.W., Heo, J.H., 1998. Isolated weakness of the fingers in cortical infarction. Neurology 50, 823-824.

Lee, S.Y., Lim, J.Y., Kang, E.K., Han, M.K., Bae, H.J., Paik, N.J., 2010. Prediction of good functional recovery after stroke based on combined motor and somatosensory evoked potential findings. J Rehabil.Med. 42, 16-20.

Legatt, A., 2014. General Principles of Somatosensory Evoked Potentials. Medscape.

Lehmann, S.J., Scherberger, H., 2013. Reach and Gaze Representations in Macaque Parietal and Premotor Grasp Areas. The Journal of Neuroscience 33, 7038-7049.

Leichnetz, G.R., 1986. Afferent and efferent connections of the dorsolateral precentral gyrus (area 4, hand/arm region) in the macaque monkey, with comparisons to area 8. J.Comp Neurol. 254, 460-492.

Lemon, R.N., 1981. Functional properties of monkey motor cortex neurones receiving afferent input from the hand and fingers. J.Physiol 311, 497-519.

Lemon, R.N., 1993. The G. L. Brown Prize Lecture. Cortical control of the primate hand. Exp.Physiol 78, 263-301.

Lemon, R.N., 1997. Mechanisms of cortical control of hand function. neuroscientist 3, 389-398.

Lemon, R.N., 2008. Descending pathways in motor control. Annu.Rev.Neurosci. 31, 195-218.

Lemon, R.N., Bennett, K.M., Werner, W., 1991. The Cortico-Motor Substrate for Skilled Movements of the Primate Hand. In: Requin, J., Stelmach, G.E. (Eds.), Tutorials in Motor Neuroscience, 62 ed. Springer Netherlands, pp. 477-495.

Lemon, R.N., Hanby, J.A., Porter, R., 1976. Relationship between the activity of precentral neurones during active and passive movements in conscious monkeys. Proc.R.Soc.Lond B Biol.Sci. 194, 341-373.

Lemon, R.N., Porter, R., 1976. Afferent input to movement-related precentral neurones in conscious monkeys. Proc.R.Soc.Lond B Biol.Sci. 194, 313-339.

Lemon, R.N., Van der Burg, J., 1979. Short-latency peripheral inputs to thalamic neurones projecting to the motor cortex in the monkey. Exp.Brain Res. 36, 445-462.

Lemon, R., 1988. The output map of the primate motor cortex. Trends in Neurosciences 11, 501-506.

Liepert, J., Hamzei, F., Weiller, C., 2000. Motor cortex disinhibition of the unaffected hemisphere after acute stroke. Muscle & Nerve 23, 1761-1763.

Liu, Y., Rouiller, E.M., 1999. Mechanisms of recovery of dexterity following unilateral lesion of the sensorimotor cortex in adult monkeys. Exp.Brain Res. 128, 149-159.

Ludbrook, J., Dudley, H., 1998. Why Permutation Tests Are Superior to t and F Tests in Biomedical Research. The American Statistician 52, 127-132.

Luppino, G., Matelli, M., Camarda, R.M., Gallese, V., Rizzolatti, G., 1991. Multiple representations of body movements in mesial area 6 and the adjacent cingulate cortex: An intracortical microstimulation study in the macaque monkey. The Journal of Comparative Neurology 311, 463-482.

Macpherson, J.M., Marangoz, C., Miles, T.S., Wiesendanger, M., 1982. Microstimulation of the supplementary motor area (SMA) in the awake monkey. Exp Brain Res 45, 410-416.

Maier, M.A., Armand, J., Kirkwood, P.A., Yang, H.W., Davis, J.N., Lemon, R.N., 2002. Differences in the corticospinal projection from primary motor cortex and supplementary motor area to macaque upper limb motoneurons: an anatomical and electrophysiological study. Cereb.Cortex 12, 281-296.

Maitre, N.L., Barnett, Z.P., Key, A.P.F., 2012. Novel Assessment of Cortical Response to Somatosensory Stimuli in Children With Hemiparetic Cerebral Palsy. Journal of Child Neurology 27, 1276-1283.

Manzano, G.M., Kohn, A.F., 2000. Proximal receptors and the mechanical stimulation of the fingers: a somatosensory evoked potential study. Electromyogr.Clin.Neurophysiol. 40, 21-29.

Marshall, W.H., Woolsey, C.N., Bard, P., 1941. Observations on cortical somatic sensory mechanisms of cat and monkey. Journal of Neurophysiology 4, 1-24.

Marshall, W.H., Woolsey, C.N., Bard, P., 1937. Cortical representation of tactile sensibility as indicated by cortical potentials. Science 85, 388-390.

Matelli, M., Luppino, G., Fogassi, L., Rizzolatti, G., 1989. Thalamic input to inferior area 6 and area 4 in the macaque monkey. The Journal of Comparative Neurology 280, 468-488.

Matelli, M., Luppino, G., Rizzolatti, G., 1985. Patterns of cytochrome oxidase activity in the frontal agranular cortex of the macaque monkey. Behavioural Brain Research 18, 125-136.

Mauguière, F., 2011. Somatosensory-evoked potentials: Normal Responses, Abnormal Waveforms, and Clinical Applications in Neurologic Diseases. In: Schomer, D.L., Lopes da Silva, F.H. (Eds.), Niedermeyer's Electroencephalography: Basic Principles, Clinical Applications, and Related Fields, 6th ed. Lippincott Williams & Wilkins, pp. 1003-1056.

Mauguière, F., Desmedt, J.E., Courjon, J., 1983. Neural generators of N18 and P14 far-field somatosensory evoked potentials studied in patients with lesion of thalamus or thalamo-cortical radiations. Electroencephalography and Clinical Neurophysiology 56, 283-292.

McCarthy, G., Wood, C.C., Allison, T., 1991. Cortical somatosensory evoked potentials. I. Recordings in the monkey *Macaca fascicularis*. J Neurophysiol 66, 53-63.

McLaughlin, D., Makeig, S., 1995. Human Electrophysiological Responses to Tactile Stimuli Presented at Different Rates. Naval Health Research Center.

McLaughlin, D.F., Kelly, E.F., 1993. Evoked potentials as indices of adaptation in the somatosensory system in humans: a review and prospectus. Brain Res.Brain Res.Rev. 18, 151-206.

Merzenich, M.M., Nelson, R.J., Kaas, J.H., Stryker, M.P., Jenkins, W.M., Zook, J.M., Cynader, M.S., Schoppmann, A., 1987. Variability in hand surface representations in areas 3b and 1 in adult owl and squirrel monkeys. Journal of Comparative Neurology 258, 281-296.

Mitz, A.R., Wise, S.P., 1987. The somatotopic organization of the supplementary motor area: intracortical microstimulation mapping. The Journal of Neuroscience 7, 1010-1021.

Monzée, J., Lamarre, Y., Smith, A.M., 2003. The Effects of Digital Anesthesia on Force Control Using a Precision Grip. Journal of Neurophysiology 89, 672-683.

Mott, F.W., Sherrington, C.S., 1894. Experiments upon the influence of sensory nerves upon movement and nutrition of the limbs. Preliminary communication. Proceedings of the Royal Society of London 57, 481-488.

Murata, A., Fadiga, L., Fogassi, L., Gallese, V., Raos, V., Rizzolatti, G., 1997. Object Representation in the Ventral Premotor Cortex (Area F5) of the Monkey. Journal of Neurophysiology 78, 2226-2230.

Murata, Y., Higo, N., Oishi, T., Yamashita, A., Matsuda, K., Hayashi, M., Yamane, S., 2008. Effects of motor training on the recovery of manual dexterity after primary motor cortex lesion in macaque monkeys. J Neurophysiol 99, 773-786.

Murphy, J.T., Kwan, H.C., MacKay, W.A., Wong, Y.C., 1978. Spatial organization of precentral cortex in awake primates. III. Input-output coupling. J Neurophysiol. 41, 1132-1139.

Murphy, J.T., Wong, Y.C., Kwan, H.C., 1975. Afferent-efferent linkages in motor cortex for single forelimb muscles. Journal of Neurophysiology 38, 990-1014.

Nakanishi, T., Takita, K., Toyokura, Y., 1973. Somatosensory evoked responses to tactile tap in man. Electroencephalography and Clinical Neurophysiology 34, 1-6.

Napier, J.R., 1956. The prehensile movements of the human hand. J Bone Joint Surg.Br 38-B, 902-913.

Napier, J.R., 1961. Prehensility an opposability in the hands of primates. Symposia of the Zoological Society,London 5, 115-132.

Napier, J., 1962. The evolution of the hand. Scientific American 207, 56-62.

Napier, J., 1993. Hands. Princeton University Press, Princeton, New Jersey.

Netz, J., Lammers, T., Homberg, V., 1997. Reorganization of motor output in the non-affected hemisphere after stroke. Brain 120 (Pt 9), 1579-1586.

Nishimura, Y., Onoe, H., Morichika, Y., Perfiliev, S., Tsukada, H., Isa, T., 2007. Time-Dependent Central Compensatory Mechanisms of Finger Dexterity After Spinal Cord Injury. Science 318, 1150-1155.

Nudo, R.J., Friel, K.M., Delia, S.W., 2000. Role of sensory deficits in motor impairments after injury to primary motor cortex. Neuropharmacology 39, 733-742.

Nudo, R.J., Milliken, G.W., 1996. Reorganization of movement representations in primary motor cortex following focal ischemic infarcts in adult squirrel monkeys. J Neurophysiol 75, 2144-2149.

Nuwer, M.R., Aminoff, M., Desmedt, J., Eisen, A.A., Goodin, D., Matsuoka, S., Mauguière, F., Shibasaki, H., Sutherling, W., Vibert, J.F., 1994. IFCN recommended standards for short latency somatosensory evoked potentials. Report of an IFCN committee. International Federation of Clinical Neurophysiology. Electroencephalogr.Clin.Neurophysiol 91, 6-11.

Onofrj, M., Basciani, M., Fulgente, T., Bazzano, S., Malatesta, G., Curatola, L., 1990. Maps of somatosensory evoked potentials (SEPs) to mechanical (tapping) stimuli: comparison with P14, N20, P22, N30 of electrically elicited SEPs. Electroencephalogr.Clin.Neurophysiol 77, 314-319.

Park, M.C., Belhaj-Saïf, A., Gordon, M., Cheney, P.D., 2001. Consistent features in the forelimb representation of primary motor cortex in rhesus macaques. J Neurosci. 21, 2784-2792.

Park, M.C., Belhaj-Saïf, A., Cheney, P.D., 2004. Properties of Primary Motor Cortex Output to Forelimb Muscles in Rhesus Macaques. Journal of Neurophysiology 92, 2968-2984.

Passingham, R.E., Perry, V.H., Wilkinson, F., 1983. The long-term effects of removal of sensorimotor cortex in infant and adult rhesus monkeys. Brain 106, 675-705.

Penfield, W., Boldrey, E., 1937. Somatic motor and sensory representation in the cerebral cortex of man as studied by electrical stimulation. Brain 60, 389-443.

Penfield, W., Jasper, H.H., 1954. Epilepsy and the Functional Anatomy of the Human Brain. Little, Brown.

Penfield, W., Rasmussen, T., 1950. The cerebral cortex of man; a clinical study of localization of function.

Perot, P.L.Jr., Vera, C.L., Fountain, E.L., 1983. Elimination of EMG interference during recording of somatosensory evoked potentials elicited by posterior tibial nerve stimulation in patients with cervical spinal cord injury. Electroencephalogr.Clin.Neurophysiol 56, 104-109.

Pizzimenti, M.A., Darling, W.G., Rotella, D.L., McNeal, D.W., Herrick, J.L., Ge, J., Stilwell-Morecraft, K.S., Morecraft, R.J., 2007. Measurement of reaching kinematics and prehensile dexterity in nonhuman primates. J Neurophysiol. 98, 1015-1029.

Pokorny, C., Breitwieser, C., Muller-Putz, G.R., 2013. A Tactile Stimulation Device for EEG Measurements in Clinical Use. IEEE Trans.Biomed.Circuits.Syst.

Pons, T.P., Garraghty, P.E., Cusick, C.G., Kaas, J.H., 1985. The somatotopic organization of area 2 in macaque monkeys. The Journal of Comparative Neurology 241, 445-466.

Popescu, M., Barlow, S., Popescu, E.A., Estep, M.E., Venkatesan, L., Auer, E.T., Brooks, W.M., 2010. Cutaneous stimulation of the digits and lips evokes responses with different adaptation patterns in primary somatosensory cortex. Neuroimage. 52, 1477-1486.

Pratt, H., Amlie, R.N., Starr, A., 1979a. Short latency mechanically evoked somatosensory potentials in humans. Electroencephalography and Clinical Neurophysiology 47, 524-531.

Pratt, H., Politoske, D., Starr, A., 1980. Mechanically and electrically evoked somatosensory potentials in humans: effects of stimulus presentation rate. Electroencephalogr.Clin.Neurophysiol 49, 240-249.

Pratt, H., Starr, A., Amlie, R.N., Politoske, D., 1979b. Mechanically and electrically evoked somatosensory potentials in normal humans. Neurology 29, 1236.

Qi, H.X., Jain, N., Collins, C.E., Lyon, D.C., Kaas, J.H., 2010. Functional organization of motor cortex of adult macaque monkeys is altered by sensory loss in infancy. Proc.Natl.Acad.Sci.USA 107, 3192-3197.

Qi, H.X., Stepniewska, I., Kaas, J.H., 2000. Reorganization of primary motor cortex in adult macaque monkeys with long-standing amputations. J Neurophysiol. 84, 2133-2147.

Rathelot, J.A., Strick, P.L., 2006. Muscle representation in the macaque motor cortex: an anatomical perspective. Proc.Natl.Acad.Sci.USA 103, 8257-8262.

Regan, D., 1989. Human brain electrophysiology: evoked potentials and evoked magnetic fields in science and medicine. Elsevier.

Reuter, E.M., Voelcker-Rehage, C., Vieluf, S., Godde, B., 2014. Effects of age and expertise on tactile learning in humans. European Journal of Neuroscience 40, 2589-2599.

Riquelme, I., Padron, I., Cifre, I., Gonzalez-Roldan, A.M., Montoya, P., 2014. Differences in somatosensory processing due to dominant hemispheric motor impairment in cerebral palsy. BMC Neurosci. 15, 10.

Rizzolatti, G., Camarda, R., Fogassi, L., Gentilucci, M., Luppino, G., Matelli, M., 1988. Functional organization of inferior area 6 in the macaque monkey. II. Area F5 and the control of distal movements. Exp Brain Res 71, 491-507.

Rosén, I., Asanuma, H., 1972. Peripheral afferent inputs to the forelimb area of the monkey motor cortex: input-output relations. Exp.Brain Res. 14, 257-273.

Rosner, B.S., Goff, W.R., 1967. Electrical Responses of the Nervous System and Subjective Scales of Intensity. In: Neff, W.D. (Ed.), Contributions to Sensory Physiology, Volume 2. Elsevier, pp. 169-221.

Rothwell, J.C., Traub, M.M., Day, B.L., Obeso, J.A., Thomas, P.K., Marsden, C.D., 1982. Manual motor performance in a deafferented man. Brain 105 (Pt 3), 515-542.

Rouiller, E.M., Babalian, A., Kazennikov, O., Moret, V., Yu, X.H., Wiesendanger, M., 1994. Transcallosal connections of the distal forelimb representations of the primary and supplementary motor cortical areas in macaque monkeys. Exp.Brain Res. 102, 227-243.

Rouiller, E.M., Moret, V., Tanne, J., Boussaoud, D., 1996. Evidence for direct connections between the hand region of the supplementary motor area and cervical motoneurons in the macaque monkey. Eur.J Neurosci. 8, 1055-1059.

Rouiller, E.M., Olivier, E., 2004. Functional recovery after lesions of the primary motor cortex. Prog.Brain Res. 143, 467-475.

Rouiller, E.M., Tanne, J., Moret, V., Boussaoud, D., 1999. Origin of thalamic inputs to the primary, premotor, and supplementary motor cortical areas and to area 46 in macaque monkeys: a multiple retrograde tracing study. J Comp Neurol. 409, 131-152.

Rouiller, E.M., Tanne, J., Moret, V., Kermadi, I., Boussaoud, D., Welker, E., 1998a. Dual morphology and topography of the corticothalamic terminals originating from the primary, supplementary motor, and dorsal premotor cortical areas in macaque monkeys. J.Comp Neurol. 396, 169-185.

Rouiller, E.M., Yu, X.H., Moret, V., Tempini, A., Wiesendanger, M., Liang, F., 1998b. Dexterity in adult monkeys following early lesion of the motor cortical hand area: the role of cortex adjacent to the lesion. Eur.J.Neurosci. 10, 729-740.

Sanes, J.N., Mauritz, K.H., Evarts, E.V., Dalakas, M.C., Chu, A., 1984. Motor deficits in patients with large-fiber sensory neuropathy. Proc.Natl.Acad.Sci.USA 81, 979-982.

Sasaki, K., Gemba, H., 1984. Compensatory motor function of the somatosensory cortex for the motor cortex temporarily impaired by cooling in the monkey. Exp.Brain Res 55, 60-68.

Sawaki, L., Wu, C.W., Kaelin-Lang, A., Cohen, L.G., 2006. Effects of somatosensory stimulation on use-dependent plasticity in chronic stroke. Stroke 37, 246-247.

Schaechter, J.D., van Oers, C.A., Groisser, B.N., Salles, S.S., Vangel, M.G., Moore, C.I., Dijkhuizen, R.M., 2012. Increase in sensorimotor cortex response to somatosensory stimulation over subacute poststroke period correlates with motor recovery in hemiparetic patients. Neurorehabil Neural Repair 26, 325-334.

Schaffelhofer, S., Agudelo-Toro, A., Scherberger, H., 2015. Decoding a Wide Range of Hand Configurations from Macaque Motor, Premotor, and Parietal Cortices. The Journal of Neuroscience 35, 1068-1081.

Schieber, M.H., 1991. Individuated finger movements of rhesus monkeys: a means of quantifying the independence of the digits. J Neurophysiol. 65, 1381-1391.

Schieber, M.H., 2001. Constraints on somatotopic organization in the primary motor cortex. J Neurophysiol 86, 2125-2143.

Schieber, M.H., Hibbard, L.S., 1993. How somatotopic is the motor cortex hand area? Science 261, 489-492.

Schieber, M.H., 1999. Somatotopic gradients in the distributed organization of the human primary motor cortex hand area: evidence from small infarcts. Exp Brain Res 128, 139-148.

Schieber, M.H., Lang, C.E., Reilly, K.T., McNulty, P., Sirigu, A., 2009. Selective Activation of Human Finger Muscles after Stroke or Amputation. In: Sternad, D. (Ed.), Progress in Motor Control, Advances in Experimental Medicine and Biology, Volume 629. Springer US, pp. 559-575.

Schieber, M.H., Poliakov, A.V., 1998. Partial Inactivation of the Primary Motor Cortex Hand Area: Effects on Individuated Finger Movements. The Journal of Neuroscience 18, 9038-9054.

Schmidlin, E., Wannier, T., Bloch, J., Rouiller, E.M., 2004. Progressive plastic changes in the hand representation of the primary motor cortex parallel incomplete recovery from a unilateral section of the corticospinal tract at cervical level in monkeys. Brain Res. 1017, 172-183.

Schmidlin, E., Brochier, T., Maier, M.A., Kirkwood, P.A., Lemon, R.N., 2008. Pronounced Reduction of Digit Motor Responses Evoked from Macaque Ventral Premotor Cortex after Reversible Inactivation of the Primary Motor Cortex Hand Area. The Journal of Neuroscience 28, 5772-5783.

Serrien, D.J., Strens, L.H., Cassidy, M.J., Thompson, A.J., Brown, P., 2004. Functional significance of the ipsilateral hemisphere during movement of the affected hand after stroke. Exp.Neurol. 190, 425-432.

Sessle, B.J., Wiesendanger, M., 1982. Structural and functional definition of the motor cortex in the monkey (*Macaca fascicularis*). J Physiol 323, 245-265.

Shimazu, H., Maier, M.A., Cerri, G., Kirkwood, P.A., Lemon, R.N., 2004. Macaque ventral premotor cortex exerts powerful facilitation of motor cortex outputs to upper limb motoneurons. J Neurosci. 24, 1200-1211.

Shimizu, T., Hosaki, A., Hino, T., Sato, M., Komori, T., Hirai, S., Rossini, P.M., 2002. Motor cortical disinhibition in the unaffected hemisphere after unilateral cortical stroke. Brain 125, 1896-1907.

Shindo, K., Shima, K., Tanji, J., 1995. Spatial distribution of thalamic projections to the supplementary motor area and the primary motor cortex: A retrograde multiple labeling study in the macaque monkey. The Journal of Comparative Neurology 357, 98-116.

Shoham, D., Grinvald, A., 2001. The cortical representation of the hand in macaque and human area S-I: high resolution optical imaging. J.Neurosci. 21, 6820-6835.

Slimp, J.C., Tamas, L.B., Stolov, W.C., Wyler, A.R., 1986. Somatosensory evoked potentials after removal of somatosensory cortex in man. Electroencephalogr.Clin.Neurophysiol 65, 111-117.

Smith, A.M., 2009. The neurohaptic control of the hand. In: Nowak, D.A., Hermsdörfer, J. (Eds.), Sensorimotor Control of Grasping: Physiology and Pathophysiology. Cambridge University Press, pp. 178-192.

Soininen, K., Jarvilehto, T., 1983. Somatosensory evoked potentials associated with tactile stimulation at detection threshold in man. Electroencephalogr.Clin.Neurophysiol 56, 494-500.

Sonoo, M., Shimpo, T., Takeda, K., Genba, K., Nakano, I., Mannen, T., 1991. SEPs in two patients with localized lesions of the postcentral gyrus. Electroencephalogr.Clin.Neurophysiol 80, 536-546.

Spinks, R.L., Kraskov, A., Brochier, T., Umilta, M.A., Lemon, R.N., 2008. Selectivity for grasp in local field potential and single neuron activity recorded simultaneously from M1 and F5 in the awake macaque monkey. J.Neurosci. 28, 10961-10971.

Starr, A., Pratt, H., Burke, D., 1982. Natural stimuli evoking somatosensory potentials. Ann.N.Y.Acad.Sci. 388, 702-706.

Stepniewska, I., Preuss, T.M., Kaas, J.H., 1993. Architectonics, somatotopic organization, and ipsilateral cortical connections of the primary motor area (M1) of owl monkeys. Journal of Comparative Neurology 330, 238-271.

Stohr, M., Dichgans, J., Voigt, K., Buettner, U.W., 1983. The significance of somatosensory evoked potentials for localization of unilateral lesions within the cerebral hemispheres. J Neurol.Sci. 61, 49-63.

Stoney, S.D.Jr., Thompson, W.D., Asanuma, H., 1968. Excitation of pyramidal tract cells by intracortical microstimulation: effective extent of stimulating current. J Neurophysiol 31, 659-669.

Strick, P.L., 1976. Anatomical analysis of ventrolateral thalamic input to primate motor cortex. Journal of Neurophysiology 39, 1020-1031.

Strick, P.L., Preston, J.B., 1982. Two representations of the hand in area 4 of a primate. II. Somatosensory input organization. J.Neurophysiol. 48, 150-159.

Strick, P.L., 1975. Multiple sources of thalamic input to the primate motor cortex. Brain Research 88, 372-377.

Strick, P.L., Preston, J.B., 1978. Sorting of somatosensory afferent information in primate motor cortex. Brain Research 156, 364-368.

Tanji, J., Wise, S.P., 1981. Submodality distribution in sensorimotor cortex of the unanesthetized monkey. J.Neurophysiol. 45, 467-481.

Tanji, J., 1994. The supplementary motor area in the cerebral cortex. Neuroscience Research 19, 251-268.

Terao, Y., Hayashi, H., Kanda, T., Tanabe, H., 1993. Discrete cortical infarction with prominent impairment of thumb flexion. Stroke 24, 2118-2120.

Thielbar, K., Lord, T., Fischer, H., Lazzaro, E., Barth, K., Stoykov, M., Triandafilou, K., Kamper, D., 2014. Training finger individuation with a mechatronic-virtual reality system leads to improved fine motor control post-stroke. Journal of NeuroEngineering and Rehabilitation 11, 171.

Thompson, W.D., Stoney, S.D.Jr., Asanuma, H., 1970. Characteristics of projections from primary sensory cortex to motorsensory cortex in cats. Brain Res 22, 15-27.

Townsend, B.R., Subasi, E., Scherberger, H., 2011. Grasp Movement Decoding from Premotor and Parietal Cortex. The Journal of Neuroscience 31, 14386-14398.

Tsuji, S., Murai, Y., Kadoya, C., 1988. Topography of somatosensory evoked potentials to median nerve stimulation in patients with cerebral lesions. Electroencephalogr.Clin.Neurophysiol 71, 280-288.

Tzvetanov, P., Rousseff, R.T., 2005. Predictive value of median-SSEP in early phase of stroke: a comparison in supratentorial infarction and hemorrhage. Clin.Neurol.Neurosurg. 107, 475-481.

Tzvetanov, P., Rousseff, R.T., Atanassova, P., 2005. Prognostic value of median and tibial somatosensory evoked potentials in acute stroke. Neurosci.Lett. 380, 99-104.

Umilta, M.A., Brochier, T., Spinks, R.L., Lemon, R.N., 2007. Simultaneous Recording of Macaque Premotor and Primary Motor Cortex Neuronal Populations Reveals Different Functional Contributions to Visuomotor Grasp. Journal of Neurophysiology 98, 488-501.

Uribe Roca, C., Gatto, E.M., Micheli, F., 2002. Isolated weakness of index finger due to small cortical infarction. Neurology 59, 2010-2012.

Uttal, W.R., Cook, L., 1964. Systematics of the evoked somatosensory cortical potential: a psychophysical-electrophysiological comparison. Annals of the New York Academy of Sciences 112, 60-80.

Valeriani, M., Le Pera, D., Niddam, D., Arendt-Nielsen, L., Chen, A.C., 2000. Dipolar source modeling of somatosensory evoked potentials to painful and nonpainful median nerve stimulation. Muscle Nerve 23, 1194-1203.

van de Wassenberg, W.J., van der Hoeven, J., Leenders, K., Maurits, N., 2008. Multichannel recording of median nerve somatosensory evoked potentials. Neurophysiol Clin. 38, 9-21.

van den Broek, S.P., Reinders, F., Donderwinkel, M., Peters, M.J., 1998. Volume conduction effects in EEG and MEG. Electroencephalogr.Clin.Neurophysiol. 106, 522-534.

Vanhatalo, S., Jousmäki, V., Andersson, S., Metsäranta, M., 2009. An Easy and Practical Method for Routine, Bedside Testing of Somatosensory Systems in Extremely Low Birth Weight Infants. Pediatr Res 66, 710-713.

Vaughan, H.G.Jr., 1982. The neural origins of human event-related potentials. Ann.N.Y.Acad.Sci. 388, 125-138.

Vitek, J.L., Ashe, J., DeLong, M.R., Alexander, G.E., 1994. Physiologic properties and somatotopic organization of the primate motor thalamus. Journal of Neurophysiology 71, 1498-1513.

Walsh, P., Kane, N., Butler, S., 2005. The clinical role of evoked potentials. J Neurol.Neurosurg.Psychiatry 76 Suppl 2, ii16-ii22.

Wannier, T.M., Maier, M.A., Hepp-Reymond, M.C., 1991. Contrasting properties of monkey somatosensory and motor cortex neurons activated during the control of force in precision grip. J Neurophysiol. 65, 572-589.

Watanabe, Y., Shikano, M., Ohba, M., Ohkubo, M., Niwa, T., 1989. Correlation between somatosensory evoked potentials and sensory disturbance in stroke patients. Clin.Electroencephalogr. 20, 156-161.

Wiesendanger, M., 1973. Input from muscle and cutaneous nerves of the hand and forearm to neurones of the precentral gyrus of baboons and monkeys. The Journal of physiology 228, 203-219.

Wilson, T.W., Godwin, D.W., Czoty, P.W., Nader, M.A., Kraft, R.A., Buchheimer, N.C., Daunais, J.B., 2009. A MEG investigation of somatosensory processing in the rhesus monkey. Neuroimage 46, 998-1003.

Wong, P.K., Lombroso, C.T., Maysumiya, Y., 1982. Somatosensory evoked potentials: variability analysis in unilateral hemispheric disease. Electroencephalogr.Clin.Neurophysiol 54, 266-274.

Wong, Y.C., Kwan, H.C., MacKay, W.A., Murphy, J.T., 1978. Spatial organization of precentral cortex in awake primates. I. Somatosensory inputs. J Neurophysiol. 41, 1107-1119.

Woolsey, C.N., 1958. Organization of somatic sensory and motor areas of the cerebral cortex. In: Harlow, H.F., Woolsey, C.N. (Eds.), Biological and biochemical bases of behavior. The University of Wisconsin Press, pp. 63-81.

Woolsey, C.N., 1964. Cortical localization as defined by evoked potential and electrical stimulation studies. Cerebral localization and organization, 17-26.

Woolsey, C.N., Erickson, T.C., 1950. Study of the postcentral gyrus of man by the evoked potential technique. Trans.Am.Neurol Assoc. 51, 50-52.

Woolsey, C.N., Erickson, T.C., Gilson, W.E., 1979. Localization in somatic sensory and motor areas of human cerebral cortex as determined by direct recording of evoked potentials and electrical stimulation. J Neurosurg. 51, 476-506.

Woolsey, C.N., Marshall, W.H., Bard, P., 1942. Representation of cutaneous tactile sensibility in the cerebral cortex of the monkey as indicated by evoked potentials. Bull Johns Hopkins Hosp 70, 399-441.

Woolsey, C.N., Settlage, P.H., Meyer, D.R., Sencer, W., Pinto Hamuy, T., Travis, A.M., 1952. Patterns of localization in precentral and "supplementary" motor areas and their relation to the concept of a premotor area. Res.Publ.Assoc.Res.Nerv.Ment.Dis. 30, 238-264.

Wyss, A.F., Hamadjida, A., Savidan, J., Liu, Y., Bashir, S., Mir, A., Schwab, M.E., Rouiller, E.M., Belhaj-Saïf, A., 2013. Long-term motor cortical map changes following unilateral lesion of the hand representation in the motor cortex in macaque monkeys showing functional recovery of hand functions. Restor.Neurol Neurosci. 31, 733-760.

Xerri, C., Merzenich, M.M., Peterson, B.E., Jenkins, W., 1998. Plasticity of primary somatosensory cortex paralleling sensorimotor skill recovery from stroke in adult monkeys. J Neurophysiol. 79, 2119-2148.

York, D.H., 1985. Somatosensory evoked potentials in man: differentiation of spinal pathways responsible for conduction from the forelimb vs hindlimb. Prog.Neurobiol. 25, 1-25.

Zaaimi, B., Edgley, S.A., Soteropoulos, D.S., Baker, S.N., 2012. Changes in descending motor pathway connectivity after corticospinal tract lesion in macaque monkey. Brain 135, 2277-2289.

Zeller, D., Litvak, V., Friston, K.J., Classen, J., 2014. Sensory Processing and the Rubber Hand Illusion – An Evoked Potentials Study. Journal of Cognitive Neuroscience 27, 573-582.

Zeman, B.D., Yiannikas, C., 1989. Functional prognosis in stroke: use of somatosensory evoked potentials. J Neurol.Neurosurg.Psychiatry 52, 242-247.

CHAPTER 4

Adaptation of the cortical somatosensory evoked potentials following a repeated tactile stimulation of the fingertips in macaque monkeys

Anne-Dominique Gindrat, Eric M Rouiller and Arko Ghosh

Abstract

The integration of sensory inputs originating from the fingers allows us to feel and skillfully manipulate objects. Taking advantage of the high temporal resolution of our scalp EEG recording method, we studied some properties of tactile processing from the fingertips in non-human primates. We recorded tactile SSEPs by using scalp EEG after 2-ms-long repeated touch stimuli applied to the right thumb tip, index fingertip and middle fingertip of three anaesthetised macaque monkeys. SSEPs in response to repeated electrical stimuli to the median nerve at the wrist were obtained as well in one of these monkeys for comparison. For both stimulation paradigms, we used a 1-Hz repetition rate precisely to avoid a massive amplitude adaptation, as usually reported to occur in case of high stimulus repetition rate.

A careful data examination revealed a novel observation: surprisingly, we noticed a significant linearly increasing latency shift of the cortical tactile component over time, for the three stimulated fingertips. More specifically, the latency adaptation for each fingertip stimulation developed regularly but distinctly during successive 50-trial blocks, and distinctly in each monkey as well. For instance, the latency increased by 1.8 ms to 8 ms over the 600-800 trials analysed after middle fingertip stimulation in each of the three monkeys. Conversely, there was no consistent adaptation in the cortical amplitude of tactile SSEPs across the animals. For comparison, a modest latency increase accompanied by a much stronger amplitude decrease over time characterised specifically the processing of the first 700 trials of electrical stimulation to the median nerve.

Taken together, our findings indicate, first, that the cortical processing of repeated stimulations was open to significant fluctuations within an experimental EEG session, meaning that cortical plasticity can operate rapidly. Second, our results suggest that these linear and at the same time finger-specific and subject-specific evolutions of latency over time reflect dynamic processes that are highly consistent in macaque monkeys and very specifically linked to the processing of tactile sensory inputs from the fingertips. We may therefore have stressed a unique and specific “cortical signature” of fingertip tactile stimulation. Our results clearly demonstrate that latency adaptation is a significant process that should be carefully considered in case of repeated tactile stimulations, even at a low stimulus repetition rate.

In the discussion, we provide evidence supporting that the adaptation in tactile SSEPs arguably did not result from a general side effect of anaesthesia. In addition, we propose some hypotheses about the origin of these adaptation patterns and we suggest that this temporal shift may enable the brain to prioritise novel stimuli by delaying the sensory processing of repeated meaningless inputs.

Introduction

In our daily life, we are often continuously exposed to a large amount of stimuli from the environment but our brain is able to select only the most relevant features to adapt our behaviour at best to such fluctuating situations. In many cases, repeated stimuli instead of isolated stimuli are experienced, for instance during the manipulation of objects or the motor exploration by palpation. In these cases, sensory inputs from sequences of repeated events separated by a fraction of millisecond to minutes are integrated to allow us to feel and skillfully manipulate objects. How the brain processes such a huge amount of continuous information and integrates stimuli at the time scale of tens to hundreds of milliseconds remains largely unknown.

Remarkably, the different sensory systems share some common principles of organisation: for instance, as a general rule, a specific type of stimulus energy is transduced into electrical signal by specialised receptors and then transmitted to a specific area of the brain by passing and being processed from one neuron to the next in a sensory afferent pathway (Frings, 2012; Gardner and Johnson, 2013; Hendry and Hsiao, 2013; Purves et al., 2004; Torre et al., 1995). In addition, the successive structures processing afferent information usually have a conserved and precise pattern of topographical organisation (Gardner and Johnson, 2013; Hendry and Hsiao, 2013; Kaas, 1997). Moreover, the contrast of stimuli is enhanced during information processing by amplifying differences in the activity of neighbouring neurons, which is called lateral or surround inhibition (Hendry and Hsiao, 2013; Severens et al., 2010; see e.g. Von Békésy, 1967).

Stimulus-specific adaptation of neural responses is another common fundamental feature of sensory processing. In case of repeated or continuous sensory stimulation (usually with high repetition rate), the nervous system and the brain in particular generally reduce their responsiveness by adapting their cortical responses, usually in the form of a

rapid decrease in response amplitude (see e.g. Pérez-González and Malmierca, 2014). The resulting advantages are presumably to optimise stimulus processing by reducing redundancy (Adibi et al., 2013; Müller et al., 1999; Wissig and Kohn, 2012) and thus to adjust sensitivity to detect changes in stimulus (Goble and Hollins, 1993; Goble and Hollins, 1994; Greenlee and Heitger, 1988; Maravall et al., 2007; Musall et al., 2014; Ohzawa et al., 1982; Pérez-González and Malmierca, 2014; Regan and Beverley, 1985; Tannan et al., 2007; Von Békésy, 1960; von der Behrens et al., 2009; Wang et al., 2010) and more relevant novel environmental inputs (Andrade et al., 2015; Kadohisa and Wilson, 2006; Tannan et al., 2006). In a very recent study in rats, adaptation was prevented by optogenetic optical activation of the barrel cortex in S1 (Musall et al., 2014). When the animals were then presented with behavioural tasks, they showed a strong improvement of stimulus detection and discrimination of stimulus frequency, but at the cost of reducing fidelity under steady-state conditions. This very elegant study clearly demonstrates the critical role of sensory adaptation in the perception of stimulus patterns. Instead of being merely a "fatigue" of sensory structures as previously claimed (see e.g. Wedell and Cummings, 1938), the adaptation to repeated stimulations corresponds in fact to a process of adjustment or "tuning" of the sensory system involved towards the most pertinent inputs. Cortical adaptation to repeated sensory inputs in the form of a rapid modification in response represents a form of short-term plasticity.

Deficit in adaptation can lead to pathological states, such as autism spectrum conditions. Processing of repeated tactile stimulations was reported to be impaired in autistic people, resulting in a sensory over-responsivity (Blakemore et al., 2006; Marco et al., 2011; Tavassoli et al., 2014), and a decreased adaptation response (assessed by tactile defensiveness, see e.g. Baranek et al., 1997; and Baranek and Berkson, 1994; Puts et al., 2014; Tannan et al., 2008). A strong decrease in GABAergic inhibition has been hypothesised to explain these impairments, based on the observed mutations in genes coding for specific GABA receptor proteins (Fatemi et al., 2002; Hussman, 2001; Ma et al., 2005). Schizophrenic patients may suffer from an impaired adaptation as well (Haigh et al., 2015a; Haigh et al., 2015b).

Adaptation in response to a repeated stimulation has been highlighted at different spatial scales, from the single neuron (see e.g. Li et al., 1993; Ringo, 1996) or individual sensory receptor level (see e.g. Fraser et al., 2006; Zufall and Leinders-Zufall, 2000), at the

level of small neuronal populations (see e.g. Kaliukhovich and Vogels, 2012), up to the level of hemodynamic changes (see e.g. Henson et al., 2002) or electrical activity recorded at the scalp (see e.g. Andrade et al., 2015; Bradley et al., 2014; Löfberg et al., 2013; Van Olphen et al., 1979) for instance, corresponding to the activity of several millions of neurons.

In addition, the neural repetition effects of adaptation have been observed at different temporal scales, lasting from some milliseconds (see e.g. Maravall et al., 2007; Ulanovsky et al., 2004), some tens of second (see e.g. Netser et al., 2011; Ulanovsky et al., 2004; Zufall and Leinders-Zufall, 2000), some minutes (see e.g. Regan and Beverley, 1985) or even some days (see e.g. van Turennout et al., 2000; van Turennout et al., 2003).

Moreover, a wealth of studies has described and characterised the repetition-related reductions of activity by sensory adaptation in different sensory systems. In the auditory system for instance, adaptation is of prime importance to faithfully encode auditory information (Pérez-González and Malmierca, 2014) and temporal integration (May et al., 2015). This phenomenon was observed in AEPs (Ballachanda et al., 1992; Debruyne, 1986; Zhang et al., 2009). More detailed investigations revealed that adaptation occurs at several levels in the auditory pathway (Pérez-González and Malmierca, 2014): as early as in the auditory nerve (Meyer et al., 2007; Smith et al., 1983), in the ventral cochlear nucleus (Loquet et al., 2003; Loquet et al., 2004; Loquet and Rouiller, 2002; Meyer et al., 2007), in the inferior colliculus (Dahmen et al., 2010) and in the auditory cortex (Herrmann et al., 2015; Löfberg et al., 2013; May et al., 2015; Ulanovsky et al., 2004; von der Behrens et al., 2009) among others.

Adaptation plays a key role in the vestibular system as well (Cohen et al., 1992; Gonshor and Jones, 1976a; Gonshor and Jones, 1976b; Lisberger and Miles, 1980; Miles and Eighmy, 1980; Watt et al., 1986) to keep sensitivity to slight linear and angular accelerations of the head in spite of constant and much stronger inputs from gravitational forces.

Olfaction is also subjected to adaptation (Cain, 1974; Dalton, 2000; Kadohisa and Wilson, 2006; McBurney, 1984; Sobel et al., 2000; Stevenson and Wilson, 2007; Stuck et al., 2014; Thomas-Danguin et al., 2014; Wilson and Rennaker, 2009; Yoder et al., 2014; Zufall and Leinders-Zufall, 2000). In brief, the sustained exposure to an odor typically results in a rapid decrease of the receptor sensitivity (Zufall and Leinders-Zufall, 2000)

associated with a rapid decrease of neuronal response in the olfactory bulb and piriform cortex (Dalton, 2000; Kadohisa and Wilson, 2006; Sobel et al., 2000; Stevenson and Wilson, 2007; Thomas-Danguin et al., 2014; Wilson and Rennaker, 2009), leading to an increase in threshold detection of a subsequent odor (Dalton, 2000; Yoder et al., 2014).

Evidence of adaptation was demonstrated in the visual cortex as well (Andrade et al., 2015; Cattan et al., 2014; Hawken et al., 1996; Müller et al., 1999; Ohzawa et al., 1982; Sclar et al., 1985; Wissig and Kohn, 2012). For instance, adapted neurons in the primary visual cortex become more sensitive to orientation change near the adapting orientation, enhancing visual discrimination (Müller et al., 1999; Wissig and Kohn, 2012).

Regarding the somatosensory processing, adaptation characteristics have been already investigated in detail in the rodent whisker-barrel cortex system. More specifically, repeated deflections of facial whiskers in rodents result in a rapid decrease in amplitude of synaptic responses in the trigeminal ganglion cells (Fraser et al., 2006, repetition rate of 1-40 Hz), in the brainstem (Minnery and Simons, 2003), in the thalamus (Chung et al., 2002; Katz et al., 2006; Khatri et al., 2004; Sosnik et al., 2001; Wang et al., 2010) and even more pronounced in the barrel cortex (Adibi et al., 2013; Ahissar et al., 2001; Chung et al., 2002; Garcia-Lazaro et al., 2007; Katz et al., 2006; Khatri et al., 2004; Maravall et al., 2007; Miu et al., 2011; Musall et al., 2014; Wang et al., 2010) with increasing number of stimulations. Short-term depression of thalamocortical inputs to the S1 cortex was proposed to be responsible for the rapid adaptation observed at sensory cortical level (Chung et al., 2002; Katz et al., 2006; Khatri et al., 2004).

There is adaptation in touch processing as well. For instance, we rapidly become unaware of the pressure of our clothes on the body. But as soon as we move an arm, for instance, we immediately and transiently perceive again the sleeve of our shirt. Adaptation in touch processing from the primate hand has been studied in detail along different levels of the somatosensory pathways. For instance, by using microneurography (Vallbo and Hagbarth, 1968), it was demonstrated that a sophisticated processing of touch stimulation begins already in the skin, similarly to early visual processing in ganglion cells (Hubel and Wiesel, 1960; Kuffler, 1953). More specifically, two types of mechanoreceptor afferents with contrasting properties of adaptation of firing rate in response to a single stimulus were discovered: slowly adapting mechanoreceptor afferents (Merkel cell-neurite complexes innervated by SA-I afferents and Ruffini endings innervated by SA-II

afferents) were characterised by a sustained firing rate during skin indentation and exhibited only very mild decline in activity to the indented stimulus. Conversely, activity in rapidly adapting mechanoreceptor afferents (Meissner corpuscles innervated by FA-I or RA afferents and Pacinian corpuscles innervated by FA-II or PC afferents) was rapidly changing and restricted to modifications in stimulation, i.e. the initial presentation of the stimulus and its removal, in the form of brief bursts of action potentials (Bensmaia et al., 2005; Johansson and Vallbo, 1976; Johansson and Vallbo, 1979; Johansson and Vallbo, 1983; Leung et al., 2005; Talbot et al., 1968; Vallbo and Johansson, 1984). This type of adaptation in primary afferents occurs within a second or less and results at least partly from the properties of the encapsulated structures of the mechanoreceptors themselves, such as the particular structure of Pacinian corpuscles (Loewenstein and Skalak, 1966) or, as proposed for vibratory adaptation, from an increase in spiking thresholds produced by cation influx through mechanosensitive ion channels in the receptor membrane of the afferent fibres (Bensmaia et al., 2005; Leung et al., 2005). By recording SSEPs after repeated stimulations (either stimulus pairs or stimulus trains of high frequency), adaptation was observed at several levels in the ascending somatosensory pathway, in the form of component amplitude attenuation, and the effect usually increased going towards higher-order structures: at subcortical level, e.g. in the cuneate nucleus (Kaji and Sumner, 1987 (stimulus repetition rate of 17-1000 Hz); O'Mara et al., 1988; Wiederholt, 1978), in the medial lemniscus (Emori et al., 1991, stimulus repetition rate of 7-330 Hz), in the thalamus (Emori et al., 1991), and in S1 (Allison, 1962 (stimulus repetition rate of 2-330 Hz); Emori et al., 1991; for a review, see McLaughlin and Kelly, 1993; Shagass and Schwartz, 1964 (stimulus repetition rate of 10-1000 Hz)). Later somatosensory ERPs were also decreased in amplitude in response to repeated tactile or electrical stimulations (Kekoni et al., 1992; Kekoni et al., 1997). In MEG studies, adaptation to tactile stimulations of the fingertips in human was characterised by a reduction in the dipole strength generated in S1 as early as the second tactile stimulation (Popescu et al., 2010; Venkatesan et al., 2010, stimulus repetition rate of 2-8 Hz). There is some *in vivo* and *in vitro* evidence that modifications in the patterns of adaptation to repeated stimuli observed in S1 can be explained by intracortical dynamics in S1 itself (Lee et al., 1992; Lee and Whitsel, 1992). Nevertheless, although the large amount of studies reporting adaptation in different sensory systems, the precise neuronal mechanisms underlying this crucial integration process remain poorly understood.

In addition to modification at the neuronal level, adaptation to a constant stimulation was shown to be accompanied by adaptation in perception, namely an increase in detection threshold of the stimulus being repeated (Berglund and Berglund, 1970; Gescheider et al., 1995; Hollins et al., 1990; Hollins et al., 1991; Laskin and Spencer, 1979; Leung et al., 2005; McLaughlin and Kelly, 1993; Wang et al., 2010).

The fingertips are very densely endowed with various mechanoreceptors presenting distinct properties of adaptation to repeated stimulations (Darian-Smith and Kenins, 1980; Johansson and Vallbo, 1979; Johansson and Vallbo, 1983; Paré et al., 2002; Vallbo and Johansson, 1984) and this is correlated with an extended representation of the fingers at the somatosensory cortical level (Merzenich et al., 1987) and an exquisite tactile spatial acuity (Johnson and Phillips, 1981; Sathian and Zangaladze, 1996; Van Boven and Johnson, 1994). Actually, the fingertips may be compared with the fovea within the retina, both regions possessing a great sensitivity resulting from a high density of receptors with small receptive fields and a high sensory magnification factor of the peripheral representation at the cortical level (Hendry and Hsiao, 2013). The integration of sensory inputs originating from the fingertips is of prime importance when small objects are detected, inspected and skillfully manipulated (Johansson and Flanagan, 2008; Johansson and Vallbo, 1976; Johansson, 1998; Johansson and Flanagan, 2009a; Johansson and Flanagan, 2009b; Johansson and Vallbo, 1979; Johansson and Westling, 1990; Johansson and Westling, 1991; Vallbo and Johansson, 1984). Many questions still remain about the crucial phenomenon of sensory adaptation occurring in the somatosensory pathway responsible for processing the cutaneous afferent inputs associated with hand sensorimotor control.

In this study, by measuring the cortical activity at the scalp in 3 adult macaque monkeys, we aimed at characterising the short-term effects of repeated stimulations to the fingertips on the brain activity, by applying a physiologically naturalistic tactile stimulus. We focused on the fingertips as they contain a high density of tactile sensors (Darian-Smith and Kenins, 1980; Johansson and Vallbo, 1979; Johansson and Vallbo, 1983; Paré et al., 2002; Vallbo and Johansson, 1984). Based on the large amount of existing literature about adaptation to repeated sensory stimulations (see above), our working hypothesis was that tactile processing of a large number of repeated sensory stimuli from the distal forelimb in non-human primates was characterised by an adaptation in the amplitude of

cortical activity over time. To test this hypothesis, we measured evoked brain activity by using 32 EEG electrodes at the scalp in response to a large number of repeated light tactile stimulations (jittered around 1 Hz) to the fingertips of the hand in 3 macaque monkeys. Moreover, in order to assess the specificity of processing of repeated tactile stimulations from the fingertips, one monkey was also exposed to repeated electrical stimulations to the median nerve at the wrist (1-Hz repetition rate). By using scalp electrodes we were able to detect the neuronal activity in a large population of neurons to survey the overall changes in signal processing as a consequence of stimulus repetition.

Materials and Methods

Monkeys

This experiment was performed on 3 intact adult female macaque monkeys (Mk-AN: 9 years old at the time of the experiment, weight: 5 kg; Mk-CA: 9 years old at the time of the experiment, weight: 5.6 kg; and Mk-DI: 9 years old at the time of the experiment, weight: 3.6 kg). Mk-AN and Mk-CA were housed in the same conditions as Mk-DI (see **Chapter General Materials and Methods**). All procedures and animal care were conducted in accordance with the Guide for the Care and Use of Laboratory Animals (Committee for the Update of the Guide for the Care and Use of Laboratory Animals and National Research Council, 2011) and were approved by local (Canton of Fribourg) and federal (Swiss) veterinary authorities. The present experiments were covered by the official veterinary authorisations FR 18/10 and 2014_42_FR. The general procedures introduced in **Chapters 1** and **2** regarding the anaesthesia, EEG acquisition and electrical stimulation (except the modifications mentioned below) apply here again, as well as the tactile stimulation protocol described in **Chapter 3**.

EEG and tactile stimulation

Briefly, cortical activity at the scalp was measured by using high-density EEG recording, as already described in detail previously (see Gindrat et al., 2014 in **Chapter 1**, and **Chapter 2**), following repeated peripheral tactile stimulations delivered randomly and individually to the volar pad of the tips of the right thumb, index finger and middle fin-

ger (see **Chapter 3**) in the 3 monkeys under sevoflurane anaesthesia. For reminder, the tappers delivered single pulses of 2-ms-long suprathreshold touch stimulus (square wave pulse) with an interstimulus interval of 1000 ± 250 ms (i.e. jittered around 1 Hz), resulting in a <0.4-mm indentation on the pulp (a 0.4-mm skin indentation was measured in human but because of the thicker fingertip skin in monkeys than in human, the indentation generated in monkeys was probably somewhat less prominent than in human). We used this repetition rate precisely to avoid massive amplitude adaptation to the repeated stimulation. Note that the tappers were always carefully positioned on the monkeys' fingertips by the same experimenter (AG) to reproduce a similar tapper positioning across the monkeys as best as possible.

Between 600 and 850 stimulations were delivered to each fingertip depending on the monkey, the variable number of trials between the fingers in a given monkey resulting from the purely random design of stimulation. The tactile stimulation experiment lasted for about 1 hour (58 min for Mk-AN, 57 min for Mk-CA and 63 min for Mk-DI). The present study is based on the sole first session of EEG recording of repeated tactile stimulus processing for each monkey because we were interested here to investigate in particular the phenomena of adaptation to repeated stimuli and we needed therefore to avoid some learning effects that could have appeared in the following sessions. For reminder, the EEG signals were recorded with a 5-kHz sampling rate.

EEG and electrical stimulation

In parallel with tactile stimulation of the fingertips, the brain activity was also recorded in one monkey (Mk-CA) subjected to a large number of repeated electrical stimulations delivered to the median nerve at the right wrist (2-mA intensity, resulting in a stimulation slightly above the visible motor threshold; 1-Hz repetition rate; square wave pulse; 400-μs duration; total of 1000 stimulations; lasting for 20 minutes, from 149 min after the induction of the anaesthesia). Here again, we used a 1-Hz repetition rate to avoid massive amplitude adaptation to the repeated stimulation that usually appears at high stimulus repetition rate. This measurement on Mk-CA was performed just after completion of the tactile stimulation protocol, during the same EEG session. Except the much

larger number of stimulations delivered and the doubled repetition rate, the rest of the electrical stimulation procedure was similar to the one described in **Chapters 1** and **2**.

Anaesthesia

Atropine was administrated to Mk-AN and Mk-CA as premedication (Atropinum sulf®, 0.5 mg/ml, Sintetica SA, 0.015 mg/kg, i.m.) in order to reduce bronchial secretions. For reminder, EEG recordings were performed under general anaesthesia induced by a facial mask with 6.5% sevoflurane in a mix of 50% air and 50% O_2, without any other pre-anaesthesia. Then, for the continuation of the experiment, the concentration of sevoflurane was reduced and maintained between 5% and 4% (0.8 ℓ/min air; 0.8 ℓ/min O_2) in Mk-AN, between 5.5% and 5% (0.85 ℓ/min air; 0.85 ℓ/min O_2) in Mk-CA and at 4% (0.7 ℓ/min air; 0.7 ℓ/min O_2) in Mk-DI, adjusted on the basis of the cardiac pulse frequency and the respiratory frequency. The complete procedure from the initiation of the anaesthesia until the waking up of the monkey lasted for 3 hours at the most. As the monkeys were anaesthetised, the recordings could be fully insulated from movements, muscular artifacts as well as cardiovascular and autonomic responses (e.g. increase in heart rate and blood pressure) that typically result from the exposure to unanticipated non-noxious tactile stimuli in conscious subjects. We were therefore able to detect very small changes in sensory processing with high sensitivity. Moreover, the use of anaesthesia ensured that the animals were exposed exclusively to purely passive touch stimulation (in case of fingertip stimulation).

Data analysis

Offline data analysis was performed using the Cartool software (Brunet et al., 2011): the EEG signals in response to both tactile and electrical stimulations were re-referenced offline to the average signal from all the scalp electrodes (average reference), band-pass filtered between 1 Hz and 80 Hz, notched at 50 Hz when necessary, and baseline corrected with a pre-stimulation period of 10 ms. We applied here this selective filtering in order to specifically show adaptation processes on relatively low-frequency EEG signal. SSEPs (total average) were then obtained in each monkey by separately averaging (from

-10 ms to +80 ms) all the 600-850 stimuli associated with each fingertip, and all the 1000 stimuli delivered to the median nerve in Mk-CA.

In order to assess the presence of adaptation in processing of repeated stimuli, SSEP signal was then also averaged by using non-overlapping successive blocks of 50 trials. The total average was used to determine the electrode with the largest positive cortical potential. Signal from this electrode was then considered in greater detail in the successive 50-trial averages. In practical terms, the amplitude and latency of the main cortical component were measured in each 50-trial block. Simple linear regressions between the temporal position of the 50-trial blocks in the sequence and the latency, respectively amplitude, of the SSEPs were computed with the corresponding Pearson's correlation coefficient in MATLAB® (MATLAB R2013b).

Results

Adaptation resulting from tactile stimulation of the fingertips

As already demonstrated in **Chapter 3**, repeated light tactile stimulations to the volar pad of the thumb tip, index fingertip and middle fingertip consistently elicited clear brain potentials measured at the scalp in all three monkeys. More specifically, SSEPs were characterised by a prominent positive cortical potential recorded over the contralateral hemisphere with maximal amplitude in the 3 monkeys between 28.6 ms and 31.4 ms after thumb tip stimulation, between 26.2 ms and 30 ms after index fingertip stimulation and between 32.2 ms and 33.2 ms after middle fingertip stimulation (latencies based on the total average of all the trials of a given stimulation site, in each animal, see **Supplementary Figure 1** at the end of te chapter). Based on the latency, we are confident that these potentials were generated at the cortical level (Gardner et al., 1984). There was a large inter-individual variability in the shape of the SSEP waveform, the amplitude and the location of the maximal positivity at the scalp. Note for instance that in Mk-DI specifically, there was a component at around 25 ms fused with the larger subsequent potential for the 3 fingertip potentials (**Supplementary Figure 1**).

In order to assess the presence of adaptation to repeated tactile stimulations of the fingertips, the trials obtained in each monkey were averaged into non-overlapping, successive blocks of 50 of them, separately for each fingertip (**Figure 1A, D**, **Figure 2A** and

Supplementary Figure 2). Interestingly, the presence of two distinct components in Mk-DI became then even more obvious: in middle fingertip-associated SSEPs for instance, the earliest blocks showed a much larger first component at around 25 ms as compared to the 2nd component. The relative amplitude of both components inverted then throughout the successive 50-trial blocks, finally resulting in a larger amplitude of the 2nd component than the amplitude of the first component (**Figure 1D** and **Supplementary Figure 2C**). Because of this special pattern, we considered both the first and the second cortical components for the subsequent analyses after stimulation of the 3 fingertips in Mk-DI.

Figures 1 and **2A-C** present the detailed time course of changes in latency and amplitude of the tactile cortical potential as a function of the temporal position of the 50-trial blocks in the sequence, in response to repeated tactile stimulations of the thumb tip, index fingertip and middle fingertip. Interestingly, one can immediately notice that there were substantial block-to-block variations in the cortical responses to identical stimulus presentations, for every fingertip stimulation, in each monkey.

Simple linear regressions between the temporal position of the 50-trial blocks in the sequence and the latency, respectively the amplitude, of the cortical component were computed for each stimulated fingertip.

As far as the latency of index fingertip SSEPs over time was concerned, we noticed unexpectedly a strongly significant positive relationship between the temporal position of the 50-trial blocks in the sequence and the change in latency of the cortical component from the first 50-trial block for all three monkeys (**Figure 1B,** the coefficients of correlation R and the associated p-values are indicated directly in the figure). Essentially, the more trials were processed, meaning the later from the repeated stimulation onset, the longer was the latency of the tactile cortical potential in the 50-trial averages. The shift in latency ranged from 1.8 ms to 8 ms over the 600-800 trials analysed in each of the three monkeys. In addition, the relationship was highly significant as well when latencies from all animals were considered together. The presence of a significant shift in latency throughout the repeated stimulations to the index fingertip in all monkeys, suggesting temporal adaptation, indicates that this phenomenon was highly conserved across all three animals, although the slope of the regression line, i.e. the first derivative of latency, corresponding to the rate of adaptation, was clearly steeper in Mk-DI (for

both components) than in Mk-AN and Mk-CA (Mk-DI>Mk-AN>Mk-CA, **Table 1**). Moreover, note that here both the first and second cortical components in Mk-DI exhibited similar shift in latency during the time course of the experiment.

A similar pattern of latency adaptation was observed in middle fingertip SSEPs (**Figure 1E**), characterised by significant positive linear regressions between the temporal position of the 50-trial blocks in the sequence and the change in latency of the cortical component in each monkey and in the whole population as well. Here, however, the latency increase was more modest, ranging only from 1.4 ms to 3 ms over the 650-850 trials analysed in each of the three monkeys, meaning less abrupt regression lines than the ones described for index fingertip SSEPs (**Table 1**). Here again, although there was a significant shift in latency in each monkey, the rate of adaptation reflected by the regression slope was variable (Mk-DI>Mk-AN>Mk-CA) and did not covary with the one of index finger SSEPs.

Regarding the evolution of latency in thumb tip-associated SSEPs over time (**Figure 2B**), a significant linear increase in latencies was observed throughout the successive 50-trial blocks in each monkey but Mk-CA, and in the whole population as well, ranging from 3.2 ms to 4.8 ms over the 650-750 trials analysed in Mk-AN and Mk-DI. Note however that the regressions, when significant, were not as significant here as the ones observed after stimulations of the index or middle fingertips (**Table 1**). Second, here again, the rate of adaptation was variable across animals (Mk-AN>Mk-DI). Third, the regression slopes of thumb SSEPs covaried neither with those of index finger SSEPs nor with those of middle finger SSEPs in either animal (**Table 1**).

To sum up so far, we observed a conserved adaptation in latency of the cortical component for the three fingertip stimulations, except for thumb tip SSEPs in Mk-CA, in the form of a linear increase in latency throughout the repeated stimulations of the individual fingertips in each monkey and in the whole population as well. However, equally importantly, the patterns of latency adaptation of the three fingertip SSEPs were variable in a given monkey, the pattern of latency adaptation for a given fingertip SSEP was variable across the monkeys, and there was no consistency in the fingertip SSEPs exhibiting the strongest, the 2nd strongest, or the weakest adaptation, respectively, across the animals (**Table 1**).

Regarding now the amplitude of the cortical component, we intended to avoid inducing a massive amplitude adaptation by delivering the stimulation at a 1-Hz repetition rate. In accordance with our expectation, there was no consistent feature across the animals for any stimulation condition (**Figure 1C, F**, **Figure 2C and Table 1**). Index fingertip SSEPs were characterised by a significant negative linear relationship between the temporal position of the 50-trial blocks in the sequence and the change in amplitude of the cortical component from the first 50-trial block in Mk-CA and Mk-DI, meaning a linear decrease in amplitude over time. Conversely the cortical amplitudes of the index finger SSEPs in Mk-AN and in the whole population were unrelated to the increasing time course of the experiment (**Figure 1C**). Amplitude adaptation was even more restricted after stimulation to the middle fingertip (**Figure 1F**): while there was a significant linear decrease in amplitude over time for the first component in Mk-DI, the same cortical amplitudes in Mk-AN, Mk-CA and the one of 2nd cortical component in Mk-DI were unrelated to the increasing time course of the experiment and neither significant adaptation in amplitude emerged when all the data were pooled. Finally, no significant adaptation in amplitude was observed in any monkey or in the whole population after tactile stimulation to the thumb tip (**Figure 2C**). Simply put, we did not observe any consistent pattern of amplitude adaptation of the cortical potential neither for each of the three fingertips across the monkeys, nor between the three stimulated fingers in a given monkey (**Table 1**).

In sum, in all three monkeys, we saw a consistent latency adaptation or shift in latency of the cortical SSEPs over time in response to repeated tactile stimulations of the thumb tip, index fingertip and middle fingertip although the rates of adaptation were not consistent neither across the animals for any given fingertip nor across fingertips in any given monkey. Conversely, no clear pattern of amplitude adaptation of the cortical potential emerged for any stimulation site.

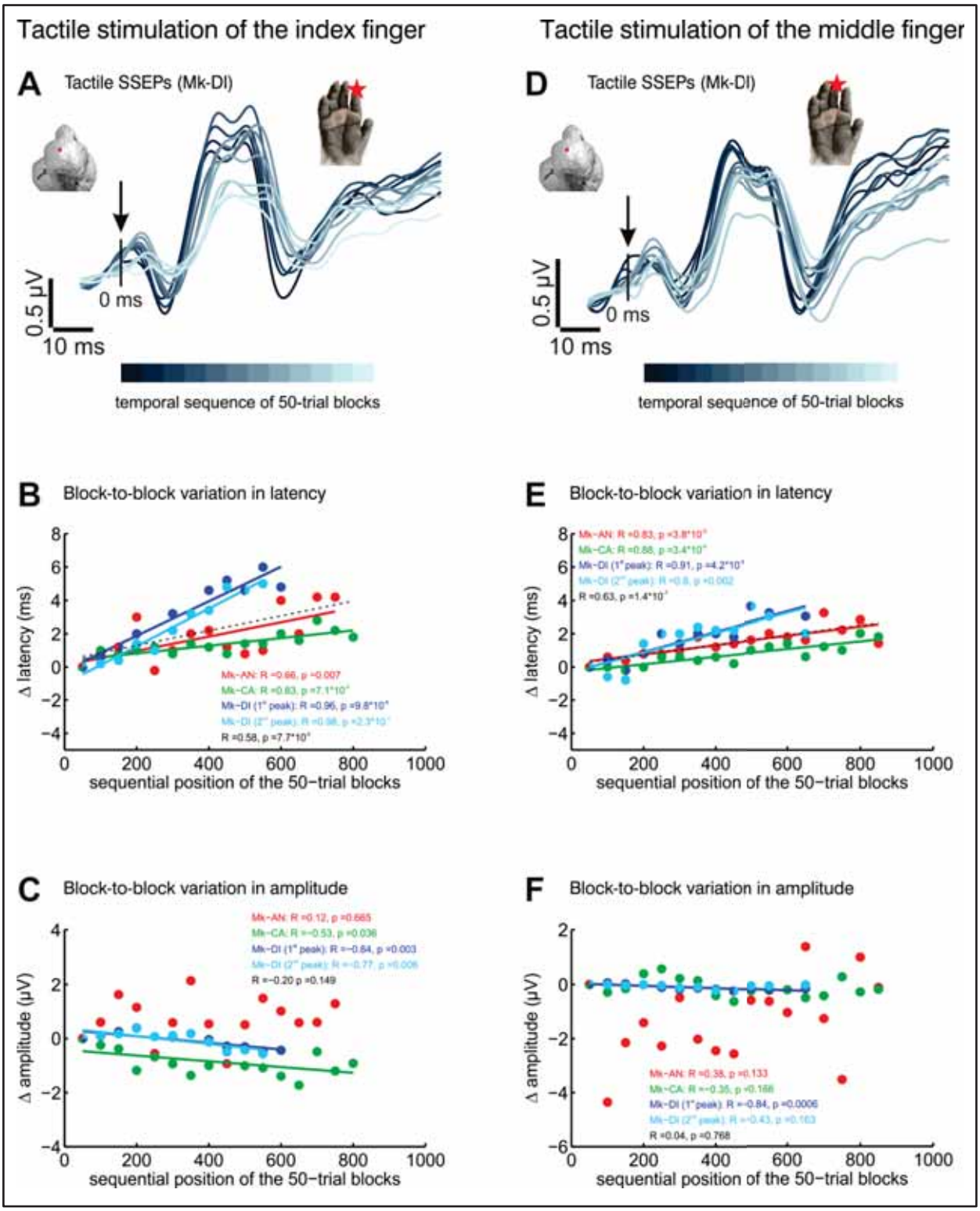

Figure 1: In macaque monkeys, the cortical processing of tactile stimuli from the fingertips is associated with a temporal adaptation in the form of an increasing cortical latency over time.

(A) The cortical potential after tactile stimulation of the right index fingertip was captured with maximal positivity from the contralateral scalp electrode indicated in red in Mk-DI. Each

superimposed trace was obtained by averaging a block of 50 trials. The temporal sequence of the successive and non-overlapping blocks is reflected by the colour gradient (first 50-trial block in dark blue to last 50-trial block in light blue). The arrow above the traces points at the tactile stimulation onset (i.e. 0 ms). (B) Correlation between the temporal position of the 50-trial blocks in the sequence, during tactile stimulation, and the change in latency of the cortical component assessed in 50-trial blocks. The latency of the first 50-trial average in ms was considered as the reference and the values of the subsequent averages were then expressed in the form of variations (Δ ms) from this initial latency. Each point represents a block of 50 trials in a given monkey. Each colour corresponds to a monkey (Mk-AN in red, Mk-CA in green, 1st and 2nd cortical components in Mk-DI in dark, respectively light blue). Significant regression lines with Pearson's correlation coefficients (R) and associated p-values are indicated for each animal with the same colour code and for the whole population (black dotted line and black annotation). (C) Correlation between the temporal position of the 50-trial blocks in the sequence, during tactile stimulation, and the change in amplitude of the cortical component assessed in 50-trial blocks. Similarly here, the amplitude of the first 50-trial average in µV was considered as the reference and the values of the subsequent averages were then expressed in the form of variations (Δ µV) from this initial amplitude. Same conventions as in (B). Panels (D), (E) and (F): same as (A), (B) and (C), but for tactile stimulation of the right middle fingertip. Note that we used the same latency scale and range in panels (B) and (E), and the same amplitude scale in panels (C) and (F).

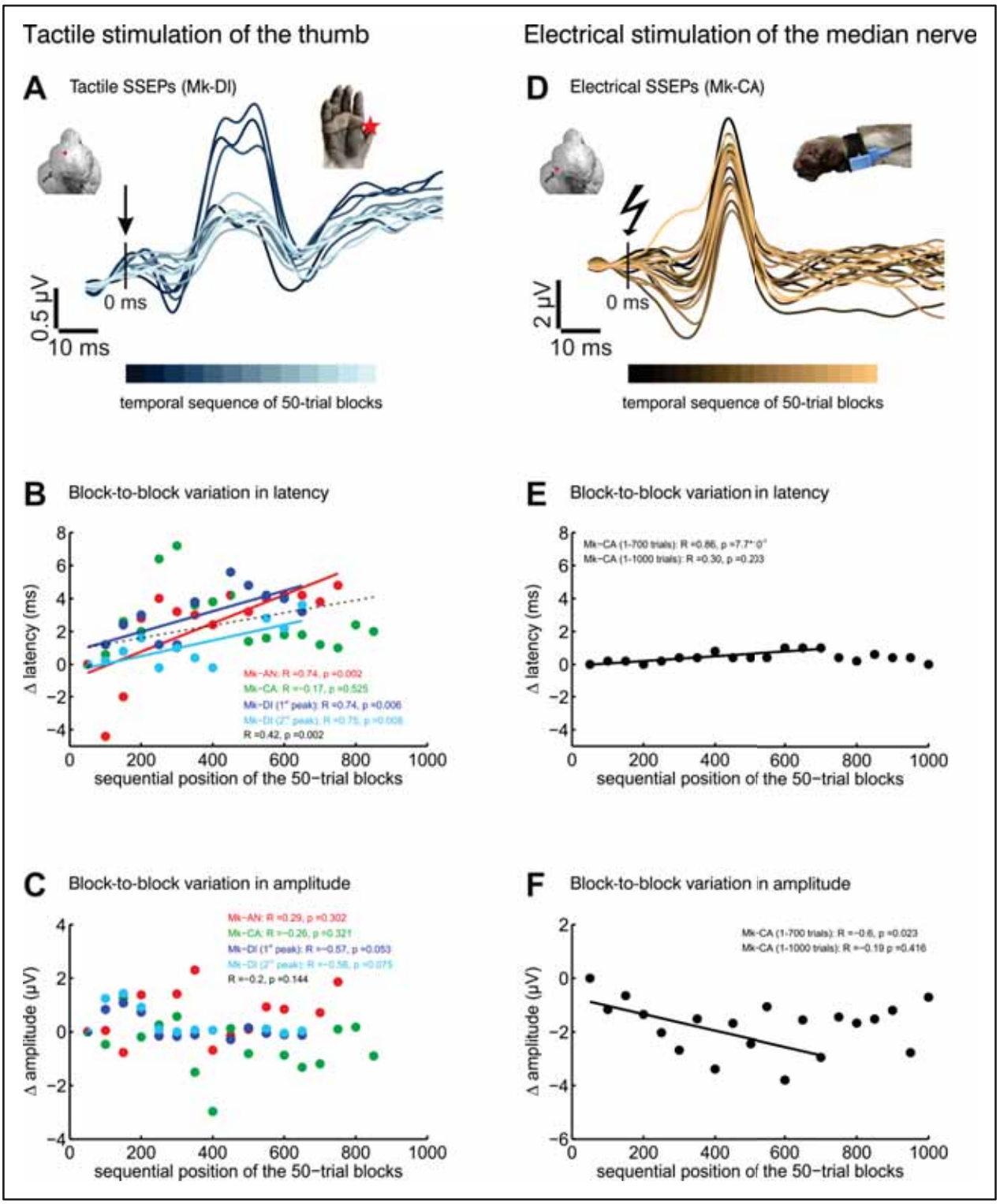

Figure 2 : Latency and amplitude adaptation in thumb tip SSEPs and median nerve SSEPs

Panels (A), (B) and (C): same as (A), (B) and (C) in Figure 1 but for tactile stimulation of the right thumb tip. (D) The cortical potential in response to electrical stimulation of the right median nerve at the wrist was captured with maximal positivity from the contralateral scalp electrode indicated in red in Mk-CA. Each superimposed trace was obtained by averaging a block of 50 trials. The

temporal sequence of the successive and non-overlapping blocks is reflected by the colour gradient (first 50-trial block in black to last 50-trial block in light copper). The zigzag arrow above the traces points at the electrical stimulation onset (i.e. 0 ms). (E) Correlation between the temporal position of the 50-trial blocks in the sequence, during electrical stimulation, and the change in latency of the cortical component assessed in 50-trial blocks in Mk-CA. Coefficients of correlation were computed both across the first 700 trials and across all trials. Same conventions as in Figure 1B. (F) Correlation between the temporal position of the 50-trial blocks in the sequence during electrical stimulation and the change in amplitude of the cortical component assessed in 50-trial blocks in Mk-CA. Same conventions as in (E) and in Figure 1B. The same latency scale and range as in Figure 1 was applied here in panels (B) and (E). Similarly, the same amplitude scale as in Figure 1 was applied here in panels (C) and (F).

		thumb tip	index fingertip	middle fingertip
Mk-AN	Δ ms/trial	8.61 **	4.3 **	2.74 ***
	Δ µV/trial	1.18	0.44	2.27
Mk-CA	Δ ms/trial	-1.27	2.3 ***	2.25 ***
	Δ µV/trial	-0.99	-1.06 *	-0.47
Mk-DI (1st component)	Δ ms/trial	6.22 **	10.35 ***	6.01 ***
	Δ µV/trial	-1.29	-1.23 **	-0.45 ***
Mk-DI (2nd component)	Δ ms/trial	4.74 **	11.27 ***	5.87 **
	Δ µV/trial	-1.52	-1.44 **	-0.19

Table 1: Slope, i.e. first derivative, of the regression lines computed between the temporal position of the 50-trial blocks in the sequence and the changes in latency (Δ ms/trial), respectively amplitude (Δ µV/trial), of the cortical potential after tactile stimulation of the right thumb tip, index fingertip and middle fingertip, in the 3 monkeys. Both first and second cortical components were considered in Mk-DI. For the sake of readability, all values were multiplied by 10^3. The significance of each regression slope is indicated: * : p <0.05, ** : p <0.01, *** : p <0.001.

Adaptation resulting from electrical stimulation of the median nerve at the wrist

In addition to tactile stimulation of the fingertips, Mk-CA was subjected to repeated electrical stimulations (n =1000) of the right median nerve at the wrist. With a stimulation frequency at 1 Hz, the major component of electrical SSEPs was a large positive cortical potential recorded with maximal amplitude over the contralateral parietal hemisphere at a mean latency of 23.2 ms (latency based on the total average of all trials). The same measurements of latency and amplitude of the cortical component in the successive 50-trial blocks were applied here, as in tactile SSEPs. The detailed time course of changes in latency and amplitude of the cortical potential as a function of the temporal position of the 50-trial blocks in the sequence, after repeated electrical stimulations of the median nerve, is presented in **Figure 2D-F**. Here again, the plots revealed some block-to-block fluctuations in the cortical responses to identical electrical stimulations.

In contrast to tactile stimulations, no consistent pattern of latency change from the first to the last 50-trial block was observed over the successive averages ($R = 0.30$, $p = 0.203$) (**Figure 2E**). Nevertheless, by considering the first 700 trials only, a significantly positive linear relationship was visible between the temporal position of the 50-trial blocks in the sequence and the latency change ($R = 0.86$, $p = 7.7*10^{-5}$), corresponding to a 1-ms latency increase over the first 700 trials analysed in Mk-CA. A magnification of the graph shows this pattern more clearly (**Supplementary Figure 3A**).

Similarly, the change in amplitude of the cortical component from the first to the last 50-trial block was not related to the increasing number of previously processed trials ($R = -0.19$, $p = 0.416$). But we observed a significant strong decrease in the amplitude of the potential from the first 50-trial block in the course of the first 700 trials only, with a maximal decrease of 3.8 µV ($R = -0.6$, $p = 0.023$) (**Figure 2F**). A magnification of the graph is presented in **Supplementary Figure 3B**.

To sum up, repeated electrical stimulations of the median nerve at the wrist induced a latency increase and an amplitude decrease of the cortical component over time but only visible in the course of the first 700 trials. Conversely, the processing of additional trials did not follow the same pattern because the latency and amplitude changes became again smaller. But more importantly, note that the latency shift observed here is much

smaller than the one described in the processing of tactile stimulation to the fingertips. On the other hand, the adaptation in amplitude is much stronger in the electrical stimulation processing than the one observed in the tactile stimulation processing when it was significant.

Discussion

Here, by using either tactile stimulation of the fingertips or electrical stimulation of the median nerve at the wrist in 3 intact adult macaque monkeys, we demonstrated that brain activity was dynamically modulated over time and that both types of repeated stimulations were able to induce cortical adaptation to a repeated stimulus. More specifically, the major finding of this study was that adaptation to repeated peripheral stimulations (about 1-Hz repetition rate) was not limited to the typical depression of brain potential with the increasing number of stimulations, but a latency adaptation did develop over time as well. In particular, the repeated tactile stimulation paradigm elicited a consistent prominent latency increase of cortical activity over time although the rates of adaptation did not correlate neither across the animals for any given fingertip SSEP nor across fingertip SSEPs in any given monkey. This suggests that latency changes were independently regulated for each tactile stimulus location. A much more modest latency increase emerged by applying 700 electrical stimulations to the median nerve at the wrist. As intended, no consistent pattern of amplitude adaptation of tactile elicited brain signal over time emerged for any finger stimulation site. Conversely, we observed a prominent amplitude decrease in cortical activity in the course of 700 electrical stimulations. Our results suggest that there were different adaptation patterns in S1 associated with each somatosensory processing from the upper limb. Moreover, remarkably, the adaptation processes described here were observed by using a low stimulus repetition rate as compared to most studies interested in this topic.

About the use of *adaptation* rather than *fatigue* or *habituation*

Following repeated peripheral stimulations, several types of experience-dependent plastic modifications of the sensory response may appear in the nervous system, namely ad-

aptation, fatigue and habituation. In our study we favoured the term *adaptation* over the other two for the following reasons:

The *adaptation* can be distinguished from the *fatigue* in the sense that a sensory receptor being adapted to a repeated unchanging stimulus is still able to answer *very rapidly* to a novel stimulus (Adrian and Zotterman, 1926) whereas a neuron showing fatigue cannot (Matthews, 1931). The fatigue increases the threshold of the cells by inducing depletion of neurotransmitters, leading to the complete abolition of neurotransmission (Burgess and Perl, 1973). This distinction is commonly used in the auditory system for instance (Eggermont, 1985). With the repetition rates used in the present study (1 Hz), it is highly improbable that we created a fatigue of the peripheral receptors. Rather this phenomenon usually occurs at high repetition rate. Moreover, after electrical stimulation, we observed adaptation during the first 700 trials but this trend then completely disappeared in the next 300 trials, followed by a re-increase in amplitude, and a re-decrease in latency, tending towards the values observed at the beginning of the episode of repeated stimulations. This clearly indicates that, at least for electrical stimulation, the neuronal populations were still able to respond after a large number of repeated stimulations.

The *adaptation* can be distinguished from the *habituation* in the sense that the latter usually refers to a perceptual and behavioural phenomenon with a behavioural response decrement after repeated stimulations (Groves and Thompson, 1970; Rankin et al., 2009; Thompson and Spencer, 1966) and therefore is more closely linked with learning and cognitive processes (Pérez-González and Malmierca, 2014). Habituation occurs with repeated stimuli as well but corresponds to an effect of attention (Cheung et al., 2008). The phenomenon of habituation is illustrated for instance by the loss of awareness of a ticking clock over time when we shift our attention away from the clock. If we focus back towards the clock, we immediately become aware again of the ticking sound. This clearly indicates that habituation does not result from either stimulus failure or receptor desensitisation but is rather an effect of attention.

Mechanoreceptors involved in tactile SSEPs from the fingertips

By dealing with tactile stimulation and sensory adaptation, a first important issue is to determine which mechanoreceptors were actually activated by the touch stimulus. The very punctate stimulation used here (single pulse of tactile stimulation lasting for 2 ms, <0.4-mm-indentation, square wave pulse, repetition rate jittered around 1 Hz) activated most probably predominantly FA-II receptors (Pacinian corpuscles) and to a lesser extent FA-I receptors (Meissner corpuscles) due to the very high frequency content of every punctate stimulus (estimated at about 2000 Hz) (Prof. Roland Johansson, personal communication, April 24, 2015). Contrary to what was traditionally thought, FA-I receptors respond on a much broader range of frequency (up to >1000 Hz), explaining why they could contribute to the tactile processing here as well, though a larger skin deformation (i.e. a higher threshold) is needed for FA-I receptors than for FA-II receptors to be activated (Prof. Roland Johansson, personal communication, April 24, 2015).

Another important concern is about the adaptation of the mechanoreceptors themselves to repeated stimulations. Here, by using an interstimulus time interval of 1000 ms ± 250 ms and randomly delivered stimuli across the 3 fingertips, meaning that the interstimulus interval for a given finger might have been actually much longer than 1000 ms ± 250 ms, we are confident that the repeated stimulations probably did not induce any adaptation at the level of the firing rate of the activated mechanoreceptors from one trial to the next because the interstimulus time interval was actually very long (Prof. Roland Johansson, personal communication, April 24, 2015).

Inter-individual variability in tactile SSEPs from the fingertips

As already reported in **Chapter 3**, tactile stimuli applied to the volar pad of the fingertips of non-human primates were shown to be effective in evoking cortical SSEP signals. But by considering the **Supplementary Figures 1** and **2**, one can immediately notice that there was a large inter-individual variability in the SSEPs (amplitude, latency, shape of the waveform). This was associated with inter-individual variability in the rate of latency and amplitude adaptation as well (see **Table 1**), suggesting a subject-dependent pattern of adaptation. One can probably attribute this variability to a large extent to some inter-individual differences in intrinsic properties of the nervous system, such as

the density of mechanoreceptors at the fingertips and the concomitant threshold of sensation (Löfvenberg and Johansson, 1984), the extent of the hand representation at the cortical level (Jain et al., 1998; Juliano and Whitsel, 1985; Merzenich et al., 1987; Qi and Kaas, 2004), the neuroanatomical organisation of the brain (Krubitzer et al., 2004; Krubitzer and Seelke, 2012), the orientation of current sources within the brain, the background activity of the brain itself, or the signal-to-noise-ratio of the signal, for instance. In addition, one can expect that every monkey processed tactile inputs from the fingertips in a use-dependent manner, as human does, leading to large inter-individual variability in the SSEPs (see for instance the large variability in the individual human potentials in **Chapter 6**, **Figure 2D** and **E** and **Figure 3A** and **B**; and in **Chapter 7**, **Figure 1C** and **Figure 2A** and **D**). Moreover, one cannot exclude that the inter-individual variability in the scalp tactile potentials exhibited by the 3 monkeys resulted, to a lesser extent, from variability in the positioning of the EEG cap at the scalp across the monkeys, or from slight differences in the position of the tappers across the 3 animals, even though they were always carefully positioned by the same experimenter (AG) to reduce such bias.

One could consider this large inter-individual variability in the data as a drawback but it is actually the opposite. The inconsistency in waveforms across the three animals goes really in favour of meaningful EEG signals reflecting a true biological process within the brain in response to repeated tactile stimulations, i.e. the processing of a naturalistic stimulus. This constitutes in fact the power of tactile SSEPs as compared to the more standardised and reproducible potentials and voltage topographies at the scalp obtained after electrical stimulation to the median nerve for instance (see e.g. Gindrat et al., 2014 in **Chapter 1**). Simply put, the more variability in a signal, the more it may potentially reflect the influence of variable external attributes (see for instance **Chapters 6** and **7**), increasing the relevance of the brain signal.

In spite of the large inter-individual variability in the tactile signal associated with the fingertips, the consistency of a strong latency shift, but not amplitude shift, over the time course of the tactile stimulations to the fingertips exhibited by all the animals for the 3 stimulation sites (except Mk-CA for the thumb tip SSEPs) suggests that it is actually a unique and specific feature to the tactile stimulation and can be considered as the "corti-

cal signature" of fingertip tactile stimulation (Juliano and Whitsel, 1985; Whitsel and Juliano, 1984).

Note that the tactile cortical SSEPs observed here are not identical to those described in **Chapter 3** simply because the filter settings, the artifact rejection settings and the number of trials averaged, among others, were different in both studies. The same is true for the median nerve cortical SSEPs described here as compared to those shown in **Chapters 1** and **2**.

Intra-individual variability in tactile SSEPs and in adaptation patterns across the fingers

The repeated tactile stimulations resulted in distinct averaged SSEPs (see **Supplementary Figure 1**) and in distinct rates of adaptation, both in latency and amplitude (see **Table 1**), across the three fingertips in a given monkey. Interestingly, the middle finger cortical SSEP had a longer latency than the thumb or index finger cortical SSEPs, consistently in all 3 monkeys. Moreover, the thumb tip exhibited less consistency in adaptation as compared to the other two fingertips. These results suggest, first, that tactile processing and adaptation were finger-specific and, second, that tactile processing and adaptation associated with each fingertip reflected complex neural processes that are not easy to interpret. Namely, we expect that the potentials associated with the 3 fingertips originate from a very close cortical region in S1.

A first hypothesis to explain the differences in averaged SSEPs and adaptation across the fingertips relies on use-dependent plasticity. Namely, we expect that the variations in tactile processing and in sensory adaptation across the fingertips most probably reflect differences in sensorimotor use of the different fingers experienced by the monkeys in their daily life (see e.g. Jenkins et al., 1990; Jenkins and Merzenich, 1987; Nudo et al., 1996; Recanzone et al., 1992; Wang et al., 1995), very similarly to what was observed in human (see e.g. **Chapter 6** and **7**). In particular, the thumb tip and index fingertip are usually more involved than the middle fingertip in fine skilled hand movements such as the precision grip, leading to different sensory experiences associated with each finger and therefore to different SSEPs.

Inter-finger variations in the density of mechanoreceptors at the fingertips may play a role as well. More specifically, we can expect that, for similar stimulated skin extents, the activity elicited from the thumb tip was different to the activity from the index and middle fingertips, respectively, given that the density of Pacinian corpuscles, in particular, is larger on the thumb tip than on the other fingertips (Paré et al., 2002). This may then lead to differences in the mechanoreceptor representation of the three fingers in S1. Note that although the stimulations were completely randomly delivered to the three fingertips, each finger received nearly equal number of stimulations in a given monkey, suggesting that meaningful differences in the amount of tactile inputs provided to each finger cannot be expected. But then, how differences in the finger representation in S1 reflect in variability of sensory adaptation across the fingers is not known.

Are there differences in the mechanisms of central integration along lemniscal and thalamocortical systems across the three fingers? Probably, but the present data do not allow to answer this question.

Finally, we cannot completely rule out that the different averaged SSEPs and the different rates in adaptation exhibited by the 3 fingertips in a given animal result from differences in the signal-to-noise-ratio in the SSEPs associated with each fingertip. In the same way, we cannot be fully sure that we positioned the tappers to the exactly same position across the 3 fingertips of an animal.

Even though we are not fully confident about the origin of the differences observed in adaptation patterns across the fingertips, our results further confirm the uniqueness of the thumb among the other fingers, as already shown in macaque monkeys in **Chapter 3** and as will be presented in human in **Chapter 6**.

Differences between adaptation after tactile versus electrical stimulation

In this study, we compared adaptation properties of both tactile stimulation and electrical stimulation because, as already reviewed in **Chapters 2** and **3**, both stimulation paradigms (i.e. naturalistic vs artificial stimulation) have different advantages and drawbacks (for a review, see e.g. McLaughlin and Kelly, 1993). Regarding adaptation to repeated stimulations, we observed here that both processings were characterised by different patterns, suggesting that adaptation mechanisms were highly specific to the in-

volved pathways. More specifically, tactile SSEPs were characterised by a stronger temporal adaptation than electrical SSEPs. Conversely, electrical SSEPs showed a more pronounced amplitude adaptation, at least in the first part of the stimulation episode. This suggests that the strong latency shift described here is specific to tactile stimulation. Discrepancies in adaptation patterns following either a repeated artificial electrical stimulation or a repeated naturalistic mechanical stimulation were already observed in human S1 (Pratt et al., 1980).

Of prime importance here is the fact that by bypassing the sensory receptors of the skin (Brown, 1984; Starr et al., 1982), the electrical stimulation prevents a natural activation of the somatosensory system and engages different types of sensory afferent and efferent fibres in abnormal patterns (McLaughlin and Kelly, 1993). The differential patterns of cortical adaptation as a function of the stimulation paradigm may partly result from differences in the afferent volleys produced in the peripheral nerve by those two types of stimulation because of the contributions of different neuronal fibres (Larsson and Prevec, 1970). Tactile stimulation to the fingertips specifically activated the rapidly adapting mechanoreceptor afferents, i.e. the FA-II receptors predominantly, and the FA-I receptors to a lesser extent. Conversely, an electrical stimulation also activates some other large myelinated sensory fibres with low activation threshold conveying proprioception, thermal and painful information (Allison et al., 1991; Aminoff and Eisen, 1998; Desmedt, 1987; Legatt and Benbadis, 2014; Walsh et al., 2005; York, 1985). These discrepancies in inputs are expected to contribute to the large differences observed between tactile and electrical SSEPs. More specifically, a repeated tactile stimulation activates a relatively homogeneous population of afferent fibres that project to specific and highly focal cortical regions with spatially restricted dynamic mechanisms because neuronal networks are engaged in a more natural manner than after electrical stimulation of a peripheral nerve (McLaughlin and Kelly, 1993). Moreover, the unspecific activation of fibres by electrical stimulation is known to increase abnormal afferent interactions (primarily inhibition of some cutaneous afferent inputs by lateral inhibition from the faster muscle afferents). Conversely, mechanical stimulation was not demonstrated to trigger similar abnormal interactions (Burke et al., 1982; McLaughlin and Kelly, 1993; Schmidt, 1973; Willis and Coggeshall, 2004). This effect may influence adaptation at subcortical and cortical levels.

Surprisingly, we observed significant linear adaptation in amplitude and latency only over the first 700 trials of electrical stimulation. Then the pattern over the last 300 trials completely changed to tend again towards cortical amplitude and latency values observed at the beginning of the stimulation episode. Nevertheless, even a power fit failed to represent all the data, both for amplitude and latency values. Therefore, we chose to represent here only the first significant linear relationship. Nevertheless, we cannot completely rule out that the electrical stimulation partly failed during the last 300 stimulations, even though we were still able to observe a regular twitch of the thumb at the end of the episode of repeated electrical stimulations, making this hypothesis not very likely. Nonetheless, for reminder, these observations are based on a single monkey and need to be confirmed.

Latency adaptation in the literature

Most studies reporting adaptation of the cortical response to repeated stimulations commonly used a stimulus repetition rate that was substantially larger than the one we used in the present study (see the examples provided in the *Introduction*) and adaptation was usually characterised by an amplitude decay over time. Only few studies reported adaptation in the time domain as well.

A latency shift specific to each component was observed at the level of single trial in BAEPs already after 5 trials (10-ms interstimulus interval) and this adaptation was maintained for clicks of different intensities (Ballachanda et al., 1992). The authors explained their results on the basis of the specific firing profile of the several populations of neurons involved in each component being adapted.

Gandevia and Ammon (1992) performed continuous electrical stimulation of the index finger in human over as long as 7 days (8-10 hours a day) and reported a progressive increase in the latency of the potential recorded over the contralateral sensorimotor hand representation at the scalp when brain activity evoked by electrical stimulation of this specific finger was regularly recorded in the course of the 7-day stimulation period (total increase of about 0.8 ms-1 ms). Conversely, no change in amplitude of the cortical potential was observed. At the same time, changes in peripheral conduction velocity and saturation of cortical activity by constant afferent inputs were excluded. The latency

shift over the 7 days was hypothesised to reflect gradual modification in processing along the somatosensory pathway.

Equally interestingly, in a study about auditory late EPs to repeated tone bursts, a reduction in amplitude accompanied by a reduction in latency in the time course of the EPs over time was reported (Zhang et al., 2009). The authors proposed that the decrease in latency over time might result from a faster recovery speed from adaptation and/or refractoriness in neurons with shorter latencies as compared to those neurons firing with longer latencies.

Hypotheses about the origin of adaptation

Adaptation to repeated stimulations has been traditionally considered as the reduction of brain activity when stimuli were repeated with a high repetition rate. Although the underlying neural mechanisms are still not fully understood, two models have been proposed to explain such diminution in amplitude of brain response (Grill-Spector et al., 2006): (i) a fatigue model characterised by a proportionally equivalent decrease in the response of all neurons in the involved neuronal networks, with repeated stimulations, maybe by firing-rate adaptation, or reduction in synaptic efficacy (Finlayson and Cynader, 1995). This results in a reduction of the population activity without any change in the temporal domain; (ii) a sharpening model where fewer neurons –the ones that were initially optimally tuned to the repeated stimulation– in the involved neuronal networks are still responding after repeated stimulations. Conversely, the neurons initially coding for irrelevant features of the stimulus are inhibited. This results in a reduced number of activated neurons with the repeated stimulation. Lateral inhibition may contribute to some repetition-induced cortical dynamics.

Here, we will focus primarily on *tactile* SSEPs because we were able to reproduce our results in three animals. Conversely, *electrical* SSEPs were obtained from a single monkey and these results still need to be confirmed.

Tactile stimulation repetition did not induce parallel evolutions of latencies and amplitudes of the cortical component over time. More specifically, while there was a consistent and significant linear increase in the latency of cortical component over the temporal position of the 50-trial blocks in the sequence, the amplitude of this potential did

not display consistently such significant linear relationship over time, but rather either a modest linearly increase or a modest linearly decrease over time, depending on the stimulated fingertips and on the monkeys. Thus, the amplitude and the latency of tactile SSEPs can be clearly considered as two separate measurements probably reflecting different underlying mechanisms, as previously suggested for VEPs (von Knorring et al., 1978).

The exact mechanism accounting for the specific shift in latency of the cortical potential found here is not fully understood. Actually, the shift in latency was unexpected based on the large body of available literature about cortical adaptation to repeated stimulations. Moreover, we used a relatively low stimulus repetition rate precisely to avoid massive cortical adaptation. In the following sections, we will consider some of the mechanisms that may underlie the results described in this study. Note that they remain hypotheses and that they are not mutually exclusive.

Side-effect of anaesthesia ?

The first hypothesis is linked to the anaesthesia. Namely, one may argue that the patterns of adaptation described here merely reflect a side-effect from the anaesthesia used to record EEG. We are aware that anaesthetics, and sevoflurane more specifically here, do have a profound impact on brain activity (see e.g. Boisseau et al., 2002; Jantti et al., 1998; Ku et al., 2002; Rehberg et al., 1998; Rytky et al., 1999; Schwender et al., 1998; Vaughan et al., 2001; Young and Apfelbaum, 1995). For instance, SSEPs recorded at the level of EEG burst suppression with sevoflurane anaesthesia were characterised by a larger positive component with longer latency in patients under anaesthesia as compared to the same component recorded in the same awake patients while all other components usually present in awake patients were largely reduced during anaesthesia (Jantti et al., 1998; Rytky et al., 1999).

We cannot objectively rule out a side-effect of the anaesthesia but there are several lines of evidence making this hypothesis unlikely. Comparing the adaptation patterns across the animals is not suitable because the anaesthesia could have induced in each animal a very specific adaptation pattern that may not be correlated between the animals, depending on the individual intrinsic responsiveness to the anaesthesia. Nevertheless, it

would have been highly suspect if we had observed the very same adaptation in latency and the very same adaptation in amplitude in all monkeys, which is not the case. This could have indicated for instance that our data were contaminated by noise. Similarly, a direct comparison between tactile SSEPs and electrical SSEPs is of course not appropriate here because both processings are so much different (for more information, see the *Discussion* in **Chapter 3**) that we could expect they can be differently affected by anaesthesia.

The time interval between the induction of the anaesthesia and the actual beginning of the tactile stimulation was variable across the animals (64 min in Mk-AN, 77 min in Mk-CA, 90 min in Mk-DI), corresponding to the time needed to prepare the monkey for the experiment (EEG cap installation, impedance minimisation, etc, see **Chapter 1** and **Chapter 2** for greater detail). Even so, when it was significant in all three animals, the slope of the regression lines of latency changes (Mk-DI>Mk-AN>Mk-CA for both index and middle finger SSEPs) did not correlate with that time interval from anaesthesia induction, suggesting that the patterns of adaptation did not depend on the time interval from anaesthesia induction. However, one can still oppose that each monkey is expected to react differently to the anaesthesia, meaning that variable concentrations of sevoflurane and/or variable time intervals are needed across the animals to obtain probably the same anaesthesia depth.

More interestingly, our best control, at least for tactile SSEPs, lies in the direct comparison between tactile potentials elicited from the 3 fingertips in a given monkey. Namely, in case of a systemic effect induced by the anaesthesia on the general brain activity, we would have expected very parallel patterns of latency, respectively amplitude, adaptation in terms of slope of the regression lines for all the 3 fingertip-associated SSEPs in a given monkey because the processes underlying the generation of these potentials are expected to be similar. To put it another way, the anaesthesia in a given monkey should have affected the potential associated with the 3 fingertips very similarly. Here, the absence of any consistent pattern of latency, respectively amplitude, adaptation across the three stimulation sites in each animal (see **Table 1**) strongly suggests that block-to-block amplitude and latency changes were very finger-specific. Consequently, these observations are really in favour of a true biological process within the brain in response to repeated tactile stimulations of each fingertip.

In addition, in Mk-AN and Mk-CA, the concentration of delivered anaesthetic was gradually decreased in the course of the experiment on the basis of vital parameters (Δ =-1% in Mk-AN and Δ =-0.5% in Mk-CA in total). Nevertheless, we observed in both animals a significant linear increase in SSEP cortical latency over time, like in Mk-DI for which the whole EEG recording was performed under constant anaesthetic level. It is known from the literature that cortical SSEP latencies increase and cortical SSEP amplitudes are depressed with increasing concentration of sevoflurane in human (Boisseau et al., 2002; Ku et al., 2002; Rehberg et al., 1998; Schindler et al., 1996; Schwender et al., 1998). Therefore, in case the anaesthesia would have strongly influenced SSEP potentials in the present study, we should have observed a decrease of latency going with an increase in amplitude over time, at least in Mk-AN and Mk-CA, but we actually observed the opposite pattern regarding cortical latency while no systematic amplitude modifications were observed in each animal for the 3 fingers. In sum, the increasing latency shift and the inconsistency in amplitude changes over recording time go really in favour of a true biological process in response to repeated tactile stimulations of the fingertips instead of anaesthesia-induced side-effects.

Given that it would be difficult to reproduce the same experiment in awake monkeys (the presence of movements and muscular artifact would require to increase the number of trials in order to get a good signal-to-noise ratio, in addition to the need to restrain the monkeys' arm for a long time period (at least more than 1 hour) and the impossibility to ensure a purely passive tactile stimulation), the ultimate proof against anaesthesia-induced side-effects would be provided by performing the same EEG acquisition by using another type of anaesthesia which is known to induce very different effects on brain activity, such as propofol (for greater detail, see e.g. Banoub et al., 2003; Boisseau et al., 2002). Then in case we could reproduce the same consistent latency shift as described here, we would be even more confident about the negligible impact of anaesthesia on the adaptation patterns.

To sum up, our findings suggest that latency and amplitude adaptations were primarily a function of the stimulation site and not merely a function of the consciousness state linked to the anaesthesia. Even though there may have been some effects of the anaesthesia on SSEPs, still we observed some interesting different patterns of adaptation across the 3 fingertips in every monkey.

Peripheral effect ?

Adaptation may already take place at the level of the receptor itself (see e.g. Fraser et al., 2006; Zufall and Leinders-Zufall, 2000). In case it was true here as well, we hypothesise that the passive spread of the receptor potential from the nerve ending (mostly Pacinian corpuscles) of the primary somatosensory neuron to the first node of Ranvier may change over time. To elaborate, the passive electrical propagation of the receptor potential along this very short but unmyelinated dendrite segment may become slower with stimulus repetition, resulting in a progressive decrease in the rising slope of the receptor potential. As a result, the generator potential may be created progressively later at the first node of Ranvier and the generation of an action potential, in case the threshold is reached, may be progressively delayed as well. In sum, the whole transduction may be progressively delayed with stimulus repetition.

Nevertheless, we are confident that the mechanoreceptors activated by the touch stimulus used in the present study (namely FA-II predominantly and FA-I to a lesser extent) did not themselves experience adaptation to the repeated stimuli because of the very long interstimulus time interval (Prof. Roland Johansson, personal communication, April 24, 2015). Actually, we may expect to observe adaptation at the level of the mechanoreceptor itself by using a high stimulus repetition rate, for instance 100 Hz.

Changes in the pattern of contribution of neuronal populations to the cortical component ?

SSEPs reflect the sum of electrical activity within several simultaneously active but anatomically or physiologically separate populations of cortical neurons (Gloor, 1985; Kandel et al., 2013; Speckmann et al., 2011). Let a cortical potential be generated by the combined contribution of several distinct populations of cortical neurons, each firing at a very precise latency. The sum of all these activities constitutes the cortical potential recorded at the scalp. Regarding tactile SSEPs, we reported here a consistent shift in latency while the amplitude of the cortical potential was less strongly modified. This means that the total number of neuronal populations involved in the generation of the cortical potential might have remained largely stable (some modifications are possible because a slight shift in amplitude was sometimes observed, though not as prominent as

the shift in latency) but the temporal sequence of their activation might have been modified by the repeated stimulation. We think that the following mechanisms may be responsible for these repetition-induced modifications:

First, we propose that repeated tactile stimulations may have led to a progressive delayed activation of those neuronal populations that were normally responding with short latency, i.e. contributing to the early portion of the SSEP component generated by the synchronous activation of all neuronal populations involved. More specifically, neuronal populations firing at short latencies might have a slower recovery speed from adaptation than neuronal populations usually responding at longer latencies (i.e. contributing to the later portion of the SSEP component generated by the synchronous activation of all neuronal populations involved). Alternatively, the spiking threshold of faster-firing neuronal populations may have changed (Fontaine et al., 2014). As a consequence, without having changed their activity, those neuronal populations responding at long latencies may now be found to be activated progressively earlier than the previously faster-firing neuronal populations because these latter may be now responding progressively later (Zhang et al., 2009). As a result, one may observe a progressive increase in the SSEP component latency with repeated stimulations, without any decrease in the amplitude of the response because as many neuronal populations still contribute to the cortical potential throughout the stimulation repetition but in another temporal sequence.

Alternatively, the repeated stimulation may have progressively suppressed the activation of early-firing neuronal populations and at the same time progressively recruited a corresponding number of later-firing neuronal populations, resulting here again in a delayed potential at the scalp with a quite similar amplitude. By simply completely inhibiting early-firing neuronal populations, we would have observed a systematic increase in latency going with a systematic decrease in amplitude, reflecting merely classic repetition suppression, which is not the case for tactile stimulation adaptation described in the present study.

Another process of adaptation to repeated stimulations might be a decrease in the firing frequency of cortical neurons in response to repeated stimulations. We do not think that this mechanism alone can explain the adaptation of tactile SSEPs because this phenomenon results in a decrease in amplitude of the scalp signal in addition to an increase in the

latency. Nevertheless, this may help to understand the adaptation described after electrical stimulation, at least in the first part, where latency increased and amplitude decreased over the first 700 trials.

Spike-timing dependent plasticity ?

Given the very complex nature of the EEG signal, it is difficult to interpret modification observed in scalp signal by going back directly to the level of single synapses. Only hypotheses can be proposed. The aforementioned changes in the pattern of contribution of neuronal populations to the cortical component may be achieved in the following way:

S*pike-timing dependent plasticity* or STDP (Dan and Poo, 2006; Feldman, 2012; Shulz and Feldman, 2013; Sjöström and Gerstner, 2010) leading to weakening of synaptic efficacy by LTD may potentially explain the increase in SSEP latency with repeated tactile stimulation. STDP is a special form of Hebbian learning (Hebb, 1949) based on a tight temporal correlation and critical order between presynaptic and postsynaptic neuronal activity (Bi and Poo, 1998; Debanne and Poo, 2010; Levy and Steward, 1983; Markram et al., 2012; Markram et al., 1997; Zhang et al., 1998). Essentially, when repeated presynaptic activity (resulting in EPSP) appears a few milliseconds *before* postsynaptic action potentials, a LTP develops in this synapse because the presynaptic activity allows the postsynaptic activity to reach the threshold for spiking. Conversely, when the presynaptic neuron fires repeatedly *after* the postsynaptic spikes, a LTD occurs in that synapse (Song et al., 2000). In sum, the synaptic efficacy can be bidirectionally modified depending on the order and the precise timing between afferent presynaptic activity (EPSP) and postsynaptic spiking (action potential) (Debanne and Poo, 2010). LTP results in an increase in the postsynaptic peak amplitude, an increase in the integral of the postsynaptic response or in a reduced postsynaptic response latency. On the contrary, LTD leads to a reduction of the postsynaptic potential amplitude and/or an increased latency (Frégnac et al., 2010). This model of brain plasticity was already proven to be valid in several biological situations (for a review, see Dan and Poo, 2006; Shulz and Feldman, 2013).

An increase in latency over time may be explained in the following way:

Let a postsynaptic neuron be connected to N presynaptic excitatory neurons firing sequentially (1, 2, 3, ..., N-1, N) over a time period of several milliseconds. In case the pre-

synaptic neurons systematically fire after the postsynaptic neurons (i.e. postsynaptic action potential before presynaptic EPSPs), the STDP model implies that the connections from the N presynaptic neurons to the postsynaptic neuron will be weakened because synapses that repeatedly fail to participate to the post-synaptic neuronal activity will be depressed (Stent, 1973). With the increasing number of repetitions of the same stimulus, the postsynaptic neuron will fire later and later because of the weaker inputs from the presynaptic neurons. As a result, we will observe the postsynaptic neuron firing with an increasing latency over time. To put it another way, the STDP function will weaken the synapses because the presynaptic neurons were activated after the postsynaptic neuron. With the repetition of stimulation over time, the new synaptic weights make the postsynaptic neuron fire later (Sjöström and Gerstner, 2010).

Whatever are the underlying mechanisms involved in the achievement of the latency shift over time, we think that delaying the sensory processing of repeated inputs could induce the reduction of responsivity to consistent and repeated environmental inputs. The resulting temporal prioritisation may free brain resources for being more receptive and then amplify novel and potentially more relevant stimuli. A similar role has already been proposed in case of adaptation to repeated stimuli (Andrade et al., 2015; Kadohisa and Wilson, 2006; Tannan et al., 2006). More specifically here, experiments were performed under general anaesthesia to ensure that the monkeys received exclusively purely *passive* tactile stimulation to the fingertips, meaning that the stimulation episode was in no way accompanied by any use of the hand. Tactile inputs that were artificially delivered to the fingertips were therefore completely meaningless and irrelevant for the monkeys in this particular situation. As a consequence, the CNS, and the brain in particular, might have delayed the efficiency of synaptic transmission and processing in response to these irrelevant peripheral inputs from the mechanoreceptors innervating the fingertips (Gandevia and Ammon, 1992).

Originality of the present study

We recorded EEG with a high sampling rate, namely 5000 Hz, corresponding to a 0.2-ms time resolution. We would probably have missed the shift in latency revealed here by

recording brain activity at a lower sampling rate, such as the ones commonly used in clinics or in research, for instance 250 Hz (Pineda et al., 1991), 500 Hz (Andrade et al., 2015; Herrmann et al., 2015) or 1000 Hz (Gindrat et al., 2015). Or at least we would not have been able to document the precise evolution of latency and amplitude changes over time. Actually, latency adaptation may have been unnoticed until now in most studies investigating adaptation to repeated stimulations simply because the sampling rate of the EEG acquisition devices was not high enough to highlight small latency shifts. The consistency of the temporal shift in tactile SSEPs among the 3 monkeys involved in this study clearly indicates that it is a significant process that should be carefully considered in case of repeated tactile stimulations, even with a low stimulus repetition rate. We therefore recommend using the full capacity offered by the current EEG acquisition systems by setting the sampling rate at high level in order to assess the presence of temporal adaptation. This phenomenon may be of significant importance depending on the processes investigated.

In addition, we took advantage of the presence of two clearly distinct peaks contributing to the main cortical component in Mk-DI to document adaptation both in early and in later tactile sensory processing. We observed actually a very similar pattern of changes over time for both peaks in Mk-DI.

Finally, we provided here a direct comparison of adaptation pattern in two types of peripheral stimulation paradigm: after tactile stimulation to the fingertips and electrical stimulation to the median nerve, allowing to demonstrate the specificity of the strong adaptation in latency for tactile stimulation.

Relevance of the present study

Even though clinical diagnoses by means of SSEPs are often obtained by delivering electrical stimulation to a peripheral nerve (see e.g. Lascano et al., 2009), SSEPs elicited by repeated tactile stimulation to the skin have proven to be relevant as well, for instance to localise the somatosensory cortex of the hand before a surgery in epileptic patients (Lascano et al., 2014) or to investigate somatosensory impairments in patients with cerebral palsy (Riquelme et al., 2014). However, not all alterations in SSEPs signal are linked to the patients but some of them may be related to the recording conditions

themselves. Consequently, identifying such confounding factors, such as adaptation of the signal in latency and in amplitude during the repetition of a large number of stimulations is crucial to try to decrease these factors and therefore to improve the yield of EPs for anatomical localisation or diagnosis, for instance. To put it another way, it is of prime importance to fully understand the characteristics of the EPs being investigated and the potential distractions that may affect them, in order to further use these signals and correctly interpret them.

Moreover, tactile or touchscreen devices keep developing and are of growing interest nowadays (see for instance **Chapter 6** and **7**), with applications for instance to haptic displays, prosthetic devices, and teleoperation systems (see e.g. Bhattacharjee et al., 2013; Chowriappa et al., 2013; Elayaperumal et al., 2013; Lim et al., 2014; Pacchierotti et al., 2014a; Pacchierotti et al., 2014b; Rinderknecht et al., 2013; Tanaka et al., 2013; Xibo and Jiting, 2013; Yeangjin et al., 2013). Most of these devices rely on repeated tactile stimuli. Consequently, a full understanding of adaptation processes is of prime importance to improve their development.

Prospects

In the present study, repeated electrical stimulations to the median nerve were delivered in only one monkey (Mk-CA) during the very first EEG recording session. In addition, we restricted the fingertip tactile stimulation protocol to a single repetition rate. Systematic recordings of electrical SSEPs and testing additional stimulus repetition rates might probably improve the robustness of future experiments (see e.g. Hollins et al., 1990; Pratt et al., 1980), but this was actually prevented here by the need to obtain a sufficiently large number of trials for each fingertip while keeping the overall duration of the experiment within three hours at most.

As sensorimotor processing may be influenced by hand preference and hand dominance (see e.g. Mori et al., 2015; Patel and Mehta, 2012), we could extend the present investigations to fingertips of both hands in order to assess whether a lateralisation bias in adaptation does exist as well.

A great improvement to fully address the question about the peripheral versus central contribution to the adaptation recorded at the scalp in response to repeated tactile

stimulations would be to add several bipolar recording electrodes along the stimulated afferent pathway, especially over the median nerve at the wrist and at the Erb's point, to follow in greater detail the afferent volleys from the fingertips to the cortex. Briefly, in case the SSEPs recorded at the wrist level would already exhibit some features of adaptation, one could infer some early contribution of peripheral structures in the adaptation recorded at the scalp.

Another interesting question would be to assess adaptation to repeated tactile stimulations of the fingertips in human as well by using a similar stimulation protocol (but in awake subjects here), to investigate whether comparable patterns of adaption are reproduced in human, especially the adaptation in the temporal domain. Such a comparative analysis between human and macaque monkeys may be relevant, especially if we keep in mind that there are some important differences in the skin organisation and its innervation at the fingertips between both species. For instance, SA-II receptors (Ruffini endings) are present in monkeys as well, contrary to what had been suggested previously (Dong et al., 2013; Johnson, 2001; Paré et al., 2002), but they are located much more deeply in the skin than in human (Prof. Roland Johansson, personal communication, April 24, 2015). Moreover, it is known that the distal part of the mechanoreceptors is amply branching (i.e. 8-16 terminals/axonal fibre) in the human glabrous skin, corresponding to the multiple strongly responding points observed in a given receptive field (Johansson, 1978). In monkeys, such branching does occur as well but it is less numerous and more scattered than in human (Johansson, 1978). Finally, differences are visible already by eyes: for instance, the skin of the fingertips is much thicker in monkeys than in human, but at the same time, the pulp of the monkeys' fingertips is more "spongy" than in human. Such differences in the skin anatomy may induce different patterns of adaptation between both species because the encoding properties of the mechanoreceptors strongly depend on the complex properties of the tissues between the stimulus and the nerve endings (Maeno et al., 1998; Srinivasan and Dandekar, 1996).

Conclusion

In sum, the present study provides new findings by showing that the adaptation to repeated stimulations was not only characterised by a well-known decrement in ampli-

tude, but the temporal domain was concerned as well, as reflected by a prominent and consistent increasing latency shift in the course of repeated tactile stimulations. It is important to remind here that we used a relatively low stimulus repetition rate as compared to those typically used in other studies describing adaptation phenomena. We may therefore have highlighted a unique and specific "cortical signature" of fingertip tactile stimulation. Our results clearly demonstrated that latency adaptation is a significant process that should be carefully considered in case of repeated tactile stimulations, even with a low stimulus repetition rate.

This chapter finishes off the EEG investigations in macaque monkeys performed within the framework of the present PhD thesis. By using high-density EEG recordings at the scalp, we were able to observe different types of brain plasticity operating at different temporal scales. The **Chapters 2** and **3** supported the idea of lesion-induced plasticity developing within the brain over the whole post-lesion recovery period. When considering now the brain plasticity of primates in more "natural" situations, cortical somatosensory representations can be reshaped, for instance when some fingers are involved in a specific task for several hours a day (see e.g. Jenkins et al., 1990; Jenkins and Merzenich, 1987; Nudo et al., 1996; Recanzone et al., 1992; Wang et al., 1995). Plastic changes (enlargement of the receptive fields) were demonstrated to occur already after 1-2 hours of electrical stimulation of the ulnar nerve in cats (Recanzone et al., 1990). In the present study, we studied adaptation as a form of plasticity working in a very short period of time: we highlighted that a large number of repeated successive tactile and electrical stimulations did not result in stable and invariant responses at the scalp over time of repeated stimulations, but rather that this cortical sensory processing was subjected to significant dynamic fluctuations within an experimental session. To go deeper into the different forms of brain plasticity, the **Chapters 6** and **7** will exemplify the notion of use-dependent plasticity.

Acknowledgements

The Cartool software (http://www.fbmlab.com/cartool-software/) has been programmed by Denis Brunet, from the Functional Brain Mapping Laboratory, Geneva,

Switzerland, and is supported by the Center for Biomedical Imaging (CIBM) of Geneva and Lausanne.

References

Adibi, M., McDonald, J.S., Clifford, C.W.G., Arabzadeh, E., 2013. Adaptation Improves Neural Coding Efficiency Despite Increasing Correlations in Variability. The Journal of Neuroscience 33, 2108-2120.

Adrian, E.D., Zotterman, Y., 1926. The impulses produced by sensory nerve endings: Part 3. Impulses set up by Touch and Pressure. J Physiol 61, 465-483.

Ahissar, E., Sosnik, R., Bagdasarian, K., Haidarliu, S., 2001. Temporal Frequency of Whisker Movement. II. Laminar Organization of Cortical Representations. Journal of Neurophysiology 86, 354-367.

Allison, T., McCarthy, G., Wood, C.C., Jones, S.J., 1991. Potentials evoked in human and monkey cerebral cortex by stimulation of the median nerve. A review of scalp and intracranial recordings. Brain 114 (Pt 6), 2465-2503.

Allison, T., 1962. Recovery functions of somatosensory evoked responses in man. Electroencephalography and Clinical Neurophysiology 14, 331-343.

Aminoff, M.J., Eisen, A.A., 1998. AAEM minimonograph 19: somatosensory evoked potentials. Muscle Nerve 21, 277-290.

Andrade, G.N., Butler, J.S., Mercier, M.R., Molholm, S., Foxe, J.J., 2015. Spatio-temporal dynamics of adaptation in the human visual system: a high-density electrical mapping study. European Journal of Neuroscience 41, 923-937.

Ballachanda, B.B., Moushegian, G., Stillman, R.D., 1992. Adaptation of the auditory brainstem response: effects of click intensity, polarity, and position. J Am Acad Audiol 3, 275-282.

Banoub, M., Tetzlaff, J.E., Schubert, A., 2003. Pharmacologic and physiologic influences affecting sensory evoked potentials: implications for perioperative monitoring. Anesthesiology 99, 716-737.

Baranek, G.T., Berkson, G., 1994. Tactile defensiveness in children with developmental disabilities: Responsiveness and habituation. J Autism Dev Disord 24, 457-471.

Baranek, G.T., Foster, L.G., Berkson, G., 1997. Tactile Defensiveness and Stereotyped Behaviors. American Journal of Occupational Therapy 51, 91-95.

Bensmaia, S.J., Leung, Y.Y., Hsiao, S.S., Johnson, K.O., 2005. Vibratory adaptation of cutaneous mechanoreceptive afferents. J Neurophysiol. 94, 3023-3036.

Berglund, U., Berglund, B., 1970. Adaption and recovery in vibrotactile perception. Percept.Mot.Skills 30, 843-853.

Bhattacharjee, T., Jain, A., Vaish, S., Killpack, M.D., Kemp, C.C., 2013. Tactile sensing over articulated joints with stretchable sensors., World Haptics Conference (WHC), 2013, pp. 103-108.

Bi, G.q., Poo, M.m., 1998. Synaptic Modifications in Cultured Hippocampal Neurons: Dependence on Spike Timing, Synaptic Strength, and Postsynaptic Cell Type. The Journal of Neuroscience 18, 10464-10472.

Blakemore, S.J., Tavassoli, T., Calò, S., Thomas, R.M., Catmur, C., Frith, U., Haggard, P., 2006. Tactile sensitivity in Asperger syndrome. Brain and Cognition 61, 5-13.

Boisseau, N., Madany, M., Staccini, P., Armando, G., Martin, F., Grimaud, D., Raucoules-Aime, M., 2002. Comparison of the effects of sevoflurane and propofol on cortical somatosensory evoked potentials. Br.J Anaesth. 88, 785-789.

Bradley, C., Joyce, N., Garcia-Larrea, L., 2014. Adaptation in human somatosensory cortex as a model of sensory memory construction: a study using high-density EEG. Brain Struct Funct, 1-11.

Brown, W.F., 1984. Evoked potentials. In: Brown, W.F. (Ed.), The Physiological and Technical Basis of Electromyography. Butterworth-Heinemann, pp. 169-221.

Brunet, D., Murray, M.M., Michel, C.M., 2011. Spatiotemporal analysis of multichannel EEG: CARTOOL. Comput.Intell.Neurosci. 2011 (ID 813870), 15 pages.

Burgess, P.R., Perl, E.R., 1973. Cutaneous Mechanoreceptors and Nociceptors. In: Iggo, A. (Ed.), Somatosensory System, 2nd ed. Springer Berlin Heidelberg, pp. 29-78.

Burke, D., Gandevia, S.C., McKeon, B., Skuse, N.F., 1982. Interactions between cutaneous and muscle afferent projections to cerebral cortex in man. Electroencephalography and Clinical Neurophysiology 53, 349-360.

Cain, W.S., 1974. Perception of odor intensity and the time course of olfactory adaptation. ASHRAE Transactions 80, 53-75.

Cattan, S., Bachatene, L., Bharmauria, V., Jeyabalaratnam, J., Milleret, C., Molotchnikoff, S., 2014. Comparative analysis of orientation maps in areas 17 and 18 of the cat primary visual cortex following adaptation. European Journal of Neuroscience 40, 2554-2563.

Cheung, B., van Erp, J.B.F., Cholewiak, R.W., 2008. Anatomical, neurophysiological and perceptual issues of tactile perception. In: van Erp, J.B.F., Self, B.P. (Eds.), Tactile displays for orientation, navigation and communication in air, sea and land environments. NATO Research and Technology Organisation, Neuilly-sur-Sein Cedex (France), pp. 1-18.

Chowriappa, A., Wirz, R., Seo, Y.W., Reddy, A., Kesavadas, T., Scott, P., Guru, K., Kesavadas, T., 2013. A predictive model for haptic assistance in robot assisted trocar insertion., World Haptics Conference (WHC), 2013, pp. 121-126.

Chung, S., Li, X., Nelson, S.B., 2002. Short-Term Depression at Thalamocortical Synapses Contributes to Rapid Adaptation of Cortical Sensory Responses In Vivo. Neuron 34, 437-446.

Cohen, H., Cohen, B., Raphan, T., Waespe, W., 1992. Habituation and adaptation of the vestibuloocular reflex: a model of differential control by the vestibulocerebellum. Exp Brain Res 90, 526-538.

Committee for the Update of the Guide for the Care and Use of Laboratory Animals, National Research Council, 2011. Guide for the Care and Use of Laboratory Animals: Eighth Edition. The National Academies Press.

Dahmen, J.C., Keating, P., Nodal, F.R., Schulz, A.L., King, A.J., 2010. Adaptation to Stimulus Statistics in the Perception and Neural Representation of Auditory Space. Neuron 66, 937-948.

Dalton, P., 2000. Psychophysical and Behavioral Characteristics of Olfactory Adaptation. Chemical Senses 25, 487-492.

Dan, Y., Poo, M.m., 2006. Spike timing-dependent plasticity: from synapse to perception. Physiol Rev. 86, 1033-1048.

Darian-Smith, I., Kenins, P., 1980. Innervation density of mechanoreceptive fibres supplying glabrous skin of the monkey's index finger. J Physiol 309, 147-155.

Debanne, D., Poo, M.m., 2010. Spike-timing dependent plasticity beyond synapse - pre- and post-synaptic plasticity of intrinsic neuronal excitability. Frontiers in Synaptic Neuroscience 2.

Debruyne, F., 1986. Influence of age and hearing loss on the latency shifts of the auditory brainstem response as a result of increased stimulus rate. International Journal of Audiology 25, 101-106.

Desmedt, J.E., 1987. Physiologie et physiopathologie des sensations somatiques étudiées chez l'Homme par la méthode des potentiels évoqués, [Physiology and physiopathology of somatic sensations studied in man by the method of evoked potentials]. J Physiol (Paris) 82, 64-136.

Dong, Y., Mihalas, S., Kim, S.S., Yoshioka, T., Bensmaia, S., Niebur, E., 2013. A simple model of mechanotransduction in primate glabrous skin. Journal of Neurophysiology 109, 1350-1359.

Eggermont, J.J., 1985. Peripheral auditory adaptation and fatigue: A model oriented review. Hearing Research 18, 57-71.

Elayaperumal, S., Bae, J.H., Christensen, D., Cutkosky, M.R., Daniel, B.L., Black, R.J., Costa, J.M., Faridian, F., Moslehi, B., 2013. Mr-compatible biopsy needle with enhanced tip force sensing., World Haptics Conference (WHC), 2013, pp. 109-114.

Emori, T., Yamada, T., Seki, Y., Yasuhara, A., Ando, K., Honda, Y., Leis, A.A., Vachatimanont, P., 1991. Recovery functions of fast frequency potentials in the initial negative wave of median SEP. Electroencephalography and Clinical Neurophysiology 78, 116-123.

Fatemi, S.H., Halt, A.R., Stary, J.M., Kanodia, R., Schulz, S.C., Realmuto, G.R., 2002. Glutamic acid decarboxylase 65 and 67 kDa proteins are reduced in autistic parietal and cerebellar cortices. Biological Psychiatry 52, 805-810.

Feldman, D.E., 2012. The spike-timing dependence of plasticity. Neuron 75, 556-571.

Finlayson, P.G., Cynader, M.S., 1995. Synaptic depression in visual cortex tissue slices: an in vitro model for cortical neuron adaptation. Exp Brain Res 106, 145-155.

Fontaine, B., Peña, J.L., Brette, R., 2014. Spike-Threshold Adaptation Predicted by Membrane Potential Dynamics *In Vivo*. PLoS Comput Biol 10, e1003560.

Fraser, G., Hartings, J.A., Simons, D.J., 2006. Adaptation of trigeminal ganglion cells to periodic whisker deflections. Somatosensory & Motor Research 23, 111-118.

Frégnac, Y., Pananceau, M., René, A., Huguet, N., Marre, O., Levy, M., Shulz, D.E., 2010. A re-examination of Hebbian-covariance rules and spike timing-dependent plasticity in cat visual cortex in vivo. Frontiers in Synaptic Neuroscience 2.

Frings, S., 2012. Primary Processes in Sensory Cells: Current Advances. In: López-Larrea, C. (Ed.), Sensing in Nature. Springer US, pp. 32-58.

Gandevia, S.C., Ammon, K., 1992. Selective temporal shift in the somatosensory evoked potential produced by chronic stimulation of the human index finger. Exp.Brain Res. 88, 219-223.

Garcia-Lazaro, J.A., Ho, S.S.M., Nair, A., Schnupp, J.W.H., 2007. Shifting and scaling adaptation to dynamic stimuli in somatosensory cortex. European Journal of Neuroscience 26, 2359-2368.

Gardner, E.P., Hamalainen, H.A., Warren, S., Davis, J., Young, W., 1984. Somatosensory evoked potentials (SEPs) and cortical single unit responses elicited by mechanical tactile stimuli in awake monkeys. Electroencephalogr.Clin.Neurophysiol 58, 537-552.

Gardner, E.P., Johnson, K.O., 2013. Coding of sensory information. In: Kandel, E.R., Schwartz, J.H., Jessell, T.M., Siegelbaum, S.A., Hudspeth, A.J. (Eds.). McGraw-Hill, pp. 449-474.

Gescheider, G.A., Santoro, K.E., Makous, J.C., Bolanowski, S.J., 1995. Vibrotactile forward masking: effects of the amplitude and duration of the masking stimulus. The Journal of the Acoustical Society of America 98, 3188-3194.

Gindrat, A.D., Quairiaux, C., Britz, J., Brunet, D., Lanz, F., Michel, C.M., Rouiller, E.M., 2014. Whole-scalp EEG mapping of somatosensory evoked potentials in macaque monkeys. Brain Struct.Funct., 1-22.

Gindrat, A.D., Chytiris, M., Balerna, M., Rouiller, E.M., Ghosh, A., 2015. Use-Dependent Cortical Processing from Fingertips in Touchscreen Phone Users. Current Biology 25, 109-116.

Gloor, P., 1985. Neuronal Generators and the Problem of Localization in Electroencephalography: Application of Volume Conductor Theory to Electroencephalography. Journal of Clinical Neurophysiology 2.

Goble, A.K., Hollins, M., 1993. Vibrotactile adaptation enhances amplitude discrimination. J Acoust.Soc.Am. 93, 418-424.

Goble, A.K., Hollins, M., 1994. Vibrotactile adaptation enhances frequency discrimination. The Journal of the Acoustical Society of America 96, 771-780.

Gonshor, A., Jones, G.M., 1976a. Extreme vestibulo-ocular adaptation induced by prolonged optical reversal of vision. The Journal of physiology 256, 381-414.

Gonshor, A., Jones, G.M., 1976b. Short-term adaptive changes in the human vestibulo-ocular reflex arc. The Journal of physiology 256, 361-379.

Greenlee, M.W., Heitger, F., 1988. The functional role of contrast adaptation. Vision Research 28, 791-797.

Grill-Spector, K., Henson, R., Martin, A., 2006. Repetition and the brain: neural models of stimulus-specific effects. Trends in Cognitive Sciences 10, 14-23.

Groves, P.M., Thompson, R.F., 1970. Habituation: A dual-process theory. Psychological review 77, 419-450.

Haigh, S.M., Murphy, T.K., Butera, C.D., Salisbury, D.F., 2015a. Is the Complex Pattern Deviant MMN Healthy in Schizophrenia? Schizophrenia Bulletin 41, S18.

Haigh, S.M., Murphy, T.K., Butera, C.D., Salisbury, D.F., 2015b. MMN to complex patter deviants in schizophrenia., Biological Psychiatry, At Toronto, ON, Canada. Society of Biological Psychiatry.

Hawken, M.J., Shapley, R.M., Grosof, D.H., 1996. Temporal-frequency selectivity in monkey visual cortex. Visual Neuroscience 13, 477-492.

Hebb, D.O., 1949. The Organization of Behavior: A Neuropsychological Theory. John Wiley & Sons, Inc., New York.

Hendry, S.H., Hsiao, S.S., 2013. Fundamentals of Sensory Systems. In: Spitzer, L.R.S. (Ed.), Fundamental Neuroscience (Fourth Edition). Academic Press, San Diego, pp. 499-511.

Henson, R.N.A., Shallice, T., Gorno-Tempini, M.L., Dolan, R.J., 2002. Face Repetition Effects in Implicit and Explicit Memory Tests as Measured by fMRI. Cerebral Cortex 12, 178-186.

Herrmann, B., Henry, M.J., Kim Fromboluti, E., McAuley, J.D., Obleser, J., 2015. Statistical Context Shapes Stimulus-Specific Adaptation in Human Auditory Cortex. Journal of Neurophysiology.

Hollins, M., Delemos, K.A., Goble, A.K., 1991. Vibrotactile adaptation on the face. Percept.Psychophys. 49, 21-30.

Hollins, M., Goble, A.K., Whitsel, B.L., Tommerdahl, M., 1990. Time course and action spectrum of vibrotactile adaptation. Somatosens.Mot.Res 7, 205-221.

Hubel, D.H., Wiesel, T.N., 1960. Receptive fields of optic nerve fibres in the spider monkey. The Journal of physiology 154, 572-580.

Hussman, J.P., 2001. Letters to the Editor: Suppressed GABAergic Inhibition as a Common Factor in Suspected Etiologies of Autism. J Autism Dev Disord 31, 247-248.

Jain, N., Catania, K.C., Kaas, J.H., 1998. A histologically visible representation of the fingers and palm in primate area 3b and its immutability following long-term deafferentations. Cereb.Cortex 8, 227-236.

Jantti, V., Sonkajarvi, E., Mustola, S., Rytky, S., Kiiski, P., Suominen, K., 1998. Single-sweep cortical somatosensory evoked potentials: N20 and evoked bursts in sevoflurane anaesthesia. Electroencephalogr.Clin.Neurophysiol 108, 320-324.

Jenkins, W.M., Merzenich, M.M., Ochs, M.T., Allard, T., Guic-Robles, E., 1990. Functional reorganization of primary somatosensory cortex in adult owl monkeys after behaviorally controlled tactile stimulation. J Neurophysiol. 63, 82-104.

Jenkins, W.M., Merzenich, M.M., 1987. Reorganization of neocortical representations after brain injury: a neurophysiological model of the bases of recovery from stroke. Progress in brain research 71, 249-266.

Johansson, R., Flanagan, J., 2008. Tactile Sensory Control of Object Manipulation in Humans., Volume 6: Somatosensation, 6th ed. Elsevier, pp. 67-86.

Johansson, R., Vallbo, A.B., 1976. Skin mechanoreceptors in the human hand: an inference of some population properties. In: Zotterman, Y. (Ed.), Sensory Functions of the Skin in Primates, Wenner–Gren Center International Symposium Series. Pergamon, pp. 171-184.

Johansson, R.S., 1978. Tactile sensibility in the human hand: receptive field characteristics of mechanoreceptive units in the glabrous skin area. The Journal of physiology 281, 101-125.

Johansson, R.S., 1998. Sensory input and control of grip. In: Bock, G.R., Goode, J.A. (Eds.), Novartis Foundation Symposium 218 - Sensory Guidance of Movement. Wiley, Chichester, pp. 45-63.

Johansson, R.S., Flanagan, J.R., 2009a. Coding and use of tactile signals from the fingertips in object manipulation tasks. Nat Rev Neurosci 10, 345-359.

Johansson, R.S., Flanagan, J.R., 2009b. Sensorimotor Control of Manipulation. In: Squire, L.R. (Ed.), Encyclopedia of Neuroscience. Academic Press, Oxford, pp. 583-594.

Johansson, R.S., Vallbo, A.B., 1979. Tactile sensibility in the human hand: relative and absolute densities of four types of mechanoreceptive units in glabrous skin. The Journal of physiology 286, 283-300.

Johansson, R.S., Westling, G., 1990. Tactile afferent signals in the control of precision grip., Attention and Performance, vol. XIII. Lawrence Erlbaum Associates, Inc, pp. 677-713.

Johansson, R.S., Westling, G., 1991. Afferent signals during manipulative tasks in humans. In: Franzén, O., Westman, J. (Eds.), Somatosensory Mechanisms. Macmillan Academic Press, London, p. 25.

Johansson, R.S., Vallbo, A.B., 1983. Tactile sensory coding in the glabrous skin of the human hand. Trends in Neurosciences 6, 27-32.

Johnson, K.O., Phillips, J.R., 1981. Tactile spatial resolution. I. Two-point discrimination, gap detection, grating resolution, and letter recognition. Journal of Neurophysiology 46, 1177-1192.

Johnson, K.O., 2001. The roles and functions of cutaneous mechanoreceptors. Current Opinion in Neurobiology 11, 455-461.

Juliano, S.L., Whitsel, B.L., 1985. Metabolic labeling associated with index finger stimulation in monkey SI: Between animal variability. Brain Research 342, 242-251.

Kaas, J.H., 1997. Topographic maps are fundamental to sensory processing. Brain Res.Bull. 44, 107-112.

Kadohisa, M., Wilson, D.A., 2006. Olfactory Cortical Adaptation Facilitates Detection of Odors Against Background. J Neurophysiol 95, 1888-1896.

Kaji, R., Sumner, A.J., 1987. Bipolar recording of short–latency somatosensory evoked potentials after median nerve stimulation. Neurology 37, 410.

Kaliukhovich, D.A., Vogels, R., 2012. Stimulus repetition affects both strength and synchrony of macaque inferior temporal cortical activity. Journal of Neurophysiology 107, 3509-3527.

Kandel, E.R., Schwartz, J.H., Jessell, T.M., Siegelbaum, S.A., Hudspeth, A.J., 2013. Principles of Neural Science, Fifth Edition. McGraw-Hill Education.

Katz, Y., Heiss, J.E., Lampl, I., 2006. Cross-Whisker Adaptation of Neurons in the Rat Barrel Cortex. The Journal of Neuroscience 26, 13363-13372.

Kekoni, J., Hämäläinen, H., Saarinen, M., Gröhn, J., Reinikainen, K., Lehtokoski, A., Näätänen, R., 1997. Rate effect and mismatch responses in the somatosensory system: ERP-recordings in humans. Biological Psychology 46, 125-142.

Kekoni, J., Tiihonen, J., Hämäläinen, H., 1992. Fast decrement with stimulus repetition in ERPs generated by neuronal systems involving somatosensory SI and SII cortices: Electric and magnetic evoked response recordings in humans. International Journal of Psychophysiology 12, 281-288.

Khatri, V., Hartings, J.A., Simons, D.J., 2004. Adaptation in thalamic barreloid and cortical barrel neurons to periodic whisker deflections varying in frequency and velocity. J.Neurophysiol. 92, 3244-3254.

Krubitzer, L., Huffman, K.J., Disbrow, E., Recanzone, G., 2004. Organization of area 3a in macaque monkeys: contributions to the cortical phenotype. J Comp Neurol. 471, 97-111.

Krubitzer, L.A., Seelke, A.M., 2012. Cortical evolution in mammals: the bane and beauty of phenotypic variability. Proc.Natl.Acad.Sci.USA 109 Suppl 1, 10647-10654.

Ku, A.S., Hu, Y., Irwin, M.G., Chow, B., Gunawardene, S., Tan, E.E., Luk, K.D., 2002. Effect of sevoflurane/nitrous oxide versus propofol anaesthesia on somatosensory evoked potential monitoring of the spinal cord during surgery to correct scoliosis. Br.J Anaesth. 88, 502-507.

Kuffler, S.W., 1953. Discharge patterns and functional organization of mammalian retina. Journal of Neurophysiology 16, 37-68.

Larsson, L.E., Prevec, T.S., 1970. Somato-sensory response to mechanical stimulation as recorded in the human EEG. Electroencephalography and Clinical Neurophysiology 28, 162-172.

Lascano, A.M., Brodbeck, V., Lalive, P.H., Chofflon, M., Seeck, M., Michel, C.M., 2009. Increasing the diagnostic value of evoked potentials in multiple sclerosis by quantitative topographic analysis of multichannel recordings. J Clin.Neurophysiol 26, 316-325.

Lascano, A.M., Grouiller, F., Genetti, M., Spinelli, L., Seeck, M., Schaller, K., Michel, C.M., 2014. Surgically relevant localization of the central sulcus with high-density somatosensory-evoked potentials compared with functional magnetic resonance imaging. Neurosurgery 74, 517-526.

Laskin, S.E., Spencer, W.A., 1979. Cutaneous masking. I. Psychophysical observations on interactions of multipoint stimuli in man. Journal of Neurophysiology 42, 1048-1060.

Lee, C.J., Whitsel, B.L., 1992. Mechanisms Underlying Somatosensory Cortical Dynamics: I. In vivo Studies. Cerebral Cortex 2, 81-106.

Lee, C.J., Whitsel, B.L., Tommerdahl, M., 1992. Mechanisms Underlying Somatosensory Cortical Dynamics: II. In vitro Studies. Cerebral Cortex 2, 107-133.

Legatt, A., Benbadis, S.R., 2014. General Principles of Somatosensory Evoked Potentials. Medscape.

Leung, Y.Y., Bensmaia, S.J., Hsiao, S.S., Johnson, K.O., 2005. Time-course of vibratory adaptation and recovery in cutaneous mechanoreceptive afferents. J Neurophysiol. 94, 3037-3045.

Levy, W.B., Steward, O., 1983. Temporal contiguity requirements for long-term associative potentiation/depression in the hippocampus. Neuroscience 8, 791-797.

Li, L., Miller, E.K., Desimone, R., 1993. The representation of stimulus familiarity in anterior inferior temporal cortex. Journal of Neurophysiology 69, 1918-1929.

Lim, S.C., Lee, H.K., Park, J., 2014. Role of combined tactile and kinesthetic feedback in minimally invasive surgery. The International Journal of Medical Robotics and Computer Assisted Surgery.

Lisberger, S.G., Miles, F.A., 1980. Role of primate medial vestibular nucleus in long-term adaptive plasticity of vestibuloocular reflex. Journal of Neurophysiology 43, 1725-1745.

Loewenstein, W.R., Skalak, R., 1966. Mechanical transmission in a Pacinian corpuscle. An analysis and a theory. The Journal of physiology 182, 346-378.

Löfberg, O., Julkunen, P., Tiihonen, P., Pääkkönen, A., Karhu, J., 2013. P 1. Repetition suppression in sensorimotor system to adapt cortex to stimuli. Clinical Neurophysiology 124, e63-e64.

Löfvenberg, J., Johansson, R.S., 1984. Regional differences and interindividual variability in sensitivity to vibration in the glabrous skin of the human hand. Brain Research 301, 65-72.

Loquet, G., Meyer, K., Rouiller, E.M., 2003. Effects of intensity of repetitive acoustic stimuli on neural adaptation in the ventral cochlear nucleus of the rat. Exp Brain Res 153, 436-442.

Loquet, G., Pelizzone, M., Valentini, G., Rouiller, E.M., 2004. Matching the Neural Adaptation in the Rat Ventral Cochlear Nucleus Produced by Artificial (Electric) and Acoustic Stimulation of the Cochlea. Audiology and Neurotology 9, 144-159.

Loquet, G., Rouiller, E.M., 2002. Neural adaptation to pulsatile acoustical stimulation in the cochlear nucleus of the rat. Hearing Research 171, 72-81.

Ma, D.Q., Whitehead, P.L., Menold, M.M., Martin, E.R., Ashley-Koch, A.E., Mei, H., Ritchie, M.D., DeLong, G.R., Abramson, R.K., Wright, H.H., Cuccaro, M.L., Hussman, J.P., Gilbert, J.R., Pericak-Vance, M.A., 2005. Identification of Significant Association and Gene-Gene Interaction of GABA Receptor Subunit Genes in Autism. The American Journal of Human Genetics 77, 377-388.

Maeno, T., Kobayashi, K., Yamazaki, N., 1998. Relationship between the Structure of Human Finger Tissue and the Location of Tactile Receptors. JSME International Journal Series C 41, 94-100.

Maravall, M., Petersen, R.S., Fairhall, A.L., Arabzadeh, E., Diamond, M.E., 2007. Shifts in Coding Properties and Maintenance of Information Transmission during Adaptation in Barrel Cortex. PLoS Biol 5, e19.

Marco, E.J., Hinkley, L.B.N., Hill, S.S., Nagarajan, S.S., 2011. Sensory Processing in Autism: A Review of Neurophysiologic Findings. Pediatr Res 69, 48R-54R.

Markram, H., Gerstner, W., Sjostrom, P.J., 2012. Spike-timing-dependent plasticity: a comprehensive overview. Front Synaptic.Neurosci. 4, 2.

Markram, H., Lübke, J., Frotscher, M., Sakmann, B., 1997. Regulation of Synaptic Efficacy by Coincidence of Postsynaptic APs and EPSPs. Science 275, 213-215.

Matthews, B.H.C., 1931. The response of a single end organ. The Journal of physiology 71, 64-110.

May, P.J.C., Westö, J., Tiitinen, H., 2015. Computational modelling suggests that temporal integration results from synaptic adaptation in auditory cortex. European Journal of Neuroscience 41, 615-630.

McBurney, D.H., 1984. Taste and Olfaction: Sensory Discrimination., Comprehensive Physiology. John Wiley & Sons, Inc., pp. 1067-1086.

McLaughlin, D.F., Kelly, E.F., 1993. Evoked potentials as indices of adaptation in the somatosensory system in humans: a review and prospectus. Brain Res.Brain Res.Rev. 18, 151-206.

Merzenich, M.M., Nelson, R.J., Kaas, J.H., Stryker, M.P., Jenkins, W.M., Zook, J.M., Cynader, M.S., Schoppmann, A., 1987. Variability in hand surface representations in areas 3b and 1 in adult owl and squirrel monkeys. Journal of Comparative Neurology 258, 281-296.

Meyer, K., Rouiller, E.M., Loquet, G., 2007. Direct comparison between properties of adaptation of the auditory nerve and the ventral cochlear nucleus in response to repetitive clicks. Hearing Research 228, 144-155.

Miles, F.A., Eighmy, B.B., 1980. Long-term adaptive changes in primate vestibuloocular reflex. I. Behavioral observations. Journal of Neurophysiology 43, 1406-1425.

Minnery, B.S., Simons, D.J., 2003. Response Properties of Whisker-Associated Trigeminothalamic Neurons in Rat Nucleus Principalis. Journal of Neurophysiology 89, 40-56.

Miu, K.K., Webber, R.M., Stanley, G.B., 2011. Cortical Adaptation to Aperiodic Tactile Stimuli.

Mori, H., Yamamoto, S., Aihara, T., Uehara, S., 2015. The role of handedness-dependent sensorimotor experience in the development of mirroring. Neuroscience Letters 584, 119-122.

Müller, J.R., Metha, A.B., Krauskopf, J., Lennie, P., 1999. Rapid Adaptation in Visual Cortex to the Structure of Images. Science 285, 1405-1408.

Musall, S., von der Behrens, W., Mayrhofer, J.M., Weber, B., Helmchen, F., Haiss, F., 2014. Tactile frequency discrimination is enhanced by circumventing neocortical adaptation. Nat Neurosci 17, 1567-1573.

Netser, S., Zahar, Y., Gutfreund, Y., 2011. Stimulus-Specific Adaptation: Can It Be a Neural Correlate of Behavioral Habituation? The Journal of Neuroscience 31, 17811-17820.

Nudo, R.J., Milliken, G.W., Jenkins, W.M., Merzenich, M.M., 1996. Use-dependent alterations of movement representations in primary motor cortex of adult squirrel monkeys. J Neurosci 16, 785-807.

O'Mara, S., Rowe, M.J., Tarvin, R.P., 1988. Neural mechanisms in vibrotactile adaptation. Journal of Neurophysiology 59, 607-622.

Ohzawa, I., Sclar, G., Freeman, R.D., 1982. Contrast gain control in the cat visual cortex. Nature 298, 266-268.

Pacchierotti, C., Abayazid, M., Misra, S., Prattichizzo, D., 2014a. Steering of flexible needles combining kinesthetic and vibratory force feedback., Intelligent Robots and Systems (IROS 2014), 2014 IEEE/RSJ International Conference on, pp. 1202-1207.

Pacchierotti, C., Abayazid, M., Misra, S., Prattichizzo, D., 2014b. Teleoperation of Steerable Flexible Needles by Combining Kinesthetic and Vibratory Feedback. Haptics, IEEE Transactions on 7, 551-556.

Paré, M., Smith, A.M., Rice, F.L., 2002. Distribution and terminal arborizations of cutaneous mechanoreceptors in the glabrous finger pads of the monkey. The Journal of Comparative Neurology 445, 347-359.

Patel, A., Mehta, A., 2012. A Comparative Study Of Nerve Conduction Velocity Between Left And Right Handed Subjects. International journal of basic and applied physiology 1, 19-21.

Pérez-González, D., Malmierca, M.S., 2014. Adaptation in the auditory system: an overview. Frontiers in Integrative Neuroscience 8.

Pineda, J.A., Holmes, T.C., Foote, S.L., 1991. Intensity-amplitude relationships in monkey event-related potentials: parallels to human augmenting-reducing responses. Electroencephalogr.Clin.Neurophysiol 78, 456-465.

Popescu, M., Barlow, S., Popescu, E.A., Estep, M.E., Venkatesan, L., Auer, E.T., Brooks, W.M., 2010. Cutaneous stimulation of the digits and lips evokes responses with different adaptation patterns in primary somatosensory cortex. Neuroimage. 52, 1477-1486.

Pratt, H., Politoske, D., Starr, A., 1980. Mechanically and electrically evoked somatosensory potentials in humans: effects of stimulus presentation rate. Electroencephalogr.Clin.Neurophysiol 49, 240-249.

Purves, D., Augustine, G.A., Fitzpatrick, D., Hall, W., LaMantia, A.-S., McNamara, J.O., Williams, S.M., 2004. Neuroscience, 3rd ed. Sinauer Associates, Incorporated.

Puts, N.A.J., Wodka, E.L., Tommerdahl, M., Mostofsky, S.H., Edden, R.A.E., 2014. Impaired tactile processing in children with autism spectrum disorder. Journal of Neurophysiology 111, 1803-1811.

Qi, H.X., Kaas, J.H., 2004. Myelin stains reveal an anatomical framework for the representation of the digits in somatosensory area 3b of macaque monkeys. J.Comp Neurol. 477, 172-187.

Rankin, C.H., Abrams, T., Barry, R.J., Bhatnagar, S., Clayton, D., Colombo, J., Coppola, G., Geyer, M.A., Glanzman, D.L., Marsland, S., McSweeney, F., Wilson, D.A., Wu, C.F., Thompson, R.F., 2009. Habituation Revisited: An Updated and Revised Description of the Behavioral Characteristics of Habituation. Neurobiology of learning and memory 92, 135-138.

Recanzone, G.H., Merzenich, M.M., Jenkins, W.M., Grajski, K.A., Dinse, H.R., 1992. Topographic reorganization of the hand representation in cortical area 3b owl monkeys trained in a frequency-discrimination task. J.Neurophysiol. 67, 1031-1056.

Regan, D., Beverley, K.I., 1985. Postadaptation orientation discrimination. J.Opt.Soc.Am.A 2, 147-155.

Rehberg, B., Ruschner, R., Fischer, M., Ebeling, B.J., Hoeft, A., 1998. Konzentrationsabhängige Veränderungen der Latenz und Amplitude somatosensorisch evozierter Potentiale durch Desfluran, Isofluran und Sevofluran, [Concentration-dependent changes in the latency and amplitude of somatosensory-evoked potentials by desflurane, isoflurane and sevoflurane]. Anasthesiol.Intensivmed.Notfallmed.Schmerzther. 33, 425-429.

Rinderknecht, M.D., Yeongmi, K., Santos-Carreras, L., Bleuler, H., Gassert, R., 2013. Combined tendon vibration and virtual reality for post-stroke hand rehabilitation., World Haptics Conference (WHC), 2013, pp. 277-282.

Ringo, J.L., 1996. Stimulus specific adaptation in inferior temporal and medial temporal cortex of the monkey. Behavioural Brain Research 76, 191-197.

Riquelme, I., Padron, I., Cifre, I., Gonzalez-Roldan, A.M., Montoya, P., 2014. Differences in somatosensory processing due to dominant hemispheric motor impairment in cerebral palsy. BMC Neurosci. 15, 10.

Rytky, S., Huotari, A.M., Alahuhta, S., Remes, R., Suominen, K., Jantti, V., 1999. Tibial nerve somatosensory evoked potentials during EEG suppression in sevoflurane anaesthesia. Clin.Neurophysiol 110, 1655-1658.

Sathian, K., Zangaladze, A., 1996. Tactile spatial acuity at the human fingertip and lip Bilateral symmetry and interdigit variability. Neurology 46, 1464.

Schindler, E., Thiel, A., Müller, M., Milosevic, M., Langer, C., Hempelmann, G., 1996. Veränderungen somatosensorisch evozierter Potentiale nach Sevofluran und Isofluran - Eine randomisierte Phase III-Studie, [Changes in somatosensory evoked potentials after sevoflurane and isoflurane. A randomized phase III study]. Der Anaesthesist 45, S52-S56.

Schmidt, R.F., 1973. Control of the Access of Afferent Activity to Somatosensory Pathways. In: Iggo, A. (Ed.), Somatosensory System, 2nd ed. Springer Berlin Heidelberg, pp. 151-206.

Schwender, D., End, H., Daunderer, M., Fiedermutz, M., Peter, K., 1998. Sevofluran und Nervensystem, [Sevoflurane and the nervous system]. Anaesthesist 47 Suppl 1, S37-S42.

Sclar, G., Ohzawa, I., Freeman, R.D., 1985. Contrast gain control in the kitten's visual system. Journal of Neurophysiology 54, 668-675.

Severens, M., Farquhar, J., Desain, P., Duysens, J., Gielen, C., 2010. Transient and steady-state responses to mechanical stimulation of different fingers reveal interactions based on lateral inhibition. Clin.Neurophysiol 121, 2090-2096.

Shagass, C., Schwartz, M., 1964. Recovery functions of somatosensory peripheral nerve and cerebral evoked responses in man. Electroencephalography and Clinical Neurophysiology 17, 126-135.

Shulz, D.E., Feldman, D.E., 2013. Spike Timing-Dependent Plasticity. In: Rakic, J.L.R. (Ed.), Neural Circuit Development and Function in the Brain. Academic Press, Oxford, pp. 155-181.

Sjöström, J., Gerstner, W., 2010. Spike-timing dependent plasticity. Scholarpedia 5, 1362.

Smith, R.L., Brachman, M.L., Goodman, D.A., 1983. Adaptation in the auditory periphery. Annals of the New York Academy of Sciences 405, 79-93.

Sobel, N., Prabhakaran, V., Zhao, Z., Desmond, J.E., Glover, G.H., Sullivan, E.V., Gabrieli, J.D.E., 2000. Time Course of Odorant-Induced Activation in the Human Primary Olfactory Cortex. Journal of Neurophysiology 83, 537-551.

Song, S., Miller, K.D., Abbott, L.F., 2000. Competitive Hebbian learning through spike-timing-dependent synaptic plasticity. Nat.Neurosci. 3, 919-926.

Sosnik, R., Haidarliu, S., Ahissar, E., 2001. Temporal Frequency of Whisker Movement. I. Representations in Brain Stem and Thalamus. Journal of Neurophysiology 86, 339-353.

Speckmann, E.J., Elger, C.E., Gorji, A., 2011. Neurophysiologic basis of EEG and DC potentials. In: Niedermeyer, E., Schomer, D.L., da Silva, F.H.L. (Eds.), Niedermeyer's Electroencephalography: Basic Principles, Clinical Applications, and Related Fields. Wolters Kluwer Health/Lippincott Williams & Wilkins, pp. 17-31.

Srinivasan, M.A., Dandekar, K., 1996. An Investigation of the Mechanics of Tactile Sense Using Two-Dimensional Models of the Primate Fingertip. Journal of Biomechanical Engineering 118, 48-55.

Starr, A., Pratt, H., Burke, D., 1982. Natural stimuli evoking somatosensory potentials. Ann.N.Y.Acad.Sci. 388, 702-706.

Stent, G.S., 1973. A Physiological Mechanism for Hebb's Postulate of Learning. Proc.Natl.Acad.Sci.USA 70, 997-1001.

Stevenson, R.J., Wilson, D.A., 2007. Odour perception: an object-recognition approach. Perception-London 36, 1821-1833.

Stuck, B.A., Fadel, V., Hummel, T., Sommer, J.U., 2014. Subjective Olfactory Desensitization and Recovery in Humans. Chemical Senses 39, 151-157.

Talbot, W.H., Darian-Smith, I., Kornhuber, H.H., Mountcastle, V.B., 1968. The sense of flutter-vibration: comparison of the human capacity with response patterns of mechanoreceptive afferents from the monkey hand. J Neurophysiol. 31, 301-334.

Tanaka, Y., Nagai, T., Sakaguchi, M., Fujiwara, M., Sano, A., 2013. Tactile sensing system including bidirectionality and enhancement of haptic perception by tactile feedback to distant part., World Haptics Conference (WHC), 2013, pp. 145-150.

Tannan, V., Simons, S., Dennis, R.G., Tommerdahl, M., 2007. Effects of adaptation on the capacity to differentiate simultaneously delivered dual-site vibrotactile stimuli. Brain Research 1186, 164-170.

Tannan, V., Holden, J.K., Zhang, Z., Baranek, G.T., Tommerdahl, M.A., 2008. Perceptual metrics of individuals with autism provide evidence for disinhibition. Autism Research 1, 223-230.

Tannan, V., Whitsel, B.L., Tommerdahl, M.A., 2006. Vibrotactile adaptation enhances spatial localization. Brain Research 1102, 109-116.

Tavassoli, T., Miller, L.J., Schoen, S.A., Nielsen, D.M., Baron-Cohen, S., 2014. Sensory over-responsivity in adults with autism spectrum conditions. Autism 18, 428-432.

Thomas-Danguin, T., Sinding, C., Romagny, S., El Mountassir, F., Atanasova, B., Le Berre, E., Le Bon, A.M., Coureaud, G., 2014. The perception of odor objects in everyday life: a review on the processing of odor mixtures. Frontiers in Psychology 5.

Thompson, R.F., Spencer, W.A., 1966. Habituation: a model phenomenon for the study of neuronal substrates of behavior. Psychological review 73, 16.

Torre, V., Ashmore, J.F., Lamb, T.D., Menini, A., 1995. Transduction and adaptation in sensory receptor cells. The Journal of Neuroscience 15, 7757-7768.

Ulanovsky, N., Las, L., Farkas, D., Nelken, I., 2004. Multiple Time Scales of Adaptation in Auditory Cortex Neurons. The Journal of Neuroscience 24, 10440-10453.

Vallbo, A.B., Hagbarth, K.E., 1968. Activity from skin mechanoreceptors recorded percutaneously in awake human subjects. Experimental Neurology 21, 270-289.

Vallbo, A.B., Johansson, R.S., 1984. Properties of cutaneous mechanoreceptors in the human hand related to touch sensation. Hum Neurobiol 3, 3-14.

Van Boven, R.W., Johnson, K.O., 1994. The limit of tactile spatial resolution in humans: Grating orientation discrimination at the lip, tongue, and finger. Neurology 44, 2361.

Van Olphen, A.F., Rodenburg, M., Verwey, C., 1979. Influence of the stimulus repetition rate on brain-stem-evoked responses in man. International Journal of Audiology 18, 388-394.

van Turennout, M., Bielamowicz, L., Martin, A., 2003. Modulation of Neural Activity during Object Naming: Effects of Time and Practice. Cerebral Cortex 13, 381-391.

van Turennout, M., Ellmore, T., Martin, A., 2000. Long-lasting cortical plasticity in the object naming system. Nat Neurosci 3, 1329-1334.

Vaughan, D.J.A., Thornton, C., Wright, D.R., Fernandes, J.R., Robbins, P., Dore, C., Brunner, M.D., 2001. Effects of different concentrations of sevoflurane and desflurane on subcortical somatosensory evoked responses in anaesthetized, non-stimulated patients. British Journal of Anaesthesia 86, 59-62.

Venkatesan, L., Barlow, S., Popescu, M., Popescu, A., Auer, E.T., 2010. TAC-Cell inputs to human hand and lip induce short-term adaptation of the primary somatosensory cortex. Brain Res. 1348, 63-70.

Von Békésy, G., 1967. Sensory inhibition. Princeton University Press, Princeton.

Von Békésy, G., 1960. Just-noticeable differences of amplitude and frequency. In: Von Békésy, G., Wever, E.G. (Eds.), Experiments in hearing. McGraw-Hill New York, pp. 207-238.

von der Behrens, W., Bäuerle, P., Kössl, M., Gaese, B.H., 2009. Correlating Stimulus-Specific Adaptation of Cortical Neurons and Local Field Potentials in the Awake Rat. The Journal of Neuroscience 29, 13837-13849.

von Knorring, L., Monakhov, K., Perris, C., 1978. Augmenting/Reducing: an Adaptive Switch Mechanism to Cope with Incoming Signals in Healthy Subjects and Psychiatric Patients. Neuropsychobiology 4, 150-179.

Walsh, P., Kane, N., Butler, S., 2005. The clinical role of evoked potentials. J Neurol.Neurosurg.Psychiatry 76 Suppl 2, ii16-ii22.

Wang, Q., Webber, R.M., Stanley, G.B., 2010. Thalamic synchrony and the adaptive gating of information flow to cortex. Nat.Neurosci. 13, 1534-1541.

Wang, X., Merzenich, M.M., Sameshima, K., Jenkins, W.M., 1995. Remodelling of hand representation in adult cortex determined by timing of tactile stimulation. Nature 378, 71-75.

Watt, D.G.D., Money, K.E., Tomi, L.M., 1986. M.I.T./Canadian vestibular experiments on the Spacelab-1 mission: 3. Effects of prolonged weightlessness on a human otolith-spinal reflex. Exp Brain Res 64, 308-315.

Wedell, C.H., Cummings, S.B.Jr., 1938. Fatigue of the vibratory sense. Journal of Experimental Psychology 22, 429-438.

Whitsel, B.L., Juliano, S.L., 1984. Imaging the responding neuronal population with 14C-2-DG: the cerebral cortical signature of a tactile stimulus. Somatosensory Mechanisms, Wenner-Gren International Symposium, 61-80.

Wiederholt, W.C., 1978. Recovery function of short latency components of surface and depth recorded somatosensory evoked potentials in the cat. Electroencephalography and Clinical Neurophysiology 45, 259-267.

Willis, W.D.Jr., Coggeshall, R.E., 2004. Sensory Mechanisms of the Spinal Cord: Volume 1 Primary Afferent Neurons and the Spinal Dorsal Horn, 1st ed. Springer Science & Business Media.

Wilson, D.A., Rennaker, R.L., 2009. Cortical Activity Evoked by Odors., The Neurobiology of Olfaction. CRC Press, pp. 353-366.

Wissig, S.C., Kohn, A., 2012. The influence of surround suppression on adaptation effects in primary visual cortex. Journal of Neurophysiology 107, 3370-3384.

Xibo, W., Jiting, L., 2013. A tele-rehabilitation system with bilateral haptic feedback to both the therapist and the patient via time-delay environment., World Haptics Conference (WHC), 2013, pp. 331-334.

Yeangjin, K., Yaungjin, N., Ahn, B., Jung, K., 2013. Advanced 2D machine palpation for tissue abnormality localization in a simulated environment., World Haptics Conference (WHC), 2013, pp. 133-138.

Yoder, W.M., Munizza, O., Lyman, M., Smith, D.W., 2014. A Technique for Characterizing the Time Course of Odor Adaptation in Mice. Chemical Senses 39, 631-640.

York, D.H., 1985. Somatosensory evoked potentials in man: differentiation of spinal pathways responsible for conduction from the forelimb vs hindlimb. Prog.Neurobiol. 25, 1-25.

Young, C.J., Apfelbaum, J.L., 1995. Inhalational anesthetics: desflurane and sevoflurane. J Clin.Anesth. 7, 564-577.

Zhang, F., Eliassen, J., Anderson, J., Scheifele, P., Brown, D., 2009. The time course of the amplitude and latency in the auditory late response evoked by repeated tone bursts. Journal of the American Academy of Audiology 20, 239-250.

Zhang, L.I., Tao, H.W., Holt, C.E., Harris, W.A., Poo, M.m., 1998. A critical window for cooperation and competition among developing retinotectal synapses. Nature 395, 37-44.

Zufall, F., Leinders-Zufall, T., 2000. The Cellular and Molecular Basis of Odor Adaptation. Chemical Senses 25, 473-481.

Supplementary Figures

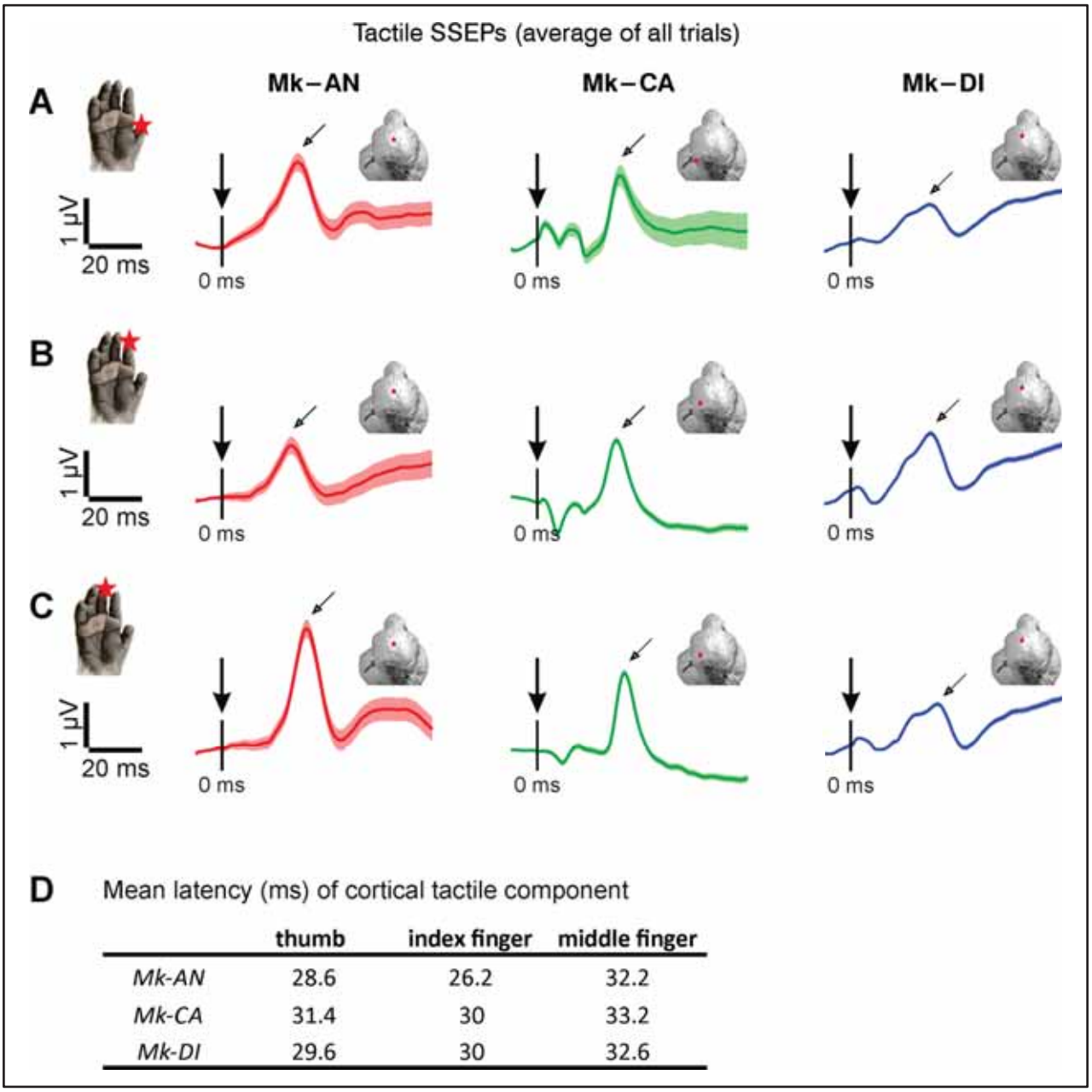

D Mean latency (ms) of cortical tactile component

	thumb	index finger	middle finger
Mk-AN	28.6	26.2	32.2
Mk-CA	31.4	30	33.2
Mk-DI	29.6	30	32.6

Supplementary Figure 1: Average tactile SSEPs in each monkey. Tactile SSEPs ± SEM (lighter shade) from the contralateral scalp electrode (red dot) with maximal cortical positivity (small oblique arrows), obtained by averaging all trials after tactile stimulation delivered to the right thumb tip (A), index fingertip (B) and middle fingertip (C) in Mk-AN, Mk-CA and Mk-DI. The arrow above the trace points at the stimulation onset (i.e. 0 ms). The time and amplitude scales are the same for the 3 animals. (D) Mean latency of the cortical tactile component (in ms) resulting from the average of all trials for each stimulation site in each monkey.

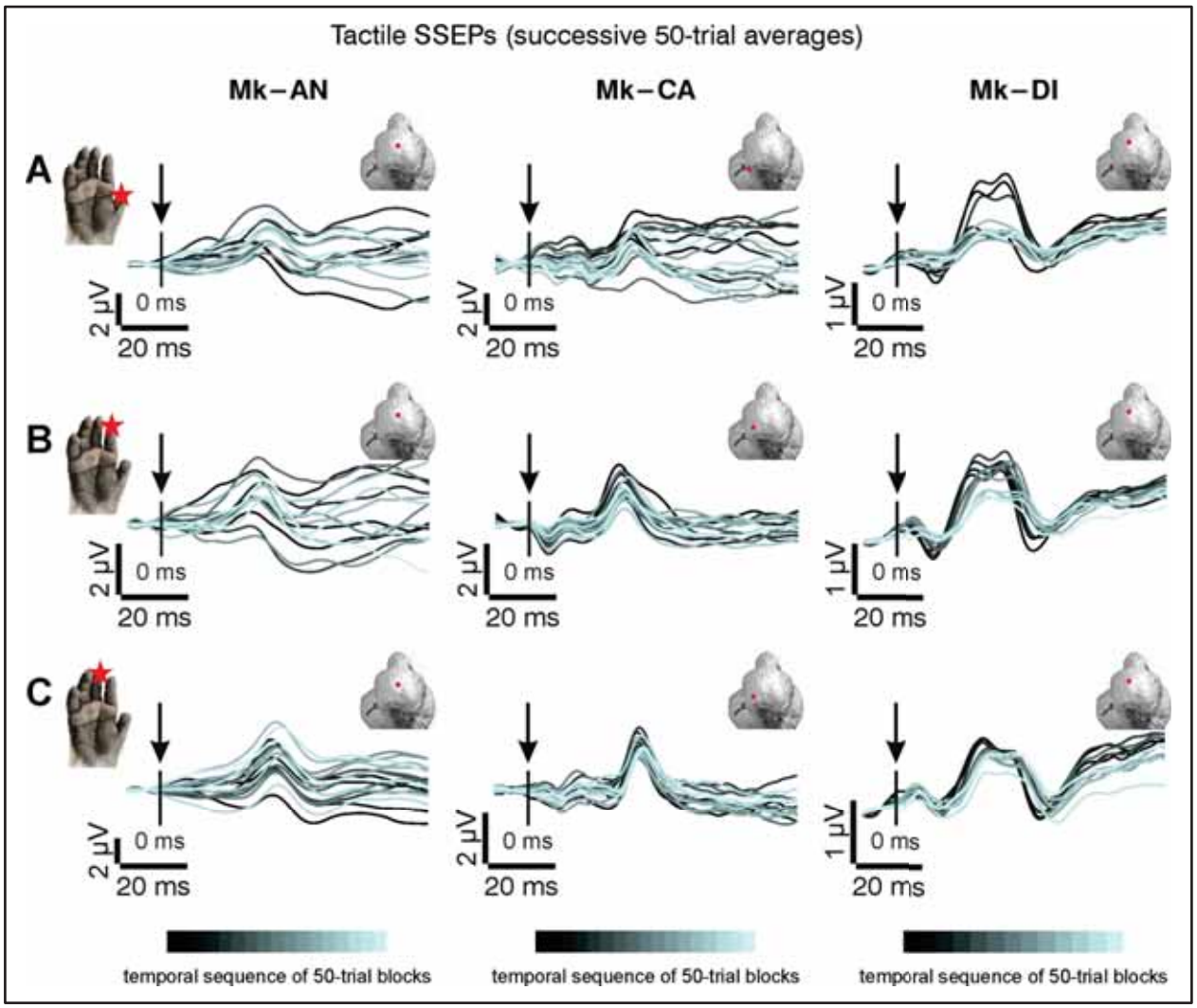

Supplementary Figure 2: Successive 50-trial averages of tactile SSEPs over time in each monkey. The same data as in Supplementary Figure 1 were then averaged into non-overlapping successive blocks of 50 trials in each animal. (A) right thumb tip SSEPs, (B) index fingertip SSEPs, (C) middle fingertip SSEPs (C). Each superimposed trace represents the average of a block of 50 trials. The temporal sequence of the blocks is reflected by the colour gradient (from first 50-trial block in dark blue to last 50-trial block in light blue). The arrow above the traces points at the stimulation onset (i.e. 0 ms). Note that here the amplitude scale was adapted to every finger in each monkey.

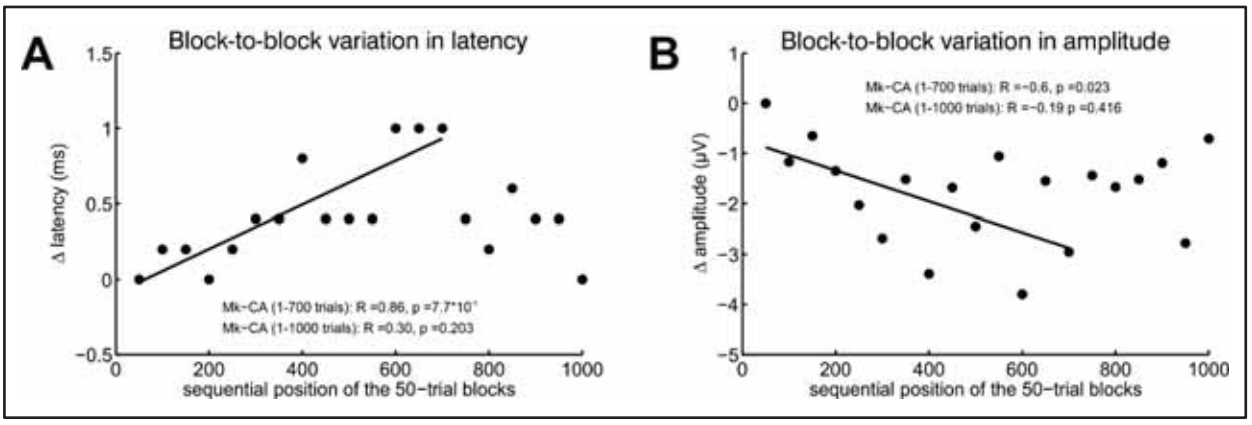

Supplementary Figure 3: (A) Latency and (B) amplitude adaptation in SSEPs, after electrical stimulation to the right median nerve at the wrist. Same data as those presented in Figure 2E and F but here, the y-axis was adapted so as to better visualise the block-to-block variability. See legend of Figure 2 for greater detail.

CHAPTER 5

Sensorimotor functional recovery of manual dexterity in non-human primates following a motor cortex lesion assessed with the Brinkman box task

Anne-Dominique Gindrat, Alexander F Wyss (AFW), Mélanie Kaeser (MK), Cindy Leuthard and Eric M Rouiller

Abstract

A *Brinkman box task* was developed to assess fine manual dexterity in macaque monkeys during retrieval of small food pellets from horizontal and vertical wells on a board by using the precision grip, in the context of motor cortex lesions. The specificity and advantage of this test over the other ones currently used in our laboratory were the possibility to perform the task either under visual feedback or without visual feedback. Without visual feedback, we expected to challenge the sensorimotor control of manual dexterity relying mainly on tactile and proprioceptive inputs from the fingers and on blind exploratory motor ability. A detailed video analysis was used to precisely document the time course of the task as well as hand movements, finger use and errors in pellet picking. After several weeks of training, seven adult macaque monkeys reached a plateau of performance. The animals were then subjected to a unilateral permanent lesion located predominantly in the hand representation in M1. Following the lesion, the contralesional manual dexterity was strongly impaired, characterised by a decrease in the speed of motor execution, some deficits in fine finger movements and in wrist deviations as well as a worse proficiency of the animals to collect the pellets. Moreover the amount of these deficits was usually correlated with the extent of the lesion. As expected, we also observed that the contralesional functional recovery of performance in the Brinkman box task with vision was better than in the task without vision. But more interestingly, some subtle post-lesion impairments emerged more specifically in the task without vision, such as a striking prominent deficit of finger use, some somatosensory-related deficits, as well as impairments following a cortical biopsy. Taken together, these results suggested, first, that the Brinkman box task was very sensitive and relevant to test the exploratory ability and tactile sense in blind condition in a lesional context. Second, we further confirmed that an M1 lesion may result in somatosensory deficits or a disruption of M1-S1 connections in addition to pure motor impairments, emphasizing the role of somatosensory feedback during motor actions.

Introduction

The outstanding primate hand

By looking at a pianist performing a piece of music at full speed, or a watchmaker meticulously mounting a watch, one immediately realises that the hand represents a very intricate and sophisticated mechanism. Indeed the basic skeleton of the human wrist and hand contains a total of 27 bones (8 carpal bones, 5 metacarpal bones and 14 phalanges) and 29 joints, at least 123 ligaments; hand movements are controlled by about 35 muscles and tendons innervated by 3 nerves (median, ulnar, and radial) that diverge then into innumerable smaller branches innervating the papillae of the palmar pads and dorsal skin (Alexander, 1993; Brorsson, 2012; Gray, 1893; Napier, 1993; Taylor and Schwarz, 1955). The interaction of all these muscles, tendons, bones, joints and nerves allows this complex apparatus to perform a huge range of movements (Brorsson, 2012) –from multi-finger grasping to fine and individuated movements of single fingers– and to assume important functions, such as the sense of touch or communication for instance (Napier, 1993; Schieber and Santello, 2004). Given that "*the hand is the mirror of the brain*" (Napier, 1993, p. 25), the outstanding properties of this organ are correlated with extended and detailed hand and finger representations at the level of motor cortex (especially in M1 and PMv) (e.g. Dechent and Frahm, 2003; Dum and Strick, 1996; Kleinschmidt et al., 1997; Lemon, 1993; Lemon, 1997; Penfield and Rasmussen, 1950; Rizzolatti et al., 1988; Schieber and Hibbard, 1993; Woolsey et al., 1952) and S1 (e.g. Kaas et al., 1979; Krubitzer and Disbrow, 2005; Martuzzi et al., 2014; Nelson et al., 1980; Overduin and Servos, 2004; Penfield and Rasmussen, 1950).

One special feature of human and Old World monkeys is their ability to perform very fine and independent finger movements (Courtine et al., 2007; Darian-Smith, 1984; Darian-Smith et al., 1996; Napier, 1962), exemplified by the precision grip (Napier, 1956), namely the full opposition of the thumb and the flexor aspects of the fingers (usually the index finger) to pinch objects. Unlike the power grip, the precision grip is used when fine motor control has to be favoured as compared to power (Napier, 1962). These refined prehensile abilities of the hand arose in the evolution of primates (**Figure 1**) with the acquisition of an independent control of the thumb and the index finger and with the emergence of a fully opposable thumb in Old World monkeys, meaning that it can rotate around the carpometacarpal joint to establish contact of its finger pad with

the pads of the index and middle fingers (Darian-Smith, 1984; Darian-Smith et al., 1996; Napier, 1962).

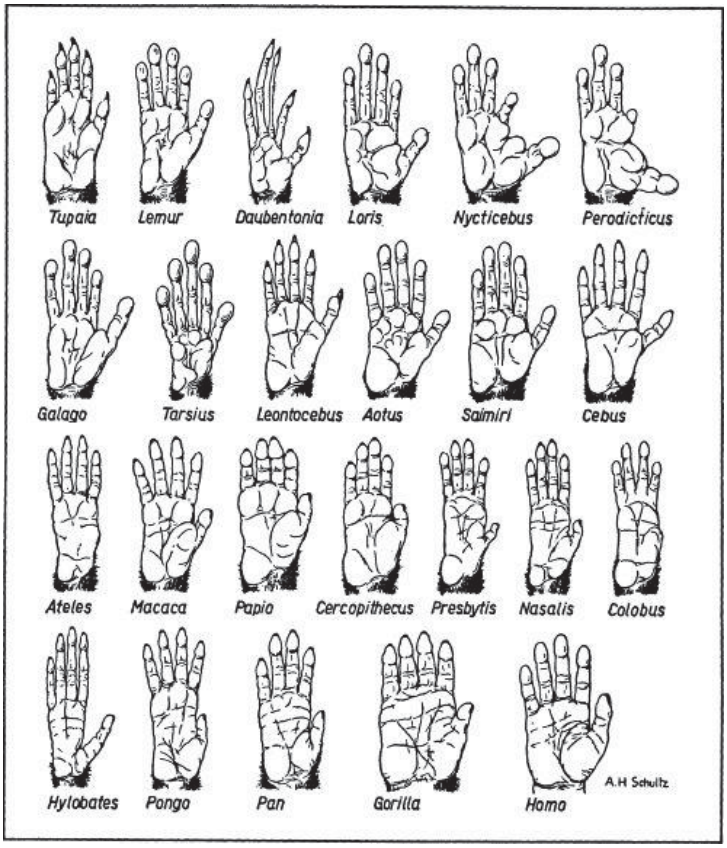

Figure 1: Right hand of different primates, from Tupaia to modern human. The most striking feature of primates is their highly manipulative grasping hands (and feet). The grasping hands arose in primates living in the trees and the emergence of an opposable thumb allowed them to grasp branches. During evolution, claws disappeared. Most actual primates have instead flat fingernails and larger fingertip pads. The opposable thumbs allow primates to manipulate objects in order to carefully investigate their environment. More specifically, the human thumb is longer in relation to the other fingers than the thumb of most other primates. This long thumb and its ability to fully touch the other fingers give human the capability to both firmly grasp (by using power grip) and finely manipulate objects of many different shapes (precision grip) (Napier, 1962; figure from Schultz, 1969; Young, 2003).

The complex biomechanical architecture of the hand makes it vulnerable to injuries, diseases and dysfunctions of motor control, especially after a stroke (Nowak, 2008), leading to an increasing interest in understanding the mechanisms of brain plasticity following such an event and in finding strategies to promote functional recovery. Due to the large similarities in nervous system organisation between human and macaque monkeys, especially with regard to the highly accomplished hand motor control achieved by the latter (Capitanio and Emborg, 2008; Courtine et al., 2007; Lemon, 2012), and the largely similar hand anatomy and function in both these primate genera, macaque monkeys constitute a model of choice to investigate the mechanisms of brain plasticity after a lesion affecting the hand motor control. For instance, several studies showed that a per-

manent focal lesion of the hand representation of M1 in monkeys resulted in a strong deficit in manual dexterity of the contralesional hand characterised by an initial complete loss of finger movements followed by a spontaneous gradual functional recovery. In most cases, although some relatively independent finger movements were restored, allowing to perform some precision grip, the ability to perform fine fractionated finger movements remained permanently altered as well as the ability to perform wrist deviations (e.g. Darling et al., 2014; Frost et al., 2003; Glees and Cole, 1950; Hoogewoud et al., 2013; Liu and Rouiller, 1999; Nudo and Milliken, 1996; Passingham et al., 1983; Pizzimenti et al., 2007; Rouiller et al., 1998; Rouiller and Olivier, 2004; Wyss et al., 2013). Changes in precision grip strategies were observed as well over the post-lesion time (Murata et al., 2008). Similarly, a unilateral section of the CST fibres controlling the distal upper limb muscles induced a severe impairment of ipsilesional hand motor control in macaque monkeys followed by a more or less strong recovery of hand dexterity (Freund et al., 2006; Freund et al., 2009; Galea and Darian-Smith, 1997; Hoogewoud et al., 2013; Lawrence and Kuypers, 1968; Nishimura et al., 2007; Schmidlin et al., 2004; Zaaimi et al., 2012).

Assessment of the fine manual dexterity in non-human primates

In the aforementioned studies and in others, more or less elaborated behavioural tests based on the use of the precision grip were employed to quantify fine manual dexterity in non-human primates.

The first behavioural tasks for monkeys involving reward picking were designed by Heinrich Klüver in the 1930s, such as the "auto-multi-stimulation reaction board" task. This bimanual test consisted in a board "*from which food [could] be obtained only by using one hand for lifting and holding a plate and the other for removing a brass square and the food*." (Klüver and Bucy, 1938; Klüver, 1935).

Later, J. Brinkman and H.G.J.M. Kuypers (1972; 1973) developed a task requiring visually-guided movements of one upper limb to reach and pick up small food pellets from wells in split-brain monkeys (**Figure 2A**). A board was designed in such a way that food morsels were visible but not palpable before collecting them, so as to avoid tactile guidance: many (the exact number was not mentioned in the original paper!) circular wells –

each filled with a food pellet– were randomly distributed on the board, each of them being interconnected through radially-oriented grooves with 1 to 3 other wells to facilitate the pellet retrieval. The task was made more difficult by adding some disturbing tactile cues on the board. In addition, J. Brinkman and H.G.J.M. Kuypers (1972; 1973) used much more simple tests based on food pellet retrieval from a forceps or from the experimenter's fingers. The original board was then refined by C. Brinkman (1984) by replacing the circular wells with 43 rounded rectangular wells in four different orientations and by removing the interconnections between the wells (**Figure 2B**). The size of the wells was designed so as to allow the macaque monkeys to insert a single finger in them and collect then the pellet by making a precision grip (Brinkman, 1984). This test has been used in our laboratory since many years in a further improved version –the modified Brinkman board task (**Figure 2C**) (Bashir et al., 2012; Chatagny et al., 2013; Freund et al., 2006; Freund et al., 2009; Hoogewoud et al., 2013; Kaeser et al., 2010; Kaeser et al., 2013; Kaeser et al., 2014; Kermadi et al., 1997; Liu and Rouiller, 1999; Rouiller et al., 1998; Schmidlin et al., 2011; Wyss et al., 2013). A full description of the task is provided in **Chapter General Materials and Methods** and in the **Appendix 2**. In brief, the animal has to unimanually or bimanually collect small banana pellets from 25 vertically- and 25 horizontally-oriented wells randomly distributed on a rectangular board. This task is performed freely, i.e. with complete visual feedback and with neither constraint of time nor reduced space limiting the degrees of freedom of the arm performing the task. Since its introduction in our laboratory, additional tests have been then derived from the modified Brinkman board task, namely the rotating Brinkman board task and the Brinkman box task (Schmidlin et al., 2011). The latter will be presented in greater detail below. The rotating Brinkman board task consists in unimanually retrieving banana pellets from 32 wells organised in 4 concentric circles on a rotating board (clockwise or counter-clockwise). Asanuma and Arissian (1984) used a quite similar rotating board based on the original Brinkman board as well.

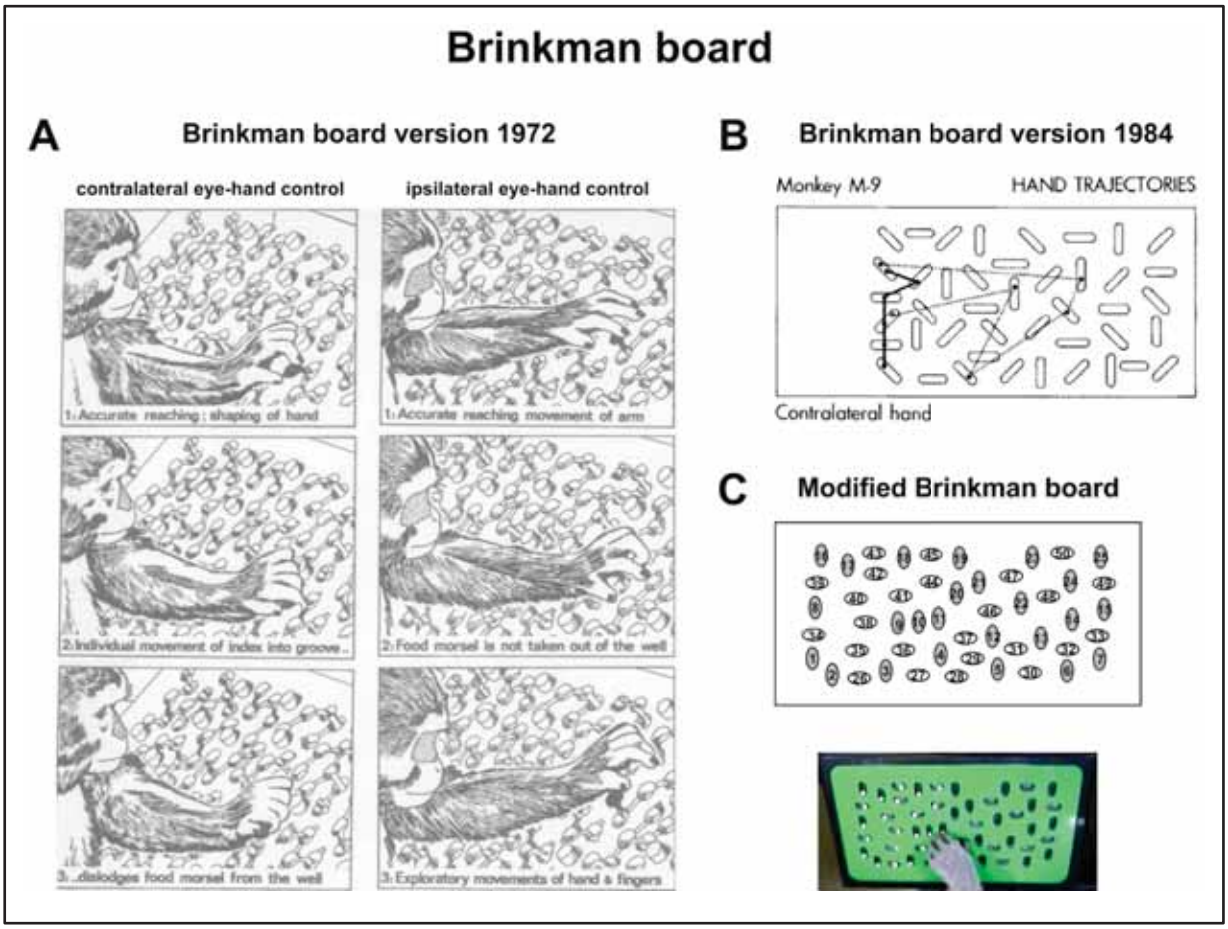

Figure 2: Brinkman board. (A) Original drawing from J. Brinkman illustrating a split-brain rhesus monkey, with one eye covered (left eye on the left side and right eye on the right side), collecting food pellets from a board. Under right eye visual guidance, the animal was easily able to perform precision grip with the left hand to retrieve the food pellets. On the contrary, under left eye visual guidance, the split-brain monkey showed deficits to use its left hand. Essentially, the animal showed exploratory behaviour as if it was blind (from Brinkman and Kuypers, 1972). (B) Second version of the Brinkman board. The macaque monkey was facing the shorter side of the board and had to fully extend its arm in order to collect the most distant pellets. Two picking sequences are drawn (solid lines: control monkey; dotted lines: monkey one week after a right SMA ablation) (from Brinkman, 1984). (C) Modified Brinkman board (50 wells) currently used in our laboratory. The board is presented with its largest side facing the macaque monkey.

Another task of choice commonly used in laboratories working on non-human primate models to test visually-guided reaching behaviours is the so-called Klüver board task (**Figure 3**) (Brochier et al., 1999; Dancause et al., 2005; Dancause et al., 2006; Darling et al., 2009; Darling et al., 2010; Eisner-Janowicz et al., 2008; Friel et al., 2005; Friel and

Nudo, 1998; Friel et al., 2000; Frost et al., 2003; Glees, 1956; Lawrence and Kuypers, 19681; Mason et al., 1998; McNeal et al., 2010; Murata et al., 2008; Nudo et al., 1992; Nudo et al., 1996; Nudo et al., 1997; Nudo et al., 2000; Passingham et al., 1983; Pizzimenti et al., 2007; Plautz et al., 2000; Plautz et al., 2003; Sugiyama et al., 2013; Xerri et al., 1998). Several adaptations were performed from the original test –the "dexterity board"– proposed by Cole and Glees in the 1950s (**Figure 3A**) (Cole, 1952; Glees, 1956). The more "modern" versions of the test require a board with 4 to 24 cylindrical wells of different diameters allowing to insert from several fingers to a single finger in order to unimanually collect the food pellet located in each well (**Figure 3B-D**).

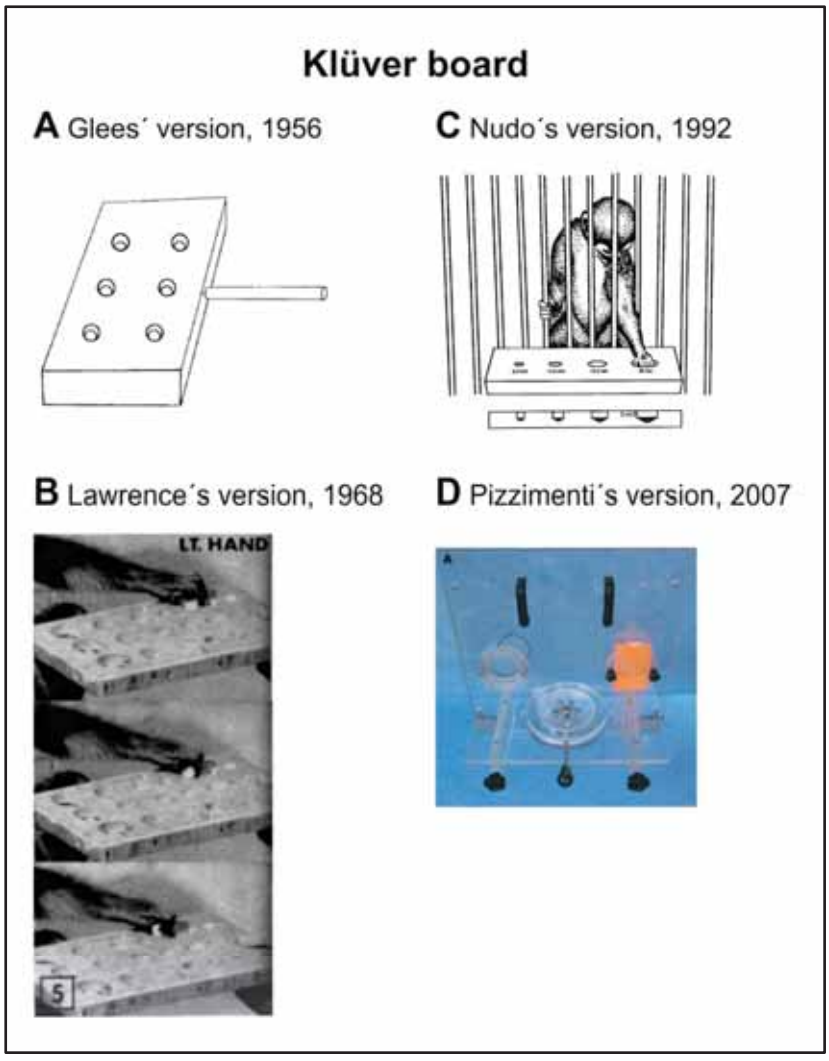

Figure 3: Klüver board. (A) Original version of the Klüver board for macaque monkeys, called at that time "dexterity board", developed by Glees, with 2 x 3 wells of equal size and depth. Other models contained 3 x 4 similar wells (Glees, 1956). (B) Macaque monkey performing a refined version of the Klüver board task based on 3 (different diameters) x 8 wells, with the left hand, 2 months after a bilateral CST lesion (Lawrence and Kuypers, 1968)[15]. (C) Squirrel monkey performing the Klüver board task. The Nudo's version of the board contains here 4 wells of graded diameters, needing the monkey to adapt its picking strategy to collect the food pellet located in each well (from the insertion of the whole hand into the largest well to the use of only

[15] Original video sequences from Lawrence and Kuypers' experiments are available as supplementary material in Lemon et al. (2012). Supplementary Video 1 in particular shows a control monkey performing the Klüver board task.

one or two fingers into the smallest well) (Nudo et al., 1992; Nudo et al., 1997). (D) Front view of Pizzimenti's version of the Klüver board, with 5 wells on a rotating board. Portals allow to restrain the use of one hand while the other is working (Pizzimenti et al., 2007).

In the most historical studies about experimental cortical lesion, the functional recovery was essentially described qualitatively (Brinkman, 1984; Brinkman and Kuypers, 1972; Brinkman and Kuypers, 1973; Klüver and Bucy, 1938; Lawrence and Kuypers, 1968). Then, analysis methods were developed to objectively quantify the fine manual dexterity. The performance in the modified Brinkman board and rotating Brinkman board tasks (see the aforementioned references), for instance, has been usually expressed in the form of a number of rewards collected in a given time period, the time needed to collect each reward, the wrist deviation needed to collect the rewards, the first finger used in the precision grip and some specific errors. In addition, the temporal sequence of reward picking was investigated in some studies (Kaeser et al., 2013; Kaeser et al., 2014; Schmidlin et al., 2011), as already attempted by Brinkman (1984) (see **Figure 2B**). In the Klüver board task, the hand preference, the number of finger flexions per retrieval, the finger surface used, the different sequences of movement, the percentage of successful trials, the reach duration, the accuracy, the grip aperture, the first manipulation duration, the manipulation attempts, and specific errors were generally extracted from the data (see the aforementioned references).

Some additional tests were developed and used more sporadically: in addition to the Klüver board task, Passingham and collaborators (1983) used two behavioural tasks to assess the functional recovery of rhesus monkeys after a permanent lesion of the sensorimotor cortex: the hand preference was assessed by using a very straightforward reaching and picking up task through the bars of the monkeys' cage. A slot task was described as well, consisting of retrieving food morsels from slots (circular central part in the middle of 2 grooves) in 4 different orientations (Passingham et al., 1983). Additional more sophisticated reaching tasks on the vertical plane were used as well in order to challenge the movements of the whole hand, wrist and forearm. Galea and Darian-Smith used a reach-and-retrieve task during which macaque monkeys had to do a precision grip in the vertical plane to collect a small sugar pellet held between the jaws of a clamp (Darian-Smith and Ciferri, 2005; Darian-Smith, 2007; Galea and Darian-Smith, 1997, see their magnificent Fig. 1). Manual dexterity was assessed in the form of percentage of

successful trials, the pattern of finger movements and the time of finger contact with the rewards. Japanese experimenters trained macaque monkeys to perform the so-called vertical slot task, consisting of reaching for small food morsels driven on a point through a narrow vertical slit by using the precision grip (Higo et al., 2009; Murata et al., 2008; Murata et al., 2015; Nishimura et al., 2007; Sasaki et al., 2004; Sugiyama et al., 2013). They essentially documented the performance by measuring the percentage of successful trials and, in some cases, the amount of rewards collected in a given time period. A quite similar grasping task of collecting food morsels driven on a rod was introduced by Darling and collaborators (2006; 2009; 2010) but now with the set-up in horizontal position and with an elaborated system to measure forces and torques applied to retrieve the rewards. Much less demanding tests were used as well, requiring the monkeys to simply collect isolated food rewards presented in front of their home cage (Spinozzi et al., 2004) or based on a foraging board covered with artificial turf allowing to hidden some food pellets inside (Darling et al., 2014).

A more challenging task is currently used in our laboratory in parallel with the different Brinkman board tasks, namely the reach and grasp drawer task (Kaeser et al., 2014; Schmidlin et al., 2011). The current set-up has been derived and upgraded from a previously described version (Kazennikov et al., 1994; Kazennikov et al., 1998; Kazennikov et al., 1999; Kermadi et al., 1997; Kermadi et al., 1998; Kermadi et al., 2000; Wannier et al., 2002). In brief, the macaque monkey is facing an automatic drawer containing an internal hollow filled with a banana pellet. By using several sensors, the different phases of the reaching and grasping can be assessed when the monkey is unimanually opening the drawer and then collecting the food pellet still with the same hand. Different resistances against the drawer opening can be applied to challenge the ability of the monkey to generate load force.

The bimanual coordination to retrieve food pellets was largely studied as well, first in split-brain monkeys (Mark and Sperry, 1968), then in monkeys subjected to a lesion in SMA for instance (Brinkman, 1981) or more recently in naive macaque monkeys in order to assess their manual preference and dominance (see Chatagny et al., 2013 in **Appendix 3**). Essentially, the set-up consisted of a horizontal board perforated with several small cylindrical slots and the monkey had to use one finger, usually the index one, to push out (up or down) a food morsel located in each slot and then to collect it ei-

ther from below or from above with the other hand. In the study by Chatagny et al. (2013), the monkeys were presented with a tube task (Hopkins, 1995) and a bimanual drawer task as well. The tube task involved a tube (sized according to the monkey's hand) with a small slot at the bottom that was filled with a food morsel. The animal had to hold the suspended tube with one hand and reach the reward within the tube with the other hand. The bimanual drawer task is a more elementary version of the reach and grasp drawer task described above and required the monkey to open the drawer with one hand in order to collect the food pellet located inside by using the other hand.

More complex delayed grasping tests based on different kinds of power and precision grips were developed as well (Baumann et al., 2009; Fluet et al., 2010; Overduin et al., 2008; Schaffelhofer et al., 2015a; Schaffelhofer et al., 2015b; Vargas-Irwin et al., 2010).

The first visually-guided reaching tasks were usually performed with the monkey free in its home cage, and the animal was presented with the board either through the bars of the cage (see **Figure 3C**) or directly in its home cage (Cole, 1952; Glees, 1956; Lehman, 1978; Nudo et al., 1992). Testing conditions, such as the specific use of the tested hand or the distance between the animal and the board, were difficult to manage and consequently not fully reproducible. Nudo and co-workers (2000) introduced therefore the use of a restraining jacket, but still in the home cage, to ensure that the animals –squirrel monkeys– were actually only working with the hand to be tested. A different way to circumvent this problem was proposed by Pizzimenti et al. (2007) by allowing only a restricted access to the testing board by using Plexiglas tunnels with portals through which the monkeys had to introduce the hand in order to collect the reward (see **Figure 3D**). Another approach has been the use of a primate chair with sliding doors, allowing to easily manage the hand to be tested and the monkey-board distance (Bliss-Moreau et al., 2013; Gisolfi et al., 1978; Schmidlin et al., 2011 in **Appendix 2**).

All the tasks presented so far have been performed under full visual feedback. There are only few studies on non-human primates involving precision grip tasks achieved without visual feedback (Kilintari et al., 2011; Nelissen and Vanduffel, 2011) and few reports of tasks performed both under visual control and without visual control by the same subjects (Darian-Smith, 2007; Hikosaka et al., 1985). Some studies used such a paradigm in human (Karl et al., 2013; Proteau et al., 1987; Proteau, 1992; Troise et al., 2014). This is astonishing if we consider the large amount of evidence about the role of vision during

haptic touch (see the *Discussion* for greater detail). Tactile discrimination tasks by palpation were designed for monkeys either only without visual feedback (Semmes and Porter, 1972) or both under and then without visual control (Kruger and Porter, 1958).

Present study

There is now a wealth of evidence that M1 plays a significant role in somatosensory processing during the execution of motor actions (for a systematic review, see Asanuma, 1981; as well as Jones, 1986). Indeed, previous studies reported somatosensory changes following a lesion affecting the motor cortex. For instance, an increase of activity in S1 forelimb area was shown in macaque monkeys during the reversible inactivation of the M1 forelimb area (Sasaki and Gemba, 1984). In addition, after an ischemic lesion of the hand representation of caudal M1, squirrel monkeys were prone to sensory errors by performing the Klüver board task: in some trials, the animals failed to collect the food reward but needed then to visually inspect their empty hand to realise that they actually did not retrieve it. Remarkably, the authors observed a positive correlation between the increase in sensory errors and the deterioration of the manual dexterity, suggesting that functional deficit after a motor cortex lesion may be due to some extent to sensory impairment or sensorimotor disconnection (Darling et al., 2014; Friel et al., 2005; Nudo et al., 2000). Somatosensory feedbacks to M1 are of prime importance particularly in active motor exploration by palpation in the absence of visual feedback (Lemon, 1981). As a matter of fact, as already suggested by many, the motor and somatosensory systems of primates should be considered more globally as a functional sensorimotor system instead of two distinct entities (Jones, 1986; Kaas, 2004a; Kaas, 2004b; Kaas, 2008; Tanji and Wise, 1981; Uematsu et al., 1992; Wise and Tanji, 1981; Woolsey, 1964).

These considerations motivated us to investigate in greater detail the integrity of the somatosensory component of the sensorimotor system in our macaque monkeys subjected to a permanent cortical lesion of the hand representation in M1. To this aim, we developed a specific behavioural task involving the precision grip –the Brinkman box task– allowing to assess the role of somatosensory inputs during motor exploration by palpation in our monkeys before and after the M1 lesion. In particular, our hypothesis is that after a lesion in M1, the somatosensory component of the sensorimotor system will be affected in parallel with the motor control itself. We also hypothesise that the result-

ing somatosensory impairments can be highlighted with the Brinkman box task, especially when performed in the absence of visual feedback.

Materials and Methods

Macaque monkeys

Experiments were conducted on 7 adult macaque monkeys (*Macaca fascicularis*) (5 males: Mk-AV, Mk-JA, Mk-JO, Mk-RO, Mk-VA, and 2 females: Mk-DI, Mk-GE). They ranged from 2.5 to 5.5 years old at initiation of behavioural training. Details about their age and weight ranges at the time of the experiments can be found in **Table 1**. All data used in the present study were collected before September 2010 by AFW and MK, except Mk-DI's data. At that time, Mk-AV, Mk-GE, Mk-JA, Mk-JO, Mk-RO and Mk-VA were housed in the animal facility in groups of 2 to 5 congeners, each group in a 15-m^3 interior housing space (12 hours light/12 hours dark cycle), with no regular access to an outside facility. For reminder, Mk-DI lived with 4 other monkeys in a 45-m^3 room (12 hours light/12 hours dark cycle), with a regular access to an outside facility (21 m^3) for a part of the day or night, and with a higher degree of enrichment (trees, branches, ladders, large pipes to hide, different toys, foraging devices, etc.). No monkey included in this study was transferred from the 15-m^3 to the 45-m^3 housing facility. This consideration is important here because an increased enrichment may largely favour manual dexterity (Lutz and Novak, 2005). The housing conditions for each animal can be found in **Table 1**. The animals were on no account food- or water-deprived (see e.g. Kaeser et al., 2010; Schmidlin et al., 2011). All procedures and animal care were conducted in accordance with the *Guide for the Care and Use of Laboratory Animals* (Committee for the Update of the Guide for the Care and Use of Laboratory Animals and National Research Council, 2011) and were approved by local (Canton of Fribourg) and federal (Swiss) veterinary authorities. The present experiments were covered by the official veterinary authorisations FR 166/03, FR 166e/05, FR 156/04, FR 157/03, FR 157e/04, FR 157e/06, FR 17/09, FR 18/10 and FR 23765. Experimental procedures were designed to minimise the animals' pain and suffering.

	Mk-DI#	Mk-GE	Mk-RO§	Mk-VA	Mk-AV°	Mk-JO	Mk-JA*
Treatment	None	None	None	Anti-Nogo-A antibody	Sham cell therapy	Cell therapy	Cell therapy
Age at time of lesion (rounded to 0.5 year)	9.5	5	4	5.5	3.5	3.5	4
Weight at time of lesion (kg)	3.6	2.8	3.2	4.9	4.3	3.4	4.3
Volume of ibotenic acid injected (µl)	39.7	13	18	15.5	15	15	38
Number of sites injected with ibotenic acid	21	13	12	11	10	10	38
Total volume of lesion (mm^3) in the gray matter (motor cortex + post-central gyrus)	68.4	48.7	14	20	33.2	33.6	22.2
Volume of lesion in post-central gyrus (mm^3)	?	7.6	0	5.8	0	3.8	2.5
Spread of lesion to subcortical white matter	yes	no	no	no	yes	yes	yes
Volume of prefrontal cortical biopsy (mm^3)	-	-	-	-	44	20.3	8.8

Table 1: Detailed information about the monkeys involved in this study (orange: control untreated animals; blue: anti-Nogo-A antibody treated animal; green: animals involved in a protocol of adult neural progenitor cell therapy; see below for greater detail).

 # The cortical lesion in Mk-DI affected a restricted part of PM and a small portion of the area 3a in addition to M1, as explained in the Chapter 2.

§ Mk-RO was subjected to 3 successive cortical lesions because the first two did not produce the expected impairment of contralesional manual dexterity assessed with the modified Brinkman board task. Day 0 was defined as the time of the 3rd lesion.

° The cortical lesion in Mk-AV affected more PM than M1.

*** Immediately after the lesion, Mk-JA was treated with an anti-epileptic drug, producing a neuroprotective effect against the cortical lesion. As a consequence, the animal recovered nearly completely its pre-lesion contralesional manual dexterity. A second lesion was therefore performed 7 months after the first one. Day 0 was defined as the time of the 2nd lesion. This resulted in a small volume of lesioned tissue in relation to the volume of ibotenic acid injected.**

Brinkman box task

We assessed the integrity of the monkeys' sensorimotor system from a behavioural point of view by using the Brinkman box task. This test has been specifically designed to challenge the motor exploration by palpation and precision grip ability without visual feedback in macaque monkeys by relying mostly on tactile sense and proprioceptive in-

puts. Such fine fractionated movements of the fingers during active tactile exploration without visual feedback involve the activation of M1 neurons through glabrous afferent inputs (Lemon, 1981).

This board was derived from the modified Brinkman board currently used for manual dexterity tests in our laboratory (see **Chapter General Materials and Methods** and **Appendix 2** for a full description). The Brinkman box set-up consisted of a transparent Plexiglas® board (11.6 cm x 11.8 cm) containing 10 vertically- and 10 horizontally-oriented rounded rectangular wells (15 mm x 7.5 mm, 6 mm deep) (**Figure 4A**). This board itself was located in a box (13.4 cm x 13.3 cm x 23 cm, 20° angle above the horizontal) whose top could be opened or closed, corresponding either to a condition with visual feedback (called *with vision* condition, **Figure 4B**) or to a condition without visual feedback (called *without vision* condition, **Figure 4C**). The bottom of the box was made of transparent Plexiglas® and a lighting system was included on the internal side of the sliding top, allowing to record the task from under the box with a standard digital camera (Sony Handycam DCR-SX33, 25 frames/s). For Mk-DI, an additional similar camera was positioned in the midline above the set-up in front of the animal's head in order to visualise the complete movement of the monkey's arm from the box to the head and vice versa.

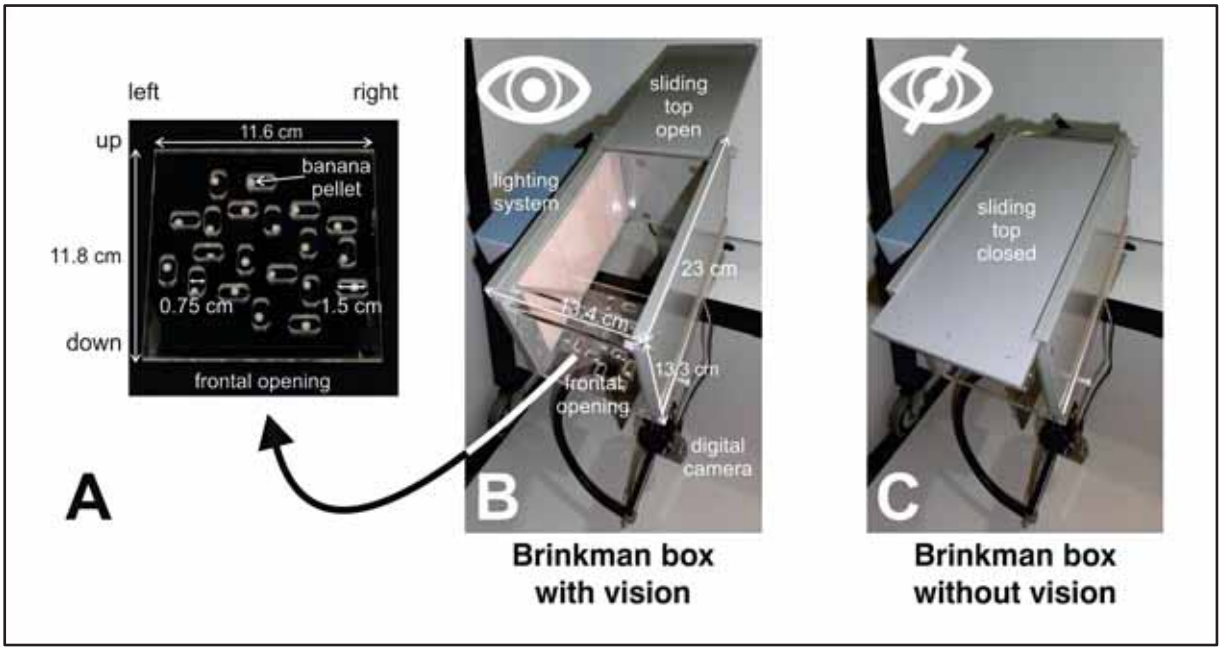

Figure 4: Brinkman box set-up. (A) Transparent Plexiglas® board containing 10 vertically- and 10 horizontally-oriented wells, each filled with a banana pellet. (B) Whole set-up in the condition with

vision. The animal was facing the set-up from the frontal opening. Note the position of the digital camera under the box. (C) Whole set-up in the condition without vision.

The task for the monkeys consisted of unimanually retrieving a 45-mg banana pellet (Bio-Serv, US and Canada, www.bio-serv.com) from each well. A fine finger motor control was required to perform the task, usually achieved by first introducing one finger (mostly the index finger or the thumb) into the well to establish a contact with the pellet, followed by the contact of a second finger (primarily the thumb or the index finger) to grasp the pellet with a precision grip while keeping the 3 other fingers flexed. To this aim, the monkeys were sat in a Plexiglas® primate chair with two sliding doors, allowing the animals to work with either hand individually while the other hand did not have access to the board (Schmidlin et al., 2011). The monkeys were facing the frontal opening of the Brinkman box with the door of the tested hand centred in the middle of the set-up. The distance between the door and the set-up was about 3 cm and the height at the basis of the board fitted the height at the basis of the door of the primate chair. Tests were conducted with each hand individually with and without vision (therefore 4 conditions per monkey), and alternating between the first tested hand from one session to the other. According to the monkeys' motivation and character, some animals (Mk-AV, Mk-GE, Mk-JA, Mk-JO, Mk-RO, Mk-VA) performed first the task without vision, followed by the task with vision with the first hand, and then the same with the other hand, whereas another animal (Mk-DI) first executed the task with vision, followed by the task without vision with the first hand, and then the same with the other hand. When performed with vision, it was a straightforward task to learn for the monkeys because they were simply reaching for food. In addition, this task was actually very similar to the modified Brinkman board task performed in parallel, except the smaller number of wells and the presence of the lateral walls of the box, limiting the degrees of freedom for the arm. Without vision, the task was more challenging, relying mostly on tactile and proprioceptive inputs from the fingers and on spatial memory. Importantly, the animals performed the task in a free-will basis, meaning that there was neither constraint of score level nor speed to achieve. To maintain a high level of motivation to complete the task, the animals were usually rewarded randomly in time during the task without vision (dried fruits, candies, cereal flakes), in addition to the banana pellets collected. Moreover, be-

havioural tests were usually performed with a musical background to mask disturbing noise from outside. Typically, these tests were conducted from twice to five times a week. Short video sequences illustrating the task performed with and without vision are available at http://www.unifr.ch/neuro/rouiller/research/BB.php. In addition to the Brinkman box task, the monkeys performed also the modified Brinkman board task (see **Chapter 2**), the rotating Brinkman board task and the reach and grasp drawer task but the results of these tests are not presented here (for greater detail, see Schmidlin et al., 2011 in **Appendix 2**). Data were usually collected over an extended pre-lesion period but the present report focuses only on the pre-lesion period once the task had been acquired in the form of a stable level of performance, and does not consider the learning period. Note that the present analyses were based on already existing video sequences for all the monkeys except Mk-DI.

Data analysis

Video sequences of the Brinkman box task performed in each of the 4 conditions (with/without vision with each hand individually), recorded from under the box, were analysed frame by frame (25 frames/s) with the software Kinovea (http://www.kinovea.org/). All video sequences were analysed by the same experimenter to avoid introducing a bias in the interpretation of the videos. However, the experimenter was neither blind to the lesioned/non-lesioned hand nor to the presence/absence of treatment given to the monkeys at the time of the analysis (retrospective study). Data were saved in Excel files and then further processed by using a customised MATLAB® script (MATLAB R2013b). A summary of the analysed parameters is provided in **Figure 5**.

Figure 5 (next page): Summary of the data analysis. The time course of successful retrieval of two successive pellets in the Brinkman box task without vision is exemplified, with the relevant time points, time intervals and collected parameters. The inset at the bottom right shows some different kinds of errors observed. The analysis was exactly the same for data obtained from the Brinkman box task with vision.

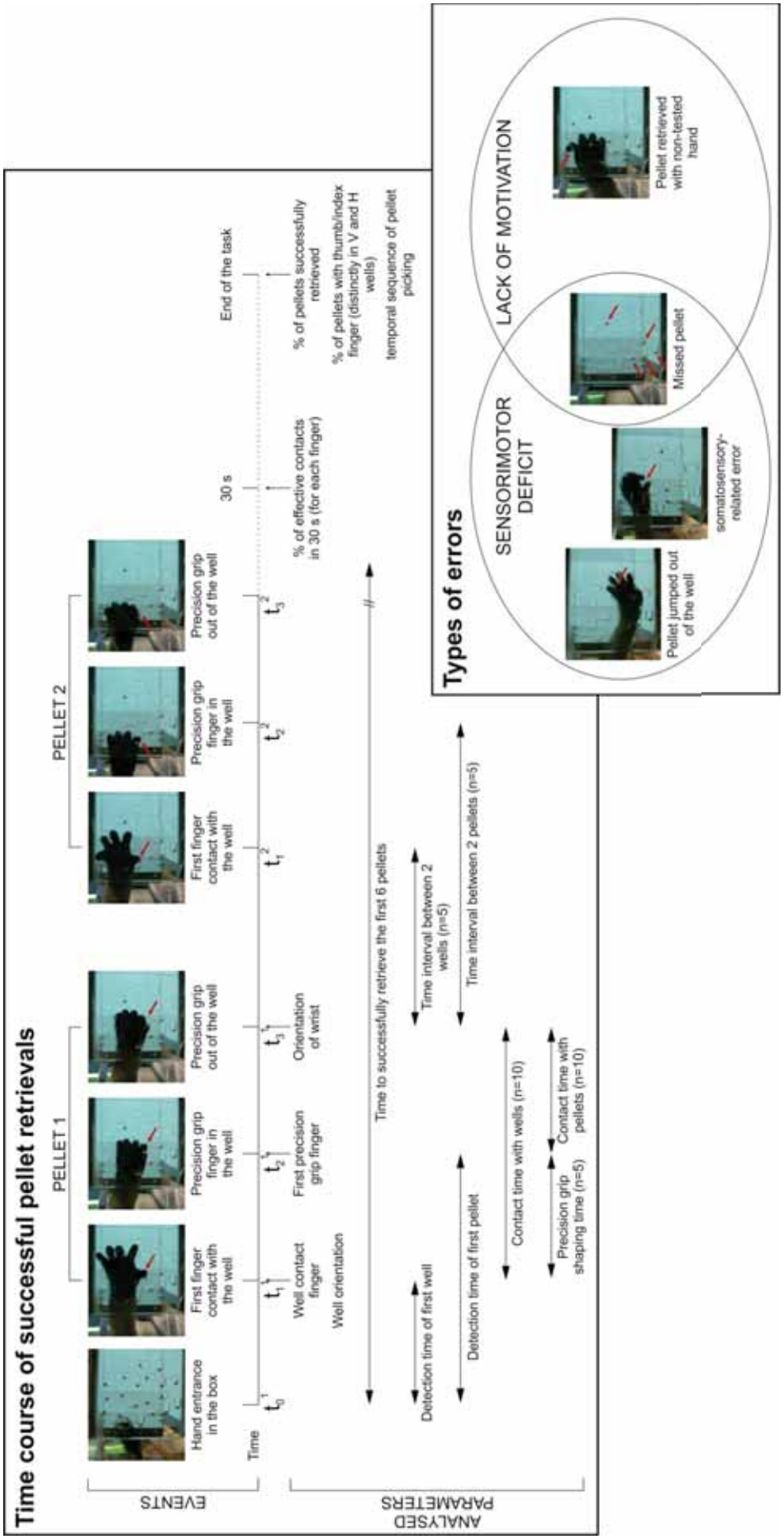
Time course of successful pellet retrievals
PELLET 1
PELLET 2
EVENTS
ANALYSED PARAMETERS
Time
Hand entrance in the box
First finger contact with the well
Precision grip finger in the well
Precision grip out of the well
Well contact finger
Well orientation
First precision grip finger
Orientation of wrist
30 s
End of the task
% of effective contacts in 30 s (for each finger)
% of pellets successfully retrieved
% of pellets with thumb/index finger (distinctly in V and H wells)
temporal sequence of pellet picking
Time to successfully retrieve the first 6 pellets
Detection time of first well
Time interval between 2 wells (n=5)
Detection time of first pellet
Time interval between 2 pellets (n=5)
Contact time with wells (n=10)
Precision grip shaping time (n=5)
Contact time with pellets (n=10)
Types of errors
SENSORIMOTOR DEFICIT
LACK OF MOTIVATION
Pellet jumped out of the well
somatosensory-related error
Missed pellet
Pellet retrieved with non-tested hand

Four event time markers (t^n, for the n^{th} pellet) were picked out for each visited well (unless otherwise mentioned), allowing then further analyses:

t_0^1: *Hand entrance in the box* (only for the first well): origin time point

t_1^n: *First finger contact with the well*: time point at first contact between the finger used to detect the well and the well

t_2^n: *Precision grip finger in the well*: time point at first contact between the finger used then in precision grip and the pellet. Often and in particular in the task without vision, the monkeys detected a well with a given finger and then brought another finger (usually the index finger or the thumb) to retrieve the pellet with a precision grip. Therefore, we differentiated the event *First finger contact with the well* (t_1^n) from the event *precision grip finger in the well* (t_2^n).

t_3^n: *Precision grip out of the well*: time point at fingers going out of the well with the pellet

Several time intervals were then derived from these events:

a) *Detection time of first well*: t_1^1 -t_0^1
b) *Detection time of first pellet*: t_2^1 -t_0^1, i.e. time needed to perform the first precision grip
c) *Contact time with wells* (for the first 10 wells): considered separately for the vertical and horizontal wells, t_3^n -t_1^n
d) *Contact time with pellets* (for the first 10 pellets): considered separately for the vertical and horizontal pellets, t_3^n -t_2^n
e) *Precision grip shaping time* (for the first 5 wells): t_2^n -t_1^n, i.e. time to conform a precision grip
f) *Time interval between 2 wells* (for the first 5 intervals between 2 wells): t_1^{n+1} -t_3^n
g) *Time interval between 2 pellets* (for the first 5 intervals between 2 pellets): t_2^{n+1} -t_3^n
h) *Time to successfully retrieve the first 6 pellets:* t_3^6 -t_0^1

Moreover, we were interested in the following parameters and measurements:

i) *Well contact finger*: (D1-D5) at t_1^n. We quantified for each well being detected which was the first finger used to detect this given well, and divided the total score of each finger by the total number of wells visited to express the use of each finger as a percentage of the total finger use (*% of well finger use*).

j) *First precision grip finger* (D1-D5) at t_2^n. We quantified for each pellet being collected using a precision grip which was the first finger in contact with this given pellet, and divided the total score of each finger by the number of pellets retrieved to express the use of each finger as a percentage of the total finger use (*% of first finger use*).

k) *Well orientation* (horizontal, vertical). We quantified the number of vertical, respectively horizontal, wells visited (i.e. leading to the pellet being collected or jumped), separately for the thumb and the index finger used to retrieve the pellet.

l) *Orientation of wrist* (radial deviation, ulnar deviation, neutral position) at the end of the precision grip (t_3^n).

The motor performance at the wrist level was quantified by using the *percentage of wrist orientation*. Both ulnar and radial deviations were especially needed to retrieve pellets from horizontal wells (see e.g. Chatagny et al., 2013; Hoogewoud et al., 2013) whereas collecting pellets from the vertical wells could be performed less challengingly with the wrist in a neutral position.

m) *Percentage of effective contacts in 30 s* established with each finger in the first 30 s of the task, defined as the number of pellets successfully retrieved in the first 30 s divided by the number of contacts established with pellets in the first 30 s, for each individual finger

n) *Percentage of pellets successfully retrieved* at the end of the task

o) *Percentage of pellets retrieved with the thumb/index finger* in vertical/horizontal wells

p) *Temporal sequence* of pellet retrieval, reflecting the motor habits of the animal, as previously reported (Kaeser et al., 2013; Kaeser et al., 2014). We

defined a gradient of wells from the left to the right side of the board and another one from the top to the bottom of the board.

Additionally, several errors were noticed, divided into 3 types:

1) Sensorimotor deficit:
   - *Pellet jumped out of the well*, allowing to calculate the *percentage of pellets successfully retrieved.*
   - *somatosensory-related error*, defined as a precision grip and hand back to the mouth without pellet
2) Lack of motivation:
   - *Pellet retrieved with the non-tested hand*, allowing to calculate the *percentage of pellets successfully retrieved.*
3) Combination of sensorimotor deficit and lack of motivation:
   - *Missed pellet*, allowing to calculate the *percentage of pellets successfully retrieved*.

We considered only the first five/ten time intervals (c, d and e), the first five intervals between 2 successive trials (f and g) and focused on the time to successfully retrieve only the first 6 pellets (h) as well as the effective contacts in the first 30 s (m) because we assumed that the retrieval of the first pellets was the most representative of the ability of the monkey to perform the task. Namely, the values from all wells/pellets were collected but then we realised that the performance often decreased after retrieving some pellets in parallel with an increase in the variability of the data because this task was highly demanding for the animal, especially when performed without visual feedback. Moreover, depending on the monkey, we observed some drop in motivation in the time course of the task, especially in post-lesion sessions, motivating us therefore to focus on the first pellets only. Similar observations were already reported in the modified Brinkman board task as well (Kaeser, 2010).

For the parameters under investigation here, we defined then a pre-lesion plateau of performance and a post-lesion plateau of performance (same dates for each parameter, based on visual appreciation, with the goal to find the time period being the most stable across the different parameters under consideration). *Median* plateaux were computed

here for numerical variables (e.g. time intervals) to be consistent with the use of Mann-Whitney test, except for *mean* plateaux for the *precision grip shaping time* where very small values often close to or equal to 0 were obtained. Therefore, the median of such values would often have resulted to 0, which is not convenient for the following analyses such as the computation of the percentage of recovery, entailing to divide one median value by another median value. For categorical variables (e.g. finger use, wrist orientation, …), plateaux represented the proportions (*100) of the given parameters among all observations. The percentage of functional recovery was defined for appropriate parameters as (post-lesion plateau/pre-lesion plateau)*100 when a higher plateau value means a better performance and as 1/(post-lesion plateau/pre-lesion plateau)*100 when a lower plateau value represents a better performance. The plateaux were compared with a Mann-Whitney test, or a z-test for comparing proportions, as the case may be. We chose to perform Mann-Whitney tests even in some cases when a t-test was possible, in order to be fully consistent across the data. Moreover, in case of small sample size, such as the data sample considered in each plateau, Mann-Whitney tests are known to perform better than t-tests (Fay and Proschan, 2010; Ludbrook and Dudley, 1998). Statistical analyses were performed with SigmaPlot 12.5. Simple linear regressions and Pearson's correlation coefficients R ($p < 0.05$) were computed in MATLAB.

We chose to express several parameters in the form of percentage instead of absolute number/score to avoid the bias that results from the duration of the task and consequently from the number of pellets that may be collected. This makes sense especially immediately after the lesion or when the task was performed without vision both before and after the lesion: the experimenter sometimes decided to interrupt the task before the board was completely empty when the monkey was simply not able to perform the task or obviously did not want to continue it, reducing therefore the maximal number of pellets to be collected.

Lesion

When the monkeys reached a stable behavioural plateau in manual dexterity tests, they were subjected to a permanent cortical lesion, performed unilaterally in the hand representation of M1 by infusion of ibotenic acid. The lesion protocol for Mk-DI is presented in the **Chapter General Materials and Methods**. The procedure for the other 6 mon-

keys differed from Mk-DI's one in the sense that the lesion was performed in each monkey based on a previously established individualised ICMS mapping (Sessle and Wiesendanger, 1982). The ICMS and lesion procedures were described in detail elsewhere (Kaeser et al., 2010; Liu and Rouiller, 1999; Schmidlin et al., 2005; Wyss et al., 2013). Briefly, a chronic recording chamber was implanted over the left sensorimotor cortex in order to perform the ICMS mapping of the hand representation in left M1. Once all the pre-lesion behavioural and electrophysiological data were collected, a unilateral permanent lesion of the M1 hand area on the left hemisphere was performed by multiple microinfusions of ibotenic acid (10 µg/µl in phosphate-buffered saline, 0.1 M, pH 7.2, either Fluka 99% or Sigma 95%) using a Hamilton microsyringe (10 µl) driven by a micromanipulator. Injections were performed at the sites along ICMS electrode penetrations where hand movements had been previously elicited at low stimulation threshold. Thus ibotenic acid was injected (1 µl or 1.5 µl per site depth over a period of 2 min, and making a pause of 3-5 min between each injection) at 1, 2 or 3 different depths along an individual ICMS penetration. The aim was to cover the whole hand representation of M1. A total volume of ibotenic acid ranging from 13 µl to 38 µl was injected in each monkey (see **Table 1** for further detail).

The Brinkman box task was carried out similarly before and after the lesion, with and without vision.

Treatments

After the lesion, Mk-DI, Mk-GE and Mk-RO did not receive any treatment (control untreated monkeys). Mk-VA was treated with anti-Nogo-A antibody (for greater detail, see Hamadjida et al., 2012; Kaeser et al., 2010; Wyss et al., 2013). Mk-AV, Mk-JA and Mk-JO were involved in an adult neural progenitor cell therapy protocol (for further detail, see Brunet et al., 2005; Kaeser et al., 2011). To this end, a cortical biopsy in the right dorsolateral prefrontal cortex (dlPFC) was performed several weeks before the lesion and the cells were put in culture to be subsequently reimplanted after the lesion. Mk-JO and Mk-JA were subjected to cell therapy whereas Mk-AV was transplanted with culture medium only and was therefore classified as a control untreated monkey with regard to the treatment (but note that Mk-AV did have a dlPFC biopsy) (**Table 1**). For more detail about the whole procedure, please consult Brunet et al. (2005) and Kaeser et al. (2011).

Histology

At the end of the experiments (behavioural tests, electrophysiological investigations, cell reimplantations or anti-Nogo-A treatment, and tracer injections), the animals were sacrificed according to a similar protocol as the one described for Mk-DI in **Chapter General Materials and Methods** and already reported for these animals (Kaeser et al., 2010). The brains were cut in the frontal plane (50-µm thickness) into 5 to 8 series of sections and two series were prepared for Nissl staining and SMI-32 staining, respectively.

As described in the **Chapter 2**, histological analyses and reconstructions of the extent and location of the lesions in the frontal plane were then performed with Neurolucida based on the Cavalieri method by using consecutive series of Nissl-stained sections and SMI-32-stained sections (see Wyss et al., 2013), allowing three-dimensional mapping and volume quantifications of the cortical lesioned areas. The extent and location of the lesions were transposed onto a lateral view of the cortical surface of the lesioned hemisphere (**Figure 6**).

Results

We present here only the most relevant data. The complete collection of graphs for each analysed parameter, for each monkey, in the four conditions of the task, is provided in **Supplementary Figures 1** and **2** at the end of the chapter.

Extent of the lesions

The extent of the lesion was assessed in each animal by using histological sections (either Nissl-stained sections or SMI-32-stained sections). These data were already available for all monkeys (Hamadjida et al., 2012; Hoogewoud et al., 2013; Kaeser et al., 2011; Rouiller et al., 1993; Wyss et al., 2013) except Mk-DI (see **Chapter 2** for more detail about the lesion in Mk-DI). The total gray matter lesion volumes ranged from 14 mm^3 in Mk-RO to 68.4 mm^3 in Mk-DI. A representation on the extent of the lesion projected on the surface of the cortex is shown for each animal in **Figure 6**. For reminder, see the important details about the lesions in **Table 1** above.

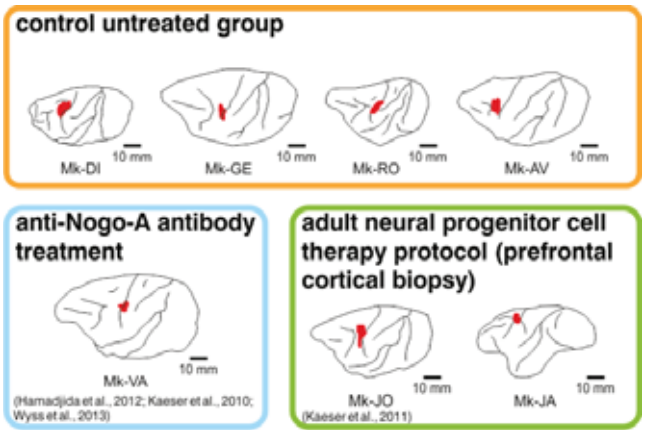

Figure 6: Projection of the gray matter lesioned area on a lateral view of the brains, based on consecutive frontal histological sections (Nissl and SMI-32 stainings). The animals are grouped according to the post-lesion treatment (see above).

Post-lesion deficits

After several weeks of training (note that the data from the learning period were not included in the present report; but see Kaeser et al., 2014), the seven monkeys performed the Brinkman box task smoothly and reached a pre-lesion plateau of performance with each hand and in both with vision and without vision conditions, illustrated e.g. by the *percentage of pellets successfully retrieved*, the *temporal sequence of pellet picking*, the *contact time* with the pellets, the *orientation of the wrist* or the *precision grip shaping time*. See the complete collection of graphs for all animals in the four conditions of the task in **Supplementary Figures 1** and **2.**

As expected, the cortical lesion of the M1 hand representation induced several deficits in each animal, especially with the contralesional, right hand. See e.g. the detailed data for Mk-DI already presented in the **Chapter 3**. Immediately after the lesion, the monkeys were completely unable to perform the Brinkman box task because of hand paralysis/paresis going with a complete loss of fine finger control for one to several days, depending on the animal (see e.g. graphs for Mk-DI with missing data or data at 0 for several days after the lesion), followed then by a period of slow, progressive functional recovery, though remaining largely incomplete. In the Brinkman box task without vision with the contralesional, right hand, the lesion usually resulted in a decreased speed of motor execution, in altered movements of the wrist, in a modified use of the fingers, in lower abilities of motor exploration by palpation and in a lower proficiency in pellets retrieval due to a larger amount of errors. Furthermore, the deficits visible in the task without vision were clearly more prominent than in the task with visual feedback. In

addition, there was a very large inter-individual variability in the different behavioural parameters of the task without visual control, affected at various degrees, possibly due to the variable extent and precise location of the lesions across individuals. Conversely, the effect of the lesion on the ipsilesional, left hand on both conditions was usually only transitory (**Supplementary Figure 3**).

These different aspects will be developed in the following sections.

Impact of the lesion on contralesional manual dexterity without vision

By considering the post-lesion time course of the different behavioural parameters of the task without vision in each monkey (**Supplementary Figure 1**), one already notices at a glance a very large variability, first, intra-individual in the form of some parameters being much more sensitive to the lesion than others, and second, inter-individual with a given parameter affected at various degrees across the monkeys, possibly due to the variable extent and location of the lesion across individuals. We were therefore interested to investigate whether there were some general trends in the effect of the lesion on the dexterity of the contralesional hand in the task without vision at the whole population level. To this end, simple regression analyses with Pearson's correlation coefficients were computed between the post-lesion recovery of the different parameters studied and the volume of the cortical lesion estimated by using histological sections (either Nissl-stained sections or SMI-32-stained sections) in the 7 animals included in this study. The percentage of recovery was determined based on the pre- and post-lesion plateaux (see *Materials and methods* for greater detail). Some significant correlations appeared (**Figure 7**).

The M1 lesion induced a decrease in the speed of motor execution (combining the ability to perform blind motor exploration by palpation as well as the travelling time between the box and the mouth and the reverse) at the population level, as exemplified by a significant negative correlation between the volume of the lesion and the post-lesion recovery of the *time interval between 2 pellets* ($R = -0.77$, $p = 0.044$) (**Figure 7A**). In brief, the larger the cortical lesion, the longer the post-lesion time intervals between 2 successive pellets as compared to the pre-lesion time intervals. Once the wells were detected by the *well contact finger*, the time needed to conform a precision grip –the *precision grip*

shaping time– increased as well, as illustrated by a significant negative correlation between the volume of the lesion and the post-lesion recovery of the *precision grip shaping time* (R =-0.79, p =0.036) (**Figure 7B**): monkeys with a larger lesion spent significantly more time to initiate a precision grip once a well had been detected. Consequently, the time spent in wells increased and the post-lesion recovery of the *contact time with wells* was negatively correlated with the volume of lesion, both in vertical (R =-0.8, p =0.03) (**Figure 7C**) and horizontal (R =-0.85, p =0.016) (**Figure 7D**) wells. In the same way, the precision grip *per se* was altered as well, reflected by a significant negative correlation between the volume of the lesion and the post-lesion recovery of the *contact time with pellets*, both for vertical (R =-0.77, p =0.045) (**Figure 7E**) and for horizontal pellets (R =-0.91, p =0.004) (**Figure 7F**). To put it another way, the more extended the lesion, the worse was the functional recovery and the much longer time was spent in the wells to adjust the fine finger movements to collect pellets.

We observed a significant positive correlation between the volume of the lesion and the post-lesion occurrence of *neutral* deviations of the contralesional wrist (R =0.88, p =0.008) (**Figure 7G**), in parallel with a non-significant negative trend between the volume of the lesion and the recovery of the ability to perform *ulnar* deviations with the contralesional wrist (R =-0.67, p =0.1) (**Figure 7H**). The correlation between the volume of the lesion and the ability to perform radial deviation is not highly relevant at the population level because this wrist position was already very infrequent before the lesion in some animals (resulting in a plateau at 0, see for instance Mk-AV, Mk-DI, and Mk-RO). This result means that monkeys with a larger lesion were more impaired to move the contralesional wrist in a challenging position, such as in the direction of ulnar deviation and favoured more a neutral wrist position after the lesion.

Moreover, we observed a significant negative correlation between the volume of the lesion and the post-lesion recovery of the ability to visit *horizontal* wells (*well orientation*) (R =-0.82, p =0.024) (**Figure 7I**), going with a significant positive correlation between the volume of the lesion and the post-lesion recovery in the ability to visit *vertical* wells (R =0.78, p =0.04) (**Figure 7J**). Taken together, both these correlations indicate that the more extended the lesion was, the more the animals favoured the less challenging vertical wells to the detriment of the horizontal ones, because these latter usually required a

deviation of the wrist in addition to the precision grip, confirming here again that the larger the lesion, the more the animals were impaired to perform wrist deviations.

Finally, there was a positive correlation between the volume of the cortical lesion and the recovery of the ability to use the *index finger* to detect the wells (R =0.76, p =0.049) (**Figure 7K**) to the detriment of the use of the *thumb*, although the correlation between the volume of the lesion and this latter parameter was above the significance threshold (R =-0.69, p =0.084) (**Figure 7L**). To put it another way, after the cortical lesion, monkeys with a larger lesion relied more on their contralesional index finger to detect the wells, to the detriment of the thumb as the use of the latter usually required an additional wrist deviation, this behaviour being more impaired in animals with a larger lesion, as already mentioned. Note that for nearly all parameters presented here, the animal with the smallest lesion extent (Mk-RO, 14 mm^3) usually recovered almost completely or even showed an improved post-lesion performance as compared to the pre-lesion one.

Basically, when the animals were considered at the whole population level, more prominent deficits of the contralesional hand were observed after a larger cortical lesion, in the Brinkman box task performed without vision.

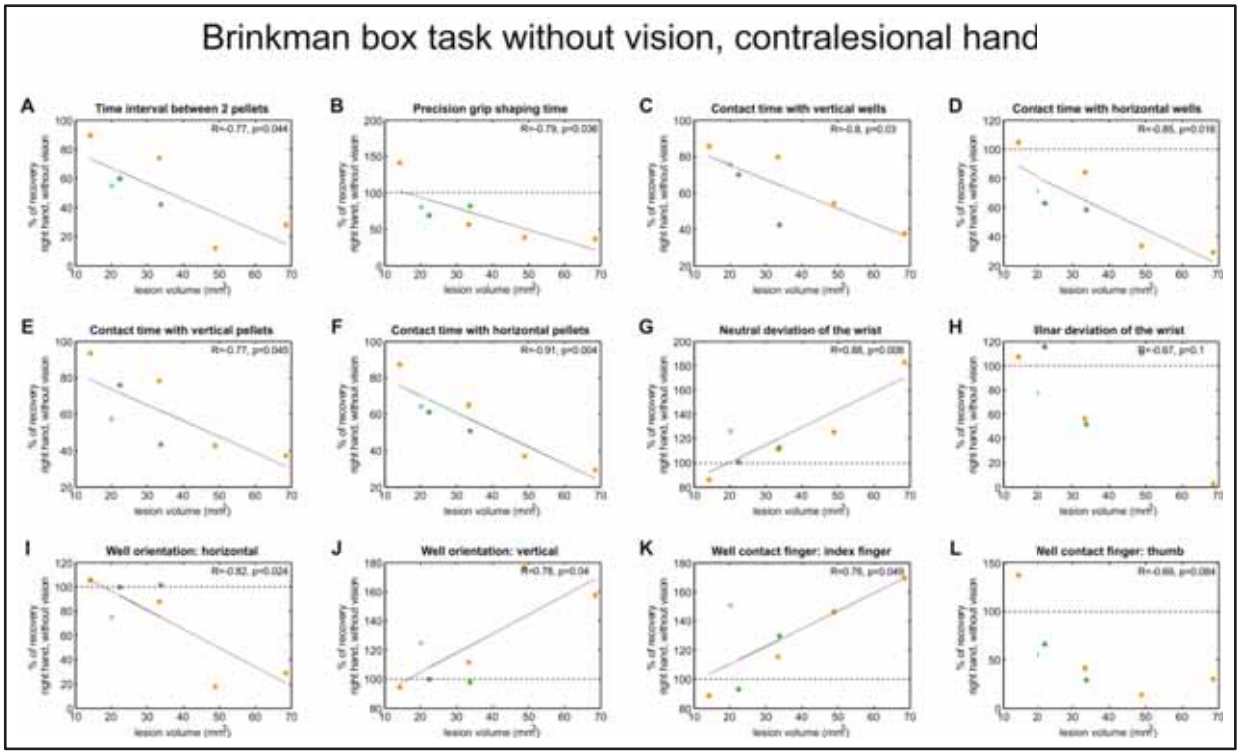

Figure 7 (previous page): Impact of the cortical lesion on the fine manual dexterity of the contralesional, right hand in the Brinkman box task without vision in all monkeys, in the form of linear regressions (black lines) between the volume of the lesion (mm^3) and the post-lesion recovery of (A) the time interval between 2 successive pellets, (B) the precison grip shaping time, (C) the contact time with vertical wells, (D) the contact time with horizontal wells, (E) the contact time with vertical pellets, (F) the contact time with horizontal pellets, (G) the occurrence of neutral deviations of the wrist, (H) the ability to perform ulnar deviations of the wrist, (I) the ability to visit horizontal wells, (J) the ability to visit vertical wells, (K) the ability to use the index finger to detect the wells, and (L) the ability to use the thumb to detect the wells. Each point depicts an individual monkey and the colour indicates the post-lesion treatment as in Table 1 and Figure 5 (orange: control untreated animals; blue: anti-Nogo-A antibody treated animal; green: animals involved in a protocol of adult neural progenitor cell therapy). For points located below the 100-% line (horizontal dotted line), post-lesion level<pre-lesion level, and conversely for points located above the 100-% line, post-lesion level>pre-lesion level. The Pearson's correlation coefficient and the p-value of each regression line are indicated at the top-right corner of the corresponding graph. Non significant regression lines were not displayed.

Impact of the lesion on contralesional manual dexterity with vision

Similar correlations between the volume of the lesion and the post-lesion recovery assessed with the different parameters were evaluated now in the Brinkman box task with vision with the contralesional hand. Some comparable results were obtained. Essentially, we observed here again that the speed of motor execution was slower in animals subjected to a larger cortical lesion, demonstrated by significant negative correlations between the volume of the lesion on the one hand and the post-lesion recovery of the *time to successfully retrieve the first 6 pellets* (R =-0.9 p =0.005) (**Figure 8A**), the post-lesion recovery of the *time interval between 2 pellets* (R =-0.91, p =0.005) (**Figure 8B**), (both reflecting here the ability to perform motor exploration assisted by visual control as well as the travelling time between the box and the mouth and the reverse), and the post-lesion recovery of the *time interval between 2 wells* (R =-0.92, p =0.003) (**Figure 8C**) (reflecting the travelling time between the box and the mouth and the reverse), respectively, on the other hand.

The impairment to perform wrist deviation was visible here as well, with a significant positive correlation between the volume of the lesion and the post-lesion occurrence of *neutral* deviations of the contralesional wrist (R =0.8, p =0.03) (**Figure 8D**), in parallel with a significant general decrease in the ability to perform *ulnar* deviations (R =-0.87, p =0.011) (**Figure 8E**).

What appeared in this condition as well is the direct link between the extent of the lesion and the proficiency of the animals to collect the pellets, exemplified by a negative correlation between the volume of the lesion and, first, the post-lesion recovery of the *percentage of effective contacts in 30 s with the index finger* (R =-0.82, p =0.024) (**Figure 8F**) and, second, the success rate, namely the post-lesion recovery of the *percentage of pellets successfully retrieved* (R =-0.95, p =0.001) (**Figure 8G**).

Similarly, as in the task without vision, the animals with small lesion extent (Mk-RO, Mk-VA and Mk-JA) usually recovered almost completely or even showed an improved post-lesion performance as compared to the pre-lesion one.

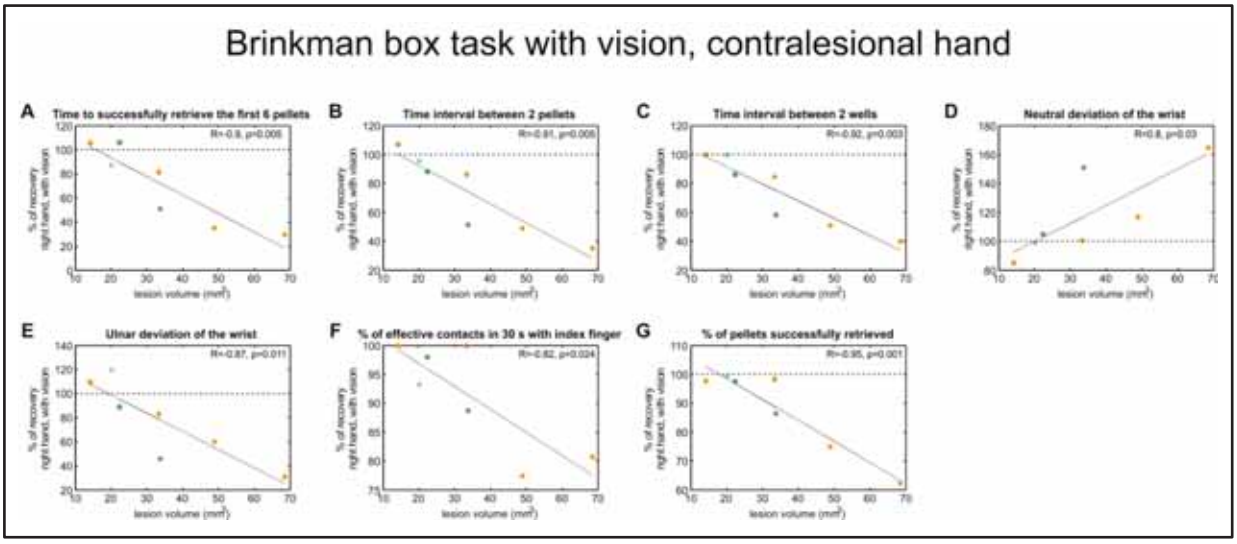

Figure 8: Impact of the cortical lesion on the fine manual dexterity of the contralesional, right hand in the Brinkman box task with vision in all monkeys, in the form of linear regressions between the volume of the lesion (mm^3) and the post-lesion recovery of (A) the time to successfully retrieve the first 6 pellets, (B) the time interval between 2 successive pellets, (C) the time interval between 2 successive wells, (D) the occurrence of neutral deviations of the wrist, (E) the ability to perform ulnar deviations of the wrist, (F) the percentage of effective contacts established in the first 30 s with the index finger, and (G) the percentage of pellets successfully retrieved. Same conventions as in Figure 7.

In short, when the monkeys performed the Brinkman box task with the contralesional hand with vision, comparable kinds of deficits correlated with the extent of the lesion were observed as in the task without vision, by considering the whole population of monkeys.

A similar analysis was performed based on data from the ipsilesional, left hand, both in the task with and without vision. The results are proposed in **Supplementary Figure 3**.

Impact of visual feedback on contralesional functional recovery from the lesion

Whereas comparable *kinds* of contralesional impairments were observed in both tasks with and without vision, what about their relative *extent*? Was the post-lesion functional recovery in one condition better than in the other? Moreover, were the levels of functional recovery in both conditions linked?

To address these questions, we examined the relationship between the levels of post-lesion recovery of the different parameters studied when the task was performed without vision versus with vision with the contralesional, right hand. First we considered the 7 animals as a single population. Interestingly, some significant positive linear relationships emerged between the percentage of recovery without vision and the percentage of recovery with vision, for instance regarding the speed of motor execution assessed with the *time interval between 2 wells* (R =0.82, p =0.024) (**Figure 9A**) as well as *between 2 pellets* (R =0.88, p =0.01) (**Figure 9B**), the fine manipulation of the pellets assessed with the *contact time with vertical pellets* (R =0.86, p =0.013) (**Figure 9C**), and finally the proficiency of motor exploration assessed with the *percentage of effective contacts in 30 s with the index finger* (R =0.82, p =0.025) (**Figure 9D**). Moreover, as expected, we observed that the post-lesion contralesional recovery was usually better when the monkeys performed the Brinkman box task with vision than without vision, corresponding to the majority of points in these graphs located on the left to the identity line. As intuitively expected, it means that the task performed without vision was more challenging than with vision. Note that there is here no strict link between the recovery in both conditions and lesion size (the latter is indicated by the size of the symbols in **Figure 9A-D**).

Equally interestingly, a discrepancy of performance in both conditions of the task could be even extreme at the single-monkey level: in Mk-DI for instance, we observed a strong opposite pattern in the evolution of the finger use (here the first finger in contact with a pellet in a precision grip) over post-lesion time according to the task: whereas there was a partial normalisation of thumb and index finger use when the task was performed with vision in the recovery period after the lesion (**Figure 9E**), the use of the thumb further decreased over post-lesion time and never recovered in the task without vision, in favour of the index finger (**Figure 9F**). This was already discussed in the **Chapter 3**.

To sum up, we observed a linear relationship between the functional recovery of manual dexterity in both tasks and, as expected, the functional recovery in the Brinkman box task performed with vision was usually more prominent than when performed without vision, both at the population level and at the individual level.

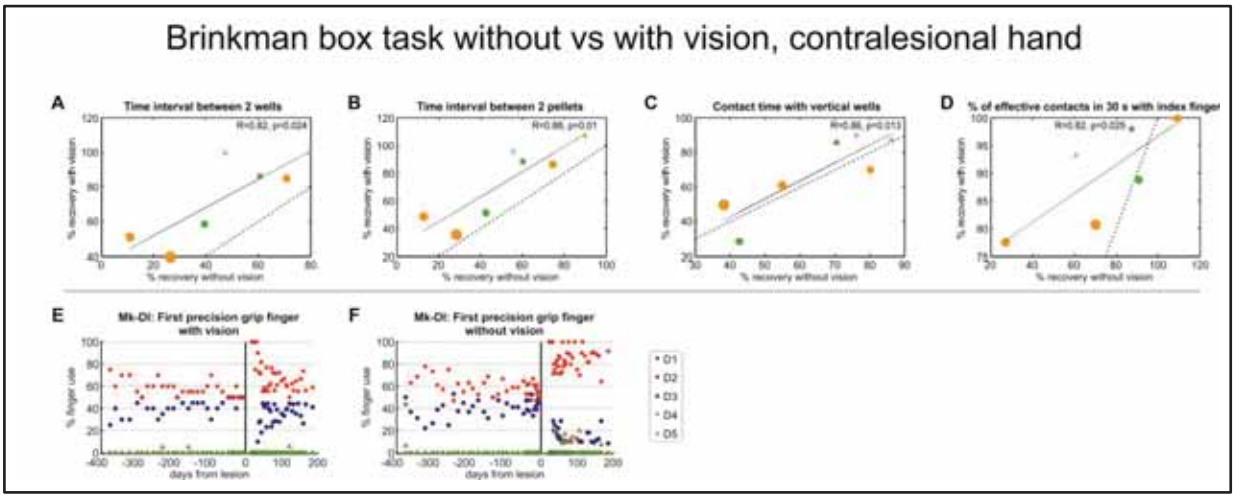

Figure 9: Impact of the visual feedback on the post-lesion functional recovery of the contralesional hand. Correlation between the percentage of post-lesion recovery without vision (x-axis) and the percentage of post-lesion recovery with vision (y-axis) at the whole population level, regarding (A) the time interval between 2 wells, and (B) between 2 pellets, (C) the contact time with vertical pellets, and (D) the percentage of effective contacts in 30 s with the index finger. The diameter of the points indicates the lesion extent (large diameter: large lesion volume and conversely). Same conventions as in Figure 7. For points located on the left to the unitary line (dotted line), recovery with vision>recovery without vision. (E-F) Opposite post-lesion evolution of the use of the first precision grip fingers according to the task, in Mk-DI. Time course of the % of first finger use in the task with vision (E) and without vision (F). The finger colour code is given on the right.

Somatosensory-related errors in contralesional manual dexterity without vision

By reading so far, one may conclude that the cortical lesions resulted globally in comparable contralesional deficits in both with vision and without vision conditions of the task, although the deficits were more prominent in the latter than in the former condition. But that would be simplistic. In addition to the striking differential post-lesion deficits in finger use according to the task observed in Mk-DI (see above), some subtle post-lesion somatosensory-related deficits of the contralesional hand dexterity emerged when the task was performed without vision.

After the motor cortex lesion, in addition to the expected deterioration of manual dexterity with the contralesional, right hand, several animals exhibited a very special behaviour in the Brinkman box task without vision: in some trials they did a precision grip but failed to grasp the pellet, withdrew then the hand from the well and from the box, brought the hand to or near the mouth, and supinated the hand to *visually* inspect the empty palm and only at that time realised that they actually did not retrieve any pellet (**Figure 10**). This erroneous behaviour –referred to as *somatosensory-related errors*– was especially present in Mk-VA in the first 50 days after the lesion and, but to a lesser extent, in Mk-GE, Mk-AV, Mk-JA and MK-JO as well (**Figure 11A-E**). Conversely, this misbehaviour was much more infrequently observed (but not completely absent) before the lesion, as well as in the other 3 conditions of the task (see **Supplementary Figure 1**) as compared to the task performed without vision with the right hand, suggesting that these errors were linked to the lesion itself. Mk-DI also showed very few occurrences of somatosensory-related errors, but they were not specific to the right hand in the task without vision. Interestingly Mk-AV already made this kind of somatosensory-related errors transiently after the cortical biopsy performed in the ipsilateral dlPFC when the right hand performed the task without vision. The animal completely recovered to a normal behaviour but exhibited again this misbehaviour transiently immediately after the lesion. These errors seem to be linked neither to the volume of the lesion nor to a lesion spread into the postcentral gyrus in addition to M1, given that the most prominent misbehaviour was observed in Mk-VA having a small lesion volume (20 mm^3), followed then by Mk-GE, and then by Mk-AV, and the latter did not exhibit any spread of the lesion in S1. Conversely, Mk-DI exhibited a large lesion extending into a small por-

tion of the area 3a, but showed this misbehaviour only very infrequently and not specifically with the contralesional hand.

Figure 10 (next 2 pages): Sequence of frames captured at 80-ms intervals, simultaneously from the digital camera positioned in front of the animal (left part of the composite picture) and from the other camera located under the board (right part of the composite picture). This sequence illustrates a typical somatosensory-related error observed in several animals in the Brinkman box task without vision with the contralesional, right hand. Here the data were obtained from Mk-DI. This animal actually did not make this misbehaviour very often but was selected here for illustrative purpose given that the quality of the video sequence was much better than for the other animals. The monkey initiated a precision grip by contacting a pellet in a vertical well with the index finger (see 240-ms frame), moved the thumb closer to the pellet to make the precision grip (see 800-ms frame) but the pellet then jumped from the pinched fingers to the next horizontal well located just more in the midline (see 1040-ms frame). The animal withdraw then its hand from the box, brought it towards the mouth (from 1360-ms frame) and had to visually inspect its empty hand to realise that the pellet had not been collected (from 1680-ms frame). The red arrows on the pictures point the precise aforementioned events.


0 ms


80 ms


160 ms


240 ms


320 ms


400 ms


480 ms


560 ms


640 ms


720 ms


800 ms


880 ms


960 ms


1040 ms


1120 ms


1200 ms


1280 ms


1360 ms


1440 ms


1520 ms


1600 ms


1680 ms


1760 ms


1840 ms

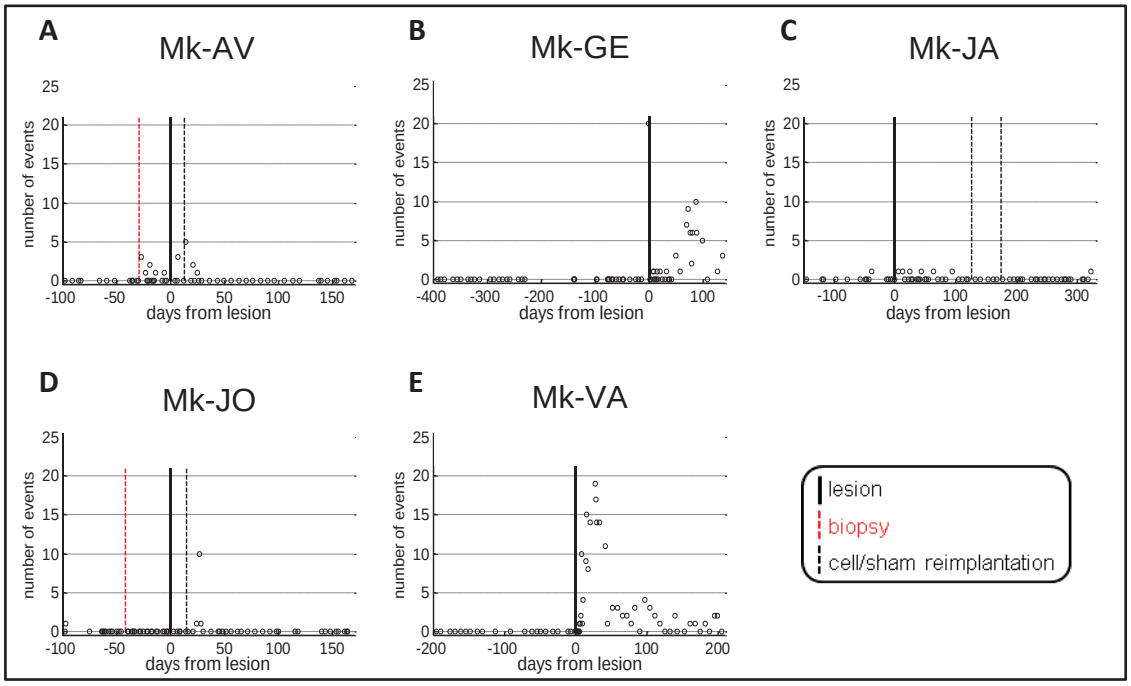

Figure 11: Time course of occurrence of the somatosensory-related errors exhibited by five monkeys (A to E) in the Brinkman box task without vision performed with the contralesional, right hand. The cortical lesion was performed at day 0 (x-axis). The time at biopsy and the time at cell/sham reimplantation for Mk-AV, Mk-JA and Mk-JO are indicated by red and black dashed lines, respectively.

In short, we demonstrated here that the post-lesion contralesional deficits in manual dexterity were also characterised by very subtle somatosensory-related impairments most probably linked to the absence of visual feedback because these misbehaviours were mostly observed in the Brinkman box task without vision.

Relationship between the contra- and the ipsilesional hand functional recovery

By considering the conflicting literature about the presence (see e.g. Kaeser et al., 2010) or absence (see e.g. Pandian and Arya, 2013) of relationship between the motor performance of the affected and non-affected body sides, we investigated here whether there was a link between the amount of post-lesion functional recovery exhibited by both hands. To this aim, we calculated Pearson's correlation coefficients between the level of functional recovery of the right hand and the level of recovery of the left hand in the Brinkman box task without vision, among the seven animals considered, for each stud-

ied parameter. We focused here only on the task without vision because it showed the most pronounced post-lesion effects.

For convenience, we speak here about post-lesion *recovery* of the ipsilesional hand as well, in the same way as for the contralesional hand, to express the post-lesion performance as a percentage of the pre-lesion performance even though the latter may be higher than the pre-lesion one.

Surprisingly, a single statistically significant correlation emerged between the levels of recovery of both hands among all the parameters investigated in our study, and concerned the use of the *wrist in a neutral deviation*: the recovery of the right hand was significantly negatively linked with the performance of the left hand ($R = -0.83$, $p = 0.021$) (**Figure 12A**). To put it another way, the monkeys that massively increased the use of the less challenging neutral wrist position with the right hand after the lesion were those that did not increase the use of the neural position with the ipsilesional, left wrist, meaning that they conversely favoured radial and/or ulnar deviations with the intact wrist. On the contrary, the animals that did not change the use of the neutral wrist position with the right hand increased this behaviour with the ipsilesional, left wrist.

Even though the very small number of significant correlations observed between the recovery of both hands in the task without vision, there was, as expected, a general trend towards a better post-lesion/pre-lesion performance with the ipsilesional hand as compared to the contralesional hand, depicted on the graphs by the points on the left side of the identity line. This was exemplified by the *time interval between 2 pellets* (**Figure 12B**), the *time to successfully retrieve the first 6 pellets* (**Figure 12C**), the *contact time* with the horizontal wells (**Figure 12D**), the *contact time* with the vertical (**Figure 12E**) and horizontal pellets (**Figure 12F**) and the *percentage of pellets successfully retrieved* (**Figure 12G**). For the other parameters under investigation, we did not observe any clear tendency. Moreover, in these graphs, no clear trend appeared regarding the ratio of recovery and the extent of the lesion.

In sum, the functional recovery of the non-affected upper limb was usually higher than the one of the affected upper limb when the whole population of animals was considered.

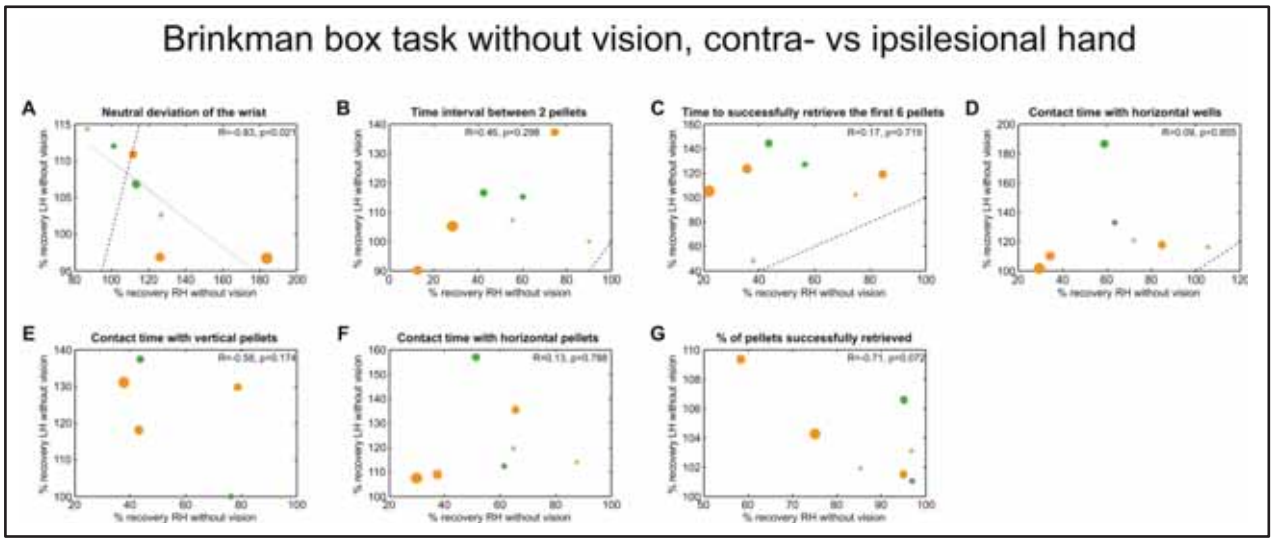

Figure 12: Correlation between the contralesional (right, RH) and the ipsilesional (left, LH) functional recoveries in the Brinkman box task without vision, regarding (A) the occurrence of neutral deviations of the wrist, (B) the time interval between 2 pellets, (C) the time to successfully retrieve the first 6 pellets, (D) the contact time with horizontal wells, (E) the contact time with vertical pellets, (F) the contact time with horizontal pellets, and (G) the percentage of pellets successfully retrieved. For points located to the left of the 100-% line (dotted line), LH recovery>RH recovery, and conversely for points located to the right of the 100-% line, RH recovery>LH recovery. The diameter of the points indicates the lesion extent (large diameter: large lesion volume and conversely). Same conventions as in Figure 7. Note that the % range is different on both axes.

Strategy of prehension

It is well established in the literature that primates, facing prehension tasks under visual control involving many objects presented simultaneously, develop strategies with increasing practice in order to be efficient in object retrieval (Brinkman, 1984; Kaeser et al., 2013; Kaeser et al., 2014; Schmidlin et al., 2011). In practical terms, in the modified Brinkman board task for instance, control monkeys usually tended to repeat the same temporal sequence of object prehension, session after session, either from the left (respectively right) to the right (respectively left) side of the board, or from the middle to the extremities (Kaeser et al., 2013; Kaeser et al., 2014; Schmidlin et al., 2011). A left-right strategy was expected in this task given the rectangular shape of the board. These previous observations motivated us to investigate the temporal sequence of pellet pick-

ing in the Brinkman box task as well. More specifically, we were interested to assess, first, whether the monkeys would develop a strategy of prehension in the Brinkman box task, both with vision and without vision and, second, in case it was present before the lesion, whether the lesion would impact on the acquired strategy.

Some monkeys in this study showed a clear strategy in their sequence of pellet picking when the task was performed with vision with either hand before the lesion, in the form of a picking sequence starting usually at the bottom and finishing at the top of the board (down-to-up preference: Mk-JA, Mk-JO (**Figure 13A, B**), Mk-RO, all three with both hands; Mk-DI with left hand only). The complete collection of graphs displaying the prehension strategies for each monkey is provided in **Supplementary Figure 2.** Mk-AV used a down-to-up strategy with right hand and an opposite up-to-down strategy with the left hand. Although the left-to-right extent of the board in the Brinkman box was much smaller than in the modified Brinkman board (11.6 cm vs 22 cm), some animals also developed a left-right strategy (Mk-AV, Mk-DI (**Figure 13C**), Mk-JA) which was sometimes superimposed on the up-down one.

The M1 lesion resulted in transiently more chaotic strategies (see e.g. Mk-JO, right hand in **Figure 13B**) and some monkeys usually favoured then the most accessible pellets with the contralesional hand (see e.g. Mk-DI, Mk-JO, Mk-VA in **Supplementary Figure 2**), resulting in an altered temporal sequence of pellet picking after the lesion. On the other hand, as expected, the picking strategy developed with the ipsilesional, left hand was maintained after the lesion, except in Mk-VA: interestingly, while Mk-VA did not present any clear prehension strategy with the left hand before the lesion, the monkey progressively developed a strategy that evolved during the post-lesion period (from an up-to-down preference to a down-to-up preference) (**Figure 13D**).

On the other hand, no clear strategy was observed when the task was performed without vision (**Supplementary Figure 2**), suggesting that the blind task was usually performed based on tactile exploration rather than on previously learned picking sequences involving spatial memory.

In short, the majority of monkeys adopted strategies to collect pellets in a quite fixed temporal sequence when the task was performed with visual feedback whereas the task without vision relied much more on motor exploration by palpation than on such acquired strategies.

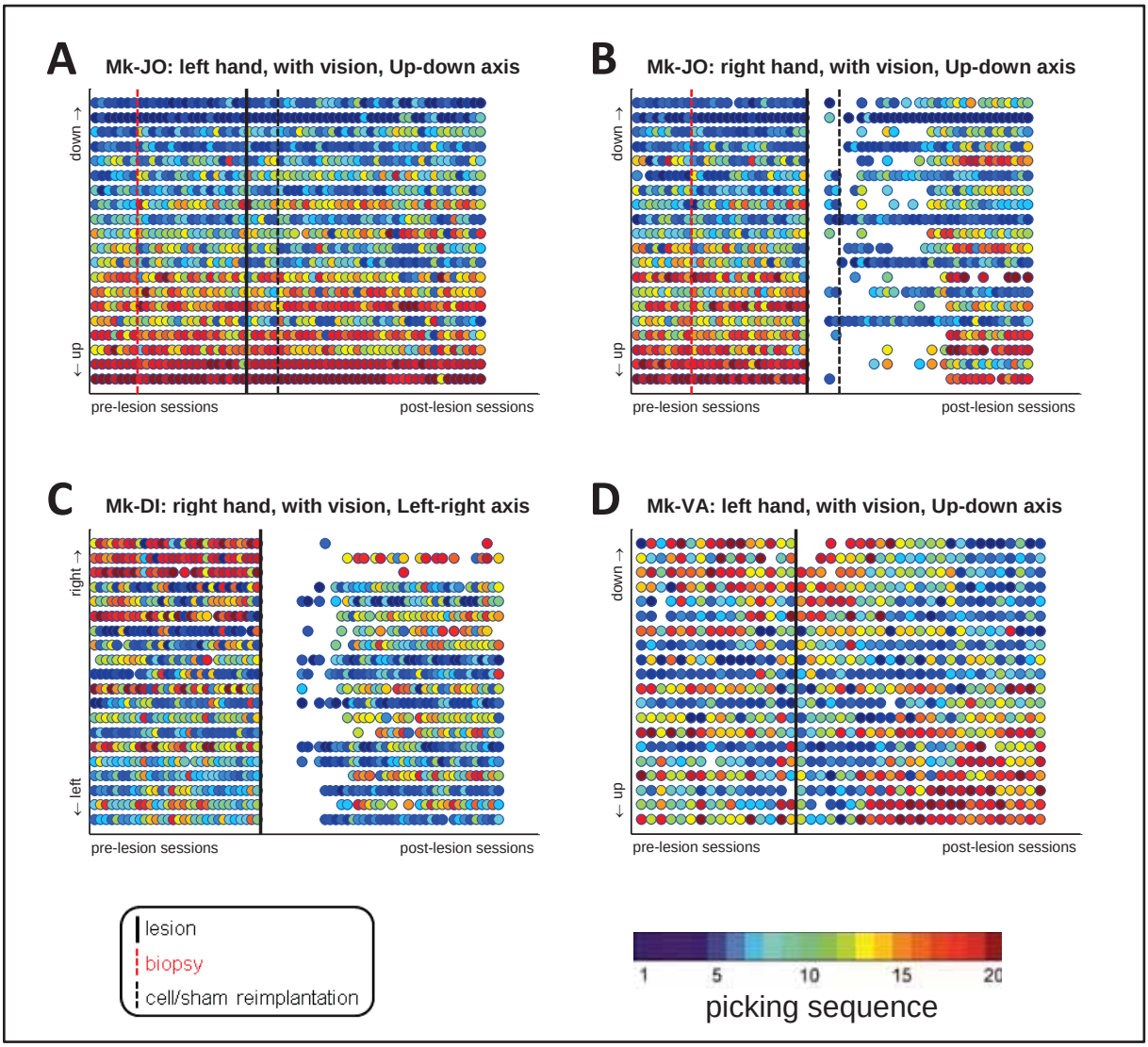

Figure 13: Colour-coded sequences of pellet picking in the Brinkman box task with vision. The x-axis represents the time in sessions: each column corresponds to one behavioural session and each collected pellet is a circle whose colour indicates its position in the temporal sequence of picking. The first collected pellets are the bluemost and the last collected pellets are the redmost. The left-right, respectively up-down, gradient is expressed on the y-axis. (A) Down-to-up strategy in Mk-JO with the left hand. (B) Down-to-up strategy in Mk-JO with the right hand. (C) Left-to-right strategy in Mk-DI. (D) Development and evolution of a post-lesion prehension strategy on the up-down axis in Mk-VA. Thick vertical black line: day at lesion; dashed vertical red line: day at dlPFC biopsy (see

the section below *Impact of a prefrontal cortical biopsy on manual dexterity*); dashed vertical black line: day at cell reimplantation (see below).

Impact of a prefrontal (dlPFC) cortical biopsy on manual dexterity

A previous study showed that a large cortical biopsy performed in the dlPFC in *M. fascicularis* induced profound modifications in the temporal sequence used to retrieve food pellets from the modified Brinkman board (Kaeser et al., 2013). For instance, in this task, Mk-AV usually scanned the board from the left side to the right side with the right hand (ipsilesional to the biopsy) before the right dlPFC biopsy. After the biopsy (44 mm^3), the animal changed completely its motor habits, scanning then the board from the right side to the left side (see their figure 4B, right hand). This change in motor strategy was nevertheless transitory and the pre-biopsy behaviour was recovered after about 20 days post-biopsy (**Figure 14A**). Conversely, the lesion did not induce any further change in strategy. The right dlPFC biopsy had an even more severe effect on the left hand because the post-biopsy alteration in motor strategy was maintained on the long-term and never recovered to the normal pre-biopsy state (Kaeser, 2010; Kaeser et al., 2013).

This very special post-biopsy alteration highlighted with the modified Brinkman board task motivated us to investigate in greater detail the temporal sequence of pellet picking in the monkeys subjected to a dlPFC biopsy given that they performed both tasks in parallel. Data related to the effect of the biopsy were obtained from Mk-AV and Mk-JO. For Mk-JA, the biopsy was performed a long time before the 2^{nd} lesion considered here and therefore the pre-biopsy data were not included in the present study. Details about the histology of the biopsy were previously reported in Kaeser et al. (2013). Briefly, some portions of both areas 9 and 46 in dlPFC had been removed during the biopsy, corresponding to a 44-mm^3 volume in Mk-AV and a 20.3-mm^3 volume in Mk-JO.

The most interesting results were obtained in Mk-AV. This animal used the same pre-biopsy strategy (i.e. scanning from the left to the right side of the board) to retrieve the pellets with the right hand (ipsilateral to the biopsy) both in the Brinkman box task with vision and in the modified Brinkman board task (**Figure 14A** and **B**), as we may have expected given both tasks are very similar. What is more, after the dlPFC biopsy, the monkey also changed its motor strategy in the same way in both tasks, i.e. usually scan-

ning both boards from the right to the left side. But, interestingly, in the Brinkman box task, this altered motor strategy never returned then to the pre-biopsy state. The subsequent cortical lesion did not induce further modification in strategy and the biopsy effect was maintained during all the post-lesion sessions (**Figure 14B**). Conversely, for reminder, the alteration in motor strategy observed after the biopsy in the modified Brinkman board task was only transitory (about 20 days) (**Figure 14A**). But still the subsequent cortical lesion did not alter the motor strategy in both tasks.

Figure 14 (next page): Impact of the dlPFC biopsy in Mk-AV. (A) Colour-coded sequences of pellet picking in the modified Brinkman board task with the right hand (modified from Kaeser, 2010; and Kaeser et al., 2013). (B) Colour-coded sequences of pellet picking in the Brinkman box task with vision with the right hand. Same conventions as in Figure 13. (C) Time course of the time to successfully retrieve the first 6 pellets in the Brinkman box task without vision with the right hand. Plateaux were compared with Mann-Whitney tests. When data were partly or completely missing, primarily after the lesion, a red star was indicated at the highest value for the corresponding date.

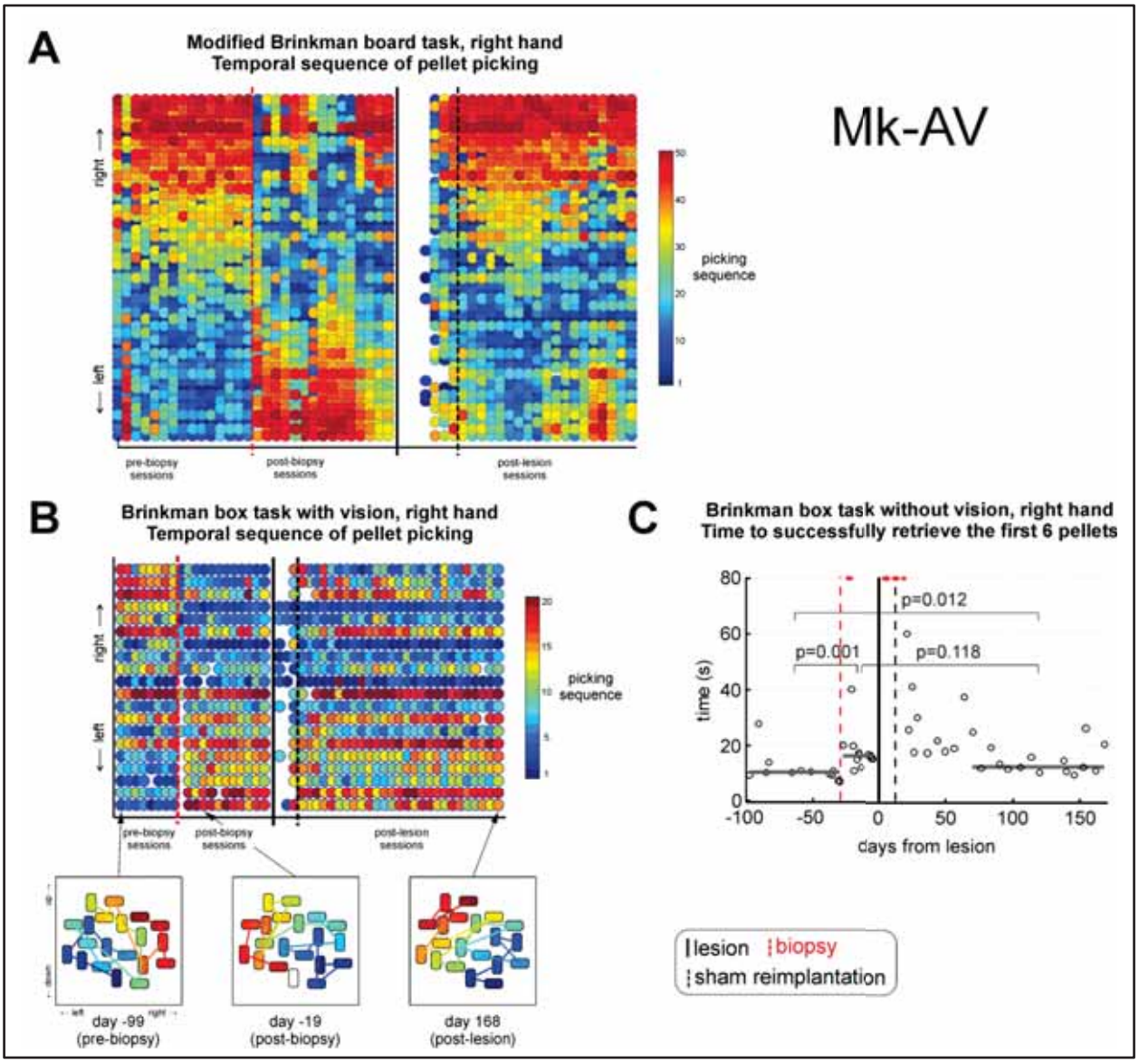

Regarding Mk-AV's left hand (contralesional to the biopsy), the monkey usually scanned the modified Brinkman board from the middle of the board to both right and left sides. Conversely, the animal adopted a systematic right-to-left strategy in the Brinkman box task with vision (**Supplementary Figure 2**). Then the biopsy effect was not consistent in both tasks either. Whereas Mk-AV used a different post-biopsy strategy to retrieve the pellets in the modified Brinkman board task (pre-biopsy: from the middle to the extremities vs post-biopsy: from the right side to the left side), no change in temporal sequence of pellet picking was observed in the Brinkman box task with vision (usually scanning from the right to the left side) (**Supplementary Figure 2**).

Kaeser et al. (2013) demonstrated that the dlPFC biopsy had a very specific impact on the motor strategy and did not affect the motor performance itself, whether the fine

manual dexterity or the speed of movement execution. We tested this statement here for the Brinkman box task without vision and observed that the biopsy did actually impair the motor performance itself as well, in addition to the pure motor strategy. More specifically, the cortical biopsy induced for instance a significant increase in the time needed to successfully collect the first 6 pellets –a measure of the speed of movement execution– (pre-biopsy median: 10.46 s vs post-biopsy median: 16.62 s, p =0.001, Mann-Whitney test) with the right hand in the task without vision (**Figure 14C**). Here again, the subsequent cortical lesion had no long-term impact on this parameter because the post-biopsy alteration was further maintained in the post-lesion plateau (post-biopsy median: 16.62 s vs post-lesion median: 12.4 s, p =0.118, Mann-Whitney test). Furthermore, as already mentioned above, Mk-AV exhibited a slight increase in the occurrence of somatosensory-related errors after the biopsy, but this change in behaviour was not specific to the biopsy given that a similar transitory increase was observed after the subsequent cortical lesion as well (**Figure 11A**).

To conclude, we confirmed here with an additional task that the dlPFC biopsy induced modifications in the picking strategy of small objects. In addition, we suggested some deficits in the speed of motor execution in the absence of visual feedback.

Discussion

Here we presented a behavioural task involving the use of the precision grip either under or without visual feedback in macaque monkeys, before and after a focal permanent motor cortex lesion of the hand representation. Following the lesion, we observed strong impairments of manual dexterity, especially when the task was performed with the contralesional hand, in the form of a decrease in the speed of motor execution, some deficits in fine finger movements and in wrist deviations as well as a worse proficiency of the animals to collect the pellets, the amount of these deficits being usually correlated with the extent of the lesion. In addition, as expected, the contralesional functional recovery of performance in the Brinkman box task with vision was better than in the task without vision. But more interestingly, some subtle post-lesion impairments emerged more specifically in the task without vision, such as a striking prominent deficit of finger use, somatosensory-related deficits, as well as impairments following a cortical biopsy,

demonstrating the relevance to test manual dexterity in blind condition as well after a cortical lesion.

Relevance of our analysis method to assess manual dexterity in non-human primates

We presented here a detailed analysis of fine manual dexterity in macaque monkeys subjected to a motor cortex lesion based on a large range of behavioural parameters. A first strength of our study rests on the use of a "manual" analysis of behavioural data. We decided to rely on such kind of analysis instead of a more automatised one because we think that post-lesion deficits in particular are so variable and complex that it is impossible to analyse them automatically without making errors. Even though time consuming, only a detailed visual assessment by human eye (i.e. frame by frame) of the video sequences allows to precisely quantify the post-lesion deficits and to detect very subtle impairments such as the somatosensory-related errors observed here.

Another strength of the present study is the large range of behavioural parameters assessed. Some previous studies reported nearly full post-lesion recovery of manual dexterity, for instance after CST lesion in non-human primates (Nishimura et al., 2009; Nishimura and Isa, 2009; Nishimura et al., 2007). Nevertheless, they based their conclusions on a single endpoint measurement in a behavioural task, namely the success ratio of precision grip. We demonstrated here that a cortical lesion resulted in a large range of deficits and by considering carefully the detailed results in each animal (**Supplementary Figure 1**), one can notice different levels of functional recovery according to the considered parameters. To put it another way, restricting the behavioural analysis to a single motor behavioural parameter is misleading because each measurement has its own limits and can on no account capture all the impairments, then probably resulting in underestimations of the impacts of lesions. The importance of a detailed assessment of behaviour, based for instance of kinematic analysis of movements, was already reported in rodents (McKenna and Whishaw, 1999; Whishaw et al., 1991; Whishaw et al., 1998). For example, even though rats completely recovered the pre-lesion success rate in pellet reaching in a few days after a unilateral lesion of the dorsal column, a very detailed video analysis of behavioural tasks revealed that the rotation of the affected upper

forelimb remained permanently altered, indicating a compensatory change in strategy (McKenna and Whishaw, 1999). In the same way, similar alterations in pronation and supination of forelimb during a reaching task were observed in rats subjected to a motor cortex lesion, by using a detailed video analysis (Whishaw et al., 1991). Lawrence and Kuypers themselves admitted that motor impairments in rhesus monkeys following a CST lesion could be greater than what they described because the behavioural tasks used to assess functional recovery could be not specific enough and animals were in fact able to use compensatory strategies (Kuypers, 1974), underestimating the dramatic effects of the lesion. As a matter of fact the best approach to assess the effects of a lesion on behaviour is to combine different tasks (see e.g. Schmidlin et al., 2011 in **Appendix 2**), each of them challenging a particular component of the behaviour and allowing therefore to highlight very specific deficits. In sum, detailed behavioural analyses in addition to outcome measurements are essential to exhaustively describe the behavioural effects of a cortical lesion.

Furthermore, the significant relationships highlighted between the extent of the lesion and the behavioural recovery in the different conditions of the task, even though our monkey sample was small and heterogeneous (3 treatment groups), indicate that the Brinkman box task documents objectively and reproducibly the functional impairments of non-human primates following a cortical damage.

Finally, the relevance of the parameters we selected for our analysis was already demonstrated in previous studies. The *precision grip shaping time* for instance seems to correspond to the "well time" assessed by Frost et al. (2003) and which was shown to be significantly increased for the contralesional hand in squirrel monkeys performing the Klüver board task after an ischemic lesion of the hand representation in M1. The *contact time with pellets*, corresponding to the "total manipulation time" in Pizzimenti et al. (2007) specifically reflects the true grasping abilities by quantifying the time of manipulation of the pellet by the fingers before collecting it. This measure has already been successfully used in our laboratory and was shown to be reliable and meaningful to capture post-lesion deficits following a spinal cord lesion (Freund et al., 2009) or a motor cortex lesion (Hoogewoud et al., 2013; Kaeser et al., 2011) and to characterise hand preference and hand dominance (see Chatagny et al., 2013 in **Appendix 3**) in our macaque monkeys. The proficiency of the animal to collect food pellets in the modified Brinkman

board task is currently measured by using the score in 30 s, a readout reflecting the combination of the pellet manipulation, arm reaching, arm withdrawal, and transport of the pellet to the mouth. Similarly to the contact time, this measure has been already proven to be relevant to document post-lesion deficits (see e.g. Kaeser et al., 2011) and was shown to covary elegantly with lesion extent (Freund et al., 2009; Kaeser et al., 2010; Wyss et al., 2013). Here, we had to express the performance in the form of a percentage rather than a raw score given that the task was usually arbitrarily stopped by the experimenter before the animal completely emptied the board, especially in the condition without visual feedback. Nevertheless, the *percentage of pellets successfully retrieved* is very similar to the score in 30 s to capture the monkeys' manual dexterity. What is more, in addition to already existing ones, we introduced some new parameters that appeared to be highly relevant in the blind task in particular, such as the distinction between the *well contact finger* and the *first precision grip finger* (for reminder, see e.g. **Figure 9F**).

Relevance of a blind task

One may argue that the task without visual feedback relies much more on spatial memory than on true motor exploration by palpation, which would completely challenge the relevance of our task to highlight somatosensory impairments after an M1 lesion. Nevertheless the present data allow to rule out this possibility. Namely, the absence of any motor strategy of pellet picking in all seven monkeys in the Brinkman box task without vision with either hand, whereas usually present in the task with visual feedback, strongly suggests that the monkeys did not acquire any precise strategy of pellet picking involving spatial memory during the training sessions. This observation indicates on the contrary that the animals usually performed the task primarily based on tactile exploration.

When behavioural tasks are performed under full visual control, as it is the case in most studies in non-human primates so far, active touch is involved, meaning that motor and sensory contributions are confounded. As mentioned in the *Introduction*, there are surprisingly very few reports about behavioural tasks assessing the precision grip both with and without visual control in the same subjects. The present results demonstrate the relevance to combine both visual conditions in a behavioural test of manual dexteri-

ty for monkeys involved in a lesion protocol, in order to test the somatosensory performance after a motor cortex lesion. Without the blind task, we would not have been able to highlight some very subtle adverse effects of the lesion such as the aforementioned sensorimotor-related errors, the impairment of finger use specific to this condition or an additional effect of the dlPFC biopsy. This indicates that the task without vision is very sensitive to reveal subtle sensorimotor deficits that emerge neither in tasks with full visual control nor in the general behaviour of the monkeys, such as the feeding, the grooming, or the interactions with the provided enrichment.

In sum, the Brinkman box task coupled with a detailed analysis method can be used to quantitatively assess fine manipulation abilities and document the time course of recovery following an insult in the nervous system by combining two complementary conditions of visual feedback.

Somatosensory-related errors

At a first glance, the misbehaviour illustrated in **Figure 10**, where the monkeys had to visually inspect their empty hand to realise that no pellet was collected actually, seems to be very similar to the sensory errors previously reported by Nudo and collaborators (Friel et al., 2005; Nudo et al., 2000) in squirrel monkeys after a lesion affecting specifically the caudal part of M1. The authors suggested a link with tactile agnosia as observed in human after a lesion in parietal lobe. However, a striking difference is that we observed this error especially when the Brinkman box task was performed without vision whereas the monkeys of Nudo's studies exhibited this sensory error when they collected rewards under full visual control from a Klüver board. There is unfortunately no mention about the behaviour of these monkeys in blind condition.

This behaviour suggests a somatosensory-related deficit. Namely, while a pure lesion of S1 in monkeys resulted in some transient motor impairments, strong tactile deficits were produced: Kruger and Porter (1958) reported that after a complete ablation of the postcentral gyrus, rhesus monkeys were able to open a box, reach for the food morsel contained inside but then closed the hand without the reward and brought the empty hand to the mouth. Others reported that tactile deficits resulting from a lesion of the hand representation of S1 in monkeys were partially compensated when visual input

was provided (Cole and Glees, 1954). More precise descriptions after a pure lesion of S1 hand representation mentioned that the animals were visually inspecting their hands after food picking to confirm that they actually collected the food morsel before eating it (Pavlides et al., 1993; Xerri et al., 1998). Conversely, this kind of behaviour was never observed in monkeys after unilateral or bilateral ablation of the precentral gyrus (see e.g. Kruger and Porter, 1958; Semmes and Porter, 1972) before Nudo's studies (Darling et al., 2014; Friel et al., 2005; Nudo et al., 2000), suggesting a somatosensory-related deficit.

Interestingly, the somatosensory-related errors described here are reminiscent of deficits of integrative sensitivity associated with an astereognosis reported in some human patients following a lesion in parietal cortex (Prof. Jean-Marie Annoni, personal communication, April 17, 2015). These latter observations are not incompatible with our data given the strong interconnectivity between the frontal and parietal areas. Moreover, comparable deficits of object recognition by touch were reproduced by locally anaesthetising the fingertips of human subjects who were then asked to perform object manipulation in the absence of visual feedback, such as picking up small objects from a dish (Johansson, talk given at the Institue of Neuroinformatics, University and ETH Zürich, April 24, 2015). The resulting astereognosis demonstrated the critical role of tactile inputs from the fingertips for object manipulation.

Nevertheless, one could argue that these deficits are not due to any somatosensory impairment but result merely from the absence of visual feedback as observed for instance in young male patients with Duchenne muscular dystrophy (Troise et al., 2014). In fact these deficits together with the completely reverse pattern of finger use according to the task observed in Mk-DI should be considered with the electrophysiological evidence from **Chapter 3**, strongly suggesting that tactile perception may be altered after a dominant motor cortical lesion and therefore further confirm the key role of M1 in somatosensory processing during the execution of a motor task (Lemon, 1981). M1 cannot be considered as a purely motor structure. Although its primary function is obviously motor, M1 processes cutaneous, muscle and joint afferents as well, due to its strong connections with the somatosensory cortex and the direct connections with the periphery through the thalamus (Asanuma, 1959; Tanji and Wise, 1981; Wannier et al., 1991).

Consequently, deficits after a motor cortex lesion should be considered as sensorimotor deficits as well rather than purely motor deficits.

The nearly complete absence of these errors under visual control suggests that monkeys were usually able to compensate, at least partly, the tactile impairment when vision was involved. There is a wealth of evidence that providing visual feedback can help tactile perception (Cardini et al., 2012; Guest and Spence, 2003; Johnson et al., 2006; Kennett et al., 2001; Schaefer et al., 2006; Serino et al., 2007; Serino et al., 2009; Taylor-Clarke et al., 2004; Yatani et al., 2012), proprioception (Ghez et al., 1995; Gordon et al., 1995; Hepp-Reymond et al., 2009; Rothwell et al., 1982) and object manipulation (Jenmalm et al., 2000) in human. For the sense of touch specifically, Haggard called this process "*visual enhancement of touch*" (Cardini et al., 2012; Haggard et al., 2003; Kennett et al., 2001; Rothwell et al., 1982). This phenomenon is well exemplified in mirror therapy: long-term improvement in tactile perception was observed in patients watching the mirror image of their unaffected limb in a mirror during tactile training (Moseley and Wiech, 2009). Conversely, removing visual feedback further deteriorated tactile performance after deafferentation (Rothwell et al., 1982). This strongly suggests that processings in the different sensory modalities influence each other, resulting in multisensory rather than purely unisensory perceptions. This is reminiscent of both M1 and S1 working together in the form of the functional sensorimotor cortex rather than two completely separated entities (Jones, 1986; Kaas, 2004a; Kaas, 2004b; Kaas, 2008; Tanji and Wise, 1981; Uematsu et al., 1992; Wise and Tanji, 1981).

Correlation between lesion extent and manual dexterity

As one may have intuitively expected, the level of functional recovery with the contralesional hand was inversely correlated with the extent of the lesion, as already observed in rodents (Freret et al., 2006; Goldstein and Davis, 1990; Rogers et al., 1997; Whishaw et al., 1991) and in stroke human patients (Alexander et al., 2010; Lövblad et al., 1997) for instance. In addition, our observations further confirm what had been reported in previous studies in our laboratory. For instance, Wyss et al. (2013) already investigated the functional contralesional recovery of some macaque monkeys (both control and anti-Nogo-A treated animals) included in our study by using at that time the modified Brinkman board task and they demonstrated that the level of recovery, assessed with the

number of pellets collected in the first 30 s of the task, was significantly negatively correlated with the volume of the lesion when all individuals were considered together, meaning very similar results as we observed in the Brinkman box task. They were even further able to show the beneficial effect of anti-Nogo-A treatment because more animals were included in each group as compared to our study.

Of course, highlighting a significant linear relationship between the extent of lesion in a given structure and behavioural deficits helps to interpret the role of that lesioned tissue in the impairments. Nevertheless, the presence of such a correlation does not mean the absence of involvement of other structures. Reciprocally, the absence of such a correlation would not necessarily mean the absence of involvement of that structure in generating the behaviour under consideration. Indeed, the scenario may be much more complex than a simple single and direct relationship between one or some brain structures and behavioural outcomes. Behavioural performances may be determined in fact by the integrity of a more complex brain network influenced itself by others cerebral structures. Then, a lesion damaging some components of this network (but sparing the influencing cerebral structures) or affecting some of the influencing cerebral structures (sparing the brain network) might result in behavioural impairments even if the influencing cerebral structures, respectively the brain network, which are known to be involved in producing the behaviour under consideration, are intact. To put it another way, functional impairments may be observed even if one of the structures normally controlling these functions remains intact. Then, by refining the correlations analyses, other factors probably contributing to the functional deficits as well may emerge. For instance, it was demonstrated that motor impairments in chronic stroke patients were significantly correlated with the level of atrophy in spared cortical tissue as well in addition to the extent of the lesion itself (Gauthier et al., 2011).

Moreover, some other measurements than the volume of the lesion itself may better correlate with the functional impairment: Pineiro et al. (2000) demonstrated for instance that functional deficits in stroke patients were significantly linearly correlated with "*the maximum proportional cross-sectional area of the corticospinal mask occupied by stroke*". On the other hand, they showed a cubic rather than linear relationship between the extent of the lesion and the functional deficits.

Remarks on the effects of the treatments

The seven monkeys of this study were divided into 3 treatment groups, namely four control animals, one animal treated post-lesion with anti-Nogo-A antibody and the last two treated post-lesion with autologous adult neural progenitor cells. We could therefore ideally expect to observe differences in the behaviour of the 3 groups of animals. Nevertheless, the very small sample size did not allow to perform statistical analysis in order to compare groups. Therefore we decided to group all the animals together for the correlation analyses. But we did not observe any trend in the 3 groups of animals, for instance in the form of treated animals forming a separate cluster of points distinct from another cluster containing the control animals in some of our regression plots. Nevertheless, the absence of any clear effect of the treatment here does not mean that the different treatments were inefficient. Previous reports already demonstrated the beneficial effects of anti-Nogo-A-antibody treatment (Schwab, 2010) in rodents subjected to spinal cord injury (Bandtlow et al., 1990; Bareyre et al., 2002; Bregman et al., 1995; Brösamle et al., 2000; Buchli et al., 2007; Buchli and Schwab, 2005; Fouad et al., 2001; Liebscher et al., 2005; Markus et al., 2005; Merkler et al., 2001; Raineteau et al., 1999; Raineteau et al., 2002; Schnell and Schwab, 1990; Schwab, 1996; Schwab, 1998; Schwab, 2002; Schwab, 2004; Schwab and Bartholdi, 1996; Thallmair et al., 1998; von Meyenburg et al., 1998), or to cortical lesion (Buchli and Schwab, 2005; Cheatwood et al., 2008; Emerick et al., 2003; Emerick and Kartje, 2004; Gillani et al., 2010; Lindau et al., 2014; Markus et al., 2005; Papadopoulos et al., 2002; Seymour et al., 2005; Tsai et al., 2011; Tsai et al., 2007; Wahl et al., 2014). Then similar beneficial effects were observed in studies extended to non-human primates subjected to spinal cord injury (Fouad et al., 2004; Freund et al., 2006; Freund et al., 2007; Freund et al., 2009) or, more recently, following motor cortex lesion (Hamadjida et al., 2012; Wyss et al., 2013) (see **Chapter 8** for further detail). In parallel, monkeys treated with adult neural progenitor cell therapy showed an improved functional recovery as compared to control animals as well (Kaeser et al., 2011). All these studies were based on a larger sample of monkeys while we were here limited by the very restricted number of animals performing the Brinkman box task.

Comparison between contra- and ipsilesional manual dexterity

Here we demonstrated that the contralateral performance usually decreased with increasing lesion extent. We also suggested that monkeys with a large lesion allotted less resource after the lesion than before the lesion to perform not very challenging behaviour (visiting vertical wells, neutral wrist position) with their intact hand in favour of more challenging motor control (visiting horizontal wells, ulnar wrist deviation) (for reminder, see **Supplementary Figure 3**). This indicates that ipsilesional motor control was usually not altered by a large lesion but quite the contrary.

A study in the laboratory (Kaeser et al., 2010) previously demonstrated a remarkably strong significant correlation between the post-lesion performance of the contra- and ipsilesional hands in the **modified Brinkman board task**, here again by grouping together animals from different treatment groups (control monkeys, anti-Nogo-A treated monkeys and monkeys treated with autologous adult neural progenitor cell therapy), some of them being involved in our study as well. They focused in particular on the long-term post-lesion performance (i.e. 100-300 days after the lesion), corresponding usually to the post-lesion periods considered in our study as well. The major difference with our results in the **Brinkman box task** lies in that they observed that the better the recovery with the contralesional hand, the better the long-term performance with the ipsilesional hand *as well*. Equally interesting, those animals with a good contralesional functional recovery showed an enhanced ipsilesional performance as compared to the pre-lesion one as well. Conversely, animals exhibiting a bad contralesional recovery also had a decrease in performance of the ipsilesional upper limb after the lesion. They interpreted this latter result as an increase of activity in the ipsilesional hemisphere (PM, SMA, CMA) in animals with bad recovery, which may putatively result in a long-lasting increase in callosal inhibition onto the intact hemisphere. Thus, the intact hemisphere being more inhibited, then the performance of the ipsilesional forelimb decreases. Moreover, to explain the increase of ipsilesional performance in animals with good recovery, the authors did not exclude a subcortical mechanism, for instance through the rubro- or reticulospinal pathways that may induce facilitation of the intact hemisphere on the ipsilesional hand.

How can we conciliate both studies, showing inconsistent results regarding the relationship between the contralesional recovery and the ipsilesional performance? The Brink-

man box task is unquestionably more challenging and more demanding than the modified Brinkman board task. Even with visual feedback, the presence of the lateral sides of the box somewhat limits movements of the upper limb. We suggest therefore that the link between recovery levels of both hands depends on the complexity of the task. Simply put, in case of a very demanding task (e.g. Brinkman box task), the monkeys with a large lesion, meaning large contralesional deficits, seem not to be able to allocate resources on both body sides but favour the existing best hand to perform difficult tasks. Conversely, animals with a small lesion recover quite well with the contralesional hand and do not need to improve their ipsilesional motor control. Then when the task is more straightforward (e.g. modified Brinkman board task), monkeys try to improve behaviour with both affected and intact upper limbs: the better the recovery with the contralesional hand, the better the performance with the ipsilesional hand as well. In case of a good contralesional functional recovery, this can even result in an enhanced ipsilesional performance as compared to the pre-lesion one as well. Conversely, animals with a bad contralesional recovery do not improve their ipsilesional motor control after the lesion.

Effect of a prefrontal cortical biopsy on ipsilesional manual dexterity

The permanent change in motor habit highlighted here for Mk-AV's right hand in the **Brinkman box task** with vision is in accordance with the previous study by Kaeser et al. (2013) that reported similar alterations in the temporal sequence of pellet picking both in the **modified Brinkman board task** and in the **rotating Brinkman board task,** in two monkeys (MK-AV and Mk-JO). Therefore, our results further confirm that the dlPFC is important for the representation of motor habits in motor tasks involving sequential manipulations of many objects, and more specifically in a free-will task as well. Namely, the role of dlPFC in strategy was originally demonstrated in conditional tasks involving visuo-spatial working memory (Constantinidis et al., 2001; Constantinidis and Procyk, 2004; Curtis and D'Esposito, 2004; D'Esposito et al., 2000; Funahashi et al., 1989; Goldman and Rosvold, 1970; Postle et al., 2000; Qi et al., 2010; Tanji and Hoshi, 2008) (for an elaborated discussion about the implication of these results, please consult directly Kaeser et al., 2013).

Moreover in Kaeser's study (2013), the effect of the biopsy was shown to be more prominent in the modified Brinkman board task (the strategy with both hands was affected),

involving 50 pellets, than in the rotating Brinkman board task (the strategy in sole counterclockwise rotation was dramatically altered, but motor strategy from both hands was still affected), involving only 32 pellets, and these effects were more visible in Mk-AV, the monkey with the largest biopsy. Here with the Brinkman box task involving only 20 pellets, we observed a rather local but still permanent effect, limited to the right, ipsilateral (to the biopsy) hand of Mk-AV. Conversely, we did not observe any change in motor strategy in Mk-JO that had a smaller biopsy than Mk-AV. Taken both studies together, this suggests that the behavioural impact of the dlPFC biopsy depended on both the extent of the biopsy and the complexity of the task (here in the form of the number of objects involved in the task).

A new finding with our task as compared with Kaeser's study (2013) is that the biopsy impact was not limited to pure motor strategy changes but the motor performance itself was affected as well, in the form of a decrease in motor execution speed. This was exemplified by a significant increase in the time needed to collect the first 6 pellets after the biopsy and this alteration was further maintained and remained unchanged over the entire post-lesion plateau period. Remarkably, this deficit was observed only when the task was performed without vision. Nevertheless, we are aware that a more rigorous analysis is required to fully conclude on the effects of the dlPFC biopsy on motor performance. For instance, we should investigate the same parameters affected by the biopsy in a larger sample of animals. Moreover, we should also include more specifically animals that had a control surgery such as the implantation of a recording chamber (e.g. by extending data analysis in Mk-VA and Mk-JA to the time before the implantation of the chronic recording chamber), what was rigorously performed in Kaeser's study. This way of processing aimed at distinguishing the effect of the biopsy itself from the side-effects induced by the surgery such as the craniotomy, the anaesthesia and the medication that went with (Kaeser et al., 2013). As things stand, more analyses on additional monkeys are required. But still, given the large inter-individual variability in the way the animals react after a surgery according to our experience and as visible in Kaeser's study (Kaeser et al., 2013), an inter-individual comparison may be risky. Conversely, we believe that the best control remains the same animal itself by comparing the effect of a surgery alone with the effect of the surgery followed by the biopsy. This strategy of intra-individual comparison was used to address the effect of a craniotomy on EEG signals recorded at the scalp in one of our monkey (see Gindrat et al., 2014 in **Chapter 1**). In a

few words, with the available data, we cannot confirm nor invalidate the real effects of the dlPFC biopsy on motor performance, but still data may suggest that the biopsy does not affect the sole motor strategy but the speed of motor execution may be altered as well. Interesting behavioural data from four other monkeys subjected to a similar dlPFC biopsy in our laboratory may be available in the next future.

Post-lesion deficits

The severe post-lesion deficits in contralesional manual dexterity described here are in accordance with previous reports of motor cortex lesions of the hand representation in non-human primates performed in our laboratory (Hoogewoud et al., 2013; Kaeser et al., 2011; Liu and Rouiller, 1999; Rouiller et al., 1998; Wyss et al., 2013), and in other groups (Darling et al., 2014; Frost et al., 2003; Glees and Cole, 1950; Nudo and Milliken, 1996; Pizzimenti et al., 2007; Plautz et al., 2003). The only exception is the somatosensory-related deficits, previously reported only by Nudo and collaborators (Darling et al., 2014; Friel et al., 2005; Nudo et al., 2000). Following an initial complete loss of fine finger movements, some gradual but incomplete functional recovery was observed, reflecting a general trend towards lower contralesional manual skills as compared to the ipsilesional hand.

The large inter-individual variability in the different behavioural parameters affected at distinct degrees by the lesion, in particular in the task without visual feedback, may probably result from the variable extent and location of the cortical lesion across monkeys. This variability may also reflect a wide range of restitution and/or substitution strategies underlying the functional recovery. Moreover, we should not forget that the age, sex and simply motivation to perform the task could impact on the performance as well.

The neural mechanisms underlying this functional recovery are still not fully known but the recruitment of adjacent and remote areas (such as PM or SMA) in the same hemisphere or in the intact hemisphere highly depends on the extent of the lesion (Dancause et al., 2005; Dancause, 2006; Dancause and Nudo, 2011; Eisner-Janowicz et al., 2008; Frost et al., 2003; Liu and Rouiller, 1999; McNeal et al., 2010; Murata et al., 2015; Nudo, 1999; Nudo, 2006a; Nudo, 2006b; Nudo, 2007; Nudo, 2013; Nudo, 2006c; Rouiller et al.,

1998; Rouiller and Olivier, 2004). For greater detail and some hypotheses, please consult **Chapter 2** and **Chapter 3**.

Further remarks

We should keep in mind that our study presents some limitations: first, this study is based on 7 animals only from 3 different treatment groups. Obviously we would need to extend the sample of monkeys to better evaluate the effects of the treatment on manual dexterity assessed here with the Brinkman box task after a lesion of the M1 hand representation. Second, there were some inter-individual variations in the protocol, e.g. the time extent of the post-lesion period and differences in lesions (size, location). Nevertheless, such confounding factors correspond to the actual situation in clinics and therefore should not be considered as a true drawback in our data if we are interested to put them back into a clinical context.

The present data, especially the very specific errors and impairments highlighted in the task without visual feedback, strongly suggest that tactile perception may be altered after a motor cortical lesion. Therefore, we could refine the general battery of behavioural tasks currently used in our laboratory by adding, for instance, tests of tactile perceptions, both active and passive.

Conclusion

Here we confirmed at the behavioural level the results obtained in the previous chapters by using EEG (**Chapters 2** and **3**). The present data strongly suggest, first, that an M1 lesion may result in a somatosensory deficit or a disruption of M1-S1 connections in addition to pure motor impairments. Therefore, deficits in fine motor control after M1 lesions may be actually partly attributed to an impaired somatosensory processing within M1 itself and/or decreased inputs from S1 or from the thalamus to M1. Second, these somatosensory-related impairments can be highlighted by using specific tasks. In the present case, the Brinkman box task was shown to be very sensitive and relevant to quantify the exploratory ability and tactile sense in a lesional context. It enabled to detect subtle impairments and highlighted the importance of somatosensory feedback, es-

pecially in the task performed without visual control. In conclusion, we advise to combine behavioural tasks with and without visual feedback to exhaustively document the effects of a motor cortex lesion and thus to avoid underestimating them.

References

Alexander, L., Black, S., Gao, F., Szilagyi, G., Danells, C., McIlroy, W., 2010. Correlating lesion size and location to deficits after ischemic stroke: the influence of accounting for altered peri-necrotic tissue and incidental silent infarcts. Behavioral and Brain Functions 6, 6.

Alexander, R.M., 1993. Joints and muscles of hands and paws. In: Preuschoft, H., Chivers, D.J. (Eds.), Hands of Primates. Springer Vienna, pp. 199-205.

Asanuma, H., 1959. Microelectrode studies on the evoked activity of a single pyramidal tract cell in the somato-sensory area in cats. Jpn.J Physiol 9, 94-105.

Asanuma, H., 1981. Functional role of sensory inputs to the motor cortex. Prog.Neurobiol. 16, 241-262.

Asanuma, H., Arissian, K., 1984. Experiments on functional role of peripheral input to motor cortex during voluntary movements in the monkey. J.Neurophysiol. 52, 212-227.

Bandtlow, C., Zachleder, T., Schwab, M.E., 1990. Oligodendrocytes arrest neurite growth by contact inhibition. J Neurosci. 10, 3837-3848.

Bareyre, F.M., Haudenschild, B., Schwab, M.E., 2002. Long-lasting sprouting and gene expression changes induced by the monoclonal antibody IN-1 in the adult spinal cord. J Neurosci. 22, 7097-7110.

Bashir, S., Kaeser, M., Wyss, A., Hamadjida, A., Liu, Y., Bloch, J., Brunet, J.F., Belhaj-Saïf, A., Rouiller, E.M., 2012. Short-term effects of unilateral lesion of the primary motor cortex (M1) on ipsilesional hand dexterity in adult macaque monkeys. Brain Struct.Funct. 217, 63-79.

Baumann, M.A., Fluet, M.C., Scherberger, H., 2009. Context-specific grasp movement representation in the macaque anterior intraparietal area. J Neurosci 29, 6436-6448.

Bliss-Moreau, E., Theil, J.H., Moadab, G., 2013. Efficient cooperative restraint training with rhesus macaques. Journal of Applied Animal Welfare Science 16, 98-117.

Bregman, B.S., Kunkel-Bagden, E., Schnell, L., Dai, H.N., Gao, D., Schwab, M.E., 1995. Recovery from spinal cord injury mediated by antibodies to neurite growth inhibitors. Nature 378, 498-501.

Brinkman, C., 1984. Supplementary motor area of the monkey's cerebral cortex: short- and long-term deficits after unilateral ablation and the effects of subsequent callosal section. J Neurosci. 4, 918-929.

Brinkman, C., 1981. Lesions in supplementary motor area interfere with a monkey's performance of a bimanual coordination task. Neuroscience Letters 27, 267-270.

Brinkman, J., Kuypers, H.G., 1972. Splitbrain Monkeys: Cerebral Control of Ipsilateral and Contralateral Arm, Hand, and Finger Movements. Science 176, 536-539.

Brinkman, J., Kuypers, H.G., 1973. Cerebral control of contralateral and ipsilateral arm, hand and finger movements in the split-brain rhesus monkey. Brain 96, 653-674.

Brochier, T., Boudreau, M.J., Paré, M., Smith, A.M., 1999. The effects of muscimol inactivation of small regions of motor and somatosensory cortex on independent finger movements and force control in the precision grip. Exp Brain Res 128, 31-40.

Brorsson, S., 2012. Biomechanical studies on hand function in rehabilitation. Human Musculoskeletal Biomechanics.

Brösamle, C., Huber, A.B., Fiedler, M., Skerra, A., Schwab, M.E., 2000. Regeneration of lesioned corticospinal tract fibers in the adult rat induced by a recombinant, humanized IN-1 antibody fragment. J Neurosci. 20, 8061-8068.

Brunet, J.F., Rouiller, E.M., Wannier, T., Villemure, J.G., Bloch, J., 2005. Primate adult brain cell autotransplantation, a new tool for brain repair? Exp.Neurol. 196, 195-198.

Buchli, A.D., Rouiller, E., Mueller, R., Dietz, V., Schwab, M.E., 2007. Repair of the injured spinal cord. A joint approach of basic and clinical research. Neurodegener.Dis. 4, 51-56.

Buchli, A.D., Schwab, M.E., 2005. Inhibition of Nogo: a key strategy to increase regeneration, plasticity and functional recovery of the lesioned central nervous system. Ann.Med. 37, 556-567.

Capitanio, J.P., Emborg, M.E., 2008. Contributions of non-human primates to neuroscience research. Lancet 371, 1126-1135.

Cardini, F., Longo, M.R., Driver, J., Haggard, P., 2012. Rapid enhancement of touch from non-informative vision of the hand. Neuropsychologia 50, 1954-1960.

Chatagny, P., Badoud, S., Kaeser, M., Gindrat, A.D., Savidan, J., Fregosi, M., Moret, V., Roulin, C., Schmidlin, E., Rouiller, E.M., 2013. Distinction between hand dominance and hand preference in primates: a behavioral investigation of manual dexterity in nonhuman primates (macaques) and human subjects. Brain and Behavior 3, 575-595.

Cheatwood, J.L., Emerick, A.J., Schwab, M.E., Kartje, G.L., 2008. Nogo-A expression after focal ischemic stroke in the adult rat. Stroke 39, 2091-2098.

Cole, J., 1952. Three tests for the study of motor and sensory abilities in monkeys. Journal of comparative and physiological psychology 45, 226.

Cole, J., Glees, P., 1954. Effects of small lesions in sensory cortex in trained monkeys. J Neurophysiol. 17, 1-13.

Committee for the Update of the Guide for the Care and Use of Laboratory Animals, National Research Council, 2011. Guide for the Care and Use of Laboratory Animals: Eighth Edition. The National Academies Press.

Constantinidis, C., Franowicz, M.N., Goldman-Rakic, P.S., 2001. Coding Specificity in Cortical Microcircuits: A Multiple-Electrode Analysis of Primate Prefrontal Cortex. The Journal of Neuroscience 21, 3646-3655.

Constantinidis, C., Procyk, E., 2004. The primate working memory networks. Cognitive, Affective, & Behavioral Neuroscience 4, 444-465.

Courtine, G., Bunge, M.B., Fawcett, J.W., Grossman, R.G., Kaas, J.H., Lemon, R.N., Maier, I., Martin, J., Nudo, R.J., Ramon-Cueto, A., Rouiller, E.M., Schnell, L., Wannier, T., Schwab, M.E., Edgerton, V.R., 2007. Can experiments in nonhuman primates expedite the translation of treatments for spinal cord injury in humans? Nat.Med. 13, 561-566.

Curtis, C.E., D'Esposito, M., 2004. The effects of prefrontal lesions on working memory performance and theory. Cognitive, Affective, & Behavioral Neuroscience 4, 528-539.

D'Esposito, M., Postle, B.R., Rypma, B., 2000. Prefrontal cortical contributions to working memory: evidence from event-related fMRI studies. Exp Brain Res 133, 3-11.

Dancause, N., 2006. Vicarious function of remote cortex following stroke: recent evidence from human and animal studies. Neuroscientist. 12, 489-499.

Dancause, N., Barbay, S., Frost, S.B., Plautz, E.J., Chen, D., Zoubina, E.V., Stowe, A.M., Nudo, R.J., 2005. Extensive cortical rewiring after brain injury. J.Neurosci. 25, 10167-10179.

Dancause, N., Barbay, S., Frost, S.B., Zoubina, E.V., Plautz, E.J., Mahnken, J.D., Nudo, R.J., 2006. Effects of small ischemic lesions in the primary motor cortex on neurophysiological organization in ventral premotor cortex. J Neurophysiol 96, 3506-3511.

Dancause, N., Nudo, R.J., 2011. Shaping plasticity to enhance recovery after injury. Progress in brain research 192, 273-295.

Darian-Smith, C., Ciferri, M.M., 2005. Loss and recovery of voluntary hand movements in the macaque following a cervical dorsal rhizotomy. J.Comp Neurol. 491, 27-45.

Darian-Smith, C., 2007. Monkey Models of Recovery of Voluntary Hand Movement After Spinal Cord and Dorsal Root Injury. ILAR Journal 48, 396-410.

Darian-Smith, I., 1984. The Sense of Touch: Performance and Peripheral Neural Processes. In: Brookhart, J.M., Mountcastle, V.B. (Eds.), Handbook of Physiology, The Nervous System, Sensory Processes. John Wiley & Sons, Inc., pp. 739-788.

Darian-Smith, I., Galea, M.P., Darian-Smith, C., Sugitani, M., Tan, A., Burman, K., 1996. Introduction., The Anatomy of Manual Dexterity, Advances in Anatomy Embryology and Cell Biology, Volume 133. Springer Berlin Heidelberg, pp. 1-16.

Darling, W.G., Morecraft, R.J., Rotella, D.L., Pizzimenti, M.A., Ge, J., Stilwell-Morecraft, K.S., Zhang, H., Soliman, H., Seecharan, D., Edwards, I., McNeal, D., Nudo, R.J., Cheney, P., 2014. Recovery of precision grasping after motor cortex lesion does not require forced use of the impaired hand in macaca mulatta. Exp Brain Res.

Darling, W.G., Peterson, C.R., Herrick, J.L., McNeal, D.W., Stilwell-Morecraft, K.S., Morecraft, R.J., 2006. Measurement of coordination of object manipulation in non-human primates. Journal of Neuroscience Methods 154, 38-44.

Darling, W.G., Pizzimenti, M.A., Rotella, D.L., Hynes, S.M., Ge, J., Stilwell-Morecraft, K.S., Vanadurongvan, T., McNeal, D.W., Solon-Cline, K.M., Morecraft, R.J., 2010. Minimal forced use without constraint stimulates spontaneous use of the impaired upper extremity following motor cortex injury. Exp Brain Res 202, 529-542.

Darling, W.G., Pizzimenti, M.A., Rotella, D.L., Peterson, C.R., Hynes, S.M., Ge, J., Solon, K., McNeal, D.W., Stilwell-Morecraft, K.S., Morecraft, R.J., 2009. Volumetric effects of motor cortex injury on recovery of dexterous movements. Experimental Neurology 220, 90-108.

Dechent, P., Frahm, J., 2003. Functional somatotopy of finger representations in human primary motor cortex. Hum.Brain Mapp. 18, 272-283.

Desrosiers, J., Bourbonnais, D., Bravo, G., Roy, P.M., Guay, M., 1996. Performance of the Unaffected Upper Extremity of Elderly Stroke Patients. Stroke 27, 1564-1570.

Dum, R.P., Strick, P.L., 1996. The Corticospinal System: A Structural Framework for the Central Control of Movement., Comprehensive Physiology. John Wiley & Sons, Inc.

Eisner-Janowicz, I., Barbay, S., Hoover, E., Stowe, A.M., Frost, S.B., Plautz, E.J., Nudo, R.J., 2008. Early and late changes in the distal forelimb representation of the supplementary motor area after injury to frontal motor areas in the squirrel monkey. J Neurophysiol 100, 1498-1512.

Emerick, A.J., Neafsey, E.J., Schwab, M.E., Kartje, G.L., 2003. Functional reorganization of the motor cortex in adult rats after cortical lesion and treatment with monoclonal antibody IN-1. J Neurosci. 23, 4826-4830.

Emerick, A.J., Kartje, G.L., 2004. Behavioral recovery and anatomical plasticity in adult rats after cortical lesion and treatment with monoclonal antibody IN-1. Behavioural Brain Research 152, 315-325.

Fay, M.P., Proschan, M.A., 2010. Wilcoxon-Mann-Whitney or t-test? On assumptions for hypothesis tests and multiple interpretations of decision rules. Statistics surveys 4, 1.

Fluet, M.C., Baumann, M.A., Scherberger, H., 2010. Context-Specific Grasp Movement Representation in Macaque Ventral Premotor Cortex. The Journal of Neuroscience 30, 15175-15184.

Fouad, K., Klusman, I., Schwab, M.E., 2004. Regenerating corticospinal fibers in the Marmoset (*Callitrix jacchus*) after spinal cord lesion and treatment with the anti-Nogo-A antibody IN-1. Eur.J Neurosci. 20, 2479-2482.

Fouad, K., Dietz, V., Schwab, M.E., 2001. Improving axonal growth and functional recovery after experimental spinal cord injury by neutralizing myelin associated inhibitors. Brain Research Reviews 36, 204-212.

Freret, T., Chazalviel, L., Roussel, S., Bernaudin, M., Schumann-Bard, P., Boulouard, M., 2006. Long-term functional outcome following transient middle cerebral artery occlusion in the rat: Correlation between brain damage and behavioral impairment. Behavioral Neuroscience 120, 1285-1298.

Freund, P., Schmidlin, E., Wannier, T., Bloch, J., Mir, A., Schwab, M.E., Rouiller, E.M., 2006. Nogo-A-specific antibody treatment enhances sprouting and functional recovery after cervical lesion in adult primates. Nat.Med. 12, 790-792.

Freund, P., Schmidlin, E., Wannier, T., Bloch, J., Mir, A., Schwab, M.E., Rouiller, E.M., 2009. Anti-Nogo-A antibody treatment promotes recovery of manual dexterity after unilateral cervical lesion in adult primates--re-examination and extension of behavioral data. Eur.J Neurosci. 29, 983-996.

Freund, P., Wannier, T., Schmidlin, E., Bloch, J., Mir, A., Schwab, M.E., Rouiller, E.M., 2007. Anti-Nogo-A antibody treatment enhances sprouting of corticospinal axons rostral to a unilateral cervical spinal cord lesion in adult macaque monkey. J Comp Neurol. 502, 644-659.

Friel, K.M., Barbay, S., Frost, S.B., Plautz, E.J., Hutchinson, D.M., Stowe, A.M., Dancause, N., Zoubina, E.V., Quaney, B.M., Nudo, R.J., 2005. Dissociation of sensorimotor deficits after rostral versus caudal lesions in the primary motor cortex hand representation. J Neurophysiol. 94, 1312-1324.

Friel, K.M., Nudo, R.J., 1998. Recovery of motor function after focal cortical injury in primates: compensatory movement patterns used during rehabilitative training. Somatosens.Mot.Res. 15, 173-189.

Friel, K.M., Heddings, A.A., Nudo, R.J., 2000. Effects of Postlesion Experience on Behavioral Recovery and Neurophysiologic Reorganization after Cortical Injury in Primates. Neurorehabilitation and Neural Repair 14, 187-198.

Frost, S.B., Barbay, S., Friel, K.M., Plautz, E.J., Nudo, R.J., 2003. Reorganization of remote cortical regions after ischemic brain injury: a potential substrate for stroke recovery. J Neurophysiol 89, 3205-3214.

Funahashi, S., Bruce, C.J., Goldman-Rakic, P.S., 1989. Mnemonic coding of visual space in the monkey's dorsolateral prefrontal cortex. Journal of Neurophysiology 61, 331-349.

Galea, M.P., Darian-Smith, I., 1997. Manual dexterity and corticospinal connectivity following unilateral section of the cervical spinal cord in the macaque monkey. J Comp Neurol. 381, 307-319.

Gauthier, L.V., Taub, E., Mark, V.W., Barghi, A., Uswatte, G., 2011. Atrophy of Spared Gray Matter Tissue Predicts Poorer Motor Recovery and Rehabilitation Response in Chronic Stroke. Stroke.

Ghez, C., Gordon, J., Ghilardi, M.F., 1995. Impairments of reaching movements in patients without proprioception. II. Effects of visual information on accuracy. J Neurophysiol. 73, 361-372.

Gillani, R.L., Tsai, S.Y., Wallace, D.G., O'Brien, T.E., Arhebamen, E., Tole, M., Schwab, M.E., Kartje, G.L., 2010. Cognitive recovery in the aged rat after stroke and anti-Nogo-A immunotherapy. Behavioural Brain Research 208, 415-424.

Gindrat, A.D., Quairiaux, C., Britz, J., Brunet, D., Lanz, F., Michel, C.M., Rouiller, E.M., 2014. Whole-scalp EEG mapping of somatosensory evoked potentials in macaque monkeys. Brain Struct.Funct., 1-22.

Gisolfi, C.V., Mora, F., Nattermann, R., Myers, R.D., 1978. New apparatus for exercising a monkey seated in a primate chair. Journal of Applied Physiology 44, 129-132.

Glees, P., 1956. Die Organisation der Motorischen Rinde. Deutsche Zeitschrift für Nervenheilkunde 175, 155-162.

Glees, P., Cole, J., 1950. Recovery of skilled motor functions after small repeated lesions of motor cortex in macaque. Journal of Neurophysiology 13, 137-148.

Goldman, P.S., Rosvold, H.E., 1970. Localization of function within the dorsolateral prefrontal cortex of the rhesus monkey. Experimental Neurology 27, 291-304.

Goldstein, L.B., Davis, J.N., 1990. Influence of lesion size and location on amphetamine-facilitated recovery of beam-walking in rats. Behavioral Neuroscience 104, 320-327.

Gordon, J., Ghilardi, M.F., Ghez, C., 1995. Impairments of reaching movements in patients without proprioception. I. Spatial errors. J Neurophysiol. 73, 347-360.

Gray, H., 1893. Anatomy, descriptive and surgical. Lea Brothers & Company.

Guest, S., Spence, C., 2003. What role does multisensory integration play in the visuotactile perception of texture? International Journal of Psychophysiology 50, 63-80.

Haggard, P., Taylor-Clarke, M., Kennett, S., 2003. Tactile perception, cortical representation and the bodily self. Current Biology 13, R170-R173.

Hamadjida, A., Wyss, A.F., Mir, A., Schwab, M.E., Belhaj-Saïf, A., Rouiller, E.M., 2012. Influence of anti-Nogo-A antibody treatment on the reorganization of callosal connectivity of the premotor cortical areas following unilateral lesion of primary motor cortex (M1) in adult macaque monkeys. Exp.Brain Res. 223, 321-340.

Hepp-Reymond, M.C., Chakarov, V., Schulte-Mönting, J., Huethe, F., Kristeva, R., 2009. Role of proprioception and vision in handwriting. Brain Research Bulletin 79, 365-370.

Hermsdörfer, J., Laimgruber, K., Kerkhoff, G., Mai, N., Goldenberg, G., 1999a. Effects of unilateral brain damage on grip selection, coordination, and kinematics of ipsilesional prehension. Exp Brain Res 128, 41-51.

Hermsdörfer, J., Ulrich, S., Marquardt, C., Goldenberg, G., Mai, N., 1999b. Prehension With the Ipsilesional Hand After Unilateral Brain Damage. Cortex 35, 139-161.

Higgins, J., Mayo, N.E., Desrosiers, J., Salbach, N.M., Ahmed, S., 2005. Upper-limb function and recovery in the acute phase poststroke. J Rehabil Res Dev 42, 65-76.

Higo, N., Nishimura, Y., Murata, Y., Oishi, T., Yoshino-Saito, K., Takahashi, M., Tsuboi, F., Isa, T., 2009. Increased expression of the growth-associated protein 43 gene in the sensorimotor cortex of the macaque monkey after lesioning the lateral corticospinal tract. The Journal of Comparative Neurology 516, 493-506.

Hikosaka, O., Tanaka, M., Sakamoto, M., Iwamura, Y., 1985. Deficits in manipulative behaviors induced by local injections of muscimol in the first somatosensory cortex of the conscious monkey. Brain Research 325, 375-380.

Hoogewoud, F., Hamadjida, A., Wyss, A.F., Mir, A., Schwab, M.E., Belhaj-Saïf, A., Rouiller, E.M., 2013. Comparison of functional recovery of manual dexterity after unilateral spinal cord lesion or motor cortex lesion in adult macaque monkeys. Front Neurol. 4, 101.

Hopkins, W.D., 1995. Hand preferences for a coordinated bimanual task in 110 chimpanzees (*Pan troglodytes*): Cross-sectional analysis. Journal of Comparative Psychology 109, 291-297.

Jenmalm, P., Dahlstedt, S., Johansson, R.S., 2000. Visual and Tactile Information About Object-Curvature Control Fingertip Forces and Grasp Kinematics in Human Dexterous Manipulation. Journal of Neurophysiology 84, 2984-2997.

Johansson, R.S., 2015. Information in first-order human tactile neurons., Talk given at the Institue of Neuroinformatics, University and ETH Zürich, April 24, 2015.

Johnson, R.M., Burton, P.C., Ro, T., 2006. Visually induced feelings of touch. Brain Research 1073–1074, 398-406.

Jones, E.G., 1986. Connectivity of the Primate Sensory-Motor Cortex. In: Jones, E.G., Peters, A. (Eds.), Sensory-Motor Areas and Aspects of Cortical Connectivity, 5th ed. Springer US, pp. 113-183.

Kaas, J.H., 2004a. Evolution of somatosensory and motor cortex in primates. Anat.Rec.A Discov.Mol.Cell Evol.Biol. 281, 1148-1156.

Kaas, J.H., 2004b. Evolution of the Large, Complex Sensorimotor Systems of Anthropoid Primates. In: Pellis, S., Marino, L. (Eds.), Special Issue: Evolution of the Vertebrate Brain and Behavior, International Journal of Comparative Psychology 17, pp. 34-52.

Kaas, J.H., 2008. The evolution of the complex sensory and motor systems of the human brain. Brain Res.Bull. 75, 384-390.

Kaas, J.H., Nelson, R.J., Sur, M., Lin, C.S., Merzenich, M.M., 1979. Multiple representations of the body within the primary somatosensory cortex of primates. Science 204, 521-523.

Kaeser, M., 2010. Transplantation of autologous adult brain progenitor cells in a non-human primate model of motor cortex lesion. Doctoral thesis. University of Fribourg, Imprimerie Saint-Paul.

Kaeser, M., Brunet, J.F., Wyss, A., Belhaj-Saïf, A., Liu, Y., Hamadjida, A., Rouiller, E.M., Bloch, J., 2011. Autologous adult cortical cell transplantation enhances functional recovery following unilateral lesion of motor cortex in primates: a pilot study. Neurosurgery 68, 1405-1416.

Kaeser, M., Chatagny, P., Gindrat, A.D., Savidan, J., Badoud, S., Fregosi, M., Moret, V., Roulin, C., Schmidlin, E., Rouiller, E.M., 2014. Variability of manual dexterity performance in non-human primates (*Macaca fascicularis*). International Journal of Comparative Psychology 27, 295-325.

Kaeser, M., Wannier, T., Brunet, J.F., Wyss, A., Bloch, J., Rouiller, E.M., 2013. Representation of motor habit in a sequence of repetitive reach and grasp movements performed by macaque monkeys: evidence for a contribution of the dorsolateral prefrontal cortex. Cortex 49, 1404-1419.

Kaeser, M., Wyss, A.F., Bashir, S., Hamadjida, A., Liu, Y., Bloch, J., Brunet, J.F., Belhaj-Saïf, A., Rouiller, E.M., 2010. Effects of unilateral motor cortex lesion on ipsilesional hand's reach and grasp performance in monkeys: relationship with recovery in the contralesional hand. J Neurophysiol 103, 1630-1645.

Karl, J.M., Schneider, L.R., Whishaw, I.Q., 2013. Nonvisual learning of intrinsic object properties in a reaching task dissociates grasp from reach. Exp Brain Res 225, 465-477.

Kazennikov, O., Hyland, B., Corboz, M., Babalian, A., Rouiller, E.M., Wiesendanger, M., 1999. Neural activity of supplementary and primary motor areas in monkeys and its relation to bimanual and unimanual movement sequences. Neuroscience 89, 661-674.

Kazennikov, O., Hyland, B., Wicki, U., Perrig, S., Rouiller, E.M., Wiesendanger, M., 1998. Effects of lesions in the mesial frontal cortex on bimanual co-ordination in monkeys. Neuroscience 85, 703-716.

Kazennikov, O., Wicki, U., Corboz, M., Hyland, B., Palmeri, A., Rouiller, E.M., Wiesendanger, M., 1994. Temporal structure of a bimanual goal-directed movement sequence in monkeys. Eur.J Neurosci. 6, 203-210.

Kennett, S., Taylor-Clarke, M., Haggard, P., 2001. Noninformative vision improves the spatial resolution of touch in humans. Current Biology 11, 1188-1191.

Kermadi, I., Liu, Y., Rouiller, E.M., 2000. Do bimanual motor actions involve the dorsal premotor (PMd), cingulate (CMA) and posterior parietal (PPC) cortices? Comparison with primary and supplementary motor cortical areas. Somatosens.Mot.Res. 17, 255-271.

Kermadi, I., Liu, Y., Tempini, A., Calciati, E., Rouiller, E.M., 1998. Neuronal activity in the primate supplementary motor area and the primary motor cortex in relation to spatio-temporal bimanual coordination. Somatosens.Mot.Res. 15, 287-308.

Kermadi, I., Liu, Y., Tempini, A., Rouiller, E.M., 1997. Effects of reversible inactivation of the supplementary motor area (SMA) on unimanual grasp and bimanual pull and grasp performance in monkeys. Somatosens.Mot.Res. 14, 268-280.

Kilintari, M., Raos, V., Savaki, H.E., 2011. Grasping in the Dark Activates Early Visual Cortices. Cerebral Cortex 21, 949-963.

Kleinschmidt, A., Nitschke, M.F., Frahm, J., 1997. Somatotopy in the Human Motor Cortex Hand Area. A High-Resolution Functional MRI Study. European Journal of Neuroscience 9, 2178-2186.

Klüver, H., Bucy, P.C., 1938. An analysis of certain effects of bilateral temporal lobectomy in the rhesus monkey, with special reference to "psychic blindness". The Journal of Psychology: Interdisciplinary and Applied 5, 33-54.

Klüver, H., 1935. An auto-multi-stimulation reaction board for use with sub-human primates. The Journal of Psychology 1, 123-127.

Krubitzer, L., Disbrow, E.A., 2005. The Evolution of Parietal Areas Involved in Hand Use in Primates. In: Kaas, J.H., Gardner, E.P. (Eds.), The senses: a comprehensive reference, Volume 6: Somatosensation. Elsevier, pp. 183-214.

Kruger, L., Porter, P., 1958. A behavioral study of the functions of the rolandic cortex in the monkey. The Journal of Comparative Neurology 109, 439-469.

Kuypers, H.G., 1974. Recovery of Motor Function in Rhesus Monkeys. Neurosci.Res.Program Bull. 12, 240-244.

Lawrence, D.G., Kuypers, H.G., 1968. The functional organization of the motor system in the monkey. I. The effects of bilateral pyramidal lesions. Brain 91, 1-14.

Lehman, R.A.W., 1978. The handedness of rhesus monkeys—I: Distribution. Neuropsychologia 16, 33-42.

Lemon, R.N., 1981. Functional properties of monkey motor cortex neurones receiving afferent input from the hand and fingers. J.Physiol 311, 497-519.

Lemon, R.N., 1993. The G. L. Brown Prize Lecture. Cortical control of the primate hand. Exp.Physiol 78, 263-301.

Lemon, R.N., 1997. Mechanisms of cortical control of hand function. neuroscientist 3, 389-398.

Lemon, R.N., 2012. Nonhuman Primate Models of the Motor System., Nonhuman Primates in Biomedical Research (Second Edition). Academic Press, Boston, pp. 783-794.

Lemon, R.N., Landau, W., Tutssel, D., Lawrence, D.G., 2012. Lawrence and Kuypers (1968a, b) revisited: copies of the original filmed material from their classic papers in Brain. Brain.

Liebscher, T., Schnell, L., Schnell, D., Scholl, J., Schneider, R., Gullo, M., Fouad, K., Mir, A., Rausch, M., Kindler, D., Hamers, F.P., Schwab, M.E., 2005. Nogo-A antibody improves regeneration and locomotion of spinal cord-injured rats. Ann.Neurol. 58, 706-719.

Lindau, N.T., Bänninger, B.J., Gullo, M., Good, N.A., Bachmann, L.C., Starkey, M.L., Schwab, M.E., 2014. Rewiring of the corticospinal tract in the adult rat after unilateral stroke and anti-Nogo-A therapy. Brain 137, 739-756.

Liu, Y., Rouiller, E.M., 1999. Mechanisms of recovery of dexterity following unilateral lesion of the sensorimotor cortex in adult monkeys. Exp.Brain Res. 128, 149-159.

Lövblad, K.O., Baird, A.E., Schlaug, G., Benfield, A., Siewert, B., Voetsch, B., Connor, A., Burzynski, C., Edelman, R.R., Warach, S., 1997. Ischemic lesion volumes in acute stroke by diffusion-weighted magnetic resonance imaging correlate with clinical outcome. Ann.Neurol 42, 164-170.

Ludbrook, J., Dudley, H., 1998. Why Permutation Tests Are Superior to t and F Tests in Biomedical Research. The American Statistician 52, 127-132.

Luke, L.M., Allred, R.P., Jones, T.A., 2004. Unilateral ischemic sensorimotor cortical damage induces contralesional synaptogenesis and enhances skilled reaching with the ipsilateral forelimb in adult male rats. Synapse 54, 187-199.

Lutz, C.K., Novak, M.A., 2005. Environmental enrichment for nonhuman primates: theory and application. ILAR.J 46, 178-191.

Mark, R.F., Sperry, R.W., 1968. Bimanual coordination in monkeys. Experimental Neurology 21, 92-104.

Markus, T.M., Tsai, S.Y., Bollnow, M.R., Farrer, R.G., O'Brien, T.E., Kindler-Baumann, D.R., Rausch, M., Rudin, M., Wiessner, C., Mir, A.K., Schwab, M.E., Kartje, G.L., 2005. Recovery and brain reorganization after stroke in adult and aged rats. Annals of Neurology 58, 950-953.

Martuzzi, R., van der Zwaag, W., Farthouat, J., Gruetter, R., Blanke, O., 2014. Human finger somatotopy in areas 3b, 1, and 2: a 7T fMRI study using a natural stimulus. Hum.Brain Mapp. 35, 213-226.

Mason, C.R., Miller, L.E., Baker, J.F., Houk, J.C., 1998. Organization of Reaching and Grasping Movements in the Primate Cerebellar Nuclei as Revealed by Focal Muscimol Inactivations. Journal of Neurophysiology 79, 537-554.

McKenna, J.E., Whishaw, I.Q., 1999. Complete Compensation in Skilled Reaching Success with Associated Impairments in Limb Synergies, after Dorsal Column Lesion in the Rat. The Journal of Neuroscience 19, 1885-1894.

McNeal, D.W., Darling, W.G., Ge, J., Stilwell-Morecraft, K.S., Solon, K.M., Hynes, S.M., Pizzimenti, M.A., Rotella, D.L., Tyler, V., Morecraft, R.J., 2010. Selective long-term reorganization of the corticospinal projection from the supplementary motor cortex following recovery from lateral motor cortex injury. Journal of Comparative Neurology 518, 586-621.

Merkler, D., Metz, G.A., Raineteau, O., Dietz, V., Schwab, M.E., Fouad, K., 2001. Locomotor recovery in spinal cord-injured rats treated with an antibody neutralizing the myelin-associated neurite growth inhibitor Nogo-A. J Neurosci. 21, 3665-3673.

Moseley, G.L., Wiech, K., 2009. The effect of tactile discrimination training is enhanced when patients watch the reflected image of their unaffected limb during training. Pain 144, 314-319.

Murata, Y., Higo, N., Oishi, T., Yamashita, A., Matsuda, K., Hayashi, M., Yamane, S., 2008. Effects of motor training on the recovery of manual dexterity after primary motor cortex lesion in macaque monkeys. J Neurophysiol 99, 773-786.

Murata, Y., Higo, N., Hayashi, T., Nishimura, Y., Sugiyama, Y., Oishi, T., Tsukada, H., Isa, T., Onoe, H., 2015. Temporal Plasticity Involved in Recovery from Manual Dexterity Deficit after Motor Cortex Lesion in Macaque Monkeys. The Journal of Neuroscience 35, 84-95.

Nakayma, H., Jørgensen, H.S., Raaschou, H.O., Olsen, T.S., 1994. Compensation in recovery of upper extremity function after stroke: The Copenhagen Stroke Study. Archives of Physical Medicine and Rehabilitation 75, 852-857.

Napier, J.R., 1956. The prehensile movements of the human hand. J Bone Joint Surg.Br 38-B, 902-913.

Napier, J., 1962. The evolution of the hand. Scientific American 207, 56-62.

Napier, J., 1993. Hands. Princeton University Press, Princeton, New Jersey.

Nelissen, K., Vanduffel, W., 2011. Grasping-Related Functional Magnetic Resonance Imaging Brain Responses in the Macaque Monkey. The Journal of Neuroscience 31, 8220-8229.

Nelson, R.J., Sur, M., Felleman, D.J., Kaas, J.H., 1980. Representations of the body surface in postcentral parietal cortex of *Macaca fascicularis*. J.Comp Neurol. 192, 611-643.

Nishimura, Y., Isa, T., 2009. Compensatory changes at the cerebral cortical level after spinal cord injury. neuroscientist 15, 436-444.

Nishimura, Y., Morichika, Y., Isa, T., 2009. A subcortical oscillatory network contributes to recovery of hand dexterity after spinal cord injury. Brain 132, 709-721.

Nishimura, Y., Onoe, H., Morichika, Y., Perfiliev, S., Tsukada, H., Isa, T., 2007. Time-Dependent Central Compensatory Mechanisms of Finger Dexterity After Spinal Cord Injury. Science 318, 1150-1155.

Nowak, D.A., 2008. The impact of stroke on the performance of grasping: Usefulness of kinetic and kinematic motion analysis. Neuroscience & Biobehavioral Reviews 32, 1439-1450.

Nudo, R.J., 1999. Recovery after damage to motor cortical areas. Curr.Opin.Neurobiol. 9, 740-747.

Nudo, R.J., 2006a. Mechanisms for recovery of motor function following cortical damage. Curr.Opin.Neurobiol. 16, 638-644.

Nudo, R.J., 2006b. Plasticity. NeuroRx. 3, 420-427.

Nudo, R.J., 2007. Postinfarct cortical plasticity and behavioral recovery. Stroke 38, 840-845.

Nudo, R.J., 2013. Recovery after brain injury: mechanisms and principles. Front Hum.Neurosci. 7, 887.

Nudo, R.J., Friel, K.M., Delia, S.W., 2000. Role of sensory deficits in motor impairments after injury to primary motor cortex. Neuropharmacology 39, 733-742.

Nudo, R.J., Jenkins, W.M., Merzenich, M.M., Prejean, T., Grenda, R., 1992. Neurophysiological correlates of hand preference in primary motor cortex of adult squirrel monkeys. The Journal of Neuroscience 12, 2918-2947.

Nudo, R.J., Milliken, G.W., 1996. Reorganization of movement representations in primary motor cortex following focal ischemic infarcts in adult squirrel monkeys. J Neurophysiol 75, 2144-2149.

Nudo, R.J., Milliken, G.W., Jenkins, W.M., Merzenich, M.M., 1996. Use-dependent alterations of movement representations in primary motor cortex of adult squirrel monkeys. J Neurosci 16, 785-807.

Nudo, R.J., Plautz, E.J., Milliken, G.W., 1997. Adaptive Plasticity in Primate Motor Cortex as a Consequence of Behavioral Experience and Neuronal Injury. Seminars in Neuroscience 9, 13-23.

Nudo, R.J., 2006c. Mechanisms for recovery of motor function following cortical damage. Current Opinion in Neurobiology 16, 638-644.

Olsen, T.S., 1989. Improvement of Function and Motor Impairment After Stroke. Neurorehabilitation and Neural Repair 3, 187-192.

Overduin, S.A., Servos, P., 2004. Distributed digit somatotopy in primary somatosensory cortex. Neuroimage. 23, 462-472.

Overduin, S.A., d'Avella, A., Roh, J., Bizzi, E., 2008. Modulation of Muscle Synergy Recruitment in Primate Grasping. The Journal of Neuroscience 28, 880-892.

Pandian, S., Arya, K.N., 2013. Motor impairment of the ipsilesional body side in poststroke subjects. Journal of Bodywork and Movement Therapies 17, 495-503.

Papadopoulos, C.M., Tsai, S.Y., Alsbiei, T., O'Brien, T.E., Schwab, M.E., Kartje, G.L., 2002. Functional recovery and neuroanatomical plasticity following middle cerebral artery occlusion and IN–1 antibody treatment in the adult rat. Annals of Neurology 51, 433-441.

Passingham, R.E., Perry, V.H., Wilkinson, F., 1983. The long-term effects of removal of sensorimotor cortex in infant and adult rhesus monkeys. Brain 106, 675-705.

Pavlides, C., Miyashita, E., Asanuma, H., 1993. Projection from the sensory to the motor cortex is important in learning motor skills in the monkey. J Neurophysiol. 70, 733-741.

Penfield, W., Rasmussen, T., 1950. The cerebral cortex of man; a clinical study of localization of function.

Pineiro, R., Pendlebury, S.T., Smith, S., Flitney, D., Blamire, A.M., Styles, P., Matthews, P.M., 2000. Relating MRI Changes to Motor Deficit After Ischemic Stroke by Segmentation of Functional Motor Pathways. Stroke 31, 672-679.

Pizzimenti, M.A., Darling, W.G., Rotella, D.L., McNeal, D.W., Herrick, J.L., Ge, J., Stilwell-Morecraft, K.S., Morecraft, R.J., 2007. Measurement of reaching kinematics and prehensile dexterity in nonhuman primates. J Neurophysiol. 98, 1015-1029.

Plautz, E.J., Barbay, S., Frost, S.B., Friel, K.M., Dancause, N., Zoubina, E.V., Stowe, A.M., Quaney, B.M., Nudo, R.J., 2003. Post-infarct cortical plasticity and behavioral recovery using concurrent cortical stimulation and rehabilitative training: a feasibility study in primates. Neurol.Res. 25, 801-810.

Plautz, E.J., Milliken, G.W., Nudo, R.J., 2000. Effects of repetitive motor training on movement representations in adult squirrel monkeys: role of use versus learning. Neurobiol.Learn.Mem. 74, 27-55.

Pohl, P.S., Winstein, C.J., 1999. Practice effects on the less-affected upper extremity after stroke. Archives of Physical Medicine and Rehabilitation 80, 668-675.

Postle, B.R., Berger, J.S., Taich, A.M., D'Esposito, M., 2000. Activity in human frontal cortex associated with spatial working memory and saccadic behavior. J Cogn Neurosci 12 Suppl 2, 2-14.

Proteau, L., 1992. On the specificity of learning and the role of visual information for movement control. Advances in psychology 85, 67-103.

Proteau, L., Marteniuk, R.G., Girouard, Y., Dugas, C., 1987. On the type of information used to control and learn an aiming movement after moderate and extensive training. Human Movement Science 6, 181-199.

Qi, X., Katsuki, F., Meyer, T., Rawley, J.B., Zhou, X., Douglas, K.L., Constantinidis, C., 2010. Comparison of neural activity related to working memory in primate dorsolateral prefrontal and posterior parietal cortex. Frontiers in Systems Neuroscience 4.

Raineteau, O., Fouad, K., Bareyre, F.M., Schwab, M.E., 2002. Reorganization of descending motor tracts in the rat spinal cord. Eur.J Neurosci. 16, 1761-1771.

Raineteau, O., Z'Graggen, W.J., Thallmair, M., Schwab, M.E., 1999. Sprouting and regeneration after pyramidotomy and blockade of the myelin-associated neurite growth inhibitors NI 35/250 in adult rats. Eur.J Neurosci. 11, 1486-1490.

Rizzolatti, G., Camarda, R., Fogassi, L., Gentilucci, M., Luppino, G., Matelli, M., 1988. Functional organization of inferior area 6 in the macaque monkey. II. Area F5 and the control of distal movements. Exp Brain Res 71, 491-507.

Rogers, D.C., Campbell, C.A., Stretton, J.L., Mackay, K.B., 1997. Correlation Between Motor Impairment and Infarct Volume After Permanent and Transient Middle Cerebral Artery Occlusion in the Rat. Stroke 28, 2060-2066.

Rothwell, J.C., Traub, M.M., Day, B.L., Obeso, J.A., Thomas, P.K., Marsden, C.D., 1982. Manual motor performance in a deafferented man. Brain 105 (Pt 3), 515-542.

Rouiller, E.M., Moret, V., Liang, F., 1993. Comparison of the connectional properties of the two forelimb areas of the rat sensorimotor cortex: support for the presence of a premotor or supplementary motor cortical area. Somatosens.Mot.Res. 10, 269-289.

Rouiller, E.M., Olivier, E., 2004. Functional recovery after lesions of the primary motor cortex. Prog.Brain Res. 143, 467-475.

Rouiller, E.M., Yu, X.H., Moret, V., Tempini, A., Wiesendanger, M., Liang, F., 1998. Dexterity in adult monkeys following early lesion of the motor cortical hand area: the role of cortex adjacent to the lesion. Eur.J.Neurosci. 10, 729-740.

Sasaki, K., Gemba, H., 1984. Compensatory motor function of the somatosensory cortex for the motor cortex temporarily impaired by cooling in the monkey. Exp.Brain Res 55, 60-68.

Sasaki, S., Isa, T., Pettersson, L.G., Alstermark, B., Naito, K., Yoshimura, K., Seki, K., Ohki, Y., 2004. Dexterous finger movements in primate without monosynaptic corticomotoneuronal excitation. J Neurophysiol 92, 3142-3147.

Schaefer, M., Flor, H., Heinze, H.J., Rotte, M., 2006. Dynamic modulation of the primary somatosensory cortex during seeing and feeling a touched hand. Neuroimage 29, 587-592.

Schaffelhofer, S., Sartori, M., Scherberger, H., Farina, D., 2015a. Musculoskeletal Representation of a Large Repertoire of Hand Grasping Actions in Primates. Neural Systems and Rehabilitation Engineering, IEEE Transactions on 23, 210-220.

Schaffelhofer, S., Agudelo-Toro, A., Scherberger, H., 2015b. Decoding a Wide Range of Hand Configurations from Macaque Motor, Premotor, and Parietal Cortices. The Journal of Neuroscience 35, 1068-1081.

Schieber, M.H., Hibbard, L.S., 1993. How somatotopic is the motor cortex hand area? Science 261, 489-492.

Schieber, M.H., Santello, M., 2004. Hand function: peripheral and central constraints on performance. J Appl.Physiol 96, 2293-2300.

Schmidlin, E., Kaeser, M., Gindrat, A.D., Savidan, J., Chatagny, P., Badoud, S., Hamadjida, A., Beaud, M.L., Wannier, T., Belhaj-Saïf, A., Rouiller, E.M., 2011. Behavioral assessment of manual dexterity in non-human primates. J.Vis.Exp., e3258.

Schmidlin, E., Wannier, T., Bloch, J., Belhaj-Saïf, A., Wyss, A.F., Rouiller, E.M., 2005. Reduction of the hand representation in the ipsilateral primary motor cortex following unilateral section of the corticospinal tract at cervical level in monkeys. BMC.Neurosci. 6, 56.

Schmidlin, E., Wannier, T., Bloch, J., Rouiller, E.M., 2004. Progressive plastic changes in the hand representation of the primary motor cortex parallel incomplete recovery from a unilateral section of the corticospinal tract at cervical level in monkeys. Brain Res. 1017, 172-183.

Schnell, L., Schwab, M.E., 1990. Axonal regeneration in the rat spinal cord produced by an antibody against myelin-associated neurite growth inhibitors. Nature 343, 269-272.

Schultz, A.H., 1969. The life of primates. Universe Books.

Schwab, M.E., 1996. Structural plasticity of the adult CNS. Negative control by neurite growth inhibitory signals. Int.J Dev.Neurosci. 14, 379-385.

Schwab, M.E., 1998. Regenerative Nerve Fiber Growth in the Adult Central Nervous System. News Physiol Sci. 13, 294-298.

Schwab, M.E., 2002. Repairing the injured spinal cord. Science 295, 1029-1031.

Schwab, M.E., 2004. Nogo and axon regeneration. Curr.Opin.Neurobiol. 14, 118-124.

Schwab, M.E., Bartholdi, D., 1996. Degeneration and regeneration of axons in the lesioned spinal cord. Physiol Rev. 76, 319-370.

Schwab, M.E., 2010. Functions of Nogo proteins and their receptors in the nervous system. Nat Rev Neurosci 11, 799-811.

Semmes, J., Porter, L., 1972. A Comparison of Precentral and Postcentral Cortical Lesions on Somatosensory Discrimination in the Monkey. Cortex 8, 249-264.

Serino, A., Farnè, A., Rinaldesi, M.L., Haggard, P., Làdavas, E., 2007. Can vision of the body ameliorate impaired somatosensory function? Neuropsychologia 45, 1101-1107.

Serino, A., Padiglioni, S., Haggard, P., Làdavas, E., 2009. Seeing the hand boosts feeling on the cheek. Cortex 45, 602-609.

Sessle, B.J., Wiesendanger, M., 1982. Structural and functional definition of the motor cortex in the monkey (*Macaca fascicularis*). J Physiol 323, 245-265.

Seymour, A.B., Andrews, E.M., Tsai, S.Y., Markus, T.M., Bollnow, M.R., Brenneman, M.M., O'Brien, T.E., Castro, A.J., Schwab, M.E., Kartje, G.L., 2005. Delayed treatment with monoclonal antibody IN-1 1 week after stroke results in recovery of function and corticorubral plasticity in adult rats. J Cereb.Blood Flow Metab 25, 1366-1375.

Spinozzi, G., Truppa, V., Lagana, T., 2004. Grasping behavior in tufted capuchin monkeys (*Cebus apella*): grip types and manual laterality for picking up a small food item. Am.J Phys.Anthropol. 125, 30-41.

Sugiyama, Y., Higo, N., Yoshino-Saito, K., Murata, Y., Nishimura, Y., Oishi, T., Isa, T., 2013. Effects of early versus late rehabilitative training on manual dexterity after corticospinal tract lesion in macaque monkeys. Journal of Neurophysiology 109, 2853-2865.

Tanji, J., Wise, S.P., 1981. Submodality distribution in sensorimotor cortex of the unanesthetized monkey. J.Neurophysiol. 45, 467-481.

Tanji, J., Hoshi, E., 2008. Role of the Lateral Prefrontal Cortex in Executive Behavioral Control. Physiological Reviews 88, 37-57.

Taylor, C.L., Schwarz, R.J., 1955. The anatomy and mechanics of the human hand. Artif.Limbs. 2, 22-35.

Taylor-Clarke, M., Kennett, S., Haggard, P., 2004. Persistence of visual–tactile enhancement in humans. Neuroscience Letters 354, 22-25.

Thallmair, M., Metz, G.A.S., Z'Graggen, W.J., Raineteau, O., Kartje, G.L., Schwab, M.E., 1998. Neurite growth inhibitors restrict plasticity and functional recovery following corticospinal tract lesions. Nature neuroscience 1, 124-131.

Troise, D., Yoneyama, S., Resende, M.B., Reed, U., Xavier, G.F., Hasue, R., 2014. The influence of visual and tactile perception on hand control in children with Duchenne muscular dystrophy. Developmental Medicine & Child Neurology 56, 882-887.

Tsai, S.Y., Papadopoulos, C.M., Schwab, M.E., Kartje, G.L., 2011. Delayed anti-nogo-a therapy improves function after chronic stroke in adult rats. Stroke 42, 186-190.

Tsai, S.Y., Markus, T.M., Andrews, E.M., Cheatwood, J.L., Emerick, A.J., Mir, A., Schwab, M.E., Kartje, G.L., 2007. Intrathecal treatment with anti-Nogo-A antibody improves functional recovery in adult rats after stroke. Exp Brain Res 182, 261-266.

Uematsu, S., Lesser, R.P., Gordon, B., 1992. Localization of sensorimotor cortex: the influence of Sherrington and Cushing on the modern concept. Neurosurgery 30, 904-912.

Vargas-Irwin, C.E., Shakhnarovich, G., Yadollahpour, P., Mislow, J.M.K., Black, M.J., Donoghue, J.P., 2010. Decoding Complete Reach and Grasp Actions from Local Primary Motor Cortex Populations. The Journal of Neuroscience 30, 9659-9669.

Vaughan, H.G.Jr., Costa, L.D., 1962. Performance of patients with lateralized cerebral lesions. II. Sensory and motor tests. The Journal of Nervous and Mental Disease 134.

von Meyenburg, J., Brösamle, C., Metz, G.A., Schwab, M.E., 1998. Regeneration and sprouting of chronically injured corticospinal tract fibers in adult rats promoted by NT-3 and the mAb IN-1, which neutralizes myelin-associated neurite growth inhibitors. Exp.Neurol. 154, 583-594.

Wahl, A.S., Omlor, W., Rubio, J.C., Chen, J.L., Zheng, H., Schröter, A., Gullo, M., Weinmann, O., Kobayashi, K., Helmchen, F., Ommer, B., Schwab, M.E., 2014. Asynchronous therapy restores motor control by rewiring of the rat corticospinal tract after stroke. Science 344, 1250-1255.

Wannier, T., Liu, J., Morel, A., Jouffrais, C., Rouiller, E.M., 2002. Neuronal activity in primate striatum and pallidum related to bimanual motor actions. Neuroreport 13, 143-147.

Wannier, T.M., Maier, M.A., Hepp-Reymond, M.C., 1991. Contrasting properties of monkey somatosensory and motor cortex neurons activated during the control of force in precision grip. J Neurophysiol. 65, 572-589.

Whishaw, I.Q., Gorny, B., Sarna, J., 1998. Paw and limb use in skilled and spontaneous reaching after pyramidal tract, red nucleus and combined lesions in the rat: behavioral and anatomical dissociations. Behavioural Brain Research 93, 167-183.

Whishaw, I.Q., Pellis, S.M., Gorny, B.P., Pellis, V.C., 1991. The impairments in reaching and the movements of compensation in rats with motor cortex lesions: an endpoint, videorecording, and movement notation analysis. Behavioural Brain Research 42, 77-91.

Wise, S.P., Tanji, J., 1981. Neuronal responses in sensorimotor cortex to ramp displacements and maintained positions imposed on hindlimb of the unanesthetized monkey. Journal of Neurophysiology 45, 482-500.

Woolsey, C.N., 1964. Cortical localization as defined by evoked potential and electrical stimulation studies. Cerebral localization and organization, 17-26.

Woolsey, C.N., Settlage, P.H., Meyer, D.R., Sencer, W., Pinto Hamuy, T., Travis, A.M., 1952. Patterns of localization in precentral and "supplementary" motor areas and their relation to the concept of a premotor area. Res.Publ.Assoc.Res.Nerv.Ment.Dis. 30, 238-264.

Wyss, A.F., Hamadjida, A., Savidan, J., Liu, Y., Bashir, S., Mir, A., Schwab, M.E., Rouiller, E.M., Belhaj-Saïf, A., 2013. Long-term motor cortical map changes following unilateral lesion of the hand representation in the motor cortex in macaque monkeys showing functional recovery of hand functions. Restor.Neurol Neurosci. 31, 733-760.

Xerri, C., Merzenich, M.M., Peterson, B.E., Jenkins, W., 1998. Plasticity of primary somatosensory cortex paralleling sensorimotor skill recovery from stroke in adult monkeys. J Neurophysiol. 79, 2119-2148.

Yatani, K., Gergle, D., Truong, K., 2012. Investigating effects of visual and tactile feedback on spatial coordination in collaborative handheld systems. ACM, pp. 661-670.

Young, R.W., 2003. Evolution of the human hand: the role of throwing and clubbing. J Anat. 202, 165-174.

Zaaimi, B., Edgley, S.A., Soteropoulos, D.S., Baker, S.N., 2012. Changes in descending motor pathway connectivity after corticospinal tract lesion in macaque monkey. Brain 135, 2277-2289.

Supplementary Data

Supplementary Figure 1 (next 35 pages): Collections of graphs illustrating the time course of all the parameters considered in the present analysis (see Figure 5) for each monkey (A to G), each hand, in the task without vision and in the task with vision. Graphs are arranged in such a way that one line represents the same parameter in the four conditions for a given animal. The x-axis represents the time in days from the lesion: each point or series of vertically aligned points corresponds to one behavioural session. Thick vertical black line: day at lesion; dashed vertical red line: time at dlPFC biopsy (Mk-AV, Mk-JO); dashed vertical black line: time at cell/sham reimplantation (Mk-AV, Mk-JA, Mk-JO); dotted vertical blue line: previous lesions (Mk-RO). The key regarding each graph is shown on the right. For parameters expressed in s, the scale has been voluntarily fixed to be the same in the four conditions in a given monkey. Pre- and post-lesion (and post-biopsy, when applicable) plateaux were computed and are indicated in the same colour as the corresponding data (see the section *Data analysis* for further detail). When data were partly or completely missing, primarily after the lesion, a red star was indicated at the highest value for the corresponding date. Note that the drop in performance observed in Mk-GE from day -134 with the ipsilesional left hand is due to an accidental finger amputation, resulting in a transient alteration of manual dexterity.

(A) Mk-AV (p. 504 to 508): sham cell therapy

(B) Mk-DI (p. 509 to 513): no treatment

(C) Mk-GE (p. 514 to 518): no treatment

(D) Mk-JA (p. 519 to 523): cell therapy

(E) Mk-JO (p. 524 to 528): cell therapy

(F) Mk-RO (p. 529 to 533): no treatment

(G) Mk-VA (p. 534 to 538): anti-Nogo-A antibody

A

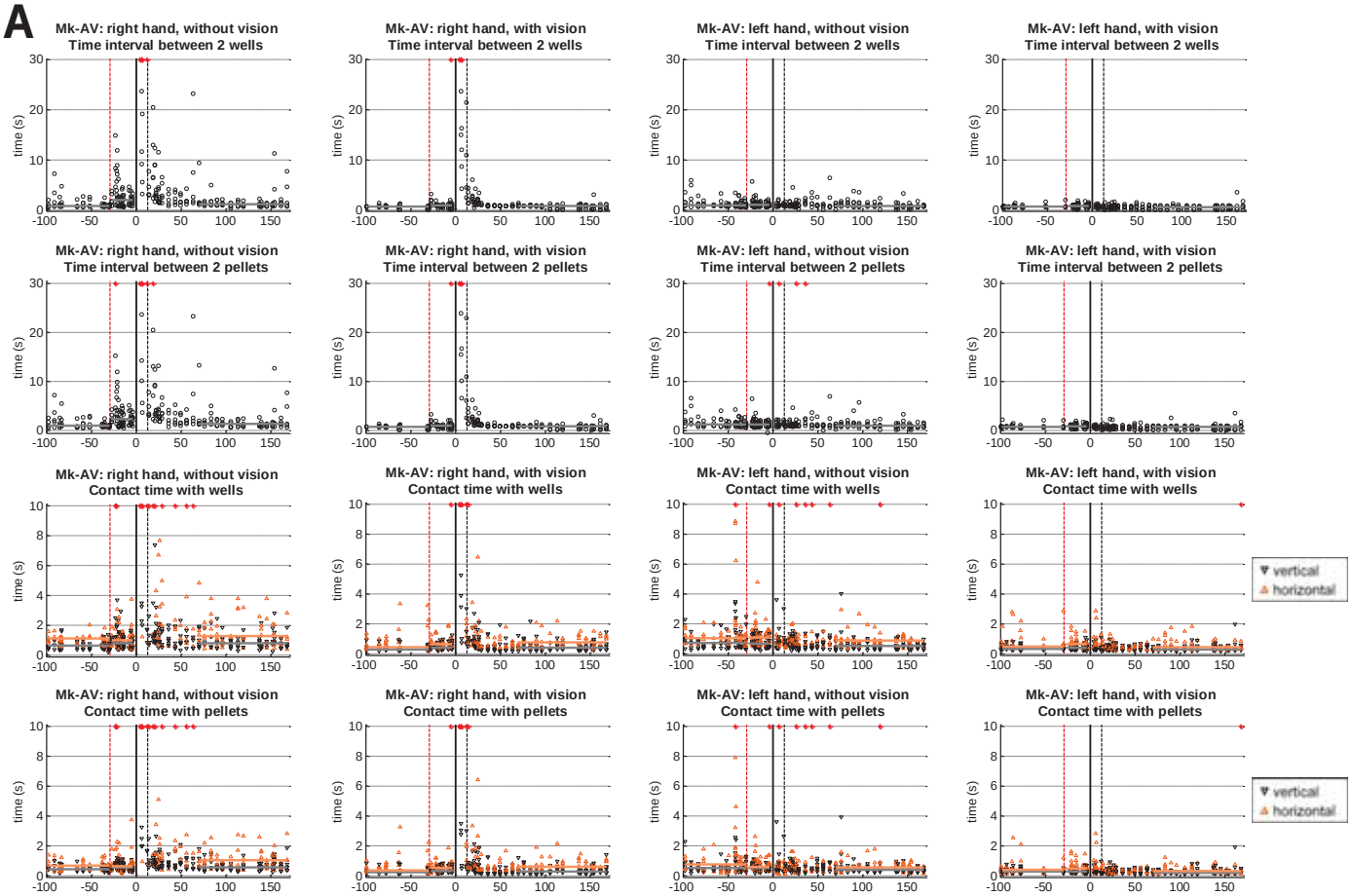
Mk-AV: right hand, without vision
Time interval between 2 wells
Mk-AV: right hand, with vision
Time interval between 2 wells
Mk-AV: left hand, without vision
Time interval between 2 wells
Mk-AV: left hand, with vision
Time interval between 2 wells
Mk-AV: right hand, without vision
Time interval between 2 pellets
Mk-AV: right hand, with vision
Time interval between 2 pellets
Mk-AV: left hand, without vision
Time interval between 2 pellets
Mk-AV: left hand, with vision
Time interval between 2 pellets
Mk-AV: right hand, without vision
Contact time with wells
Mk-AV: right hand, with vision
Contact time with wells
Mk-AV: left hand, without vision
Contact time with wells
Mk-AV: left hand, with vision
Contact time with wells
Mk-AV: right hand, without vision
Contact time with pellets
Mk-AV: right hand, with vision
Contact time with pellets
Mk-AV: left hand, without vision
Contact time with pellets
Mk-AV: left hand, with vision
Contact time with pellets
time (s)
vertical
horizontal

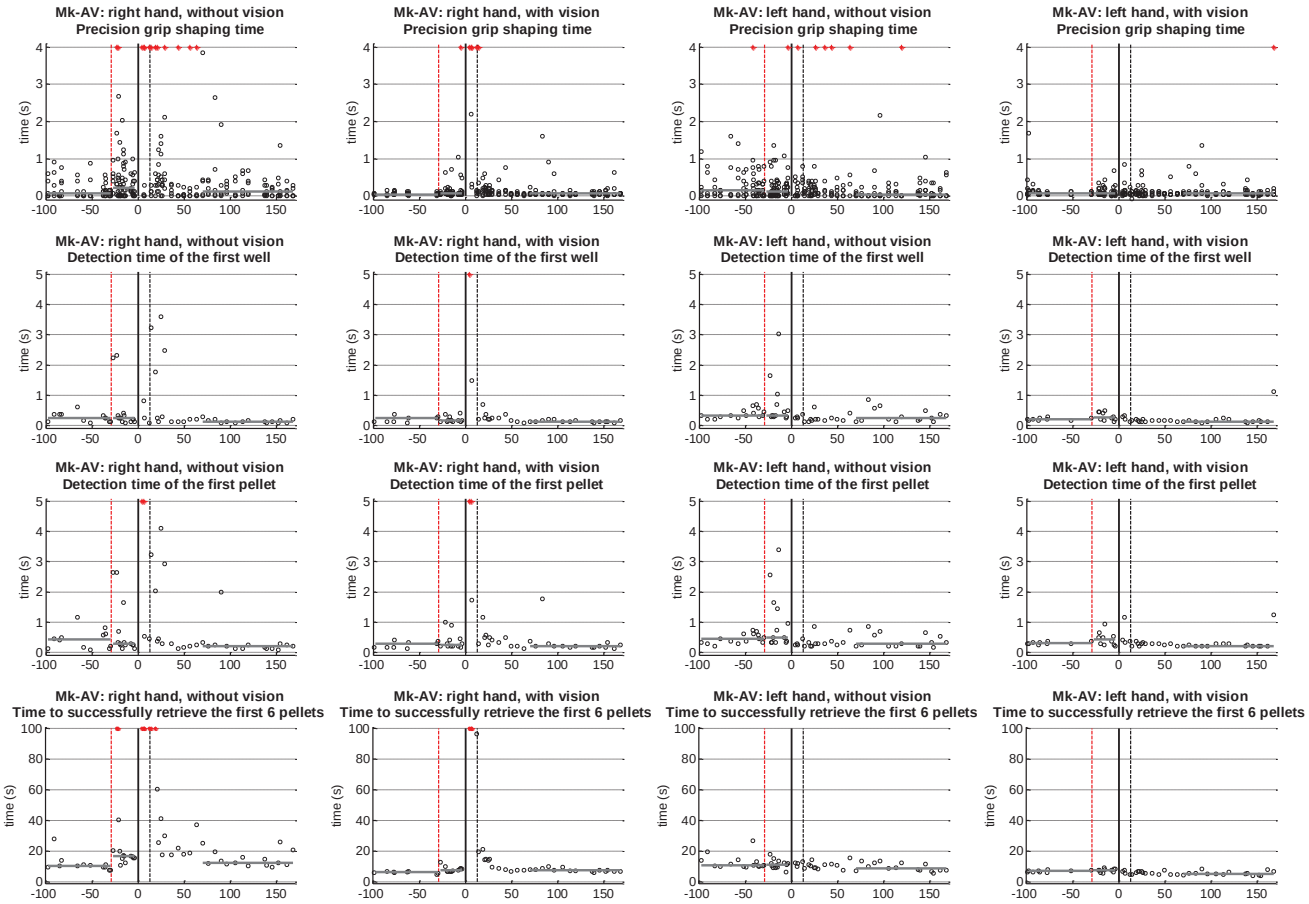
Mk-AV: right hand, without vision
Precision grip shaping time
Mk-AV: right hand, with vision
Precision grip shaping time
Mk-AV: left hand, without vision
Precision grip shaping time
Mk-AV: left hand, with vision
Precision grip shaping time
Mk-AV: right hand, without vision
Detection time of the first well
Mk-AV: right hand, with vision
Detection time of the first well
Mk-AV: left hand, without vision
Detection time of the first well
Mk-AV: left hand, with vision
Detection time of the first well
Mk-AV: right hand, without vision
Detection time of the first pellet
Mk-AV: right hand, with vision
Detection time of the first pellet
Mk-AV: left hand, without vision
Detection time of the first pellet
Mk-AV: left hand, with vision
Detection time of the first pellet
Mk-AV: right hand, without vision
Time to successfully retrieve the first 6 pellets
Mk-AV: right hand, with vision
Time to successfully retrieve the first 6 pellets
Mk-AV: left hand, without vision
Time to successfully retrieve the first 6 pellets
Mk-AV: left hand, with vision
Time to successfully retrieve the first 6 pellets
time (s)

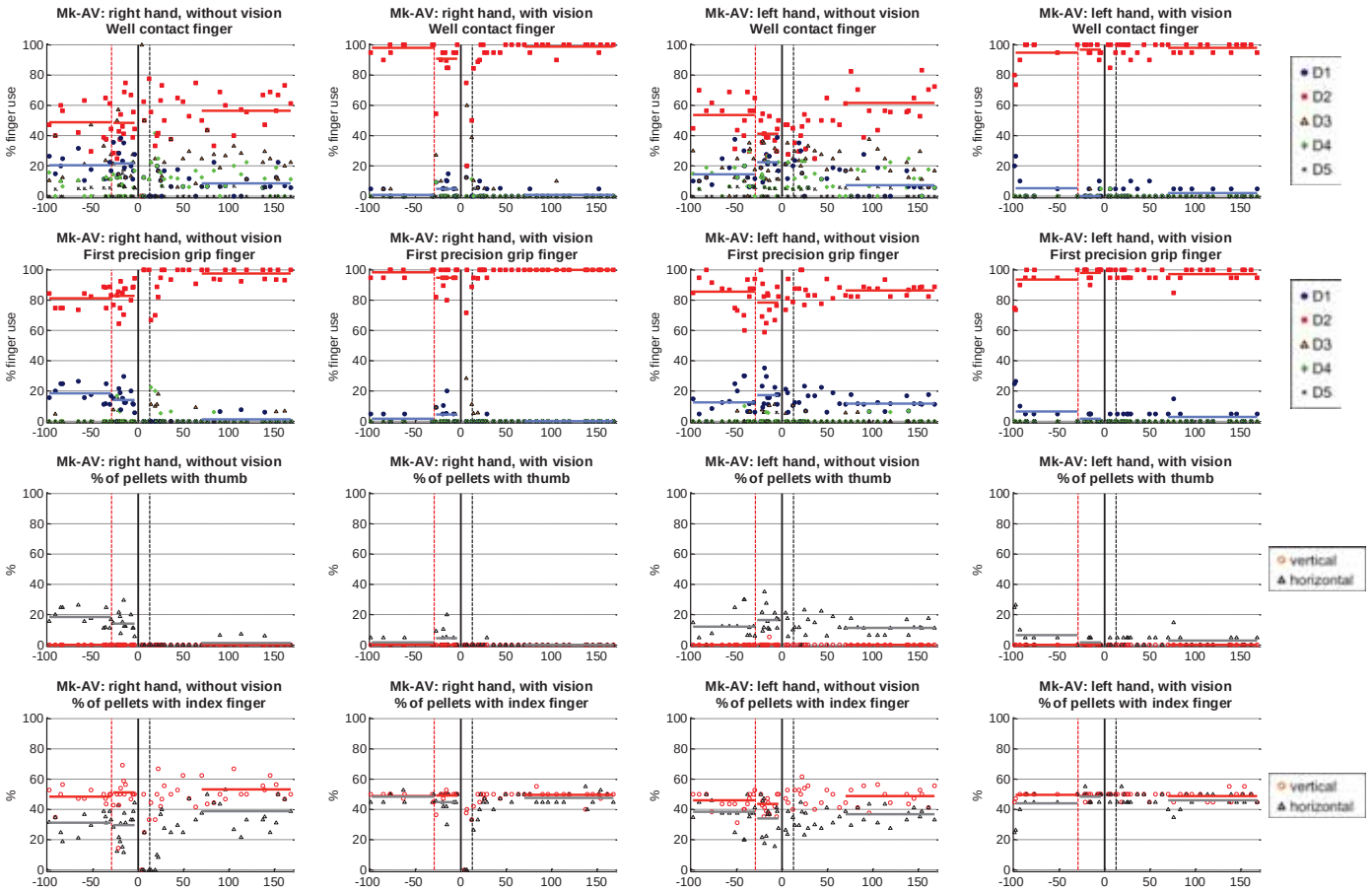
Mk-AV: right hand, without vision
Well contact finger
Mk-AV: right hand, with vision
Well contact finger
Mk-AV: left hand, without vision
Well contact finger
Mk-AV: left hand, with vision
Well contact finger
Mk-AV: right hand, without vision
First precision grip finger
Mk-AV: right hand, with vision
First precision grip finger
Mk-AV: left hand, without vision
First precision grip finger
Mk-AV: left hand, with vision
First precision grip finger
Mk-AV: right hand, without vision
% of pellets with thumb
Mk-AV: right hand, with vision
% of pellets with thumb
Mk-AV: left hand, without vision
% of pellets with thumb
Mk-AV: left hand, with vision
% of pellets with thumb
Mk-AV: right hand, without vision
% of pellets with index finger
Mk-AV: right hand, with vision
% of pellets with index finger
Mk-AV: left hand, without vision
% of pellets with index finger
Mk-AV: left hand, with vision
% of pellets with index finger
% finger use
%
D1
D2
D3
D4
D5
vertical
horizontal

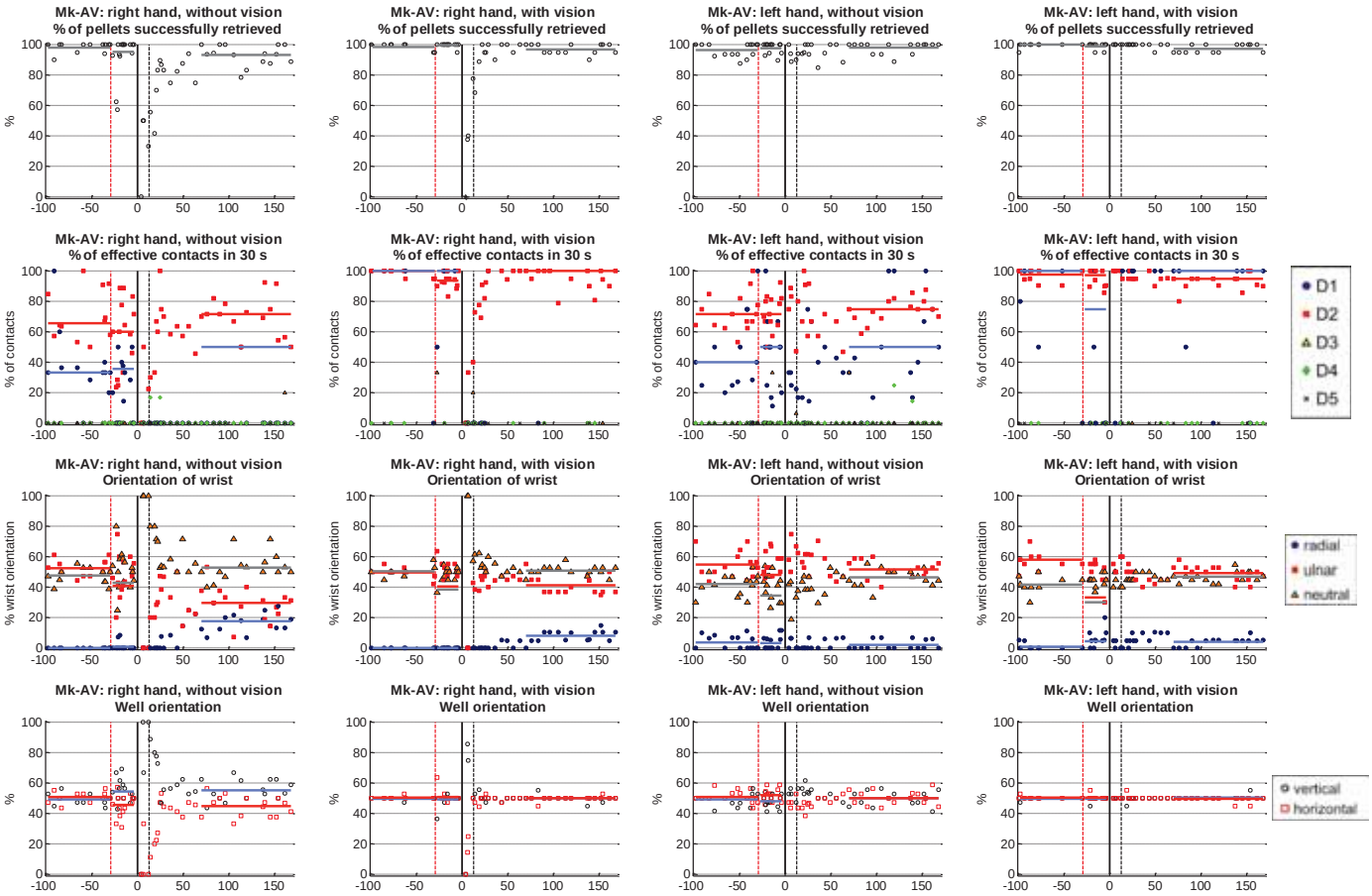
Mk-AV: right hand, without vision
% of pellets successfully retrieved
Mk-AV: right hand, with vision
% of pellets successfully retrieved
Mk-AV: left hand, without vision
% of pellets successfully retrieved
Mk-AV: left hand, with vision
% of pellets successfully retrieved
Mk-AV: right hand, without vision
% of effective contacts in 30 s
Mk-AV: right hand, with vision
% of effective contacts in 30 s
Mk-AV: left hand, without vision
% of effective contacts in 30 s
Mk-AV: left hand, with vision
% of effective contacts in 30 s
Mk-AV: right hand, without vision
Orientation of wrist
Mk-AV: right hand, with vision
Orientation of wrist
Mk-AV: left hand, without vision
Orientation of wrist
Mk-AV: left hand, with vision
Orientation of wrist
Mk-AV: right hand, without vision
Well orientation
Mk-AV: right hand, with vision
Well orientation
Mk-AV: left hand, without vision
Well orientation
Mk-AV: left hand, with vision
Well orientation
%
% of contacts
% wrist orientation
D1
D2
D3
D4
D5
radial
ulnar
neutral
vertical
horizontal

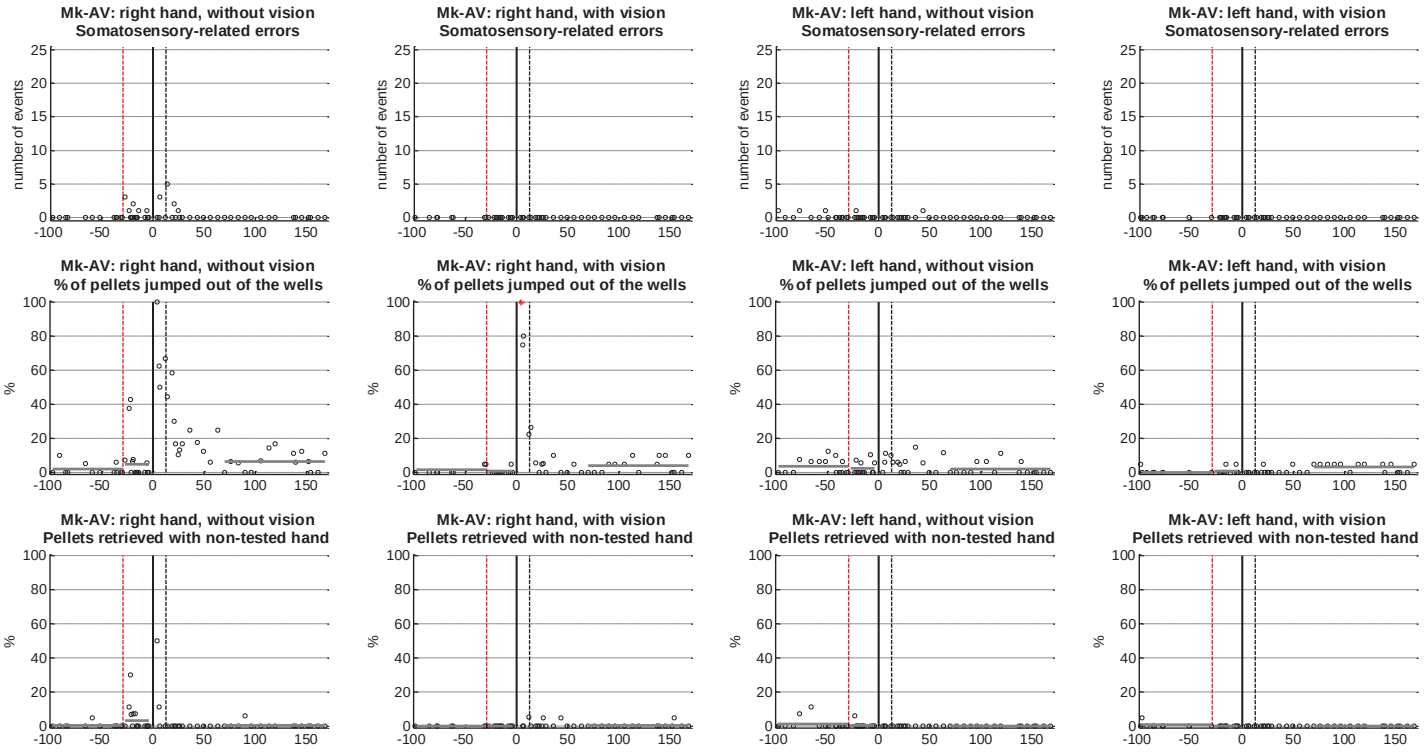
Mk-AV: right hand, without vision
Somatosensory-related errors
Mk-AV: right hand, with vision
Somatosensory-related errors
Mk-AV: left hand, without vision
Somatosensory-related errors
Mk-AV: left hand, with vision
Somatosensory-related errors
number of events
Mk-AV: right hand, without vision
% of pellets jumped out of the wells
Mk-AV: right hand, with vision
% of pellets jumped out of the wells
Mk-AV: left hand, without vision
% of pellets jumped out of the wells
Mk-AV: left hand, with vision
% of pellets jumped out of the wells
%
Mk-AV: right hand, without vision
Pellets retrieved with non-tested hand
Mk-AV: right hand, with vision
Pellets retrieved with non-tested hand
Mk-AV: left hand, without vision
Pellets retrieved with non-tested hand
Mk-AV: left hand, with vision
Pellets retrieved with non-tested hand

B

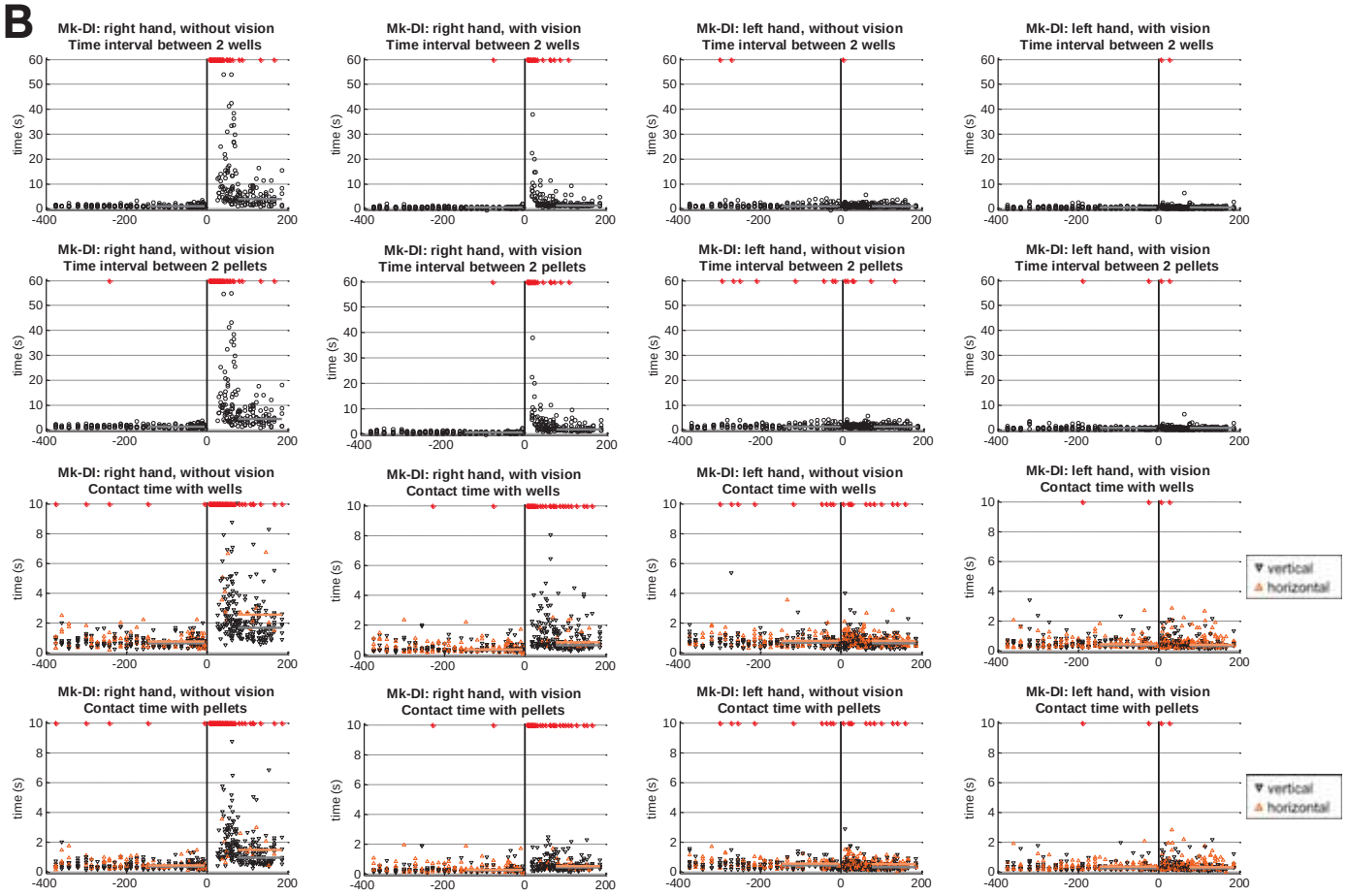
Mk-DI: right hand, without vision
Time interval between 2 wells
Mk-DI: right hand, with vision
Time interval between 2 wells
Mk-DI: left hand, without vision
Time interval between 2 wells
Mk-DI: left hand, with vision
Time interval between 2 wells
Mk-DI: right hand, without vision
Time interval between 2 pellets
Mk-DI: right hand, with vision
Time interval between 2 pellets
Mk-DI: left hand, without vision
Time interval between 2 pellets
Mk-DI: left hand, with vision
Time interval between 2 pellets
Mk-DI: right hand, without vision
Contact time with wells
Mk-DI: right hand, with vision
Contact time with wells
Mk-DI: left hand, without vision
Contact time with wells
Mk-DI: left hand, with vision
Contact time with wells
Mk-DI: right hand, without vision
Contact time with pellets
Mk-DI: right hand, with vision
Contact time with pellets
Mk-DI: left hand, without vision
Contact time with pellets
Mk-DI: left hand, with vision
Contact time with pellets
time (s)
vertical
horizontal

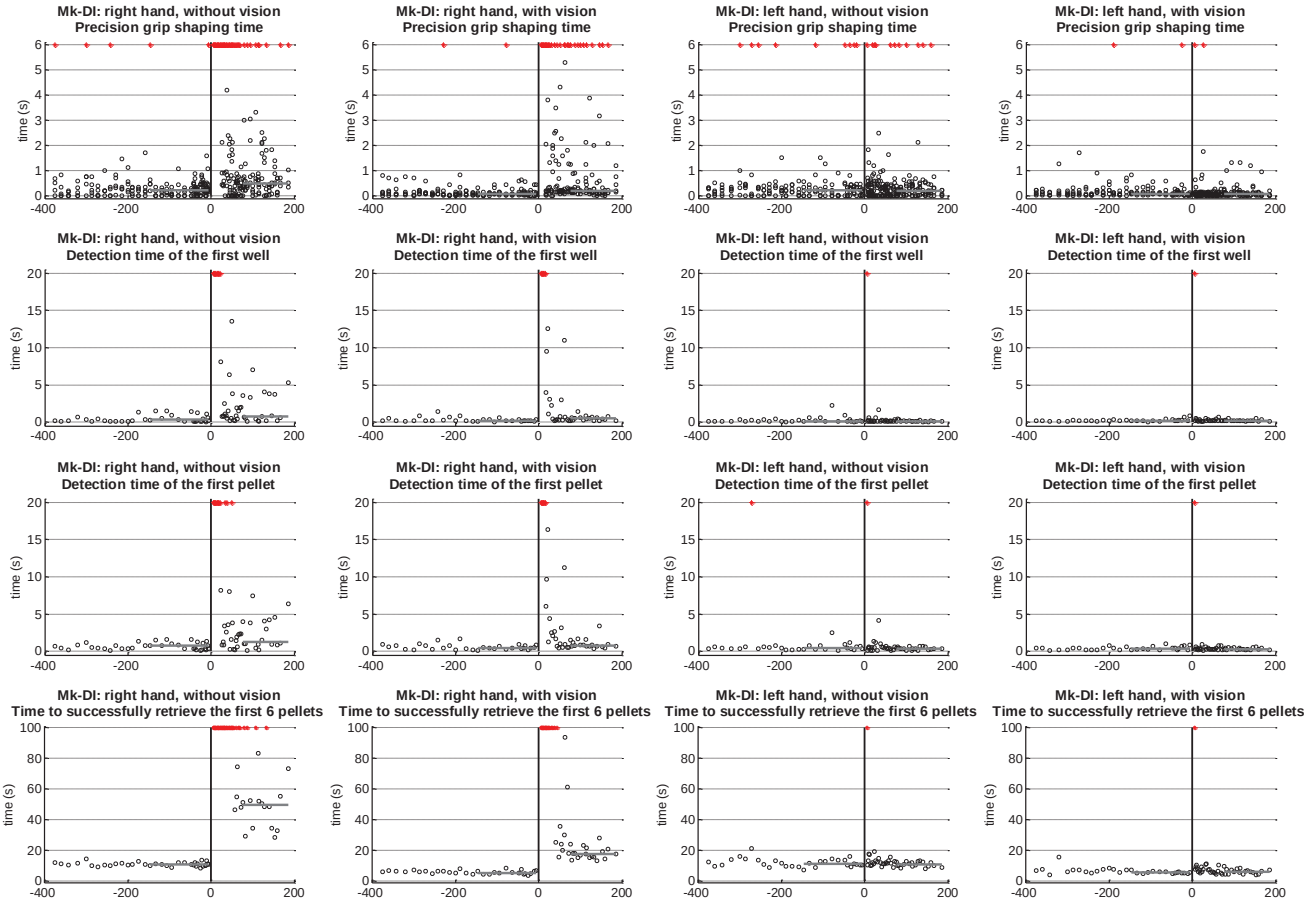
Mk-DI: right hand, without vision
Precision grip shaping time
Mk-DI: right hand, with vision
Precision grip shaping time
Mk-DI: left hand, without vision
Precision grip shaping time
Mk-DI: left hand, with vision
Precision grip shaping time
Mk-DI: right hand, without vision
Detection time of the first well
Mk-DI: right hand, with vision
Detection time of the first well
Mk-DI: left hand, without vision
Detection time of the first well
Mk-DI: left hand, with vision
Detection time of the first well
Mk-DI: right hand, without vision
Detection time of the first pellet
Mk-DI: right hand, with vision
Detection time of the first pellet
Mk-DI: left hand, without vision
Detection time of the first pellet
Mk-DI: left hand, with vision
Detection time of the first pellet
Mk-DI: right hand, without vision
Time to successfully retrieve the first 6 pellets
Mk-DI: right hand, with vision
Time to successfully retrieve the first 6 pellets
Mk-DI: left hand, without vision
Time to successfully retrieve the first 6 pellets
Mk-DI: left hand, with vision
Time to successfully retrieve the first 6 pellets
time (s)

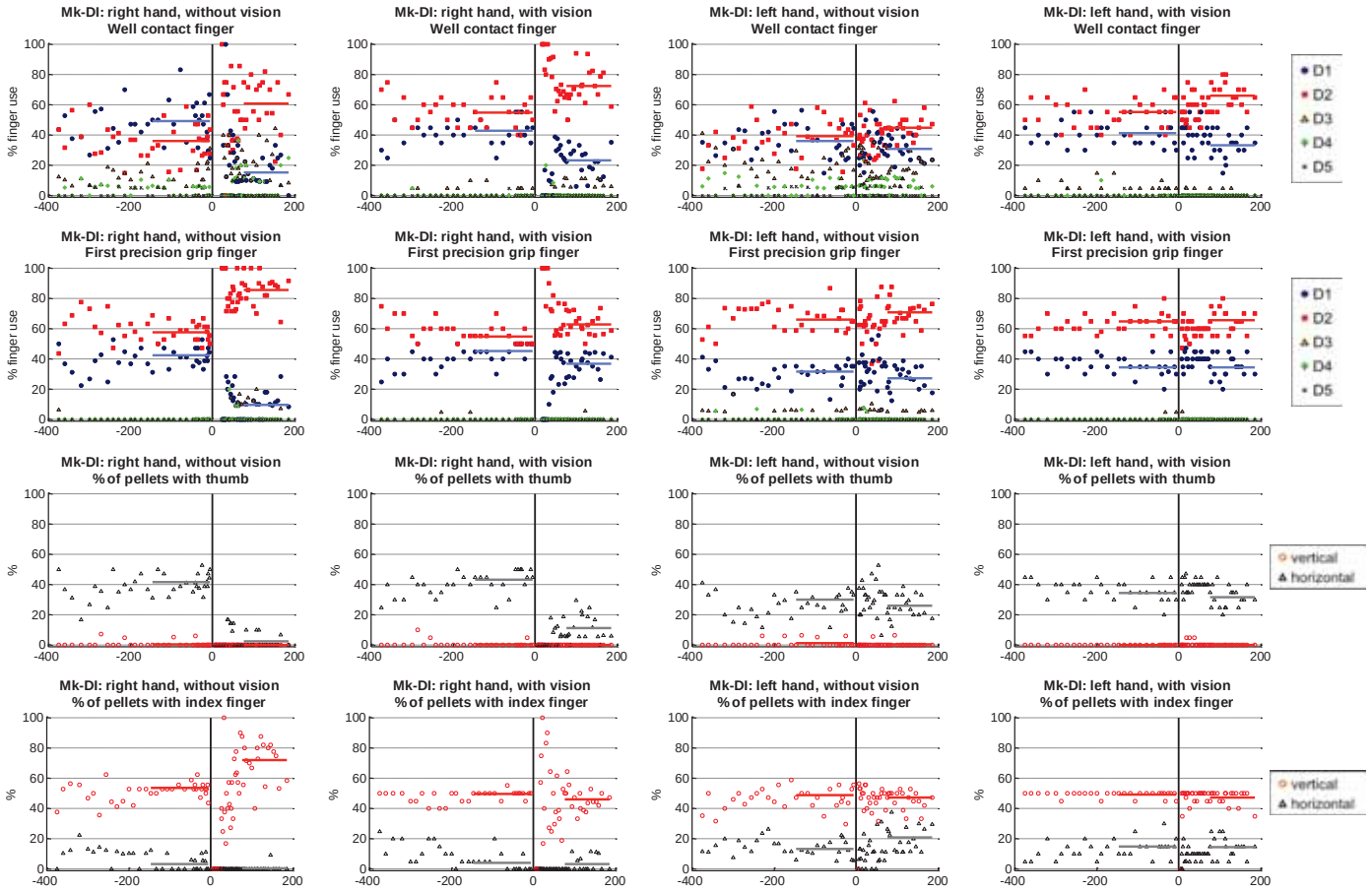
Mk-DI: right hand, without vision
Well contact finger
Mk-DI: right hand, with vision
Well contact finger
Mk-DI: left hand, without vision
Well contact finger
Mk-DI: left hand, with vision
Well contact finger
% finger use
D1
D2
D3
D4
D5
Mk-DI: right hand, without vision
First precision grip finger
Mk-DI: right hand, with vision
First precision grip finger
Mk-DI: left hand, without vision
First precision grip finger
Mk-DI: left hand, with vision
First precision grip finger
Mk-DI: right hand, without vision
% of pellets with thumb
Mk-DI: right hand, with vision
% of pellets with thumb
Mk-DI: left hand, without vision
% of pellets with thumb
Mk-DI: left hand, with vision
% of pellets with thumb
%
vertical
horizontal
Mk-DI: right hand, without vision
% of pellets with index finger
Mk-DI: right hand, with vision
% of pellets with index finger
Mk-DI: left hand, without vision
% of pellets with index finger
Mk-DI: left hand, with vision
% of pellets with index finger

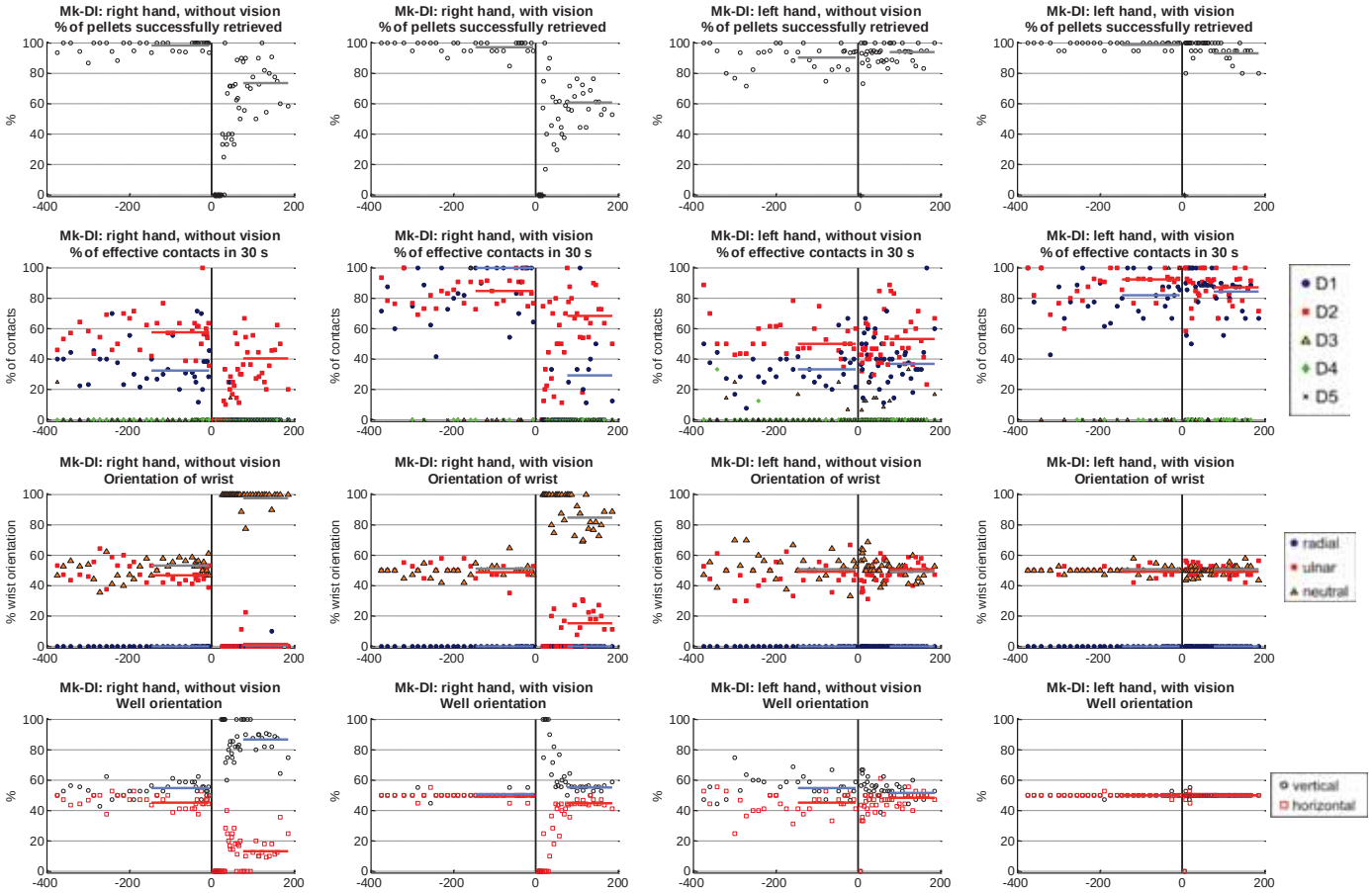
Mk-DI: right hand, without vision
% of pellets successfully retrieved
Mk-DI: right hand, with vision
% of pellets successfully retrieved
Mk-DI: left hand, without vision
% of pellets successfully retrieved
Mk-DI: left hand, with vision
% of pellets successfully retrieved
Mk-DI: right hand, without vision
% of effective contacts in 30 s
Mk-DI: right hand, with vision
% of effective contacts in 30 s
Mk-DI: left hand, without vision
% of effective contacts in 30 s
Mk-DI: left hand, with vision
% of effective contacts in 30 s
Mk-DI: right hand, without vision
Orientation of wrist
Mk-DI: right hand, with vision
Orientation of wrist
Mk-DI: left hand, without vision
Orientation of wrist
Mk-DI: left hand, with vision
Orientation of wrist
Mk-DI: right hand, without vision
Well orientation
Mk-DI: right hand, with vision
Well orientation
Mk-DI: left hand, without vision
Well orientation
Mk-DI: left hand, with vision
Well orientation
%
% of contacts
% wrist orientation
D1
D2
D3
D4
D5
radial
ulnar
neutral
vertical
horizontal

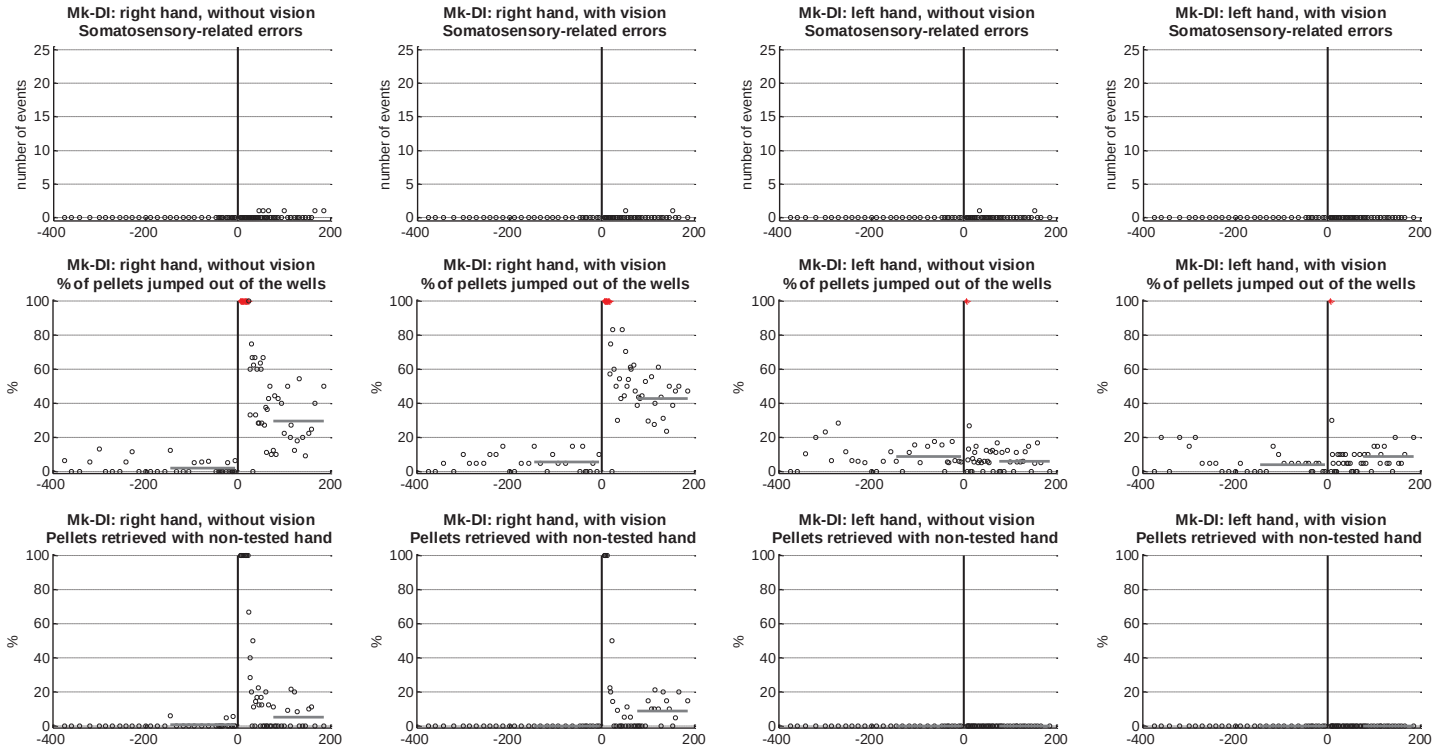
Mk-DI: right hand, without vision
Somatosensory-related errors
Mk-DI: right hand, with vision
Somatosensory-related errors
Mk-DI: left hand, without vision
Somatosensory-related errors
Mk-DI: left hand, with vision
Somatosensory-related errors
number of events
Mk-DI: right hand, without vision
% of pellets jumped out of the wells
Mk-DI: right hand, with vision
% of pellets jumped out of the wells
Mk-DI: left hand, without vision
% of pellets jumped out of the wells
Mk-DI: left hand, with vision
% of pellets jumped out of the wells
%
Mk-DI: right hand, without vision
Pellets retrieved with non-tested hand
Mk-DI: right hand, with vision
Pellets retrieved with non-tested hand
Mk-DI: left hand, without vision
Pellets retrieved with non-tested hand
Mk-DI: left hand, with vision
Pellets retrieved with non-tested hand
-400
-200
0
200

C

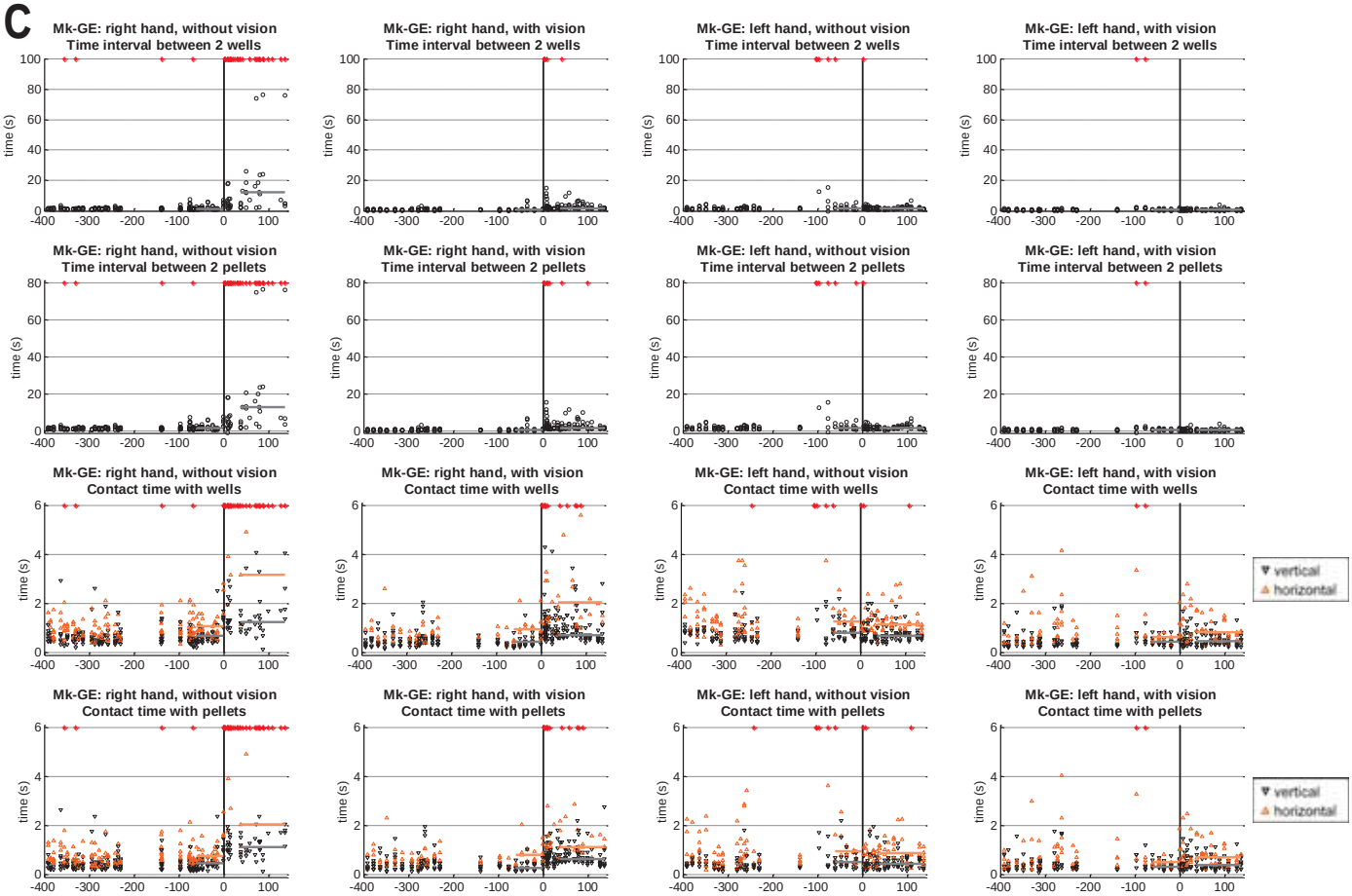
Mk-GE: right hand, without vision
Time interval between 2 wells
Mk-GE: right hand, with vision
Time interval between 2 wells
Mk-GE: left hand, without vision
Time interval between 2 wells
Mk-GE: left hand, with vision
Time interval between 2 wells
Mk-GE: right hand, without vision
Time interval between 2 pellets
Mk-GE: right hand, with vision
Time interval between 2 pellets
Mk-GE: left hand, without vision
Time interval between 2 pellets
Mk-GE: left hand, with vision
Time interval between 2 pellets
Mk-GE: right hand, without vision
Contact time with wells
Mk-GE: right hand, with vision
Contact time with wells
Mk-GE: left hand, without vision
Contact time with wells
Mk-GE: left hand, with vision
Contact time with wells
Mk-GE: right hand, without vision
Contact time with pellets
Mk-GE: right hand, with vision
Contact time with pellets
Mk-GE: left hand, without vision
Contact time with pellets
Mk-GE: left hand, with vision
Contact time with pellets
time (s)
vertical
horizontal

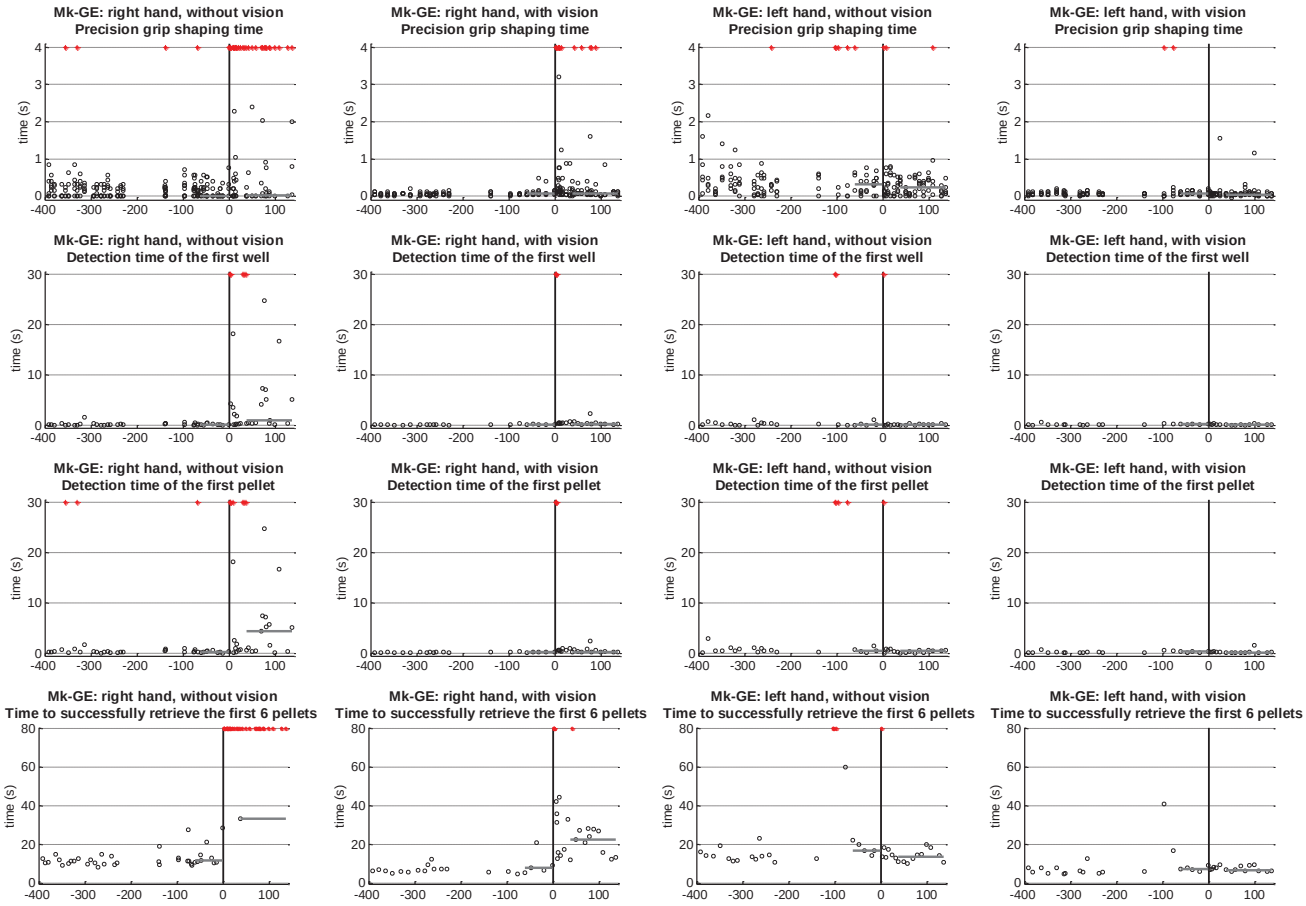
Mk-GE: right hand, without vision
Precision grip shaping time
Mk-GE: right hand, with vision
Precision grip shaping time
Mk-GE: left hand, without vision
Precision grip shaping time
Mk-GE: left hand, with vision
Precision grip shaping time
Mk-GE: right hand, without vision
Detection time of the first well
Mk-GE: right hand, with vision
Detection time of the first well
Mk-GE: left hand, without vision
Detection time of the first well
Mk-GE: left hand, with vision
Detection time of the first well
Mk-GE: right hand, without vision
Detection time of the first pellet
Mk-GE: right hand, with vision
Detection time of the first pellet
Mk-GE: left hand, without vision
Detection time of the first pellet
Mk-GE: left hand, with vision
Detection time of the first pellet
Mk-GE: right hand, without vision
Time to successfully retrieve the first 6 pellets
Mk-GE: right hand, with vision
Time to successfully retrieve the first 6 pellets
Mk-GE: left hand, without vision
Time to successfully retrieve the first 6 pellets
Mk-GE: left hand, with vision
Time to successfully retrieve the first 6 pellets
time (s)

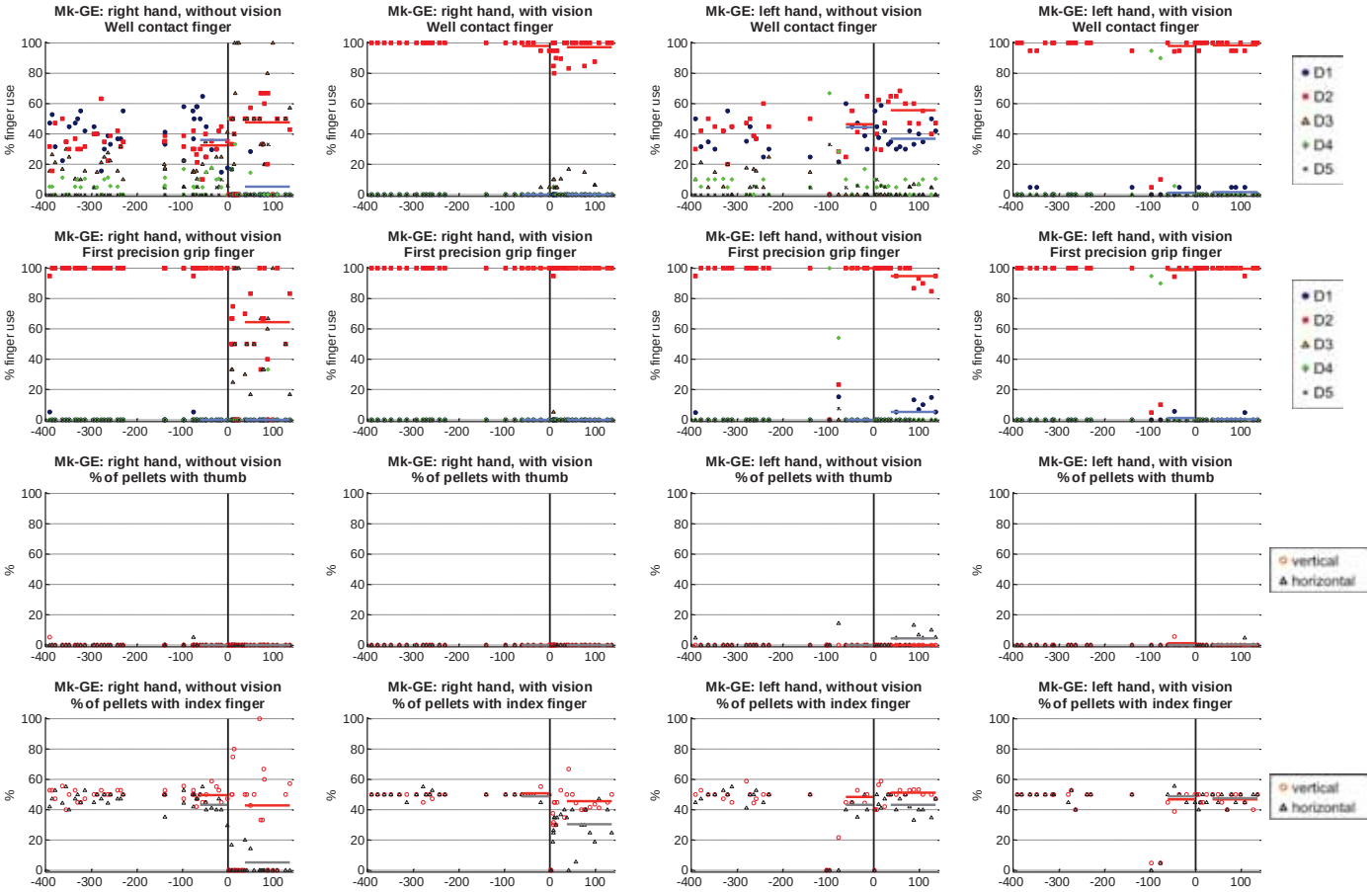
Mk-GE: right hand, without vision
Well contact finger
Mk-GE: right hand, with vision
Well contact finger
Mk-GE: left hand, without vision
Well contact finger
Mk-GE: left hand, with vision
Well contact finger
% finger use
D1
D2
D3
D4
D5
Mk-GE: right hand, without vision
First precision grip finger
Mk-GE: right hand, with vision
First precision grip finger
Mk-GE: left hand, without vision
First precision grip finger
Mk-GE: left hand, with vision
First precision grip finger
Mk-GE: right hand, without vision
% of pellets with thumb
Mk-GE: right hand, with vision
% of pellets with thumb
Mk-GE: left hand, without vision
% of pellets with thumb
Mk-GE: left hand, with vision
% of pellets with thumb
%
vertical
horizontal
Mk-GE: right hand, without vision
% of pellets with index finger
Mk-GE: right hand, with vision
% of pellets with index finger
Mk-GE: left hand, without vision
% of pellets with index finger
Mk-GE: left hand, with vision
% of pellets with index finger

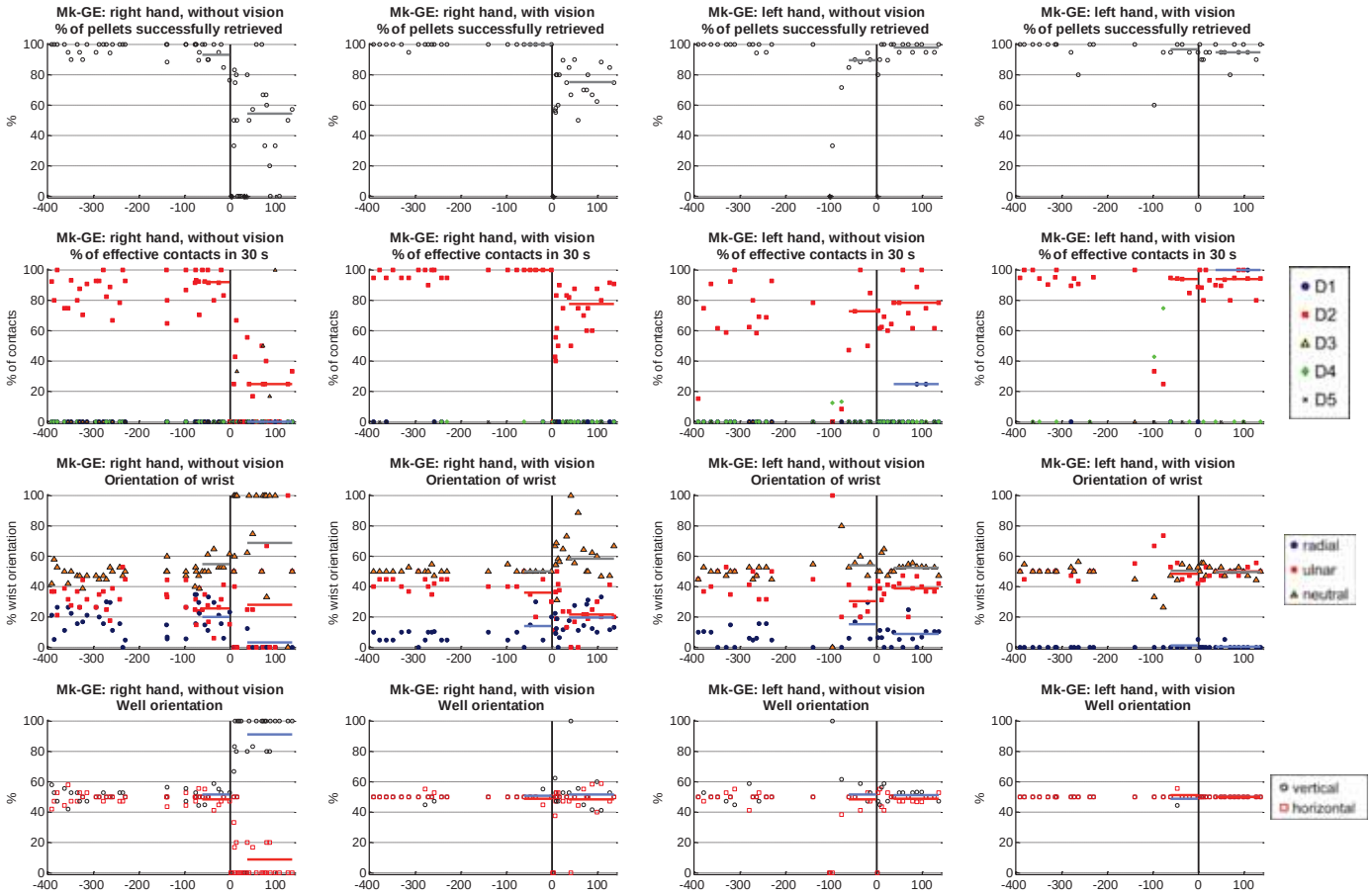
Mk-GE: right hand, without vision
% of pellets successfully retrieved
Mk-GE: right hand, with vision
% of pellets successfully retrieved
Mk-GE: left hand, without vision
% of pellets successfully retrieved
Mk-GE: left hand, with vision
% of pellets successfully retrieved
Mk-GE: right hand, without vision
% of effective contacts in 30 s
Mk-GE: right hand, with vision
% of effective contacts in 30 s
Mk-GE: left hand, without vision
% of effective contacts in 30 s
Mk-GE: left hand, with vision
% of effective contacts in 30 s
Mk-GE: right hand, without vision
Orientation of wrist
Mk-GE: right hand, with vision
Orientation of wrist
Mk-GE: left hand, without vision
Orientation of wrist
Mk-GE: left hand, with vision
Orientation of wrist
Mk-GE: right hand, without vision
Well orientation
Mk-GE: right hand, with vision
Well orientation
Mk-GE: left hand, without vision
Well orientation
Mk-GE: left hand, with vision
Well orientation
%
% of contacts
% wrist orientation
D1
D2
D3
D4
D5
radial
ulnar
neutral
vertical
horizontal

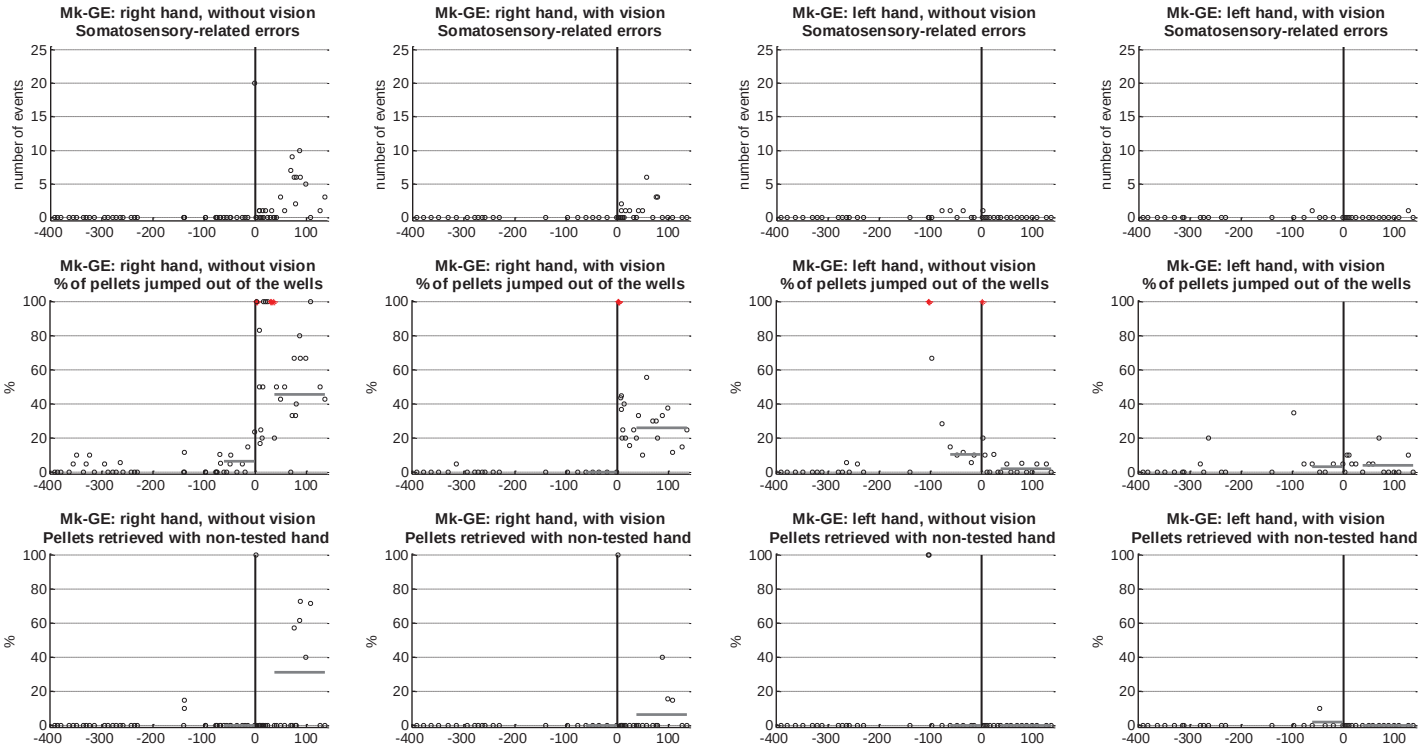
Mk-GE: right hand, without vision
Somatosensory-related errors
Mk-GE: right hand, with vision
Somatosensory-related errors
Mk-GE: left hand, without vision
Somatosensory-related errors
Mk-GE: left hand, with vision
Somatosensory-related errors
number of events
Mk-GE: right hand, without vision
% of pellets jumped out of the wells
Mk-GE: right hand, with vision
% of pellets jumped out of the wells
Mk-GE: left hand, without vision
% of pellets jumped out of the wells
Mk-GE: left hand, with vision
% of pellets jumped out of the wells
%
Mk-GE: right hand, without vision
Pellets retrieved with non-tested hand
Mk-GE: right hand, with vision
Pellets retrieved with non-tested hand
Mk-GE: left hand, without vision
Pellets retrieved with non-tested hand
Mk-GE: left hand, with vision
Pellets retrieved with non-tested hand

D

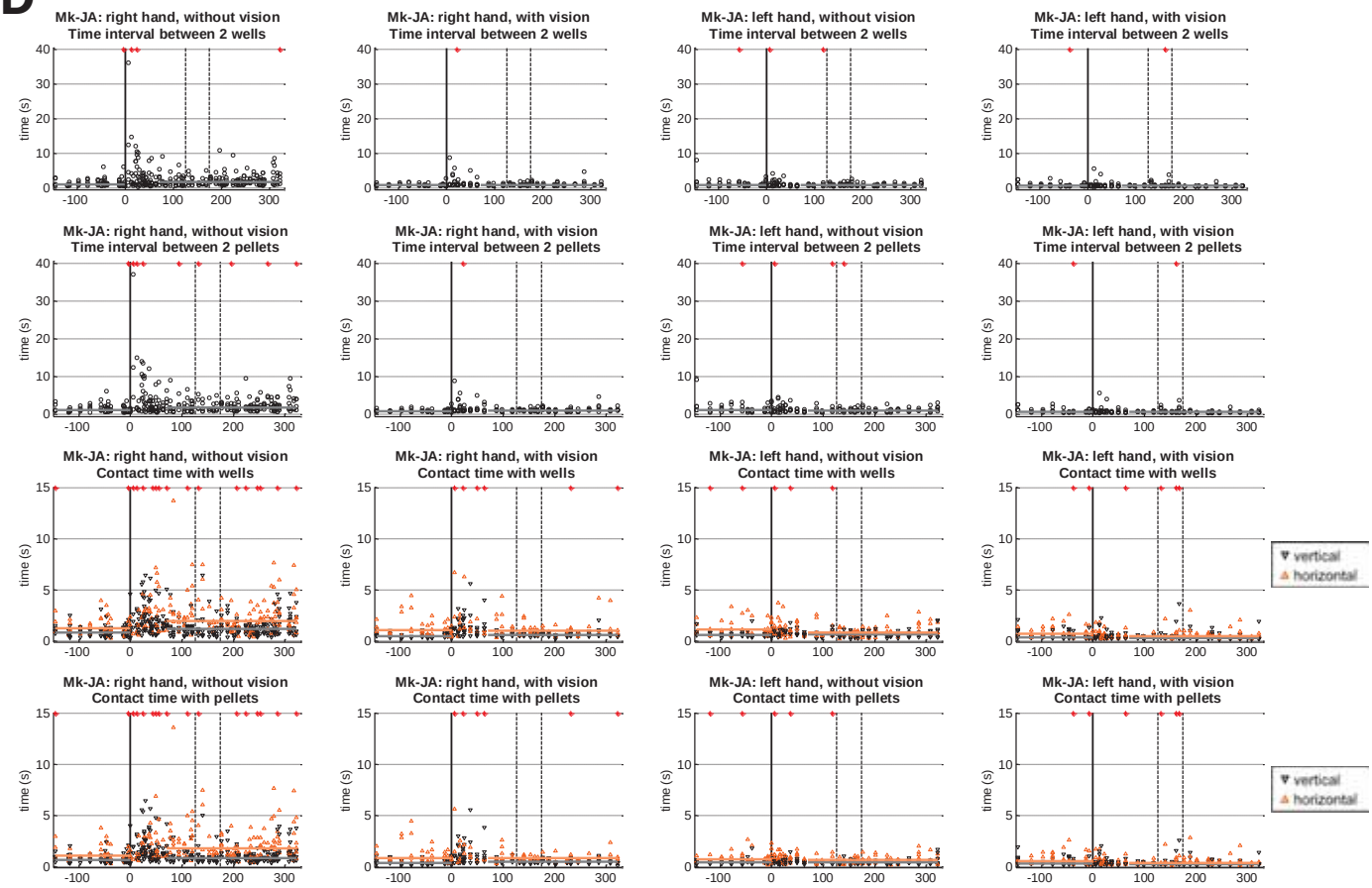
Mk-JA: right hand, without vision
Time interval between 2 wells
Mk-JA: right hand, with vision
Time interval between 2 wells
Mk-JA: left hand, without vision
Time interval between 2 wells
Mk-JA: left hand, with vision
Time interval between 2 wells
Mk-JA: right hand, without vision
Time interval between 2 pellets
Mk-JA: right hand, with vision
Time interval between 2 pellets
Mk-JA: left hand, without vision
Time interval between 2 pellets
Mk-JA: left hand, with vision
Time interval between 2 pellets
Mk-JA: right hand, without vision
Contact time with wells
Mk-JA: right hand, with vision
Contact time with wells
Mk-JA: left hand, without vision
Contact time with wells
Mk-JA: left hand, with vision
Contact time with wells
Mk-JA: right hand, without vision
Contact time with pellets
Mk-JA: right hand, with vision
Contact time with pellets
Mk-JA: left hand, without vision
Contact time with pellets
Mk-JA: left hand, with vision
Contact time with pellets
time (s)
vertical
horizontal

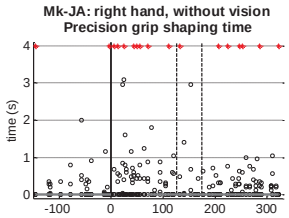

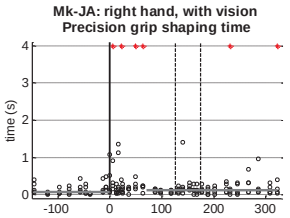

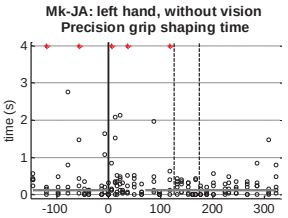

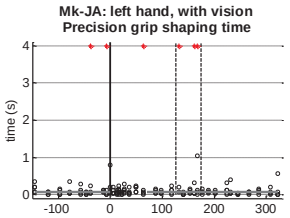

Not applicable because the monkey was able to see the first pellet.

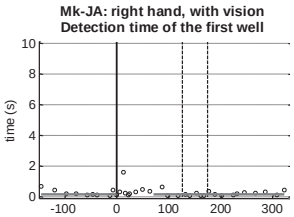

Not applicable because the monkey was able to see the first pellet.

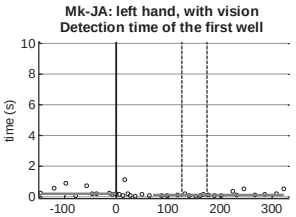

Not applicable because the monkey was able to see the first pellet.

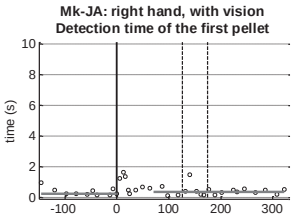

Not applicable because the monkey was able to see the first pellet.

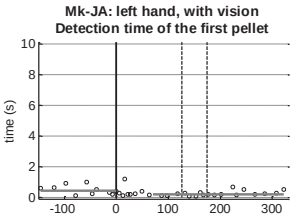

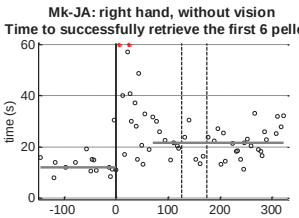

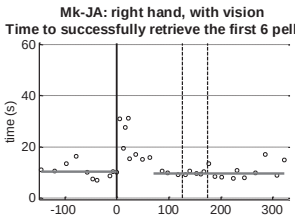

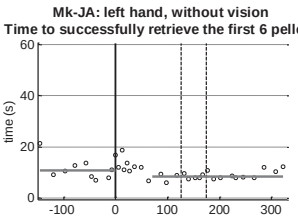

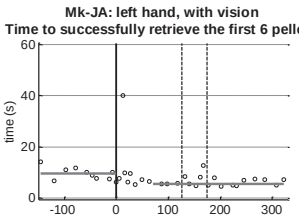

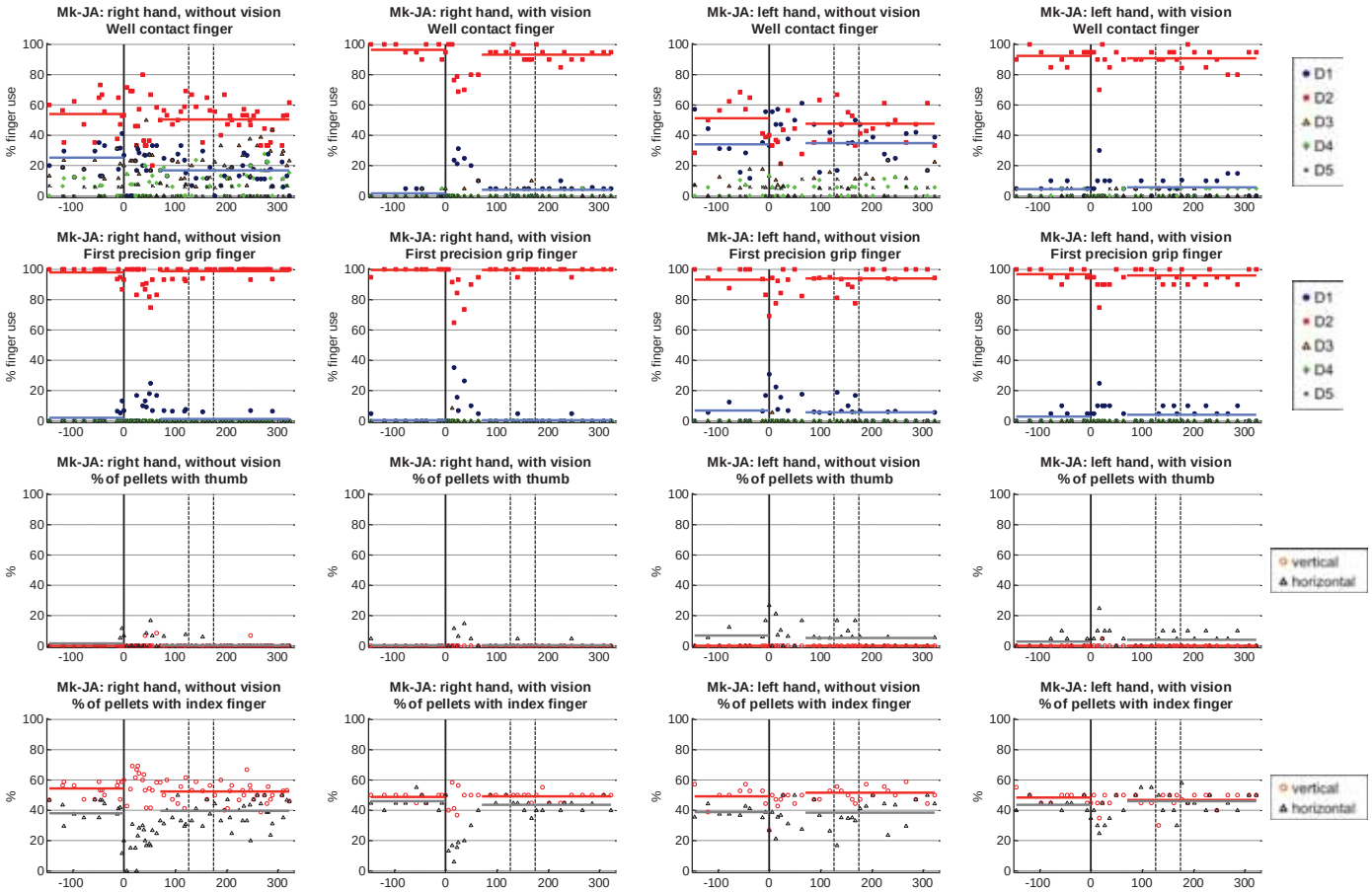
Mk-JA: right hand, without vision
Well contact finger
Mk-JA: right hand, with vision
Well contact finger
Mk-JA: left hand, without vision
Well contact finger
Mk-JA: left hand, with vision
Well contact finger
% finger use
D1
D2
D3
D4
D5
Mk-JA: right hand, without vision
First precision grip finger
Mk-JA: right hand, with vision
First precision grip finger
Mk-JA: left hand, without vision
First precision grip finger
Mk-JA: left hand, with vision
First precision grip finger
Mk-JA: right hand, without vision
% of pellets with thumb
Mk-JA: right hand, with vision
% of pellets with thumb
Mk-JA: left hand, without vision
% of pellets with thumb
Mk-JA: left hand, with vision
% of pellets with thumb
%
vertical
horizontal
Mk-JA: right hand, without vision
% of pellets with index finger
Mk-JA: right hand, with vision
% of pellets with index finger
Mk-JA: left hand, without vision
% of pellets with index finger
Mk-JA: left hand, with vision
% of pellets with index finger

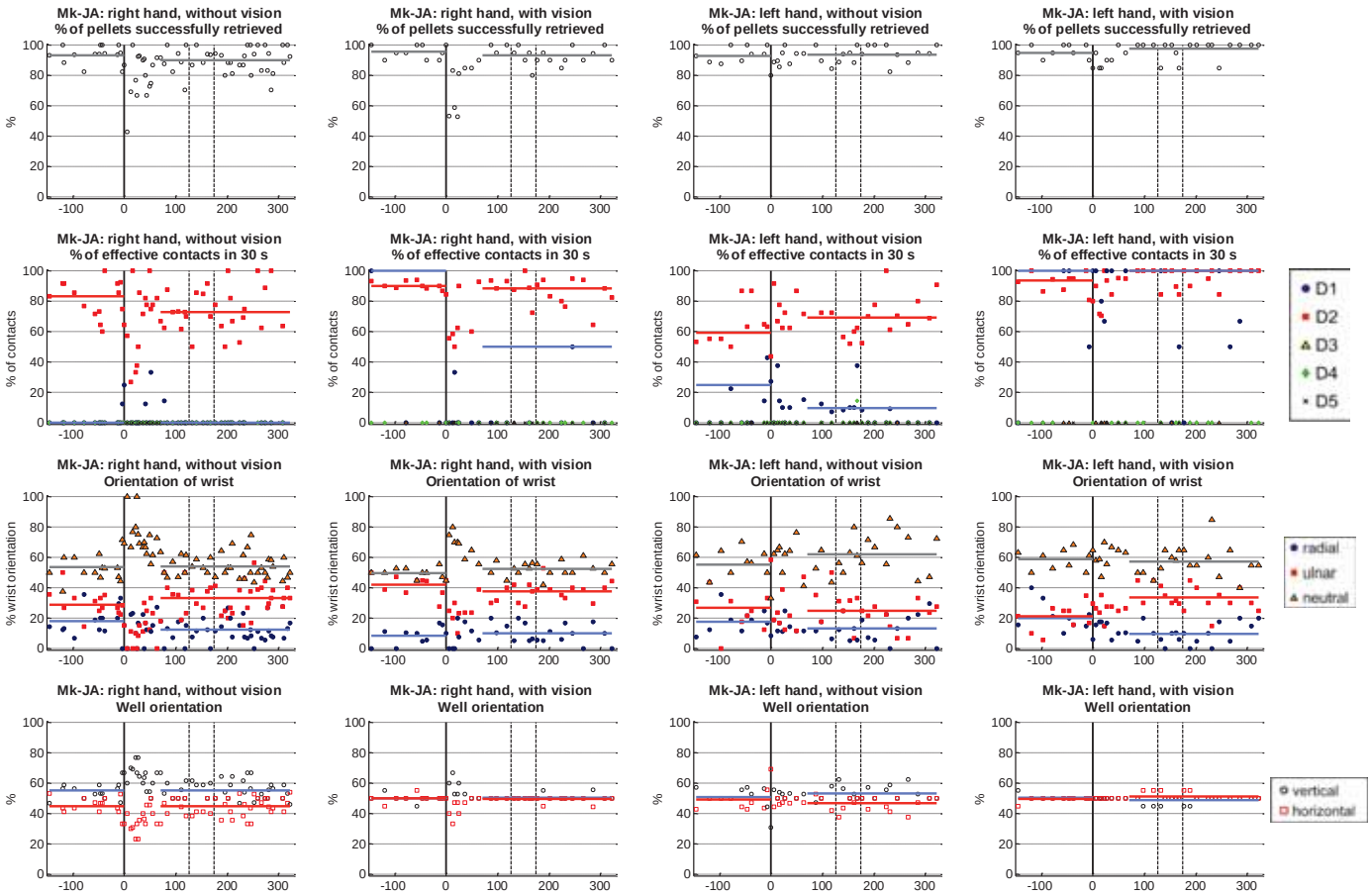
Mk-JA: right hand, without vision
% of pellets successfully retrieved
Mk-JA: right hand, with vision
% of pellets successfully retrieved
Mk-JA: left hand, without vision
% of pellets successfully retrieved
Mk-JA: left hand, with vision
% of pellets successfully retrieved
Mk-JA: right hand, without vision
% of effective contacts in 30 s
Mk-JA: right hand, with vision
% of effective contacts in 30 s
Mk-JA: left hand, without vision
% of effective contacts in 30 s
Mk-JA: left hand, with vision
% of effective contacts in 30 s
Mk-JA: right hand, without vision
Orientation of wrist
Mk-JA: right hand, with vision
Orientation of wrist
Mk-JA: left hand, without vision
Orientation of wrist
Mk-JA: left hand, with vision
Orientation of wrist
Mk-JA: right hand, without vision
Well orientation
Mk-JA: right hand, with vision
Well orientation
Mk-JA: left hand, without vision
Well orientation
Mk-JA: left hand, with vision
Well orientation
%
% of contacts
% wrist orientation
D1
D2
D3
D4
D5
radial
ulnar
neutral
vertical
horizontal

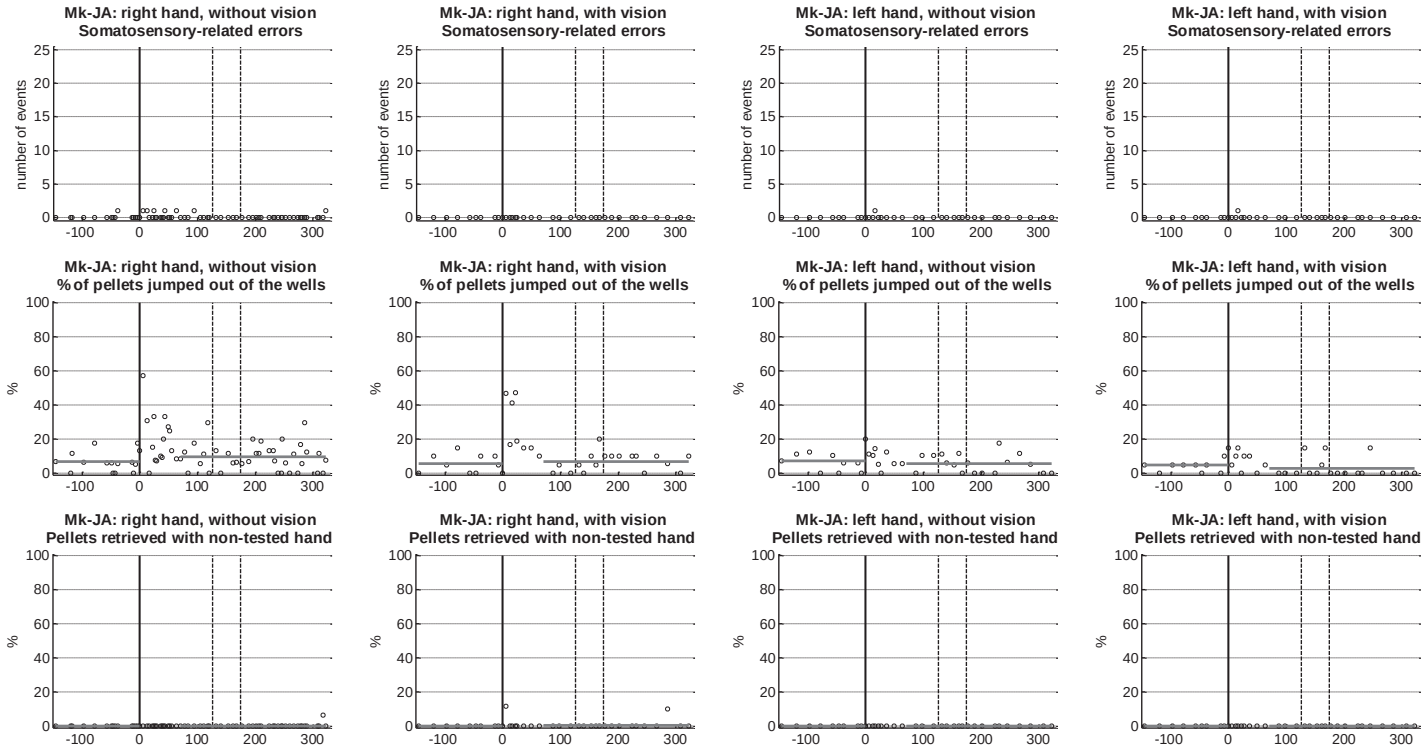
Mk-JA: right hand, without vision
Somatosensory-related errors
Mk-JA: right hand, with vision
Somatosensory-related errors
Mk-JA: left hand, without vision
Somatosensory-related errors
Mk-JA: left hand, with vision
Somatosensory-related errors
number of events
Mk-JA: right hand, without vision
% of pellets jumped out of the wells
Mk-JA: right hand, with vision
% of pellets jumped out of the wells
Mk-JA: left hand, without vision
% of pellets jumped out of the wells
Mk-JA: left hand, with vision
% of pellets jumped out of the wells
%
Mk-JA: right hand, without vision
Pellets retrieved with non-tested hand
Mk-JA: right hand, with vision
Pellets retrieved with non-tested hand
Mk-JA: left hand, without vision
Pellets retrieved with non-tested hand
Mk-JA: left hand, with vision
Pellets retrieved with non-tested hand

E

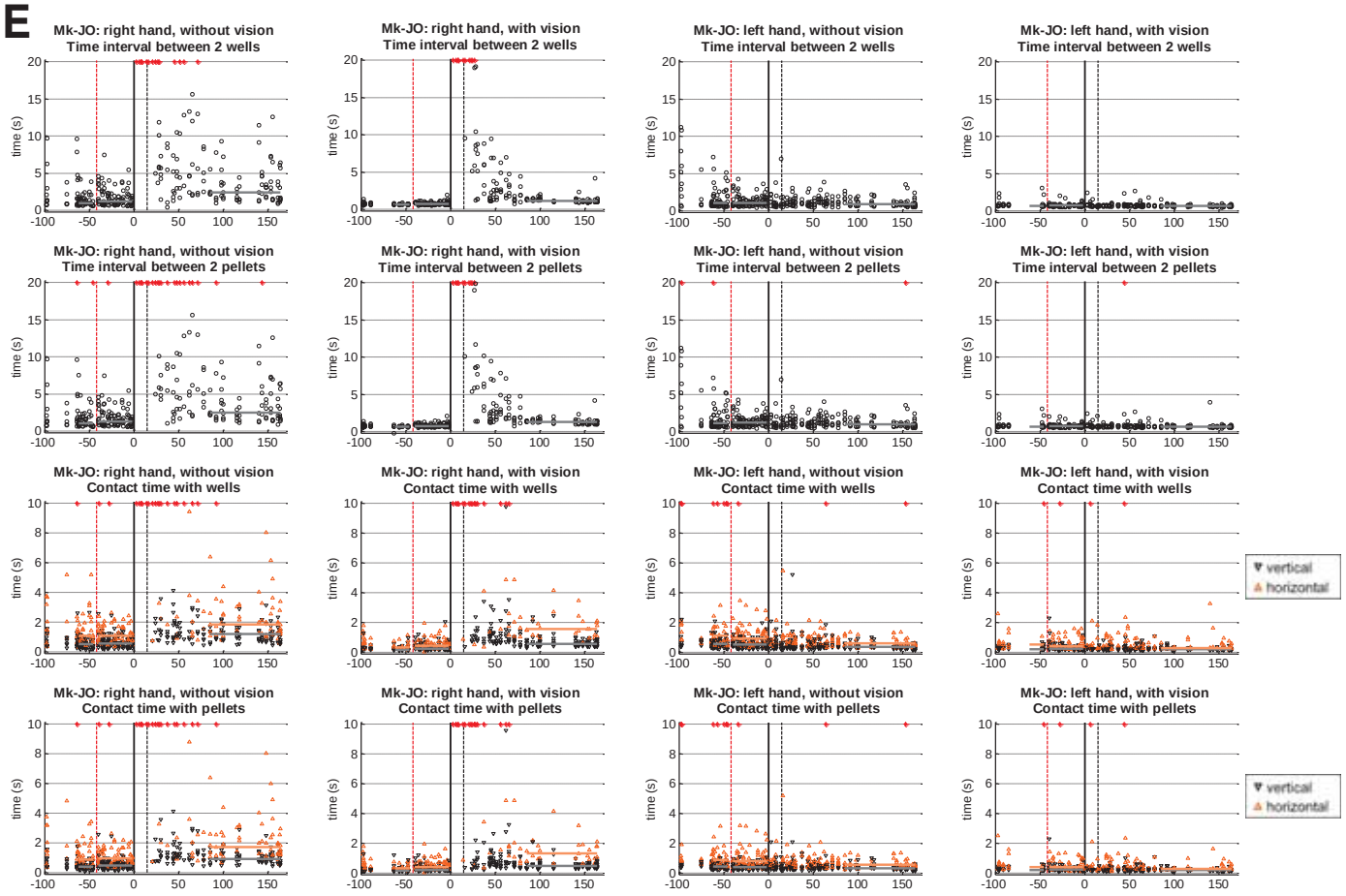
Mk-JO: right hand, without vision
Time interval between 2 wells
Mk-JO: right hand, with vision
Time interval between 2 wells
Mk-JO: left hand, without vision
Time interval between 2 wells
Mk-JO: left hand, with vision
Time interval between 2 wells
Mk-JO: right hand, without vision
Time interval between 2 pellets
Mk-JO: right hand, with vision
Time interval between 2 pellets
Mk-JO: left hand, without vision
Time interval between 2 pellets
Mk-JO: left hand, with vision
Time interval between 2 pellets
Mk-JO: right hand, without vision
Contact time with wells
Mk-JO: right hand, with vision
Contact time with wells
Mk-JO: left hand, without vision
Contact time with wells
Mk-JO: left hand, with vision
Contact time with wells
Mk-JO: right hand, without vision
Contact time with pellets
Mk-JO: right hand, with vision
Contact time with pellets
Mk-JO: left hand, without vision
Contact time with pellets
Mk-JO: left hand, with vision
Contact time with pellets
time (s)
vertical
horizontal

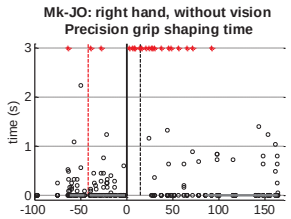

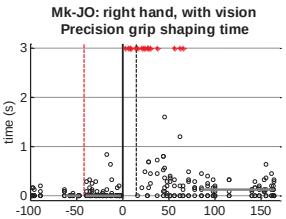

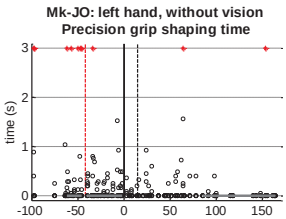

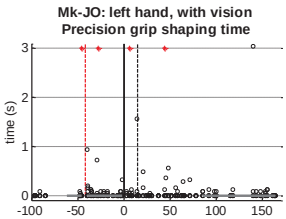

Not applicable because the monkey was able to see the first pellet.

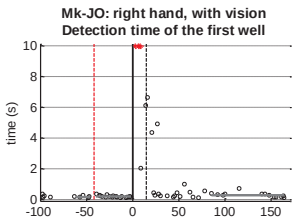

Not applicable because the monkey was able to see the first pellet.

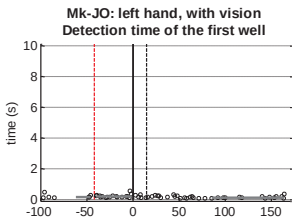

Not applicable because the monkey was able to see the first pellet.

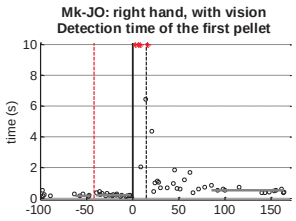

Not applicable because the monkey was able to see the first pellet.

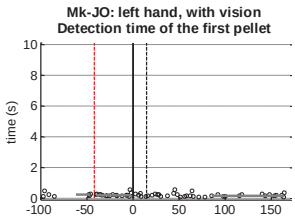

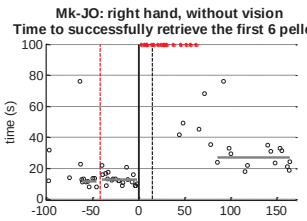

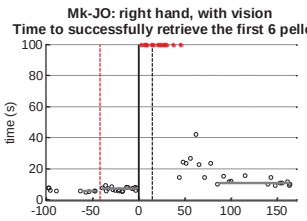

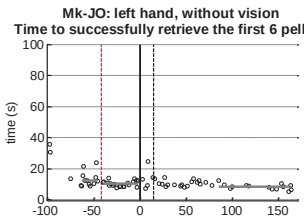

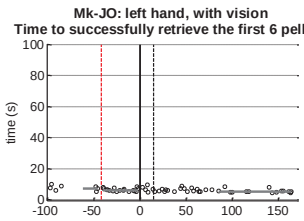

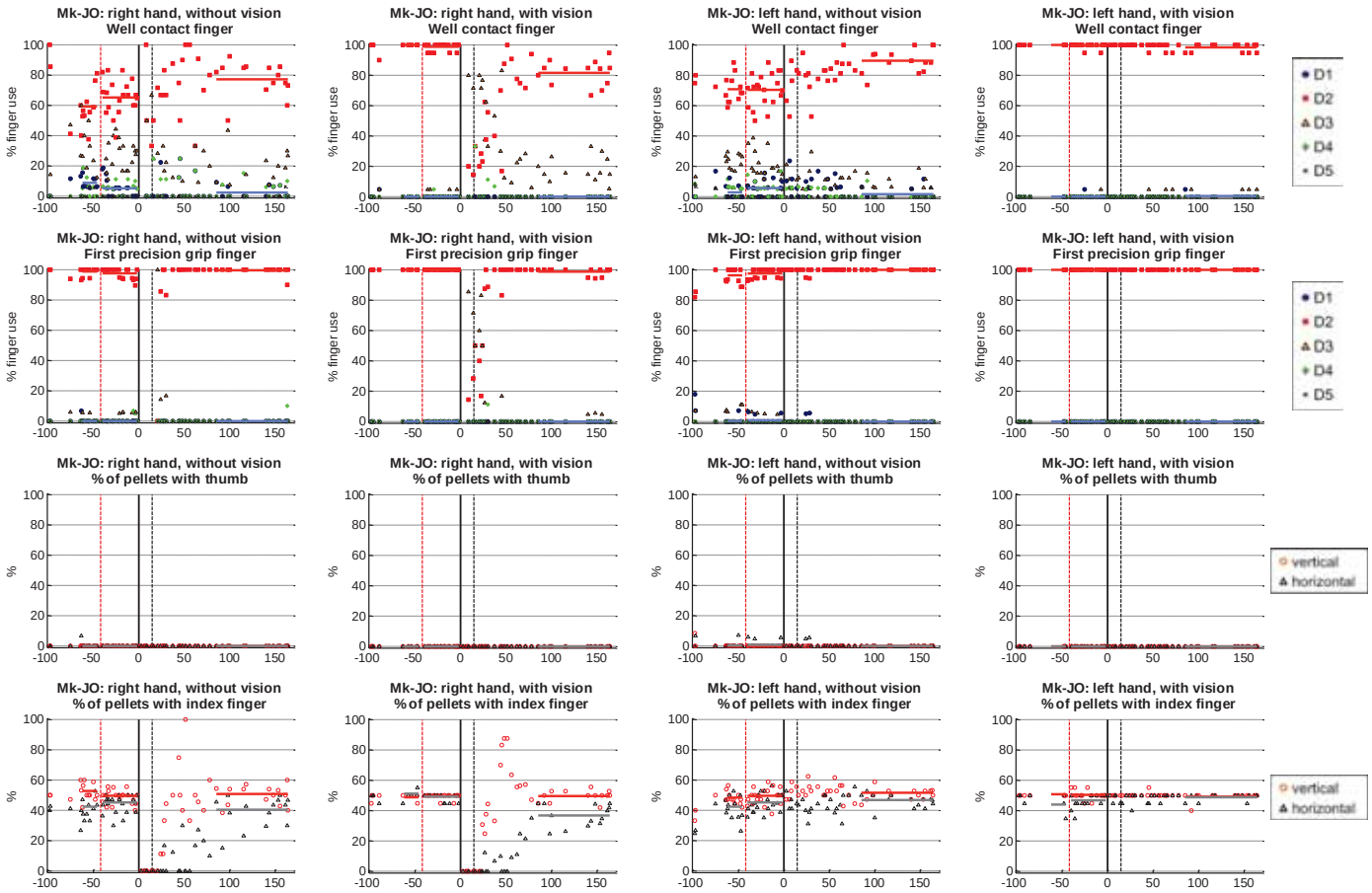
Mk-JO: right hand, without vision
Well contact finger
Mk-JO: right hand, with vision
Well contact finger
Mk-JO: left hand, without vision
Well contact finger
Mk-JO: left hand, with vision
Well contact finger
% finger use
D1
D2
D3
D4
D5
Mk-JO: right hand, without vision
First precision grip finger
Mk-JO: right hand, with vision
First precision grip finger
Mk-JO: left hand, without vision
First precision grip finger
Mk-JO: left hand, with vision
First precision grip finger
% finger use
D1
D2
D3
D4
D5
Mk-JO: right hand, without vision
% of pellets with thumb
Mk-JO: right hand, with vision
% of pellets with thumb
Mk-JO: left hand, without vision
% of pellets with thumb
Mk-JO: left hand, with vision
% of pellets with thumb
%
vertical
horizontal
Mk-JO: right hand, without vision
% of pellets with index finger
Mk-JO: right hand, with vision
% of pellets with index finger
Mk-JO: left hand, without vision
% of pellets with index finger
Mk-JO: left hand, with vision
% of pellets with index finger
%
vertical
horizontal

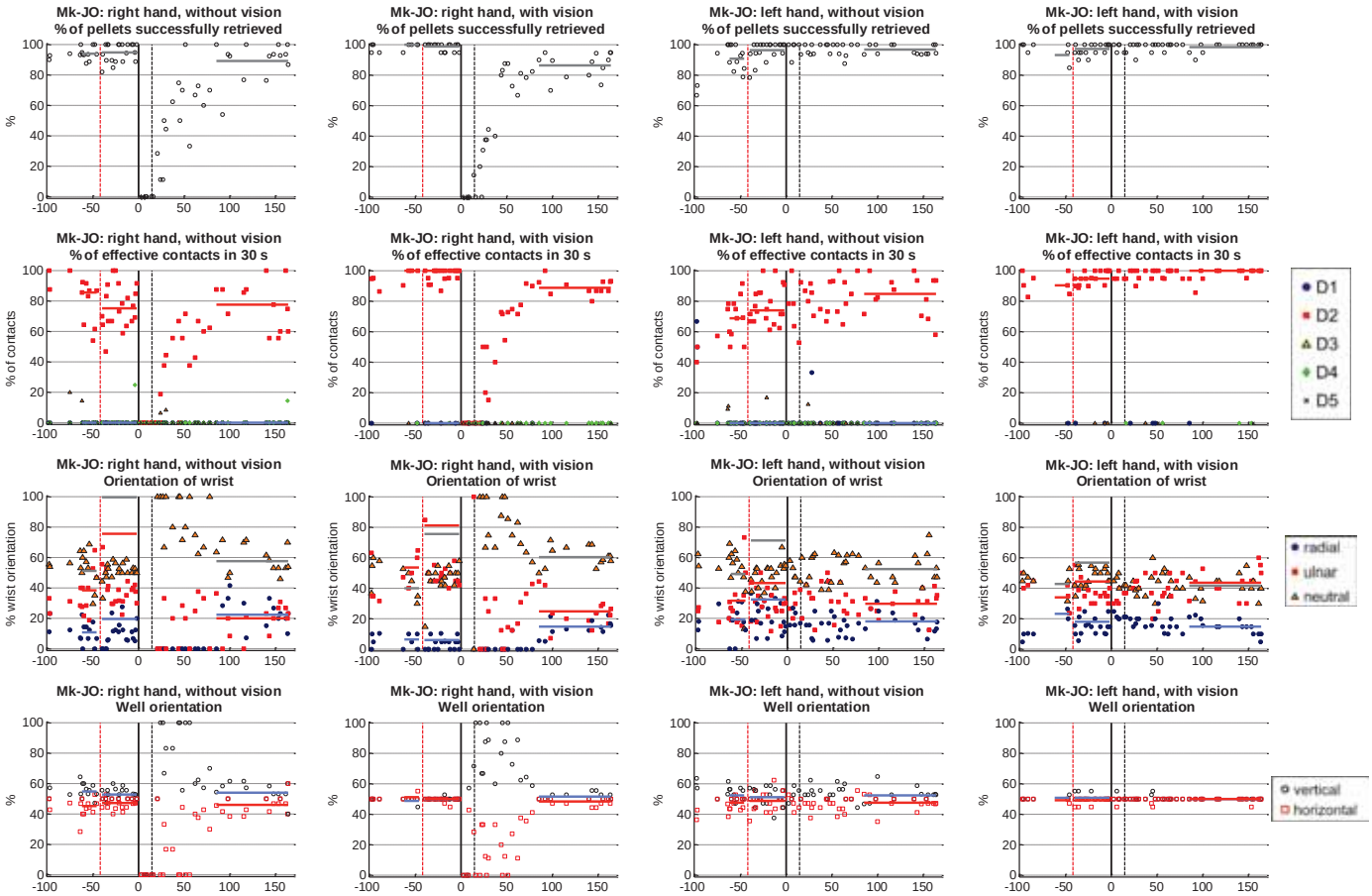
Mk-JO: right hand, without vision
% of pellets successfully retrieved
Mk-JO: right hand, with vision
% of pellets successfully retrieved
Mk-JO: left hand, without vision
% of pellets successfully retrieved
Mk-JO: left hand, with vision
% of pellets successfully retrieved
Mk-JO: right hand, without vision
% of effective contacts in 30 s
Mk-JO: right hand, with vision
% of effective contacts in 30 s
Mk-JO: left hand, without vision
% of effective contacts in 30 s
Mk-JO: left hand, with vision
% of effective contacts in 30 s
% of contacts
D1
D2
D3
D4
D5
Mk-JO: right hand, without vision
Orientation of wrist
Mk-JO: right hand, with vision
Orientation of wrist
Mk-JO: left hand, without vision
Orientation of wrist
Mk-JO: left hand, with vision
Orientation of wrist
% wrist orientation
radial
ulnar
neutral
Mk-JO: right hand, without vision
Well orientation
Mk-JO: right hand, with vision
Well orientation
Mk-JO: left hand, without vision
Well orientation
Mk-JO: left hand, with vision
Well orientation
%
vertical
horizontal

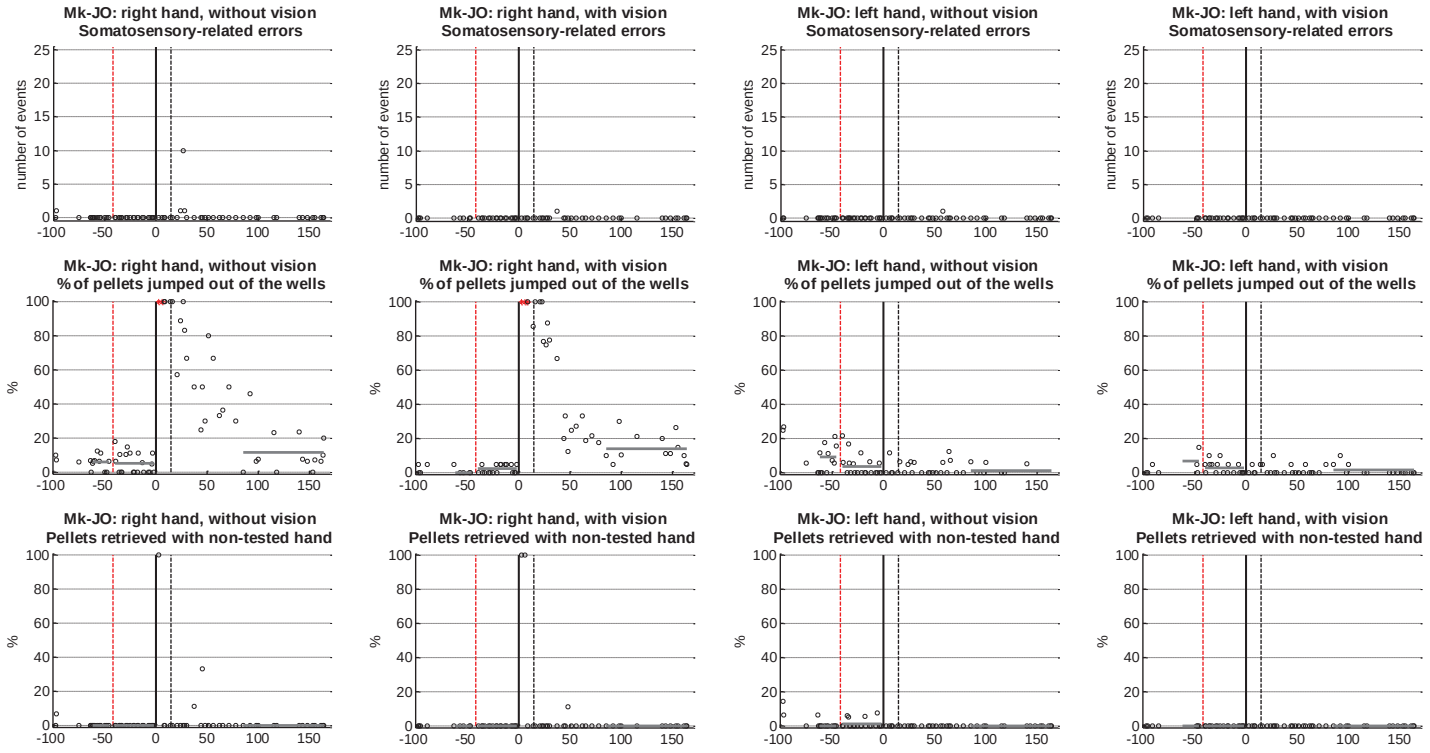
Mk-JO: right hand, without vision
Somatosensory-related errors
Mk-JO: right hand, with vision
Somatosensory-related errors
Mk-JO: left hand, without vision
Somatosensory-related errors
Mk-JO: left hand, with vision
Somatosensory-related errors
number of events
Mk-JO: right hand, without vision
% of pellets jumped out of the wells
Mk-JO: right hand, with vision
% of pellets jumped out of the wells
Mk-JO: left hand, without vision
% of pellets jumped out of the wells
Mk-JO: left hand, with vision
% of pellets jumped out of the wells
%
Mk-JO: right hand, without vision
Pellets retrieved with non-tested hand
Mk-JO: right hand, with vision
Pellets retrieved with non-tested hand
Mk-JO: left hand, without vision
Pellets retrieved with non-tested hand
Mk-JO: left hand, with vision
Pellets retrieved with non-tested hand

F

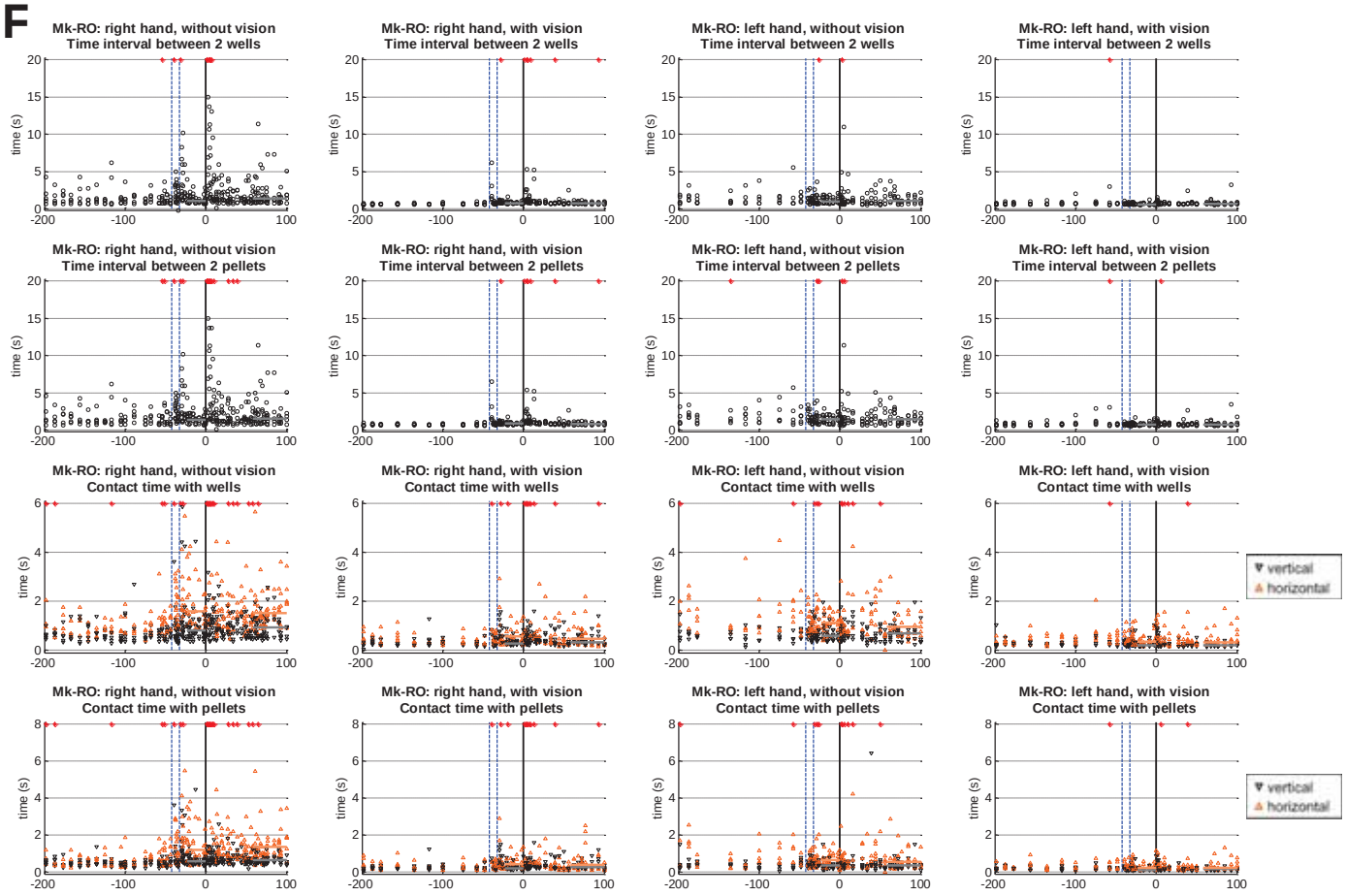
Mk-RO: right hand, without vision
Time interval between 2 wells
Mk-RO: right hand, with vision
Time interval between 2 wells
Mk-RO: left hand, without vision
Time interval between 2 wells
Mk-RO: left hand, with vision
Time interval between 2 wells
Mk-RO: right hand, without vision
Time interval between 2 pellets
Mk-RO: right hand, with vision
Time interval between 2 pellets
Mk-RO: left hand, without vision
Time interval between 2 pellets
Mk-RO: left hand, with vision
Time interval between 2 pellets
Mk-RO: right hand, without vision
Contact time with wells
Mk-RO: right hand, with vision
Contact time with wells
Mk-RO: left hand, without vision
Contact time with wells
Mk-RO: left hand, with vision
Contact time with wells
Mk-RO: right hand, without vision
Contact time with pellets
Mk-RO: right hand, with vision
Contact time with pellets
Mk-RO: left hand, without vision
Contact time with pellets
Mk-RO: left hand, with vision
Contact time with pellets
time (s)
vertical
horizontal

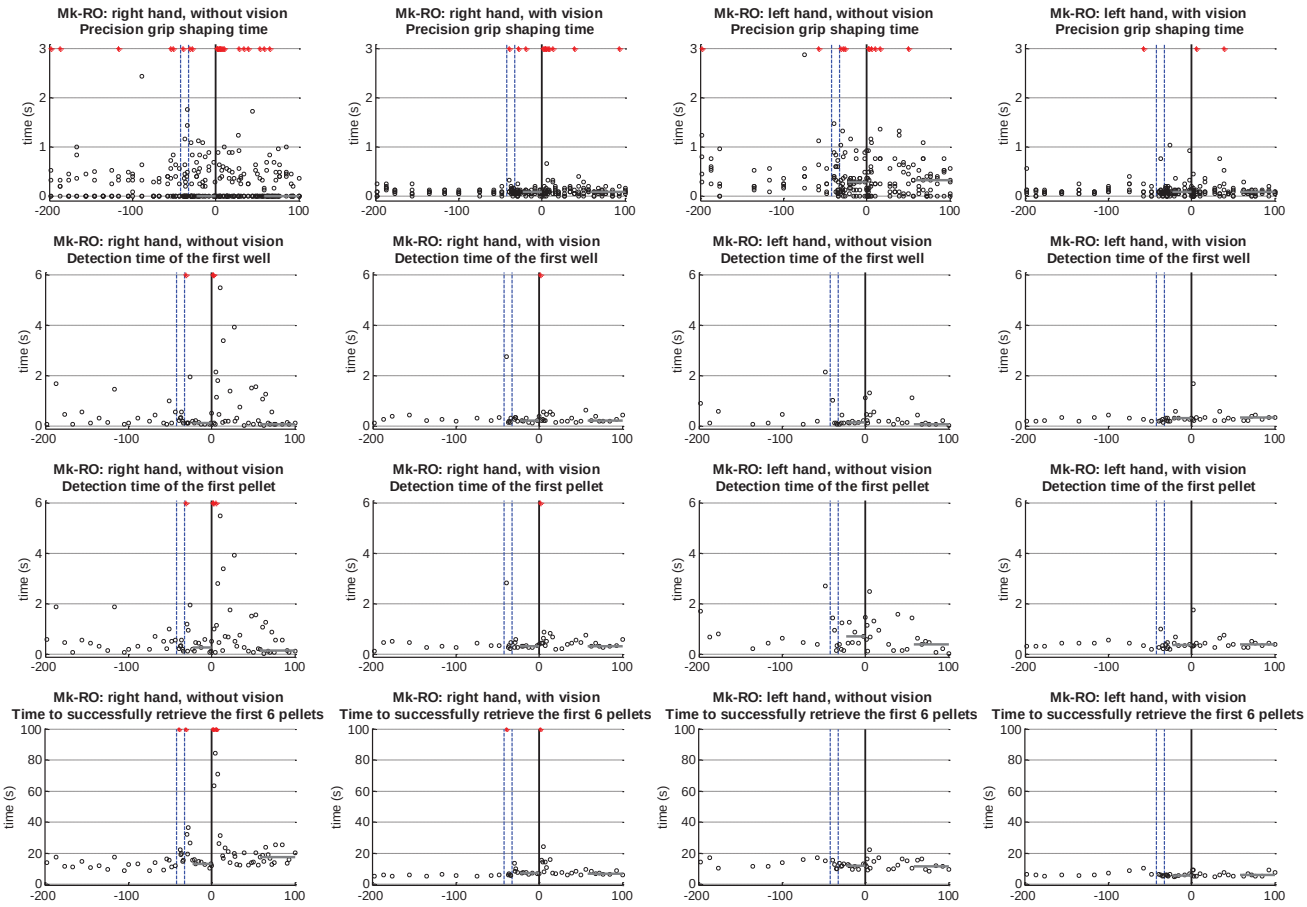
Mk-RO: right hand, without vision
Precision grip shaping time
Mk-RO: right hand, with vision
Precision grip shaping time
Mk-RO: left hand, without vision
Precision grip shaping time
Mk-RO: left hand, with vision
Precision grip shaping time
Mk-RO: right hand, without vision
Detection time of the first well
Mk-RO: right hand, with vision
Detection time of the first well
Mk-RO: left hand, without vision
Detection time of the first well
Mk-RO: left hand, with vision
Detection time of the first well
Mk-RO: right hand, without vision
Detection time of the first pellet
Mk-RO: right hand, with vision
Detection time of the first pellet
Mk-RO: left hand, without vision
Detection time of the first pellet
Mk-RO: left hand, with vision
Detection time of the first pellet
Mk-RO: right hand, without vision
Time to successfully retrieve the first 6 pellets
Mk-RO: right hand, with vision
Time to successfully retrieve the first 6 pellets
Mk-RO: left hand, without vision
Time to successfully retrieve the first 6 pellets
Mk-RO: left hand, with vision
Time to successfully retrieve the first 6 pellets
time (s)

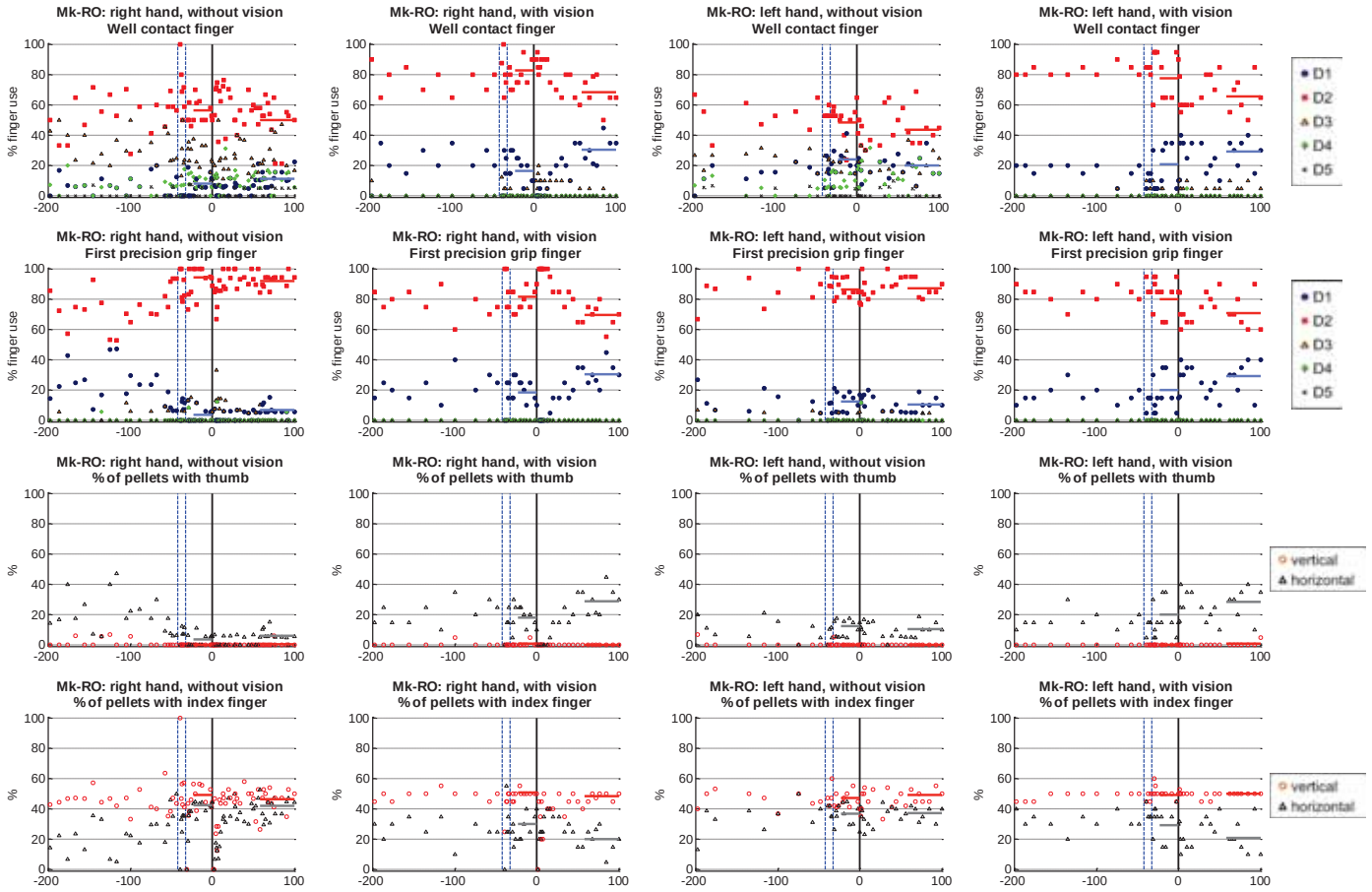
Mk-RO: right hand, without vision
Well contact finger
Mk-RO: right hand, with vision
Well contact finger
Mk-RO: left hand, without vision
Well contact finger
Mk-RO: left hand, with vision
Well contact finger
% finger use
D1
D2
D3
D4
D5
Mk-RO: right hand, without vision
First precision grip finger
Mk-RO: right hand, with vision
First precision grip finger
Mk-RO: left hand, without vision
First precision grip finger
Mk-RO: left hand, with vision
First precision grip finger
Mk-RO: right hand, without vision
% of pellets with thumb
Mk-RO: right hand, with vision
% of pellets with thumb
Mk-RO: left hand, without vision
% of pellets with thumb
Mk-RO: left hand, with vision
% of pellets with thumb
%
vertical
horizontal
Mk-RO: right hand, without vision
% of pellets with index finger
Mk-RO: right hand, with vision
% of pellets with index finger
Mk-RO: left hand, without vision
% of pellets with index finger
Mk-RO: left hand, with vision
% of pellets with index finger

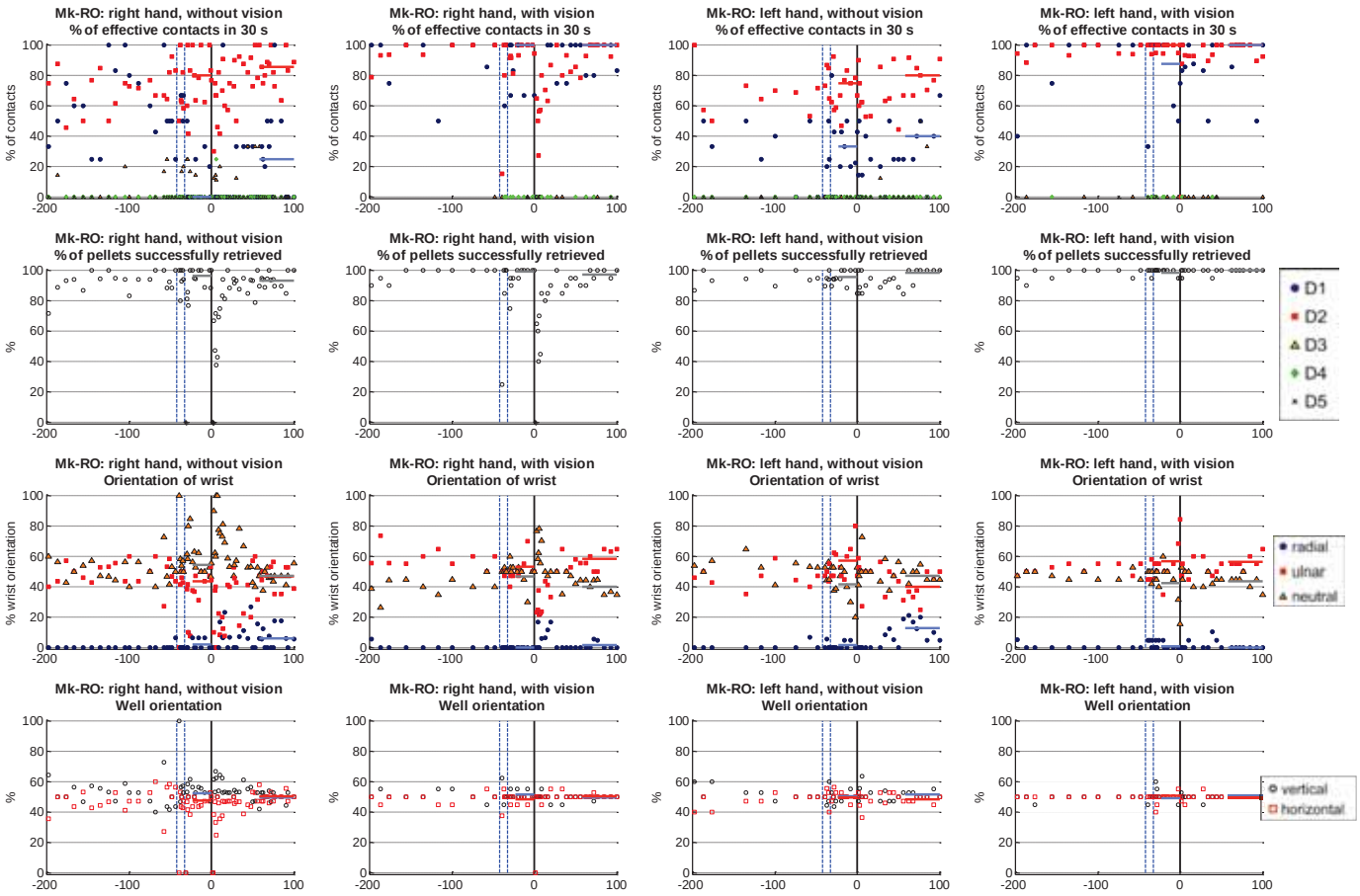
Mk-RO: right hand, without vision
% of effective contacts in 30 s
Mk-RO: right hand, with vision
% of effective contacts in 30 s
Mk-RO: left hand, without vision
% of effective contacts in 30 s
Mk-RO: left hand, with vision
% of effective contacts in 30 s
% of contacts
Mk-RO: right hand, without vision
% of pellets successfully retrieved
Mk-RO: right hand, with vision
% of pellets successfully retrieved
Mk-RO: left hand, without vision
% of pellets successfully retrieved
Mk-RO: left hand, with vision
% of pellets successfully retrieved
%
D1
D2
D3
D4
D5
Mk-RO: right hand, without vision
Orientation of wrist
Mk-RO: right hand, with vision
Orientation of wrist
Mk-RO: left hand, without vision
Orientation of wrist
Mk-RO: left hand, with vision
Orientation of wrist
% wrist orientation
radial
ulnar
neutral
Mk-RO: right hand, without vision
Well orientation
Mk-RO: right hand, with vision
Well orientation
Mk-RO: left hand, without vision
Well orientation
Mk-RO: left hand, with vision
Well orientation
vertical
horizontal

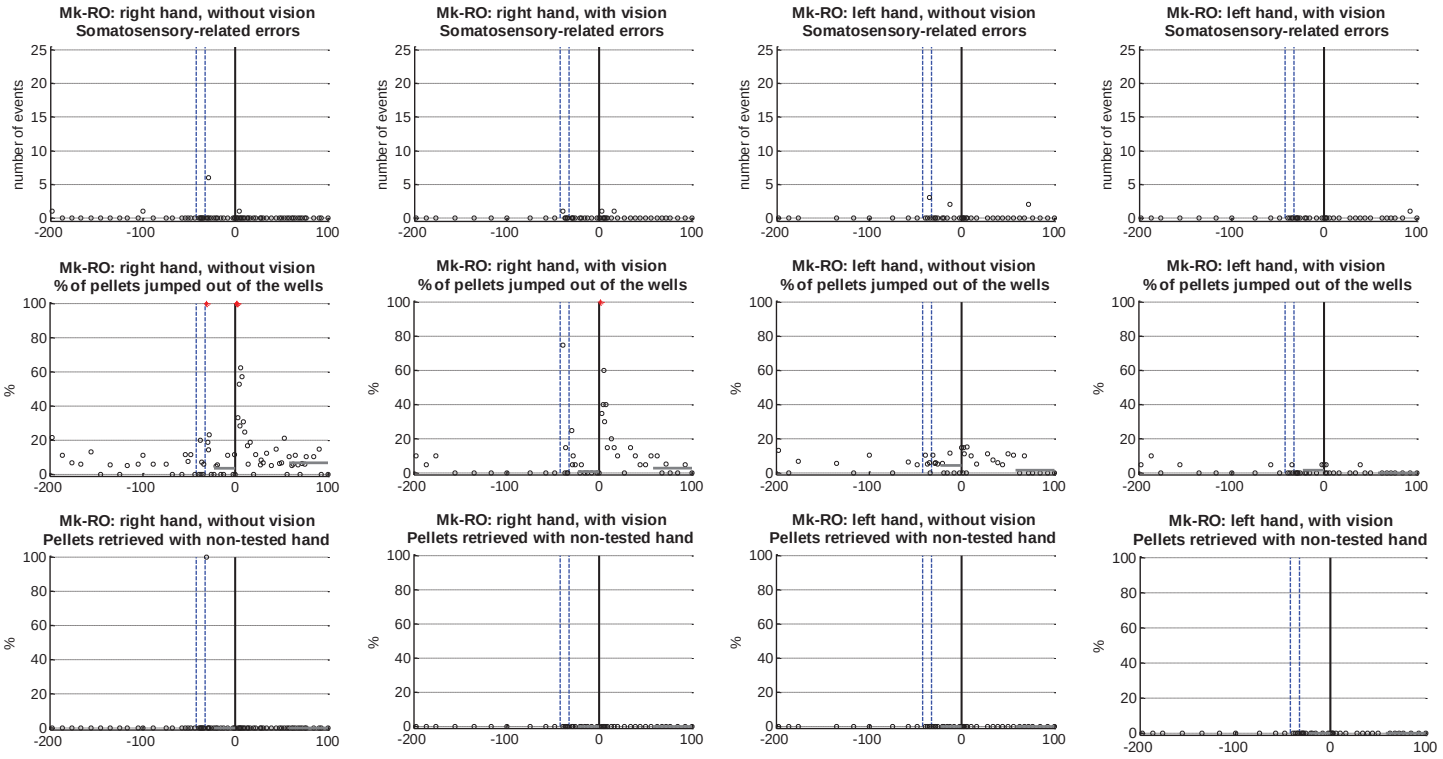
Mk-RO: right hand, without vision
Somatosensory-related errors
Mk-RO: right hand, with vision
Somatosensory-related errors
Mk-RO: left hand, without vision
Somatosensory-related errors
Mk-RO: left hand, with vision
Somatosensory-related errors
number of events
Mk-RO: right hand, without vision
% of pellets jumped out of the wells
Mk-RO: right hand, with vision
% of pellets jumped out of the wells
Mk-RO: left hand, without vision
% of pellets jumped out of the wells
Mk-RO: left hand, with vision
% of pellets jumped out of the wells
%
Mk-RO: right hand, without vision
Pellets retrieved with non-tested hand
Mk-RO: right hand, with vision
Pellets retrieved with non-tested hand
Mk-RO: left hand, without vision
Pellets retrieved with non-tested hand
Mk-RO: left hand, with vision
Pellets retrieved with non-tested hand

G

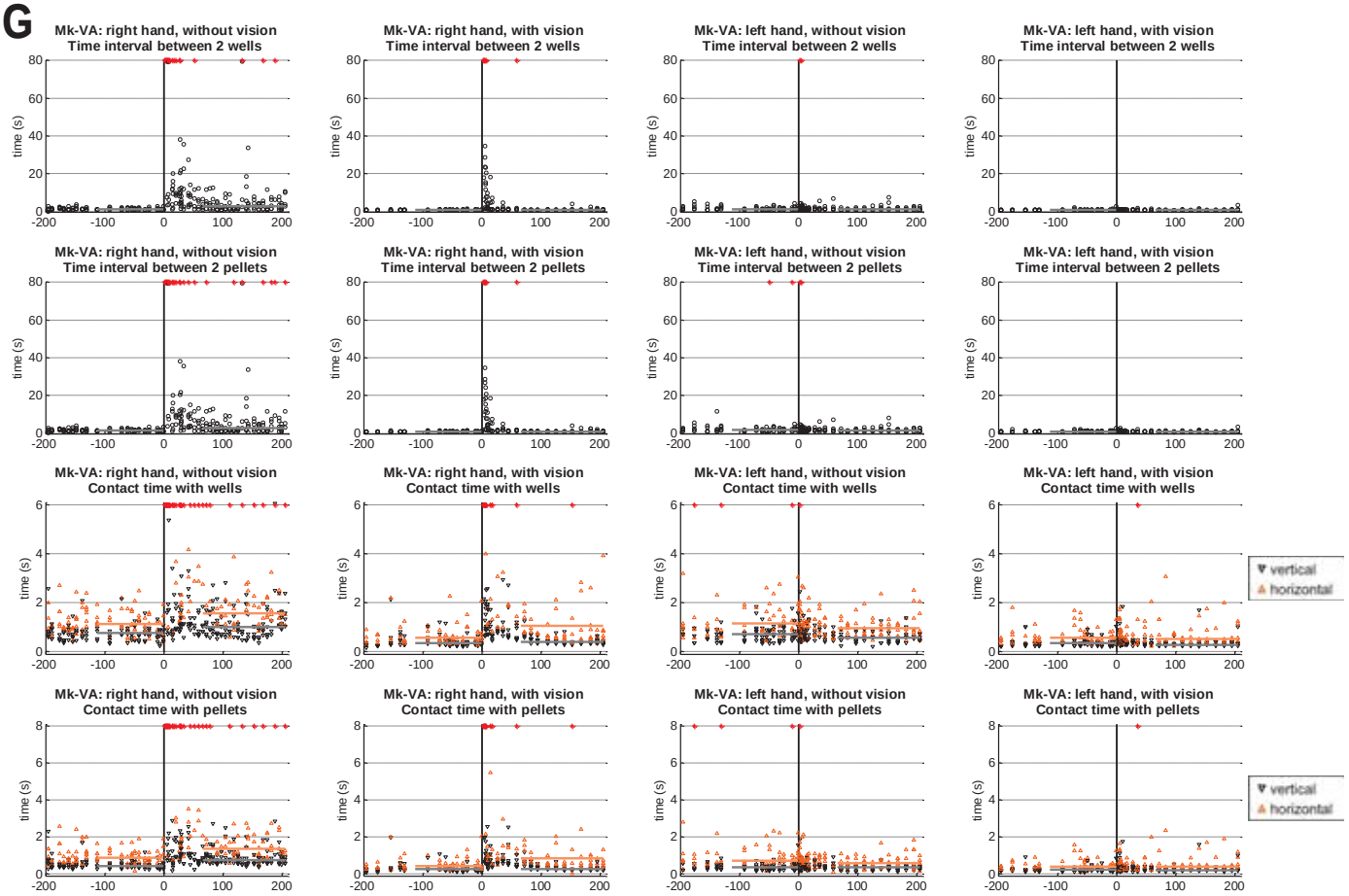
Mk-VA: right hand, without vision
Time interval between 2 wells
Mk-VA: right hand, with vision
Time interval between 2 wells
Mk-VA: left hand, without vision
Time interval between 2 wells
Mk-VA: left hand, with vision
Time interval between 2 wells
Mk-VA: right hand, without vision
Time interval between 2 pellets
Mk-VA: right hand, with vision
Time interval between 2 pellets
Mk-VA: left hand, without vision
Time interval between 2 pellets
Mk-VA: left hand, with vision
Time interval between 2 pellets
Mk-VA: right hand, without vision
Contact time with wells
Mk-VA: right hand, with vision
Contact time with wells
Mk-VA: left hand, without vision
Contact time with wells
Mk-VA: left hand, with vision
Contact time with wells
Mk-VA: right hand, without vision
Contact time with pellets
Mk-VA: right hand, with vision
Contact time with pellets
Mk-VA: left hand, without vision
Contact time with pellets
Mk-VA: left hand, with vision
Contact time with pellets
time (s)
vertical
horizontal

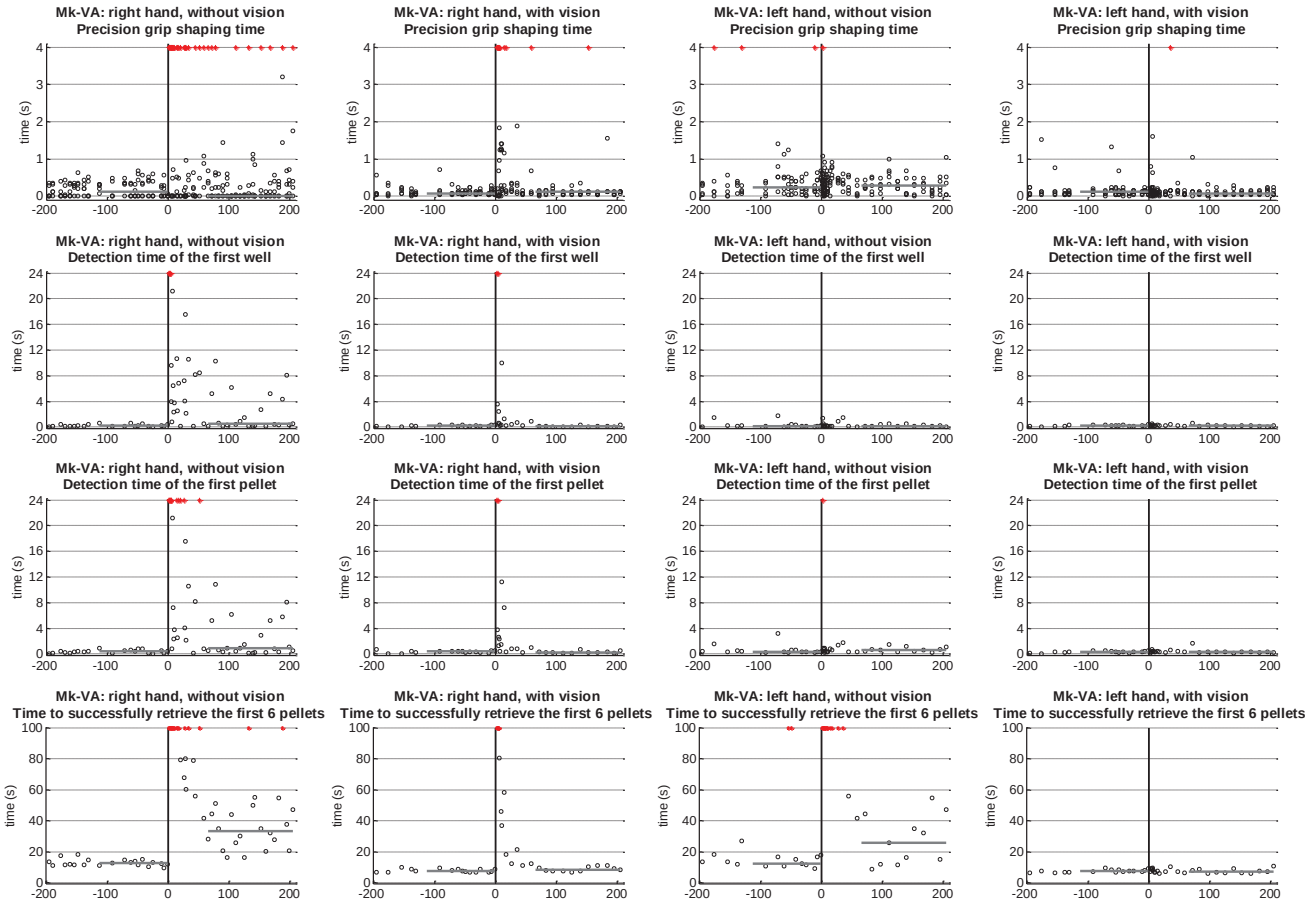
Mk-VA: right hand, without vision
Precision grip shaping time
Mk-VA: right hand, with vision
Precision grip shaping time
Mk-VA: left hand, without vision
Precision grip shaping time
Mk-VA: left hand, with vision
Precision grip shaping time
Mk-VA: right hand, without vision
Detection time of the first well
Mk-VA: right hand, with vision
Detection time of the first well
Mk-VA: left hand, without vision
Detection time of the first well
Mk-VA: left hand, with vision
Detection time of the first well
Mk-VA: right hand, without vision
Detection time of the first pellet
Mk-VA: right hand, with vision
Detection time of the first pellet
Mk-VA: left hand, without vision
Detection time of the first pellet
Mk-VA: left hand, with vision
Detection time of the first pellet
Mk-VA: right hand, without vision
Time to successfully retrieve the first 6 pellets
Mk-VA: right hand, with vision
Time to successfully retrieve the first 6 pellets
Mk-VA: left hand, without vision
Time to successfully retrieve the first 6 pellets
Mk-VA: left hand, with vision
Time to successfully retrieve the first 6 pellets
time (s)

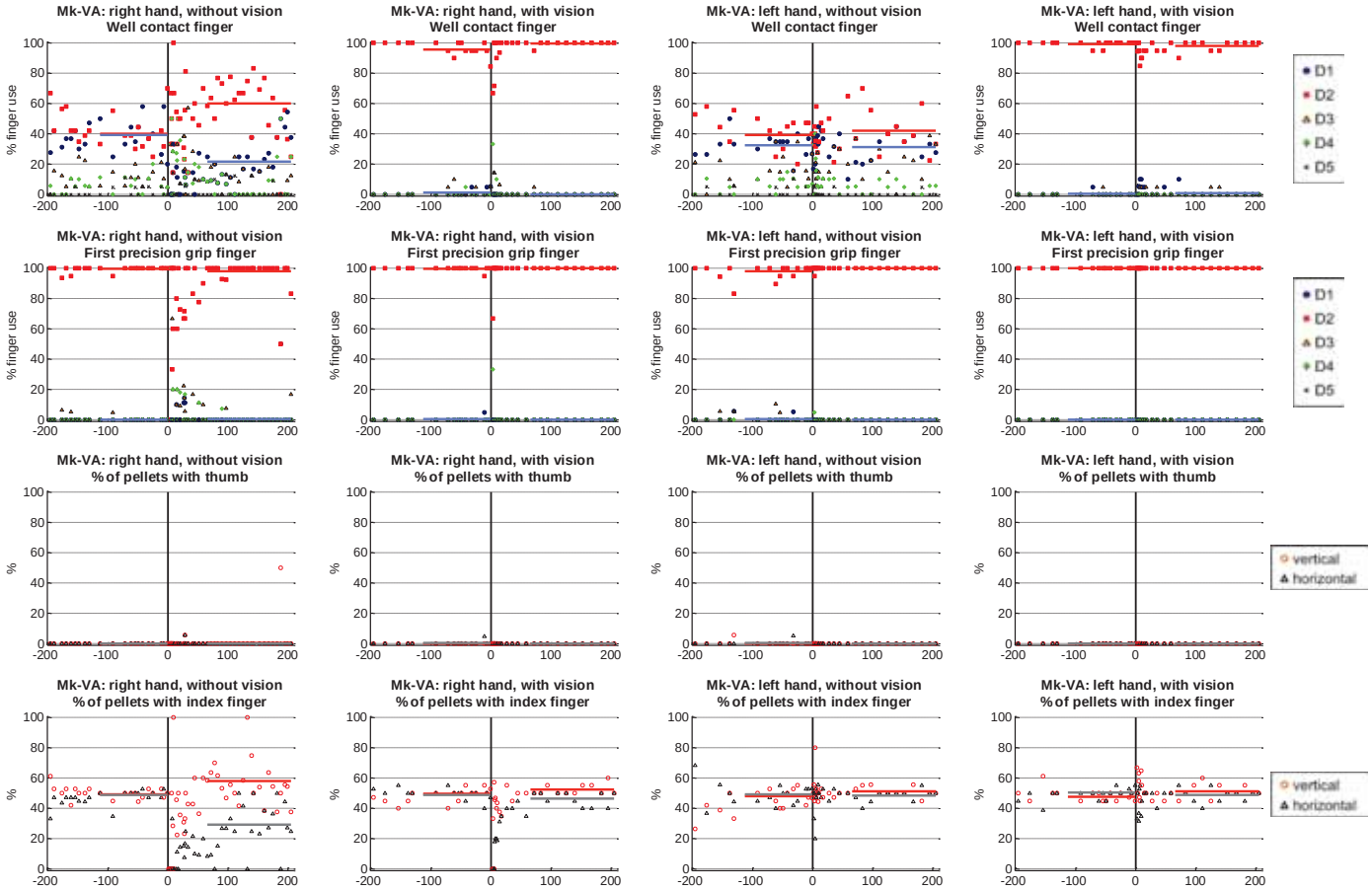
Mk-VA: right hand, without vision
Well contact finger
Mk-VA: right hand, with vision
Well contact finger
Mk-VA: left hand, without vision
Well contact finger
Mk-VA: left hand, with vision
Well contact finger
% finger use
D1
D2
D3
D4
D5
Mk-VA: right hand, without vision
First precision grip finger
Mk-VA: right hand, with vision
First precision grip finger
Mk-VA: left hand, without vision
First precision grip finger
Mk-VA: left hand, with vision
First precision grip finger
Mk-VA: right hand, without vision
% of pellets with thumb
Mk-VA: right hand, with vision
% of pellets with thumb
Mk-VA: left hand, without vision
% of pellets with thumb
Mk-VA: left hand, with vision
% of pellets with thumb
%
vertical
horizontal
Mk-VA: right hand, without vision
% of pellets with index finger
Mk-VA: right hand, with vision
% of pellets with index finger
Mk-VA: left hand, without vision
% of pellets with index finger
Mk-VA: left hand, with vision
% of pellets with index finger

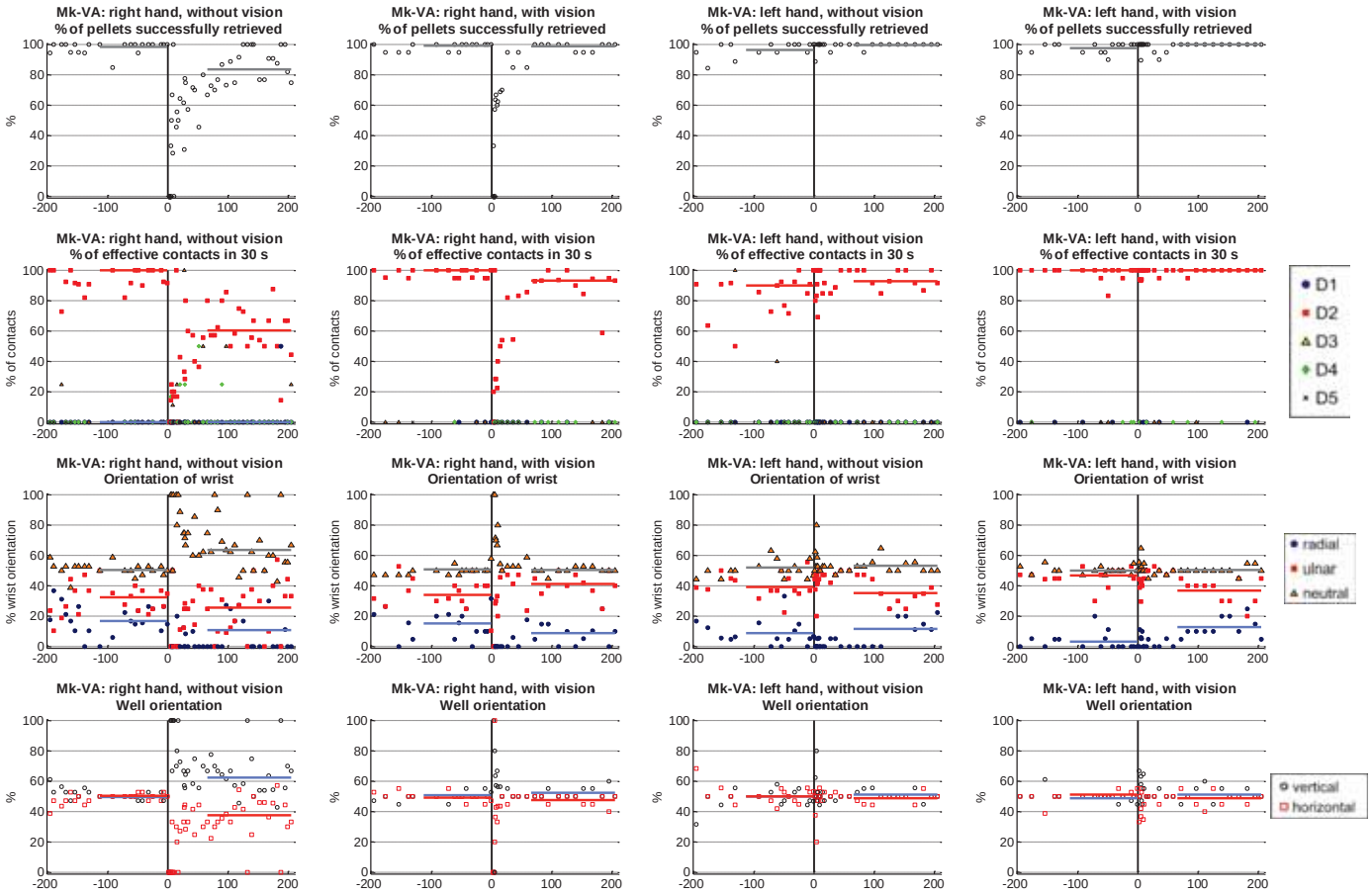
Mk-VA: right hand, without vision
% of pellets successfully retrieved
Mk-VA: right hand, with vision
% of pellets successfully retrieved
Mk-VA: left hand, without vision
% of pellets successfully retrieved
Mk-VA: left hand, with vision
% of pellets successfully retrieved
Mk-VA: right hand, without vision
% of effective contacts in 30 s
Mk-VA: right hand, with vision
% of effective contacts in 30 s
Mk-VA: left hand, without vision
% of effective contacts in 30 s
Mk-VA: left hand, with vision
% of effective contacts in 30 s
Mk-VA: right hand, without vision
Orientation of wrist
Mk-VA: right hand, with vision
Orientation of wrist
Mk-VA: left hand, without vision
Orientation of wrist
Mk-VA: left hand, with vision
Orientation of wrist
Mk-VA: right hand, without vision
Well orientation
Mk-VA: right hand, with vision
Well orientation
Mk-VA: left hand, without vision
Well orientation
Mk-VA: left hand, with vision
Well orientation
%
% of contacts
% wrist orientation
D1
D2
D3
D4
D5
radial
ulnar
neutral
vertical
horizontal

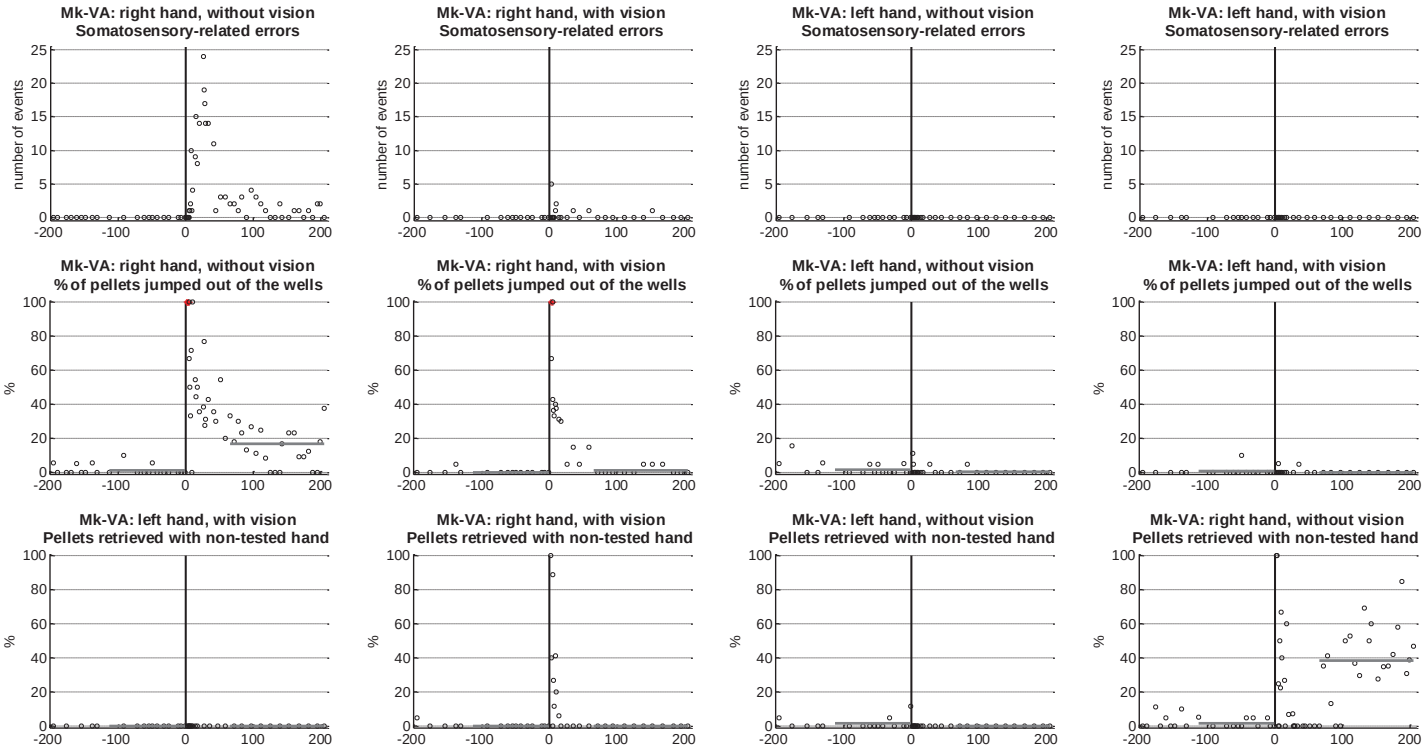
Mk-VA: right hand, without vision
Somatosensory-related errors
Mk-VA: right hand, with vision
Somatosensory-related errors
Mk-VA: left hand, without vision
Somatosensory-related errors
Mk-VA: left hand, with vision
Somatosensory-related errors
number of events
Mk-VA: right hand, without vision
% of pellets jumped out of the wells
Mk-VA: right hand, with vision
% of pellets jumped out of the wells
Mk-VA: left hand, without vision
% of pellets jumped out of the wells
Mk-VA: left hand, with vision
% of pellets jumped out of the wells
%
Mk-VA: left hand, with vision
Pellets retrieved with non-tested hand
Mk-VA: right hand, with vision
Pellets retrieved with non-tested hand
Mk-VA: left hand, without vision
Pellets retrieved with non-tested hand
Mk-VA: right hand, without vision
Pellets retrieved with non-tested hand

Supplementary Figure 2 (next 7 pages): Colour-coded sequences of pellet picking for each monkey (A to G), each hand, in the task without vision and in the task with vision. The x-axis represents the time in sessions: each column corresponds to one behavioural session and each collected pellet is a circle whose colour indicates its position in the temporal sequence of picking. The first collected pellets are the bluemost and the last collected pellets are the redmost. The temporal sequence of pellet picking was analysed according to a left-right gradient (left column) and an up-down gradient (right column), expressed on the y-axis. Thick vertical black line: day at lesion; dashed vertical red line: time at dlPFC biopsy (Mk-AV, Mk-JO); dashed vertical black line: time at cell/sham reimplantation (Mk-AV, Mk-JA, Mk-JO); dotted vertical blue line: previous lesions (Mk-RO).

(A) Mk-AV (p. 540): sham cell therapy

(B) Mk-DI (p. 541): no treatment

(C) Mk-GE (p. 542): no treatment

(D) Mk-JA (p. 543): cell therapy

(E) Mk-JO (p. 544): cell therapy

(F) Mk-RO (p. 545): no treatment

(G) Mk-VA (p. 546): anti-Nogo-A antibody

Supplementary Figure 2

A

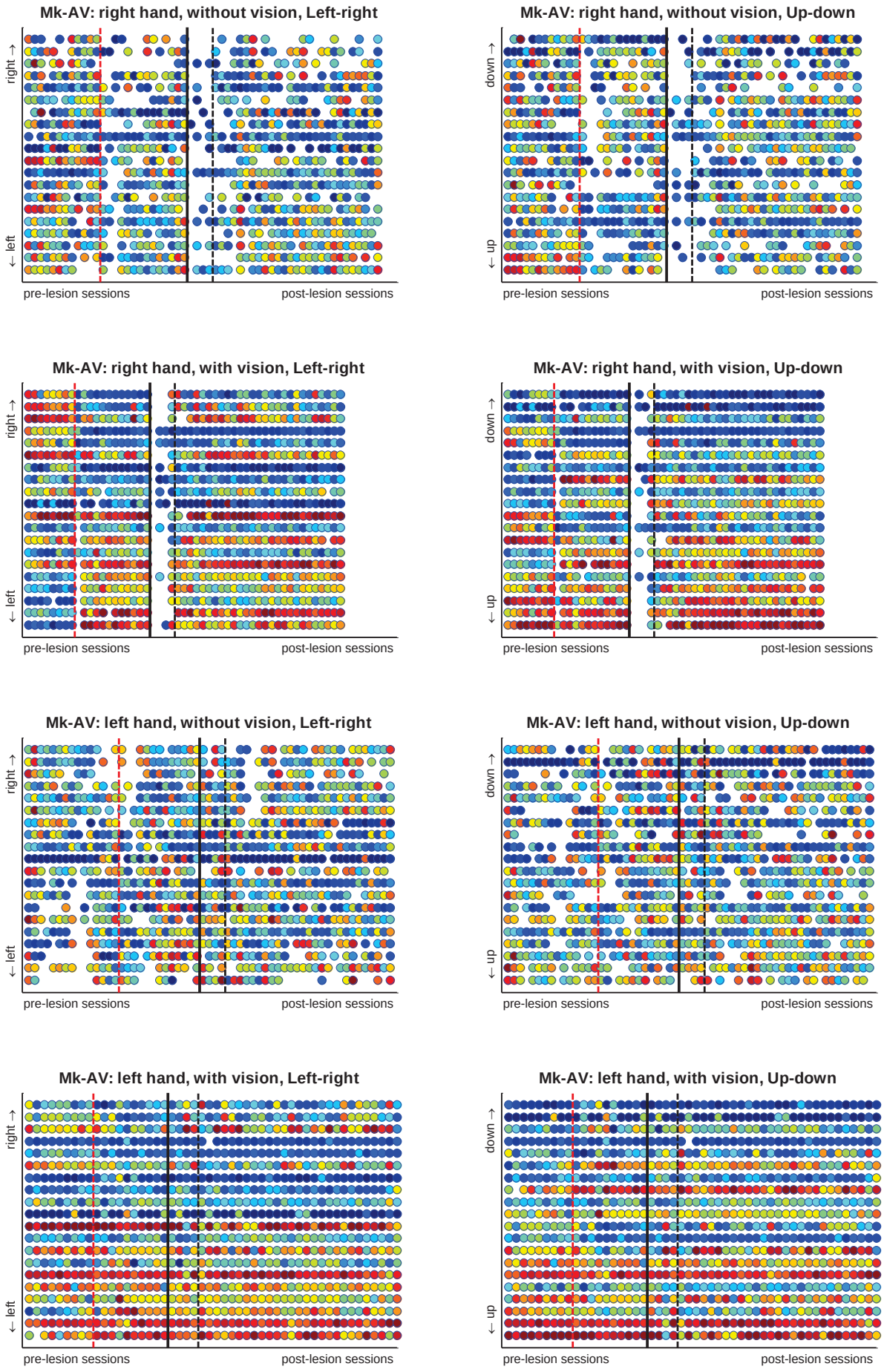

B

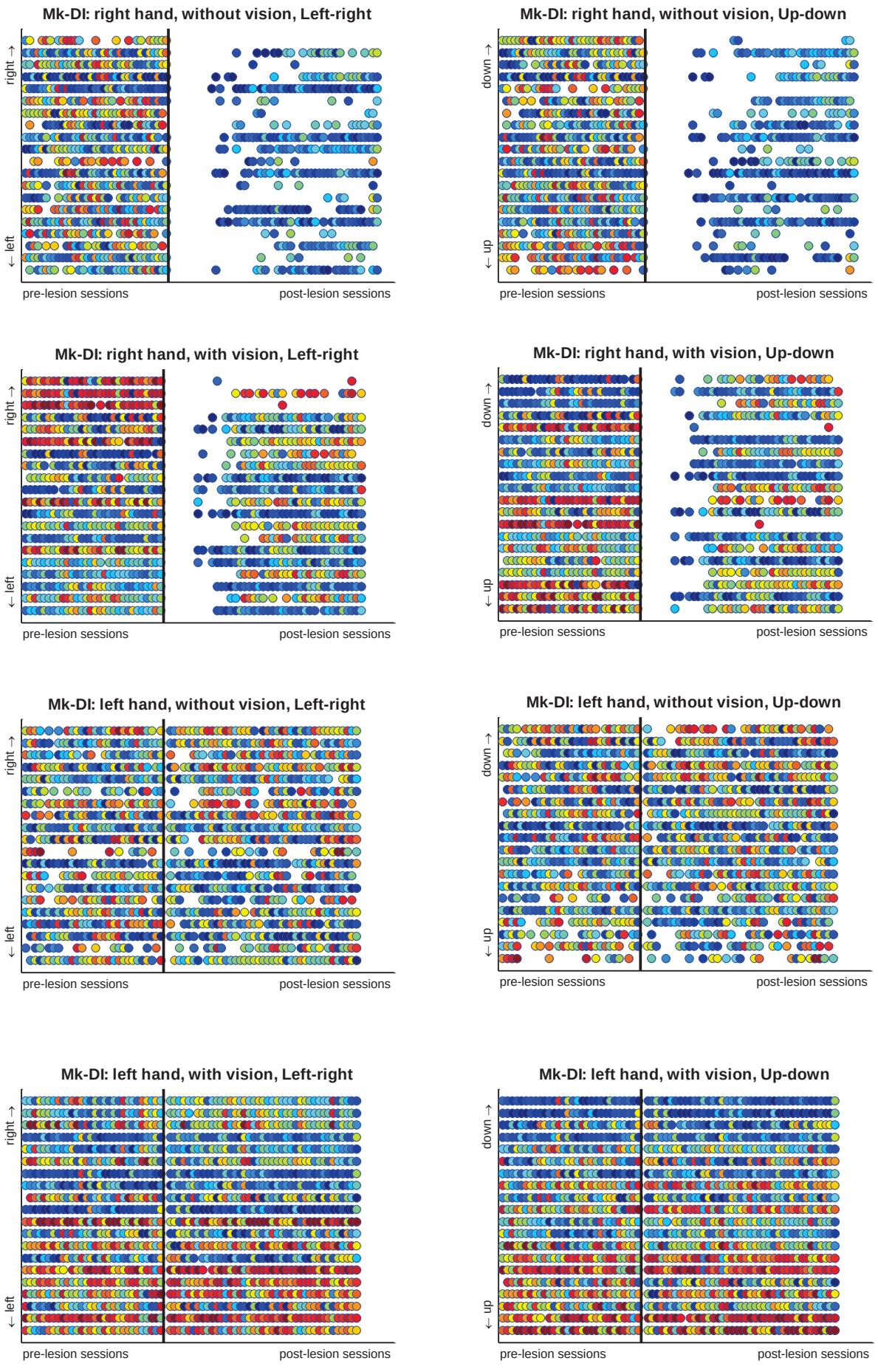
Mk-DI: right hand, without vision, Left-right
Mk-DI: right hand, without vision, Up-down
Mk-DI: right hand, with vision, Left-right
Mk-DI: right hand, with vision, Up-down
Mk-DI: left hand, without vision, Left-right
Mk-DI: left hand, without vision, Up-down
Mk-DI: left hand, with vision, Left-right
Mk-DI: left hand, with vision, Up-down
right →
← left
down →
← up
pre-lesion sessions
post-lesion sessions
lesion
previous lesion
biopsy
cell/sham reimplantation
1
5
10
15
20
picking sequence

C

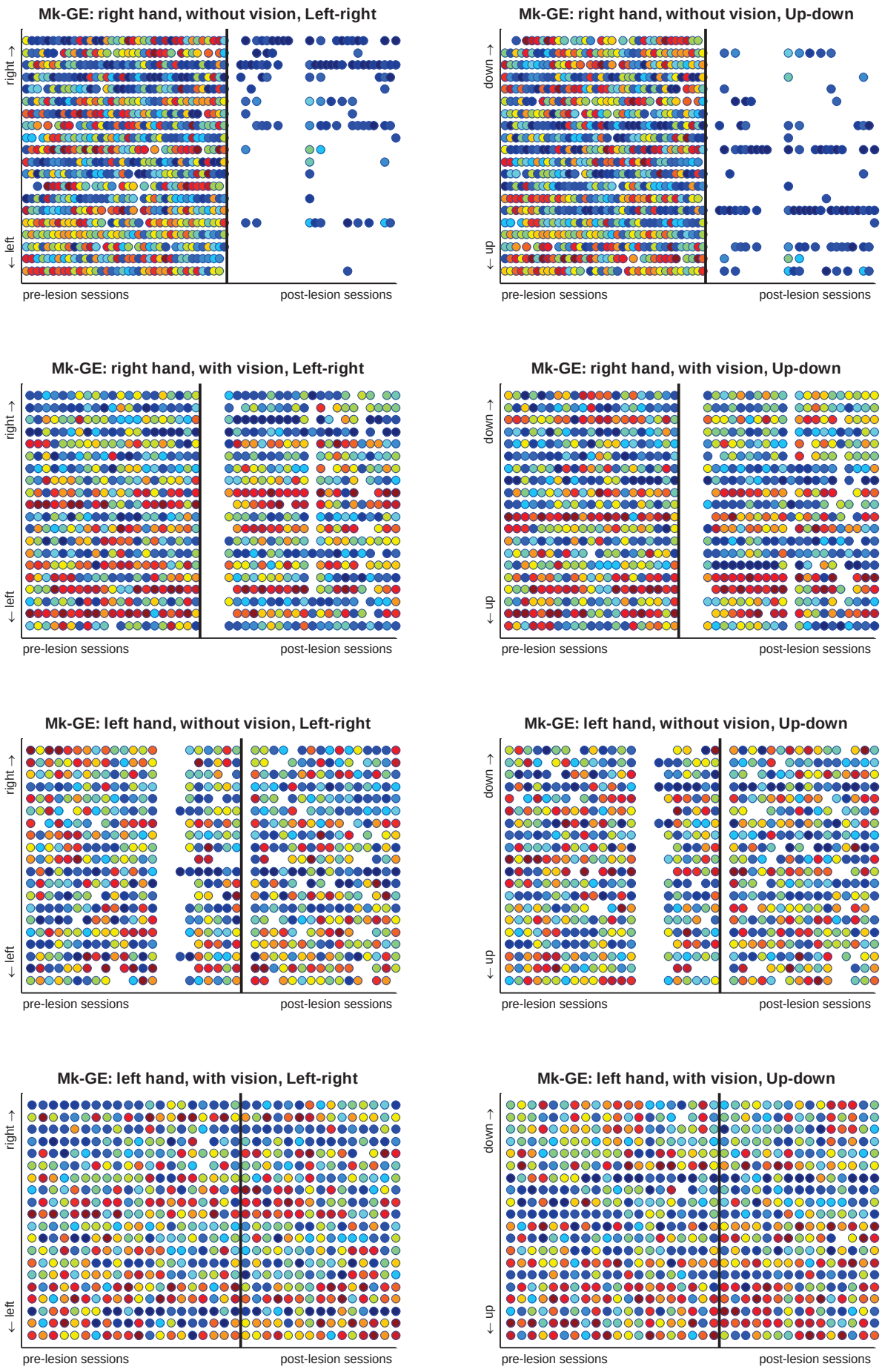
Mk-GE: right hand, without vision, Left-right
right →
← left
pre-lesion sessions
post-lesion sessions
Mk-GE: right hand, without vision, Up-down
down →
← up
pre-lesion sessions
post-lesion sessions
Mk-GE: right hand, with vision, Left-right
right →
← left
pre-lesion sessions
post-lesion sessions
Mk-GE: right hand, with vision, Up-down
down →
← up
pre-lesion sessions
post-lesion sessions
Mk-GE: left hand, without vision, Left-right
right →
← left
pre-lesion sessions
post-lesion sessions
Mk-GE: left hand, without vision, Up-down
down →
← up
pre-lesion sessions
post-lesion sessions
Mk-GE: left hand, with vision, Left-right
right →
← left
pre-lesion sessions
post-lesion sessions
Mk-GE: left hand, with vision, Up-down
down →
← up
pre-lesion sessions
post-lesion sessions
lesion
previous lesion
biopsy
cell/sham reimplantation
1
5
10
15
20
picking sequence

D

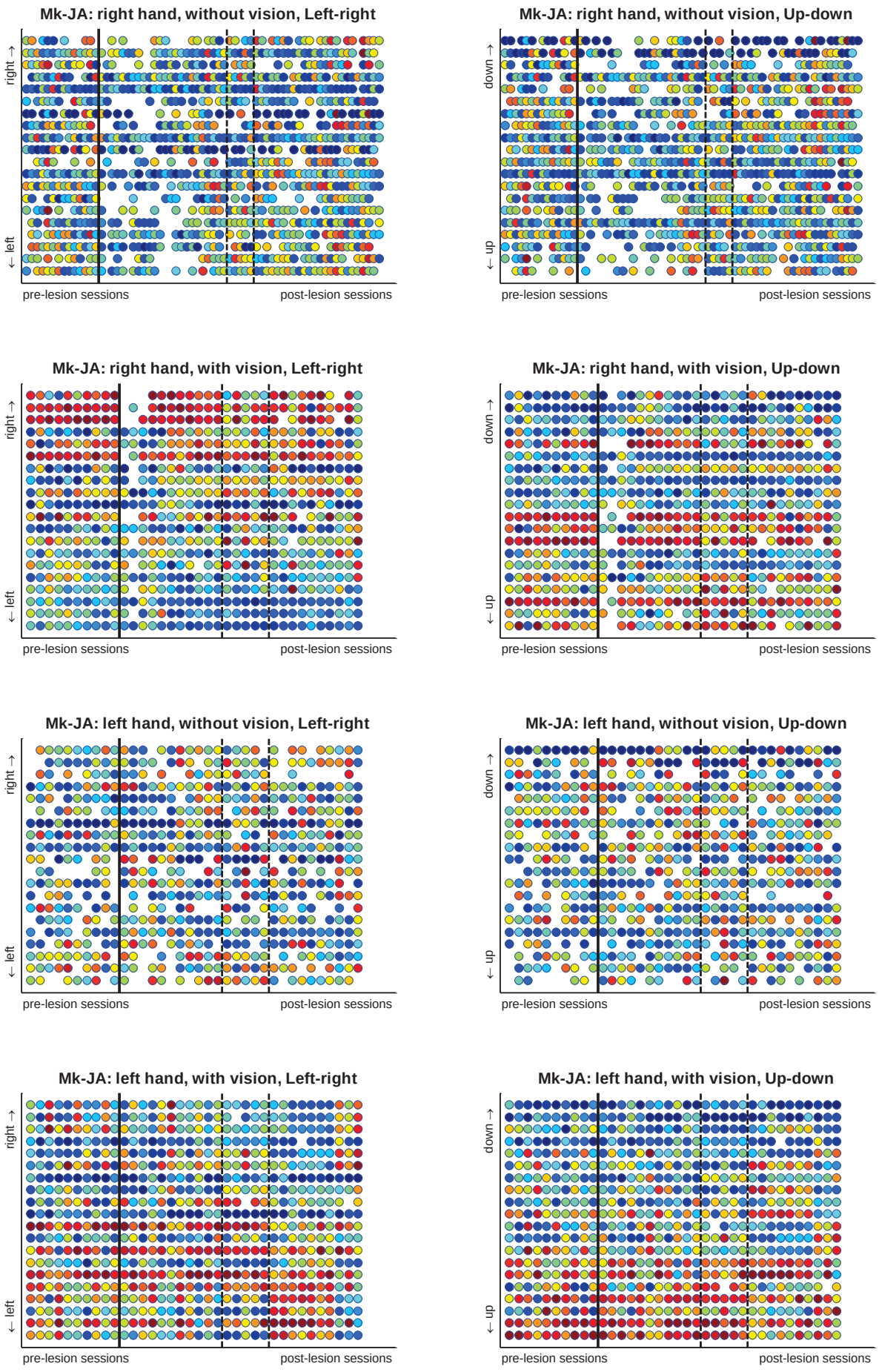
Mk-JA: right hand, without vision, Left-right
Mk-JA: right hand, without vision, Up-down
Mk-JA: right hand, with vision, Left-right
Mk-JA: right hand, with vision, Up-down
Mk-JA: left hand, without vision, Left-right
Mk-JA: left hand, without vision, Up-down
Mk-JA: left hand, with vision, Left-right
Mk-JA: left hand, with vision, Up-down
right →
← left
down →
← up
pre-lesion sessions
post-lesion sessions
lesion
previous lesion
biopsy
cell/sham reimplantation
1
5
10
15
20
picking sequence

E

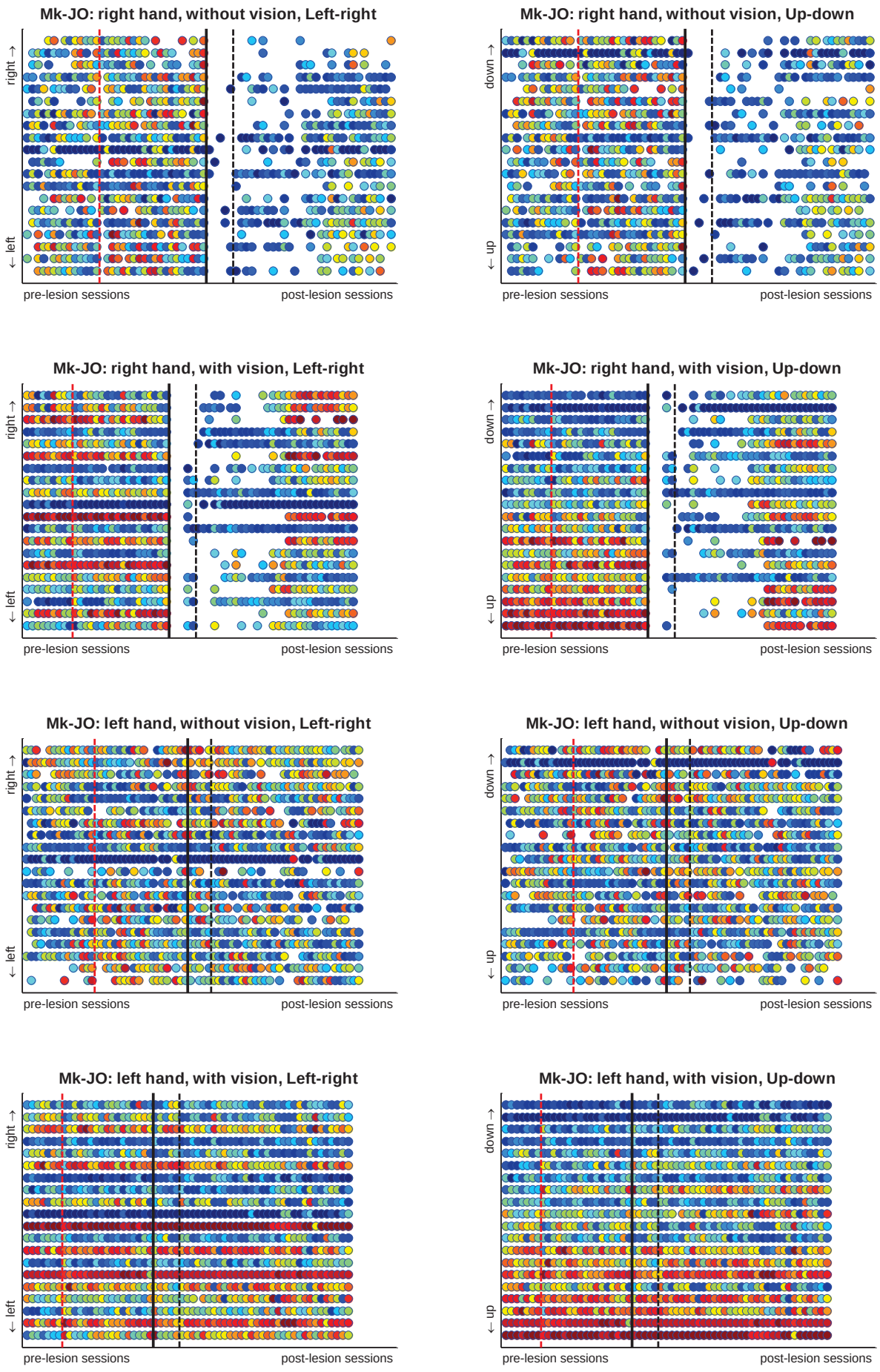
Mk-JO: right hand, without vision, Left-right
Mk-JO: right hand, without vision, Up-down
Mk-JO: right hand, with vision, Left-right
Mk-JO: right hand, with vision, Up-down
Mk-JO: left hand, without vision, Left-right
Mk-JO: left hand, without vision, Up-down
Mk-JO: left hand, with vision, Left-right
Mk-JO: left hand, with vision, Up-down
right →
← left
down →
← up
pre-lesion sessions
post-lesion sessions
lesion
previous lesion
biopsy
cell/sham reimplantation
1
5
10
15
20
picking sequence

F

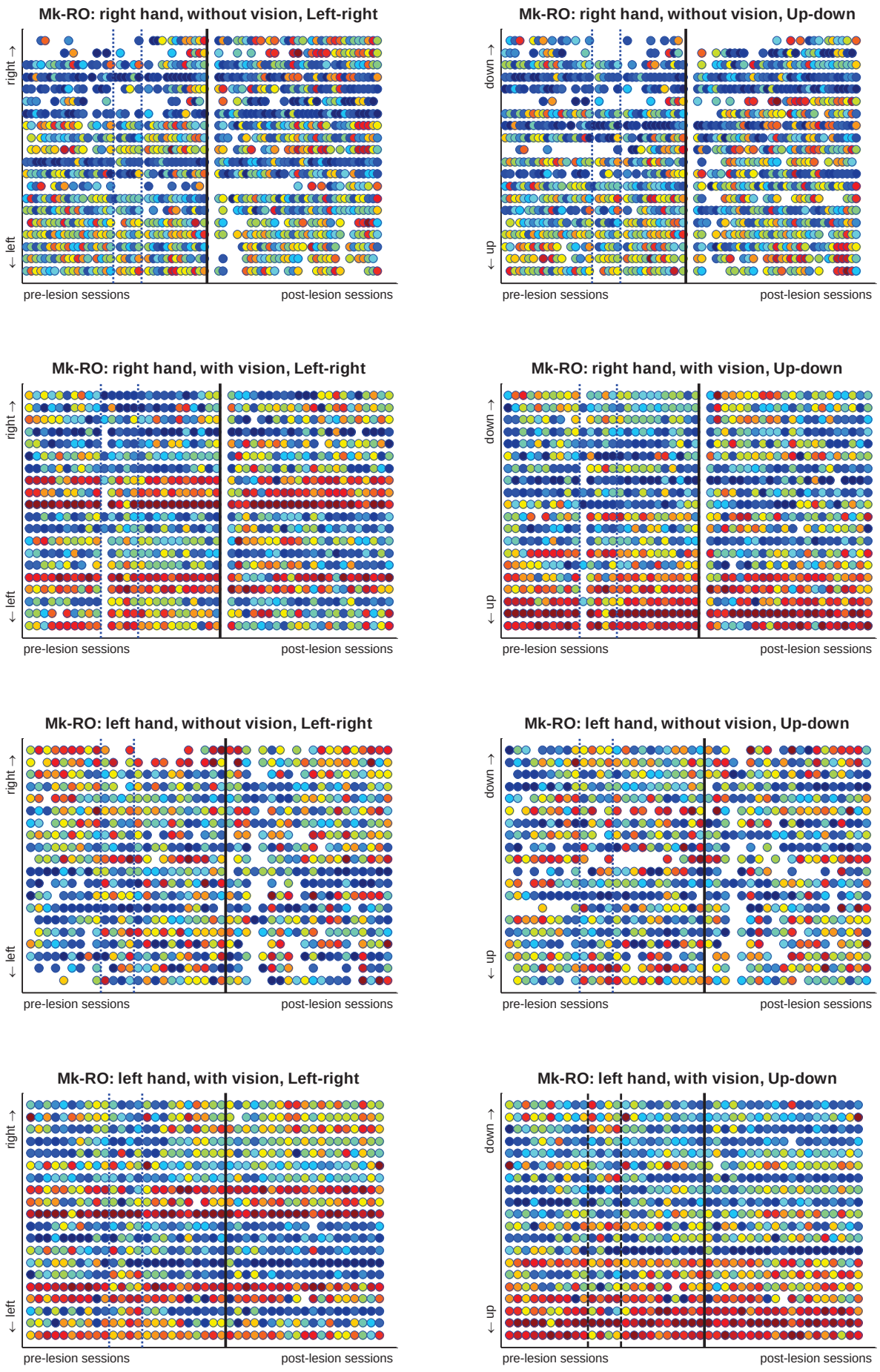
Mk-RO: right hand, without vision, Left-right
Mk-RO: right hand, without vision, Up-down
Mk-RO: right hand, with vision, Left-right
Mk-RO: right hand, with vision, Up-down
Mk-RO: left hand, without vision, Left-right
Mk-RO: left hand, without vision, Up-down
Mk-RO: left hand, with vision, Left-right
Mk-RO: left hand, with vision, Up-down
right →
← left
down →
← up
pre-lesion sessions
post-lesion sessions
lesion
previous lesion
biopsy
cell/sham reimplantation
1
5
10
15
20
picking sequence

G

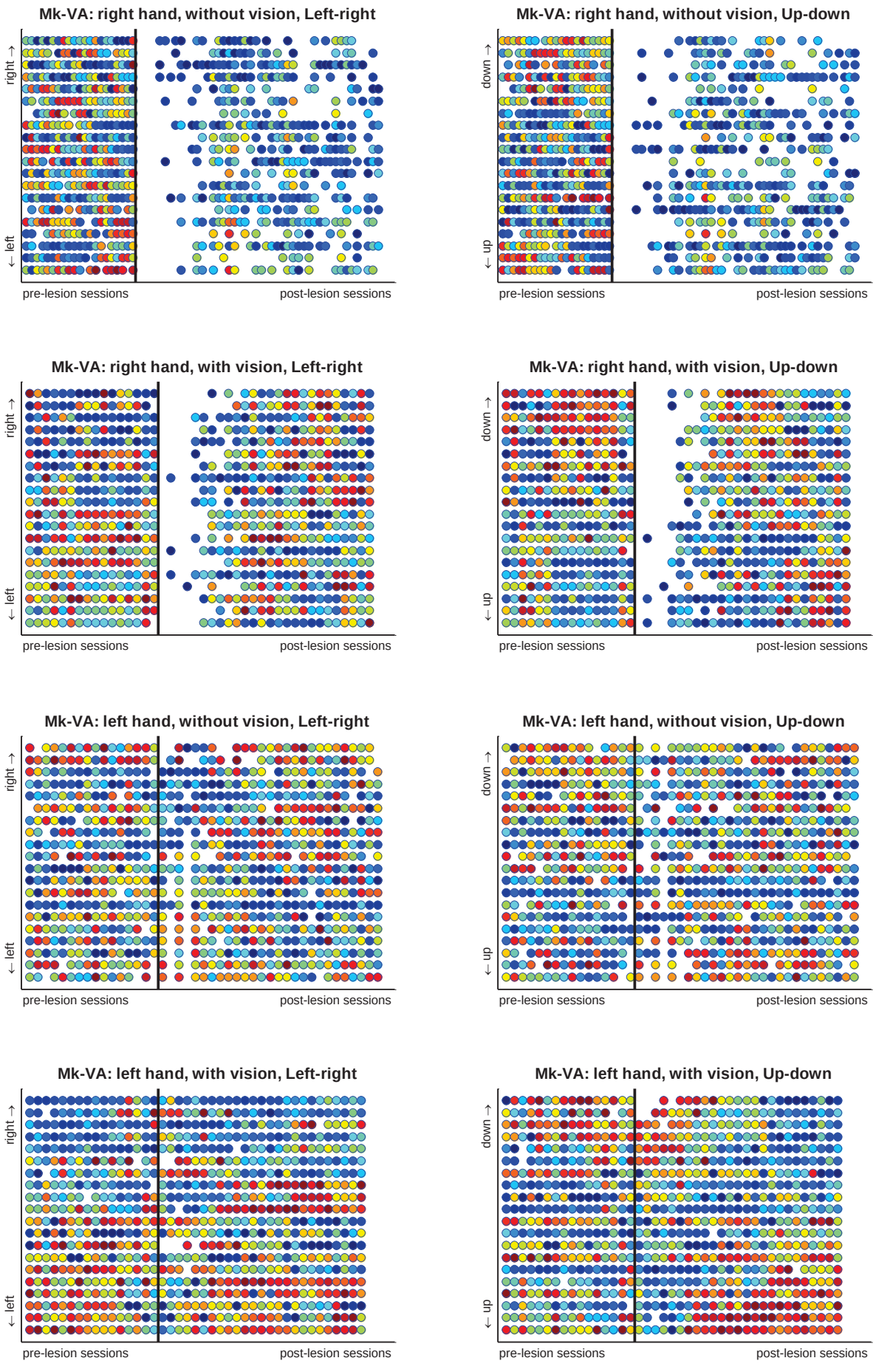
Mk-VA: right hand, without vision, Left-right
right →
← left
pre-lesion sessions
post-lesion sessions
Mk-VA: right hand, without vision, Up-down
down →
← up
pre-lesion sessions
post-lesion sessions
Mk-VA: right hand, with vision, Left-right
right →
← left
pre-lesion sessions
post-lesion sessions
Mk-VA: right hand, with vision, Up-down
down →
← up
pre-lesion sessions
post-lesion sessions
Mk-VA: left hand, without vision, Left-right
right →
← left
pre-lesion sessions
post-lesion sessions
Mk-VA: left hand, without vision, Up-down
down →
← up
pre-lesion sessions
post-lesion sessions
Mk-VA: left hand, with vision, Left-right
right →
← left
pre-lesion sessions
post-lesion sessions
Mk-VA: left hand, with vision, Up-down
down →
← up
pre-lesion sessions
post-lesion sessions
lesion
previous lesion
biopsy
cell/sham reimplantation
1
5
10
15
20
picking sequence

Impact of the lesion on ipsilesional manual dexterity

Already a quick inspection of the graphs of the individual behavioural parameters in each monkey (**Supplementary Figures 1** and **2**) shows that the effects of the lesion on the ipsilesional, left hand in both conditions were usually much less prominent and only transient as compared to the contralesional hand. Nevertheless, there are many reports that a brain lesion may influence the motor control of the ipsilesional body side as well, inducing either an improvement (Kaeser et al., 2010; Luke et al., 2004; Nakayma et al., 1994; Olsen, 1989; Pohl and Winstein, 1999) or an impairment of motor function (Bashir et al., 2012; Desrosiers et al., 1996; Hermsdörfer et al., 1999a; Hermsdörfer et al., 1999b; Higgins et al., 2005; Pandian and Arya, 2013; Pizzimenti et al., 2007; Vaughan and Costa, 1962).

Based on these observations, we computed correlations between the volume of the lesion and the post-lesion recovery assessed with the different parameters for the ipsilesional, left hand, similarly to what we did for the contralesional, right hand. As expected, the impact of the cortical lesion was much less obvious on the ipsilesional manual dexterity than on the contralesional one.

When the task was performed without vision, the only very clear correlations that emerged from the data were linked to the orientation of visited wells. Essentially, we observed that animals with a large lesion visited less often *vertical wells* ($R = -0.91$, $p = 0.005$) (**Supplementary Figure 3A**) in favour of *horizontal wells* ($R = 0.91$, $p = 0.004$) (**Supplementary Figure 3B**) with their ipsilesional hand after the lesion. Conversely, the less extended the lesion was, the more often the animals visited the vertical wells to the detriment of the horizontal ones. Another interesting negative correlation was observed between the volume of the lesion and the post-lesion/pre-lesion occurrence of the *neutral position of the wrist* ($R = -0.8$, $p = 0.032$) (**Supplementary Figure 3C**): the less extended the lesion was, the more often the monkeys relied on their ipsilesional wrist in neutral position after the lesion as compared to before the lesion. Conversely, the two monkeys with the largest lesions favoured less often the use of the wrist in neutral position after the lesion.

In the task with vision, a single correlation appeared, namely between the volume of the lesion and the post-lesion/pre-lesion performance of the *index finger to detect the wells* during exploration. Briefly, the larger the lesion, the more often the animals interacted

with their ipsilesional index finger to detect the wells after the lesion as compared to before the lesion (R =0.88, p =0.01). Conversely, monkeys with a small lesion relied less on their left index finger to detect the wells after the lesion (**Supplementary Figure 3D**).

Simply put, we suggest that monkeys with a large lesion allotted less resource after the lesion than before the lesion to perform not very challenging behaviours (visiting vertical wells, neutral wrist position) with their intact hand in favour of more challenging motor control (visiting horizontal wells, ulnar wrist deviation although this latter correlation was not significant (R =0.71, p =0.076)). Conversely, animals with a small lesion used more often after the lesion than before the lesion their intact hand to perform effortless behaviours. Nevertheless, the effects of the lesion on ipsilesional behaviour were much less prominent than those observed on the contralesional hand.

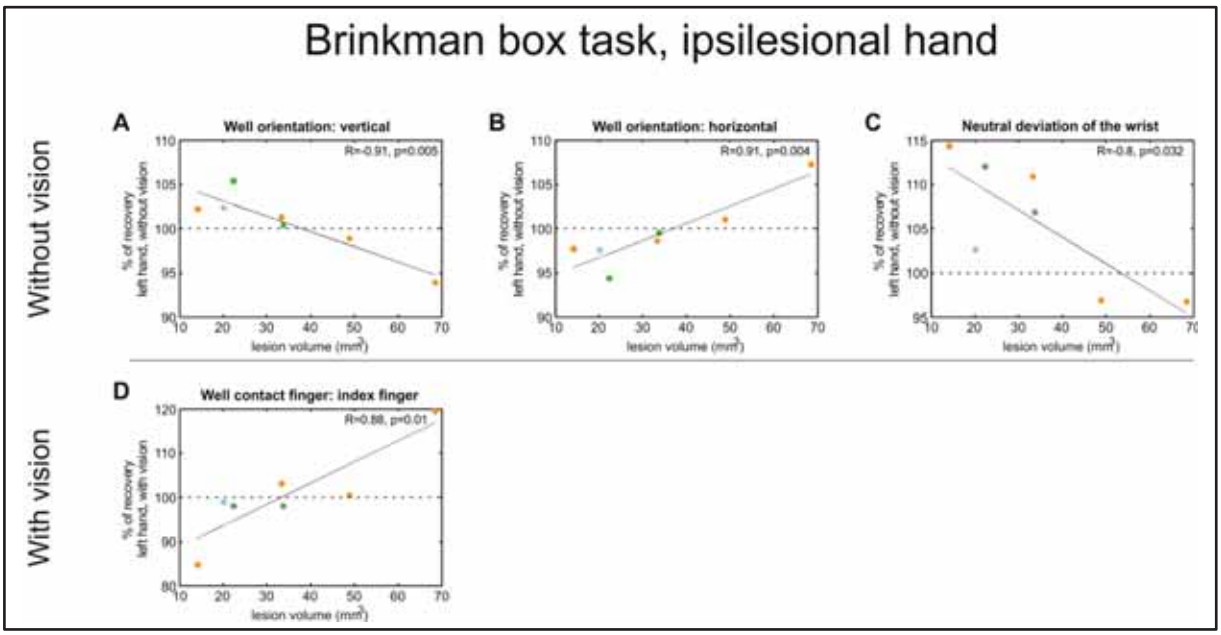

Supplementary Figure 3: Impact of the cortical lesion on the fine manual dexterity of the ipsilesional, left hand in the Brinkman box task without vision (A-C) and with vision (D) in all animals, in the form of linear regressions between the volume of the lesion (mm^3) and the post-lesion/pre-lesion (A) ability to visit vertical wells, (B) ability to visit horizontal wells, (C) occurrence of neutral deviations of the wrist, (D) ability to use the index finger to detect the wells. Same conventions as in Figure 7.

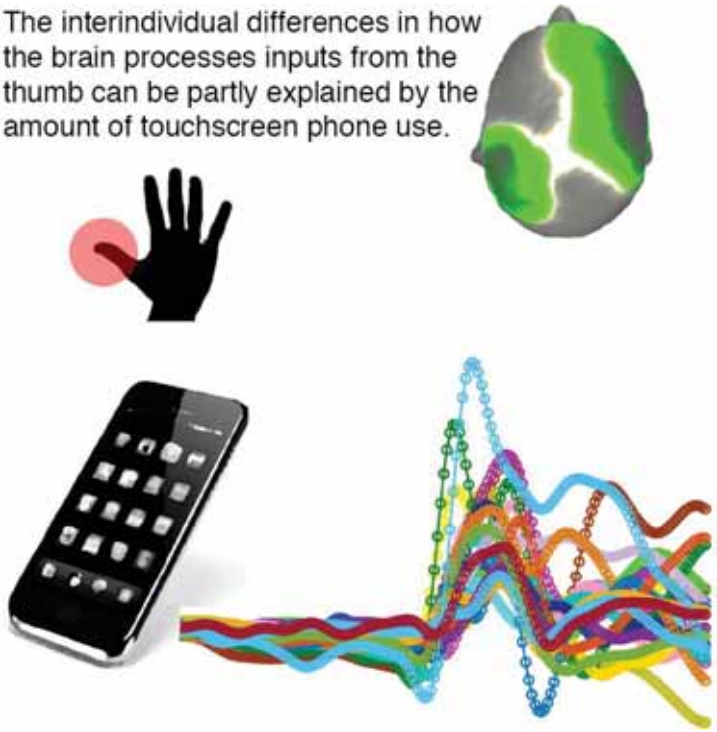

CHAPTER 6

Use-Dependent Cortical Processing from Fingertips in Touchscreen Phone Users

Gindrat AD*, Chytiris M*, Balerna M*, Rouiller EM, Ghosh A (2015). Current Biology 25(1):1-8. DOI: 10.1016/j.cub.2014.11.026

L'utilisation de smartphones façonne le traitement cortical de l'information sensorielle tactile provenant de l'extrémité des doigts. Med Sci (Paris) 31(4):363-366. DOI: 10.1051/medsci/20153104006

* Equal first authorship

Author Contributions

A.-D.G., M.C., M.B., and A.G. collected the data and performed preliminary analysis. A.G. performed formal analysis and drafted the report, and **A.-D.G.**, M.C., M.B., and E.M.R. edited its contents. A.G. provided the study concept, and **A.-D.G.**, E.M.R., and A.G. designed the experiments.

Please cite this article in press as: Gindrat et al., Use-Dependent Cortical Processing from Fingertips in Touchscreen Phone Users, Current Biology (2015), http://dx.doi.org/10.1016/j.cub.2014.11.026

Current Biology *25*, 1–8, January 5, 2015 ©2015 Elsevier Ltd All rights reserved http://dx.doi.org/10.1016/j.cub.2014.11.026

Report

Use-Dependent Cortical Processing from Fingertips in Touchscreen Phone Users

Anne-Dominique Gindrat,[1,5] Magali Chytiris,[1,2,5] Myriam Balerna,[1,2,5] Eric M. Rouiller,[1] and Arko Ghosh[2,3,4,*]
[1]Domain of Physiology, Fribourg Cognition Center, Department of Medicine, University of Fribourg, Chemin du Musée 5, Fribourg 1700, Switzerland
[2]Institute of Neuroinformatics, University of Zurich and ETH Zurich, Winterthurerstrasse 190, Zurich 8057, Switzerland
[3]Neuroscience Center Zurich, University of Zurich and ETH Zurich, Winterthurerstrasse 190, Zurich 8057, Switzerland
[4]Institute of Cognitive Neuroscience, University College London, 17 Queen Square, London WC1N 3AR, UK

Summary

Cortical activity allotted to the tactile receptors on fingertips conforms to skilful use of the hand [1–3]. For instance, in string instrument players, the somatosensory cortical activity in response to touch on the little fingertip is larger than that in control subjects [1]. Such plasticity of the fingertip sensory representation is not limited to extraordinary skills and occurs in monkeys trained to repetitively grasp and release a handle as well [4]. Touchscreen phones also require repetitive finger movements, but whether and how the cortex conforms to this is unknown. By using electroencephalography (EEG), we measured the cortical potentials in response to mechanical touch on the thumb, index, and middle fingertips of touchscreen phone users and nonusers (owning only old-technology mobile phones). Although the thumb interacted predominantly with the screen, the potentials associated with the three fingertips were enhanced in touchscreen users compared to nonusers. Within the touchscreen users, the cortical potentials from the thumb and index fingertips were directly proportional to the intensity of use quantified with built-in battery logs. Remarkably, the thumb tip was sensitive to the day-to-day fluctuations in phone use: the shorter the time elapsed from an episode of intense phone use, the larger the cortical potential associated with it. Our results suggest that repetitive movements on the smooth touchscreen reshaped sensory processing from the hand and that the thumb representation was updated daily depending on its use. We propose that cortical sensory processing in the contemporary brain is continuously shaped by the use of personal digital technology.

Results

Cortical Fingertip Representations in Touchscreen Phone Users Differ from Those Found in Nonusers

We analyzed 37 right-handed volunteers, 26 of whom used touchscreen phones and 11 of whom used old-technology mobile phones. Questionnaires provided few key insights into how the more modern phones were used. First, touchscreen users primarily used their right thumb on the screen as opposed to other fingers (Figure 1A), and none of them used a stylus. The thumb preference was expected given that hand-held phones were designed as such [5]. Second, in agreement with a US national survey on smartphone use, 80% of the touchscreen users in our study mainly used their phone for receiving and sending text messages or e-mails, as opposed to passively listening to music, watching videos, or making calls [6]. Finally, according to the self-reports, touchscreen users spent noticeably more time with their phones than did the nonusers (Figure 1B).

We investigated whether the somatosensory cortical electrical activity evoked from the fingertips differed between touchscreen phone users and nonusers. Sixty-two surface electrodes distributed over the entire scalp were used to detect cortical potentials evoked by touch on the thumb, index, and middle fingertips of the right hand. Each tactile stimulus consisted of a light mechanical contact that lasted for 2 ms, and event-related potentials (ERPs) were based on 1,250 stimulations on each fingertip. For all three fingertips tested both in touchscreen users and nonusers, the touch resulted in a dipole field around the contralateral (to stimulation) somatosensory cortex with signal onset at 32 ms and peak at 55 ms (on grand mean traces). The positive ERPs were detected in the contralateral parietal electrodes, and the negative signals were detected more medially in the contra- and ipsilateral frontal electrodes (Figures 1C–1H). Based on the latency and signal topology, we could assert that these signals originated from the primary somatosensory cortex [7–9]. We analyzed the signal differences between the touchscreen users and nonusers across all time points (50 ms prestimulation to 120 ms poststimulation) and for each electrode by using two-sample t tests corrected for multiple comparisons using 2D spatiotemporal clustering [10]. Interestingly, for all of the tested fingertips, the amplitude of the positive ERP was larger in touchscreen users compared to nonusers (Figures 1C–1H). Temporally, the positive signals differed between 39 and 68 ms for the thumbtip, between 38 and 60 ms for the index fingertip, and between 48 and 66 ms for the middle fingertip (Figures 1C, 1E, and 1G). Spatially, the statistical maps revealed that the differences were clustered on the contralateral parietal scalp for all the three fingertips (Figures 1D, 1F, and 1H). However, the spatial extent of these differences was the smallest for the middle finger (Figure 1H).

In short, touchscreen users relied mostly on their thumb to interact with the screen, but the cortical potentials associated with the first three fingertips were enhanced in comparison to nonusers. However, the spatiotemporal impact of phone use was the least prominent for the middle fingertip.

The Amount of Touchscreen Phone Use Influences Cortical Activity

The increased cortical activity in touchscreen users compared to nonusers could be due to a more intense usage of the hand, in the sense that the former group used the right thumb more than the latter group did. Alternatively, it could be due to the development of touchscreen-specific motor routines or "skills" as the movements associated with push buttons (in nonusers, who used only old-technology mobile phones)

[5]Co-first author
*Correspondence: arko@ini.uzh.ch

Please cite this article in press as: Gindrat et al., Use-Dependent Cortical Processing from Fingertips in Touchscreen Phone Users, Current Biology (2015), http://dx.doi.org/10.1016/j.cub.2014.11.026

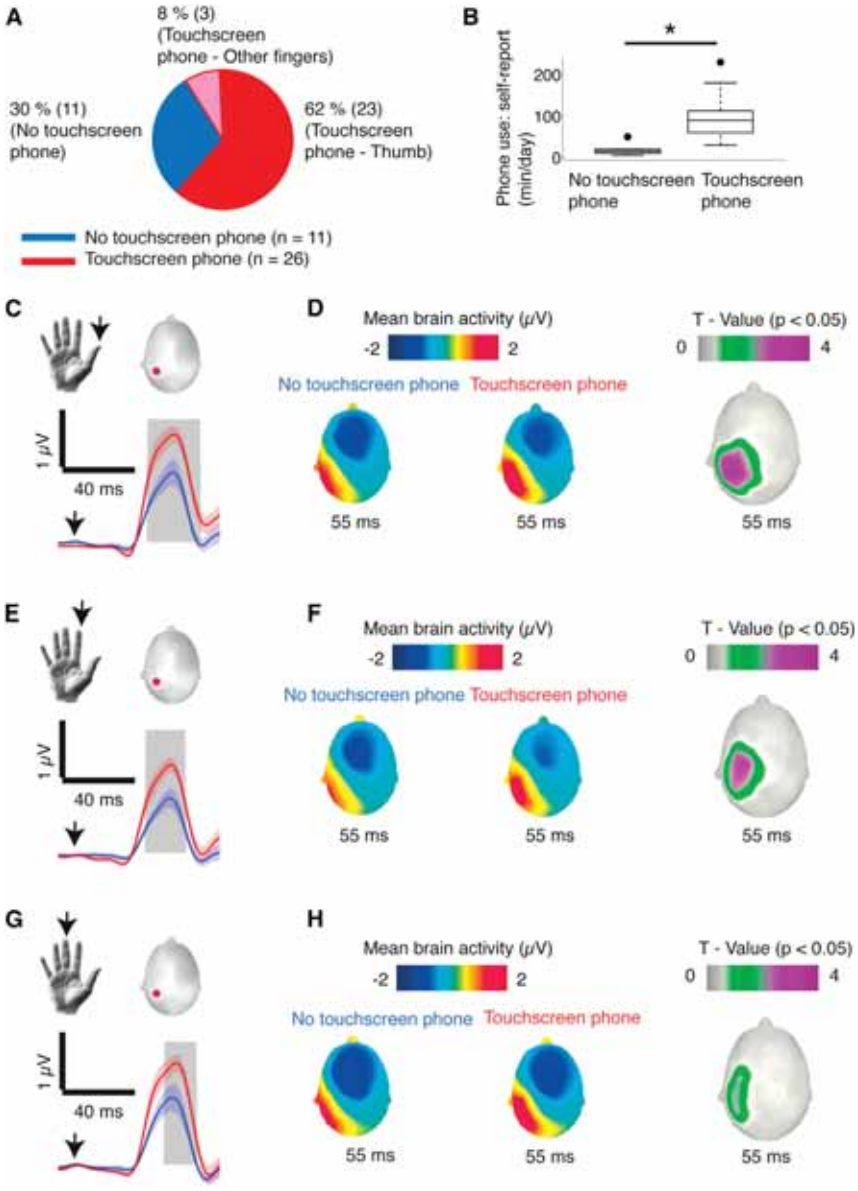

Figure 1. Tactile Event-Related Potentials in Touchscreen Phone Users and Nonusers

(A) Our study sample consisted of touchscreen phone users (red) and users of old-technology phones without touchscreens (blue), and most of the touchscreen users relied on their right thumb to interact with the screen (dark red).

(B) Box plot showing self-reported time spent using their mobile phone by touchscreen phone users and nonusers. Plot description: box, 25th and 75th percentile; whiskers, 10th and 90th percentile. Outliers are represented by black dots. *p < 0.05, Wilcoxon rank-sum test.

(C) Group means of the ERPs ± SEM (lighter shade) from the electrode with maximal positivity (red dot) in response to the right thumb tip stimulation in touchscreen users and nonusers. The gray area depicts significant differences between both groups—p < 0.05 and T > 1. The small arrow above the traces points at the stimulation onset (i.e., 0 ms).

(D) The corresponding scalp maps of the ERPs at 55 ms comparing the touchscreen users and nonusers. The multiple comparison corrected T value map revealed the electrodes with significant differences at 55 ms.

(E and F) Same as (C) and (D) but for right index fingertip.

(G and H) Same as (C) and (D) but for right middle fingertip.

versus taps or swipes on a smooth screen (in touchscreen phone users) were distinct.

To evaluate whether the cortical alterations scaled corresponding to touchscreen use, we identified three different attributes related to phone use: first, the self-reported age at which volunteers started using their touchscreen phone ("age of inception," Figure 2A). This attribute was inspired by previous reports on elite musicians and athletes in which the somatosensory representation of the corresponding body part was linked to the age at which practice began [1, 11]. Second, we quantified the history of phone use over a 10-day period by using built-in battery logs. Essentially, as the battery was drained with each phone use, the logs provided a proxy measure of finger-touchscreen interactions with a 10 min resolution, and the data were smoothed using a 50 min moving window [12]. The area under this curve was divided by the length of the recording period to derive the "phone use per hour"' (Figure 2B). Third, using the same smoothed battery signals, we estimated the time elapsed from a period of intense use—defined as the peak of battery drain—to the time of electroencephalogram (EEG) measurement ("duration from peak," Figure 2C; see also Figure S1 for scatter-plot matrix using the three variables). Based on preliminary simple linear regression between this measure and brain activity, we used the natural log of hours elapsed from the peak. Multiple regression analysis was conducted using these three phone use variables (Z′ normalized) for all time points (50 ms prestimulation to 120 ms poststimulation) and across all electrodes, resulting in event-related coefficients (ERCs) for each variable [10]. The regression statistics were corrected for multiple comparisons using 2D spatiotemporal clustering.

For the thumb tip, at the electrode with maximum mean positive ERP (grand mean of touchscreen user group), the corresponding "phone use per hour" ERC was also positive, and this linear relationship was significant between 33 and 44 ms and 53 and 61 ms (Figure 2D). Essentially, the higher the amount of phone use in the preceding 10 days, the larger the signal at the rising edge, peak, and falling edge of the positive ERP. At the electrode with the maximum mean negative ERP amplitude, the "duration from peak" ERC was significantly positive between 56 and 68 ms (Figure 2E). In other words, the longer the time elapsed from a period of intense use, the lesser the signal at the falling edge of the negative ERP. Scalp maps of the ERCs and the corresponding statistics captured the widespread impact of phone use (Figures 2F–2I). Overall, according to the R^2 value of the linear model, up to 60% of the interindividual variation in cortical activity could be

Please cite this article in press as: Gindrat et al., Use-Dependent Cortical Processing from Fingertips in Touchscreen Phone Users, Current Biology (2015), http://dx.doi.org/10.1016/j.cub.2014.11.026

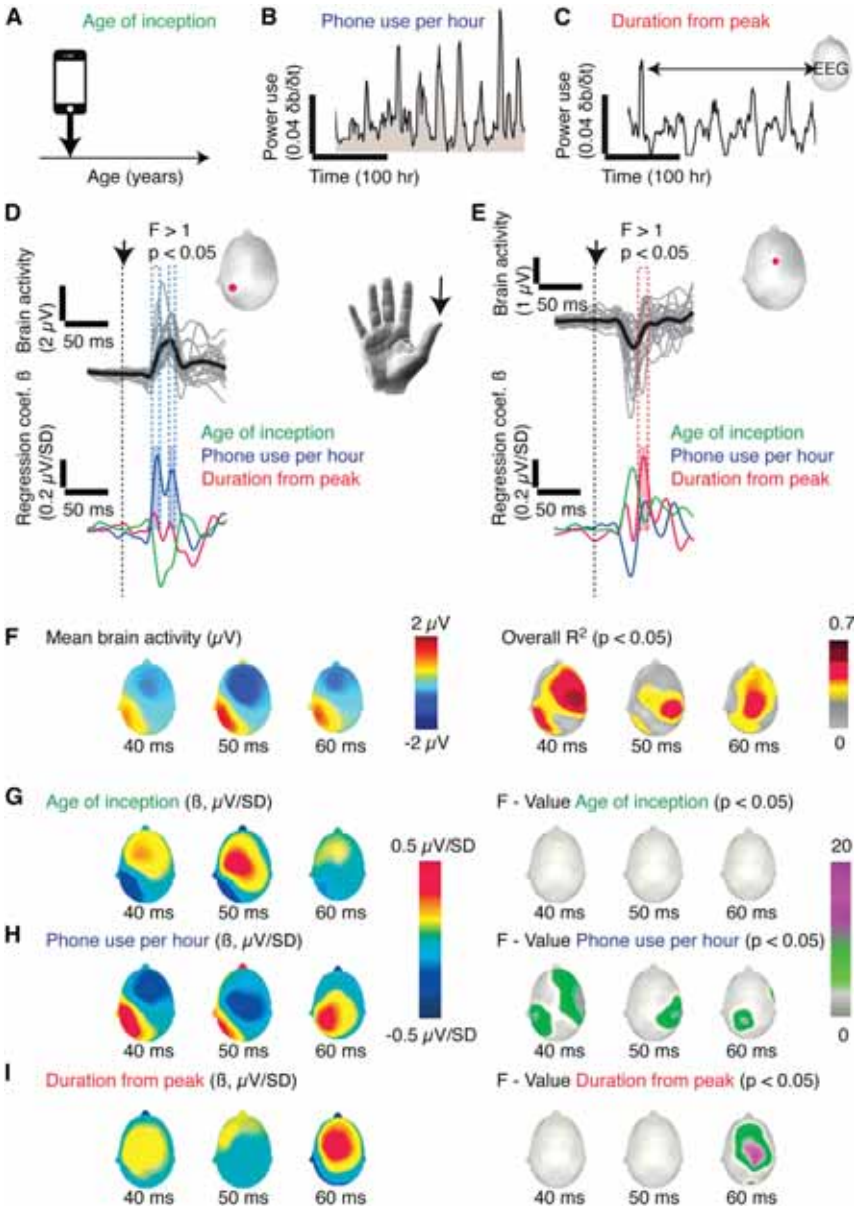

Figure 2. Interindividual Variations in Thumb ERPs Were Related to Touchscreen Phone Battery Logs

(A–C) To investigate how touchscreen use shaped cortical sensory processing, we identified three independent variables for multiregression analysis. We determined from the self-reports the age at which volunteers began using touchscreen phones ("age of inception," A). From the battery logs, we extracted the area under the curve to determine how much the phone was used in a 10-day period ("phone use per hour," B) and the "duration from peak" of use to EEG measurement expressed as natural log of hours (C). All the variables were Z′ normalized.

(D and E) The regression analysis of the right thumb tip ERPs resulted in a time series of β values or event-related coefficients (ERCs), and the β values at the positive peak ERP electrode (red dot; D) and the negative peak ERP electrode (red dot; E) are shown. Twenty-four individual positive and negative ERP traces are plotted with thin gray lines, and thick black lines depict the corresponding means. The areas in the dotted line boxes depict significant β values and are color coded according to the variable. The small arrow above the traces points at the stimulation onset (i.e., 0 ms).

(F) Scalp maps of the mean ERPs and the corresponding goodness-of-fit estimate of the full regression model (R^2) at three consecutive time points poststimulation.

(G–I) Scalp maps of the estimated β values and the corresponding F statistics for the three variables. Note that both "phone use per hour" and "duration from peak" variables were significantly related to the ERPs across several electrodes. See also Figures S1 and S2.

explained by the chosen variables (Figure 2F). Focusing on individual ERC scalp maps, for the "phone use per hour," the electrodes that detected positive ERP showed positive ERCs, and the negative ERP electrodes showed negative ERCs (Figure 2H). The pattern was distinct for "duration from peak"—here, only the negative ERP electrodes were related to the variable and the relationship was reversed, i.e., the negative ERP electrodes showed positive ERCs (Figure 2I). Although the spatiotemporal pattern of "age of inception" ERCs appeared to be converse to the "phone use per hour" ERCs, no significant relationship was found between this variable and brain activity (Figure 2G).

For the index fingertip, the linear relationships at the maximum positive and negative ERP electrodes were more restricted than for the thumb tip (Figures 3A and 3B). Essentially, a significant relationship was found between the "phone use per hour" variable and ERP, but only for the maximum positive electrode between 32 and 43 ms. Simply put, the more the phone was used over the 10 days preceding the EEG recording, the larger the signal on the rising edge of the positive ERP. According to the scalp maps, the positive ERP electrodes showed positive ERCs (Figure 3E). The rest of the variables did not show any significant relationship to brain activity (Figures 3D and 3F). Nevertheless, up to 54% of the variations were explained by the linear model (Figure 3C). For the middle fingertip, no significant ERCs were found, although the linear model explained up to 55% of the variation (see Figure S2).

In sum, the cortical potentials associated with the thumb and index fingertips reflected the touchscreen phone use history recorded by using the 10-day battery logs. The cortical activity evoked by touch to the thumb tip was directly proportional to the amount of phone use over the past 10 days and inversely proportional to the time elapsed from a period of intense use. The potential evoked by touch to the index fingertip was also related to the amount of use, albeit to a lesser extent and not related to the latter variable.

Interfingertip Inhibitory Interactions Are Not Eroded by the Touchscreen Phone Use

When neighboring fingertips are simultaneously stimulated, the magnitude of the ERP is smaller than the arithmetic sum of signals from the corresponding individual stimulations

Please cite this article in press as: Gindrat et al., Use-Dependent Cortical Processing from Fingertips in Touchscreen Phone Users, Current Biology (2015), http://dx.doi.org/10.1016/j.cub.2014.11.026

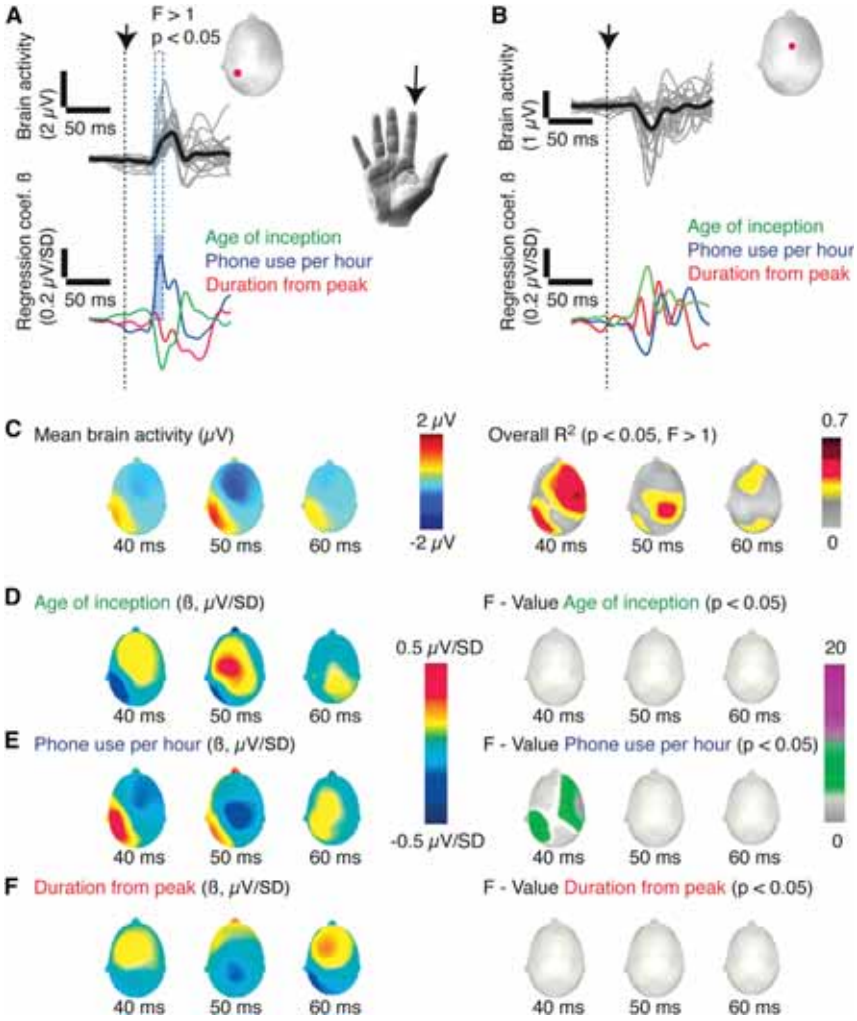

Figure 3. The "Phone Use per Hour" Variable Was Related to the Index Finger ERPs

The same variables as illustrated in Figure 2 for the thumb ERPs were used for regression analysis to model the index finger ERPs.

(A) At the positive peak ERP electrode, the area in the dotted line box depicts the significant β values or ERCs ("phone use per hour").

(B) No significant relations were found at the negative peak ERP electrode.

(C) Scalp map of the mean ERPs and the corresponding goodness-of-fit estimate of the full regression model (R^2).

(D–F) Scalp maps of individual β values and the corresponding F statistics. Note that only "phone use per hour" was significantly linked to the index finger ERPs.

The same conventions are used as in Figure 2. See also Figures S1 and S2.

[13, 14]. This difference is theoretically explained by cortical lateral inhibitory interactions between the neighboring fingers. The increased cortical activity associated with individual fingertips in touchscreen users may have come at the cost of such inhibitory interactions. Essentially, unmasking the inhibition between the neighboring fingertips may have contributed to the larger potentials in touchscreen users [4, 15]. To address this issue, we measured the difference between the predicted and real ERPs in response to simultaneous stimulation of the thumb and index fingertips (Figure 4A). Touchscreen users were compared to nonusers using two-sample t tests across all electrodes and time points (50 ms prestimulation to 120 ms poststimulation) and were corrected for multiple comparisons using 2D spatiotemporal clustering. Interestingly, the proxy measure of inhibition was significantly enhanced in touchscreen users compared to the nonusers between 40 and 57 ms (Figures 4B and 4C).

Therefore, the increased cortical signals in touchscreen phone users were not associated with a loss of intracortical inhibitory activity.

Discussion

Plasticity of cortical tactile processing has been of intense interest, but how it is applied through our daily lives remains poorly understood. Here, we found that the common use of touchscreen phones was associated with cortical reorganization. Touchscreen users showed larger amplitude of cortical potentials in response to tactile stimulation of the fingertips compared to nonusers. Furthermore, the amplitude was directly proportional to the recent phone use history quantified using battery logs built into the touchscreen phones. Intriguingly, transient cortical plasticity was induced within the monitoring period such that the thumb cortical potential was larger when volunteers' brain activity was measured soon after an episode of intense phone use than when measured later.

The scalp recordings revealed positive and negative fields in response to fingertip stimulations, and yet the effects of touchscreen use were not always symmetric on either side of the putative dipole projection. First, for all fingertips, the positive ERP, but not the negative ERP, was significantly enhanced in touchscreen users compared to nonusers. Second, only the negative thumb tip ERP, not the positive one, was linked to the duration from the peak of use. It is important to note that the signal magnitudes were also asymmetric, i.e., the magnitude of the negative potential was 60% of the positive signal. Three factors were previously raised to explain this positive-negative magnitude asymmetry [16]. First, the volume conduction of the currents may be asymmetrically distorted due to the variations in the skull and head tissue. Nevertheless, this can be eliminated as an explanation of the touchscreen use-associated asymmetry, as these physical factors were unlikely to be systematically modified by phone use. Similarly, the curvature of the cortical surface could be eliminated as an explanation. The final and the most promising candidate is linked to the notion that EEG signals reflect a "spatial average" of several current dipoles [17, 18]. In theory, the scalp signals reflect a combination of tangential and radial dipoles. The former ones generate both positive and negative fields on the scalp, and the latter ones introduce a positive or negative component depending on their orientation. Indeed,

Please cite this article in press as: Gindrat et al., Use-Dependent Cortical Processing from Fingertips in Touchscreen Phone Users, Current Biology (2015), http://dx.doi.org/10.1016/j.cub.2014.11.026

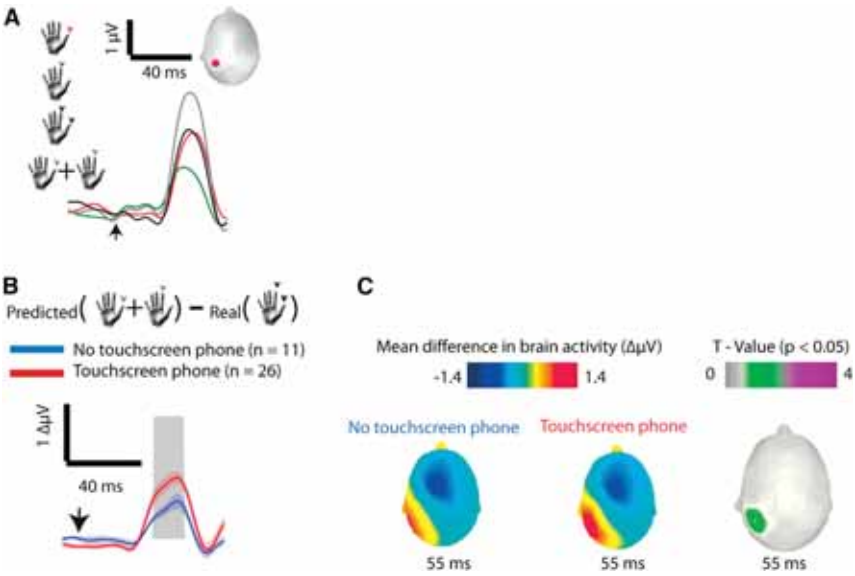

Figure 4. Sensory Integration from Thumb and Index Fingertips in Touchscreen Users and Nonusers

(A) An example measure from one volunteer depicting "inhibitory" interactions between the thumb and index fingertips. Note that the predicted (linear sum) signal magnitude (in gray) is larger than the real response evoked by simultaneous stimulations (in black).

(B) The difference between the predicted and real response magnitudes was enhanced in touchscreen phone users compared to nonusers.

(C) Scalp maps of voltage differences between the predicted and real response magnitudes in both groups and the corresponding T value map.

according to a combined EEG and magnetoencephalography (MEG) study, the primary somatosensory cortex (area 3b) generates both tangential and radial dipoles in response to electrical stimulation of the fingers [19]. Speculatively, the asymmetries described in our study may reflect touchscreen use-dependent alterations of the tangential as opposed to the radial sources. However, the exact neuronal origin of such a tangential source remains beyond the scope of our speculations, and isolating it would require a more improved theoretical understanding of how individual neurons in the somatosensory cortex contribute to the EEG signal at the scalp.

At first glance, the increased cortical activity in touchscreen phone users compared to nonusers appears to be similar to what occurs in string instrument players [1]. But a more detailed examination reveals two notable differences. First, the age at which musical practice began was strongly and linearly related to the cortical activity evoked from the little finger. However, this link between the age of inception and the cortical activity was not significant for touchscreen users. Furthermore, a daily diary of musical practice was maintained for a week, analogous to the 10-day battery logs used here. Whereas the musicians did not show any linear relationship to the recent activity, the touchscreen users did. Perhaps musicians enjoyed a more stable sensory representation than touchscreen users, shaped by disciplined practice through the early years. Notably, the minimum age of inception for musical practice was 5 years old, whereas for the touchscreen use it was 15 years old.

Based on the 10-day battery log versus brain activity correlations alone, it was not clear whether cortical processing was shaped by phone use over the past 10 days. Essentially, did the 10-day log reflect use over the past 10 days only, or was this log representative of use over a much longer period? For instance, the phone use levels may have remained stable over months and gradually shaped the cortical processing, but due to the stable usage the cortical signals may have still correlated well with the recent log. Based on previous studies, it appears that touchscreen use is at best "partially stable" [20, 21]. Among university students (studied here), several factors and their interactions may have contributed to unstable usage: as touchscreen phones are used toward educational activities, usage may have increased when approaching semester deadlines [21]. Intuitively, the usage levels varied with semester breaks as well. Intriguingly, moving from high school (where phones were generally disallowed) to university was also expected to alter how phones were used. Therefore, the 10-day log may have reflected past use on the scale of a few weeks but not years. Nevertheless, within the 10-day period of our study, phone use was uneven in each individual. Interestingly, cortical activity was significantly related to the day-to-day fluctuations, and this strongly suggested that the cortex was reshaped within this 10-day period. Essentially, volunteers who peaked their use a few days prior to the brain measurement had a larger thumb cortical potential than volunteers who had a longer gap between the peak of use and the brain measurement. Interestingly, previous laboratory experiments showed that 30 min of repeating simple taps with the thumb transiently reinforced motor cortical outputs [22]. Taken together, we speculate that both somatosensory and motor cortices conform to temporary increases in motor behavior by temporary reallocation of neuronal resources.

Although the rapidly transient cortical alterations were limited to the thumb, the cortical potentials from all the first three fingertips were enhanced in touchscreen users compared to nonusers. This suggests that the longer-term cortical alterations were not restricted to the skin surface most frequently used on the touchscreen (i.e., thumb fingertip). Kinematically, the index and middle fingers were involved in gripping and stabilizing the phone as the thumb hovered to touch the screen (data not shown) [23]. Therefore, the tactile receptors of the index and middle fingers tips were also activated during the phone use. Additionally, a less intuitive source of activations during phone use may have come from the tactile receptors on the hand, which are activated during grasping actions even without direct contact [24, 25]. Therefore, repetitive contact-based and contact-free coactivations of several receptors across the hand surface may have driven "hebbian-like" plasticity to increase the cortical potentials associated with all the fingertips [4, 26, 27]. However, this form of widespread plasticity was not triggered by the very short-term fluctuations in use, restricting the rapidly transient cortical alterations to the thumb tip only.

The mechanisms underlying cortical reorganization in touchscreen users remain unclear. The potential explanations are as follows: first, use-dependent increase in cortical activity has been previously associated with a recession of

intracortical inhibition [15, 28], but this was not found here with simultaneous stimulation of thumb and index fingertips. Still, as only the fingertips were tested, this mechanism cannot be entirely ruled out by our data. Second, touchscreen phone use may have strengthened the synapses in the somatosensory cortex, resulting in larger cortical potentials. This idea is supported by experiments involving brief periods of low-intensity direct-current stimulation of the cerebral cortex—which strengthens cortical synapses and increases the amplitude of somatosensory cortical potentials [29–32]. Third, the cortical alterations may be accompanied with subcortical alterations in touchscreen users. After amputation or spinal cord injury, nonhuman primates showed profound cortical changes, which were partly explained by the plasticity of the brainstem and thalamic circuits [33, 34]. Finally, we cannot entirely rule out peripheral modifications such as a decrease in threshold of the mechanical receptors driven by phone use, but such a use-dependent alteration of peripheral structures remains unreported in the neuroscientific literature. Furthermore, extensive research on experienced blind Braille readers provides strong evidence for central, but not peripheral, changes in people subjected to repeated tactile contacts with a fingertip [35, 36]. Nevertheless, according to dermatological research, "friction-induced dermatoses" may be observed in computer and mouse users, but only in case of severe usage (4–10 hr of daily use for 5–10 years), putatively resulting in the reduction of tactile inputs due to a build-up of extra layer of tissue over the damaged skin [37, 38]. Still, we cautiously speculate that a combination of central changes, rather than changes in the periphery, is more likely to be the underlying cause of the altered cortical potentials linked to touchscreen use.

In conclusion, touchscreen phone use reorganized the representation of the fingertips in the somatosensory cortex. The focus on regular touchscreen phone users complements the series of investigations already performed in elite athletes and musicians. Essentially, our study provided direct empirical insights into the operation of brain plasticity through our regular day-to-day activities, and this would not have been possible by studying expert groups or highly trained monkeys in a laboratory. Moreover, we unlocked a new method to non-intrusively quantify daily hand use by using battery logs, and this could be used to calibrate somatosensory potentials in basic and clinical neurophysiology. The consequences of the observed alterations may have been adaptive in the sense that they contributed to the development of useful associations between touch and phone activities. However, it is as likely that the plasticity was maladaptive. For instance, cortical plasticity in string instrument players is associated with dystonia [15, 39]. Furthermore, plasticity of the somatosensory cortex is associated with the development of chronic pain [40]. Worryingly, there is some evidence linking excessive phone use with motor dysfunctions and pain [41, 42]. More research is still needed to unravel the consequences of the altered sensory processing linked to the use of touchscreen devices.

Experimental Procedures

Volunteers

This study was conducted on 38 healthy right-handed mobile phone users between 19 and 34 years old (median: 22.9; 18 males and 20 females). Among them, 27 were touchscreen smartphone users (median: 22.9; 12 males and 15 females) and 11 were old-technology mobile phone users (median: 23.2; six males and five females). The volunteers, all university students, were recruited via mass e-mails and lecture hall announcements. By using self-reports, we eliminated hand injuries, history of neurological disorders, and medications that might have affected the nervous system. We also confirmed the volunteers' handedness using a questionnaire [43]. All volunteers were compensated for their participation with gift cards or course credits. One person (female touchscreen phone user) chose to drop out of the study by missing the brain measurement and was eliminated from all analyses. In this study, we considered a smartphone, as opposed to an old-technology mobile phone, to be any mobile phone with a fast processor and full front panel touchscreen, such as iPhone and Samsung Galaxy. Informed consent was obtained from all participants, and the Canton of Vaud approved the experimental procedures in accordance with the Swiss federal law on human experimentation.

Mobile Phone Use Survey and Battery Logs

All volunteers were probed on mobile phone use behavior via a questionnaire. This was used to extract the number of years the volunteers owned a touchscreen smartphone (i.e., leading to the age of inception) and/or an old-technology phone, to document the mobile phone model, to list any other personal digital technology owned, to estimate the time spent on the phone, and to specify the mode of interaction (stylus, voice, or touch). The questionnaire also included a list of 18 hand/finger postures on a touchscreen smartphone, and touchscreen phone users were instructed to rank them from the most-favored to the least-favored posture. Similarly, mobile phone activities were also ranked from a list of 11 actions that included text messaging and phone calls. Furthermore, the typing actions and grip style of all volunteers were also documented with a 480 fps camera.

We focused on battery logs from touchscreen phones to quantify use in a nonintrusive manner prior to the brain activity measurements over a period of 10 days. In one user, the data were available for 30 days due to rescheduling of a missed brain measurement session. However, such quantifications could not be performed with the old-technology (nontouchscreen) phones due to the lack of easy access to the battery sensors. All the touchscreen phones included in this study used similar batteries, with manufacturer's specifications on the battery life ranging from 6–8 hr of talk time on 3G, 10–14 hr of talk time on 2G, 4–7 hr of web use over 3G, and 7–10 hr of web use over Wi-Fi. The percentage of battery power was registered every 10 min when the phone was in use with the DataWiz app (Princeton EDGE Lab). The change in state of the battery over time was quantified using differences between consecutive samples (MATLAB R2011b). The negative differential indicated battery drain, and the positive differential indicated gain such as in charging of the phone. Because we were only interested in phone use, all positive values were set to 0, and remaining absolute values were used for further analysis. The data were smoothed using a 50 min moving window. The area under the differentials divided by the entire recording period (in hr) and the natural log of the time interval from the differential peak (from the entire recording period) to the time of brain measurement were extracted using MATLAB. The app malfunctioned in two volunteers due to users' error and the corresponding data were eliminated from further analysis.

Tactile Stimulations and EEG

The thumb, index, and middle fingertips of the right hand were randomly stimulated using solenoid tappers (Heijo Research Electronics), which could be precisely computer controlled in time via a stimulation box using a home-made script running on MATLAB. The tappers applied a 2-ms-long circular suprathreshold touch stimulus with an interstimulus interval of 750 ± 250 ms and made a 12.5 mm^2 contact with the fingertips. Stimulations were randomly delivered either individually to the three fingertips or simultaneously to the thumb and index fingertips. In order to cover the noise made by the tappers, we made a background white noise audible via headphones.

The EEG data were acquired from 62 electrodes mounted on an elastic cap (EasyCap) and distributed equidistantly to cover the entire scalp. Two additional electrodes were used for electro-oculogram (EOG) to monitor eye movements. The electrode locations were digitized in a 3D nasion-ear coordinate frame (ANT Neuro and Xensor software) for a representative volunteer. The EEG signals were recorded against the vertex and amplified with an alternating-current-coupled amplifier (BrainAmp, Brain Products). The data were sampled at 1,000 Hz, digitized using a 16 bit A/D converter, and rereferenced offline to the average signal from all the scalp electrodes (EEGLAB, an open source MATLAB toolbox [44]). The data were further analyzed with EEGLAB to band-pass filter between 1 and 80 Hz. All epochs that exceeded the ±70 μV threshold were eliminated to reject eye blinks from the analysis. Furthermore, trials containing statistically "abnormal" amplitudes were defined and eliminated using the kurtosis and joint

probabilities of the recordings (the threshold was set at 5 SD), and finally, eye movement artifacts and facial movement artifacts were rejected using independent component analysis (EEGLAB). ERPs for each stimulus location were obtained by averaging of 1,250 corresponding stimulations. Brain activity at each time point (−50 ms to 120 ms; 0 ms = stimulus onset; −50 to 0 ms = baseline) from each electrode and for each stimulus location was analyzed with a linear modeling approach. The two-sample t tests and multiple linear regressions (and the corresponding F tests) were corrected for multiple comparisons using 2D spatiotemporal clustering based on 1,000 bootstraps. All of the statistical and clustering analyses were conducted with LIMO EEG (MATLAB toolbox, using EEGLAB), and these tests are described here in detail [10].

Supplemental Information

Supplemental Information includes two figures and can be found with this article online at http://dx.doi.org/10.1016/j.cub.2014.11.026.

Author Contributions

A.-D.G., M.C., M.B., and A.G. collected the data and performed preliminary analysis. A.G. performed formal analysis and drafted the report, and A.-D.G., M.C., M.B., and E.M.R. edited its contents. A.G. provided the study concept, and A.-D.G., E.M.R., and A.G. designed the experiments.

Acknowledgments

This research was supported by a Society in Science Branco Weiss Fellowship, and A.G. was also supported by research grants from OPO Stiftung and Vontobel Stiftung, Zurich. We would also like to acknowledge FNS grant no. 149643 (to E.M.R.). We thank Kevan Martin and the other members at the Institute of Neuroinformatics for their support, Cyril Pernet for clarifying LIMO EEG, Nobuhiro Hagura and Roland S. Johansson for their comments, and the colleagues at the University of Fribourg for their generous help with data collection.

Received: October 5, 2014
Revised: October 31, 2014
Accepted: November 10, 2014
Published: December 23, 2014

References

1. Elbert, T., Pantev, C., Wienbruch, C., Rockstroh, B., and Taub, E. (1995). Increased cortical representation of the fingers of the left hand in string players. Science *270*, 305–307.
2. Pantev, C., Engelien, A., Candia, V., and Elbert, T. (2001). Representational cortex in musicians. Plastic alterations in response to musical practice. Ann. N Y Acad. Sci. *930*, 300–314.
3. Pascual-Leone, A., and Torres, F. (1993). Plasticity of the sensorimotor cortex representation of the reading finger in Braille readers. Brain *116*, 39–52.
4. Byl, N.N., Merzenich, M.M., and Jenkins, W.M. (1996). A primate genesis model of focal dystonia and repetitive strain injury: I. Learning-induced dedifferentiation of the representation of the hand in the primary somatosensory cortex in adult monkeys. Neurology *47*, 508–520.
5. Perry, K.B., and Hourcade, J.P. (2008). Evaluating one handed thumb tapping on mobile touchscreen devices. Proceedings of Graphics Interface 2008, 57–64.
6. Duggan, M., and Rainie, L. (2013). Pew Research Center's Internet & American Life Project: Cell Phone Activities 2012. http://pewinternet.org/Reports/2012/Cell-Activities.aspx.
7. Allison, T., McCarthy, G., and Wood, C.C. (1992). The relationship between human long-latency somatosensory evoked potentials recorded from the cortical surface and from the scalp. Electroencephalogr. Clin. Neurophysiol. *84*, 301–314.
8. Suk, J., Ribary, U., Cappell, J., Yamamoto, T., and Llinás, R. (1991). Anatomical localization revealed by MEG recordings of the human somatosensory system. Electroencephalogr. Clin. Neurophysiol. *78*, 185–196.
9. Nakamura, A., Yamada, T., Goto, A., Kato, T., Ito, K., Abe, Y., Kachi, T., and Kakigi, R. (1998). Somatosensory homunculus as drawn by MEG. Neuroimage *7*, 377–386.
10. Pernet, C.R., Chauveau, N., Gaspar, C., and Rousselet, G.A. (2011). LIMO EEG: a toolbox for hierarchical LInear MOdeling of ElectroEncephaloGraphic data. Comput. Intell. Neurosci. *2011*, 831409.
11. Murakami, T., Sakuma, K., and Nakashima, K. (2008). Somatosensory evoked potentials and high-frequency oscillations in athletes. Clin. Neurophysiol. *119*, 2862–2869.
12. Carroll, A., and Heiser, G. (2010). An analysis of power consumption in a smartphone. Proceedings of the 2010 USENIX Conference on USENIX Annual Technical Conference, 21.
13. Biermann, K., Schmitz, F., Witte, O.W., Konczak, J., Freund, H.J., and Schnitzler, A. (1998). Interaction of finger representation in the human first somatosensory cortex: a neuromagnetic study. Neurosci. Lett. *251*, 13–16.
14. Gandevia, S.C., Burke, D., and McKeon, B.B. (1983). Convergence in the somatosensory pathway between cutaneous afferents from the index and middle fingers in man. Exp. Brain Res. *50*, 415–425.
15. Tamura, Y., Ueki, Y., Lin, P., Vorbach, S., Mima, T., Kakigi, R., and Hallett, M. (2009). Disordered plasticity in the primary somatosensory cortex in focal hand dystonia. Brain *132*, 749–755.
16. Allison, T., McCarthy, G., Wood, C.C., and Jones, S.J. (1991). Potentials evoked in human and monkey cerebral cortex by stimulation of the median nerve. A review of scalp and intracranial recordings. Brain *114*, 2465–2503.
17. Murakami, S., and Okada, Y. (2006). Contributions of principal neocortical neurons to magnetoencephalography and electroencephalography signals. J. Physiol. *575*, 925–936.
18. Buzsáki, G., Anastassiou, C.A., and Koch, C. (2012). The origin of extracellular fields and currents—EEG, ECoG, LFP and spikes. Nat. Rev. Neurosci. *13*, 407–420.
19. Buchner, H., Fuchs, M., Wischmann, H.A., Dössel, O., Ludwig, I., Knepper, A., and Berg, P. (1994). Source analysis of median nerve and finger stimulated somatosensory evoked potentials: multichannel simultaneous recording of electric and magnetic fields combined with 3D-MR tomography. Brain Topogr. *6*, 299–310.
20. Dai, P., and Ho, S.S. (2014). A smartphone user activity prediction framework utilizing partial repetitive and landmark behaviors). IEEE 15th International Conference on Mobile Data Management (MDM) *1*, 205–210.
21. Rahmati, A., and Zhong, L. (2013). Studying smartphone usage: lessons from a four-month field study. IEEE Trans. Mob. Comput. *12*, 1417–1427.
22. Classen, J., Liepert, J., Wise, S.P., Hallett, M., and Cohen, L.G. (1998). Rapid plasticity of human cortical movement representation induced by practice. J. Neurophysiol. *79*, 1117–1123.
23. Goel, M., Wobbrock, J., and Patel, S. (2012). GripSense: using built-in sensors to detect hand posture and pressure on commodity mobile phones. Proceedings of the 25th Annual ACM Symposium on User Interface Software and Technology, 545–554.
24. Westling, G., and Johansson, R.S. (1987). Responses in glabrous skin mechanoreceptors during precision grip in humans. Exp. Brain Res. *66*, 128–140.
25. Hulliger, M., Nordh, E., Thelin, A.E., and Vallbo, A.B. (1979). The responses of afferent fibres from the glabrous skin of the hand during voluntary finger movements in man. J. Physiol. *291*, 233–249.
26. Byl, N.N., McKenzie, A., and Nagarajan, S.S. (2000). Differences in somatosensory hand organization in a healthy flutist and a flutist with focal hand dystonia: a case report. J. Hand Ther. *13*, 302–309.
27. Recanzone, G.H., Merzenich, M.M., and Schreiner, C.E. (1992). Changes in the distributed temporal response properties of SI cortical neurons reflect improvements in performance on a temporally based tactile discrimination task. J. Neurophysiol. *67*, 1071–1091.
28. Florence, S.L., Jain, N., and Kaas, J.H. (1997). Plasticity of somatosensory cortex in primates. Semin. Neurosci. *9*, 3–12.
29. Cheeran, B., Talelli, P., Mori, F., Koch, G., Suppa, A., Edwards, M., Houlden, H., Bhatia, K., Greenwood, R., and Rothwell, J.C. (2008). A common polymorphism in the brain-derived neurotrophic factor gene (BDNF) modulates human cortical plasticity and the response to rTMS. J. Physiol. *586*, 5717–5725.
30. Nitsche, M.A., Fricke, K., Henschke, U., Schlitterlau, A., Liebetanz, D., Lang, N., Henning, S., Tergau, F., and Paulus, W. (2003). Pharmacological modulation of cortical excitability shifts induced by transcranial direct current stimulation in humans. J. Physiol. *553*, 293–301.

31. Fritsch, B., Reis, J., Martinowich, K., Schambra, H.M., Ji, Y., Cohen, L.G., and Lu, B. (2010). Direct current stimulation promotes BDNF-dependent synaptic plasticity: potential implications for motor learning. Neuron *66*, 198–204.
32. Matsunaga, K., Nitsche, M.A., Tsuji, S., and Rothwell, J.C. (2004). Effect of transcranial DC sensorimotor cortex stimulation on somatosensory evoked potentials in humans. Clin. Neurophysiol. *115*, 456–460.
33. Kambi, N., Halder, P., Rajan, R., Arora, V., Chand, P., Arora, M., and Jain, N. (2014). Large-scale reorganization of the somatosensory cortex following spinal cord injuries is due to brainstem plasticity. Nat. Commun. *5*, 3602.
34. Florence, S.L., Hackett, T.A., and Strata, F. (2000). Thalamic and cortical contributions to neural plasticity after limb amputation. J. Neurophysiol. *83*, 3154–3159.
35. Goldreich, D., and Kanics, I.M. (2003). Tactile acuity is enhanced in blindness. J. Neurosci. *23*, 3439–3445.
36. Grant, A.C., Thiagarajah, M.C., and Sathian, K. (2000). Tactile perception in blind Braille readers: a psychophysical study of acuity and hyperacuity using gratings and dot patterns. Percept. Psychophys. *62*, 301–312.
37. Schady, W., Sheard, A., Hassell, A., Holt, L., Jayson, M.I., and Klimiuk, P. (1991). Peripheral nerve dysfunction in scleroderma. Q. J. Med. *80*, 661–675.
38. Ghasri, P., and Feldman, S.R. (2010). Frictional lichenified dermatosis from prolonged use of a computer mouse: Case report and review of the literature of computer-related dermatoses. Dermatol. Online J. *16*, 3.
39. Quartarone, A., Siebner, H.R., and Rothwell, J.C. (2006). Task-specific hand dystonia: can too much plasticity be bad for you? Trends Neurosci. *29*, 192–199.
40. Flor, H., Braun, C., Elbert, T., and Birbaumer, N. (1997). Extensive reorganization of primary somatosensory cortex in chronic back pain patients. Neurosci. Lett. *224*, 5–8.
41. Berolo, S., Wells, R.P., and Amick, B.C., 3rd. (2011). Musculoskeletal symptoms among mobile hand-held device users and their relationship to device use: a preliminary study in a Canadian university population. Appl. Ergon. *42*, 371–378.
42. Shavlovskaia, O.A. (2012). [Towards a question of formation mechanisms of hand muscular dystonia]. Fiziol. Cheloveka *38*, 113–123.
43. Oldfield, R.C. (1971). The assessment and analysis of handedness: the Edinburgh inventory. Neuropsychologia *9*, 97–113.
44. Delorme, A., and Makeig, S. (2004). EEGLAB: an open source toolbox for analysis of single-trial EEG dynamics including independent component analysis. J. Neurosci. Methods *134*, 9–21.

Supplementary Figures

Figure S1, Related to Figure 2 and 3: Scatter plot matrix of the 3 independent variables described in Fig 2A-C (with histograms) used towards regression analysis, and shown here prior to Z' normalization. Note the absence of correlations between the pairs of independent variables, and the corresponding R^2 values mentioned for each plot.

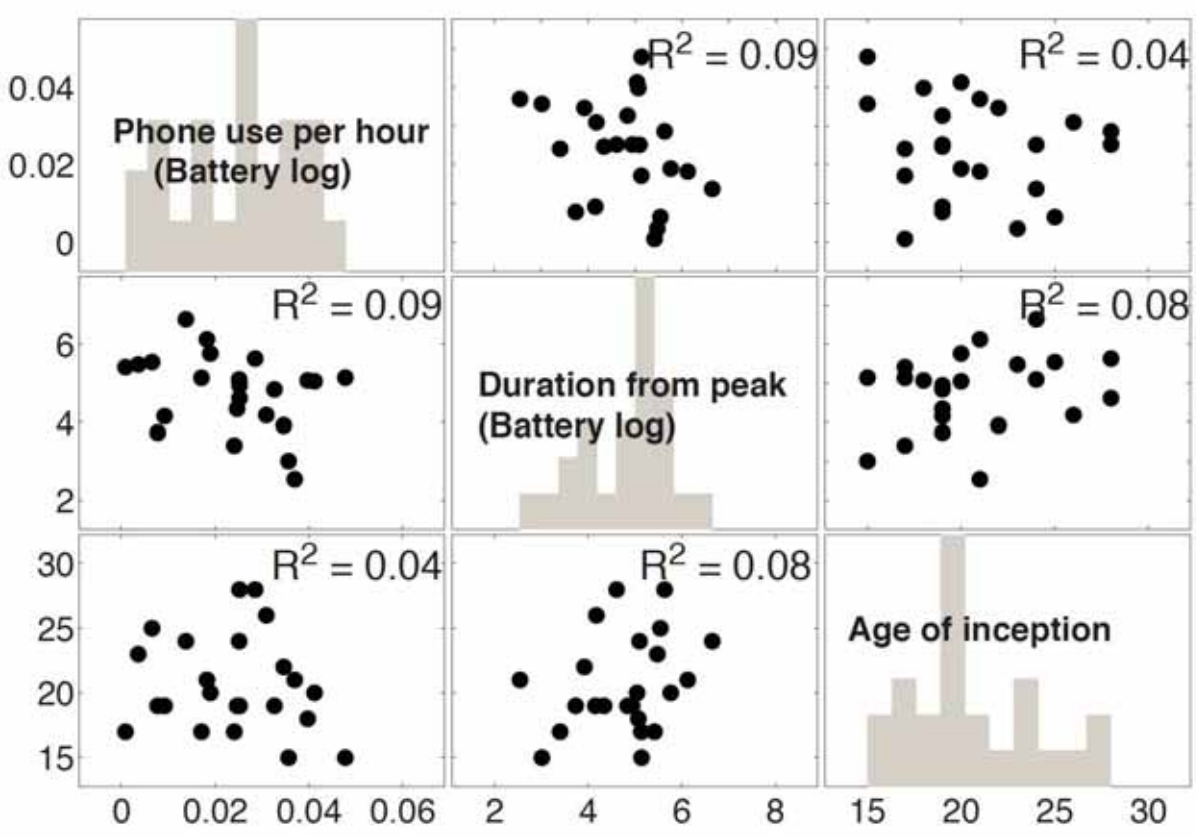

Figure S2, Related to Figures 2 and 3: *Smartphone use and the middle finger ERPs*. The same three variables used for thumb and index finger ERP analysis were also used to model the middle finger ERPs. No significant individual ß values or ERCs were detected at the peak positive (A) or peak negative (B) ERP electrodes. (C) Scalp map of mean ERPs and the corresponding goodness-of-fit estimate of the full regression model (R^2). (D-F) Scalp maps of the ERCs and the corresponding F-statistics revealed no significant relationships. The same conventions are used as in Fig. 2.

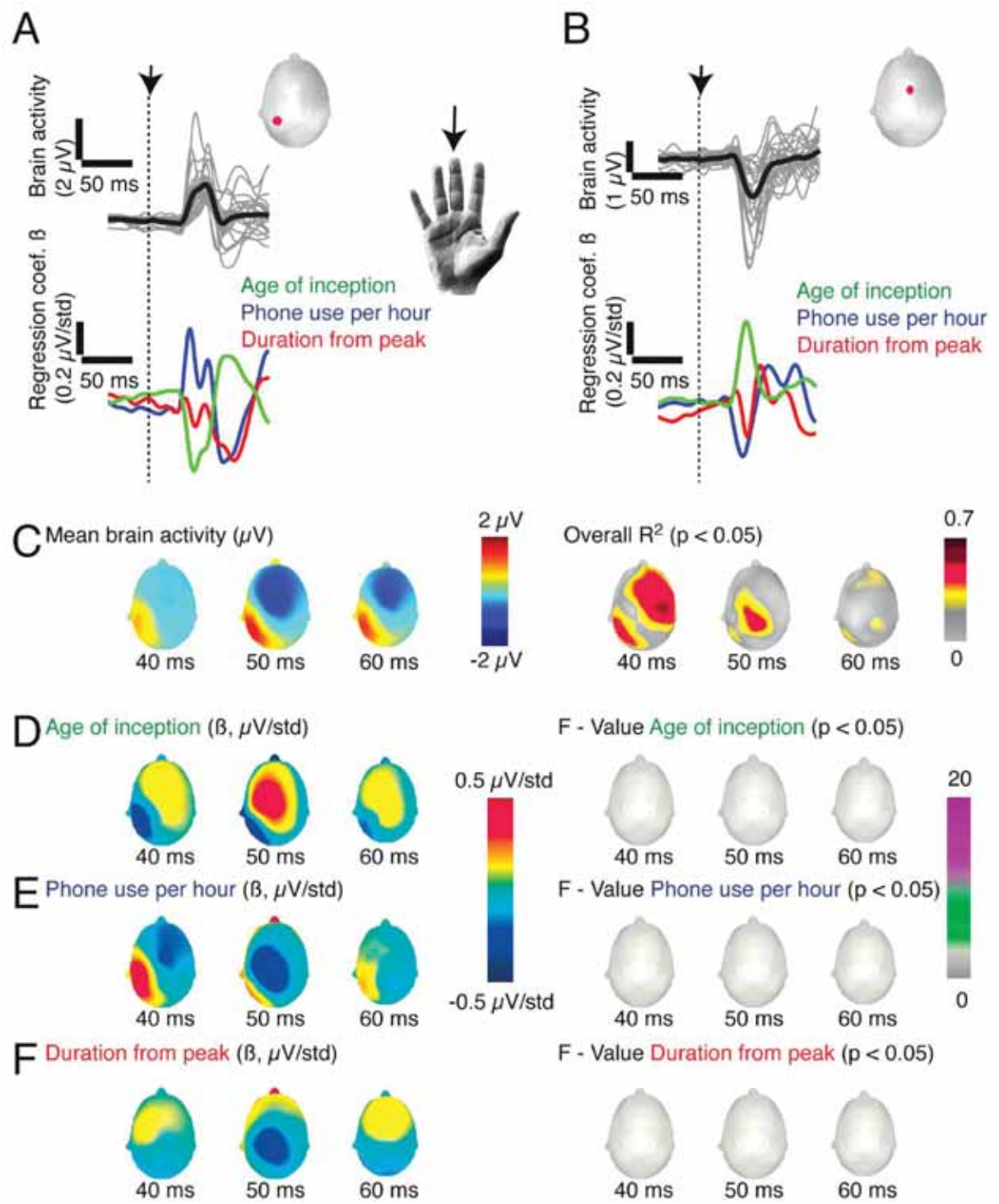

Appendix: Survey

How do you use your mobile phone?

Dear participant,

Thank you for your contribution. Your data will be used confidentially and for scientific purposes only.

1. General profile

Sex: □ Male □ Female

What is your professional activity?.....

Since when? .....

You are: □ Left-hander □ Right-hander □ Ambidextrous

Do you practise a specific art requiring a particular or intensive use of the fingers (e.g. piano)? .....

If yes, what kind?.....

Since when? ..... How often (hours per week)?.....

Have you ever severely injured your hands, your fingers? .....

If yes, when and are you still impaired?.....

Do you have any neurological dysfunction? .....

2. Information about your mobile phone

Do you own a mobile phone?.....If yes, what type of mobile phone do you currently use?

Brand (e.g. iPhone, Samsung, …):..... Model (e.g. 4S, galaxy 3S):.....

How long (in years) have /did you owned a standard mobile phone?..... a smartphone?.....

3. If you are a <u>smartphone</u> user, how often do you use your phone in the following ways? Rank the situations from the most frequent (assign number 1) to the most rare (assign number 18).

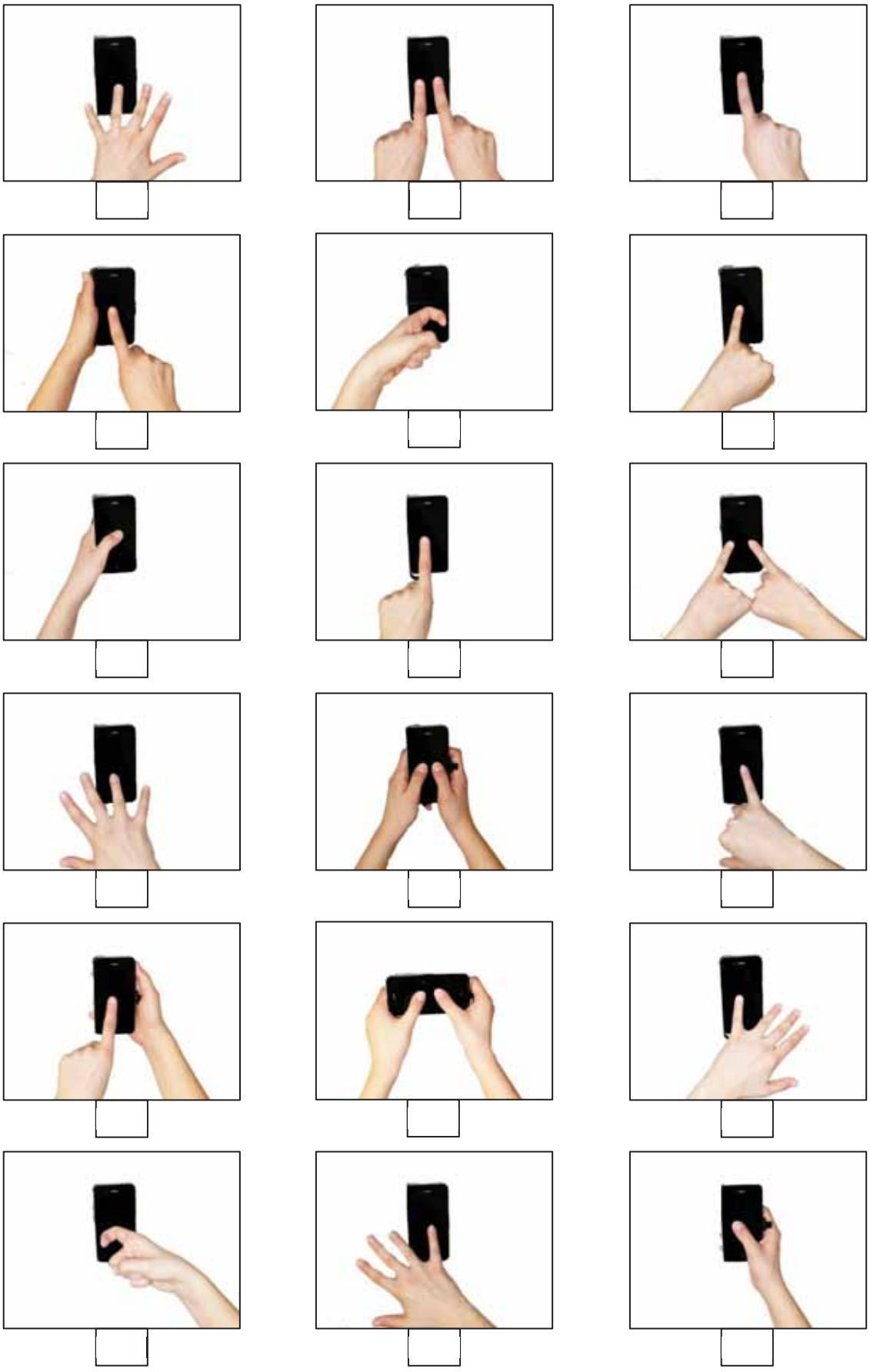

4. Do you use any of these devices? If yes, with which hand usually?

Track pad on the notebook/PC	□ No	□ Yes,	□ with the right hand	□ with the left hand
Mouse	□ No	□ Yes,	□ with the right hand	□ with the left hand
Wii	□ No	□ Yes,	□ with the right hand	□ with the left hand
Gamepad/joystick	□ No	□ Yes,	□ with the right hand	□ with the left hand
Tablet/ Touchscreen PC	□ No	□ Yes,	□ with the right hand	□ with the left hand

5. Do you use a stylus on your phone?

□ never □ rarely □ often □ always

Date..... Signature.....

L'utilisation de *smartphones* façonne le traitement cortical de l'information sensorielle tactile provenant de l'extrémité des doigts

Anne-Dominique Gindrat[1,*], Magali Chytiris[1,2,*], Myriam Balerna[1,2,*], Eric M. Rouiller[1], Arko Ghosh[2-4]

[1]Domaine de physiologie, Fribourg cognition center, département de médecine, université de Fribourg, 5 chemin du Musée, CH-1700 Fribourg, Suisse ;
[2]Institut de neuroinformatique, université de Zürich et ETH Zürich, Winterthurerstrasse 190, CH-8057 Zürich, Suisse ;
[3]Neuroscience center Zürich, Université de Zürich et ETH Zürich, Winterthurerstrasse 190, CH-8057 Zürich, Suisse ;
[4]Institut de neuroscience cognitive, university college London, 17 Queen Square, Londres, WC1N 3AR, Royaume-Uni.
anne-dominique.gindrat@unifr.ch
magalichyt@gmail.com
balerna.myriam@gmail.com
eric.rouiller@unifr.ch
arko@ini.uzh.ch
*Ces auteurs ont contribué de façon égale

La plasticité cérébrale au quotidien

L'architecture de base de notre cerveau n'est pas complètement figée mais peut évoluer dans le temps, par exemple au cours du développement du système nerveux ou, chez l'adulte, pendant les phases d'apprentissage, en fonction du degré d'utilisation des différentes parties du corps. On appelle « plasticité cérébrale par l'usage » la capacité qu'a le cerveau à augmenter sélectivement le traitement de l'information associée à une partie du corps en réponse à une plus grande utilisation de celle-ci [1-3]. Jusqu'à présent, la plasticité cérébrale par l'usage a été mise en évidence dans des situations extrêmes, que ce soit chez des patients ayant perdu une partie du corps après un traumatisme (lésion de la moelle épinière, amputation, membre immobilisé) [4, 5], ou chez des sujets montrant des habiletés extraordinaires nécessitant une utilisation particulièrement intensive d'une partie du corps, comme les sportifs d'élite [6], les aveugles lisant le Braille [7] et les musiciens [8]. Chez les joueurs d'instruments à cordes [8] par exemple, la représentation corticale de la main gauche, occupée à raccourcir la longueur des cordes de l'instrument (ce qui requiert donc une grande dextérité manuelle et une forte stimulation sensorielle), était non seulement plus étendue que celle de la main droite, qui manie si besoin l'archet, mais également plus étendue que celle de la main gauche chez des sujets contrôles. Ces exemples de plasticité cérébrale chez des sujets hors du commun conduisent alors à se demander si ce phénomène intervient aussi dans notre vie quotidienne. Les technologies digitales personnelles telles que les téléphones portables avec écran tactile ou *smartphones*, constituent des « supports » de choix pour répondre à cette question. Non seulement ces petits appareils occupent une place prépondérante dans nos vies, mais ils permettent également d'utiliser leur propre technologie pour en suivre l'utilisation faite par leur propriétaire.

L'électroencéphalographie (EEG) offre la possibilité d'étudier de manière non invasive, et avec une grande résolution temporelle, l'activité électrique générée par le cortex cérébral. L'étude relatée ici [9] a porté sur l'enregistrement de l'activité corticale par EEG de surface (62 électrodes sur le cuir chevelu) en réponse à des stimulations tactiles très focales (d'une durée de 2 ms, provoquant une légère déformation de la peau) appliquées sur la phalange distale du pouce, de l'index et du majeur droits chez 37 sujets droitiers : 26 possédaient un *smartphone* et 11 un téléphone portable d'ancienne génération, sans écran tactile. Des potentiels évoqués somatosensoriels (PES) ont été obtenus par le moyennage de 1 250 stimulations par doigt stimulé.

Les technologies digitales personnelles façonnent le traitement de l'information tactile par le cerveau

À notre plus grande surprise, alors que les utilisateurs de *smartphones* interagissaient avec l'écran tactile de leur appareil essentiellement par le pouce, l'amplitude de l'activité corticale en réponse aux stimulations tactiles des extrémités des trois doigts testés s'est avérée statistiquement plus grande chez les utilisateurs de *smartphones* que chez les utilisateurs de téléphones portables d'ancienne génération *(Figure 1A)*. Cette différence s'observait spatialement au niveau des électrodes contralatérales pariétales pour les trois sites de stimulation, bien que plus faible suite à la stimulation du majeur *(Figure 1B-C)*. Grâce à des stimulations tactiles simultanées des extrémités du pouce et de l'index, nous avons aussi démontré que l'augmentation de l'activité cérébrale chez les utilisateurs de *smartphones* ne s'était pas produite aux dépens des interactions inhibitrices [10] entre les doigts, phénomène qui permet d'augmenter la capacité de discrimination tactile.

Restait alors à expliquer l'activité corticale des adeptes du *smartphone*. Pour ce faire, des analyses de régressions multiples ont été réalisées entre l'activité cérébrale moyenne de la popula-

DOI : 10.1051/medsci/20153104006

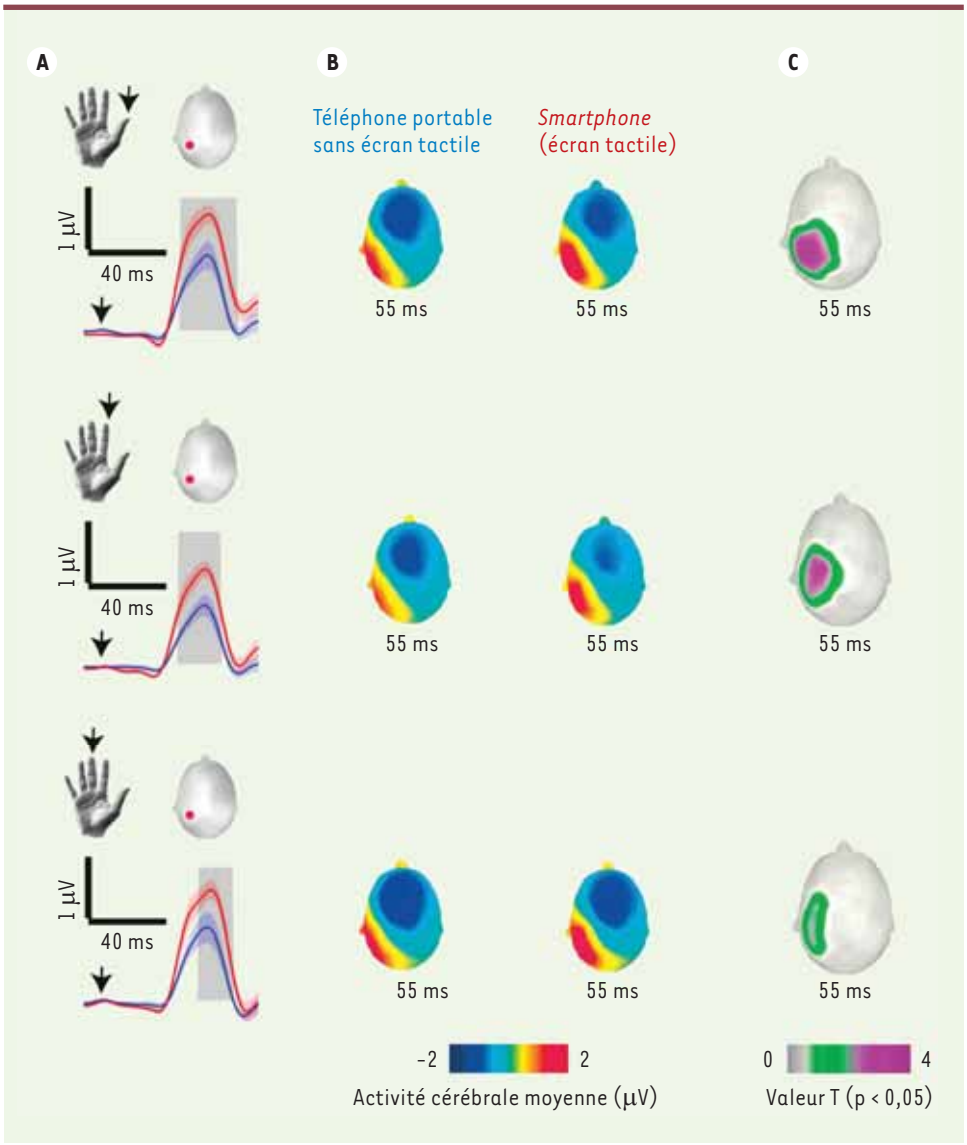

Figure 1. ***Modification du traitement de l'information tactile des doigts par l'usage de smartphones.*** ***A.*** Tracés moyennés (traits foncés) des potentiels évoqués somatosensoriels (PES) (référence moyenne) ± erreur type (zones plus claires) au niveau de chaque groupe de sujets, mesurés sur l'électrode (point rouge) montrant le plus grand PES positif en réponse à la stimulation tactile de la phalange distale du pouce droit (haut), de l'index droit (milieu) et du majeur droit (bas) chez les utilisateurs de *smartphones* (rouge) et chez les utilisateurs de téléphones portables sans écran tactile (bleu). Le rectangle gris correspond aux latences pour lesquelles il existe une différence statistiquement significative entre les deux groupes de sujets ($p < 0,05$ et $T > 1$, test *t* à deux échantillons corrigé ensuite pour les comparaisons multiples par un *clustering* spatiotemporel en 2D basé sur 1 000 *bootstraps*). Le début de la stimulation (0 ms) est indiqué par une flèche pointant en direction des tracés. ***B.*** Cartes correspondantes de la distribution du voltage mesuré sur le cuir chevelu 55 ms après la stimulation chez les utilisateurs de téléphones portables sans écran tactile et chez les utilisateurs de *smartphones*. ***C.*** Cartes des valeurs *T* ($p < 0,05$, corrigées ensuite pour les comparaisons multiples par un *clustering* spatiotemporel en 2D basé sur 1 000 *bootstraps*) indiquant la distribution des électrodes mesurant un signal significativement différent entre les deux groupes de sujets 55 ms après la stimulation (figure et légende reproduites de [9] - © 2015, avec la permission d'Elsevier).

tion d'utilisateurs de *smartphones* d'une part, et trois variables liées à l'utilisation de ces appareils d'autre part, à savoir l'âge du début de la pratique (inspiré par les résultats obtenus chez les joueurs d'instruments à cordes [8]), l'usage par heure et la durée comprise entre le pic d'utilisation du téléphone et l'acquisition EEG *(Figure 2)*. Ces deux derniers paramètres ont été dérivés directement de l'historique de l'utilisation de la batterie du *smartphone* pendant les 10 jours précédant l'acquisition EEG (évolution de la décharge de la batterie au cours du temps suivie au moyen d'une application).

Nous avons alors pu montrer que chez les utilisateurs de *smartphones*, l'activité corticale résultant de la stimulation tactile du pouce et celle liée à la stimulation tactile de l'index étaient directement proportionnelles à l'intensité de l'utilisation du téléphone (usage par heure). Deuxième fait marquant, la réponse à la stimulation tactile du pouce était sensible aux fluctuations quotidiennes de l'utilisation du *smartphone* : en effet, plus l'intervalle de temps compris entre l'épisode d'utilisation la plus intense du téléphone et la mesure de l'activité cérébrale en réponse à la stimulation du pouce était court, plus l'activité corticale associée était grande. Étant donné les grandes fluctuations de l'utilisation des *smartphones* au cours du temps en fonction de notre besoin, l'historique de l'utilisation de ces appareils

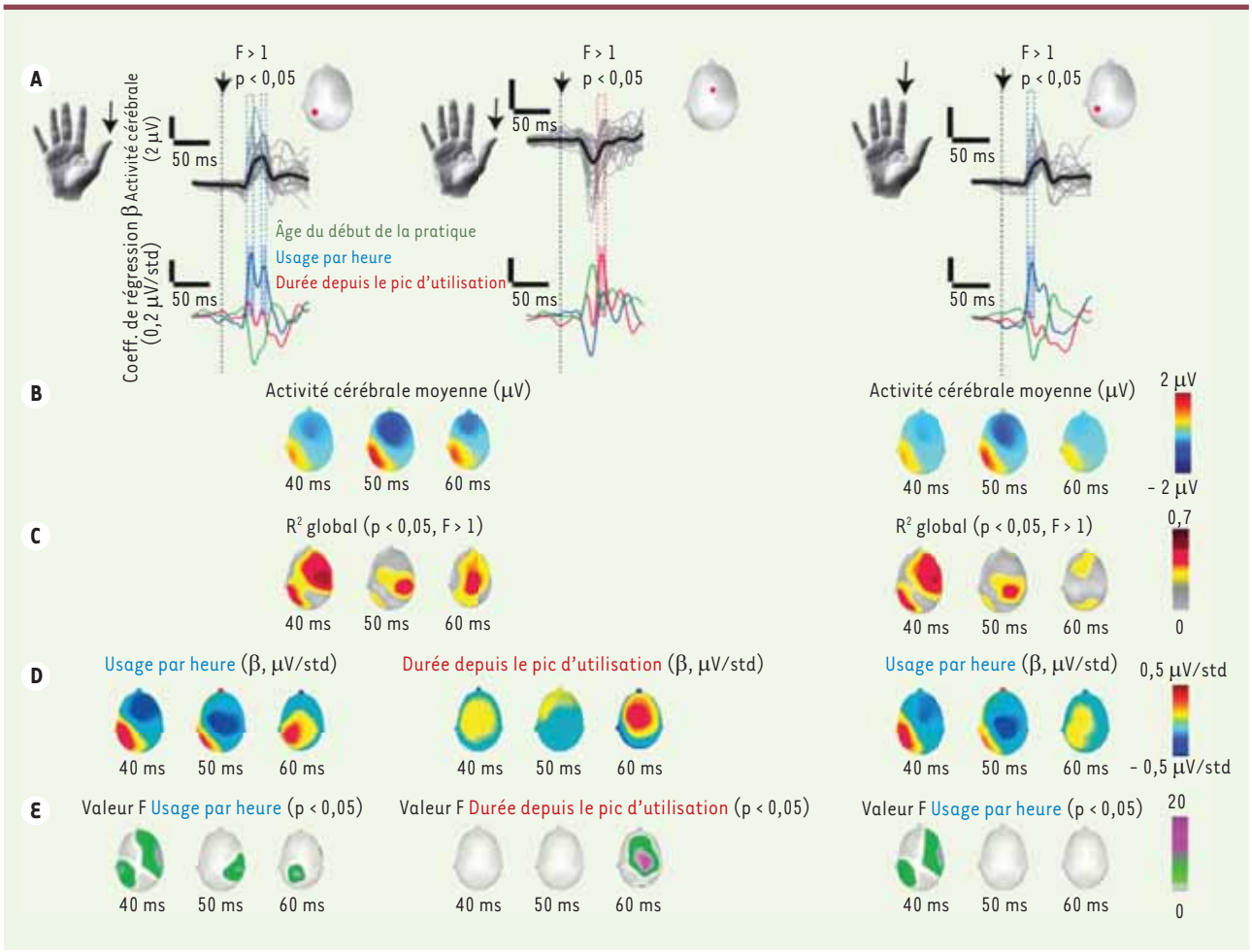

Figure 2. ***Relation entre les variations interindividuelles de l'activité corticale et l'utilisation des smartphones. A.*** Des analyses de régressions multiples ont été réalisées pour chaque site de stimulation entre les potentiels évoqués somatosensoriels (PES) (haut) et trois variables indépendantes (normalisées Z') liées à l'utilisation des *smartphones* : l'âge du début de la pratique, l'usage par heure (aire sous la courbe) et la durée depuis le pic d'utilisation (ln(h)). Des coefficients de corrélation β (bas) au cours du temps ont ainsi été obtenus pour chaque variable aux deux électrodes (point rouge) montrant le plus grand PES positif, respectivement négatif, en réponse à la stimulation tactile de chacun des trois doigts, mais seules les corrélations statistiquement significatives sont représentées ici. Les PES obtenus chez chaque utilisateur de *smartphones* (référence moyenne) sont représentés par les traits gris et la moyenne obtenue à l'intérieur de ce groupe est illustrée par le trait noir épais (haut). Le début de la stimulation (0 ms) est indiqué par une flèche pointant en direction des tracés. Les rectangles de couleur délimités par les traits pointillés correspondent aux latences auxquelles il existe une corrélation statistiquement significative (coefficients de corrélation β significatifs, $p < 0,05$, régressions corrigées ensuite pour les comparaisons multiples par un *clustering* spatiotemporel en 2D basé sur 1000 *bootstraps*) entre les PES et la variable correspondante (bas). std : écart-type. ***B.*** Cartes correspondantes de la distribution du voltage mesuré sur le cuir chevelu 40 ms, 50 ms et 60 ms après la stimulation. ***C.*** Estimation de la validité de l'ajustement correspondant pour le modèle de régression global (R^2) aux trois mêmes latences que ***B***. ***D.*** Cartes de la distribution sur le cuir chevelu des coefficients de corrélation β aux trois mêmes latences que ***B***. ***E.*** Cartes de la distribution sur le cuir chevelu des valeurs F statistiquement significatives aux trois mêmes latences que ***B***. L'usage par heure s'est avéré significativement corrélé aux PES suite à la stimulation tactile du pouce et de l'index sur certaines électrodes, alors que la durée depuis le pic d'utilisation s'est montrée significativement corrélée aux PES suite à la stimulation tactile du pouce sur certaines électrodes (figure et légende reproduites de [9], © 2015, avec la permission d'Elsevier).

basé sur les 10 jours précédant la mesure de l'activité cérébrale reflète l'utilisation à court terme seulement. Malgré cela, la relation linéaire entre l'activité corticale et les fluctuations journalières de l'utilisation des smartphones suggère qu'un remodelage du cortex a déjà pu se produire pendant cette courte période.

L'augmentation de l'activité corticale chez les utilisateurs de *smartphones* diffère de celle démontrée précédemment chez les joueurs d'instruments à

cordes [8]. Chez ces derniers, il existait une relation linéaire entre l'âge auquel les sujets avaient débuté la pratique de leur instrument et l'activité cérébrale, phénomène que nous n'avons pas observé chez les utilisateurs de *smartphones*. En revanche, nous avons pu mettre en évidence une relation linéaire entre l'utilisation récente (du *smartphone*) et l'activité corticale, lien qui n'existait pas chez les musiciens. Le fait que ces derniers aient entamé la pratique de leur instrument beaucoup plus précocement que les utilisateurs de *smartphones* l'emploi de leur téléphone, laisse à penser que ces musiciens disposaient d'une représentation sensorielle corticale beaucoup plus stable que celle des utilisateurs de *smartphones*.

Ces résultats suggèrent que les mouvements répétitifs opérés sur des écrans tactiles lisses réorganisent le traitement de l'information sensorielle à partir de la main, avec des ajustements quotidiens de la représentation corticale de l'extrémité des doigts selon l'intensité de l'utilisation du *smartphone*.

Conclusion

Loin de nous l'idée de faire sensation en nous prononçant sur un quelconque impact positif ou négatif de l'utilisation des *smartphones* sur notre vie quotidienne ! L'originalité de notre travail repose tout d'abord sur le désir d'étudier la plasticité cérébrale chez M. et Mme Tout-le-monde, mais également sur la formidable opportunité offerte par les *smartphones* d'utiliser leur propre technologie pour en quantifier l'usage. Il nous reste néanmoins encore beaucoup de facettes à explorer pour interpréter nos résultats plus en détail et les appliquer. Toutefois, il ressort de cette étude que l'utilisation de *smartphones* n'est pas anodine pour le cerveau, et qu'il faut rester attentif en cas d'utilisation très intensive. Notre approche pourrait permettre de disposer d'un outil adapté pour suivre, voire prévenir, des changements en cours (maladaptation) conduisant à un état pathologique (par exemple dysfonctions motrices ou douleur chronique neurogène). Cela nécessiterait alors d'étendre nos investigations à des sujets présentant des signes d'addiction. ◊

Smartphone use shapes cortical tactile sensory processing from the fingertips

REMERCIEMENTS

Ce projet a été financé par la Society in Science, The Branco Weiss Fellowship, OPO Stiftung et Vontobel Stiftung, Zürich (A. Ghosh) et le Fonds national suisse de la recherche scientifique (fonds n° 149643 (E.M. Rouiller). Nous remercions également Kevan Martin et les autres membres de l'Institut de neuroinformatique pour leur soutien, Cyril Pernet pour ses explications concernant LIMO EEG, Nobuhiro Hagura et Roland S. Johansson pour leurs commentaires, ainsi que les collègues de l'Université de Fribourg pour leur précieuse participation à l'étude.

LIENS D'INTÉRÊT

Les auteurs déclarent n'avoir aucun lien d'intérêt concernant les données publiées dans cet article.

RÉFÉRENCES

1. Dayan E and Cohen LG. Neuroplasticity subserving motor skill learning. *Neuron* 2011 ; 72 : 443-54.
2. Nudo RJ. Plasticity. *NeuroRx* 2006 ; 3 : 420-7.
3. Pascual-Leone A, Amedi A, Fregni F, *et al*. The plastic human brain cortex. *Annu Rev Neurosci* 2005 ; 28 : 377-401.
4. Flor H, Nikolajsen L, Staehelin JT. Phantom limb pain: a case of maladaptive CNS plasticity? *Nat Rev Neurosci* 2006 ; 7 : 873-81.
5. Langer N, Hanggi J, Muller NA, *et al*. Effects of limb immobilization on brain plasticity. *Neurology* 2012 ; 78 : 182-8.
6. Pearce AJ, Thickbroom GW, Byrnes ML, *et al*. Functional reorganisation of the corticomotor projection to the hand in skilled racquet players. *Exp Brain Res* 2000 ; 130 : 238-43.
7. Pascual-Leone A, Torres F. Plasticity of the sensorimotor cortex representation of the reading finger in Braille readers. *Brain* 1993 ; 116 : 39-52.
8. Elbert T, Pantev C, Wienbruch C, *et al*. Increased cortical representation of the fingers of the left hand in string players. *Science* 1995 ; 270 : 305-7.
9. Gindrat AD, Chytiris M, Balerna M, *et al*. Use-dependent cortical processing from fingertips in touchscreen phone users. *Curr Biol* 2015 ; 25 : 109-16.
10. Von Békésy G. *Sensory inhibition*. Princeton : Princeton University Press, 1967 : 278 p.

CHAPTER 7

Imprint of historical touchscreen minutes in cortical tactile processing

Gindrat AD*, Chytiris M*, Rouiller EM, Ghosh A

* Equal first authorship

The following part has been submitted to be considered for publication in the *Annals of Neurology*.

Author contributions and potential conflicts of interest

Author ADG performed the EEG measurements, helped gather the phone use data, and edited the manuscript. Author MC performed EEG measurements and helped gather the phone use data. Author EMR helped design the experiments and edited the manuscript. Author AG conceptualized the study, designed the experiments, helped in the data collection, analyzed the data and drafted the manuscript. None of the authors has any conflicts of interest to report.

Abstract

How experience-dependent brain plasticity is implemented in daily behavior is not known. We focused on smartphone behavior, which is characterized by bursts of touchscreen activity that last for a few seconds to minutes per episode but add up to hours of use per day. We used built-in touchscreen ON/OFF sensors to monitor this activity and relate the past experiences to cortical somatosensory evoked potentials induced from the fingertips. Our findings suggest that lower cortical somatosensory circuits are shaped at the level of individual behavioral episodes whereas higher circuits are shaped by both the aggregated durations and the unusually long episodes.

Introduction

The adult somatosensory cortex is remarkably plastic and reflects the history of sensory experiences (Pascual-Leone et al., 2005). This is vividly demonstrated by clinical neuroimaging of amputees or after spinal cord injury where the cortical body map is reorganized, resulting in phantom sensations (Brugger, 2008; Flor et al., 1995; Flor et al., 2006; Moore et al., 2000). Importantly, the specific pattern of cortical alterations corresponds to the type of experience and this has been well documented by using somatosensory evoked potentials (SEPs) in response to stimulation of the hand. For instance, after an arm is experimentally restrained for 12 hours, the magnitude of the cortical signal evoked from the corresponding body part *decreases* (Huber et al., 2006) whereas, on the contrary, the intense practice in expert string musicians *increases* the signal associated with the fingers engaged on the instrument (Elbert et al., 1995). However, much of our daily behavior occurs as spontaneous bursts of activity that are distinct from the long-lasting behavioral alterations induced by an injury or by the disciplined long durations of practice in athletes or musicians.

A significant part of our daily activities occurs on the digital network and touchscreen smartphone use is characterized by bursts of activity scattered throughout the day. Recently, by using a coarse but non-intrusive measure of phone use –in the form of built-in battery logs– we found that the SEPs induced by tactile stimuli delivered to the thumb and index fingertips were strongly related to phone use over the previous 10 days (Gindrat et al., 2015). In the present report we further leveraged the digital logs to quan-

titatively address how the duration of tactile interactions shapes cortical sensory processing. We recorded touchscreen smartphone use with built-in ON/OFF sensors for a period of 10-24 days and addressed whether the SEPs associated with the digit tips' tactile stimulation were related to the duration of individual episodes of phone use, the total duration spent on the phone per day or the presence of unusually long episodes of phone use.

Materials and Methods

Volunteers and touchscreen behavioral log

Thirty healthy right-handed touchscreen smartphone (Android operating system) users were recruited from the general public (10 females, age range 21 – 35 years, median 25 years). A custom written app (ACCAPP v1.0, available on Google Play) was used to continuously track the touchscreen on and off states with millisecond precision, from the time of installation to the EEG recording, corresponding to a period of 10 – 24 days (median 18 days). The touchscreen settings were standardized to switch off the screen upon 15 seconds of inactivity. The data were processed using MATLAB (MATLAB R2011b) to extract the mean touchscreen use duration per episode, the sum of all touchscreen use durations normalized to the number of days of recording and the kurtosis (indicator of exceptionally long episodes). Note that 2 volunteers were eliminated due to a malfunction of the app and 2 others for excessive muscular artifacts during the EEG. Two additional volunteers were eliminated from the middle finger analysis due to a malfunction of the tapper. The ethical committees of Cantons of Zurich and Vaud approved all the experimental procedures.

Touchscreen-finger interaction survey

Volunteers rank ordered a pictorial survey consisting of 18 images in accordance with their most preferred way of interacting with the touchscreen: 1 most preferred and 18 least preferred. The pictures were presented in random order on a single sheet. The images consisted of the following finger use postures on a touchscreen. The following abbreviations indicate – digits on touchscreen – 1 (thumb) to 5 (little finger), and – hand –

L (left) and R (right)): L1, R1, LR1 (touchscreen oriented in portrait), L2, R2, LR2, L3, R3, LR3, L4, R4, LR4, L5, R5, LR5, R2 (L hand-held), L2 (R hand-held), and LR1 (touchscreen oriented in landscape).

Somatosensory evoked potentials and multiple regression analysis

For EEG experiments tactile stimulations were delivered using computer-controlled solenoid tappers attached to the thumb, index and middle fingertips of the right hand (Heijo Research Electronics, UK). Each stimulus lasted for 2 ms and the digits were individually stimulated in a randomized order (inter-stimulus interval: from 750 to 1250 ms). Each digit tip was stimulated 1250 times while the volunteers watched a movie in a relaxed posture. The EEG signals were recorded by using 62 electrodes embedded in an equidistant cap (EASYCAP GmbH, Germany). The signals were amplified and digitized at 1 kHz (BrainAmp, Brain Products GmbH, Germany). Offline processing using EEGLAB (Delorme and Makeig, 2004) (open source MATLAB toolbox) involved band-pass filtering of the data between 1 to 45 Hz, baseline correction using 200 ms of pre-stimulation data, eye and muscle artifact rejection based on independent component analysis.

Multiple regression analysis was performed by using general linear modeling (LIMO-EEG, MATLAB toolbox, using EEGLAB) to link the phone use parameters and EEG signals across all 62 scalp electrodes and time points between 5 and 250 ms post-stimulation (Pernet et al., 2011). The regression analysis was corrected for multiple comparisons by using two-dimensional spatiotemporal clustering and 1000 bootstrapped samples (Pernet et al., 2011).

Results

According to the pictorial survey that ranked digit use, the right thumb interacted predominantly with the smartphone touchscreen, followed by the right index finger, whereas the middle finger was virtually never reported as a preferred finger; median ranks were 1 and 4 for the right thumb and index finger respectively on a scale of 1 to 18 where 1 was the most preferred posture. Interestingly, the touchscreen ON-OFF logs revealed a highly dynamic behavior characterized by bursts of activity spread through the

entire recording period (**Figure 1A, B**). We extracted three parameters to describe this behavior (**Figure 1B**): (1) the mean duration of a touchscreen use episode expressed in minutes per episode. (2) the sum of all the durations expressed in total number of minutes per day. (3) the Kurtosis of the distribution expressed in natural log units to normalize the population data. This measure is extremely sensitive to outliers, i.e. the presence of episodes of unusually long durations (Naik, 1989). According to paired linear regressions, these three parameters were at best only poorly linked to each other (all R^2 values were less than 0.17).

Repeated tactile stimulations of the thumb or index or middle fingertips resulted each in distinct positive peaks and a negative valley on the population mean SEP signal at peak latencies of 55 ($+^{ve}$ peak), 110 ($+^{ve}$), 160 ($-^{ve}$) and 200 ($+^{ve}$) ms over the contralateral somatosensory area. These latencies, comparable to previously reported values for similar tactile stimulations, were longer than SEP components resulting from electrical stimulation of the median nerve (Allison et al., 1992; Gindrat et al., 2015; Hämäläinen et al., 1990; Wood et al., 1988). Notably, for all the digit tips the inter-individual variability was higher in the late as opposed to the early SEP components.

We examined the statistical relationships between the phone use parameters and the SEP components by assessing the event related coefficients (ERCs) based on multiple regression analysis across all time points and electrodes. Interestingly, the pattern of ERCs varied according to the digits stimulated and latency of the SEP components. For the thumb (**Figure 1C-E**), the early cortical amplitude at 55 ms was exclusively related to the mean duration of touchscreen use. Essentially, the higher the mean duration per episode, the larger was the SEP signal amplitude at 55 ms. A more complex pattern of relationships was visible in the late components between 100 to 200 ms. Here, surprisingly, Kurtosis was directly proportional to the signal magnitude at 160 ms. Furthermore, the sum of the touchscreen use durations was directly proportional to the signal magnitude at 120 ms (falling edge of the 110 ms component on the grand mean signal described above), inversely proportional to the magnitude at 160 ms and again directly proportional at 200 ms. For the index finger (**Figure 2A-C**), a similar albeit less pronounced pattern of results was observed. In particular, significant correlations for the late SEP components were detected only from the 160 ms signal onwards. For the middle finger (**Figure 2D-F**), the results were even more different from those described for

the thumb in the sense that the early SEP components were not at all related to phone use while the late ones past 160 ms were related to all three variables.

Figure 1 (next page): Imprint of touchscreen phone use durations on somatosensory evoked potentials (SEPs) associated with the thumb tip. (A) Smartphone ON-OFF logs from a subject who was tracked for 18 days. (B) Distribution of the touchscreen use episodes from the same subject. Dashed red line: mean duration/episode. (C) SEPs recorded from an electrode over the contralateral somatosensory area in individual volunteers (gray traces) and population mean potential (black trace) in response to thumb tip tactile stimulation. The lower plot depicts the corresponding event-related coefficients (ERCs, β) and significant coefficients are shaded. Note that the positive SEP component at 55 ms revealed a positive coefficient exclusively for the mean duration per episode variable (in red) and note the surprising relationship of the negative component around 160 ms with Kurtosis (in blue), a highly sensitive measure of extraordinarily long episodes in the touchscreen history. Small arrow: stimulation onset (i.e., 0 ms). (D) Scalp maps of the grand average signal and the corresponding R^2 values for the regression model when using all the variables (full model). (E) Scalp maps of the ERCs (β) and the corresponding F-statistics for the individual phone use variables.

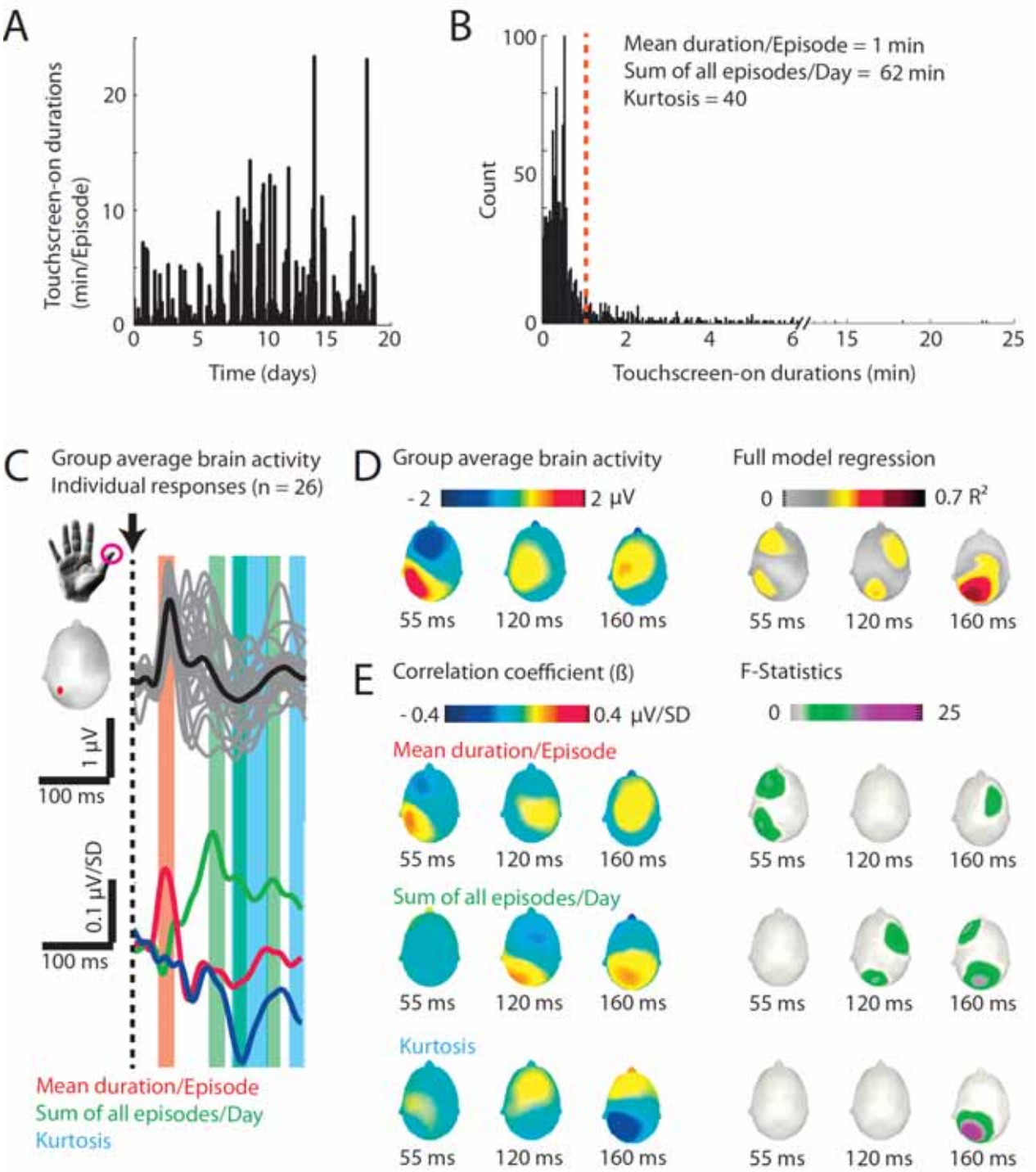
A
Touchscreen-on durations (min/Episode)
Time (days)
B
Mean duration/Episode = 1 min
Sum of all episodes/Day = 62 min
Kurtosis = 40
Count
Touchscreen-on durations (min)
C
Group average brain activity
Individual responses (n = 26)
1 µV
100 ms
0.1 µV/SD
100 ms
Mean duration/Episode
Sum of all episodes/Day
Kurtosis
D
Group average brain activity
- 2
2 µV
55 ms
120 ms
160 ms
Full model regression
0
0.7 R²
E
Correlation coefficient (ß)
- 0.4
0.4 µV/SD
F-Statistics
0
25
Mean duration/Episode
Sum of all episodes/Day
Kurtosis

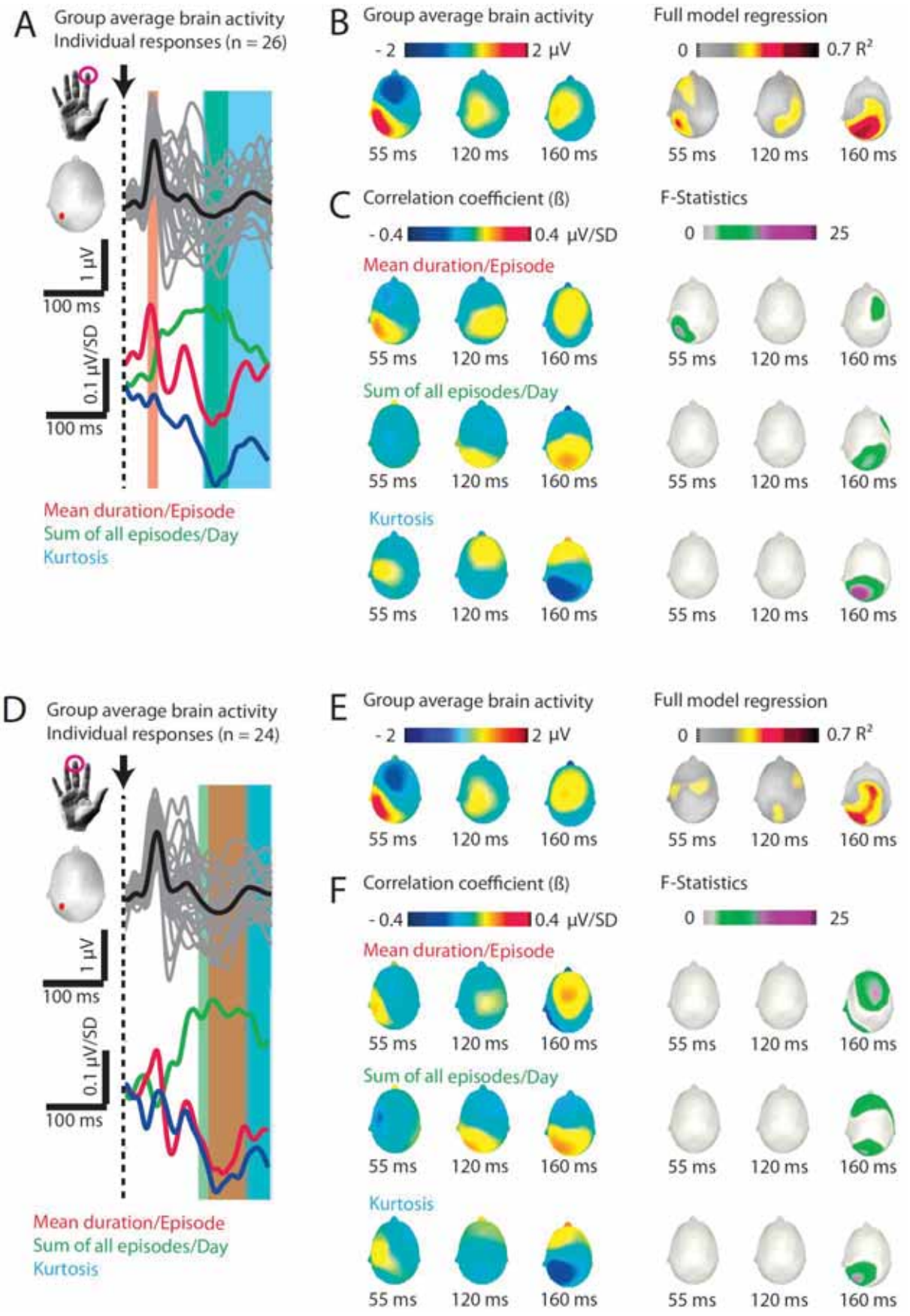
A
Group average brain activity
Individual responses (n = 26)
1 µV
100 ms
0.1 µV/SD
100 ms
Mean duration/Episode
Sum of all episodes/Day
Kurtosis
B
Group average brain activity
- 2
2 µV
55 ms
120 ms
160 ms
Full model regression
0
0.7 R²
55 ms
120 ms
160 ms
C
Correlation coefficient (ß)
- 0.4
0.4 µV/SD
Mean duration/Episode
55 ms
120 ms
160 ms
Sum of all episodes/Day
55 ms
120 ms
160 ms
Kurtosis
55 ms
120 ms
160 ms
F-Statistics
0
25
55 ms
120 ms
160 ms
55 ms
120 ms
160 ms
55 ms
120 ms
160 ms
D
Group average brain activity
Individual responses (n = 24)
1 µV
100 ms
0.1 µV/SD
100 ms
Mean duration/Episode
Sum of all episodes/Day
Kurtosis
E
Group average brain activity
- 2
2 µV
55 ms
120 ms
160 ms
Full model regression
0
0.7 R²
55 ms
120 ms
160 ms
F
Correlation coefficient (ß)
- 0.4
0.4 µV/SD
Mean duration/Episode
55 ms
120 ms
160 ms
Sum of all episodes/Day
55 ms
120 ms
160 ms
Kurtosis
55 ms
120 ms
160 ms
F-Statistics
0
25
55 ms
120 ms
160 ms
55 ms
120 ms
160 ms
55 ms
120 ms
160 ms

Figure 2 (previous page): Imprint of phone use durations on cortical processing from the index and middle fingertips. (A-C) Same conventions as in Figure 1 C-E except that SEPs were obtained from the index fingertip. (D-E) Same conventions as in Figure 1 C-E except that SEPs were obtained from the middle fingertip.

Discussion

Much of the daily behavior occurs as bursts of activity and our results show that distinct cortical sensory circuits are shaped to reflect the duration of individual behavioral episodes and their accumulated duration. Early cortical SEP components from the thumb or index fingertips were strongly related to the duration of individual touchscreen use episodes and the longer latency components were related to the sum of all the durations. Surprisingly, the late SEPs were also related to the presence of unusually long episodes (Kurtosis) of touchscreen use.

The time varying imprint of the touchscreen use parameters on the cortical SEP components may be partly due to the hierarchical nature of cortical somatosensory processing. First, it is well established that the early SEP components with a latency of around 50 ms originate in the primary somatosensory cortex and the later potentials between 100 - 200 ms originate from a more widespread network including the secondary somatosensory cortex (Allison et al., 1992; Hämäläinen et al., 1990; Hari and Forss, 1999; Wood et al., 1988). Second, according to non-human primate experiments the neuronal receptive fields lower in the sensory hierarchy represent individual digits as opposed to higher neurons that represent multiple fingertips (Fitzgerald et al., 2006). This may explain as to why the early SEP components were specifically related to touchscreen use for the digits that interacted on the screen (thumb and index finger), and why the later components were related to touchscreen use for all the three digits even though the middle finger was rarely ever engaged on the screen. Finally, the secondary somatosensory processors are implicated in sophisticated comparisons of consecutive inputs and such information processing may underlie plastic mechanisms that track the presence of unusually long durations (Chen et al., 2008; Romo et al., 2002). Interestingly, by using vibratory stimulations, a negative signal at 140 ms (N140) –which is comparable to the signal at 160 ms reported here– has been associated with the detection of deviant somatosensory inputs from an experimental stimuli train (Kekoni et al., 1997). It is tempting to

speculate that the sensory circuits that operate to detect such *unusual* stimuli overlap with the circuits engaged in the plasticity driven by *unusually* long touchscreen use episodes.

In conclusion, touchscreen use in conjunction with SEP measurements from the fingertips offered a quantitative view on experience-dependent cortical sensory processing in daily behavior. The knowledge of the behavioral parameters that imprint on the sensory processors is crucial for the search of mechanisms that enable successful day-to-day behavior. Non-intrusive personal digital histories can be related to neurological measurements and we believe that such an approach offers a fresh opportunity for personalizing neurology.

Acknowledgements

This study was supported by the Society in Science Branco Weiss Fellowship awarded to author AG, by research grants from Holcim Stiftung Wissen, OPO Stiftung and Vontobel Stiftung to author AG, and by Swiss National Science Foundation grant no. 149643 to author EMR. The authors thank Myriam Balerna who helped with data collection and Enea Ceolini who helped develop the App used to track smartphone behavior.

References

Allison, T., McCarthy, G., Wood, C.C., 1992. The relationship between human long-latency somatosensory evoked potentials recorded from the cortical surface and from the scalp. Electroencephalography and Clinical Neurophysiology/Evoked Potentials Section 84, 301-314.

Brugger, P., 2008. The phantom limb in dreams. Consciousness and Cognition 17, 1272-1278.

Chen, T.L., Babiloni, C., Ferretti, A., Perrucci, M.G., Romani, G.L., Rossini, P.M., Tartaro, A., Del Gratta, C., 2008. Human secondary somatosensory cortex is involved in the processing of somatosensory rare stimuli: An fMRI study. Neuroimage 40, 1765-1771.

Delorme, A., Makeig, S., 2004. EEGLAB: an open source toolbox for analysis of single-trial EEG dynamics including independent component analysis. J Neurosci Methods 134, 9-21.

Elbert, T., Pantev, C., Wienbruch, C., Rockstroh, B., Taub, E., 1995. Increased cortical representation of the fingers of the left hand in string players. Science 270, 305-307.

Fitzgerald, P.J., Lane, J.W., Thakur, P.H., Hsiao, S.S., 2006. Receptive Field (RF) Properties of the Macaque Second Somatosensory Cortex: RF Size, Shape, and Somatotopic Organization. The Journal of Neuroscience 26, 6485-6495.

Flor, H., Elbert, T., Knecht, S., Wienbruch, C., Pantev, C., Birbaumers, N., Larbig, W., Taub, E., 1995. Phantom-limb pain as a perceptual correlate of cortical reorganization following arm amputation. Nature 375, 482-484.

Flor, H., Nikolajsen, L., Staehelin, J.T., 2006. Phantom limb pain: a case of maladaptive CNS plasticity? Nat.Rev.Neurosci. 7, 873-881.

Gindrat, A.D., Chytiris, M., Balerna, M., Rouiller, E.M., Ghosh, A., 2015. Use-Dependent Cortical Processing from Fingertips in Touchscreen Phone Users. Current Biology 25, 109-116.

Hämäläinen, H., Kekoni, J., Sams, M., Reinikainen, K., Näätänen, R., 1990. Human somatosensory evoked potentials to mechanical pulses and vibration: contributions of SI and SII somatosensory cortices to P50 and P100 components. Electroencephalography and Clinical Neurophysiology 75, 13-21.

Hari, R., Forss, N., 1999. Magnetoencephalography in the study of human somatosensory cortical processing. Philosophical Transactions of the Royal Society B: Biological Sciences 354, 1145-1154.

Huber, R., Ghilardi, M.F., Massimini, M., Ferrarelli, F., Riedner, B.A., Peterson, M.J., Tononi, G., 2006. Arm immobilization causes cortical plastic changes and locally decreases sleep slow wave activity. Nat Neurosci 9, 1169-1176.

Kekoni, J., Hämäläinen, H., Saarinen, M., Gröhn, J., Reinikainen, K., Lehtokoski, A., Näätänen, R., 1997. Rate effect and mismatch responses in the somatosensory system: ERP-recordings in humans. Biological Psychology 46, 125-142.

Moore, C.I., Stern, C.E., Dunbar, C., Kostyk, S.K., Gehi, A., Corkin, S., 2000. Referred phantom sensations and cortical reorganization after spinal cord injury in humans. Proceedings of the National Academy of Sciences 97, 14703-14708.

Naik, D.N., 1989. Detection of outliers in the multivariate linear regression model. Communications in Statistics - Theory and Methods 18, 2225-2232.

Pascual-Leone, A., Amedi, A., Fregni, F., Merabet, L.B., 2005. The plastic human brain cortex. Annu.Rev.Neurosci. 28, 377-401.

Pernet, C.R., Chauveau, N., Gaspar, C., Rousselet, G.A., 2011. LIMO EEG: a toolbox for hierarchical LInear MOdeling of ElectroEncephaloGraphic data. Comput.Intell.Neurosci. 2011, 831409.

Romo, R., Hernandez, A., Zainos, A., Lemus, L., Brody, C.D., 2002. Neuronal correlates of decision-making in secondary somatosensory cortex. Nat.Neurosci. 5, 1217-1225.

Wood, C.C., Spencer, D.D., Allison, T., McCarthy, G., Williamson, P.D., Goff, W.R., 1988. Localization of human sensorimotor cortex during surgery by cortical surface recording of somatosensory evoked potentials. Journal of Neurosurgery 68, 99-111.

CHAPTER 8

May one conceive research in Neuroscience without animal models ?

This chapter is the written and refined version of a public conference held by A-D Gindrat at the *Société Jurassienne d'Émulation* in Porrentruy on the 14th May 2014.

Introduction

Strictly speaking, this chapter is not part of my PhD thesis project. Nevertheless, by working nowadays with macaque monkeys, we inevitably must face some increasingly incessant ethical issues concerning animal experimentation from the general population as well as from the friend and family circles. Are we allowed to inflict constraints on an animal in order to gain knowledge that will enable to cure human diseases and to improve our daily life? How do we justify the use of animals' life to safe ours? I propose here to consider this ethical dilemma from the other side by reformulating these questions as follows: *May one conceive biomedical research, especially in Neuroscience, without animal models ?*

To my mind, favouring educational initiatives, for instance by concretely illustrating some achievements obtained in Neuroscience thanks to animal models, is the easiest and best way to argue against preconceived ideas about the use of laboratory animals and to make the general population aware of their crucial role for biomedical research and, as a consequence, for our health and our life. To this end, I will illustrate here the invaluable contribution of animal models to biomedical research, with a special emphasis on Neuroscience, by means of three examples, namely (i) the development of neuroprosthetics, (ii) the development of therapies based on anti-Nogo-A antibody to promote the CNS regeneration, and (iii) the development of therapies to relieve the symptoms of Parkinson's disease.

Our brain, this fascinating organ

Human has always been fascinated by the brain. One evidence of this statement is the discovery of a stone age cranium (about 5100 BC) in a burial site in Alsace (France) showing two clear marks of trepanations (**Figure 1**) (Alt et al., 1997). Interestingly, both holes had more or less healed (the anterior hole closed completely whereas the posterior one only partially), indicating unequivocally that this "surgery" was performed *intra vitam*, on living people, and was on no account a *post mortem* ritual. This example constitutes the oldest known indication of a healing brain "surgery" on living subjects.

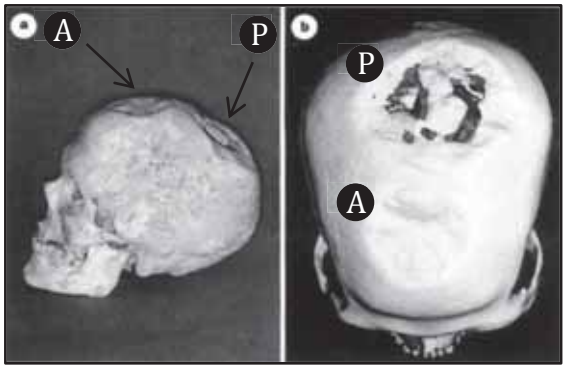

Figure 1: Oldest proof of skull "surgery" discovered in Ensisheim (Alsace, France). (a) Lateral view of the cranium. The position of both anterior (A) and posterior (P) trepanations is indicated by the arrows. (b) 3D reconstruction of the cranium by computed-tomography, seen from above (modified from Alt et al., 1997).

This pronounced interest in the brain led to the development of Neuroscience as an interdisciplinary field of science focused on understanding the development, the organisation and the functioning of the nervous system "*from genes to cognition, from molecules to mind*" (Kandel and Squire, 2000). The ultimate aims of Neuroscience are to understand the biological mechanisms of mental activity and to develop potential treatments to cure diseases and disorders affecting the nervous system (Albright et al., 2000). Nowadays, Neuroscience encompasses several disciplines, each of them focused on a specific level of organisation of the nervous system (Albright et al., 2000; Bear et al., 2007):

- *Neuroanatomy* : study of the nervous system organisation
- *Electrophysiology* : study of the electrical phenomena taking place in the nervous system
- *Molecular neurobiology* : study of the functioning of the nervous system at the molecular level
- *Cellular neurobiology* : study of the functioning of the nervous system at the cellular level
- *Systems Neuroscience* : study of the functioning of the various sensory and motor systems
- *Behavioural Neuroscience* : study of the bases of integrated behaviours, such as memory, dreams, emotions, addiction, gender-specific behaviours, etc.
- *Cognitive Neuroscience* : study of the neural mechanisms underlying high-level mental activity, such as self-awareness, cognition, language, etc.

- *Neurology and psychiatry* : study of the diseases affecting the nervous system such as depression, schizophrenia, Alzheimer's disease, Parkinson's disease, mania, multiple sclerosis, etc., and the conditions resulting from a lesion of the nervous system, such as stroke, spinal cord lesion, etc.
- *Neuropsychiatry*: study of the localisation of the biological source of mental functions.

The brain is a highly complex, if not the most complex, and fascinating organ. Several lines of evidence illustrate this assertion. If one considers the adult human brain in particular:

- The brain has $86.1 \times 10^9 \pm 8.1 \times 10^9$ neurons and $84.6 \times 10^9 \pm 9.8 \times 10^9$ glial cells (Azevedo et al., 2009; Herculano-Houzel, 2009), all of them contained in a volume as small as 1.32-1.51 dm^3 (Luders et al., 2002).
- There are about 0.15×10^{15} (quadrillion) synapses between neurons in the neocortex (Pakkenberg et al., 2003).
- The sulci on the cortex allow to obtain a cortical area equal to 2000-2500 cm^2, corresponding to an A2 paper sheet (Griffin, 1994).
- The cumulated length of the myelinated nerve fibres is about 180'000 km (Pakkenberg et al., 2003), corresponding roughly to 4.5 times the Earth perimeter!
- The brain represents about 2% of the body weight but it consumes on average 15% of the cardiac output, 20% of total body oxygen, and 25% of total body glucose (Herculano-Houzel, 2011; Magistretti et al., 1995; Raichle and Gusnard, 2002).

Ethical dilemma[16]

Nowadays, many facets of the nervous system and the brain in particular remain still largely unknown and the research in Neuroscience is interested to unravel the mechanisms of this complex machinery at all its levels of organisation. Of prime importance is to understand the mechanisms of the pathologies affecting the nervous system in order to prevent, cure or relieve them. Nevertheless, from an ethical point of view, some experiments on human subjects would be completely unacceptable. Animal models play then a critical role at this stage. Some crucial contributions of animal experimentation to biomedical research will be reviewed in the next paragraphs.

Experiments on laboratory animals imply a serious ethical dilemma because we assume that animals, vertebrates in particular, are able to suffer and feel pain. This critical issue –"*Can they suffer ?*"– was first raised by the British philosopher Jeremy Bentham (1748-1832) (Bentham, 1789). Are we allowed to inflict constraints on an animal in order to gain knowledge that will enable to cure human diseases and to improve our daily life? How do we justify the use of animals' life to safe ours? The way we solve this problem, i.e. our position with regard to animal experimentation, depends actually on the moral value we attribute to animals. Some people admit a moral value for human only. At the other extreme, others think that everything in the world has the same moral value, human being at the same level as a sand grain for instance. In between, some others consider that human has a similar moral value as the one of other primates, but larger than the one of the other living beings. In fact, many different scenarios are possible between both extreme points of view. The most important thing is to position itself according to its own conscience. If we consider that human has the highest moral value, then we take the liberty of using animals to simply live or to improve our quality of life, such as the use of production animals for food, working animals (guide dogs, police dogs and horses, beasts of burden), animals for clothing (wool, fur, leather), pets, leisure animals (in zoo, in circus, for sport) and by the same logic laboratory animals for research. Nevertheless, in this latter case, we must carry out a constant balancing of interests between, on the one hand, the benefits for human in terms of scientific knowledge that should result from the experiment and, on the other hand, the discomfort and pains inflicted on the

[16] For a more complete discussion of ethical issues of research on laboratory animals, see *The ethics of research involving animals* (Nuffield Council on Bioethics, 2005) and Hurst and Mauron (2012).

animals. To put it another way, an experiment expected to induce some pains to the animals has to be justified by the benefits obtained in return for human.

Application fields of research based on animal models

Studies on animal models were and continue to be of prime importance in several fields.

First, several basic principles of neuroanatomy and neurophysiology remain still misunderstood (see e.g. Albright et al., 2000; Cui et al., 2015; Glanzman, 2012; Kandel and Squire, 2000; Lemon, 2012) and may be unraveled only by performing experiments on animals. To put it another may, animal models may lead to meaningful progress in scientific research and improve the state of the art in Neuroscience, in particular. One could argue that basic research is sterile, completely disconnected from reality and is only for the beauty of science. In actual fact, basic research and applied research are intimately linked and benefit from each other, and only their joint contribution leads to progress in medicine. Today's basic research shall benefit to tomorrow's applied research:

"All ignorance is bad and all knowledge good. We were born into this world a long time ago. In the beginning, we knew nothing of the forces surrounding us. But for all these millions of years the human brain has been chipping away at that ignorance, storing up hard-earned wisdom. This is the greatest adventure of mankind: to find something that was never known before, or understood. Each new piece of knowledge does not need to have a specific or functional use, at least not at the moment. It is sufficient triumph that we have learned something and proved it by documentation, that had formerly been part of the darkness." (Stone, 1971)

Moreover, note that the freedom of scientific research is a fundamental right explicitly guaranteed by the Swiss Constitution (Title 2, Chapter 1, Article 20), the European Union legislation (Recital 17 and Article 8 of the revised EU Council Directive on the protection of animals used for scientific purposes -2010/63/EU; see Chapter 2 on animal research), and the United Nation Human Rights (International Covenant on Economic, Social and Cultural Rights, 1966, Article 15, Paragraph 3).

Second, the pathophysiology of many human diseases remains elusive and experiments on animals may enable to improve our understanding of them and ultimately make

some key progress in human medicine and treatments (translational medicine) (see e.g. Baumer et al., 2014; Charalambous et al., 2015; Cui et al., 2015; Hamani and Temel, 2012). Successfully treating and completely recovering from some diseases that were fatal in the past is today obvious for us. Nevertheless, without animal models, it would not have been possible to develop vaccines against diphtheria (Behring, 1913; Wadsworth et al., 1932) or poliomyelitis (Enders et al., 1949; Enders et al., 1954; Landsteiner and Popper, 1909) for instance, to develop blood transfusion (Crile, 1907), to discover insulin (Banting, 1925; Macleod, 1925) and other treatments (Szkudelski and Szkudelska, 2015) against diabetes, to discover antibiotics (for reviews, see Fantin and Carbon, 1992; Fleming, 1929; Marra, 2012; White, 2012; Zak and O'Reilly, 1991), to develop dialysis for kidney failure (Abel et al., 1914), to discover the Rhesus factor system (Landsteiner and Wiener, 1941), to develop treatments to cure cardiac diseases (Hasenfuss, 1998; Houser et al., 2012), to increase understanding of prion diseases (Gajdusek, 1976), to develop some treatments against various cancers (see e.g. Merchant et al., 2002) and leukaemia (see e.g. le Coutre et al., 1999), or to develop therapies against AIDS (see e.g. Hessell and Haigwood, 2015; Ruprecht et al., 1986). Equally important, surgical procedures were and continue to be developed through the use of animal models, such as the development of cardiac surgery (Bigelow et al., 1950; Carrel, 1912; Starr and Edwards, 1961), tissue and organ graft (Moore, 1964). More specific examples of progress in Neuroscience research established by experimenting on animals will be given below. For a detailed survey about medical advances accomplished by using animal experiments, see http://www.animalresearch.info/en/medical-advances/.

Third, while non-invasive imaging tools, among others for the human brain, are widely used nowadays and have already led to improve our understanding of the pathophysiology of many neurological disorders, we still poorly understand for example how the electrical activity at the level of single neurons within the brain does contribute to the haemodynamic response captured by fMRI (Kayser and Logothetis, 2013; Logothetis, 2008; Logothetis and Wandell, 2004) or to the electrical (in particular, the origins and mechanisms of far-field SSEPs are still under debate) and magnetic fields recorded in scalp EEG, respectively MEG. Some essential invasive and detailed neurophysiological studies at the micro- and mesoscopic levels on animal models with a brain anatomy and physiology close to human's ones are therefore of prime importance to improve our knowledge about the fundamental principles of functioning of these diagnostic tools

used in human medicine, in order to correctly interpret the data they provide and to calibrate these imaging methods appropriately (Lemon, 2012; Lopes da Silva, 2013).

Fourth, in Switzerland, the development of a new drug is a long-term process lasting for many years before the new active principle is officially authorised to be available on the market (**Figure 2**). Among the requirements is the ethical and legal obligation (according to the *Ordonnance de l'Institut suisse des produits thérapeutiques du 9 novembre 2001 sur les exigences relatives à l'autorisation de mise sur le marché des médicaments (Ordonnance sur les exigences relatives aux médicaments, OEMéd)*) to test the new drug firstly on laboratory animals to ensure that the subsequent tests on human will be safer. These studies have to be performed, at least partially, on animals anatomically or physiologically close to human, such as pigs or non-human primates. To elaborate, investigations using animal models include pharmacological and pharmacokinetics tests, tolerance essay and teratological assessment on animal fetus, teratological assessment on animal reproduction and tolerance over the short term and the long term. This means that every officially authorised pharmaceutical is linked to tests beforehand carried out on animals.

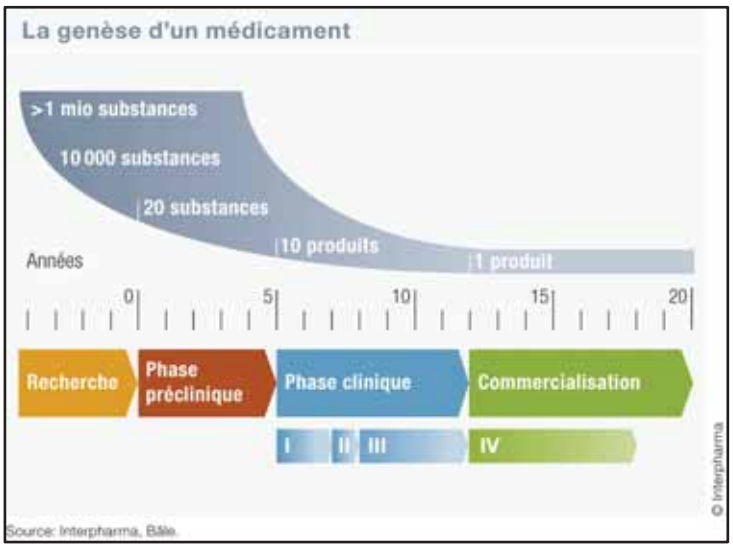

Figure 2: In Switzerland, the development of new phamaceuticals requires 4 successive steps: research, pre-clinical phase, clinical phase and launching, the whole process lasting for many years. For further detail, see the link below (from http://www.interpharma.ch/fr/faits-et-statistiques/2830-la-longue-naissance-dun-medicament).

Finally, veterinary medicine and animals themselves do benefit from advances in biomedical research. Indeed, medical research carried out by using animal models has already led directly to veterinary treatments, in addition to those addressed to human. Good illustrations of this are vaccines for feline leukaemia (Lewis et al., 1988; Mastro et

al., 1986; Olsen et al., 1987) and canine distemper (for a review, see Appel, 1999). Moreover, animal experiments led to the discovery of new veterinary medicines and vaccines that allow to reduce the risk of some diseases and improve the health status of production animals (Sang and Blecha, 2014) and endangered species (Chang et al., 2007; Turnbull et al., 2004).

Animal models involved in biomedical research

Biomedical research resorts to different animal models, from invertebrates such as drosophila or nematodes to non-human primates through zebrafish, chickens, rabbits, ferrets, hamsters, guinea pigs, sheep, pigs, rodents, cats and dogs. This list is non-exhaustive. In any case, the principle of subsidiarity has to be applied, meaning that an experiment has always to be performed using an animal model classified at the lowest rank from an evolutionary point of view. Simply put, if a hypothesis can be tested using a mouse, there is no need to test it with a non-human primate. Basic research often uses primitive organisms to unravel some fundamental principles. Examples include the first intracellular electrophysiological recordings of animal neurons performed on squid giant axons (Cole and Curtis, 1941; Curtis and Cole, 1938) that enabled to characterise the properties of action potentials (Curtis and Cole, 1942; Hodgkin and Huxley, 1939), or the famous discovery of the basic principles of learning and memory by using *Aplysia* (Bailey et al., 1996; Bailey and Kandel, 2008; Hawkins et al., 2006; see e.g. Kandel et al., 1986). Nevertheless, the more one focuses on a question such as the refinement of a protocol, the more evolutionarily high-ranking animals are used. For instance, the closer to marketing new developed pharmaceuticals are, the more the tests are performed on animals metabolically close to human.

The situation in Switzerland

In Switzerland, the total number of animals involved in research has strongly decreased in the last 30 years, going from 1'992'794 in 1983 to 606'434 in 2012 (**Figure 3A**), namely a decrease of 70%. This strong decline can be explained with the 3R principles explained below. The small increase in the number of laboratory animals observed from

2000 comes from the development of biomedical research involving in particular transgenic models. Moreover, some new diseases appeared recently, such as bovine spongiform encephalopathy (end 1990s), AIDS, Avian influenza (from 2004), all of them requiring to develop new treatments.

Animal experiments involve primarily mice and rats. Conversely, non-human primates (red line at the top of each bar in **Figure 3B**) constitute a nearly negligible amount compared with the total number of animals (from 0.04% in 2010 to 0.13% in 2000). Most experiments are classified with a severity degree of 0 (i.e. no constraint) or 1 (mild constraints) (**Figure 3C**). For comparison, statistics from Great Britain are available in **Supplementary Figure 1**.

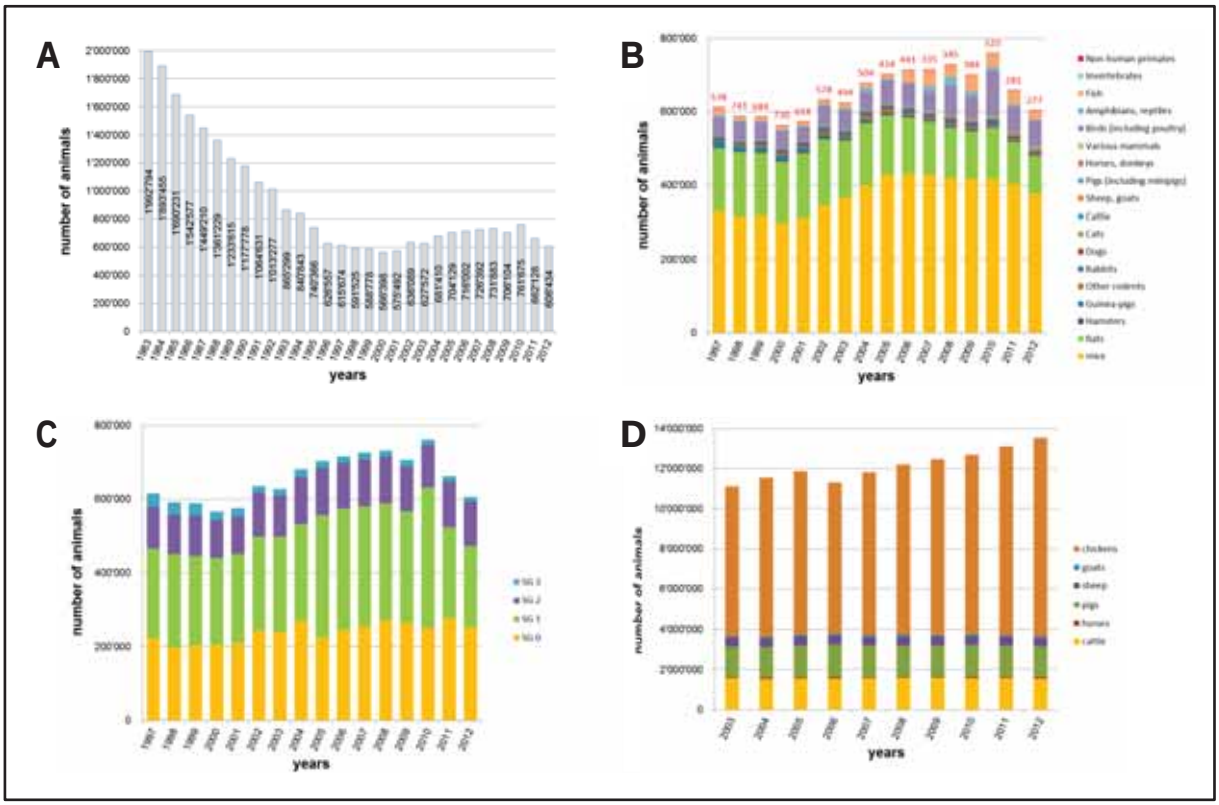

Figure 3: Number of animals used for research in Switzerland. (A) Total number of animals involved, from 1983 to 2012. The value for each year is indicated in the corresponding bar. Data from http://tv-statistik.ch/fr/statistique-simples/index.php. (B) Number of animals involved from 1997 to 2012, according to the species. Non-human primates are displayed in red at the top of each bar and the number is given in red. (C) Number of animals involved from 1997 to 2012, according to the severity degree (SG, from SG 0 to SG 3). See the text below for greater detail. B and C from

http://tv-statistik.ch/fr/statistiques-dynamiques/index.php. Note that in A, B and C, in case a laboratory animal is used for several years, it appears each year in the statistics. This is the case in particular for non-human primates that are usually involved in protocols lasting for several years. (D) For comparision, the number of production animals is given, according to species/group of species, from 2003 to 2012. Data from http://www.bfs.admin.ch/bfs/portal/fr/index/themen/07/03/blank/data/01/03.html. Note that the y-axis scale was adapted for each graph.

One immediately relativises these numbers by comparing them to the total number of production animals in Switzerland from 2003 to 2012 (**Figure 3D**). One notices then obviously that we breed overwhelmingly more animals to further eat them than the total number of animals involved in research. Even though this very small proportion of animals used for research in Switzerland, it did not prevent demonstrations, threats and attacks towards researchers from happening, from organisations against animal experimentation. For instance, in 2009, activists set fire to Daniel Vasella's holiday chalet (chief executive of the pharmaceutical company Novartis) and desecrated his mother's grave as well.

The Swiss legislation is one of the strictest in the world regarding animal experimentation, governed by the Federal law about animal welfare (*Loi fédérale sur la protection animale (LPA 2012)*) and the Edict about animal welfare (*Ordonnance sur la protection des animaux (OPAn 2008)*). This legislation deals with authorisation granting and checking animal experiments. From the 1st July 1981, corresponding to the first Edict about animal welfare coming into force, most of animal experiments need an authorisation to be performed. Swiss people clearly voted several times against banning or considerably restricting animal experimentation (70.5% rejection of federal citizen's initiative "for the abolition of vivisection" in 1985; 56.4% rejection of federal citizen's initiative "for a gradual but drastic reduction in animal experiments (An end to animal experimentation!)" in 1992; 72.2% rejection of federal people's prerogative "to abolish experimentation on animals" in 1993; 70.5% rejection of federal citizen's initiative "against the cruelty of animals and for better legal protection of animals (Initiative for instituting a lawyer for animal protection)" in 2010[17]). From 1992, animals are not considered to be things anymore and the Swiss constitution enshrined that the *dignity of creatures* should be re-

[17] From http://www.bk.admin.ch/themen/pore/vi/index.html?lang=fr

spected, at least in the German version of the Swiss Constitution while this was translated into *integrity of living beings* in the French version (language discrepancy, if not a regional cultural disparity…).

To perform a study involving animal experimentation in Switzerland, several conditions have to be fulfilled: first, the project needs financing, either from the Swiss National Science Foundation (SNSF), or from a private institution or other. To this aim, the quality, the originality and the methodology of the project had to be beforehand acknowledged. Second, a veterinary authorisation by the Cantonal Veterinary Office is mandatory (valid for 3 years at the most) (see **Supplementary Figure 2**). Researchers have to demonstrate that the benefits for society exceed the constraints inflicted on the animals during experiments (constant balancing of interests). Actually the Swiss Federal Veterinary Office has classified animal experiments according to 4 severity degrees, according to the constraints which the animals are subject to[18] (see **Figure 3C**). In addition, there have to be members from animal welfare organisations in the commissions assessing the research projects involving animal experimentation. If needed, the Federal Veterinary Office can then appeal against the authorisation by the Cantonal Veterinary Office. Moreover, all researchers who carry out or supervise animal experiments have to receive appropriate training course. (DFE Ordinance 455.109.1), in the form of an introductory course in laboratory animal science (module 1; section 2: article 23). For those planning and supervising animal experiments, an additional course is required (module 2; section 3: article 27).

The *3R Research Foundation Switzerland* is an institution jointly set up in 1987 by deputies of Swiss Parliament working on animal experiment, by the Interpharma (Association of Swiss pharmaceutical industries performing research : Actelion Ltd, Merck Serono International SA, Novartis Pharma SA, F. Hoffmann-La Roche SA, Bayer (Suisse) SA, Cilag SA and Vifor SA) and by the animal welfare organisation *Fund for Research without animal experiment* (*Fonds pour une Recherche sans expérimentation animale*), now called *Animalfree Research*. Its goal is to favour the implementation of the 3R principle (*Replace*, *Reduce*, *Refine*) in research. Experiments on animals are allowed only if there is no alternative method (*Replace*), such as *in vitro* or computer modelling approaches. Moreover, the number of animals used has to be reduced to a minimum (*Reduce*). Finally, an-

[18] For more information, see http://www.blv.admin.ch/themen/tierschutz/00777/03579/index.html?lang=fr.

imal experiments have to be designed in such a way to limit as much as possible the constraints inflicted on the animals (*Refine*), for instance by providing enough enrichment in the animal facility (Buchanan-Smith, 2011; Lutz and Novak, 2005) and by using appropriate dosages of anaesthetics and painkillers when needed (Coleman et al., 2012; Committee for the Update of the Guide for the Care and Use of Laboratory Animals and National Research Council, 2011; Murphy et al., 2012). It is important to mention that working in accordance with the 3R principles is in researchers' interest because experiments involving laboratory animals are very expensive. Moreover refined methodologies allowing to increase animal welfare are crucial because many results would be completely altered and therefore irrelevant if they were obtained on animals under stress.

The non-human primate as model of choice in Neuroscience[19]

In vitro strategies (see e.g. Puschmann et al., 2013) and substitution models (see e.g. Gerstner et al., 2012; Huang et al., 2012; Pamies et al., 2014) can prove very powerful to solve some Neuroscience issues. Nevertheless, resorting to animal models, such as rodents or non-human primates, may be required in other situations (Editorial Nature Medicine vol.19 (10), 2013; Lemon and Griffiths, 2005).

Experiments conducted on rodents have led among others to better understand the mechanisms of memory (Crystal and Alford, 2014; Halstead et al., 1967; Martin and Clark, 2007; Rosenzweig and Leiman, 1968) and those of drug addiction (Hopf and Lesscher, 2014; Quintero, 2013; Schuster and Thompson, 1969). Furthermore, rats have proved to be relevant models for some human diseases, such as in X fragile syndrome research (see e.g. Berry-Kravis et al., 2012; Henderson et al., 2012; Rotschafer and Razak, 2013).

[19] This issue is presented in detail in the Weatherall report (Weatherall et al., 2006). This key document in the field of biomedical research examined the scientific basis for the use of non-human primates in research, based on an exhaustive overview of scientific literature (376 bibliographic references!). Briefly, the Weatherall report concluded that the non-human primate is an irreplaceable model, at least for the foreseeable future, for biomedical research in infectious communicable diseases, neuroscience (pp. 59-83), reproductive biology, developmental biology, aging and for drug development, among others. The recommendations expressed in this report still apply in 2015, in particular if we consider the recent Ebola epidemic and the urge need to develop a vaccine against this devastating virus.

Nevertheless, there are major structural and functional differences between the rodent and the human nervous systems (size, complexity, neuroanatomy, neurophysiology, behaviour, inflammatory and immunological responses), meaning that in some situations the relevance of rodent models is limited and transposition of scientific results obtained in rodents to human is impossible, or at least risky (see e.g. Baker, 2013; Courtine et al., 2007; Lemon and Griffiths, 2003; Manger et al., 2008). It is then required to use animal models biologically closer to human, such as non-human primates (Courtine et al., 2007; Garbarini, 2010; Lemon and Griffiths, 2005). In Lemon's words, "*species that are more closely related to humans will have more similar phenotypes to ours*" (Lemon and Griffiths, 2003). Research involving non-human primates follows of course the highly-demanding ethical standards established in the 3R principle, meaning that these animals are used as models only when replacing them with lower-ranking animals is not possible. Typically, non-human primates remain a model of choice for research in Neuroscience. The main reasons are listed in the following paragraphs, with a special emphasis on hand motor control.

First, non-human primates and human are biologically and genetically very close given that they diverged from a common ancestor only about 65 million years ago (**Figure 4**). In particular, human and Old World monkeys such as macaques split from their common ancestor only 25 million years ago and the macaque (*Macaca mulatta*) genome is 93% similar to human's genome (Rhesus Macaque Genome Sequencing and Analysis Consortium et al., 2007). The consequence is that experiments on non-human primates are largely contested. Non-human primates used in biomedical research are both New World monkeys and Old World monkeys but experiments involving great apes are not allowed (Carlsson et al., 2004; Torres et al., 2010; Weatherall et al., 2006). Among Old World monkeys, macaques are most frequently used, especially rhesus macaques (*Macaca mulatta*), cynomologus or long-tailed macaques (*Macaca fascicularis*) and stumptailed macaques (*Macaca arctoides*). Regarding New World monkeys, common marmosets (*Callithrix jacchus*), squirrel monkeys (*Saimiri spp.*), capuchins (*Cebus spp.*), and tamarins (*Saguinus spp.*) are usually involved in scientific research.

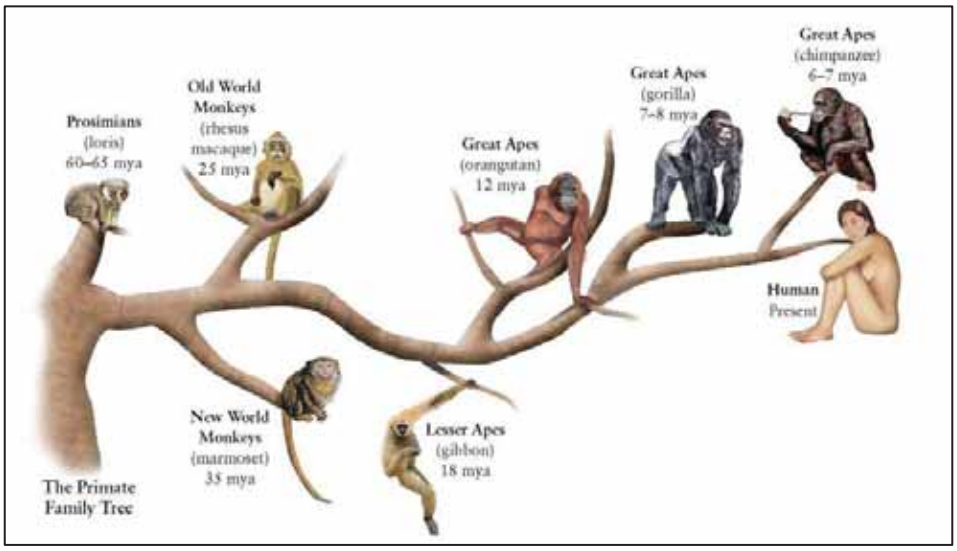

Figure 4: Evolutionary tree of primates showing, among others, the close phylogenetic relationship between macaque monkeys and human. The speciation from prosimians to human happened in 65 million years. To elaborate, there were only prosimans 65 million years ago. The prosimans split further into two groups (today's prosimians and today's simians (anthropoids)) through evolution and natural selection. The simians then split into New World monkeys (35 million years ago) and Old World monkeys (25 million years ago). This last split is characterised by the disapperance of tails in the Hominoidea superfamily (modern apes and human), unlike the cercopithecidea superfamily (modern monkeys). The hominoidea superfamily evolved then into lesser apes (18 millon years ago), orang-utans (12 million years ago), gorillas (7-8 million years ago), chimpanzees (6-7 million years ago) and finally the direct ancestors of modern human (6-7 million years ago) (from Larsen and Repcheck, 2010).

The close evolutionary relationship between non-human primates and human is reflected in many neuroanatomical and neurophysiological similarities between both groups, such as the anatomical (see e.g. Evrard et al., 2012; Evrard et al., 2014; Öngür and Price, 2000) and functional (see e.g. Wager and Yarkoni, 2012) brain organisation, the fine motor control of the hand (Courtine et al., 2007; Lemon, 2008), cognitive capabilities (see e.g. Reinhart et al., 2012) and the great social complexity (Capitanio and Emborg, 2008).

Among primates, the human brain has by far the largest amount of neurons and the most complex sulcus organisation (see **Figure 5** bottom right). Nevertheless, the organisation of the macaque's brain is close (see **Figure 5** bottom left) in terms of structures and cortical areas.

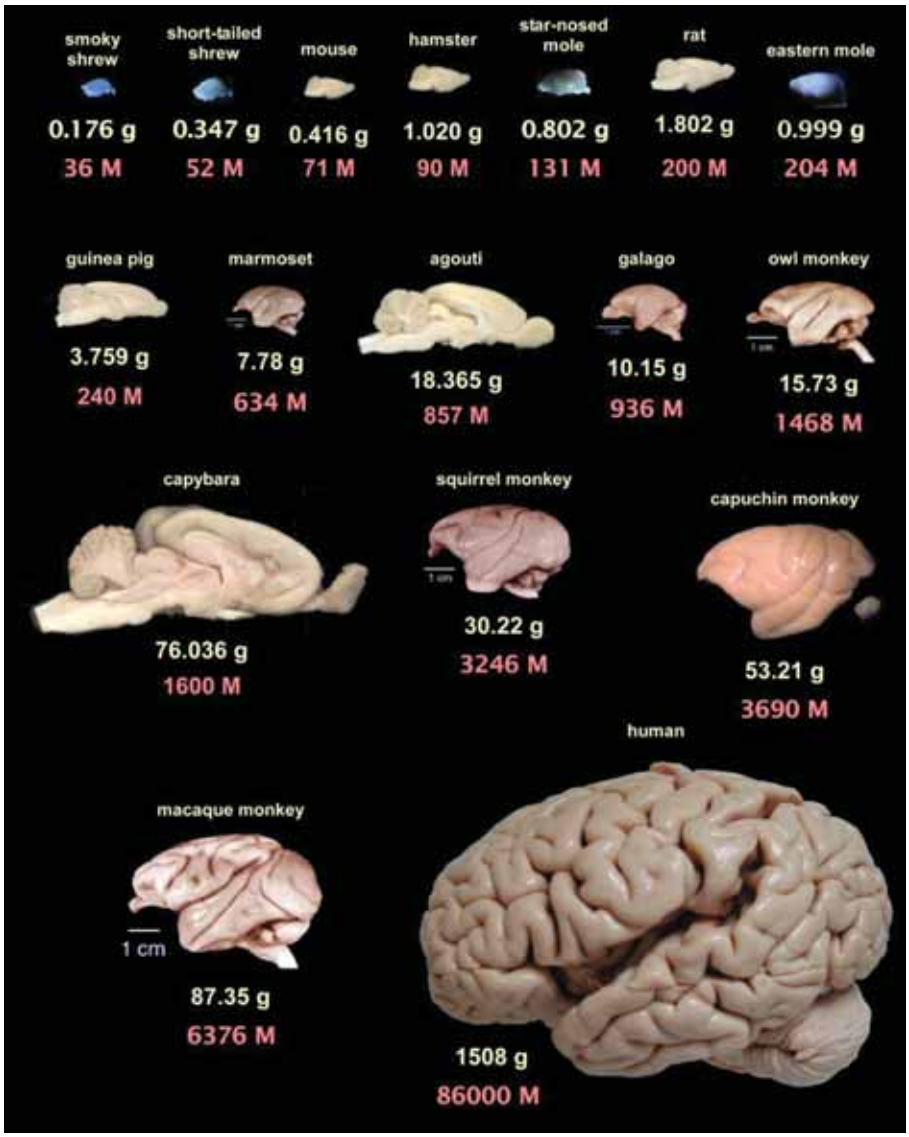

Figure 5: Lateral view of the brain of some rodents (brains pointing to the right), insectivores (in blue due to illumination conditions) and primates (brains pointing to the left), classified according to the increasing number of neurons in millions (in red, M: million). The brain weight is indicated in yellow (from Herculano-Houzel, 2009).

Regarding the motor cortex, both macaques and human share a common organisation into homologous (M1, PM, SMA, CMA) and somatotopically arranged motor cortical areas. Briefly, the homunculus found in human is homologous to the so-called simiusculus found in monkeys (Penfield and Boldrey, 1937; Penfield and Jasper, 1954; Penfield and Rasmussen, 1950; Woolsey et al., 1952), with the foot and leg control areas medial and the arm, face, mouth, and mastication control areas progressively more lateral. Last but not least, the motor representation of the face and fingers is much larger than the one of the other body parts in both species (**Figure 6**) (Penfield and Boldrey, 1937; Penfield

and Jasper, 1954; Penfield and Rasmussen, 1950; Schieber, 2001; Woolsey et al., 1952). See the **General Introduction** for greater detail.

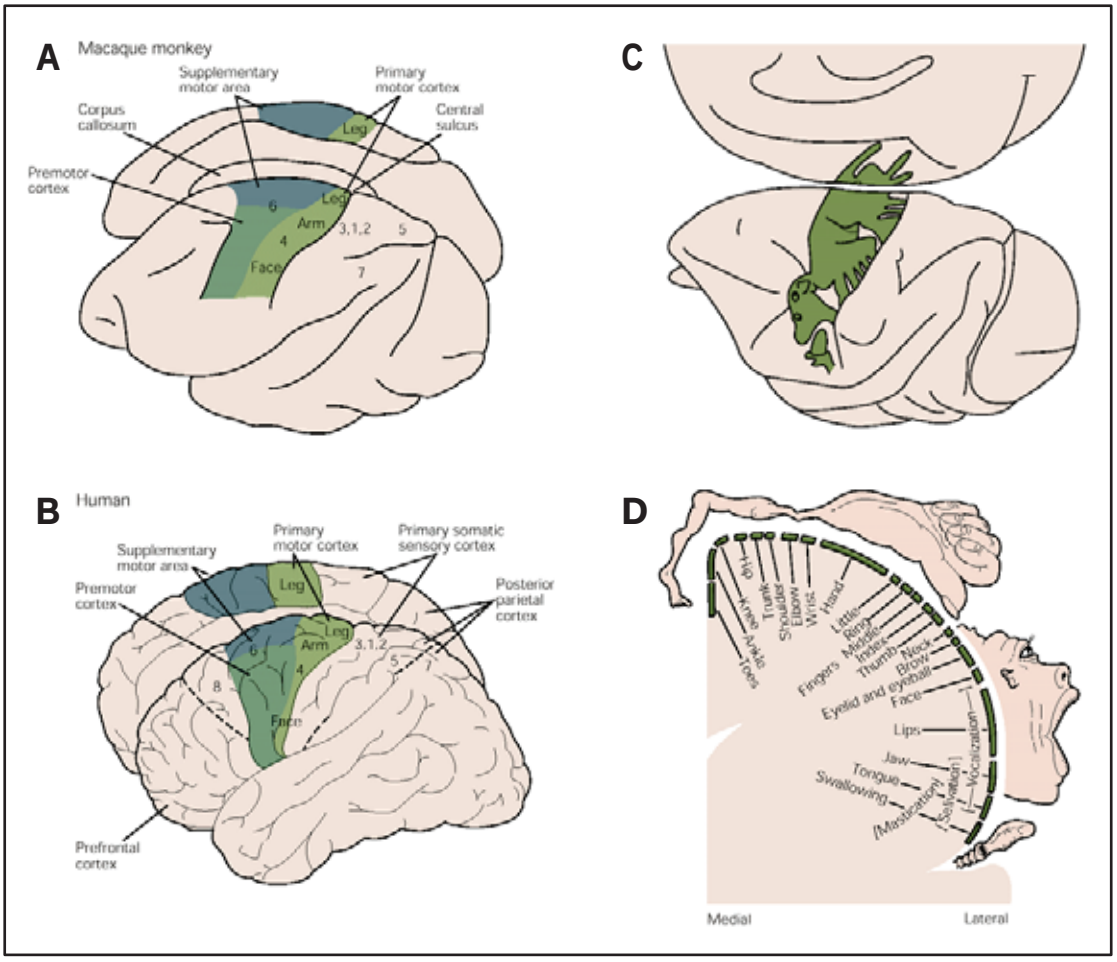

Figure 6 : Comparison of the somatotopic organisation of motor cortical areas in macaque monkey and in human. (A) Lateral view of the left hemisphere and medial aspect of the right hemisphere of a macaque monkey's brain. Motor areas are highlighted in green. The Brodmann's cytoarchitecture of the sensorimotor cortex is given. (B) Same as (A) but for a human's brain. (C) Representation of the macaque monkey's motor simiusculus on a lateral view and medial aspect of the left hemisphere. (D) Representation of the human's motor homunculus on a frontal section of M1 (from Kandel et al., 2000).

Equally important, the organisation of the descending spinal motor pathways controlling voluntary movements are homologous in non-human primates such as macaque monkeys and human (Lemon and Griffiths, 2005). In particular, both groups share similar CST and CM tract pathways, allowing the outstanding fine manual dexterity that

characterises the sole primates (**Figure 7**). To elaborate, rodents and cats have no direct connections between CST neurons and the cervical motoneurons controlling distal forelimb muscles, but interneurons are involved to transmit inputs from the motor cortex to the motoneurons. This is linked with a poor manual dexterity. Conversely, some non-human primates and human exhibit a higher manual dexterity, allowing performing refined and individuated finger movements. This is correlated with the considerable development of the neocortex at the origin of the CST and the development of the CST itself, containing direct connections between motor areas and motoneurons –the CM pathway (Courtine et al., 2007; Lemon, 2008; Lemon and Griffiths, 2005; Nakajima et al., 2000). Equally relevant regarding the hand motor control, both Old World monkeys and human share a common skeletomotor apparatus of the hand (Lemon, 2008; Napier, 1962; Napier, 1993).

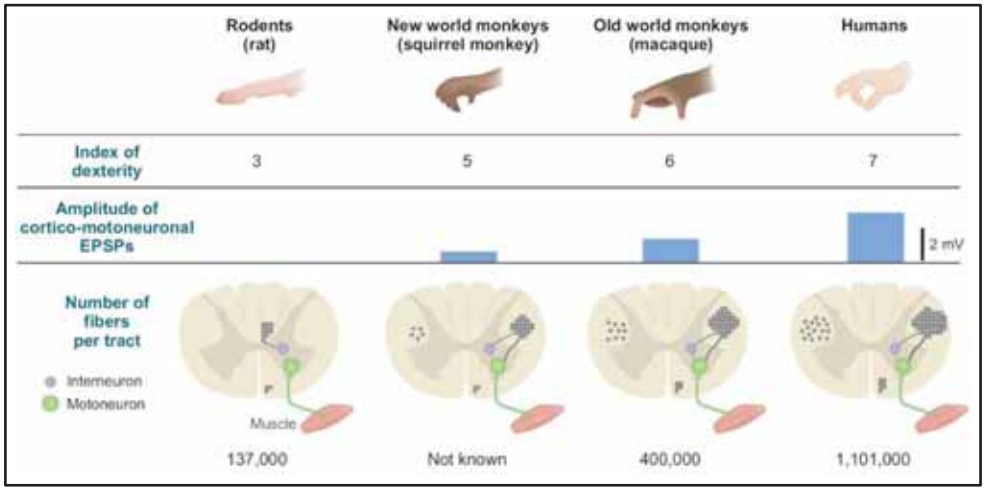

Figure 7: The acquisition of fine motor control abilities in the evolution of primates is correlated with the development of the CST. The first row depicts the manual dexterity as the ability to perform the precision grip using the thumb and the index finger. The amplitude of CM EPSPs is increasing with the development of the direct CM pathway in primates (middle row). The last row shows transversal spinal cord sections and the location of CST neurons (in gray), mostly located in the dorsal horn in rodents, while primarily in the lateral horn and to a lesser extent in the ventral horn in primates. Note the presence of ipsilateral CST fibres (10%-20%) in primates exclusively, which were proved to be of clinical relevance in case of unilateral section of the spinal cord. Moreover, rodents lack the direct CM pathway that characterises the sole primates. Rather, CST inputs from the motor cortex are conveyed through interneurons in the rodent spinal cord. Equally

relevant, the emergence and the development of CM fibres in the evolution of primates are linked with an increase in the number, diameter and conduction speed of the CST fibres (from Lemon, 2008).

In addition, non-human primates such as macaque monkeys have cognitive abilities allowing to teach them to perform quite sophisticated sensorimotor tasks, for instance involving a fine motor control of the fingers (see e.g. **Chapter 5** and **Appendix 2**).

For an extended review about the use of non-human primate models in research on the motor system, see Lemon (2012).

The visual system constitutes another example of the highly conserved neuroanatomical and neurophysiological organisation between non-human primates and human. More specifically, the primate visual cortex is largely more developed and more complex than the rodent one (**Figure 8**). Therefore, non-human primates represent prime models to study the organisation and functioning of the human visual system (see e.g. Baker, 2013; Mitchell and Leopold, 2015; Orban et al., 2004; Solomon and Rosa, 2014).

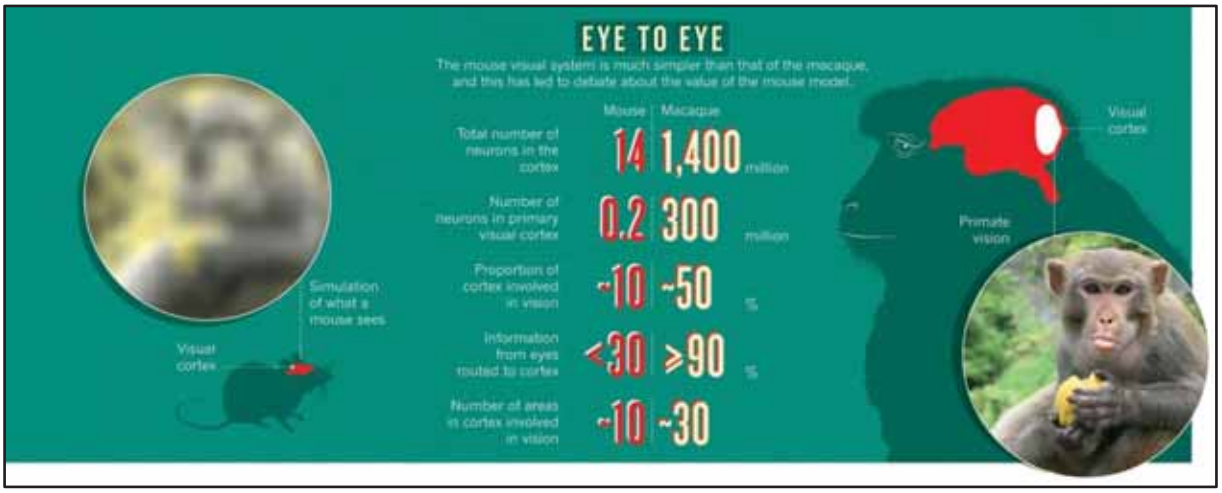

Figure 8: Comparison of the visual cortex of the mouse and the macaque. Both rodent and primate visual cortices have the same neuronal subtypes, in about similar proportions and organisation. Nevertheless, they largely differ in size: mice have less visual cortical areas and a smaller proportion of neurons involved in vision than primates and consequently mice have a much more blurred vision than primates (from Baker, 2013).

Contributions of non-human primates to biomedical progress in Neuroscience

A large body of key knowledge currently available in Neuroscience was gained thanks to experiments performed on animal models. The critical contribution of these animals to the field of Neuroscience is further illustrated by considering Nobel Prize laureates and their research field: from 1904 to 2014, 39 discoveries related to Neuroscience were rewarded with Nobel Prize and 36 of them involved experiments on animal models[20]. Non-human primates in particular led to significant advances in Neuroscience (for a short review, see Pennisi, 2007), among others the synthesis of poliomyelitis vaccines (Enders et al., 1980; Enders et al., 1949; Enders et al., 1954; Landsteiner and Popper, 1909, Nobel Prize in Physiology or Medicine 1954), a better understanding of some mechanisms of visual information processing (Hubel and Wiesel, 1968; Hubel and Wiesel, 1998, Nobel Prize in Physiology or Medicine 1981), insights into some mechanisms of brain plasticity in adult cerebral cortex (Allard et al., 1991; Jenkins et al., 1990; Kaas et al., 1983; Merzenich et al., 1983; Merzenich et al., 1984; Nudo et al., 1996; Recanzone et al., 1992; Wall et al., 1986), the discovery of the functional specialisation of brain hemispheres (Sperry, 1982, Nobel Prize in Physiology or Medicine 1981), deeper knowledge about the mechanisms of reward signalling by midbrain dopaminergic neurons (Schultz et al., 1993; Schultz et al., 1997), the development of technologies such as neuroprosthetics (see below), the discovery of molecules promoting the regeneration of neural fibres after a lesion (see below), the development of treatments against degenerating diseases such as Parkinson's disease (see below), or the development of medical imaging techniques such as MRI (Nobel Prize in Physiology or Medicine 2003) and Diffusion Tensor Imaging (Filler, 2009).

Three examples of the invaluable contribution of animal models to Neuroscience, with a special emphasis on non-human primates, will be developed in greater detail in the following paragraphs.

[20]Combined information from http://fbresearch.wsol.net/nobelprize/, http://www.nobelprize.org/nobel_prizes/medicine/fields.html, http://www.aphb.uwa.edu.au/courses/honours/Neuroscience/history#1900s, and http://www.dls.ym.edu.tw/chudler/nobel.html.

Neuroprosthetics

Neural prostheses or neuroprosthetics are artificial extentions of the body directly controlled by re-routeing brain signals from the subject, in order to replace or restore some neural deficiencies (Leuthardt et al., 2014; Nicolelis, 2001). There are two types of neuroprosthetic devices: (i) *output* neural interfaces, converting brain activity to control artificial devices performing external actions, such as brain-computer interfaces or brain-machine interfaces to restore the function of a lost limb in amputees or paralysed patients (Collinger et al., 2013; Hochberg et al., 2006; Hochberg et al., 2012; Ifft et al., 2013; Nicolelis, 2003; O'Doherty et al., 2011; Velliste et al., 2008; Wodlinger et al., 2015; Wolpaw et al., 1991); (ii) *input* neural interfaces, collecting information from the environment and converting it into perceptions, such as retinal and epiretinal implants to restore impaired vision (Chow et al., 2004; da Cruz et al., 2013; Ghezzi et al., 2013; Mandel et al., 2013; Saunders et al., 2014; Stingl et al., 2013), or cochlear implants to restore impaired audition (Brand et al., 2014; Clark, 2015; Gantz et al., 2006; Kim et al., 2012; Mudry and Mills, 2013).

Regarding more specifically brain-machine interfaces, one of the ultimate ambitions of developing such neuroprosthetic devices has always been to restore some voluntary motor control by using neural interface, for instance in paralysed patients. To this end, Velliste et al. (2008) developed a rhesus monkey model able to control a robotic arm allowing to grasp rewards. They implanted intracortical microelectrode arrays (64-100 microelectrodes per hemisphere) in M1 that derived and decoded monkeys' brain activity in order to control in all three dimensions and in real time a mechanised arm with a gripper at its extremity, during a self-feeding task. This was the first successful demonstration of an embodied neuroprosthetic device allowing a multi-degree-of-freedom control to physically interact with his "owner". Some short movies illustrating this technological advance are provided by the authors at http://www.nature.com/nature/journal/v453/n7198/suppinfo/nature06996.html.

Hochberg et al. (2006; 2012) were then able to transpose this technical achievement to long-standing tetraplegic human patients to restore in them some mobility and some independence. To elaborate, a neural interface containing a 96-microelectrode array was implanted in a small, local neuronal population of M1 to record and then process spiking activity directly into signals allowing to control in all three dimensions and in

real time an articulated dexterous robotic arm. Most outstanding, the patients were able to reach and grasp objects such as a bottle already after a very short period of familiarisation with the device (less than 15 minutes). Short movie sequences illustrating this achievement are provided by the authors at http://www.nature.com/nature/journal/v485/n7398/full/nature11076.html. Such technological approach was later successfully used in a tetraplegic patient to control an anthropomorphic prosthetic limb freely and in the three dimensions. Remarkably, the patient was able to perform dexterous and coordinated reach and grasp movements (Collinger et al., 2013). Very recently, the motor control of the hand of these anthropomorphic prosthetic devices was even refined by extracting additional brain signals, allowing patients to achieve movements with no less than 10 degrees of freedom (Wodlinger et al., 2015).

Controlling a prosthetic arm by using neural interfaces in human would never have been possible without more than 40 years of collaborative research in several various fields, primarily using non-human primates (Collinger et al., 2014; Jackson, 2012), beginning with the study of neuronal mechanisms underlying the arm motor control (Donoghue et al., 1998; Evarts, 1974; Evarts, 1964; Georgopoulos et al., 1982; Georgopoulos, 1987; Humphrey et al., 1970; Sanes and Donoghue, 1993), followed by the development and implementation of microelectrodes allowing to properly derive brain activity (Jones et al., 1992; Maynard et al., 1997; Nordhausen et al., 1994), then the development of neural interfaces to decode neural activity in rhesus monkey (Serruya et al., 2002; Taylor et al., 2002; Vargas-Irwin et al., 2010; Velliste et al., 2008; Wessberg et al., 2000) and eventually the transposition of brain-controlled dexterous robotic hands to human tetraplegic patients (Collinger et al., 2013; Hochberg et al., 2006; Hochberg et al., 2012; Wang et al., 2013) (**Figure 9**).

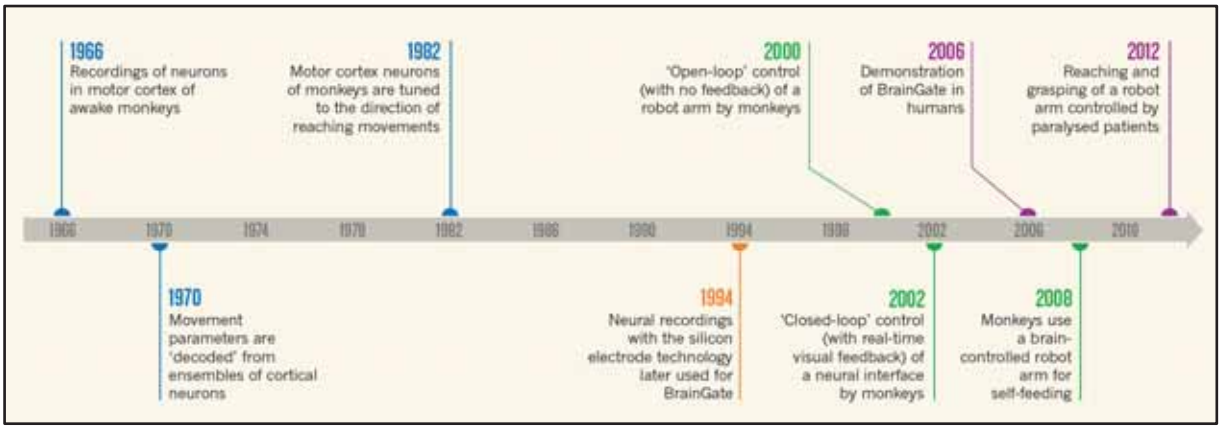

Figure 9: Key steps of research, primarily conducted on non-human primates, that led to the successful development of dexterous prosthetic arms for human patients, controlled through a neural interface: advances in decoding brain activity that controls arm movements (blue), development of microelectrodes (orange), development of neural interfaces for monkeys (green), application of the prosthetic arm technology to human patients (purple) (from Jackson, 2012).

The successful story of anti-Nogo-A: examples of CNS lesions

Partly due to the increase in lifespan, diseases and lesions of the nervous system, such as stroke (**Figure 10**), keep affecting a growing proportion of people and often result in severe after-effects and impairments, inducing significant and increasing costs for the healthcare system as well (Annoni et al., 2006; Mühl and Vuadens, 2011; Schwab and Buchli, 2012). Therefore, there is a urgent need for finding therapeutic approaches allowing to "repair" lesioned tissues and several of them have already been identified (Filli and Schwab, 2012; Hulsebosch, 2002; Maier and Schwab, 2006; Rossignol et al., 2007; Wahl and Schwab, 2014). Here we will focus in particular on animal models for spinal cord lesion and stroke.

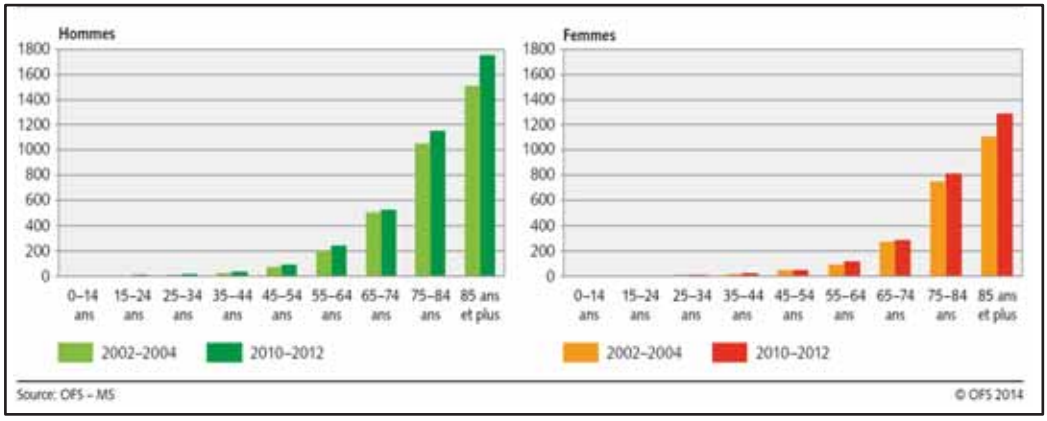

Figure 10: Number of patients (rate for 100'000 people) having been hospitalised due to a stroke in 2002-2004 and 2010-2012, in Switzerland, separately for males (left panel) and females (right panel). Data from the *Swiss Health Survey 2014*, available at http://www.bfs.admin.ch/bfs/portal/fr/index/themen/14/01/new/nip_detail.html?gnpID=2014-371.

It has been already observed from a long time that the CNS and the PNS have differential regeneration properties (Benfey and Aguayo, 1982; David and Aguayo, 1981; Ramon y Cajal, 1928; Schwab and Thoenen, 1985). In adult but not in embryo (Chen et al., 1995), a section of a CNS fibre results in a strong inhibition of spontaneous regeneration of the lesioned fibre, contrary to a lesion of a PNS fibre. As a result, a lesion affecting the adult spinal cord (for a review, see Schwab and Bartholdi, 1996) or the brain usually leads to dramatic consequences.

The development of a therapy based on the so-called anti-Nogo-A antibodies, first for spinal cord injured human patients and potentially later for patients with brain cortical lesions as well, results from the close collaboration between different research groups working on rodents, on monkeys and on human. An overview of the key steps is given in the following paragraphs.

Interesting observations were performed in late 1980s on *in vitro* neuronal cultures in the laboratory of Prof. Martin Schwab in Zürich. To elaborate, cell adhesion, neurite growth and fibroblast spreading of rodent nerve cells were strongly prevented when these cells were cultured with differenciated oligodendrocytes (i.e CNS myelin) from rats or chicks. In particular two membrane-bound proteins (35kd and 250kd, the latter is now called Nogo-A) in myelin extract were responsible for creating this strongly nonpermissive and hostile substrate. Conversely, myelin from rodent PNS nerves had

permissive properties for rat nerve cells (Bandtlow et al., 1990; Caroni and Schwab, 1988b; Schwab and Caroni, 1988). In case the CNS myelin substrate or directly a substrate made of oligodendrocytes were added with monoclonal antibodies IN-1 (later called anti-Nogo-A) or IN-2 raised against both myelin-associated proteins with inhibitory substrate properties, then nerve fibres were able to grow (Bandtlow et al., 1990; Caroni and Schwab, 1988a; Schwab and Caroni, 2008; Spillmann et al., 1997), meaning that both antibodies IN-1 or IN-2 made the substrate permissive. The authors therefore concluded that the nonpermissive substrate properties of CNS white matter were achieved *in vivo* by myelin, more specifically by both myelin-associated proteins (Cadelli and Schwab, 1991; Caroni and Schwab, 1988a; for a review, see Filbin, 2003; Savio and Schwab, 1989). The gene coding for one of the potent inhibitors (IN-1 antigen) of neurite growth was cloned and called Nogo-A (Chen et al., 2000; for a review, see Goldberg and Barres, 2000).

The *in vivo* function of Nogo-A protein during the normal development of CNS was studied in newborn rats by suppressing its production or inhibiting its action. In this way, it was concluded that immediately after birth, nerve fibres were growing towards their targets, in the absence of myelin (Pernet et al., 2008; Schwegler et al., 1995; Vanek et al., 1998), but then, as soon as myelin formation began, oligodendrocytes started producing the inhibitory molecule Nogo-A that has both boundary and guidance functions that restrict sprouting (Schwegler et al., 1995) and channel, regulate and finally block the axonal growth, resulting in a restricted axonal growth and in the stabilisation of connections in adult CNS (Cadelli and Schwab, 1991; Schwab, 1996; Schwab and Schnell, 1991) (**Figure 11A**). Moreover, Nogo-A was demonstrated to be involved, among others, in synaptic plasticity and regulation of learning of skilled movements in the motor cortex (Zemmar et al., 2014). In sum, Nogo-A is a developmental neurite growth regulatory factor that strongly regulates plastic reorganisation and thus stabilises connectivity in adult CNS (Petrinovic et al., 2010; for reviews, see Schmandke et al., 2014; Schwab, 2010; and Schwab and Strittmatter, 2014).

Based on these observations, the antibody IN-1 in particular, later called anti-Nogo-A, was proposed to be a potential new substance that may favour the regeneration on CNS lesioned nerve fibres and thus promote plasticity. Simply put, the anti-Nogo-A strategy consists in neutralising the myelin-associated neurite growth inhibitory protein Nogo-A

present around lesions located in adult CNS, by using the antibody anti-Nogo-A, raised against Nogo-A. In this way, axonal outgrowth is favoured and the regeneration of nerve fibres is promoted (**Figure 11B**) (for reviews, see Gonzenbach and Schwab, 2008; and Grandpré and Strittmatter, 2001).

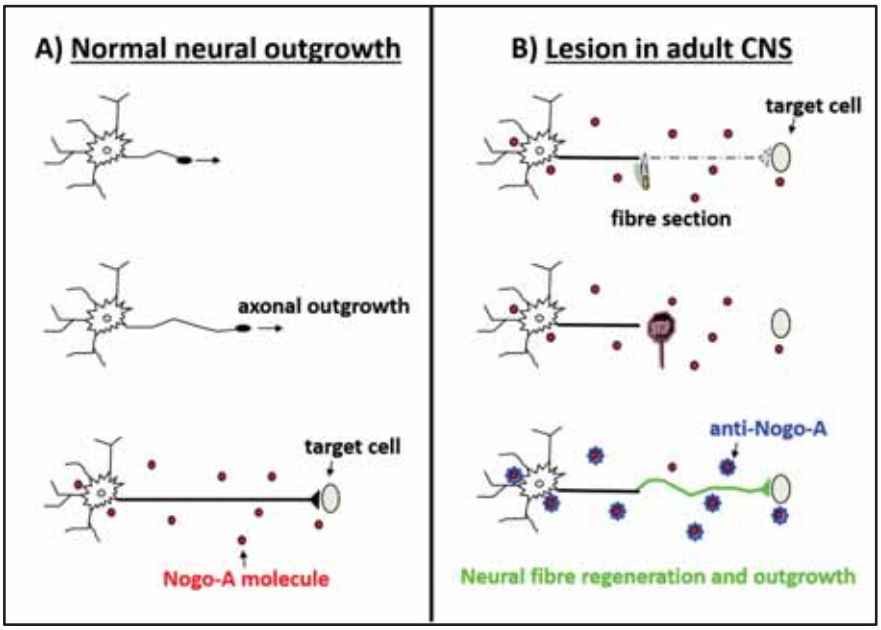

Figure 11: (A) The axonal outgrowth in developing CNS is regulated by the Nogo-A molecule. Without myelin, axonal fibres grow. During myelination, oligodendrocytes produce Nogo-A proteins that act then by channeling the growth of the fibres towards target cells, preventing further outgrowth and thus stabilising connections. Myelinated fibres are represented by thick black lines. (B) The regeneration of lesioned nerve fibres in adult CNS is prevented by Nogo-A. The anti-Nogo-A strategy consists then in neutralising Nogo-A molecules by using monoclonal antibody anti-Nogo-A. As a result, the lesioned axon can then grow towards its target and regenerate (modified from a figure generously provided by Prof. Eric M. Rouiller).

The anti-Nogo-A strategy was first tested on rodents after spinal cord transection. More specifically, studies on adult rats subjected to a CST transection demonstrated that anti-Nogo-A antibody considerably favoured the regeneration of lesioned spinal cord fibres over long distance (up to 7-11 mm beyond the lesion), such that prominent sprouting of fibres was observed rostral to the lesion and some regenerated fibres circumvent or even crossed the lesion through spared tissue bridges towards the caudal spinal cord and then grew down the spinal cord over several mm (**Figure 12B**). Conversely, there was no fibre regeneration over long distance in control rats (**Figure 12A**) (Bareyre et al., 2002; Bregman et al., 1995; Brösamle et al., 2000; Buchli and Schwab, 2005; Fouad et al.,

2001; Liebscher et al., 2005; Raineteau et al., 1999; Raineteau et al., 2002; Schnell and Schwab, 1990; Schwab, 1996; Schwab, 1998; Schwab, 2002; Schwab, 2004; Schwab and Bartholdi, 1996; Thallmair et al., 1998; von Meyenburg et al., 1998). In addition, anti-Nogo-A-treated rats, but not control rats, showed substantial sensorimotor functional recovery, demonstrated by using several tests, such as the swim test (**Figure 12C**) (Bregman et al., 1995; Buchli et al., 2007; Buchli and Schwab, 2005; Fouad et al., 2001; Liebscher et al., 2005; Maier et al., 2009; Merkler et al., 2001; Schwab, 2004; Thallmair et al., 1998; von Meyenburg et al., 1998). Importantly, these studies dismissed the presence of side-effects such as pain or spasticity that may have indicated some abberant reorganisation after the lesion (Merkler et al., 2001).

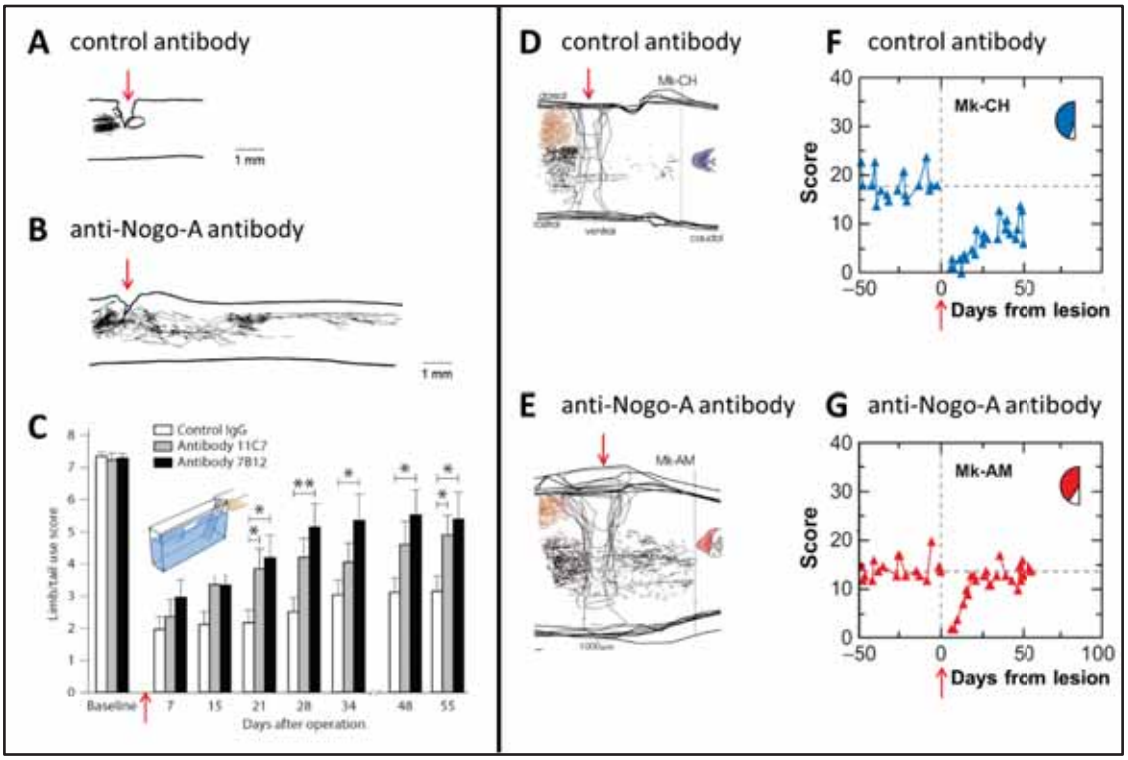

Figure 12: The anti-Nogo-A antibody promotes the regeneration of lesioned fibres in the spinal cord and the functional recovery in adult rodents and macaque monkeys. (A) *Camera lucida* **reconstruction of consecutive parasagittal spinal cord sections at the lower thoracic level of a control rat subjected to a unilateral CST lesion (red arrow, dorsolateral hemisection at T8 level). (B) Same as (A) but in a rat treated with anti-Nogo-A antibody (here a recombinant, humanized IN-1 antibody fragment). Axonal fibres were labelled with BDA marker (A and B from Brösamle et al., 2000). (C) Behavioural evaluation of motor functional recovery by using the swim test performed regularly after spinal cord lesion (red arrow) in control antibody treated rats (white) and in anti-**

Nogo-A-treated rats (gray and black: 2 forms of the antibody were tested here, each one directed against a defined region of Nogo-A), * p <0.01; ** p <0.001 (from Buchli et al., 2007; Liebscher et al., 2005). (D) *Camera lucida* **reconstruction of consecutive parasagittal spinal cord sections at the cervical level of a control macaque monkey subjected to a unilateral CST lesion (red arrow, dorsolateral hemisection at C7-C8 border, lesion extent and location shown in the small inset on the right). (E) Same as (D) but in a macaque monkey treated with anti-Nogo-A antibody after the lesion. Axonal fibres were labelled with BDA marker (D and E from Freund et al., 2007). Motor functional recovery regularly evaluated by using the modified Brinkman board task in (F) the control monkey and in (G) the anti-Nogo-A-treated monkey, before and after the lesion (red arrow, lesion extent represented in the small inset on the right). The score corresponds to the total number of pellets collected in the first 30 s of the task with the ipsilesional hand (F and G from Freund et al., 2006).**

Even though the very promising results obtained on the rodent model, it would have been inconceivable to transpose the anti-Nogo-A therapy directly to spinal cord injured human patients because, as already mentioned above, the anatomical and functional organisation of the nervous system, and in particular here of the spinal cord, is largely different between rodents and human. To meet current legislation, the safety and effectiveness of the anti-Nogo-A strategy were consequently assessed on a non-human primate model. To this end, 13 adult macaque monkeys were subjected to a cervical hemitransection of the CST. Anti-Nogo-A antibody treated monkeys (n =7) showed substantially more sprouting of CST axons both rostal (Freund et al., 2007) and caudal (Freund et al., 2006) to the lesion compared with the control antibody treated monkeys (n =6) (**Figure 12D, E**). The enhanced nerve fibre regeneration was usually associated with a faster and larger functional recovery of ipsilesional manual dexterity in the modified Brinkman board task in anti-Nogo-A antibody treated monkeys compared with the lower spontaneous functional recovery observed in most control animals (**Figure 12F, G**). In brief, the functional recovery as a function of the extent of CST lesion was better in anti-Nogo-A antibody treated monkeys than in control monkeys (Freund et al., 2006; Freund et al., 2009). Studies performed on other non-human primates confirmed these results (Fouad et al., 2004). The absence of chronic pain in anti-Nogo-A antibody treated animals was confirmed in monkeys as well (Freund et al., 2006).

Taken together, data from both rodent and macaque monkey models clearly indicated the effectiveness of anti-Nogo-A therapy in relieving of spinal cord injury in those

species. These encouraging results thus paved the way for clinical trials in human patients. Phase I clinical trials, corresponding to assessement of antibody pharmacokinetics, safety, tolerance and appropriate dose, were successfully carried out from 2006 on paraplegic and tetraplegic human patients (Zorner and Schwab, 2010). Phase II clinical trials are expected to begin in an immediate future.

The cerebral cortex represents an additional level of complexity in both structure and function as compared to the spinal cord, meaning that results from spinal cord injury models cannot be directly transposed to cerebral cortex injuries. As a consequence, rodent models of focal cortical lesions were developed to test the potential of the anti-Nogo-A strategy in such kinds of lesions. More specifically, rats were subjected to a focal lesion in the sensorimotor cortex, resulting in a strong motor deficit of contralesional forelimb. In those rats that were subsequently treated with the anti-Nogo-A antibody, but not in control animals, an enhanced neuronal plasticity was observed, in the form of a strong regeneration of nerve fibres and enlarged synaptic modifications (**Figure 13A**). In addition, anti-Nogo-A antibody treated rodents showed a significantly better and long-lasting functional recovery after the lesion as compared to control rats (**Figure 13B, C**) (Buchli and Schwab, 2005; Cheatwood et al., 2008; Emerick et al., 2003; Emerick and Kartje, 2004; Gillani et al., 2010; Lindau et al., 2014; Markus et al., 2005; Papadopoulos et al., 2002; Seymour et al., 2005; Tsai et al., 2011; Tsai et al., 2007; Wahl et al., 2014).

Similar studies are currently ongoing in our laboratory on a macaque monkey model of cortical lesion. Briefly, several macaque monkeys were subjected to a restricted, permanent and unilateral cortical lesion of the hand representation in M1 (see **Chapter General Materials and Methods** and **Chapter 5** for further detail). Preliminary results indicate that the functional recovery of the contralesional manual dexterity is enhanced in anti-Nogo-A antibody treated monkeys compared with control animals with a similar lesion extent (**Figure 13D**) (Hamadjida et al., 2012; Wyss et al., 2013). Moreover, in order to fulfil the *refine* principle advocated by the 3R, we have developed and then largely used the non-invasive method of scalp EEG recordings presented in **Chapters 1** to **4** to document in greater detail the post-lesion reorganisation, in addition to information obtained with behavioural tests.

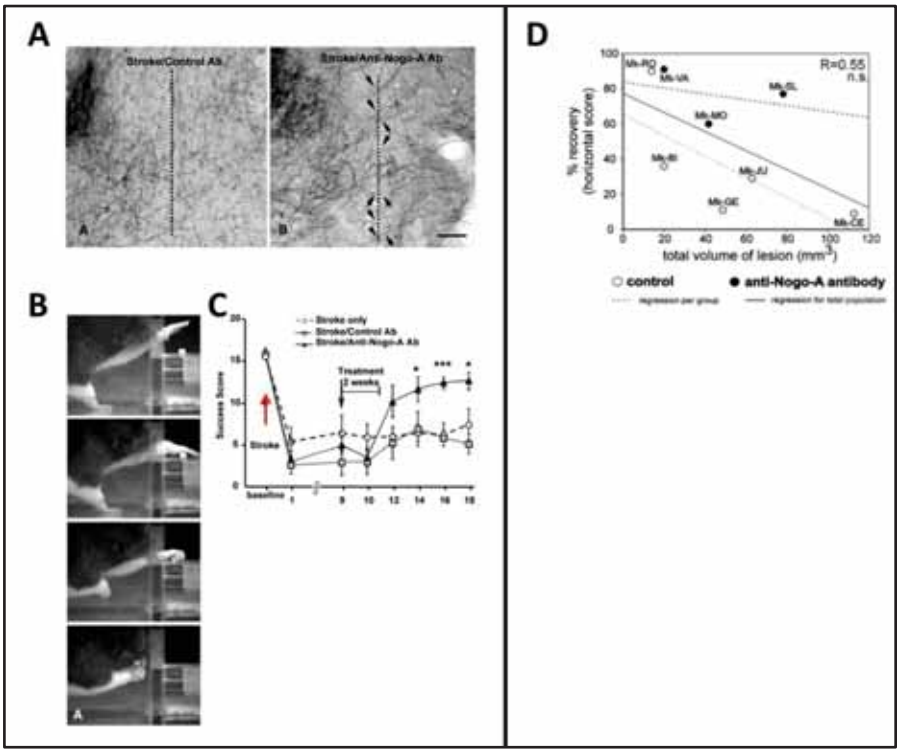

Figure 13: Anti-Nogo-A antibody promotes the regeneration of lesioned fibres in the cortex and functional recovery in rodents and in macaque monkeys. (A) Photomicrographs showing corticorubral fibres crossing (small black arrows) the midline (dotted line) more densely in stroke rats subsequently treated with anti-Nodo-A antibody (right) than in control animals (left). Axonal fibres were labelled with BDA marker. (B) Selected pictures showing a rat performing the "skilled forelimb reaching task". This test was used to behaviourally assess functional recovery and consisted in retrieving a small food pellet by introducing the forelimb through a slit. (C) Success score ± SEM in the skilled forelimb reaching task for the contralesional forelimb before and after stroke (red arrow) in rats with stroke only (white circles), in rats with stroke and subsequent control-antibody treatment (gray squares) and in rats with stroke and subsequent anti-Nogo-A antibody treatment (black triangles). Treatment, when present, began 9 days after the lesion and was delivered for 2 weeks. All 3 groups of rats had severe functional deficits immediately after the lesion. But then, after treatment, there was a significant strong functional recovery in this task only in those rats that were treated with anti-Nogo-A antibody, * p <0.05, ** p <0.01, *** p <0.001. (A, B and C from Tsai et al., 2011). (D) Functional recovery of contralesional manual dexterity in the modified Brinkman board task as a function of cortical lesion extent. The percentage of recovery was expressed as (post-lesion score in 30 s in horizontal wells/pre-lesion score in 30 s in horizontal wells)*100, both in 5 control monkeys (white circles) and in 3 anti-Nogo-A antibody treated monkeys (black circles). There was no significant correlation between the lesion extent and the

functional recovery but for a comparable lesion extent, anti-Nogo-A-treated monkeys usually recovered better than control monkeys (from Wyss et al., 2013).

The anti-Nogo-A story is by far still not at its end. In the same way as the development of neuroprosthetics exemplified above, it illustrates the very long-term processes that are required in the development of new treatments and the crucial information that are collected at every step by working on several animal models, before transposition to human.

Parkinson's disease

Parkinson's disease is a chronical and progressive neurodegenerative disease beginning on average at about 60 years old and characterised among others by hypokinesia, bradykinesia, rigidity, resting tremor, gait impairment, postural changes, postural instability (**Figure 14**) and various other non-motor symptoms, such as automomic dysfunctions, sleep-wake disorders, sensory disorders and neuropsychiatric disorders (Apetauerova, 2012; Wolters et al., 2014).

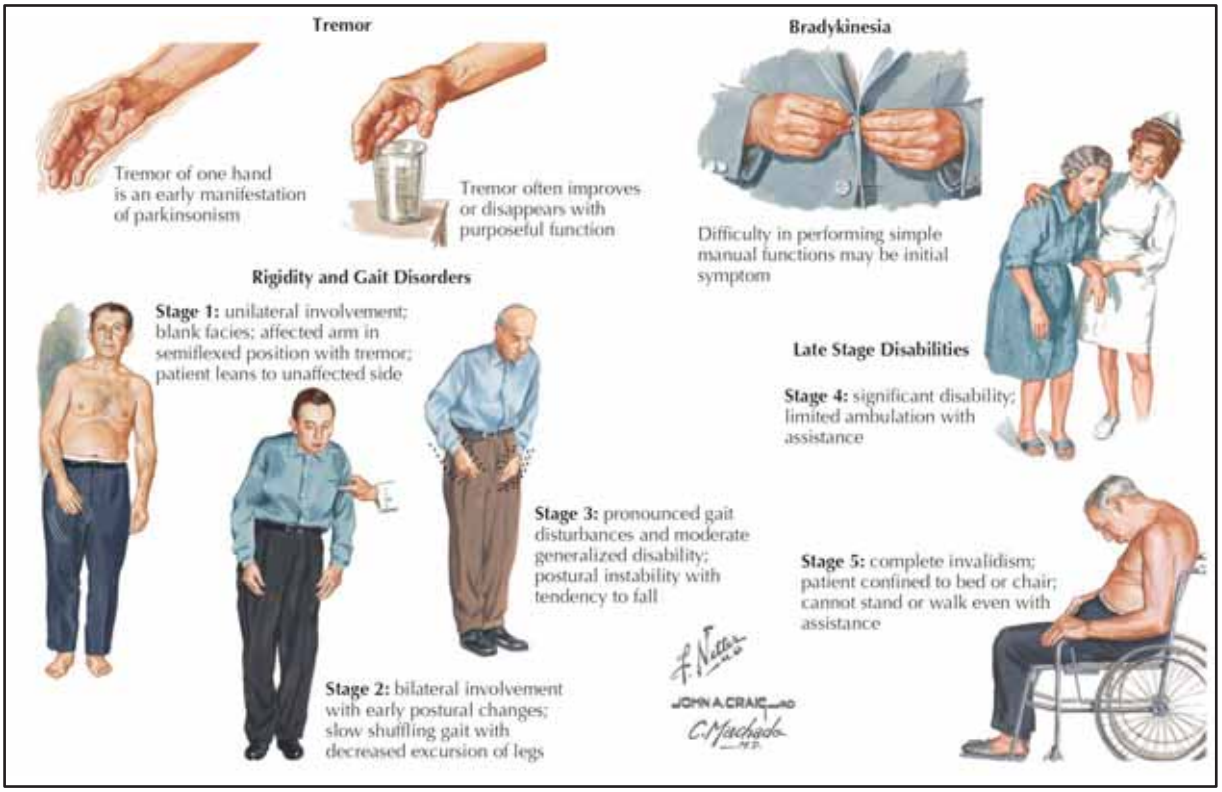

Figure 14: Major clinical manifestations of Parkinson's disease (from Apetauerova, 2012).

Research on animal models enabled to understand several pathophysiological mechanisms of the disease and led to the treatments currently used in the clinics (L-Dopa, deep brain stimulation, stem cells) to improve the patients' quality of life. One of the Nobel prize laureates in Medicine-Physiology in 2000, Arvid Carlsson, demonstrated in 1959 already, by experimenting on rabbits and mice, that Parkinson's disease might result from dopamine depletion (Carlsson, 1960; Carlsson, 2001) (**Figure 15**): he administrated animals with reserpine, a molecule mimicking very faithfully the symptoms of Parkinson's disease also in animals. As a results, the animals showed impairments close to the ones observed in parkinsonian patients. By injecting then these animals with L-Dopa, a precursor of dopamine, a dramatic reversal of the symptoms was induced, indicating that reserpine was actually depleting dopamine. These first experiments allowed to establish the critical role of dopamine in Parkinson's disease.

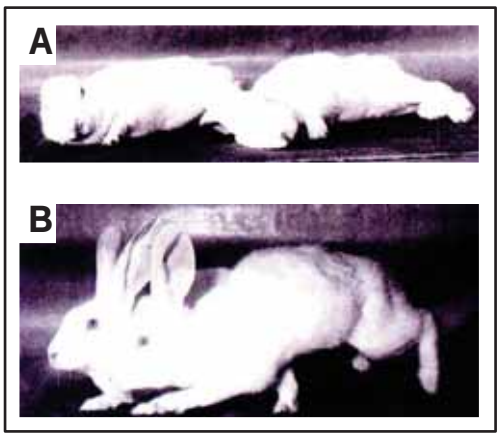

Figure 15: Rabbits treated with reserpine, inducing similar symptoms as observed in parkinsonian patients, before (A) and (B) after treatment with L-Dopa (Carlsson, 1960; Carlsson, 2001).

Later on, other studies were performed on brains of pigeons and allowed to demonstrate that dopamine was accumulated in basal ganglia homologous to the mammalian corpus striatum, some structures being involved among others in motor control (Juorio and Vogt, 1967; Karle et al., 1996; Reiner et al., 1998) (**Figure 16**). Taken these results together, it was therefore concluded that basal ganglia in parkinsonian people degenerate, inducing a depletion of dopamine in the nervous system and leading to an imbalance in the activity between the basal ganglia. Treatment of Parkinson's disease with L-Dopa was therefore established to restore the dopamine concentration in the brain (see e.g. Barbeau, 1981; Birkmayer and Hornykiewicz, 1962; Birkmayer and Hornykiewicz, 1964). This therapy is effective during the first years of the disease (Poewe et al., 2010). Nevertheless, many parkinsonian patients become progressively

resistant to L-Dopa, meaning that the drug becomes less and less effective and induces strong side-effects a few years after therapy onset (Poewe et al., 2010; Tarsy, 2012).

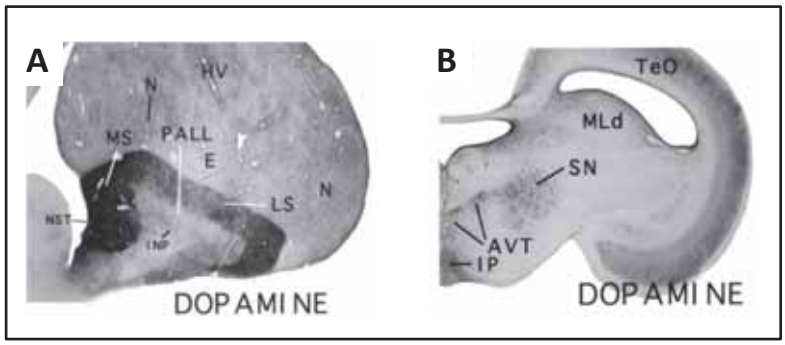

Figure 16: Dopamine immunolabelling on transverse sections of (A) the right telencephalic hemisphere of a pigeon through mid-basal ganglia, (B) the right half of midbrain at the level of the substantia nigra. Abbreviations: E, ectostriatum; HV, hyperstriatum ventrale; INP, intrapeduncular nucleus; LS, lateral striatum; MS, medial striatum; N, neostriatum; NST, nucleus of the stria terminalis; PALL, pallidum. Dopamine is strongly accumulated in basal ganglia (from Reiner et al., 1998).

To go deeper in investigating the role of basal ganglia in Parkinson's disease, non-human primate models of parkinsonism were developed by injecting them with the neurotoxin MPTP (1-methyl-4-phenyl-1,2,3,6-tetrahydropyridine) (Blume, 1983; Burns et al., 1983; Kolata, 1983; Langston et al., 1983b; Miller and DeLong, 1987). This protocol was based on the discovery by accident of strong parkinsonian symptoms induced on drug addicts that used illicit drugs contaminated with MPTP, and on a chemist daily exposed to MPTP (Blume, 1983; Langston et al., 1983a; Langston et al., 1983b; Langston, 1983). In these subjects, MPTP was suggested to selectively destruct dopaminergic neurons in the substantia nigra pars compacta (Langston et al., 1983a), which was confirmed in MPTP monkeys (Burns et al., 1983; Langston et al., 1983b). Later on, it was observed that the subthalamic nucleus and the globus pallidus internus became overactive in MPTP rhesus monkeys (Bergman et al., 1994; Miller and DeLong, 1987). Consequently, based first on the principle that stimulating these overactive brain structures could decrease their overactivity, restore the balance of activity between basal ganglia and attenuate symptoms of Parkinson's disease (Wichmann et al., 1994) and, second, in order to circumvent the resistance to L-Dopa that may develop in the course of the therapy, another approach to treat Parkinson's disease was then developed, namely the deep brain stimulation or DBS (for a review, see Mehanna and Lai, 2013).

Before applying DBS directly to human, this technique was developed first in rats (Benazzouz et al., 2000; Spieles-Engemann et al., 2010) and then in monkeys (Benazzouz et al., 1993; Hashimoto et al., 2003; Johnson et al., 2009; Meissner et al., 2005). From the first report in 1993, but actually already performed in 1987 (see e.g. Benabid et al., 1993), many pharmacologically resistant parkinsonian patients have been treated using high-frequency DBS (Anderson et al., 2005; Ashkan et al., 2004; Deuschl et al., 2006; Fleury et al., 2013; Follett et al., 2010; Huys et al., 2014; Krack et al., 1997; Mehanna and Lai, 2013; Odekerken et al., 2013; Odekerken et al., 2015; Okun et al., 2009; Ramdhani et al., 2015; Rothlind et al., 2007; Weaver et al., 2009; Weaver et al., 2012). To this aim, electrodes are chronically implanted into the basal ganglia, usually either the subthalamic nucleus or the globus pallidus internus. These electrodes are then connected via cables to small power generators implanted under the skin. They send then high-frequency electrical discharges that inhibit the abnormal neuronal activities of these strucures, immediately relieving some symptoms of Parkinson's disease, such as resting tremor. The main advantage of DBS is that it is reversible and may be adjusted according to the patients' needs. Some movie sequences illustrating the striking effectiveness of DBS are available for instance at http://www.medtronicdbs.com/parkinsons/about/introduction-to-dbs-therapy/index.htm.

Nowadays, L-Dopa remains one of the gold standards of oral treatment of Parkinson's disease (Connolly and Lang, 2014; Poewe et al., 2010). Then, DBS is one prime alternative for those patients having developed resistance reactions to L-Dopa. Nevertheless, both L-Dopa supplementation and DBS act on the symptoms of the disease but do not address the underlying cause itself, i.e the degeneration of dopaminergic cells within the brain. Until now, there is still no cure for Parkinson's disease. However ongoing research is carried out aiming at directly replacing degenerated cells by using cell therapy (for a review, see e.g. Wakeman et al., 2011), for instance with fetal neural stem cells or autologous cells (this topic in particular is under ongoing investigation in the laboratory of Prof. Eric Rouiller). Preliminary studies have been performed on rodents (Andereggen et al., 2009; Thompson and Parish, 2013) and on monkeys (Bjugstad et al., 2005; Bjugstad et al., 2008; Bloch et al., 2014; Gonzalez et al., 2015; Redmond et al., 2007; Redmond et al., 2013; Wakeman et al., 2014a; Wakeman et al., 2014b), and very promising trials have been recently carried out on human, suggesting

that a treatment based on grafted cells may be possible in human as well. In particular, two parkinsonian patients had intrastriatal grafts of human fetal ventral mesencephalic tissue, rich in dopaminergic neuroblasts (Kefalopoulou et al., 2014). They were then clinically assessed regularly for 15 and 18 years, respectively. Both of them clearly improved their motor performance during the years following the graft (**Figure 17A**) and were able to live completely free of L-Dopa. This was correlated with the recovery of dopaminergic innervation in the striatum (**Figure 17B**). To be continued carefully!

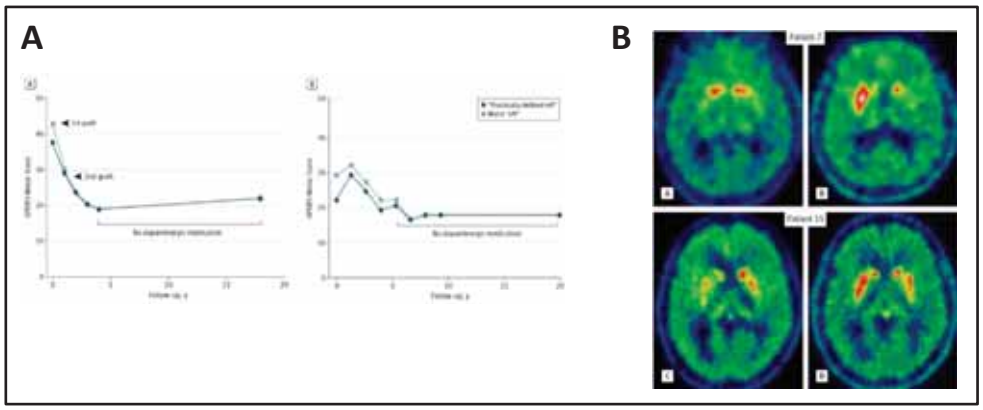

Figure 17: Long-term assessment of the effects of intrastriatal grafts of dopaminergic fetal cells in two parkinsonian patients. (A) Motor performance evaluated with the Unified Parkinson's Disease Rating Scale (UPDRS motor scale). Severe symptoms are indicated by high values whereas the complete absence of symptom corresponds to 0. Both patients clearly showed a progressive decrease in parkinsonian symptoms after the fetal cell grafts (day 0). (B) 6-L-Fluorodopa F 18 PET-scan showing the location of the dopaminergic cells (in red) within the brain before (left) and after (right) the fetal cell graft in both patients. In both cases, the number of dopaminergic cells increased after the graft, indicating that the graft did successfully restore the dopaminergic innervation that had been lost during the evolution of the disease (from Kefalopoulou et al., 2014).

Concluding remarks

Going back to the main question of this chapter, namely *May one conceive biomedical research, especially in Neuroscience, without animal models ?*, it emerges among others from the different examples presented above that animal models played and continue to play an invaluable role in biomedical research, and more specifically here in Neuroscience. As a consequence, the answer is a strong no, at least at the moment.

Indeed with the increasing incidence of pathologies and damages affecting the nervous system, resorting to animal models with a physiology and a phenotype closely related to human ones, such as non-human primates, is at the moment of prime importance for biomedical research in Neuroscience. However, one must bear in mind that non-human primate models represent only a very small percentage of laboratory animals in Switzerland.

Nevertheless, one can actually expect that the growing strong opposition to animal experimentation on the one hand, and the highly expensive costs resulting from using laboratory animals for experimental research on the other hand, will further motivate the development of effective alternative solutions. Therefore, if we think ahead what may happen in the much longer term, say 15-20 years, maybe one day one will be in a position to do with much less animal experimentation. Nevertheless, I think we will never be able to simulate the real complexity of a living being, even with the best *in vitro* model (such as the "brain-on-a-chip", Pamies et al., 2014), because an organism is largely much more than just the sum of all its isolated components. This is especially true for the brain, that is by far the most complex organ of our boby (Koch and Laurent, 1999). In Watson's words: "*The brain is the last and grandest biological frontier, the most complex thing we have yet discovered in our universe. It contains hundreds of billions of cells interlinked through trillions of connections. The brain boggles the mind*." (Watson, J.D., *Foreword*, p iii, in Ackerman, 1992).

It is important to keep in mind the consequences that might result from a complete abolition on animal experimentation in Switzerland. They may be actually highly prejudicial in several respects. First of all, several entire research areas may move abroad. Certainly the number of laboratory animals involved in experimental research would drastically decrease in Switzerland but, most probably, at the expense of animal experiments carried out abroad according to less restricting legal and ethical standards. For reminder, Switzerland has one of the strictest legislation in the world about animal experimentation by attaching much importance to animal welfare, whether regarding housing and care of laboratory animals or regarding experimental constraints. Second, transfering whole sectors of Swiss biomedical research abroad may result in a fall of competitiveness of all Swiss Universities, Federal Institutes of Technology and pharmaceutical industries, which may be highly deleterious for the high level of

scientific excellence achieved in Swizerland. Third, this may lead to a very hypocritical and absurd situation where most people would be against animal experimentation but even so, in case they would become seriously sick or disabled, they would not be ready to give up benefit from innovative medical treatments developed abroad by using laboratory animals. We must actually assume our choice of wanting to always have a cutting edge medicine by accepting all what it involves. In case we cannot for some ethical reasons, therefore we must do without medicine benefits as well. Everyone should position himself/herself in all conscience regarding animal experimentation, but should then remain fully consistent as well regarding the fact of benefiting or not from medical treatments.

The most important is therefore to favour educational initiatives to inform the public clearly and with full transparency about what is carried out in the laboratories using animal models.

By way of conclusion, I have always had a profound respect and a deep gratitude for animals and in particular for the macaque monkeys I was daily in charge of and working with. Nevertheless I acknowledge the unvaluable contribution of laboratory animals to get a better understanding about biological processes and develop effective medical treatments. Therefore I accept the use of animals in research in spite of the obvious constraints to them, provided experiments are carried out rigorously and properly in accordance with current legislation and ethical standards.

References

Abel, J.J., Rowntree, L.G., Turner, B.B., 1914. On the removal of diffusible substances from the circulating blood of living animals by dialysis. Journal of Pharmacology and Experimental Therapeutics 5, 275-316.

Ackerman, S., 1992. Discovering the brain. National Academies Press.

Albright, T.D., Jessell, T.M., Kandel, E.R., Posner, M.I., 2000. Neural science: a century of progress and the mysteries that remain. Cell 100 Suppl, S1-55.

Allard, T., Clark, S.A., Jenkins, W.M., Merzenich, M.M., 1991. Reorganization of somatosensory area 3b representations in adult owl monkeys after digital syndactyly. J Neurophysiol. 66, 1048-1058.

Alt, K.W., Jeunesse, C., Buitrago-Tellez, C.H., Wachter, R., Boes, E., Pichler, S.L., 1997. Evidence for stone age cranial surgery. Nature 387, 360.

Andereggen, L., Meyer, M., Guzman, R., Ducray, A.D., Widmer, H.R., 2009. Effects of GDNF pretreatment on function and survival of transplanted fetal ventral mesencephalic cells in the 6-OHDA rat model of Parkinson's disease. Brain Research 1276, 39-49.

Anderson, V.C., Burchiel, K.J., Hogarth, P., Favre, J., Hammerstad, J.P., 2005. Pallidal vs subthalamic nucleus deep brain stimulation in parkinson disease. Archives of Neurology 62, 554-560.

Annoni, J.M., Staub, F., Bruggimann, L., Gramigna, S., Bogousslavsky, J., 2006. Emotional disturbances after stroke. Clinical and Experimental Hypertension 28, 243-249.

Apetauerova, D., 2012. Parkinson Disease. In: Jones, H.R., Srinivasan, J., Allam, G.J., Baker, R.A. (Eds.), Netter's Neurology, 2nd ed. Elsevier Health Sciences, pp. 287-298.

Appel, M.J.G., 1999. Forty years of canine vaccination. In: Schultz, R. (Ed.), Advances in Veterinary Medicine, volume 41. Academic Press, pp. 309-324.

Ashkan, K., Wallace, B., Bell, B.A., Benabid, A.L., 2004. Deep brain stimulation of the subthalamic nucleus in Parkinson's Disease 1993–2003: where are we 10 years on? British Journal of Neurosurgery 18, 19-34.

Azevedo, F.A., Carvalho, L.R., Grinberg, L.T., Farfel, J.M., Ferretti, R.E., Leite, R.E., Jacob, F.W., Lent, R., Herculano-Houzel, S., 2009. Equal numbers of neuronal and nonneuronal cells make the human brain an isometrically scaled-up primate brain. J Comp Neurol 513, 532-541.

Bailey, C.H., Bartsch, D., Kandel, E.R., 1996. Toward a molecular definition of long-term memory storage. Proceedings of the National Academy of Sciences 93, 13445-13452.

Bailey, C.H., Kandel, E.R., 2008. Synaptic remodeling, synaptic growth and the storage of long-term memory in *Aplysia*. In: Sossin, W.S., Lacaille, J.C., Castellucci, V.F., Belleville, S. (Eds.), Progress in Brain Research, Essence of Memory, volume 169. Elsevier, pp. 179-198.

Baker, M., 2013. Neuroscience: Through the eyes of a mouse. Nature 502, 156-158.

Bandtlow, C., Zachleder, T., Schwab, M.E., 1990. Oligodendrocytes arrest neurite growth by contact inhibition. J Neurosci. 10, 3837-3848.

Banting, F.G., 1925. Diabetes and Insulin. Nobel Lecture Physiology or Medicine.

Barbeau, A., 1981. The use of L-DOPA in Parkinson's disease: a 20 year follow-up. Trends in Pharmacological Sciences 2, 297-299.

Bareyre, F.M., Haudenschild, B., Schwab, M.E., 2002. Long-lasting sprouting and gene expression changes induced by the monoclonal antibody IN-1 in the adult spinal cord. J Neurosci. 22, 7097-7110.

Baumer, D., Talbot, K., Turner, M.R., 2014. Advances in motor neurone disease. J R.Soc.Med. 107, 14-21.

Bear, M.F., Connors, B.W., Paradiso, M.A., 2007. Neuroscience: exploring the brain. Lippincott Williams & Wilkins.

Behring, E., 1913. Ueber ein neues Diphtherieschutzmittel. DMW-Deutsche Medizinische Wochenschrift 39, 873-876.

Benabid, A.L., Pollak, P., Seigneuret, E., Hoffmann, D., Gay, E., Perret, J., 1993. Chronic VIM Thalamic Stimulation in Parkinson's Disease, Essential Tremor and Extra-Pyramidal Dyskinesias. In: Meyerson, B.A., Broggi, G., Martin-Rodriguez, J., Ostertag, C., Sindou, M. (Eds.), Advances in Stereotactic and Functional Neurosurgery 10, vol 58. Springer Vienna, pp. 39-44.

Benazzouz, A., Gao, D.M., Ni, Z.G., Piallat, B., Bouali-Benazzouz, R., Benabid, A.L., 2000. Effect of high-frequency stimulation of the subthalamic nucleus on the neuronal activities of the substantia nigra pars reticulata and ventrolateral nucleus of the thalamus in the rat. Neuroscience 99, 289-295.

Benazzouz, A., Gross, C., Féger, J., Boraud, T., Bioulac, B., 1993. Reversal of rigidity and improvement in motor performance by subthalamic high–frequency stimulation in MPTP–treated monkeys. European Journal of Neuroscience 5, 382-389.

Benfey, M., Aguayo, A.J., 1982. Extensive elongation of axons from rat brain into peripheral nerve grafts. Nature 296, 150-152.

Bentham, J., 1789. An introduction to the principles of morals and legislation. Available from http://www.econlib.org/library/Bentham/bnthPML18.html; accessed 29 April 2015; Internet.

Bergman, H., Wichmann, T., Karmon, B., DeLong, M.R., 1994. Parkinsonian Tremor is Associated with Low Frequency Neuronal Oscillations in Selective Loops of the Basal Ganglia. In: Percheron, G., McKenzie, J.S., Féger, J. (Eds.), The Basal Ganglia IV, vol 41. Springer US, pp. 317-325.

Berry-Kravis, E.M., Hessl, D., Rathmell, B., Zarevics, P., Cherubini, M., Walton-Bowen, K., Mu, Y., Nguyen, D.V., Gonzalez-Heydrich, J., Wang, P.P., Carpenter, R.L., Bear, M.F., Hagerman, R.J., 2012. Effects of STX209 (arbaclofen) on neurobehavioral function in children and adults with fragile X syndrome: a randomized, controlled, phase 2 trial. Sci.Transl.Med. 4, 152ra127.

Bigelow, W.G., Callaghan, J.C., Hopps, J.A., 1950. General Hypothermia for Experimental Intracardiac Surgery: The Use of Electrophrenic Respirations, an Artificial Pacemaker for Cardiac Standstill, and Radio-Frequency Rewarming in General Hypothermia. Annals of Surgery 132, 531-537.

Birkmayer, W., Hornykiewicz, O., 1962. Der L-Dioxyphenylalanin (=L-DOPA)-Effekt beim Parkinson-Syndrom des Menschen: Zur Pathogenese und Behandlung der Parkinson-Akinese. Archiv für Psychiatrie und Zeitschrift f.d.ges.Neurologie 203, 560-574.

Birkmayer, W., Hornykiewicz, O., 1964. Weitere experimentelle Untersuchungen über L-DOPA beim Parkinson-Syndrom und Reserpin-Parkinsonismus. Archiv für Psychiatrie und Zeitschrift f.d.ges.Neurologie 206, 367-381.

Bjugstad, K.B., Redmond, D.E.Jr., Teng, Y.D., Elsworth, J.D., Roth, R.H., Blanchard, B.C., Snyder, E.Y., Sladek, J.R.Jr., 2005. Neural stem cells implanted into MPTP-treated monkeys increase the size of endogenous tyrosine hydroxylase-positive cells found in the striatum: a return to control measures. Cell Transplant. 14, 183-192.

Bjugstad, K.B., Teng, Y.D., Redmond, D.E.Jr., Elsworth, J.D., Roth, R.H., Cornelius, S.K., Snyder, E.Y., Sladek, J.R.Jr., 2008. Human neural stem cells migrate along the nigrostriatal pathway in a primate model of Parkinson's disease. Exp Neurol 211, 362-369.

Bloch, J., Brunet, J.F., McEntire, C.R.S., Redmond, D.E.Jr., 2014. Primate adult brain cell autotransplantation produces behavioral and biological recovery in 1-methyl-4-phenyl-1,2,3,6-tetrahydropyridine-induced parkinsonian St. Kitts monkeys. Journal of Comparative Neurology 522, 2729-2740.

Blume, E., 1983. Street drugs yield primate parkinson's model. JAMA : the journal of the American Medical Association 250, 13-14.

Brand, Y., Senn, P., Kompis, M., Dillier, N., Allum, J.H., 2014. Cochlear implantation in children and adults in Switzerland. Swiss.Med Wkly. 144, w13909.

Bregman, B.S., Kunkel-Bagden, E., Schnell, L., Dai, H.N., Gao, D., Schwab, M.E., 1995. Recovery from spinal cord injury mediated by antibodies to neurite growth inhibitors. Nature 378, 498-501.

Brösamle, C., Huber, A.B., Fiedler, M., Skerra, A., Schwab, M.E., 2000. Regeneration of lesioned corticospinal tract fibers in the adult rat induced by a recombinant, humanized IN-1 antibody fragment. J Neurosci. 20, 8061-8068.

Buchanan-Smith, H.M., 2011. Environmental enrichment for primates in laboratories. Adv.Sci.Res 5, 41-56.

Buchli, A.D., Rouiller, E., Mueller, R., Dietz, V., Schwab, M.E., 2007. Repair of the injured spinal cord. A joint approach of basic and clinical research. Neurodegener.Dis. 4, 51-56.

Buchli, A.D., Schwab, M.E., 2005. Inhibition of Nogo: a key strategy to increase regeneration, plasticity and functional recovery of the lesioned central nervous system. Ann.Med. 37, 556-567.

Burns, R.S., Chiueh, C.C., Markey, S.P., Ebert, M.H., Jacobowitz, D.M., Kopin, I.J., 1983. A primate model of parkinsonism: selective destruction of dopaminergic neurons in the

pars compacta of the substantia nigra by N-methyl-4-phenyl-1,2,3,6-tetrahydropyridine. Proc.Natl.Acad.Sci.USA 80, 4546-4550.

Cadelli, D.S., Schwab, M.E., 1991. Myelin-associated inhibitors of neurite outgrowth and their role in CNS regeneration. Ann.N.Y.Acad.Sci. 633, 234-240.

Capitanio, J.P., Emborg, M.E., 2008. Contributions of non-human primates to neuroscience research. Lancet 371, 1126-1135.

Carlsson, A., 1960. Zur Frage der Wirkungsweise einiger Psychopharmaka. European Neurology 140, 220-222.

Carlsson, A., 2001. Nobel Lecture: A Half-Century of Neurotransmitter Research: Impact on Neurology and Psychiatry. Bioscience Reports 21, 691-710.

Carlsson, H.E., Schapiro, S.J., Farah, I., Hau, J., 2004. Use of primates in research: a global overview. Am.J Primatol. 63, 225-237.

Caroni, P., Schwab, M.E., 1988a. Antibody against myelin-associated inhibitor of neurite growth neutralizes nonpermissive substrate properties of CNS white matter. Neuron 1, 85-96.

Caroni, P., Schwab, M.E., 1988b. Two membrane protein fractions from rat central myelin with inhibitory properties for neurite growth and fibroblast spreading. J Cell Biol. 106, 1281-1288.

Carrel, A., 1912. Suture of Blood-Vessels and Transplantation of Organs. Nobel Lecture Physiology or Medicine.

Chang, G.J., Davis, B.S., Stringfield, C., Lutz, C., 2007. Prospective immunization of the endangered California condors (*Gymnogyps californianus*) protects this species from lethal West Nile virus infection. Vaccine 25, 2325-2330.

Charalambous, C.C., Bowden, M.G., Adkins, D.L., 2015. Motor Cortex and Motor Cortical Interhemispheric Communication in Walking After Stroke: The Roles of Transcranial Magnetic Stimulation and Animal Models in Our Current and Future Understanding. Neurorehabilitation and Neural Repair.

Cheatwood, J.L., Emerick, A.J., Schwab, M.E., Kartje, G.L., 2008. Nogo-A expression after focal ischemic stroke in the adult rat. Stroke 39, 2091-2098.

Chen, D.F., Jhaveri, S., Schneider, G.E., 1995. Intrinsic changes in developing retinal neurons result in regenerative failure of their axons. Proc.Natl.Acad.Sci.USA 92, 7287-7291.

Chen, M.S., Huber, A.B., van der Haar, M.E., Frank, M., Schnell, L., Spillmann, A.A., Christ, F., Schwab, M.E., 2000. Nogo-A is a myelin-associated neurite outgrowth inhibitor and an antigen for monoclonal antibody IN-1. Nature 403, 434-439.

Chow, A.Y., Chow, V.Y., Packo, K.H., Pollack, J.S., Peyman, G.A., Schuchard, R., 2004. The artificial silicon retina microchip for the treatment of vision loss from retinitis pigmentosa. Arch.Ophthalmol 122, 460-469.

Clark, G.M., 2015. The multi-channel cochlear implant: Multi-disciplinary development of electrical stimulation of the cochlea and the resulting clinical benefit. Hearing Research 322, 4-13.

Cole, K.S., Curtis, H.J., 1941. Membrane potential of the squid giant axon during current flow. The Journal of General Physiology 24, 551-563.

Coleman, K., Bloomsmith, M.A., Crockett, C.M., Weed, J.L., Schapiro, S.J., 2012. Behavioral Management, Enrichment, and Psychological Well-being of Laboratory Nonhuman Primates. In: Morris, C.R.A. (Ed.), Nonhuman Primates in Biomedical Research (Second Edition). Academic Press, Boston, pp. 149-176.

Collinger, J.L., Kryger, M.A., Barbara, R., Betler, T., Bowsher, K., Brown, E.H.P., Clanton, S.T., Degenhart, A.D., Foldes, S.T., Gaunt, R.A., Gyulai, F.E., Harchick, E.A., Harrington, D., Helder, J.B., Hemmes, T., Johannes, M.S., Katyal, K.D., Ling, G.S.F., McMorland, A.J.C., Palko, K., Para, M.P., Scheuermann, J., Schwartz, A.B., Skidmore, E.R., Solzbacher, F., Srikameswaran, A.V., Swanson, D.P., Swetz, S., Tyler-Kabara, E.C., Velliste, M., Wang, W., Weber, D.J., Wodlinger, B., Boninger, M.L., 2014. Collaborative Approach in the Development of High-Performance Brain–Computer Interfaces for a Neuroprosthetic Arm: Translation from Animal Models to Human Control. Clinical and Translational Science 7, 52-59.

Collinger, J.L., Wodlinger, B., Downey, J.E., Wang, W., Tyler-Kabara, E.C., Weber, D.J., McMorland, A.J.C., Velliste, M., Boninger, M.L., Schwartz, A.B., 2013. High-performance neuroprosthetic control by an individual with tetraplegia. The Lancet 381, 557-564.

Committee for the Update of the Guide for the Care and Use of Laboratory Animals, National Research Council, 2011. Guide for the Care and Use of Laboratory Animals, Eighth ed. The National Academies Press.

Connolly, B.S., Lang, A.E., 2014. Pharmacological treatment of parkinson disease: A review. JAMA : the journal of the American Medical Association 311, 1670-1683.

Courtine, G., Bunge, M.B., Fawcett, J.W., Grossman, R.G., Kaas, J.H., Lemon, R.N., Maier, I., Martin, J., Nudo, R.J., Ramon-Cueto, A., Rouiller, E.M., Schnell, L., Wannier, T., Schwab, M.E., Edgerton, V.R., 2007. Can experiments in nonhuman primates expedite the translation of treatments for spinal cord injury in humans? Nat.Med. 13, 561-566.

Crile, G., 1907. The Technique of Direct Transfusion of Blood. Annals of Surgery 46, 329-332.

Crystal, J.D., Alford, W.T., 2014. Validation of a rodent model of source memory. Biol.Lett. 10, 20140064.

Cui, X., Gooch, H., Groves, N.J., Sah, P., Burne, T.H., Eyles, D.W., McGrath, J.J., 2015. Vitamin D and the brain: Key questions for future research. The Journal of Steroid Biochemistry and Molecular Biology 148, 305-309.

Curtis, H.J., Cole, K.S., 1938. Transverse electric impedance of the squid giant axon. The Journal of General Physiology 21, 757-765.

Curtis, H.J., Cole, K.S., 1942. Membrane resting and action potentials from the squid giant axon. Journal of Cellular and Comparative Physiology 19, 135-144.

da Cruz, L., Coley, B.F., Dorn, J., Merlini, F., Filley, E., Christopher, P., Chen, F.K., Wuyyuru, V., Sahel, J., Stanga, P., Humayun, M., Greenberg, R.J., Dagnelie, G., for the Argus II Study Group, 2013. The Argus II epiretinal prosthesis system allows letter and word reading and long-term function in patients with profound vision loss. British Journal of Ophthalmology 97, 632-636.

David, S., Aguayo, A.J., 1981. Axonal elongation into peripheral nervous system "bridges" after central nervous system injury in adult rats. Science 214, 931-933.

Deuschl, G., Schade-Brittinger, C., Krack, P., Volkmann, J., Schäfer, H., Bötzel, K., Daniels, C., Deutschländer, A., Dillmann, U., Eisner, W., Gruber, D., Hamel, W., Herzog, J., Hilker, R., Klebe, S., Kloss, M., Koy, J., Krause, M., Kupsch, A., Lorenz, D., Lorenzl, S., Mehdorn, H.M., Moringlane, J.R., Oertel, W., Pinsker, M.O., Reichmann, H., Reuss, A., Schneider, G.H., Schnitzler, A., Steude, U., Sturm, V., Timmermann, L., Tronnier, V., Trottenberg, T., Wojtecki, L., Wolf, E., Poewe, W., Voges, J., 2006. A Randomized Trial of Deep-Brain Stimulation for Parkinson's Disease. New England Journal of Medicine 355, 896-908.

Donoghue, J.P., Sanes, J.N., Hatsopoulos, N.G., Gaal, G., 1998. Neural discharge and local field potential oscillations in primate motor cortex during voluntary movements. J Neurophysiol 79, 159-173.

Editorial Nature Medicine vol.19 (10), 2013. Animal research: a balancing act. Nat.Med 19, 1191.

Emerick, A.J., Neafsey, E.J., Schwab, M.E., Kartje, G.L., 2003. Functional reorganization of the motor cortex in adult rats after cortical lesion and treatment with monoclonal antibody IN-1. J Neurosci. 23, 4826-4830.

Emerick, A.J., Kartje, G.L., 2004. Behavioral recovery and anatomical plasticity in adult rats after cortical lesion and treatment with monoclonal antibody IN-1. Behavioural Brain Research 152, 315-325.

Enders, J.F., Robbins, F.C., Weller, T.H., 1980. Classics in infectious diseases. The cultivation of the poliomyelitis viruses in tissue culture by John F. Enders, Frederick C. Robbins, and Thomas H. Weller. Rev Infect.Dis. 2, 493-504.

Enders, J.F., Robbins, F.C., Weller, T.H., 1954. The cultivation of the poliomyelitis viruses in tissue culture. Nobel Lecture, 448-467.

Enders, J.F., Weller, T.H., Robbins, F.C., 1949. Cultivation of the Lansing strain of poliomyelitis virus in cultures of various human embryonic tissues. Science 109, 85-87.

Evarts, E.V., 1974. Precentral and postcentral cortical activity in association with visually triggered movement. J Neurophysiol. 37, 373-381.

Evarts, E.V., 1964. Temporal patterns of discharge of pyramidal tract neurons during sleep and waking in the monkey. Journal of Neurophysiology 27, 152-171.

Evrard, H.C., Forro, T., Logothetis, N.K., 2012. Von Economo Neurons in the Anterior Insula of the Macaque Monkey. Neuron 74, 482-489.

Evrard, H.C., Logothetis, N.K., Craig, A.D., 2014. Modular architectonic organization of the insula in the macaque monkey. Journal of Comparative Neurology 522, 64-97.

Fantin, B., Carbon, C., 1992. In vivo antibiotic synergism: contribution of animal models. Antimicrobial Agents and Chemotherapy 36, 907-912.

Filbin, M.T., 2003. Myelin-associated inhibitors of axonal regeneration in the adult mammalian CNS. Nat.Rev.Neurosci. 4, 703-713.

Filler, A., 2009. Magnetic resonance neurography and diffusion tensor imaging: origins, history, and clinical impact of the first 50,000 cases with an assessment of efficacy and utility in a prospective 5000-patient study group. Neurosurgery 65, A29-A43.

Filli, L., Schwab, M.E., 2012. The rocky road to translation in spinal cord repair. Annals of Neurology 72, 491-501.

Fleming, A., 1929. On the Antibacterial Action of Cultures of a Penicillium, with Special Reference to their Use in the Isolation of B. influenzae. British journal of experimental pathology 10, 226-236.

Fleury, V., Wider, C., Horvath, J., Zacharia, A., Bally, J., Pollak, P., Pollo, C., Vingerhoets, F.J.G., Burkhard, P.R., 2013. Successful long-term bilateral subthalamic nucleus deep brain stimulation in VPS35 Parkinson's disease. Parkinsonism & Related Disorders 19, 707-708.

Follett, K.A., Weaver, F.M., Stern, M., Hur, K., Harris, C.L., Luo, P., Marks, W.J., Rothlind, J., Sagher, O., Moy, C., Pahwa, R., Burchiel, K., Hogarth, P., Lai, E.C., Duda, J.E., Holloway, K., Samii, A., Horn, S., Bronstein, J.M., Stoner, G., Starr, P.A., Simpson, R., Baltuch, G., De Salles, A., Huang, G.D., Reda, D.J., 2010. Pallidal versus Subthalamic Deep-Brain Stimulation for Parkinson's Disease. New England Journal of Medicine 362, 2077-2091.

Fouad, K., Klusman, I., Schwab, M.E., 2004. Regenerating corticospinal fibers in the Marmoset (*Callitrix jacchus*) after spinal cord lesion and treatment with the anti-Nogo-A antibody IN-1. Eur.J Neurosci. 20, 2479-2482.

Fouad, K., Dietz, V., Schwab, M.E., 2001. Improving axonal growth and functional recovery after experimental spinal cord injury by neutralizing myelin associated inhibitors. Brain Research Reviews 36, 204-212.

Freund, P., Schmidlin, E., Wannier, T., Bloch, J., Mir, A., Schwab, M.E., Rouiller, E.M., 2006. Nogo-A-specific antibody treatment enhances sprouting and functional recovery after cervical lesion in adult primates. Nat.Med. 12, 790-792.

Freund, P., Schmidlin, E., Wannier, T., Bloch, J., Mir, A., Schwab, M.E., Rouiller, E.M., 2009. Anti-Nogo-A antibody treatment promotes recovery of manual dexterity after unilateral cervical lesion in adult primates--re-examination and extension of behavioral data. Eur.J Neurosci. 29, 983-996.

Freund, P., Wannier, T., Schmidlin, E., Bloch, J., Mir, A., Schwab, M.E., Rouiller, E.M., 2007. Anti-Nogo-A antibody treatment enhances sprouting of corticospinal axons rostral to a unilateral cervical spinal cord lesion in adult macaque monkey. J Comp Neurol. 502, 644-659.

Gajdusek, D.C., 1976. Unconventional viruses and the origin and disappearance of kuru. Nobel Lecture Physiology or Medicine.

Gantz, B.J., Turner, C., Gfeller, K.E., 2006. Acoustic plus Electric Speech Processing: Preliminary Results of a Multicenter Clinical Trial of the Iowa/Nucleus Hybrid Implant. Audiology and Neurotology 11 (suppl 1), 63-68.

Garbarini, N., 2010. Primates as a model for research. Dis.Model.Mech. 3, 15-19.

Georgopoulos, A.P., 1987. Cortical mechanisms subserving reaching. In: CIBA Foundation Symposium (Ed.), Motor Areas of the Cerebral Cortex. Wiley, pp. 125-141.

Georgopoulos, A.P., Kalaska, J.F., Caminiti, R., Massey, J.T., 1982. On the relations between the direction of two-dimensional arm movements and cell discharge in primate motor cortex. The Journal of Neuroscience 2, 1527-1537.

Gerstner, W., Sprekeler, H., Deco, G., 2012. Theory and simulation in neuroscience. Science 338, 60-65.

Ghezzi, D., Antognazza, M.R., Maccarone, R., Bellani, S., Lanzarini, E., Martino, N., Mete, M., Pertile, G., Bisti, S., Lanzani, G., Benfenati, F., 2013. A polymer optoelectronic interface restores light sensitivity in blind rat retinas. Nat Photon 7, 400-406.

Gillani, R.L., Tsai, S.Y., Wallace, D.G., O'Brien, T.E., Arhebamen, E., Tole, M., Schwab, M.E., Kartje, G.L., 2010. Cognitive recovery in the aged rat after stroke and anti-Nogo-A immunotherapy. Behavioural Brain Research 208, 415-424.

Glanzman, D.L., 2012. Behavioral Neuroscience: No Easy Path from Genes to Cognition. Current Biology 22, R302-R304.

Goldberg, J.L., Barres, B.A., 2000. Neurobiology: Nogo in nerve regeneration. Nature 403, 369-370.

Gonzalez, R., Garitaonandia, I., Crain, A., Poustovoitov, M., Abramihina, T., Noskov, A., Jiang, C., Morey, R., Laurent, L.C., Elsworth, J.D., 2015. Proof of Concept Studies Exploring the Safety and Functional Activity of Human Parthenogenetic-Derived Neural Stem Cells for the Treatment of Parkinson's Disease. Cell transplantation 24, 681-690.

Gonzenbach, R.R., Schwab, M.E., 2008. Disinhibition of neurite growth to repair the injured adult CNS: Focusing on Nogo. Cell.Mol.Life Sci. 65, 161-176.

Grandpré, T., Strittmatter, S.M., 2001. Nogo: A Molecular Determinant of Axonal Growth and Regeneration. the neuroscientist 7, 377-386.

Griffin, L.D., 1994. The intrinsic geometry of the cerebral cortex. J Theor.Biol. 166, 261-273.

Halstead, W.C., Rucker, W.B., McMahon, J.P., 1967. Memory. Annu.Rev Med. 18, 1-14.

Hamadjida, A., Wyss, A.F., Mir, A., Schwab, M.E., Belhaj-Saïf, A., Rouiller, E.M., 2012. Influence of anti-Nogo-A antibody treatment on the reorganization of callosal connectivity of the premotor cortical areas following unilateral lesion of primary motor cortex (M1) in adult macaque monkeys. Exp.Brain Res. 223, 321-340.

Hamani, C., Temel, Y., 2012. Deep Brain Stimulation for Psychiatric Disease: Contributions and Validity of Animal Models. Science Translational Medicine 4, 142rv8.

Hasenfuss, G., 1998. Animal models of human cardiovascular disease, heart failure and hypertrophy. Cardiovascular Research 39, 60-76.

Hashimoto, T., Elder, C.M., Okun, M.S., Patrick, S.K., Vitek, J.L., 2003. Stimulation of the Subthalamic Nucleus Changes the Firing Pattern of Pallidal Neurons. The Journal of Neuroscience 23, 1916-1923.

Hawkins, R.D., Kandel, E.R., Bailey, C.H., 2006. Molecular Mechanisms of Memory Storage in Aplysia. The Biological Bulletin 210, 174-191.

Henderson, C., Wijetunge, L., Kinoshita, M.N., Shumway, M., Hammond, R.S., Postma, F.R., Brynczka, C., Rush, R., Thomas, A., Paylor, R., Warren, S.T., Vanderklish, P.W., Kind, P.C., Carpenter, R.L., Bear, M.F., Healy, A.M., 2012. Reversal of disease-related pathologies in the fragile X mouse model by selective activation of GABA(B) receptors with arbaclofen. Sci.Transl.Med. 4, 152ra128.

Herculano-Houzel, S., 2009. The human brain in numbers: a linearly scaled-up primate brain. Front Hum.Neurosci. 3, 31.

Herculano-Houzel, S., 2011. Scaling of brain metabolism with a fixed energy budget per neuron: implications for neuronal activity, plasticity and evolution. PLoS One 6, e17514.

Hessell, A.J., Haigwood, N.L., 2015. Animal models in HIV-1 protection and therapy. Current Opinion in HIV and AIDS 10.

Hochberg, L.R., Bacher, D., Jarosiewicz, B., Masse, N.Y., Simeral, J.D., Vogel, J., Haddadin, S., Liu, J., Cash, S.S., van der Smagt, P., Donoghue, J.P., 2012. Reach and grasp by people with tetraplegia using a neurally controlled robotic arm. Nature 485, 372-375.

Hochberg, L.R., Serruya, M.D., Friehs, G.M., Mukand, J.A., Saleh, M., Caplan, A.H., Branner, A., Chen, D., Penn, R.D., Donoghue, J.P., 2006. Neuronal ensemble control of prosthetic devices by a human with tetraplegia. Nature 442, 164-171.

Hodgkin, A.L., Huxley, A.F., 1939. Action potentials recorded from inside a nerve fibre. Nature 144, 710-711.

Hopf, F.W., Lesscher, H.M., 2014. Rodent models for compulsive alcohol intake. Alcohol 48, 253-264.

Houser, S.R., Margulies, K.B., Murphy, A.M., Spinale, F.G., Francis, G.S., Prabhu, S.D., Rockman, H.A., Kass, D.A., Molkentin, J.D., Sussman, M.A., Koch, W.J., 2012. Animal Models of Heart Failure: A Scientific Statement From the American Heart Association. Circulation Research 111, 131-150.

Huang, Y., Williams, J.C., Johnson, S.M., 2012. Brain slice on a chip: opportunities and challenges of applying microfluidic technology to intact tissues. Lab on a Chip 12, 2103-2117.

Hubel, D.H., Wiesel, T.N., 1968. Receptive fields and functional architecture of monkey striate cortex. J.Physiol 195, 215-243.

Hubel, D.H., Wiesel, T.N., 1998. Early exploration of the visual cortex. Neuron 20, 401-412.

Hulsebosch, C.E., 2002. Recent advances in pathophysiology and treatment of spinal cord injury. Adv.Physiol Educ. 26, 238-255.

Humphrey, D.R., Schmidt, E.M., Thompson, W.D., 1970. Predicting Measures of Motor Performance from Multiple Cortical Spike Trains. Science 170, 758-762.

Hurst, S., Mauron, A., 2012. Expérimentation animale: une pesée en déséquilibre., 5 ed, pp. 20-22.

Huys, A.C.M.L., Bally, J.F., Pollak, P., 2014. Deep Brain Stimulation in Parkinson's Disease. In: Wolters, E.C.M.J., Baumann, C. (Eds.), Parkinson Disease and Other Movement Disorders: Motor Behavioural Disorders and Behavioural Motor Disorders. International Association of Parkinsonism and Related Disorders & VU University Press, Amsterdam, pp. 271-285.

Ifft, P.J., Shokur, S., Li, Z., Lebedev, M.A., Nicolelis, M.A.L., 2013. A Brain-Machine Interface Enables Bimanual Arm Movements in Monkeys. Science Translational Medicine 5, 210ra154.

Jackson, A., 2012. Neuroscience: Brain-controlled robot grabs attention. Nature 485, 317-318.

Jenkins, W.M., Merzenich, M.M., Ochs, M.T., Allard, T., Guic-Robles, E., 1990. Functional reorganization of primary somatosensory cortex in adult owl monkeys after behaviorally controlled tactile stimulation. J Neurophysiol. 63, 82-104.

Johnson, M.D., Vitek, J.L., McIntyre, C.C., 2009. Pallidal stimulation that improves parkinsonian motor symptoms also modulates neuronal firing patterns in primary motor cortex in the MPTP-treated monkey. Exp Neurol 219, 359-362.

Jones, K.E., Campbell, P.K., Normann, R.A., 1992. A glass/silicon composite intracortical electrode array. Annals of biomedical engineering 20, 423-437.

Juorio, A.V., Vogt, M., 1967. Monoamines and their metabolites in the avian brain. The Journal of physiology 189, 489-518.

Kaas, J.H., Merzenich, M.M., Killackey, H.P., 1983. The reorganization of somatosensory cortex following peripheral nerve damage in adult and developing mammals. Annu.Rev.Neurosci. 6, 325-356.

Kandel, E.R., Schwartz, J., Jessell, T.M., 2000. Principles of neural science, 4th ed. McGraw-Hill, Health Professions Division.

Kandel, E.R., Klein, M., Castellucci, V.F., Schacher, S., Goelet, P., 1986. Some principles emerging from the study of short- and long-term memory. Neuroscience Research 3, 498-520.

Kandel, E.R., Squire, L.R., 2000. Neuroscience: Breaking Down Scientific Barriers to the Study of Brain and Mind. Science 290, 1113-1120.

Karle, E.J., Anderson, K.D., Medina, L., Reiner, A., 1996. Light and electron microscopic immunohistochemical study of dopaminergic terminals in the striatal portion of the pigeon basal ganglia using antisera against tyrosine hydroxylase and dopamine. Journal of Comparative Neurology 369, 109-124.

Kayser, C., Logothetis, N.K., 2013. The Electrophysiological Background of the fMRI Signal. In: Ulmer, S., Jansen, O. (Eds.), fMRI. Springer Berlin Heidelberg, pp. 25-36.

Kefalopoulou, Z., Politis, M., Piccini, P., Mencacci, N., Bhatia, K., Jahanshahi, M., Widner, H., Rehncrona, S., Brundin, P., Bjorklund, A., Lindvall, O., Limousin, P., Quinn, N., Foltynie, T., 2014. Long-term clinical outcome of fetal cell transplantation for Parkinson disease: two case reports. JAMA Neurol 71, 83-87.

Kim, J.H., Min, K.S., Jeong, J.S., Kim, S.J., 2012. Challenges for the Future Neuroprosthetic Implants. In: Jobbágy, Á. (Ed.), 5th European Conference of the International Federation for Medical and Biological Engineering, volume 37. Springer Berlin Heidelberg, pp. 1214-1216.

Koch, C., Laurent, G., 1999. Complexity and the Nervous System. Science 284, 96-98.

Kolata, G., 1983. Monkey model of Parkinson's disease. Science (New York, NY) 220, 705.

Krack, P., Pollak, P., Limousin, P., Benazzouz, A., Benabid, A.L., 1997. Stimulation of subthalamic nucleus alleviates tremor in Parkinson's disease. The Lancet 350, 1675.

Landsteiner, K., Popper, E., 1909. Uebertragung der Poliomyelitis acuta auf Affen. Z Immunitätsforsch 2, 377-390.

Landsteiner, K., Wiener, A.S., 1941. Studies on an agglutinogen (Rh) in human blood reacting with anti-rhesus sera and with human isoantibodies. The Journal of Experimental Medicine 74, 309-320.

Langston, J.W., 1983. Parkinson's Disease in a Chemist Working with 1-Methyl-4-Phenyl-L,2,5,6-Tetrahydropyridine. New England Journal of Medicine 309, 310.

Langston, J.W., Ballard, P., Tetrud, J.W., Irwin, I., 1983a. Chronic Parkinsonism in humans due to a product of meperidine-analog synthesis. Science 219, 979-980.

Langston, J.W., Langston, E.B., Irwin, I., 1983b. MPTP-induced parkinsonism in human and non-human primates--clinical and experimental aspects. Acta neurologica Scandinavica.Supplementum 100, 49-54.

Larsen, C.S., Repcheck, J., 2010. Our Origins: Discovering Physical Anthropology. W. W. Norton, Incorporated.

le Coutre, P., Mologni, L., Cleris, L., Marchesi, E., Buchdunger, E., Giardini, R., Formelli, F., Gambacorti-Passerini, C., 1999. In Vivo Eradication of Human BCR/ABL-Positive Leukemia Cells With an ABL Kinase Inhibitor. Journal of the National Cancer Institute 91, 163-168.

Lemon, R.N., 2008. Descending pathways in motor control. Annu.Rev.Neurosci. 31, 195-218.

Lemon, R.N., 2012. Nonhuman Primate Models of the Motor System., Nonhuman Primates in Biomedical Research (Second Edition). Academic Press, Boston, pp. 783-794.

Lemon, R.N., Griffiths, J., 2003. Is the rat a good model for human neurological disease? Nat Rev Neurosci 3.

Lemon, R.N., Griffiths, J., 2005. Comparing the function of the corticospinal system in different species: organizational differences for motor specialization? Muscle Nerve 32, 261-279.

Leuthardt, E.C., Roland, J.L., Ray, W.Z., 2014. Neuroprosthetics.

Lewis, M.G., Lafrado, L.J., Haffer, K., Gerber, J., Sharpee, R.L., Olsen, R.G., 1988. Feline leukemia virus vaccine: New developments. Veterinary Microbiology 17, 297-308.

Liebscher, T., Schnell, L., Schnell, D., Scholl, J., Schneider, R., Gullo, M., Fouad, K., Mir, A., Rausch, M., Kindler, D., Hamers, F.P., Schwab, M.E., 2005. Nogo-A antibody improves regeneration and locomotion of spinal cord-injured rats. Ann.Neurol. 58, 706-719.

Lindau, N.T., Bänninger, B.J., Gullo, M., Good, N.A., Bachmann, L.C., Starkey, M.L., Schwab, M.E., 2014. Rewiring of the corticospinal tract in the adult rat after unilateral stroke and anti-Nogo-A therapy. Brain 137, 739-756.

Logothetis, N.K., 2008. What we can do and what we cannot do with fMRI. Nature 453, 869-878.

Logothetis, N.K., Wandell, B.A., 2004. Interpreting the BOLD Signal. Annual Review of Physiology 66, 735-769.

Lopes da Silva, F.H., 2013. EEG and MEG: relevance to neuroscience. Neuron 80, 1112-1128.

Luders, E., Steinmetz, H., Jancke, L., 2002. Brain size and grey matter volume in the healthy human brain. Neuroreport 13, 2371-2374.

Lutz, C.K., Novak, M.A., 2005. Environmental enrichment for nonhuman primates: theory and application. ILAR.J 46, 178-191.

Macleod, J.J.R., 1925. The physiology of insulin and its source in the animal body. Nobel Lecture Physiology or Medicine.

Magistretti, P.J., Pellerin, L., Martin, J.L., 1995. Brain energy metabolism: an integrated cellular perspective. In: Bloom, F.E., Kupfer, D.J. (Eds.), Psychopharmacology : the fourth generation of progress. Raven Press, New York, pp. 657-670.

Maier, I.C., Ichiyama, R.M., Courtine, G., Schnell, L., Lavrov, I., Edgerton, V.R., Schwab, M.E., 2009. Differential effects of anti-Nogo-A antibody treatment and treadmill training in rats with incomplete spinal cord injury. Brain 132, 1426-1440.

Maier, I.C., Schwab, M.E., 2006. Sprouting, regeneration and circuit formation in the injured spinal cord: factors and activity. Philos.Trans.R.Soc.Lond B Biol.Sci. 361, 1611-1634.

Mandel, Y., Goetz, G., Lavinsky, D., Huie, P., Mathieson, K., Wang, L., Kamins, T., Galambos, L., Manivanh, R., Harris, J., Palanker, D., 2013. Cortical responses elicited by photovoltaic subretinal prostheses exhibit similarities to visually evoked potentials. Nat Commun 4.

Manger, P.R., Cort, J., Ebrahim, N., Goodman, A., Henning, J., Karolia, M., Rodrigues, S.L., Strkalj, G., 2008. Is 21st century neuroscience too focussed on the rat/mouse model of brain function and dysfunction? Front Neuroanat. 2, 5.

Markus, T.M., Tsai, S.Y., Bollnow, M.R., Farrer, R.G., O'Brien, T.E., Kindler-Baumann, D.R., Rausch, M., Rudin, M., Wiessner, C., Mir, A.K., Schwab, M.E., Kartje, G.L., 2005. Recovery and brain reorganization after stroke in adult and aged rats. Annals of Neurology 58, 950-953.

Marra, A., 2012. A Review of Animal Models Used for Antibiotic Evaluation. In: Dougherty, T.J., Pucci, M.J. (Eds.), Antibiotic Discovery and Development. Springer US, pp. 1009-1033.

Martin, S.J., Clark, R.E., 2007. The rodent hippocampus and spatial memory: from synapses to systems. Cell Mol.Life Sci. 64, 401-431.

Mastro, J.M., Lewis, M.G., Mathes, L.E., Sharpee, R., Tarr, M.J., Olsen, R.G., 1986. Feline leukemia vaccine: Efficacy, contents and probable mechanism. Veterinary Immunology and Immunopathology 11, 205-213.

Maynard, E.M., Nordhausen, C.T., Normann, R.A., 1997. The Utah Intracortical Electrode Array: A recording structure for potential brain-computer interfaces. Electroencephalography and Clinical Neurophysiology 102, 228-239.

Mehanna, R., Lai, E., 2013. Deep brain stimulation in Parkinson's disease. Translational Neurodegeneration 2, 22.

Meissner, W., Leblois, A., Hansel, D., Bioulac, B., Gross, C.E., Benazzouz, A., Boraud, T., 2005. Subthalamic high frequency stimulation resets subthalamic firing and reduces abnormal oscillations. Brain 128, 2372-2382.

Merchant, M.S., Woo, C.W., Mackall, C.L., Thiele, C.J., 2002. Potential Use of Imatinib in Ewing's Sarcoma: Evidence for In Vitro and In Vivo Activity. Journal of the National Cancer Institute 94, 1673-1679.

Merkler, D., Metz, G.A., Raineteau, O., Dietz, V., Schwab, M.E., Fouad, K., 2001. Locomotor recovery in spinal cord-injured rats treated with an antibody neutralizing the myelin-associated neurite growth inhibitor Nogo-A. J Neurosci. 21, 3665-3673.

Merzenich, M.M., Kaas, J.H., Wall, J., Nelson, R.J., Sur, M., Felleman, D., 1983. Topographic reorganization of somatosensory cortical areas 3b and 1 in adult monkeys following restricted deafferentation. Neuroscience 8, 33-55.

Merzenich, M.M., Nelson, R.J., Stryker, M.P., Cynader, M.S., Schoppmann, A., Zook, J.M., 1984. Somatosensory cortical map changes following digit amputation in adult monkeys. J Comp Neurol 224, 591-605.

Miller, W.C., DeLong, M.R., 1987. Altered Tonic Activity of Neurons in the Globus Pallidus and Subthalamic Nucleus in the Primate MPTP Model of Parkinsonism. In: Carpenter, M.B., Jayaraman, A. (Eds.), The Basal Ganglia II, vol 32. Springer US, pp. 415-427.

Mitchell, J.F., Leopold, D.A., 2015. The marmoset monkey as a model for visual neuroscience. Neuroscience Research 93, 20-46.

Moore, F.D., 1964. Give and take: The development of tissue transplantation. Saunders.

Mudry, A., Mills, M., 2013. The early history of the cochlear implant: A retrospective. JAMA Otolaryngology-Head & Neck Surgery 139, 446-453.

Mühl, A., Vuadens, P., 2011. Intérêt et coût de la réadaptation neurologique des patients cérébrolésés, [Interest and costs of neurorehabilitation of brain injury patients]. Revue médicale suisse 7, 948-951.

Murphy, K.L., Baxter, M.G., Flecknell, P.A., 2012. Anesthesia and Analgesia in Nonhuman Primates. In: Morris, C.R.A. (Ed.), Nonhuman Primates in Biomedical Research (Second Edition). Academic Press, Boston, pp. 403-435.

Nakajima, K., Maier, M.A., Kirkwood, P.A., Lemon, R.N., 2000. Striking differences in transmission of corticospinal excitation to upper limb motoneurons in two primate species. J Neurophysiol. 84, 698-709.

Napier, J., 1962. The evolution of the hand. Scientific American 207, 56-62.

Napier, J., 1993. Hands. Princeton University Press, Princeton, New Jersey.

Nicolelis, M.A., 2003. Brain-machine interfaces to restore motor function and probe neural circuits. Nat Rev Neurosci 4, 417-422.

Nicolelis, M.A.L., 2001. Actions from thoughts. Nature 409, 403-407.

Nordhausen, C.T., Rousche, P.J., Normann, R.A., 1994. Optimizing recording capabilities of the Utah Intracortical Electrode Array. Brain Research 637, 27-36.

Nudo, R.J., Milliken, G.W., Jenkins, W.M., Merzenich, M.M., 1996. Use-dependent alterations of movement representations in primary motor cortex of adult squirrel monkeys. J Neurosci 16, 785-807.

Nuffield Council on Bioethics, 2005. The ethics of research involving animals.

O'Doherty, J.E., Lebedev, M.A., Ifft, P.J., Zhuang, K.Z., Shokur, S., Bleuler, H., Nicolelis, M.A.L., 2011. Active tactile exploration using a brain-machine-brain interface. Nature 479, 228-231.

Odekerken, V.J.J., Boel, J.A., Geurtsen, G.J., Schmand, B.A., Dekker, I.P., de Haan, R.J., Schuurman, P.R., de Bie, R.M.A., The NSTAPS Study Group, 2015. Neuropsychological outcome after deep brain stimulation for Parkinson disease. Neurology 84, 1355-1361.

Odekerken, V.J.J., van Laar, T., Staal, M.J., Mosch, A., Hoffmann, C.F., Nijssen, P.C., Beute, G.N., van Vugt, J.P., Lenders, M.W.P.M., Contarino, M.F., Mink, M.S.J., Bour, L.J., van den Munckhof, P., Schmand, B.A., de Haan, R.J., Schuurman, P.R., de Bie, R.M.A., 2013. Subthalamic nucleus versus globus pallidus bilateral deep brain stimulation for advanced Parkinson's disease (NSTAPS study): a randomised controlled trial. The Lancet Neurology 12, 37-44.

Okun, M.S., Fernandez, H.H., Wu, S.S., Kirsch-Darrow, L., Bowers, D., Bova, F., Suelter, M., Jacobson, C.E., Wang, X., Gordon, C.W., Zeilman, P., Romrell, J., Martin, P., Ward, H., Rodriguez, R.L., Foote, K.D., 2009. Cognition and mood in Parkinson's disease in subthalamic nucleus versus globus pallidus interna deep brain stimulation: The COMPARE Trial. Annals of Neurology 65, 586-595.

Olsen, R.G., Lewis, M.G., Lafrado, L.J., Mathes, L.E., Haffer, K., Sharpee, R., 1987. Feline leukemia virus: current status of the feline induced immune depression and immunoprevention. Cancer Metast Rev 6, 243-260.

Öngür, D., Price, J.L., 2000. The Organization of Networks within the Orbital and Medial Prefrontal Cortex of Rats, Monkeys and Humans. Cerebral Cortex 10, 206-219.

Orban, G.A., Van Essen, D., Vanduffel, W., 2004. Comparative mapping of higher visual areas in monkeys and humans. Trends in Cognitive Sciences 8, 315-324.

Pakkenberg, B., Pelvig, D., Marner, L., Bundgaard, M.J., Gundersen, H.J., Nyengaard, J.R., Regeur, L., 2003. Aging and the human neocortex. Exp.Gerontol. 38, 95-99.

Pamies, D., Hartung, T., Hogberg, H.T., 2014. Biological and medical applications of a brain-on-a-chip. Experimental Biology and Medicine 239, 1096-1107.

Papadopoulos, C.M., Tsai, S.Y., Alsbiei, T., O'Brien, T.E., Schwab, M.E., Kartje, G.L., 2002. Functional recovery and neuroanatomical plasticity following middle cerebral artery occlusion and IN–1 antibody treatment in the adult rat. Annals of Neurology 51, 433-441.

Penfield, W., Boldrey, E., 1937. Somatic motor and sensory representation in the cerebral cortex of man as studied by electrical stimulation. Brain 60, 389-443.

Penfield, W., Jasper, H.H., 1954. Epilepsy and the Functional Anatomy of the Human Brain. Little, Brown.

Penfield, W., Rasmussen, T., 1950. The cerebral cortex of man; a clinical study of localization of function.

Pennisi, E., 2007. Boom time for monkey research. Science 316, 216-218.

Pernet, V., Joly, S., Christ, F., Dimou, L., Schwab, M.E., 2008. Nogo-A and myelin-associated glycoprotein differently regulate oligodendrocyte maturation and myelin formation. J Neurosci. 28, 7435-7444.

Petrinovic, M.M., Duncan, C.S., Bourikas, D., Weinman, O., Montani, L., Schroeter, A., Maerki, D., Sommer, L., Stoeckli, E.T., Schwab, M.E., 2010. Neuronal Nogo-A regulates neurite fasciculation, branching and extension in the developing nervous system. Development 137, 2539-2550.

Poewe, W., Antonini, A., Zijlmans, J.C., Burkhard, P.R., Vingerhoets, F., 2010. Levodopa in the treatment of Parkinson's disease: an old drug still going strong. Clinical interventions in aging 5, 229.

Puschmann, T.B., Zanden, C., De Pablo, Y., Kirchhoff, F., Pekna, M., Liu, J., Pekny, M., 2013. Bioactive 3D cell culture system minimizes cellular stress and maintains the in vivo-like morphological complexity of astroglial cells. Glia.

Quintero, G.C., 2013. Role of nucleus accumbens glutamatergic plasticity in drug addiction. Neuropsychiatr.Dis.Treat. 9, 1499-1512.

Raichle, M.E., Gusnard, D.A., 2002. Appraising the brain's energy budget. Proceedings of the National Academy of Sciences 99, 10237-10239.

Raineteau, O., Fouad, K., Bareyre, F.M., Schwab, M.E., 2002. Reorganization of descending motor tracts in the rat spinal cord. Eur.J Neurosci. 16, 1761-1771.

Raineteau, O., Z'Graggen, W.J., Thallmair, M., Schwab, M.E., 1999. Sprouting and regeneration after pyramidotomy and blockade of the myelin-associated neurite growth inhibitors NI 35/250 in adult rats. Eur.J Neurosci. 11, 1486-1490.

Ramdhani, R.A., Patel, A., Swope, D., Kopell, B.H., 2015. Early Use of 60 Hz Frequency Subthalamic Stimulation in Parkinson's Disease: A Case Series and Review. Neuromodulation: Technology at the Neural Interface.

Ramon y Cajal, S., 1928. Degeneration & regeneration of the nervous system, 1st ed. Oxford University Press, Humphrey Milford.

Recanzone, G.H., Merzenich, M.M., Jenkins, W.M., Grajski, K.A., Dinse, H.R., 1992. Topographic reorganization of the hand representation in cortical area 3b owl monkeys trained in a frequency-discrimination task. J.Neurophysiol. 67, 1031-1056.

Redmond, D.E.Jr., Bjugstad, K.B., Teng, Y.D., Ourednik, V., Ourednik, J., Wakeman, D.R., Parsons, X.H., Gonzalez, R., Blanchard, B.C., Kim, S.U., Gu, Z., Lipton, S.A., Markakis, E.A., Roth, R.H., Elsworth, J.D., Sladek, J.R.Jr., Sidman, R.L., Snyder, E.Y., 2007. Behavioral improvement in a primate Parkinson's model is associated with multiple homeostatic effects of human neural stem cells. Proc.Natl.Acad.Sci.USA 104, 12175-12180.

Redmond, D.E.Jr., McEntire, C.R.S., Kingsbery, J.P., Leranth, C., Elsworth, J.D., Bjugstad, K.B., Roth, R.H., Samulski, R.J., Sladek, J.R.Jr., 2013. Comparison of Fetal Mesencephalic Grafts, AAV-delivered GDNF, and Both Combined in an MPTP-induced Nonhuman Primate Parkinson's Model. Mol Ther 21, 2160-2168.

Reiner, A., Perera, M., Paullus, R., Medina, L., 1998. Immunohistochemical localization of DARPP32 in striatal projection neurons and striatal interneurons in pigeons. Journal of Chemical Neuroanatomy 16, 17-33.

Reinhart, R.M., Heitz, R.P., Purcell, B.A., Weigand, P.K., Schall, J.D., Woodman, G.F., 2012. Homologous mechanisms of visuospatial working memory maintenance in macaque and human: properties and sources. J Neurosci. 32, 7711-7722.

Rhesus Macaque Genome Sequencing and Analysis Consortium, Gibbs, R.A., Rogers, J., Katze, M.G., Bumgarner, R., Weinstock, G.M., Mardis, E.R., Remington, K.A., Strausberg, R.L., Venter, J.C., Wilson, R.K., Batzer, M.A., Bustamante, C.D., Eichler, E.E., Hahn, M.W., Hardison, R.C., Makova, K.D., Miller, W., Milosavljevic, A., Palermo, R.E., Siepel, A., Sikela, J.M., Attaway, T., Bell, S., Bernard, K.E., Buhay, C.J.,

Chandrabose, M.N., Dao, M., Davis, C., Delehaunty, K.D., Ding, Y., Dinh, H.H., Dugan-Rocha, S., Fulton, L.A., Gabisi, R.A., Garner, T.T., Godfrey, J., Hawes, A.C., Hernandez, J., Hines, S., Holder, M., Hume, J., Jhangiani, S.N., Joshi, V., Khan, Z.M., Kirkness, E.F., Cree, A., Fowler, R.G., Lee, S., Lewis, L.R., Li, Z., Liu, Y.s., Moore, S.M., Muzny, D., Nazareth, L.V., Ngo, D.N., Okwuonu, G.O., Pai, G., Parker, D., Paul, H.A., Pfannkoch, C., Pohl, C.S., Rogers, Y.H., Ruiz, S.J., Sabo, A., Santibanez, J., Schneider, B.W., Smith, S.M., Sodergren, E., Svatek, A.F., Utterback, T.R., Vattathil, S., Warren, W., White, C., Chinwalla, A.T., Feng, Y., Halpern, A.L., Hillier, L.W., Huang, X., Minx, P., Nelson, J.O., Pepin, K.H., Qin, X., Sutton, G.G., Venter, E., Walenz, B.P., Wallis, J.W., Worley, K.C., Yang, S.P., Jones, S.M., Marra, M.A., Rocchi, M., Schein, J.E., Baertsch, R., Clarke, L., Csürös, M., Glasscock, J., Harris, R.A., Havlak, P., Jackson, A.R., Jiang, H., Liu, Y., Messina, D.N., Shen, Y., Song, H.X.-Z., Wylie, T., Zhang, L., Birney, E., Han, K., Konkel, M.K., Lee, J., Smit, A.F.A., Ullmer, B., Wang, H., Xing, J., Burhans, R., Cheng, Z., Karro, J.E., Ma, J., Raney, B., She, X., Cox, M.J., Demuth, J.P., Dumas, L.J., Han, S.G., Hopkins, J., Karimpour-Fard, A., Kim, Y.H., Pollack, J.R., Vinar, T., Addo-Quaye, C., Degenhardt, J., Denby, A., Hubisz, M.J., Indap, A., Kosiol, C., Lahn, B.T., Lawson, H.A., Marklein, A., Nielsen, R., Vallender, E.J., Clark, A.G., Ferguson, B., Hernandez, R.D., Hirani, K., Kehrer-Sawatzki, H., Kolb, J., Patil, S., Pu, L.L., Ren, Y., Smith, D.G., Wheeler, D.A., Schenck, I., Ball, E.V., Chen, R., Cooper, D.N., Giardine, B., Hsu, F., Kent, W.J., Lesk, A., Nelson, D.L., O'Brien, W.E., Prüfer, K., Stenson, P.D., Wallace, J.C., Ke, H., Liu, X.M., Wang, P., Xiang, A.P., Yang, F., Barber, G.P., Haussler, D., Karolchik, D., Kern, A.D., Kuhn, R.M., Smith, K.E., Zwieg, A.S., 2007. Evolutionary and Biomedical Insights from the Rhesus Macaque Genome. Science 316, 222-234.

Rosenzweig, M.R., Leiman, A.L., 1968. Brain functions. Annu.Rev Psychol. 19, 55-98.

Rossignol, S., Schwab, M., Schwartz, M., Fehlings, M.G., 2007. Spinal cord injury: time to move? J Neurosci. 27, 11782-11792.

Rothlind, J.C., Cockshott, R.W., Starr, P.A., Marks, W.J., 2007. Neuropsychological performance following staged bilateral pallidal or subthalamic nucleus deep brain stimulation for Parkinson's disease. Journal of the International Neuropsychological Society 13, 68-79.

Rotschafer, S., Razak, K., 2013. Altered Auditory Processing in a Mouse Model of Fragile X Syndrome. Brain Res.

Ruprecht, R.M., O'Brien, L.G., Rossoni, L.D., Nusinoff-Lehrman, S., 1986. Suppression of mouse viraemia and retroviral disease by 3'-azido-3'-deoxythymidine. Nature 323, 467-469.

Sanes, J.N., Donoghue, J.P., 1993. Oscillations in local field potentials of the primate motor cortex during voluntary movement. Proc.Natl.Acad.Sci.USA 90, 4470-4474.

Sang, Y., Blecha, F., 2014. Alternatives to Antibiotics in Animal Agriculture: An Ecoimmunological View. Pathogens 4, 1-19.

Saunders, A.L., Williams, C.E., Heriot, W., Briggs, R., Yeoh, J., Nayagam, D.A.X., McCombe, M., Villalobos, J., Burns, O., Luu, C.D., Ayton, L.N., McPhedran, M., Opie, N.L., McGowan,

C., Shepherd, R.K., Guymer, R., Allen, P.J., 2014. Development of a surgical procedure for implantation of a prototype suprachoroidal retinal prosthesis. Clinical & Experimental Ophthalmology 42, 665-674.

Savio, T., Schwab, M.E., 1989. Rat CNS white matter, but not gray matter, is nonpermissive for neuronal cell adhesion and fiber outgrowth. J Neurosci. 9, 1126-1133.

Schieber, M.H., 2001. Constraints on somatotopic organization in the primary motor cortex. J Neurophysiol 86, 2125-2143.

Schmandke, A., Schmandke, A., Schwab, M.E., 2014. Nogo-A: Multiple Roles in CNS Development, Maintenance, and Disease. the neuroscientist 20, 372-386.

Schnell, L., Schwab, M.E., 1990. Axonal regeneration in the rat spinal cord produced by an antibody against myelin-associated neurite growth inhibitors. Nature 343, 269-272.

Schultz, W., Apicella, P., Ljungberg, T., 1993. Responses of monkey dopamine neurons to reward and conditioned stimuli during successive steps of learning a delayed response task. J Neurosci. 13, 900-913.

Schultz, W., Dayan, P., Montague, P.R., 1997. A neural substrate of prediction and reward. Science 275, 1593-1599.

Schuster, C.R., Thompson, T., 1969. Self administration of and behavioral dependence on drugs. Annu.Rev Pharmacol. 9, 483-502.

Schwab, M.E., 1996. Structural plasticity of the adult CNS. Negative control by neurite growth inhibitory signals. Int.J Dev.Neurosci. 14, 379-385.

Schwab, M.E., 1998. Regenerative Nerve Fiber Growth in the Adult Central Nervous System. News Physiol Sci. 13, 294-298.

Schwab, M.E., 2002. Repairing the injured spinal cord. Science 295, 1029-1031.

Schwab, M.E., 2004. Nogo and axon regeneration. Curr.Opin.Neurobiol. 14, 118-124.

Schwab, M.E., Bartholdi, D., 1996. Degeneration and regeneration of axons in the lesioned spinal cord. Physiol Rev. 76, 319-370.

Schwab, M.E., Caroni, P., 1988. Oligodendrocytes and CNS myelin are nonpermissive substrates for neurite growth and fibroblast spreading in vitro. J Neurosci. 8, 2381-2393.

Schwab, M.E., Schnell, L., 1991. Channeling of developing rat corticospinal tract axons by myelin-associated neurite growth inhibitors. J Neurosci. 11, 709-721.

Schwab, M.E., Thoenen, H., 1985. Dissociated neurons regenerate into sciatic but not optic nerve explants in culture irrespective of neurotrophic factors. The Journal of Neuroscience 5, 2415-2423.

Schwab, M.E., 2010. Functions of Nogo proteins and their receptors in the nervous system. Nat Rev Neurosci 11, 799-811.

Schwab, M.E., Buchli, A.D., 2012. Drug research: Plug the real brain drain. Nature 483, 267-268.

Schwab, M.E., Caroni, P., 2008. Reflections. Neuron 60, 404-405.

Schwab, M.E., Strittmatter, S.M., 2014. Nogo limits neural plasticity and recovery from injury. Current Opinion in Neurobiology 27, 53-60.

Schwegler, G., Schwab, M.E., Kapfhammer, J.P., 1995. Increased collateral sprouting of primary afferents in the myelin-free spinal cord. J Neurosci. 15, 2756-2767.

Serruya, M.D., Hatsopoulos, N.G., Paninski, L., Fellows, M.R., Donoghue, J.P., 2002. Brain-machine interface: Instant neural control of a movement signal. Nature 416, 141-142.

Seymour, A.B., Andrews, E.M., Tsai, S.Y., Markus, T.M., Bollnow, M.R., Brenneman, M.M., O'Brien, T.E., Castro, A.J., Schwab, M.E., Kartje, G.L., 2005. Delayed treatment with monoclonal antibody IN-1 1 week after stroke results in recovery of function and corticorubral plasticity in adult rats. J Cereb.Blood Flow Metab 25, 1366-1375.

Sigg, H., 2011. L'expérimentation animale en Suisse. BioFokus 84.

Solomon, S.G., Rosa, M.G.P., 2014. A simpler primate brain: the visual system of the marmoset monkey. Frontiers in Neural Circuits 8.

Sperry, R., 1982. Some effects of disconnecting the cerebral hemispheres. Science 217, 1223-1226.

Spieles-Engemann, A.L., Collier, T.J., Sortwell, C.E., 2010. A functionally relevant and long-term model of deep brain stimulation of the rat subthalamic nucleus: advantages and considerations. Eur.J Neurosci 32, 1092-1099.

Spillmann, A.A., Amberger, V.R., Schwab, M.E., 1997. High Molecular Weight Protein of Human Central Nervous System Myelin Inhibits Neurite Outgrowth: an Effect which can be Neutralized by the Monoclonal Antibody IN-1. European Journal of Neuroscience 9, 549-555.

Starr, A., Edwards, M.L., 1961. Mitral Replacement: Clinical Experience with a Ball-Valve Prosthesis. Annals of Surgery 154, 726-740.

Stingl, K., Bartz-Schmidt, K.U., Gekeler, F., Kusnyerik, A., Sachs, H., Zrenner, E., 2013. Functional Outcome in Subretinal Electronic Implants Depends on Foveal Eccentricity Subretinal Electronic Implants. Investigative Ophthalmology & Visual Science 54, 7658-7665.

Stone, I., 1971. The passions of the mind: a novel of Sigmund Freud. Doubleday & Company, Inc., New York.

Szkudelski, T., Szkudelska, K., 2015. Resveratrol and diabetes: from animal to human studies. Biochimica et Biophysica Acta (BBA) - Molecular Basis of Disease 1852, 1145-1154.

Tarsy, D., 2012. Treatment of parkinson disease: A 64-year-old man with motor complications of advanced parkinson disease. JAMA : the journal of the American Medical Association 307, 2305-2314.

Taylor, D.M., Tillery, S.I.H., Schwartz, A.B., 2002. Direct Cortical Control of 3D Neuroprosthetic Devices. Science 296, 1829-1832.

Thallmair, M., Metz, G.A.S., Z'Graggen, W.J., Raineteau, O., Kartje, G.L., Schwab, M.E., 1998. Neurite growth inhibitors restrict plasticity and functional recovery following corticospinal tract lesions. Nature neuroscience 1, 124-131.

Thompson, L.H., Parish, C.L., 2013. Transplantation of fetal midbrain dopamine progenitors into a rodent model of Parkinson's disease. Methods Mol.Biol. 1059, 169-180.

Torres, L.B., Silva Araujo, B.H., Gomes de Castro, P.H., Romero, C.F., Sarges, M.K., Silva, A.M., Gomes da, S.S., Muniz, J.A., Cavalheiro, E.A., 2010. The use of new world primates for biomedical research: an overview of the last four decades. Am.J Primatol. 72, 1055-1061.

Tsai, S.Y., Papadopoulos, C.M., Schwab, M.E., Kartje, G.L., 2011. Delayed anti-Nogo-A therapy improves function after chronic stroke in adult rats. Stroke 42, 186-190.

Tsai, S.Y., Markus, T.M., Andrews, E.M., Cheatwood, J.L., Emerick, A.J., Mir, A., Schwab, M.E., Kartje, G.L., 2007. Intrathecal treatment with anti-Nogo-A antibody improves functional recovery in adult rats after stroke. Exp Brain Res 182, 261-266.

Turnbull, P.C.B., Tindall, B.W., Coetzee, J.D., Conradie, C.M., Bull, R.L., Lindeque, P.M., Huebschle, O.J.B., 2004. Vaccine-induced protection against anthrax in cheetah (*Acinonyx jubatus*) and black rhinoceros (*Diceros bicornis*). Vaccine 22, 3340-3347.

Vanek, P., Thallmair, M., Schwab, M.E., Kapfhammer, J.P., 1998. Increased lesion-induced sprouting of corticospinal fibres in the myelin-free rat spinal cord. Eur.J Neurosci. 10, 45-56.

Vargas-Irwin, C.E., Shakhnarovich, G., Yadollahpour, P., Mislow, J.M.K., Black, M.J., Donoghue, J.P., 2010. Decoding Complete Reach and Grasp Actions from Local Primary Motor Cortex Populations. The Journal of Neuroscience 30, 9659-9669.

Velliste, M., Perel, S., Spalding, M.C., Whitford, A.S., Schwartz, A.B., 2008. Cortical control of a prosthetic arm for self-feeding. Nature 453, 1098-1101.

von Meyenburg, J., Brösamle, C., Metz, G.A., Schwab, M.E., 1998. Regeneration and sprouting of chronically injured corticospinal tract fibers in adult rats promoted by NT-3 and the mAb IN-1, which neutralizes myelin-associated neurite growth inhibitors. Exp.Neurol. 154, 583-594.

Wadsworth, A., Quigley, J.J., Sickles, G.R., 1932. The purification and concentration of diphtheria toxoid. The Journal of Experimental Medicine 55, 815-828.

Wager, T.D., Yarkoni, T., 2012. Establishing homology between monkey and human brains. Nat.Methods 9, 237-239.

Wahl, A.S., Omlor, W., Rubio, J.C., Chen, J.L., Zheng, H., Schröter, A., Gullo, M., Weinmann, O., Kobayashi, K., Helmchen, F., Ommer, B., Schwab, M.E., 2014. Asynchronous therapy restores motor control by rewiring of the rat corticospinal tract after stroke. Science 344, 1250-1255.

Wahl, A.S., Schwab, M.E., 2014. Finding an optimal rehabilitation paradigm after stroke: Enhancing fiber growth and training of the brain at the right moment. Frontiers in Human Neuroscience 8.

Wakeman, D.R., Redmond, D.E.Jr., Dodiya, H.B., Sladek, J.R.Jr., Leranth, C., Teng, Y.D., Samulski, R.J., Snyder, E.Y., 2014a. Human Neural Stem Cells Survive Long Term in the Midbrain of Dopamine-Depleted Monkeys After GDNF Overexpression and Project Neurites Toward an Appropriate Target. Stem Cells Transl Med.

Wakeman, D.R., Dodiya, H.B., Kordower, J.H., 2011. Cell Transplantation and Gene Therapy in Parkinson's Disease. Mount Sinai Journal of Medicine: A Journal of Translational and Personalized Medicine 78, 126-158.

Wakeman, D.R., Weiss, S., Sladek, J.R., Elsworth, J.D., Bauereis, B., Leranth, C., Hurley, P.J., Roth, R.H., Redmond, D.E.Jr., 2014b. Survival and Integration of Neurons Derived From Human Embryonic Stem Cells in MPTP-Lesioned Primates. Cell transplantation 23, 981-994.

Wall, J.T., Kaas, J.H., Sur, M., Nelson, R.J., Felleman, D.J., Merzenich, M.M., 1986. Functional reorganization in somatosensory cortical areas 3b and 1 of adult monkeys after median nerve repair: possible relationships to sensory recovery in humans. J Neurosci. 6, 218-233.

Wang, W., Collinger, J.L., Degenhart, A.D., Tyler-Kabara, E.C., Schwartz, A.B., Moran, D.W., Weber, D.J., Wodlinger, B., Vinjamuri, R.K., Ashmore, R.C., Kelly, J.W., Boninger, M.L., 2013. An Electrocorticographic Brain Interface in an Individual with Tetraplegia. PLoS One 8, e55344.

Weatherall, D., Goodfellow, P., Harris, J., Hinde, R., Johnson, L., Morris, R., Ross, N., Skehel, J., Tickell, C., 2006. The use of non-human primates in research. Academy of Medical Sciences, Medical Research Council, The Royal Society and Wellcome Trust, London, United Kingdom.

Weaver, F.M., Follett, K., Stern, M., Hur, K., Harris, C., Marks, W.J., Rothlind, J., Sagher, O., Reda, D., Moy, C.S., Pahwa, R., Burchiel, K., Hogarth, P., Lai, E.C., Duda, J.E., Holloway, K., Samii, A., Horn, S., Bronstein, J., Stoner, G., Heemskerk, J., Huang, G.D., for the CSP, 2009. Bilateral Deep Brain Stimulation vs Best Medical Therapy for Patients With

Advanced Parkinson Disease: A Randomized Controlled Trial. JAMA : the journal of the American Medical Association 301, 63.

Weaver, F.M., Follett, K.A., Stern, M., Luo, P., Harris, C.L., Hur, K., Marks, W.J., Rothlind, J., Sagher, O., Moy, C., Pahwa, R., Burchiel, K., Hogarth, P., Lai, E.C., Duda, J.E., Holloway, K., Samii, A., Horn, S., Bronstein, J.M., Stoner, G., Starr, P.A., Simpson, R., Baltuch, G., De Salles, A., Huang, G.D., Reda, D.J., 2012. Randomized trial of deep brain stimulation for Parkinson disease: Thirty-six-month outcomes. Neurology 79, 55-65.

Wessberg, J., Stambaugh, C.R., Kralik, J.D., Beck, P.D., Laubach, M., Chapin, J.K., Kim, J., Biggs, S.J., Srinivasan, M.A., Nicolelis, M.A.L., 2000. Real-time prediction of hand trajectory by ensembles of cortical neurons in primates. Nature 408, 361-365.

White, R., 2012. The Early History of Antibiotic Discovery: Empiricism Ruled. In: Dougherty, T.J., Pucci, M.J. (Eds.), Antibiotic Discovery and Development. Springer US, pp. 3-31.

Wichmann, T., Baron, M., DeLong, M.R., 1994. Local Inactivation of the Sensorimotor Territories of the Internal Segment of the Globus Pallidus and the Subthalamic Nucleus Alleviates Parkinsonian Motor Signs in MPTP Treated Monkeys. In: Percheron, G., McKenzie, J.S., Féger, J. (Eds.), The Basal Ganglia IV, vol 41. Springer US, pp. 357-363.

Wodlinger, B., Downey, J.E., Tyler-Kabara, E.C., Schwartz, A.B., Boninger, M.L., Collinger, J.L., 2015. Ten-dimensional anthropomorphic arm control in a human brain–machine interface: difficulties, solutions, and limitations. Journal of Neural Engineering 12, 016011.

Wolpaw, J.R., McFarland, D.J., Neat, G.W., Forneris, C.A., 1991. An EEG-based brain-computer interface for cursor control. Electroencephalography and Clinical Neurophysiology 78, 252-259.

Wolters, E.C.M.J., de Munter, H., Steinbusch, H., 2014. Parkinson's Disease. In: Wolters, E.C.M.J., Baumann, C. (Eds.), Parkinson Disease and Other Movement Disorders: Motor Behavioural Disorders and Behavioural Motor Disorders. International Association of Parkinsonism and Related Disorders & VU University Press, Amsterdam, pp. 149-162.

Woolsey, C.N., Settlage, P.H., Meyer, D.R., Spencer, W., Pinto Hamuy, T., Travis, A.M., 1952. Patterns of localization in precentral and "supplementary" motor areas and their relation to the concept of a premotor area. Res.Publ.Assoc.Res.Nerv.Ment.Dis. 30, 238-264.

Wyss, A.F., Hamadjida, A., Savidan, J., Liu, Y., Bashir, S., Mir, A., Schwab, M.E., Rouiller, E.M., Belhaj-Saïf, A., 2013. Long-term motor cortical map changes following unilateral lesion of the hand representation in the motor cortex in macaque monkeys showing functional recovery of hand functions. Restor.Neurol Neurosci. 31, 733-760.

Zak, O., O'Reilly, T., 1991. Animal models in the evaluation of antimicrobial agents. Antimicrobial Agents and Chemotherapy 35, 1527-1531.

Zemmar, A., Weinmann, O., Kellner, Y., Yu, X., Vicente, R., Gullo, M., Kasper, H., Lussi, K., Ristic, Z., Luft, A.R., Rioult-Pedotti, M., Zuo, Y., Zagrebelsky, M., Schwab, M.E., 2014. Neutralization of Nogo-A enhances synaptic plasticity in the rodent motor cortex and improves motor learning in vivo. J Neurosci. 34, 8685-8698.

Zorner, B., Schwab, M.E., 2010. Anti-Nogo on the go: from animal models to a clinical trial. Ann N.Y.Acad.Sci. 1198 Suppl 1, E22-E34.

Supplementary Figures

Supplementary Figure 1 (below and next page): Total number of animals used for different purposes, among them research, in Great Britain (from Nuffield Council on Bioethics, 2005).

Examples of the numbers of animals used for different purposes by humans

Use	Numbers used
Animal research (see Appendix 2)	UK (2003): 2.79 million[1]
Food[2]	UK (2003): Total 900 million – 1 billion Including:
Poultry	UK (2003): 871 million broiler chickens (for meat) 27 million hens for egg production
Cattle	UK (2003): 10.4 million
Sheep	UK (2003): 33.6 million
Pigs	UK (2003): 4.6 million
Fish	UK (2003): 631,400 tonnes[3]
Working animals	
Guide Dogs	UK (2004): 5,000[4]
Police Dogs	England and Wales (2003): 2,500[5]
Clothing	
Wool	UK (2002/03): 24.9 million sheep[6]
Fur	Fur farming is now prohibited in the UK[7]
Leisure/ Education	
Wildlife observation	not available
Companion animals/Pets	UK (1995): More than half of all households have a pet – 7.2 million cats,[8] 6.5 million dogs, 1.2 million rabbits, 135 million ornamental fish[9]
Zoo	UK (2003): 160 registered zoos[10]
Circus	UK (1997): 21 circuses with animal acts, 545 wild and exotic animals[11]
Hunting/shooting	UK (1999): 178 fox hunts, 3 deer hunts, 83 hare hunts and 20 mink hunts per year[12], approximately 4,000 hounds a year put down[13]
Sport	
Horse racing	UK (2005): 14,000 horses in training[14]
Greyhound racing	UK (2005): 10,000 new greyhounds registered with the National Greyhound Racing Club each year[15]
Pest control	[UK (2002): 1,300 pest-control companies – mice, rats, wasps, bees [16]]

1 Home Office (2004) *Statistics of Scientific Procedures on Living Animals Great Britain 2003* (Norwich: HMSO).

2 DEFRA (2003) *Statistics in Animal Health & Welfare Strategy for GB: The Evidence Base*, available at: http://www.scotland.gov.uk/library5/environment/ahwseb.pdf. Accessed on: 3 May 2005; see also RSPCA (2005) *Farm Animals*, available at: http://www.rspca.org.uk/servlet/Satellite?pagename=RSPCA/Publications/FarmAnimalsPublications&articleid=0. Accessed on: 3 May 2005.

3 DEFRA (2004) *United Kingdom Sea Fisheries Statistics* 2003, available at: http://statistics.defra.gov.uk/esg/publications/fishstat/uksfs03.pdf. Accessed on: 3 May 2005.

4 Royal National Institute of the Blind (2005) *Facts and Myths about people with sight problems*, available at: http://www.rnib.org.uk/xpedio/groups/public/documents/PublicWebsite/public_empfacts.hcsp. Accessed on: 4 May 2005.

5 BBC (2003) *Crime Fighters: Policing – Police Dog Unit*, available at: http://www.bbc.co.uk/crime/fighters/policedogunit.shtml. Accessed on: 4 May 2005.

6 The British Wool Marketing Board (2004) *Wool statistics*, available at: http://www.britishwool.org.uk/a-factsheet4.asp. Accessed on: 4 May 2005.

7 Under the Fur Farming (Prohibition) Act (2000) mink farming was banned in the UK from the beginning of 2003. British Fur Trade Association: see British Fur Trade Association (2004) available at: http://www.britishfur.co.uk. Accessed on: 3 May 2005.

8 A survey estimated that domestic cats kill 300 million wild animals annually, see The Mammal Society (1998) *Look what the cat's brought in!*, available at http://www.mammal.org.uk/catkills.htm. Accessed on: 3 May 2005; A four-year cat predation study done at the University of Wisconsin estimated that rural free-roaming cats kill at least 7.8 million and perhaps as many as 217 million birds a year in Wisconsin. See Coleman JS and SA Temple (1995) How many birds do cats kill? *Wildlife Control Technology* **44**.

9 Animal Aid, available at http://www.animalaid.org.uk/youth/topics/sport/intro.htm. Accessed on: 3 May 2005.

10 Zoos UK (2003), available at: http://www.zoos.50megs.com. Accessed on: 3 May 2005.

11 BBC News (1998) *Protect Circus animals call*, available at: http://news.bbc.co.uk/1/hi/uk_politics/201483.stm. Accessed on: 3 May 2005.

12 Burns Committee report on hunting with dogs (submitted to Secretary of State for the Home Department in 2000).

13 Burns Committee report on hunting with dogs (submitted to Secretary of State for the Home Department in 2000).

14 The Jockey Club (2005) *Key facts*, available at: http://www.thejockeyclub.co.uk/about/aboutframeset.html. Accessed on: 4 May 2005.

15 National Greyhound Racing Club (2005) *Frequently asked questions*, available at: http://www.ngrc.org.uk/default.asp?articletype=Fact%20Sheets. Accessed on: 4 May 2005.

16 Office of Fair Trading (2002) Review of undertakings given by Rentokill Initial plc: A consultation paper, available at: http://www.oft.gov.uk/NR/rdonlyres/A4D14148-39FB-42F7-8C11-AE3CE796DE85/0/oft392.pdf. Accessed on: 3 May 2005.

Supplementary Figure 2: Licensing process to perform animal experimentation (example from the Canton of Zürich). To perform an animal experiment, an application for license has to be submitted, containing an extensive description of the experimental aims, of the methodologies to be used and of the balancing of interests (i.e. constraints for the animal versus anticipated benefits in the form of acquired knowledge for human) to demonstrate the indispensability of the experiment. For experiments inducing contraints for the animals, a long procedure of application review by the Cantonal Commission for Animal Experiments takes place, resulting in Cantonal Commission recommendations. If the application is in accordance with current legislation and ethical standards, the license for the experiment is approved. The Federal Veterinary Office supervises the process and can oppose the Cantonal Commission decision (from Sigg, 2011 and http://www.tierschutz.uzh.ch/bewilligungen/tierversuche_en.html#2).

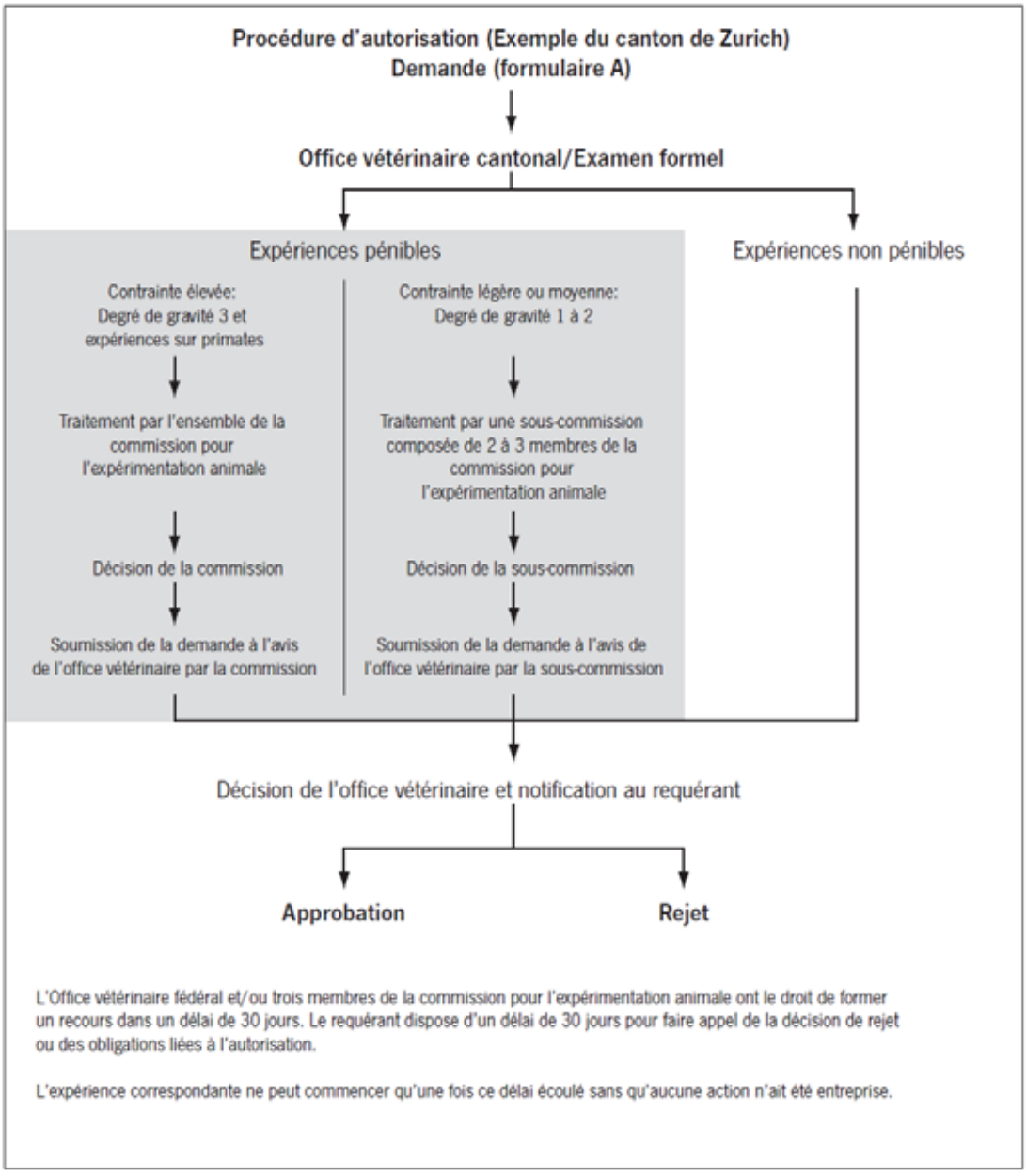

GENERAL DISCUSSION

Summary of the main results

At the end of the present thesis, it is time to sum up our main results. The first cornerstone of our work is the description of a methodological approach allowing to investigate brain activity in anaesthetised macaque monkeys by using whole-scalp EEG recording of SSEPs. We achieved the development of non-invasive EEG recordings with intra- and inter-individual reproducible signals. To this aim, we based on state-of-the-art electrical neuroimaging tools already established in human (Michel et al., 2001; Michel et al., 2004) and in rodents (Mégevand et al., 2008). The main advantages of an EEG approach over other brain imaging techniques are its submillisecond temporal resolution, its non-invasiveness, its sampling from the whole scalp and not from a restricted zone, its user-friendly nature, and not insignificantly its low cost. Furthermore, contrary to brain imaging tools such as fMRI or PET, EEG offers a direct, real-time monitoring of neuronal activity at the scalp, not a correlate of it, by non-invasively directly detecting the electrical activity of the neurons within the brain. Obviously, our goal was not to replace these already well-established brain imaging tools but rather to provide an additional and complementary approach to decipher the spatiotemporal dynamics of brain activity in non-human primates.

Based on this first achievement, we demonstrated then that a craniotomy performed in the context of a cortical lesion did not induce major distortions in the EEG signal measured at the scalp. This represented a prerequisite towards validating our EEG methodology for long-term investigations of large-scale neuronal networks in macaque monkeys and their reorganisation after lesions requiring a craniotomy. From then on, we were able to confidently use this EEG technique to investigate the effects of a cortical lesion on brain activity and the mechanisms involved in subsequent cortical reorganisation.

Our second key result was obtained by regularly performing EEG measurements of SSEPs in response to electrical stimulation to the median nerve, before and after a lesion located predominantly in the motor cortex, in one monkey, in order to test the integrity of the somatosensory processing. Until now, most studies in the laboratory have focused on the post-lesion reorganisation taking place in the motor system itself, after an M1 lesion (Hamadjida et al., 2012; Liu and Rouiller, 1999; Rouiller et al., 1998; Rouiller and Olivier, 2004; Wyss et al., 2013). Conversely, relatively little attention has been given to the reorganisation of the somatosensory system after an M1 lesion. Essentially, we

found here that the lesion induced extensive alterations in somatosensory processing as well, confirming that M1 is important for somatosensory processing. More specifically, experiments revealed that plastic modifications of neural circuits were not restricted to the sensorimotor cortical level, but surprisingly affected the subcortical level as well. Thus we provided additional information about the post-lesion compensatory mechanisms of subcortical structures interacting with the cortex, pointing to another facet of **lesion-induced plasticity**.

Our third important result was obtained by implementing EEG recording of SSEPs elicited by a more naturalistic, tactile stimulation to the fingertips, in order to overcome some major drawbacks inherent to peripheral electrical stimulations, which are actually very artificial and experimental. Indeed, we cannot infer detail about the processing of every day encountered sensory inputs based on the processing of artificial stimuli. Basically, we observed that a dominant M1 lesion induced drastic alterations in tactile sensory processing from the fingertips, especially from the thumb tip, although the lesion affected the entire hand representation in M1, and these cortical modifications were associated with differential alterations and recovery of the use of the different fingers in a precision grip task. By focusing more deeply on behaviour, in particular by using a task performed without visual control, we were able to confirm that a dominant motor cortex lesion induced somatosensory-related behavioural deficits in other monkeys as well.

In sum, by studying brain activity and behaviour on monkeys subjected to a dominant motor cortex lesion, we confirmed that **lesion-induced plasticity** developed within the somatosensory system representations over the post-lesion recovery period in adult macaque monkeys in the sense that sustained changes in motor output and sensorimotor connectivity induced by a motor cortex lesion were sufficient to deeply reorganise the somatosensory processing, in addition to the control of fine manual dexterity itself. Last but not least, our results further demonstrated that the motor cortex is definitely not a purely motor structure but, on the contrary, M1 is also important for somatosensory processing in primates (see below for further detail).

Our fourth main finding arose from studying in detail the effects of a repeated peripheral stimulation on somatosensory processing in intact monkeys. Such an investigation is an important concern for all EEG studies dealing with repeated stimulations. By using a 1-Hz stimulation repetition rate, which is actually low as compared to many other studies

using repeated stimulations, we were able to observe that cortical adaptation is not limited to the well-known reduction in amplitude of cortical activity over time, but surprisingly we demonstrated here that the latency of EEG signal was adapting over time, specifically after a repeated tactile stimulation to each of the fingertips. Simply put, a slowly repeated sensory input could rapidly impact on the timing of tactile sensory processing in the brain. We may therefore have stressed a unique and specific "cortical signature" of fingertip tactile stimulations that may enable the brain to prioritise novel stimuli by delaying the sensory processing of repeated and thus meaningless inputs. This study opened thus a new window on **rapid plastic modifications** operating at the somatosensory cortical level. Our results clearly demonstrated that latency adaptation is a significant process that should be carefully considered in case of repeated tactile stimulation, even at a low stimulus repetition rate. It is indeed of prime importance to fully understand the characteristics of the EPs being investigated and the potential distractions that may affect them, in order to further use these signals and correctly interpret them.

Last but not least, we obtained fresh and significant insights into **use-dependent plasticity** by moving from EEG investigations on macaque monkeys to EEG investigations on human. While most studies on use-dependent plasticity have usually focused on expert people so far, implying consequently the intense practice of a particular skill, we decided to investigate how this phenomenon operates in daily, unconstrained conditions. More specifically, we examined the plasticity of the sensorimotor cortex in relation to the use of touchscreen smartphones by taking advantage of the own technology of these devises to store built-in battery logs, providing a direct measure of our activity on them. In this way, we were able to demonstrate that the repetitive interactions on a smooth touchscreen led to deep reshaping of tactile sensory processing from the fingers. Remarkably, we demonstrated that use-dependent plasticity can operate very rapidly by daily updating cortical representations (here the thumb more specifically), depending on the use of the corresponding body part. In a second study, we investigated in greater detail how the statistics of the behavioural episodes experienced on the touchscreen are imprinted through the different stages of sensory processing in the cerebral cortex. In short, we observed that different temporal aspects of touchscreen experiences and related hand actions are strongly imprinted at distinct stages of tactile sensory processing in the brain experiencing new technologies throughout the daily live. Thus, our studies

on smartphone users complement the wealth of observations about use-dependent plasticity already performed on extremely skilled people such as Braille readers, professional musicians or athletes, for instance, by showing that the normal daily use of personal digital technology was able to continuously update the cortical sensory processing in our brain and thus that use-dependent plasticity does operate in ordinary, unconstrained conditions as well. In other words, past sensory experiences of daily life significantly shape the adult cerebral cortex as well. Equally important, our results suggest that touchscreen smartphone users may represent an interesting, easily accessible population for further investigations on how daily experiences shape cortical sensory processing in adults. Indeed, considerable work remains to be done to fully understand the mechanisms of use-dependent plasticity in these subjects, particularly in terms of the impacts of these plastic modifications on behaviour, i.e. is such cortical plasticity adaptive or maladaptive? This question is highly relevant if we consider the increasing popular use of touchscreen devices, especially in young children. Nevertheless we cannot answer it based on the present data. More knowledge about this meaningful topic could be obtained by extending our investigations to subjects that became pathologically dependent on their smartphone, for instance. Furthermore, it would be interesting as well to measure EEG over the long term on very new adult smartphone users to resolve the neural correlate of the acquisition of a new dexterous behaviour in adults, in particular about the time course for plastic changes to develop and then stabilise, and to investigate whether the acquisition of such a new practice in adults requires different mechanism from the maintenance of an already acquired behaviour observed in regular smartphone users. Another line of research would be to include older smartphone users as well because they seem to rely on different finger behaviour to interact on the touchscreen as compared to the young population investigated here (i.e. median age: 22.9 years old). Consequently, is their EEG cortical signature different from the one described here?

Potential limitations of our studies and perspectives

Due to unexpected events with two other monkeys, the lesion study presented here (i.e. post-lesion EEG mapping of SSEPs after electrical stimulation to the median nerve in **Chapter 2** and after tactile stimulations to the fingertips in **Chapter 3**) was based on a

single monkey and we acknowledge that we did not succeed in inducing a pure M1 lesion. As a consequence, our results should be considered as a case report and still need to be verified by reproducing the same experiments on additional animals. Thus, it is difficult to propose any direct implications of our results but we have rather opened up the way for further investigations by describing some interesting observations. In other words, we should not consider the present studies as being some purely fundamental research but they are rather located in a continuum between fundamental research and applied research.

The very specific post-lesion EEG signature to each stimulus type needs to be confirmed in a larger sample of animals, at least with two other monkeys subjected to a lesion of the hand representation in M1. In case our results are verified on other animals, the present data may become much more relevant. Indeed, this means that we would have highlighted a conserved complex reorganisation process taking place both at subcortical and cortical levels in the primate sensorimotor cortex after a focal M1 lesion. In such a case, the precise nature of the subcortical potential and the mechanisms leading to this alterations would need to be refined, for instance by using non-invasive simultaneous EEG-fMRI recordings, or invasive investigations such as simultaneous recordings of intracorical brain activity with scalp EEG (see below for greater detail).

Nevertheless, our results are already interesting because further investigations on other monkeys will be inevitably associated with inter-individual variability in lesion location and size. Consequently, we think that comparing the brain activity before and after the lesion in the same animal remains the best control. Such inter-individual variability in lesion location and size should nevertheless not be considered as a real drawback because it actually mimics the large inter-individual variability in brain damages observed in the clinics as well, such as among stroke patients.

Even though our investigations were mostly focused on one animal, we tried to document at best the effects of a cortical lesion on somatosensory processing by investigating different facets of somatosensory processing in this animal, in order to fulfil the *reduce* principle advocated by the 3R. Thus we introduced the naturalistic, tactile stimulation to the fingertips as a complement to the already well established but artificial electrical stimulation to the median nerve at the wrist. In this way, we were able to get additional insight into lesion-induced plasticity taking place in the somatosensory processing by

demonstrating, for instance, that the processing from the thumb was much more sensitive to the lesion than the processing from the index and middle fingers.

A very relevant improvement to EEG measurements of SSEPs on monkeys would be to add several bipolar recording electrodes along the stimulated afferent pathway, especially over the median nerve at the wrist and at the Erb's point, to follow in greater detail the afferent volleys from the stimulation site to the cortex. Thus we may better understand the mechanisms of somatosensory processing taking place already at the periphery and more specifically about the adaptation to repeated peripheral stimulations. Briefly, in case the SSEPs recorded at the wrist level would already exhibit some features of adaptation, one could infer some early contribution of peripheral structures in the adaptation recorded at the scalp.

The EEG investigations described here were performed on anaesthetised monkeys for several reasons: first, the preparation of the monkeys in terms of EEG cap installation would have been obviously less convenient and more time-consuming to achieve the same very low electrode impedances on awake and moving monkeys as we succeeded in anaesthetised monkeys, especially as the minimisation of electrode impedance may be a disagreeable step for the animals. Second, EEG recordings under general anaesthesia ensured highly controlled conditions (e.g. decreased muscular and movement artifacts, as well as reduced cardiovascular and autonomic responses such as increase in heart rate and blood pressure that typically result from the exposure to unanticipated non-noxious stimuli in conscious subjects), allowing to increase the sensitivity to detect at the scalp small changes in brain signals between different conditions. Third, regarding the finger tactile stimulation protocol in particular, we were interested to obtain purely passive tactile stimulation in our macaque monkeys. Due to the low signal-to-noise ratio of such tactile SSEPs, this stimulation paradigm requires a high number of stimulations to be averaged (Krarup and Trojaborg, 1994; Starr et al., 1982; York, 1985) and recordings should be insulated from movements and muscular artifacts as much as possible in order to obtain a reliable signal at the scalp. Additionally, the monkey's hand needs to be fully inactive to be purely passively touched. These requirements could be suited with ease by performing EEG recordings on monkeys under anaesthesia. We acknowledge that the requirement for anaesthesia and the use of passive stimulations are far from natural conditions and therefore somewhat limits the relevance of the EEG signal ob-

tained here as an approach to document the natural sensorimotor integration from the hand in monkeys, even though this was actually not the aim of this thesis.

A major improvement would be to transpose our EEG methodological approach on awake monkeys to investigate whether the complex somatosensory processing of peripheral electrical and tactile stimuli before and after the lesion is achieved similarly under more natural conditions. It would nevertheless imply to solve some technical issues, such as restraining the monkey's head and immobilising the stimulated limb. Moreover, powerful artifact rejections methods should be used and naturally quiet animals should be favoured in such experiments in order to minimise muscular artifacts. The animal should be for instance regularly provided with liquid rewards in order to maintain it cooperative while avoiding massive muscular artifacts from the jaw. A trade-off should be found between the optimal duration of the recording leading to enough data on the one hand, and the time extent during which the animal stays cooperative, on the other hand. Actually, EEG recordings from the scalp in awake monkeys were already reported (Gilda-Costa et al., 2013) and promising EEG acquisitions of audio-visual EPs on awake macaque monkeys are currently under development in our laboratory and may provide a first step towards the development of EEG recording of SSEPs in awake monkeys.

The next and actually ultimate step towards understanding the impact of a cortical lesion on the real sensorimotor integration of somatosensory stimuli under natural conditions could be achieved by chronically implanting multielectrode arrays (Nicolelis et al., 2003) over the sensorimotor cortex on monkeys to record brain activity in freely moving animals. Such outstanding technology is under development from several years in the context of brain-machine interfaces (for reminder, see the section *Neuroprosthetics* in **Chapter 8**). Very promising results have been reported recently using wireless electrode implants in macaque monkeys, allowing to record large-scale brain activity from up to 1800 neurons, simultaneously with the extracellular activity of about 500 cortical neurons, for 5 years (Schwarz et al., 2014).

Regarding behavioural investigations, a key message of the present thesis is the relevance to test manual dexterity successively with visual feedback and without visual feedback to exhaustively document the sensorimotor deficits resulting from of a motor cortex lesion and thus to avoid underestimating them. More specifically, a better understanding of the link between cortical reorganisation assessed by EEG and functional re-

covery may be obtained by systematically using such tasks in monkeys involved in a motor system lesion protocol.

Plasticity as the driving force of brain activity

Taken all these results together, EEG measurements provided a unique window into the brain to investigate one of its most fascinating properties and at the same time one of the most significant in terms of repercussions, namely brain plasticity, the first main theme of the present thesis. By highlighting 3 distinct forms of brain plastic modifications in adult primates, i.e. lesion-induced plasticity, rapid cortical plastic modifications in response to repeated stimulations, and use-dependent plasticity, we realise even more how much the brain activity cannot be dissociated from the concept of brain plasticity, as already proposed since the first outstanding observations by Merzenich in 1983 (Kaas et al., 1983; Merzenich et al., 1983a; Merzenich et al., 1983b). In other words, brain plasticity is a driving force of brain activity.

EEG as an imaging tool

The second main theme of the present thesis was EEG.

The brain is a large *terra incognita*. Until recently, investigations about the brain functioning were limited due to the lack of appropriate technology to investigate this organ. The localisation of some brain functions was then based on clinical observations of some patients with specific deficits and the subsequent *post mortem* analysis of their brain (such as the famous observations on Phineas Gage or those on Broca's aphasic patients). Remember **Figure 1** in the **Chapter General Introduction**, showing that in 1988, there were still large fields of Neuroscience that were under-investigated simply because no available method existed at that time. But the recent huge development of brain imaging technologies led to impressive progresses in deciphering the brain activity at the macroscopic scale and even in the electrophysiology of individual neurons. We are now able to really view the brain in action using fMRI or PET, for instance. Nevertheless, we still do not fully understand some mechanisms underlying the perception of stimulus or the production of behaviour because they rely on the real-time interactions of large popula-

tions of neurons from different locations within the brain. Such submillisecond processes escape the low temporal resolution of fMRI, for example. Conversely, they can be resolved by the outstanding temporal resolution of EEG, one of the most commonly used tools for investigating brain activity, at least in human, for both clinical applications and neurophysiological research. Here in particular, we demonstrated how powerful EEG is in unravelling some submillisecond processes such as the adaptation patterns resulting from the repetition of a large number of stimulations. Actually, the strength of EEG resides in its huge temporal resolution.

On the other hand, the complex nature of the EEG signal (Buzsáki et al., 2012) is far from full understanding and still constitutes a major limitation in the interpretation of scalp EEG signals. For instance, we still do not know exactly how the spatiotemporal organisation of individual neuronal populations in the cortex contributes to the EEG signal at the scalp, and the volume-conduction of EEG signal towards the scalp remains elusive. The precise configuration of neural generators within the brain cannot be simply resolved based on EEG signal measured at the scalp because the inverse solution problem is far more complex. It is especially true for monkeys where no routine protocol already existed, as it is the case in human EEG. In **Chapter 1**, we presented preliminary steps of inverse solution applied to median nerve SSEPs, and obviously this electrical neuroimaging approach will need additional improvements in order to use it in monkeys as efficiently as it is currently used in human.

Moreover, as a consequence of the volume-conduction properties of the brain, the electrical activity from the neuronal populations is blurred on its way towards the scalp and thus the spatial resolution of EEG is reduced as compared to fMRI, for instance. This problem is partially overcome by using a high density of electrodes at the scalp, as presented in our thesis.

We identified at least three other possible ways to substantially improve the interpretability of EEG signal, first in monkeys and then potentially translated to human. First, a significant and promising advance in brain imaging has been performed by combining the high temporal resolution of high-density EEG recordings with the high spatial resolution of fMRI into simultaneous EEG-fMRI recordings. This multimodal approach has already led to promising results in human subjects (Jorge et al., 2014) since we are now able to efficiently remove the MRI-associated artifacts in EEG signal (Iannotti et al.,

2015; Jorge et al., 2015). An example is the non-invasive localisation of epileptic foci that may help to increase knowledge about epileptic networks in human patients (for reviews, see Pittau et al., 2014a; and Pittau et al., 2014b). One can expect that such combinations of different non-invasive imaging tools, each of them offering specific advantages, for instance in terms of spatial resolution or temporal resolution, will rapidly lead to other important discoveries by providing unique information about the spatio-temporal dynamics of brain functions. In particular, it would represent a great improvement to acquire simultaneous EEG-fMRI signals in our macaque monkeys to gain fresh insights into the precise location of SSEPs generators and to decipher the complex mechanisms of their post-lesion reorganisation. Technically, customised MRI-compatible EEG caps are already available for monkeys, meaning that such combined EEG-fMRI acquisitions should be possible in the near future.

Second, by using transient inactivations of some brain regions, either chemically induced by performing microinfusion of the GABA agonist muscimol, or magnetically induced by using TMS, or optogenetically induced, we may acquire significant knowledge about the contribution of the different cortical areas to the EEG signal captured at the scalp.

Third, we expect that the complex nature of EEG signal will be better understood by simultaneously recording the EEG signal at the scalp and invasively the intracranial activity at the level of the generators. This multimodal technical approach has been already used successfully in rodents (see e.g. Mahon et al., 2001) and is currently under development in monkeys and represents actually the only way to localise the EEG generators without ambiguity. Promising results were already obtained by performing simultaneous surface EEG measurements along with intracortical recordings of local field potentials (LFPs) in the primary visual cortex of behaving macaque monkeys (Musall et al., 2014; Whittingstall and Logothetis, 2009). Briefly, these authors demonstrated, among others, that the neural synchrony alone was sufficient to modulate the EEG signal at the scalp, independently from the changes in amplitude of local neural activity, providing significant understanding about how the activity of neuronal populations contributes to the EEG measured at the scalp, at least in the visual cortex.

Evidently, even though the latest generations of EEG approaches allow for the recording and localisation of neural activity with an increasing spatial resolution, additional inves-

tigations in this field need to be performed, primarily by resorting to invasive recordings on animals, especially on monkeys, in order to fully understand how the EEG signal is generated and therefore to better apprehend its significance. From then on, we will be in a position to use EEG as a true brain imaging method, as proposed by Michel and Murray (2012), both in monkeys and in human, at the same level as other non-invasive neuroimaging techniques such as fMRI, in particular by combining EEG and fMRI acquisitions. However, note in passing that the mechanisms of generation of the BOLD signal captured by fMRI still remain largely elusive as well (Kayser and Logothetis, 2013; Logothetis, 2008; Logothetis and Wandell, 2004).

Taken all together, we can fully appreciate how investigations on animals and on monkeys in particular, are of prime importance to unravel the complex mechanisms of brain activity, and to understand the relevance of the signal obtained with the different available brain imaging methods.

Importance to comprehend the sensorimotor system as a whole

A third important message of this thesis is that the motor system is not only involved in executing movements and the processing of somatosensory information does not culminate and finish in S1. Rather, there is a large body of evidence that both somatosensory and motor cortices are integrated into a more global and more complex functional sensorimotor cortex involved in motor control. The sensorimotor integration (of tactile and proprioceptive inputs) underlies motor behaviour. Indeed, sensory inputs to M1 may be involved in the sequencing of voluntary movements by facilitating and/or setting up the excitability level of corticofugal neurons in M1 by positive feedback, both before and during voluntary movements (Lemon, 1981; Liepert et al., 2003; Murray and Keller, 2011) and may be particularly important for the learning of motor skills (Lemon, 1981; Pavlides et al., 1993). Tactile exploration (Darian-Smith, 2007) and real-time adjustments during object manipulation (Gardner et al., 2007; Monzée et al., 2003; Wannier et al., 1991) with the fingers and the hand in particular were shown to strongly depend on a continuous afferent positive feedback of peripheral inputs to M1 (Lemon, 1981).

In the present thesis, we had the opportunity to investigate different aspects of the functioning of the sensorimotor system both in macaque monkeys and in human. Note that

we focused on the motor component only on monkeys, by using the modified Brinkman board task and the Brinkman box task. Conversely, the somatosensory processing was investigated deeply in both species by using EEG.

In case our lesion results are confirmed on additional monkeys, they may have relevant implications in the field of neurorehabilitation addressed to patients presenting a brain insult, for instance. Briefly, by showing that a motor cortex lesion was accompanied by modifications in somatosensory processing as well, our results may suggest that motor recovery is tightly linked with somatosensory recovery and therefore promoting somatosensory recovery may help towards motor recovery as well. More specifically, neurorehabilitation strategies should be oriented towards intense somatosensory rehabilitation as well in parallel with the recovery of motor functions themselves, as already initiated in some studies (see e.g. Byl et al., 2003; Laible et al., 2012; Sawaki et al., 2006).

Uniqueness of the thumb

Interestingly, investigations on both monkeys and human revealed that the sensorimotor processing associated with the thumb was distinct from the processing associated with the index or middle fingers. For reminder, we observed in monkeys that the sensorimotor processing from the thumb tip and the motor behaviour of this finger were more affected by a lesion of the M1 hand representation than the other fingers (see **Chapter 3**). Moreover, the pattern of cortical adaptation to repeated stimulations was less consistent for the thumb tip as compared to the other fingertips (see **Chapter 4**). Then, in human smartphone users, we demonstrated that the tactile cortical potentials associated with the thumb specifically reflected the daily variability in smartphone use (see **Chapters 6**). Our findings confirm the uniqueness of the primate thumb. It is most probably linked to the fully opposable nature of this finger that emerged in Old World monkeys during the primate evolution and that assisted them in fine motor skills such as grasping, manipulating and handling objects more efficiently than the other primates lacking in it (Darian-Smith, 1984; Darian-Smith et al., 1996; Napier, 1962). Please, see the discussion of **Chapter 3** for a more elaborated review about the sensorimotor control of the thumb.

Conclusion

By way of conclusion, brain imaging such as EEG measurement is a rapidly evolving field in Neuroscience that has allowed to demonstrate one of the most exciting findings of contemporary Neuroscience, namely that the adult primate brain is not hard-wired. Conversely, brain imaging techniques have enabled to visualise plastic cortical modifications taking place within the brain, demonstrating that brain activity in adult primates cannot be dissociated from the concept of brain plasticity. Brain plasticity is an intrinsic property of the nervous system, operating in our normal daily life. Our brain is continuously remodeled during life according to learning and our sensory experiences. In addition, brain plasticity is involved in triggering functional recovery after a cortical lesion. By investigating on animals, we are in a position to better comprehend mechanisms that remain elusive in human, such as the post-lesion reorganisation of brain activity and the nature of signal detected with the different brain imaging methods. We hope that the results presented here will open up the way for further investigations that may eventually contribute to a better understanding of the normal and post-injury brain activity in human.

References

Buzsáki, G., Anastassiou, C.A., Koch, C., 2012. The origin of extracellular fields and currents - EEG, ECoG, LFP and spikes. Nat Rev Neurosci 13, 407-420.

Byl, N., Roderick, J., Mohamed, O., Hanny, M., Kotler, J., Smith, A., Tang, M., Abrams, G., 2003. Effectiveness of sensory and motor rehabilitation of the upper limb following the principles of neuroplasticity: patients stable poststroke. Neurorehabil Neural Repair 17, 176-191.

Darian-Smith, C., 2007. Monkey Models of Recovery of Voluntary Hand Movement After Spinal Cord and Dorsal Root Injury. ILAR Journal 48, 396-410.

Darian-Smith, I., 1984. The Sense of Touch: Performance and Peripheral Neural Processes. In: Brookhart, J.M., Mountcastle, V.B. (Eds.), Handbook of Physiology, The Nervous System, Sensory Processes. John Wiley & Sons, Inc., pp. 739-788.

Darian-Smith, I., Galea, M.P., Darian-Smith, C., Sugitani, M., Tan, A., Burman, K., 1996. Introduction., The Anatomy of Manual Dexterity, Advances in Anatomy Embryology and Cell Biology, Volume 133. Springer Berlin Heidelberg, pp. 1-16.

Gardner, E.P., Ro, J.Y., Babu, K.S., Ghosh, S., 2007. Neurophysiology of prehension. II. Response diversity in primary somatosensory (S-I) and motor (M-I) cortices. J.Neurophysiol. 97, 1656-1670.

Gil-da-Costa, R., Stoner, G.R., Fung, R., Albright, T.D., 2013. Nonhuman primate model of schizophrenia using a noninvasive EEG method. Proc.Natl.Acad.Sci.USA 110, 15425-15430.

Hamadjida, A., Wyss, A.F., Mir, A., Schwab, M.E., Belhaj-Saïf, A., Rouiller, E.M., 2012. Influence of anti-Nogo-A antibody treatment on the reorganization of callosal connectivity of the premotor cortical areas following unilateral lesion of primary motor cortex (M1) in adult macaque monkeys. Exp.Brain Res. 223, 321-340.

Iannotti, G.R., Pittau, F., Michel, C.M., Vulliemoz, S., Grouiller, F., 2015. Pulse Artifact Detection in Simultaneous EEG–fMRI Recording Based on EEG Map Topography. Brain Topogr 28, 21-32.

Jorge, J., Grouiller, F., Ipek, Ö., Stoermer, R., Michel, C.M., Figueiredo, P., van der Zwaag, W., Gruetter, R., 2015. Simultaneous EEG–fMRI at ultra-high field: Artifact prevention and safety assessment. Neuroimage 105, 132-144.

Jorge, J., van der Zwaag, W., Figueiredo, P., 2014. EEG–fMRI integration for the study of human brain function. Neuroimage 102, Part 1, 24-34.

Kaas, J.H., Merzenich, M.M., Killackey, H.P., 1983. The reorganization of somatosensory cortex following peripheral nerve damage in adult and developing mammals. Annu.Rev.Neurosci. 6, 325-356.

Kayser, C., Logothetis, N.K., 2013. The Electrophysiological Background of the fMRI Signal. In: Ulmer, S., Jansen, O. (Eds.), fMRI. Springer Berlin Heidelberg, pp. 25-36.

Krarup, C., Trojaborg, W., 1994. Compound sensory action potentials evoked by tactile and by electrical stimulation in normal median and sural nerves. Muscle Nerve 17, 733-740.

Laible, M., Grieshammer, S., Seidel, G., Rijntjes, M., Weiller, C., Hamzei, F., 2012. Association of Activity Changes in the Primary Sensory Cortex With Successful Motor Rehabilitation of the Hand Following Stroke. Neurorehabil Neural Repair 26, 881-888.

Lemon, R.N., 1981. Functional properties of monkey motor cortex neurones receiving afferent input from the hand and fingers. J.Physiol 311, 497-519.

Liepert, J., Gorsler, A., van Eimeren, T., Münchau, A., Weiller, C., 2003. Motor excitability in a patient with a somatosensory cortex lesion. Clinical Neurophysiology 114, 1003-1008.

Liu, Y., Rouiller, E.M., 1999. Mechanisms of recovery of dexterity following unilateral lesion of the sensorimotor cortex in adult monkeys. Exp.Brain Res. 128, 149-159.

Logothetis, N.K., 2008. What we can do and what we cannot do with fMRI. Nature 453, 869-878.

Logothetis, N.K., Wandell, B.A., 2004. Interpreting the BOLD Signal. Annual Review of Physiology 66, 735-769.

Mahon, S., Deniau, J.M., Charpier, S., 2001. Relationship between EEG Potentials and Intracellular Activity of Striatal and Cortico-striatal Neurons: an In Vivo Study under Different Anesthetics. Cerebral Cortex 11, 360-373.

Mégevand, P., Quairiaux, C., Lascano, A.M., Kiss, J.Z., Michel, C.M., 2008. A mouse model for studying large-scale neuronal networks using EEG mapping techniques. Neuroimage. 42, 591-602.

Merzenich, M.M., Kaas, J.H., Wall, J., Nelson, R.J., Sur, M., Felleman, D., 1983a. Topographic reorganization of somatosensory cortical areas 3b and 1 in adult monkeys following restricted deafferentation. Neuroscience 8, 33-55.

Merzenich, M.M., Kaas, J.H., Wall, J.T., Sur, M., Nelson, R.J., Felleman, D.J., 1983b. Progression of change following median nerve section in the cortical representation of the hand in areas 3b and 1 in adult owl and squirrel monkeys. Neuroscience 10, 639-665.

Michel, C.M., Murray, M.M., 2012. Towards the utilization of EEG as a brain imaging tool. Neuroimage 61, 371-385.

Michel, C.M., Murray, M.M., Lantz, G., Gonzalez, S., Spinelli, L., Grave de Peralta, R., 2004. EEG source imaging. Clin.Neurophysiol 115, 2195-2222.

Michel, C.M., Thut, G., Morand, S., Khateb, A., Pegna, A.J., Grave de Peralta, R., Gonzalez, S., Seeck, M., Landis, T., 2001. Electric source imaging of human brain functions. Brain Res.Brain Res.Rev. 36, 108-118.

Monzée, J., Lamarre, Y., Smith, A.M., 2003. The Effects of Digital Anesthesia on Force Control Using a Precision Grip. Journal of Neurophysiology 89, 672-683.

Murray, P.D., Keller, A., 2011. Somatosensory response properties of excitatory and inhibitory neurons in rat motor cortex. J Neurophysiol 106, 1355-1362.

Musall, S., von Pföstl, V., Rauch, A., Logothetis, N.K., Whittingstall, K., 2014. Effects of Neural Synchrony on Surface EEG. Cerebral Cortex 24, 1045-1053.

Napier, J., 1962. The evolution of the hand. Scientific American 207, 56-62.

Nicolelis, M.A.L., Dimitrov, D., Carmena, J.M., Crist, R., Lehew, G., Kralik, J.D., Wise, S.P., 2003. Chronic, multisite, multielectrode recordings in macaque monkeys. Proceedings of the National Academy of Sciences 100, 11041-11046.

Pavlides, C., Miyashita, E., Asanuma, H., 1993. Projection from the sensory to the motor cortex is important in learning motor skills in the monkey. J Neurophysiol. 70, 733-741.

Pittau, F., Grouiller, F., Spinelli, L., Seeck, M., Michel, C.M., Vulliemoz, S., 2014a. The role of functional neuroimaging in pre-surgical epilepsy evaluation. Frontiers in Neurology 5.

Pittau, F., Mégevand, P., Sheybani, L., Abela, E., Grouiller, F., Spinelli, L., Michel, C.M., Seeck, M., Vulliemoz, S., 2014b. Mapping epileptic activity: sources or networks for the clinicians? Frontiers in Neurology 5.

Rouiller, E.M., Olivier, E., 2004. Functional recovery after lesions of the primary motor cortex. Prog.Brain Res. 143, 467-475.

Rouiller, E.M., Yu, X.H., Moret, V., Tempini, A., Wiesendanger, M., Liang, F., 1998. Dexterity in adult monkeys following early lesion of the motor cortical hand area: the role of cortex adjacent to the lesion. Eur.J.Neurosci. 10, 729-740.

Sawaki, L., Wu, C.W., Kaelin-Lang, A., Cohen, L.G., 2006. Effects of somatosensory stimulation on use-dependent plasticity in chronic stroke. Stroke 37, 246-247.

Schwarz, D.A., Lebedev, M.A., Hanson, T.L., Dimitrov, D.F., Lehew, G., Meloy, J., Rajangam, S., Subramanian, V., Ifft, P.J., Li, Z., Ramakrishnan, A., Tate, A., Zhuang, K.Z., Nicolelis, M.A.L., 2014. Chronic, wireless recordings of large-scale brain activity in freely moving rhesus monkeys. Nat Meth 11, 670-676.

Starr, A., Pratt, H., Burke, D., 1982. Natural stimuli evoking somatosensory potentials. Ann.N.Y.Acad.Sci. 388, 702-706.

Wannier, T.M., Maier, M.A., Hepp-Reymond, M.C., 1991. Contrasting properties of monkey somatosensory and motor cortex neurons activated during the control of force in precision grip. J Neurophysiol. 65, 572-589.

Whittingstall, K., Logothetis, N.K., 2009. Frequency-Band Coupling in Surface EEG Reflects Spiking Activity in Monkey Visual Cortex. Neuron 64, 281-289.

Wyss, A.F., Hamadjida, A., Savidan, J., Liu, Y., Bashir, S., Mir, A., Schwab, M.E., Rouiller, E.M., Belhaj-Saïf, A., 2013. Long-term motor cortical map changes following unilateral lesion of the hand representation in the motor cortex in macaque monkeys showing functional recovery of hand functions. Restor.Neurol Neurosci. 31, 733-760.

York, D.H., 1985. Somatosensory evoked potentials in man: differentiation of spinal pathways responsible for conduction from the forelimb vs hindlimb. Prog.Neurobiol. 25, 1-25.

APPENDIXES

In addition to the work and published papers presented in the previous chapters, I was included as a co-author in 4 others studies as well during my stay in the laboratory of Professor Eric Rouiller. The corresponding papers are proposed in the **Appendixes 1** to **4**.

Appendix 1

Follow-up of cortical activity and structure after lesion with laser speckle imaging and magnetic resonance imaging in nonhuman primates

Peuser J*, Belhaj-Saif A*, Hamadjida A, Schmidlin E**, Gindrat AD**, Volker AC, Zakharov P, Hoogewoud HM, Rouiller EM, Scheffold F (2011). Journal of Biomedical Optics 16(9):096011-1-096011-11. DOI:10.1117/1.3625287

I participated as a Master student in this study investigating the time course of cortical reorganisation following a permanent M1 lesion in two macaque monkeys by combining laser speckle imaging and MRI.

Appendix 1

Journal of Biomedical Optics 16(9), 096011 (September 2011)

Follow-up of cortical activity and structure after lesion with laser speckle imaging and magnetic resonance imaging in nonhuman primates

Jörn Peuser,[a,*] Abderraouf Belhaj-Saif,[b,*] Adjia Hamadjida,[b] Eric Schmidlin,[b] Anne-Dominique Gindrat,[b] Andreas Charles Völker,[a] Pavel Zakharov,[a] Henri-Marcel Hoogewoud,[c] Eric M. Rouiller,[b,†] and Frank Scheffold[a,†]
[a]University of Fribourg, Department of Physics, Ch. du Musée 3, CH-1700 Fribourg, Switzerland
[b]University of Fribourg, Department of Medicine, Program in Neurosciences, Ch. du Musée 5, CH-1700 Fribourg, Switzerland
[c]HFR (Hôpital Fribourgeois), Fribourg, Hôpital cantonal, Department of Radiology, CH-1708 Fribourg, Switzerland

Abstract. The nonhuman primate model is suitable to study mechanisms of functional recovery following lesion of the cerebral cortex (motor cortex), on which therapeutic strategies can be tested. To interpret behavioral data (time course and extent of functional recovery), it is crucial to monitor the properties of the experimental cortical lesion, induced by infusion of the excitotoxin ibotenic acid. In two adult macaque monkeys, ibotenic acid infusions produced a restricted, permanent lesion of the motor cortex. In one monkey, the lesion was monitored over 3.5 weeks, combining laser speckle imaging (LSI) as metabolic readout (cerebral blood flow) and anatomical assessment with magnetic resonance imaging (T2-weighted MRI). The cerebral blood flow, measured online during subsequent injections of the ibotenic acid in the motor cortex, exhibited a dramatic increase, still present after one week, in parallel to a MRI hypersignal. After 3.5 weeks, the cerebral blood flow was strongly reduced (below reference level) and the hypersignal disappeared from the MRI scan, although the lesion was permanent as histologically assessed post-mortem. The MRI data were similar in the second monkey. Our experiments suggest that LSI and MRI, although they reflect different features, vary in parallel during a few weeks following an excitotoxic cortical lesion. [DOI: 10.1117/1.3625287]

Keywords: monkey; motor cortex; ibotenic acid; cerebral blood flow; excitotoxic lesion.

Paper 11074RR received Feb. 18, 2011; revised manuscript received Jul. 19, 2011; accepted for publication Jul. 20, 2011; published online Sep. 2, 2011.

1 Introduction

The spontaneous capacity of the brain to functionally recover from a lesion is limited, as it is the case after stroke, for instance. A crucial step toward feasible, safe, and efficient clinical application of a therapeutic strategy requires basic investigations and proofs of principle in animal models. The nonhuman primate model is often mandatory to address safety issues and scientific concerns, especially to take into consideration exquisite neural functions present only in primates,[1,2] such as manual dexterity.[3] The nonhuman primate model of the macaque monkey was extensively used in our laboratory to assess the extent and mechanisms of spontaneous recovery from spinal cord or motor cortex lesion and to test strategies aimed at enhancing recovery.[4–12]

The nonhuman primate model is suitable to study the consequences of a lesion of the motor cortex, produced by various interventions (surgical lesion, block of a cerebral artery, chemical lesion),[11–17] and to establish possible mechanisms of recovery.[4,14] The interpretation of the behavioral data is strongly dependent on the properties of the lesion, such as its extent (volume) and its precise location. Furthermore, the dynamics of the lesion procedure is also likely to influence the magnitude of the deficit and the extent of recovery. In our nonhuman primate model of motor cortex lesion,[4,11,12] the hand representation in the primary motor cortex (M1) was first delineated with intracortical microstimulation and then damaged by infusion of the excitotoxic ibotenic acid at the most excitable sites, leading to a permanent damage of the corresponding brain area. The precise time course of the devastating effect of ibotenic acid on the cortical tissue is not known, as well as the follow-up of the appearance of the cortical lesion site produced by ibotenic acid infusion in M1 on magnetic resonance imaging (MRI) scans during the weeks post-lesion. To fill this gap, we have implemented in parallel a functional readout [a measure of cerebral blood flow based on laser speckle imaging (LSI) technique] and a structural readout (MRI scan) at consecutive time points post-lesion.

The LSI method[18,19] is relatively low-cost and easy to implement, and it was broadly used in biomedical studies on small animals over the last decade.[20–30] The main field of application consisted of creating maps of capillary and perfusion blood flow in tissue. A number of improvements with regard to signal processing and quantitative data analysis have been reported in the literature.[31–36] The LSI technique can be applied to the exposed cerebral cortex or, in some cases, to the intact (surgically thinned) skull,[33,36] albeit at reduced performance. Applications for larger animals or humans are impractical due to the limited coherent penetration of light into the skull, although

*Equal first authorship.
†Equal senior authorship.

Address all correspondence to: Eric Rouiller, University of Fribourg, Medicine, Musee 5 - Fribourg, Fribourg 1700 Switzerland. Tel: 41 26 300 86 09; Fax: 41 26 300 96 75; E-mail: Eric.Rouiller@unifr.ch.

1083-3668/2011/16(9)/096011/11/$25.00

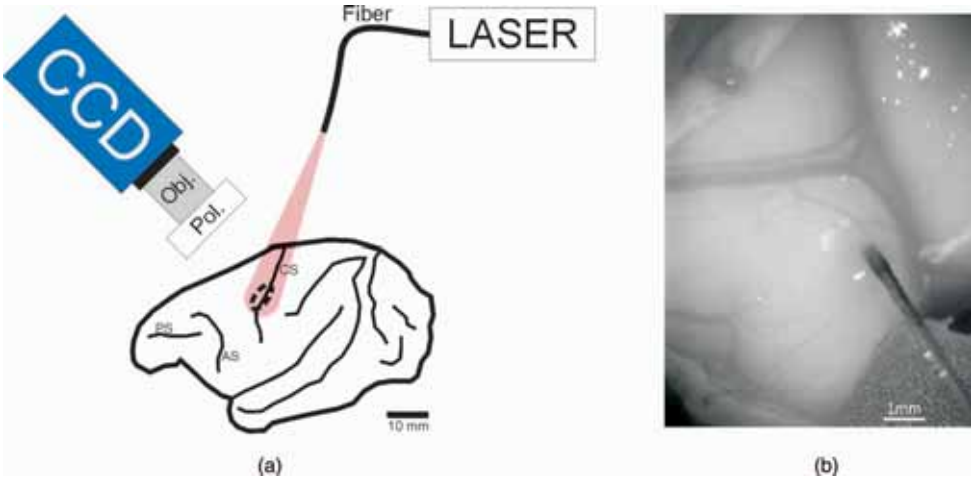

Fig. 1 (a) Setup of the LSI experiment, schematized over a standard lateral view of the left hemisphere of the macaque monkey. CS = central sulcus; AS = arcuate sulcus; PS = principal sulcus. (b) Time integrated image of the cortical surface, taken with the CCD camera. A vertically oriented blood vessel on the right follows the central sulcus, whereas another blood vessel of large diameter is horizontally oriented over the pre-central gyrus. The image was taken when the needle of an Hamilton syringue was inserted into the motor cortex, rostral to the central sulcus, to perform one of the six penetrations along which ibotenic acid was infused.

intraoperative use of LSI as a monitoring tool in neurosurgery has been reported.[37]

Despite the importance and widespread use of the LSI technique in neurosciences using rodents, a successful application in nonhuman primates is still missing, to our knowledge. The present study thus uses LSI to monitor, in nonhuman primate and over several weeks, the variation of cerebral blood flow of a cortical territory subjected to a permanent lesion induced by infusion of ibotenic acid and, in parallel, the changes of structural properties of the same territory assessed with MRI. A more specific goal was to measure, with LSI, changes of cerebral blood flow during surgery in real time when ibotenic acid was infused in the cerebral cortex to generate a permanent excitotoxic lesion. A further goal was to refine the LSI technique in order to improve the quality of the image by introducing a sliding window processing scheme, as well as to reduce the interference due to movements related to heart beat.

2 Materials and Methods

2.1 *Lesion of the Motor Cortex*

LSI and MRI data were collected in parallel from an adult macaque monkey (a male macaca fascicularis: Mk-JH), 7 years old and weighting 7 kg at the time of the cortical lesion. Additional MRI data were obtained from a second male macaque monkey (Mk-BI; 5 years old, 5 kg body weight). All procedures were conducted in accordance to the Guide for Care and Use of Laboratory Animals (ISBN 0–309-05377–3; 1996) and approved by local veterinary authorities. As previously reported,[11] the monkeys were housed in our animal facilities in rooms of 12 m^3, in which usually two to four monkeys were free to move and to interact among each other. (A new Swiss regulation was introduced in September 2010 requesting a volume of 45 m^3 at least to be given to a group of up to five macaque monkeys.) The monkeys had free access to water and were not food deprived.

To perform the lesion of M1 in both monkeys (Mk-JH and Mk-BI) and, subsequently, to measure cerebral blood flow with LSI in Mk-JH, the animals were subjected to the following surgical procedures. The monkeys were first tranquilized with ketamine (Ketalar®; Parke-Davis, 5 mg/kg, intramuscularly); atropine was injected (0.05 mg/kg, intramuscularly) in order to reduce bronchial secretions. Before surgery, the animals were treated with the analgesic Carprofen (Rimadyl®, 4 mg/kg, subcutaneously) and the antibiotic Albipen® (Ampiciline 10%, 30 mg/kg, subcutaneously). Subsequently, Mk-JH and Mk-BI were anaesthetized with intravenous perfusion of 1% propofol (Fresenius®) mixed with a 5% glucose solution (1 volume of propofol and 2 volumes of glucose solution); ketamine was added to the perfusion solution (65 mg/100 ml). To prevent edema, Methylprednisolone (Solu-medrol, Pfizer®) was added to the propofol/glucose solution (1 mg/ml). The level of anesthesia was kept at an optimal level with a perfusion rate of the propofol/glucose mixture of 0.1 ml/min/kg. All surgeries were performed under sterile conditions. Heart rate, respiration rate, expired CO_2, arterial O_2 saturation, and rectal temperature were monitored throughout the surgery. After surgery, the monkey received Carprofen (pills of Rimadyl® mixed with food) daily and Albipen® (subcutaneously; same dose as above) every two days during one to two weeks.

A squared osseous sector of about 30 × 30 mm was opened above the central sulcus, centered at a medio-lateral coordinate (15 mm from midline) corresponding to the expected position of the hand area in M1. The dura-mater was incised and reclined in order to expose the central sulcus as well as the precentral and postcentral gyri. In monkey Mk-JH, ibotenic acid (Sigma 95%) was injected at six sites in the precentral gyrus, at a position roughly corresponding to the hand area based on its coordinate and the shape of the central sulcus at this location. The extent of the cortical territory, in which ibotenic acid was injected in Mk-JH, corresponded to the area of cortex captured by the charge-coupled device (CCD) camera for LSI measurements (Fig. 1). Acquisitions of cerebral blood flow with LSI (see below) were performed before and then after each individual injection of ibotenic acid. A volume of 3 μl of

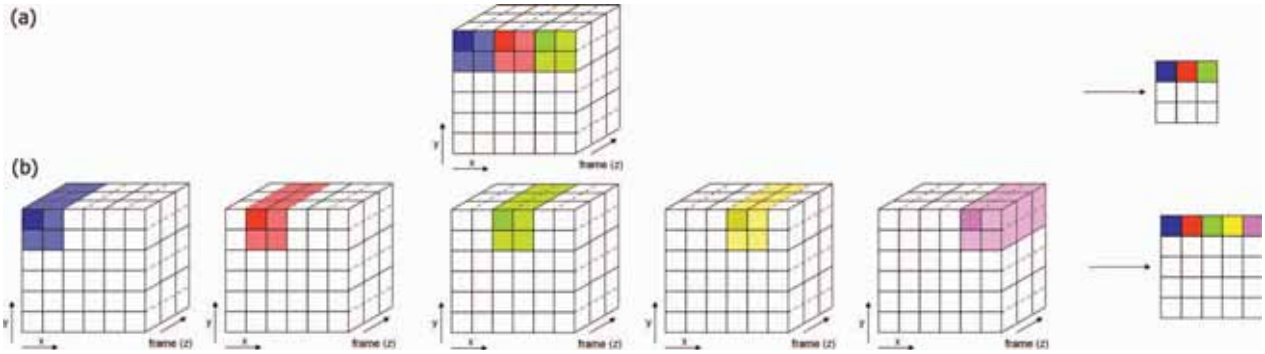

Fig. 2 (a) Standard (temporal) LSI scheme. (b) High resolution LSI introducing a sliding window in space.

ibotenic acid solution (10 μg/μl in phosphate-buffered saline) was injected at each site by using a Hamilton microsyringe, positioned at 2 mm below the pial surface (Fig. 1). The total volume of ibotenic acid injected in Mk-JH was 18 μl, an amount representative of volumes injected in monkeys used for behavioral studies.[4,11,12] In Mk-BI, from which only MRI data were derived, ibotenic acid was injected at 29 sites defined based on intracortical microstimulation,[11] at which a volume of 1 μl was infused (total amount 29 μl). The volume of ibotenic acid injected was larger in Mk-BI, because this animal was involved in the behavioral protocol,[12] requesting a lesion affecting the entire hand representation in M1. In contrast, Mk-JH was exclusively involved in the present LSI protocol and, therefore, the lesion was adapted to the cortical territory covered by the CCD camera rather than covering the entire hand representation in M1. In addition, in Mk-JH the infusion sites were somewhat more distant than in Mk-BI, and therefore, the volume injected at each infusion site in Mk-JH was larger. At the end of this experimental session aimed at lesioning the motor cortex, the dura mater was put back in place and sutured. The craniotomy was not closed. The muscle and skin were then sutured.

2.2 *Laser Speckle Imaging*

2.2.1 *Data acquisition and image processing*

For each subsequent LSI recording session conducted in Mk-JH only (at 1 and 3.5 weeks post-lesion, also under anesthesia as described above for the initial session), the skin was incised, the muscles reclined, and the dura was reopened as described above. For such a time interval between sessions, there were no adhesions between the dura and the blood vessels. A selected part of the surface of the cerebral cortex was homogeneously illuminated with a 785 nm single frequency laser (Toptica®, Munich, Germany), feeding a single mode fiber attached to a collimating lens (Schaefter + Kirchhoff®, Hamburg, Germany; Fig. 1). The whole illuminating device and the CCD camera have been positioned using a stereotaxic frame. The total laser power incident on the brain cortex was about 3 mW distributed over an area of several cm^2, thus preventing any physiological effects or superficial heating of cortical tissue. The diffuse reflected light was monitored in the image plane in the crossed polarization channel with a CCD camera (PCO Pixelfly, 640 × 480 pixels, 12 bit, exposure time 12 ms). A region of 10 mm by 7.5 mm of the cortex was imaged onto the 1/2″ CCD chip at 0.64× magnification.

Individual measurements of 15 s duration at 50 frames per second (total 750 frames) have been streamed at full resolution to the hard disk using the Streampix 3 software package (NorPix Inc.®, Montreal, Quebec, Canada). The local speckle contrast K was computed from a b × b square of pixels and typically 40 successive frames,[24,32,38] setting the actual time resolution of the experiment to 0.8 s. The image quality was further improved by implementation of a sliding window average (Figs. 2 and 3), where essentially all camera pixels are replaced by a metapixel (value K). Only a few pixels at the image border need to be excluded from the final image due to the lack of sufficient neighbors. For a raw image with 640 × 480 pixels, and typically b = 5, this procedure provides a speckle image with a nominal resolution of 636 × 476 pixels (Fig. 3). The Labview® and Matlab® source codes are available free of charge from the authors (with no support) at http://physics.unifr.ch/en/page/54/.

2.2.2 *Heartbeat filter*

During the experiment the recorded image sequences exhibited a small periodic movement of the cerebral cortex due to the heartbeat/blood pressure variation of the animal. This movement leads to a measurable change in contrast (roughly +/− 10%) and in turn slightly blurs the image, when averaging over a sequence of images. To minimize this effect, we have implemented a software filter that allowed us to select images at a certain reference point in the heart beat cycle (Fig. 4). As expected, we found that the contrast time course essentially follows the heart beat with a frequency of approximately 80 beats per minute. A high pass filter was applied to select only the frames of the sequence with an average region of interest (ROI) contrast higher than a specified threshold. All other frames were discarded for the processing of the laser speckle image, thus roughly reducing the number of analyzed raw images by a factor of four to five. As can be seen in Fig. 4, this procedure allows us to reduce the systematic error due to heartbeat from more than 10 to about 3%.

Residual movements of the skull were observed leading to minute shifts in *x*-/*y*-directions during a long time recording sequence. It was not straightforward to compensate these movements within our measurement scheme. The presence of these small drifts thus imposes a limit to the total recording time, and therefore, the statistical accuracy of the measurements, in order to avoid blurring effects. Here, we have chosen the image acquisition time such that the influence of these drifts is negligible.

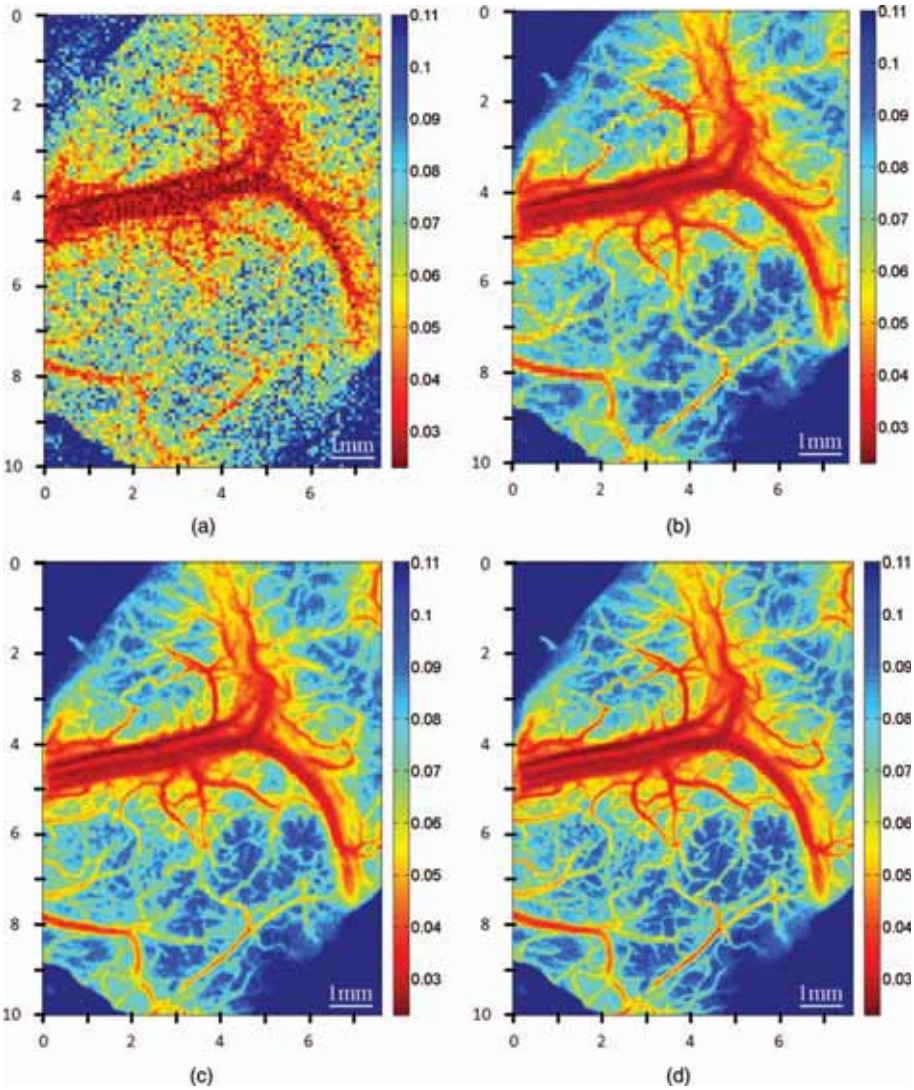

Fig. 3 Typical LSI in our experiment is constructed from 40 individual frames (resolution 640 × 480 pixels) and a spatial average of 5 × 5 camera pixels is performed at each point resolution in a final image with a nominal resolution of 636 × 476 pixels. Laser speckle images of the cerebral motor cortex calculated with different parameter settings: spatial averaging box size is set to 5^2 pixels for (a), (b), and (c); for (d) it is 2^2 pixels. (a) No time average, single frame, standard resolution scheme. (b) Time averaging over 40 frames, standard resolution scheme. (c) Time averaging over 40 frames, high resolution scheme (sliding window). (d) Time averaging over 250 frames, high resolution scheme (sliding window). The number of raw pixels used for the calculation of one LSI metapixels is 1000 for (b), (c), and (d) (example: box size * frames = 5^2 pixels * 40 frames = 1000 pixels). Axes labeling: *x-y* display the camera pixel at 0.64 magnification. The speckle contrast is color coded as shown by the color bar on the right of each LSI.

2.3 *Magnetic Resonance Imaging Acquisition*

The MRI data were acquired in Mk-JH and Mk-BI using a 1.5 Tesla Siemens© Symphony magnetic resonance scanner. To allow direct comparison of the extent of the cortical lesion at regular time points after the lesion, the anesthetized animal was placed in a decubitus ventral position with his head stabilized into a nonferromagnetic fixation frame with ear, mouth, and eye bars. MRI was performed under heavy sedation induced with subcutaneous injections of ketamine (Graeub® 10 mg/kg) associated with medetomidine (Graeub® 1 mg/kg). At the end of the acquisition, the anesthesia was reversed with Atipamezol (Pfizer®, 0.25 mg/kg). The acquisition parameters of the MRI data were the following: total of 19 images, slice thickness 2 mm, 2 TSE (TR 4500 ms and TE 129 ms), field of view 107 mm × 140 mm.

2.4 *Necropsy and Histology*

At the end of the experiment, the monkeys were sacrificed[5,7] for histological analysis of the lesion. Mk-JH was sacrificed a few days after the last LSI session, whereas Mk-BI was sacrificed several months post-lesion as it was involved in a study of functional recovery.[12] The monkeys were sacrificed under deep anesthesia [initiated first with an i.m. ketamine injection followed by an i.p. lethal dose of sodium pentobarbital (90 mg/kg)] by transcardiac perfusion with 0.9% saline (400 ml) continued with fixative (three liters of four paraformaldehyde in 0.1 M phosphate

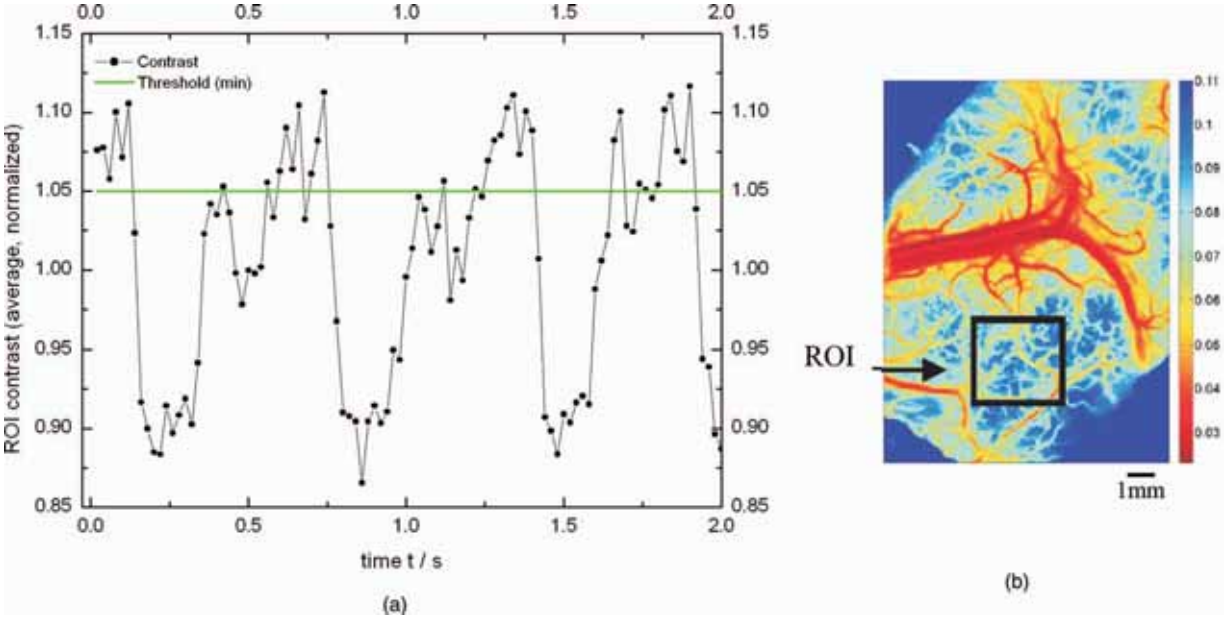

Fig. 4 (a) Heart beat signal computed from the average contrast in a ROI of 100 × 100 pixels from successive individual frames. The data were normalized and baseline corrected. The green line shows the minimum threshold, all other frames below that line will not be used to calculate a high resolution contrast image. (b) LSIs of the cerebral motor cortex calculated from 5^2 pixels and 40 successive frames. The ROI analyzed for the heartbeat correction is indicated by the black square.

buffer, pH = 7.6) and solutions (two liters each) of the same fixative containing increasing concentrations of sucrose (10, 20, and 30%). The brain was removed, dissected, and stored in a sucrose solution (30%) for 1.5 to 2 weeks. Frozen sections of the brain were then cut in the frontal plane at a thickness of 50 μm. Eight series of sections were collected with a cryotome (HM560, MICROM®, Switzerland). Among these series, one was Nissl-stained and one was immunocytochemically treated (SMI-32 antibody against a non-phosphorylated neurofilament epitope), as previously reported.[7,39] Furthermore, additional series were processed for other markers, such as Neuronal Nuclei [(NeuN) neuronal marker] and glial fibrillary acidic protein [(GFAP) glial marker], following previously described protocols.[40]

3 Results

3.1 *Injections of Ibotenic Acid*

In the first LSI recording session conducted in Mk-JH, LSI acquisition was immediately made after incision of the dura in order to establish the cerebral blood flow level corresponding to the reference state under stable propofol anesthesia. Then, this first session comprised the procedure of ibotenic acid infusion in the motor cortex in order to produce a permanent cortical lesion, comparable to lesions made in the course of previous studies in our laboratory.[4,11,12] Six penetrations with the needle of a Hamilton syringe were performed (Fig. 5), in the part of cerebral cortex rostral to the central sulcus, corresponding to M1.

3.2 *Speckle Contrast Imaging (Laser Speckle Imaging)*

The LSI in the reference state exhibited a high contrast [Figs. 6(a) and 7], corresponding to a moderate blood flow. As expected, the infusion of ibotenic acid at the first site of injection (Fig. 5) produced an immediate decrease of contrast, in line with an increase of cerebral blood flow (Fig. 7). Note, however, that the contrast slightly increased in the few minutes following the infusion of ibotenic acid at one site, as shown by the three LSI data points taken at 1.5 min intervals following the first post-infusion LSI acquisition. The same time course of contrast change was observed at all six injection sites during the few minutes following the actual infusion [Fig. 7(a)]. The next infusion at sites #2 and #3 produced a further decrease of contrast (increase of blood flow) [Fig. 7(a)]. As of the fourth injection site, the contrast reached a stable lowest level (maximal blood flow), although the small rebound of contrast was still

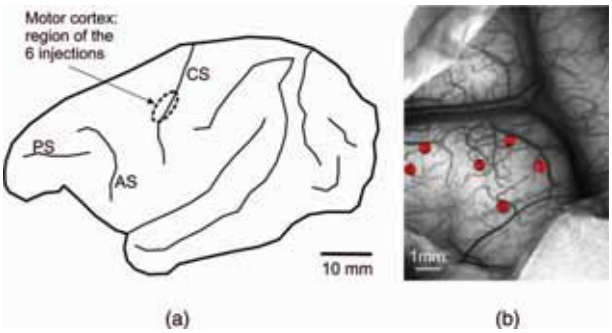

Fig. 5 (a) Lateral view of the left hemisphere of Mk-JH, showing the cortical territory (circle) in which a lesion of the motor cortex was performed with infusion of ibotenic acid along six penetrations in the pre-central gyrus. The ROI is presumably located in the zone corresponding to the hand area. (b) CCD image (slightly tilted to the left) of the cortical surface in the pre-central gyrus, with location on the cortical surface of the six syringe penetrations (one to six). Same orientation as in the right panel of Fig. 1.

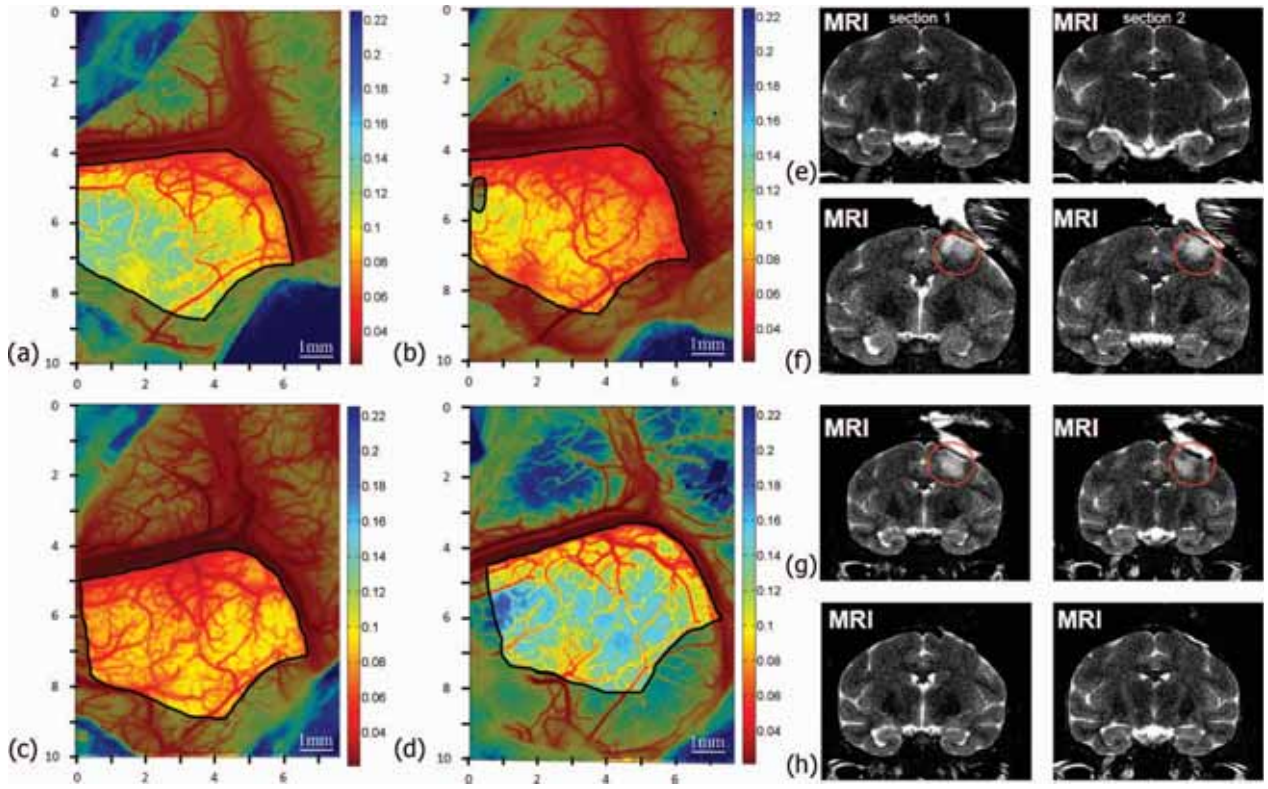

Fig. 6 LSI [(a),(b),(c),(d)] and MRI [(e),(f),(g),(h)] are compared in Mk-JH within a time frame of 3.5 weeks; (a), (e) reference before the injections; (b), (f) LSI taken 60 min post-lesion, MRI at one day post-lesion; (c), (g) LSI and MRI at one week post-lesion (one day apart from each other); (d), (h) LSI and MRI 3.5 weeks post-lesion (one day apart from each other). The highlighted area in the LSI figures shows the ROI wherein the average contrast was calculated for the quantitative data shown in Fig. 7. Calculation parameters for the LSI: 250 frames out of 750, HBC filter, sliding box, box $= 5^2$ pixels. The left and right MRI images on the same horizontal panel are taken at two rostro-caudal levels, distant by 2 mm, intercepting the ROI in the motor cortex.

present in the few minutes following each individual injection [Fig. 7(a)]. LSI was acquired during 25 more minutes after injection at the last site (site #6), taken at roughly 5 min intervals: there was a slow increase of contrast, finally reaching a stable level after about 75 min, situated in between those observed after the second and third injections of ibotenic acid. This contrast level at plateau is illustrated for the ROI in Fig. 6(b), showing that it was clearly diminished as compared to the reference state [Fig. 6(a)].

At that step, the dura was sutured (together with muscles and skin), the anesthesia was discontinued and the monkey was returned to the animal room. LSI was reacquired one week later and the contrast level was comparable to that observed about one hour after lesion [Figs. 6(c) and 7(b)]. The next LSI data point was acquired 3.5 weeks post-lesion, showing a dramatic increase of contrast, reaching a value higher than the initial reference value [Figs. 6(d) and 7(b)]. These data are indicative of a substantial decrease of blood flow at 3.5 weeks post-lesion, in line with the notion that ibotenic acid infusion produces a permanent lesion of the cortical tissue.

3.3 *Comparison of Laser Speckle Imaging, Magnetic Resonance Imaging and Histology*

LSI and MRI were not acquired the very same day as the two facilities are located at distant sites. The first MRI image [Fig. 6(e)] was taken two days before the first LSI recording acquisition [Fig. 6(a)], both representing the reference state pre-lesion. The second MRI image was acquired one day after the first LSI session during which the ibotenic acid was infused at six sites. The zone of infusion corresponds to a marked hypersignal [red circle in Fig. 6(f)] present in the pre-central gyrus. The hypersignal in the MRI was found to be maintained in the same area [red circle in Fig. 6(g)] one week later, in parallel to the decrease of contrast in the LSI [Figs. 6(c) and 7(b)], associated to an increase of cerebral blood flow. The last MRI image was taken 3.5 weeks post-lesion [Fig. 6(h)], showing a complete disappearance of the hypersignal, in parallel to the dramatic decrease of cerebral blood flow at the same time point, reflected by the increase of LSI contrast [Figs. 6(d) and 7(b)]. The LSI and MRI signals in the ROI follow a parallel time course, at least for the four time points considered in the present study (reference, briefly after lesion, one week post-lesion, and 3.5 days post-lesion). The lesion generated by ibotenic acid infusion in the motor cortex is visible with both LSI and MRI only during a few days (at least one week). Later on, after 3.5 weeks, the signals in both LSI and MRI returned in the direction of the reference appearance pre-lesion [compare Figs. 6(a) and 6(d) for LSI; Figs. 6(e) and 6(h) for MRI], although the LSI signal had a higher contrast, corresponding to a decrease of cerebral blood flow. Evidence for the presence of a permanent cortical lesion was provided by the histology post-mortem for Mk-JH (Fig. 8). As shown in SMI-32

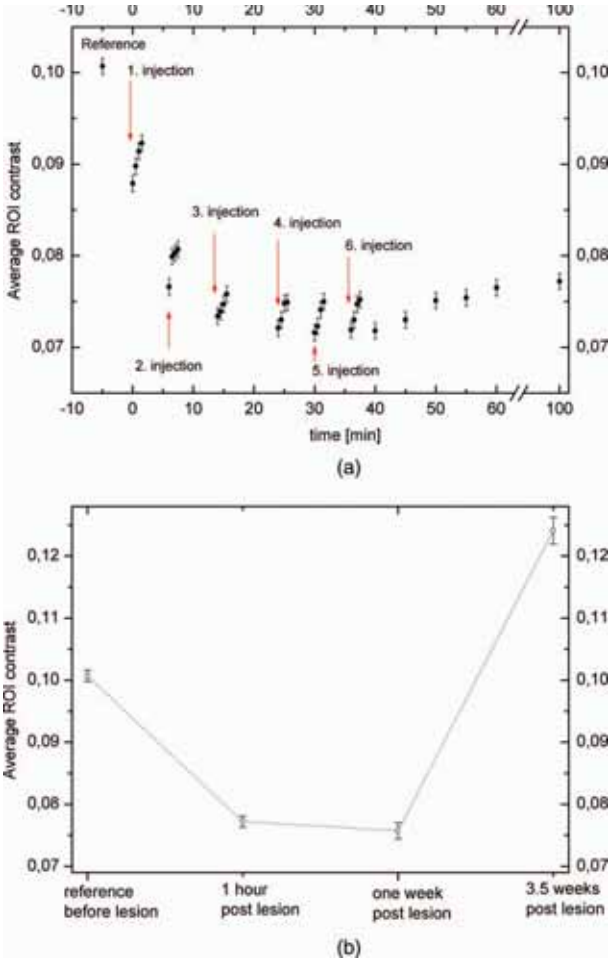

Fig. 7 Time course of maximum, minimum, and average ROI contrast on (a) the day of ibotenic acid injection in Mk-JH as well as (b) at two further distant time points. In (a), the data points related to the six infusions of ibotenic acid were acquired after offset of the injection (the needle was removed from the tissue). In (b), the data point at reference and at one hour post-lesion corresponds to the data point at reference and at 100 min in the upper panel (errors bars were estimated from the time course of the measurements). The data at one and 3.5 weeks were derived from six and five independent measurements, respectively.

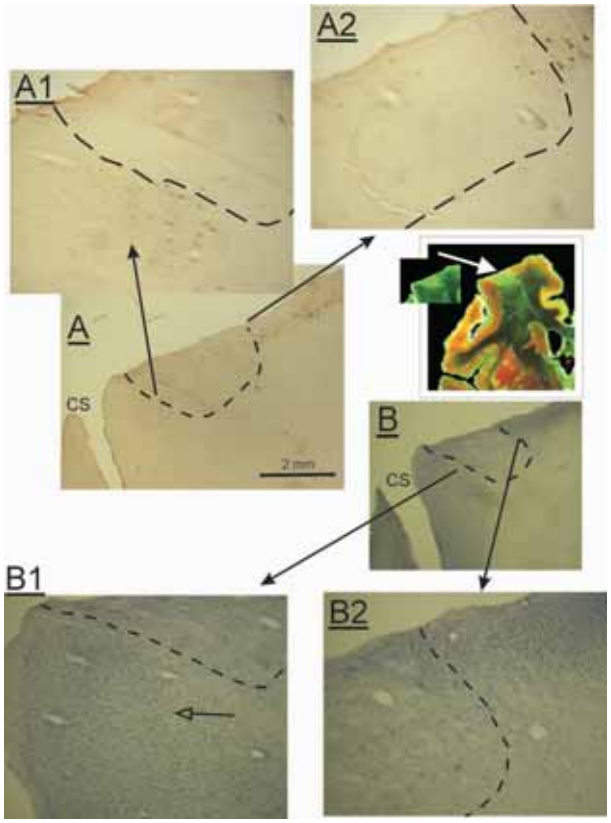

Fig. 8 Histological assessment of the permanent lesion in the motor cortex in Mk-JH, on a frontal section of the motor cortex. Panel A is a low magnification of the lesion area, as seen with the marker SMI-32. In the top row, the panels A1 and A2 are higher magnification of the lateral and medial edges of the lesion territory, respectively, also in SMI-32 material. The damaged territory corresponds to an interruption of the layers III and V pyramidal neurons stained with SMI-32. In the middle, panel B is a low magnification in Nissl material of the lesion area. The panels B1 and B2 in the bottom row show at higher magnification the edges of the lesion with Nissl staining. In all panels, the dashed line delimits the lesion territory. The open arrow in panel B1 points to large Nissl stained neurons in layer V in an intact territory located slightly more lateral than the lesion. The inset in the middle at the right is a low magnification view of the lesion (white arrow), as seen in a combined NeuN (red) and GFAP (green) stained material. The corresponding lesion area is shown for GFAP labeling alone (in green), next to the white arrow. CS = central sulcus.

stained material (Fig. 8), the infusion of ibotenic acid produced a clear disruption of the cortical layers in the lesion site (delineated with the dashed line) without SMI-32 labeled pyramidal cells, whereas in the intact tissue adjacent to the lesion territory the cortical layers III and V are clearly visible by the presence of pyramidal neurons stained with SMI-32 (panels A1 and A2 in Fig. 8 at higher magnification). The appearance of the lesion is similar to that previously shown in monkeys subjected to such lesion and involved in our functional recovery protocols.[11] The focal cortical lesion does not generate a cavity in the gray matter but, as seen on Nissl staining, it corresponds to a homogeneous territory with loss of neuronal cell bodies in all cortical layers (Fig. 8, panels B1 and B2; comparable to a previous description in the rat: see Fig. 1 in Leroux et al.[41]). Furthermore, the lesioned territory seen with the above two markers (SMI-32 and Nissl) matches the zone corresponding to an interruption of the neuronal marker NeuN and, in contrast, an increase of the glial marker GFAP (Fig. 8, middle inset). The MRI data obtained in Mk-BI (not shown) exhibit a similar time course of the hypersignal associated to the ibotenic acid lesion in M1, as illustrated for Mk-JH in Fig. 6.

3.4 *Comparison of the Lesion Size Assessed with Magnetic Resonance Imaging, or Post-mortem on Histological Sections or with Laser Speckle Imaging*

Based on consecutive histological sections as the one illustrated in Fig. 8 and using an ad-hoc function of the Neurolucida software (based on the Cavalieri method) as previously described,[11] the volume of the histological permanent lesion affecting the

gray matter was estimated to be 18.8 mm^3 in Mk-JH (after sacrifice, one month post-lesion). For comparison, the volume of the lesion as reflected by the hypersignal in the MRI scan (computed with the software OsiriX®) was 436 mm^3 at one day post-lesion, 405 mm^3 after one week, and 341 mm^3 after two weeks. After 3.5 weeks, the lesion was no longer visible on the MRI scan [Fig. 6(h)]. In the second monkey (Mk-BI), the volume of the lesion assessed based on the hypersignal on the MRI scan was 262 mm^3 one day post-lesion, 146 mm^3 one week after lesion, 135 mm^3 two weeks after lesion, and 97 mm^3 three weeks after the lesion, whereas, 10 months post-lesion, the volume of the permanent lesion was estimated at 20.1 mm^3 on SMI-32 stained histological material.

As expected, mostly due to edema in the days following the cortical lesion, the volume of the lesion derived from the MRI scans is clearly larger than the final volume histologically determined, by a factor of about 10 to 20. The difference may also comprise a deviation between the two methods to measure the volume of the lesion: although the infusion was aimed to the gray matter, some spread to the white matter is likely, which may be detected on the MRI scans, whereas the histological assessment was limited to the gray matter.

Finally, for comparison, the volume of the lesion was tentatively calculated from the LSI data at the time point at which a territory with reduced blood flow was observed, corresponding to the lesion. Based on an estimation of the surface of the cortical territory with reduced cerebral blood flow as seen after 3.5 weeks in Mk-JH [Fig. 6(d)] and considering an average cortical thickness of 2 mm, the volume of the cortical lesion as derived from LSI data is estimated to be around 58 mm^3. Again, this figure is larger than the actual volume of the lesion histologically determined, but only by a factor of two to three in the comparison between LSI after 3.5 weeks and histology after four weeks. As the LSI approach does not permit an assessment of the cortical thickness in which cerebral blood flow is modified, one may compare in Mk-JH the extent of cortical surface exhibiting an increase of cerebral blood flow detected with LSI during the excitotoxic phase (immediately after infusion of ibotenic acid and one week later) with the cortical surface of the hypersignal observed from MRI one day and one week post-lesion. The cortical surface of the MRI hypersignal was 78.3 mm^2 at one day and 71.7 mm^2 at one week post-lesion, whereas the zone of increased blood flow corresponded to a cortical surface estimated at 22 mm^2, both on the day of ibotenic acid infusion and one week later.

4 Discussion

The present study, based on a parallel assessment of a cortical lesion using LSI and MRI in nonhuman primates, provides evidence that LSI and MRI are tools suitable to monitor the time course of a cortical lesion, for subsequent correlation with the behavioral recovery curve, at least in the present experimental conditions (monkey, ibotenic acid cortical lesion). Although the time course of LSI and MRI signals change in parallel in a time window of a few weeks post-lesion, there is no evidence for a direct relation between LSI and MRI signals, as the former measures cerebral blood flow whereas the latter reflects mostly edema (see below) and tissue infarct – degeneration. The real time LSI data during the surgery show that, when ibotenic acid is infused in the cerebral cortex at multiple adjacent sites in a bit less than an hour, there is an immediate increase of cerebral blood flow, which is still present after one week (Fig. 7). As far as the extent of the cortical lesion is concerned, the present study provides estimates of the ratio between the sizes of the lesion derived from LSI data and from MRI data during the few weeks following the damage, as well as with the size of the corresponding permanent lesion histologically assessed.

Moreover, the LSI and MRI data may contribute to a better understanding of mechanisms underlying functional recovery after cerebral cortex lesion, such as collateral blood or reperfusion after ischemic stroke.[28,30] The LSI method may also be suitable to assess whether cortical areas adjacent to the lesion change their activity, as they may contribute to the recovery, as shown in a rat model of M1 lesion.[26] The improvements of the LSI analysis method [heart beat compensation (HBC) filter, high resolution and low noise LSI] have successfully been applied to the present data set, revealing detailed and additional information on cerebral blood flow that are not visible in the MRI. The LSI adapted technique permitted here to monitor online the cerebral blood flow while ibotenic acid was infused in the cerebral cortex of macaque monkey to produce a permanent lesion. At the onset of ibotenic acid infusion, the cerebral blood flow dramatically increased almost immediately, followed by a slight reversal during the next five minutes (Fig. 7).

Follow-up studies are available in human subjects after stroke, during time windows ranging from 12 h,[42] one month,[43] and up to four months.[44] MRI is a standard tool used in the clinical evaluation of acute stroke, mainly based on the weighted-diffusion imaging setting, offering the best sensitivity to assess acute ischemic lesions for instance.[45,46] In the present study, the T2-weighted imaging setting was chosen as it provides better sensitivity and resolution to detect a chronic cortical lesion and, therefore, is better suited to conduct a longitudinal study over several weeks. Nevertheless, the T2 setting allowed detection of the ibotenic acid lesion in Mk-JH and in Mk-BI already relatively early, about 24 h post-lesion. This observation contrasts with previous T2 data in humans after stroke, exhibiting no hypersignal either immediately post-infarct or after 24 h.[43] This discrepancy may be explained by the different type of lesion, stroke in humans, and ibotenic acid in the macaque monkeys Mk-JH and Mk-BI. More consistent is the situation observed after about a week, with a hypersignal detected with T2 in both humans[43] and monkeys Mk-JH and Mk-BI (present study). After three to four weeks, there was again a discrepancy, as the T2 hypersignal was present in human subjects[43] but no longer in Mk-JH and Mk-BI. In human subjects after stroke, a T2 hypersignal was still present after four months.[44] However, the latter authors reported that the volume of the infarct lesion in humans significantly diminished in the chronic phase, possibly due to lesion consolidation-related changes. In Mk-JH and Mk-BI, similar changes may have happened, but even more rapidly in the present case of a much smaller ibotenic acid lesion, corresponding to a total disappearance of the lesion after 3.5 weeks in MRI. In macaque monkeys, in contrast to the present study, an ibotenic acid lesion in the hippocampus remained visible about 4 years later,[47] but the lesion was performed at the neonatal stage (12 to 16 days after birth), whereas in Mk-JH and Mk-BI the lesion took place at the adult stage, thus possibly accounting for this discrepancy (at least in part). After lesion of the hippocam-

pal formation in adult macaques with ibotenic acid infusion,[48] a prominent hypersignal was found in T2-weighted images after one week post-lesion (as is the case in the present study), but the hypersignal then weakened at two weeks post-lesion, before it gradually disappeared. The optimal time for post-lesion scan was thus identified as less than two weeks.[48]

The time course of the neurotoxic lesion observed here in the nonhuman primate is generally consistent with that reported from MRI data for the same type of lesion in the rat, either in the cerebral cortex[49] or in the striatum,[50,51] namely a hypersignal during a few days, followed then by a progressive decrease after one to two weeks. From the time course of the cortical lesion in the rat derived from MRI,[49] it was concluded that functional and behavioral investigations should be initiated about two weeks after the neurotoxic lesion to avoid transient confounding factors.

As far as cortical lesion produced by ibotenic acid injection in monkeys is concerned,[4,11,12,16,52–54] the present parallel LSI and MRI study extends previous information in the time dimension. As a result of ibotenic acid infusion, the excitotoxic increase of activity, as reflected by an increase of cerebral blood flow visualized with LSI, does not last only a few hours but it is still present after at least a week. The clinical consequence of the ibotenic acid infusion in M1 in monkeys has a very rapid time course as the flaccid paralysis of the contralateral hand occurs already 10 to 15 min after the infusion of ibotenic acid.[4] Based on the parallel time course of both LSI and MRI, the present data suggest that the MRI hypersignal is possibly associated, at least in part, to the excitotoxic activity of the ibotenic acid injections. After 3.5 weeks, the excitotoxic activity has disappeared in both LSI and MRI. The disappearance of the hypersignal in T2-weighted images could be correlated with the decrease of the cytotoxic edema, as previously reported in the rat.[49] This observation would then be in line with the time course reported after ibotenic acid injection in the hippocampal formation,[48] as well as with excitotoxic lesion in rats.[49–51] It remains to be determined at which precise time point (between one and 3.5 weeks) the excitotoxic activity disappears, to turn into a cortical region with diminished cerebral blood flow, as compared to the pre-lesion reference level. However, as previously claimed based on ibotenic acid lesion in the hippocampus of monkeys, the edema associated to the lesion may, to a large extent, contribute to the hypersignal in the MRI imaging during a few weeks post-lesion.[48] Interestingly, the same authors found that T2-weighted imaging obtained after one to two weeks post-lesion was an accurate predictor of the extent of the lesion determined a year later from post-mortem histology. In a study on macaque monkeys subjected to ibotenic acid lesion of the cortical areas MT (middle temporal) and MST (medial superior temporal),[54] the hypersignal in T2-weighted MRI imaging associated to the lesion remained visible after several months. However, the lesions were much larger than the present lesions in M1, as the total amount of ibotenic acid injected in MT and MST were about five to eight times bigger.

LSI was previously used in rats (ministroke models) to monitor the changes of cerebral flow at the surface of the cerebral cortex during and after blood vessels occlusion,[25–29] as well as the reperfusion after reversal of vascular ligation.[28] In these studies, the blood flow was measured with LSI during minutes and hours after the lesion, and up to 24 h in the reperfusion model.[28] Besides the very different type of lesion, ibotenic acid initially provoking (for at least a week) an increase of cerebral blood flow reflecting over-excitation, whereas vessels' occlusion generates a dramatic decrease of perfusion, the present study provides LSI measurements at much more distant time points from the lesion (one and 3.5 weeks). The permanent lesional property, characterized by a reduced cerebral blood flow, is established only between one and 3.5 weeks after infusion of ibotenic acid.

Due to limitations, mainly for ethical reasons, on the use of nonhuman primates in biomedical research, the present pilot experiment aimed at applying LSI on macaque monkeys was restricted to a single animal (acute experiment lasting about one month). As a consequence, no statistical data on LSI measurements could be provided. Based on the present pilot LSI data, the next step may be to develop a LSI chronic recording site from the cortical surface (below a transparent artificial dura, as previously reported[55–58]), including the lesion site (for instance M1) as well as adjacent cortical areas possibly contributing to the functional recovery (e.g., the premotor cortex). This approach may replace the monitoring of the cortical lesion based on MRI, in case the latter facility is not accessible for nonhuman primates, with the restriction however that LSI is invasive (chronic recording chamber). As LSI and MRI provides parallel data with respect to the time course of changes of the cortical lesion, if available, MRI may be preferred as it is noninvasive. Moreover, the present study gives an approximation on how much the size of the cortical lesion assessed by MRI during the few weeks post-lesion overestimates the lesion extent observable post-mortem on histological sections.

5 Conclusion

Using in-parallel morphological (MRI) and functional imaging (LSI) methods in a macaque monkey, the present study shows that a restricted excitotoxic lesion of the motor cortex in nonhuman primate leads to a marked hypersignal in parallel to a dramatic increase in blood flow, at least up to a week post-lesion. Traces of the lesion were still detectable using LSI after several weeks (about three to four weeks) in the form of a diminished cerebral blood flow as compared to pre-lesion, a time point at which the MRI signal had already returned to baseline. The presence of the lesion on a stable and long-term basis was corroborated by the histological post-mortem analysis.

Acknowledgments

The authors wish to thank the technical assistance of Dr. J. F. Brunet, Véronique Moret, Christine Roulin, Françoise Tinguely, and Christiane Marti (histology); Josef Corpataux, Laurent Bossy, Bernard Bapst and Bernard Morandi (animal house keeping); André Gaillard (mechanics), Bernard Aebischer (electronics), Laurent Monney (informatics), and Joël Baechler (MRI technician). We are grateful to Professor Bruno Weber and Dr. Fabrizio Croccolo for important discussions and help. This research was supported by the Swiss National Science Foundation [Grant Nos. 310000–110005 and 31003A-132465 to EMR, the National Centre of Competence in Research (NCCR) on "Neural plasticity and repair" (EMR), No. 2000020 – 126772 and 200020-117762 to FS].

References

1. G. Courtine, M. B. Bunge, J. W. Fawcett, R. G. Grossman, J. H. Kaas, R. Lemon, I. Maier, J. Martin, R. J. Nudo, A. Ramon-Cueto, E. M. Rouiller, L. Schnell, T. Wannier, M. E. Schwab, and V. R. Edgerton, "Can experiments in nonhuman primates expedite the translation of treatments for spinal cord injury in humans?," *Nat. Med.* **13**, 561–566 (2007).
2. J. P. Capitanio and M. E. Emborg, "Contributions of non-human primates to neuroscience research," *Lancet* **371**, 1126–1135 (2008).
3. R. N. Lemon, "Descending pathways in motor control," *Annu. Rev. Neurosci.* **31**, 195–218 (2008).
4. Y. Liu and E. M. Rouiller, "Mechanisms of recovery of dexterity following unilateral lesion of the sensorimotor cortex in adult monkeys," *Exp. Brain Res.* **128**, 149–159 (1999).
5. E. Schmidlin, T. Wannier, J. Bloch, and E. M. Rouiller, "Progressive plastic changes in the hand representation of the primary motor cortex parallel incomplete recovery from a unilateral section of the corticospinal tract at cervical level in monkeys," *Brain Res.* **1017**, 172–183 (2004).
6. E. Schmidlin, T. Wannier, J. Bloch, A. Belhaj-Saif, A. Wyss, and E. M. Rouiller, "Reduction of the hand representation in the ipsilateral primary motor cortex following unilateral section of the corticospinal tract at cervical level in monkeys," *BMC Neurosci.* **6**, 56 (2005).
7. T. Wannier, E. Schmidlin, J. Bloch, and E. M. Rouiller, "A unilateral section of the corticospinal tract at cervical level in primates does not lead to measurable cell loss in motor cortex," *J. Neurotrauma* **22**, 703–717 (2005).
8. P. Freund, E. Schmidlin, T. Wannier, J. Bloch, A. Mir, M. E. Schwab, and E. M. Rouiller, "Nogo-A-specific antibody treatment enhances sprouting and functional recovery after cervical lesion in adult primates," *Nat. Med.* **12**, 790–792 (2006).
9. P. Freund, T. Wannier, E. Schmidlin, J. Bloch, A. Mir, M. E. Schwab, and E. M. Rouiller, "Anti-Nogo-A antibody treatment enhances sprouting of corticospinal axons rostral to a unilateral cervical spinal cord lesion in adult macaque monkey," *J. Comp. Neurol.* **502**, 644–659 (2007).
10. P. Freund, E. Schmidlin, T. Wannier, J. Bloch, A. Mir, M. E. Schwab, and E. M. Rouiller, "Anti-Nogo-A antibody treatment promotes recovery of manual dexterity after unilateral cervical lesion in adult primates–re-examination and extension of behavioral data," *Eur. J. Neurosci.* **29**, 983–996 (2009).
11. M. Kaeser, A. F. Wyss, S. Bashir, A. Hamadjida, Y. Liu, J. Bloch, J. F. Brunet, A. Belhaj-Saif, and E. M. Rouiller, "Effects of unilateral motor cortex lesion on ipsilesional hand's reach and grasp performance in monkeys: relationship with recovery in the contralesional hand," *J. Neurophysiol.* **103**, 1630–1645 (2010).
12. M. Kaeser, J. F. Brunet, A. F. Wyss, A. Belhaj-Saif, Y. Liu, A. Hamadjida, E. M. Rouiller, and J. Bloch, "Autologous adult cortical cell transplantation enhances functional recovery following unilateral lesion of motor cortex in primates: a pilot study," *Neurosurg.* **68**, 1405–1417 (2011).
13. S. B. Frost, S. Barbay, K. M. Friel, E. J. Plautz, and R. J. Nudo, "Reorganization of remote cortical regions after ischemic brain injury: a potential substrate for stroke recovery," *J. Neurophysiol.* **89**, 3205–3214 (2003).
14. N. Dancause, S. Barbay, S. B. Frost, E. J. Plautz, D. F. Chen, E. V. Zoubina, A. M. Stowe, and R. J. Nudo, "Extensive cortical rewiring after brain injury," *J. Neurosci.* **25**, 10167–10179 (2005).
15. N. Dancause, S. Barbay, S. B. Frost, E. V. Zoubina, E. J. Plautz, J. D. Mahnken, and R. J. Nudo, "Effects of small ischemic lesions in the primary motor cortex on neurophysiological organization in ventral premotor cortex," *J. Neurophysiol.* **96**, 3506–3511 (2006).
16. Y. Murata, N. Higo, T. Oishi, A. Yamashita, K. Matsuda, M. Hayashi, and S. Yamane, "Effects of motor training on the recovery of manual dexterity after primary motor cortex lesion in macaque monkeys," *J. Neurophysiol.* **99**, 773–786 (2008).
17. D. G. Darling, M. A. Pizzimenti, D. L. Rotella, C. R. Peterson, S. M. Hynes, J. Ge, K. Solon, D. W. McNeal, K. S. Stilwell-Morecraft, and R. J. Morecraft, "Volumetric effects of motor cortex injury on recovery of dexterous movements," *Exp. Neurol.* **220**, 90–108 (2009).
18. A. F. Fercher and J. D. Briers, "Flow visualization by means of single exposure speckle photography," *Opt. Commun.* **37**, 326–330 (1981).
19. J. D. Briers, "Laser Doppler, speckle and related techniques for blood perfusion mapping and imaging," *Physiol, Meas* **22**(4), R35–R66 (2001).
20. A. K. Dunn, A. Devor, H. Bolay, M. L. Andermann, M. A. Moskowitz, A. M. Dale, and D. A. Boas, "Simultaneous imaging of total cerebral hemoglobin concentration, oxygenation, and blood flow during functional activation," *Opt. Lett.* **28**, 28–30 (2003).
21. A. K. Dunn, H. Bolay, M. A. Moskowitz, and D. A. Boas, "Dynamic imaging of cerebral blood flow using laser speckle," *J. Cereb. Blood Flow Metab.* **21**,195–201 (2001).
22. C. Ayata, A. K. Dunn, Y. Gursoy-Ozdemir, Z. Huang, D. A. Boas, and M. A. Moskowitz, "Laser speckle flowmetry for the study of cerebrovascular physiology in normal and ischemic mouse cortex," *J Cereb. Blood Flow Metab.* **24**, 744–755 (2004).
23. T. Durduran, M. G. Burnett, G. Yum, C. Zhoum, D. Furuyam, A. G. Yodh, J. A. Detrem, and J. H. Greenbergm, "Spatiotemporal quantification of cerebral blood flow during functional activation in rat somatosensory cortex using laser-speckle flowmetry," *J. Cereb. Blood Flow Metab.* **24**, 518–525 (2004).
24. B. Weber, C. Burger, M. T. Wyss, G. K. von Schulthess, F. Scheffold, and A. Buck, "Optical imaging of the spatiotemporal dynamics of cerebral blood flow and oxidative metabolism in the rat barrel cortex," *Eur. J. Neurosci.* **20**, 2664–2670 (2004).
25. J. S. Paul, A. R. Luft, E. Yew, and F. S. Sheu, "Imaging the development of an ischemic core following photochemically induced cortical infarction in rats using laser speckle contrast analysis (LASCA)," *Neuroimage* **29**, 38–45 (2006).
26. J. S. Paul, S. Fwu-Shan, and A. R. Luft, "Early adaptation in somatosensory cortex after focal ischemic injury to motor cortex," *Exp. Brain Res.* **168**, 178–185 (2006).
27. Z. Wang, P. Li, W. Luo, S. Chen, and Q. Luo, "Peri-infarct temporal changes in intrinsic optical signal during spreading depression in focal ischemic rat cortex," *Neurosci. Lett.* **424**, 133–138 (2007).
28. W. Luo, Z. Wang, P. Li, S. Zeng, and Q. Luo, "A modified mini-stroke model with region-directed reperfusion in rat cortex," *J. Cereb. Blood Flow Metab.* **28**, 973–983 (2008).
29. J. Luckl, C. Thou, T. Durduran, A. G. Yodh, and J. H. Greenberg, "Characterization of periinfarct flow transients with laser speckle and doppler after middle cerebral artery occlusion in the rat," *J. Neurosci. Res.* **87**, 1219–1229 (2009).
30. G. A. Armitage, K. G. Todd, A. Shuaib, and I. R. Winship, "Laser speckle contrast imaging of collateral blood flow during acute ischemic stroke," *J. Cereb. Blood Flow Metab.* **30**, 1432–1436 (2010).
31. W. J. Tom, A. Ponticorvo, and A. K. Dunn, "Efficient processing of laser speckle contrast images," *IEEE Trans. Med. Imaging* **27**, 1728–1738 (2008).
32. P. Zakharov, A. Völker, A. Buck, B. Weber, and F. Scheffold, "Quantitative modeling of laser speckle imaging," *Opt. Lett.* **31**, 3465–3467 (2006).
33. P. Zakharov, A. C. Völker, M. T. Wyss, F. Haiss, N. Calcinaghi, C. Zunzunegui, A. Buck, F. Scheffold, and B. Weber, "Dynamic laser speckle imaging of cerebral blood flow," *Opt. Express* **17**, 13904–13917 (2009).
34. A. C. Völker, P. Zakharov, B. Weber, A. Buck, and F. Scheffold, "Laser speckle imaging with an active noise reduction scheme," *Opt. Express* **13**, 9782–9787 (2005).
35. A. B. Parthasarathy, W. J. Tom, A. Gopal, Zhang, and A. K. Dunn, "Robust flow measurement with multi-exposure speckle imaging," *Opt. Express* **16**, 1975–1989 (2008).
36. P. C. Li, S. Ni, L. Zhang, S. Zeng, and Q. Luo, "Imaging cerebral blood flow through the intact rat skull with temporal laser speckle imaging," *Opt. Lett.* **31**, 1824–1826 (2006).
37. N. Hecht, J. Woitzik, J. P. Dreier, and P. Vajkoczy, "Intraoperative monitoring of cerebral blood flow by laser speckle contrast analysis," *Neurosurg. Focus* **27**(4), E11 (2009).
38. H. Cheng, Q. Luo, S. Zeng, S. Chen, J. Cen, and H. Gong, "Modified laser speckle imaging method with improved spatial resolution," *J. Biomed. Opt.* **8**, 559–564 (2003).
39. M. L. Beaud, E. Schmidlin, T. Wannier, P. Freund, J. Bloch, A. Mir, M. E. Schwab, and E. M. Rouiller, "Anti-Nogo-A antibody treatment does not prevent cell body shrinkage in the motor cortex in adult monkeys subjected to unilateral cervical cord lesion," *BMC Neurosci.* **9**, 5 (2008).

40. J. Bloch, M. Kaeser, Y. Sadeghi, E. M. Rouiller, D. E. Redmond Jr., and J. F. Brunet, "Doublecortin-positive cells in the adult primate cerebral cortex and possible role in brain plasticity and development," *J. Comp. Neurol*. **519**, 775–789 (2011).
41. P. Leroux, C. Hennebert, J. Cateau, N. Legros, O. Hennebert, V. Laudenbach, and S. Marret, "Neuroprotective effects vary across nonsteroidal anti-inflammatory drugs in a mouse model of developing excitotoxic brain injury," *Neuroscience* **167**, 716–723 (2010).
42. Y. Ozsunar, P. E. Grant, T. A. G. M. Huisman, P. W. Schaefer, O. Wu, A. G. Sorensen, W. J. Koroshetz, and R. G. Gonzalez, "Evolution of water diffusion and anisotropy in hyperacute stroke: significant correlation between fractional anisotropy and T2," *AJNR Am. J. Neuroradiol*. **25**, 699–705 (2004).
43. M. Thurnher, "Brain Ischemia – Imaging in acute stroke," *The Radiology Assistant*, www.radiologyassistant.nl/en/483910a4b6f14 (2008).
44. A. Ritzl, S. Meisel, H. J. Wittsack, G. R. Fink, M. Stiebler, U. Mödder, and R. J. Seitz, "Development of brain infarct volume as assessed by magnetic resonance imaging (MRI): follow-up of diffusion-weighted MRI lesions," *J. Magn. Reson. Imaging* **20**, 201–207 (2004).
45. J. L. Sunshine, R. W. Tarr, C. F. Lanzieri, D. M. D. Landis, W. R. Selman, and J. S. Lewin, " Hyperacute stroke: ultrafast MR imaging to triage patients prior therapy," *Radiology* **212**, 325–332 (1999).
46. A. E. Baird and S. Warach, "Magnetic resonance imaging of acute stroke," *J. Cereb. Blood Flow. Metab.* **18**, 583–609 (1998).
47. P. Lavenex, P. Banta Lavenex, and D. G. Amaral, "Spatial relational learning persists following neonatal hippocampal lesions in macaque monkeys," *Nat. Neurosci.* **10**, 234–239 (2007).
48. L. Malkova, C. K. Lex, M. Mishkin, and R. C. Saunders, "MRI-based evaluation of locus and extent of neurotoxic lesions in monkeys," *Hippocampus* **11**, 361–370 (2001).
49. N. Ben-Horin, S. Hazvi, P. Bendel, and R. Schul, "The ontogeny of a neurotoxic lesion in rat brain revealed by combined MRI and histology," *Brain Res*. **718**, 97–104 (1996).
50. J. John, V. Govindaraju, P. Raghunathan, and V. M. Kumar, "Magnetic resonance imaging of temporal changes of neurotoxic lesion in the rat," *Brain Res. Bull.* **40**, 273–277 (1996).
51. N. Shemesh, O. Sadan, E. Melamed, D. Offen, and Y. Cohen, "Longitudinal MRI and MRSI characterization of the quinolinic acid rat model for excitotoxicity: peculiar apparent diffusion coefficients and recovery of N-acetyl aspartate levels," *NMR Biomed*. **23**, 196–206 (2010).
52. W. T. Newsome, R. H. Wurtz, M. R. Dürsteler, and A. Mikami, "Deficits in visual motion processing following ibotenic acid lesions of the middle temporal visual area of the macaque monkey," *J. Neurosci*. **5**, 825–840 (1985).
53. W. H. Merigan, T. A. Nealey, and J. H. Maunsell, "Visual effects of lesions of cortical area V2 in macaques," *J. Neurosci.* **13**, 3180–3191 (1993).
54. K. Rudolf and T. Pasternak, "Transient and permanent deficits in motion perception after lesions of cortical areas MT and MST in the macaque monkey," *Cereb. Cortex* **9**, 90–100 (1999).
55. E. Shtoyerman, A. Arieli, H. Slovin, I. Vanzetta, and A. Grinvald, "Long-term optical imaging and spectroscopy reveal mechanisms underlying the intrinsic signal and stability of cortical maps in V1 of behaving monkeys," *J. Neurosci.* **20**, 8111–8121 (2000).
56. A. Arieli, A. Grinvald, and H. Slovin, "Dural substitute for long-term imaging of cortical activity in behaving monkeys and its clinical implications," *J. Neurosci. Methods* **114**,119–133 (2002).
57. L. M. Chen, B. Heider, G. V. Williams, F. L. Healy, B. M. Ramsden, and A. W. Roe, "A chamber and artificial dura method for long-term optical imaging in the monkey," *J. Neurosci. Methods* **113**, 41–49 (2002).
58. B. Heider, G. Jando, and R. M. Siegel, "Functional architecture of retinotopy in visual association cortex of behaving monkeys," *Cereb. Cortex* **15**, 460–478 (2005).

Appendix 2

Behavioral assessment of manual dexterity in non-human primates

Schmidlin E*, Kaeser M*, **Gindrat AD**, Savidan J, Chatagny P, Badoud S, Hamadjida A, Beaud ML, Wannier T, Belhaj-Saif A, Rouiller EM (2011). Journal of Visualized Experiments (57) e3258. DOI: 10.3791/3258

In this paper we gave a comprehensive description of the different behavioural tasks currently used in the laboratory to assess fine manual dexterity in macaque monkeys.

jove Journal of Visualized Experiments www.jove.com

Video Article

Behavioral Assessment of Manual Dexterity in Non-Human Primates

Eric Schmidlin*, Mélanie Kaeser*, Anne- Dominique Gindrat, Julie Savidan, Pauline Chatagny, Simon Badoud, Adjia Hamadjida, Marie-Laure Beaud, Thierry Wannier, Abderraouf Belhaj-Saif, Eric M. Rouiller

Department of Medicine, University of Fribourg

*These authors contributed equally

Correspondence to: Eric M. Rouiller at Eric.Rouiller@unifr.ch

URL: http://www.jove.com/details.php?id=3258

DOI: 10.3791/3258

Keywords: Neuroscience, Issue 57, monkey, hand, spinal cord lesion, cerebral cortex lesion, functional recovery,

Date Published: 11/11/2011

Citation: Schmidlin, E., Kaeser, M., Gindrat, A.D., Savidan, J., Chatagny, P., Badoud, S., Hamadjida, A., Beaud, M., Wannier, T., Belhaj-Saif, A., Rouiller, E.M. Behavioral Assessment of Manual Dexterity in Non-Human Primates. J. Vis. Exp. (57), e3258, DOI : 10.3791/3258 (2011).

Abstract

The corticospinal (CS) tract is the anatomical support of the exquisite motor ability to skillfully manipulate small objects, a prerogative mainly of primates[1]. In case of lesion affecting the CS projection system at its origin (lesion of motor cortical areas) or along its trajectory (cervical cord lesion), there is a dramatic loss of manual dexterity (hand paralysis), as seen in some tetraplegic or hemiplegic patients. Although there is some spontaneous functional recovery after such lesion, it remains very limited in the adult. Various therapeutic strategies are presently proposed (e.g. cell therapy, neutralization of inhibitory axonal growth molecules, application of growth factors, etc), which are mostly developed in rodents. However, before clinical application, it is often recommended to test the feasibility, efficacy, and security of the treatment in non-human primates. This is especially true when the goal is to restore manual dexterity after a lesion of the central nervous system, as the organization of the motor system of rodents is different from that of primates[1,2]. Macaque monkeys are illustrated here as a suitable behavioral model to quantify manual dexterity in primates, to reflect the deficits resulting from lesion of the motor cortex or cervical cord for instance, measure the extent of spontaneous functional recovery and, when a treatment is applied, evaluate how much it can enhance the functional recovery.

The behavioral assessment of manual dexterity is based on four distinct, complementary, reach and grasp manual tasks (use of precision grip to grasp pellets), requiring an initial training of adult macaque monkeys. The preparation of the animals is demonstrated, as well as the positioning with respect to the behavioral set-up. The performance of a typical monkey is illustrated for each task. The collection and analysis of relevant parameters reflecting precise hand manipulation, as well as the control of force, are explained and demonstrated with representative results. These data are placed then in a broader context, showing how the behavioral data can be exploited to investigate the impact of a spinal cord lesion or of a lesion of the motor cortex and to what extent a treatment may enhance the spontaneous functional recovery, by comparing different groups of monkeys (treated versus sham treated for instance). Advantages and limitations of the behavioral tests are discussed. The present behavioral approach is in line with previous reports emphasizing the pertinence of the non-human primate model in the context of nervous system diseases[2,3].

Video Link

The video component of this article can be found at http://www.jove.com/details.php?id=3258

Protocol

The overall scheme of the experiment is depicted in Figure 1.

1. Animal preparation and transfer to the behavioral laboratory

1. In the laboratory, prepare the behavioral set-up: fill the wells of the different test boards (tests 1 to 3 below) with the pellets, which serve as reward during the behavioral tests.
2. Transfer the monkey from the group housing room into a transfer cage. The monkey is trained to enter a tunnel giving access to the primate chair, with subsequent positioning of the head. The monkey's weight is measured, before transfer in the primate chair to the laboratory.

2. Test 1: Modified Brinkman board

1. This test, modified and adapted from previous reports[4,5], is the basic behavioral task of reference, to be conducted on every behavioral session. Initiate the video recording with the digital camera above the set-up (possibility also to place 2 additional cameras, one on each side of the board) and place the monkey in front of the Brinkman board.
2. Open for instance the right window on the primate chair to give access to the right hand. Using the right hand, the monkey retrieves the food pellets from the 50 slots (25 vertical and 25 horizontal).
3. After completion of the test, close the right window and refill the board with pellets.
4. Open the left window and repeat the test for the left hand.

5. Reward the animal at the end of the test with a few dried raisins or an almond, a procedure to be repeated at the end of each test to maintain the motivation during the whole daily session.

Additional information: Three digital video cameras are used to record the sequence for off-line processing, placed one above the board and one on each side of the board (to precisely assess the position of the fingers while performing the grasping). Within the same daily session, the monkey can perform another task (either task 2, and/or task 3 and/or task 4; to be distributed among the different days of the week). For the test 1, if the monkey started with the right hand on day 1, start with the left hand on day 2 and so on.

6. Optional: While the test performed above with one or the other hand separately allows comparing the performance of the left hand to the right hand (to identify the "dominant hand"), it is also possible at an early stage of the training to let the monkey perform the task with both hands simultaneously. If one hand is used more often than the other to grasp pellets, then it may be considered as the "preferred hand".

3. Test 2: Brinkman box (with and without visual control)

1. The Brinkman box comprises 20 wells (10 vertical and 10 horizontal). As compared to test 1, the monkey has to control the hand in a limited space, with reduced degrees of freedom to perform the precision grip movement. Fill the board with pellets and close the upper facet of the box, in order to conduct first the test in absence of visual control (relying on tactile exploration).
2. Place the monkey in front of the Brinkman box. Open the left window of the primate chair to test the left hand in absence of visual control. The monkey tries to retrieve the 20 pellets, while the sequence is recorded from a digital camera placed below the box.
3. Close the left window of the primate chair. Refill the board with pellets. Open the right window of the primate chair. The monkey repeats the test with the right hand in absence of visual control. Close the right window of the primate chair.
4. To test the ability to grasp pellets in the Brinkman box under visual control,open the top facet of the box.
5. Refill the box with pellets and the monkey performs the test using the right hand.
6. Close the right window of the primate chair. Refill the box with pellets.
7. Open the left window of the primate chair. The monkey performs the test using the left hand.Repeat step 2.5.

4. Test 3: Rotating Brinkman board

1. This test is comparable to the Brinkman board task (test 1), except that the board is rotating, forcing the monkey to anticipate the displacement of the board in one (clockwise) or the other (counter-clockwise) direction. Fill the board with pellets. The sequence is recorded with a digital camera placed above the set-up (possibility also to place 2 additional cameras, one on each side).
2. Open the right window of the primate chair. The monkey retrieves the pellets from the 32 wells, distributed on four concentric rows, while the board is turning clockwise.
3. Close the right window. Refill the board with pellets.
4. Open the left window of the primate chair. The monkey performs the test as in 4.2 with the left hand.
5. Repeat points 4.2 to 4.4, while the board is turning counterclockwise (one hand after the other). Repeat step 2.5.

5. Test 4: Reach and grasp drawer task

1. To combine prehension ability with the capacity to generate force, this test (derived from previous versions[6-11]) was designed so that the monkey has to open a drawer by exerting first a grip force on the knob of the drawer, followed by a load force to open the drawer, giving access to a pellet placed inside the drawer. The pellet is retrieved with the same hand while the drawer remains open, again using the precision grip. A digital camera is placed on top of the drawer, to record the trials for off-line control of the data (e.g. detection of erroneous trials).
2. Open the right window of the primate chair. The monkey performs 10 trials at each of the 5 different levels of resistance, using the right hand (to have at least 5 correct trials for each resistance level).
3. Repeat the test (50 trials) with the left hand. Repeat step 2.5.

Additional information: On the next behavioral daily session, alternate the hand with which the animal did the test first on the previous session.

6. End of behavioral session

1. After completion of the tests foreseen on that day, feed and reward the monkey with food in addition to the pellets received during the tests. Typically, the monkey receives cereals and fruits.
2. The monkey is returned to the group housing room with the mates.

The precise temporal sequence of the various tests performed is written on the protocol form.

7. Representative Results

The four behavioral tests illustrated above (**Figure 1**) have been used extensively in our laboratory in the context of studies aimed at investigating the functional recovery from lesion of the cervical spinal cord (**Figure 2A**) or of the motor cortex (**Figure 2B**), in absence or in presence of a treatment applied to enhance the spontaneous recovery[12-19].

For test 1 (*modified Brinkman board*), the analysis is focused on two parameters (**Figures 3 and 4A**): i) the score, given by the number of pellets retrieved by the monkey in the first 30 seconds, counted separately for the vertical slots and the horizontal slots (by replaying off-line the recorded video sequence); ii) the contact time (CT), defined as the time (duration) of contact between the fingers and the pellet (see also Figure 6, bottom series of pictures). It is the time interval between the insertion of the first finger (usually the index finger) into the slot to touch the pellet and the onset of retrieval of the pellet out of the well. The time interval is measured by replaying frame by frame the video sequence. The CT is measured for the first five vertical slots and the first five horizontal slots aimed by the monkey[16-18]. The graphs of the score illustrate the initial training phase, the pre-lesion plateau, the dramatic drop of score (usually to zero) immediately after the lesion, the progressive (spontaneous) functional recovery towards the post-lesion plateau. The functional recovery is expressed in % by the ratio of the median post-lesion score at plateau divided by the median pre-lesion score (plateau) *100 (**Figures 3 and 4A**). For the CT, as an increase reflects a deficit, the functional recovery expressed in % is

the ratio of the median pre-lesion CT (plateau) divided by the median post-lesion CT at plateau *100. The effect of treatments post-lesion, demonstrated based on the test 1, are illustrated in detail in previous reports from this laboratory[14,15,17]. A further analysis may address the issue of the strategy, namely the temporal sequence of slots visited by the monkey (**Figure 4B**).

For test 2 (*Brinkman box*), although the score can also be established as in test 1, a more meaningful parameter is the "total time", defined as the time interval between the picking of the pellet in the first slot and the picking of the pellet in the last (20^{th}) slot (**Figure 5**). A functional recovery can be computed and expressed in %. It is calculated using the median total time pre-lesion (plateau after training phase) divided by the median total time post-lesion at plateau *100.

For **test 3** (*rotating Brinkman board*), although the score can also be established as above (test 1), a sensitive parameter is the contact time (CT, defined as above in test 1), measured for the first ten slots (**Figure 6**).

For **test 4** (*.reach and grasp drawer task*), the set-up comprises several detectors, recording discrete events such as trial initiation (the hand interrupts a light beam placed in front of the panel), hand touching the knob, onset of drawer pulling, end of drawer opening, hand entering the slot (pick-in time), hand withdrawal from the slot (pick-out time). Force transducers on the knob allow measuring the grip force (exerted by the thumb and index finger pressing on the knob) and the load force (exerted to pull the drawer, to counteract different levels of resistance imposed on the drawer opening). The different levels of resistance opposing the opening of the drawer were obtained by changing the intensity of current applied to a rotative electromagnetic motor attached to the back of the drawer. The set-up is designed to apply a resistive force in parallel to the orientation of the opening of the drawer. Detailed scheme of the drawer set-up is available on request to the corresponding author. All these data are collected with the interface and software *Spike 2* and displayed as illustrated in **Figure 7**.

As previously reported1[4,15], these tasks represent the behavioral basis to investigate whether the spontaneous recovery from a lesion of the cervical cord may be enhanced with a specific treatment aimed at promoting axonal regeneration (**Figure 8**).

The retrieval score and the contact time parameters reflect different components of the manual dexterity: the first one includes the entire motor sequence (reaching, grasping, withdrawal of the hand, transport of the pellet to the mouth), whereas the second one is focused on the grasping phase only. These two parameters are particularly accurate and complementary for the modified and the rotating Brinkman board tasks. Whereas the score represents largely redundant information in these two tasks, the contact time in contrast provides more task-specific information due to the variability of the slots' positions in the rotating Brinkman board task, as compared to their static position in the modified Brinkman board task. The Brinkman box task differs from the two above mentioned tasks, as the degrees of freedom of movements with the hand are limited by the closed space. As a consequence, the positions of the different slots on the board within the Brinkman box play an important role in terms of difficulty to perform the manual prehension, due to the exiguity of the box. For instance, the grasping with the hand from the slots located on the right side of the box interferes with right lateral wall.

Consequently, the assessment of retrieval score limited to 30 seconds as in the modified Brinkman board would be biased depending on the position of the slots actually visited by the monkey during this restricted time period, generating a substantial variability from one session to another. For this reason, it is more appropriate to involve all slots (n=20) and therefore the parameter total time was chosen. In the modified Brinkman board, the total time was not considered, as the monkey may in some case loose motivation (for instance post-lesion) due to the large number of slots to be performed (n=50). Along the same line, the analysis of the contact time would implicate to take all the slots of the Brinkman box into consideration (whereas only the first five slots in the modified Brinkman board were considered as the position of the selected slots has little, if no impact on this parameter). Therefore, for the Brinkman box, we recommend in a first approach to determine the total time, as it was observed to be a highly pertinent and informational parameter, at least in our studies with monkeys subjected to a motor cortex lesion (no data available for spinal cord lesioned monkeys). Nevertheless, the contact time may be considered for the Brinkman box, but in a second step including all twenty slots, separately however for the horizontal and vertical slots (not shown).

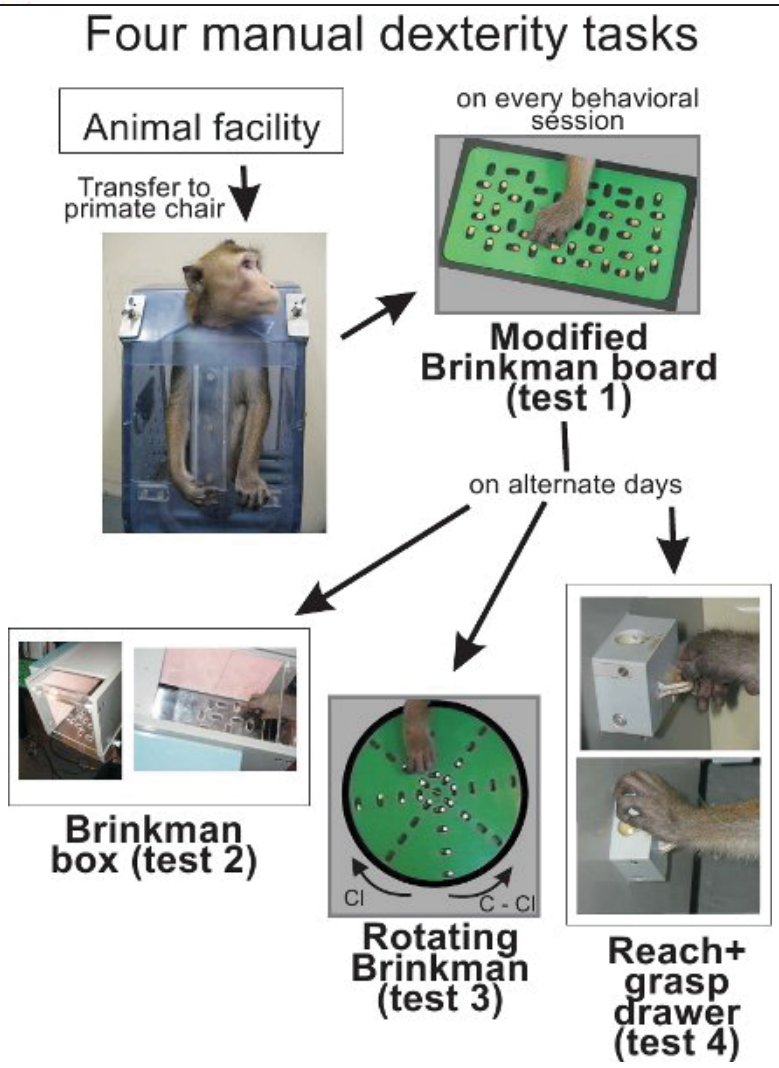

Figure 1. Overall scheme of the experiment. The animal is transferred from the animal facility into the primate chair, transported then to the behavioral laboratory. On each daily session, the monkey performs the test 1. On alternate days, the monkey then performs test 2, and/or test 3, and/or test 4. Some monkeys (especially motivated) may perform all tests on the same daily session. Food pellets (used as reward) were made of dried banana or glucose powder that is compressed in a round shape of about 4 mm in diameter. In all our behavioral tests, we use dustless precision pellets (45 mg) provided by BioServ, One 8th street, Suite One, Frenchtown, NJ 08825, USA.

The dimension of the modified Brinkman board is 240mm long and 140 mm wide, whereas the dimension of the slots is 15 mm long, 8 mm wide and 6 mm deep. The diameter of the board in the rotative Brinkman board is 114 mm.

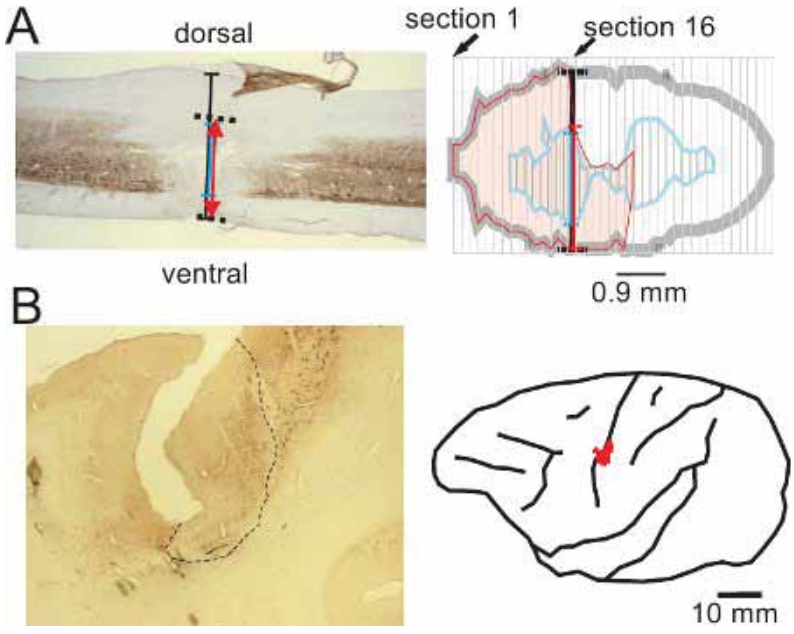

Figure 2. Representative (surgical) lesion of the cervical cord (panel A; modified from[15]) and (chemical) lesion of the motor cortex (panel B; modified from[16]), derived from corresponding histological sections, processed for SMI-32 staining. The maximal extent of the cervical cord lesion has been reconstructed from consecutive sagittal sections of the spinal cord (panel A), whereas the extent and position of the motor cortex lesion has been reconstructed from consecutive frontal sections of the brain and re-positioned on a lateral view of the corresponding brain hemisphere (red spot in panel B). The cervical cord lesion resulted from a transection with a surgery blade at the level C7-C8, resulting in a sub-hemisection interrupting unilaterally the main CS tract component in the dorsolateral funiculus, above the motoneurons controlling hand muscles[14,15,20]. The permanent cortical lesion was produced by infusion of ibotenic acid[13,16,17], at sites covering the hand representation previously established using intracortical microstimulation (ICMS, see[16,21,22]). The cortical lesion territory appears as an abrupt interruption of the SMI-32 staining of neurons in layers III and V in the rostral bank of the central sulcus (area delineated with the dashed line in panel B).

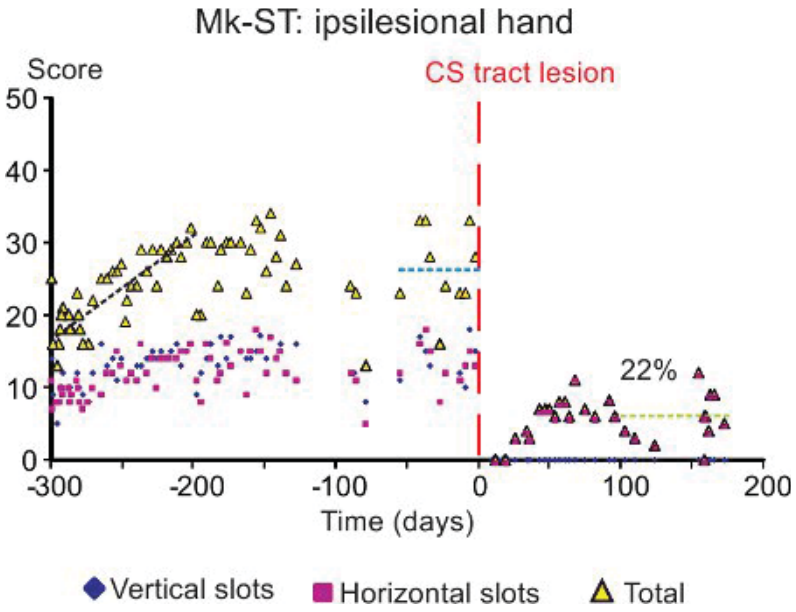

Figure 3. Representative data derived from the modified Brinkman board task (test 1) performed by a monkey subjected to a lesion of the spinal cord (as illustrated in Figure 2A). The graph shows the score (ordinate), separately for the vertical slots (blue symbols) and the horizontal slots (red symbols). The yellow symbols are for the sum of vertical and horizontal scores on a given daily session. In the abscissa, the time is for the consecutive days of the behavioral sessions. The vertical dashed redline (day 0) is the day at which the lesion was performed. Three different periods are highlighted: the first one (black dashed line) corresponds to the training period, the second one (blue dashed line) to the plateau of performance before the lesion, and the third one (green dashed line) to the plateau of recovered performance. Data modified from[15].

Figure 4A

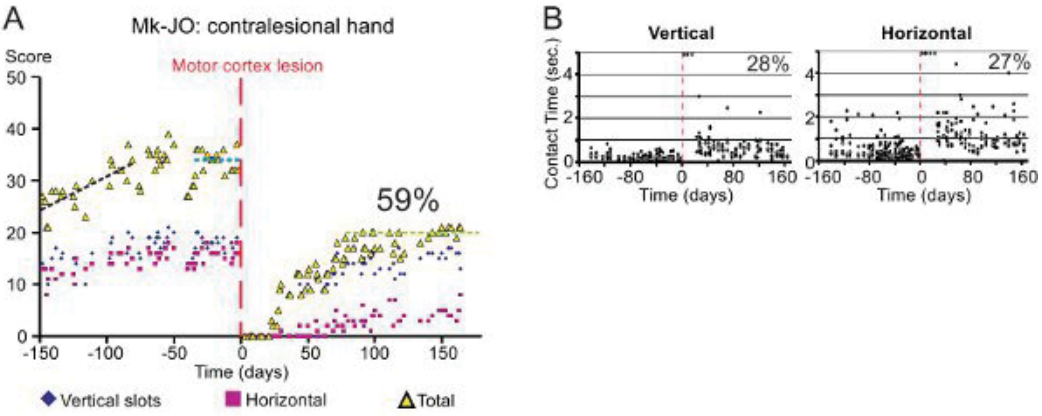

Figure 4B

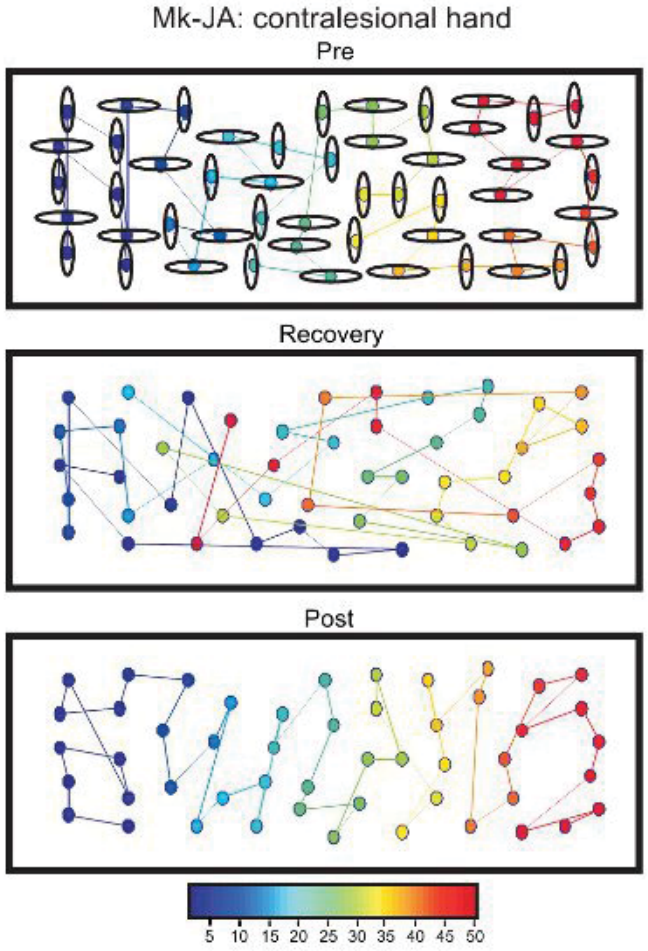

Figure 4A. Same as in Figure 3 (**test 1**), but in a monkey subjected to a lesion of the motor cortex (as illustrated in Figure 2B). The graphs show the score (panel A; same conventions as in Figure 3) and the contact time (CT; panel B) data. In the abscissa, the time is for the consecutive days of the behavioral sessions. The vertical dashed redline (day 0) is the day at which the lesion was performed. In panel B, each dot corresponds to the time of contact between the finger and the pellet in one slot (5 trials per orientation for each session; the grey bar represents the median value). Note that for the trials in which the animal could not perform the task (immediately after the lesion), the CT appears as a saturated value at 5 seconds. Data modified from[16,17].

Figure 4B. Analysis of strategy adopted in the modified Brinkman board task performed with the contralesional hand, before lesion of the motor cortex (Pre), during the recovery phase (Recovery) and post-lesion at plateau (Post). The color of each slot indicates the sequential order of the slots visited by the monkey in one session (the first slot visited is depicted by the darkest blue and the last slot visited by the darkest red). Note that pre-lesion, the monkey started on the left side of the board and scanned systematically towards right. During the recovery, the sequential order was changed. At plateau post-lesion, the strategy adopted pre-lesion re-appeared (systematic scan from left to right).

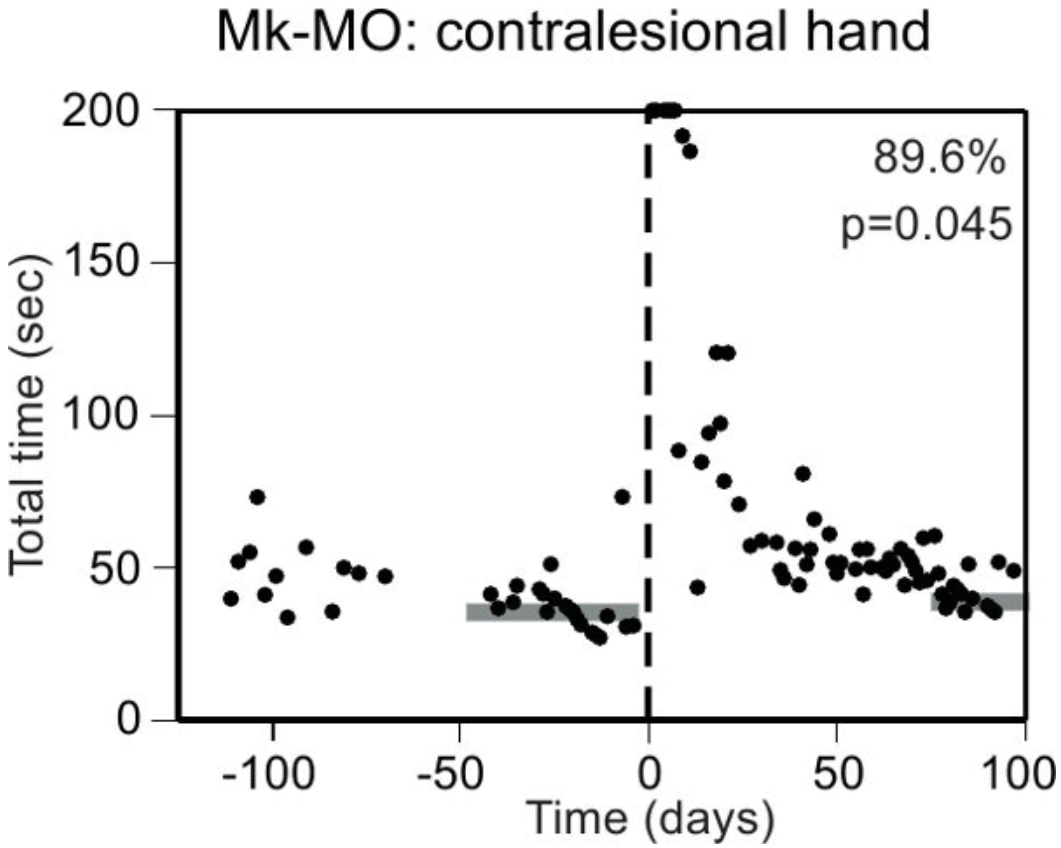

Figure 5. Representative data derived from the Brinkman box (test 2), for a monkey performing the task under visual control. The ordinate is the total time needed to empty the 20 wells along the daily sessions (abscissa), conducted before and after a lesion of the motor cortex (vertical dashed line). The dimensions of the accessible volume within the box are 1360 cm^3 (120mm*110mm*103mm). Note an initial phase of training, characterized by a larger variability of the total time from one session to the next. Immediately after the cortical lesion, the monkey was not able to perform the task (data points saturated at 200 seconds). The p value is statistically significant for the difference between the median total time pre-lesion (middle of the horizontal gray rectangle at the left) and the median total time post-lesion in the last sessions (middle of the horizontal gray rectangle at the right). The percentage of functional recovery is 89.6% whereas the volume of the motor cortex lesion was 41.8 mm^3. Data modified from[19].

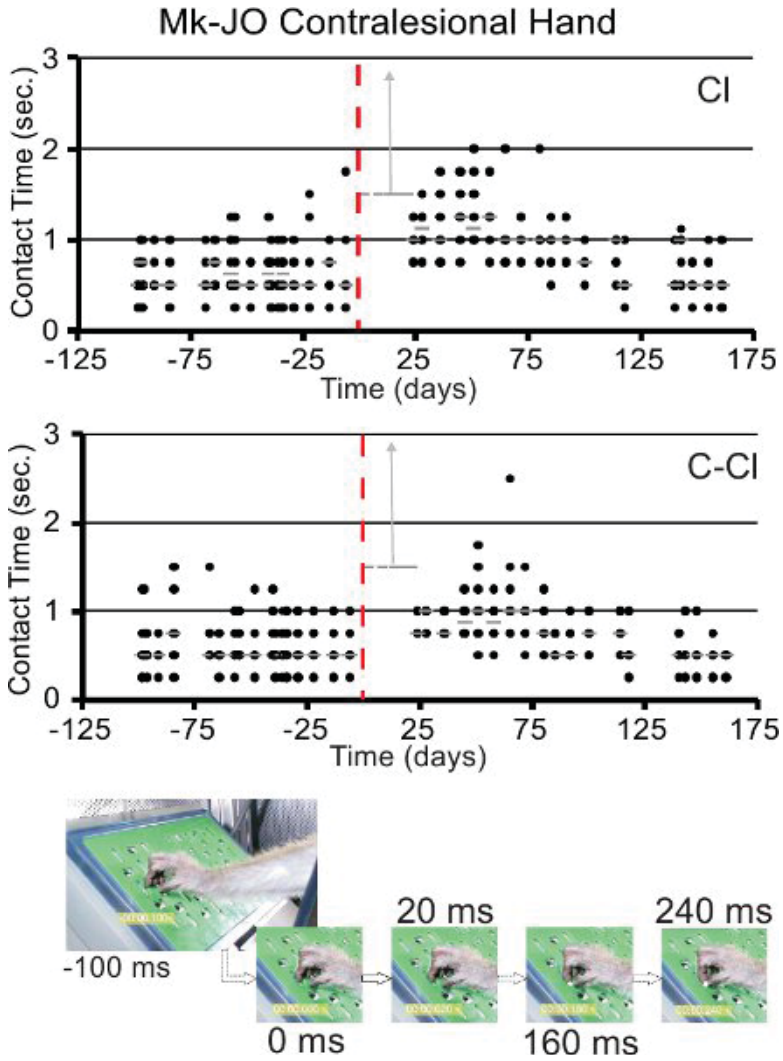

Figure 6. Representative results (top two graphs) derived from the rotative Brinkman board task (**test 3**), with illustration of the contact time measured pre-lesion and post-lesion, with the same conventions as in Figure 4A (panel B), for a monkey subjected to a lesion of the motor cortex (data modified from[17]). The top graph is for a clockwise ("CI") rotation of the board, whereas the bottom graph is for a counterclockwise ("C-CI") rotation of the board. The two vertical gray arrows indicate that the contact time was infinitely long in few sessions immediately after the lesion, as the monkey was unable to perform the task with the contralesional hand. The series of pictures at the bottom of the figure illustrate the method to measure the contact time (valid for both the modified Brinkman board and the rotating Brinkman board). The leftmost picture shows the hand approaching the slot containing the pellet (100 ms before contact between the index finger and the pellet). The next frame on the right corresponds to the time point of contact (0 ms). Then the contact time is defined as the time interval (in ms) running until reaching the frame (rightmost one) corresponding to the time point at which the pellet is taken out of the slot. The contact time here is 240 ms.

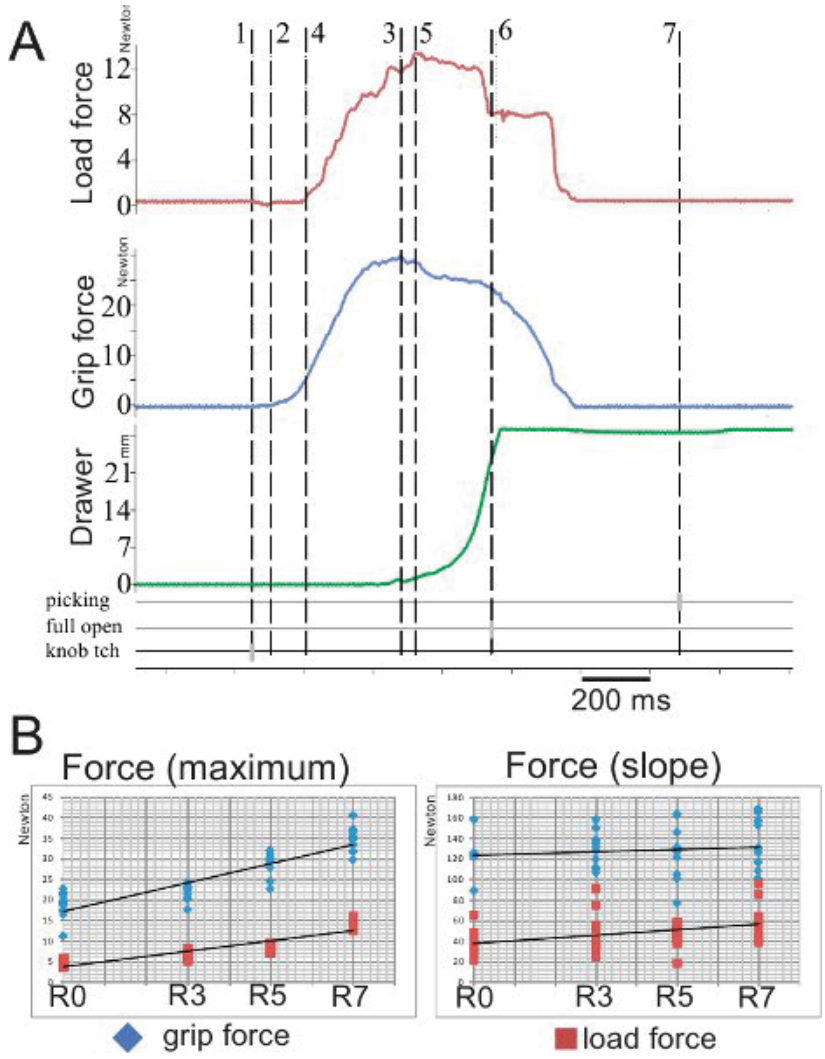

Figure 7. Representative data derived from a session performed by one monkey on the reach and grasp drawer task (**test 4**).

Panel A: Raw data corresponding to three parameters acquired online during a single trial: load force in red, grip force in blue and displacement of the drawer in green. Several markers were also acquired during the task: picking time corresponds to the time of the reward grasping, full open to the full opening of the drawer and knob touch (tch) to the time point when the animal first touches the knob. For the analysis, seven cursors were placed at critical time points in the unfolding task (e.g. 3 gray cursors on the bottom three horizontal lines): 1) time locked to the touch of the knob by the animal; 2) onset of grip force; 3) maximal grip force; 4) onset of load force; 5) maximal load force; 6) time locked when the drawer is fully open; 7) time locked to the picking time.

Panel B: Representation of the quantitative results for two parameters recorded during the task: the grip force (force used to grasp the knob between the index finger and the thumb) and the load force (force used to open the drawer) in two diagrams: the maximal value (left graph) and the slope value (from the onset to the max.; right graph).

Four out of the five different relative levels of resistance have been illustrated here: R0 (0 Newton), R3 (1.4 N), R5 (2.75 N) to R7 (5 N). The knob of the drawer has a triangular and flat shape. The base of the triangle attached to the drawer measures 20mm and the top (15 mm from the base) consists in a circular contour of 7 mm of diameter. The drawer itself has the following dimensions: length=50 mm; width=27 mm and height= 45mm.

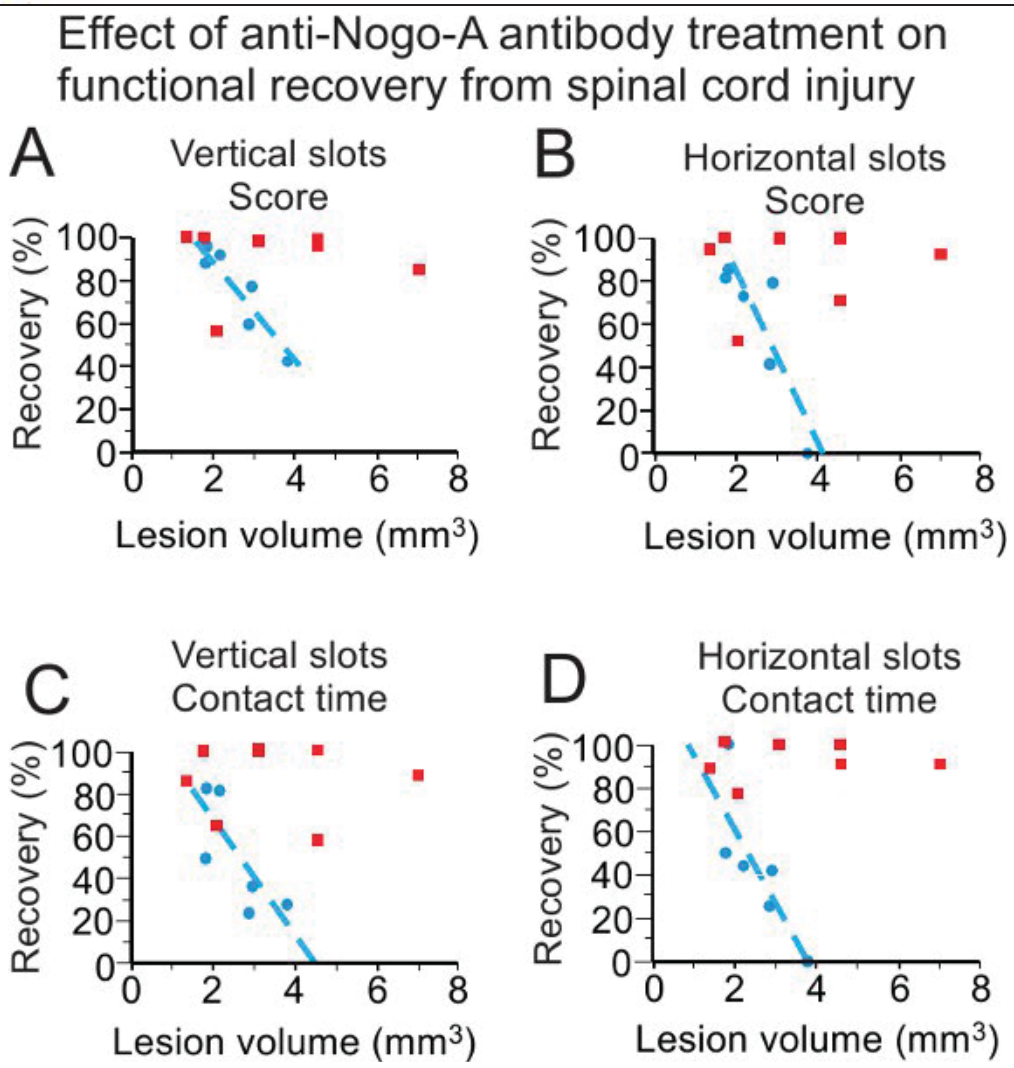

Figure 8. Reminder (modified from[15]) of the use of the behavioral **test 1** to investigate the possible effect of a treatment (anti-Nogo-A antibody) on the functional recovery from cervical cord lesion. For both scores and contact time, as well as for both slot orientations, the group of control antibody treated monkeys (blue symbols; n=6) recovers manual dexterity less well than the group of anti-Nogo-A antibody treated monkeys (red symbols; n=7), especially for large volumes of lesion. The 2 groups differ significantly with p=0.035 (panel A), p=0.022 (panel B), p=0.035 (panel C) and p=0.008 (panel D).

Discussion

Although the present behavioral tasks have been considered so far in our laboratory in the context of studies related to lesion of the cervical cord or to lesion of the motor cortex with the aim to test various treatments (see[14,15,17] and http://www.unifr.ch/neuro/rouiller >select "research" in the top bar menu, then > "motor system" > "recovery after lesion"), they may also have a broader application, as manual dexterity is also an aspect to consider in other pathologies, such as Parkinson disease (MPTP monkeys) or in case of sensory de-afferentation affecting proprioception and/or the sense of touch (especially the **test 2** in absence of visual control).

The behavioral tests proposed here are suitable to investigate the motor control of distal movements of the forelimb, as involved in manual dexterity. The specificity of the tests is demonstrated by the absence of deficit (except for a couple of days) in case of a lesion which does not impair relevant components of the control system: indeed, in case of a lesion placed more caudal than the motoneurons controlling hand muscles, there was no deficit. The pertinence of the test 1 can be appreciated by comparing on video sequences taken at two time points of the post-lesion recovery curve, which differ by an enhancement of functional recovery of 25%, possibly in relation to a cell therapy treatment[17].

In spite of some initial, relatively short training phase at beginning (lasting generally 2-3 months), the behavioral tests proposed here are relatively "natural" and straightforward, as compared to complex (e.g. conditional) tasks for which the training of the monkey may take nearly a year or more. The positive reinforcement is based on solid food, which is less sensitive on the ethical point of view than water deprivation, usually used in more complex tasks[23]. There is no need to deprive the monkeys from food to obtain stable and consistent results. The pellets received during the tasks represent the first access to the food on the day of the behavioral session (assuming that the monkey does not eat during the preceding night; however additional food may be given until the end of the afternoon of the preceding day). It is crucial that each monkey performs the behavioral session at the same time of the day, as well as respecting the same sequential order between the different monkeys forming a group in the housing room. As the monkeys are sensitive to external disturbing events, the behavioral tasks should be conducted in presence of background music, masking potential disturbing noise coming from neighboring rooms or laboratories. It is crucial that during the whole duration of the experiment (from initial training up to the last daily experimental session, a period of several months if not years), a given monkey is placed daily under the supervision of the same experimenter.

The present behavioral tests, used since several years in our laboratory to quantify manual dexterity, are to some extent comparable to other tests of manual dexterity recently reported in the literature[24-28]. There is however a crucial need to standardize tests across different laboratories (for better comparison), which is a tentative goal of the present report. On demand, the detailed properties of the set-ups illustrated here for tests 1-4 can be provided by the corresponding author, in order to replicate them. Beyond the issue of regenerative medicine (recovery from lesion of spinal cord or cerebral cortex), the present palette of tests may be suitable to address in normal non-human primates developmental issues (e.g. time course of motor development of dexterous movements), to investigate lateralization aspects (hand preference/dominance) and to decipher evolutionary questions by comparing the motor abilities of different species of primates, including human subjects. Note however that the dimensions of the apparatuses should be adapted according to the digits' size (thickness and length) of the primate species, as it may influence the task performance. In the present study, the tests were conducted on macaca fascicularis monkeys, ranging from 2.5 to 8 years old and weighing between 2.5 and 8 kg. The length of the index finger (used first to manipulate the pellets) ranges from 32 to 35 mm, whereas the circumference of the distal phalanx (tip) of the index finger was between 22 and 25 mm in the monkeys included in our studies. As tested in previous experiments, the same grasping tests are suitable for macaca mulatta as well.

All experiments were conducted in accordance with the *Guide for the Care and Use of Laboratory Animals* (1996) and approved by local (Swiss) veterinary authorities. All experimental procedures on the monkeys, as well as the detention conditions in the animal facility, were described in detail in recent reports from our laboratory: see references 12-18.

Disclosures

No conflicts of interest declared.

Acknowledgements

The authors would like to thank Prof. M.E. Schwab, Dr. P. Freund, Dr. A. Wyss, Dr. S. Bashir, Dr. A. Mir, Dr. J. Bloch, Dr. J.F. Brunet, Dr. J. Aebischer, Dr. A. Meszaros, Dr. V. Goetschman for their contribution to previous experiments and analyses. The experimental set-ups were constructed by André Gaillard, Bernard Aebischer and Laurent Monney. In the animal facility, the monkeys were placed under the supervision of professional animal caretakers: Josef Corpataux, Laurent Bossy and Jacques Maillard. The behavioral tests and analysis of the data, as well as histology, were conducted with the highly valuable contributions of laboratory technicians: Véronique Moret (also web master), Françoise Tinguely, Christine Roulin, Monica Bennefeld, Christiane Marti and Georgette Fischer. This work was supported by the Swiss National Science Foundation, grants No 31-61857.00, 310000-110005, 31003A-132465 (EMR), 310030-118357, 31003A-104061 (TW), 310030-120411 (ABS), PZ00P3_121646 (ES), Novartis Foundation; The National Centre of Competence in Research (NCCR) on "Neural plasticity and repair".

References

1. Lemon, R.N. Descending pathways in motor control. *Annu. Rev. Neurosci.* **31**, 195-218 (2008).
2. Courtine, G., *et al.* Can experiments in nonhuman primates expedite the translation of treatments for spinal cord injury in humans? *Nat. Med.* **13**, 561-566 (2007).
3. Capitanio, J.P. & Emborg, M.E. Contributions of non-human primates to neuroscience research. *Lancet.* **371**, 1126-1135 (2008).
4. Brinkman, C. Supplementary motor area of the monkey's cerebral cortex: short- and long-term deficits after unilateral ablation and the effects of subsequent callosal section. *J. Neurosci.* **4**,918-929 (1984).
5. Brinkman, J. & Kuypers, H.G. Cerebral control of contralateral and ipsilateral arm, hand and finger movements in the split-brain rhesus monkey. *Brain.*, 653-674 (1973).
6. Kazennikov, O., *et al.* Temporal structure of a bimanual goal-directed movement sequence in monkeys. *Eur. J. Neurosci.* **6**, 203-210 (1994).
7. Kazennikov, O., *et al*. Neural activity of supplementary and primary motor areas in monkeys and its relation to bimanual and unimanual movement sequences. *Neuroscience.* **89**, 661-674 (1999).
8. Kermadi, I., Liu, Y., Tempini, A., & Rouiller, E.M. Effects of reversible inactivation of the supplementary motor area (SMA) on unimanual grasp and bimanual pull and grasp performance in monkeys. *Somatosens. Mot. Res.* **14**, 268-280 (1997).
9. Kermadi, I., Liu, Y., Tempini, A., Calciati, E., & Rouiller, E.M. Neuronal activity in the primate supplementary motor area and the primary motor cortex in relation to spatio-temporal bimanual coordination. *Somatosens. Mot. Res.* **15** , 287-308 (1998).
10. Kermadi, I., Liu, Y., & Rouiller, E.M. Do bimanual motor actions involve the dorsal premotor (PMd), cingulate (CMA) and posterior parietal (PPC) cortices? Comparison with primary and supplementary motor cortical areas. *Somatosensory and Motor Research.* **17**, 255-271 (2000).
11. Wannier, T., Liu, J., Morel, A., Jouffrais, C.& Rouiller,E.M. Neuronal activity in primate striatum and pallidum related to bimanual motor actions. *NeuroReport.* **13**, 143-147 (2002).
12. Rouiller, E.M. *et al.* Dexterity in adult monkeys following early lesion of the motor cortical hand area: the role of cortex adjacent to the lesion. *Eur. J. Neurosci.* **10**, 729-740 (1998).
13. Liu,Y., & Rouiller, E.M. Mechanisms of recovery of dexterity following unilateral lesion of the sensorimotor cortex in adult monkeys. *Exp. Brain. Res.* **128**, 149-159 (1999).
14. Freund, P. *et al.* Nogo-A-specific antibody treatment enhances sprouting and functional recovery after cervical lesion in adult primates. *Nature. Med.* **12**, 790-792 (2006).
15. Freund, P. *et al.* Anti-Nogo-A antibody treatment promotes recovery of manual dexterity after unilateral cervical lesion in adult primates--re-examination and extension of behavioral data. *Eur. J. Neurosci.* **29**, 983-996 (2009).
16. Kaeser, M. *et al.* Effects of Unilateral Motor Cortex Lesion on Ipsilesional Hand's Reach and Grasp Performance in Monkeys: Relationship With Recovery in the Contralesional Hand. *J. Neurophysiol.* **103**, 1630-1645 (2010).
17. Kaeser, M. *et al*. Autologous adult cortical cell transplantation enhances functional recovery following unilateral lesion of motor cortex in primates: a pilot study. *Neurosurgery.* **68**, 1405-1417 (2011).
18. Bashir, S. *et al.* Short-term effects of unilateral lesion of the primary motor cortex (M1) on Ipsilesional hand dexterity in adult macaque monkeys. *Brain Structure and Function.* (In Press, 2011).
19. Hamadjida, A. *et al.* Influence of anti-Nogo-A treatment on the reorganization of callosal connectivity of the premotor cortical areas following unilateral lesion of primary motor cortex (M1) in adult macaque monkeys (Submitted, 2011).
20. Jenny, A.B. & Inukai, J. Principles of motor organization of the monkey cervical spinal cord. *J. Neurosci.* **3**, 567-575 (1983).
21. Schmidlin, E., *et al*. Progressive plastic changes in the hand representation of the primary motor cortex parallel incomplete recovery from a unilateral section of the corticospinal tract at cervical level in monkeys. *Brain Research.* **1017**, 172-183 (2004).

22. Schmidlin, E., *et al*. Reduction of the hand representation in the ipsilateral primary motor cortex following unilateral section of the corticospinal tract at cervical level in monkeys. *BMC Neuroscience.* **6:56**, (2005).
23. Prescott, M.J., *et al*. Refinement of the use of food and fluid control as motivational tools for macaques used in behavioural neuroscience research: report of a Working Group of the NC3Rs. *J. Neurosci. Methods.* 193,167-188 (2010).
24. Darling, W.G., *et al*. Volumetric effects of motor cortex injury on recovery of dexterous movements. *Exp. Neurol.* **220**, 90-108 (2009).
25. Darling, W.G., *et al*. Minimal forced use without constraint stimulates spontaneous use of the impaired upper extremity following motor cortex injury. *Exp. Brain. Res.* **202**, 529-542 (2010).
26. McNeal, D.W., *et al*. Selective long-term reorganization of the corticospinal projection from the supplementary motor cortex following recovery from lateral motor cortex injury. *J. Comp. Neurol.* **518**, 586-621 (2010).
27. Nishimura, Y., *et al*. Time-dependent central compensatory mechanisms of finger dexterity after spinal cord injury. *Science.* 318, 1150-1155 (2007).
28. Pizzimenti, M.A., *et al*. Measurement of reaching kinematics and prehensile dexterity in nonhuman primates. *J. Neurophysiol.* **98**, 1015-1029 (2007).

Appendix 3

Distinction between hand dominance and hand preference in primates: a behavioral investigation of manual dexterity in nonhuman primates (macaques) and human subjects

Chatagny P*, Badoud S*, Kaeser M, **Gindrat AD**, Savidan J, Fregosi M, Moret V, Roulin C, Schmidlin E, Rouiller EM (2013). Brain and Behavior 3:575-595, DOI: 10.1002/brb3

Several behavioural tasks were used here in our macaque monkeys as well as in humans to distinguish hand dominance and hand preference, either notion being commonly misunderstood and wrongly substituted for the other.

Brain and Behavior

Open Access

Distinction between hand dominance and hand preference in primates: a behavioral investigation of manual dexterity in nonhuman primates (macaques) and human subjects

Pauline Chatagny*, Simon Badoud*, Mélanie Kaeser, Anne-Dominique Gindrat, Julie Savidan, Michela Fregosi, Véronique Moret, Christine Roulin, Eric Schmidlin & Eric M. Rouiller

Unit of Physiology, Department of Medicine, Faculty of Sciences and Fribourg Center for Cognition, University of Fribourg, Chemin du Musée 5, CH-1700 Fribourg, Switzerland

Keywords
Bimanual coordination, handedness, intermanual difference, motor performance, precision grip

Correspondence
Eric M. Rouiller, Unit of Physiology, Department of Medicine, Faculty of Sciences and Fribourg Center for Cognition, University of Fribourg, Chemin du Musée 5, CH-1700 Fribourg, Switzerland.
Tel: +41 26 300 86 09; Fax: +41 26 300 96 75; E-mail: eric.rouiller@unifr.ch

Funding Information
This study was supported by Swiss National Science Foundation, grants No. 31-61857.00, 310000-110005, 31003A-132465, and FZFS-0_144990 (E. M. R.), 31-121646 (E. S.); the Novartis Foundation; the National Centre of Competence in Research (NCCR) on "Neural plasticity and repair" and the Christopher Reeves Foundation (Springfield, NJ).

Received: 2 January 2013; Revised: 29 June 2013; Accepted: 30 June 2013

doi: 10.1002/brb3.160

*Equal first authorship.

Abstract

Background: The present study aimed to determine and confront hand preference (hand chosen in priority to perform a manual dexterity task) and hand dominance (hand with best motor performance) in eight macaques (*Macaca fascicularis*) and in 20 human subjects (10 left-handers and 10 right-handers). **Methods:** Four manual dexterity tests have been executed by the monkeys, over several weeks during learning and stable performance phases (in controlled body position): the modified Brinkman board, the reach and grasp drawer, the tube and the bimanual board tasks. Three behavioral tests, adapted versions from the monkeys tasks (modified Brinkman board, tube and bimanual board tasks), as well as a handedness questionnaire, have been conducted in human subjects. **Results:** In monkeys, there was a large disparity across individuals and motor tasks. For hand dominance, two monkeys were rather right lateralized, three monkeys rather left lateralized, whereas in three monkeys, the different parameters measured were not consistent. For hand preference, none of the eight monkeys exhibited a homogeneous lateralization across the four motor tasks. *Macaca fascicularis* do not exhibit a clear hand preference. Furthermore, hand preference often changed with task repetition, both during training and plateau phases. For human subjects, the hand preference mostly followed the self-assessment of lateralization by the subjects and the questionnaire (in the latter, right-handers were more lateralized than left-handers), except a few discrepancies based on the tube task. There was no hand dominance in seven right-handers (the other three performed better with the right hand) and in four left-handers. Five left-handers showed left-hand dominance, whereas surprisingly, one left-hander performed better with the right hand. In the modified Brinkman board task, females performed better than males, right-handers better than left-handers. **Conclusions:** The present study argues for a distinction between hand preference and hand dominance, especially in macaque monkeys.

Introduction

How is handedness defined? Commonly, handedness means hand preference. For most people, the preferred hand is the hand which is most efficient to perform specific manual dexterity tasks (e.g., writing, manipulating objects or tools, etc.). In the present study, in line with a previously proposed concept (e.g., Hopkins et al. 1992; Triggs et al. 2000), we propose to emphasize the distinction between two hand attributes: hand preference and hand dominance.

The hand of preference is defined as the hand with which subjects prefer to work on a specific task, instinctively and without concern whether this hand is actually the most efficient one. In bimanual tasks for instance (e.g., tapping a nail with a hammer, knitting, eating with a fork, and a knife, etc.), the preferred hand is the hand which executes the most complex action or the manipulative role, whereas the nonpreferred hand acts mainly as postural support. In the above mentioned bimanual tasks, they need to be learned, whereas other bimanual tasks are

more instinctive and they are also observed in nonhuman primates (e.g., peeling a fruit, cracking a nut with a stone, etc.). In contrast to hand preference, hand dominance refers to the hand which shows the best efficiency to perform a particular unimanual action (Serrien et al. 2006), thus reflecting an intermanual difference of motor performance. The general aim of the present study was to assess separately hand preference and hand dominance in eight adult long-tailed macaque monkeys (*Macaca fascicularis*) and in 20 young adult human subjects.

Population-level right-handedness (preference for the right hand) was considered for a long time as a feature of human being (Raymond et al. 1996). During the last 20 years, several studies demonstrated that handedness for specific manual tasks is also present in nonhuman primates, from prosimians to great apes (e.g., Masataka 1989; Ward et al. 1990, 1993; Fagot and Vauclair 1991; Spinozzi et al. 1998; Lacreuse et al. 1999; Hopkins et al. 2011). Whereas 90% of humans are right-handed (Coren and Porac 1977; Raymond and Pontier 2004), the percentage and the direction of the lateralization vary among the nonhuman primates (see e.g., Papademetriou et al. 2005; mainly for reaching tasks). Concerning the great apes, a recent study by Hopkins et al. (2011) showed population right-handedness, except for Orangutans, which tend to use preferentially the left hand. These results are consistent with other studies (Lacreuse et al. 1999; Wesley et al. 2001; Hopkins et al. 2002, 2003, 2004, 2005; Sherwood et al. 2007). Baboons were also found to be right-handed at population level (Fagot and Vauclair 1988; Vauclair et al. 2005). However, some divergent observations were reported (Pouydebat et al. 2010), concluding to the difficulty to establish a stable handedness among Gorillas, based on different behavioral tasks. In Old World monkeys, handedness seems to be less consistent among the family (Westergaard et al. 1997, 2001a,b), as it appears to depend on the species, especially in Macaques. Although some macaques, such as *Macaca mulatta*, exhibited population-level left-handedness when they performed a specific task (also *Macaca fuscata*, see Murata et al. 2008), other species like *M. fascicularis* did not exhibit any manual bias at the population-level for the same tasks (tube task, reaching to food morsel; Westergaard et al. 1997, 2001a,b; see also Lehman 1980b). The above data for *M. mulatta* are not consistent with previous observations derived from food reaching tests (Lehman 1978a), which showed roughly equal numbers of right- and left-handed individuals. Furthermore, the latter author and others reported that handedness was accentuated with monkeys' age, as well as with task repetition (e.g., Lehman 1978a,b, 1980a,b; Westergaard and Suomi 1996; Westergaard and Lussier 1999; Zhao et al. 2012). Similarly, Hopkins (2004) found a less prominent handedness among Old and New World monkeys in comparison to the great apes. It is, however, interesting to highlight that, for some investigators (e.g., Lehman 1980a, 1989; Hopkins et al. 1989; Fagot and Vauclair 1991; Uomini 2009), these disparate results may depend on the task used to determine handedness (see also Spinozzi et al. 1998, 2007). Indeed, these authors showed that the complexity of the task plays an important role. A high-level manual activity involves, most of the time, a manual bias at the population-level, whereas a simple and low-level task does not. A typical example of high-level manual performance is the precision grip (opposition of thumb and usually index finger to grasp an object), requiring the cooperation of several muscles of hand and arm, tendons, ligaments, and the stabilization of the upper limb to ensure a better effectiveness (e.g., Lemon 1993, 2008; Porter and Lemon 1993). Bimanual tasks are considered as high-level ones, involving a coordination of different limbs and movements. As demonstrated in squirrel monkeys, hand preference is correlated to an asymmetry in functional topography of motor cortex between the two hemispheres, with a greater distal forelimb representation in the dominant hemisphere, opposite the preferred hand (Nudo et al. 1992). Asymmetries in the primary motor cortex related to handedness was reported in great apes (Hopkins and Pilcher 2001; Hopkins et al. 2002, 2010; Hopkins and Cantalupo 2004; Dadda et al. 2006; Sherwood et al. 2007) and in humans (e.g., Dassonville et al. 1997).

Hand preference and hand dominance were each determined based on three adapted manual tasks, which belong to high-level manual activities, for both human subjects and monkeys (*M. fascicularis*). Two tests are bimanual coordinated tasks: the bimanual Brinkman board task (Mark and Sperry 1968) and the tube task (Hopkins 1995), whereas the third test is the modified Brinkman board task (original test: Brinkman and Kuypers 1973; see also Brinkman 1984), performed either unimanually or with both hands at the same time. Monkeys had to perform an additional task, the reach and grasp drawer task, whereas humans had to answer a handedness questionnaire, which allowed us to confirm the self-assessment of each subject and, then, to compare the self-assessment with the results derived from the manual dexterity tests. More specifically, the aim of the study was to test the hypothesis that, in *M. fascicularis*, hand preference is variable across tasks and individuals, the dominant hand does not systematically correspond to the preferred hand, whereas human subjects exhibit more systematic lateralization (hand preference) and the preferred hand generally corresponds to the most dexterous hand (dominant hand).

Material and Methods

Nonhuman primate subjects

The experiments were conducted on eight adult female monkeys (*M. fascicularis*), aged between 6 and 7 years old at the beginning of the tests (weight: 3–3.9 kg) and housed in 45 m^3 rooms with four other animals. The monkeys were neither food nor water deprived (see e.g., Kaeser et al. 2010; Schmidlin et al. 2011). None of the animals had executed the different manual dexterity tasks before, so they were totally naïve. The experimental protocol has been approved by the local ethical committee on animal experimentation and it was in accordance with the *Guidelines for the Care and Use of Laboratory Animals* (ISBN 0-309-05377-3; 1996), as well as authorized by local (Canton of Fribourg) and federal (Swiss) veterinary authorities. The present experiments were covered by the official authorization numbers FR 192/07E, FR 206/08, FR 17/09, FR 18/10, FR 22010. The experimental procedures were designed to minimize pain and suffering for the animals. In the part of the present study on monkeys, the protocol was restricted to behavioral assessment, without any surgical or pharmacological intervention. The macaque monkeys originate initially from an officially recognized breeding center in China and were imported via a quarantine center in Europe (Harlan, Milano, Italy), where they stayed during a few months within a large group of a couple of dozen animals from the same origin. After arrival in our animal facility, the animals were habituated during 1–2 months to the new environment, before starting the habituation procedure (2–3 months duration) aimed at transferring the monkey on a free-will basis to the primate chair (see Schmidlin et al. 2011). The present behavioral experiments were then initiated when the monkeys were comfortable with the primate chair.

During each behavioral test, the monkey sat in a primate chair (see Schmidlin et al. 2011), made of Plexiglas® (Transparent PVC, Notz Plastik AG, Biel, Switzerland), with an adjustable opening on top allowing free head movements although the monkey is restrained. The primate chair also comprises two independent sliding doors at the front, allowing execution of manual dexterity tasks with both hands, separately or simultaneously (Schmidlin et al. 2011). Each experimental session was recorded with one to three digital video cameras, depending on the task (drawer, tube, and bimanual board tasks with one camera; modified Brinkman board task with three cameras; Schmidlin et al. 2011). The duration of a typical daily behavioral session was about 60 min and the experiments were conducted with background music to cover possible disturbing, external noise. At the end of the session, the animals received their daily ration of food, composed of cereals, fruits, and vegetables, in addition to the rewards (food pellets) received during the tests.

Human subjects

The human subjects were 20 persons (students) aged between 18 and 30 years old. The human experiments were conducted in the context of practical courses for students at the University of Fribourg and the subjects gave their full consent to the experimental protocol. They agreed that the data may be used anonymously for the present study. The human subjects first declared themselves either as left- or as right-handers and it corresponded to the hand they used to write. Based on this initial self-declaration, there were ten left-handers (six men and four women) and ten right-handers (four men and six women). The size of each of these two groups ($n = 10$) was chosen as to approximately match the group size of monkeys ($n = 8$). Given the human population bias for right-hand preference (about 90%), self-declared left-handers were deliberately recruited, thanks to a large pool of students available on the campus. It is expected that the self-declared left-handers are less lateralized than the self-declared right-handers.

Each human subject was enrolled in a single behavioral session (lasting about 60–90 min) and he/she executed three manual dexterity tasks, before responding to the handedness questionnaire at the end of the session. The set-ups for the three manual dexterity tasks were positioned on a table and the behavioral session was recorded with a digital video camera. The subjects began with the modified Brinkman board task, followed by the bimanual board task, and finally, the tube task. Before the beginning of the tests, the subjects sat on a chair in the middle and in front of the experimental table. They had to adjust the height of the chair to feel comfortable.

Behavioral tasks

The assessment of handedness was based on a palette of behavioral manual dexterity tasks, in which macaque monkeys ($n = 8$) and human subjects ($n = 20$) were enrolled. For both monkeys and human subjects, typical video sequences illustrating the various behavioral tasks described below can be visualized on the following website: http://www.unifr.ch/neuro/rouiller/research/PM/pm1.html.

Modified Brinkman board task

The modified Brinkman board and its different adapted versions from the original test of Brinkman and Kuypers (1973) were used routinely for behavioral and motor control studies in macaques (Brinkman 1984; Rouiller

et al. 1998; Liu and Rouiller 1999; Freund et al. 2009; Kaeser et al. 2010, 2011, 2013; Schmidlin et al. 2011). The modified Brinkman board for monkeys (Fig. 1A, left panel) is made of a rectangular board of Perspex® with 50 rounded rectangular slots: 25 slots are oriented horizontally and 25 vertically. Each slot measures 6 mm deep, 14 mm long, and 7 mm wide. The board itself measures 22 cm length, 12 cm wide, and 1.2 cm thick. At the beginning of the test, each slot is filled with a banana or sugar flavored pellet (diameter 4 mm). The size of slots permits the monkeys to grasp the pellets only by performing the precision grip, generally using the thumb and the index finger (or rarely another finger, with a flexion of the distal phalanx). Retrieval from the horizontal slots is more difficult than from the vertical ones, because it involves also a rotation of the wrist, either a radial deviation or an ulnar deviation, depending on the position of the corresponding slot on the board (Freund et al. 2009). The board was positioned in front of the monkey with 40° of inclination from horizontal. During each daily session, the animal has used firstly both hands, then each individual hand successively by alternating daily the hand used first. The daily protocol for this task thus comprises three consecutive tests, with retrieval of 50 pellets in each, lasting overall about 10 min, including the time interval to refill the modified Brinkman board with pellets in between the three tests. With respect to the board, the monkey was placed in a middle position (when performing the task with both hand simultaneously), or slightly at the left, or at the right, when using only the right or the left hand, respectively, in such a manner that the hand performing the task is aligned to the set-up. Video sequences illustrating this task can be visualized on the website: http://www.unifr.ch/neuro/rouiller/research/PM/pm1.html (video sequences 1–3) or in a recent visualized experimental report (Schmidlin et al. 2011).

The Brinkman board model, adapted for human subjects (Fig. 1A, right panel), is made of a wooden board of 58 cm long and 28.5 cm wide and it comprises 50 rounded rectangular slots of 4.3 cm long, 2.2 cm wide, and 1.8 cm deep (25 oriented vertically and 25 oriented horizontally). It is tilted with a 30-degree angle from horizontal. Before the beginning of a session, each slot is filled with a bolt (external diameter: 1.8 cm, internal diameter: 1 cm). The bolts replace the food pellets used for the same tests on monkeys. The slots were designed in a manner that subjects have to use the precision grip to retrieve the bolts, and their spatial arrangement is identical to that of the modified Brinkman

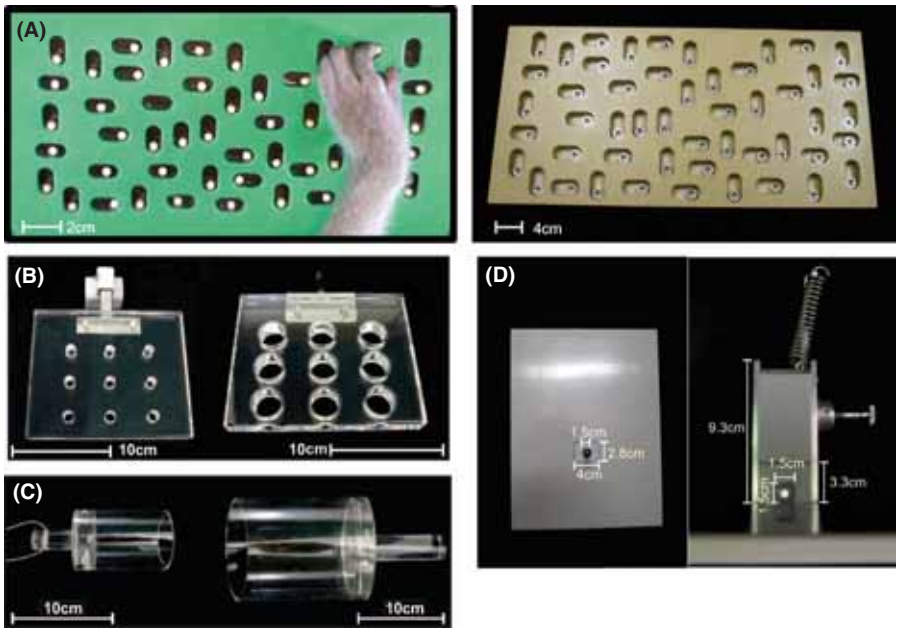

Figure 1. Pictures illustrate the experimental set-ups used in the different behavioral tasks for monkeys and for human subjects. In panel (A), the modified Brinkman board used for monkeys is shown on the left, with each slots filled with a banana pellet, whereas its version adapted for human subjects is shown on the right with each slot filled with a bolt. See text for dimensions of the board and slots. Panel (B) shows the bimanual Brinkman board used for monkeys (on the left) and for humans (on the right). Similarly, in panel (C), the tube used for monkeys is shown on the left and the version adapted for humans on the right. See text for dimensions of the boards, slots, and tubes. In panel (D), the bimanual reach and grasp drawer set-up (used for monkeys only) is shown in a front view (left picture) and from top (right picture). In the top view, the slot in the drawer is clearly visible (with one white pellet inside), as well as the spring at the back of the drawer, imposing to hold the drawer open with one hand while grasping the pellet with the other hand.

board used for monkeys. In a single behavioral session, the human subjects had to execute the grasping of the 50 bolts as fast as possible, taking one bolt at a time, and putting it into a plastic box located in front of the board in a middle position. The human subjects were not allowed to throw the bolt into the box. These rules contributed normalizing the test. The subjects performed the task 20 times, using alternatively 10 times the right hand and 10 times the left hand (right, left, right, etc.). The experimenter determined with which hand the subject had to begin (see http://www.unifr.ch/neuro/rouiller/research/PM/pm1.html [video sequences 4–5]).

Bimanual Brinkman board task

This task was adapted from the bimanual coordinated task of Mark and Sperry (1968). Our bimanual board is made of transparent acrylic glass (PMMA or Plexiglas®); Fig. 1B). The model for monkeys (Fig. 1B, left panel) measures 15.8 cm long, 13.1 cm large, and has a thickness of 2 cm. It comprises nine holes. Each hole has an upper diameter of 9.5 mm and a lower diameter of 7 mm and contains a sticky reward, like sultana or a little piece of apple. The board is fixed with an inclination of 20–30° from horizontal. The primate chair was placed in the front of the board and the two sliding doors were opened to allow access with both hands simultaneously. The monkeys had to retrieve the reward using both hands at the same time and following one or the other of two possible strategies (see below: analysis of data). One daily session included three to five repetitions of the whole board, with retrieval of each reward. Each hole represented an individual trial (see http://www.unifr.ch/neuro/rouiller/research/PM/pm1.html [video sequence 6]).

The model of the bimanual board adapted for human subjects (Fig. 1B, right panel) is a transparent acrylic glass board of 16 cm long, 13 cm wide, 2 cm thick, and comprising nine holes (diameter of 2.2 cm). The board is fixed with 30° of inclination from horizontal. Before the test started, each hole was filled with a pellet in modeling clay. Using both hands, the human subjects had to take only one pellet at a time and to put it into a plastic box placed in the front of the board. In one session, the subject had to empty the board 20 times. Each hole represented an individual trial (see http://www.unifr.ch/neuro/rouiller/research/PM/pm1.html [video sequence 7]).

The tube task

This bimanual task was inspired by the tube task of Hopkins (1995), used to determine handedness in Chimpanzees and later in Old World monkeys (Zhao et al. 2012). Our tube, in transparent acrylic glass (PPMA or Plexiglas®), was adapted to macaques with the following dimensions: the handle measures 4 cm long and 2 cm diameter, the tube itself is 9 cm long from the outside and 7 cm deep from the inside, with an external diameter of 6 cm and an internal diameter of 5 cm. At the bottom of the tube, there is a slot of 0.5 cm in diameter and 0.7 cm deep (Fig. 1C; left panel). The slot was filled with a sticky reward like sultana or little pieces of apple. The tube was attached to a rope by the handle and hung, in such a way that it was placed in front of the primate chair, aligned with the central bar between the sliding doors. The basis of the tube was positioned at the level as the basis of the sliding doors. The test was performed with the two sliding doors open and the animal had to hold the suspended tube with one hand while reaching the reward in the tube with the other hand and bring it to the mouth. A daily session comprised 10–20 trials (see http://www.unifr.ch/neuro/rouiller/research/PM/pm1.html [video sequence 8]).

The model of the tube adapted for human subjects is also made of acrylic glass tube (PPMA or Plexiglas®) with the following dimensions (Fig. 1C, right panel): the tube itself measures 14.7 cm long, 12.8 cm deep, with an external diameter of 12 cm and an internal diameter of 11 cm. The handle is 9.5 cm long and has a diameter of 3 cm. The slot positioned at the bottom of the tube is 2.2 cm in diameter and 0.9 cm deep. The reward was a candy (*Yupi strawberry kiss* or *Yupi MarshMallow*). A second tube was available for human subjects with smaller hands: the dimensions are the same, except the external diameter of 9 cm and the internal diameter of 8 cm. The tube was positioned vertically on the table, with the handle upwards. Starting with the hands placed on the table on each side of the tube, the human subjects had to collect the reward from the tube using both hands. They had the possibility to eat the reward or to give it to the experimenter. Then, the human subjects had to put the tube back on the table at its initial location. The task was performed 20 times to complete the session. One trial was achieved when the human subjects grabbed the tube with one hand while, simultaneously, they took the reward with the other hand (see http://www.unifr.ch/neuro/rouiller/research/PM/pm1.html [video sequence 9]).

Reach and grasp drawer task

This bimanual task was used for the monkeys only and it is a simplified version of the set-up previously described (Kazennikov et al. 1994; Kermadi et al. 1998, 2000; Schmidlin et al. 2011). The primate chair was placed in front of the drawer with both sliding doors opened, so that the monkey used both hands. Because of a spring mechanism, once open, the drawer had to be maintained with one hand to avoid that it closed back, while the monkey

used the other hand to grasp the pellet, which was initially placed in a slot dig inside the drawer. The dimensions of the object are indicated on the Figure 1D. During one session, the animal executed about five to 15 trials. One trial was achieved when the monkey opened the drawer with one hand, kept it open, and grasped the pellet with the other hand (see http://www.unifr.ch/neuro/rouiller/research/PM/pm1.html [video sequence 10]).

Handedness questionnaire

At the end of the manual dexterity tasks, the human subjects were asked to answer a handedness questionnaire, elaborated by MacManus (2009). It was chosen because it fills several pertinent criteria to assess handedness in human subjects (Oldfield 1971). The questions dealt with actions of daily life such as: with which hand do you write, do you hold a potato while you are peeling it, do you throw a ball, etc.

Analysis of data

The data of the behavioral tasks were analyzed manually from the recorded video sequences. The software VirtualDubMpeg2® (Developper Avery Lee, free software, www.virtualdub.org) allowed visualizing the video sequences frame by frame, corresponding to a time resolution of 40 msec (acquisition at 25 frames per second). The data were processed first in Excel® worksheets, before they were transferred to Sigmastat®/Sigmaplot® (Systat Software Inc., www.sigmaplot.com) and SPSS® (SPSS Inc., Chicago, IL) allowing more elaborated graphic representation and statistical analysis.

The hand dominance was determined based on a single task, the modified Brinkman board task performed with one hand imposed at a time. Two types of data were analyzed for the monkeys (Schmidlin et al. 2011). (i) The score, defined as the number of pellets correctly retrieved during the first 30 sec; (ii) The contact time (CT), defined as the time interval between the first contact of a finger (most often the index finger) with the pellet and the moment when the fingers left the slot with the reward. The CT is a pertinent parameter in addition to the score, as the latter can sometimes be biased. Indeed, the animal may be disturbed by external noises, or may exhibit a lack of motivation or concentration. In such cases, the monkey may interrupt the test, leading to a distortion of the score. Moreover, the CT truly measures the actual manipulation of the pellets with the fingers. The CT was measured for the first five horizontal and the first five vertical slots in the 20 last daily sessions at plateau, whereas the score was calculated for every daily session. The onset of the plateau was defined, when the learning curve tended to saturate (as estimated by visual inspection), as the first value in the nearly flat curve of the score that was not exceeded by one of the five following score values. For human subjects, the analysis of hand dominance was based mainly on the score in 30 sec, although the CT was also established for comparison in a sample of subjects.

The hand preference for monkeys was determined based on four tests: the modified Brinkman board task, when the animal was free to use both hands simultaneously, the reach and grasp drawer task, the tube task, and the bimanual Brinkman board task. For human subjects, two tests were considered, the tube task and the bimanual Brinkman board task, as well as the questionnaire indicating their self-assessed hand preference. For the tube task, the preferred hand was defined as the hand used to grasp the reward into the tube, playing the manipulative role, whereas the other hand, holding the tube, played the postural role. The preferred hand (left hand or right hand) was determined for each tube task trial performed by the subject (humans and monkeys), in order to calculate the handedness index (HI) (see below). For the bimanual board task, the subjects (humans and monkeys) used two different strategies to retrieve the reward. In the first one, the hand above the board pushed the reward while the other hand collected it below the board. In the second one, the hand positioned below the board pushed up the reward using one finger (usually the index finger) and the other hand grasped it above the board, performing the precision grip. In the first strategy (adopted in more than 98% of trials in five out of eight monkeys), the preferred hand is the one pushing the reward. Indeed its role is manipulative, whereas the role of the other hand is postural. For the second strategy, the preferred hand is the one retrieving the reward, as its action is more manipulative and more challenging (precision grip), as compared to the role of the other hand (one finger used). Additionally, the board has an inclination, making this movement still more difficult. This second strategy was used in about half of the trials in one monkey (Mk-MI) and it was predominant in two other monkeys (Mk-CA and Mk-AN; 68% and 98%, respectively). For the reach and grasp drawer task (in monkeys only), the preferred hand is the hand grasping the reward (manipulative role) while the other hand, the postural one, holds the drawer.

For these three tasks (bimanual Brinkman board task, reach and grasp drawer task, tube task), we computed the HI (Westergaard et al. 1997; Spinozzi et al. 1998; Hopkins et al. 2004; Schmitt et al. 2008), defined as follows: the number of trials the right hand (R) was used as preferred hand minus the number of times the left hand (L) was used as preferred hand, divided by the total number of trials:

$$HI = (R-L)/(R+L)$$

Consequently, a negative HI reflects a left bias whereas a positive HI reflects a right bias. The HI (lateralization) ranges between +1 (strongly right-handed) and −1 (strongly left-handed).

For the modified Brinkman board task, we measured the score in 30 sec when the animal was free to use both hands, and counted the number of pellets grasped with each hand. The hand with the highest score is considered as the preferred hand.

For the questionnaire, we calculated a handedness score by using the criteria of MacManus (2009):

> *"Laterality scores (laterality indices):*
> *Score all the items as −1 = Always left, −0.5 = Usually left, 0 = Either, +0.5 = Usually right and +1 = Always right. For items 4 (dish), 6 (jar), and 9 (potato) a strong right-hander would answer left. These three items should therefore be reverse scored by changing the sign on the values given previously (i.e., +1 = Always left, etc.). Having done this, then one can obtain the overall laterality score, an average of all 11 items."*

The score was then transformed into percentage (−100% indicating strongly left-handed and +100%, strongly right-handed).

The statistical analysis was conducted as follows. For the tube task, the reach and grasp drawer task, and the bimanual Brinkman board task, we used a binomial test (SPSS®; see Fig. 7). For the scores of the modified Brinkman board task, we used either the paired *t*-test or the Wilcoxon signed-rank test (Sigmastat®). Finally, for the CT derived from the modified Brinkman board task, we used either the unpaired *t*-test or the Mann–Whitney *U* test (Sigmastat®).

In order to limit the duration of the behavioral session with human subjects to a reasonable extent, the modified Brinkman board task using both hands simultaneously, as well as the reach and grasp drawer task, were not performed with human subjects. These tests, aimed in the monkeys to determine their preferred hand, were considered redundant for human subjects with the handedness questionnaire.

Results

Hand dominance: unimanual modified Brinkman board task

Monkeys

For monkeys, the hand dominance was determined based on the total score in 30 sec (sum of vertical and horizontal slots in all behavioral sessions) and the CT (measured for the first five horizontal and the first five vertical slots) in the 20 last recorded sessions of the modified Brinkman board task, at plateau. The performance of one hand was compared to the performance of the other hand, measured in the two consecutive unimanual tests carried out on the same day. The dominant hand is the hand exhibiting a higher score, respectively, a shorter CT, than the opposite hand. For this specific analysis of hand dominance, only the score at plateau was taken into consideration (see Fig. 2A). A typical example of the score data is illustrated for one monkey (Mk-AT: left and right hand for total, vertical and horizontal slots) in Figure 2A, with a vertical dashed line separating the plateau phase from the preceding learning phase.

The top panel of Figure 2B represents the distribution of the scores for the left and the right hands for each monkey at plateau, in the form of box and whiskers plots. In Mk-DI, immediately after the end of the learning phase, there was a transient period with a decrease in the number of grasped pellets (most likely due to a temporary drop of motivation), corresponding to a first plateau. Later, the level of score corresponding to the end of the learning phase reappeared, corresponding to a second plateau, which was considered for the data of the top panel in Figure 2B. Overall, three monkeys exhibited a significant difference of manual dexterity reflected by the score between the hands, namely Mk-AN, Mk-CA, and Mk-MA. The first one performed better with the left hand ($P = 0.036$), whereas Mk-CA and Mk-MA were more dexterous with the right hand ($P = 0.002$ and $P < 0.001$, respectively). Mk-AT, Mk-DI, Mk-LO, Mk-MI, and Mk-TH did not show any significant difference of manual dexterity between hands at plateau, as far as the total score is concerned.

The CT data are plotted in the two bottom panels of Figure 2B. As the combination of movements required to grasp pellets were different for the two slot orientations, the CT was plotted separately for the vertical slots (middle panel in Fig. 2B) and for the horizontal slots (bottom panel in Fig. 2B). Overall, and as expected, the CTs for the vertical slots tended to be shorter (less challenging task) than the CTs for the horizontal slots. It is important to recall that the shorter the CTs, the better the performance. For the vertical slots, the CTs were significantly shorter for the left hand in Mk-AN and Mk-DI ($P = 0.002$ and $P = 0.005$, respectively), whereas they were significantly shorter for the right hand in Mk-CA and Mk-LO ($P < 0.001$ for both). For the other monkeys (Mk-AT, Mk-MA, Mk-MI, and Mk-TH), there was no significant difference of CTs between the two hands for the vertical slots. Considering the horizontal slots, the CTs were significantly different between the two hands for seven out of the eight monkeys, as only Mk-AN

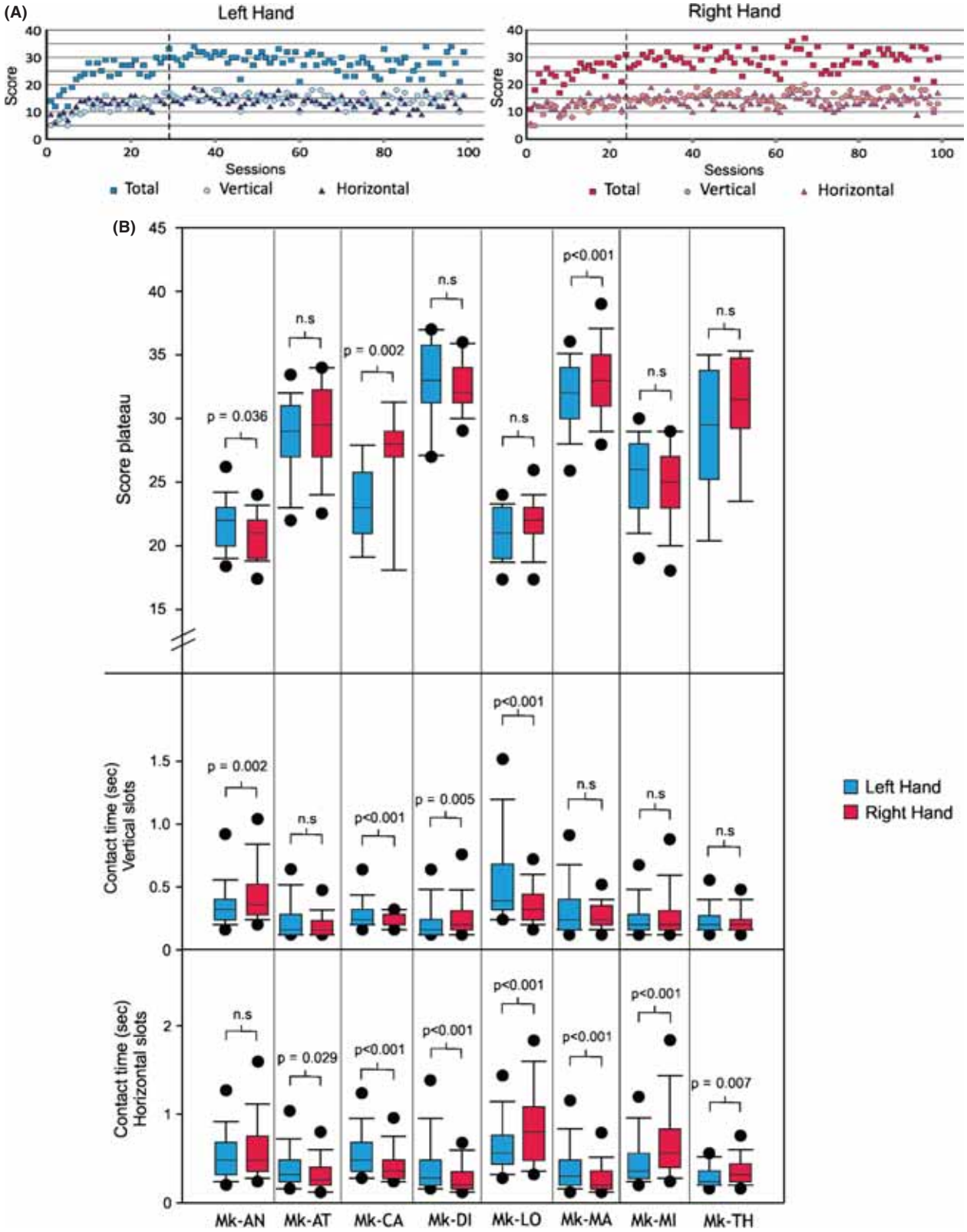

Figure 2. Hand dominance analysis for monkeys. An example of scores (Mk-AT) for the left and the right hand when the use of the hand was imposed in the modified Brinkman board task is shown in panel (A). Along the abscissa, the values refer to the consecutive daily session numbers, incremented by one for each individual session, irrespective of the actual date of the session. The regular interval between two consecutive sessions is thus not representative of the number of actual days separating the two sessions. In panel (B), three graphs in the form of box and whiskers plots represent for each monkey the distribution of the total scores (sum of horizontal and vertical slots) at the plateau (top graph), the distribution of contact times (CT, in seconds) for the vertical slots (middle graph) and for the horizontal slots (bottom graph), for the left hand (blue) and the right hand (red). These data concern the results when the use of one hand was imposed in the unimanual modified Brinkman board task. The statistical comparisons between the two hands in each daily session were performed using the paired *t*-test (normality test passed) or the nonparametric Wilcoxon rank signed test (normality test failed) for the score data (paired for the left hand and the right hand in a given daily session). In contrast, the CT data (five values per daily session for each slot orientation) are not paired and therefore the statistical comparisons between the two hands were performed using the unpaired *t*-test (normality test passed) or the nonparametric Mann–Whitney test (normality test failed) on the CT values pooled from 20 daily sessions.

exhibited comparable CTs for the left and the right hand. In four monkeys (Mk-AT, Mk-CA, Mk-DI, and Mk-MA), the CTs were shorter for the right hand, whereas the CTs were shorter for the left hand in three monkeys (Mk-LO, Mk-MI, and Mk-TH). Considering both the vertical and the horizontal slots, note that in two monkeys (Mk-DI and Mk-LO) exhibiting a significant difference of CTs between the two hands for both slot orientations, surprisingly the hand with the shortest CTs was not the same for the vertical and the horizontal slots.

Human subjects

The hand dominance was determined for the human subjects by comparing the total score (sum of vertical and horizontal slots visited in 30 sec) between each hand in the unimanual modified Brinkman board task. Graphs derived from one self-assessed right-hander (AG) and one self-assessed left-hander (AH) are shown in Figure 3A, with the total score for each hand in the ten consecutive trials. Generally, there was a training effect along the sessions, as most subjects increased their performance (total score) after a few trials. In two human subjects, the learning effect was rapid (plateau reached after two trials) but of limited extent (small increase of score). In the other human subjects, the learning phase was longer, 4–6 trials in most cases. The gain in total score was for most subjects in the order of 10 additional bolts collected in 30 sec at plateau as compared to the score observed for the first trial, although overall the gain in total score ranged from about 5–15 additional bolts collected in 30 sec. Moreover, most subjects developed strategies (motor habits) to increase their performance: for instance, they began to grasp bolts from the vertical slots and then bolts from the horizontal ones, or they began each trial on one side and systematically scanned the board to the other extremity. Additionally, in this sample of 20 human subjects, the right-handers performed significantly better than the left-handers ($P < 0.001$; Mann–Whitney test) and women exhibited higher total scores than men ($P = 0.009$; Mann–Whitney test).

The hand dominance was determined by comparing the total scores between the left hand and the right hand in each subject (Fig. 3B). Generally, the total score ranged between 15 and 40. Out of the twenty subjects, only nine showed a significant hand dominance. In the left-handed subjects (ID initials in blue in Fig. 3B; $n = 10$), five people exhibited a significant left-hand dominance: AB, AH, AP, MF, and VC ($P = 0.038$, $P = 0.002$, $P < 0.001$, $P = 0.045$, and $P < 0.001$, respectively), whereas one self-declared left-hander surprisingly showed a significant right-hand dominance (SB with $P = 0.015$). In the other four left-handers, there was no significant hand dominance. In the population of right-handed subjects (ID initials in red in Fig. 3B; $n = 10$), three of them showed a right-hand dominance (AG, JG, and MS, with $P = 0.025$, $P = 0.004$, and $P = 0.005$, respectively), whereas there was no significant hand dominance in the other seven self-declared right-handed subjects.

The CT was assessed in the human subjects as well, separately for the vertical and horizontal slots and illustrated in Figure 4 for four representative subjects. The subjects AP and MS were representative of lateralized humans, self-declared as left-hander and right-hander, respectively, and showed a dominance of the corresponding hand (left in AP and right in MS), with statistically shorter CTs as compared to the opposite hand. The CTs of two other subjects are displayed in Figure 4, one fast subject (AG) and one slow subject (MB), as exhibited in Figure 3B by their high and low scores, respectively. The fast subject (AG), declared as right-hander, also exhibited shorter CTs with the corresponding hand (the difference with the opposite hand was statistically significant only for the vertical slots). In contrast, the slow subject (MB), declared as left-hander, exhibited comparable CTs for both hands. As compared to monkeys (Fig. 2B), the human CT data (Fig. 4) reflect a somewhat shorter time interval needed to successfully grasp the object from the slots, especially for the horizontal slots. This species difference may be explained by the object properties, as the bolt with its angular contour and surface with a hole in it is easier to grasp than the round shape of the pellets presented to the monkeys.

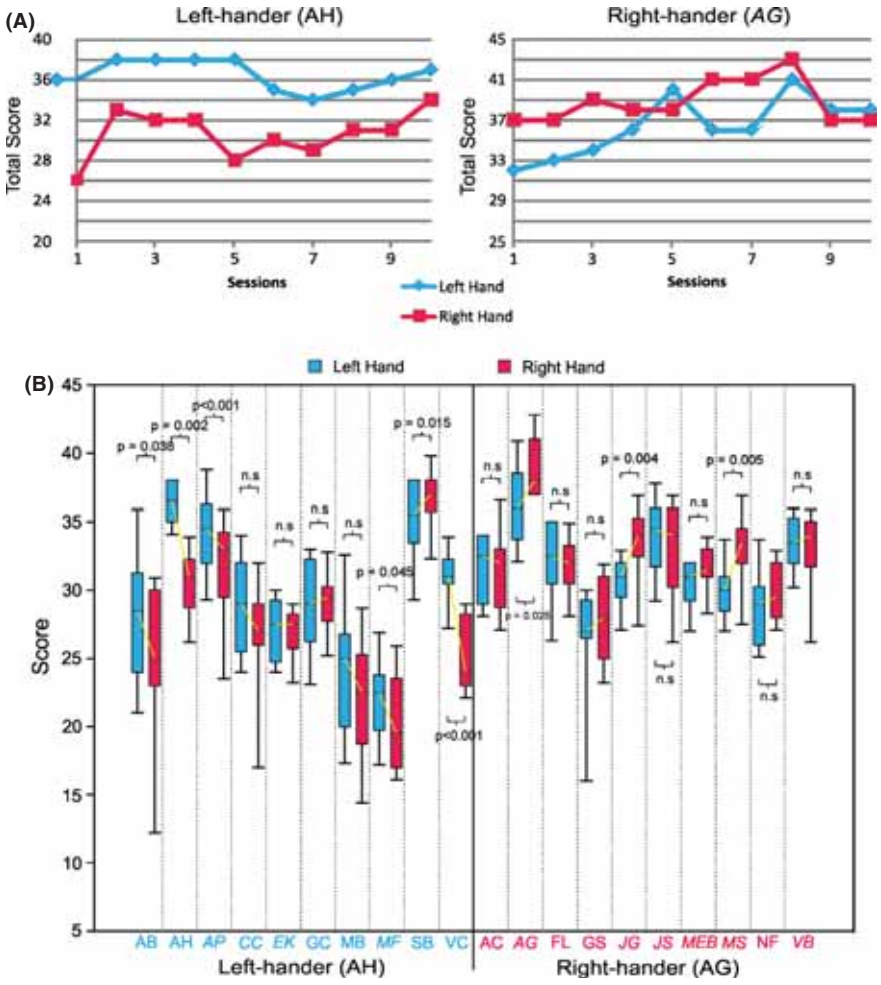

Figure 3. Hand dominance analysis for human subjects (women in italic), derived from the unimanual modified Brinkman board task. Examples of the total score (sum of the number of horizontal and vertical slots visited in 30 sec) for a left-handed subject (AH) and a right-handed subject (AG) are shown in panel (A). In panel (B), the box and whiskers plots represent the distribution of the total scores observed for the left hand (blue) and the right hand (red), for each human subject tested (n = 20, indicated by their ID initials). The ID initials of the subjects are in blue versus red, when the subjects presented themselves as left-hander versus right-hander, respectively. The ID initials of males and females are shown with normal and italic type, respectively. The statistical comparisons of total score between the two hands in each of the 10 trials were performed using the paired t-test (normality test passed) or the nonparametric Wilcoxon rank signed test (normality test failed). In each subject, a yellow line connects the median values of the left and the right hands, in order to emphasize the intermanual comparison.

Hand preference

Monkeys

As reminder, the hand preference in monkeys was determined based on the results of the modified Brinkman board, when the use of the two hands was free, as well as on the results of three other specific tasks: the bimanual board, the tube, and the drawer tasks.

For the modified Brinkman board task (executed with both hands simultaneously), we made a distinction among the scores according to different phases, each characterized by distinct patterns of manual use. Indeed, the monkeys evolved in their manner to execute the task and in the choice of one hand to the detriment of the other along the daily sessions. There were mainly three different behavioral profiles exhibited by the animals (Fig. 5). In the first profile (for instance Mk-AN in Fig. 5A), the monkey used nearly always the same hand in phase I, whereas in phase II (to the right of the vertical dashed line), both hands were used more or less at the same frequency. In the second profile (for instance Mk-LO in Fig. 5B), one of the hands was less used than the other hand along all daily sessions. However, two phases were distinguished, phase I corresponding to a minimal use of one hand followed, in phase II, by an increased contribution of the less used hand. The third profile (for instance Mk-MA, Fig. 5C) is the opposite to the first one: both hands were used more or less at the same frequency during phase I, whereas one hand was then less used than the other hand during phase II.

After determining the different phases corresponding to different profiles (manual patterns), we compared the score for the right hand with the one for the left hand, separately in the vertical (Fig. 6A) and in the horizontal slots (Fig. 6B), in each phase in each monkey. In the vertical slots in phase I, four monkeys exhibited a significant preference to use one hand over the other (left-hand preference in Mk-AN and Mk-TH; right-hand preference in Mk-DI and Mk-LO), whereas the other four monkeys did not show any significant hand preference (Mk-AT, Mk-CA, Mk-MA, and Mk-MI). In phase II, most of the scores for the vertical slots did not exhibit a significant

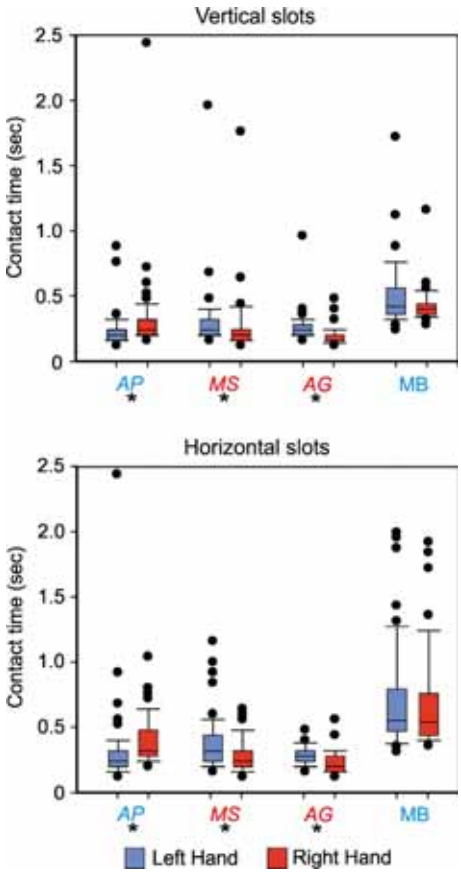

Figure 4. Hand dominance analysis for human subjects, derived from CTs obtained in the unimanual modified Brinkman board task, for four representative human subjects (see text), when the use of one hand was imposed. Both graphs, in the form of box and whiskers plots, represent the distribution of CTs in seconds, for the vertical slots (top graph) and for the horizontal slots (bottom graph), and separately for the left hand (blue) and the right hand (red). The CT data (five values per daily session for each slot orientation) are not paired and the statistical comparisons between the two hands were performed using the unpaired *t*-test (normality test passed) or the nonparametric Mann–Whitney test (normality test failed) on the CT values pooled from the 10 sessions. Same ID initial code as in Figure 3.

difference between both hands, except for Mk-LO and Mk-MA, with a significant preference for their right hand. In the horizontal slots (Fig. 6B), in phase I, all monkeys but Mk-MA showed a significant hand preference. Four monkeys (Mk-AN, Mk-AT, Mk-MI, and Mk-TH) used preferably their left hand, whereas three monkeys (Mk-CA, Mk-DI, and Mk-LO) used more often their right hand. In phase II, five out of eight monkeys showed a preference for one hand over the other, with a left-hand preference in Mk-AT and Mk-MI, whereas Mk-CA, Mk-LO, and Mk-MA exhibited a right-hand preference. Overall, there were clearly more significant hand preferences observed for the horizontal slots than for the vertical slots (Fig. 6).

The HI, derived from the three other tasks performed by the monkeys (the bimanual board task (Fig. 1B), the tube task (Fig. 1C), and the drawer task (Fig. 1D), were plotted on the same bar graph (Fig. 7A, rightmost part of the graph, separated from human subjects by a vertical black line). In most cases, these three tasks were lateralized (large positive or negative HI). Mk-TH was the only monkey to exhibit a coherent hand preference for all three tasks, with a systematically positive HI, corresponding to a significant right-hand preference ($P < 0.05$; binomial test). In the other seven animals, there was an absence of systematic consistency across tasks.

Three monkeys (Mk-AN, Mk-CA, and Mk-DI) exhibited a preference for the right hand in the bimanual board and the tube tasks (positive HI) and a preference for the left hand in the drawer task (negative HI). These HI values were statistically significant (meaning lateralized; binomial test $P < 0.05$), except in Mk-CA for the tube task (Fig. 7A).

Mk-LO and Mk-MI shared a comparable general pattern of HI distribution among the three tasks (Fig. 7A), namely a clearly positive HI (>0.5) for the bimanual board and the drawer tasks, whereas the HI was strongly negative for the tube task (Fig. 7A). In these two animals, all HI values were statistically significant (lateralized; $P < 0.05$).

The last three monkeys had each a unique general pattern of HI distribution among the three tasks. Mk-AT exhibited a significant preference for the right hand in the bimanual board task ($P < 0.05$), whereas a significant left-hand preference was present for the tube and the drawer tasks ($P < 0.05$). In Mk-MA, there was a significant left hand preference for the first two tasks ($P < 0.05$), whereas for the drawer task the right hand was preferred ($P < 0.05$).

Human subjects

Two tasks, namely the tube and the bimanual Brinkman board tasks, as well as the handedness questionnaire were used to assess the hand preference in human subjects. The observed HI values obtained for the bimanual board and for the tube tasks were plotted on the same graph for all subjects (Fig. 7A, left and middle parts of the graph, separated from the rightmost part concerning monkeys by the solid vertical black line). Most human subjects exhibited a HI near to −1 or 1. The *P*-value for each test and for each subject was statistically significant ($P < 0.05$; binomial test), except for the tube task in the subject FL ($P > 0.05$). The results for both tasks (Fig. 7A) showed that most self-declared left-handers indeed used their left hand as the preferred hand (HI negative), and similarly most self-

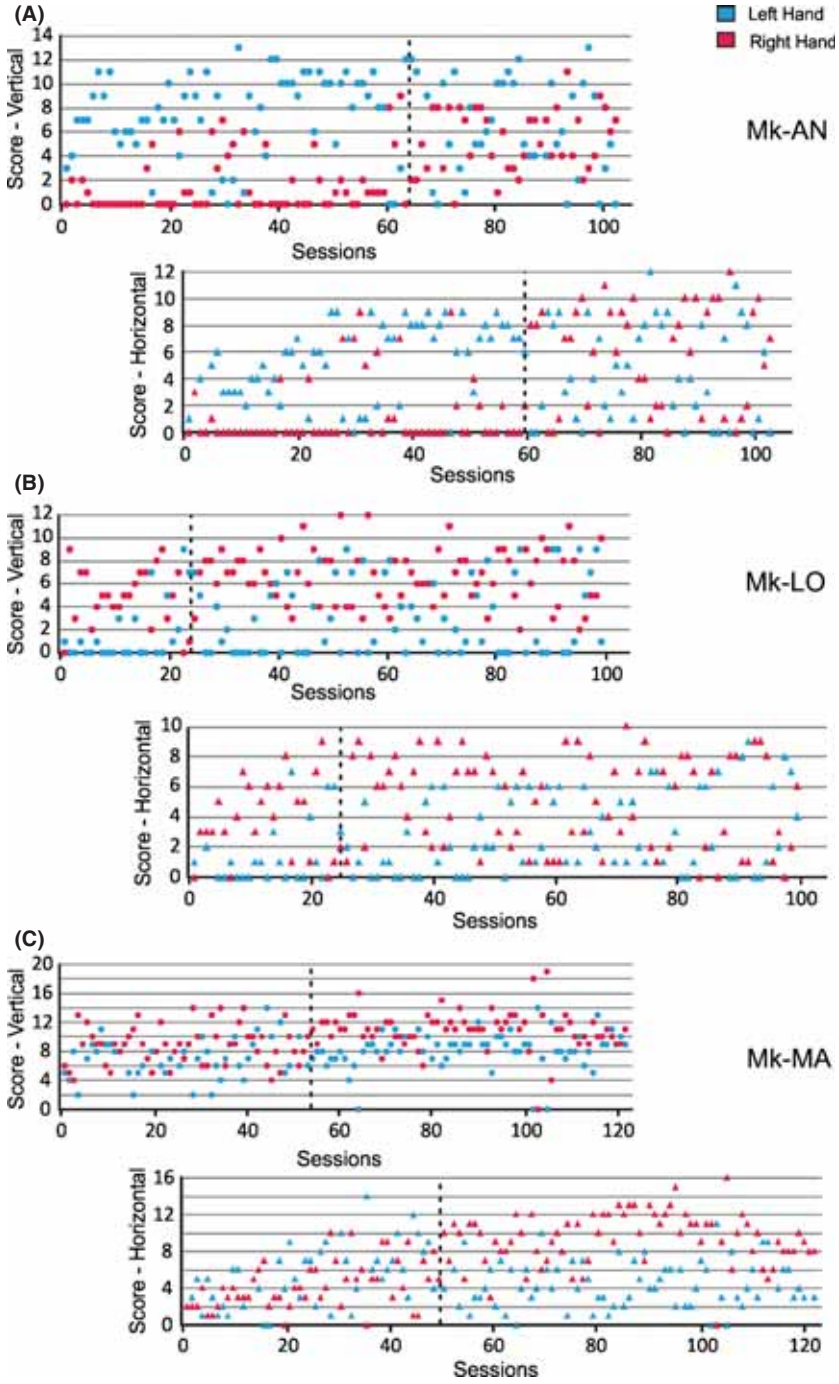

Figure 5. Hand preference in monkeys: distinction between different phases in the modified Brinkman board task, when the use of both hands was free. Different behaviors appear among monkeys. In panel (A), the scores for the vertical and horizontal slots for Mk-AN are shown. The vertical dotted line separates two phases: phase I in which the right hand (in red) was hardly ever used and phase II during which both hands were used more or less at the same frequency (see the corresponding statistical tests in Fig. 6). In panel (B), scores for vertical and horizontal slots for Mk-LO are shown. The vertical dotted line also separates two phases, but the distinction is here less marked. In phase I, the left hand was hardly ever used, whereas it was used more in phase II. However, the right hand seems to be more used in the two phases than the left one (see statistical tests in Fig. 6). In panel (C), scores for vertical and horizontal slots for Mk-MA are shown. The vertical dotted line separates two phases as well: phase I in which both hands were used more or less at the same frequency, and phase II, in which conversely the left hand was less used than the right hand (statistical tests in Fig. 6). As emphasis was put on the comparison between the two hands in each condition, the ordinate maximal values were variable among conditions.

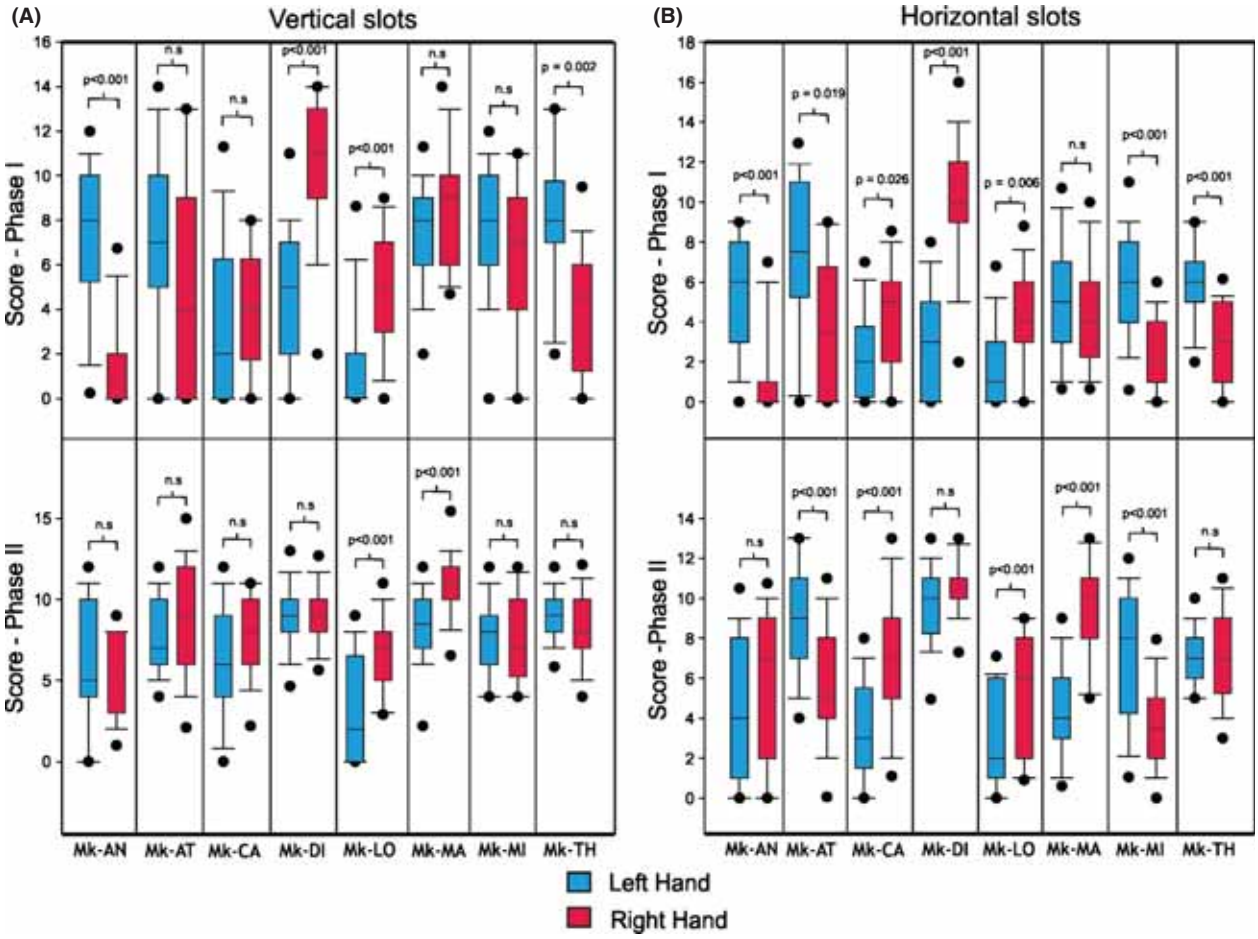

Figure 6. Hand preference statistical analysis for monkeys, applied to the modified Brinkman board task data, with free use of the two hands simultaneously, as illustrated in Figure 5, and represented by box and whiskers plots. Scores for vertical slots for phases I and II are shown for all monkeys in panel (A) and scores for the horizontal slots for phases I and II are displayed in panel (B).

declared right-handers indeed used their right hand as the preferred hand (HI positive). Only three left-handers exhibited a preference for the right hand in the tube task (subjects AP, CC, and MB). One of these three left-handed subjects (CC) furthermore showed a preference for the right hand in the bimanual board task. In the population of self-declared right-handers (Fig. 7A), four of them (subjects AC, GS, JG, and NF) showed a preference for their left hand in the tube task, whereas another right-handed subject (MS) exhibited a preference for the left hand in the bimanual board task. Statistical comparisons (*t*-test or Mann–Whitney) between the groups of right-handers versus left-handers for the tube task (blue bars in Fig. 7A) did not reveal any significant difference ($P > 0.05$) for both the real HI values and the absolute HI values. On the other hand, for the bimanual board task (gray bars in Fig. 7A), there was a significant difference for the real HI values between the right-handers and the left-handers ($P = 0.002$), but not for the absolute HI values ($P = 0.33$), indicating that the degree of lateralization is comparable in both groups.

The scores derived from the handedness questionnaire was calculated and transformed into percentages (Fig. 7B). The overall questionnaire scores for the self-announced right-handers (ID initials in red in Fig. 7B) were clearly positive, ranging between 53.85% and 100%. The questionnaire scores derived from the self-announced left-handers (ID initials in blue in Fig. 7B) were mostly negative, ranging between −30.77% and −73.08%. The exception was the subject AB, who surprisingly showed a positive questionnaire score (26.92%). The absolute values of laterality score were significantly larger in the right-handers than in the left-handers ($P = 0.007$), confirming the well-established notion that right-handers are more lateralized.

An overview of all results is available in Table 1, separately for the monkeys (Part A) and for the human subjects (Part B). Generally, it can be concluded that comparable numbers of left- and right-handed occurrences appeared

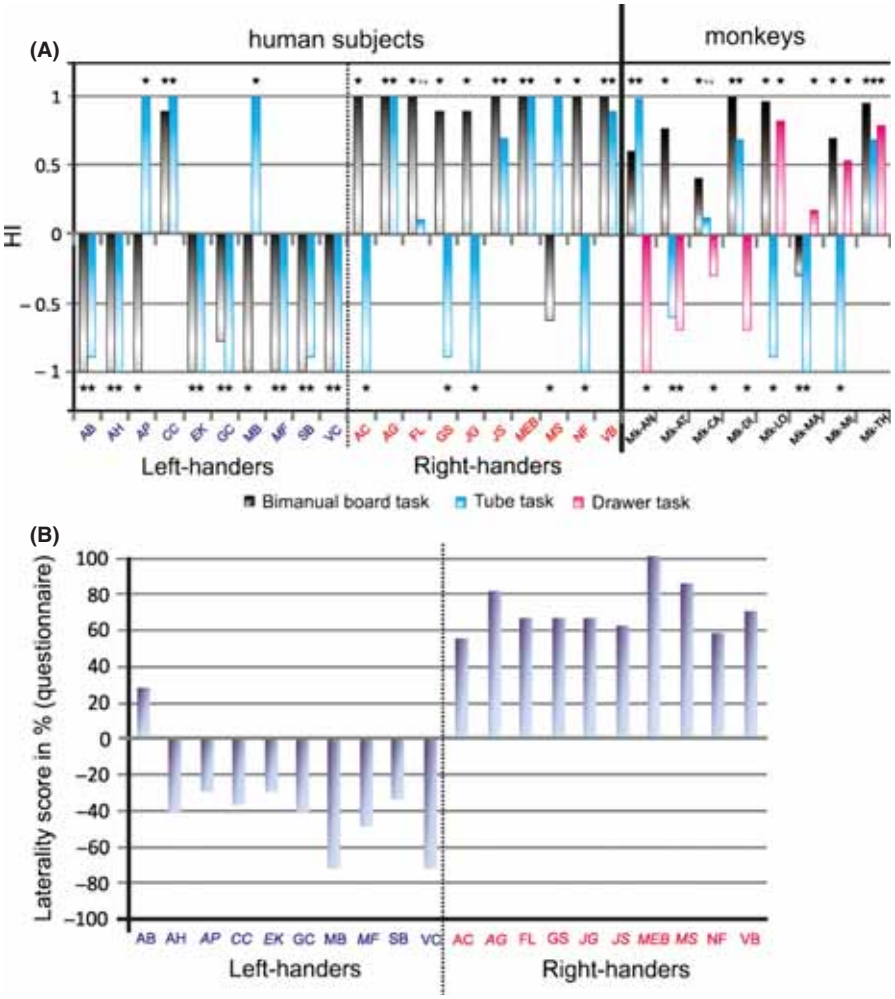

Figure 7. Hand preference analysis for monkeys and human subjects. In panel (A), the bar graph displays the handedness index (HI) for the bimanual Brinkman board and the tube tasks in human subjects and for the bimanual Brinkman board, the tube and the reach and grasp drawer tasks in monkeys. The solid vertical black line separates human subjects (left) from monkeys (right) and the vertical dotted line separates the human subjects who presented themselves as left-handers (left) from the subjects who presented themselves as right-handers (right). For each task and for each subject, the stars indicate a $P \leq 0.05$ obtained in a binomial statistical test (ns = not significant, $P > 0.05$), above or below each corresponding bar graph. In panel (B), the bar graph represents the overall laterality score from the handedness questionnaire in percentage for each human subject. The ID initials of the subjects are in blue versus red for the self-announced left-handers versus right-handers, respectively. See text for statistical analysis. For human subjects, same ID initial code as in Figure 3 (women in italic).

among monkeys, concerning both the hand dominance and the hand preference (Table 1, Part A). However, there was no general consistency in hand dominance or in hand preference in monkeys, neither between individuals nor within each individual. On the contrary, as far as human subjects are concerned, the hand preferences revealed by the two manual tests and the questionnaire were largely coherent with the self-assessment by the subject (Table 1, Part B), although the tube task revealed a few more discrepancies. There were less systematic occurrences of hand dominance (assessed with the unimanual modified Brinkman board task; Table 1, Part B) although, when present, it was consistent with the lateralization of the hand preference (except in the subject SB). We also observed that hand dominance was somewhat more frequent in left-handers than in right-handers.

Discussion

At least to the best of our knowledge, the present study introduced several new aspects of handedness assessment in primates, with emphasis on manual dexterity (use of precision grip). First of all, the data support the concept of separation of two hand attributes, namely the hand dominance and the hand preference. In monkeys, these two attributes were not systematically consistent, and in

Table 1. Overview of the results. The panel (A) shows a summary of all results derived from the eight monkeys. VS and HS mean vertical and horizontal slots, respectively. Pl refers to plateau. Pl.I/Pl.II mean phases I and II of the plateau. The letter L indicates a left-hand dominance/preference and the letter R, a right-hand dominance/preference, whereas ns means a statistically nonsignificant difference ($P > 0.05$). The panel (B) shows an overview of all results in human subjects for the self-announced right-handers (ID initials in red) and left-handers (ID initials in blue). The letters L and R indicate a statistically significant left and right dominance/preference, respectively. ns means a statistically nonsignificant difference.

(A)				Mk-AN	Mk-AT	Mk-CA	Mk-DI	Mk-LO	Mk-MA	Mk-MI	Mk-TH
Hand dominance	Modified Brinkman board task	Total	Score learning	ns	ns	ns	R	R	L	L	ns
			Score Pl	L	ns	R	ns	ns	R	ns	ns
		VS	CT	L	ns	R	L	R	ns	ns	ns
		HS	CT	ns	R	R	R	L	R	L	L
Hand preference	Modified Brinkman board task	VS	Score Pl.I	L	ns	ns	R	R	ns	ns	L
			Score Pl.II	ns	ns	ns	ns	R	R	ns	ns
		HS	Score Pl.I	L	L	R	R	R	ns	L	L
			Score Pl.II	ns	L	R	ns	R	R	L	ns
	Bimanual board task			R	R	R	R	R	L	R	R
	Tube task			R	L	ns	R	L	L	L	R
	Drawer task			L	L	L	L	R	R	R	R

		Left-handers										Right-handers									
(B)		AB	AH	AP	CC	EK	GC	MB	MF	SB	VC	AC	AG	FL	GS	JG	JS	MEB	MS	NF	VB
Hand dominance	Modified Brinkman board task	L	L	L	ns	ns	ns	ns	L	R	L	ns	R	ns	ns	R	ns	ns	R	ns	ns
Hand preference	Bimanual board task	L	L	L	R	L	L	L	L	L	L	R	R	R	R	R	R	R	L	R	R
	Tube task	L	L	R	R	L	L	R	L	L	L	L	R	ns	L	L	R	R	R	L	R
	Handedness questionnaire	R	L	L	L	L	L	L	L	L	L	R	R	R	R	R	R	R	R	R	R

human subjects the hand preference was not systematically accompanied by consistent hand dominance, at least for the modified Brinkman board task (Table 1). This may be different for more challenging manual dexterity tasks. Second, the present study is original in comparing nonhuman primates and human subjects with respect to their handedness, based on a set of comparable manual dexterity tasks performed by macaque monkeys and human subjects (see also Lacreuse and Fragaszy 1997; for a comparison between capuchin monkeys and humans). In particular, the modified Brinkman board task widely and classically used in monkeys (e.g., Brinkman and Kuypers 1973; Brinkman 1984; Liu and Rouiller 1999; Kaeser et al. 2010, 2011, 2013; Schmidlin et al. 2011) was tested in human subjects for the first time. Third, the manual performance in nonhuman primates was conducted here in well-defined conditions, such as reproducible posture and position of the animal with respect to the behavioral set-up, thanks to the use of the primate chair placed in the same position from one daily session to the next (in contrast to observations in the wild or in the detention cage). The primate chair offers also the possibility to test separately the left hand from the right hand, as needed to assess hand dominance for instance. Finally, in monkeys, the assessment of manual performance was not restricted to a single or very few time points, but it was monitored in daily sessions over several weeks or months.

Overall, the results confirmed our hypothesis that hand preference in *M. fascicularis* is variable across manual tasks and individuals (Table 1). Furthermore, the hand preference in monkeys did not systematically correspond to the hand dominance in the modified Brinkman board task (four out of eight monkeys: see Table 1). In contrast, human subjects are more lateralized and the correspondence between hand preference and hand dominance was systematic in the vast majority of cases (one exception out of 20 subjects: see Table 1).

As expected, our results related to hand preference show that left-handers are not a mirror image of right-handers, at least based on the questionnaire (Fig. 7B). Right-handers are clearly more lateralized, as laterality scores (absolute values) were significantly larger in right-handers than in left-handers. In monkeys, based on the three tasks they performed (Fig. 7A), only one animal exhibited a consistent lateralization (Mk-TH: right-hander), whereas in the others, the preferred hand was largely task dependent.

The part of the present study focused on human subjects, in spite of a relatively limited sample of subjects (n = 20, comprising 10 men and 10 women distributed in 10 right-handers and 10 left-handers based on their self-assessment) revealed some interesting differences. First, the questionnaire data showed that left-handers are less lateralized than right-handers (Fig. 7B), as previously reported (see e.g., Kastner-Koller et al. 2007) and in line with our hypothesis (see Introduction and Methods). However, this lateralization difference between self-declared left- and right-handers reflected by the questionnaire was not found for the two bimanual tasks tested here: as shown in Table 1, there was a comparable number of hand preference deviations in each group (four right hand deviations in the left-handers and five left hand deviations in the right-handers). Second, in the context of hand dominance assessment based on the modified Brinkman board task, right-handers performed significantly better than left-handers, in the 10 trials conducted for each subject during the unique behavioral session. Whether this difference would be maintained along multiple sessions conducted at subsequent days remains an open question. Third, women performed significantly better than men in the modified Brinkman board task, as reflected by a higher total score. This result is in line with the previously reported notion that females perform better than males in tasks requiring high levels of manual dexterity (Kimura 2000). The gender difference was opposite in a computer-pointing task (Rohr 2006), with motor times shorter in men, favoring speed, than women, highlighting accuracy.

In the present study, fairly comparable results were obtained for human subjects and monkeys, as far as the hand dominance is concerned. Indeed, 62% of monkeys and 55% of human subjects did not show any statistically significant hand dominance, as assessed by the score derived from the modified Brinkman board task. Concerning the CTs, the results are more difficult to interpret in monkeys. The CTs were fully coherent with the score in one case only (Mk-CA), whereas for the other monkeys, there was no, or less, consistency (Table 1). As reminder, the CT is a parameter additional to the score, which eliminates possible biases in the score, due to inattention and/or lack of motivation of the monkey. In other words, it does not take into account the time interval between two slot manipulations. Moreover, we had taken into consideration only the last 20 sessions at plateau, to focus on the supposedly most stable daily behavioral sessions. It may, however, be interesting to consider the CT in more sessions in the plateau phase for a stricter comparison with the score for the very same sessions, although, in previous studies (e.g., Kaeser et al. 2010, 2011), the CTs were largely stable during the entire plateau phase. The discrepancy between score and CTs is likely to be due to other parameters, such as diverted attention in between the grasping of two consecutive pellets. It may also originate from the different motor habits reflected by the temporal sequence followed by the animal

to visit the slots (e.g., the monkey scans the board systematically from one side to the other or from the middle and then to the sides; see Kaeser et al. 2013). Moreover, at a given time point, the animal may change prehension strategy (e.g., collect two pellets at a time). As long as the new strategy is not fully mastered, the hand dominance may vary, although the CTs remain short. In human subjects, as for the score data, the CT data showed that the hand dominance is generally consistent with the hand preference.

The present study offers the opportunity to compare the hand dominance and the hand preference for both human subjects and nonhuman primates. As reminder, the human subjects exhibiting hand dominance showed, most of the time, the same laterality for hand preference. This was not the case for the monkeys, where the laterality of the hand dominance did not systematically correspond to the one of the hand preference (Table 1). The same conclusion was met in a study conducted on four female *M. fuscata* Japanese monkeys (Kinoshita 1998).

Concerning the hand preference, the results in human subjects are very consistent with their self-assessment. Indeed, for most subjects, the preferred hand revealed by the different tasks corresponded to the hand they used to write, except for the tube task, where the results were more disparate (Table 1). The tube task thus appears less appropriate than the bimanual Brinkman board task and the questionnaire to determine the hand preference in human subjects. This raises then the question whether this task is adequate to assess hand preference in monkeys. The results related to hand preference in monkeys were highly disparate. Only two animals showed similar results (Mk-DI and Mk-AN) and, for each monkey, there was no systematic hand preference among all the tasks performed. Considering the questionable suitability of the tube task in human subjects (see above), it was tried to eliminate the tube test from the monkey data: omitting the tube task data did not modify substantially the results, except for Mk-LO, which was a right-hander for each task except the tube one. Two conclusions maybe drawn from these results: either the tasks used here are not fully appropriate to determine the hand preference in monkeys, or the *M. fascicularis* monkeys do not show a stable and systematic hand preference for the present panel of tasks. In human subjects, the bimanual Brinkman board appears to be an adequate test, but is it also the case for the nonhuman primates? This question highlights the limits of our experiment. On the one hand, we compare for the first time handedness in human subjects and in nonhuman primates for the same tasks directly but, on the other hand, these manual tasks may not be equally relevant in both species. The complexity and the representation of the different tasks may well be different for nonhuman primates and for human subjects. A difference is already present at the level of training. Clearly, human subjects reached more rapidly plateau values than monkeys, especially for the modified Brinkman board task. Human subjects are obviously more often engaged in bimanual coordination tasks in their everyday life than monkeys, a difference which may bias the comparison between the two groups performing the same manual tasks. At onset time of behavioral testing, the human subjects were already strongly lateralized, whereas this was most likely not the case in the nonhuman subjects. In the monkeys, the present data demonstrate that hand preference is more prominently revealed by a more challenging task (horizontal slots) than an easier task (vertical slots in the modified Brinkman board task, executed with both hands simultaneously; see Table 1). In the comparison between monkeys and humans, it has to be emphasized that reinforcement is not of the same nature (food in monkeys, a bolt in human) and therefore the motivational context is different. Furthermore, human subjects were asked to perform the task as rapidly as possible, whereas there was no such time constraint in monkeys. However, as the task represented the first access to food on that day, the monkeys were motivated and therefore they were fast too.

As compared to previous studies available in the literature, several aspects deserve further comments. As already mentioned above, few of the previous studies clearly distinguished hand dominance from hand preference, especially in nonhuman primates. Consequently, in previous studies conducted in monkeys with the aim to investigate the effect of different lesions of the central nervous system on the manual dexterity, it is often mentioned that a unilateral lesion was performed on the contralateral side with respect to the "dominant" hand. From the present study, such statement remains unclear as it is not obvious to distinguish whether the hand was more proficient (better motor performance reflecting hand dominance as defined here) or selected in priority (preferred hand) by the animal to perform a specific manual dexterity task. The difficulty is even increased when considering the data presented in Figure 5, demonstrating that the hand preference may vary with time along the daily behavioral sessions.

Focusing on hand preference (as defined in the present report), several studies showed similar results to ours, confirming an individual-level hand preference associated to different tasks (Old World Monkey in Westergaard et al. 2001a,b and Chapelain et al. 2006; Prosimians in Leliveld et al. 2008 and Hanbury et al. 2010). For Chapelain et al. (2006), this individual preference is an evidence of endogenous laterality, but to explain the differences between the animals, they propose an influence of differ-

ent factors dependent on the task specificity. Hopkins (2006) reached similar conclusions in great apes. Linked to this observation, several studies suggested dependence between handedness and task complexity (Lehman 1989; Fagot and Vauclair 1991; Hopkins 1995; Hopkins and Rabinowitz 1997; Spinozzi et al. 1998; Hopkins and Cantalupo 2005). Indeed, the more complex the task, the more prominent the hand preference. This is in line with the larger occurrences of hand preference observed here in the horizontal slots of the modified Brinkman board task, as compared to the less challenging vertical slots (Table 1). Overall, in our study, all tasks in which the monkeys were engaged may be considered as complex, so it explains why, for most of them, we found an individual manual laterality (hand preference; see Table 1). Moreover, previous studies emphasized the significance of the body position in relation to the task in order to determine the manual laterality (Hopkins and Cantalupo 2005; Meunier et al. 2011). In our study, the position of the animal was highly reproducible and this parameter thus did not influence our results.

Unlike to the first aforementioned studies, Hopkins et al. (2002), Westergaard et al. (1997), and Wesley et al. (2001) found a population-level handedness in macaques and chimpanzees, but the methods used to assess hand preference were a bit different. Indeed, Hopkins et al. (2002) and Westergaard et al. (1997) tested the hand preference using a lower number of tasks.

Concerning the different results obtained from human subjects and monkeys, several explanations appear pertinent. Sociability plays an important role for the handedness (Hopkins 2006). Indeed, pedagogical or cultural pressures can influence the hand preference in humans, which is not considered to be the case in nonhuman primates. The postural origin theory of handedness offers a possible explanation for the monkey data (MacNeilage et al. 1987). Indeed, several studies showed a right-hand preference for more terrestrial species, whereas a left-hand preference was found for more arboreal animals (Masataka 1989; Singer and Schwibbe 1999; Hopkins et al. 2011; Meguerditchian et al. 2012; Zhao et al. 2012). In our case, our animal model, the *M. fascicularis*, is considered to be both arboreal and terrestrial (Fooden 2006; South Asian Primate C.A.M.P. Report, 2003; http://www.zooreach.org/downloads/ZOO_CAMP_PHVA_reports/2003%20Primate%20Report.pdf). Our results in *M. fascicularis* monkeys, showing a right- or left-hand preference depending on the tasks, is thus in line with the postural origin theory, in the sense that our animals did not show a clear right- or left-handedness, but an intermediate and variable position, consistent with the mixed arboreal and terrestrial status of *M. fascicularis*. These data are consistent with hand preference observations derived from simple food reaching task, also in cynomolgus (*M. fascicularis*) monkeys (Lehman 1980b). In a longitudinal study (from birth to weaning) conducted on a large number of monkeys (*M. fascicularis*), and based also on a task using a slot board but emphasizing more the attribute of hand dominance than hand preference (Brinkman and Smithson 2007), it was found that the infant monkeys showed a "dominant" hand at individual level (but bimodal distribution at population level). Their hand "dominance" was the same as that of their mother and, moreover, their pattern of grip movement resembled their mothers', suggesting imitation (Brinkman and Smithson 2007). In line with Hopkins (2004), the present data in *M. fascicularis* show that, as far as hand preference is concerned, they considerably diverge from human subjects (highly lateralized), whereas apes can be placed in between the two groups, with intermediate hand preference characteristics. This wide range of behavioral lateralization is consistent with its multifactorial origin (see e.g., Rogers 2009; Schaafsma et al. 2009; Uomini 2009; Forrester et al. 2013).

Acknowledgments

The authors wish to thank the technical assistance of Josef Corpataux, Laurent Bossy and Jacques Maillard (animal house keeping), André Gaillard (mechanics), Bernard Aebischer (electronics), Laurent Monney (informatics). This study was supported by Swiss National Science Foundation, grants No. 31-61857.00, 310000-110005, 31003A-132465, and FZFS-0_144990 (E. M. R.), 31-121646 (E. S.); the Novartis Foundation; the National Centre of Competence in Research (NCCR) on "Neural plasticity and repair" and the Christopher Reeves Foundation (Springfield, NJ). The experiments were conducted in the framework of the SPCCR (Swiss Primate Center for Competence in Research), financed by the State Secretariat for Education and Research.

Conflict of Interest

None declared.

References

Brinkman, C. 1984. Supplementary motor area of the monkey's cerebral cortex: short- and long-term deficits after unilateral ablation and the effects of subsequent callosal section. J. Neurosci. 4:918–929.

Brinkman, J., and H. G. J. M. Kuypers. 1973. Cerebral control of contralateral and ipsilateral arm, hand and finger movements in the split-brain rhesus monkey. Brain 96:653–674.

Brinkman, C., and M. Smithson. 2007. Determinants of hand preference in monkeys (*M. fascicularis*): birth to weaning. Aust. J. Psychol. 59(Suppl. 1):21.

Chapelain, A., P. Bec, and C. Blois-Heulin. 2006. Manual laterality in Campbell's Monkeys (*Cercopithecus c. campbelli*) in spontaneous and experimental actions. Behav. Brain Res. 173:237–245.

Coren, S., and C. Porac. 1977. Fifty centuries of right-handedness: the historical record. Science 198:631–632.

Dadda, M., C. Cantalupo, and W. D. Hopkins. 2006. Further evidence of an association between handedness and neuroanatomical asymmetries in the primary motor cortex of chimpanzees (*Pan troglodytes*). Neuropsychologia 44:2582–2586.

Dassonville, P., X. H. Zhu, K. Uurbil, S. G. Kim, and J. Ashe. 1997. Functional activation in motor cortex reflects the direction and the degree of handedness. Proc. Natl. Acad. Sci. USA 94:14015–14018.

Fagot, J., and J. Vauclair. 1988. Handedness and manual specialization in the baboon. Neuropsychologia 26:795–804.

Fagot, J., and J. Vauclair. 1991. Manual laterality in nonhuman primates: a distinction between handedness and manual specialization. Psychol. Bull. 109:76–89.

Fooden, J. 2006. Comparative review of fascicularis-group species of macaques (Primates: Macaca). Fieldiana Zool. 107:1–44.

Forrester, G. S., C. Quaresmini, D. A. Leavens, D. Mareschal, and M. S. C. Thomas. 2013. Human handedness: an inherited evolutionary trait. Behav. Brain Res. 237:200–2006.

Freund, P., E. Schmidlin, T. Wannier, J. Bloch, A. Mir, M. E. Schwab, et al. 2009. Anti-Nogo-A antibody treatment promotes recovery of manual dexterity after unilateral cervical lesion in adult primates–re-examination and extension of behavioral data. Eur. J. Neurosci. 29:983–996.

Hanbury, D. B., K. D. Edens, D. A. Bunch, C. E. Legg, and S. L. Watson. 2010. Multiple measures of laterality in Garnett's bushbaby (*Otolemur garnettii*). Am. J. Primatol. 72:206–216.

Hopkins, W. D. 1995. Hand preferences for a coordinated bimanual task in 110 chimpanzees (*Pan troglodytes*): cross-sectional analysis. J. Comp. Psychol. 109:291–297.

Hopkins, W. D. 2004. Laterality in maternal cradling and infant positional biases: implications for the development and evolution of hand preferences in nonhuman primates. Int. J. Primatol. 25:1243–1265.

Hopkins, W. D. 2006. Comparative and familial analysis of handedness in great apes. Psychol. Bull. 132:538–559.

Hopkins, W. D., and C. Cantalupo. 2004. Handedness in chimpanzees (*Pan troglodytes*) is associated with asymmetries of the primary motor cortex but not with homologous language areas. Behav. Neurosci. 118: 1176–1183.

Hopkins, W. D., and C. Cantalupo. 2005. Individual and setting differences in the hand preferences of chimpanzees (*Pan troglodytes*): a critical analysis and some alternative explanations. Laterality 10:65–80.

Hopkins, W. D., and D. L. Pilcher. 2001. Neuroanatomical localization of the motor hand area with magnetic resonance imaging: the left hemisphere is larger in great apes. Behav. Neurosci. 115:1159–1164.

Hopkins, W. D., and D. M. Rabinowitz. 1997. Manual specialisation and tool use in captive chimpanzees (*Pan troglodytes*): the effect of unimanual and bimanual strategies on hand preference. Laterality 2:267–277.

Hopkins, W. D., D. A. Washburn, and D. M. Rumbaugh. 1989. Note on hand use in the manipulation of joysticks by rhesus monkeys (*Macaca mulatta*) and chimpanzees (*Pan troglodytes*). J. Comp. Psychol. 103:91–94.

Hopkins, W. D., D. A. Washburn, L. Berke, and M. Williams. 1992. Behavioral asymmetries of psychomotor performance in rhesus monkeys (*Macaca mulatta*): a dissociation between hand preference and skill. J. Comp. Psychol. 106:392–397.

Hopkins, W. D., C. Cantalupo, M. J. Wesley, A. B. Hostetter, and D. L. Pilcher. 2002. Grip morphology and hand use in chimpanzees (*Pan troglodytes*): evidence of a left hemisphere specialization in motor skill. J. Exp. Psychol. Gen. 131:412–423.

Hopkins, W. D., M. Hook, S. Braccini, and S. J. Schapiro. 2003. Population-level right handedness for a coordinated bimanual task in chimpanzees: replication and extension in a second colony of apes. Int. J. Primatol. 24:677–689.

Hopkins, W. D., M. J. Wesley, M. K. Izard, M. Hook, and S. J. Schapiro. 2004. Chimpanzees (*Pan troglodytes*) are predominantly right-handed: replication in three populations of apes. Behav. Neurosci. 118:659–663.

Hopkins, W. D., J. L. Russell, C. Cantalupo, H. Freeman, and S. J. Schapiro. 2005. Factors influencing the prevalence and handedness for throwing in captive chimpanzees (*Pan troglodytes*). J. Comp. Psychol. 119:363–370.

Hopkins, W. D., J. P. Taglialatela, J. L. Russell, T. M. Nir, and J. Schaeffer. 2010. Cortical representation of lateralized grasping in chimpanzees (*Pan troglodytes*): a combined MRI and PET study. PLoS One 5:e13383.

Hopkins, W. D., K. A. Phillips, A. Bania, S. E. Calcutt, M. Gardner, J. Russell, et al. 2011. Hand preferences for coordinated bimanual actions in 777 great apes: implications for the evolution of handedness in hominins. J. Hum. Evol. 60:605–611.

Kaeser, M., A. F. Wyss, S. Bashir, A. Hamadjida, Y. Liu, J. Bloch, et al. 2010. Effects of unilateral motor cortex lesion on ipsilesional hand's reach and grasp performance in monkeys: relationship with recovery in the contralesional hand. J. Neurophysiol. 103:1630–1645.

Kaeser, M., J. F. Brunet, A. Wyss, A. Belhaj-Saif, Y. Liu, A. Hamadjida, et al. 2011. Autologous adult cortical cell transplantation enhances functional recovery following unilateral lesion of motor cortex in primates: a pilot study. Neurosurgery 68:1405–1416.

Kaeser, M., T. Wannier, J. F. Brunet, A. Wyss, J. Bloch, and E. M. Rouiller. 2013. Representation of motor habit in a sequence of repetitive reach and grasp movements performed by macaque monkeys: evidence for a

contribution of the dorsolateral prefrontal cortex. Cortex 49:1404–1419.
Kastner-Koller, U., P. Deimann, and J. Bruckner. 2007. Assessing handedness in pre-schoolers: construction and initial validation of a hand preference test for 4–6 year olds. Psychol. Sci. 49:239–254.
Kazennikov, O., U. Wicki, M. Corboz, B. Hyland, A. Palmeri, E. M. Rouiller, et al. 1994. Temporal structure of a bimanual goal-directed movement sequence in monkeys. Eur. J. Neurosci. 6:203–210.
Kermadi, I., Y. Liu, A. Tempini, E. Calciati, and E. M. Rouiller. 1998. Neuronal activity in the primate supplementary motor area and the primary motor cortex in relation to spatio-temporal bimanual coordination. Somatosens. Mot. Res. 15:287–308.
Kermadi, I., Y. Liu, and E. M. Rouiller. 2000. Do bimanual motor actions involve the dorsal premotor (PMd), cingulate (CMA) and posterior parietal (PPC) cortices? Comparison with primary and supplementary motor cortical areas. Somatosens. Mot. Res. 17:255–271.
Kimura, D. 2000. Sex and cognition. MIT Press, Cambridge, MA.
Kinoshita, M. 1998. Do monkeys choose the more skillful hand in manual problem-solving? Percept. Mot. Skills 87:83–89.
Lacreuse, A., and D. M. Fragaszy. 1997. Manual exploratory procedures and asymmetries for a haptic search task: a comparison between capuchins (*Cebus apella*) and humans. Laterality 2:247–266.
Lacreuse, A., L. A. Parr, H. M. Smith, and W. D. Hopkins. 1999. Hand preferences for a ahptic task in chimpanzees (*Pan troglodytes*). Int. J. Primatol. 20:867–881.
Lehman, R. A. 1978a. The handedness of rhesus monkeys: I. Distribution. Neuropsychologia 16:33–42.
Lehman, R. A. 1978b. The handedness of rhesus monkeys: II. Concurrent reaching. Cortex 14:190–196.
Lehman, R. A. 1980a. The handedness of rhesus monkeys: III. Consistency within and across activities. Cortex 16:197–204.
Lehman, R. A. 1980b. Distribution and changes in strength of hand preferences of cynomolgus monkeys. Brain Behav. Evol. 17:209–217.
Lehman, R. A. 1989. Hand preferences of rhesus monkeys on differing tasks. Neuropsychologia 27:1193–1196.
Leliveld, L. M., M. Scheumann, and E. Zimmermann. 2008. Manual lateralization in early primates: a comparison of two mouse lemur species. Am. J. Phys. Anthropol. 137:156–163.
Lemon, R. N. 1993. Cortical control of the primate hand. Exp. Physiol. 78:263–301.
Lemon, R. N. 2008. Descending pathways in motor control. Annu. Rev. Neurosci. 31:195–218.
Liu, Y., and E. M. Rouiller. 1999. Mechanisms of recovery of dexterity following unilateral lesion of the sensorimotor cortex in adult monkeys. Exp. Brain Res. 128:149–159.
MacManus, I. C. 2009. Brief handedness questionnaire. Available at http://www.ucl.ac.uk/medical-education/other-studies/laterality/laterality-questionnaires/BriefHandednessQuestionnaire2009.pdf (accessed 22 July 2013).
MacNeilage, P. F., M. G. Studert-Kennedy, and B. Lindblom. 1987. Primate handedness reconsidered. Behav. Brain Sci. 10:247–303.
Mark, R. F., and R. W. Sperry. 1968. Bimanual coordination in monkeys. Exp. Neurol. 21:92–104.
Masataka, N. 1989. Population-level asymetry of hand preference in lemurs. Behaviour 110:244–247.
Meguerditchian, A., J. Donnot, S. Molesti, R. Francioly, and J. Vauclair. 2012. Sex difference in squirrel monkey's handedness for unimanual and bimanual coordinated tasks. Anim. Behav. 83:635–643.
Meunier, H., C. Blois-Heulin, and J. Vauclair. 2011. A new tool for measuring hand preference in non-human primates: adaptation of Bishop's Quantifying Hand Preference task for Olive baboons. Behav. Brain Res. 218:1–7.
Murata, Y., N. Higo, T. Oishi, A. Yamashita, K. Matsuda, M. Hayashi, et al. 2008. Effects of motor training on the recovery of manual dexterity after primary motor cortex lesion in macaque monkeys. J. Neurophysiol. 99:773–786.
Nudo, R. J., W. M. Jenkins, M. M. Merzenich, T. Prejean, and R. Grenda. 1992. Neurophysiological correlates of hand preference in primary motor cortex of adult squirrel monkeys. J. Neurosci. 12:2918–2947.
Oldfield, R. C. 1971. The assessment and analysis of handedness: the Edinburgh inventory. Neuropsychologia 9:97–113.
Papademetriou, E., C. F. Sheu, and G. F. Michel. 2005. A meta-analysis of primate hand preferences, particularly for reaching. J. Comp. Psychol. 119:33–48.
Porter, R., and R. Lemon. 1993. Corticospinal function and voluntary movement. Clarendon Press, Oxford.
Pouydebat, E., E. Reghem, P. Gorce, and V. Bels. 2010. Influence of the task on hand preference: individual differences among gorillas (*Gorilla gorilla gorilla*). Folia Primatol. (Basel) 81:273–281.
Raymond, M., and D. Pontier. 2004. Is there geographical variation in human handedness? Laterality 9:35–51.
Raymond, M., D. Pontier, A. B. Dufour, and A. P. Moller. 1996. Frequency-dependent maintenance of left handedness in humans. Proc. Biol. Sci. 263:1627–1633.
Rogers, L. J. 2009. Hand and paw preferences in relation to the lateralized brain. Philos. Trans. R. Soc. Lond. B Biol. Sci. 364:943–954.
Rohr, L. E. 2006. Gender-specific movement strategies using a computer-pointing task. J. Mot. Behav. 38:431–437.
Rouiller, E. M., X. H. Yu, V. Moret, A. Tempini, M. Wiesendanger, and F. Liang. 1998. Dexterity in adult monkeys following early lesion of the motor cortical hand area: the role of cortex adjacent to the lesion. Eur. J. Neurosci. 10:729–740.

Schaafsma, S. M., B. J. Riedstra, K. A. Pfannkuche, A. Bouma, and T. G. Groothuis. 2009. Epigenesis of behavioural lateralization in humans and other animals. Philos. Trans. R. Soc. Lond. B Biol. Sci. 364:915–927.

Schmidlin, E., M. Kaeser, A. D. Gindrat, J. Savidan, P. Chatagny, S. Badoud, et al. 2011. Behavioral assessment of manual dexterity in non-human primates. J. Vis. Exp. 57:3258.

Schmitt, V., S. Melchisedech, K. Hammerschmidt, and J. Fischer. 2008. Hand preferences in Barbary macaques (*Macaca sylvanus*). Laterality 13:143–157.

Serrien, D. J., R. B. Ivry, and S. P. Swinnen. 2006. Dynamics of hemispheric specialization and integration in the context of motor control. Nat. Rev. Neurosci. 7:160–166.

Sherwood, C. C., E. Wahl, J. M. Erwin, P. R. Hof, and W. D. Hopkins. 2007. Histological asymmetries of primary motor cortex predict handedness in chimpanzees (*Pan troglodytes*). J. Comp. Neurol. 503:525–537.

Singer, S. S., and M. H. Schwibbe. 1999. Right or left, hand or mouth: general-specific preferences in marmosets and tamarins. Behaviour 136:119–145.

Spinozzi, G., M. G. Castorina, and V. Truppa. 1998. Hand preferences in unimanual and coordinated-bimanual tasks by tufted capuchin monkeys (*Cebus apella*). J. Comp. Psychol. 112:183–191.

Spinozzi, G., T. Lagana, and V. Truppa. 2007. Hand use by tufted capuchins (*Cebus apella*) to extract a small food item from a tube: digit movements, hand preference, and performance. Am. J. Primatol. 69:336–352.

Triggs, W. J., R. Calvanio, M. Levine, R. K. Heaton, and K. M. Heilman. 2000. Predicting hand preference with performance on motor tasks. Cortex 36:679–689.

Uomini, N. T. 2009. The prehistory of handedness: archaeological data and comparative ethology. J. Hum. Evol. 57:411–419.

Vauclair, J., A. Meguerditchian, and W. D. Hopkins. 2005. Hand preferences for unimanual and coordinated bimanual tasks in baboons (*Papio anubis*). Brain Res. Cogn. Brain Res. 25:210–216.

Ward, J. P., G. W. Milliken, D. L. Dodson, D. K. Stafford, and M. Wallace. 1990. Handedness as a function of sex and age in a large population of Lemur. J. Comp. Psychol. 104:167–173.

Ward, J. P., G. W. Milliken, and D. K. Stafford. 1993. Patterns of lateralized behavior in prosimians. Pp. 43–74 *in* J. P. Ward and W. D. Hopkins, eds. Primate laterality: current behavioral evidence of primate asymmetries. Springer, New-York, NY.

Wesley, M. J., S. Fernandez-Carriba, A. Hostetter, D. Pilcher, S. Poss, and W. D. Hopkins. 2001. Factor analysis of multiple measures of hand use in captive chimpanzees: an alternative approach to the assessment of handedness in non-human primates. Int. J. Primatol. 23:1155–1168.

Westergaard, G. C., and I. D. Lussier. 1999. Left-handedness and longevity in primates. Int. J. Neurosci. 99:79–87.

Westergaard, G. C., and S. J. Suomi. 1996. Hand preference for a bimanual task in tufted capuchins (*Cebus apella*) and rhesus macaques (*Macaca mulatta*). J. Comp. Psychol. 110:406–411.

Westergaard, G. C., M. Champoux, and S. J. Suomi. 1997. Hand preference in infant rhesus macaques (*Macaca mulatta*). Child Dev. 68:387–393.

Westergaard, G. C., I. D. Lussier, and J. D. Higley. 2001a. Familial influences on hand preference: genotypic variation between closely related primate species. Dev. Neuropsychol. 20:605–617.

Westergaard, G. C., I. D. Lussier, and J. D. Higley. 2001b. Between-species variation in the development of hand preference among macaques. Neuropsychologia 39:1373–1378.

Zhao, D., W. D. Hopkins, and B. Li. 2012. Handedness in nature: first evidence on manual laterality on bimanual coordinated tube task in wild primates. Am. J. Phys. Anthropol. 148:36–44.

Appendix 4

Variability of manual dexterity performance in non-human primates (*Macaca fascicularis*)

Kaeser M*, Chatagny P*, **Gindrat AD**, Savidan J, Badoud S, Fregosi M, Moret V, Roulin C, Schmidlin E, Rouiller EM (2014). International Journal of Comparative Psychology 27(2):295-325

In the context of large inter-individual variability in fine manual dexterity in control macaque monkeys, we proposed here a detailed analysis of hand motor performance in the modified Brinkman board task and in the reach and grasp drawer task, both during the learning phase and the plateau phase, with the aim to find some predictors of the stable motor performance at plateau already during the learning phase.

Appendix 4

INTERNATIONAL JOURNAL OF COMPARATIVE PSYCHOLOGY

2014, 27 (2), 295-325
A. Blaisdell & W. D. Stahlman
Special Issue
Peer-reviewed

Variability of manual dexterity performance in non-human primates (*Macaca fascicularis*)

Mélanie Kaeser*, Pauline Chatagny*, Anne-Dominique Gindrat, Julie Savidan, Simon Badoud, Michela Fregosi, Véronique Moret, Christine Roulin, Eric Schmidlin[#] and Eric M. Rouiller[#]
Domain of Physiology, Department of Medicine and Fribourg Center for Cognition, University of Fribourg, Chemin du Musée 5, CH-1700 Fribourg, Switzerland.

The goal of this study was to quantify the inter-individual and intra-individual variability of manual (digits) skill in adult macaque monkeys, over a motor learning phase and, later on, when motor skills were consolidated. The hypothesis is that several attributes of the stable manual dexterity performance can be predicted from learning characteristics. The behavioral data were collected from 20 adult *Macaca fascicularis*, derived from their dominant hand, defined as the hand exhibiting a better performance than the other. Two manual dexterity tasks were tested: (i) the "modified Brinkman board" task, consisting in the retrieval of food pellets placed in 50 slots in a board, using the precision grip (opposition of the thumb and index finger); (ii) the "reach and grasp drawer" task, in which the grip force and the load force were continuously monitored while the monkey opened a drawer against a resistance, before grasping a pellet inside the drawer. The hypothesis was verified for the performance of manual dexterity after consolidation, correlated with the initial score before learning. Motor habit, reflected by the temporal order of sequential movements executed in the modified Brinkman board task, was established very early during the learning phase. As mostly expected, motor learning led to an optimization of manual dexterity parameters, such as score, contact time, as well as a decrease in intra-individual variability. Overall, the data demonstrate the substantial inter-individual variability of manual dexterity in non-human primates, to be considered for further pre-clinical applications based on this animal model.

In the common language, some people are described as clumsy whereas others have recognized talents to practice challenging motor tasks with great manual (digits) dexterity, such as musicians, top sports performers, as well as in some professional activities requiring high degree of precision in motor control (e.g., handmade watchmakers). Such inter-individual variability of motor skill is accompanied by some degree of intra-individual variability as the manual dexterity of a human being is subjected to variations from one day to the next, as well as to improvement resulting from motor practice. Manual dexterity corresponds to the skill to control independently and precisely each finger. From an evolutionary point of view, exquisite manual dexterity is largely considered as a prerogative of primates, as other mammalian orders do not exhibit such a high degree of manual dexterity, in spite of some recent findings providing evidence in favor of some manual skill in rodents for instance (see e.g., Sacrey, Alaverdashvili, & Whishaw, 2009; Whishaw, Whishaw, & Gorny, 2008; Whishaw, Travis, Koppe, Sacrey, Gholamrezaei, & Gorny, 2010; but see also Klein, Sacrey, Whishaw, & Dunnett, 2012). The specialty of primates for manual dexterity is based on the specific anatomical organization of the primate motor system, comprising the direct cortico-spinal projection called the cortico-motoneuronal (CM) system (see Lawrence & Hopkins, 1976; Lawrence, Porter, & Redman, 1985;

* shared first authorship, [#] shared senior authorship

Please send correspondence to Prof. Eric M. Rouiller, Domain of Physiology, Department of Medicine and Fribourg Center for Cognition, University of Fribourg, Chemin du Musée 5, CH-1700 Fribourg, Switzerland, Phone: +41 26 300 86 09; Fax: +41 26 300 96 75. (Email: eric.rouiller@unifr.ch)

Lemon, 2008). The progressive evolution of the CM system across mammalian species is correlated with an increasing manual skill (see e.g., Courtine et al., 2007). Consequently, the non-human primates represent a unique animal model to study mechanisms involved in manual dexterity, which are also applicable to human subjects. For instance, monkeys have been used extensively to investigate experimentally the consequences on manual dexterity of various types of lesions affecting the motor system (e.g., Bashir et al., 2012; Beaud et al., 2008; Beaud et al., 2012; Bihel et al., 2010; Brinkman, 1984; Brinkman & Kuypers, 1973; Dancause & Nudo, 2011; Dancause et al., 2005; Dancause et al., 2006; Darling et al., 2009; Darling et al., 2010; Darling et al., 2011; Darling et al., 2013; Eisner-Janowicz et al., 2008; Friel & Nudo, 1998; Friel, Heddings & Nudo, 2000; Frost, Barbay, Friel, Plautz & Nudo, 2003; Galea & Darian-Smith 1997; Glees & Cole, 1950; Hoogewoud et al., 2013; Kaeser et al., 2010; Kaeser et al., 2013; Liu & Rouiller 1999; Marshall et al., 2003; McNeal et al., 2010; Murata et al., 2008; Nishimura et al., 2007; Nudo & Milliken, 1996; Nudo, Wise, SiFuentes, & Milliken, 1996; Ogden & Franz, 1917; Passingham, Perry, & Wilkinson, 1983; Pizzimenti et al., 2007; Roitberg et al., 2003; Rouiller et al., 1998; Sasaki & Gemba, 1984; Schmidlin, Wannier, Bloch, & Rouiller, 2004; Schmidlin et al., 2005; Schmidlin et al., 2011; Travis, 1955; Wannier, Schmidlin, Bloch, & Rouiller, 2005) and, in some cases, also to test the potential of various treatments after such lesions (e.g., Freund et al., 2006; Freund et al., 2007; Freund et al., 2009; Hamadjida et al., 2012; Kaeser et al., 2011; Plautz et al., 2003; Sugiyama et al., 2013; Wyss et al., 2013).

Numerous studies shed light on the anatomical, physiological and developmental aspects underlying manual dexterity in monkeys (e.g., Alstermark et al., 2011, Alstermark & Isa, 2002, 2012; Armand, Edgley, Lemon, & Olivier, 1994; Armand, Olivier, Edgley, & Lemon, 1997; Borra, Belmalih, Gerbella, Rozzi, & Luppino, 2010; Bortoff & Strick, 1993; Darian-Smith, Galea, & Darian-Smith, 1996; Darian-Smith et al., 1996; Darian-Smith, Burman, & Darian-Smith, 1999; Flament, Hall, & Lemon, 1992; Galea & Darian-Smith, 1994, 1995; Iwaniuk, Pellis, & Whishaw, 1999; Kinoshita et al., 2012; Lacroix et al., 2004; Lemon, Johansson, & Westling, 1996; Lemon, 1999; Maier et al., 2002; Manoel & Connolly, 1995; Ogihara & Oishi, 2012; Olivier, Edgley, Armand, & Lemon, 1997; Padberg et al., 2007; Rathelot & Strick, 2009; Rouiller, Moret, Tanné, & Boussaoud, 1996; Sasaki et al., 2004). Furthermore, various aspects linked with manual dexterity were studied, such as manual coordination and strategies, handedness and tool use, as well as phylogenetic characteristics (e.g., Chalmeau, Visalberghi, & Gallo, 1997; Chatagny et al., 2013; Christel & Billard, 2002; Costello & Fragaszy, 1988; Falk, Pyne, Helmkamp, & DeRousseau, 1988; Fragaszy & Adams-Curtis, 1997; Gash et al., 1999; Fragaszy, 1998; Iwaniuk & Whishaw, 1999, 2000; King, 1986; King & Landau, 1993; Lacreuse & Fragaszy, 1999; Leca, Gunst, & Huffman, 2011; Lemon & Griffiths, 2005; Lindshield & Rodrigues, 2009; Nahallage & Huffman, 2007; Pouydebat, Laurin, Gorce, & Bels, 2008; Pouydebat, Gorce, Coppens, & Bels, 2009; Pouydebat, Reghem, Borel, & Gorce, 2011; Van Schaik, Deaner, & Merrill, 1999; Spinozzi, Castorina, & Truppa, 1998; Spinozzi, Truppa, & Lagana, 2004; Spinozzi, Lagana, & Truppa, 2007; Wiesendanger, 1999; Zhao, Hopkins, & Li, 2012).

In the present study, our goal was to use two complementary manual dexterity tasks, namely the *modified Brinkman board* task and the *reach and grasp drawer* task, to quantify the inter-individual variability of manual skill in adult macaque monkeys, as well as the intra-individual variations along a motor learning phase and, later on, during motor skills consolidation. More specifically, our main hypothesis is that manual dexterity performance and variability in the modified Brinkman board task, when acquired, can be predicted from the duration of the learning phase, and/or from the learning slope and/or from the initial score before any training took place. For the two tasks, it is also expected that the learning phase contributes: (i) to significantly reduce the intra-individual variability of manual skills, when a plateau of performance is reached; (ii) to optimize several attributes of manual dexterity, underlying the better motor performance reached at plateau. Nevertheless, in line with the principle of motor equivalence (see Lashley, 1930), the same motor goals with comparable levels of performance can be achieved using highly different motor strategies, as reflected by a wide inter-individual variability in manual skill parameters exhibited by adult macaque monkeys.

Method

Subjects

The behavioral experiments were conducted on 20 adult macaque monkeys (see Table 1 for individual parameters related to sex, weight, age, etc). Detailed information about the detention conditions of the monkeys, the veterinary authorizations, reward procedures and inclusion of the monkeys in previous studies can be found in the supplementary Methods and Results. As illustrated previously in the form of a video sequence (Schmidlin et al., 2011), the first experimental step (lasting 1-3 months) was to habituate the monkeys to be transferred into a primate chair, without direct manipulation of the animals by the experimenters, a procedure reducing the stress on the animals and the risks for the experimenters. Placed in the primate chair, the monkeys were weighed, and then transferred to the behavioral set-up in the laboratory.

Procedure

On each behavioral session (3-5 days a week), the monkeys systematically performed the modified Brinkman board task (derived from the initial task of Brinkman & Kuypers, 1973; Brinkman, 1984), representing the basic manual dexterity task on which the present data are based. In addition, shifting from one session to the next, the monkeys performed additional tasks (rotating Brinkman board task; Brinkman box task; reach and grasp drawer task; as illustrated in Schmidlin et al., 2011). In the present report, only the reach and grasp drawer task is considered as an additional behavioral test to the modified Brinkman board task and in a subgroup of the monkeys only as this quantitative test was introduced fairly recently.

Taking advantage of two separate windows in front of the primate chair, each hand was tested separately and the first hand tested was alternated at each session. Typically, a daily behavioral session lasted about one hour, to test separately each hand. All behavioral tests were videotaped for off-line analysis. The present report is however restricted to data derived from the **dominant hand**, defined as the hand exhibiting the highest score in the modified Brinkman board task at plateau, to be distinguished from the preferred hand defined as the hand preferably chosen to perform a task when the monkey had the choice to use one or the other hand, irrespective of the performance (see Chatagny et al., 2013).

Materials and Measures

The modified Brinkman board task requires the precision grip (opposition of thumb and index finger) to grasp food pellets from 50 slots dug in a perspex board (see Schmidlin et al., 2011), placed in front of the monkey (see also Figure 5D). The 50 slots are divided into 25 vertically oriented slots and 25 horizontally oriented slots, randomly distributed on the board. Banana flavor 45 mg pellets were used (*Bio-Serv, US and Canada: www.bio-serv.com)*.

As previously reported (Schmidlin et al., 2011), the following 4 parameters were analyzed in the modified Brinkman board task: i) the **score** (number of food pellets retrieved during the first 30 seconds); ii) the **contact time** (CT = duration in seconds of contact between the fingers and the food pellets in the slot), determined for the first 5 vertical slots and the first 5 horizontal slots; iii) the **temporal sequence** followed by the monkey's hand to visit the 50 slots of the board; iv) the **types of movements** and **strategies** used to retrieve the pellets from the slots, as well as the quantification of errors of grasping.

The reach and grasp drawer task also measures the ability to unimanually catch a food pellet in a well, but this action is preceded by the opening of a drawer, requiring to counteract a variable resistance opposing the pulling. The test thus allows quantifying via sensors the force applied to hold the knob of the drawer in between the thumb and the index finger (grip force), as well as the load force (applied to pull the drawer). Moreover, several other sensors allow quantifying distinct consecutive phases of the task (Figure 6A; Schmidlin et al., 2011). In the reach and grasp drawer task, emphasis was put on aspects not covered by the modified Brinkman board task, namely the ability of the monkey to generate different levels of force to counteract the resistances opposing the opening of the drawer (load force), while precisely controlling the grip force between the thumb and index finger to prevent the loss of contact with the drawer knob (see Schmidlin et al., 2011). The following parameters were specifically analyzed in the reach and grasp drawer task: i) the **maximal grip force**; ii) the **maximal load force**; iii) the **duration of the grip force** application; iv) the **duration of the load force** application. The load force is believed to be initiated only when the grip force has reached a sufficient level to prevent sliding of the fingers on the knob due to the resistance opposing the opening of the drawer. Further details about the behavioral set-ups were described earlier (Schmidlin et al., 2011).

The behavioral data were represented graphically and analyzed statistically using the Sigmaplot 12.0 software package (*www.sigmaplot.com*). Accordingly, group comparisons were based on parametric tests (paired or unpaired t-tests) when the normality criteria were satisfied or, if not, on non-parametric tests (Wilcoxon rank-sum test or Mann-Whitney U test). Relationships between two behavioral parameters were assessed based on the Pearson correlation test.

Results

Modified Brinkman Board Task

The modified Brinkman board task is largely intuitive in the sense that an experimentaly-naïve monkey placed in front of the board rapidly starts to grasp flavored food pellets, thus representing a fairly *natural* motor task. However, as a result of practice, the performance measured by the number of pellets retrieved in 30 seconds (score) increased from one session to the next, during the learning phase (Figure 1 and Supplementary Figure 1). The use of the precision grip to perform the task is also naturally adopted by all monkeys, although there may be subtle variations in the prehension pattern itself (see below). Furthermore, as there is no time constraint imposed to visit the 50 slots, the monkeys perform the task at their own pace depending on their motivation, a task thus assimilated to a voluntary behavior. In absence of strong constraints imposing a learning schedule and a level of performance on the monkeys, there is the possibility to assess the inter-individual variability related to manual skill, both during the learning phase and the plateau phase. The data will be first, and mainly, described based on the total score.

Learning phase: Total score. The learning phase of the modified Brinkman board task appeared quite variable from one animal to the next. A unique case is Mk-RO (Figure 1), exhibiting more a substantial decrease in variability along the 146 days of practice than a true increase in performance (modest regression line slope; see also Table 1). Another particular case is Mk-MO (Figure 1), with an impressive score from beginning, maintained during more than 100 days, before a moderate enhancement of score taking place at day 110, considered as the end of the learning phase. The regression line with a slightly negative slope is meaningless (Table 1), reflecting the absence of progressive improvement of score during the first 110 days.

All other monkeys exhibited a progressive increase in score, although the slope and the duration of the corresponding learning period were highly variable across animals (see Figure 1 and Supplementary Figure 1; Table 1). Four monkeys were characterized by a very steep learning slope (Figure 2 panel A; Table 1): Mk-AT (see also Figure 1), Mk-DI (see also Supplementary Figure 1), Mk-WI and Mk-CE. In the rest of the monkeys, the learning slope ranged from low to medium values (Figure 2 panel A), as illustrated for instance by Mk-JO (Figure 1; Table 1).

Another parameter of interest in relation to the learning phase is the intercept of the learning regression line with the y-axis (score), yielding an estimate of the initial performance at the onset of the training. As shown in Figure 2 (panel B: filled circles), the intercept values are quite variable from one monkey to the next, without however forming separate clusters. In Figure 1, three monkeys illustrate a low initial value (Mk-AN), a medium initial score (Mk-JA) and a high initial value (Mk-MO), respectively.

Highly variable also was the duration of the learning phase (Figure 2 panel C). With the exception of Mk-RO (as discussed above), the end of the learning phase was defined using the following criterion (as already used in a recent study on hand dominance/preference: Chatagny et al., 2013): when the progressive increase in score approached a plateau perceived by visual inspection, as observed in most monkeys, the first score value considered as the onset of the plateau is the score which is not exceeded by another value among the five next score values. Consequently, the end of the learning phase, indicated by the vertical dashed line in

Table 1
List of monkeys and relevant parameters for the modified Brinkman board task

	Sex+	Weight*	Age*	Learning phase (days)[&]	Plateau (days)[&]	First score value[& ç]	Median plateau value[&]	Mean plateau value[&]	*SD* plateau value[&]	Slope learning phase[&]	Score plateau[#] Comparison H vs V slots	Median contact time at plateau V slots	Median contact time at plateau H slots	Mean errors (learning; plateau)
Mk-AN	f [1,b]	3.2	6	151	44	8.894	22	21.889	1.987	0.0795	H>V	0.32	0.48	5; 0 (c)
Mk-AT	f [1,b]	3.4	7	32	129	18.266	30	29.507	3.521	0.418	**V>H (W)**	0.16	0.26	4.5; 1.2 (c)
Mk-CA	f [1,b]	3.7	7	210	30	12.177	28	26.875	4.303	0.0598	**V>H (t)**	0.2	0.36	3.8; 2.1 (e)
Mk-LO	f [1,b]	3	7	97	92	12.302	22	21.528	2.408	0.0827	**V>H (t)**	0.32	0.8	2.3; 0.4 (c)
Mk-MA	f [1,b]	3.2	7	89	133	17.416	33	33.179	2.984	0.176	**V>H (t)**	0.24	0.2	16; 0.7 (c)
Mk-MI	f [1,b]	3.1	7	86	85	19.846	26	25.465	3.397	0.0611	**V>H (t)**	0.2	0.36	9.8; 1.4 (c)
Mk-TH	f [1,b]	3.9	6	101	26	16.77	31.5	30.938	4.389	0.15	**V>H (t)**	0.2	0.32	7; 0.5 (c)
Mk-DI	f [1,b]	3.4	7	41	109	20.516	31	31.154	3.294	0.410	**H>V (W)**	0.2	0.2	4.8; 1 (c)
Mk-EN	m [3,a]	4.2	5	213	216	27.816	33	32.78	2.339	0.0095	**V>H (W)**	0.2	0.32	2; 0.4 (c)
Mk-AV	m [2,b]	3.2	3	31	120	20.132	31	30.35	2.854	0.198	H>V	0.24	0.44	0; 0 (d)
Mk-JO	m [2,b]	3.2	3	63	34	24.52	34.5	34.25	2.817	0.121	**V>H (W)**	0.16	0.28	1; 0.7 (d)
Mk-JA	m [2,b]	2.5	3	163	60	22.75	28	28.2	2.783	0.0199	**V>H (t)**	0.333	0.867	0; 0.7 (d)
Mk-WI	m [2,b]	2.7	3.5	16	234	30.116	35	34.95	3.306	0.409	**V>H (W)**	0.24	0.32	3.8; 0.2 (c)
Mk-VA	m [2,a]	3.4	3.5	64	404	24.12	26.5	26.875	4.463	0.0937	**V>H (W)**	0.333	0.6	2.3; 0 (c)
Mk-BI	m [2,a]	3.7	4.5	163	142	29.567	34.5	33.817	3.362	0.0336	**V>H (W)**	0.18	0.32	0.7; 0.3 (d)
Mk-MO	m [2,a]	4	4.5	110	114	33.318	35	34.424	2.681	-0.00370	**V>H (t)**	0.133	0.267	1; 0.5 (c)
Mk-GE	f [2,a]	3.5	5	70	447	17.751	21	20.955	4.817	0.0516	**V>H (t)**	0.34	0.56	1.9; 0.1 (c)
Mk-RO	m [2,a]	3.7	3	146	181	23.651	28	27.667	2.087	0.0288	**V>H (W)**	0.44	0.52	6.1; 0.9 (c)
Mk-CE	m [2,a]	3.5	4	21	77	21.75	25.5	23.5	4.468	0.274	**V>H (t)**	0.667	0.8	0.8; 0.9 (d)
Mk-DG	m [3,a]	5.2	4	107	64	20.58	31	31.68	4.13	0.119	**V>H (t)**	0.23	0.32	2.3; 1.8 (e)

Notes. + f = female; m = male. The following number ([1], [2] or [3]) indicates the housing conditions: 1 = 45 m^3 housing facility; 2 = 15 m^3 facility; 3 = transfer from 15 m^3 to 45 m^3 (data acquired however after transfer). The following letter ([a], [b]) indicates whether the animal has been subjected to preliminary habituation to the behavioral set-up (a) or not (b), before data collection.

* at beginning of training (age rounded 0.5).

& established for total score in the modified Brinkman board task (all monkeys).

ç intercept of regression line with y-axis in score plot.

Bold characters are for statistically significant differences between H (horizontal slots) and V (vertical slots): paired t-test (**t**) or Wilcoxon (**W**) test; see also text for learning phase.

In the rightmost column, c, d and e correspond to three different error profiles (see text).

Figure 1 and Supplementary Figure 1, precedes the first score value defined as the onset of the plateau. Mk-AV is representative of a very quick learning (Supplementary Figure 1), with a plateau reached after only 31 days. At the other extremity, Mk-EN exhibited a very long learning phase, with a weak slope, completed after 213 days (Supplementary Figure 1). An average duration of learning phase is illustrated by Mk-MA (Supplementary Figure 1), with a plateau reached after about 3 months.

The difference between the average score at plateau and the initial score before training yields an estimate of the score enhancement obtained during the learning phase. This value is represented for the total score by crosses in Figure 2 (panel B). As one might have expected, there is a trend towards a larger improvement of score during the learning phase in the monkeys with a low initial score as compared to those with a higher initial score characterized by a limited score progression. The two (interdependent to some extent) parameters of initial score and score improvement during learning appear to present a difference with respect to sex. As shown in Figure 2 panel B, the nine females (identified by "f" the x-axis) exhibit lower initial values than most males. The average initial score was 15.99 pellets in 30 seconds in females (*SD* = 3.95) whereas, in males, it was 25.3 pellets in 30 seconds (*SD* = 4.3). This difference between females and males is statistically significant ($p < 0.001$; unpaired t-test). Consequently, females exhibited a larger margin of score progression during learning (average 10.84 pellets in 30 seconds; *SD* = 4.23) than males (average 5.47 pellets in 30 seconds; *SD* = 3.42); this difference related to sex is also statistically significant ($p = 0.006$; unpaired t-test). The other two parameters related to learning (learning slope and duration of training) did not differ between the sex groups (Figure 2 panels A and C).

Plateau phase: Total score. As illustrated in Figure 1 and Supplementary Figure 1, the plateau phase starts after the vertical dashed line. The average and median score values reached at plateau were also variable among monkeys, ranging from 21 to 35 pellets (Figure 2 panels E and F; Table 1). A relevant parameter at plateau is the intra-individual variability from one daily session to the next, estimated by the standard deviation (*SD*) of the score values during the entire plateau phase (Table 1). The *SD* was highly variable across monkeys (Figure 2 panel D), ranging from 1.99 to 4.82. A "typical" monkey is represented by Mk-AN (Figure 1), whereas a monkey exhibiting an atypical performance at plateau is illustrated by Mk-MI (Supplementary Figure 1).

To assess whether the performance reached at plateau (score and variability) depends on learning properties, such as the duration of the learning phase, the slope of the learning regression line or the initial score before training, the average score at plateau and its *SD* were plotted for the 20 monkeys as a function of the corresponding learning parameters (Supplementary Figure 2). There was correlation neither between the learning duration (in days) and the average score at plateau, nor between the learning duration and the *SD* of the score at plateau (top two panels in Supplementary Figure 2). The same absence of correlations was found during the first five learning sessions. Similarly, the speed of learning, estimated by the slope of the learning regression line, was not correlated with the manual performance at plateau (score or *SD*; bottom two panels in Supplementary Figure 2). In contrast, the initial score before training was to some extent a predictor of the score at plateau, as there was a statistically significant correlation between these two parameters (top right panel in Figure 3; Pearson correlation test). On the other hand, there was no correlation between the initial score before training and the variability (*SD*) of the score at plateau (middle right panel in Supplementary Figure 2).

Both the inter-individual and intra-individual variations of the total score can be better visualized when displayed in the form of box and whisker plots (Figure 3 top left panel). Some animals exhibited a fairly small variability of their total score at plateau, from one daily session to the next (Mk-AN, Mk-CA, Mk-LO, Mk-JO and Mk-RO). In these monkeys, the distance between the 25 and 75 percentiles was equal to or smaller than

3.6 pellets. At the other extreme, some monkeys were characterized by a large variability across daily sessions (Mk-GE and Mk-WI), with a distance between the 25 and 75 percentiles equal to or larger than 10 pellets.

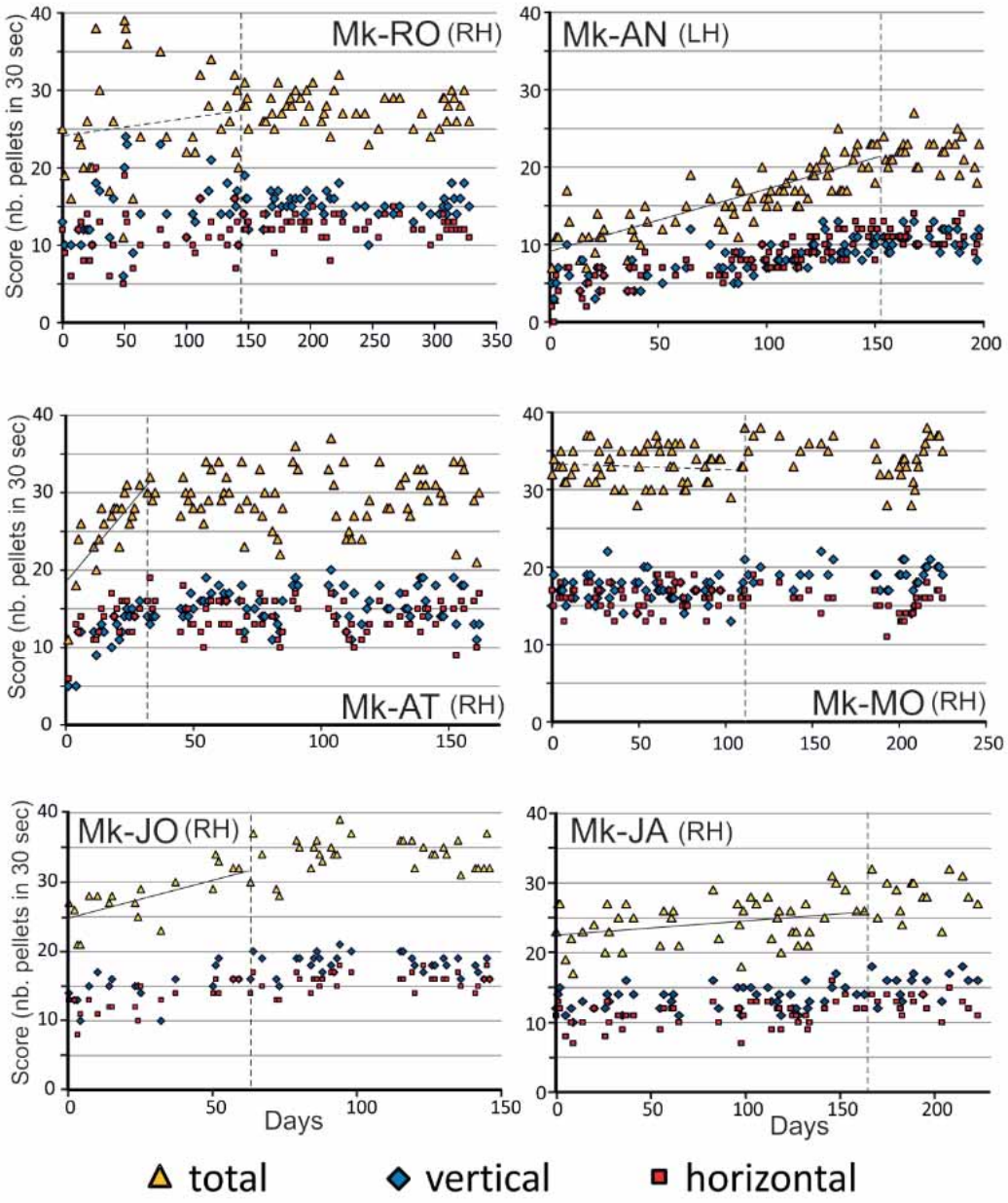

Figure 1. Plots showing the score obtained by 6 monkeys (Mk-RO, Mk-AT, Mk-JO, Mk-AN, Mk-MO, MK-JA) in the modified Brinkman board task for the dominant hand (RH=right hand; LH=left hand). Yellow triangles represent the total score, whereas the separate scores in vertical and horizontal slots are displayed by blue diamonds and purple squares, respectively. The time in days from the first day of testing is represented on the x-axis. For instance, in absence of test during the weekend, there is a delta of 3 days between tests conducted on Friday and then on next Monday. The vertical dashed lines represent the end of the learning phase and consequently the onset of the plateau phase (see text). A learning regression line on the total score is displayed for each animal (see text). The regression lines for Mk-RO and Mk-MO are represented with dashed lines as they are special cases (see text).

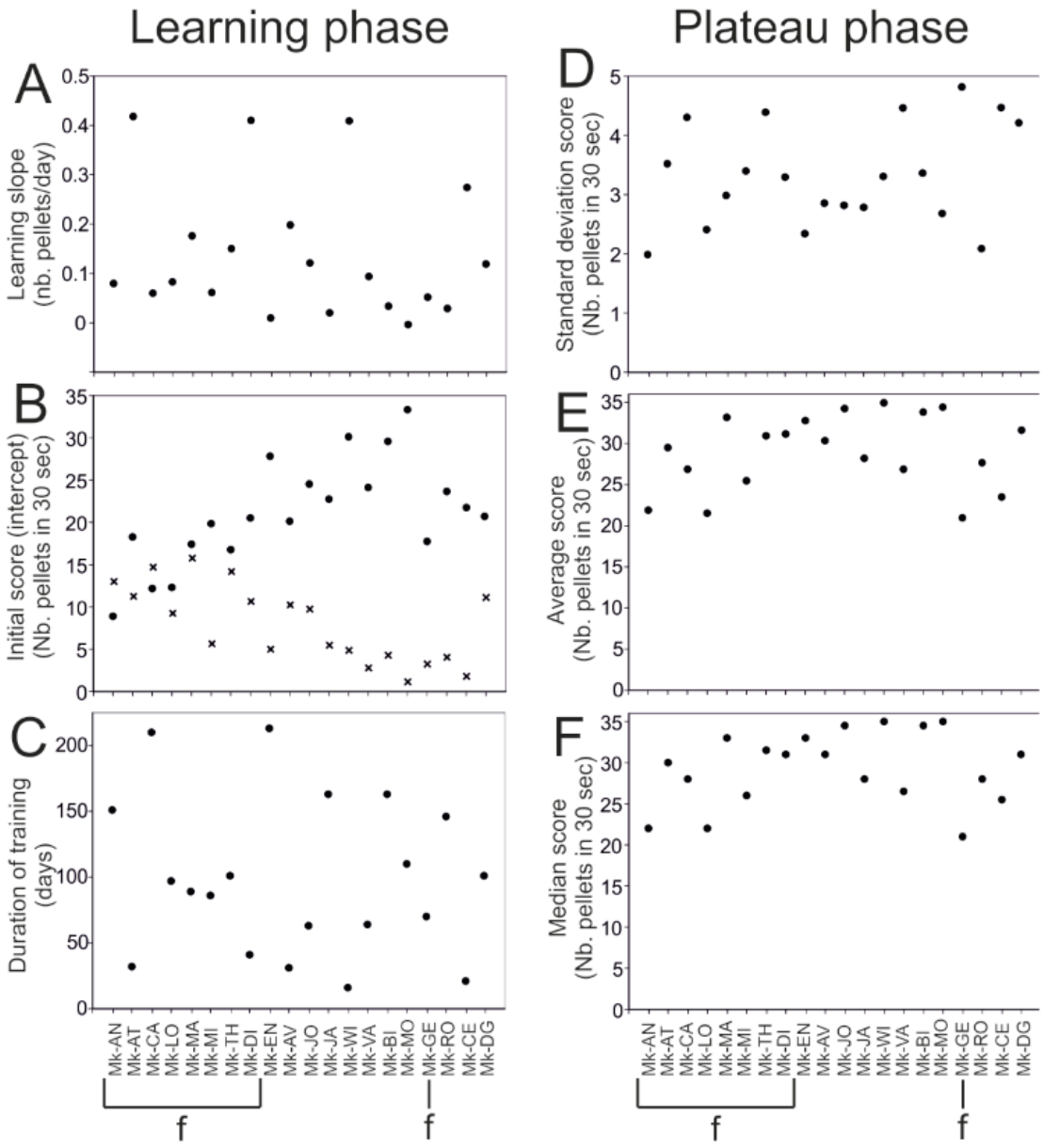

Figure 2. Plots showing relevant parameters for motor performance by all monkeys during the learning phase and the plateau phase of the modified Brinkman board task. The data concern the total score. The ID name of the monkeys appears below each bottom graphs. The 9 females monkeys are identified by "f" below the ID names. The other 11 monkeys are males. In panel B, crosses represent the progress of score obtained during the learning phase: it is the average score at plateau minus the initial score (also expressed as a number of pellets in 30 seconds; see text).

Score in vertical and horizontal slots. Pellet retrieval from the horizontal slots is more challenging than from the vertical ones (see Chatagny et al., 2013; Freund et al., 2009; Hoogewoud et al., 2013; Schmidlin et al., 2011), as the precision grip is usually accompanied by a deviation of the wrist/arm, not necessary for the vertical slots, corresponding either to an ulnar deviation or a radial deviation (see below, Variable Patterns of

Food Pellet Grasping). Below, the data are presented first at plateau, where they are more stable, and then, for comparison, during the learning phase.

At plateau, the scores were in most cases lower in the horizontal slots than in the vertical slots (Figure 1 and Supplementary Figure 1; Table 1): this difference was statistically significant in 17 monkeys ($p < 0.001$ in 15 monkeys; $p = 0.016$ in Mk-CE and $p = 0.011$ in Mk-TH; see Table 1). In contrast, in three monkeys, the horizontal scores were higher than the vertical scores, but the difference was not statistically significant ($p > 0.05$) in two monkeys (Mk-AN, see Figure 1; Mk-AV, see Supplementary Figure 1). In the third monkey (Mk-DI), the horizontal score was significantly higher than the vertical score ($p < 0.001$; see Supplementary Figure 1 and Table 1). At the plateau phase, there was no statistically significant difference between females and males in the median score for the vertical and horizontal slots taken separately, as well as for the variability of both of them (Figure 3).

The variability of the scores at plateau taken separately for the horizontal and the vertical slots can be visualized when the scores are displayed in the form of box and whisker plots (Figure 3 bottom two panels). In this way, the 20 monkeys can be distributed in three subgroups. First, in eight monkeys the variability of scores at plateau was comparable for both slot orientations. Second, the variability of scores at plateau was lower in the vertical slots in six monkeys. Third, it was the other way around in six monkeys with a lower variability in the horizontal slots.

In the learning phase, there was a positive correlation between vertical and horizontal mean scores ($r = 0.79$), indicating that the learning performance for one slot orientation is consistent with that for the other orientation. Nevertheless, no significant correlation appeared neither between vertical and horizontal *SD*s, nor between mean and *SD* for both slots orientations. However, differences between the scores observed in the vertical slots and in the horizontal slots at plateau were already visible during the learning phase (see all monkeys illustrated in Figure 1 and Supplementary Figure 1, except Mk-AT). In the three monkeys (Mk-AN, Mk-AV and Mk-DI) with a higher score in the horizontal slots at plateau, this difference was already present during the learning phase. However, it was only a trend as the differences were not statistically significant ($p > 0.05$, paired t-test or Wilcoxon rank-sum test). In the 17 monkeys exhibiting higher scores in the vertical slots at plateau, this difference was already present and statistically significant in 13 of them during the learning phase ($p < 0.05$, paired t-test or Wilcoxon rank-sum test test); it was only a trend in two monkeys (Mk-CE and Mk-EN; $p > 0.05$, paired t-test or Wilcoxon rank-sum test); there was a statistically non-significant trend towards a better score in the horizontal slots during learning in Mk-GE ($p > 0.05$, paired t-test); surprisingly, in Mk-AT, there were statistically better scores in the horizontal slots during the learning phase ($p = 0.023$, Wilcoxon rank-sum test), whereas this was the opposite at plateau (Figure 1).

Contact time (CT). The score data of the modified Brinkman board task described above involve motor components that are not purely part of the precision grip itself, such as the time of transport of the arm first towards and then away from the board. The contact time (CT) represents the time interval used by the monkey's hand to retrieve the pellets from the slots (see Method). As the precision grip movement is different with respect to slot orientation, the CT was measured separately in the horizontal and in the vertical slots in all 20 monkeys during the plateau phase (Figure 4; same plateau phase as defined for the score data). As expected, in the vast majority of monkeys ($n = 18$), the median CT at plateau was shorter in the vertical slots than in the horizontal slots (Table 1). The median CT was equal in both slot orientations in Mk-DI (0.2 second), and it was shorter in the horizontal slots in Mk-MA (Table 1). At plateau, the median CTs ranged from 0.13 sec to 0.67 sec across the 20 monkeys in the vertical slots and from 0.20 sec to 0.87 sec in the horizontal slots (see Table 1 and left panels of Figures 4A and B). The variability of the CTs at plateau (Figure 4) was greater for the horizontal slots in all monkeys. Three monkeys (Mk-CE, Mk-JA and Mk-RO) exhibited consistent highly variable CTs at plateau in both horizontal and vertical slots (Figure 4).

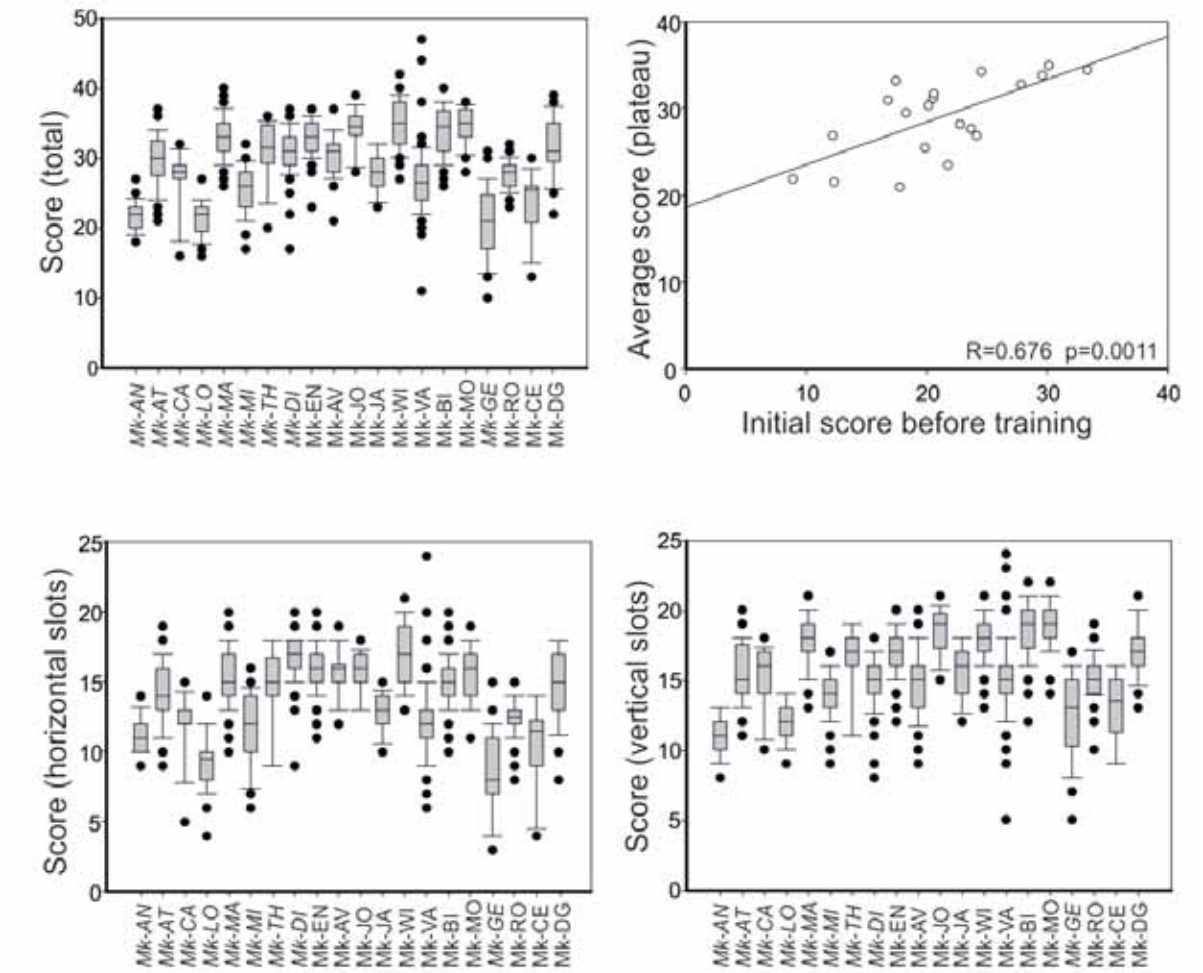

Figure 3. Scores obtained by all monkeys at **plateau phase** in the modified Brinkman board task, represented in the form of box and whisker plots. The horizontal line in the boxes represents the median value. The top and bottom of the boxes are for the 75 and 25 percentiles, respectively. The top and bottom of the whiskers represent the 90 and 10 percentiles, respectively. Black dots are for individual values above and below the 90 and 10 percentiles. The top left graph displays the total score, whereas the scores in the horizontal and vertical slots are shown in the bottom left and bottom right graphs, respectively. The ID names of females are shown in italics. The plot on the top right shows the statistically significant correlation between the average total score at plateau and the initial score before training, with the regression line. The corresponding coefficient of correlation (R) is given at the bottom right of the plot, followed by the p value (Pearson correlation test).

The CTs established at plateau were compared with those at the onset of the learning phase. The CT was assessed during the first four daily behavioral sessions (right panel in Figures 4A and B, for the horizontal and vertical slots, respectively), based on previous evidence that individual differences and intra-individual variations are greatest during the first four practice trials during motor learning (e.g., Carron & Leavitt, 1968; Marteniuk, 1974). The median CT values at onset of learning are clearly longer than those measured at plateau (Figure 4), reflecting a decrease in CT during the learning phase, corresponding to an enhancement of precision grip performance. An in-depth comparison of CTs at plateau with those at onset of learning is presented in the supplementary Methods and Results, together with supplementary Figure 3. Moreover, how

the CTs progressively decrease during the first four days of learning is also reported in the supplementary Methods and Results.

Temporal sequence of grasping (motor habit). As the modified Brinkman board task is a voluntary motor task, there was no constraint on the monkey on how to perform the task, for instance in which temporal order to visit the 50 slots. However, as previously reported (Kaeser et al., 2013; Schmidlin et al., 2011), most monkeys did not visit the 50 slots randomly at plateau, but they generally adopted a preferential temporal sequence, for instance starting to empty the slots at one extremity of the board (right side for instance) and then scanning the board progressively and systematically towards the opposite extremity (left side in this example), as illustrated by the bottom inset in Figure 5A.

Such preferential temporal sequence, generally maintained at plateau from one daily session to the next, was considered as a **motor habit** and was found to be affected by a unilateral lesion of the dorsolateral prefrontal cortex (Kaeser et al., 2013; as assessed in five monkeys). In the present study, these data were extended by investigating variability of motor habit across 20 monkeys and by assessing whether the motor habit was already introduced at the beginning of the learning phase.

Overall, the comparison of the temporal sequence at the beginning of the learning phase with that at plateau yielded a distribution of the monkeys into four profiles (Figure 5 panels A and B). Profile 1, illustrated by Mk-AV, is characterized by variable temporal sequences to visit the 50 slots across daily sessions, without significant difference between the learning phase and the plateau phase. Several monkeys (n = 10 including Mk-AV) exhibited a similar sequence pattern (Mk-AT, Mk-BI, Mk-EN, Mk-GE, Mk-LO, Mk-MA, Mk-MI, Mk-RO, Mk-TH). Profile 2, illustrated by Mk-MO, is shared by three monkeys (Mk-AN, Mk-CE, Mk-MO) also exhibiting variable daily temporal sequences to visit the 50 slots but, in addition to a daily variability, the general pattern during the learning phase appears different from the one adopted during the plateau phase. Profile 3 includes four monkeys (Mk-JA, Mk-JO, Mk-VA, Mk-WI), and is characterized by a systematic temporal sequence to visit the 50 slots, present already during the learning phase and maintained during the plateau phase (illustrated by Mk-JA in Figure 5A). Finally, Profile 4 comprises three monkeys (Mk-CA, Mk-DG, Mk-DI), in which there was also a systematic daily temporal sequence to visit the 50 slots, but the sequence was significantly different during the learning phase from the one during the plateau phase (illustrated by Mk-DG in Figure 5A). The four profiles of motor habit are illustrated quantitatively in Figure 5B, where the positions of the 50 slots were given increasing numbers going from the left extremity of the Brinkman board to the right. Then, these numbers were subtracted from the temporal order (first slot visited, second, third, etc), cumulating their absolute values yielded a low cumulative value for a systematic scan from left to right; on the contrary, a systematic scan from right to left yielded a high cumulative value.

In the above four profiles of temporal sequences to visit the 50 slots, Profiles 1 and 3 exhibited comparable patterns at both learning phase and plateau phase, corresponding quantitatively to an absence of statistically significant difference between the two phases (*ns* in Figure 5B for Mk-AV and Mk-VA for instance). In contrast, the other two profiles (2 and 4) exhibited statistically significant differences in patterns of temporal sequences between the learning phase and the plateau phase (Figure 5B, *stars*, Mk-MO and Mk-DG for instance; see legend for a description of the statistical tests used).

Variable patterns of food pellet grasping. Although the monkeys generally used the standard precision grip (opposition of thumb and index finger) to grasp the food pellets in the modified Brinkman board task, there was some subtle variability in the precise pattern of grasping. For instance, already at the beginning

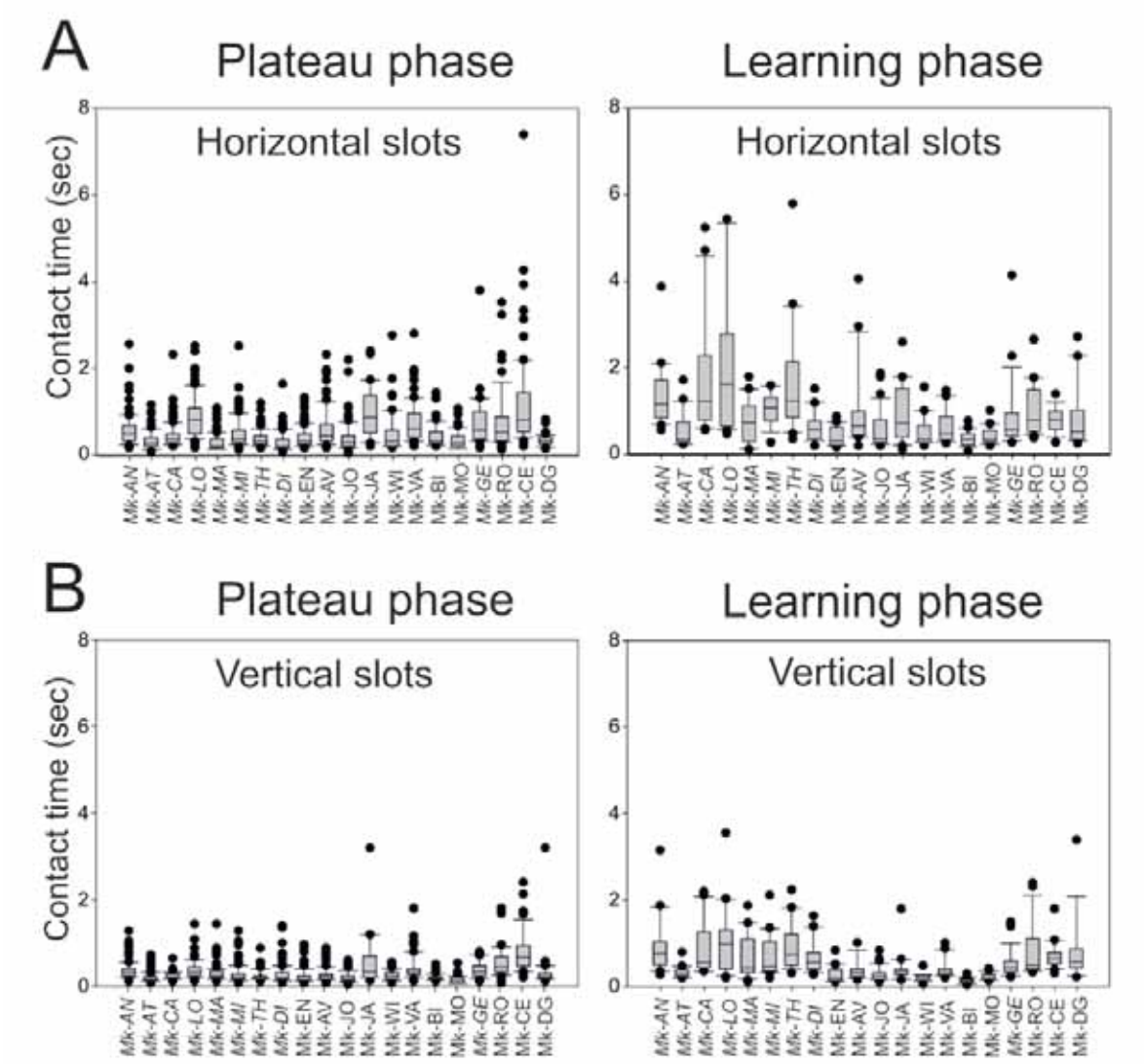

Figure 4. Contact times measured at **plateau phase** and at the **onset of the learning phase** for all monkeys in the modified Brinkman board task, in the horizontal (panel A) and vertical (panel B) slots, represented in the form of box and whiskers plots. The ID names of females are shown in italics. Same conventions as in Figure 3.

of practice, Mk-EN did not grasp a single food pellet with the left hand at a time to bring it to the mouth, as seen in the other monkeys, but grasped a first pellet, stored it in the palm of the hand, and then grasped a second pellet, before transporting both of them together to the mouth (see video sequence at http://www.unifr.ch/neuro/rouiller/ijcp/fr0.html). Conversely, single pellets were transported to the mouth with the right hand at the beginning of the learning phase. After about 10 months of practice, Mk-EN adopted frequently the strategy to collect two pellets at the same time with the left hand (Figure 5C). At the same time point, this strategy was also present for the right hand, but less systematically than for the left hand. Later, after two years of practice, Mk-EN systematically exhibited the prehension of two pellets at the same time with the left hand, extending it even to the grasping of three pellets together on a few trials (http://www.unifr.ch/neuro/rouiller/ijcp/fr0.html). This strategy to collect two pellets at the same time was also observed in few other monkeys, but more occasionally, for instance in Mk-JO and Mk-WI (Figure 5C)

during the plateau phase only, and in Mk-AV and Mk-JA, both during the learning phase and the plateau phase.

The standard grasping from the vertical slots (one single pellet after the other) was highly stereotyped among the monkeys with the use of the standard precision grip (opposition of thumb and index finger). The temporal sequence of movement was such that the monkeys first established contact between the index finger and the pellet, moved the pellet toward the bottom extremity of the vertical slot and finally put the thumb in contact with the pellet to perform the retrieval itself from the slot.

The pattern of grasping was more variable for the horizontal slots. The first contact might be performed with the index finger first (as for the vertical slots) but also sometimes with the thumb first (see a few examples in Mk-EN at http://www.unifr.ch/neuro/rouiller/ijcp/fr0.html). Seven monkeys used the strategy to contact the pellet only with index finger first (Mk-BI, Mk-CA, Mk-GE, Mk-JO, Mk-LO, Mk-MO, Mk-VA). Episodic first contacts with the thumb were observed in six monkeys (Mk-AV, Mk-CE, Mk-EN, Mk-JA, Mk-MI, Mk-WI). Finally, first contacts with the thumb were frequent in seven monkeys, amounting to about 30% of trials in Mk-DG, Mk-RO and Mk-TH; in the other four monkeys, first contact established with the thumb were as frequent (Mk-AN) or even more frequent (Mk-AT, Mk-DI, Mk-MA) than with the index finger. In two of these seven monkeys with frequent first contacts with the thumb, this behavior appeared only at the plateau phase (Mk-MA, Mk-TH), whereas for the other five monkeys it was present already during the learning phase, with increasing frequency of occurrence over time.

To retrieve pellets from the horizontal slots, in part depending on their position on the Brinkman board, the monkeys performed the precision grip with the wrist/arm either in a radial deviation posture or in an ulnar deviation posture (Figure 5D; nomenclature derived from Hoffman and Strick, 1986). In 11 monkeys, the ulnar deviation was highly predominant (Mk-AN, Mk-AT, Mk-BI, Mk-GE, Mk-LO, Mk-MA, Mk-MI, Mk-MO, Mk-RO, Mk-TH, Mk-WI; see Figure 5E for Mk-LO). In one of them, the wrist/arm in radial deviation posture occurred only during the learning phase (Mk-MA), whereas in Mk-MI and Mk-RO the radial deviation posture was observed only at the plateau phase. In the other nine monkeys, ulnar and radial deviation postures of the wrist/arm were mixed with usually fewer radial deviations (ranging mostly from 20 to 40%) than ulnar deviations in eight of them (Mk-AV, Mk-CA, Mk-DG, Mk-DI, Mk-EN, Mk-JA, Mk-JO, Mk-VA; Figure 5E for Mk-JA and Mk-DG), whereas radial deviations were as frequent as ulnar deviations in Mk-CE. Overall, in the nine monkeys using a mix of radial and ulnar deviation postures, this behavior was in most cases already present during the learning phase (Figure 5E).

Errors of food pellet grasping. In the modified Brinkman board task, the monkeys made episodic errors in the form of unsuccessful trials, for instance when the pellet was ejected from the slot instead of being grasped, or when the pellet was dropped before transport to the mouth. Three profiles were identified among the 20 monkeys. The first profile (in 13 monkeys; see (c) in the rightmost column of Table 1) is defined by a progressive decrease in the number of errors from one day to the next during the few days at onset of learning followed by a further decrease at plateau, as expected. The second profile was observed in five monkeys (see (d) in Table 1), with a surprising constant and low number of errors both at onset of the learning phase and at plateau. The third profile included two monkeys (see (e) in Table 1), in which the errors occurred randomly (low to moderate number of errors), irrespective of the phase (onset of learning or plateau). As shown in Table 1, the mean number of errors at the onset of the learning phase ranged across monkeys from 0 to 16 and at plateau from 0 to 2. There was no correlation between the mean number of errors at onset of learning and the mean number of errors at plateau.

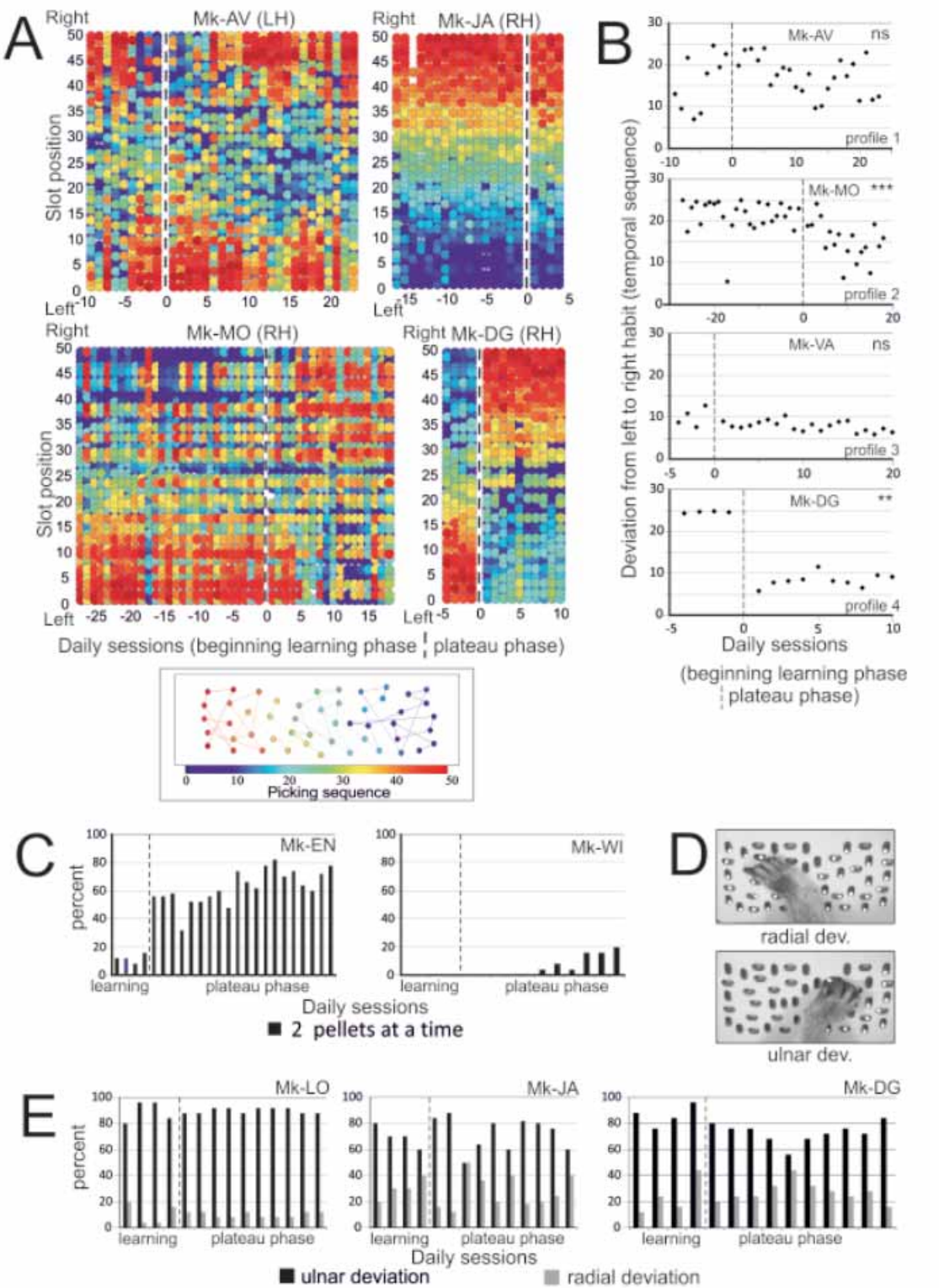

Figure 5. **Panel A:** Temporal sequence used by the monkeys to visit the 50 slots in the modified Brinkman board task. The picking sequence is shown by a color scale in the bottom inset, in which the first-visited slots are represented in blue, whereas the last visited

ones are represented in red (board scanning from right (blue slots) to left (red slots) in this example). In the top and middle displays, the temporal sequence was established for 4 monkeys, each representative of a behavioral profile (see text), both during the beginning of the learning phase (negative session numbers) and the plateau phase (positive session numbers). The x-axis displays the time in daily sessions, irrespective of the time interval (in days) between two consecutive sessions (different from the time scale in Figures 1 and Supplementary Figure 1). Each vertical column corresponds to a daily session of the modified Brinkman board task. Along each column, dots at the bottom are for slots located at the left extremity of the board, whereas dots at the top are for slots at the right extremity. RH=Right hand; LH=Left hand. **Panel B**: Quantitative assessment of the temporal sequence used to visit the 50 slots in the modified Brinkman board task for four monkeys, representative of the four profiles reported in the text. An index of systematic motor sequence (habit) was computed, indicating the extent of deviation from a systematic sequence starting from the left extremity of the board and terminating at its right extremity (corresponding to a low value for this precise sequence), and plotted in the y-axis as a function of behavioral daily sessions. The mirror sequence (systematic right to left scan) yields a high value. A small variability from one daily behavioral session to the next, indicating a reproducible motor sequence, reflects motor habit. The temporal sequence is shown qualitatively for the same monkeys Mk-AV, Mk-MO and Mk-DG in panel A. See text for detailed description of the results. The index of motor sequence was compared between the learning phase and the plateau phase with the non-parametric Mann-Whitney U test. The result of the statistical comparison is indicated at the top right of each graph: ns = statistically non-significant difference ($p > 0.05$); ** is for $p \leq 0.01$; *** is for $p \leq 0.001$. **Panel C**: Percentage of grasping patterns (at the beginning of learning and at plateau) in which two pellets were retrieved at the same time instead of a single one, in the modified Brinkman board task. In other words, the monkey grasped two pellets before transport to the mouth. In the other trials, the monkey retrieved a single pellet and brought it to the mouth. For this analysis, the vertical and horizontal slots were cumulated. **Panel D**: Usually, to retrieve pellets from the horizontal slots and depending on their position in the modified Brinkman board, the monkeys used a precision grip movement associated with a complementary wrist/arm movement. As illustrated for a right hand, on the left part of the Brinkman board, there was a trend to perform a radial deviation of the wrist/arm (top picture) whereas, on the right part of the Brinkman board, the trend was in favour of an ulnar deviation (bottom picture). **Panel E**: The distribution of wrist/arm radial deviation and ulnar deviation postures for pellet retrieval from the horizontal slots is illustrated for three monkeys over consecutive daily sessions, at the beginning of the learning phase and at plateau. For each daily session, the black bar and the gray one indicate the percentage of ulnar deviations and radial deviations, respectively. The sum of the radial and ulnar deviations is 100% in each daily session. Mk-LO is representative of 11 monkeys exhibiting a clear prevalence of ulnar deviations, during both the learning phase and the plateau phase. Mk-JA and Mk-DG also preferred ulnar deviations, but to a lesser extent.

Based on multiple correlation analyses (not shown), it turned out that the mean number of errors both at onset of the learning phase and at plateau was correlated with none of the following parameters: learning duration, slope of learning regression line, initial score value at onset of learning, median score value at plateau, *SD* of score at plateau, difference between the initial score at learning onset, or average score at plateau. Nevertheless, there was a positive correlation between the gain of score performance during practice and the mean number of errors at onset of learning ($p = 0.029$): monkeys with larger mean numbers of errors at onset of learning exhibited a larger gain of performance provided by the learning phase.

Reach and Grasp Drawer Task

Typical traces of grip force and load force recorded during a single trial of the reach and grasp drawer task are illustrated in Figure 6A, in parallel to the displacement of the drawer and discrete events, such as *touch knob*, *open onset*, *full open* and *picking*. Four monkeys were included in the analysis of the drawer task (Mk-LO, Mk-TH, Mk-DI and Mk-AT). Based on five daily sessions recorded both at the beginning of the learning phase and at plateau, the maximal grip force was measured for five correct trials at each resistance tested (R1 = 0 Newton, R2 = 1.25 N, R3 = 2.75 N, R4 = 5N) and plotted in the form of box and whisker plots (Figure 6C). Two of the monkeys (Mk-DI and Mk-TH) exhibited a systematic and statistically significant increase in the maximal grip force applied on the drawer knob when the task was performed at plateau as compared to the

learning phase (Mann-Whitney U test). A comparable result was obtained in Mk-LO for the lowest two resistances, whereas there was no statistically significant difference between the learning and plateau phases at higher resistances (R3 and R4). A reverse behavior was found in Mk-AT, exhibiting in contrast a lower maximal grip force at plateau than during the learning phase at R1, R2 and R3, although the difference was statistically significant at R2 only (Figure 6C). At R4, Mk-AT used a statistically higher maximal grip force at plateau than during the learning phase, as Mk-TH.

The maximal load force was measured from the same trials, as shown in Figure 7A, and no difference between the learning and plateau phases appeared in Mk-AT and Mk-TH with the exception in the latter of the resistance R2, at which the maximal load force was significantly higher at plateau. Mk-DI used a lower maximal load force at plateau as compared to the learning phase (Figure 7A), but the difference was statistically significant only at the resistances R2 and R3. Mk-LO presented a more variable behavior, with a higher maximal load force at plateau at R1 and R2, but statistically significant at R1 only and a lower maximal load force at plateau as compared to the learning phase at R3 and R4, but statistically significant at R4 only. As illustrated for Mk-AT and for Mk-LO (Figure 7B), in the four monkeys enrolled in the reach and grasp drawer task the transition from the learning phase to the plateau phase was accompanied by a statistically significant decrease in both the grip force duration and the load force duration (Figure 7B), except at the highest level of resistance (R4). In Mk-TH, at resistance R4 as well, both durations were also statistically shorter at plateau than at the beginning of the learning phase.

The difference in grip force (solid lines in Figure 6B left column) and in load force (solid lines in Figure 6B right column) between the beginning of the learning phase and the end of the plateau phase is illustrated in Mk-DI, together with their variability (dashed lines representing plus and minus *SDs*). These data are representative of the observation (Figure 6C) that grip force was usually stronger at plateau phase than at the beginning of the learning phase, except in Mk-AT. However, variability was clearly larger at the onset of the learning phase than at the end of the plateau. Duration of grip application was shorter at plateau phase (as seen in Figure 7B). There was less difference between the two phases in the amplitude of the load force (Figure 6B right column), as compared to the grip force. However, load force duration was shorter and less variable at the end of the plateau than at onset of the learning phase, as shown in Figure 7B (right panel).

Discussion

Survey of the Main Results

Our main hypothesis that acquired manual (digits) dexterity performance and variability can be predicted from the duration of the learning phase, from the learning slope and from the initial score before any training was not verified for the most part, based on the modified Brinkman board data. Indeed, both performance and variability of manual dexterity, precision grip in the present case, were not related to the duration of training and to the slope of the learning regression line (Supplementary Figure 2). Only the performance of manual dexterity at plateau was correlated with the initial score before learning, the higher the initial score before training, the better the score at plateau (Figure 3, top right panel). On the other hand, the initial score of manual dexterity before learning was a poor predictor of intra-individual variability at plateau (Supplementary Figure 2).

As mostly expected, motor learning led to an optimization of manual dexterity parameters in the modified Brinkman board task, such as score, CT, as well as a substantial decrease in intra-individual variability, especially for the CT (Figures 1, 4 and Supplementary Figures 1, 3), in line with current theories

(see e.g., Marteniuk 1974). The present study also demonstrates the considerable inter-individual variations in precision grip skills, reflected across monkeys both by wide ranges of motor parameters (score, CT, learning properties) and disparate qualitative characteristics of grasping patterns (e.g., grip type, hand posture, strategy, motor habit). Such large inter-individual variability is in line with the theory of motor equivalence claiming that a given motor goal can be achieved via multiple strategies. In relation to motor habit, reflected by the temporal order in which sequential movements were executed in the modified Brinkman board task, the data (Figure 5A and B) support the notion that motor habit is established very early during the learning phase in most animals. These data suggest that macaque monkeys, as most human subjects would do, adopt motor habits early, reflecting the capability to organize motor sequences following a strategy perceived as optimal, as opposed to a random scan of the board augmenting the probability of neglecting a slot and requiring more attention to detect yet unvisited slots. The early emergence of a preferential prehension sequence is present also in children (3-5 years old), as observed in the Pegboard with 12 pegs test (Kakebeeke, Caflisch, Chaouch, Rousson, Largo & Jenni, 2013; T. Kakebeeke, personal communication). In adult human subjects performing the modified Brinkman board task, a preferential prehension sequence is most often already present at first trial and then maintained over 10 repetitions of the test (data derived from Chatagny et al., 2013).

In the reach and grasp drawer task, the expectation that the monkeys would use exaggerated maximal grip and load forces to make sure to open the drawer during learning phase, then reduced at plateau to just exceed the minimal forces required, representing an energy conservation and behavioral optimization, was not verified, at least in three out of four monkeys tested (Figures 6 and 7: Mk-LO, Mk-TH and Mk-AT). This principle of optimization was observed only in one monkey (Mk-DI), for the load force but not for the grip force. On the other hand, the duration of application of both the grip force and load force was reduced at plateau as compared to the learning phase (Figure 7), as expected.

Methodological Considerations and Limitations

In the present study, emphasis was put on an individual analysis of 20 adult macaques. This individual (*differential*) strategy was prompted by the notion that "averaging data over participants (the *experimental* approach) can mask the actual individual participant and trial functions of change, as well as it can also produce learning curves that are not representative of any single individual in the group" (Adi-Japha, Karni, Parnes, Loewenschuss & Vakil, 2008; Newell, Liu & Mayer-Kress, 2001; Schmidt & Lee, 2011: Chapter 9). These concerns emitted in relation to the learning curves apply also most likely to the motor performance at plateau. Indeed the data shown in all Figures of the present study emphasize the considerable inter-individual variability of manual dexterity performance across our population of 20 macaque monkeys, although they were housed for many years in groups in the same environment and performed the same motor tasks in well controlled and reproducible laboratory conditions.

Our study presents weaknesses in the data gathering due to variations in the experimental protocol, inherent to this type of non-human primate study and its related constraints. First, as expected for a study conducted over a long period of time (15 years), several conditions changed from one animal to the next. One example is the size of the housing facility and its degree of enrichment (Table 1), adapted over the years according to changes in the legislation dealing with the protection of animals involved in scientific research. A second confounding factor is the supervision of the monkeys by different experimenters: a given experimenter is devoted to the very same monkeys every day and therefore cannot supervise more than two monkeys daily.

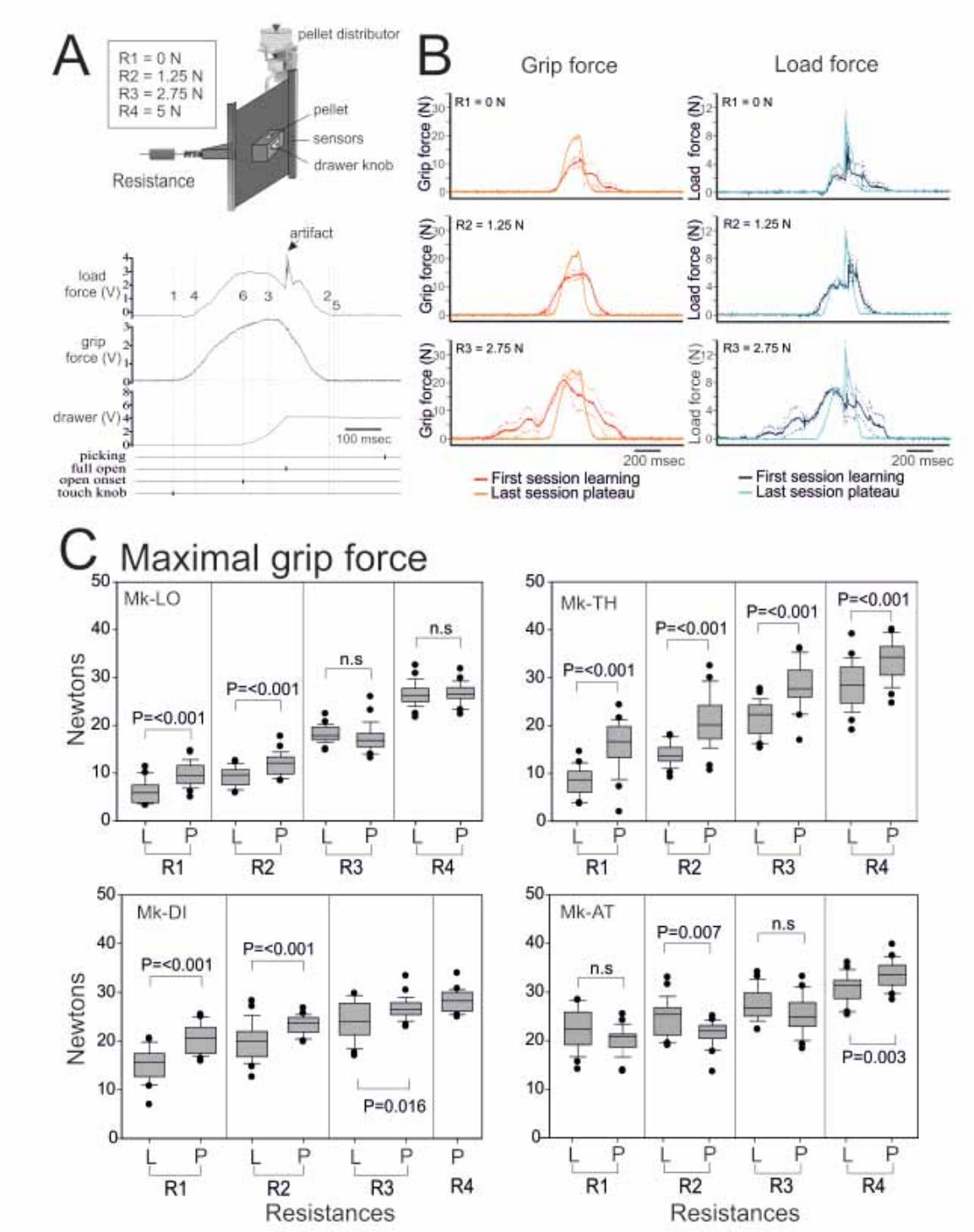

Figure 6. **Panel A**: Typical traces of the load force, grip force and drawer displacement as a function of time (from top to bottom) when a monkey executed a trial in the reach and grasp drawer task. The time occurrence of four discrete events is shown below (vertical tics). A schematic representation of the drawer set-up is shown on the top, with the four increasing resistances opposing the opening of the drawer (R1 to R4). The vertical dashed lines with numbers correspond to: *onset of grip force* (1), *offset of grip force* (2), *maximal grip*

force (3), *onset of load force* (4), *offset of load force* (5) and *maximal load force* (6). An artifact in the load force trace occurred when the drawer was blocked at its maximal opening. **Panel B**: Average traces (over 5 trials) and their variability (+/- 1 *SD*) in Newtons (N) for the grip force (left column) and load force (right column), recorded in Mk-DI. In each column, the two colors distinguish traces obtained at the beginning of the learning phase and at the end of the plateau phase. The traces are shown for three levels of resistances (R1, R2, R3; see panel A). For each curve, the variability is represented by the envelope in dashed lines. **Panel C**: Box and whisker plots (same conventions as in Fig. 3) of the maximal grip force recorded during the learning phase (L) and during the plateau phase (P), in the four monkeys involved in the reach and grasp drawer task, as a function of 4 increasing resistance levels opposing the opening of the drawer (R1, R2, R3, R4). The results of the statistical comparison between "L" and "P" are given with the corresponding p value or n.s when statistically non-significant ($p > 0.05$). Note that Mk-DI performed the task at resistance level R4 only during the plateau phase, after learning.

Moreover, the duration of the entire experiment on a given monkey may last up to two to three years and may consequently be conducted by several successive experimenters. Equally important, each experimenter develops his/her own approach to train each animal, depending also on the *personal* traits of the latter. In particular, some monkeys required a longer preliminary habituation phase than others before being actively involved in the experiment, before collecting the behavioral data for subsequent analysis (Table 1). Over the years, the monkeys originated from different sources, such as our own breeding colony (before 2010) or from different authorized suppliers (China, Mauritius Island, Vietnam), via various quarantine European centers. In spite of these multiple parameters influencing our monkey data, which cannot be strictly controlled over a 15 year period, it remains that they have most likely less impact than the even more numerous confounding factors associated with human studies, such as genetic variability, socio-cultural background, education, economical status, motivation, professional occupation, hobbies and so on.

The vast majority of lesion studies dealing with manual dexterity in non-human primates (see introduction) provide behavioral data restricted to two time points, namely before a lesion of the motor system (after reaching a plateau of performance) and after the lesion. In these studies, the data related to the learning phase of the motor tasks were rarely, if not at all, reported. The originality of the present study was to compare the manual dexterity properties of adult macaque monkeys at their plateau (before subsequent lesion) with those derived earlier from the acquisition of manual performance for two motor tasks, in the same animals. Furthermore, as the behavioral sessions took place three to five days a week, it was possible to precisely follow progressive changes in each monkey in order to assess intra-individual and inter-individual variability over a very long time frame. As the motor tests took place in the laboratory with the monkeys sitting in a primate chair, confounding factors such as the position of the monkeys with respect to the set-up and the separate use of each hand were well controlled.

Initial Score Before Training

The statistically significant correlation between the initial score before training and the score reached in the modified Brinkman board task at plateau (Figure 3, top right panel) suggests that there is a limited margin of progression during learning, meaning a ceiling effect. When the initial score was high (above 25 pellets; in four monkeys, see Table 1), the increase in score during the learning phase was modest (1-5 pellets at most; Figure 2B: crosses), corresponding to the ceiling effect, with a maximal score in the most dexterous monkeys ranging from about 30 to 35 pellets in 30 seconds. A few other monkeys ($n = 5$), in spite of a lower initial score before training (ranging from 18 to 24 pellets), also exhibited a limited gain of score during the learning phase (below 6 pellets; Figure 2B: crosses). Overall, 10 monkeys improved relatively modestly during the learning phase. In the other 10 monkeys, the margin of score progression during learning was more prominent (ranging from 9 to 16; Figure 2B: crosses). The latter monkeys were predominantly females (7 out of 10). In comparison with human subjects performing the modified Brinkman board task in 10 consecutive sessions on

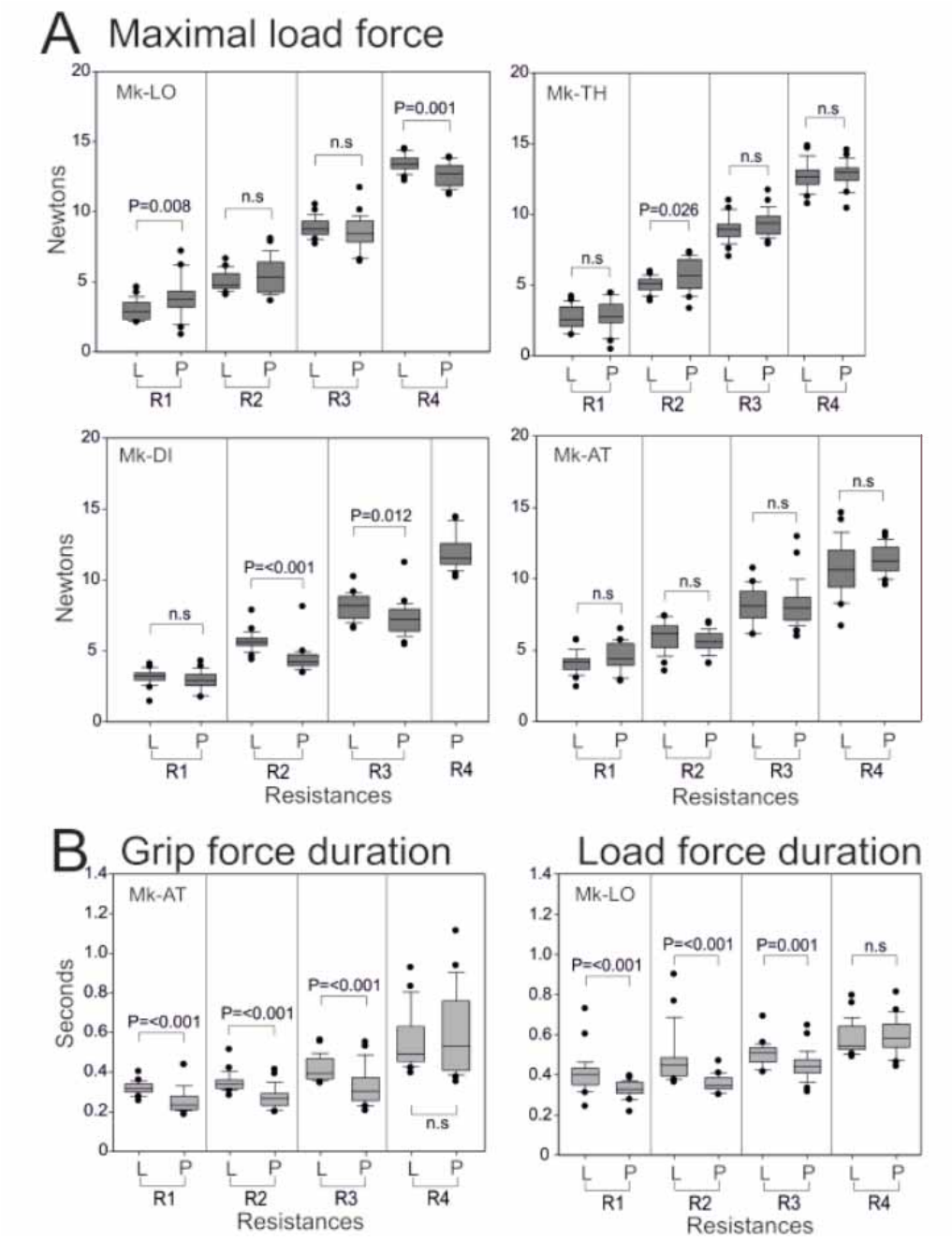

Figure 7. **Panel A**: Box and whisker plots (same conventions as in Fig. 3) of the maximal load force during the learning phase (L) and during the plateau phase (P), in the same four monkeys as in Figure 6. Same conventions as in Figure 6. **Panel B**: Grip force duration and load force duration measured in 2 animals during the learning phase (L) and the plateau phase (P), as a function of the resistance levels opposing the opening of the drawer (R1, R2, R3, R4). Same conventions as in Figure 6.

the same day, the training effect was less prominent than in monkeys (Chatagny et al., 2013), suggesting that humans started closer to the ceiling of performance.

The statistically significant lower scores in females than males (Figure 2B) is consistent with the lack of a few habituating sessions before collecting data in females, as opposed to the majority of males (Table 1). Moreover, other confounding factors might have played a role in this sex difference as well (e.g., size of housing facility, degree of enrichment; see Table 1). However, later on, when females were more familiar with the new environment and the tasks, their score increased more than in males so that the two groups exhibited largely overlapping mean or median scores at plateau (Figure 2, panels E and F). The absence of sex difference for the score at plateau in the macaque monkeys enrolled in the present study contrasts with the significantly better performance observed in women than in men in a human adapted version of the modified Brinkman board task (Chatagny et al., 2013).

Application to Lesion Studies

The large inter-individual variability of the average score at plateau (Table 1) may be considered as an inconvenience in comparing two groups of monkeys subjected to a lesion, one group receiving a treatment and the other not. Nevertheless, this drawback is actually attenuated because, in such studies and in contrast to clinical trials (see e.g., Kaeser et al., 2010), the most relevant comparison is made within the same monkey, between the pre-lesion score and the post-lesion score at plateau after functional recovery (usually incomplete; see e.g., Freund et al., 2009; Hamadjida et al., 2012). Thus, the comparison between two groups of animals is based on the percentage of functional recovery individually determined for each animal (see e.g., Freund et al., 2009; Hamadjida et al., 2012; Hoogewoud et al., 2013; Kaeser et al., 2010, 2011), which is less affected by inter-individual variability than group comparisons in clinical trials.

Learning Curves

As reviewed by Newell and collaborators (2001), the forms of the learning curves, defined as "plots of the outcome performance as a function of practice", can be highly variable: "learning curves of almost every conceivable shape can and have been found", corresponding to various mathematical functions, such as exponential, power law, S-shaped, hyperbolic, accelerating functions, etc. In the present case, one would have intuitively expected an exponential rise of performance (score) to a maximum (ceiling; see Schmidt & Lee, 2011: Chapter 10, their Figure 10.8). As illustrated in Figure 1 and Supplementary Figure 1 however, the majority of monkeys (n = 16 out of 20) exhibited a progression of performance during the learning phase that was rather better approximated by a regression line than by an exponential function. The exceptions are Mk-RO (Figure 1), Mk-DI, Mk-LO (Supplementary Figure 1) and Mk-TH (not shown). This linear learning progression observed here may be specific to the modified Brinkman board task, as well as to each monkey, in line with the proposition that the "learning rate is individual and task dependent" (Newell et al., 2001). In the same line, unlike recent studies in humans (e.g., Rosenblatt, Hurt, Latash, & Grabiner, 2014 in locomotor tasks; Wu et al., 2014 in arm movements tasks) demonstrating that a greater variability at the beginning of practice allows a faster learning rate, no such correlation was found in our monkeys performing unconditioned voluntary tasks requiring fine manual dexterity. Individual differences in motor skill learning are likely to be related to variations in the function and structure of specific brain regions, such as prefrontal, premotor and parietal cortices, as well as basal ganglia and cerebellum (Tomassini et al., 2011).

An important parameter here is the time scale when attempting to characterize the change in behavior resulting from motor learning (Newell et al., 2001). In most cases, especially in human subjects, the time range of observation of the learning phase was narrow (an hour to a single day most often; e.g., Chatagny et al., 2013). Longitudinal studies, though conducted in relation to infant motor development, are relatively rare

and therefore the present study is original thanks to the long time period of observation during the learning phase (over weeks to months). Short daily sessions, during such a long time scale, may explain the very progressive and regular improvement of performance with practice observed in the majority of monkeys. In the present learning data on macaque monkeys, the learning phase may appear rather long for a relatively natural motor task, such as the precision grip performed in the modified Brinkman board task, at least in some individuals (Table 1). This underlies the fact that precision grip is an exquisite motor function subjected to very fine and progressive adjustments with practice. For instance, it was reported that the even more sophisticated skill in rolling cigars may still improve after many years (up to seven) of practice (Crossman, 1959).

Comparison with Previous Studies

Comparing the present behavioral data with the literature is limited to some extent, as the manual dexterity performance and variability strongly depends on the animal/primate species, on practice schedule (Stelmach, 1968), on expertise level (Schorer, Baker, Fath, & Jaitner, 2007), as well as on the type of task. Individual differences are indeed strongly task specific, corresponding to the theory of specificity (see e.g., Marteniuk, 1974). Even close species such as *Macaca fascicularis* and *Macaca mulatta* have different hand size (e.g., finger length), larger for the latter, corresponding consequently to different manual dexterity abilities (see e.g., Darling et al., 2013 for more details). A direct comparison of the present macaque data with rodent data (mainly rats) remains questionable, due to the strong difference between the pincer grasp (or precision grip) in primates and the arpeggio/power grasp in rodents (Klein et al., 2012). In the context of motor specificity, a strong influence is exerted by the size and shape of the object to be manipulated, as well as by the size of the well containing the object, when applicable. In a human study focused on precision grasps (Wong & Whishaw, 2004), it was shown that there was a high degree of variability of grasping pattern within and between subjects, like in our group of monkeys. Wong and Whishaw (2004) reported up to seven grasp types in human subjects, involving the thumb and various combinations of other digits, depending on the size of the bead being held. The proper precision grip (opposition of thumb and index finger only) was highly predominant when grasping the smallest beads, whereas the involvement of other fingers increased when progressively larger beads were grasped. In the present study on monkeys, only the proper precision grip was observed (opposition of thumb and index finger) because the food pellet was small compared to the finger size. Wong and Whishaw (2004) reported also in human subjects a large variability of first contact strategy with an object, depending on which and how the first finger contacted the object. This observation is in line with the large inter-individual variability observed here for the monkeys in the first digit used to contact the pellet in the horizontal slots (see results paragraph Variable Patterns of Food Pellet Grasping). The large inter- and intra-individual variability of grasping patterns observed in our monkeys and in humans (Wong & Whishaw, 2004) is consistent with the exquisitely complex somatotopic organization in mosaics of the primary motor cortex in primates (e.g., Schieber, 2001) as well as with complex movements synergies elicited in primates by microstimulation of the primary motor cortex (Graziano, Taylor, & Moore, 2002).

In two studies conducted on *Macaca fascicularis* (Brinkman, 1984) and *Macaca mulatta* (Brinkman & Kyupers, 1973), using a very comparable task (the original Brinkman board task), the data were mostly reported in a qualitative manner (movement pattern), preventing a direct comparison with the present quantitative data. The same limitation applies to other macaque studies using different manual tasks (e.g., Glees & Cole, 1950; Ogden & Franz, 1917; Passingham et al., 1983). In several studies on non-human primates (as listed in the introduction) involving a lesion of the motor system followed by functional recovery, the pre-lesion behavioral data were often limited to very few baseline data points, if not a single one, thus strongly limiting the comparison with the present progressive training phase over weeks, followed then by a long period of performance stabilization at plateau.

An exception is the study by Pizzimenti et al. (2007) conducted on *Macaca mulatta* and using a somewhat different behavioral apparatus, modified from the often used dexterity *Klüver* board. Although different from our modified Brinkman board, the wells A and B in the dexterity board used by Pizzimenti et al. (2007) had a size comparable to our slots. The manual dexterity was assessed quantitatively in three monkeys, using the so-called performance ratio, defined as the average score divided by the *SD* of the score, derived from five pre-lesion sessions (plateau). For the preferred hand, the performance ratios ranged from 2.5 to 3.0 in well A and from 3.5 to 8 in well B, the latter being the least difficult. Taking our data from the modified Brinkman board at plateau (Table 1) and computing similarly the performance ratio, values ranging from 4.4 to 14.0 (average = 9.3) among the 20 monkeys were obtained, thus corresponding to a generally better manual dexterity performance in our monkeys. However, such direct comparison may be biased due to important differences, such as species, manual task, duration of the considered plateau phase, scoring, as well as the time interval between the sessions (1-2 weeks in Pizzimenti et al., 2007 versus 1-3 days in our study). Furthermore, the monkeys of Pizzimenti et al. (2007) worked from their home cage (in a primate chair here).

As far as the reach and grasp drawer task is concerned, slightly different versions of the original set-up (Kazennikov et al., 1994) were used along the years (Kazennikov et al., 1998; Kazennikov et al., 1999; Kermadi, Liu, Tempini, & Rouiller, 1997; Kermadi, Liu, Tempini, Calciati, & Rouiller, 1998; Kermadi, Liu, & Rouiller, 2000), with special emphasis put on the issue of inter-limb coordination. In the current report, the reach and grasp drawer task was used in its unimanual version only, with focus on the assessment of the grip and load forces, a situation more closely related to studies on human subjects performing the reach and grasp drawer task (e.g., Grichting, Hediger, Kaluzny, & Wiesendanger, 2000; Serrien & Wiesendanger, 1999; Serrien, Kaluzny, Wicki & Wiesendanger, 1999). Interestingly, as compared to intact human subjects, cerebellar patients overestimated the proactive grip force requested to pull the drawer (Serrien & Wiesendanger, 1999). It can thus be expected that the reach and grasp drawer task will also be pertinent in macaque monkeys to evaluate deficits related to various motor dysfunctions (e.g., Parkinson disease, cortical lesion, spinal cord lesion) and to follow the time course and extent of functional recovery. In particular, it will be interesting to compare the properties of the initial learning phase of a motor task with those of the re-learning phase of the same task in the same animals following a lesion, in absence (spontaneous recovery) or presence of a specific treatment (induced recovery).

Acknowledgements

The authors wish to thank the technical assistance of Françoise Tinguely, Josef Corpataux, Laurent Bossy, Jacques Maillard (animal care taking), André Gaillard (mechanics), Bernard Aebischer (electronics), Laurent Monney (informatics). Over the years, previous members of the laboratory were involved in some of the experiments: Dr. Alexander Wyss, Dr. Shahid Bashir, Dr. Yu Liu and Dr. Abderraouf Belhaj-Saif.

Informative video material: http://www.unifr.ch/neuro/rouiller/ijcp/fr0.html.

References

Adi-Japha, E., Karni, A., Parnes, A., Loewenschuss, I., & Vakil, E. (2008). A shift in task routines during the learning of a motor skill: group-averaged data may mask critical phases in the individuals' acquisition of skilled performance. *Journal of Experimental Psychology: Learning, Memory, and Cognition, 34,* 1544-1551.

Alstermark, B., & Isa, T. (2002). Premotoneuronal and direct corticomotoneuronal control in the cat and macaque monkey. *Advances in experimental medicine and biology, 508*, 281-297.

Alstermark, B., Pettersson, L. G., Nishimura, Y., Yoshino-Saito, K., Tsuboi, F., Takahashi, M., & Isa, T. (2011). Motor command for precision grip in the macaque monkey can be mediated by spinal interneurons. *Journal of Neurophysiology, 106*, 122-126.

Alstermark, B., & Isa, T. (2012). Circuits for skilled reaching and grasping. *Annual Review of Neuroscience, 35*, 559-578.

Armand, J., Edgley, S. A., Lemon, R. N., & Olivier, E. (1994). Protracted postnatal development of corticospinal projections from the primary motor cortex to hand motoneurones in the macaque monkey. *Experimental Brain Research, 101*, 178-182.

Armand, J., Olivier, E., Edgley, S. A., & Lemon, R. N. (1997). Postnatal development of corticospinal projections from motor cortex to the cervical enlargement in the macaque monkey. *Journal of Neuroscience, 17*, 251-266.

Bashir, S., Kaeser, M., Wyss, A., Hamadjida, A., Liu, Y., Bloch, J., . . . Rouiller, E. M. (2012). Short-term effects of unilateral lesion of the primary motor cortex (M1) on ipsilesional hand dexterity in adult macaque monkeys. *Brain Structure and Function, 217*, 63-79.

Beaud, M. L., Schmidlin, E., Wannier, T., Freund, P., Bloch, J., Mir, A., . . . Rouiller, E. M. (2008). Anti-Nogo-A antibody treatment does not prevent cell body shrinkage in the motor cortex in adult monkeys subjected to unilateral cervical cord lesion. *BMC Neuroscience, 9*, 5.

Beaud, M. L., Rouiller, E. M., Bloch, J., Mir, A., Schwab, M. E., Wannier, T., & Schmidlin, E. (2012). Invasion of lesion territory by regenerating fibers after spinal cord injury in adult macaque monkeys. *Neuroscience, 227*, 271-282.

Bihel, E., Pro-Sistiaga, P., Letourneur, A., Toutain, J., Saulnier, R., Insausti, R., . . . Touzani, O. (2010). Permanent or transient chronic ischemic stroke in the non-human primate: behavioral, neuroimaging, histological, and immunohistochemical investigations. *Journal of Cerebral Blood Flow and Metabolism, 30*, 273-285.

Borra, E., Belmalih, A., Gerbella, M., Rozzi, S., & Luppino, G. (2010). Projections of the hand field of the macaque ventral premotor area F5 to the brainstem and spinal cord. *Journal of Comparative Neurology, 518*, 2570-2591.

Bortoff, G. A., & Strick, P. L. (1993). Corticospinal terminations in two new-world primates: further evidence that corticomotoneuronal connections provide part of the neural substrate for manual dexterity. *Journal of Neuroscience, 13*, 5105-5118.

Brinkman, C. (1984). Supplementary motor area of the monkey's cerebral cortex: short- and long-term deficits after unilateral ablation and the effects of subsequent callosal section. *Journal of Neuroscience, 4*, 918-929.

Brinkman, J., & Kuypers, H. G. J. M. (1973). Cerebral control of contralateral and ipsilateral arm, hand and finger movements in the split-brain rhesus monkey. *Brain, 96*, 653-674.

Carron, A. V., & Leavitt, J. L. (1968). Individual differences in two motor learning tasks under massed practice. *Perceptual and Motor Skills, 27*, 499-504.

Chalmeau, R., Visalberghi, E., & Gallo, A. (1997). Capuchin monkeys, *Cebus apella* fail to understand a cooperative task. *Animal Behaviour, 54*, 1215-1225.

Chatagny, P., Badoud, S., Kaeser, M., Gindrat, A. D., Savidan, J., Fregosi, M., . . . Rouiller, E. M. (2013). Distinction between hand dominance and hand preference in primates: a behavioral investigation of manual dexterity in nonhuman primates (macaques) and human subjects. *Brain and Behavior, 3*, 575-595.

Christel, M. I., & Billard, A. (2002). Comparison between macaques' and humans' kinematics of prehension: the role of morphological differences and control mechanisms. *Behavioural Brain Research, 131*, 169-184.

Costello, M. B., & Fragaszy, D. M. (1988). Prehension in *Cebus* and *Saimiri*: I. Grip type and hand preference. *American Journal of Primatology, 15,* 235-245.

Courtine, G., Bunge, M. B., Fawcett, J. W., Grossman, R. G., Kaas, J. H., Lemon, R., . . . Edgerton, V. R. (2007). Can experiments in nonhuman primates expedite the translation of treatments for spinal cord injury in humans? *Nature Medicine, 13,* 561-566.

Crossman, E. R. F. W. (1959) A theory of the acquisition of speed-skill. *Ergonomics 2,* 153-166.

Dancause, N., Barbay, S., Frost, S. B., Plautz, E. J., Chen, D. F., Zoubina, E. V., . . .Nudo, R. J. (2005). Extensive cortical rewiring after brain injury. *Journal of Neuroscience, 25,* 10167-10179.

Dancause, N., Barbay, S., Frost, S. B., Zoubina, E. V., Plautz, E. J., Mahnken, J. D., & Nudo, R. J. (2006). Effects of small ischemic lesions in the primary motor cortex on neurophysiological organization in ventral premotor cortex. *Journal of Neurophysiology, 96,* 3506-3511.

Dancause, N., & Nudo, R. J. (2011). Shaping plasticity to enhance recovery after injury. *Progress in Brain Research, 192,* 273-295.

Darian-Smith, I., Galea, M. P., & Darian-Smith, C. (1996). Manual dexterity: how does the cerebral cortex contribute? *Clinical and Experimental Pharmacology and Physiology, 23,* 948-956.

Darian-Smith, I., Galea, M. P., Darian-Smith, C., Sugitani, M., Tan, A., & Burman, K. (1996). The anatomy of manual dexterity. The new connectivity of the primate sensorimotor thalamus and cerebral cortex. *Advances in Anatomy, Embryology and Cell Biology, 133,* 1-140.

Darian-Smith, I., Burman, K., & Darian-Smith, C. (1999). Parallel pathways mediating manual dexterity in the macaque. *Experimental Brain Research, 128,* 101-108.

Darling, W. G., Pizzimenti, M. A., Rotella, D. L., Peterson, C. R., Hynes, S. M., Ge, J., . . . Morecraft, R. J. (2009). Volumetric effects of motor cortex injury on recovery of dexterous movements. *Experimental Neurology, 220,* 90-108.

Darling, W. G., Pizzimenti, M. A., Rotella, D. L., Hynes, S. M., Ge, J., Stilwell-Morecraft, K. S., . . . Morecraft, R. J. (2010). Minimal forced use without constraint stimulates spontaneous use of the impaired upper extremity following motor cortex injury. *Experimental Brain Research, 202,* 529-542.

Darling, W. G., Pizzimenti, M. A., Hynes, S. M., Rotella, D. L., Headley, G., Ge, J., . . . Morecraft, R. J. (2011). Volumetric effects of motor cortex injury on recovery of ipsilesional dexterous movements. *Experimental Neurology, 231,* 56-71.

Darling, W. G., Helle, N., Pizzimenti, M. A., Rotella, D. L., Hynes, S. M., Ge, J., . . . Morecraft, R. J. (2013). Laterality affects spontaneous recovery of contralateral hand motor function following motor cortex injury in rhesus monkeys. *Experimental Brain Research, 228,* 9-24.

Eisner-Janowicz, I., Barbay, S., Hoover, E., Stowe, A. M., Frost, S. B., Plautz, E. J., & Nudo, R. J. (2008). Early and late changes in the distal forelimb representation of the supplementary motor area after injury to frontal motor areas in the squirrel monkey. *Journal of Neurophysiology, 100,* 1498-1512.

Falk, D., Pyne, L., Helmkamp, R. C., & DeRousseau, C. J. (1988). Directional asymmetry in the forelimb of Macaca mulatta. *American Journal of Physical Anthropology, 77,* 1-6.

Flament, D., Hall, E. J., & Lemon, R. N. (1992). The development of cortico-motoneuronal projections investigated using magnetic brain stimulation in the infant macaque. *Journal of Physiology, 447,* 755-768.

Fragaszy, D. M., & Adams-Curtis, L. E. (1997). Developmental changes in manipulation in tufted capuchins (*Cebus apella*) from birth through 2 years and their relation to foraging and weaning. *Journal of Comparative Psychology, 111,* 201-211.

Fragaszy, D. M. (1998). How non-human primates use their hands. In K. J. Connolly (Ed.), *The psychobiology of the hand* (pp. 77-96). London, UK: Mac Keith Press.

Freund, P., Schmidlin, E., Wannier, T., Bloch, J., Mir, A., Schwab, M. E., & Rouiller, E. M. (2006). Nogo-A-specific antibody treatment enhances sprouting and functional recovery after cervical lesion in adult primates. *Nature Medicine, 12,* 790-792.

Freund, P., Wannier, T., Schmidlin, E., Bloch, J., Mir, A., Schwab, M. E., & Rouiller, E. M. (2007). Anti-Nogo-A antibody treatment enhances sprouting of corticospinal axons rostral to a unilateral cervical spinal cord lesion in adult macaque monkey. *Journal of Comparative Neurology, 502,* 644-659.

Freund, P., Schmidlin, E., Wannier, T., Bloch, J., Mir, A., Schwab, M. E., & Rouiller, E. M. (2009). Anti-Nogo-A antibody treatment promotes recovery of manual dexterity after unilateral cervical lesion in adult primates--re-examination and extension of behavioral data. *European Journal of Neuroscience, 29,* 983-996.

Friel, K. M., & Nudo, R. J. (1998). Recovery of motor function after focal cortical injury in primates: compensatory movement patterns used during rehabilitative training. *Somatosensory and Motor Research, 15,* 173-189.

Friel, K. M., Heddings, A. A., & Nudo, R. J. (2000). Effects of postlesion experience on behavioral recovery and neurophysiologic reorganization after cortical injury in primates. *Neurorehabilitation and Neural Repair, 14,* 187-198.

Frost, S. B., Barbay, S., Friel, K. M., Plautz, E. J., & Nudo, R. J. (2003). Reorganization of remote cortical regions after ischemic brain injury: A potential substrate for stroke recovery. *Journal of Neurophysiology, 89,* 3205-3214.

Galea, M. P., & Darian-Smith, I. (1994). Multiple corticospinal neuron populations in the macaque monkey are specified by their unique cortical origins, spinal terminations, and connections. *Cerebral Cortex, 4,* 166-194.

Galea, M. P., & Darian-Smith, I. (1995). Postnatal maturation of the direct corticospinal projections in the macaque monkey. *Cerebral Cortex, 5,* 518-540.

Galea, M. P. & Darian-Smith, I. (1997). Corticospinal projection patterns following unilateral section of the cervical spinal cord in the newborn and juvenile macaque monkey. *Journal of Comparative Neurology, 381,* 282-306.

Gash, D. M., Zhang, Z. M., Umberger, G., Mahood, K., Smith, M., Smith, C., & Gerhardt, G. A. (1999). An automated movement assessment panel for upper limb motor functions in rhesus monkeys and humans. *Journal of Neuroscience Methods, 89,* 111-117.

Glees, P., & Cole, J. (1950). Recovery of skilled motor function after small repeated lesions of motor cortex in macaque. *Journal of Neurophysiology, 13,* 137-148.

Graziano, M. S., Taylor, C. S., & Moore, T. (2002). Complex movements evoked by microstimulation of precentral cortex. *Neuron, 34,* 841-851.

Grichting, B., Hediger, V., Kaluzny, P., & Wiesendanger, M. (2000). Impaired proactive and reactive grip force control in chronic hemiparetic patients. *Clinical Neurophysiology, 111,* 1661-1671.

Hamadjida, A., Wyss, A. F., Mir, A., Schwab, M. E., Belhaj-Saif, A., & Rouiller, E. M. (2012). Influence of anti-Nogo-A antibody treatment on the reorganization of callosal connectivity of the premotor cortical areas following unilateral lesion of primary motor cortex (M1) in adult macaque monkeys. *Experimental Brain Research, 223,* 321-340.

Hoffman, D. S., & Strick, P. L. (1986). Step-tracking movements of the wrist in humans. I. Kinematic analysis. *Journal of Neuroscience, 6,* 3309-3318.

Hoogewoud, F., Hamadjida, A., Wyss, A. F., Mir, A., Schwab, M. E., Belhaj-Saif, A., & Rouiller, E. M. (2013). Comparison of functional recovery of manual dexterity after unilateral spinal cord lesion or motor cortex lesion in adult macaque monkeys. *Frontiers in Neurology,* (in press).

Iwaniuk, A. N., Pellis, S. M., & Whishaw, I. Q. (1999). Is digital dexterity really related to corticospinal projections?: a re-analysis of the Heffner and Masterton data set using modern comparative statistics. *Behavioural Brain Research, 101,* 173-187.

Iwaniuk, A. N., & Whishaw, I. Q. (1999). How skilled are the skilled limb movements of the raccoon (*Procyon lotor*)? *Behavioural Brain Research, 99,* 35-44.

Iwaniuk, A. N., & Whishaw, I. Q. (2000). On the origin of skilled forelimb movements. *Trends in Neuroscience, 23,* 372-376.

Kaeser, M., Wyss, A. F., Bashir, S., Hamadjida, A., Liu, Y., Bloch, J., . . . Rouiller, E. M. (2010). Effects of unilateral motor cortex lesion on ipsilesional hand's reach and grasp performance in monkeys: Relationship with recovery in the contralesional hand. *Journal of Neurophysiology, 103,* 1630-1645.

Kaeser, M., Brunet, J. F., Wyss, A., Belhaj-Saif, A., Liu, Y., Hamadjida, A., . . . & Bloch, J. (2011). Autologous adult cortical cell transplantation enhances functional recovery following unilateral lesion of motor cortex in primates: a pilot study. *Neurosurgery, 68,* 1405-1416.

Kaeser, M., Wannier, T., Brunet, J. F., Wyss, A., Bloch, J., & Rouiller, E. M. (2013). Representation of motor habit in a sequence of repetitive reach and grasp movements performed by macaque monkeys: Evidence for a contribution of the dorsolateral prefrontal cortex. *Cortex, 49,* 1404-1419.

Kakebeeke, T. H., Caflisch, J., Chaouch, A., Rousson, V., Largo, R. H., & Jenni, O. G. (2013). Neuromotor development in children. Part 3: motor performance in 3- to 5-year olds. *Developmental Medicine and Child Neurology, 55,* 248-256.

Kazennikov, O., Wicki, U., Corboz, M., Hyland, B., Palmeri, A., Rouiller, E. M., & Wiesendanger, M. (1994). Temporal structure of a bimanual goal-directed movement sequence in monkeys. *European Journal of Neuroscience, 6,* 203-210.

Kazennikov, O., Hyland, B., Wicki, U., Perrig, S., Rouiller, E. M., & Wiesendanger, M. (1998). Effects of lesions in the mesial frontal cortex on bimanual co-ordination in monkeys. *Neuroscience, 85,* 703-716.

Kazennikov, O., Hyland, B., Corboz, M., Babalian, A., Rouiller, E. M., & Wiesendanger, M. (1999). Neural activity of supplementary and primary motor areas in monkeys and its relation to bimanual and unimanual movement sequences. *Neuroscience, 89,* 661-674.

Kermadi, I., Liu, Y., Tempini, A., & Rouiller, E. M. (1997). Effects of reversible inactivation of the supplementary motor area (SMA) on unimanual grasp and bimanual pull and grasp performance in monkeys. *Somatosensory and Motor Research, 14,* 268-280.

Kermadi, I., Liu, Y., Tempini, A., Calciati, E., & Rouiller, E. M. (1998). Neuronal activity in the primate supplementary motor area and the primary motor cortex in relation to spatio-temporal bimanual coordination. *Somatosensory and Motor Research, 15,* 287-308.

Kermadi, I., Liu, Y., & Rouiller, E. M. (2000). Do bimanual motor actions involve the dorsal premotor (PMd), cingulate (CMA) and posterior parietal (PPC) cortices? Comparison with primary and supplementary motor cortical areas. *Somatosensory and Motor Research, 17,* 255-271.

King, B. J. (1986). Extractive foraging and the evolution of primate intelligence. *Journal of Human Evolution, 1,* 361-372.

King, J., & Landau, V. (1993). Manual preference in varieties of reaching in squirrel monkeys. In J. Ward & W. Hopkins (Eds.), *Primate laterality* (pp. 107-124). New York, NY: Springer.

Kinoshita, M., Matsui, R., Kato, S., Hasegawa, T., Kasahara, H., Isa, K., . . . Isa, T. (2012). Genetic dissection of the circuit for hand dexterity in primates. *Nature, 487,* 235-238.

Klein, A., Sacrey, L. A., Whishaw, I. Q., & Dunnett, S. B. (2012). The use of rodent skilled reaching as a translational model for investigating brain damage and disease. *Neuroscience and Biobehavioral Reviews, 36,* 1030-1042.

Lacreuse, A., & Fragaszy, D. M. (1999). Left hand preferences in capuchins (Cebus apella): role of spatial demands in manual activity. *Laterality, 4,* 65-78.

Lacroix, S., Havton, L. A., McKay, H., Yang, H., Brant, A., Roberts, J., & Tuszynski, M. H. (2004). Bilateral corticospinal projections arise from each motor cortex in the macaque monkey: A quantitative study. *Journal of Comparative Neurology, 473,* 147-161.

Lashley, K. S. (1930) Basic neural mechanisms in behavior. *Psychological Review, 37,* 1-24.

Lawrence, D. G., & Hopkins, D. A. (1976). The development of motor control in the rhesus monkey: evidence concerning the role of corticomotoneuronal connections. *Brain, 99,* 235-254.

Lawrence, D. G., Porter, R., & Redman, S. J. (1985). Corticomotoneuronal synapses in the monkey: light microscopic localization upon motoneurons of intrinsic muscles of the hand. *Journal of Comparative Neurology, 232,* 499-510.

Leca, J. B., Gunst, N., & Huffman, M. (2011). Complexity in object manipulation by Japanese macaques (*Macaca fuscata*): A cross-sectional analysis of manual coordination in stone handling patterns. *Journal of Comparative Psychology, 125,* 61-71.

Lemon, R. N., Johansson, R. S., & Westling, G. (1996). Modulation of corticospinal influence over hand muscles during gripping tasks in man and monkey. *Canadian Journal of Physiology and Pharmacology, 74,* 547-558.

Lemon, R. N. (1999). Neural control of dexterity: what has been achieved? *Experimental Brain Research, 128,* 6-12.

Lemon, R. N., & Griffiths, J. (2005). Comparing the function of the corticospinal system in different species: organizational differences for motor specialization? *Muscle Nerve, 32,* 261-279.

Lemon, R. N. (2008). Descending pathways in motor control. *Annual Review of Neuroscience, 31,* 195-218.

Lindshield, S. M., & Rodrigues, M. A. (2009). Tool use in wild spider monkeys (*Ateles geoffroyi*). *Primates, 50,* 269-272.

Liu, Y., & Rouiller, E. M. (1999). Mechanisms of recovery of dexterity following unilateral lesion of the sensorimotor cortex in adult monkeys. *Experimental Brain Research, 128,* 149-159.

Maier, M. A., Armand, J., Kirkwood, P. A., Yang, H. W., Davis, J. N., & Lemon, R. N. (2002). Differences in the corticospinal projection from primary motor cortex and supplementary motor area to macaque upper limb motoneurons: an anatomical and electrophysiological study. *Cerebral Cortex, 12,* 281-296.

Manoel, E. J., & Connolly, K. J. (1995). Variability and the development of skilled actions. *International Journal of Psychophysiology, 19,* 129-147.

Marshall, J. W., Ridley, R. M., Baker, H. F., Hall, L. D., Carpenter, T. A., & Wood, N. I. (2003). Serial MRI, functional recovery, and long-term infarct maturation in a non-human primate model of stroke. *Brain Research Bulletin, 61,* 577-585.

Marteniuk, R. G. (1974). Individual differences in motor performances and learning. *Exercise and Sport Sciences Reviews, 2,* 103-130.

McNeal, D. W., Darling, W. G., Ge, J., Stilwell-Morecraft, K. S., Solon, K. M., Hynes, S. M., . . . Morecraft, R. J. (2010). Selective long-term reorganization of the corticospinal projection from the supplementary motor cortex following recovery from lateral motor cortex injury. *Journal of Comparative Neurology, 518,* 586-621.

Murata, Y., Higo, N., Oishi, T., Yamashita, A., Matsuda, K., Hayashi, M., & Yamane, S. (2008). Effects of motor training on the recovery of manual dexterity after primary motor cortex lesion in macaque monkeys. *Journal of Neurophysiology, 99,* 773-786.

Nahallage, C. A. D., & Huffman, M. A. (2007). Acquisition and development of stone handling behavior in infant Japanese macaques. *Behaviour, 144,* 1193-1215.

Newell, K. M., Liu, Y. T., & Mayer-Kress, G. (2001). Time scales in motor learning and development. *Psychological Review, 108,* 57-82.

Nishimura, Y., Onoe, H., Morichika, Y., Perfiliev, S., Tsukada, H., & Isa, T. (2007). Time-dependent central compensatory mechanisms of finger dexterity after spinal cord injury. *Science, 318,* 1150-1155.

Nudo, R. J., Wise, B. M., SiFuentes, F., & Milliken, G. W. (1996). Neural substrates for the effects of rehabilitative training on motor recovery after ischemic infarct. *Science, 272,* 1791-1794.

Nudo, R. J., & Milliken, G. W. (1996). Reorganization of movement representations in primary motor cortex following focal ischemic infarcts in adult squirrel monkeys. *Journal of Neurophysiology, 75,* 2144-2149.

Ogden, R., & Franz, S. I. (1917). On cerebral motor control: the recovery from experimentally produced hemiplegia. *Psychobiology, 1,* 33-49.

Ogihara, N., & Oishi, M. (2012). Muscle dimensions in the Japanese macaque hand. *Primates., 53,* 391-396.

Olivier, E., Edgley, S. A., Armand, J., & Lemon, R. N. (1997). An electrophysiological study of the postnatal development of the corticospinal system in the macaque monkey. *Journal of Neuroscience, 17,* 267-276.

Padberg, J., Franca, J. G., Cooke, D. F., Soares, J. G., Rosa, M. G., Fiorani, M. Jr., . . . Krubitzer, L. (2007). Parallel evolution of cortical areas involved in skilled hand use. *Journal of Neuroscience, 27,* 10106-10115.

Passingham, R. E., Perry, V. H., & Wilkinson, F. (1983). The long-term effects of removal of sensorimotor cortex in infant and adult rhesus monkeys. *Brain, 106 (Pt 3),* 675-705.

Pizzimenti, M. A., Darling, W. G., Rotella, D. L., McNeal, D. W., Herrick, J. L., Ge, J., . . . Morecraft, R. J. (2007). Measurement of reaching kinematics and prehensile dexterity in nonhuman primates. *Journal of Neurophysiology, 98,* 1015-1029.

Plautz, E. J., Barbay, S., Frost, S. B., Friel, K. M., Dancause, N., Zoubina, E. V., . . . Nudo, R. J. (2003). Post-infarct cortical plasticity and behavioral recovery using concurrent cortical stimulation and rehabilitative training: a feasibility study in primates. *Neurological Research, 25,* 801-810.

Pouydebat, E., Laurin, M., Gorce, P., & Bels, V. (2008). Evolution of grasping among anthropoids. *Journal of Evolutionary Biology, 21,* 1732-1743.

Pouydebat, E., Gorce, P., Coppens, Y., & Bels, V. (2009). Biomechanical study of grasping according to the volume of the object: human versus non-human primates. *Journal of Biomechanisms, 42,* 266-272.

Pouydebat, E., Reghem, E., Borel, A., & Gorce, P. (2011). Diversity of grip in adults and young humans and chimpanzees (*Pan troglodytes*). *Behavioural Brain Research, 218,* 21-28.

Rathelot, J. A., & Strick, P. L. (2009). Subdivisions of primary motor cortex based on cortico-motoneuronal cells. *Proceedings of the National Academy of Sciences of the United States of America, 106,* 918-923.

Roitberg, B., Khan, N., Tuccar, E., Kompoliti, K., Chu, Y., Alperin, N., . . . Emborg, M. E. (2003). Chronic ischemic stroke model in cynomolgus monkeys: behavioral, neuroimaging and anatomical study. *Neurological Research, 25,* 68-78.

Rosenblatt, N. J., Hurt, C. P., Latash, M. L., & Grabiner, M. D. (2014) An apparent contradiction: increasing variability to achieve greater precision? *Experimental Brain Research, 232,* 403-413.

Rouiller, E. M., Moret, V., Tanné, J., & Boussaoud, D. (1996). Evidence for direct connections between the hand region of the supplementary motor area and cervical motoneurons in the macaque monkey. *European Journal of Neuroscience, 8,* 1055-1059.

Rouiller, E. M., Yu, X. H., Moret, V., Tempini, A., Wiesendanger, M., & Liang, F. (1998). Dexterity in adult monkeys following early lesion of the motor cortical hand area: the role of cortex adjacent to the lesion. *European Journal of Neuroscience, 10,* 729-740.

Sacrey, L. A., Alaverdashvili, M., & Whishaw, I. Q. (2009). Similar hand shaping in reaching-for-food (skilled reaching) in rats and humans provides evidence of homology in release, collection, and manipulation movements. *Behavioural Brain Research, 204,* 153-161.

Sasaki, K., & Gemba, H. (1984). Compensatory motor function of the somatosensory cortex for dysfunction of the motor cortex following cerebellar hemispherectomy in the monkey. *Experimental Brain Research, 56,* 532-538.

Sasaki, S., Isa, T., Pettersson, L. G., Alstermark, B., Naito, K., Yoshimura, K., . . . Ohki, Y. (2004). Dexterous finger movements in primate without monosynaptic corticomotoneuronal excitation. *Journal of Neurophysiology, 92,* 3142-3147.

Schieber, M. H. (2001). Constraints on somatotopic organization in the primary motor cortex. *Journal of Neurophysiology, 86,* 2125-2143.

Schmidlin, E., Wannier, T., Bloch, J., & Rouiller, E. M. (2004). Progressive plastic changes in the hand representation of the primary motor cortex parallel incomplete recovery from a unilateral section of the corticospinal tract at cervical level in monkeys. *Brain Research, 1017,* 172-183.

Schmidlin, E., Wannier, T., Bloch, J., Belhaj-Saïf, A., Wyss, A., & Rouiller, E. M. (2005). Reduction of the hand representation in the ipsilateral primary motor cortex following unilateral section of the corticospinal tract at cervical level in monkeys. *BMC Neuroscience, 6:56.*

Schmidlin, E., Kaeser, M., Gindrat, A. D., Savidan, J., Chatagny, P., Badoud, S., . . . Rouiller, E. M. (2011). Behavioral assessment of manual dexterity in non-human primates. *Journal of Visualized Experiments, 57:* 3258.

Schmidt, R. A., & Lee, T. D. (2011). Individual differences and capabilities. In *Motor control and learning: a behavioral emphasis* (5th ed., pp. 297-324). Champaign, IL: Human Kinetics.

Schmidt, R. A., & Lee, T. D. (2011). Motor learning concepts and research methods. In *Motor control and learning: a behavioral emphasis* (5th ed., pp. 327-346). Champaign, IL: Human Kinetics.

Schorer, J., Baker, J., Fath, F., & Jaitner, T. (2007). Identification of interindividual and intraindividual movement patterns in handball players of varying expertise levels. *Journal of Motor Behavior, 39,* 409-421.

Serrien, D. J., & Wiesendanger, M. (1999). Grip-load force coordination in cerebellar patients. *Experimental Brain Research, 128,* 76-80.

Serrien, D. J., Kaluzny, P., Wicki, U., & Wiesendanger, M. (1999). Grip force adjustments induced by predictable load perturbations during a manipulative task. *Experimental Brain Research, 124,* 100-106.

Spinozzi, G., Castorina, M. G., & Truppa, V. (1998). Hand preferences in unimanual and coordinated-bimanual tasks by tufted capuchin monkeys (*Cebus apella*). *Journal of Comparative Psychology, 112,* 183-191.

Spinozzi, G., Truppa, V., & Lagana, T. (2004). Grasping behavior in tufted capuchin monkeys (*Cebus apella*): grip types and manual laterality for picking up a small food item. *American Journal of Physical Anthropology, 125,* 30-41.

Spinozzi, G., Lagana, T., & Truppa, V. (2007). Hand use by tufted capuchins (*Cebus apella*) to extract a small food item from a tube: digit movements, hand preference, and performance. *American Journal of Primatology, 69,* 336-352.

Stelmach, G. E. (1968). Distribution of practice in individual differences and intra-variability. *Perceptual and Motor Skills, 26,* 727-730.

Sugiyama, Y., Higo, N., Yoshino-Saito, K., Murata, Y., Nishimura, Y., Oishi, T., & Isa, T. (2013). Effects of early versus late rehabilitative training on manual dexterity after corticospinal tract lesion in macaque monkeys. *Journal of Neurophysiology, 109,* 2853-2865.

Tomassini, V., Jbabdi, S., Kincses, Z. T., Bosnell, R., Douaud, G., Pozzilli, C., . . . Johansen-Berg, H. (2011). Structural and functional bases for individual differences in motor learning. *Human Brain Mapping, 32,* 494-508.

Travis, A. M. (1955). Neurological deficiencies after ablation of the precentral motor area in *Macaca mulatta*. *Brain, 78,* 155-173.

Van Schaik, C. P., Deaner, R. O., & Merrill, M. Y. (1999). The conditions for tool use in primates: implications for the evolution of material culture. *Journal of Human Evolution, 36,* 719-741.

Wannier, T., Schmidlin, E., Bloch, J., & Rouiller, E. M. (2005). A unilateral section of the corticospinal tract at cervical level in primate does not lead to measurable cell loss in motor cortex. *Journal of Neurotrauma, 22,* 703-717.

Whishaw, I. Q., Whishaw, P., & Gorny, B. (2008). The structure of skilled forelimb reaching in the rat: a movement rating scale. *Journal of Visualized Experiments, 18*: 816.

Whishaw, I. Q., Travis, S. G., Koppe, S. W., Sacrey, L. A., Gholamrezaei, G., & Gorny, B. (2010). Hand shaping in the rat: conserved release and collection vs. flexible manipulation in overground walking, ladder rung walking, cylinder exploration, and skilled reaching. *Behavioural Brain Research, 206,* 21-31.

Wiesendanger, M. (1999). Manual dexterity and the making of tools - an introduction from an evolutionary perspective. *Experimental Brain Research, 128,* 1-5.

Wong, Y. J., & Whishaw, I. Q. (2004). Precision grasps of children and young and old adults: individual differences in digit contact strategy, purchase pattern, and digit posture. *Behavioural Brain Research, 154,* 113-123.

Wu, H. G., Miyamoto, Y. R., Gonzalez Castro, L. N., Ölveczky, B. P., & Smith, M. A. (2014) Temporal structure of motor variability is dynamically regulated and predicts motor learning ability. *Nature Neuroscience, 17*, 312-321.

Wyss, A. F., Hamadjida, A., Savidan, J., Liu, Y., Bashir, S., Mir, A., . . . Belhaj-Saif, A. (2013). Long-term motor cortical map changes following unilateral lesion of the hand representation in the motor cortex in macaque monkeys showing functional recovery of hand functions. *Restorative Neurology and Neuroscience, 31*, 733-760.

Zhao, D., Hopkins, W. D., & Li, B. (2012). Handedness in nature: first evidence on manual laterality on bimanual coordinated tube task in wild primates. *American Journal of Physical Anthropology, 148*, 36-44.

Financial Support: Swiss National Science Foundation, Grants No 31-61857.00, 310000-110005, 31003A-132465, 310030B-149643 (EMR), the National Centre of Competence in Research (NCCR) on *Neural plasticity and repair*; Novartis Foundation; The Christopher Reeves Foundation (Springfield, NJ, USA); The Swiss Primate Competence Centre for Research (SPCCR: *http://www.unifr.ch/neuro/rouiller/SPCCR*); Consortium Grant Sinergia CRSI33-125408.

Conflict of interest: none.

Submitted: *August 31st, 2013*
Resubmitted: *December 14th, 2013*
Accepted: *January 22nd , 2014*

INTERNATIONAL JOURNAL OF COMPARATIVE PSYCHOLOGY

2014, 27 (2), S1 –S5
A. Blaisdell & W. D. Stahlman
Special Issue
Peer-reviewed

Variability of manual dexterity performance in non-human primates (*Macaca fascicularis*)

Mélanie Kaeser*, Pauline Chatagny*, Anne-Dominique Gindrat, Julie Savidan, Simon Badoud, Michela Fregosi, Véronique Moret, Christine Roulin, Eric Schmidlin# and Eric M. Rouiller#
Domain of Physiology, Department of Medicine and Fribourg Center for Cognition, University of Fribourg, Chemin du Musée 5, CH-1700 Fribourg, Switzerland.

Supplementary Methods

Twenty adult macaque monkeys were included in the present study (see Table 1 for individual parameters related to sex, weight, age, etc). Before September 2010, the monkeys were kept in the animal facility in groups of 2 to 5 animals, each group in an interior housing space of 15 m^3 at most, without regular access to an outside facility. In September 2010, new guidelines were introduced in the Swiss legislation. From this time point, animals have been housed in 45 m^3 rooms, still in groups of 2-5 animals. In addition, the monkeys have access to an outside facility for a part of the day or night (ranging from 13.6 m^3 to 23 m^3). The housing conditions for each animal are indicated in Table 1. Only a couple of monkeys were transferred in 2010 from the 15 m^3 to the 45 m^3 housing facility. The degree of enrichment of the housing facilities, consisting in trees, ropes, cylinders to hide, different toys, etc, was higher in the 45 m^3 housing facility than in the previously used 15 m^3 housing facility.

Experimental procedures, limited in the current report to behavioral investigations, and animal care, were previously described in detail (e.g. Kaeser et al., 2010, 2011; Bashir et al., 2012; Hamadjida et al., 2012; Hoogewoud et al., 2013), and were conducted in accordance to the Guide for the Care and Use of Laboratory Animals (ISBN 978-0-309-15400-0; 2011). The experiments were approved first by the local (cantonal) ethical committee (surveying animal experimentation and evaluating research proposals). The experiments were finally authorized by the cantonal (Fribourg) and federal (Swiss) veterinary officers. The present experiments were covered by the following authorizations: FR 24/95/1; FR 40/96, FR 166/03, FR 166/05, FR 166E/08, FR 157e/04, FR 156/04, FR 156/06, FR 157e/06; FR 156/08, FR 185-08, FR 192/07e, FR 185/08, FR 206/08, FR 18/10, FR 17-09, FR 22010.

The monkeys had always free access to water and were not food deprived. The behavioral tests represented the first daily access to food (pellets), complemented by fruits, vegetables and cereals following the behavioral session and during the rest of the day (no food was given during the night). The body weight of the monkeys was monitored on each working day. In case of a loss of 10% or more of the body weight, the behavioral experiments were to be interrupted, a condition never met in the course of the present experiments. Due to individual behavioral differences when the monkeys were confronted to the behavioral set-up for the first time, some animals were first habituated to the modified Brinkman board task (5-15 blank sessions) whereas, for other monkeys, the collection of the data started immediately on the first session (Table 1).

* shared first authorship, # shared senior authorship

Please send correspondence to Prof. Eric M. Rouiller, Domain of Physiology, Department of Medicine and Fribourg Center for Cognition, University of Fribourg, Chemin du Musée 5, CH-1700 Fribourg, Switzerland, Phone: +41 26 300 86 09; Fax: +41 26 300 96 75. (eric.rouiller@unifr.ch)

One monkey (Mk-CE) was involved in studies performed from 1996 to 1998, whereas others were engaged in later studies (between 2000 and 2006: Mk-AV, Mk-BI, Mk-GE, Mk-JA, Mk-JO, Mk-MO, Mk-RO, Mk-VA, Mk-WI). These monkeys appeared in previous reports of the laboratory, focused on functional recovery from spinal cord or motor cortex lesion (e.g. Bashir et al., 2012; Hamadjida et al., 2012; Hoogewoud et al., 2013; Kaeser et al., 2010, 2011, 2013; Schmidlin et al., 2011). Finally, the rest of the monkeys (n=10; see Table 1) are involved in ongoing studies. In all monkeys, the ultimate goal is to train them to perform a palette of manual dexterity tasks (Schmidlin et al., 2011), before the occurrence of an experimental lesion affecting the motor system. In the present report, only the phase preceding the lesion is considered, comprising a learning phase, followed by a stable pre-lesion plateau of performance.

Supplementary Results

To better compare CTs at plateau with CTs at onset of learning phase, correlation plots were established (suppl. Fig. 3). Considering the median CTs (suppl. Fig. 3, panel A), separately for the horizontal and vertical slots, the data point are located on the right of the identity lines for most monkeys, meaning that CTs were indeed longer at onset of the learning phase than later at plateau. The median CTs observed at onset of the learning phase were predictors of the median CTs at plateau, but only to a limited extent (coefficients of correlation not statistically significant: $p=0.085$ and 0.073, respectively). The comparison of CTs' variability at plateau and at onset of the learning phase was achieved by correlating the respective distance between the 25 and 75 percentiles of the box and whisker plots (suppl. Fig. 3, panel B). The variability of CTs was larger in most cases at the beginning of the learning phase than at plateau, but the CT's variability at onset of learning was a poor predictor of CT's variability at plateau.

Human subjects exhibited a very rapid learning curve for the modified Brinkman board, reaching a plateau after 4-5 sessions in a series of 10, though performed all the same day (Chatagny et al., 2013). Do monkeys also improve their performance very early during the training phase, in the form of a rapid decrease in CTs' variability? To address this question, the CTs of the 20 monkeys in the first four days of the learning phase were pooled: there was no decrease in variability of CTs from the first day of learning to the fourth day, for both slot orientations. However, as pooling data over monkeys may produce a learning curve not representative of any single individual monkey (Newell et al., 2001; Adi-Japha et al., 2008), the variability of CTs during the first four days of learning was assessed individually in the 20 monkeys. In 13 monkeys, in line with the pooled trend, there was no clear decrease in CTs' variability during the first four days of learning, for both vertical and horizontal slots. In contrast, 4 monkeys exhibited a progressive decrease in CT's variability for both slot orientations during the first four days of learning already (Mk-DG, Mk-LO, Mk-MA, and Mk-TH). Three monkeys showed the same progressive decrease in CTs' variability, but only for the horizontal slots (Mk-AT and Mk-DI), respectively only for the vertical slots (Mk-EN). These 7 monkeys with a decrease in CTs' variability early during the learning phase did not systematically exhibit short learning durations or steep slope of learning (Table 1), except for Mk-DI and MK-TH. Overall, the learning appeared slower and more progressive in the majority of monkeys, as compared to human subjects. However, this difference may be in part related to different experimental designs: humans practiced the test 10 times on the same day whereas, in monkeys, it was restricted to one session a day.

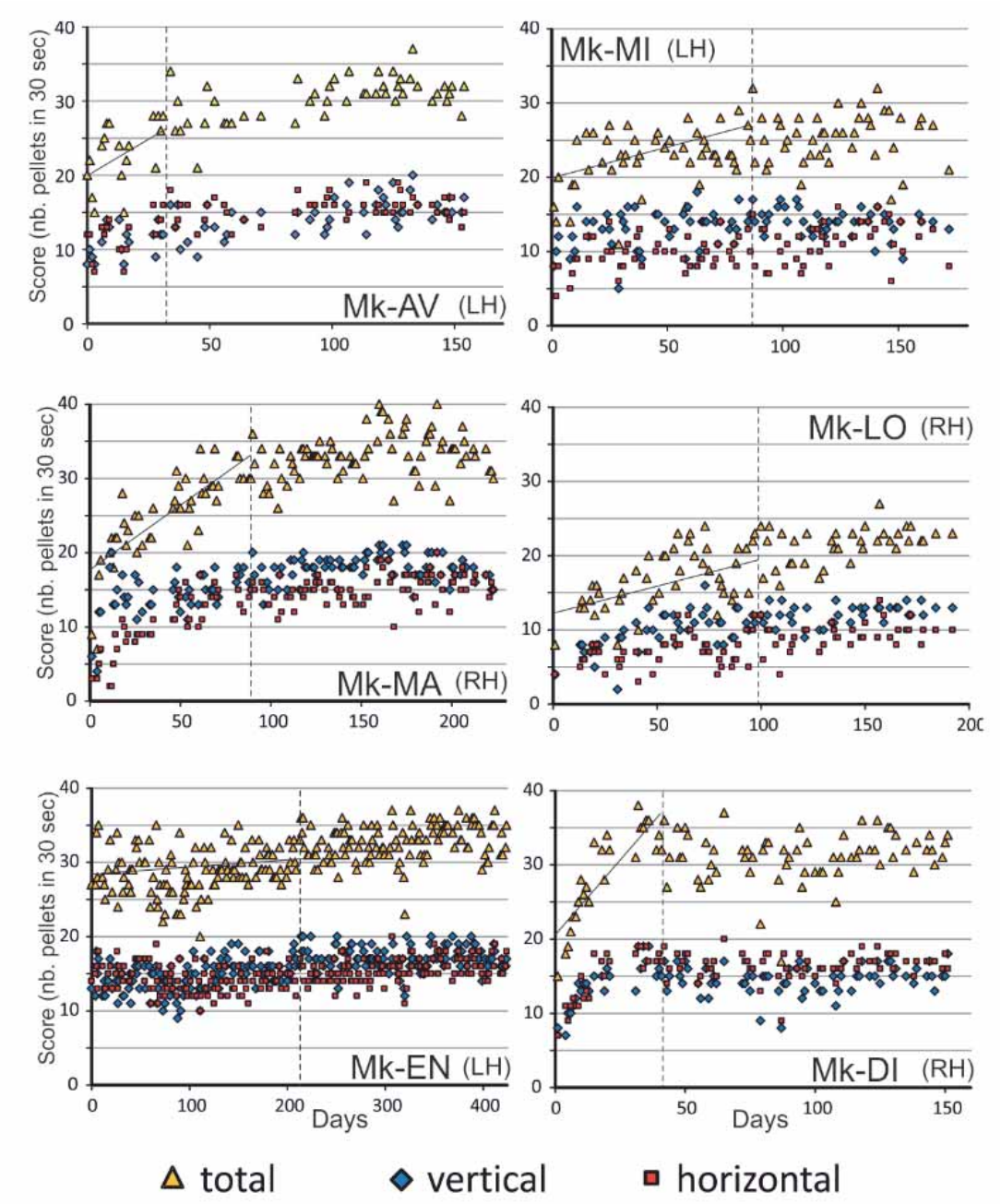

Supplementary Figure 1. Plots showing the score obtained by 6 monkeys (Mk-AV, Mk-MA, Mk-EN, Mk-MI, Mk-LO, Mk-DI) in the modified Brinkman board task for the dominant hand. Same conventions as in Figure 1.

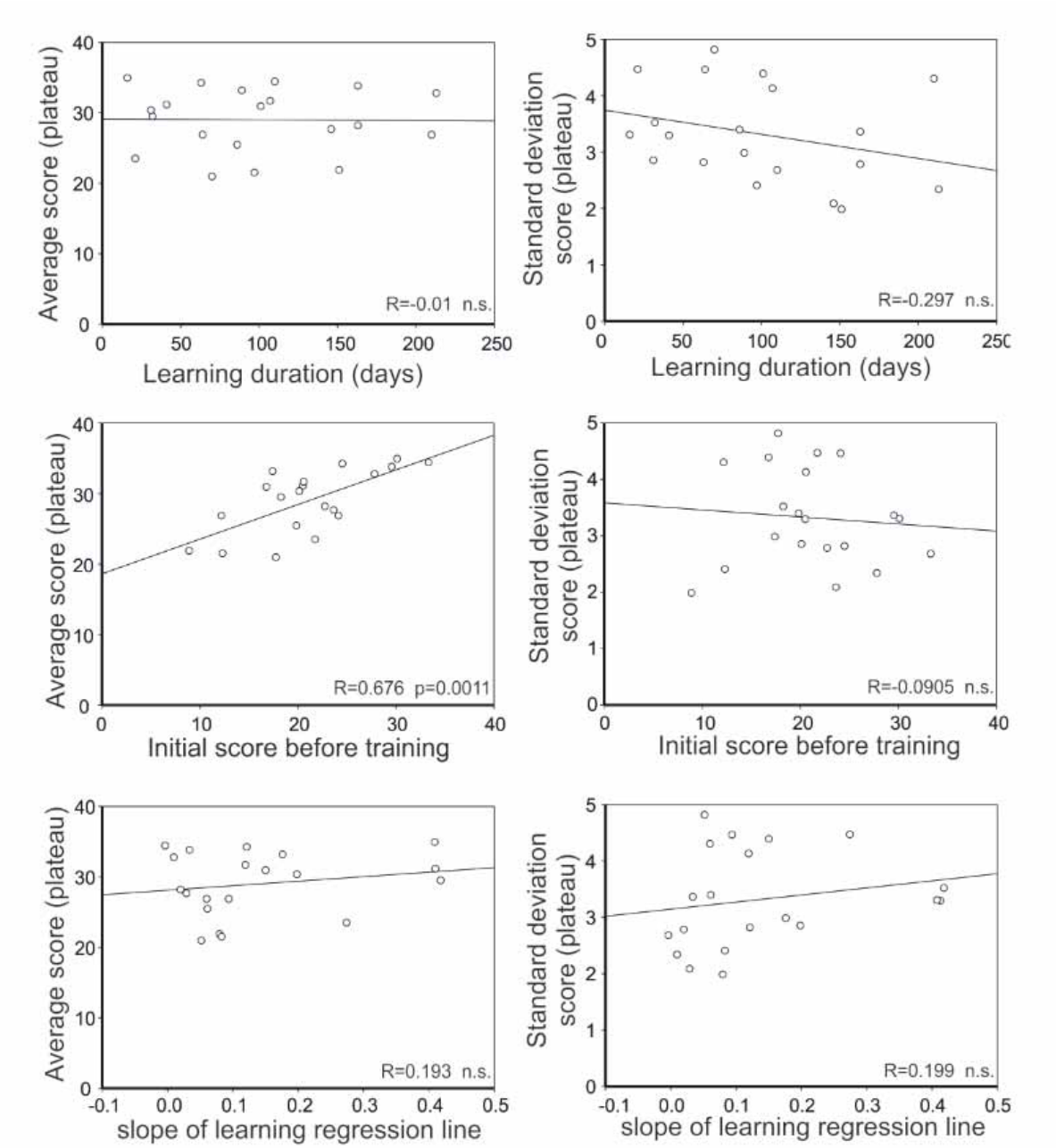

Supplementary Figure 2. Correlation plots between parameters representative of the learning phase and parameters representative of the plateau phase for the modified Brinkman board task (see text). The corresponding coefficients of correlation (R) are given at the bottom right of each graph, followed by the p value in case of statistical significance or "n.s." if the coefficient of correlation is not statistically significant (Pearson correlation test). The regression line is shown for each graph. Note that, for completeness of data illustration, the middle left panel is the same as that shown in Figure 3 (top right panel).

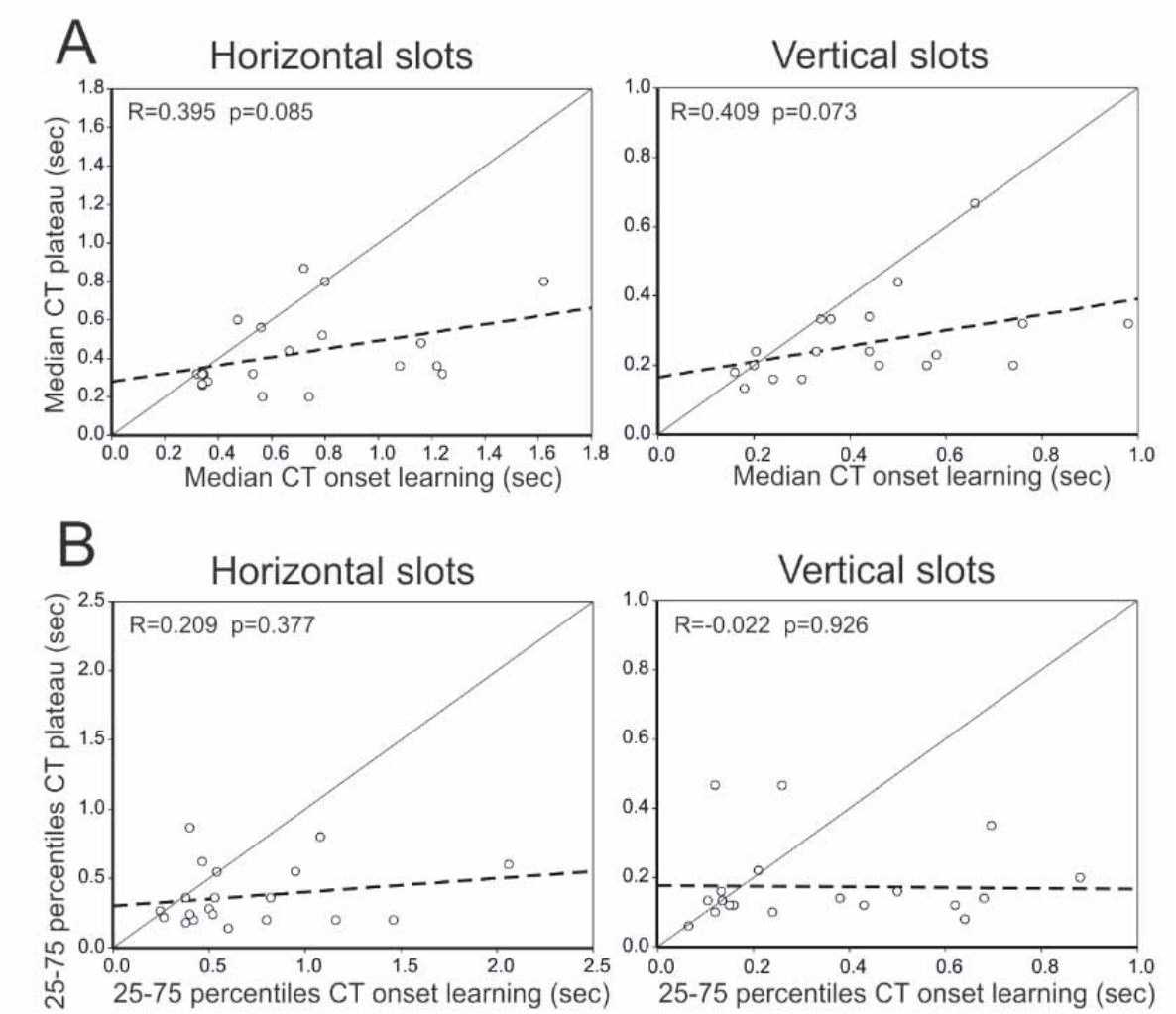

Supplementary Figure 3. **Panel A**: The median contact times (CTs) measured at plateau (y-axis) were correlated for each of the 20 monkeys with those established at the onset of the learning phase (x-axis), separately for the horizontal (left column) and the vertical (right column) slots. In each plot, the regression line is represented by the dashed line and the identity line by the solid line. The corresponding coefficients of correlation (R=) and p values are indicated at the top left of each plot. **Panel B**: The variability of CTs at plateau (y-axis) was correlated with the one at the beginning of learning phase (x-axis). Same conventions as in panel A.

Curriculum vitae

Anne-Dominique, Marie-Claire, Andrée Gindrat

Date of birth: 9th December 1985
Place of origin: La Baroche (JU, Switzerland)
Citizenship: Swiss
Civil status: Single

Work address

University of Fribourg
Department of Medicine
Domain of Physiology
Chemin du Musée 5
CH-1700 Fribourg
Switzerland
Phone: +41 26 300 86 12
E-mail: anne-dominique.gindrat@unifr.ch

Home address

Route des Arsenaux 39
CH-1700 Fribourg
Switzerland

Research interests

Neuroscience, neurophysiology, electroencephalography, sensorimotor system, hand motor control, lesion-induced brain plasticity, use-dependent brain plasticity

Education

21st September 2015	PhD in Neuroscience, laboratory of Prof. E.M. Rouiller, University of Fribourg, Switzerland PhD thesis: *A window into the plasticity of the sensorimotor system in adult primates using EEG: Insights from lesion, repeated stimulation and touchscreen use*
Dec. 2014 - Sept. 2015	Guest student at the Institute of Neuroinformatics and Neuroscience Center Zürich, University of Zürich and ETH Zürich, laboratory of Dr. Arko Ghosh
March 2010 - Sept. 2015	PhD student in Neuroscience, laboratory of Prof. E.M. Rouiller, University of Fribourg, Switzerland BeNeFri Program in Neuroscience

Sept. 2008 - Feb. 2010	MSc in Biology, University of Fribourg, Switzerland Option Developmental and Cell Biology Master thesis: *Development of an EEG cap allowing multichannel somatosensory evoked potential recordings in macaque monkey*, carried out in the laboratory of Prof. E.M. Rouiller, University of Fribourg, Switzerland
Oct. 2005 - Sept. 2008	BSc in Biology, University of Fribourg, Switzerland Options Neuroscience, Special Biology for Biology students Bachelor work: *Évolution de la performance motrice fine, des potentiels évoqués somatosensoriels et des réponses aux microstimulations intracorticales chez le macaque à longue queue suite à une lésion du cortex moteur primaire,* carried out in the laboratory of Prof. E.M. Rouiller, University of Fribourg, Switzerland
June 2005	Diplôme de maturité gymnasiale, Lycée Saint-Charles, Porrentruy, Switzerland Options Biology/Chemistry, Physics
March 2005	Preliminary English Test (PET), Cambridge ESOL Pass with Merit

Education and training in animal experiments

Sept.-Dec. 2014	LTK Module 20: Introductory Course in Laboratory Animal Science, Non-human primates
5th Sept. 2013	Practical seminar on animal anaesthesia and analgesia of various species, held by Veterinary Anaesthesia Services-International
7th-8th March 2012	Education seminar on animal anaesthesia and analgesia of various species, held by Veterinary Anaesthesia Services-International
8th-17th June 2009	RESAL Module 1: Introductory Course in Laboratory Animal Science 20 hours of theory and 20 hours of practice on laboratory rodents and rabbits, corresponds to FELASA B category course

Languages

French	Mother tongue
English	Level B2 (according to the Council of Europe Level)
German	Level B1-B2 (according to the Council of Europe Level)
Latin	Studied for 6 years

Teaching experience

April 2010 – present	Teaching assistant for practical courses of Neurophysiology for Medical students, Biomedical Sciences students, Biology and Psychology students, Domain of Physiology, University of Fribourg, Switzerland
12th May 2011	*Development of high-density scalp SSEP recordings in macaque monkeys*, Advanced PhD course in EEG recording and analysis, Lemanic Neuroscience Doctoral School

Invited talks

5th August 2015	*A window into the plasticity of the sensorimotor system in adult primates using EEG: Insights from lesion, repeated stimulation and touchscreen* use, German Primate Center, Goettingen, Germany
3rd March 2015	*What do smartphones or macaque monkeys tell us about the reorganisation of the sensorimotor cortex in primates ?*; Brain and Development Meeting, Children Hospital Zürich, Switzerland
29th January 2015	*Lesion-induced or use-dependent reorganisation of sensorimotor cortex in primates*; Max Planck Institute for Biological Cybernetics, Tuebingen, Germany
8th September 2014	*Effect of primary motor cortex lesion on cortical processing of tactile finger stimulation in adult monkeys*; Hand, Brain and Technology, CSF Conference, Monte Verità, Switzerland
14th May 2014	*La recherche en neurosciences est-elle concevable sans modèle animal ?*; Société jurassienne d'Émulation; Porrentruy, Switzerland
2nd October 2013	*The sensorimotor system in macaque monkeys following a motor cortex lesion: study from whole-scalp EEG mapping of somatosensory evoked potentials and from the Brinkman box task*; Fribourg Day of Cognition 2013, University of Fribourg, Switzerland
27th June 2012	*Recordings of high-density scalp somatosensory evoked potentials in macaque monkeys (Macaca fascicularis)*; Dep-Med Seminar, Department of Medicine, University of Fribourg, Switzerland
14th June 2011	*Feasibility of high-density somatosensory evoked potential recordings in macaque monkeys: a pilot study*; NCCR P3 progress report, ETH, Zürich, Switzerland
31st March 2010	*Development of an EEG cap allowing multichannel somatosensory evoked potential recordings in macaque monkey*; Faculty of Medicine, University of Geneva, Switzerland

Publications

Gindrat AD*, Chytiris M*, Balerna M*, Rouiller EM, Ghosh A (2015) L'utilisation de smartphones façonne le traitement cortical de l'information sensorielle tactile provenant de l'extrémité des doigts. Med Sci (Paris) 31(4):363-366. DOI: 10.1051/medsci/20153104006

Gindrat AD*, Chytiris M*, Balerna M*, Rouiller EM, Ghosh A (2015) Use-Dependent Cortical Processing from Fingertips in Touchscreen Phone Users. Current Biology 25(1):1-8. DOI: 10.1016/j.cub.2014.11.026

Kaeser M*, Chatagny P*, Gindrat AD, Savidan J, Badoud S, Fregosi M, Moret V, Roulin C, Schmidlin E, Rouiller EM (2014) Variability of manual dexterity performance in non-human primates (*Macaca fascicularis*). International Journal of Comparative Psychology 27(2):295-325

Gindrat AD*, Quairiaux C*, Britz J, Brunet D, Lanz F, Michel CM, Rouiller EM (2014) Whole-scalp EEG mapping of somatosensory evoked potentials in macaque monkeys. Brain Structure and Function 1-22. DOI: 10.1007/s00429-014-0776-y

Chatagny P*, Badoud S*, Kaeser M, Gindrat AD, Savidan J, Fregosi M, Moret V, Roulin C, Schmidlin E, Rouiller EM (2013) Distinction between hand dominance and hand preference in primates: a behavioral investigation of manual dexterity in nonhuman primates (macaques) and human subjects. Brain and Behavior 3:575-595, DOI: 10.1002/brb3

Schmidlin E, Kaeser M, Gindrat AD, Savidan J, Chatagny P, Badoud S, Hamadjida A, Beaud ML, Wannier T, Belhaj-Saif A, Rouiller EM (2011) Behavioral assessment of manual dexterity in non-human primates. Journal of Visualized Experiments (57) e3258. DOI: 10.3791/3258

Peuser J, Belhaj-Saif A, Hamadjida A, Schmidlin E, Gindrat AD, Volker AC, Zakharov P, Hoogewoud HM, Rouiller EM, Scheffold F (2011) Follow-up of cortical activity and structure after lesion with laser speckle imaging and magnetic resonance imaging in nonhuman primates. Journal of Biomedical Optics 16(9):096011-1-096011-11. DOI:10.1117/1.3625287

Media

25th March 2015	Radio	*L'impact des smartphones sur le cerveau*, Scientific broadcast (RTS la 1ère, CQFD)
14th Jan. 2015	TV	*Chez le natif digital, l'usage de la main est modifié ainsi que les effets sur le cerveau*, Swiss prime-time news (RTS, le 19h30)
2014-2015	Print	*Impact of smartphone use on sensory processing in the brain,* La Liberté, Le Quotidien Jurassien
2014-2015	Web	*That smartphone is giving your thumbs superpowers,* Various web sites, among them: Reuters, NBC News, BBC News, FOX News, Washington ost, Huffington Post, PLOS Neuroscience Community, Scientific American, le Monde, etc.

Membership

Student Member of the Swiss Society for Neuroscience

23.08.2015